LANDSLIDE RISK MANAGEMENT

PROCEEDINGS OF THE INTERNATIONAL CONFERENCE ON LANDSLIDE RISK
MANAGEMENT, VANCOUVER, CANADA, 31 MAY–3 JUNE 2005

Landslide Risk Management

Edited by

Oldrich Hungr
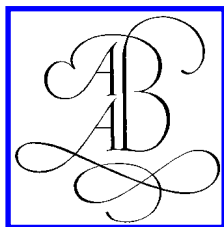*University of British Columbia, Canada*

Robin Fell
University of New South Wales, Australia

Réjean Couture
Geological Survey of Canada

Erik Eberhardt
University of British Columbia, Canada

A.A. BALKEMA PUBLISHERS   LEIDEN / LONDON / NEW YORK / PHILADELPHIA / SINGAPORE

Cover photo courtesy: D. Panaro, Ventura County, California, 2005

Table of Contents

VI

VII

Remedial works and early warning systems

VIII

Preface

Landslides rank behind earthquakes and droughts on the scale of destructiveness. Nevertheless, they represent a major type of natural hazard that extracts a steady, painful toll from inhabitants of mountains, hilly regions, escarpments and river valleys around the world. The impact of landslides is sudden and erratic in time and reliable warnings are difficult to implement. It is highly focused in area and this allows an opportunity for pro-active defense, by outlining the hazard areas beforehand and estimating the hazards and risks. The benefits of rationally-planned pro-active defense are twofold. On one hand, it saves lives and property when an impact occurs. On the other hand, it prevents excessive expenses that are often incurred by governments in futile attempts to rectify a critical situation after damage has happened. Either goal requires that landslide hazards and risks be reliably and accurately characterized before they occur. This is a considerable challenge, primarily to the applied geoscience professionals who specialize in this field.

In 1997, Professor Robin Fell called an informal meeting of specialists on landslide risk in Honolulu, Hawaii. The result of this workshop was a book, representing a fair summary of the State of the Art of landslide risk at the time (Cruden & Fell 1997). To follow up on this pilot project, the Joint Technical Committee on Landslides and Engineered Slopes (JTC-1*), in association with the Vancouver Geotechnical Society*, proposed to host an International Conference on Landslide Risk Management on the campus of the University of British Columbia in Vancouver, from May 31 to June 3, 2005. This volume represents the proceedings of the conference. It has two parts. The first part contains State of the Art and Invited lectures, prepared by teams of authors selected for their experience in specific topics assigned to them by the JTC-1 Committee. The second part is a selection of general papers submitted to the conference, most of which serve as case history illustrations of projects on landslide risk management. Thus, the book is not merely a set of conference proceedings, but a comprehensive reference, summarizing the current status of the subject as viewed by experts from around the world. Further papers presented at the conference are being published simultaneously on a Compact Disk.

Each paper in the book and CD was reviewed by at least one peer reviewer. In addition, the Chair of JTC-1, Professor Robin Fell, independently reviewed each State of the Art and Invited paper. The Editors would like to acknowledge the following Reviewers for their competent work:

Andrée Blais-Stevens, Geological Survey of Canada
Peter T. Bobrowsky, Geological Survey of Canada
Chris Bunce, CP Rail, Inc.
Giovanni Crosta, University of Milan
Dave Cruden, University of Alberta
Jonathan Fannin, University of British Columbia
Corey Froese, AMEC Earth & Environmental Ltd.
Bob Gerath, Thurber Engineering Ltd.
Jean Hutchinson, Queens University
Monica Jaramillo, Geological Survey of Canada
Serge Leroueil, Université Laval
Jacques Locat, Université Laval
Scott McDougall, University of British Columbia
Norbert Morgenstern, University of Alberta
Susan Nichol, Geological Survey of Canada
Didier Perret, Geological Survey of Canada
Dave Petley, Durham University
Doug Stead, Simon Fraser University
Alex Strouth, University of British Columbia
Dharma Wijewickreme, University of British Columbia
Reginald Hermanns, Geological Survey of Canada

Messrs. Ron Yehia and Mark Sloat from the University of British Columbia assisted ably with the organization and editing of the papers.

Thanks are also due to the organizers of the conference:

The Editors feel privileged for being a part of this exciting undertaking and hope that the present volume will be useful to many practitioners of landslide risk science and that it will, perhaps, help to reduce future losses due to landslides.

Vancouver 2005 Editors,
Oldrich Hungr, Robin Fell, Réjean Couture, Erik Eberhardt
March 1, 2005

Reference: D.M. Cruden & R.Fell (Eds.), Landslide Risk Assessment. Proceedings, Landslide Risk Workshop, Honolulu, Hawaii, Balkema, Rotterdam , 371 p.

*Contacts:
The Joint Technical Committee on Landslides and Engineered Slopes, JTC-1
    sponsored by: ISSMGE, ISRM and IAEG,
    Web address: http://www.geoforum.com/jtc1/
Vancouver Geotechnical Society
    Sponsored by the Canadian Geotechnical Society,
    Web address: http://www.vancouvergeotechnicalsociety.com/

Colour plates

(a) Post-landslide looking seaward

(b) Pre-landslide looking landward with outline of landslide debris

Plate I.   La Conchita CA Landslide 2005 (by UCSB).
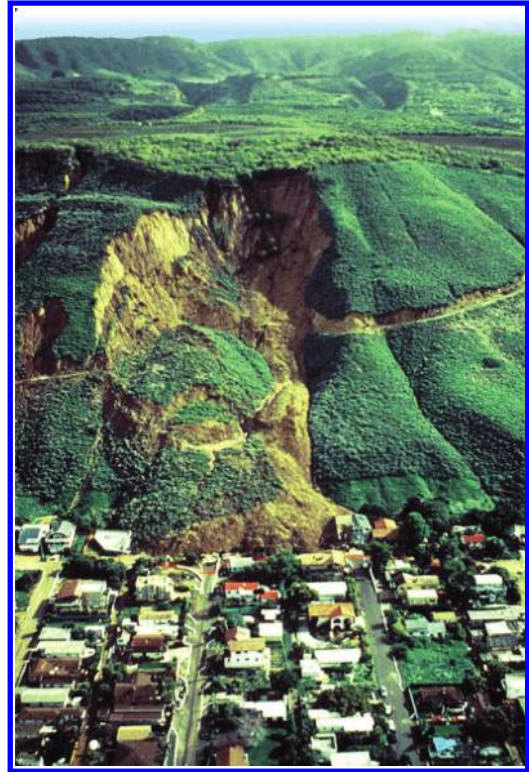
Plate II.   La Conchita CA Landslide 1995 (by USGS).
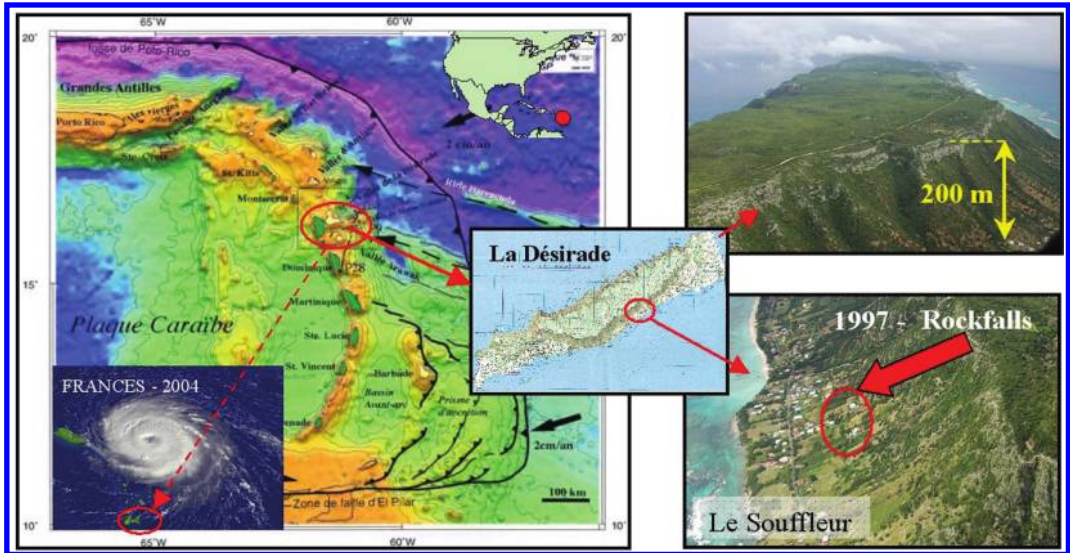
Plate III.   General context of La Désirade Island.
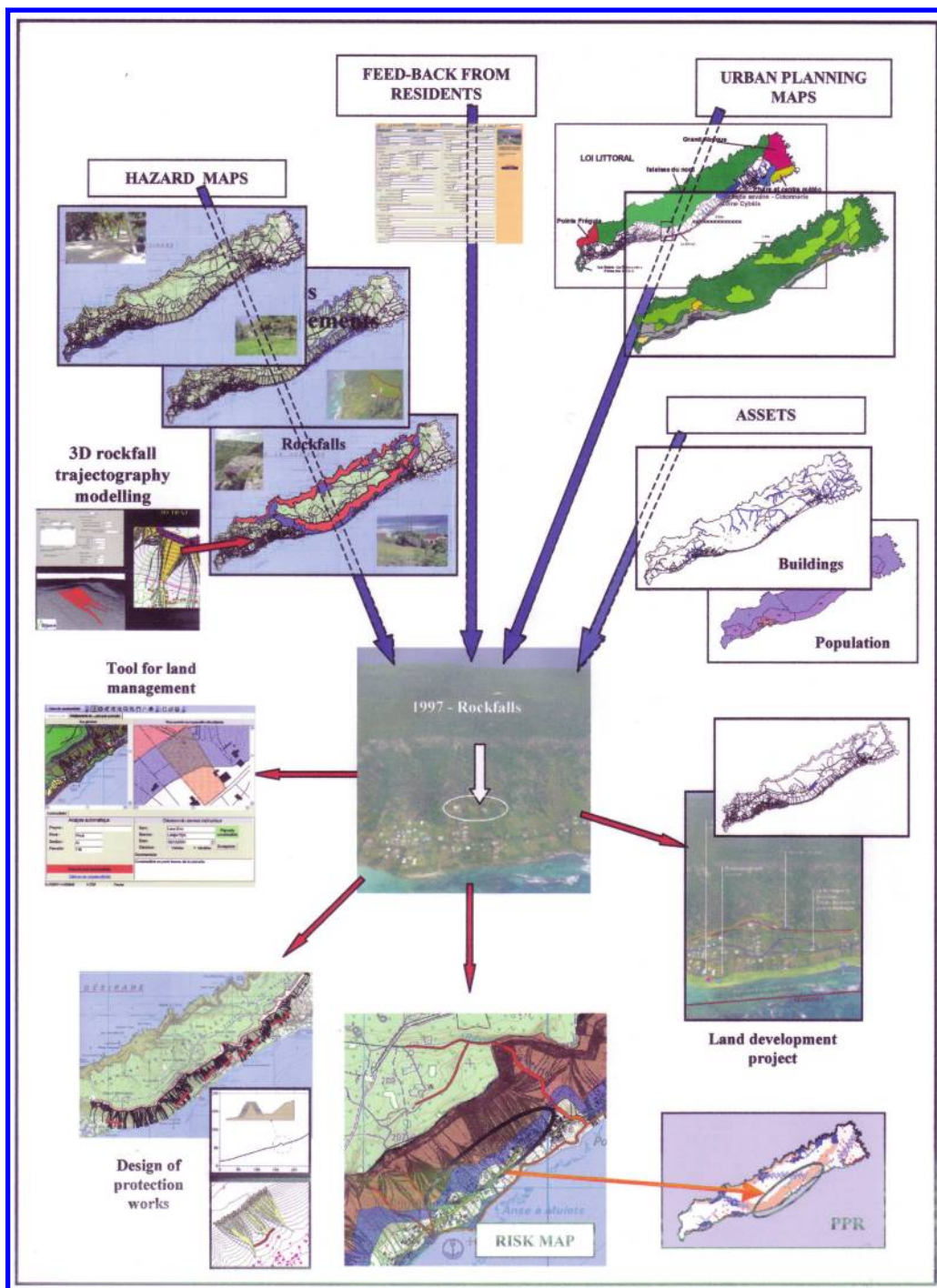
Plate IV. General framework describing work carried-out to manage landslides risks in La Désirade Island after 1997 rock-fall event.

Plate V. Annual landslide frequency (based on OAP 2003).

Legend

- ■ (red) Distressed ground (with tension cracks and slow moving landslides).

- ■ (dark red) Area of landslide clustering.

- ■ (purple) Alluvium, channelised debris flow deposit, colluvium and taluvium boulder accumulate along the drainage channels.

- ■ (light blue) Shallow landslides deposit colluvium on gully side slopes. Many landslides.

- ■ (green) Taluvial lobes downslope from intermittent rock.

- ■ (blue) Rockfall debris at the toe of rock outcrops.

- ■ (yellow) Accumulation of colluvium in topographic depressions.

- ■ (grey) Landslides occur on former steep coastal slopes.

- ■ (pale yellow) Open hillslope colluvium accumulates on relatively hillslopes. In feldsparphyric rhyolite/porphyritic microgranite shallow Terrain. Very few landslides.

- ■ (pale blue) Open hillslope colluvium on relatively shallow hillslopes (younger terrain) in the rhyolite lava/tuff terrain as a result of creep. Few landslides.

- ■ (pink) Relatively steep hillslopes in the upper portion of the rhyolite lava/tuff terrain (older terrain). Drainage channels generally have well defined convex breaks of slope at their heads but very few recent landslides.

■ (dark brown)
■ (brown)
■ (orange) — Incised and degraded / Younger — Debris fans, comprising coalescing bodies of colluvium/alluvium, have developed at the hillslope toe.
■ (light orange)
■ (pale orange)

— (red line) Study Area Boundary
— (gold line) Former Shoreline
— (green line) Former Cliffline

- ■ (dark green) Areas of saprolite along hillside spurs. Very few landslides.

- ■ (magenta) Rock outcrops.

Plate VI.   Landslide process model (OAP 2005).

760
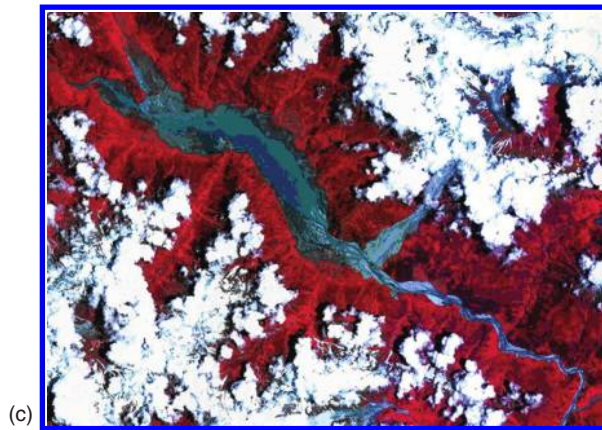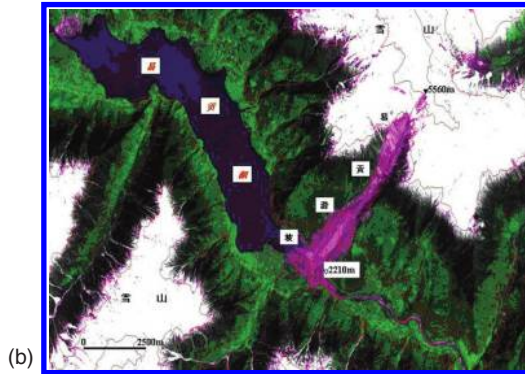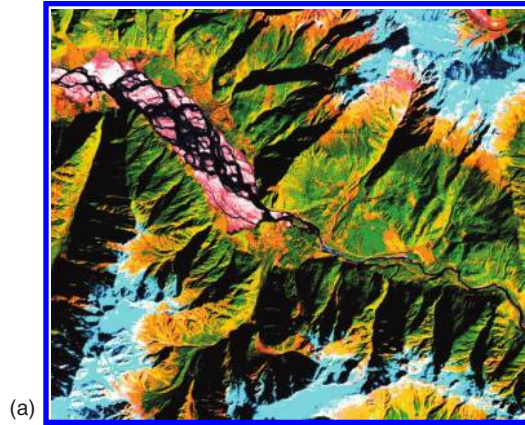
Plate VII.   Yigong landslide RS image showing from top to bottom: (a) Before landslide on 2000.4.9; (b) Landslide dammed the River; and (c) Landslide dam bursting.

761

Plate VIII.   Property in danger of landslide hazard in Pacifica, California, USA.
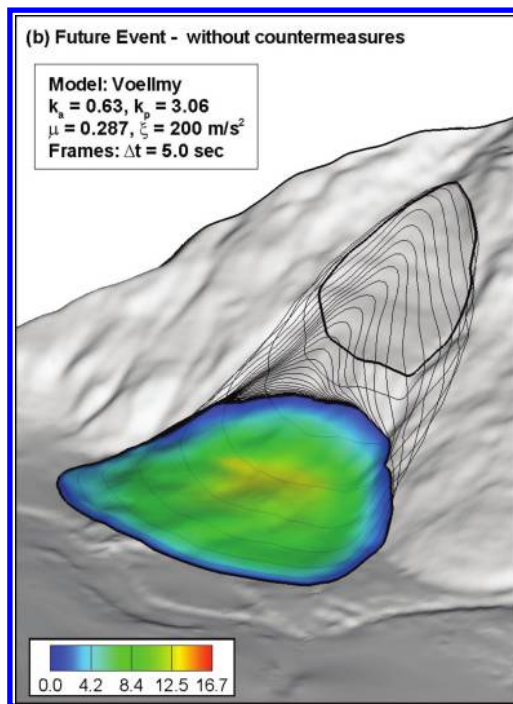
Plate IX.   Predicted time sequences of the possible landslide failure without passive countermeasures. The flood contours show the debris depth distribution (in meters) in the final deposition.

762
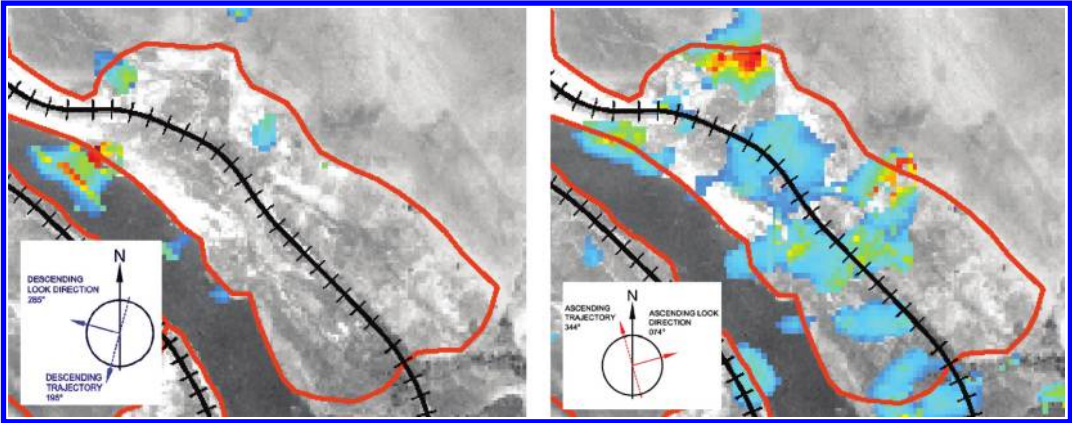
Plate X. Example of motion detected in the ascending trajectory with movement in the line of sight of the satellite (left) and the same site with motion not detected as movement is near perpendicular to the line of site (right).
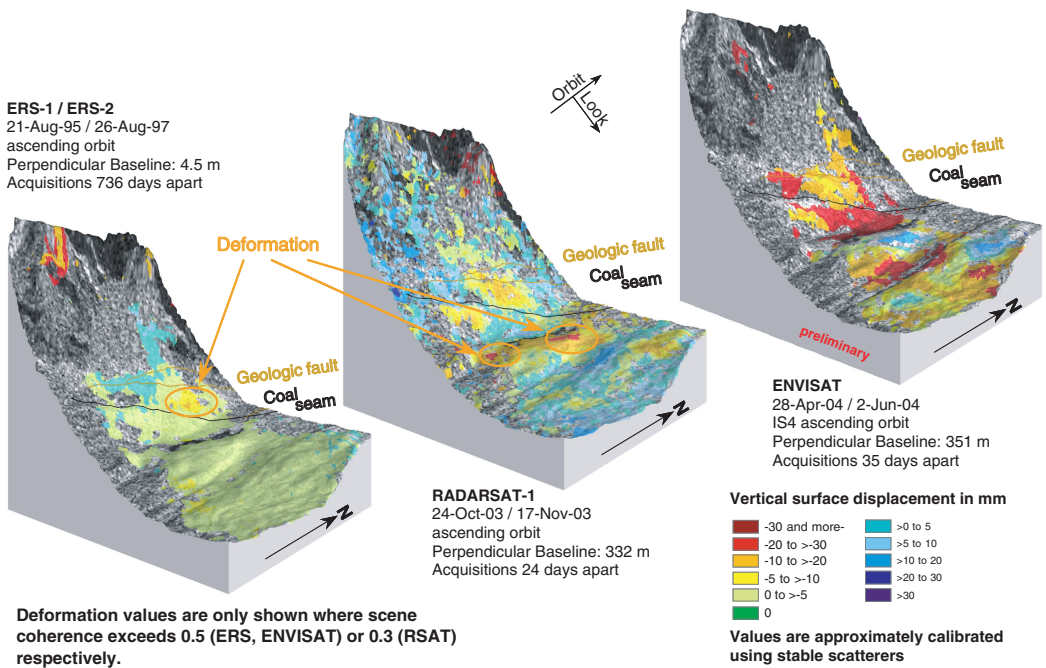
Plate XI. Surface deformation maps, interferometrically generated from ERS, RADARSAT-1, and ENVISAT ASAR data.

763
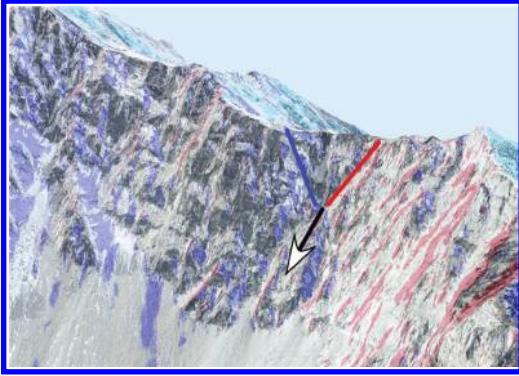
Plate XII. Wedge identified on the present scar of Frank slide (Source: Geological Survey of Canada).
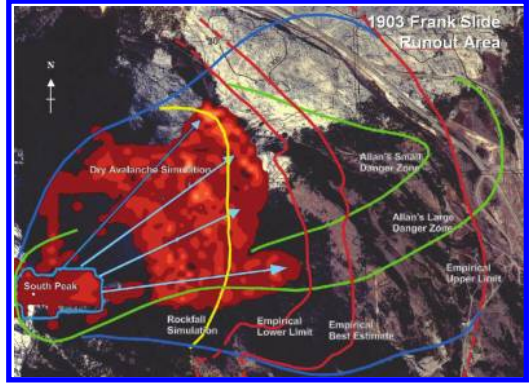
Plate XIV. Predicted range of danger zones for runout from South Peak (BGC 2000).
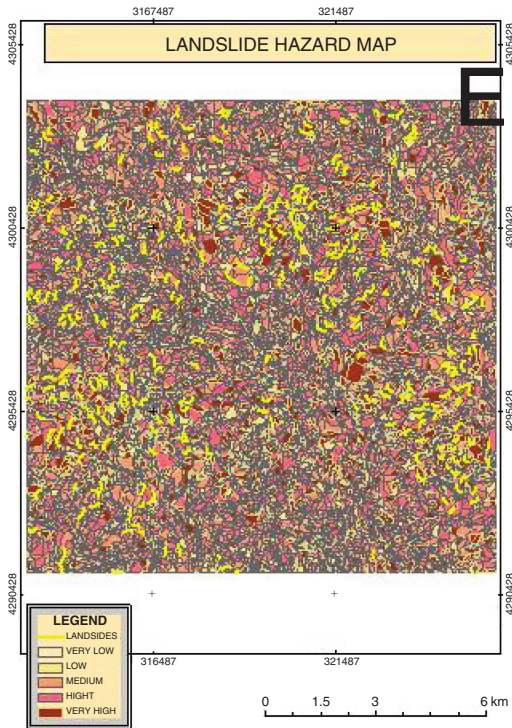
Plate XIII. Landslide hazard map.
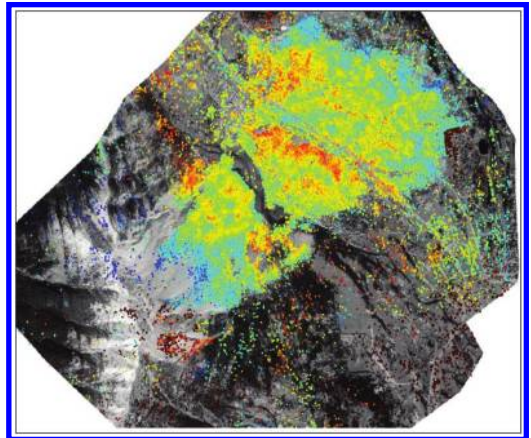
Plate XV. Data points utilized for the CTM assessment overlain on the DEM.

State of the art papers

A framework for landslide risk assessment and management

R. Fell
School of Civil and Environmental Engineering, The University of New South Wales, Sydney, Australia

K.K.S. Ho
Geotechnical Engineering Office, Civil Engineering and Development Department, Hong Kong

S. Lacasse
International Centre for Geohazards, Norwegian Geotechnical Institute, Oslo, Norway

E. Leroi
Urbater, Roquevaire, France

ABSTRACT: This paper provides a framework for landslide risk assessment and management. It outlines the processes of hazard analysis, including characterization of the landslide (the danger); frequency analysis; the risk estimation calculation; risk evaluation against risk tolerance criteria and value judgements. The paper discusses the benefits and limitations of quantitative and qualitative risk management, and gives simplified examples.

1 INTRODUCTION

Landslides and engineered slopes have always involved some form of risk assessment and management. This was often done by the use of "engineering judgement" by the Geotechnical Engineers or Engineering Geologists in consultation with owners and regulators.

The more formal applications of risk assessment and management principles, in a qualitative manner, have been practised for landslide hazard zoning for urban planning and highway slope management since the 1970's. In the 1980's, and particularly in the 1990's, these have been extended to quantitative methods, and to management of individual slopes, pipeline routes, submarine slopes and more global slope risk management.

These developments are described by Varnes (1984), Whitman (1984), Einstein (1988, 1997), Fell (1994), Leroi (1996), Wu *et al.* (1996), Fell and Hartford (1997), Nadim & Lacasse (1999) Ho *et al.* (2000) Kvalstad *et al.* (2001), Nadim *et al.* (2003), Nadim & Lacasse (2003, 2004), Hartford & Baecher (2004), and Lee & Jones (2004). Some guidelines have been developed (e.g. Australian Geomechanics Society 2000).

At this time there exists a generic framework for the use of quantitative risk assessment (QRA) for engineered slopes and landslides; including individual slopes, groups of slopes (such as cuts and fills on a length of highway), land use planning and zoning for urban development and "global" or regional landslide risk management. This paper describes this framework.

This paper also discusses the advantages, disadvantages and limitations of QRA for engineered slopes and landslides. The other seven State of the Art (SOA) papers in this Conference provide the details of the methods that can be used. The invited and submitted papers in this volume deal with specific applications, case studies, research and development.

2 TERMINOLOGY

The International Society of Soil Mechanics and Geotechnical Engineering (ISSMGE) Technical Committee on Risk Assessment and Management (TC32) developed a Glossary of Terms for Risk Assessment, based on IUGS (1997), ICOLD (2003), and National Standards such as British Standard BS 8444, Australia-New Zealand Standard AS/NZS 4360, and Canadian Standard CAN/CSA – Q 634-91. The Glossary is attached to this volume and these terms are used throughout all the SOA papers.

Readers are encouraged to use these terms so that there is consistency across the international community. The most important terms and their definitions are:

Annual exceedance probability (AEP): The estimated probability that an event of specified magnitude will be exceeded in any year.

Consequence: In relation to risk analysis, the outcome or result of a hazard being realised.

Danger (Threat): The natural phenomenon that could lead to damage, described in terms of its geometry, mechanical and other characteristics. The danger can be an existing one (such as a creeping slope) or a potential one (such as a rockfall). The characterisation of a danger or threat does not include any forecasting.

Elements at risk: Population, buildings and engineering works, infrastructure, environmental features and economic activities in the area affected by a hazard.

Frequency: A measure of likelihood expressed as the number of occurrences of an event in a given time or in a given number of trials (see also likelihood and probability).

Hazard: Probability that a particular danger (threat) occurs within a given period of time.

Individual risk to life: The increment of risk imposed on a particular individual by the existence of a hazard. This increment of risk is an addition to the background risk to life, which the person would live with on a daily basis if the facility did not exist.

Likelihood: Conditional probability of an outcome given a set of data, assumptions and information. Also used as a qualitative description of probability and frequency.

Probability: A measure of the degree of certainty. This measure has a value between zero (impossibility) and 1.0 (certainty). It is an estimate of the likelihood of the magnitude of the uncertain quantity, or the likelihood of the occurrence of the uncertain future event.

There are two main interpretations:

i) Statistical – frequency or fraction – The outcome of a repetitive experiment of some kind like flipping coins. It includes also the idea of population variability. Such a number is called an "objective" or relative frequentist probability because it exists in the real world and is in principle measurable by doing the experiment.

ii) Subjective probability (degree of belief) – Quantified measure of belief, judgement, or confidence in the likelihood of an outcome, obtained by considering all available information honestly, fairly, and with a minimum of bias. Subjective probability is affected by the state of understanding of a process, judgement regarding an evaluation, or the quality and quantity of information. It may change over time as the state of knowledge changes.

Risk: Measure of the probability and severity of an adverse effect to life, health, property, or the environment. Quantitatively, Risk = Hazard × Potential Worth of Loss. This can be also expressed as "Probability of an adverse event times the consequences if the event occurs".

Risk analysis: the use of available information to estimate the risk to individuals or populations, property or the environment, from hazards. Risk analyses generally contain the following steps: definition of scope, danger (threat) identification, estimation of probability of occurrence to estimate hazard, evaluation of the vulnerability of the element(s) at risk, consequence identification, and risk estimation. Consistent with the common dictionary definition of analysis, viz. "A detailed examination of anything complex made in order to understand its nature or to determine its essential features", risk analysis involves the disaggregation or decomposition of the system and sources of risk into their fundamental parts.

Qualitative risk analysis: An analysis which uses word form, descriptive or numeric rating scales to describe the magnitude of potential consequences and the likelihood that those consequences will occur.

Quantitative risk analysis: An analysis based on numerical values of the probability, vulnerability and consequences, and resulting in a numerical value of the risk.

Risk assessment: The process of making a decision recommendation on whether existing risks are tolerable and present risk control measures are adequate, and if not, whether alternative risk control measures are justified or will be implemented. Risk assessment incorporates the risk analysis and risk evaluation phases.

Risk control: The implementation and enforcement of actions to control risk, and the periodic re-evaluation of the effectiveness of these actions.

Risk evaluation: The stage at which values and judgement enter the decision process, explicitly or implicitly, by including consideration of the importance of the estimated risks and the associated social, environmental, and economic consequences, in order to identify a range of alternatives for managing the risks.

Risk management: The systematic application of management policies, procedures and practices to the tasks of identifying, analysing, assessing, mitigating and monitoring risk.

Risk mitigation: A selective application of appropriate techniques and management principles to reduce either likelihood of an occurrence or its adverse consequences, or both.

Societal risk: The risk of widespread or large scale detriment from the realisation of a defined risk, the implication being that the consequence would be on such a scale as to provoke a socio/political response.

Temporal (spatial) probability: The probability that the element at risk is in the area affected by the danger (threat) at the time of its occurrence.

Tolerable risk: A risk within a range that society can live with so as to secure certain net benefits. It is a range of risk regarded as non-negligible and needing to be kept under review and reduced further if possible.

Vulnerability: The degree of loss to a given element or set of elements within the area affected by a hazard. It is expressed on a scale of 0 (no loss) to 1 (total loss).

Also, a set of conditions and processes resulting from physical, social, economic, and environmental factors, which increase the susceptibility of a community to the impact of hazards.

Other terms to describe landslide classification, features and geometry are detailed in Appendix A of this volume.

3 THE RISK MANAGEMENT PROCESS

Figures 1–3 describe the overall risk management process.

Hazard analysis involves characterising the landslide (classification, size, velocity, mechanics, location,

Figure 1. Flow chart for landslide risk management.

5

(a) Landslide (danger) characterisation

(b) Hazard analysis

(c) Risk analysis

(d) Risk evaluation

(e) Risk mitigation and control
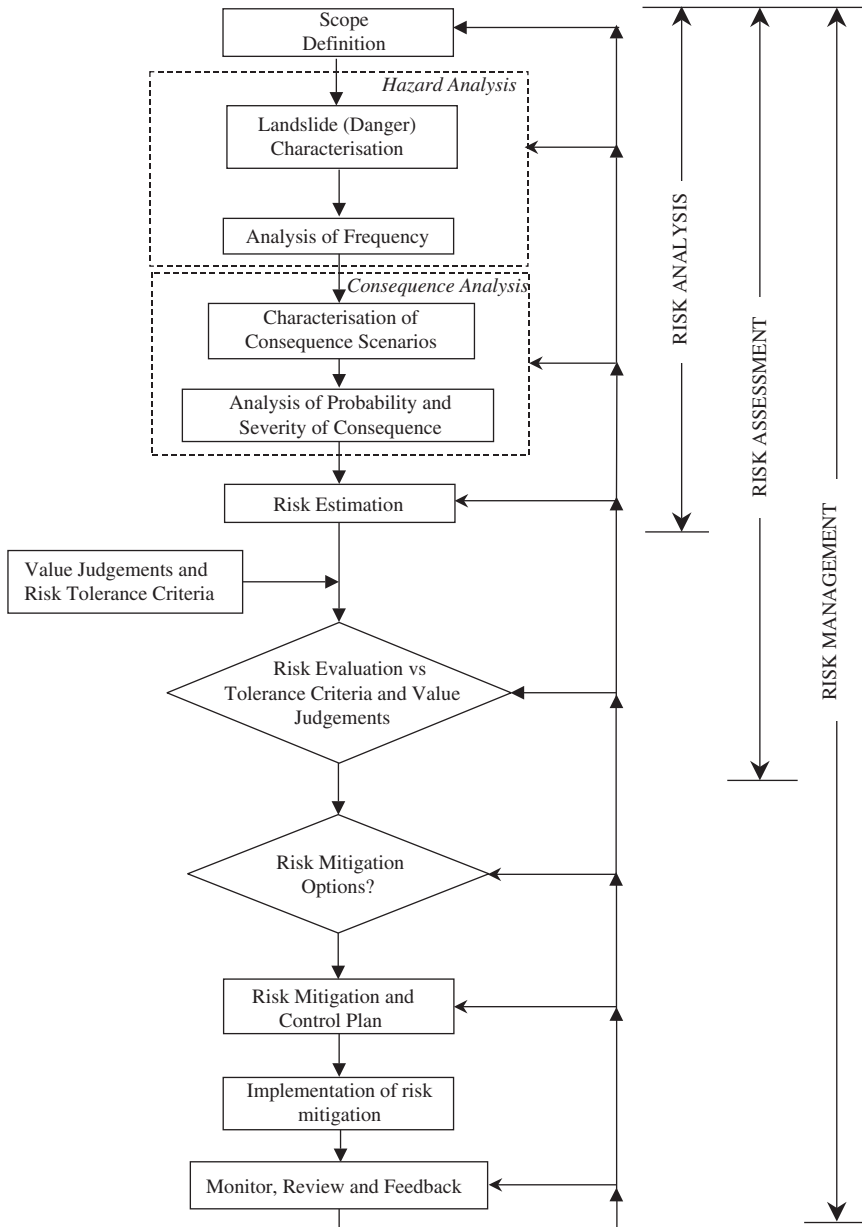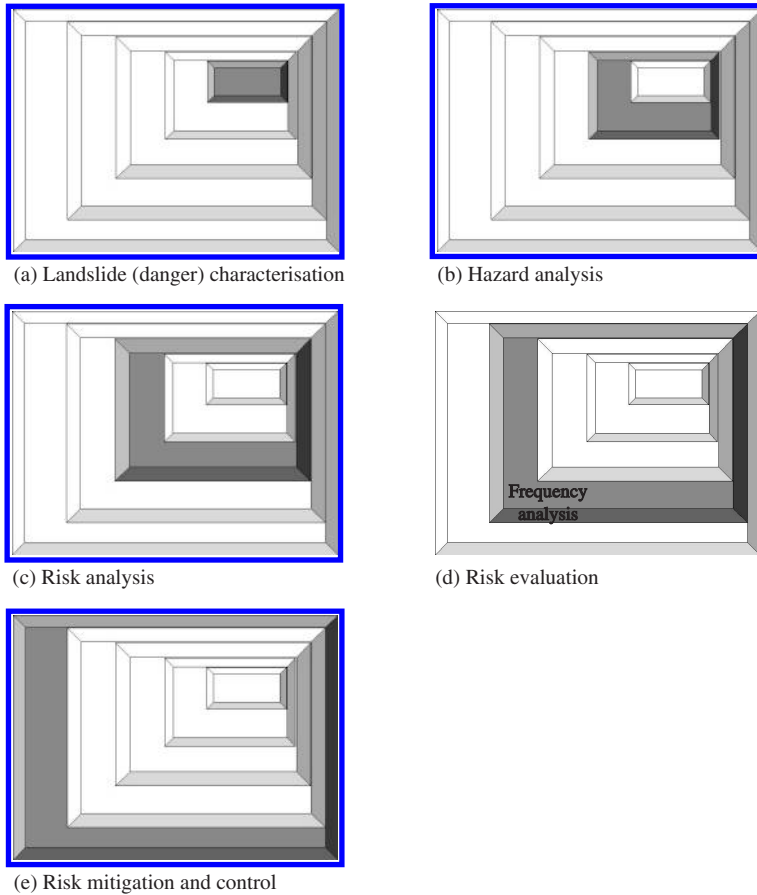
Figure 2.   Representation of 5 phases of the risk management process.

travel distance), and the corresponding frequency (annual probability) of occurrence.

Risk analysis includes hazard analysis and consequence analyses. Consequence analysis includes identifying and quantifying the elements at risk (property, persons), their temporal spatial probability, their vulnerability either as conditional probability of damage to conditional probability of damage to property, or conditional probability of loss of life or injury.

Risk assessment takes the output from risk analysis and assesses these against values judgements, and risk acceptance criteria.

Risk management takes the output from the risk assessment, and considers risk mitigation, including accepting the risk, reducing the likelihood, reducing consequences e.g. by developing monitoring, warning and evacuation plans or transferring risk (e.g. to insurance), develops a risk mitigation plan and possibly implements regulatory controls. It also includes

monitoring of the risk outcomes, feedback and iteration when needed.

The process is iterative within any one study, and should be up-dated periodically as monitoring results become available.

Landslide risk management involves a number of stakeholders including owners, occupiers, the affected public and regulatory authorities, as well as geotechnical professionals, and risk analysts.

It is an integral part of risk management that the estimated risks are compared to acceptance criteria (either quantitative or qualitative). Geotechnical professionals are likely to be involved as the risk analysts, and may help guide in the assessment and decision process, but ultimately it is for owners, regulators and governments to decide whether the calculated risks are acceptable or whether risk mitigation is required.

In some cases the absolute values of risk are not as important as the relative risks. This is often the case

6
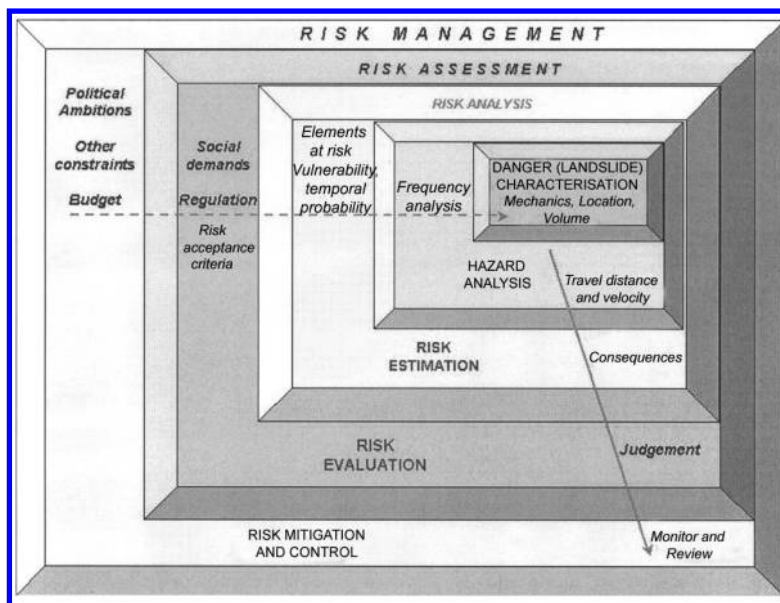
Figure 3.   Schematic representation of the integrated risk management process.

for risk assessments for cuts and fills on highways, where the risk assessment process is being used to prioritise the implementation of risk reduction measures.

The risk management process in Figure 1 can be divided in phases. Five of these are illustrated by the darker shades in Figure 2. The graphics illustrate that each new phase includes the previous one(s) and that the solution becomes more involved as one progresses through the different phases. The 5 phases together form an integrated framework schematically illustrated in the graphics in Figure 3.

4   LANDSLIDE RISK ANALYSIS

4.1   *Scope definition*

To ensure that the risk analysis addresses the relevant issues, satisfies the needs of those concerned, and to avoid misunderstandings, it is important to define the scope of the risk analysis:

(a) Is the analysis for a single site (e.g. a road cutting, or a building); a number of sites, (e.g. all the road cuttings on a length of road); hazard zoning for land-use planning; or "global risk assessment", where for example cut slopes on all roads in a local government area are being studied universally to formulate policies and prioritise mitigation actions?
(b) The geographic limits. Note that to be complete, the effects of landsliding up slope of a site, not confined to the site may need to be considered;

and the impacts of the landsliding on sites down-slope, e.g. of a road fill, may also need to be part of the analysis.
(c) Whether the analysis will be restricted to property loss or damage, or it will also include assessment of the potential for loss of life and injury.
(d) The extent of geotechnical engineering and geological studies which will form the basis of the analysis. These can control the overall standard of the risk analysis.
(e) The approach to be used to characterise the landslides, and assess the frequency of landsliding, and their consequences.
(f) Whether the analysis will be quantified or qualitative.
(g) How risk acceptance criteria will be determined, by whom, and through what process? The extent to which the stakeholders (owners, public, regulator, risk analyst) will be involved.
(h) Operational (e.g. land access) and financial constraints to the analysis.
(i) Legal responsibilities of all parties.
(j) The nature of the end product of the risk analysis – report, maps, and how these will be communicated to the interested parties.

4.2   *Hazard analysis*

Hazard analysis is the process of identification and characterisation of the potential landslides together with evaluation of their corresponding frequency of occurrence.

7

4.2.1 Landslide (Danger) characterisation

Landslide (danger) characterisation requires an understanding of the slope processes and the relationship of those processes to geomorphology, geology, hydrogeology, failure and slide mechanics, climate and vegetation. From this understanding it will be possible to:

– Classify the types of potential landsliding: the classification system as proposed by Varnes (1984) or modified by Cruden & Varnes (1996) forms suitable systems. A site may be affected by more than one type of landslide hazard e.g., slow rotational earth slides on the site, and very rapid rockfall and debris flows from above the site.
– Assess the physical extent of each potential landslide, including the location, areal extent and volume involved.
– Assess the likely initiating event(s), the physical characteristics of the materials involved, such as shear strength, pore pressures; and the slide mechanics. The latter is critical to understanding the pre and post failure behaviour of the landslide.
– Estimate the resulting anticipated travel distance, travel path, depth and velocity of movement if failure occurs, taking account of the slide mechanics, and estimating the probability that the land slide will affect the area in which the element at risk is located ($P_{T:L}$).
– Identify possible pre-failure warning signs which may be monitored.

A list of possible landslides (dangers) should be developed. Consideration must be given to hazards located off site as well as within the site as it is possible for landslides both upslope and downslope to affect the elements at risk. It is vital that the full range of hazards (e.g. from small, high frequency events to large, low frequency events) be properly characterised and considered in the risk analysis. Often the risk is dominated by the smaller, more frequent landslides. The effects of proposed development in an area should also be considered, as these effects may alter the nature and frequency of potential hazards.

It is important that geotechnical professionals with training and experience in landsliding and slope processes are involved in this stage of the analysis because the omission or under/over estimation of the effects of different landslides often can control the outcomes of the analysis.

4.2.2 Frequency analysis

The frequency of landsliding can be expressed in terms of (IUGS 1997):

– The number of landslides of a certain characteristic that may occur in a study area per year.

– The probability of a particular slope experiencing landsliding in a given period, e.g. a year.
– The driving forces exceeding the resistant forces in probability or reliability terms, with the frequency of occurrence being determined by considering the annual probability of the critical pore water pressures being exceeded in the analysis.
– This should be done for each type of landslide which has been identified and characterised as affecting the analysis.

There are several ways of calculating frequency (IUGS 1997):

(1) Historic data within the area of study, or areas with similar characteristics, e.g. geology, geomorphology.
(2) Empirical methods based on correlations in accordance with slope instability ranking systems.
(3) Use of geomorphological evidence (coupled with historical data), or based on expert judgement.
(4) Relationship to the frequency and intensity of the triggering event, e.g. rainfall, earthquake.
(5) Direct assessment based on expert judgement, which may be undertaken with reference to a conceptual model, e.g. use of a fault tree methodology.
(6) Modelling the primary variable, e.g. piezometric pressures versus the triggering event, coupled with varying levels of knowledge of geometry and shear strength.
(7) Application of probabilistic methods, taking into account the uncertainty in slope geometry, shear strength, failure mechanism, and piezometric pressures. This may be done either in a reliability framework, or taking into account the frequency of failure (for example by considering pore pressures on a frequency basis).
(8) Combinations of the above methods.

In practice it may be appropriate and advisable to use more than one method for the analysis.

Details of the methods and their applicability are given in SOA Paper 2 in this volume. It is important to express the probability of sliding in frequency (per annum) terms, because quantitative risk acceptance criteria for loss of life are usually expressed in per annum terms. Financial analysis of damage also usually requires frequency as an input.

The authors have a preference for estimating frequencies quantitatively. This gives a uniformity of outcomes in quantified terms (rather than using ill-defined subjective terms such as likely, unlikely etc.), allows risk to be compared with quantitative acceptance criteria, and allows comparison with risks from other hazards with which the parties involved may be able to associate. However it is recognised that many practitioners are not familiar with quantifying landslide frequencies, and it is important there are "sanity checks"

on the results against historical performance data, and for more important analyses, reviews by persons who are experienced in landslide risk analysis.

For most hazard analyses, the estimation of frequency based on historical data, geomorphological evidence, relationship to trigger event frequencies etc. are typically more reliable than the apparently more rigorous and detailed probabilistic analyses because of the many uncertainties involved and data constraints. Also, some of the causes or contributory factors to slope instability may not be amenable to conventional limit equilibrium analysis, e.g. effects of topography on surface water flows.

This is particularly true for smaller slopes, and for landslides on natural hillsides, where it is very difficult to estimate pore water pressures, and where small variations in strengths, and geometry and geological anomalies have large effects on the outcomes. There is also seldom sufficient data to properly model such factors as auto-correlation of parameters, so reliance is often placed on published generalised information which may not be applicable to the site under consideration.

4.3 *Consequence analysis*

Consequence analysis involves:

(a) Identifying and quantifying the elements at risk including property and persons.
(b) Assessing temporal spatial probabilities for the elements at risk ($P_{S:T}$).
(c) Assessing vulnerability of the elements at risk, in terms of property damage ($V_{prop:T}$) and loss of life/injury ($V_{D:T}$) as appropriate.

This has to be done for each of the landslide hazards.

The consequences may not be limited to property damage and loss of life/injury. Other consequences may include loss of reputation of the owner and geotechnical engineers, consequential costs (e.g. a road is closed for some time affecting businesses along the road), litigation from those injured or the relatives of those killed, potential criminal charges for those involved, political repercussions, adverse social and environmental effects. Most of these may not be readily quantifiable, but may need to be systematically considered, in consultation with owners and factored into the decision-making process as appropriate, at least for comprehensive risk analysis studies.

4.3.1 *Elements at risk*
The elements at risk include the population, buildings, engineering works, infrastructure, vehicles, environmental features and economic activities which are in the area affected by the hazard. In practical terms, this usually means on the landslide, and/or in the area onto which the landslide may travel if it occurs. It may also include property immediately adjacent to or upslope of the landslide, if the property or its value would be affected by landsliding and infrastructure which may include powerlines, water supply, sewage, drainage, roads, communication facilities. The population at risk includes persons who live, work, or travel through the area affected by the hazard.

It would be usual to categorise vehicles into cars, trucks and buses, because of the different number of persons likely to be in the vehicles.

The elements at risk are likely to be dependent on the nature of the landslide hazard e.g. for a boulder fall, or debris flow at a given site.

4.3.2 *Probability of landslide reaching the element at risk ($P_{T:L}$)*
The probability of the landslide reaching the element at risk depends on the relative location of the element at risk and the landslide source, together with the path the landslide is likely to travel below the source. It is a conditional probability between 0 and 1.

(a) For buildings which are located on the source landslide $P_{T:L} = 1$.
(b) For buildings or persons located below the source landslide and in the path of the resulting travel of the landslide, $P_{T:L}$ is calculated taking account of the travel distance of the landslide, the location of the source landslide, and the element at risk.
(c) For vehicles or persons in vehicles, or persons walking in the area below the source landslide in the path of the resulting travel (runout) of the landslide, $P_{T:L}$ is calculated taking account of the travel distance of the landslide, and the path to be followed by the vehicle or person. Whether the vehicle or person is in the path at the time of the landslide is taken account through the temporal spatial probability ($P_{S:T}$).

The methods for estimation of travel distance are described in SOA 4 of this volume. This involves some uncertainty which should be taken determined.

4.3.3 *Temporal spatial probability ($P_{S:T}$)*
The temporal spatial probability is the probability that the element at risk is in the area affected by the hazard at the time of its occurrence. It is a conditional probability, and is between 0 and 1.

(a) For buildings on or in the path of the landslide, the temporal spatial probability is 1.
(b) For a single vehicle which passes below a single landslide, it is the proportion of time in a year when it will be in the path of the landslide.
(c) For all the vehicles which pass below a single landslide, it is the proportion of time in a year when a vehicle will be in the path of the landslide. Where there are a number of potential landslides in any year, e.g. rockfalls, the calculation is

somewhat more complicated as described in SOA 5 in this volume.

(d) For persons in a building, it is the proportion of time in a year which the persons occupy the building (0–1.0). This is likely to be different for each person.

For persons in vehicles, the temporal spatial probability will be as for (b) and (c). However it may vary for say one person in a car, and four persons in a car.

The range of credible consequence scenarios will need to be considered in societal risk calculations. Details of how to calculate temporal spatial probability are given in SOA 5 of this volume.

For some situations it will be necessary to build into the calculation of temporal spatial probability, whether the person(s) at risk may have sufficient warning to evacuate from the area affected by the hazard. Persons on a landslide are more likely to observe the initiation of movement and move off the slide than those who are below a slide falling or flowing onto them.

Each case should take into account the nature of the landslide including its volume, and velocity, monitoring results, warning signs, evacuation systems, the elements at risk, and the mobility of the persons.

4.3.4 *Vulnerability ($V_{prop:T}$ and $V_{D:T}$)*

Vulnerability is the degree of loss (or damage) to a given element, or set of elements, within the area affected by the hazard. It is a conditional probability, given the landslide occurs and the element at risk is on or in the path of the landslide. For property, it is expressed on a scale of 0 (no loss or damage) to 1 (total loss or damage) for property.

For persons it is usually the probability (between 0 and 1) that given the person is on or in the path of the landslide, the person is killed. It may also include the probability of injury.

Factors that most affect vulnerability of property include:

– The volume of the landslide in relation to the element at risk.
– The position of the element at risk, e.g. on the landslide, or immediately downslope.
– The magnitude of landslide displacement, and relative displacements within the landslide (for elements located on the landslide).
– The velocity of landslide movement.

Landslides which move slowly (particularly those with a nearly planar, horizontal surface of rupture) may cause little damage, other than to structures which are on the boundaries of the landslide and hence experience differential displacement.

The rate of movement is less important for structures than it is for loss of life, except in so far as it affects the time rate of damage, i.e. buildings on a slow moving slide (which moves intermittently every year) can be expected to have a lower vulnerability than those on a fast moving one.

Factors which most affect the vulnerability of persons include:

– The velocity of landsliding. Persons are more likely to be killed by a rapid landslide than slow regardless of the landslide volume.
– Landslide volume – persons are more likely to be buried or crushed by large landslides than small.
– Whether the person(s) are in the open, or in a vehicle or building (ie. a function of the degree of protection the person(s) has from the landslide impact).
– If they are in a building, whether the building collapses upon impact by the landslide, and the nature of the collapse.

Persons who are buried by a landsliding mass have a high vulnerability. Death is more likely to result from asphyxia than from crushing or impact. SOA 5 in this volume gives detailed information on the assessment of vulnerability.

4.4 *Risk estimation*

4.4.1 *Risk calculation*

The risk can be presented in a number of ways:

(a) The annual risk (expected value) in which the probability of occurrence of the danger is multiplied by the consequences summed over all the hazards. This is expressed as \$x damage per annum; or potential loss of lives per annum.

(b) Frequency-consequence (f-N) pairs – for example for property, the annual probability of minor (\$x) damage; medium (\$y) damage and major (\$z) damage; and for risk to life, the annual probability of loss of 1 life, 5 lives, 100 lives etc.

(c) Cumulative frequency – consequence plots (F-N plots), for example a plot of the annual probability of N or more lives being lost (see section 5.2 and Fig. 4).

It is often useful to calculate all three. The annual risk for property can be calculated from:

$$R_{(prop)} = P_{(L)} \times P_{(T:L)} \times P_{(S:T)} \times V_{(prop:S)} \times E \qquad (1)$$

where

$R_{(prop)}$ is the annual loss of property value
$P_{(L)}$ is the frequency of the landsliding
$P_{(T:L)}$ is the probability of the landslide reaching the element at risk
$P_{(S:T)}$ is the temporal spatial probability of the element at risk
$V_{(prop:S)}$ is the vulnerability of the element at risk to the landslide event

10
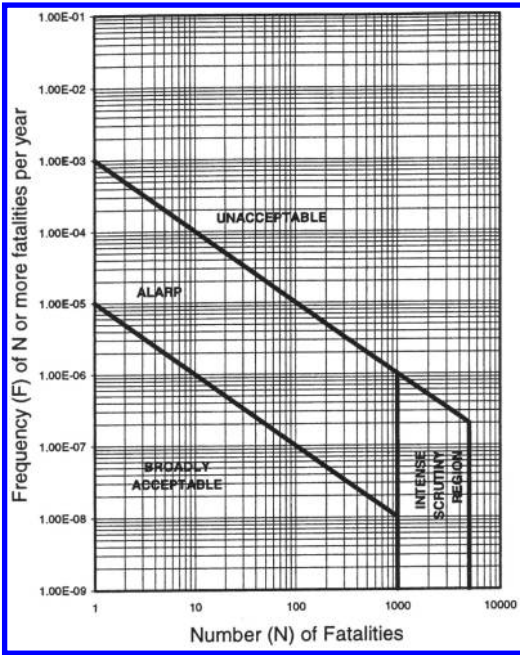
Figure 4. Interim societal risk tolerance criteria (Geotechnical Engineering Office 1998).

E   is the element at risk (e.g. the value or net present value of the property).

The annual probability that a particular person may lose his/her life can be calculated from:

$$P_{(LOL)} = P_{(L)} \times P_{(T:L)} \times P_{(S:T)} \times V_{(D:T)} \qquad (2)$$

where

$P_{(LOL)}$ is the annual probability that the person will be killed
$V_{(D:T)}$ is the vulnerability of the person to the landslide event
and $P_{(L)}$, $P_{(T:L)}$ and $P_{(S:T)}$ are as defined above.

To estimate annual loss of life risk, equation (3) is expanded to be as for equation (2) with E being the number of persons at risk.

There are a number of situations where the risks from a number of landslide hazards have to be summed to give the total risk. These include:

– Where the element at risk is exposed to a number of types of landsliding e.g. boulder fall, debris flows, and translational sliding.
– Where the landsliding may be triggered by more than one phenomena e.g. rainfall, earthquake, human activity.
– Where the element at risk is exposed to a number of different sizes of landslide of the same classification

e.g. debris flows of $50\,m^3$, $5,000\,m^3$ and $100,000\,m^3$ volume.
– Where the element at risk is exposed to a number of slopes on which landsliding can occur e.g. a vehicle driving along a road in which there are 20 cut slopes each of which is a potential source of boulder falls.

In these cases, equations (1) and (2) should be written as:

$$R_{(prop)} = \sum_{1}^{n}(P_{(L)} \times P_{(T:L)} \times P_{(S:T)} \times V_{(prop:S)} \times E) \qquad (3)$$

and

$$P_{(LOL)} = \sum_{1}^{n}(P_{(L)} \times P_{(T:L)} \times P_{(S:T)} \times V_{D:T}) \qquad (4)$$

where n is the number of landslide hazards.

This assumes that the hazards are independent of each other, which may often not be correct. If one or more of the hazards may result from the same causative event e.g. a single rain event, or earthquake, then the probabilities should be estimated using the theory of uni-modal bounds as follows:

(i) The upper bound

From de Morgan's rule, the estimated upper bound conditional probability is

$$P_{UB} = 1 - (1 - P_1)(1 - P_2) \ldots\ldots(1 - P_n) \qquad (5)$$

where
P_{UB} = estimated upper bound conditional probability.
P_1 to P_n = the estimate of several individual hazard conditional probabilities.

This calculation should be done before applying the annual probability of the common causative event. If all the conditional probabilities P_1–P_n are small (<0.01), equation 5 yields the same value, within acceptable accuracy, as obtained by adding all the estimated conditional probabilities.

(ii) The lower bound

The lower bound estimate is the maximum individual conditional probability.

4.4.2 Uncertainty and sensitivity analysis

The inputs into the risk estimation are not precise, usually involving a large contribution from engineering judgement, or uncertainty in input parameters (e.g. for formal probabilistic analysis) (Lacasse *et al.* 2003, 2004). Uncertainty describes any situation without

certainty, whether or described by a probability distribution. Uncertainty is caused by natural variation and/or incomplete knowledge (lack of understanding or insufficient data). In the context of structural safety, uncertainty can be either aleatory (inherent variability in natural properties and events) or epistemic (incomplete knowledge of parameters and the relationships between input and output values).

Often for landslide risk assessments, it is not practical to model uncertainties formally e.g. by assigning probability distributions to each input and using Monte Carlo type analysis (e.g. Morgan & Henrion 1990). However, it is possible to do sensitivity analysis by considering the effects of different assumed values for the inputs. It should be recognised that the use of upper or lower limits of input variables in order to estimate upper and lower bound results gives extremely low likelihood values, and that the analysis may be almost meaningless.

4.4.3 Qualitative risk estimation

Qualitative risk analysis uses descriptors to describe the frequency of landsliding and the consequences. This may comprise tools such as risk rating systems, risk scoring schemes, and risk ranking matries (e.g. Stewart *et al.* 2002). These can serve a useful role in landslide risk management in providing a relative comparison of risks of different sites and prioritisation of follow-up actions in addressing the risk portfolio posed by a large number of sites. In some cases, a hybrid approach may be adopted whereby qualitative risk analysis can facilitate a "first-pass" screening of the more dominant hazards in a given site so that attention can be focused on the more deserving areas or hazards, which can be evaluated in detail using quantitative methods. Qualitative risk assessment may also be used, coupled with engineering judgement, to examine whether a given landslide hazard is posing a significant risk to life (e.g. a precariously perched boulder above a busy highway with signs of distress) and the need for prompt risk reduction measures (e.g. boulder removal) in order to safeguard public safety, without the need for elaborate quantitative analysis. In general, qualitative risk assessment must be undertaken critically and preferably subject to expert review to avoid spurious outcomes and for it to be value-adding.

Table 1 gives an example adapted from AGS (2000). In this case, the "likelihood" incorporates the frequency of landsliding, the probability of the landslide reaching the element at risk, and temporal spatial probability. The consequences incorporate the vulnerability and the value of the element at risk.

Combining likelihood with consequence results in a risk matrix divided into 5 classes from very low risk (VL) to very high risk (VH).

Table 1. Example of qualitative terminology for use in assessing risk to property – adapted from AGS (2000).

Qualitative measures of likelihood of landsliding

Level	Descriptor	Description
A	Almost certain	The event is expected to occur
B	Likely	The event will probably occur under adverse conditions
C	Possible	The event could occur under adverse conditions
D	Unlikely	The event could occur under very adverse circumstances
D	Rare	The event is conceivable but only under exceptional circumstances
E	Not credible	The event is inconceivable or fanciful

Qualitative measures of consequences to property

1	Catastrophic	Structure completely destroyed or large scale damage requiring major engineering works for stabilisation
2	Major	Extensive damage to most of structure, or extending beyond site boundaries requiring significant stabilisation works
3	Medium	Moderate damage to some of structure, or significant part of site requiring large stabilisation works
4	Minor	Limited damage to part of structure, or part of site requiring some reinstatement/ stabilisation works
5	Insignificant	Little damage

Qualitative risk analysis matrix – classes of risk to property

Likelihood	Consequences to property				
	Catas-trophic	Major	Medium	Minor	Insignif-icant
Almost certain	VH	VH	H	H	M
Likely	VH	H	H	M	L-M
Possible	H	H	M	L-M	VL-L
Unlikely	M-H	M	L-M	VL-L	VL
Rare	M-L	L-M	VL-L	VL	VL
Not credible	VL	VL	VL	VL	VL

Legend – VH: very high risk; H: high risk; M: moderate risk; L: low risk VL: very low risk.

Other schemes may be developed by the geotechnical risk analyst in consultation with the owners or other stakeholders where appropriate, to best suit a given problem.

12

Qualitative risk assessment is subject to limitations, which include potentially imprecise and subjective description of the likelihood term, for example "adverse or" could occur" and hence are liable to result in wide differences in the estimated risks, together with lack of risk acceptance criteria against which the qualitatively assessed risks can be evaluated.

AGS (2000) recommended that schemes such as that shown in Table 1 are only applicable to consideration of risks to property. Extreme care must be exercised where qualitative risk assessment approaches are used for estimating risk of loss of life and decision-making on site-specific basis, especially for marginal cases, because of the associated shortcomings.

5 LANDSLIDE RISK ASSESSMENT

5.1 *Risk assessment process*

Risk assessment involves taking the outputs from the risk analysis and comparing them against values judgements and risk tolerance criteria to determine if the risks are low enough to be tolerable.

The process is one of making judgements, taking account of political, legal, environmental, regulatory and societal factors. The decision is usually the responsibility of the owner and regulator, sometimes consulting with the affected public or stakeholders. Non-technical clients may seek guidance from the risk analyst on whether to accept the risk, but from a legal viewpoint it is important that the owner and regulator make the final decision.

Assessment of the risk may involve consideration of values such as:

(a) Property or financial loss
  – Annualised risk cost
  – Financial capability
  – Impact on corporate reputations
  – Insurance available
  – For railways and roads; accidents per million tonnes of freight hauled, frequency of accidents
  – Indirect costs e.g. loss of road access
  – When mitigation measures are being considered, cost benefit ratio.
(b) Loss of life
  – Individual risk to life.
  – Societal risk e.g. as a frequency versus number of deaths (known as f – N) or cumulative frequency versus number of deaths (known as F – N) criteria.
  – Annualised potential loss of life
  – When mitigation measures are being considered, cost per statistical life saved.

5.2 *Risk acceptance criteria*

It is important to recognise the difference between acceptable and tolerable risks:

Acceptable risk: A risk which everyone impacted is prepared to accept. Action to further reduce such risk is usually not required unless reasonably practicable measures are available at low cost in terms of money, time and effort.

Tolerable risk: A risk within a range that society can live with so as to secure certain net benefits. It is a range of risk regarded as non-negligible, and needing to be kept under review and reduced further if possible.

Factors that affect an individual's attitude to acceptable or tolerable risk will include (adapted from AGS 2000):

– Resources available to reduce the risk.
– Whether there is a real choice, e.g. can the person afford to vacate a house despite the high risk?
– The individual's commitment to the property and its value relative to the individuals income.
– Age and character of the individual.
– Exposure the individual has experienced in the past, especially with regards to risk associated with landslides.
– Availability of insurance.
– Regulatory or policy requirements.
– Whether the risk analysis is perceived to be reliable.

There are some common general principles that can be applied when considering tolerable risk to loss of life criteria (IUGS 1997):

– The incremental risk from a hazard to an individual should not be significant compared to other risks to which a person is exposed in everyday life.
– The incremental risk from a hazard should, wherever reasonably practicable, be reduced, i.e. The As Low As Reasonably Practicable (ALARP) principle should apply.
– If the possible loss of life from a landslide incident is high, the likelihood that the incident might actually occur should be low. This accounts for society's particular intolerance to incidents that cause many simultaneous casualties, and is embodied in societal tolerable risk criteria.
– Persons in society will tolerate higher risks than they regard as acceptable, when they are unable to control or reduce the risk because of financial or other limitations.
– Higher risks are likely to be tolerated for existing slopes than for planned projects, and for workers in industries with hazardous slopes, e.g. mines, than for society as a whole.

These principles are common with other dangers such as Potentially Hazardous Industries (PHI) and dams. (IUGS 1997) considered that there are other

13

Table 2. AGS (2000) suggested tolerable risk criteria.

Situation	Suggested tolerable risk for loss of life
Existing engineered slopes	10^{-4}/annum person most at risk 10^{-5}/annum average of persons at risk
New engineered slopes	10^{-5}/annum person most at risk 10^{-6}/annum average of the persons at risk

principles that are applicable to risk from slopes and landslides:

– Tolerable risks are higher for landslides on natural hillsides than those from engineered slopes.
– Once a natural slope has been placed under monitoring, or risk mitigation measures have been executed, the tolerable risks approach those of engineered slopes.
– Tolerable risks may vary from country to country, as well as within a country, depending on historic exposure to landslide hazard, and the system of ownership and control of slopes and natural landslides hazards.

There are no universally established individual or societal risk acceptance criteria for loss of life due to landslides. Guidance on what has been accepted in various countries is given in SOA 6 in this volume.

The following are some examples:

(i) Individual risk

AGS (2000) suggested that, based on criteria adopted for Potentially Hazardous Industries, Australian National Committee on Large Dams (ANCOLD 1994, which were also adopted in ANCOLD 2003); and the review in Fell and Hartford (1997) the tolerable risk criteria shown in Table 2 "might reasonably be concluded to apply to engineered slopes". They suggested that acceptable risks are usually considered to be one order of magnitude smaller than these tolerable risks.

It should be noted the AGS (2000) guidelines do not represent a regulatory position. ANCOLD (2003) deleted reference to the "average of persons at risk", taking account only of the person most at risk.

(ii) Societal risk

The application of societal risk to life criteria is to reflect the reality that society is less tolerant of events in which a large number of lives are lost in a single event, than of the same number of lives are lost in a large number of separate events. Examples are public concern to the loss of large numbers of lives in airlines crashes, compared to the many more lives lost in small aircraft accidents.

The use of cumulative FN curves to reflect this is not universal. An example which has been trialled on an interim basis to assist landslide risk management of natural hillside hazards is shown in Figure 4.

Christian (2004) also discusses the use of *FN* criteria. He suggests that using the output of probabilistic analyses is hindered by the well-established fact that people, including engineers, have a lot of trouble understanding small probabilities and that in recent years, the *fN* and *FN* diagrams have proven to be useful tools for describing the meaning of probabilities and risks in the context of other risks with which society is familiar. He points out that computed absolute probabilities may not include all contributions; an effective approach is to compare probabilities of different options or alternatives. Probabilistic methodologies also provide insight into the relative contributions of different parameters to the uncertainty of the result and thus give guidance for where further investigations will be most fruitful.

Whether such quantitative criteria as the examples given are acceptable in principle will depend on the country and legal system in which the landsliding is being considered. In some societies, e.g. Australia, Hong Kong, and the United Kingdom, the use of such criteria for Potentially Hazardous Industries, and to a lesser extent dams and landslides is gaining acceptance. In others, such as France, the legal framework currently precludes the use at least in absolute terms. This is discussed further in SOA6.

As pointed out in IUGS (1997), those who use QRA for slopes and landslides should keep the following in mind when analysing, assessing and managing risk:

(a) Estimates of risk are inevitably approximate, and should not be considered as absolute values. This is best understood by allowing for the uncertainty in the input parameters, and in reporting the risk analysis outcomes.
(b) Tolerable risk criteria are themselves not absolute boundaries. Society shows a wide range of tolerance to risk, and the risk criteria are only a mathematical expression of the assessment of general societal opinion.
(c) It is often useful to use several measures of tolerable risk criteria, e.g. fN pairs, individual and societal risk, and measures such as cost to save a life and maximum justifiable cost if risk mitigation is being considered.
(d) It must be recognised that QRA is only one input to the decision process. Owners, society and regulators will also consider political, social and legal issues in their assessments and may consult the public affected by the hazard.
(e) The risk can change with time because of natural processes and development. For example:
– Depletion of debris from slopes can lead to a reduction in risk with time
– Removal of vegetation by natural processes, e.g. fire or human intervention, can lead to an increase in risk

14

– Construction of roads on a slope may increase the probability of landsliding and/or the elements at risk, and hence the risk.

(f) Extreme events should be considered as part of the spectrum of events. This is relevant to the triggering events (landslides, earthquake) the size of the landslide and the consequences. Sometimes it is the smaller, more frequent, landslides that contribute most to risk, not the low frequency very large event.

6 LANDSLIDE RISK MANAGEMENT

6.1 *Risk management process*

The outcomes of the Risk Assessment will be either:

(a) The risks are tolerable, or even acceptable and no mitigation options need be considered.

or

(b) The risks are intolerable, and risk mitigation options need to be considered.

The risk management process is iterative, requiring consideration of the risk mitigation options and the results of the implementation of the mitigation measures and of the monitoring.

Examples of options for mitigation of risks for a slope or group of slopes would include:

– Reduce the frequency of landsliding – by stabilization measures such as groundwater drainage, slope modification, anchors; or by scaling loose rocks,

– Reduce the probability of the landslide reaching the element at risk – e.g. for rockfalls, construct rock catch fences; for debris flows construct catch dams;

– Reduce the temporal spatial probability of the element at risk e.g. by installing monitoring and warning systems so persons can evacuate; relocation of buildings to be further from the landslide;

Other risk management options may include:

– Avoid the risk – e.g. abandon the project, seeking an alternative site or form of development such that the risk will be tolerable

– Transfer the risk, by requiring another authority to accept the risk, or to compensate for the risk such as by insurance (for property)

– Postpone the decision if there is sufficient uncertainty, awaiting the outcomes of further investigations, assessment of mitigation options, and monitoring. This would usually only be a temporary measure.

Finally a risk mitigation plan will be decided upon. There may be elements of control in this plan – i.e. regulations imposed by local or other governments.

For hazard analysis for land use planning, the emphasis may be on limiting building development to those areas where risks are assessed as likely to be acceptable, and using the higher hazard areas for low occupancy use such as sports field or passive recreation. In some cases mitigation measures as outlined above may be appropriate.

Apart from the consideration of risk mitigation using engineering measures, landslide risk management also consists of the use of 'soft' (or non-engineering) options, such as public education campaigns, public information services, etc. to address the issue of risk tolerance by the general public or the stakeholders and avoid unduly high expectations of the level of safety that can be achieved in practice. Risk tolerance is related, in part, to the perception and understanding of landslide risk. Risk communication to lay people forms a key element of the landslide risk management process in facilitating a better understanding of the nature and reality of landslide risk, and promoting the build-up of trust in, and credibility of, the risk analyst. Geotechnical professionals involved in landslide risk assessment and risk management have an important role to play in risk communication, which is best done using languages and means that can be easily comprehensible by the general public.

7 THE BENEFITS AND LIMITATIONS OF LANDSLIDE RISK MANAGEMENT

Some of the benefits of the use of quantitative risk assessment in landslide risk management include:

(a) It encourages a rational, systematic approach to assessing the safety of natural and engineered slopes, by requiring an assessment of the characteristics of the landslides, their travel distance and velocity, frequency of sliding, the elements at risk, their temporal spatial probability and vulnerability.

(b) It can be applied to situations which are not amenable to conventional deterministic analysis e.g. rockfalls, small landslides in cut slopes, shallow landslides and resulting debris flows on steep natural slopes.

(c) It can be applied to land-use planning, with specific loss of life acceptance criteria used to determine the zoning where building is acceptable.

(d) It allows comparison of risks across an owner's portfolio of slopes e.g. cut slopes on highways, and thereby allows prioritisation of remedial works, and potentially setting of risk-based standards for acceptable designs.

(e) Some local and regional government planners are familiar with risk management principles, and welcome landslide risk management being presented in terms they can relate to other hazards.

(f) The process requires consideration of risks for all levels of loading, rather than relying on "extreme event" loadings. Often failure paths will be identified in the analysis which have been overlooked.

(g) It focuses attention or what happens if the slope fails, including the possibility of the slide travelling rapidly onto buildings below, causing damage and loss of life.

(h) It focuses attention on liabilities and responsibilities if the parties involved.

(i) It provides a framework to put uncertainties and engineering judgement into a system. This results in an enhanced awareness of the need to consider uncertainties, and insight on what can go wrong, and their potential consequences, together with how the uncertainties and risks can be best managed

(j) It provides an open and transparent process on the nature and key contributors of landslide risk and the corresponding uncertainty for discussion with the regulators, owners, stakeholders, etc.

(k) It allows systematic consideration of risk mitigation options and cost benefit ratios, consistent with the As Low As Reasonably Practical (ALARP) principles, thus encouraging optimisation and enhancing cost benefit.

Some of the challenges and perceived limitations include (adapted from IUGS 1997):

(a) The potential uncertainty in estimating frequencies, travel distance and vulnerability. However these uncertainties can be modelled in the analysis, or sensitivity studies done to get a feel for their influence.

(b) The variety of approaches, and the need for expert judgement to assess frequency of landsliding in many cases. This requires those doing the analysis to be trained, and "calibrated". Baynes *et al* (2002) give a good example of how this can be achieved.

(c) Revisiting an assessment can lead to a significant change in the assessed risk due to increased data, or development of more advanced methods. This however is common to a "conventional deterministic" approach.

(d) Poor estimates of risk because significant hazards have been overlooked. This is a problem whichever approach is used, and can only be overcome by using well trained and experienced geotechnical professionals to do the analyses.

(e) Results of an assessment are seldom verifiable. A possible approach to overcome this is to use systematic peer review by individuals or for larger projects, panels. The first author has seen how successful this can be in risk assessment for dams. For slopes, where budgets are often smaller, peer review while still essential, is more likely to be done on a sample of the slopes being assessed, but it still should be done.

(f) Acceptable and tolerable loss of life criteria for slopes and landslides are not well established. This is an issue which has to be overcome at the country, state or local government level. It will not be practical to establish universal guidelines, although inevitably people will refer to what it is being done in societies with similar legal and social values.

(g) Some over rely on the results of risk assessments – and do not understand the uncertainty in the probabilities calculated. This is for the analyst to understand, and convey in the reporting process and when communicating with the public.

(h) The authors' experience is that many experienced practitioners are reluctant to use quantitative approaches to estimating landslide frequencies, because of their lack of experience in doing this. This needs to be addressed by systematic, on the site training and review by experienced professionals.

(i) There is still a lack of general acceptance of the method by the profession. It should be recognised that QRA is an engineering tool that may be used for an appropriate problem or to supplement other conventional tools for landslide risk management.

8 EXAMPLES OF LANDSLIDE RISK ASSESSMENT

Figures 5–7 give examples of certain elements of landslides risk assessment. These are simplified to illustrate the basic principles involved. Note that for convenience it has been assumed that the tolerable risk criteria in Table 2 and Figure 4 apply to the cases considered. Other examples can be found in Lee & Jones (2004), Lacasse (1998), Ho *et al* (2000), and Fell & Hartford (1997).

9 CONCLUDING REMARKS

(a) The risk management framework presented in this paper has been successfully used in landslide risk assessment and management for engineered and natural slopes. The framework may be adapted to suit a variety of problems, with due regard to the nature of the issues involved.

(b) Recent developments have included more widespread use of quantitative methods; more refined hazard and risk zoning which often involves use of digital technologies; improved rainfall-landslide incidence correlation models; and improved methods for assessing travel distances and travel paths.
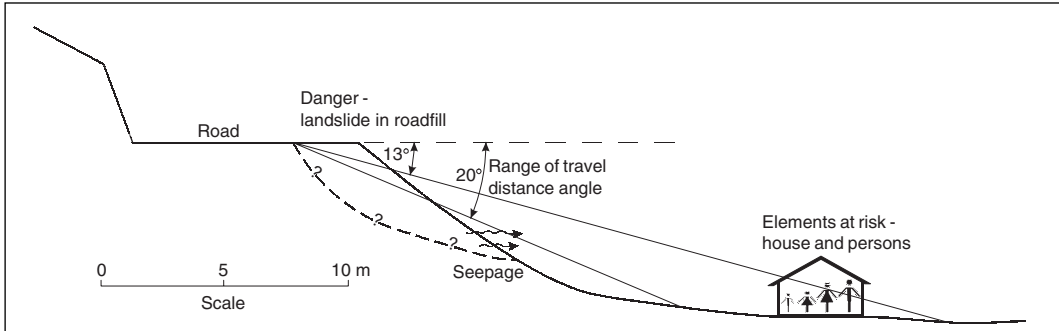
1. SCOPE DEFINITION

Calculate the risk to persons living in the house below a road as shown in the Figure. Assess the tolerability of this risk against the tolerable risk criteria shown in Table 1 and Figure 4.

2. RISK ANALYSIS

(i) Danger (Landslide) characterisation
The road was built 50 years ago, by cut and fill with a bulldozer. There was no proper compaction of the fill. The site is underlain by granitic rocks, and the fill is derived from residual soils and completely weathered granite which classifies as a silty sand. A thorough search of records has indicated that over the length of this road, which is all in similar topography, geology and climatic conditions to this fill, there have been 4 landslides in a total of 60 fills.

   Based on the geometry of the fill, and the landslides which have occurred, it is assessed that the likely volume of the slide is about $1000\,m^3$. Because of the loose, saturated nature of the fill it is anticipated that there may be a large loss of undrained shear strength on sliding ("static liquefaction") and the movement after failure is likely to be rapid.

   Using empirical methods, it is estimated that the travel distance angle will be between 13° and 20°. Based on this estimate, and the geometry of the slope, it is estimated that the probability of the landslide reaching the element at risk (the house and its occupants) $P_{T:L} = 0.4$.

(ii) Frequency analysis
Assuming this fill is similar to the other 60 fills on the road and that the 50 years of the road's performance road is representative of the future, the frequency of sliding of the fill is:

$$P_L = \frac{4}{60 \times 50} = 1.33 \times 10^{-3}\,/\,annum$$

(iii) Consequence analysis
(a) Temporal spatial probability ($P_{(S:T)}$) of the persons
Four persons live in the house. One of those persons is in the house 20 hours per day, 7 days per week; while the other three are in the house 12 hours per day, 2 days per week.

For the person most at risk:

$$P_{(S:T)} = \frac{20}{24} = 0.83$$

For the other three persons:

$$P_{(S:T)} = \frac{12}{24} \times \frac{2}{7} = 0.14$$

$$P_{(S:T)} = \frac{12}{24} \times \frac{2}{7} = 0.14 \text{ assuming no warning.}$$

(b) Vulnerability (of the persons ($V_{(D:T)}$)
Based on the volume of landsliding, its likely velocity when it hits the house, it is estimated that the vulnerability of the persons to being killed if they are in the house when the landslides hits is 0.4.

Figure 5.   Example I – landsliding in road fill.

17

(iv) Risk estimation

The annual probability of the person most at risk losing his/her life is

$$P_{(LOL)} = P_{(L)} \times P_{(T:L)} \times P_{(S:T)} \times V_{(D:T)}$$

$$= (1.33 \times 10^{-3}) \times (0.4) \times (0.83) \times (0.4) / \text{annum}$$

$$= 1.7 \times 10^{-4} / \text{annum}$$

The annual probability of four persons being in the house where it is hit by the slide (assuming the time they spend in the house overlap)

$$= (1.33 \times 10^{-3}) \times (0.4) \times (0.14)$$

$$= 0.74 \times 10^{-4} / \text{annum}$$

Since their vulnerability is 0.4, so 1.6 persons (say 1 to 2) would be killed.

3. RISK ASSESSMENT

(i) Risk evaluation

    (a) Individual Risk

    From Table 2, the tolerable individual risk for an existing slope is 1×10^{-4}/annum; so for the individual most at risk, with $P_{(LOL)} = 1.7 \times 10^{-4}$, the risk is just in the intolerable range.

    (b) Societal Risk

    From Figure 4 reproduced below, the societal risk is below the limit of tolerability line, but in the ALARP region.
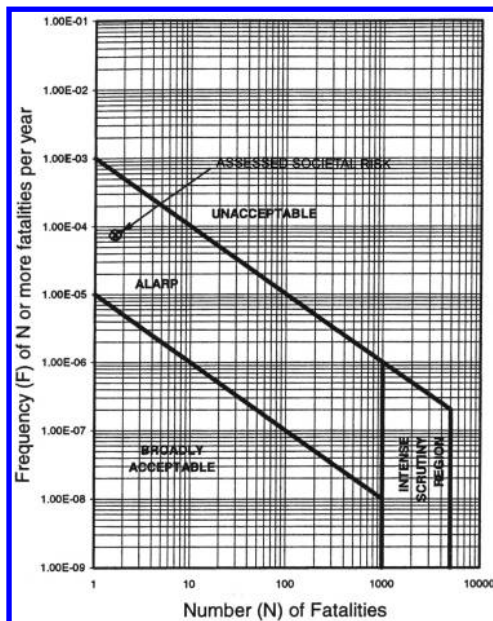
(ii) Comment

At this time, possible risk mitigation options would be considered, and the risks re-calculated. The ALARP principle might be used along with values judgements to determine a risk mitigation and/or monitoring plan, or to consider doing more geotechnical investigations to get an improved more accurate assessment of the risk.

Figure 5. (*Continued*).

18
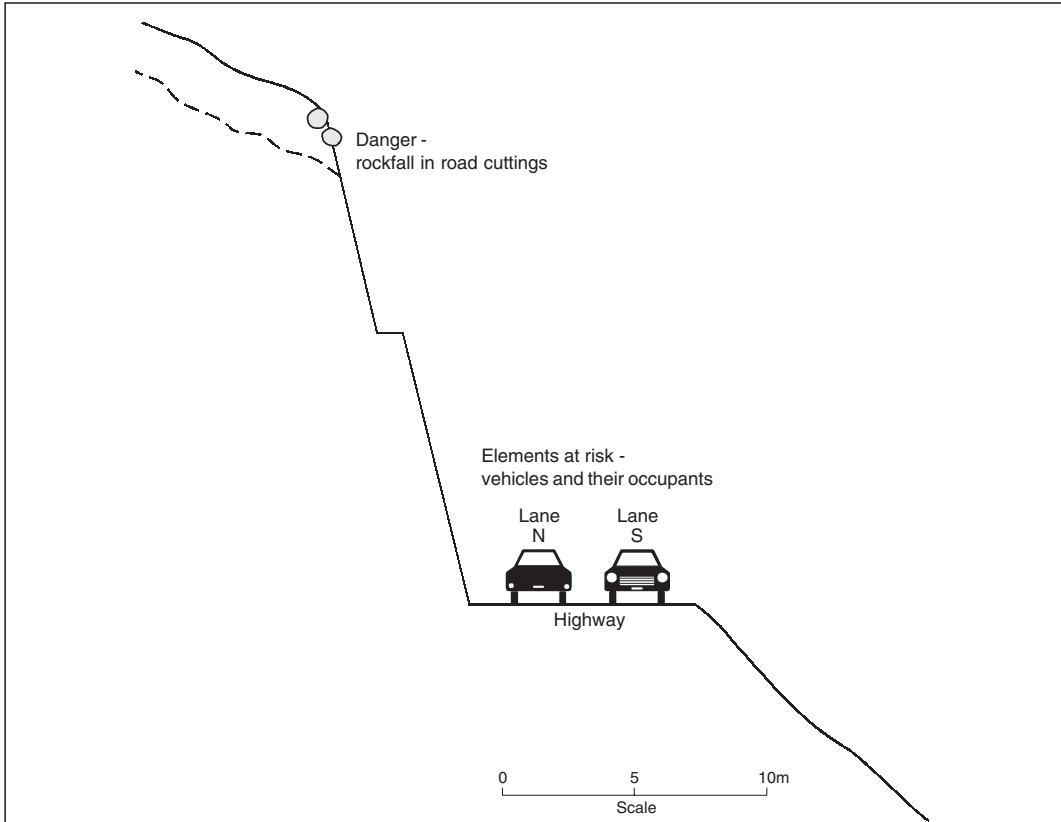
1. SCOPE DEFINITION

Calculate the risk to persons travelling on the highway as shown in the Figure. Assess the tolerability of this risk against the tolerable risk criteria shown in Table 1 and Figure 4. Only consider direct impact falls.

2. RISK ANALYSIS

(i) Danger (landslide) characterisation
The road to a ski resort is privately owned and was built 10 years ago. The 50 cuts in the road were constructed at relatively steep slopes, and without treatment to control weathering, erosion and shallow instability leading to rockfalls.

   A thorough search of the maintenance records and observations of boulder impacts on the road surface indicated that for the average cutting on the road, there have been 2 rockfalls per annum, with boulders ranging in size from 0.5 m dia to 1 m dia. The cuttings are in similar topography, geology and climatic conditions. Based on the recorded boulder impacts on the road surface, and the use of rockfall simulation programs, it is assessed that 60% of rocks falling from the slope will impact on Lane N which is closest to the cut, and 10% on Lane S.

(ii) Frequency analysis
The average frequency of rockfalls for each cutting is 2 per annum. There are a total of 50 cuts along the road, giving a total of 100 rockfalls per annum or 0.27/day, the average frequency of rockfalls (N_R) onto lane, N = $0.6 \times 0.27 = 0.16$/day, and on Lane S, = $0.1 \times 0.27 = 0.027$/day.

Figure 6. Example II – rockfalls from cuttings on a highway.

19

(iii) Consequence analysis
    (a) Temporal spatial probability ($P_{(S:T)}$) of vehicles
        The probability of a vehicle occupying the length of road onto which the rock falls is given by

$$P_{(S:T)} = \frac{N_V}{24} \bullet \frac{L}{1000} \bullet \frac{1}{V_V}$$

where N_V = average number of vehicles/day

    L = average length of vehicle (metres)
   V_V = velocity of vehicle (km/hour)

  For each lane, the average number of vehicles per day over the year is 2000, the average length of the vehicles is 6 metres, and they are travelling at 60 km/hr, ignoring the width of the boulder:

For each lane   For a particular vehicle travelling once each day in one direction

$$P_{(S:T)} = \frac{2000}{24} \bullet \frac{6}{1000} \bullet \frac{1}{60}$$
$$= 0.0083$$

$$P_{(S:T)} = \frac{1}{24} \bullet \frac{6}{1000} \bullet \frac{1}{60}$$
$$= 0.0000042$$

    (b) Vulnerability of the persons in the vehicles $V_{(D:T)}$
        Based on published information and judgement, it is estimated that the vulnerability of persons in vehicles in lane N is 0.3 and in lane S, 0.15.

(iv) Risk estimation
The annual probability of the person most at risk losing his/her life by driving along the road is:
    (a) For lane N   (b) For lane S

$$P_{(LOL)} = P_{(S)} \; x \; V_{D:T} = (1 - (1 - P_{(S:T)})^{N_R}) \; x \; V_{D:T}$$
$$= (1 - (1 - 0.0000042)^{0.16}) \; x \; 0.3$$
$$= 2.0 \; x \; 10^{-7} / annum$$

$$P_{(LOL)} = (1 - (1 - 0.0000084)^{0.027} \; x \; 0.15$$
$$= 0.3 \; x \; 10^{-7} / annum$$

      The total probability of death for the person most at risk is 2.3×10^{-7}/annum. For a person who only travels on the road once per year in each direction, $P_{(LOL)} = 6.3 \times 10^{-10}$/annum ($2.3 \times 10^{-7}$/365). The total annual risk assuming each of the 2000 vehicles/day carries an average of 3 persons is $2000 \times 365 \times 3 \times 6.3 \times 10^{-10}$/annum = 0.0014 persons/annum. The F-N plot has not been determined in this case.

3.   RISK ASSESSMENT

(i) Risk evaluation
    (a) Individual risk
      From Table 1, the tolerable individual risk for existing slopes is 1×10^{-4}/annum. So for the individual most at risk, with $P_{(LOL)} = 2.3 \times 10^{-7}$/annum, the risks are within the tolerable limit. For an individual who drives on the road only once per year, the risk is 6.3×10^{-10}/annum, which would be acceptable. The societal risk limit of tolerability for one life lost is 10^{-3}/annum (see Figure 4). The estimated probability of one or more lives lost is about 5×10^{-4}/annum, near the tolerable limit.
(ii) Comment
    (a) It is considered reasonable to sum the risks for all the road cuttings because the road is the responsibility of one organization.
    (b) At this time, risk mitigation options would be considered. These could include engineering option to reduce the frequency of rockfalls (rock-bolting, shotcreting, scaling of loose rocks in a regulated manner); reducing the probability the rocks will fall onto the road (e.g. mesh protection over the slope, catch drain); or reducing the probability of vehicles being below a rockfall when it occurs (e.g. closing the road in periods of heavy rain if it could be demonstrated that is when most rockfalls occurred).
    (c) See SOA Paper 5 for the equations for estimating risk.

Figure 6.   (*Continued*).
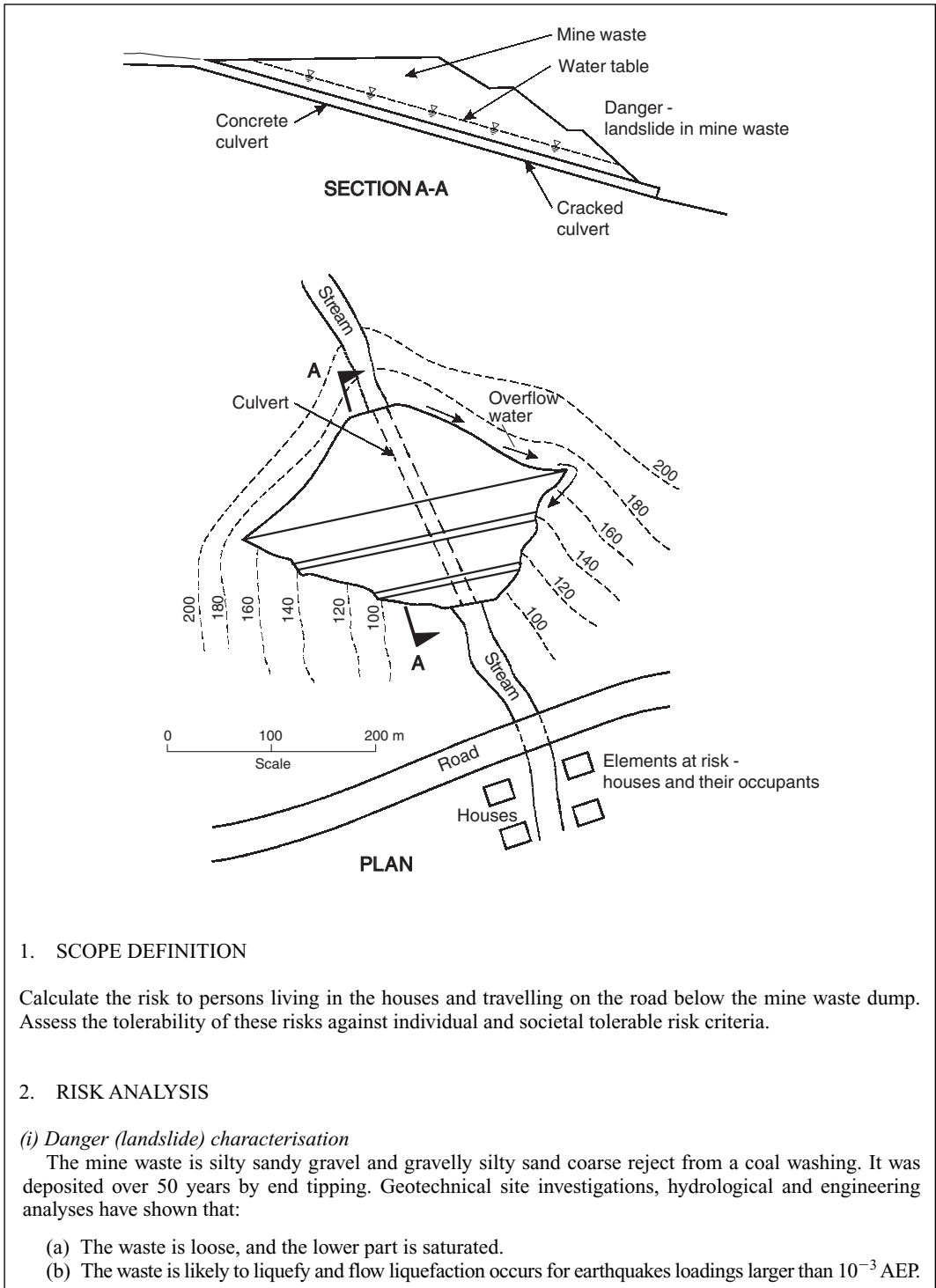
Figure 7.   Example III – landslinding of mine waste dump.

1.   SCOPE DEFINITION

Calculate the risk to persons living in the houses and travelling on the road below the mine waste dump. Assess the tolerability of these risks against individual and societal tolerable risk criteria.

2.   RISK ANALYSIS

(i) Danger (landslide) characterisation
    The mine waste is silty sandy gravel and gravelly silty sand coarse reject from a coal washing. It was deposited over 50 years by end tipping. Geotechnical site investigations, hydrological and engineering analyses have shown that:

  (a) The waste is loose, and the lower part is saturated.
  (b) The waste is likely to liquefy and flow liquefaction occurs for earthquakes loadings larger than 10^{-3} AEP.

21

(c) The culvert through the waste dump exceeds its capacity and runs full for floods greater than 0.1 AEP. For floods larger than this water flows over the sides of the waste dump and leaks onto the waste material through cracks in the culvert, increasing the pore pressures in the waste.

(d) The factor of safety of the dump under static loading is about 1.2 for water table levels which are reached annually.

(e) If the dump slides even under static loading, it is likely to flow because of its loose, saturated granular nature. The probability of this occurring given sliding occurs and the resultant debris flow reaching the houses is 0.5 based on post liquefaction shear strengths, and empirical methods for estimating travel distance.

(f) The volume of the anticipated landslide and resulting debris flow is about $100,000\,m^3$ and the debris flows are likely to be travelling at a high velocity when they reaches the road and houses.

(ii) Frequency analysis

The potential failure modes are:

(a) Culvert runs full, water leaks, saturates downstream toe, causes slide.
(b) As for (a), but a smaller slide, blocks/shears culvert, causes slide.
(c) Culvert collapses, flow saturates downstream toe, causes slide.
(d) A bigger flood, causes the culvert overflow, saturates fill, causes slide.
(e) As for (d), but scour of flowing water at toe of fill initiates slide.
(f) Rainfall infiltration, remobilizes slide.
(g) Earthquake causes liquefaction.

Based on the hydrology of the catchment, the hydraulics of the culvert, stability analyses and engineering judgement, it is estimated that the frequency of landsliding of the waste for modes (a) to (f) is 0.01/annum.

Based on an analysis of liquefaction using a Youd et al (2001) approach, and post liquefaction stability analysis, it is estimated that the frequency of landsliding for mode G is 0.005/annum.

Hence the total $P_{(L)} = 0.015$/annum.

(iii) Consequence analysis

(a) Temporal spatial probability ($P_{(S:T)}$) of the persons in the houses, and on the road

A survey of occupancy of the houses shows that the person most at risk in one of the houses is in the house on average 18 hours/day, 365 days per year, so $P_{(S:T)} = 0.75$.

Each house is occupied by a further 4 persons, for 10 hours/day, 325 days/year. Assuming they are all in the houses at the same time. So:

$$P_{(S:T)} \text{ for 16 persons} = \frac{10}{24} \times \frac{325}{365}$$
$$= 0.36$$

Vehicles on the road travel at an average velocity of 30 km/hour as they pass by the 100 metres of road potentially affected by the debris flow. So for each time the vehicle drives along the road,

$$P_{(S:T)} = \frac{100}{30,000 \times 365 \times 24}$$
$$= 3.8 \times 10^{-7}$$

If a vehicle travels along the road 250 times a year (such as the school bus)

$P_{(S:T)} = 250 \times 3.8 \times 10^{-7} = 9.5 \times 10^{-5}$

The critical vehicles for risk assessment are buses which travel 250 days/year.

(b) Vulnerability of persons ($V_{(D:T)}$)

Bases on the likely high velocity of sliding and large volume, it is estimated that the vulnerability of persons in the houses is 0.9, and in a bus, 0.8.

Figure 7. (*Continued*).

22

(iv) Risk estimation

The annual probability of the person most at risk losing his or her life is

$$P_{LOL} = p_{(L)} \text{ x } P_{(T:L)} \text{ x } P_{(S:T)} \text{ x } V_{(D:T)}$$

$$P_{LOL} = (0.015) \text{ x } (0.5) \text{ x } (0.75) \text{ x } 0.9/\text{annum}$$

$$= 5 \text{ } x \text{ } 10^{-3} / annum$$

If all four houses are hit by the landslide, 0.9×16 or say 14 of the 16 persons would be killed. The annual probability that this would happen is:

$$= 0.015 \text{ x } 0.5 \text{ x } 0.36/\text{annum}$$

$$= 2.7 \text{ x } 10^{-3}/\text{annum}$$

If a bus with 40 persons on it is hit by the landslide, $0.8 \times 40 = 32$ persons would be killed. The annual probability this would happen is:

$$= 0.015 \text{ x } 0.5 \text{ x } 9.5 \text{ x } 10^{-5}/\text{annum}$$

$$= 7.1 \text{ x } 10^{-7}/\text{annum}$$

So if loss of life of persons in other vehicles on the road is ignored, the cumulative F-N pair are:

One or more lives $F = 5 \text{ x } 10^{-3} + 2.7 \text{ } x \text{ } 10^{-3} + 7.1 \text{ } x \text{ } 10^{-7} = 7.7 \text{ } x \text{ } 10^{-3} / annum$

15 *or more lives* $= 2.7 \text{ } x \text{ } 10^{-3} + 7.1 \text{ } x \text{ } 10^{-7} = 2.7 \text{ } x \text{ } 10^{-3} / annum$

33 lives $F = 7.1 \text{ } x \text{ } 10^{-7} / annum$

3. RISK ASSESSMENT
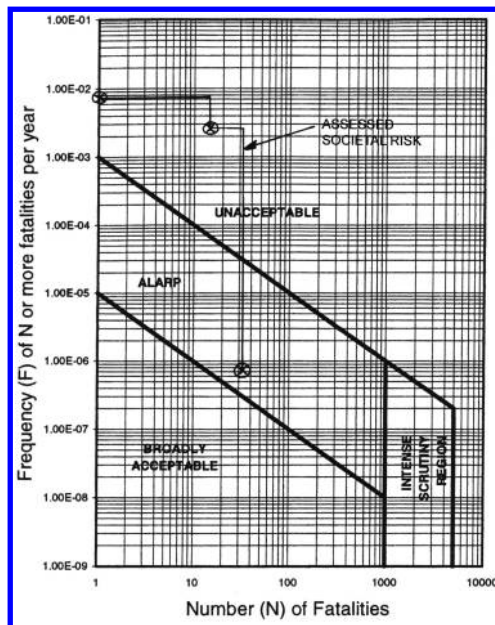
Figure 7. (*Continued*)

(a) Individual risk.

The risk for the person most at risk is 5×10^{-3}/annum which is well in excess of the tolerable individual risk in Table 1.

(b) Societal risk

The three points on the F-N curve are shown below. It can be seen that the risks are well in excess of the tolerable for 1 and 15 lives, but in the ALARP range for 33 lives lost in a bus.

(ii) Comment

At this point, possible risk mitigation options would be considered, and the risks recalculated. The mitigation options could include reducing the probability of sliding by repairing the cracks in the culvert, controlling water which overflows when the culvert capacity is exceeded; removing and replacing the outer waste well compacted so it will not flow if it fails; adding a stabilizing berm; installing a warning system so persons in the houses can be evacuated and the road blocked to traffic when movement is detected in the waste.

Figure 7.　(*Continued*)

(c) While the emphasis in this paper is on quantitative methods, current practice also involves the use of risk-based qualitative methods in many applications, including management of landslide risks for roads and railways, and in land use planning. These are valuable in that the landslide processes are systematically studied, and can lead to uniform classification of hazards and risks, which can be understood by those responsible for risk management. Qualitative approaches are better if they are underpinned by quantitative studies particularly where loss of life is an issue. RTA(2001) is an example of this for risk management of landsliding affecting highways. Other examples include the design event approach for assessing mitigation measures for natural hillside landslide hazards (Ho 2004).

(d) Adoption of quantitative methods is likely to assist in risk communication in many cases because regulators, politicians and managers of larger organizations are often familiar with quantifying risks within other parts of their responsibilities. Quantifying landslide risks allows these people to assess them in perspective with those from other hazards. In some cases the use of quantitative risk assessment is stipulated by the regulator or owner.

(e) While the nature of the problem and available methods for many studies always involve some degree of uncertainty in the risk estimates, this is not to say they should not be estimated, provided the limitations are acknowledged. Decisions have to be made despite the uncertainties, and it is better to have an approximate estimate of the risks, than none at all. The level of sophistication to be adopted in risk estimation for a particular problem only needs to be sufficient to facilitate an informed decision.

(f) There is often an overemphasis on the risk analysis, and not enough attention put on the risk assessment and management. It is important that Geotechnical Professionals involve themselves in the assessment and management process because they often have the best understanding of the nature of the hazard and the risk. However the final decisions on tolerable risks lie with owners, regulators and politicians.

(g) The authors cannot over-emphasise the need for proper geotechnical inputs to the risk analysis, particularly with respect to the hazard identification and quantification. Risk assessment is not a substitute for good geotechnical engineering knowledge and judgement. It enhances it by adding insight.

ACKNOWLEDGEMENTS

REFERENCES

ANCOLD 1994. *Guidelines on risk assessment.* Australian Committee on Large Dams.

ANCOLD 2003. *Guidelines on risk assessment*. Australian National Committee on Large Dams.

AS/NZS 4360:1999. Australian/New Zealand Standard, Risk Management Standards Australia, Standards New Zealand.

Australian Geomechanics Society 2000. *"Landslide risk management concepts and guidelines"*. Australian Geomechanics Society, Sub-Committee on Landslide Risk Management. *Australian Geomechanics* 35: 49–92.

24

Baynes, F.J., Lee, I.K. & Stewart, I.E. 2002. A study of the accuracy and precision of some landslide risk analyses. *Australian Geomechanics* 37(2): 149–156.

Canadian Standards Association 1991. "Risk analysis requirements and guidelines". CAN/CSA-Q634-91, Canadian Standards Association, Toronto, Canada, 42 pp.

Christian, J.T. 2004. Geotechnical Engineering reliability: how well do we know what we are doing? *Journal Geotechnical and Geoenvironmental Engineering* 130(10): 985–1003.

Cruden, D.M. & Varnes, D.J. 1996. Landslide types and processes: in "Landslides Investigation and Mitigation". In Turner & Schuster (eds), *Transportation Research Board Special Report 247*, National Research Council, Washington, D.C.

Einstein, H.H. 1988. Special lecture, landslide risk assessment. *Proc. 5th Int. Symp. On Landslides, Lausanne, Switzerland*. A.A. Balkema, Rotterdam, The Netherlands, 2: 1075–1090.

Einstein, H.H. 1997. Landslide risk – systematic approaches to assessment and management. In *Landslide Risk Assessment*, Cruden & Fell (eds), Balkema, Rotterdam, 25–50.

Fell, R. & Hartford, D. (1997). Landslide risk management. In *Landslide Risk Assessment*, Cruden & Fell (eds), Balkema, Rotterdam, 51–110.

Fell, R. 1994. Landslide risk assessment and acceptable risk, *Canadian Geotechnical Journal* 31: 261–272.

Geotechnical Engineering Office 1998. Landslides and Boulder Falls from Natural Terrain: Interim Risk Guidelines. GEO Report No.75, Geotechnical Engineering Office, The Government of the Hong Kong Special Administrative Region.

Hartford, D.N.D. & Baecher, G.S. 2004. Risk and uncertainty in Dam Safety. Thomas Telford, London.

Ho, K.K.S. 2004. Recent advances in geotechnology for slope stabilization and landslide mitigation – perspective from Hong Kong, in Landslides: evaluation and stabilization. Lacerda et al. (eds). Taylor and Francis Group, London, 1507–1560.

Ho, K., Leroi, E. & Roberds, B. 2000. Quantitative risk assessment. *Application, myths and future directions*. GeoEng 2000, Technomic Publishing, 269–312.

ICOLD 2003. Risk assessment in dam safety management, Draft ICOLD Bulletin. International Commission on Large Dams, Paris.

IUGS 1997. Quantitative risk assessment for slopes and landslides – the State of the Art. IUGS Working Group on Landslides, Committee on Risk Assessment, in *Landslide risk assessment*, Cruden & Fell (eds), Balkema, Rotterdam, 3–12.

Kvalstad, T.J., Nadim, F. & Harbitz, C.B. 2001. Deepwater geohazards: Geotechnical concerns and solutions. Offshore Technology Conference, OTC '01, Houston, Texas, 30 April–3 May, Paper OTC 12958., 11 p.

Lacasse, S. 1998. Risk and Reliability in Geotechnical Engineering. State-of-the-Art paper. Fourth International Conference on Case Histories in Geotechnical Engineering, St-Louis, Missouri, USA. March 1998. (NGI Report 594000–4.).

Lacasse, S. 2004. Risk Assessment for Geotechnical Solutions Offshore. Keynote Paper. OMAE2004-51144. Proc. of OMAE 2004 -23rd International Conference on Offshore Mechanics and Arctic Engineering. Vancouver, Canada. June 2004, 16 p.

Lacasse, S., Nadim, F. & Høeg, K. 2003. Risk Assessment in Soil and Rock Engineering. PanAm Conference, SARA, June 2003, pp. 2743–2750.

Lacasse, S., Nadim, F., Høeg, K. & Gregersen, O. 2004. Risk Assessment in Geotechnical Engineering: The Importance of Engineering Judgement. The Skempton Conference, Proc. London UK. Vol.2, pp. 856–867.

Lee, E.M. & Jones, D.K.C. 2004. Landslide Risk Assessment. Thomas Tilford Publishing, London.

Leroi, E. 1996. Landslide hazard – risk maps at different scales: objectives, tools and developments. In *Landslides Proc. Int. Symp. On Landslides*, Trondheim, 17–21 June, Senneset (ed), 35–52.

Morgan, M.G. & Henrion, M. 1990. Uncertainty – a guide to dealing with uncertainty in quantitative risk and policy analysis. Cambridge University Press.

Nadim, F. 2002. Probabilistic methods for geohazard problems: State-of-the-Art. Probabilistics in GeoTechnics: Technical and Economic Risk Estimation, Graz, Austria, September 15–19, pp. 333–350.

Nadim, F. & Lacasse, S. 2004. Mapping of landslide hazard and risk along the pipeline route. GeoPipe 2004. Terrain and Geohazard Challenges facing Onshore Oil and Gas Pipelines. Proc. (loose leaf binder), London, June 2004.

Nadim, F. & Lacasse, S. (1999). Probabilistic Slope Stability Evaluation. Proc. "Geotechnical Risk Management", Hong Kong Institution of Engineers, Hong Kong, 177–186.

Nadim, F. & Lacasse, S. 2003. Review of probabilistic methods for quantification and mapping of geohazards. Geohazards 2003, Edmonton, June 2003, pp. 279–286.

Nadim, F., Krunic, D. & Jeanjean, P. 2003. Probabilistic slope stability analyses of the Sigsbee Escarpment. Procs, OTC 15203, Offshore Technology Conference '03, Houston, Texas, May 2003, OTC paper 15203, 8 p.

RTA 2001. Guide to slope risk analysis version 3.1. Roads and Traffic Authority, Sydney.

Stewart, I.E., Baynes, F.J. & Lee, I.K. 2002. The RTA guide to slope risk analysis version 3.1. *Australian Geomechanics* 37(2): 115–149.

Varnes, D.J. 1984. The International Association of Engineering Geology Commission on Landslides and Other Mass Movements 1984. *Landslide hazard zonation: A review of principles and practice.* Natural Hazards, 3: 63. Paris, France. UNESCO.

Whitman, R.V. 1984. Evaluating calculated risk in geotechnical engineering, *J. Geotech. Eng., ASCE* 110(2): 145–188.

Wu, T.H., Tang, W.H. & Einstein, H.H. (1996). Landslide hazard and risk assessment; in landslides investigations and mitigation, Transportation Research Board Special Report 247, national Research Council Washington DC.

Youd, T.L., Idriss, I.M., Andrus, R.D., Arango, I., Castro, G., Christian J.T., Dobry, R., Finn, W.D.L., Harder, L.F., Hynes, M.E., Ishihara, K., Koester, J.P., Liao, S.S.C., Marcuson, W.F., Martin, G.R., Mitchell, J.K., Moriwaki, Y., Power, M.S., Robertson, P.K., Seed, R.B., & Stokoe, K.H. 2001. Liquefaction resistance of soils: summary report from the 1996 NCEER and 1998 NCEER/NSF Workshops on evaluation of liquefaction resistance of soils. *J. Geotechnical and Geoenvironmental Engineering*, ASCE 127(10): 817–834.

Hazard characterization and quantification

L. Picarelli
Seconda Universita di Napoli, Italy

F. Oboni
Oboni Associates and Riskope, Vancouver, B.C., Canada

S.G. Evans
University of Waterloo, Waterloo, Canada

G. Mostyn
Pells Sullivan Meynink, Sydney, Australia

R. Fell
School of Civil and Environmental Engineering, The University of New South Wales, Sydney, Australia

ABSTRACT: Hazard characterization and quantification involves (hazard analysis) characterizing the danger (the landslides) in terms of type, size, velocity, location, travel distance, pre-failure deformations and mechanics; and the corresponding probability of occurrence (or frequency, when records exist). This paper provides an overview of characterization; the importance of understanding the mechanics of sliding; and of methods to assess the frequency of landsliding.

1 INTRODUCTION

Landslide hazard characterization and quantification involves (hazard analysis) characterizing the danger in terms of type, size, velocity, location, travel distance, pre-failure deformations and mechanics; and the corresponding frequency (annual probability) if suitable data exists.

This requires understanding of the landsliding processes as well as frequency statistics.

This paper provides an overview of characterization; the importance of understanding sliding mechanics on analysis; and of methods to assess the frequency of landsliding.

2 DANGER (LANDSLIDE) CHARACTERISATION

2.1 *Classification of landslides*

It is extremely important that landslides are described in terms which are consistent with international practice, using a classification scheme such as that of Varnes (1978), Cruden & Varnes (1996) or Hutchinson (1988). It is important to recognise that landsliding which results in, for example debris flows, may have a source landslide which was an earth slide, or some other type of slide, and to understand the danger, both may need to be described. For this reason the Cruden & Varnes (1996) method has some advantages, although Varnes (1978) can be used to describe the source slide, and the resultant flow (for this example).

Cruden & Varnes (1996) suggested a landslide classification based on a taxonomic order. Landslide names are to be built from terms describing the following attributes, in sequential order:

– state (Table 3a)
– distribution (Table 3a)
– style (Table 3a)
– rate of movement (Tables 1 and 3(b), (c))
– water content (Tables 3(b), (c))
– type of material (Tables 3(b), (c))
– type of movement (Table 2)

Because both type of movement and rate can change during motion, the same description should be applied repeatedly to several phases of motion, if necessary. This process is rational and well-organized, but results in long names; for example "*complex, extremely rapid, dry rock fall – debris flow*". Such names make it difficult to develop typological groupings of landslide phenomena that are essential for hazard analysis

Table 1. Terms describing the velocity of a landslide (Cruden & Varnes 1996).

Velocity class	Description	Velocity (mm/sec)	Typical velocity	Human response
7	Extremely rapid			Nil
	------------	5×10^3	5 m/sec	Nil
6	Very rapid			
	------------	5×10^1	3 m/min	
5	Rapid			Evacuation
	------------	5×10^{-1}	1.8 m/hr	
4	Moderate			Evacuation
	------------	5×10^{-3}	13 m/month	
3	Slow			Maintenance
	------------	5×10^{-5}	1.6 m/year	
2	Very slow			Maintenance
	------------	5×10^{-7}	16 mm/year	
1	Extremely slow			Nil

Table 2. Abbreviated classification of slope movements (Cruden & Varnes 1996).

		Type of material	
		Engineering Soils	
Type of movement	Bedrock	Predominantly coarse	Predominantly fine
Fall	Rock fall	Debris fall	Earth fall
Topple	Rock topple	Debris topple	Earth topple
Slide	Rock slide	Debris slide	Earth slide
Spread	Rock spread	Debris spread	Earth spread
Flow	Rock flow	Debris flow	Earth flow

(e.g. Hungr et al. 2001). For some situations therefore it may be sufficient to use the abbreviated classification shown in Table 2 or the simplified version of the Varnes classification shown in Table 4.

As depicted in Figure 1, four different stages of slope movements can be considered:

– The pre-failure stage, when the slope is strained throughout, but is essentially intact.
– The onset of failure is characterized by the formation of a continuous surface of rupture (e.g. a shear band) through the slope.
– The post-failure stage, which includes movement of the material in the landslide from just after failure until it essentially stops.
– The reactivation stage, when the slope slides along one or several pre existing shear surfaces: this reactivation can be occasional or continuous with seasonal (or longer period) variations in the rate of movement.

Table 3. Glossary for forming names of landslides (Cruden & Varnes 1996).

(a) Activity

State	Distribution	Style
Active	Advancing	Complex
Reactivated	Retrogressive	Composite
Suspended	Widening	Multiple
Inactive	Enlarging	Successive
Dormant	Confined	Single
Abandoned	Diminishing	
Stabilised	Moving	
Relict		

(b) Description on first movement

Rate	Water content	Material	Type
Extremely rapid	Dry	Rock	Fall
Very rapid	Moist	Soil	Topple
Rapid	Wet	Earth	Slide
Moderate	Very wet	Debris	Spread
Slow			Flow
Very slow			
Extremely slow			

Note: Subsequent movements may be described by repeating the above descriptors as many times as necessary.

Table 4. A simplified version of the Varnes' landslide classification. The italicized names represent landslide types likely to exhibit extremely rapid velocities (more than 5 m/sec). Based on Fig. 3.1 in Varnes (1978).

	Bedrock	Debris (<80% sand and finer)	Earth (>80% sand and finer)
Falls	**Rock fall**	**Debris fall**	**Earth fall**
Topples	**Block topple**	–	**Block topple**
Slides	Rock slump	**Debris slide**	Earth slump
	Rock slide		Earth slide
Spreads	Rock spread	–	**Earth spread**
Flows	Rock creep	**Debris flow**	**Wet sand and silt**
	Slope sagging	**Debris avalanche**	**Flow**
		Soil creep	**Rapid earth flow**
		solifluction	**Loess flow**
			Dry sand flow
			Earth flow
Complex	**Rock avalanche**		
	Earth slump-Earthflow		

2.2 Geological and geotechnical inputs to landslide characterization

All site investigations, whether for natural or constructed slopes, should be carried out with a clear objective, and with a set of questions to be answered.

28
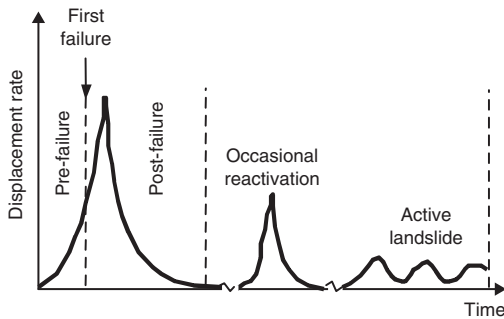
Figure 1. Different stages of slope movements (Leroueil et al. 1996).

Stapledon (1995) and Sowers & Royster (1978) (in Turner & McGuffey1996) give examples of the questions to be answered. Table 5 is developed from them, and is applicable to all classes of slopes, although clearly some questions are more applicable to large, natural landslides and other larger slopes than to a constructed fill for example.

Not all site investigation methods are applicable to all classes of slopes, or to all stages of investigation. Table 6 lists the applicability of the methods to typical classes of slope problem.

It will be seen that for:

• Shallow natural landslides there is a reliance on geological, topographical geomorphological and

Table 5. Questions to be addressed in slope stability and landslide investigations (Fell et al. 2000).

1. Topography?	1.1 In the landslide source and potential travel path
	1.2 Effect and timing of natural and human activity on the topography
2. Geological setting?	2.1 Regional stratigraphy, structure, history (e.g. glaciation, sea level submergence and emergence)
	2.2 Local stratigraphy, slope processes, structure, history
	2.3 Geomorphology of slope and adjacent areas
3. Hydrogeology?	3.1 Regional and local groundwater model?
	3.2 Piezometric pressures within and around the slide?
	3.3 Relationship of piezometric pressures to rainfall, snowfall and snowmelt, temperature, streamflows, reservoir levels, both seasonally and annually?
	3.4 Effect of natural or human activity?
	3.5 Groundwater chemistry and sources
	3.6 Annual exceedance probability (AEP) of groundwater pressures
4. History of movement?	4.1 Velocity, total displacement, and vectors of surface movement?
	4.2 Any current movements and relation to hydrogeology and other natural or human activity?
	4.3 Evidence of historic movement and incidence of sliding e.g. lacustrine deposits formed behind a landslide dam, shallow natural slides, or failures of cuts and fills
	4.4 Geomorphic or historic evidence of movement of slope or adjacent slopes
5. Geotechnical characterisation of the slide or potential slide?	5.1 Stage of movement (pre failure, post failure, reactivated, active)
	5.2 Classification of movement (e.g. slide, flow)
	5.3 Materials factors (classification, fabric, volume change, degree of saturation)
6. Mechanisms and dimensions of the slide or potential slide?	6.1 Configuration of basal, other bounding, and internal rupture surfaces?
	6.2 Is the slide part of an existing or larger slide?
	6.3 Slide dimensions, volume?
	6.4 Is a slide mechanism feasible?
7. Mechanics of shearing and strength of the rupture surface?	7.1 Relationship to stratigraphy, fabric, pre existing rupture surfaces
	7.2 Drained or undrained shear?
	7.3 First time or reactivated shear?
	7.4 Contractant or dilatant?
	7.5 Saturated or partially saturated?
	7.6 Strength pre and post failure, and stress–strain characteristics
8. Assessment of stability?	8.1 Current, and likely factors of safety allowing for hydrological, seismic and human influences?
	8.2 AEP of failure (factor of safety $\leqslant 1$)?
9. Assessment of deformations and travel distance?	9.1 Likely pre failure deformations?
	9.2 Post failure travel distance and velocity?
	9.3 Likelihood of rapid sliding?

Table 6. Application of site investigation methods to slope classes (Fell et al. 2000).

Site investigation method	Natural slopes			Constructed slopes				
	Small/shallow	Medium	Large	Existing cut	Existing fill	New cut	New fill	Soft clay
Topographic mapping and survey	A	A	A	A	A	A	A	A
Regional geology	A	A	A	A	A	A	A	A
Geological mapping of project area	B	B	A	A	B	A	B	C
Geomorphological mapping	A	A	A	B	B	B	B	D
Satellite imagery interpretation	D	D	C	D	D	D	D	D
Air photograph interpretation	A	B	A	C	C	C	C	C
Historic record	A	B	B	A	B	B(2)	B(2)	B(2)
Dating past movements	B	C	B	D	D	D	D	D
Geophysical methods	C	C	B	C	C	C	D	C
Trenches and Pits	B	A	B	B	B	B	B	C
Drilling/boring	C	A	A	C	B	B	B	A
Downhole inspection	C	B	B	C	D	C	D	D
Shafts and tunnels	D	C	B	D	D	D	D	D
In-situ testing of strength and permeability	C(3)	C(3)	C(4)	D	B(3)	C	C	A(3)
Strength and permeability monitoring pore pressures, rainfall etc.	C	A	A	A	A	C	C	A(5)
Monitoring of displacements	C	B	A	B	B	B(5)	C(5)	A(5)
Laboratory testing	C	A	B	B	B	B	C	A
Back analysis of stability	C	B	A	C	B	B(2)	C(2)	C(2)

Notes: (1) A – Strongly applicable, B – Applicable, C – May be applicable, D – Seldom applicable.
    (2) In similar areas.
    (3) SPT, CPT, CPTU.
    (4) Permeability.
    (5) During construction.

historic information without detailed drilling, sampling, laboratory testing and analysis.

- Medium natural landslides have a similar emphasis on geology, geomorphology and historic records, but a greater emphasis on sub-surface exploration, sampling, monitoring of pore pressures and laboratory testing.
- Large natural landslides there is a greater emphasis on monitoring of deformations and groundwater pressures, less emphasis on laboratory testing and more on back-analysis to assess strengths.
- Existing cuts and fills, there is a reliance on topography, geology, geomorphology and historic performance. For larger structures, more subsurface investigation, sampling and laboratory testing will be carried out.
- New cuts and fills, there is a reliance on the performance of structures in similar conditions, and monitoring post construction. It is essential that geomorphological studies be included to identify existing natural landsliding.
- Embankments and cuts in soft clays, the emphasis is on stratigraphy and strength, often obtained by in-situ tests, and careful drilling, sampling and laboratory tests.

The hazard analysis will only be as good as the geotechnical inputs so this process requires experienced geotechnical professionals who have an appreciation of hazard analysis to be involved.

2.3 Assessment of the size, location, post failure velocity and travel distance of landslides

As part of the landslide characterization it is necessary to assess:

(a) The likely size (volume, area, depth) of the potential landslides
(b) the location on the slope the slides are likely to occur
(c) The likely post failure velocity and travel distance.

This is a fundamental difference to the deterministic approach as shown in Figure 2.

For the deterministic approach the questions are:

What is …
- Geometry, Geology, Hydrogeology?
- Shear Strength?
- Pore Pressure?

30
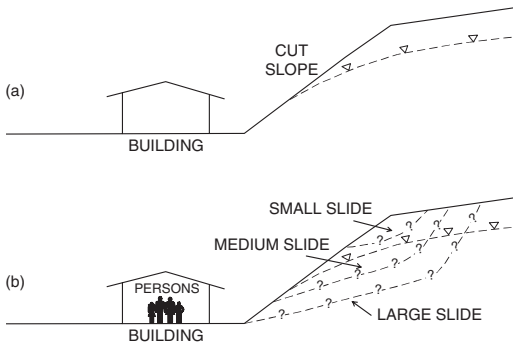
Figure 2. Comparison of a factor of safety approach to a risk assessment approach. (a) Deterministic approach (b) Risk based approach.

What is factor of safety and sensitivity to assumptions?

For the risk based approach, the questions are:

What is …
- Slope Geometry, Geology, Hydrogeology?
- Where? How big? And what is the probability of sliding?
- What will the slide mechanism be?
- How far will the slide travel? And how fast?
- Will there be warning signs?
- Will the slide reach the house/How big? How fast?

The potential volume of the slide(s) should be estimated from knowledge of the geometry of the slope, features controlling the depth and boundaries of the slide (e.g. joints, depth of colluvial soil over a rock slope etc). Judgement will be required, and there may be a range of possible slide volumes, each with a different frequency of sliding.

Similarly the locations of the potential sliding can be assessed from the slope geometry, geology, geomorphology and historic data.

The likely post failure velocity and travel distance should be assessed for each class of potential sliding accounting for the slide volume, position on the slope and slide mechanics. SOA 4 discusses the methods available for doing this.

3 THE IMPORTANCE OF LANDSLIDE MECHANICS IN PREDICTING BEHAVIOUR

3.1 General

An understanding of the mechanics of landsliding is an essential input to assessing the likelihood of sliding, the pre and post failure deformations, and the velocity of sliding post-failure. The latter is quite critical to the

consequences of sliding, particularly for life loss risks. The following provides some insights to the issues. Other papers which contribute to this general understanding include Hutchinson (1988), Picarelli (2000, 2004), Fell et al. (2000), Bromhead (2004), Leroueil (2001, 2004), Leroueil et al. (1996) and SO4 in this volume.

All classifications of slope movements are based on the description of the mechanisms of post-failure deformation and movement (Picarelli 2000). Many authors identify five main mechanisms: falling, toppling, sliding, flowing and spreading. Some of these may combine, giving rise to more complex phenomena. Every mechanism has a mechanical explanation calling for the relationships existing between the triggering factors (changes in boundary conditions and possibly, in the long term, in soil properties), and their effects in terms of stress and strain conditions. The initial stress conditions related to the geological history play a fundamental role, even if they cannot be precisely evaluated by analysis.

According to experience, different mechanisms of failure (thus landslide types), require different analytical approaches. Therefore, a correct classification of slope movement is an important tool for framing the events to be examined, predicting their behavior and magnitude, and selecting the best criteria for risk mitigation.

Some aspects of the mechanics of landslides and their effects on the magnitude of landslides, will be examined in the following, referring to the main types of landslides mentioned above, and separating these into soil and rock slopes.

3.2 Some aspects of the mechanics of soil slopes

3.2.1 Slides

Slides are slope movements caused by general shear failure. Typically, movement consists in shearing concentrated along the sliding surface located at the base of the landslide body, and in some internal deformation (Fig. 3). Internal deformation is caused by the stress redistribution associated with any change of the boundary stress conditions (as variation of the shear stress along the lower boundary) and with viscous soil properties (that produce creep or stress relaxation). In rocks or in jointed and/or layered clay, the sliding surface generally coincides with a pre-existing persistent discontinuity, whereas in intact or fissured clay, it is just a result of failure.

As shown by Skempton & Petley (1967), the slip surface is something more than a pure shear surface, but a part of a thin zone, the shear zone, that includes also minor shears (Fig. 4). Shear along the sliding surface is associated with complex, and probably, large shear deformations of the shear zone around it. For the simple theoretical case of infinite slope subjected to

31
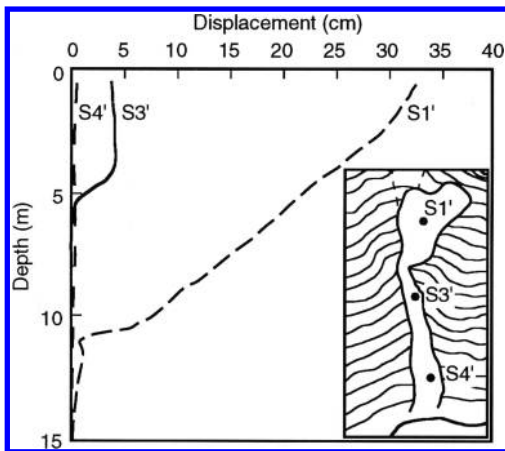
Figure 3. Displacement profiles within the same landslide characterized by minor (S4′) or significant (S1′) internal shear deformation (Picarelli et al. 1995).
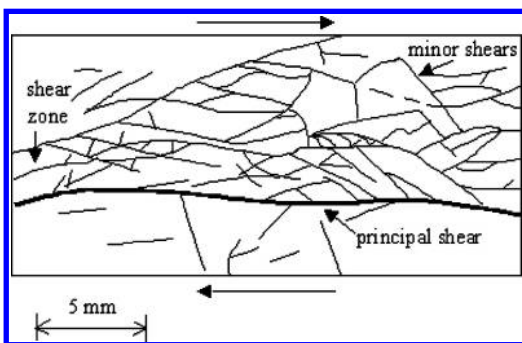
Figure 4. The shear zone recognized at the base of the Guildford landslide (from Skempton & Petley, 1967).

monotonic uniform pore pressure that rises eventually to cause slope failure, Urciuoli (2002) demonstrates that the shear zone starts forming before general slope failure and that its thickness depends on the initial state of stress, through the coefficient of earth pressure at rest: in the case of OC clay it is thin, but in the case of slightly overconsolidated clay, it could be fairly thick (Fig. 5). Some data seem to support this hypothesis (Demers et al. 1993) mentioned by Picarelli et al. 2004). Experience that is mainly concerned with slides in highly overconsolidated clay, shows that the shear zone is generally quite thin (not more than a few centimeters).

Therefore, the deformation of either the shear zone or the landslide body above, should be practically insignificant on the global mechanisms of slope movement, that is dominated by basal slipping.

During movement, the soil mass more or less maintains its shape and integrity or breaks into stiff blocks whose movements can be fairly independent.

Slides are caused by changes of boundary conditions and consequent changes in the state of stress, or by changes in the shear strength. Surcharges determine an increase in the state of stress; the opposite, i.e. a decrease in the state of stress, is caused by excavation (engineered slopes) or by natural erosion (natural slopes). A transient change in the state of stress, with possible permanent consequences on the slope, is caused by earthquakes. Frequently, slides are triggered by reduction in the shear strength, as a consequence of pore pressure changes induced by rainfall or thawing, or by soil weakening caused by weathering, softening, slaking or fatigue, while the total stress remains more or less constant. However, soil weakening is very slow and can trigger slope failure only in the very long-term.

Each of the mentioned causes of slope instability is responsible for full shear strength mobilization, but through very different stress paths (Fig. 6) that lead to different values of the mobilized shear strength that depend on the induced changes of the effective stress. Usually, the initial and the induced state of stress are not uniform, depending respectively on the past and recent stress history. Therefore, soil failure is initially localized in a small part of the slope (local slope failure, according to Urciuoli et al. 2005). Since the initial direction of the major principal stress depends on the past stress history, the orientation of the local failure plane is not unique. This implies a complex mechanism of general slope failure characterized by either propagation of failure in the slope and rotation of the direction of the principal stresses until the formation of a continuous failure surface (Urciuoli & Picarelli 2004). Only when the shear zone reaches the ground surface, infinite deformation can eventually develop and a failure takes place. If changes of boundary conditions (or the same process of failure) cause building up of deficient pore pressures, as typically occurs as a response to cutting or of erosion if it is rapid enough (Fenelli & Picarelli 1990, Potts et al. 1997), failure can be delayed.

As a consequence of movement, particle packing and internal fabric of the shear zone can progressively change. Overconsolidated clays experience increase in water content (Henkel 1957), whereas the opposite occurs in slightly overconsolidated clays (Lefebvre 1981). This is a consequence of the soil response to both shearing and change of the mean stress (Urciuoli 2002). As the magnitude of movement increases, the soil particles located near the sliding surface progressively align in the direction of shear, while the shear zone bounding the sliding surface experiences

32

$K_0 = 0.63$

displacement (m)
0.1 0.05 0

FS=1.2

depth (m)

failure plane

H_W

displacement (m)
0.1 0.05 0

FS=1.1

plastic zone

displacement (m)
0.1 0.05 0

FS~1.0

failure plane
parallel to the slope

δ

$K_0 = 0.95$

displacement (m)
0.1 0.05 0

FS=1.2

depth (m)

displacement (m)
0.1 0.05 0

FS=1.1

failure plane
parallel to the slope

displacement (m)
0.1 0.05 0

FS~1.0

failure plane

plastic zone
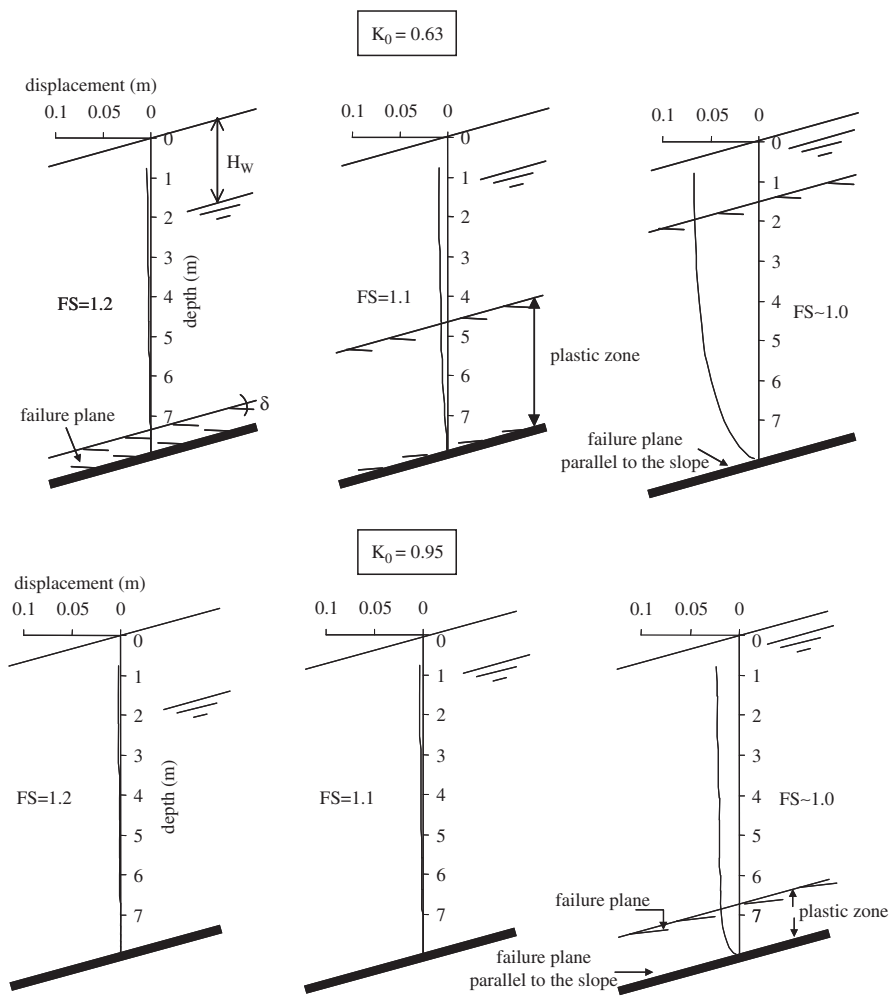
Figure 5.   Displacement profiles from the pre-failure to the failure stage calculated in two cases of infinite slope analyzed by Picarelli et al. (2004).

(a)

(b)
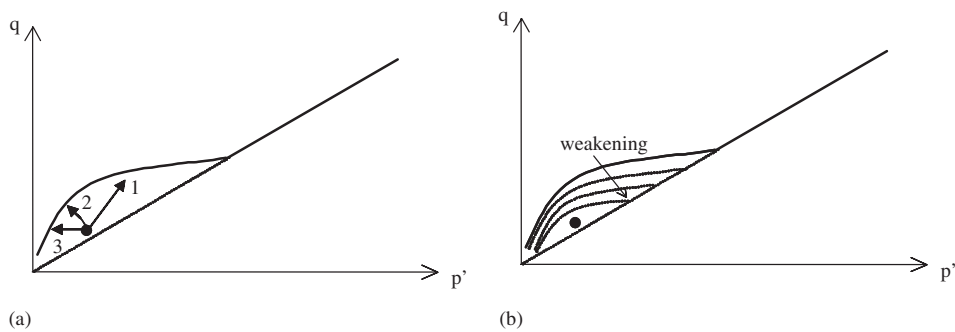
weakening

Figure 6.   Schematic local stress paths to failure: a) as a consequence of stress changes in response to surcharge (1), in response to cutting (2), in response to rainfall (3); b) as a consequence of soil weakening.

33
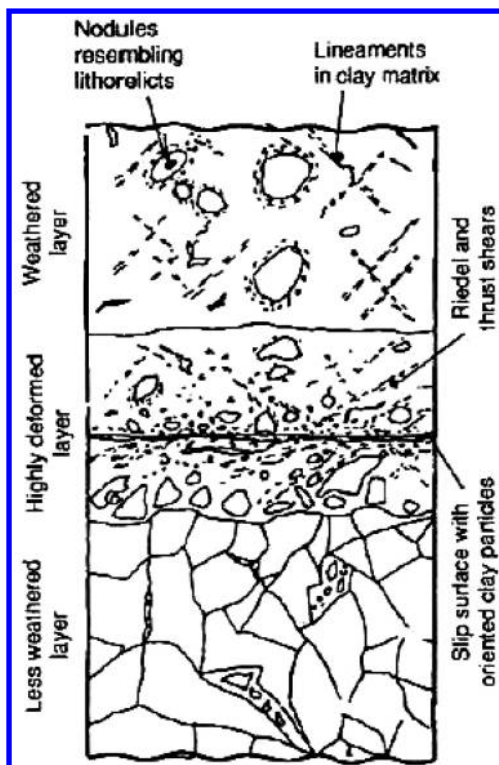
Figure 7. Shear zone of a rock subject to ice thrusting, Highvale mine, Alberta (from Tsui et al. 1988).

destructuration and remolding. Figure 7 shows the shear zone of rock mass subject to ice-thrusting, where it is possible to recognize minor shears and soil lithorelicts mixed with remolded clay (Tsui et al. 1988). As a consequence of alignment of clay particles, the mobilized shear strength along the slip surface progressively decreases. Similar phenomena have been noticed in granular soils subject to fast shearing (Agung 2004). Along rock joints or bedding surfaces, shearing causes smoothing of the joint surface, leading to a decrease in the coefficient of roughness and, friction angle.

The presence of a fossil slip surface is a major cause of landslide mobilization (reactivation). In this case the location of the slip surface dictates both the mechanism of failure and the size of the landslide body. Since in some clays the residual shear strength is much smaller than the peak strength, in areas occupied by old landslides reactivation is very likely and occurs in response to even small changes in the boundary conditions. In uncemented sand, the large strain shear strength is only slightly less than the peak strength, thus reactivation is not so usual. Reactivation can be progressive just as in first-time failure. Russo (1997)

and Picarelli (2000) describe some mechanisms of progressive reactivation.

The size of slides is extremely variable, depending on the internal structure of the slope (location and orientation of discontinuities and weak zones) and on the mechanism of slope failure.

Large landslides are mostly a heritage of past events, as valley erosion and earthquakes, but sometimes large landslides occur as a final effect of long-lasting phenomena such as soil (or rock) weakening.

Experience indicates that the velocity of slides falls within a wide range. In rock, the displacement rate is typically rapid, and the landslide can transform into a rock avalanche or a debris flow. In first-time slides in overconsolidated clay the peak velocity usually ranges between rapid and moderate. In sensitive clay it is rapid to moderate, and the mechanism typically changes into a flow slide (for definition of flow slide, see Hungr et al. 2001). In sand, movement can be either moderate or extremely rapid depending on the degree of saturation and initial density: also slides in loose saturated sand can rapidly change into flow slides.

Hungr (1981) and other Authors propose to use the displacement rate as indicator of the intensity (or magnitude) of landslides, even though a different parameter, as the momentum or kinetic energy (that account also for the size of the involved soil mass), might be more relevant for assessing the risk of landslide.

The rate of displacement depends on either slope morphology (inclination of the slip surface) or physical and mechanical properties of soil. The problem can be examined in the light of energetic considerations (Leroueil et al. 1996). When available potential; energy cannot be fully spent in shearing, the soil mass must accelerate. Its velocity depends on the Generalised Brittleness Index defined by D'Elia et al. (1998) that represents the rate of shear strength decrease. This mechanical process justifies fast slides in rock and stiff soils, such as OC clays. D'Elia et al. (1998) use this simple scheme to justify the different kinematics of two landslides (Fig. 8) triggered by excavations in the S. Barbara mine, one in a brittle OC clay, the other one in a ductile highly fissured clay.

Deformability of soil must be accounted for. It must be considered that: i) slope failure is progressive; ii) the soil mass can experience internal plastic deformation; iii) in saturated clay any change in the state of stress, if fast enough, can generate excess pore pressures (Comegna & Picarelli 2005). The first consideration suggests that the average mobilised strength at failure can be is lower than the peak. According to the second consideration, during post-failure movement the potential energy is partially dissipated into plastic internal deformation. The third point suggests that excess pore pressures can affect the mean effective stress at failure and so the amount of energy dissipated by friction. In addition, negative values, as in the case

34
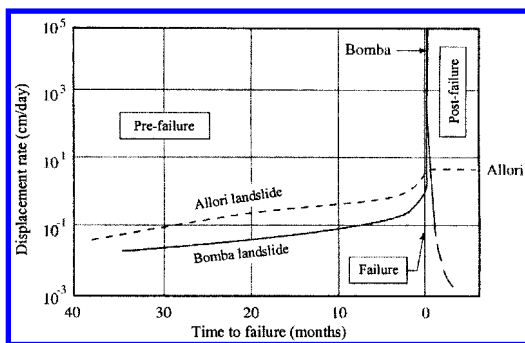
Figure 8. Pre and post-failure displacements of two land-slides in the S. Barbara mine: the Bomba landslide in brittle OC clay and the Allori landslide in a ductile highly fissured clay (D'Elia et al. 1998).

of cuttings and, in general, of highly OC clay, can delay the time of failure (Potts et al. 1997). Globally, in OC soils the influence of soil deformability should oppose full transformation of potential energy into kinetic energy. As will be discussed below, in loose sands and in sensitive clays, static liquefaction can play a prominent role, determining a transformation of slide type landslides into flow-like landslides.

The travel distance of slides mainly depends on the length of the slope, shape of the slip surface and soil brittleness.

3.2.2 *Flows*

Flow-like landslides can involve all types of geomaterials, such as fractured rocks, sands, silts including loess and volcanic ashes, sensitive and stiff fissured clays and organic soils (Hungr et al. 2001). Flow-like landslides occur in subaerial and submarine environment, and can involve either natural slopes or earthworks. Their features are very similar to those of other natural phenomena of mass transport, such as hyperconcentrated flows, floods, lava flows, snow avalanches, lahars and so on (Picarelli 2004, Meunier 1993).

As a result of the variability of phenomena and materials, the terminology is quite confused: in fact, same terms can be used to indicate different types of movement. Attempts to establish a unique terminology of flow-like slope movements have been recently made by Hungr et al. (2001) and Hutchinson (2004), but a real globalisation of the terminology will be probably attained only when the mechanics of movement will be definitely highlighted, allowing to clearly distinguish among different events.

Typically, flow-like landslides reveal themselves only in the post-failure stage. They often represent the evolution of landslides having a different initial deformation pattern: in fact, rock slides or falls can turn into rock avalanches or debris flows, slides can turn into flow slides or mudslides and so on (Picarelli 2000).

The main characteristics of flow-like landslides are:

– diffuse and apparently non-localized large deformations, often giving rise to movements very similar to those exhibited by viscous fluids;
– a high mobility and capability to spread over the land, covering large distances, much larger than by other types of landslides;
– capability to adapt themselves to the slope morphology, entering and running within natural tracks or spreading laterally over flat slopes.

These characteristics depend on the mechanics of rupture and post-rupture deformation that is affected by the nature and state of the materials involved, but also by other parameters as slope morphology, initial state of stress, etc.

In the following, only some types of flow-like landslides will be dealt with, i.e. rock avalanches (and debris flows), flow slides and mudslides. Reported data and considerations provide a partial framework of this complex category of slope movements allowing to identify some of the factors that govern their initiation and evolution.

3.2.2.1 Flow slides

Flow slides typically involve cohesionless soils such as gravelly sand, sand, silty sand, or clayey silts of low plasticity and so-called "sensitive clays". Hungr et al. (2001) and Hutchinson (2004) categorize flow slides as flow-like slope movements triggered by a complete or partial soil liquefaction. Such a definition, that is adopted also in this report, implies that at the onset of flow initiation involved material must be practically saturated. Many examples of flow slides in saturated materials are reported in literature. Some of them concern coastal flow slides, as alongside the Dutch coast (Silvis & de Groot 1995), or in the Nerlek underwater berm (Sladen et al. 1985). General considerations about submarine flowslides are reported by Lee & Locat (2004). Other examples of flow slides in saturated soils concern tailing impoundments (Blight & Fourie 2004) and sensitive clays (Potvin et al. 2001). However, literature reports also many catastrophic rainfall-induced flow slides involving natural slopes covered by unsaturated granular materials, suggesting that these movements can develop, once a high saturation degree has been attained (Olivares & Picarelli 2003).

Since flow slides occur with very little warning, and run hundreds of metres in a few minutes, there is a lack of well documented field data. Therefore our present knowledge comes from speculation supported by laboratory testing and physical modelling. In particular, modelling by laboratory and in situ flume tests, or by centrifuge tests, is providing a lot of interesting data that allow to check some ideas about the mechanics of flow slides.

35

Laboratory tests enable investigation of the soil state and stress conditions that are responsible for liquefaction in granular soils. Undrained strain rate controlled monotonic triaxial tests show that loose soils can experience a strong shear strength decrease after peak (static liquefaction). In stress controlled conditions, failure is sudden and unstoppable. A well defined line, the so-called Steady State Line (SSL), subdivides the compression plane (p′, e) in two parts. If the initial void ratio is well above the SSL, the soil displays an unstable behaviour: for a very high void ratio, a complete liquefaction can occur (Castro 1969, Casagrande 1971, Poulos 1981, Yamamuro & Lade 1997). In particular, if in the stress plane (q, p′) the initial state of stress falls inside the zone located between the SSL and the so-called Instability Line, IL (Lade & Pradel 1990), i.e. the initial stress conditions are highly anisotropic, even a small undrained stress change can lead soil to collapse. If the initial void ratio is well below the SSL, the soil displays stable behaviour with strength increase with strain. Hence, for loose undrained soil, instability seems capable to generate flow-like movements, thus assessment of the soil density could help to recognize sloping natural soil deposits as liquefiable or not liquefiable. However, it is worth noting that, according to Sassa (2000), mechanisms of "sliding surface liquefaction" is possible also in dense soils, as a consequence of grain crushing during failure.

Laboratory testing shows other factors, besides void ratio and initial effective mean stress that govern the undrained soil behaviour after peak. In particular, liquefaction is favoured by uniform grain size and presence of non plastic silt (Yamamuro & Lade 1997). In addition, the stress path to failure has some influence on soil behaviour: in fact, liquefaction seems more likely following an extension than a compression stress path. Chu et al. (2002) discussed the consequences of paths reproducing the effects of pore pressure rising.

Many flow slides involve highly permeable geomaterials. Hence, field evidence of excess pore pressures are lacking. Hutchinson (2004) cites a unique case of direct evidence of excess pore pressures within a flow slide. It involved sensitive clays embedded within thick low permeability silty clays, at Furre, Norway. Since the excess pore pressures persisted for several months after slope failure, piezometer measurements allowed them to be measured.

Recent catastrophic flow slides occurred in Sarno and in other small villages in Italy (1998), reached a size of some hundreds of thousands cubic metres, running kilometres with a peak velocity of about 20 m/sec. Such a velocity has been calculated from damage to buildings and other structures using a back analysis of the kinetic energy possessed by the landslide mass at the instant of the impact (Faella 2003).

Physical modelling, even if generally conducted on small-scale slopes, helps in the investigation of the mechanisms of flow-like movements. Some experiments conducted at the end of the Eighties (Iverson & Lahusen 1989, Eckersley 1990) showed that flowslide initiation is really associated with building up of excess pore pressures, confirming the role of soil liquefaction. Further experiments carried out later through flume tests on soils saturated by lateral seepage provided more information (Spence & Guymer 1997, Wang & Sassa 2001, Orense et al. 2002). They showed that liquefaction is a consequence of soil saturation and remarked that excess pore pressure develops just after rupture, as a consequence, more than as a cause of it (Fig. 9). Therefore, even if slope failure occurs in fully drained conditions, it can be followed by a mechanism of undrained deformation and flow.

The most likely mechanism of excess pore pressure generation is due to the tendency of loose granular soils to contract as a consequence of deviator stresses. Therefore, failure of saturated soils, if fast enough, can give rise to building up of excess pore pressure. However, rapid local stress changes can induce the same effect in the zones of the subsoil where total stress increases. Experiments by Okada et al. (2002) and by Moriwaki et al. (2004) show in detail the effects of pore pressure rising in complex models characterised by slope changes. Moriwaki et al. (2004) conducted a flume test on a practically full-scale model slope, instrumented with a number of transducers located at different depths that gave a clear representation of the pore pressure regime before and after failure. They show that excess pore
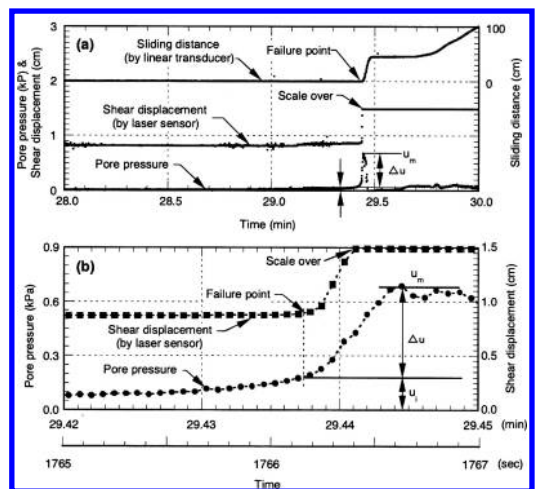
Figure 9. Shear displacement and pore pressure measured at the base of a model slope led to failure by seeping (from Wang & Sassa 2001).

36

pressures can be generated by either shear (mostly upslope) or compression (mostly downslope). They also remark a diffuse pore pressure increase within the soil mass, that experience large internal deformation even though a slip surface can be recognized as a consequence of localised shear (Fig. 10).

These data support the idea that progressive failure can develop also through an undrained process, as hypothized by Bernarder (1984) for landslides in sensitive clays.

Flow slides in unsaturated soils can develop as a consequence of volumetric collapse induced by saturation. In this case, failure is a consequence of water infiltration from the ground surface and progressive soil saturation. The process of saturation is governed by stratigraphy of the subsoil (layering and possible local lack of layering) and boundary conditions (permeability of the bedrock, possible seepage occurring also from the bedrock etc.). However, Olivares et al. (2002) remark that a flowslide can develop only if at the onset of rupture as the soil attains a practically full saturation. According to this idea, steep slopes are less susceptible to flow-like movement since rupture can occur in still unsaturated conditions, giving rise to a fast slide (or to a debris flow) because of dramatic loss of cohesion due to suction decrease, but not to a flow slide. Therefore, in unsaturated soils, the triggering of a flow slide depends also on slope morphology. For slope inclinations larger than a critical value, it is not likely, even in soils that are susceptible to liquefaction.

However, rapid loading and liquefaction of saturated material entrained from the path of the landslide

during movement can still produce a flow-like landslide (e.g. Hungr & Evans 2004).

Flume and centrifuge tests on unsaturated slopes brought to failure by artificial rainfall have been carried out by some research centres (Okura et al. 2002, Damiano 2003, Take et al. 2004).

So as to trigger liquefaction, Damiano carried out flume tests on 40° quasi-infinite slopes, built of volcanic silty sand of pyroclastic origin (volcanic ash), having a friction angle of 38°. In this case, failure occurs just when the soil reaches a condition of full saturation. In the tests, suction, pore pressure and displacements were continuously recorded. As a consequence of saturation, loose soils experience increasing vertical compression due to suction decrease, and failure, followed by sudden pore pressure increase that locally reaches a value very close to the total stress (Olivares & Damiano 2004). In contrast, dense soil displays only small strains, then failure, pore pressures remaining more or less constant. In fact, while in the first case the slope experienced a clear liquefaction, in the second one, even though fast, movement did not display a well defined flow-like movement pattern. These data suggest that a careful monitoring of soil deformation could help in the prediction of flow slide generation, since unsaturated loose soils can experience large pre-failure deformation as a consequence of suction decrease associated with increase of the saturation degree.

Following considerations by Savage & Hutter (1989), Musso & Olivares (2004) demonstrate that soil liquefaction can be followed by fluidization, that
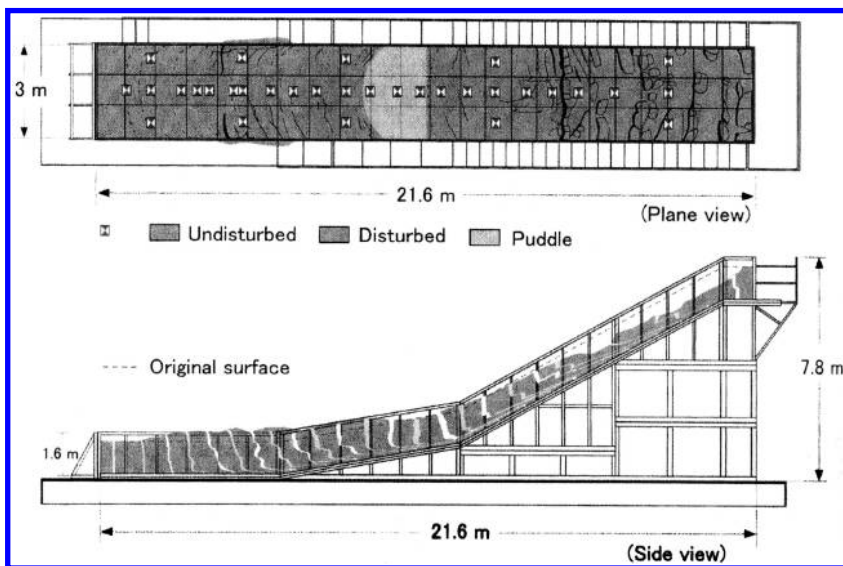
Figure 10. The deformation pattern induced by failure in a full-scale flume test (Moriwaki et al. 2004).

37

is characterized by a complete loss of contact among soil particles, as a consequence of dynamic interaction with water. This has been proven for volcanic ashes investigated by Damiano (Olivares & Damiano 2004). Only a strong deceleration, due for instance to a slope change, can favour "restructuration", development of friction, and arrest.

Take et al. (2004) report results of similar tests carried out on a decomposed granite from Hong Kong in the centrifuge of the Oxford University. In such a case, true liquefaction did not occur because the soil did not attain complete saturation.

Recently, tests are being carried out in the field on natural slopes. The interpretation of these experiments is more complicated because of natural conditions, i.e. inhomogeneity characterising morphology, initial conditions and soil properties. Ochiai et al. (2004) report the results of an experience on an instrumented slope constituted by decomposed granites ruptured as a consequence of artificial rainfall. This experimental data confirm all the considerations reported above. More than in other cases, the non-homogeneous state of stress reflects itself on the mechanisms of rupture that is characterised by progressive failure.

3.2.2.2 Mudslides

Mudslides (that are also named earth flows, by North American researchers) typically involve stiff clays and indurated fine-grained materials (clay shales, mudstones, marls). Their classification in the domain of flow-like landslides is debated and sometimes criticized, because of significant differences with other phenomena in the same category. In fact, Hutchinson & Bandhari (1971) and Cruden (1993) claim that in some cases they might be better classified as slides, as they often advance by sliding quite slowly on discrete slip surfaces, determining a clear discontinuity in the displacement profile. However, Picarelli (2001) remarks that a flow-like deformation pattern can be really recognized in the early stage of movement, often following a slide failure (complex slide-earthflow, according to Varnes 1978). In this stage, the mobilised soil mass actually moves as a highly viscous fluid, reaching a fairly high velocity, if the soil mass enters a channel and runs within it forming a fan at the foot. Then, the movement progressively decelerates taking the features of a slide. This final sliding stage can be very long, while in the case of debris and flow-slides, the deceleration leads to a practically immediate and complete stop, that does not show any change in the deformation pattern of the soil mass.

Well documented examples of mudslides have been reported by English researchers concerning several areas in U.K. and in Ireland (Hutchinson 1970, 1988, Moore & Brunsden 1996). Further significant examples are provided by Italian (D'Elia 1979, Cotecchia & Del Prete 1984, Iaccarino et al. 1995,

Angeli & Silvano 2004) and other researchers (Malet et al. 2004, Savage et al. 2004). As flow slides, it is worth noting that mudslides can involve also engineered slopes. D'Elia & Tancredi (1979) report the Valle del Pero mudslide that involved an earthfill constituted by fine-grained materials.

The size of mudslides is extremely variable. The huge Slumgullion mudslide, 8 km long, has been investigated for a long time by American and Italian researchers (Pariseau et al. 2004). Large mudslides are typical of the Apennine landscape, in Italy (Carboni et al. 1996, Picarelli & Napoli 2003). Their velocity is also very variable. While in the first stage of movement it can reach a peak of some tens of metres per hour, in the final long-lasting stage, the displacement rate can be in the order of millimetres per year.

Mudslides are mainly triggered by rainfall and earthquakes. The Irpinia earthquake (1980) triggered a number of large mudslides in Southern Apennines (Cotecchia & Del Prete 1984, D'Elia et al. 1985). In some cases, the delay of flow-like movement after the seismic shock was some hours (D'Elia et al. 1985), even if probably some small displacement occurred soon. A definite explanation of this mechanism has not been provided. Possibly, the movement developed as a progressive failure, starting from zones where excess pore pressures had been generated by the shock.

Often mudslides present an arched accumulation zone characterised by high scarps (Cotecchia et al. 1984, Picarelli & Napoli 2003, Savage et al. 2004), that bound a gentle terrace, or depletion zone (Fig. 11). Slides or mudslides display scarps showing retrogression of the landslide that indents the slope above, progressing upslope. Fresh material accumulated over the terrace moves towards the track supplying the mudslide body; once discharged in the track, it can run downslope as a surge. Lateral alimentation by erosion, slides or smaller mudslides can also supply the main track. At the foot the mudslide forms a thick fan that grows laterally and in thickness as a consequence of continuous accumulation. Therefore, the movement can arrest only once alimentation stops. This depends on the geomorphological features of the slope.

Iaccarino et al. (1995) remark that movement can continue for as long as hundreds of years through periodical mechanisms of reactivation-deceleration caused not only by volume increase provided by
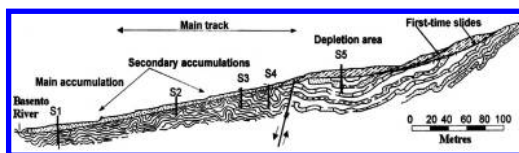
Figure 11. The Brindisi di Montagna mudslide (from Cotecchia et al. 1984).

38

erosion or landslides, but also by rainfall or earthquakes. However, even though alimentation stops, the movement can continue for a long-time as a consequence of erosion of the toe, pore pressure fluctuations within the landslide and creep. Moore & Brunsden (1996) assume that in some cases, continuous movements can be induced by seasonal changes in the pore water chemistry. Moreover, Picarelli (1993) and Picarelli et al. (1998) stress that mechanical degradation of the material (stiff clay, clay shale or mudstone) can contribute to continuous movement caused by a slow decrease of stiffness and shear strength. These degradation phenomena transform the stiff and often "structured" original material into a mixture of small hard residual fragments (lithorelicts) and a rather soft clay matrix (Skempton & Hutchinson 1969, Vallejo 1989, Picarelli 1993), whose soft component increases continuously with time.

Developing an idea firstly proposed by Hutchinson & Bandhari (1971), Picarelli (1988) and Pellegrino et al. (2004) assume that the mechanisms of acceleration-deceleration described above essentially depend on cyclic building up of excess pore pressures followed by consolidation. Some causes of excess pore pressure generation are described by Picarelli et al. (2005) as follows:

(a) Static loading caused by accumulation of debris discharged on the mudslide body from the main or secondary scarps (Hutchinson & Bhandari 1971);
(b) Quasi static loading induced by surges travelling over the landslide body (Vallejo 1984);
(c) Redistribution of the total state of stress caused by internal mechanisms of rupture or reactivation (Comegna & Picarelli 2005);
(d) Compressive deformation of the landslide body associated with restraint met during movement, as narrowing of the main track or local variations of the slope of the sliding surface (Picarelli & Russo 2004);
(e) Seismic loading.

Pore pressure increases can determine either a complete collapse of the entire mudslide body that can reach velocities up to tens of metres per hour, or moderate acceleration of parts of the mass that interact with other parts at its boundaries.

The mechanism of alimentation described above can be interpreted within this framework. In fact, it is very likely that the mechanism of accumulation at the foot of the lateral scarps can generate high excess pore pressures in the same sliding mass under its own weight (Pellegrino et al. 2004); then it can move as a surge over the soil filling the track, down to the accumulation zone. As a consequence of undrained loading caused by the surge, the underlain mudslide body in turn accelerates interacting with soil masses located above and ahead, thus causing pore pressure

changes also in these parts of the landslide. On the other hand, as a consequence of stress release caused by sliding, the main scarp bounding the depletion zone experiences negative excess pore pressures, that delay further movements, as discussed by Bromhead & Dixon (1984) for coastal landslides in the U.K. This can explain the steepness and height often presented by these slopes.

Such considerations about the role of pore pressures in the mechanics of mudslides are supported by field observations and measurements.

Hutchinson & Bandhari (1971) reported the results of field pore pressure measurements in a mudslide, showing a sudden pore pressure increase caused by a surge approaching the instrumented zone. Picarelli (1988) discussed the high pore pressure measured with a Casagrande type piezometer in the accumulation zone of the Brindisi di Montagna mudslide, and the following subsidence of the ground surface around the piezometer, attributed to consolidation of the soil mass. Further data were reported by Picarelli et al. (1995) for the Masseria Marino mudslide, showing sudden pore pressure increases following acceleration of movement. More recently, Pellegrino et al. (2004) reported well documented additional data of pore pressures measured with a vibrating wire transducer, showing that soil acceleration is associated with increase of the piezometer level of about 5 m, leaving the water level about 3 m above the ground surface (Fig. 12). Considering that the cell was located at a depth of about 3 m, this caused a dramatic effective stress decrease. Even though liquefaction does not occur as in the case of flow slides, such a shear strength decrease certainly has a strong influence on the mudslide behaviour.

These data are confirmed by some considerations by Comegna et al. (2004) about pore pressures measured with Casagrande type piezometers in the same Masseria Marino mudslide, but in a different period of time. Analysis of data show that in non active or slowly moving parts of the mudslide pore pressures
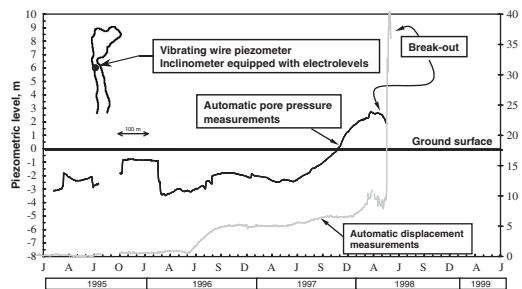
Figure 12. Displacement of a mudslide body and pore pressure measured at depth (from Pellegrino et al. 2004).

39
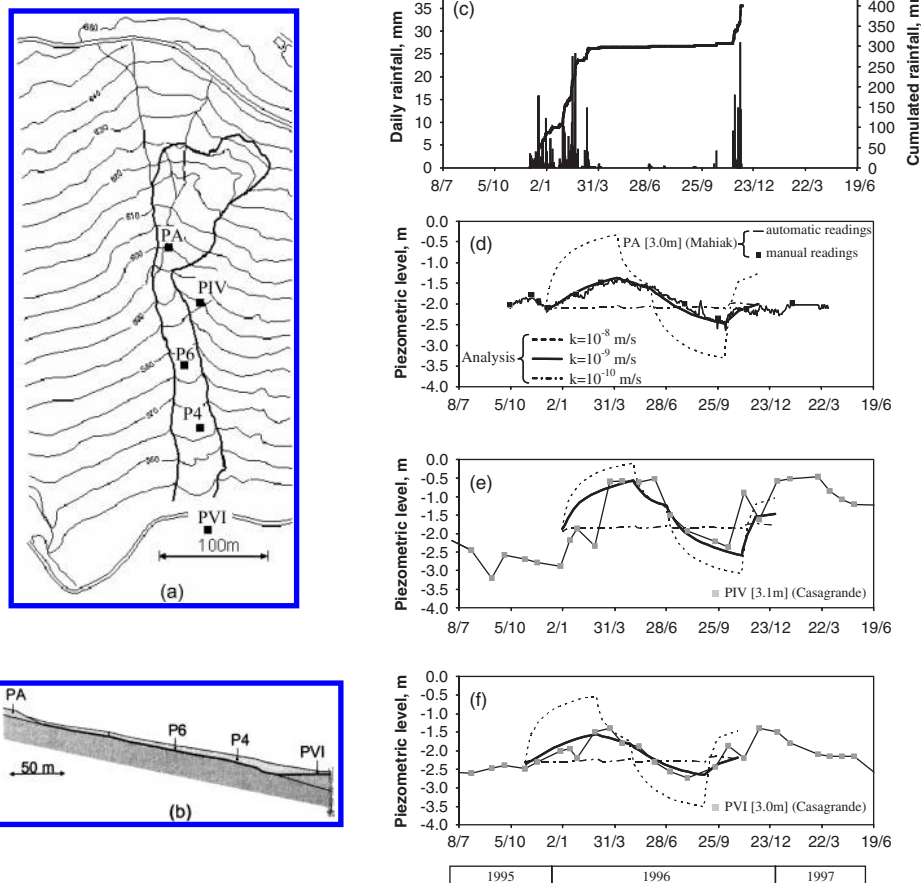
Figure 13. Comparison between measured and calculated pore pressures in non active (a) and active (b) zones of the Masseria Marino mudslide (from Comegna et al. 2004).

fluctuation is quite regular and consistent with seasonal precipitation, while in active parts they are very irregular and are not consistent with data collected with a rainfall gauge. Using a simple model to correlate pore pressures to changes of the hydraulic boundary conditions, they demonstrate that in the first case a good agreement exist between results of the analysis and measured pore pressures, while in the second case the same analysis cannot reproduce the measured values (Fig. 14): in particular some peaks in the water level, followed by rapid drops, are significantly higher than the calculated values. These anomalous peaks have been explained by excess pore pressures built up as a consequence of total stress changes associated with deformation of the soil mass.

Picarelli et al. (1995) and Russo (1997) have analysed some possible scenarios of mudslide mobilization through simple numerical schemes (schemes 1 and 2

reported above). They assume that local mobilisation is due to undrained compression caused by mobilisation of the mudslide body upslope, as a consequence of a surge travelling over the ground surface or of a different cause.

Comegna (2004) and Comegna & Picarelli (2005) report further analyses to examine the interplay between movements and pore pressures in non catastrophic stages of landslide evolution (scheme 3 above). It is assumed that pore pressure rising due to rainfall and infiltration can cause local failure, triggering a soil deformation rapid enough to cause excess pore pressures. The analysis has been carried out using as reference the Masseria Marino mudslide (Fig. 15). The shear zone is bounded by a sliding surface, which has been simulated by an interface element. The soil behaviour has been reproduced by the "Soft-Soil Model". The parent formation located below the shear

40
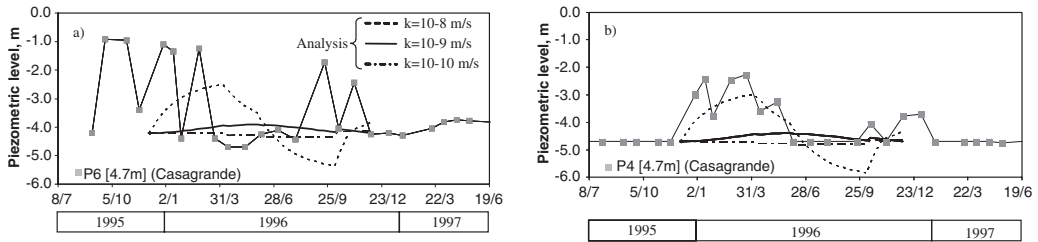
Figure 14.   Case examined by Comegna & Picarelli (2005): plastic zones induced by pore pressure rising.
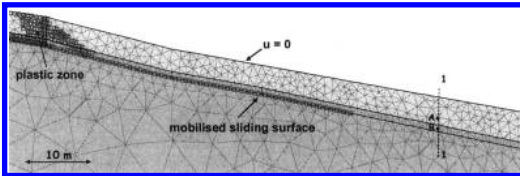
Figure 15.   Plastic zones induced by pore pressure rising in part of the landslide in Figure 13 (from Comegna & Picarelli 2005).

zone has been considered as a stiff bedrock. Initially the global safety factor is much larger than one, even if along a steeper intermediate part of the slope it is close to one (Fig. 15). The pore pressure rise caused by rainfall was also simulated. As the pore pressure increases, the state of stress in the mudslide body changes and a part of the soil mass tends to slip because of the shear strength mobilisation along the sliding surface. In order to simulate a failure in the landside body, a vertical cut is imposed in the plastic zone. The consequent new situation has been investigated by a "short-term" (undrained) analysis; then, the associated excess pore pressures have been allowed to equalize. It is worth mentioning that in this way any excess pore pressure that could be induced by soil deformation caused by pore pressure rising, is concentrated at the instant of cracking. Figure 14 reports the evolution of pore pressures calculated at two points in the same section, one in the shear zone, and the other one in the landslide body. The different stiffness of the two materials is responsible for different excess pore pressures. In the following complex phase of consolidation, pore pressures once again abruptly change as a consequence of the non-uniform distribution of piezometer heads around the two points. Such a result can explain apparent anomalous cyclic changes of the pore pressure observed in active zones. The resultant pore pressure increase is due to continuing infiltration.

3.2.3   Identification of classes of slope subject to rapid landsliding

There are several classes of soil slope within which a landslide (once slope failure has been triggered)

develops into a slide of rapid post-failure velocity: (i) flow slides in saturated (or near-saturated), essentially granular soils that are contractive on shearing under the effective stress conditions imposed by the slope geometry and pore-pressure conditions and reach a flow liquefaction condition as shearing continues, e.g., loose road, railway, or other constructed fills, mine waste stockpiles, mine tailings, hydraulic fills, and submarine slopes; (ii) slides in sensitive clays (or quick clays) such as occur, for example, in parts of Scandinavia and Canada; (iii) slides in steep cut slopes in residual soil, colluvium, or completely weathered rock, either through the soil or weathered rock mass or controlled by defects; and (iv) slides of debris in natural slopes with steep source area slope angles.

Landslides in saturated or near-saturated soils that are initially contractive on shearing (i.e. flow slides) will virtually always reach rapid post-failure velocities, regardless of the geometry of the surface of rupture and the slope geometry below the slide. Landslides in soils that are initially dilative on shearing, will usually be slow. However they may develop into debris flows of rapid post-failure velocity or debris slides. The development of a landslide in a soil that is initially dilative on shearing into a debris flow of rapid – post-failure velocity generally requires the initial failure to occur in a steep slope and (or) the slope immediately below the slide source area to be steep.

Hence, it is important to distinguish between soils that are either contractive or dilative on initial shearing. For soils that are initially contractive on shearing it is important to then identify if a liquefaction condition can develop and flow sliding occur.

Based on an analysis of 350 case studies and an understanding of the mechanics of contractive sols, Hunter & Fell (2003) determined that the approximate bounds of particle-size distribution of loose fills susceptible to static liquefaction and flow sliding are as shown in Figure 16. The coarse boundary, representative of sandy gravels with a trace of mostly silty fines (from coal mine waste dumps), is probably an upper bound particle-size distribution due to permeability constraints. Materials with such coarse particle-size distributions are likely to be sufficiently permeable

41
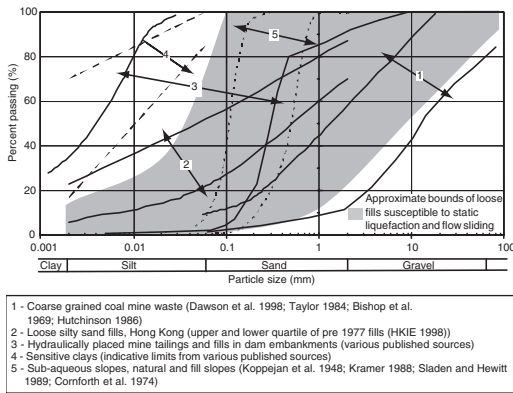
Figure 16. Particle size distributions of soils susceptible to static liquefaction and rapid flow sliding (Hunter & Fell 2003).

that pore-water pressures developed on contraction can be dissipated.

Based on a review of the literature, Hunter & Fell (2003) found that an approximate guide to soils that are susceptible to flow liquefaction and hence potential rapid post-failure velocity of the slide mass include the following: (i) clean sands with relative density less than about 15%–30% (i.e. very loose to loose sands); this is likely to vary depending on the particle-size distribution and the particle shape (Cubrinovski & Ishihara 2000); (ii) silty sands with relative densities up to 45%–60% (i.e. very loose to medium dense); (iii) silty sands with clay contents less than about 10%–20%, such as those derived from decomposed granite with density ratios below 85%–90% of standard maximum dry density (HKIE 1998); flow slides in these materials are typically of shallow depth (up to 3–4 m) and on slopes steeper than about 30°–40°; and (iv) sandy gravels and gravely sands (in coal waste spoil piles and coking coal stockpiles) with trace to some silty fines (less than 5%–10% finer than 75 μm) at void ratios greater about 0.3 (Dawson 1994, Eckersley 1986); field studies in these material types (Eckersley 1990, Dawson et al. 1998) show that the moisture content at placement and the method of placement have a significant effect on the initial void ratio and therefore the potential for flow sliding.

Flow slides in mine waste spoil piles generally occur where the spoil pile has been placed by tipping from low height onto the crest of the active dump. No cases of flow slides have been reported in spoil piles formed by dumping from a height such as by dragline. Foundation slope is also an important factor for flow slides in mine waste spoil piles, with most failures occurring on relatively steep hillsides. For the failure case studies in coal mine waste spoil piles the hillside slope averaged 25° for the flow slides in

British Columbia (Golder Associates Limited 1992) and 17° for those in South Wales.

Sensitive clays are susceptible to large loss of strength on shearing and development of retrogressive flow sliding. The soil properties and conditions for which retrogression is likely to occur are summarized by Tavenas (1984), Leroueil et al. (1996), Lefebvre (1996), and Trak & Lacasse (1996).

A useful guide to whether sandy and silty sand soils are likely to be susceptible to liquefaction and rapid flow can be obtained from Standard Penetration Test N values as shown in Figure 17.

Rapid post-failure velocity of the slide mass from slides initiating in natural slopes generally occurs on slopes where the source area and immediate down slope angle is greater than about 25° but can occur on slopes down to about 18–20°. The likelihood of rapid landsliding is almost certain on slopes steeper than 35° and likely to high likely on slopes of 30–35°.

On cut slopes, rapid sliding is almost certain for slopes steeper than 35°. These slopes apply regardless of whether the soils are contractive or dilative.

3.3 Characteristics of large landslides which travel slowly and rapidly on failure

3.3.1 General

The classification and mechanics of landsliding are important in determining whether large (greater than 1 million m³) landslides on natural slopes will travel rapidly or slowly after failure. Glastonbury (2002), Glastonbury and Fell (2002a, b, c, 2005a, b, c) studied an extensive database of large rock and soil natural landslides, and based on the case studies and an understanding of the mechanics of sliding developed some guidance for determining whether a slide will travel rapidly or slowly on failure. A summary of the results of the study appears in Bonnard & Glastonbury (2005), in this volume.

Glastonbury & Fell (2002c) and (2005c) also present a decision analysis approach to ascertaining the likelihood of a slide will be rapid or slow on failure.

4 ASSESSMENT OF THE FREQUENCY OF LANDSLIDING

4.1 General

The estimation of the frequency (annual probability) of landsliding is one of the most critical components of the assessment of landslide hazard for natural and constructed slopes.

There are a number of methods for doing this:

(a) Assessment of the historic record of landsliding.
(b) Relating the history of landsliding to geomorphology and geology.
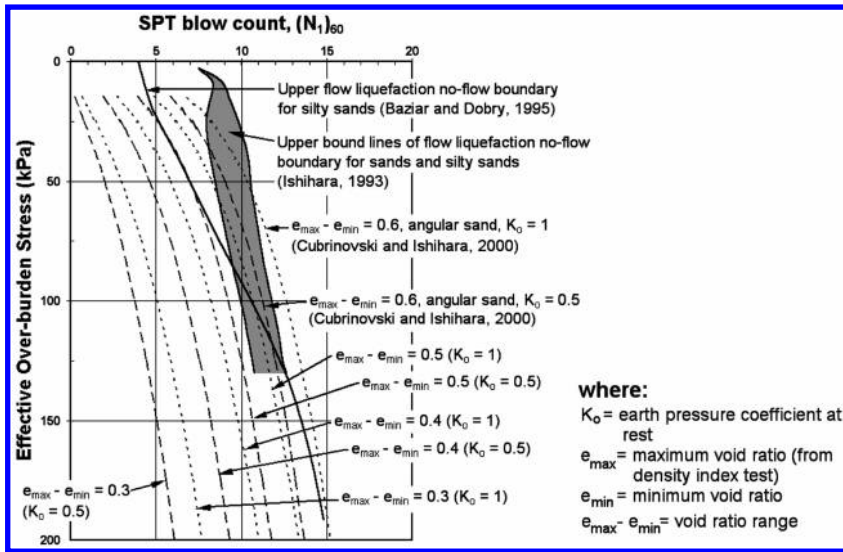
Figure 17. Comparison of flow liquefaction no-flow boundaries (in terms of SPT $(N_1)_{60}$ for sands and silty sands from monotonic laboratory undrained tests and earthquake-triggered field cases (after Cubrinovski and Ishihara 2000). $e_{max} - e_{min}$ void ratio range; K_o earth pressure coefficient at rest. (Hunter & Fell 2003).

(c) Relating the historic record of landsliding to geomorphology, geology, geometry and other factors (multi-variate analysis).

(d) Relating the historic record of landsliding to rainfall intensity and duration, slope geometry and their factors.

(e) Relating the historic record of rainfall, slope geometry and geotechnical properties, and landsliding.

(f) Modelling piezometric levels in the landslide versus rainfall, relating this to the incidence of sliding or calculated factors of safety less than 1.0.

(g) Event tree methods, including the use of expert opinion.

(h) Formal probabilistic or reliability methods.

This section gives an overview of the methods based largely on the authors experience, but referencing examples from elsewhere. The objective is to outline the methods and discuss their applicability and limitation. Formal probabilistic and reliability methods are discussed in SOA 3 and are not further discussed here.

4.2 Assessment of the historic record of landsliding

4.2.1 Simple data analysis for cuts and fills

In the simplest form this method consists of recording the number of landslides which occur each year in an area of interest, such as along a road or railway. It may be extended to include the type of sliding, e.g. on natural or constructed slopes, or on cuts and fills, and characteristics such as volume or area of landsliding.

Chowdhury & Flentje (1998) discuss the use of a database to record such data in a systemic way.

The method is only valid if the cuts or fills are of a similar geometry, in consistent geological and climatic conditions. It usually requires gathering of historic data for the road or railway in question, because data from other areas cannot be used elsewhere.

Examples of this approach are given in: Morgan et al. (1992) where the historic record of landsliding was used to assess the magnitude and probability of debris flows; Fell et al. (1996a), where records collected by the Geotechnical Engineering Office of Hong Kong were used to estimate the annual average probability of cut, fill, and retaining wall failures; examples which include rock fall are described in Moon et al. (1992), Cruden (1997) and Moon et al. (1996).

This method can be a useful way of estimating the average annual probability of landsliding, but usually does not discriminate between individual slopes and does not allow for the dependence of the landsliding on triggering factors, such as rainfall. A long representative period of record is needed, and even then there are potentially difficulties because of the nonlinear relationship between the triggering event, e.g. rainfall and number of landslides, the influence of development changes in vegetation, and run-on and run-off of water. However, it can be a very valuable method for smaller landslides (e.g. in road cuts and fills), and as a check on more sophisticated methods.

The historical data on landsliding on engineered slopes e.g. rock falls from road cuttings; fill failures on

43

a highway; can be obtained from maintenance records, newspaper reports, files on reconstruction works and traffic incidents; and by inspection e.g. of the fill slopes to see signs of sliding. On natural slopes, air photographs can be a valuable source of data, by using photos taken at different times as described in Ho (2004).

4.2.2 *Landslide magnitude-frequency relationships*

Analysis and use of the magnitude and frequency (m/f) relations of landslides, recently reviewed in some detail by Malamud et al. (2004), is a comparatively recent development in landslide hazard assessment. The approach is based to some extent on the well-known Gutenberg-Richter power-law relation (Gutenberg & Richter 1956) for earthquakes:

$$\log N\,(m) = aM^{-b} \qquad (1)$$

where $N(m)$ = cumulative frequency equal to or greater than M; M = earthquake magnitude; and a and b are constants.

Because of its scale-invariance and universal characteristic (1) has formed the basis for seismic hazard assessment methodologies world-wide based on the analysis of earthquake occurrences recorded in historical earthquake catalogues supplemented by geological evidence for prehistoric earthquakes.

In its application to landslides, magnitude (m) has been taken to be some measure of landslide size based on area (A) or volume (V). Further, magnitude expressed in terms of area may be expressed as source area (A_s), area of deposit (A_d), or the total area of the landslide site itself (A_t). These parameters may be readily measured from maps, aerial photographs, or satellite images. The most common expression of magnitude, however, is total area (A_t). Magnitude expressed in terms of volume (V) may be expressed in terms of volume of source landslide (V_S) or the volume of the resulting debris (V_d). Volume is calculated on direct estimates of source volume and/or debris thicknesses. In addition, it may be calculated using some empirical equation relating volume to area derived from field measured data (e.g., Simonett 1967, Hovius et al. 1997, Evans 2003, Guthrie & Evans 2004 a, b).

Frequency (f) may be expressed in a simple cumulative (or rank-ordering), in a non-cumulative manner (see discussion in Guzzetti et al. 2002), or in terms of frequency density, i.e., the number of landslides in any given magnitude bin divided by the bin size (Guzzetti et al. 2003). Frequency may also be expressed directly as an annual frequency (cumulative number per year) if, as discussed below, the dataset is time constrained.

The methodology is applied utilizing spatial datasets (landslide inventories) for a region representing landslide occurrence in one of four types of temporal records; Type 1 – collected at one time (e.g., from a flight of aerial photographs flown on a certain date). In this record all landslides are mapped and are of varying ages from very old to very recent. The landslide dataset is thus a cumulative record of landslide occurrence over an undefined long period of time prior to the mapping timeline (e.g., Guzzetti et al. 2002, Malamud et al. 2004); Type 2 – a record of landslide occurrence within a defined time interval (or time intervals), for example, from mapping of landslides from successive aerial photography or remote sensing images, which constitute multiple time slices (e.g., Guthrie & Evans 2004b); Type 3 – from a continuous inventory of landslide occurrences within a region or along a transportation corridor, as in the case of road/railway maintenance inventories. These records constitute continuous datasets (e.g., Hungr et al. 1999, Dai & Lee 2001, Guzzetti et al. 2003, 2004); Type 4 – a record of landslide occurrence from one very short period of time, for example, the mapping of new landslides after a rainstorm or earthquake-triggering event representing an instantaneous one-time slice (e.g., Pelletier et al. 1997, Guthrie & Evans 2004a, Malamud et al. 2004).

The m/f methodology may also be applied at an engineering site where landslides (e.g., rockfalls, debris flows) are recurrent in time and historical data exists on their magnitude and frequency; in this situation the m/f record may be extended back into prehistory by mapping out prehistoric events and dating them by such techniques such as radiocarbon dating (e.g., Hungr 2004). A site record of this type represents a Type 5 temporal record.

(a) The structure of landslide m/f relations

Early work by Fuji (1969) analysed the m/f relationship for 650 rainfall-triggered events and found that the frequency of landslides is inversely related to their volume and can be defined by a power law similar to the Gutenburg-Richter relation in (1). Whitehouse & Griffiths (1983) found a similar relationship for rock avalanches in New Zealand. Later work by Ohmori & Hirano (1988) and Sugai et al. (1994) further showed that landslide m/f relations are power law functions of magnitude.

However, it was the work of Hovius et al. (1997) and Pelletier et al. (1997) that initiated the current interest in landslide magnitude and frequency by deriving what can be described as the characteristic form of the magnitude/frequency relation (Fig. 18). Hovius et al. (1997) analysed multiple sets of air photos between 1948 and 1986 in the western Southern Alps of New Zealand. They found that m/f relations for the area of landslide scars (A_s) are scale invariant

44
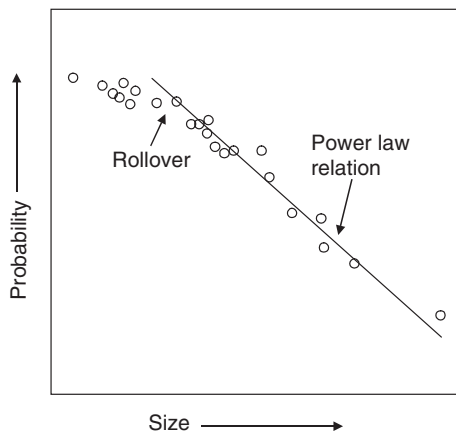
Figure 18. The characteristic form of the landslide magnitude/cumulative frequency relation on a log-log plot.

and had a robust power law m/f distribution over approximately two orders of area magnitude with a flattening of the curve at lower magnitudes. Pelletier et al. (1997) analysed three data sets in which magnitude was expressed in terms of area (A); a Type 1 data set of landslides in Japan, in which landslide area included the run-out zone (A_t), a Type 1 data set of landslides in Bolivia, and a Type 4 record of 11,111 landslides triggered by the 1994 Northridge earthquake over an area of 10,000 km^2. All three m/f plots showed a linear segment characterized by a power law and a flattening of the curve at small landslide magnitudes similar to Figure 18. They also found that A_t scales in the same way as A_i.

Thus the m/f log–log plots of Hovius et al. (1997) and Pelletier (1997) show two characteristics; first a liner segment at small to large magnitudes and second, a flattening of the curve at small magnitudes which has been termed "rollover" (Fig. 18). The linear portion of the m/f plot obeys a power law of general form in:

$$N(A) \sim A^{-b} \qquad (2)$$

where A = landslide area; N(A) = number of events greater than V; and b is a constant parameter.

Rollover in Figure 18 implies fewer landslides of smaller magnitude below a certain threshold. The rollover occurs at small magnitudes greater than the resolution of the dataset implying some lower physical geotechnical and/or geomorphological limit on the occurrence of landsliding within a given region. However, the rollover may also be in part due to incomplete recording and/or incomplete detection of landslide occurrence at lower magnitudes (cf. Guthrie & Evans 2004a, b).

Subsequent studies on different types of landslides in different geological environments have found similar results and m/f plots of similar shape to that in Figure 18. Hungr et al. (1999) analysed maintenance records for the volume and frequency of rockfall along transportation routes in British Columbia and found m/f relations charcterised by a power law. Other studies of the m/f of rockfall and rock slope failure, using volume as magnitude, were carried out by Chau et al. (2003) in Hong Kong, Guzzetti et al. (2003) in Yosemite, Singh and Vick (2003) in British Columbia, and Guzzetti et al. (2004) in central Italy. All these studies found broadly similar m/f relations. In a comprehensive study, Dussauge-Pressier et al. (2002) and Dussauge et al. (2003) found that datasets of rockfalls from Yosemite and the Grenoble area as well as rockslides and rock avalanches from a global data set followed a m/f relation characterised by a power law in (2).

Dai & Lee (2001) studied a record of a variety of rainfall triggered landslides in Hong Long in the period 1992–1997. In their study, magnitude was expressed as volume and they found a power law relationship with b = −0.791 (max. vol. of 100,000 m^3). Martin et al. (2002) analysed the magnitude (expressed as area) and frequency of a Type 1 record (with a temporal constraint based on an assumption of forest growth rates) on the Queen Charlotte Islands, British Columbia. Shallow soil slips and debris slides showed a less robust power law relation at magnitudes in excess of the rollover, manifested in some steepening of the curve at higher magnitudes. This suggests some landscape limiting factor on landslide magnitude. Guzzetti et al. (2002) examined two data sets; one was a Type 1 record containing 16,809 landslides in Umbria-Marche area (Central Italy) and the other was a Type 4 record of 4,233 landslides triggered by a snow-melt event in the same region. Both records correlated well with a power-law relation using non-cumulative frequency-area data.

M/f relations of rain-induced landslides triggered by individual storms has been analysed by Crosta et al. (2003), Malamud et al. (2004), Guthrie & Evans (2004a, b). The characteristic m/f relation was obtained by all these studies with some variation in the b value in (2). Malamud et al. (2004) examined the contribution of individual triggering events (e.g., a rapid snowmelt trigger) to the complete record of landslide occurrence in a region.

There have been two attempts to formalize the complete m/f relation, including the rollover. Stark and Hovius (2002) proposed a Double Pareto distribution fit for the m/f relation based on the assumption that the rollover is a function of mapping scale and subsequent under-sampling at small landslide magnitudes. Guthrie & Evans (2004a, b) present an argument that the rollover is a real effect reflecting slope stability processes. Malamud et al. (2004) suggest a more com-

45

plex inverse gamma distribution fit for the m/f of flows and slides. Their success in fitting three datasets to this distribution is impressive. Significantly, Malamud et al. (2004) suggest that the m/f behaviour of rockfalls and rockslides is characterized by a different process, perhaps related to rock fragmentation.

Thus the structure of landslide m/f relations is characterized by scale invariance (i.e. the power-law segment of the m/f plot is linear over several orders of landslide magnitude); similar shaped m/f plots are obtained for various measures of landslide magnitude consisting of area and volume, different landslide types, in different geological environments both in space and time, and with different triggers. The characteristic relation is obtained from the analysis of the five types of temporal record defined above. The characteristic m/f relation also applies to landslides from natural and artificial slopes in natural and human-modified terrain. The power law structure of the m/f relation makes it possible to predict the frequency of larger landslides (for which a record may not exist) based on the slope of the linear part of the m/f plot derived from the occurrence of smaller landslides, assuming that the record of smaller landslides is complete.

These apparently universal characteristics of landslide m/f relations result in their extreme usefulness for landslide hazard assessment; they form a type of hazard model (Lee & Jones 2004) which may be used in the quantification of landslide hazard which, as seen below, serves as input into a quantitative risk calculation.

(b) Use of landslide m/f relations in landslide hazard assessment and estimates of landslide risk

Once a magnitude and frequency relation has been established for a region or a site, it may be used to estimate the probability of occurrence of a landslide of a certain magnitude providing the length of the record is known (e.g., Hungr et al. 1999, Dussauge et al. 2003). This gives a quantitative estimate of hazard which when combined with vulnerability data can give a quantitative estimate of landslide risk.

The first application of landslide m/f relations to formal landslide hazard and risk assessment was by Hungr et al. (1999). In this study, m/f relations were derived for rockfalls from natural and artificial slopes in transportation corridors in southwestern British Columbia utilizing a set of very complete Type 3 records. These data gave the probability of rockfalls of a given size occurring in the narrow linear road and rail corridors. Combined with traffic density data for a segment of a corridor, the risk of a fatal accident due to rockfall impact was calculated (Hungr et al. 1999). It is also possible to use the m/f relations derived by Hungr et al. (1999) to calculate the probability of such scenarios as total blockage of a given corridor by a large landslide involving rock slope failure.

This approach was further developed by Guzzetti et al. (2003, 2004) who took the m/f relations, derived from Type 3 records, and used them to condition input into a 3D rockfall simulation program which simulated rockfall trajectories over topography. The results of the 3D simulation were linked to a GIS and zones of rockfall impact were thus mapped out. The number of rockfalls impacting within a given GIS cell were taken as a proxy for the probability of occurrence. In this approach a risk map is obtained by overlaying the simulation results by a map showing infrastructural elements and community locations. Guzzetti et al. (2004) extended the risk assessment to determine the effectiveness of rockfall defensive structures in reducing risk. In a probabilistic rockfall hazard assessment Singh & Vick (2003) utilized rockfall m/f relations derived from maintenance records, together with encounter and effects analysis to calculate relative risk of rockfall-vehicle collisions along a mountain highway.

Landslide m/f relations may also be used at engineering sites to determine landslide hazard and risk. Hungr (2004) reports the results of a site investigation on the Cheekye Fan in southwestern British Columbia. The fan was considered as a site for urban development and had been built up during the Holocene by successive debris flows from the Cheekye River which drains the western flank of Mount Garibaldi, an extinct Pleistocene stratovolcano. A geological history of debris flow occurrences and debris flow magnitudes (expressed as area of the fan covered) was assembled from surface and subsurface data and the frequency of these events was determined by radiocarbon dating. An m/f relation for these events showed a power law form and was used to determine the hazard to locations on the fan resulting in quantitative risk estimates for the development.

(c) Assumptions and limitations in the m/f approach to landslide hazard assessment

Despite the accumulating evidence of a characteristic, possibly universal landslide m/f signature there are some assumptions and limitations that should be kept in mind in the application of the methodology to landslide hazard assessment.

A major difficulty is the assumption of invariance in the occurrence of landslides in time, i.e., that the rate of occurrence implicit in the Type 1–5 temporal records will persist at the same rates into the future, at least in terms of engineering time scales. Landslide occurrence reflects to some extent the frequency of landslide triggers (e.g., rainstorms and earthquakes). In this regard climate change may affect the frequency and intensity of rainfall triggers such that regional landslide events may be more frequent in the future. This could increase the frequency and thus the hazard of rainfall-triggered landslide events. In the same way, adverse effects of

human activity (e.g., forest harvesting) can also result in an increase in landslide frequency (cf. Guthrie & Evans 2004b). At geological time scales, Cruden & Hu (1993) have argued that the probability of occurrence of large rockslides in the Rocky Mountains of Canada is decaying with time as the number of rockslide sites conditioned by Pleistocene glaciation becomes exhausted by Holocene rockslide occurrence. This is in contrast to the implicit assumption of steady state landslide occurrence in landslide m/f relations.

Further limitations are associated with the quality of the landslide dataset. As discussed by Malamud et al. (2004), the accuracy of landslide magnitude measurement, whether it be expressed in terms of area or volume, is an important consideration. A related problem is that of record completeness. Erosion censoring of large magnitude landslides over long time periods removes them from long-time-period records (Whitehouse & Griffiths 1983). At the other end of the magnitude scale, the non-recording of smaller events may condition the onset of rollover in the characteristic landslide m/f plot (Fig. 18). In addition, the scale of spatial inventories determines the resolution of the record and the frequency count of smaller landslides.

Two other problems associated with deriving frequency estimates from landslide inventory data were mentioned by Hungr (2004): The analyses routinely assume data *homogeneity*, while real data is often heterogeneous, as clusters of landslide activity triggered by individual storms or earthquakes alternate with periods of relative quiescence. The second problem is data *stationarity*. If a storm causes widespread landsliding in an area, slopes are modified by it and another storm occurring short time later may not be able to de-stabilize the same locations. These issues have not yet been adequately addressed in research.

Despite these assumptions and limitations, the analysis of landslide m/f relations, increasingly provides a key element in landslide hazard assessment and subsequent risk evaluation at regional and site scales.

4.2.3 *Application of landslide magnitude-frequency models to engineering scale slopes*

Landslide magnitude-frequency models can be a useful way of analysing and presenting historical landslide data. As discussed by Moon et al. (2005) in this volume, presenting size-frequency models graphically such as shown in Figure 18 has the advantage of showing how observations, interpretations and judgements are interrelated, and allows patterns to be recognised.

The example in Figure 19 is for an engineering scale slope. Other examples are given in Moon et al. (1996), Hantz et al. (2003), also been used on a larger scale.

4.3 *Relating the history of landsliding to geomorphology and geology*

This method is based on the principle but forward by Varnes (1984) that the past and present are guides to the future:

- Hence it is likely that landsliding will occur where it has occurred in the past, and
- Landslides are likely to occur in similar geological geo-morphological and hydrological conditions as they have in the past.

The method is the one most widely used in hazard and risk zoning studies, for sliding on natural slopes, and is often done on a judgemental, experience based approach, without quantification of the probability. Hence, the outputs are in qualitative terms, e.g. low, medium, high hazard.

Baynes & Lee (1998) discuss the role of geomorphology in landslide hazard assessment.

The general issues in estimating the probability of landsliding in this method are discussed in Hutchinson (1988), Leroi (1996), and Soeters & Van Westen (1996). Some examples for specific projects are given in Siddle et al. (1991), Lee et al. (1991), Hutchinson & Chandler (1991), Hutchinson et al. (1991), Morgan et al. (1992), Mostyn & Fell (1997), Carrera et al. (1991, 1992). Some details are given in Fell & Hartford (1997). Examples of where this method has been developed to a semi-quantitative level include Moon et al. (1992) and Fell et al. (1996b).

Fell et al. (1996b) present two examples of semi-quantitative assessment of the probability of landsliding in an area which had a history of deep seated, slow moving landsliding, which was studied by Finlay (1996). The area was mapped geo-morphologically, the history of landsliding determined and relative probabilities of landsliding within the study area determined based on:

- whether there had been historic landslides
- whether slide planes were known to be present (in road cuttings)
- the presence of scarps, benches, uneven ground; and whether the slope was concave, convex or planar
- the present of springs or moist areas
- whether the area was cleared of trees, or reshaped by building roads or benching and filling for houses.

The system was subjective, and there was a difficulty in using the historic data to calibrate the probabilities because most of the historic landsliding had occurred in the 1800s when the area had been cleared of all trees. These had since regrown, but then in the 1970s the area was further subdivided with extensive house building with associated earthworks and changes to drainage. There were also some inherent

47
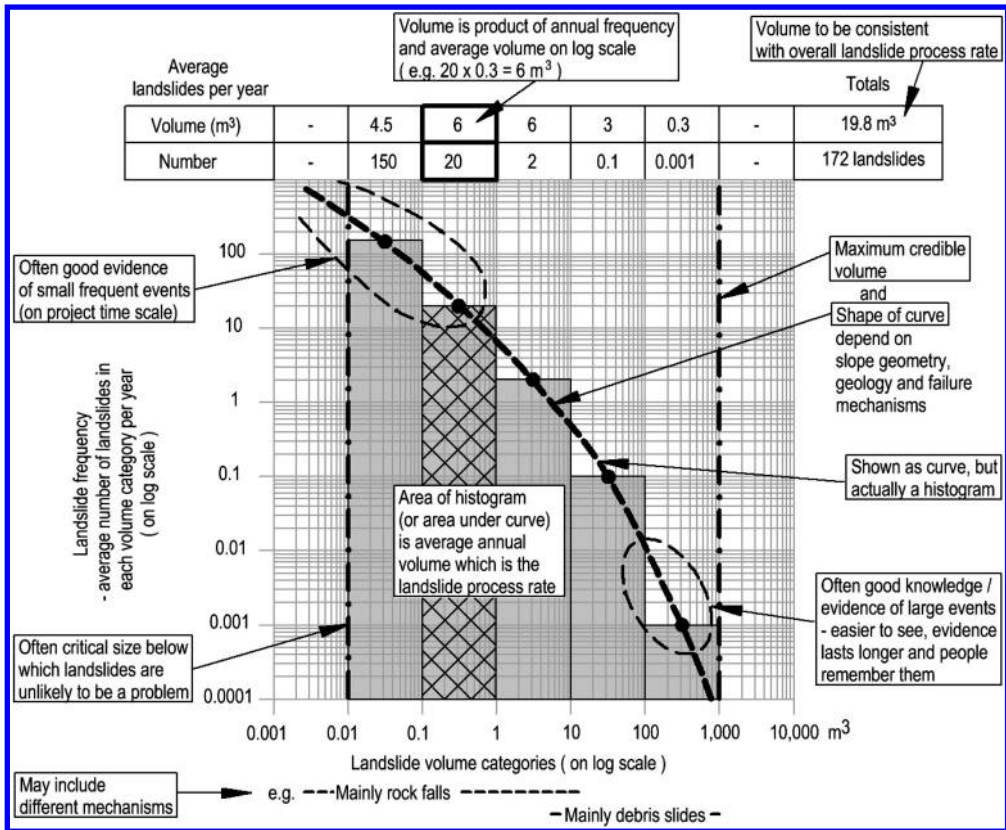
Figure 19. Example of a landslide size-frequency model (Moon et al. 2005).

assumptions, e.g. that sliding was more likely on concave (gully) areas, than convex which might not be correct elsewhere.

The second approach in Fell et al. (1996b) is a more general method for assessing the probability of landsliding based on geomorphological, geological and historic data. The method is in the form of a flow chart which is reproduced in Figure 20.

The most contentious part of the flow chart is the probability values. Those shown were based on the authors' judgement and were felt to be applicable to areas similar to the Sydney Basin, where there are interbedded sedimentary rocks, with most landsliding being of a relatively slow and intermittent nature, e.g. moving say 0.01 m to 1 m every 6 to 25 years, with depths of 1 m to 30 m, and where geo-morphological evidence was apparent, at least to experienced persons. The approach would be applicable in other areas of similar geology, and for example in areas underlain by weathered basalts.

The flow chart lacks rigorous calibration and would need, in any case, to be modified and calibrated for other areas. The main benefit of such an approach is to assist in achieving some uniformity between different practitioners in the assessments of probability, and providing an open transparent system for local assessment.

Overall, these methods are considered to be a vital and valuable approach, which if well done, and calibrated with historic data, can lead to reasonable estimates of the probability of landsliding. There are problems with their use, including reliance on the skill and experience of the person doing the mapping, and studies being done with too little ground-truthing; i.e. lack of inspection on the ground, and subsurface information. There are also situations where the basic premise on which the method is based does not apply, e.g. where debris flows may deplete the source material, leaving the probability of further debris flows diminished possibly even to zero.

4.4 Relating the historic record of landsliding to geomorphology geology, geometry and other factors (multivariate analyses)

The use of geomorphology, geology and landslide records can be extended to include other factors such

48
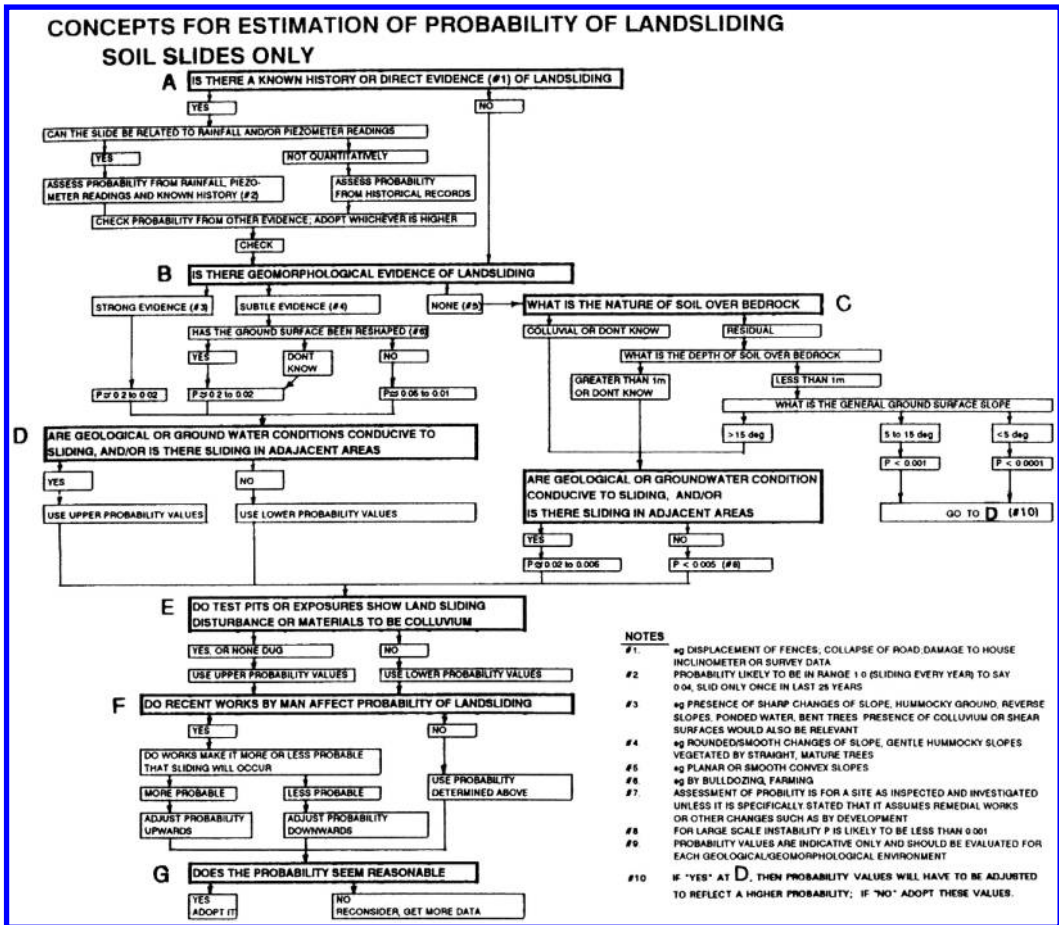
Figure 20. Flow chart for the assessment of the probability of landsliding (Fell et al. 1996b).

as slope angle, slope drainage, slope age, presence of groundwater, and evidence and history of instability, provided records are kept of such data.

Attributes of potential landslide areas may be compared to corresponding attributes of existing landslides areas. Most important attributes are first selected and the critical ranges or values of an attribute can be identified using GIS-based approaches for querying and analysing. For example, different geological units can be ranked in order of failure susceptibility and the same can be done with slope inclination, geomorphology and other factors (Meisina et al. 2001).

An alternative approach, valuable when looking at regional scale can be developed within a GIS-based (database) environment (Abbot et al. 1988a, b) using a number of "themes" or attributes representing the key influencing factors for landslide susceptibility and developing suitable relationships leading to a hazard rating or, best, to a probability of occurrence

of a landslide of a given magnitude. Generally previous knowledge, research and professional experience within a particular geographical area (D'Amato et al. 2003) facilitate the correct selection of "themes" which are of key importance to landslides occurrence in a given region.

Recent examples of these GIS-based and other approaches are given in Zezere et al. (2004), Saboya et al. (2004), Saro & Ryu (2004), Lee et al. (2004), Garcia & Zezere (2004), Jaboyedoff et al. (2004), Coe et al. (2004), Fallsvik et al. (2003), Nassalacqua & Bouetto (2003), Ho (2004) describes extensive work in Hong Kong to develop landslide susceptibility maps. Details are given in Lee et al. (2002), Evans & King (1998), Dai & Lee (2002).

Finlay (1996) and reported in Fell et al. (1996a) carried out a multivariate analysis of engineered slopes using the Geotechnical Engineering Office's (GEO) data for 3,000 landslides in Hong Kong. In this

49

approach the probability of landsliding for individual slopes was assessed, using factors calibrated on the past performance of the slopes over a 10 year period.

In some cases quantification was possible on a reasonably rigorous basis, e.g. for slopes or cuts, but in others, a considerable degree of judgement was necessary. It also became apparent that the quality of the data was a limitation, because of difficulties in obtaining information on a slope in difficult conditions, e.g. rain, darkness etc.

A more detailed study was also carried out by Finlay (1996) using GEO data on 180 cut slopes (of which about half had failed), for which 300 variables were defined. This took the form of a discriminate between those slopes which were stable and those which were unstable). Reasonable discrimination was achieved, but sometimes with variables which one would not intuitively expect to be critical. A large amount of time and money was needed to develop the database and while this might be reduced by more judicious selection of variables, it will usually be a fairly costly exercise.

In effect, many schemes for ranking slopes for prioritisation of remedial works (e.g. Koirala & Watkins 1988, for Hong Kong) are a form of this method. However, these are usually based on judgement for the factors to be included, may not be properly calibrated and are therefore inaccurate, and are unable to quantify the probabilities. These are described in SOA 8.

4.5 *Relating the historic record of landsliding to rainfall intensity and duration, slope geometry and other factors*

These methods relate the historic occurrence of landsliding to rainfall intensity and duration, and in some cases, to antecedent rainfall. They have been used in rural areas (e.g. by Siddle et al. 1985, Kim et al. 1992) to delineate rainfall which is likely to lead to extensive landsliding. Figure 21 shows the results of Kim et al.'s (1992) study of shallow landslides in steep, tree covered hill slopes in Korea. A degree of quantification of the extent of sliding is introduced as shown.

Lumb (1976), Brand et al. (1984) and Premchitt et al. (1994) and more recently Ko (2003) have developed methods for relating rainfall intensity of landsliding in constructed and natural slopes in Hong Kong. These, and the Kim et al. (1992), methods have largely been developed to determine what rain conditions lead to extensive landsliding, so that warning systems can be instituted, to keep the population away from the high hazard areas in such times. Fell et al. (1988) carried out an analysis of rainfall in a suburb of Newcastle, and assessed a number of algorithms for antecedent rainfall, relating the incidence of landsliding (in this case relatively large, deep slides, compared to those studied by Korea or Hong Kong and
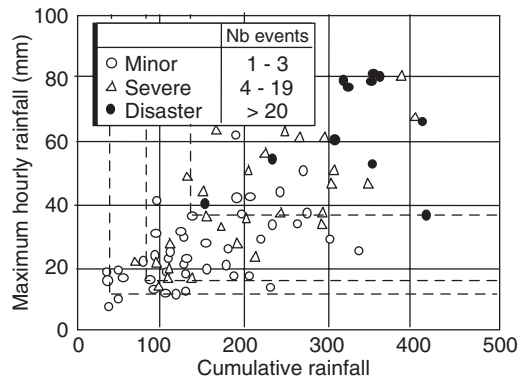
Figure 21. Relationship between landsliding and rainfall (Kim et al. 1992).

referenced above) to the 24 hour rainfall and antecedent rain. The intention in this case was to assess the frequency of such landslides in a given study area. Given the landslides were largely reactivations of existing landslides, the method could be used to crudely assess the average probability of landsliding for those identified landslides. Similarly, for Hong Kong, where the population of slopes is known, it could be possible to approximately assign the average probability of landsliding for each slope.

These methods generally have their uses, but are unable to allow discrimination between the relative probability of landsliding for different slopes within the population. In addition, they need to be carefully applied to determine the critical rainfall duration, and period of antecedent rainfall. For example, Premchitt et al. (1994) have found that the 1 hour intensity is the most critical factor for Hong Kong's relatively small, shallower slides in constructed and natural slopes and that antecedent rainfall was not important, but Fell et al. (1988) found that the prediction was best including with the 1 hour data, antecedent rainfall up to 30 to 60 days for the larger, deeper landslides in their study.

Finlay (1996), reported in Finlay et al. (1997), has extended these approaches to relate the number of landslides to the rainfall intensity, duration and antecedent rainfall, using records of landsliding in Hong Kong taken by the Geotechnical Engineering Office, and very detailed rainfall data (5 and 15 minute data was used).

The concept developed allows the prediction of the number of landslides which may occur for say a 1 in 100 AEP rain event, within a given area. However, in this case and probably more generally), the incidence of landsliding varies non linearly with rainfall, and is markedly affected by data from a small number of heavy rain events. This makes the extrapolation uncertain. In addition, it becomes apparent that a critical feature is the areal extent of the rain event, yet such

50

data is seldom available. As for the other examples of this method, it is not possible to assess the probability of landsliding of individual slopes, only the average (assuming the population of slopes is known).

Some recent examples of these approaches are given in Okada et al. (2003), Gonzalez-Garcia & Mayorga-Marquez (2004), and Corominas et al. (2004).

Some studies have been recently aimed at understanding the relationships between immediate or antecedent rainfall, groundwater and the occurrence of landslides (Celestino et al. 2001, Picarelli et al. 2004, Terranova 2002). In this specific field, more than in any other, local oddities as well as climate pattern (tropical, temperate, alpine, climate changes etc.) and geological/geotechnical conditions drive the future behaviour of a slope.

A recent paper discussed in detail how, under similar stimulus, three slopes behaved quite differently based on their initial hydro-geological conditions (Franciosi et al. 2001), under a major rain event coupled with a rapid snowmelt in Switzerland (Lateltin et al. 2001). Also, it can be noted that the influence of antecedent rains can go from practically nil (Brand et al. 1984), to very long intervals (Bonnard and Noverraz 2001) and present infinite aspects depending on the depth, geology and local conditions (Capecchi & Focardi 1988, Dapporto et al. 2003).

4.6 Relating the historic record of rainfall, slope geometry and geotechnical properties, and landsliding

The methods described in section 4.5 have been extended by some authors to include the slope of the ground, potential depth of sliding, and piezometric pressure parameters which are linked to rainfall and infiltration. Some of the more recent models model partially saturated soil behaviour, and flows from the rock beneath the colluvium which is susceptible to sliding. Examples are given in Keefer et al. (1987), Omura & Hicks (1992), Fourie (1996), Pradel & Raad (1993), Sun et al. (1998), Tarantino & Mongiovi (2003), Olivares et al. (2003), Rabuffetti (2003), Dapporto et al. (2003), Cascine et al. (2003), Berti & Simoni (2003), and Savage et al. (2004).

These methods have the apparent virtue of properly modelling the sliding process, e.g. for shallow sliding leading to debris slides. However, they sometimes oversimplify the piezometric pressure component of the analysis, which in factor dominates the calculation, by for example:

- using constant infiltration rates and/or permeability
- ignoring the non linear effects of partial saturation on infiltration
- ignoring the heterogeneity of the slope – e.g. ignoring layering in the soil, root holes, infiltration from the rock below the soil as shown in Figure 22.

- Not modelling 3 dimensional (or sometimes even 2 dimensional) effects across and up and down slope
- Not modelling the rainfall intensity-duration properly.

A further problem is that the analytical models sometimes do not model the actual slide mechanisms properly, and are really modeling detachment (sliding), not the debris flow initiation which is often what is critical for the slope.

The real situation is generally however far too complex to model successfully – the real slope often has roots, root holes, fissures, desiccation cracks, variable soil properties with depth e.g. higher permeability colluvial soils underlain by lower permeability residual soils and completely weathered rock; colluvium is commonly stratified. Alternating layers notably differing in permeability, create perched and pressurized bodies of ground-water which are frequent causes of shallow slope failures; seepage inflow from the underlying rock etc; soil "pipes" (in some situations), and potentially complex mechanics e.g. collapse surface controlling failure rather than peak strength. Hence the calculations are at worst simply misleading giving those doing the analyses a feeling of rigor in their analyses. At best, they can be "calibrated" against real slope performance, but then it is questionable whether it is worth going through the steps of the stability analysis, and whether it would be better simply to calibrate slope performance against rainfall, evaporation and slope characteristics such as slope, catchment area above the slope, and geo-morphological characteristics.

The more complex models such as those of Savage et al. (2004) being developed are addressing these issues and no doubt will be better than earlier attempts.

In situ tests have been developed for studying rain influence, using artificial rain to reduce the variability of the main parameter (Springman & Teysseire 2001) and concluded also to the great variability of the rain-slide response time and the influence of the density of the slope's material. Only very few studies are aimed at identifying a model capable of predicting slopes movements based on hydro-geological modelling (Parriaux et al. 2001) and focus their attention on the meshing of thin and discontinuous aquifers, the modeling of perched aquifer, real 3D geology and short steps transient flow simulations, thus trying to bridge the gap between actual conditions and the simplistic water table model assumed by most methodologies.

4.7 Modelling piezometric levels versus rainfall

The method outlined in Fell et al. (1991) is an example of this approach, where piezometric levels recorded over some period (in that case 3 years) are related to rainfall, and the probability of various

51

RUN-ON

RAINFALL

EVAPOTRANSPIRATION

SOIL

GROUNDWATER INFLOW

INFILTRATION

RUN-OFF

ROCK

GROUND WATER PIEZOMETRIC HEAD

GROUNDWATER OUTFLOW

RECHARGE
(= INFILTRATION IN
SIMPLEST MODELS)

(a) Idealised slope

EVAPOTRANSPIRATION

RAINFALL

GROUND-
WATER
INFLOW

VEGETATION

INTERCEPTION

ROOTS

COLLUVIUM
(HIGH PERMEABILITY)

FISSURED RESIDUAL SOIL (MEDIUM PERMEABILITY)

NON-FISSURED RESIDUAL SOIL (LOW PERMEABILITY)

SEEPAGE

NETT RAINFALL

SOIL 'PIPES'

SAND INFILLED
JOINTS

SEEPAGE

SEEPAGE

COMPLETELY WEATHERED
ROCK (LOW PERMEABILITY)

WEATHERED, JOINTED
ROCK (MEDIUM PERMEABILITY)

GROUNDWATER
OUTFLOW

(b) Actual slope

Figure 22.   Hydro-geological conditions in shallow landslides on natural slopes Idealised slope (b) Actual slope. (Fell et al. 2000). These simplifications are necessary to make the problem solvable, but in the process of simplification, reality may be lost.

piezometric levels being reached is assessed by analyzing the modeled piezometric levels for the period of record of the dam (in that case 100 years). Other examples are given in Haneberg (1991) and

Okunushi & Okumura (1987), Wiggington & Meuris (1988).

The method is ideal in principle for a single, relatively deep seated landslide. However, in reality it is

52

difficult to achieve any accuracy in the modeling because of the complex infiltration processes involved, heterogeneity of the soil and rock in the slope, and groundwater seeping into the slide from below. It is also apparent that a lengthy period of calibration (years) is likely to be necessary, to experience a range of rainfall and piezometric conditions including high rainfalls after long droughts for example.

Moreover, stress relief and other mechanical factors can greatly influence the behaviour of the piezometric levels (Bromhead & Dixon 1984, Hulla et al. 1984) before and during the occurrence of a landslide or a reactivation of an existing landslide.

When studying potential landslide hazards outside the boundaries of existing landslides, or approaching an existing landslide at the inception of a monitoring program, modeling and simulations based on probabilistic models (Cherubini & Masi 2002), Oboni et al. 1984) as well as Bayesian approaches, to update probabilities estimates as new monitoring information is acquired, are the tools of preference. Interesting approaches based on geomorphological and "reconstruction of landscape evolution" approaches have been presented in recent years (Perini et al. 2001).

4.8 Event tree methods, including the use of expert opinion

It is sometimes practical to simulate the sequence of events which may lead to an individual slope failing using an event tree, and estimate the frequency of landsliding in this manner. This is particularly applicable where slope instability may be triggered by liquefaction due to earthquake, or where the issue is given landsliding occurs, will it be contractive and travel rapidly, or dilative and not travel far at all. In other words, the event trees can be used to model the uncertainty. An example of this approach is given in Hsi & Fell (2005) in this volume.

4.9 Some detailed issues in estimating frequency of landsliding

4.9.1 Introduction

When the frequency of landslide is estimated or rock falls from a cliff, sliding of cuts and fills on roads or railways, and small scale landsliding from natural slopes, the result is often in a form which requires manipulation to be used in quantitative risk analysis.

The following examples are presented to aid readers in considering this data.

4.9.2 Boulder falls from cliff above a dwelling

On the cliff line which has length L_c, historic data indicates that x falls occur per annum, and the boulders which fall are an average width w. If it is
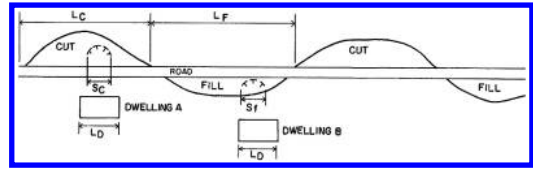
Figure 23.   Plan of road cuts and fills above dwellings.

assumed all potential boulders are equally likely to fall, the annual probability of any rock falling is given by

$$P_{rf} = \frac{xw}{L_c} \tag{3}$$

The dwelling has a length L_D, so the number of boulders on the cliff which are directly above the dwelling is

$$\frac{L_D}{w} \tag{4}$$

The annual probability of one or more of these boulders above the dwelling falling (P_D) is given by

$$P_D = 1 - (1 - P_{rf})^{\frac{L_D}{w}} \tag{5}$$

For P_{rf} is less than about 0.01, this can be approximated as

$$P_D = \frac{L_D}{w} P_{rf} \tag{6}$$

Whether the dwelling is impacted by the boulder fall depends on the travel distance of the boulders.

4.9.3 Landsliding of cuts and fills on a road or railway above dwellings

Here are a number of cuts and fills on the road shown in Figure 23. Historic performance data indicates that there have been x landslides from a total of 7 fills on the road in a period of z years. Assuming that the fills are all identical, and that the period of record is representative the annual probability of a landslide occurring on any one fill (P_{rf}) is given by

$$P_{rf} = \frac{x}{yz} \text{ per annum} \tag{7}$$

If we consider the fill above dwelling B, whether the landslide occurs in a position within the fill above the dwelling must be considered when doing the risk analysis.

53
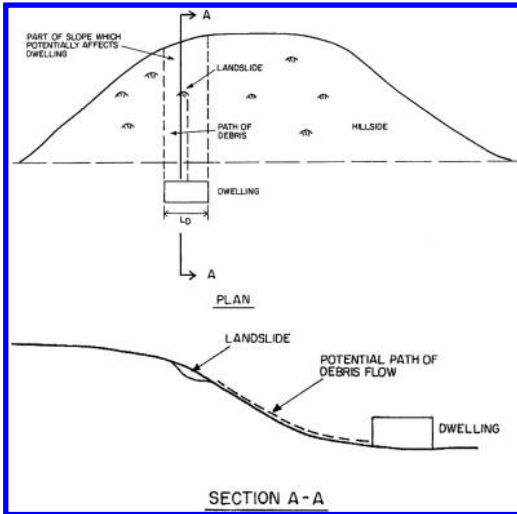
Figure 24.   Plan and section of dwelling below natural slope.

If the estimated length of the slide is S_f, the length of the average fill is L_F, and the length of the dwelling is L_D then the annual probability of one or more of these slides occurring wholly above the dwelling (P_{DW}) is given by

$$P_{DW} = 1 - (1 - P_{ff})^{\frac{L_D}{L_F}} \qquad (9)$$

Landslides may also occur so they are only partly above the dwelling. The annual probability of one or more of these slides occurring (P_{DP}) is given by

$$P_{DW} = 1 - (1 - P_{ff})^{\frac{2S_f}{L_F}} \qquad (10)$$

Similar equations would apply to landslides in the cut slope above dwelling A.

4.9.4 *Landsliding on natural slopes above dwellings*

Figure 24 shows a plan and section of a natural hillslide above a dwelling. Historic performance data indicates that a 0.1 annual exceedance probability rainfall initiates on average x landslides/square kilometre of natural slope. The source landslides are an average area of y square metres.

If the part of the slope which is above the dwelling has an area of z square metres, the annual probability of one or more landslides occurring in this area is given by

$$P_{NSD} = 1 - (1 - P_{NS})^{\frac{z}{y}} \qquad (11)$$

$$\text{where } P_{NS} = 0.1 \left(1 - \left(\frac{y}{1000} \right)^x \right) \qquad (12)$$

P_{NS} is the annual probability of one or more slides occurring on any area of y square metres (To determine the total probability of landsliding, it would be necessary to consider the full range of rain events – annual probability of 0.9, 0.1, 0.01, 0.001 annual probability of exceedance, and integrate the outcomes.

Whether the slides would impact on the dwelling would depend on the travel distance.

5   CONCLUSION

Hazard characterization is the most difficult and important step in any risk-based landslide assessment. We must remember that thorough understanding of the varied processes involved in destabilization and failure of slopes lies at the foundation of any subsequent analysis, especially if quantitative results need to be achieved. No amount of analytical or statistical analysis, or even testing and instrumentation, can substitute for such understanding. Landslide hazard characterization calls on the entire spectrum of skills and experience available to an applied geoscience professional. The thought processes needed to solve the related problems cannot be summarized in any textbook or manual. This paper presents and discusses several available tools.

REFERENCES

Abbott, B., Bruce, I., Keegan, T., Oboni, F. & Savigny, W. 1988a. A methodology for the assessment of rockfall hazard and risk along linear transportation corridors, *IUGS Conference*, Vancouver.

Abottt, B., Bruce, I., Keegan, T., Oboni, F. & Savigny, W. 1988b. Application of a new methodology for the management of rockfall risk along a railway, *IUGS Conference*, Vancouver.

Agung, M.W., Sassa, K., Fukuoka, H. & Wang, G. (2004). Evolution of shear-zone structure in undrained ring shear tests. *Landslides* 1(2): 101–112.

Angeli, M.G. & Silvano, S. 2004. Two cases of mudslides in different geological and climatic environments. Proc. Int. Workshop, "Occurrence and Mechanisms of Flow-Like Landslides in Natural Slopes and Earthfills", Sorrento: 209–216, Picarelli (ed.), Patron, Bologna.

Baum, R.L., Savage, W.Z. & Wasowski, J. 2004. Mechanics of earthflows. Proc. Int. Workshop "Occurrence and Mechanisms of Flow-Like Landslides in Natural Slopes and Earthfills", Sorrento: 185–190, Picarelli (ed), Patron, Bologna.

Baziar, M.H. & Dobry, R. 1995. Residual strength and large deformation potential of loose silty sands. *Journal of Geotechnical Engineering*, ASCE 121(12): 896–906.

Bernarder, S. On formation of progressive failures in slopes. *Proceed. 10th ISSMFE*, Stockholm.

Berti, M. & Simoni, A. 2003. Debris flow initiation in an highly-conductive soil. In Picarelli (ed.), *Proceedings of Int. Conf. Fast Slope Movements, Prediction and*

Prevention for Risk Mitigation. 29–36. Naples, May 2003. Patron editore, Bologna.

Bishop, A.W., Hutchinson, J.N., Penman, A.D.M. & Evans, H.E. 1969. Geotechnical investigation into the causes and circumstances of the disaster of 21 October 1966. In A selection of technical reports submitted to the Aberfan Tribunal. HMSO, The Stationary Office Ltd., Norwich, U.K., 1–80 (Item 1).

Blight, G.E. & Fourie, A.B. 2004. A review of catastrophic flow failures of deposits of mine waste or municipal refuse. Proceed. int. workshop "Occurrence and Mechanisms of Flow-Like Landslides in Natural Slopes and Earthfills", Sorrento: 19–36, Picarelli (ed.), Patron, Bologna.

Bonnard, C. & Noverraz, F. 2001. Influence of climate change on large scale landslides: assessment of long-term movements and trends. In *International Conference on Landslides, Causes, Impacts and Counter Measures*, June 2001, 121–138, 17–21, Davos, Switzerland.

Brand, E., Premchitt, J. & Phillipson, H. 1984. Relationship between rainfall and landslides in Hong Kong. In *Landslides, Proc. Fourth International Symposium on Landslides*, Toronto, Canada. BiTech Publishers, Vancouver, Canada.

Bromhead, E.N. & Dixon, N. 1984. Pore-water pressure observations in the coastal clay cliffs at the Isle of Sheppey, England. In *IV International Symposium on Landslides – ISL*, September 16th–21st 1984, 1: 385–390, Canadian Geotechnical Society, Toronto, Canada.

Bromhead, E.N. & Dixon, N. 1984. Pore water pressure observations in the coastal cliffs in the Isle of Sheppey, England. Proceed. 4th Int. Symp. on Landslides, Toronto, 1:385–390.

Brunsden, D. 1984. Mudslides. In: Slope Instability: 363–410, Brunsden & Prior (eds.), J. Wiley & Sons, New York.

Capecchi, F. & Focardi, P. 1988. Rainfall and landslides: research into a critical precipitation coefficient in an area of Italy. In Bonnard (ed.), *Landslides*, July 10th–15th 1988, Lausanne, 2, 1131–1136. Lausanne-EPFL, Switzerland.

Carboni, R., Casagli, N., Iotti, A., Monti, L., Tarchiani, U. & Vannini, S. 1996. La frana di Silla (Gaggio Montano, BO): indagini, interventi e monitoraggio. Proc. Conf. "La Prevenzione delle Catastrofi Idrogeologiche: il Contributo della Ricerca Scientifica", Alba, 1: 107–115, Luino (ed.).

Carrera, A., Cardinali, M. & Guzzetti F. 1992. Uncertainty in assessing landslide hazard and risk. *ITC Journal* 1992(2): 172–183.

Carrera, A., Cardinali, M., Detti, R. Guzzetti F., Pasqui, V. & Reichenbach, P. 1991. GIS techniques and statistical models in evaluating landslide hazard. *Earth Surface Processes and Landforms* 16(5): 427–445.

Casagrande, A. 1976. Liquefaction and cyclic deformations of sands – a critical review. Harvard Soil Mechanics Series no 88, Cambridge, Massachussets.

Cascini, L., Sorbino, G. & Cuomo, S. 2003. Modelling of flowslide triggering in pyroclastic soils. In Picarelli (ed.), *Proceedings of Int. Conf. Fast Slope Movements, Prediction and Prevention for Risk Mitigation.* 93–100. Naples, May 2003. Patron editore, Bologna.

Castro, G. 1969. Liquefaction of sand. PhD Thesis, Division of Engineering and Applied Physics, Harvard University.

Celestino, B., Lins, P. & Prado de Campos, L. 2001. Theoretical estimates of the relationships between rainfall and the occurrence of landslides. In *International Conference on Landslides, Causes, Impacts and Counter Measures*, 17–21 June 2001, 147, Davos, Switzerland.

Chau, K.T., Wong, R.H.C. & Lee, C.F. 2003. Rockfall hazard analysis for Hong Kong based on rockfall inventory. *Rock Mechanics and Rock Engineering* 36: 383–408.

Cherubini, C. & Masi, P. 2002. Probabilisitic and fuzzy reliability analysis in stability assessment In McInnes & Jakeways (eds.), *Instability Planning and Management, Seeking Sustainable Solutions to Ground Movements Problems*, 20–23 May 2002, 209–217, Isle of Wight, UK.

Chowdhury, R.N. & Flentje, P.N. 1998. A landslide database for landslide database for landslide hazard assessment. In Sivakumar & Chowdhury (eds.), *Proceeding Second International Conference on Environmental Management*. Feb. 10–13. Wollongong, Australia. 1229–1239, Elsevier, London.

Chu, J., Leroueil, S. & Leong, W.K. 2003. Unstable behaviour of sand and implications for slope instability. *Canadian Geotechnical Journal* 40: 873–885.

Coe, J.A. and Godt, J.W., Baum, R.L., Bucknam, R.C. & Michael, J.A. 2004. Landslide susceptibility from topography in Guatemala. In Lacerda et al. (eds.), *Landslides evaluation and stabilization,* 69–78, Balkema Leiden.

Comegna, L. 2005. Considerazioni sulla meccanica delle colate in argilla. PhD Thesis, Seconda Università di Napoli, Aversa.

Comegna, L. & Picarelli, L. 2005. The interplay between pore pressures and slope movements in fine-grained materials. Proceed. 11th IACMAG, Turin, in press.

Comegna, L., Urciuoli, G. & Picarelli, L. 2004. The role of pore pressures on the mechanics of mudslides. Proc. 9th Int. Symp. on Landslides, Rio de Janeiro, 2: 1183–1188, Lacerda et al. (eds.), Balkema, Rotterdam.

Cornforth, D.H., Worth, E.G. & Wright, W.L. 1974. Observation and analysis of a flow slide in sand fill. In *Proceedings of the Symposium on field Instrumentation in Geotechnical Engineering,* U.K. Edited by British Geotechnical Society. Butterworths, London, U.K., 136–151.

Corominas, J., Moya, J., Masachs, I. & Baeza, C. 2004. Reconstructing recent activity of Pyrenean landslides by means of dendrogeomorphological techniques. In Lacerda et al. (eds.), *Landslides evaluation and stabilization,* 363–370, Balkema Leiden.

Cotecchia, V. & Del Prete, M. 1984. The reactivation of large flows in the parts of southern Italy affected by the earthquake of November 1980, with reference to the evolutive mechanism. Proceed. 4th Int. Symp. on Landslides, Toronto, 2: 33–38.

Cotecchia, V., Del Prete, M., Federico, A., Fenelli, G.B., Pellegrino, A. & Picarelli, L. 1984. Some observations on a typical mudslide in a highly tectonized formation in Southern Apennines. Proceed. 4th Int. Symp. on Landslides, Toronto, 2: 39–44.

Crosta, G.B., Dal Negro, P. & Frattini, P. 2003. Soil slips and debris flows on terraced slopes. *Natural Hazards and Earth System Sciences* 3: 31–42.

Cruden, D. 1993. Slope stability and protection. Proceed. int. symp. "The Geotechnical Engineering of Hard Soils – Soft Rocks", Athens, Anastagnopulos et al. (eds.), 3: 1967–1984. Balkema, Rotterdam.

Cruden, D.M. 1997. Estimating the risks from landslides using historical data. In Cruden & Fell (eds.), "Landslide Risk Assessment", 277–284, Balkema.

Cruden, D.M. & Varnes, D.J. 1996. Landslide types and processes. In Turner & Schuster (eds.), *Landslides – Investigation and Mitigation Transportation Research Board Special Report No.247*. 36–75. National Academic Press, Washington DC.

Cruden, D.M. & Hu, X.Q. 1993. Exhaustion and steady state models for predicting landslide hazards in the Canadian Rocky Mountains. *Geomorphology* 8: 279–285.

Cubrinovski, M. & Ishihara, K. 2000. Flow potential of sandy soils with different grain compositions. *Soils and Foundations* 40(4): 103–119.

D'amato Avanzi G., Giannecchini, R. & Puccinelli, A. 2003. A contribution to an evaluation of landslide susceptibility in the Apuan Alps (Italy): Geologic and Geomorphic factors of the 1996 soil slip-debris flows. In Picarelli (ed.), *International Conference, Fast Slope Movements Prediction and Prevention for Risk Mitigation*, 125–130, 11–13 May 2003. Naples, Italy.

D'Elia, B. 1979. Caratteri cinematici delle colate: interventi di stabilizzazione. *Rivista Italiana di Geotecnica* 13: 122–136.

D'Elia, B., Esu, F., Pescatore, T.S. & Pellegrino, A. 1985. Some effects on natural slope stability induced by the 1980 Italian earthquake. Proceed. 11th ICSMFE, San Francisco, 4: 1943–1949.

D'Elia, B., Picarelli, L., Leroueil, S. & Vaunat, J. 1998. Geotechnical characterisation of slope movements in structurally complex clay soils and stiff jointed clays. *Rivista Italiana di Geotecnica* 32(3): 5–47.

D'Elia, B. & Tancredi, G. 1979. Colate permanenti e temporanee. *Geologia Applicata e Idrogeologia* 14: 23–39.

Dai, F.C. & Lee, C.F. 2001. Frequency-volume relation and prediction of rainfall-induced landslides. *Engineering Geology* 59: 253–266.

Dai, F.C. & Lee, C.F. 2002. Terrain-based mapping of landslide susceptibility using a geographic information system: a case study. *Canadian Geotechnical Journal* 38: 911–923.

Damiano, E. 2004. Meccanismi d'innesco di colate di fango in terreni piroclastici. PhD Thesis, Seconda Università di Napoli, Aversa.

Dapporto, S., Falorni, G., Tofani, V. & Vannocci, P. 2003. Analysis of pore pressure conditions leading to slope instability during November 2000 event in Tuscany. In Picarelli (ed.), *International Conference, Fast Slope Movements Prediction and Prevention for Risk Mitigation,* 131–137, 11–13 May 2003. Naples, Italy.

Dapporto, S., Falorni, G., Tofani, V. & Vannocci, P. 2003. Analysis of pore pressure conditions leading to slope instability during November 2000 event in Tuscany. In Picarelli (ed.), *Proceedings of Int. Conf. Fast Slope Movements, Prediction and Prevention for Risk Mitigation.* 131–137. Naples, May 2003. Patron editore, Bologna.

Dawson, R.F. 1994. Mine waste geotechnics. PhD thesis, Department of Civil Engineering, University of Alberta, Edmonton, Alta.

Dawson, R.F., Morgenstern, N.R. & Stokes, A.W. 1998. Liquefaction flowslides in Rocky Mountain coal mine waste dumps. *Canadian Geotechnical Journal* 35: 328–343.

Demers, D., Leroueil, S. & D'Astous, J. 1993. In situ testing in a landslide area at Maskinongé, Québec. Proceed. 46th Canadian Geotechnical Conf., Saskatoon: 465–474.

Dussauge, C., Grasso, J-R. & Helmstetter, A. 2003. Statistical analysis of rockfall volume distributions: implications for rockfall dynamics. *Journal of Geophysical Research* 108(B6): ETG 2-1 to ETG 2-11.

Dussauge-Peisser, C., Helmstetter, A., Grasso, J-R., Hantz, D., Desvarreux, P., Jeannin, M. & Giraud, A. 2002. Probabilistic approach to rock fall hazard assessment: potential of historical data analysis. *Natural Hazards and Earth System Sciences* 2: 15–26.

Eckersley, D. 1990. Instrumented laboratory flowslides. *Géotechnique* 40: 489–502.

Eckersley, J.D. 1986. The initiation and development of slope failures with particular reference to flowslides. PhD thesis, Department of Civil and Systems Engineering, James Cook University of North Queensland, Townsville, Queensland, Australia.

Eckersley, J.D. 1990. Instrumental laboratory flowslides. *Géotechnique* 40(3): 489–502.

Evans, S.G. 2003. Characterizing landslide risk in Canada. Proceedings 3rd Canadian Conference on Geotechnique and Natural Hazards, Canadian Geotechnical Society, Edmonton Canada: 19–34.

Evans, N. & King, J. 1998. The natural terrain landslide study: debris avalanche susceptibility. Technical Note No. TN 1/98, 96. Geotechnical Engineering Office, Hong Kong.

Faella, C. & Nigro, E. 2004. Dynamic impact of the debris flows on the constructions during the hydrogeological disaster in Campania – 1988: failure mechanical models and evaluation of the impact velocity. Proceed. int. conf. "Fast Slope Movements – Prediction and Prevention for Risk Mitigation", Napoli, 1:179–186, Picarelli (ed.), Patron, Bologna.

Fallsvik, J., Rankka, K., Viberg, L. & Nisser, M. 2003. Survey mapping of this stability conditions in gullies and slopes in till and coarse sediment soils in Sweden. In Picarelli (ed.), *Proceedings of Int. Conf. Fast Slope Movements, Prediction and Prevention for Risk Mitigation.* 205–211. Naples, May 2003. Patron editore, Bologna.

Fell, R. & Hartford, D. 1997. Landslide risk management. In Cruden & Fell (eds.) *Landslide Risk Assessment*, 51–110, Rotterdam: Balkema.

Fell, R., Finlay, P.J. & Mostyn, G.R. 1996a. Framework for assessing the probability of sliding of cut slopes. *Proc. Seventh International Symposium on Landslides*, Trondheim, The Netherlands, 1, 201–208. Rotterdam: Balkema.

Fell, R., Hungr, O., Leroueil, S. & Riemer, W. 2000. Keynote Lecture – Geotechnical engineering of the stability of natural slopes, and cuts and fills in soil, GeoEng 2000, 1, 21–120. Invited Papers, Technomic Publishing, Lancaster, ISBN: 1-58716-067-6, November 2000.

Fell, R., Mostyn, G., O'Keeffe, L. & Maguire, P. 1988. Assessment of the probability of rain induced landsliding. *Fifth Australia-New Zealand Conference on Geomechanics*, 72–77.

Fell, R., Walker, B.F. & Finlay, P.J. 1996b. Estimating the probability of landsliding. *Proc. 7th Australia New Zealand Conf. on Geomechanics*, Adelaide. Institution of Engineers Australia, Canberra, 304–311.

Fenelli, G.B. & Picarelli, L. 1990. The pore pressure field built up in a rapidly eroded soil mass. *Canadian Geotechnical Journal* 27: 387–392.

Finlay, P.J. 1996. The risk assessment of slopes. PhD Thesis, School of Civil Engineering, University of New South Wales.

Finlay, P.J., Fell, R. & Maguire, P.K. 1997. The relationship between the probability of landslide occurrence and rainfall. *Canadian Geotech. Journal* 34(6): 811–824.

Fourie, A.B. 1996. Predicting rainfall-induced slope instability. *Proc. Instn. Civ. Engrs. Geotech. Eng.* 119: 221–218.

Franciosi, G., Tullen, P., Marcuard, C., Joliquin, P. & Clément, I. 2001. Difference responses of landslides in the Swiss rhôcatchment to the 1999 extreme hydrological event. In *International Conference on Landslides, Causes, Impacts and Counter Measures,* 149–155, 17–21 June 2001. Davos, Switzerland.

Fuji, Y. 1969. Frequency distribution of the magnitude of the landslides caused by heavy rainfall. *Journal of the Seismological Society of Japan* 22: 244–247.

Garcia, R.A.C. & Zêzere, J.L. 2004. Abadia Basin (Torres Vedras, Portugal) – A case study of landslide susceptibility assessment and validation. In Lacerda et al. (eds.), *Landslides evaluation and stabilization,* 137–142, Balkema Leiden.

Glastonbury, J. & Fell R. 2002b. Report on the analysis of slow, very slow and extremely slow natural landslides. *UNICIV Report No.R-402,* ISBN85841 369 8, School of Civil and Environmental Engineering, The University of New South Wales.

Glastonbury, J. & Fell, R. 2002a. Report on the analysis of rapid natural rock slope failures. *UNICIV Report No. R-390,* ISBN 85841 357 4, School of Civil and Environmental Engineering, The University of New South Wales.

Glastonbury, J. & Fell, R. 2002c. A decision analysis framework for assessing post-failure velocity of natural rock slopes. *UNICIV Report No. R-409,* ISBN: 85841 376 0. School of Civil and Environmental Engineering, The University of New South Wales.

Glastonbury, J. & Fell, R. 2005c. A decision analysis framework for the assessment of likely post failure velocity of large/natural rock slope failures. Submitted to Canadian Geotechnical Journal.

Glastonbury, J.P. & Fell, R. 2005a. The geotechnical characteristics of large slow, very slow and extremely slow landslides. Submitted to Canadian Geotechnical Journal.

Glastonbury, J.P. & Fell, R. 2005b. The geotechnical characteristics of large rapid landslides. Submitted to Canadian Geotechnical Journal.

Golder Associates Limited 1992. Runout characteristics of debris from dump failures in mountainous terrain. Stage 1: data collection. Interim Report to Department of Supply and Services, Contract No. 23440-0-9198/01-X8G. Golder Associates Limited, Burnaby, B.C.

González-García, A.J. & Mayorga-Márquez, R. 2004. Thresholds for rainfall events that induce landslides in Colombia. In Lacerda et al. (eds.), *Landslides evaluation and stabilization,* 349–356, Balkema Leiden.

Guthrie, R.H. & Evans, S.G. 2004a. Magnitude and frequency of landslides triggered by a storm event, Loughborough Inlet, British Columbia. *Natural Hazards and Earth System Sciences* 4: 475–483.

Guthrie, R.H. & Evans, S.G. 2004b. Analysis of landslide frequencies and characteristics in a natural system, Coastal British Columbia. *Earth Surface Processes and Landforms* 29: 1321–1339.

Guzzetti, F., Malamud, B.D., Turcotte, D.L. & Reichenbach, P. 2002. Power-law correlations of landslide areas in central *Italy. Earth and Planetary Science Letters* 195: 169–183.

Guzzetti, F., Reichenbach, P. & Ghigi, S. 2004. Rockfall hazard and risk assessment along a transportation corridor in the Nera Valley, Central Italy. *Environmental Management* 34: 191–208.

Guzzetti, F., Reichenbach, P. & Wieczorek, G.F. 2003. Rockfall hazard and risk assessment in the Yosemite valley, California, USA. *Natural Hazards and Earth System Sciences* 3: 491–503.

Haneberg, W. 1991. Observation and analysis of pore pressure fluctuations in a thin colluvial landslide complex near Cincinnati, Ohio. *Engineering Geology* 31: 159–184.

Hantz, D., Dussauge-Peisser, C., Jeannin, M. & Vengeon, J-M. 2003. Rock fall hazard assessment: from qualitative to quantitative failure probability. In Picarelli (ed.), *Proceedings of Int. Conf. Fast Slope Movements, Prediction and Prevention for Risk Mitigation.* 263–267. Naples, May 2003. Patron editore, Bologna.

Henkel, D.J. 1956. Discussion on: Earth movement affecting L.T.E. railway in deep cutting east Uxbridge. Proceed. ICE, part II: 320–323.

His, J. & Fell, R. 2005. Landslide risk assessment of coal refuse emplacement. *Proceedings International Conference on Landslide Risk Management,* Vancouver, May 2005.

Hovius, N., Stark, C.P. & Allen, P.A. 1997. Sediment flux from a mountain belt derived by landslide mapping. *Geology* 25: 231–234.

HKIE, 1998. Soil nails in loose fill: a preliminary study (draft report). Hong Kong Institution of Engineers (HKIE), Geotechnical Division, Hong Kong.

Hulla, J., Turcek, P. & Ravinger, R. 1984. Water movement in landslide slopes. In *IV International Symposium on Landslides – ISL,* 405–410. 16th–21st September, 1984, Toronto, Canadian Geotechnical, Toronto, Canada.

Hungr, O. 1981. Dynamics of rock avalanches and other types of slope movements. PhD Thesis, University of Alberta, Edmonton.

Hungr, O. 2004. Geotechnique and management of landslide hazard. Proceedings, 57th. Canadian Geotechnical Conference, Québec City, (Paper 33.411, Session 4C, pp. 1–10).

Hungr, O., Evans, S.G. & Hazzard, J. 1999. Magnitude and frequency of rock falls and rock slides along the main transportation corridors of southwestern British Columbia. *Canadian Geotechnical Journal* 36: 224–238.

Hungr, O., Evans, S.G., Bovis, M.J. & Hutchinson, J.N. 2001. A review of the classification of landslides of flow type. *Environmental and Engineering Geoscience* 7(3): 1–18.

Hungr, O. & Evans, S.G., 2004. Entrainment of debris in rock avalanches; an analysis of a long run-out mechanism. *Bulletin, Geological Society of America* 116(9/10): 1240–1252.

Hunter, G. & Fell, R. 2003. Travel distance angle for "rapid" landslides in constructed and natural soil slopes. *Canadian Geotechnical Journal,* 40: 6, 1123–1141. National Research Council, Ottawa, Canada, ISSN 1208–6010.

Hutchinson, J.N. 1970. A coastal mudflow on the London Clay cliffs at Beltinge, North Kent. *Géotechnique* 20: 412–438.

Hutchinson, J.N. 1986. A sliding-consolidation model for flow slides. *Canadian Geotechnical Journal* 23: 115–126.

Hutchinson, J.N. 1988. General Report: Morphological and geotechnical parameter of landslides in relation to geology and hydrogeology. In Bonnard (ed.) Landslides, *Proc. Fifth Int. Symp. on Landslides*, Lausanne, Switzerland, 1, 3–35.

Hutchinson, J.N. 1992. Flow slides from natural slopes and waste tips. *3rd National Symposium on Avalanches and Lakdslides*, 827–841. La Coruna, Spain.

Hutchinson, J.N. 2004. Review of flow-like mass movements in granular and fine-grained materials. Proc. Int. Workshop "Occurrence and Mechanisms of Flow-Like Landslides in Natural Slopes and Earthfills", Sorrento: 3–16, Picarelli (ed.), Patron, Bologna.

Hutchinson, J.N. & Bhandari, R. 1971. Undrained loading: a fundamental mechanism of mudflows and other mass movements. *Géotechnique* 21: 353–358.

Hutchinson, J.N., Brunsden, D. & Lee, E.M. 1991. The geomorphology of the landslide complex at Ventnor, Isle of Wight. In Chandler (ed.), Slope Stability Engineering, Developments and Applications. *Proc. Int. Conf. on Slope Stability, Isle of Wight,* 197–206. Thomas Telford.

Hutchinson, J.N., Prior, D,B. & Stephens, N. 1974. Potentially dangerous surges in an Antrim mudslide. *Quarterly Journal Engineering Geology* 7: 363–376.

Iaccarino, G., Peduto, F., Pellegrino, A. & Picarelli, L. 1995. Principal features of earthflows in part of Southern Apennine. Proceed. 11th ECSMFE, Copenhagen, 4: 354–359. Danish Geotechnical Society.

Ishihara, K. 1993. Liquefaction and flow failure during earthquakes. *Géotechnique* 43(3): 351–415.

Iverson, R.M. & Lahusen, R.G. 1989. Dynamic pore pressure fluctuations in rapidly shearing granular materials. *Science* 246: 796–799.

Jaboyedoff, M., Baillifard, F., Couture, R., Locat, J. & Locat, P. 2004. New insight of geomorphology and landslide prone area detection using Digital Elevation Model(s). In Lacerda et al. (eds.), *Landslides evaluation and stabilization,* 191–198, Balkema Leiden.

Keefer, D.K., Wilson, R.C., Mark, R.K., Brabb, E.E., Brown, W.M., Ellen, S.D., Harp, F.L., Wieczoreck, O.F., Alger, C.S. & Zatkin, R.S. 1987. Real time landslide warning during heavy rainfall. *Science* 238: 921–925.

Kim, S.K., Hong, W.P. & Kim, Y.M. 1992. Prediction of rainfall-triggered landslides in Korea. In Landslides, *Proc. Sixth Int. Symp. on Landslides*, Christchurch, New Zealand. Rotterdam: Balkema.

Ko, F.W.Y 2003. Correlation between rainfall and natural terrain landslide occurrence in *Hong Kong Special Project Report No. SPR 7/2003*, Geotechnical Engineering Office, Hong Kong.

Koirala, N.P. & Watkins, A.T. 1988. Bulk appraisal of slopes in Hong Kong. In Bonnard (ed.), Landslides, *Proc. Of the Fifth Int. Symp. on Landslide,* Lausanne, Switzerland. 2, 1181–1186. Rotterdam: Balkema.

Koppejan, A.W., Wamelen, B.M. & Weinberg, L.J.H. 1948. Coastal flow slides in the Dutch province of Zeeland. In *Proceedings of the 2nd International Conference on Soil Mechanics and Foundation Engineering*, Rotterdam. Vol. 5. American Association of Civil Engineers, New York, 89–96.

Kramer, S.L. 1988. Triggering of liquefaction flow slides in coastal soil deposits. *Engineering Geology* 26: 17–31.

Lade, P.V. & Pradel, V. 1990. Instability and plastic flow of soils. I: Experimental observations. *Journal of Engineering Mechanics, ASCE* 116(11): 2532–2550.

Lampitiello, S. 2004. Resistenza non drenata e suscettività alla liquefazione di ceneri vulcaniche della Regione Campania. Ph.D. Thesis, Seconda Università di Napoli, Aversa.

Lateltin, O., Bolliger, D., Hegg, C. & An Kreusen, H. 2001. The analysis of the 1999 landslides in Switzerland. In *International Conference on Landslides, Causes, Impacts and Counter Measures,* 159–167, 17–21 June 2001. Davos, Switzerland.

Lee, E.M. & Jones, D.K.C. 2004. Landslide Risk Assessment. Thomas Telford, London. 454 p.

Lee, C.F., ye, H., Yeung, M.R., Chan, X. & Chen, G. 2002. Application of artificial intelligence to natural terrain landslide susceptibility mapping in Hong Kong. *Proc. of Conf. on Natural Terrain – A Constraint to Development?* 223–237. Institution of Mining and Metallurgy (Hong Kong Branch).

Lee, E.M., Doorkamp, J.C., Brundsen, D. & Norton, N.H. 1991. Ground movement in Ventnor, Isle of Wight. Research Contract No. PECD 7/1/272. A Report by Geomorphological Services ltd. For the Department of the Environment.

Lee, H.J. & Locat, J. 2004. Mobilization of submarine flows: examples and questions. Proceed. int. work. "Occurrence and Mechanisms of Flow-Like Landslides in Natural Slopes and Earthfills", Sorrento: 273–288, Picarelli (ed.). Patron, Bologna.

Lee, S. & Ryu, J-H. 2004. Landslide susceptibility analysis and its verification using likelihood ratio, logistic regression and artificial neural network methods: case study of Yongin, Korea. In Lacerda et al. (eds.), *Landslides evaluation and stabilization,* 91–96, Balkema Leiden.

Lee, S., Choi, J. & Ryu, J-H. 2004. Probabilistic landslide hazard mapping using GIS and remote sensing data at Boun, Korea. In Lacerda et al. (eds.), *Landslides evaluation and stabilization,* 85–90, Balkema Leiden.

Lefebvre, G. 1981. Strength and slope stability in Canadian soft clay deposits. *Canadian Geotechnical Journal* 18: 420–442.

Lefebvre, G. 1996. Soft sensitive clays. In Turner & Schuster (eds.), *Landslides – investigation and mitigation*. U.S. Transportation Research Board, Special Report 247. 607–619.

Leroi, E. 1996. Landslide hazard – Risk maps at different scales: objectives, tools and developments. In Senneset (ed.), Landslides, *Proc. Int. Symp. on Landslides*, Trondheim, 35–52.

Leroueil, S., Locat, J., Vaunat, J., Picarelli, L. & Faure, R. 1996. Geotechnical characterisation of slope movements. In Senneset (ed.), *Proceedings of the Seventh International Symposium on landslides,* 1, 53–74. Trondheim, Norway, Rotterdam: Balkema.

Leroueil. S., Vaunat, J., Picarelli, L., Locat, J. & Faure, R. 1996. Geotechnical characterization of slope movements. Proceed. 7th Int. Symp. on Landslides, Trondheim, 1: 53–74, Senneset (ed.), Balkema, Rotterdam.

Lumb, P. 1975. Slope failures in Hong Kong. *Quarterly Journal of Engineering Geology* 8: 31–65.

MacKay, C.H. 1997. Management of rock slopes on the Canadian Pacific Highway, in Cruden & Fell (eds.), *Landslide Risk Assessment*, 271–276, Rotterdam: Balkema.

Malamud, B.D., Turcotte, D.L., Guzzetti, F. & Reichenbach, P. 2004. Landslide inventories and their statistical properties. *Earth Surface Processes and Landforms* 29: 687–711.

Malet, J.P. & Maquaire, O. 2003. Black marl earthflow mobility and long-term seasonal dynamic in Southeastern France. Proceed. int. conf. "Fast Slope Movements – Prediction and Prevention for Risk Mitigation", Napoli, 1: 333–240, Picarelli (ed.), Patron, Bologna.

Mancini, M. & Rabuffettii, D. 2003. Sensitivity of rainfall thresholds triggering soil slip to soil hydraulic parameter and hillslope geometry. In Picarelli (ed.), *Proceedings of Int. Conf. Fast Slope Movements, Prediction and Prevention for Risk Mitigation.* 349355. Naples, May 2003. Patron editore, Bologna.

Martin, Y., Rood, K., Schwab, J.W. & Church, M. 2002. Sediment transfer by shallow landsliding in the Queen Charlotte Islands, British Columbia. *Canadian Journal of Earth Sciences* 39:189–205.

Meisina, C., Piccio, A. & Tocchio, A. 2001. Some aspects of landslide susceptibility in sorba valley (western Alps, Italy). In *International Conference on Landslides, Causes, Impacts and Counter Measures*, pp. 547–556, 17–21 June 2001. Davos, Switzerland.

Meunier, M. 1993. Classification of stream flows. Proceed. Pierre Beghin int. workshop "Rapid Gravitational Mass Movements", Grénoble: 231–236.

Moon, A., Robertson, M. & Davies, W. 1996. Quantifying rockfall risk using a probabilistic toppling failure model. In Senneset (ed), *Proc. 7th Int. Symp. On Landslides*, Trondheim, 17–21 June 1996. Rotterdam: Balkema.

Moon, A.T., Olds, R.J., Wilson, R.A. & Burman, B.C. 1992. Debris flow zoning at Montrose, Victoria. In Bell (ed.), Landslides, *Proc. Sixth Int. Symp. on Landslides*, Christchurch, New Zealand, 2, 1015–1022, Rotterdam: Balkema.

Moon, A.T., Wilson, R.A. & Flentje, 2005. Developing and using landslide frequency models. *Proceedings International Conference on Landslide Risk Management,* Vancouver, May 2005.

Moore, R. & Brunsden, D. 1996. Physical-chemical effects on the behaviour of a coastal mudslide. *Géotechnique* 46(2): 259–278.

Morgan, G.C., Rawlings, G.E. & Sobkowicz, J.C. 1992. Evaluating total risk to communities from large debris flows. In Geotechnique and Natural Hazards, *Proc. Geohazards '92 Symposium* 225–236. BiTech Publishers, Canada..

Moriwacki, H., Inokuchi, T., Hattanji, T., Sassa, K., Ochiai, H. & Wang, G. 2004. Failure processes in a full-scale landslide experiment using a rainfall simulator. *Landslides* 1(4): 277–288.

Mostyn, G. & Fell, R. 1997. Quantitative and Semi quantitative estimation of the probability of landslides. In Cruden & Fell (eds.), *Landslide Risk Assessment*, 297–316. Rotterdam: Balkema.

Musso, A. & Olivares, L. 2004. Post-failure evolution in flow-slide: transition from static liquefaction to fluidization. Proceed. int. workshop "Occurrence and Mechanisms of Flow-Like Landslides in Natural Slopes and Earthfills", Sorrento: 117–128, Picarelli (ed.). Patron, Bologna.

Oboni, F., Bourdeau, P.L. & Bonnard, C. 1984. Probabilistic analysis of Swiss landslides. In *IV International Symposium on Landslides – ISL*, 2, 473–478, 16th–21st September 1984. Toronto, Canadian Geotechnical Society, Toronto, Canada.

Ochiai, H., Okada, Y., Furuya, G., Okura, Y., Matsui, T., Sammori, T., Terajima, T. & Sassa, K. 2004. A fluidized landslide on a natural slope by artificial rainfall. *Landslides* 1(3): 211–220.

Ohmori, H. & Hirano, M. 1988. Magnitude, frequency and geomorphological significance of rocky mud flows, landcreep and the collapse of steep slopes. *Zeitschrift fur Geomorphologie (Suppl. Bd.)* 101: 149–164.

Okada, K., Sugiyama, T., Fujii, T., Ota, N., Nunokawa, O. & Akiyama, Y. 2003. A risk assessment method of rain-induced slope failure on railway embankment based on critical rainfall. In Picarelli (ed.), *Proceedings of Int. Conf. Fast Slope Movements, Prediction and Prevention for Risk Mitigation.* 383–390. Naples, May 2003. Patron editore, Bologna.

Okunishi, K. & Okumura, T. 1987. Groundwater models for mountain slopes. In Anderson & Richards (eds.), *Slope Stability*. 265–285. Wiley.

Okura, Y., Ochiai, H. & Sammori, T. 2002. Flow failure generation caused by monotonic liquefaction. Proceed. Int. Symp. on "Landslide Risk Mitigation and Protection of Cultural and Natural Heritage", Kyoto: 155–172.

Olivares, L., Andreozzi, L., Damiano, E., Avolio, B. & Picarelli, L. 2003. Hydrologic response of a steep slope in unsaturated pyroclastic soils. In Picarelli (ed.), *Proceedings of Int. Conf. Fast Slope Movements, Prediction and Prevention for Risk Mitigation.* 391–397. Naples, May 2003. Patron editore, Bologna.

Olivares, L. & Damiano, E. 2004. Post-failure mechanics of landslides – flowslides in pyroclastic soils. Proceed. 9th Int. Symp. on Landslides, Rio de Janeiro, 2: 1343–1354, Lacerda et al (ed.), Balkema, Rotterdam.

Olivares, L. & Picarelli, L. 2003. Shallow flowslides triggered by intense rainfalls on natural slopes covered by loose unsaturated pyroclastic soils. *Géotechnique* 53(2): 283–288.

Olivares, L., Picarelli, L., Andreozzi, L., Avolio, B., Damiano, E. & Lampitiello, S. 2002. Scenari di pericolosità di frana in terreni sciolti di natura piroclastica. Proceed. XXI Convegno Nazionale di Geotecnica, L'Aquila: 173–181.

Omura, H. & Hicks, D. 1992. Probability of landslides in hill country. In Landslides, *Proc. Sixth Int. Symp. on Landslides*, Christchurch, New Zealand, Rotterdam: Balkema.

Orense, R., Shimoma, S., Maeda, K., Farooq, K. & Towhata, I. 2002. Laboratory model tests on rainfall-induced landslides. Proc. Int. Symp. "Landslide Risk Mitigation and Protection of Cultural and Natural Heritage", Kyoto: 61–72.

Parise, M., Coe, J.A., Savage, W.Z. & Varnes, D.J. 2004. The Slumgullion landslide (Southwestern Colorado, USA): investigation and monitoring. Proceed. int. workshop "Occurrence and Mechanisms of Flow-Like Landslides in Natural Slopes and Earthfills", Sorrento: 253–264, Picarelli (ed.), Patron, Bologna.

Parriaux, A., Tullen, P., Tacher, L. & Turberg, P. 2001. Hydrogeological modelling of slopesL a tool for movement forecasting. In *International Conference on Landslides, Causes, Impacts and Counter Measures,* 179–188, 17–21 June 2001. Davos, Switzerland.

Passalacqua, R. & Baretto, A. 2003. Landslides and rock-falls predictions by GIS in Western Liguria. In Picarelli

(ed.), *Proceedings of Int. Conf. Fast Slope Movements, Prediction and Prevention for Risk Mitigation.* 421–429. Naples, May 2003. Patron editore, Bologna.

Pelletier, J.D., Malamud, B.D., Blodgett, T. & Turcotte, D.L. 1997. Scale-invariance od soil moisture variability and its implications for the frequency-size distribution of landslides. *Engineering Geology* 48: 255–268.

Pellegrino, A., Picarelli, L. & Urciuoli. G. (2004c). Experiences of mudslides in Italy. Proceed. int. workshop "Occurrence and Mechanisms of Flow-Like Landslides in Natural Slopes and Earthfills", Sorrento: 191–206, Picarelli (ed.), Patron, Bologna.

Perini, P., Ferreli, L., Guarneri, E., Hormes, A., Michetti, A. & Rovinelli, W. 2001. Recent landscape evolution in the upper part of Valtellina (Italian Alps) and the characterization of geological and hydrological hazard. In *International Conference on Landslides, Causes, Impacts and Counter Measures,* 189–197, 17–21 June 2001, Davos, Switzerland.

Picarelli, L. 1988. Modellazione e monitoraggio di una colata in formazioni strutturalmente complesse. Proceed. Conf. "Cartografia e Monitoraggio dei Movimenti Franosi", Bologna: 119–130, L. Cascini ed.

Picarelli, L. 1993. Structure and properties of clay shales involved in earthflows. Proceed. Int. Symp. "The Geotechnical Engineering of Hard Soils-Soft Rocks", Athens, 3: 2009–2019, Anagnastopoulos et al. (eds). Balkema, Rotterdam.

Picarelli, L. 2000. Mechanics and rates of slope movements in fine grained soils. In *GeoEng 2000*, Technomic, Basel, 1618–1670.

Picarelli, L. 2001. Transition from slide to earthflow, and the reverse. Proceed. conf. "Transition from Slide to Flow – Mechanisms and Remedial Measures", Karadeniz Technical University, Trabzon.

Picarelli, L. 2004. Opening. Proceed. Int. Workshop "Occurrence and Mechanisms of Flow-Like Landslides in Natural Slopes and Earthfills", Sorrento: XVI–XVII, Picarelli (ed.), Patron, Bologna.

Picarelli, L., Di Maio, C., Olivares, L. & Urciuoli, G. 1998. Properties and behaviour of tectonized clay shales in Italy. Proceed. 2nd int. symp. "The Geotechnics of Hard Soils-Soft Rocks", Napoli, 3: 1211–1242, Evangelista & Picarelli (eds), Balkema, Rotterdam.

Picarelli, L., Leroueil, S., Urciuoli, G., Guerriero, G. & Delisle, M.C. 1997. Occurrence and features of shear zones in clay. Proceed. Int. Symp. "Localisation and Bifurcation Theory for Soils and Rocks", Gifu: 259–270.

Picarelli, L. & Napoli, V. 2003. Some features of two large earthflows in intensely fissured tectonized clay shales and criteria for risk mitigation. Proceed. Int. Conf. "Fast Slope Movements – Prediction and Prevention for Risk Mitigation", Napoli, 1: 431–438, Picarelli (ed.), Patron, Bologna.

Picarelli, L. & Russo, C. 2004. Remarks on the mechanics of slow active landslides and the interaction with man-made works. Proceed. 9th Int. Symp. on Landslides, Rio de Janeiro, 2: 1141–1176, Lacerda et al. (ed.), Balkema, Rotterdam.

Picarelli, L., Russo, C. & Urciuoli, G. 1995. Modelling earthflows based on experiences. Proceed. 11th ECSMFE, Copenhagen, 6: 157–162. Danish Geotechnical Society.

Picarelli, L., Urciuoli, G. & Russo, C. 2004. Effect of groundwater regime on the behaviour of clayey slopes. *Canadian Geotechnical Journal* 41(3): 467–484.

Picarelli, L., Urciuoli, G. Ramondini, M. & Comegna, L. 2005. Main features of mudslides in tectonized highly fissured clay shales. Landslides, in press.

Potts, D.M., Kovacevic, N. & Vaughan, P.R. 1997. Delayed collapse of cut slopes in stiff clay. *Géotechnique* 47(5): 953–982.

Potvin, J., Pellerin, F., Demers, F., Robitaille, D., La Rochelle, P. & Chagnon, J.Y. 2001. Revue et investigation complémentaire du site du glissement de Saint-Jean-Vianney. Proceed. 54th Geotechnical Soc. Conf., Calgary: 792–800.

Poulos, S.J. The steady state of deformation. *Journal of Geotechnical Engineering Division, ASCE* 107: 553–561.

Pradel, D. & Raad, G. 1993. Effect of permeability on surficial stability of homogeneous slopes. *ASCE J. Geotech Eng.* 119(2): 315–332.

Premchitt, J., Brand, E.W. & Chen, P.Y.M. 1994. Rain-induced landslides in Hong Kong 1972–1992. *Asia Engineer*, June: 43–51.

Roberds, W.J. 1990. Methods for developing defensible subjective probability assessments. *Proceedings of the Transportation Research Board, No. 1288*, 183–190. National Research Council, Washington DC.

Russo, C. 1997. Caratteri evolutivi dei movimenti traslativi e loro interpretazione meccanica mediante l'analisi numerica. PhD Thesis, Università di Napoli Federico II.

Saboya, F. Jr., Pinto, W.D. & Gatts, C.E.N. 2004. Fuzzy mapping of great areas susceptible to slope failure. In Lacerda, et al. (eds.), *Landslides evaluation and stabilization,* 371–378, Balkema Leiden.

Sassa, K. 2000. Mechanism of flows in granular soils. Proceed. GeoEng2000, int. conf. "Geotechnical and Geological Engineering", Melbourne, 1: 1671–1702. Technomic Publ. Co.

Savage, S.B. & Hutter, K. 1989. The motion of a finite mass of granular material down of a rough incline. *Journal of Fluid Mechanics* 199: 177–215.

Savage, W.Z., Godt, J.W. & Baum, R.L. 2004. Modelling time-dependent areal slope stability. In Lacerda et al. (eds.), *Landslides evaluation and stabilization,* 23–38, Balkema Leiden.

Siddle, H.J., Jones, D.B. & Payne, H.R. 1991. Development of a methodology for landslip potential mapping in the Rhondda Valley. In Chandler (ed.), Slope Stability, Isle of Wight, 137–148. Thomas Telford.

Silvis, G.F. & de Groot, M.B. 1995. Flow slides in the Netherlands: experience and engineering practice. *Canadian Geotechnical Journal* 32: 1086–1092.

Simonett, D.S. 1967. Landslide distribution and earthquakes in the Bewani and Torricelli Mountains, New Guinea. In Landform Studies from Australia and New Guinea. Jennings & Mabbutt (eds.). Cambridge University Press, p. 64–84.

Singh, N.K. & Vick, S.G. 2003. Probabilistic rockfall hazard assessment for roadways in mountainous terrain. Proceedings, 3rd Canadian Conference on Geotechnique and Natural Hazards, Canadian Geotechnical Society, Edmonton, p. 253–260.

Skempton, A.W. & Hutchinson, J.N. 1969. Stability of natural slopes and embankment foundations. Proc. 7th ICSMFE, Mexico City, 4: 291–340.

Skempton, A.W. & Petley, D. 1967. The strength along structural discontinuities in stiff clays. Proc. Geotechnical Conference, Oslo, 2: 55–69. Aas&Wahls Boktrykkeri, Oslo.

Sladen, J.A., D'Hollander, R.D., Krahn, J. & Mitchell, D.E. 1985. Back-analysis of the Nerlerk berm liquefaction slides. *Canadian Geotechnical Journal* 22: 564–578.

Sladen, J.A. & Hewitt, K.J. 1989. Influence of placement method on the in situ density of hydraulic sand fills. *Canadian Geotechnical Journal* 26: 453–466.

Soeters, R. & van Westen, C.J. 1996. Slope instability recognition, analysis, and zonation. In Turner &Schuster (eds.), Landslides Investigation and Mitigation. 129–177. Transportation Research Board, National Research Council.

Stapledon, D.H. 1995. Keynote paper: Geological modeling in landslide investigation. In Bell (ed.), *Proc. Sixth Int. Symp. on Landslides*, Christchurch 1992. 1499–1524. Rotterdam: Balkema.

Sun, H.W., Wong, H.N. & Ho, K.K.S. 1998. Analysis of infiltration in unsaturated ground.. *Proc. Annual Seminar on Slope Engineering in Hong Kong*, 101–109. Hong Kong: Balkema.

Stark, C.P. & Hovius, N. 2001. The characterization of landslide size distributions. *Geophysical Research Letters* 28: 1091–1094.

Sugai, T., Ohmori, H., & Hirano, M. 1994. Rock control on magnitude-frequency distribution of landslides. *Transactions Japanese Geomorphological Union* 15: 233–251.

Take, W.A., Bolton, M.D., Wong, P.C.P. & Yeung, F.J. 2004. Evaluation of landslide triggering mechanisms in model fill slopes. *Landslides* 1(3): 173–184.

Tarantino, A. & Mongiovì, L. 2003. Numerical modeling of shallow landslides triggered by rainfall. In Picarelli (ed.), *Proceedings of Int. Conf. Fast Slope Movements, Prediction and Prevention for Risk Mitigation.* 491–495. Naples, May 2003. Patron editore, Bologna.

Tavenas, F. 1984. Landslides in Canadian sensitive clays – a state-of-the-art. In *Proceedings of the 4th International Symposium on Landslides, Toronto.* Vol.1. BiTech Publishers Ltd., Vancouver, B.C., 141–153.

Taylor, R.K. 1984. Composition and engineering properties of British colliery discard. Report to National Coal Board, Mining Department.

Terranova, O. 2002. Risk analysis of potentially damaging rainfall events. In McInnes & Jakeways (eds.), *Instability Planning and Management, Seeking Sustainable Solutions to Ground Movements Problems,* 389–397, 20–23 May 2002. Isle of Wight, UK.

Trak, B. & Lacasse, S. 1996. Soils susceptible to flow slides and associated failure mechanisms. In Senneset (ed.), *Proceedings of the 7th International Symposium on Landslides.* Trondheim, Norway, 1: 497–506. Rotterdam: Balkema.

Tsui, P.C., Cruden, D.M. & Thomson, S. 1988. Mesofabric, microfabric and submicrofabric of ice-thrust bedrock, Highvale mine, Wabamun Lake area, Alberta. *Canadian Journal of Earth Sciences* 25: 1420–1431.

Turner, A.K. & McGuffey, V.C. 1996. Organisation of investigation process. In Turner & Schister (eds.), *Landslides Investigation and Mitigation.* 121–128. Transportation Research Board Special Report 247. National Academy Press.

Urciuoli, G. 2002. Strain preceding failure in infinite slopes. *Int. Journal of Geomechanics* 2(1): 93–112.

Urciuoli, G. & Picarelli, L. 2004. The shear strength mobilised in first-time slides in highly overconsolidated clays. Proc. "Advances in Geotechnical Engineering. The Skempton Conference", London, 2: 1005–1016.

Urciuoli, L., Picarelli, L. & Leroueil, S. 2005. Local soil failure before general slope failure. *Journal of Geotechnical and Geoenvironmental Engineering, ASCE*, submitted for publication.

Vallejo, L. 1984. Analysis of the mobilization of submarine landslides. Proceed. 4th Int. Symp. on Landslides, Toronto, 2: 361–366.

Vallejo, L. 1989. An extension of the particulate model of stability analysis for mudflows. *Soils and Foundations* 29: 1–13.

Varnes, D.J. 1978. Slope movement types and processes. Landslides, Analysis and Control, Transportation Research Board, Spec. Rep. n. 176: 11–23.

Varnes, D.J. and the International Association of Engineering Geology Commission on Landslides and Other Mass Movements 1984. Landslide hazard zonation: A review of principles and practice. Natural Hazards, 3, UNESCO, 63. Paris, France.

Walker, B.F. 2002. Probability calculations for a number of events. *Australian Geomechanics* 37(2), 83–86.

Wang, G. & Sassa, K. 2001. Factors affecting rainfall-induced landslides in laboratory flume tests. *Géotechnique* 51(7): 587–600.

Yamamuro, J.A. & Lade, P.V. 1997. Static liquefaction of very loose sands. *Canadian Geotechnical Journal* 34: 905–917.

Zêrere, J.L., Rodrigues, ML., Reis, E., Garcia, R., Oliveira, S., Vieira, G. & Ferreira, A.B. 2004. Spatial and temporal data management for the probabilistic landslide hazard assessment considering landslide typology. In Lacerda et al. (eds.), *Landslides evaluation and stabilization,* 117–124, Balkema Leiden.

Probabilistic stability analysis for individual slopes in soil and rock

F. Nadim
Norwegian Geotechnical Institute/International Centre for Geohazards, Oslo, Norway

H. Einstein
Department of Civil and Environmental Eng., Massachusetts Institute of Technology, Cambridge, USA

W. Roberds
Golder Associates, Seattle, USA

ABSTRACT: The state-of-the-art in probabilistic stability analysis for individual soil and rock slopes is reviewed. It is demonstrated that probabilistic analyses complement the conventional deterministic analyses in achieving a safe design, and add great value to the results by modest additional effort.

1 INTRODUCTION

The state-of-the-art in probabilistic slope stability analysis for individual soil and rock slopes is reviewed in this paper. Example applications demonstrate that probabilistic analyses complement conventional deterministic safety factor and/or deformation-based analyses in achieving safe design, and add great value to the results with a modest additional effort.

The paper starts with two sections providing necessary background knowledge, specifically Section 2 contrasts deterministic and probabilistic formats of slope stability analysis and Section 3 discusses sources of uncertainty. The central part of the paper is in Sections 4 and 5, which review approaches to slope stability analysis in continua (mostly soils) and discontinua (mostly rock masses), respectively. The discussions in Sections 4 and 5 are differently structured with emphasis on different probabilistic approaches in Section 4 and using the underlying mechanics as an introduction to probabilistic approaches in Section 5. Nevertheless, there are many common aspects, which appear throughout both sections and which lead to the conclusions in Section 7.

The readers should also consult the companion State of Art Papers 1 (A framework for landslide risk assessment and management), 4 (Travel distance and velocity) and 5 (Temporal probability and vulnerability) in these proceedings for completeness.

2 DETERMINISTIC AND PROBABILISTIC SAFETY FORMATS FOR SLOPE STABILITY ASSESSMENT

Often the stability situation for natural and man-made slopes is expressed by the factor of safety. The factor of safety is defined as the ratio of the characteristic resisting force to the characteristic load (driving force). The conventional approach does not address the uncertainty in load and resistance in a consistent manner. The ambiguous definition of "characteristic" values allows the engineer to implicitly account for uncertainties by choosing conservative values of load (high) and resistance parameters (low). The choice, however, is somewhat arbitrary. Slopes with nominally the same factor of safety could have significantly different safety margins because of the uncertainties and how they are dealt with. Duncan (2000) pointed out that "Through regulation or tradition, the same value of safety factor is often applied to conditions that involve widely varying degrees of uncertainty. This is not logical." As shown in Figure 1, a low safety factor does not necessarily correspond to a high probability of failure and vice versa. The relationship between the factor of safety and probability of failure depends on the uncertainties in load and resistance.

Probability theory and reliability analyses provide a rational framework for dealing with uncertainties and decision making under uncertainty. Depending
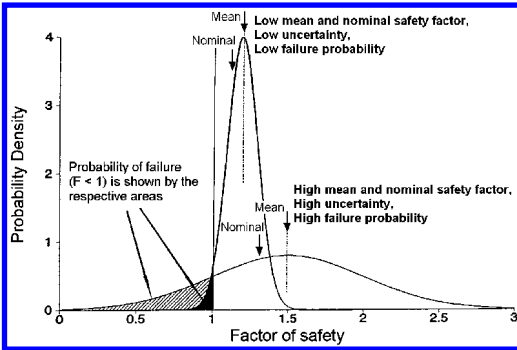
Figure 1. Comparison of two situations with different factors of safety and uncertainty.

Table 1. Comparative probabilities of failure for James Bay dikes, after Christian *et al.* (1994).

Caste	Factor of safety, F	Probability of failure, P_f
H = 6 m, single stage	1.58	$2.53 \cdot 10^{-2}$
H = 12 m, single stage	1.53	$4.73 \cdot 10^{-3}$
H = 23 m, multiple stage	1.50	$7.13 \cdot 10^{-4}$

on the level of sophistication, the analyses provide one or more of the following outputs:

– Probability of failure (or probability of unsatisfactory performance)
– Reliability index
– The most probable combination of parameters leading to failure
– Sensitivity of result to any change in parameters

Christian *et al.* (1994) gave an example of the use of comparative probabilities. Three heights of dikes were proposed for the James Bay project: 6, 12, and 23 m. The first two are single stage dikes; the last, a composite dike built in stages. Table 1 gives the estimated factors of safety and probabilities of failure for the three designs. Although the factors of safety are similar, the probabilities of failure are quite different. The 23-m dike has a lower probability of failure, which is not reflected in the factor of safety.

One way to use these results in engineering design is to consider the desirable target probability of failure (see State of Art Paper on "Risk criteria assessment and management" by Leroi *et al.* in this conference proceedings). However, the computed failure probability is sometimes difficult to interpret as it is dominated by our lack of knowledge. Therefore it is often more useful to compare probabilities of failure for different alternative courses of action than to rely on the absolute probability of failure.

Christian (2004) discussed the pros and cons of deterministic and probabilistic safety formats for the evaluation of the stability of existing slopes. The deterministic approach requires that a number of troublesome issues be addressed, including what is meant by the conventional factor of safety and how close is the slope to failure. Simple idealized examples and actual case studies show that slopes with high calculated factors of safety are not necessarily the safest. Well-established reliability methods, such as the first-order second-moment approximation (FOSM), the first-order reliability method (FORM) and Monte Carlo simulation are useful techniques for determining the reliability of the slope and for estimating the probability of failure. The reliability methods also reveal which parameters contribute most to the uncertainty in the stability. A simple prescription of a factor of safety to be achieved in all instances is not realistic and may lead to either overdesign or underdesign.

2.1 *Probabilistic analysis methods*

The first step in application of any probabilistic method is to decide on what constitutes unsatisfactory performance or failure. Mathematically, this is achieved by defining a performance function $G(X)$, such that $G(X) \geq 0$ means satisfactory performance and $G(X) < 0$ means unsatisfactory performance or "failure". X is a vector of basic random variables including resistance parameters, load effects, geometry parameters and modeling uncertainty.

In the methods described below, the failure mechanisms that are related to deterministic stability models serve as the basis for probabilistic analyses. There are, however, some probabilistic analyses which are not based on deterministic models, e.g. fault tree, statistical analysis, etc. It is informative in this context to emphasize that there is a significant difference between reliability analyses, essentially dealing with the probability of failure, and risk analysis which associates probability of failure with the consequences. While this paper deals mostly with probability of failure (reliability), it must be emphasized that this should always be done in the context of risk, see Roberds (2001), Roberds *et al.* (2002), and State of the Art Paper 1 in these proceedings. Vick (2002) provides a more extensive discussion of these issues.

2.1.1 *FOSM – reliability index*
The FOSM (First-Order, Second-Moment) approach (Ang & Tang 1984) provides analytical approximations for the mean and standard deviation of the safety factor as a function of the mean and standard deviations of the various input factors, and their correlations. One must assume the distribution function

Table 2. Risk format and reliability index β (Li & Lumb 1987).

G(X)	β
$R - S$	$\dfrac{F-1}{\sqrt{F^2 CoV_R^2 + CoV_S^2}}$
$\dfrac{R}{S} - 1$	$\dfrac{F-1}{F\sqrt{CoV_R^2 + CoV_S^2}}$
$\ln \dfrac{R}{S}$	$\dfrac{\ln F}{\sqrt{CoV_R^2 + CoV_S^2}}$

Figure 2. Relationship between reliability index, β, and probability of failure, P_f (assuming a Gaussian distribution).

for the safety factor beforehand to estimate the failure probability. The "reliability index", defined as

$$\beta = \frac{\mu_G}{\sigma_G} \tag{1}$$

in which μ_G and σ_G are respectively the mean and standard deviation of the performance function, is often used as an alternative risk measure to the factor of safety (Li & Lumb 1987, Christian *et al.* 1994, Roberds & Ho 1997, Duncan 2000).

The reliability index provides more information about the stability of the slope than is obtained from a factor of safety alone. It is directly related to the probability of failure and the computational procedures used to evaluate the reliability index reveal which parameters contribute most to the uncertainty in the factor of safety. This is useful information that can guide the engineer in further investigations. However, the reliability index estimated using the FOSM approach is not "invariant". Table 2 shows the reliability indices for different formats of the performance function using the FOSM method. R and S in the table represent respectively the total resisting force and the driving force acting on the slope. CoV_R and CoV_S in the table denote the coefficients of variation of the resisting and the loading forces respectively ($CoV = \sigma/\mu$, where σ denotes the standard deviation and μ denotes the mean value) and $F = \mu_R/\mu_S$.

2.1.2 *First- and second-order reliability methods (FORM and SORM)*

Hasofer & Lind (1974) proposed an invariant definition for the reliability index. The approach is referred to as the first-order reliability method (FORM). As mentioned earlier, the starting point for FORM is the definition of the performance function G(X), where X is the vector of basic random variables. If the joint probability density function of all random variables $F_x(X)$ is known, then the probability of failure P_f is given by

$$P_f = \int_L F_x(X)\, dX \tag{2}$$

where L is the domain of *X* where G(*X*) < 0.

In general, the above integral cannot be solved analytically. In the FORM approximation, the vector of random variables *X* is transformed to the standard normal space *U*, where *U* is a vector of independent Gaussian variables with zero mean and unit standard deviation, and where G(*U*) is a linear function. The probability of failure P_f is then (P[…] means probability that …):

$$P_f = P\left[G(\boldsymbol{U}) < 0\right] = P\left[\sum_{i=1}^{n} \alpha_i U_i - \beta < 0\right] = \Phi(-\beta) \tag{3}$$

where α_i is the direction cosine of random variable U_i, β is the distance between the origin and the hyperplane G(*U*) = 0, n is the number of basic random variables X, and Φ is the standard normal distribution function.

The vector of the direction cosines of the random variables (α_i) is called the vector of sensitivity factors, and the distance β is the reliability index. The relationship between the reliability index and probability of failure defined by Equation (3) is shown in Figure 2.

The square of the direction cosines or sensitivity factors (α_i^2), whose sum is equal to unity, quantifies in a relative manner the contribution of the uncertainty in each random variable X_i to the total uncertainty.

In summary the FORM approximation involves:

1. transforming a general random vector into a standard Gaussian vector,
2. locating the point of maximum probability density (most likely failure point, design point, or simply β-point) within the failure domain, and
3. estimating the probability of failure as $P_f \approx \Phi(-\beta)$, in which Φ(.) is the standard Gaussian cumulative distribution function.

An illustration of the design point and graphical representation of β is given in Figure 3.

65
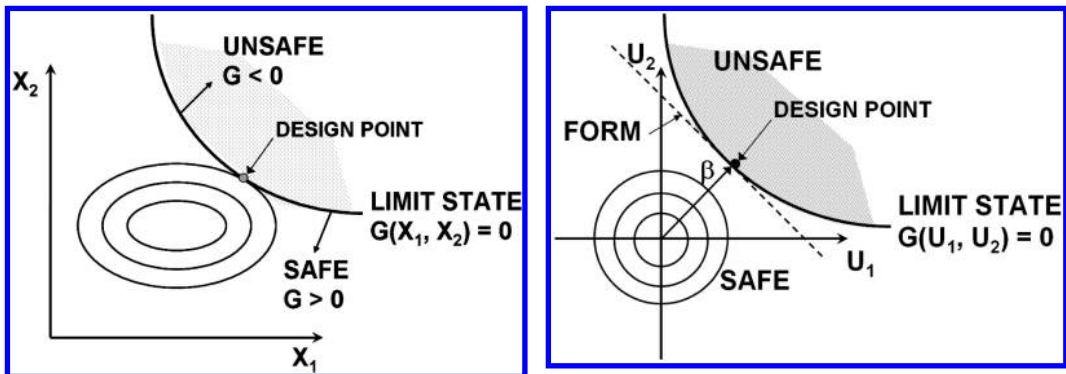
Figure 3. The FORM approximation (right) and definition of β and design point.
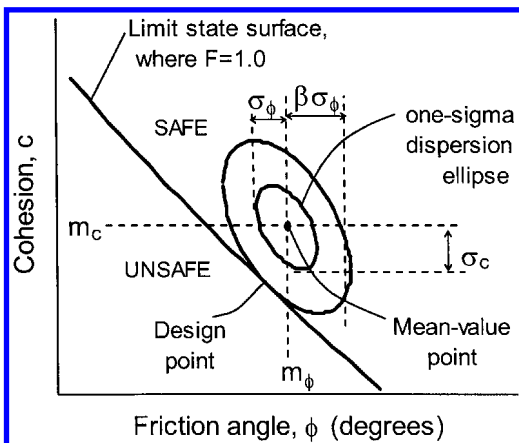
Figure 4. Illustration of β in the plane of original variables (Low 2003).

Low (2003) presented a method for finding the reliability index in the original space.

$$\beta = \min \sqrt{(X-m)^T C^{-1}(X-m)} \text{ for } \{X : G(X) \leq 0\} \quad (4)$$

in which $X = (x_1, x_2, \dots, x_n)$, m = mean vector of X, and C = covariance matrix of X.

Geometrically, for two-variable problems this can be interpreted as finding the smallest ellipsoid (of the probability distribution of the variables) tangent to the limit state surface, see Figure 4.

The key advantage of this formulation is that it can be implemented using built-in functions in EXCEL without programming and EXCEL is widely available on PCs (Phoon & Nadim 2004).

In the second-order reliability method (SORM), the limit state function is defined as in FORM, but the resulting limit state function is approximated by a second order function (Breitung 1984). For geo-problems the probabilities of failure obtained with SORM analyses have been very close to the values obtained with FORM (Lacasse & Nadim 1999).

2.1.3 *Monte-Carlo simulation*
A Monte-Carlo simulation is a repeated simulation of problem solution with randomly selected values of variables. A recent example is provided by El-Ramly *et al.* (2004). The method applies to all problems but can require a large number of simulations. Monte Carlo simulation can be optimized by stratified sampling techniques, for example Latin Hypercube sampling (Iman & Conover 1982). These "organized" sampling techniques considerably reduce the number of simulations required for a reliable distribution of the response.

Monte Carlo simulation is a powerful technique that is applicable to both linear and non-linear problems. The technique is implemented in some commercial slope stability analysis packages (e.g. Geo-Slope 2003). However, when the probability of failure is very small, the number of simulations required to obtain an accurate result directly is so large that, except for very simple (or simplified) problems, it renders the application impractical. In these situations the conditional probability of failure can be determined for various low probability scenarios, and then combined, considering the scenario probabilities.

3 SOURCES AND TYPES OF UNCERTAINTY

Slope failures often occur due to a combination of factors. The evaluation of slope stability requires estimating these factors; a task which always involves some uncertainty. Working with uncertainty is an essential aspect of engineering – the larger the uncertainties

66

and the closer to critical, the greater the need for evaluating their effect(s) on the results. Uncertainty in slope stability evaluation is due to:

– Inherent spatial and temporal variability
– Measurement errors (random and/or systematic)
– Statistical fluctuations
– Model uncertainty
– Uncertainty in load and load effects
– Omissions

It is conceptually useful to classify the uncertainty in the mechanical soil/rock properties and load effects (e.g. design seismic acceleration coefficient) into two groups:

Aleatory uncertainty, representing the natural randomness of a variable. For example, the variation of the soil characteristics in the horizontal direction is often aleatory, the variation in the peak acceleration of an earthquake is aleatory. The aleatory uncertainty is also called the inherent uncertainty. Aleatory uncertainty cannot be reduced.

Epistemic uncertainty, representing the uncertainty due to lack of knowledge on a variable. Epistemic uncertainty includes measurement uncertainty, statistical uncertainty (due to limited information), and model uncertainty. Epistemic uncertainty can be reduced, for example by increasing the number of tests or by improving the measurement method.

To characterize the uncertainties in soil and/or rock properties, the engineer needs to combine, in addition to actual data, knowledge about the quality of the data, knowledge on the geology and, most importantly, engineering judgment. The discussions below apply, in principle, to both soil and rock with the exception of Section 3, which deals with specific rock-related aspects.

3.1 *Uncertainties due to measurement of soil properties*

The first rule, when determining the uncertainties related to a soil property and using statistical methods, is to ensure that consistent data populations are used. Major uncertainties have been introduced in the past because of inconsistent data sets. The inconsistency can originate from different soils, different stress conditions, different test methods, stress history, different codes of practice, testing errors or imprecisions that are not reported, different interpretations of the data, sampling disturbance, etc.

It can be useful to establish data banks for different types of parameters or geographical locations, or to review the literature and compare one's values to values used by others. These estimates can be biased by the beliefs of the designer. The probabilistic analysis will, however, single out the importance of the hypotheses on the results.

Table 3. Typical coefficient of variation and distribution of soil properties.

Soil property	Soil type	PDF[*]	CoV (%)
Cone resistance	Sand	LN	Varies greatly from site to site
	clay	N/LN	
Undrained shear strength	Clay (triax)	LN	5–20
	Clay (Index s_u)[**]	LN	10–35
	Clayey silt	N	10–30
Ratio s_u/σ'_{vo}	Clay	N/LN	5–15
Plastic limit	Clay	N	3–20
Submerged unit weight	All soils	N	1–8
Friction angle	Sand	N	2–5
Void ratio, Porosity	All soils	N	7–30
Overconsolidation ratio	Clay	N/LN	10–35

[*] N = Normal, LN = Log-normal
[**] s_u estimated from index tests

A review was made on test results in NGI's files and data available from the literature. Suspicious data were eliminated. The variability, in terms of coefficient of variation (CoV) and the probability distribution functions (PDF) are listed in Table 3.

3.2 *Spatial variation of soil properties*

It is common to describe the soil property into a trend component and a random component with zero mean (Li & Lumb 1987, Lacasse & Nadim 1996, El-Ramly *et al.* 2002):

$$Y(x) = g(x) + \varepsilon(x) \tag{5}$$

where $Y(x)$ is the value of a soil property at a point $x = (x, y, z)$, $g(x)$ is the trend component and $\varepsilon(x)$ is the random component. Properties that vary over time (temporal variability) can be described in a similar way by replacing x with "time" in Equation 5. Temporal variability is discussed in the companion State of Art Paper 5 by Roberds *et al.*

Theoretical random field models (Vanmarcke 1984) and field data suggest that $\varepsilon(x)$ exhibits a spatial structure. The information about the spatial structure of the data can be exploited for stochastic interpolation between the data points and for reducing the uncertainty in soil parameters averaged over large areas or volumes. The degree of spatial correlation can be expressed through an autocovariance function, $C(r)$, where r is the vector of separation distance between two points. The normalized form of the autocovariance function $C(r)/C(0)$ is known as the autocorrelation function, where $C(0)$ is the variance of data. The

67

three autocovariance functions most often used to model soil properties are:

$$\text{Exponential: } C(r) = \sigma^2 e^{-(r/r_0)} \qquad (6a)$$

$$\text{Squared exponential: } C(r) = \sigma^2 e^{-(r/r_0)^2} \qquad (6b)$$

$$\text{Spherical: } C(r) = \sigma^2 \left[1 - \frac{3r}{2r_0} + \frac{r^3}{2r_0^3} \right] \qquad (6c)$$

Other autocorrelation functions (second-order autoregressive model, cosine exponential) can be found in Li & Lumb (1987). The parameter r_0 in the above equations is called "range" or "autocorrelation distance", i.e. distance beyond which the parameters become more-or-less independent. Table 4 lists typical values of autocorrelation distance (range) for cone penetration resistance quoted in the literature.

3.2.1 Effects of spatial averaging on uncertainty

The effect of the spatial variability on the computed performance (probability of failure and reliability index) of a slope is to reduce the variability of the soil shear strength. The reason for the reduction is that the variability is averaged over a volume, and only the averaged contribution to the uncertainty is of interest. This is shown schematically in Figure 5.

The scale of fluctuation shown in Figure 5 is the distance over which a soil property shows relatively strong correlation from point to point. The scale of fluctuation is between 1.4 and 2.0 times the autocorrelation distance for the exponential, squared exponential and spherical autocorrelation functions (Vanmarcke 1984).

The variance of the averaged random process may be obtained by applying a variance function $\gamma(T)$ to the variance of the underlying process. This reduction factor is referred to as the variance function:

$$\sigma_{X_T}^2 = \gamma(T)\sigma_X^2 \qquad (7)$$

Vanmarcke (1984) suggested that the variance reduction for most autocorrelations functions used in geotechnical engineering could be approximated by a unique curve, which results in a simple relation between reduction factor and distance over which the soil parameter is averaged. The simplified equation for the variance function $\gamma(T)$ is shown in Figure 6.

The results listed in Table 4 suggest that the scale of fluctuation for a typical engineering soil property within a geologically distinct soil unit is in the order of 10–100 m in the horizontal direction, and 0.5–5 m in the vertical direction.

Taking advantage of the spatial structure of a particular soil property (provided that such structure could be identified) would reduce significantly the aleatory uncertainty in the averaged property. It should be noted, however, that the epistemic uncertainty about the

Table 4. Autocorrelation distance for cone penetration resistance.

Soil	Direction	Autocorrelation distance (m)	Reference
Offshore soils	Horizontal	30	Høeg & Tang(1976), Tang (1979)
Offshore sand	Horizontal	14–38	Keaveny et al. (1989)
Silty clay	Horizontal	5–12	Lacasse & Lamballerie (1995)
Clean sand	Vertical	3	Alonzo & Krizek (1975)
Mexico clay	Vertical	1	Alonzo & Krizek (1975)
Clay	Vertical	1	Vanmarcke (1977)
Sensitive clay	Vertical	2	Chiasson et al. (1995)
Silty clay	Vertical	1	Lacasse & Lamballerie (1995)
Soft clay	Vertical	0.2–0.5	Gauer & Lunne (2002)
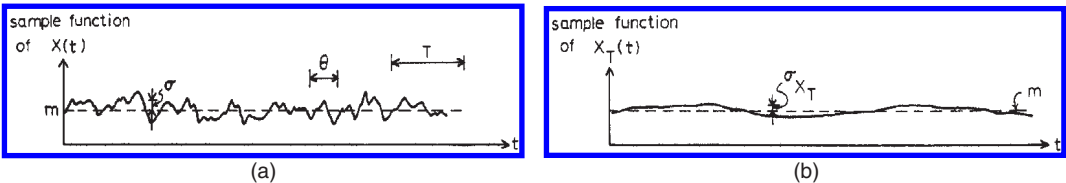
Figure 5. Effects of spatial averaging on reducing the variability (Vanmarcke 1984).
(a) Sample function of a random process X(t) with mean m, standard deviation σ, and scale of fluctuation θ. (b) Sample function of the local average process $X_{T(t)}$ obtained by averaging X(t) over a moving interval of size T.

68
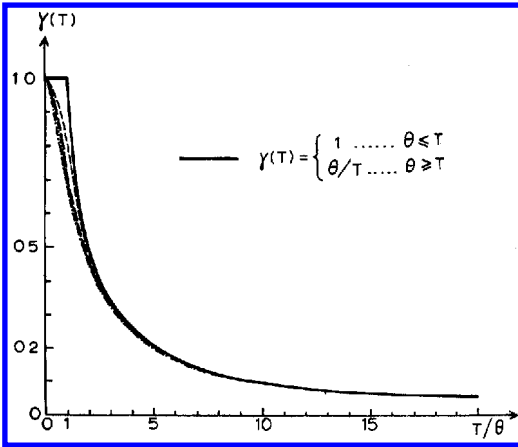
Figure 6. Variance function $\gamma(T)$ vs. normalized averaging interval T/θ for correlation functions defined by Eqs. 6a through 6c, and simplified equation for $\gamma(T)$ (Vanmarcke 1984).

mean value of soil parameters would not be reduced by spatial averaging.

El-Ramly *et al.* (2002) demonstrated the importance of the reduction in the uncertainty due to soil variability as a result of spatial correlation of soil parameters. The uncertainty in the computed value of foundation capacity was reduced by 70–80% when variance reduction was incorporated in the calculations to account for spatial correlation.

The importance of the point variability of a soil parameter on the computed probability of failure of a slope is reduced because the variability is averaged over a volume, and only the averaged contribution to the uncertainty is of interest. For quantities averaging linearly, the amount of variance reduction depends on the autocorrelation distance. Figure 7 (after El-Ramly *et al.* 2002) shows that as the averaging area is increased, the coefficient of variation of the local averages drops from 1.55 to 0.28 and the minimum and maximum values become closer to the mean.

It would be overly conservative to assume that the uncertainty in the average strength equals the
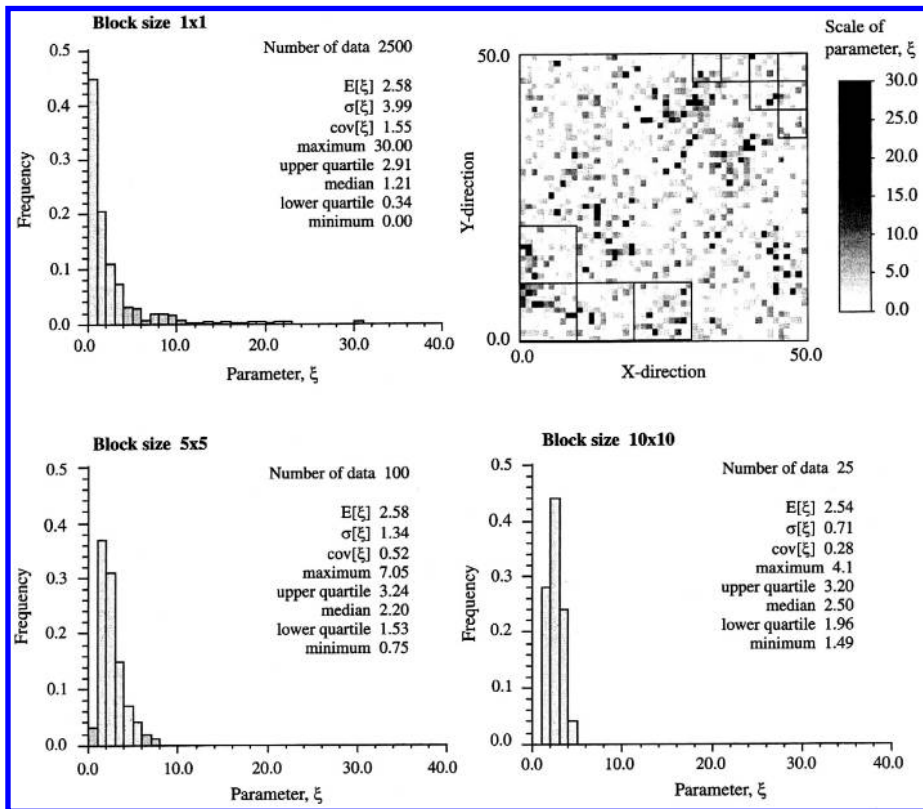
Figure 7. Variance reduction due to spatial averaging over blocks of sizes 1×1, 5×5 and 10×10 (El-Ramly *et al.* 2002).

69
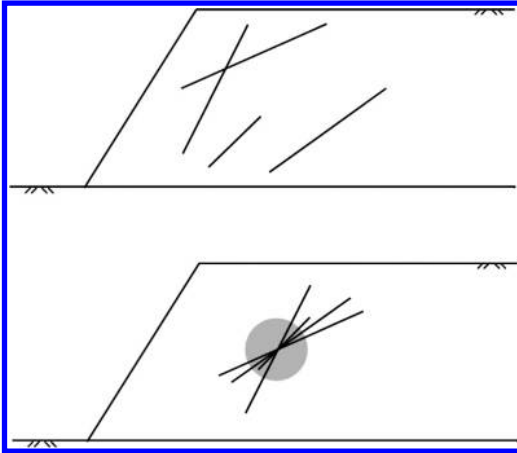
Figure 8. Lumped modeling. The actual association of orientation and location (top) is lost in the lumped (bottom) (Einstein 1996).

uncertainty in small-scale measurements, which some researchers have done in the past. It should also be noted that there will be some variability in the average strength on various potential failure surfaces, with the lowest average governing.

3.3 *Uncertainty in rock parameters*

Rock slope stability is strongly affected by discontinuities. The uncertainty in geometry and mechanical properties of discontinuities and the concept of "persistence" will be discussed in detail in Section 5. In this section only a particular aspect of the uncertainty in geometry of discontinuities and shear strength are discussed.

The geometry of rock joints are represented by attitude, spacing, extent (length or size) and aperture. Although the distributions of joint attitude, spacing and extent provide information on the uncertainty of joint patterns, they unfortunately eliminate an important piece of information. The distributions are so-called "lumped" models, i.e. data from joints are collected from different locations in space, but represented as if they were occurring all at the same location, thereby removing spatial correlation, see Figure 8. As in soil, care must be taken to identify the geological units that can be treated as statistically uniform units.

Another important parameter for stability of rock slopes is the shear strength of rock discontinuities Duzgun *et al.* (2002) developed an uncertainty assessment model for the peak friction angle of the rock discontinuities, in which the uncertainty is decomposed into two parts such as inherent variability and discrepancies between the laboratory measured and field values.

3.4 *Model uncertainty*

One of the main reasons to place focus on model uncertainty is that it is generally large, and in some cases it can be reduced. Model uncertainty is due to errors introduced by mathematical approximations and simplifications. In probabilistic analysis, model uncertainty is often represented by a parameter (error function) with a normal or lognormal distribution. Model uncertainty is difficult to assess and should be evaluated on the basis of:

– Comparisons of relevant model tests with deterministic calculations
– Expert opinions
– Relevant case studies of "prototypes"
– Information from the literature

To make a reliable estimate of model uncertainty, all relevant mechanisms should be identified and included in the probabilistic models. An important aspect of model uncertainty is the form it takes in the equilibrium function. Model uncertainty is best included in one of three ways:

– Factor on each random variable in the analysis
– Factor on specific components
– Global factor on the limit state function

A general discussion on model uncertainty in geotechnical engineering is provided in Phoon & Kulhawy (2003). More specific discussions on model uncertainty for evaluation of stability of soil and rock slopes are provided in Sections 4 and 5 below.

4 SLOPES IN CONTINUA – STABILITY OF SOIL SLOPES

An overview of deterministic slope stability analysis can be found in Duncan (1992) and Duncan (1996). The overview includes the factor of safety approach, equilibrium methods of slope stability analysis (Janbu's generalized method of slices, Bishop's method, Spencer's method, Morgenstern and Price's method among others), techniques for searching for the critical slip surface, both circular and non-circular, three dimensional analyses of slope stability, analyses of the stability of reinforced slopes, drained and undrained conditions, and total stress and effective stress analyses.

As long as a deterministic model to analyze a geotechnical problem exists, a probabilistic analysis can always be established. Figure 9 shows the steps involved in deterministic and probabilistic slope stability evaluation. Other probabilistic approaches (e.g. statistically-based) are also available.

70
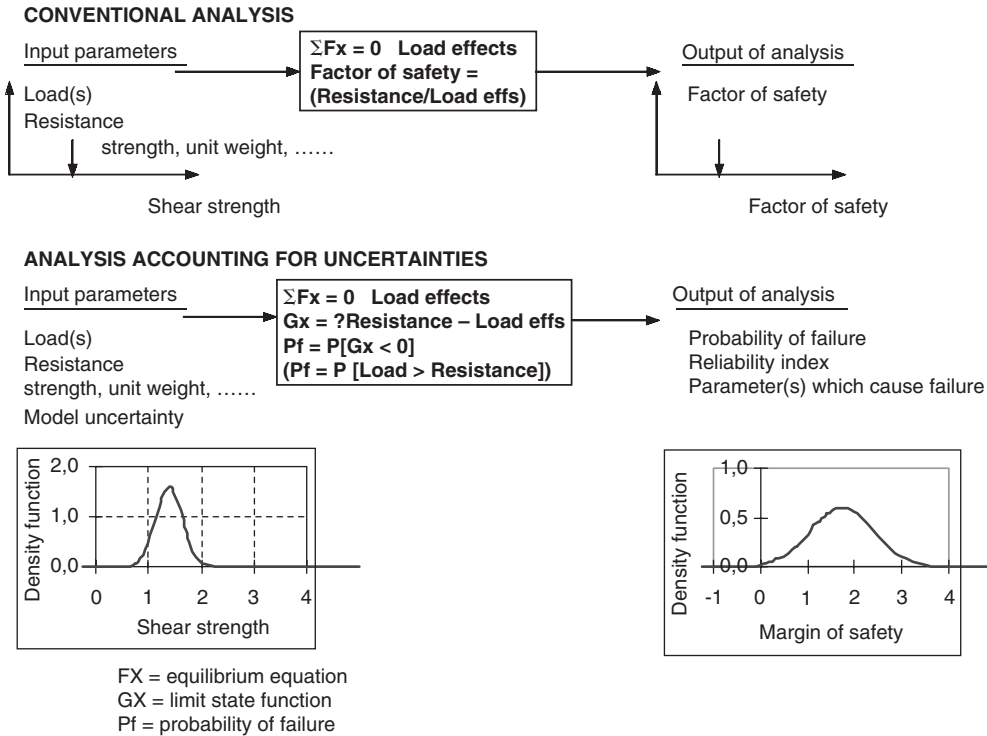
Figure 9.   Comparison of deterministic and probabilistic analyses.

4.1   *Examples of probabilistic slope stability analyses*

Many examples are available in the literature. Below are a few that illustrate the particular issues discussed.

FORM: Nadim & Lacasse (1999)
Nadim & Lacasse (1999) demonstrated the application of the FORM approach to undrained slope stability analysis. They evaluated the factor of safety and probability of failure of a slope consisting of 2 clay layers with assessed large-scale average property distributions for static and seismic conditions, Figure 10. Their analyses showed that the critical surface with the lowest safety factor is not identical with the critical surface that has the highest probability of failure, Figure 11. Slip surface 1, which cuts through both soil layers, has the lowest deterministic safety factor. However, due to spatial averaging effects, the uncertainty in the computed safety factor is significantly less than that for slip surface 2, which only cuts through the top layer.

FOSM: Christian et al. (1994)
Christian *et al.* (1994) showed the application of the FOSM method for designing embankment dams on

Variable (large-scale ave.)	Distribution function	Mean	CoV
s_u in Layer 1	Log-normal	75 kPa	25%
γ_t in Layer 1	Normal	17.5 kN/m^3	5%
s_u in Layer 2	Log-normal	150 kPa	15%
γ_t in Layer 2	Normal	17.5 kN/m^3	5%
Model uncertainty, ε	Normal	1.0	10%
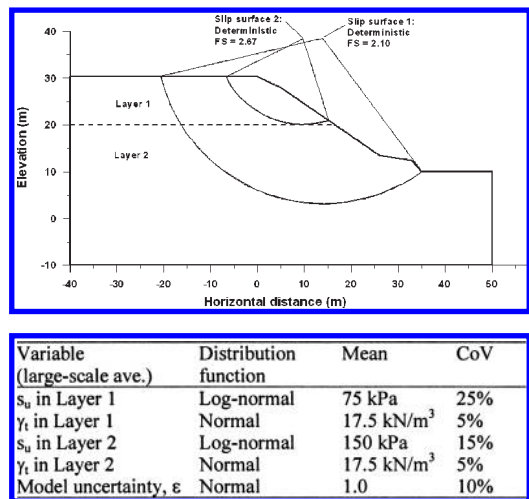
Figure 10.   Slope considered by Nadim & Lacasse (1999).

soft sensitive clays for the James Bay hydroelectric project in northern Quebec. Figure 12 shows the cross section for the single- or multistage construction of dikes for the project (Ladd *et al.* 1983).

71

The first alternative was the construction of the embankment in a single stage, either to a height of 6 or 12 m, with one berm. The distribution of large-scale average undrained shear strength values were obtained from field vane tests, and the stability analyses were done by the simplified Bishop method. The second alternative called for multistage construction.

The FOSM method was used to calculate the contribution to the variance in the safety factor from the variance of the variables.

Table 5 gives a summary of the reliability results and effects of model error for the three cases. The table shows that when the mean of the model uncertainty parameter is greater than unity (i.e. the model is biased), the computed reliability index can increase or decrease when the effects of model uncertainty are introduced. For an unbiased model, including model uncertainty will always lead to a smaller reliability index.
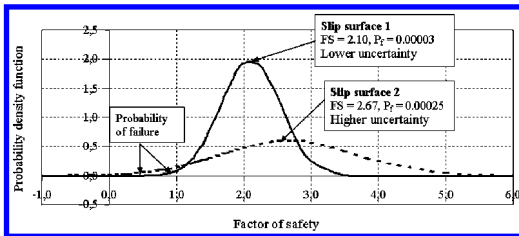
Figure 11. Computed distribution of safety factors for slip surfaces 1 and 2 of Fig. 10 (Nadim & Lacasse 1999).
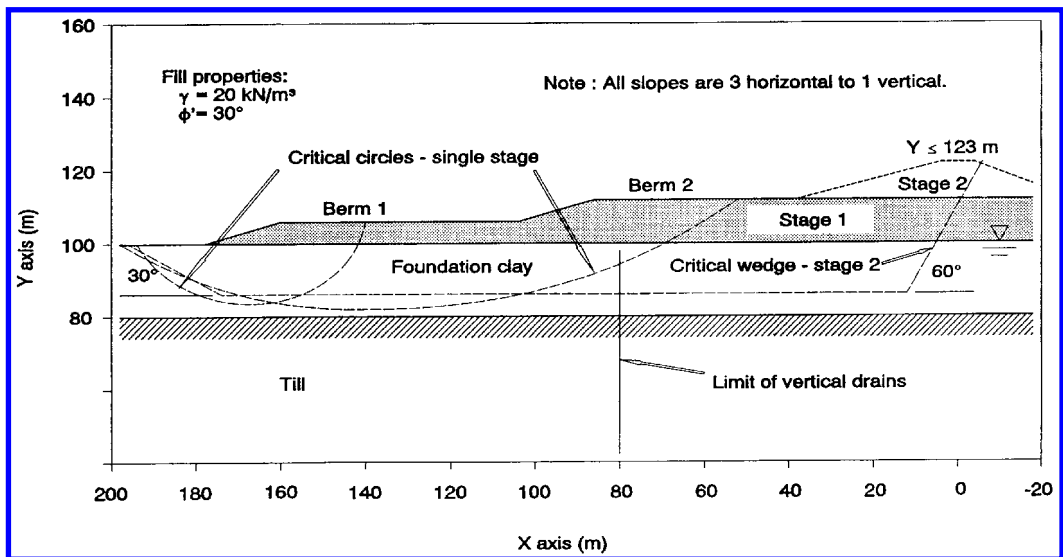
Figure 12. Cross section of SEBJ design problem (Ladd *et al.* 1983).

Table 5. Summary of the reliability results and effects of model error for the three cases considered by Christian *et al.* (1994).

| | E[F][a] | Reduced spatial | σ^2[F] (variance of safety factor) | | | | |
			Prior systematic	Model error[b]	Total	$\beta = (E[F] - 1.0)/\sigma[F]$
Sgl., H = 6 m						
without model error	1.500	0.050	0.024	–	0.074	1.84
with model error	1.575	0.050	0.024	0.012	0.086	1.96
Sgl., H = 12 m						
without model error	1.453	0.009	0.020	–	0.029	2.66
with model error	1.526	0.009	0.020	0.011	0.041	2.60
Multi, H = 23 m						
without model error	1.427	0.0012	0.0122	–	0.0134	3.69
with model error	1.498	0.0012	0.0012	0.011	0.0244	3.19

[a] E[F] = expected value of safety factor with model error = E[F] without model error × 1.05
[b] $\sigma^2_{model\ error}$ = (0.07 × increased E[F])^2

72

To extrapolate their results to other conditions, Christian *et al.* (1994) considered two possible simplifications. One could assume that for a basic geometry the variance and standard deviation of F is constant and calculate the reliability index as:

$$\beta = \frac{E[F]-1.0}{\sigma[F]} \qquad (8)$$

On the other hand, one could assume the coefficient of variation is constant and apply

$$\beta = \frac{E[F]-1.0}{E[F] \cdot CoV[F]} \qquad (9)$$

The consequences of the two assumptions are shown on Figure 13. Figure 14 shows the projected nominal probabilities of failure as functions of the computed factors of safety for the example stability problems.
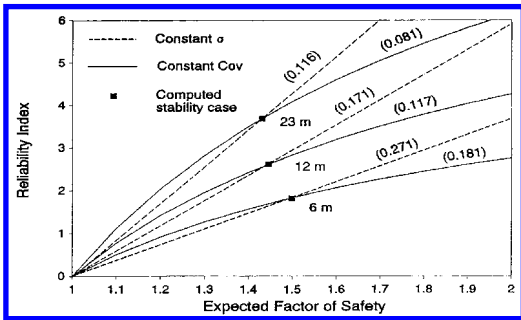
Figure 13.   Projection of reliability index versus factor of safety (without model error) (Christian *et al.* 1994).
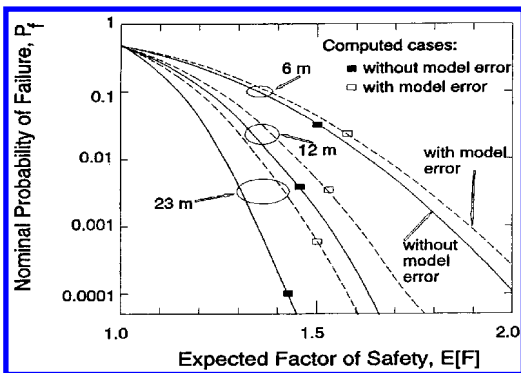
Figure 14.   Nominal probability of failure versus computed factor of safety for Example problems (Christian *et al.* 1994).

The probabilities are computed on the assumption that F is normally distributed. Curves are plotted for results both with and without the effects of model uncertainty. Note that the model used by Christian *et al.* (1994) is biased. Otherwise inclusion of model error would reduce the reliability index, not increase it. For further discussion of the problem shown in Figure 12, see Duncan *et al.* (2003).

Random field modeling of soil properties: Li & Lumb (1987)

Li & Lumb (1987) applied the FORM approach to a case study of the Selset landslide reported in Skempton & Brown (1961). The following assumptions were used in their analysis:

1. In the analysis, only the effective cohesion (*c*), the density (γ), the coefficient of shearing resistance (*t*) and the pore pressure (*u*) were taken as random variables. Other loads are taken as zero.
2. For practical purposes the strength components *c* and *t* were regarded as independent. The assumption of mutual independence simplifies the computation and errs on the conservative side because they would typically be negatively correlated. The cross correlation of γ with *c* and *t* can be neglected without incurring significant errors.
3. The soil properties were modeled as random fields.
4. The pore water pressure was speculated to consist of two random components with different scales of fluctuation. In theory, the pore-water pressure can also be modeled as a random field. In the analyses a simple model was used where the pore-water pressure ratio, described as the ratio of the excess pore water pressure to the effective vertical stress in hydrostatic condition, was assumed to be perfectly spatially-correlated within the slope, i.e. it was regarded as a single variable.

Since the scale of fluctuation δ was not known, two values of δ for undrained shear strength were used (1.5 m and 4.6 m) to calculate β. Figure 15 shows that the computed failure probability is very sensitive to the scales of fluctuation.

The result indicated that the locations of the critical slip circle with minimum safety factor F and the slip circle with minimum reliability index β (highest failure probability) are not coincident, but very close to each other. Consequently, the location of the critical slip surface with the minimum F can be used as a good initial trial location for the search for the slip surface with the minimum reliability index.

Li & Lumb (1987) concluded that the main advantage of using a probabilistic approach is to provide an operational procedure by which the uncertainties of the design can be considered in the analysis. It also helps the engineer to quantify his/her experience by way of building up knowledge on the values of the

73

statistical parameters such as the covariance or scales of fluctuations of the local soils.

Monte Carlo Simulation: El-Ramly et al. (2003)
El-Ramly *et al.* (2003) performed probabilistic slope analysis using Monte Carlo simulation to evaluate the stability of a section of the Syncrude Tailings Dyke in Fort McMurray, Canada, Figure 16. The dyke was approximately 44 m high. The performance of the dyke was governed by uncertainties about material properties and pore-water pressures, in particular in the disturbed clay-shale (Kca) layer, and the sandy till at toe of the dyke.

The residual shear strength of this material was evaluated from shear box tests on 80 specimens. Based on

Figure 15. Variation of safety factor and failure probability with height of slope for Selset landslide (Li & Lumb 1987).

the histogram of the results obtained from the tests, and spatial averaging to the appropriate scale, the residual friction angle was assumed to have a lognormal probability density function with a mean of 7.5° and a standard deviation of 2.1° in the Monte Carlo simulations.

Substantial amounts of pore pressure data were available from numerous pneumatic and standpipe piezometers along the dyke. Figure 17 shows a plot of the pore pressure ratio r_u, defined as the ratio of excess pore pressure to effective vertical stress for hydrostatic conditions, at a section along the dyke profile in March of 1994. The measurements are scattered. It seems that the pore pressure ratio tends to decrease towards the dyke toe. A linear trend fitted to the data using the method of least squares is shown on the plot. The standard deviation of the pore pressure ratio around the mean trend is calculated to be 0.12.

The measured peak friction angles of the sandy till layer belonged to different statistical populations and grouping them together increased the estimate of uncertainty. When all measurements were combined for an approximate statistical assessment, the measured values ranged between 33.3° and 39.2°. The mean and standard deviation of the peak friction angle were calculated to be 35.7° and 2°, respectively.

The pore water pressure in the sandy till layer was assessed from data from 14 piezometers at different depths and locations along Section 53+000E. The pore pressure ratio varied between 0.1 and 0.46 with a mean of 0.30. Due to a large increase in pore pressure ratio towards the dyke toe, the data were divided into two subgroups and the pore pressure ratio modeled by two random variables representing the middle portion of the slope and the toe area respectively.

A model of dyke geometry, soil stratigraphy and properties, and pore water pressures was developed in an Excel spreadsheet. The Bishop method of slices was used in the model with the limit equilibrium equations rearranged to account for the noncircular portion of the slip surface. Five input parameters are considered
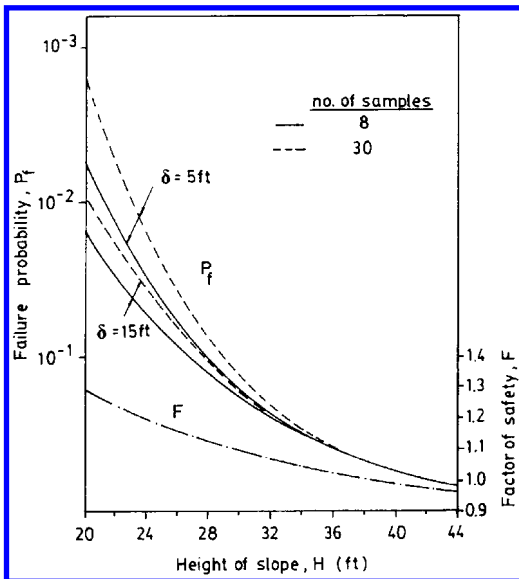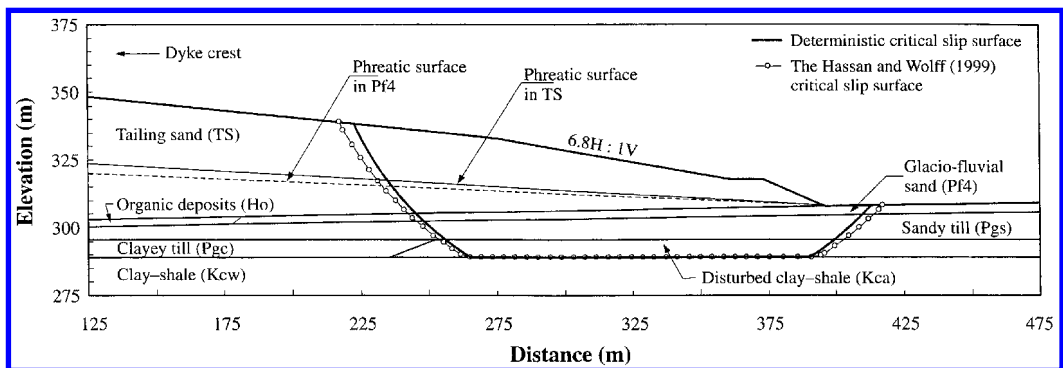
Figure 16. Dyke profile and stratigraphy of the Syncrude Tailings Dyke analyzed by El-Ramly *et al.* 2003.

74

variables: the residual friction angle of Kca clay-shale, the peak friction angle of the sandy till, the residual pore pressure ratio in the Kca clay-shale and the pore pressure ratios at the middle and at the toe of the slope in the sandy till. Monte Carlo simulation was performed using @Risk and the prepared spreadsheet model. Figure 18 shows the histogram of results and the inferred probability distribution function of the factor of safety. Figure 19 shows the probability of unsatisfactory performance, based on the results of only 25 simulations. The mean probability of unsatisfactory performance is estimated to be $1.6 \cdot 10^{-3}$, with the 95% confidence interval around the mean ranging between $1.5 \cdot 10^{-3}$ and $1.7 \cdot 10^{-3}$.

Regional classification of slopes: Poschmann et al. (1983)

In parts of Ontario, Canada, the slope stability has been classified by means of safety factors calculated on the basis of regional shear strength parameters (Poschmann *et al.* 1983). Stability analysis for 400 stable and 1000 unstable slopes were carried out using regional shear strength parameters of $c' = 10$ kPa, $\phi' = 33°$, $\gamma = 16.45$ kN/m^3, and pore pressure ratio $r_u = 0.62$.
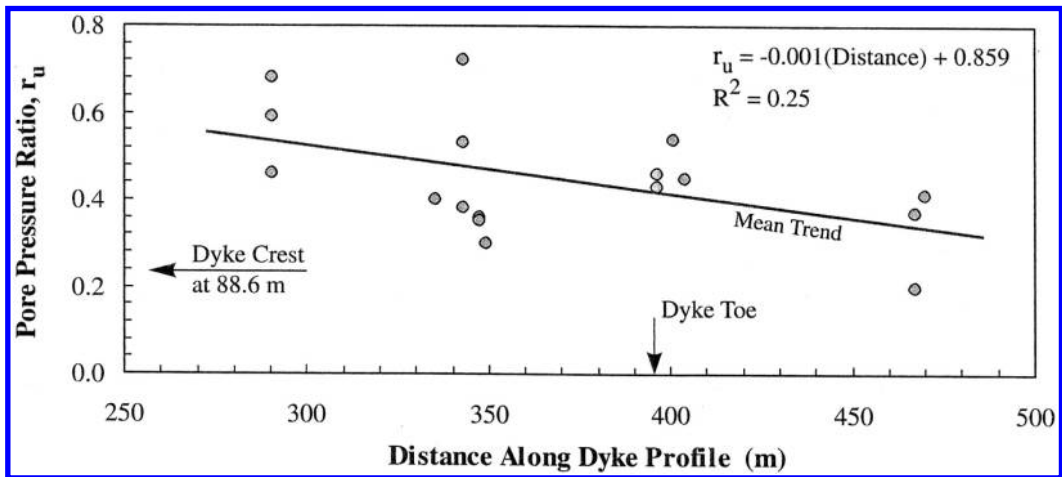
Figure 17. Profile of pore pressure ratio in the Kca layer along dyke cross-section, March 1994 (El-Ramley *et al.* 2003).
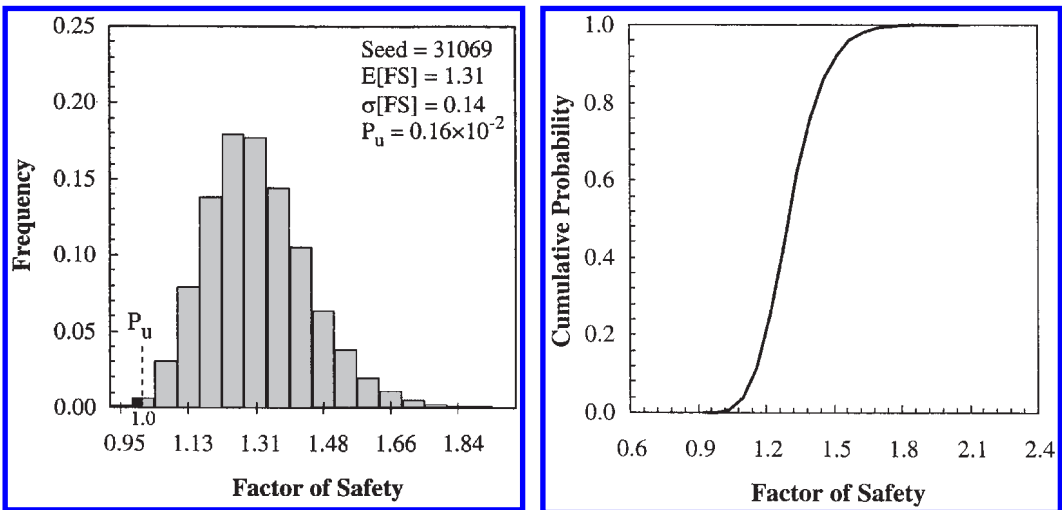
Figure 18. Histogram and probability distribution function of the factor of safety – number of simulation iterations equals 34000 (El-Ramly *et al.* 2003).

75

The results of this analysis are shown in Figure 20. A similar hazard rating system has been developed in Hong Kong (Roberds 2002).

This type of calculation works in a general sense, but the stability for individual slopes may be underestimated or overestimated. It is emphasized that this type of stability classification is semi-quantitative and its use is restricted to be a guide for planning, not as a basis for engineering design.
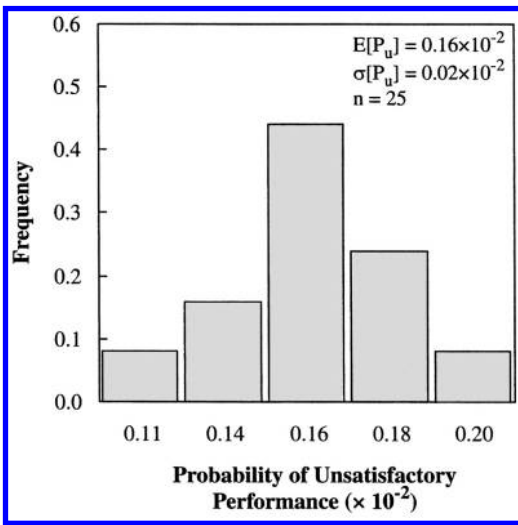
Figure 19.   Histogram of the probability of unsatisfactory performance (El-Ramly *et al.* 2003).

Effects of water level and correlation among parameters: Rahhal & Germani (2003)

Rahhal & Germani (2003) studied the stability of a 24-m long and 12-m high clayey slope with a phreatic surface. A parametric study was conducted to investigate the effects of the presence of the water, uncertainty in the level of phreatic surface, variation of the correlation coefficient between cohesion and pore water pressure, and variation of the correlation coefficient between angle of friction and pore water pressure.

Correlation coefficients between cohesion and pore water pressure (ρ_{cu}), friction angle and pore water pressure ($\rho_{\Phi u}$), cohesion and friction angle ($\rho_{c\Phi}$) were varied between 0 and -1. Figure 21 shows that $\rho_{c\Phi}$ has asymptotic behavior for β. The reliability index β is higher both for a negatively greater correlation coefficient $\rho_{\Phi u}$ and a negatively greater correlation coefficient ρ_{cu}.

The most probable failure surface for different correlation coefficients moves further apart from the deterministic failure surface: the more negative $\rho_{c\Phi}$, the shallower the critical failure surface, see Figure 22. The deepest failure surface was obtained in the deterministic calculations. The most probable failure point (design point) was strongly affected by $\rho_{c\Phi}$, and not by $\rho_{\Phi u}$ or ρ_{cu}.

The probability of failure increased with a shallower water table level. The reliability index β for the clayey slope was calculated for different positions of the water table and the results are shown on Figure 23. The relationship between the reliability index for the
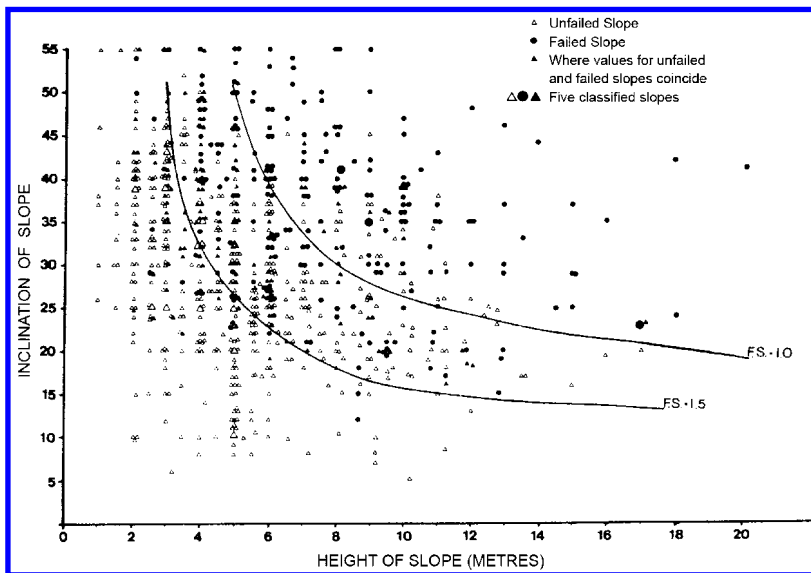
Figure 20.   Analysis of stable and failed slopes using regional shear strength parameters (Poschmann *et al.* 1983).

76

slope and the position of the water table is almost linear for this case.

Submarine slopes and sensitivity factors: Nadim et al. (2005)

The use of reliability methods for evaluation of soil slope stability is more common in the offshore petroleum industry than in the conventional land-based engineering, e.g. Nadim *et al.* (2002) and Nadim *et al.* (2005). The huge investments and potentially catastrophic consequences of failure require that the risk associated with potential seabed instabilities are quantified to the extent possible.

A comprehensive probabilistic slope stability analysis was carried out by Nadim *et al.* (2005) for the slopes in the Ormen Lange gas field in the Norwegian Sea. The Ormen Lange gas field is located within the slide scar of the enormous Storegga Slide that took place about 8200 years ago. There are strong indications that the Storegga slide generated a tsunami wave hitting the coastlines of Norway, Scotland and the Faeroes. The headwalls of the Storegga slide are steep and their current deterministic safety factor could be as low as 1.5.

Nadim *et al.* (2005) evaluated the probability for new submarine slides along the suggested pipeline routes from the Ormen Lange field and their potential consequences, Figure 24. The potential triggering mechanisms for inducing a submarine slide in the area were extensively evaluated. Both natural triggers (such as earthquake, sea floor displacements due to tectonic faulting, temperature increase caused by climate change, excess pore pressure due to rapid sedimentation during glacial periods, and gas hydrate melting due to climate change with increased sea water temperature after glacial periods) and man-made triggers (such as
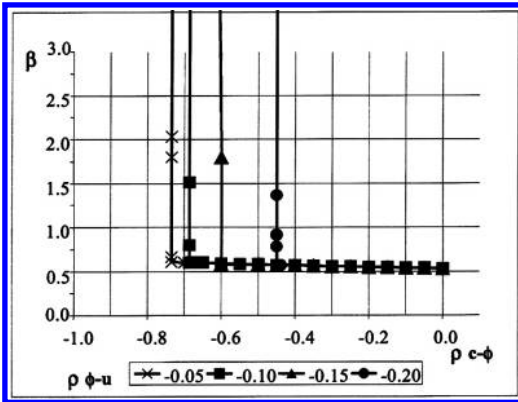
Figure 21. Reliability Index β as a function of correlation coefficients $\rho_{\Phi u}$ and $\rho_{c\Phi}$ (Rahhal & Germani 2003).
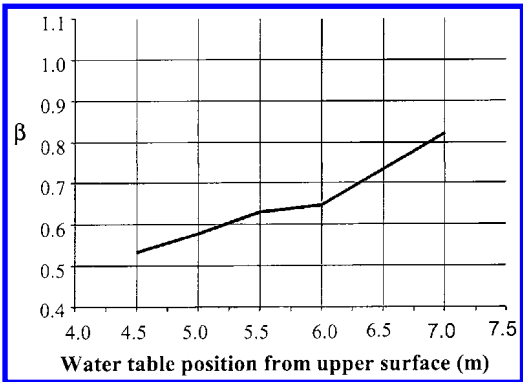
Figure 23. Variation of the reliability index β as a function of water table level (Rahhal & Germani, 2003).
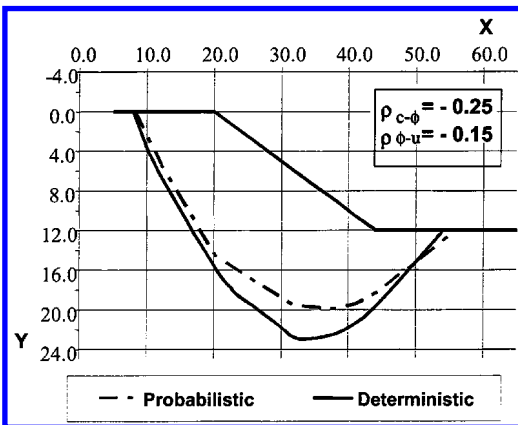
Figure 22. Deterministic and probabilistic failure mechanisms.
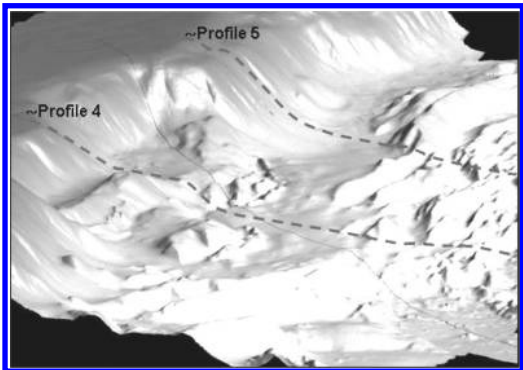
Figure 24. Seabed topography showing alternative pipeline routes in the Ormen Lange area and the critical profiles analyzed (Nadim *et al.* 2005).
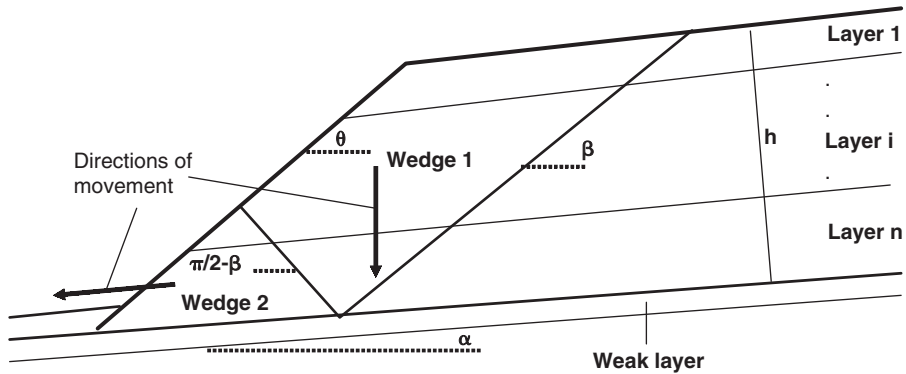
Figure 25.   The 2-wedge failure mechanism considered by Nadim *et al*. (2005).
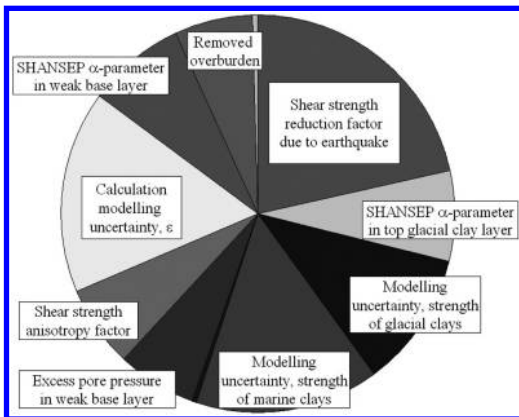
Figure 26.   Sensitivity factors for random variables – Profile 5, shallow failure mechanism, post-earthquake stability.

Figure 27.   Effect of discontinuity space scale: (a) needs to be treated as discontinuum, (b) needs to be treated as continuum.

sections along the pipeline route is 10^{-5}-10^{-6}. The random variables contributing most to the uncertainty in the safety margin were identified through the sensitivity factors, as shown in Figure 26.

5   SLOPES IN DISCONTINUA – STABILITY OF ROCK SLOPES

The distinction between rock and soil slopes is mostly related to the prevalence of discontinuities (weak planes) in rock masses. These discontinuities will usually be joints (fractures) but can also be faults or bedding planes and foliation surfaces. There are soils containing distinct weakness surfaces and these are often treated with the same or similar approaches as discontinuous rock masses. On the other hand, if the spacing of the rock discontinuities is small relative to the scale of the slope, or other engineering problems, it is possible to treat these with continuum approaches based on soil mechanics principles (Fig. 27).

Discontinuum approaches require a distinction between geometrical and mechanical properties (Fig. 28). Since nature defines the potential weakness surfaces (individual fractures etc.), stability problems in discontinua are to some extent better defined than

anchor forces from ships or floating platforms, rock-filling for pipeline supports, temperature change around wells in the field development area, underground blow-out, reservoir depletion and subsidence, including induced seismicity) were considered. Of all the potential triggering mechanisms considered, only a strong earthquake was shown to be realistically capable of triggering a new slide.

The critical failure mechanism for the slopes analyzed was sliding on a weak marine clay layer and formation of a 2-wedge mechanism as shown on Figure 25. The shear strength of the clay layers was derived using the SHANSEP approach (Ladd & Foott 1974).

Nadim *et al.* (2005) used a closed-form solution for the safety factor of the 2-wedge mechanism shown on Figure 25 and the FORM approximation to estimate the annual failure probability of the critical slopes. The analyses showed that the annual probability of earthquake-induced failure for the most critical

78

Figure 28. Discontinuity modeling: discontinuity patterns and individual discontinuity.
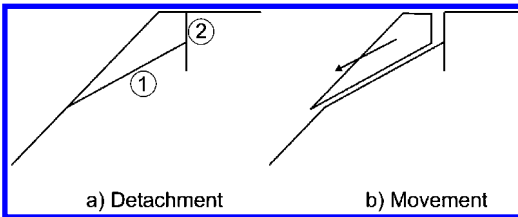
Figure 29. Detachment and movement: (a) detach, start to slide at 1, separate in tension at 2, (b) move.
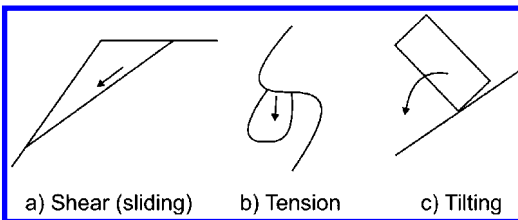
Figure 30. Detachment mechanisms: (a) shear (sliding), (b) tension, (c) tilting.

Figure 31. Translational (1) and rotational (2) sliding of a block.
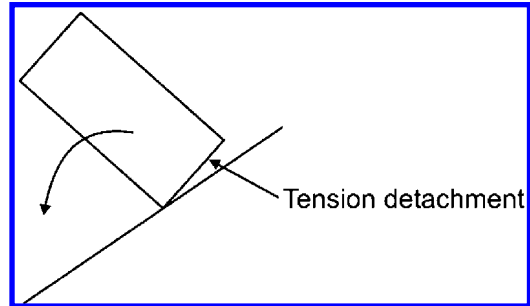
Figure 32. Tension detachment during tilting.

those in continua where "searches for critical failure surfaces" have to be conducted in the analyses. On the other hand, the discontinuities vary in space producing significant inherent spatial uncertainty. As will be seen later in this section, the uncertainties which might be probabilistically expressed are related to the spatial, geometric variability of the discontinuity pattern and the variability of the mechanical properties of the individual discontinuity and, possibly, the intact rock, as well as slopes geometry and loads.

5.1 *Mechanisms*

In description of the basic failure mechanisms in rock (discontinuum) slopes, it is necessary to distinguish between the detachment (initiation) mechanisms and the following movement mechanisms (Fig. 29) as these

mechanisms may be quite different. Nevertheless, many analyses inherently combine the two. The separate treatment below is done for reasons of clarity.

5.1.1 *Detachment*
Detachment can occur in shear, tension or tilting (Fig. 30). Shear may be either translational, rotational or both (Fig. 31). While tension detachment can occur by itself, tilting detachment usually occurs in combination with tension (Fig. 32). As a matter of fact, rather than distinguishing tilting as such, one could call this rotational tension detachment and thus have a more logical categorization: shear and tension detachment each with the subcategories of translational/rotational. Since tilting, and the subsequent toppling, is an often-used description, it will be used here interchangeably with rotational tension.

At this point, one of the most important complications of discontinuum behavior has to be introduced, namely "persistence". This expresses the fact that most discontinuities are not through-going/continuous separations of the parent rock along a plane, but consist of discontinuous (fractured) and intact rock (rock bridge) portions. This is schematically shown in Figure 33. It is, therefore, necessary to look at the above-mentioned shear and tension mechanisms both for persistent and impersistent discontinuities.

Shearing along persistent discontinuities and the discontinuous parts of impersistent discontinuities, is governed by the material properties of the adjacent
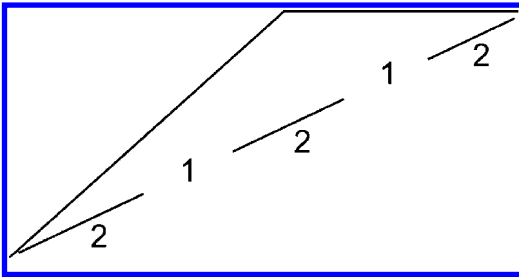
Figure 33. Persistence. Sketch shows impersistent discontinuity with intact rock bridges (1) and discontinuous portions (2).
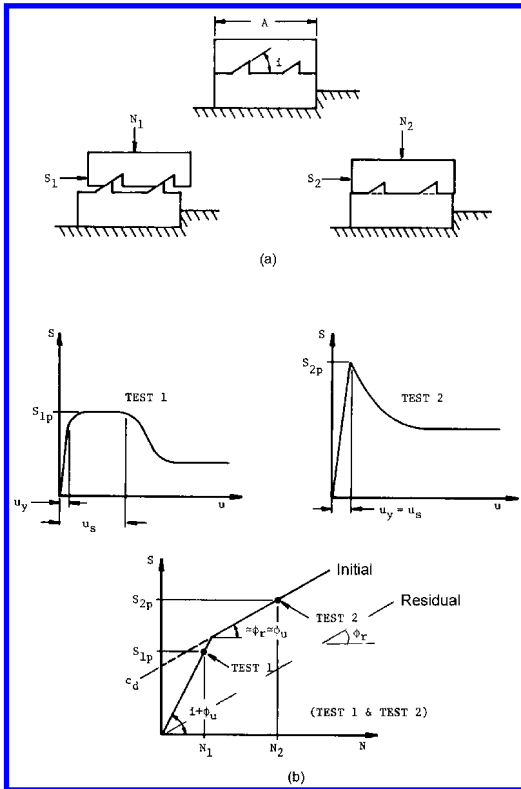
Figure 34. Shearing resistance of individual rough discontinuity.

rock and the geometry (deviation from an ideal planar surface often called roughness) of the discontinuity. This interaction of material and geometric properties leads, in simplified terms, to bilinear or curved τ-σ envelopes (see e.g. Goldstein *et al.* 1966, Patton 1966), see Figure 34. As will be also seen later, the geometry or roughness is spatially variable and can be considered

in appropriate probabilistic approaches. Also shown in Figure 34 is the residual τ-σ envelope which is important to movement beyond the initial detachment. Detachment of a persistent discontinuity in shear will occur when the applied shear stress (force) exceeds the shearing resistance for the particular normal stress (force), which applies both to translation and rotation.

The nonlinear shear failure behavior of rock discontinuities makes the use of linear Coulomb criterion questionable. Especially, the existence of cohesion for rock discontinuities is only satisfied when there are perfectly mating discontinuities such as undisturbed bedding planes. As an alternative to Coulomb, the Barton-Bandis (Barton & Bandis 1990) nonlinear shear failure criterion is mostly considered in practice since it is relatively simple compared to other nonlinear shear failure criteria proposed in the literature (e.g. Jaeger 1971, Hsu-Jun 1979, Swan 1981, Dight & Chiu 1981, Swan & Zonqi 1985, Davis & Salt 1986, Desai & Fishman 1987, Kane & Drumm 1987, Plesha 1987, Benjelloun *et al.* 1990, Handanyan *et al.* 1990, Hack & Price 1995, Power & Hencher 1996, Dong & Pan 1996, Maksimovic 1996, Archambault *et al.* 1996).

Tensile failure (detachment) of a persistent discontinuity simply occurs when the applied normal, tensile force (stress) exceeds the existing normal compressive force (stress) the latter usually caused by gravity. This consideration also applies to rotational tension.

Things become more complicated when dealing with the intact rock bridges. In principle, shearing through intact rock could be expressed by exceeding the shearing resistance represented by a linear Coulomb or curved envelope in the τ-σ relation, i.e. the shear stress exceeds the shear resistance along a plane through the intact rock bridge. As has been originally shown by Lajtai (1969) and as has been confirmed by many other researchers (e.g. Nemat-Nasser & Horii 1982, Einstein *et al.* 1980) this occurs only at relatively high normal stresses. At low normal stresses, intact rock bridge failure occurs through initiation and propagation of tensile cracks which coalesce to form a failure surface (Fig. 35). This leads to lower quasi-shear resistance (if plotted in a τ-σ diagram) than assuming shearing failure along the fracture surface. Very often failure does not occur along a plane through the rock bridge between two discontinuous portions but stepping up or down between the discontinuous portions (Fig. 36).

Tensile detachment through intact rock is straightforward, i.e. the applied tensile stress exceeds the tensile strength. This also applies to rotational tension for which, however, the non-uniform stress distribution will have to be considered.

It will, therefore, be necessary in the analysis to consider these different failure mechanisms, as well as keeping in mind that they can occur simultaneously or in close sequence.

80
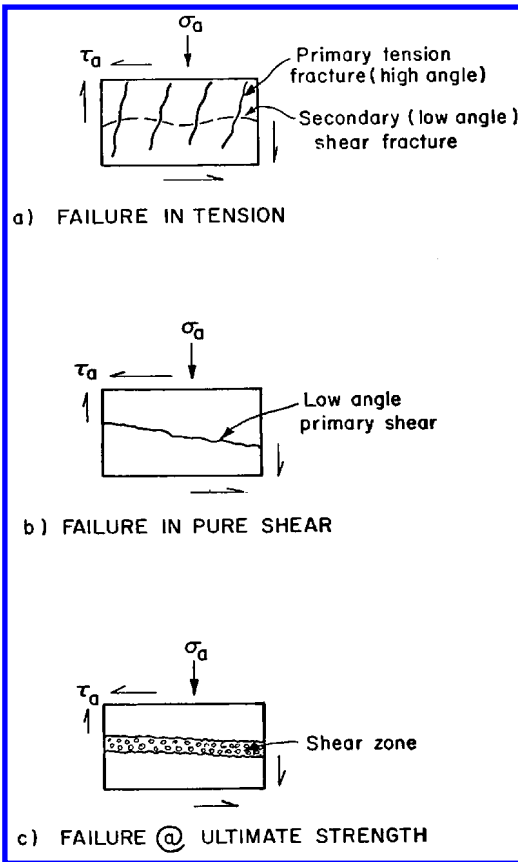
Figure 35. Failure modes of intact rock in direct shear (based on work by Lajtai 1969).

Figure 36. "In-Plane" or "Out-of-Plane" (Step) failure of intact rock bridges.

When reviewing the detachment mechanisms described above, one can identify the following factors which influence them: slope geometry, discontinuity geometry (orientation and persistence), shearing resistance and tensile resistance of the intact material and discontinuities, external static and dynamic (cyclic) loads, vegetation, and water (including ice). Water will act in a number of different ways:

– Driving force/pressure (Fig. 37a)
– Reduction of resisting force/stress; the "classic" effective stress effect (Fig. 37b)
– Water in form of ice can block discontinuities and lead to an increase in water pressure (Fig. 37c)
– Freeze-thaw cycles and the fact that ice has a greater volume than liquid water causes crack/ fracture propagation

5.1.2 *Movement of detached bodies*
Since an entire State-of-the-Art paper at this conference is devoted to runout (see State-of-the-Art paper on "Estimating distance and velocity" by Hungr *et al.* in this volume), only brief comments are made here. Movement may occur in form of sliding, rolling, jumping and falling naturally also in combinations.

Sliding is governed by the shearing resistance between the sliding block and the underlying surface with the shearing resistance usually decreasing with increased displacement. Rolling is analogously governed by the rolling frictional resistance which is not only related to material properties but to the shape of the "rolling" body. Jumping is a more complicated but well defined, at least in principle, mechanism affected by coefficients of restitution (rotational and translational) and to some extent also the shearing resistance between the moving body and underlying surface. Falling, in principle and disregarding aerodynamic drag, is governed by the mass of the moving body.

The influencing factors are to a large extent the same for detachment but with different importance. Slope geometry has an overriding effect on which type of the movement occurs, in addition to affecting acceleration and deceleration. Discontinuity geometry, on the other hand, has a minor effect once detachment has occurred. Water, both in liquid and solid form, has only a small effect on individual body

Copyright 2005 by Taylor & Francis Group
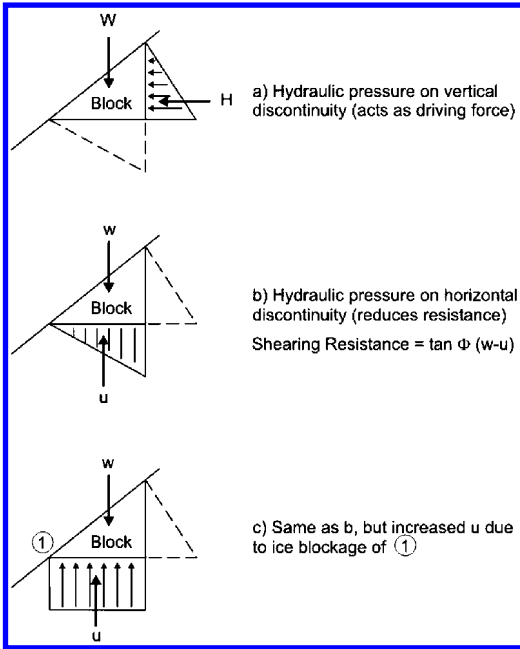
Figure 37.   Water pressure effects on a block.

Figure 38.   Different wedges/blocks defined by discontinuities (from Heuzé & Goodman 1972).

movement. However, when water is combined with a mass of many solid bodies, it will have a major effect through reduction of shearing resistance and creation of suspension. Vegetation will very often have a major effect in deceleration of moving bodies.

What has been alluded to in the preceding comments is the fact that movement following detachment in discontinua often involves not single bodies but assemblies. This may be caused by breakup of bodies or by individual bodies destabilizing simultaneously or briefly after each other. Such movements of assembled bodies are often quite complex and are affected by entrainment of air (gas) and water with associated pore pressure effects or they may be granular mobility movements (Bagnold 1956) or combinations.

5.2 *Deterministic analyses*

Deterministic analyses are introduced and briefly discussed because they provide, in most cases, the basic models on which probabilistic analyses are based. The basic detachment mechanisms, described above are considered together with the geometry of the destabilized body defined by discontinuities. As will be seen, the analyses can be grouped into two major categories. One category is "rigid body analyses" in which the stress distribution along the detachment surfaces is not considered and the analysis is done through limit

equilibrium approaches. The other category represents approaches which in one way or the other consider stress distribution.

5.2.1 *Single body detachment – rigid body analyses*

Discontinuities can form a variety of bodies (blocks, wedges) the geometry of which have been schematized by Heuzé & Goodman (1972) (Fig. 38). As can be seen in this figure, detachment can occur along one or several detachment surfaces. For this discussion, consideration of Cases 1, 4 and 9 is sufficient. Before these cases are discussed in more detail, it is, however, convenient and necessary to subdivide the stability analysis into kinematic and kinetic stability analyses. All the cases in Figure 38 and Case a in Figure 39 are kinematically free to move while Cases b and c in Figure 39 cannot move. Only kinematically unstable cases need to be further considered in the subsequent a kinetic analysis, which leads back to Cases 1, 4, 9 in Figure 38.

Case 9 is the simplest one in which the body can only move along a single plane; this movement is, in most cases, translational. If forces other than gravity are acting, rotation is possible. In Case 4, detachment can occur 1) through shear detachment along one and tensile detachment on the other plane or 2) shear detachment along both planes or 3) tensile detachment from both planes. Finally for Case 1 destabilization is either through:

– Shear detachment on two planes with tensile detachment from the third plane

82
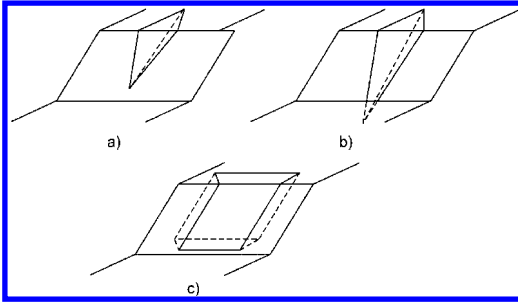
Figure 39. Kinematically possible/impossible movements. Only wedge a can kinematically destabilize; b and c cannot.

– Shear detachment on one plane with tensile detachment from the two other planes
– Tensile detachment from all planes

What has so far been mentioned regarding Cases 4 and 1 is only considering translation. Rotational movements on the planes, around edges and around corners are also possible. A comprehensive treatment of all possible cases has been provided by Wittke (1964). Most other and more recent approaches concentrate on translational movements (e.g. Hendron *et al.* 1971, Hoek & Bray 1981). Given the rigid body assumptions, the analyses are done in form of vector analyses either graphically, purely analytically or in combinations. Driving forces including weight (gravity), water pressure and external loads are combined and compared to resisting forces, which are a combination of shearing and tensile resistance and artificial resisting forces such as bolts. In deterministic analyses, factors of safety, i.e. "Resisting forces/driving forces" or safety margins, i.e. "Resisting forces – Driving forces" are calculated. Note that as long as all forces act through a single point, only force equilibrium can be considered, otherwise moment equilibrium should also be considered. Clearly many computer programs exist to do so. It should be noticed that limit equilibrium analyses usually consider shearing resistance through the sample shearing mechanism represented by the Coulomb relation $\tau = C + N \tan \phi$, possibly expanded by including persistence according to Jennings (1970) (Fig. 40).

A special case regarding a single body detachment is toppling of a single block. In simple terms this can be handled by moment equilibrium as shown for the case of a toppling block on plane (Fig. 41). The above-mentioned cases when wedges or blocks rotate around bounding edges or corners can be handled analogously.

5.2.2 *Analysis considering stress distribution and numerical analyses*

Limit equilibrium analysis with its rigid body assumption precludes deformation and thus any knowledge on

$$K = Persistence = \frac{\Sigma a_i}{\Sigma a_i + \Sigma b_i} = \frac{A_j}{A_j + A_r} = \frac{A_j}{A}$$

$c_a = (1-K)c_i + (K)c_j$
$tg\ \Phi_a = (1-K)tg\ \Phi_i + (K)tg\ \Phi_k$
$\tau = c_a + \sigma\ tg\ \Phi_a$
$c_i, c_j = $ Cohesion (intact, joint)
$\Phi_i, \Phi_j = $ Friction angle (intact, joint)
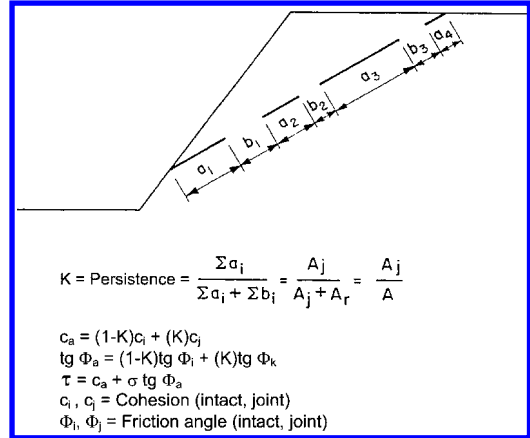
Figure 40. Consideration of persistence (Jennings 1970).
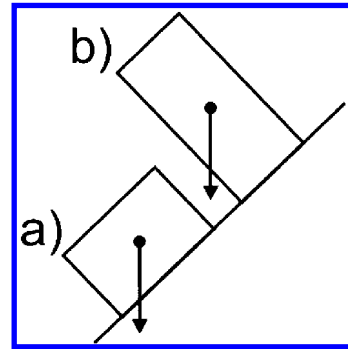
Figure 41. Toppling: blocks stable (a) and unstable (b) against toppling.

stresses acting in the joint planes. Not being able to determine the stress distribution makes the problem indeterminate. In the normally employed force analysis, assumptions are required with regard to direction or even magnitude of forces to make unique solutions possible. As indicated above, the exclusion of moments is a frequent assumption. The other common simplifying assumption is the normality of reactions on the discontinuity planes, an assumption that is often not explicitly stated. However, assuming normal reactions only can have severe consequences. Stability predictions can deviate considerably from the real situation and often on the unsafe side.

The normality assumption can be eliminated and more realistic force assumptions made if one considers the stiffness of discontinuities or the state of stress in the slope (and the potentially unstable wedge or block). Obviously, these are artificial means to introduce the effect of stresses in a rigid body analysis method.

83

They are, however, justified since the wedge itself is still considered to be a rigid body, but is acted upon by stresses (forces) determined via discontinuity stiffnesses or related to the stress state in the slope. The standard normality assumptions for discontinuity plane reactions imply that there is no shear stiffness (the ratio of normal stiffness to shear stiffness is infinite) and that the ratio of lateral to vertical "K" is 1. Stated in this way, one becomes aware how far from reality one may be. This is the reason why research both on stiffness approaches (Mahtab & Goodman 1970, St. John 1971) and on stress approaches (Steiner 1977) was conducted and led to improved analyses. However, these initial approaches were limited e.g. by considering only symmetric wedges and only frictional resistance.

Significant additional development of both approaches was conducted by Glynn (Glynn 1979, Einstein *et al.* 1980) to make them applicable to a broader range of 2-discontinuity wedge geometries and particularly to include all the other capabilities of wedge stability analysis. These generalized approaches were then compared to the simplifying normality assumption. Using the stiffness approach, it was shown that, particularly for narrow wedges or wedges with one steep discontinuity, considerable deviations in stability predictions result – the required friction angle (an expression of safety) can be up to 30° greater than for the normality assumption, i.e. the normality assumption is unsafe. A lateral stress ratio different from $K = 1$ (implying non-normal reactions) is particularly significant if the wedges have relatively flat lying lines of intersection. $K > 1$ underestimates the factor of safety, while $K < 1$ overestimates it compared to $K = 1$.

The definite need to eliminate the restrictive normality assumption in wedge stability analysis was thus established. Another consequence of the work on stiffness and stress approaches was the clarification of their relative significance. The stress approach correctly models the behavior of a wedge in the natural environment subject basically to its own weight. This is so because the history of a slope has led to a certain stress state which governs the current stability of wedges. Discontinuity stiffnesses in contrast can only be used to determine stress changes due to additional loads, the stiffnesses cannot provide information on the present natural state of stress. The stiffness approach can, therefore, be used to make predictions on the effect of additional loads.

The reason for discussing all this in such detail is that it has implication on the main topic of this paper, namely the treatment of uncertainty. The different approaches and particularly the resulting substantial differences in stability determination is an expression of model uncertainty. On the other hand, both the stiffness and the stress approaches require additional information. Normal and shear stiffness values of rock discontinuities have been collected by a number of researchers (e.g. Goodman 1970, Kulhawy 1975, Einstein & Dowding 1981); there is a wide variety of values. Stress distribution in rock masses, particularly near slopes, are known to vary over short distances. The stiffness and stress approaches demonstrate the classic dilemma: Using them improves model accuracy but the need for additional, quite variable, parameters increases uncertainty.

Finite element analyses, boundary element analyses and combined analyses have been used to solve the single body detachment problems (for an overview, see e.g. Hudson *et al.* 1993). These methods are not constrained by the rigid body assumption. However the uncertainties related to stiffness and stress conditions apply.

5.3 Multiple body detachment

Given the prevalence of discontinuities, a rock slope will usually consist of a number of potentially unstable wedges and blocks rather than the single one which has been discussed so far. If the blocks do not interfere with each other, slope stability analyses can be simplified to consideration of one or several representative bodies. However, in many cases, a block can only be detached if another one moves – largely a geometric (kinematic) problem. However, the multiple block detachment process often involves also mechanical interaction. The following sections are devoted to these two considerations.

5.3.1 Kinematics of multiple block detachment – key block approach

Figure 42 shows what was alluded to above. Block 1 needs to be removed to have blocks 2 move, and so on. Goodman & Shi (1985) developed the keyblock theory to handle this. Figures 43 and 44 explain the basics of block theory in 2-dimensions. The theory is also applicable to 3-dimensional blocks.

The keyblock theory is of greatest interest in constrained conditions such as underground openings and displacement of rock socketed piers (To *et al.* 2003), but clearly has major applicability also in rock slope design. Goodman & Shi (1985) devote a chapter to this problem domain. It should be mentioned that the keyblock theory, which looks at the kinematics of the problem can be combined with kinetic consideration.

Goodman & Shi (1985) do this to some extent. A fully kinematically/kinetic integrated approach for the keyblock problem was developed by Warburton (1981).

5.3.2 Kinetic (mechanical) and kinematic (geometric) interaction during multiple block detachment (and movement)

This topic is best discussed in the context of toppling although it applies also to multiple-body sliding as discussed above. Figure 45 shows an example of
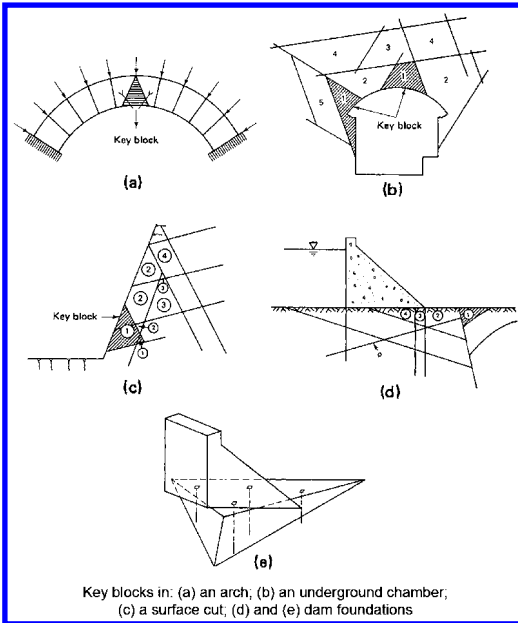
Figure 42. Key blocks in: (a) an arch, (b) and underground chamber, (c) a surface cut, (d) and (e) dam foundations (from Goodman & Shi 1985).
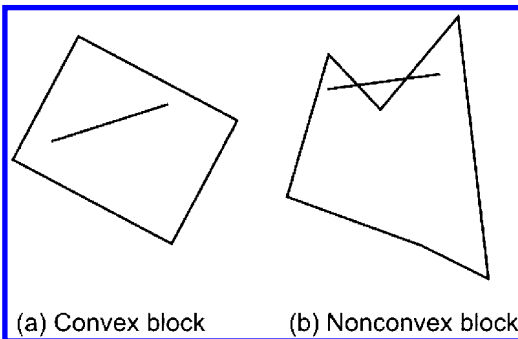
Figure 43. Convex and non-convex blocks.

multiple-body toppling and it is clear that one "slice" has to move before the next one can do so. Looking at the idealized schematical (Fig. 45) it is evident that mechanical interaction between blocks/slides must occur which is shown in detail in Figures 46a–c. Goodman & Bray (1977) developed a closed-form approach for this. The toppling mechanism also led to one of the major numerical model developments, namely that of distinct element modeling (Cundall 1971). Best known are the UDEC and 3DEC approaches, which are further developments of Cundall's (1971) original model. Others (e.g. Kafritsas *et al.* 1987, 1984) have developed similar approaches.
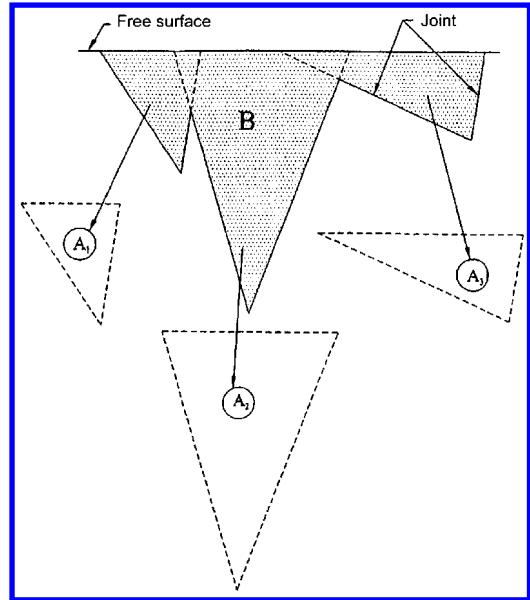
Figure 44. Decomposition of non-convex block into three convex blocks.

It should be noted that the present distinct element models allow one to consider a wide variety of shapes and can also consider water pressure in the discontinuity. Both the closed-form and the distinct element approach require one to make assumptions regarding interblock force direction or contact conditions. A good overview of the state-of-the-art of distinct element models is given by Jing (2003).

5.4 Movement of bodies

The analytical solution by Goodman & Bray (1977), to some extent, and the distinct element approaches, definitely, allow one to also consider the movement of the bodies.

The single body detachment analyses can, to a limited extent, be extended to consider movement essentially by replacing the initial resistance parameters. For instance, for sliding, full persistence can be assumed during movement with the resistance parameters being residual values. In cases where vegetation increases shear resistance, higher resistance values during movement can be assumed.

5.5 Field observations – overall stability of individual slopes

Numerous studies exist in which actual failures of natural rock slopes were observed or where evidence of past failure was recorded. In order to be useful for

85
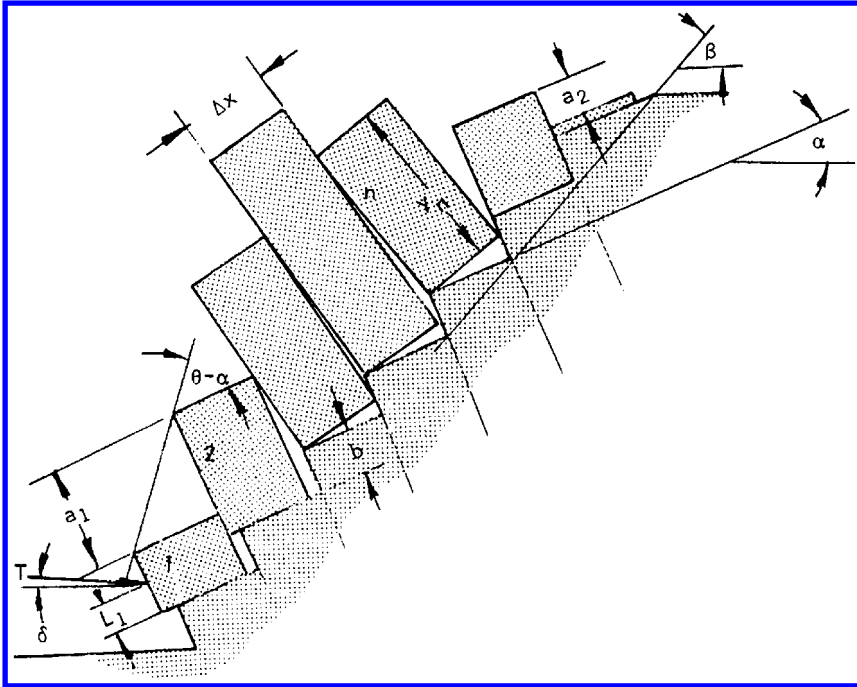
Figure 45.   Model for limiting equilibrium analysis of toppling on a stepped base (Hoek & Bray 1981).
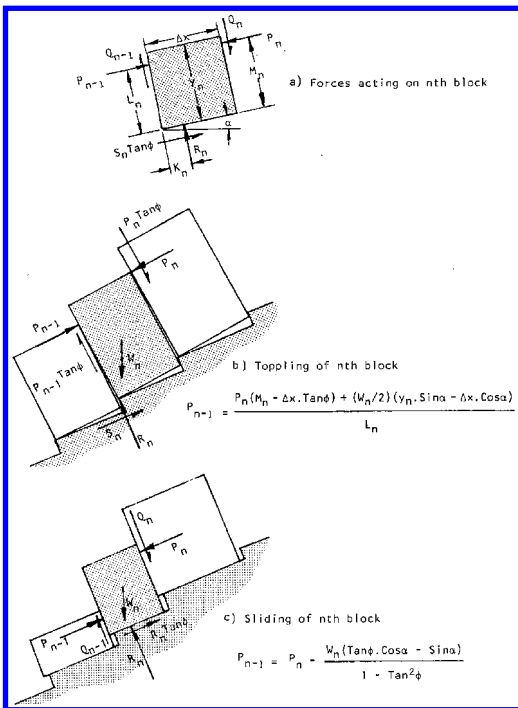
Figure 46.   Limiting equilibrium conditions for toppling and for siding of the n'th block (Hoek & Bray 1981).

application to other than the specific slope, such studies should include a number of slopes with similar rock mass characteristic and climatic conditions. Given the fact that several slopes are considered, there is a statistical aspect and one could argue that this section should actually be in the following probabilistic treatment. Two such studies are briefly summarized below to provide examples.

Patton (1966) studied slopes in the Big Horn Mountains, specifically 101 sandstone slopes and 146 slopes in carbonatic rocks. He distinguished stable, unstable and failed slopes on the basis of the criteria developed from his observations, see Table 6. Figure 47 presents the histograms from Patton's observations. In addition to relating the criteria of Table 1 with the dip of the critical discontinuity, Patton also observed where possible, the average irregularity angle "i" and deducted this from the observed Φa, leading to a range of values of $\Phi \mu$ which can be considered the residual angle of a sliding friction. Note that Patton discussed the use of second order (steep, small scale) and first order (relatively flat, large scale) irregularities and concluded that only the latter should be considered in this correction.

Bjerrum & Jørstad (1968) studied the stability of rock slopes in Norway. They collected data from 300 unstable areas and locations where rock falls and rock slides had occurred. A distinction was made between rock falls, which are caused by active processes near

86

Table 6. Physical characteristics used to classify rock slopes in the Bighorn Mountains (after Patton 1966).

Stable	No visible evidence of past or present slope movements
Unstable	Tension cracks at top of slope Shear movements along slope-sides Slopes bulging at their midpoints Slope separated into blocks, showing rel. displacements Evidence of crushed and sheared rock along potential failure planes at toe of slope Audible cracking and popping noises at toe of slope Evidence of mylonitic zones and slickensided fractures associated with recent movements Rock units at top of slope, which has already failed and – which rests on discontinuity whose dip is approx. the same as that of the missing rock unit
Failed	Rock units missing along steep rock slopes, not caused by water or wind erosion Rock units completely broken up and only remaining near original position due to buttress type support by debris at toe of slope

Figure 47. Classification of natural slopes in Big Horn Mountain (Patton 1966).

the rock surface, and rock slides, which are due to processes working at larger depths. The main conclusion of their study was that the problems of stability in the hard Norwegian rocks cannot be solved by theoretical methods only. This is due principally to the fact that the stability of a slope in these rocks is entirely dependent on the extent and continuity of joint systems, the presence of internal residual stresses, local stress concentrations, etc.; a whole set of factors whose size and effect are largely uncertain and incapable of treatment in a conventional [deterministic] stability analysis.

5.6 Probabilistic analysis

Probabilistic analyses can be considered as an expansion of the deterministic analyses in which rather than single-valued parameters, parameter distributions are included. This was the main reason for going into detail when discussing detachment and movement mechanisms and the associated deterministic analyses. There are, however, some specific issues regarding the probabilistic treatment which have to be taken into account and which will be introduced at the end of this section.

As was mentioned before, of the relevant sources of uncertainty introduced in Section 3, only a spatial (temporal) variability and the non-corrected measurement errors will be considered in this probabilistic treatment. In addition, there will be some discussion of model uncertainty and load uncertainty, the latter related to earthquakes.

The following factors influencing slope stability are uncertain:

– Discontinuity geometry (orientation, size, spacing)
– Discontinuity resistance either directly described by friction angle and cohesion or indirectly through roughness/irregularities and infillings
– Resistance of intact rock related to the persistence effect
– Water pressure/Ice pressure
– Vegetation
– Support
– Slope geometry

Most of these parameters were discussed and considered in the deterministic treatment. The specific, additional probabilistic issue is spatial correlation which needs to be formally considered. If it is not considered this should be clearly stated, since it may contribute to model uncertainty.

5.6.1 Stochastic discontinuity models
As was described in Section 3 geometric descriptions in space are often simplified through the use of so-called "lumped" models (Fig. 8), which are the basis of the well known pole diagrams and associated distributions (Fig. 48). These are actually one of the first systematic representations of spatial variability (Schmidt 1932). Nevertheless using these lumped models, one loses information in that a particularly oriented discontinuity can be located at a particular location and have particular other geometric and mechanical properties such as schematically illustrated in Figure 49.

This deficiency led to a number of geometric stochastic models starting from Snow's (1965, 1968) essentially orthogonal model, to the 2-dimensional Poisson model by Priest & Hudson (1976), and the Veneziano (1979) and Baecher (Baecher & Lanney

87
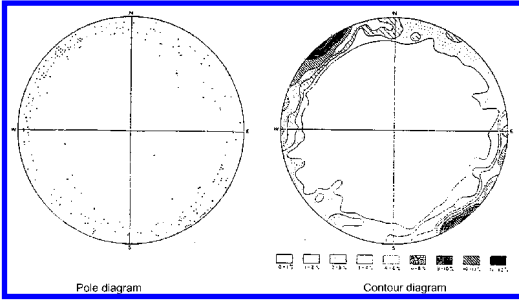
Figure 48.   Typical discontinuity orientation records.
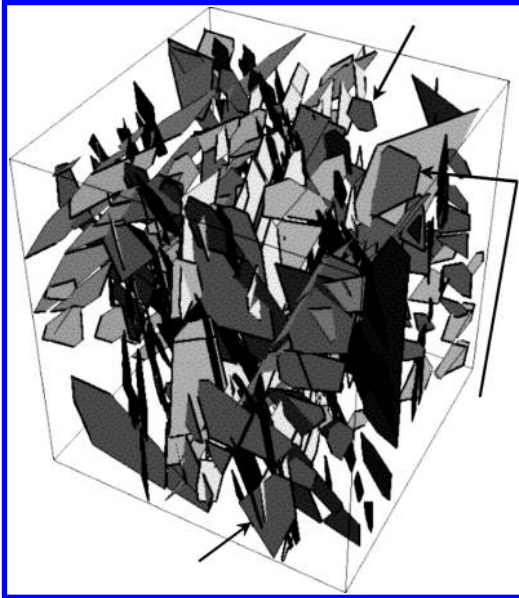
Figure 49.   Stochastic discontinuity modeling – One realization.

Figure 50.   Stochastic discontinuity modeling – Geofrac. Four sequential processes: (a) primary, (b) secondary, (d) tertiary, (e) & (f) quarternary.

1978) models, all of which have been summarized together with some treatment of spatial tessellation by Einstein & Dershowitz (1988). Most recently all this has been substantially expanded with a model by Dershowitz (1981) which eventually led to the commercially available and widely known FRACMAN (Dershowitz *et al.* 1993) and Geofrac (Ivanova 1998) software packages. The processes of Geofrac are shown in Figure 50. It should be noted that these stochastic models use standard input measured in the field, namely: discontinuity orientation, spacing, and trace lengths (see e.g. Ivanova & Einstein 2004). Also, it is possible to not only include geometric but also mechanical discontinuity properties, although this has been done to a limited degree only.

5.6.2   *Simplified probabilistic analyses of single/multiple body detachment*

The simplifications involved are the assumption of lumped orientation distributions and the consideration of persistence (if at all) based on Jennings assumptions. McMahon (1971) was probably first to formally propose probabilistic wedge/block analyses. In the mid- and late 1970's many researchers and practicing engineers proposed more advanced but still simplified approaches. Examples are those by Piteau (1971), Canmet/Coates (1976/77), Glynn (1979a, b) and Einstein *et al.* (1980). Glynn introduced a formal subdivision into kinematic and kinetic probability of instability and proposed an approach to express the kinematic probability of failure as a percentage of wedge intersection lines falling into the kinematically unstable region. Probability of wedge failure can thus be expressed as:

$$P_f = P[F_{kinematic}] \times P[F_{kinetic}| F_{kinematic}] \qquad (10)$$

i.e. the product of the kinematic failure probability and a conditional kinetic failure probability. The latter in turn can be expressed as the percentage of kinematically unstable bodies whose shearing resistance is less than a limiting resistance. This is schematically shown in Figure 51. Shearing resistance distributions are usually obtained from measured discontinuity friction angles. It is also possible to include cohesion distributions (correlated with friction angle) and as

88
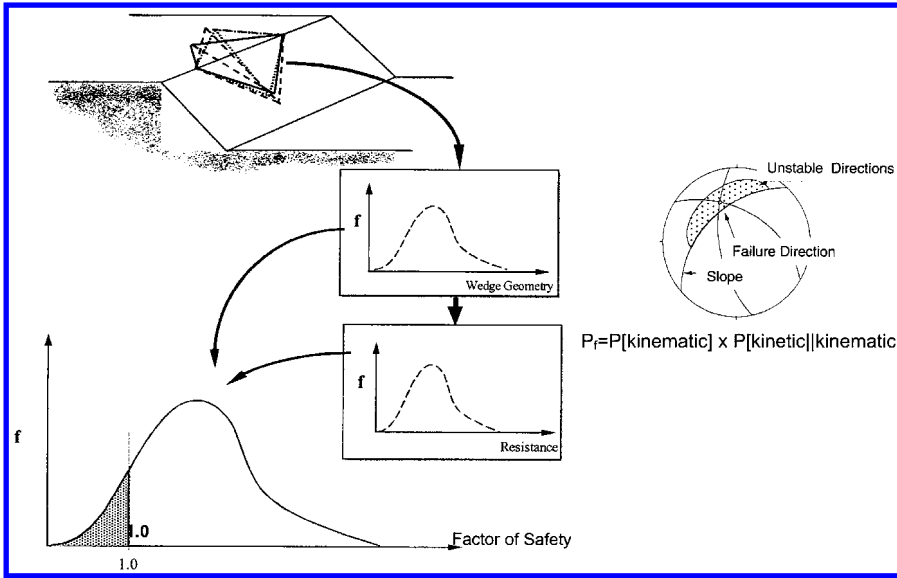
Figure 51. Probabilistic stability model for wedge failure.

mentioned earlier, the intact rock bridge components of the Jennings equation. When using the latter, it is, however, better to go a step further and introduce the stochastic nature of discontinuity geometry which will be described in the next section.

Despite their limitations, the simplified probabilistic wedge/block analyses have the advantage that a quick check without sophisticated geometric and mechanical data collection can be done. Accordingly, a corresponding attempt at providing a probabilistic approach to the keyblock analysis exists (Chan & Goodman 1983).

Piteau & Martin (1977) are among the earliest users of Monte Carlo simulation for rock slope stability analysis. They determined the probability of occurrence of unstable wedge blocks which could spill over the berms of Cassiar Mine by Monte Carlo simulation. Kim *et al.* (1978a) and Kim *et al.* (1978b) described the usage of Monte Carlo simulation for plane, step path and 3-D wedge stability analysis. McPhail & Fourie (1980) presented results of slope stability analysis by Monte Carlo simulation with a comparison of probabilistic and deterministic analysis results. McCracken (1983), Morriss & Stoter (1983), Priest & Brown (1985), Rosenbaum & Jarvis (1985), Kulatilake (1988), Esterhuizen (1990), Özgenoğlu & Fotoohi (1991), Muralha (1991), Muralha & Trunk (1993) are among the researchers who implemented the Monte Carlo simulation technique to analyze different failure modes of rock slopes.
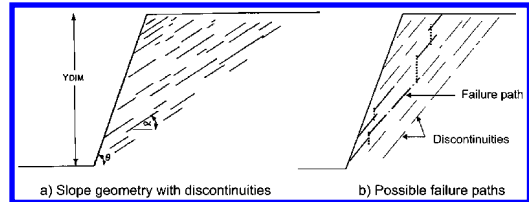
Figure 52. Slope geometry with discontinuities (a) and with possible failure paths (b).

5.6.3 *Probabilistic analyses for single/multiple block detachment based on stochastic models*

This is where the full power but also the complexity of the probabilistic treatment enters. These approaches originated from attempts to treat persistence more rationally. This requires a consideration of both the actual, stochastic geometry of discontinuities in a rock slope and the mechanism by which failure through intact rock, and thus connecting existing discontinuities, occurs. Examples are approaches by Glynn (1979), Call *et al.* (1976) and Call & Nichols, (1978). The most advanced is still the one proposed by O'Reilly (1980) (see also Einstein *et al.* 1980, 1983), which is summarized below.

Figure 52 shows a slope with as set of parallel but impersistent discontinuities. It also shows potential failure paths involving the discontinuities and the intact rock bridges. The figure represents a single realization of the geometric stochastic model simulation for the particular slope and discontinuity set. In each

89
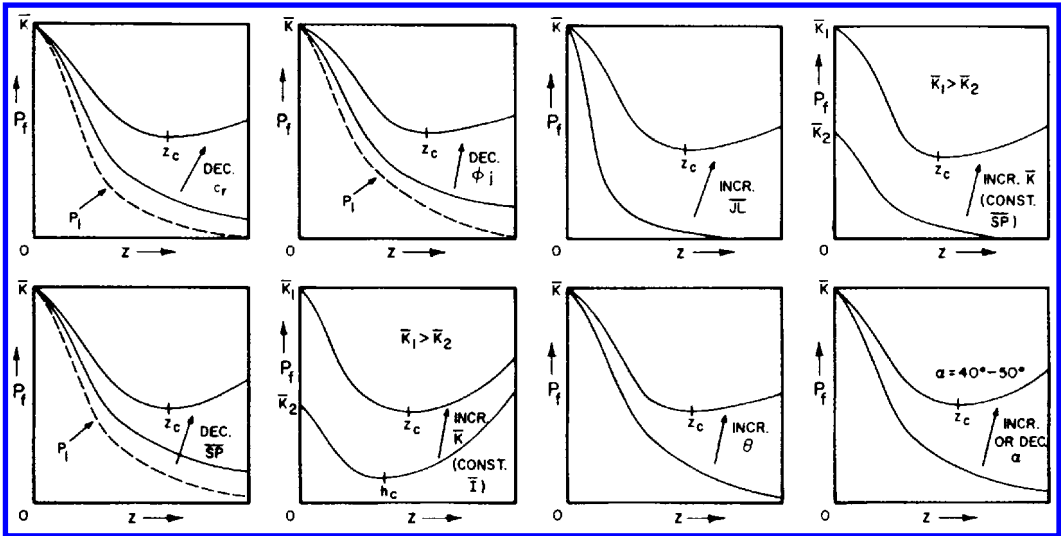
Figure 53. Failure probability (reliability) as a function of slope height Z. Other parameters: friction, cohesion, discontinuity size and spacing, persistence, slope angle, discontinuity indicator.

realization, the most critical failure path is determined. Each failure path has a probability of failure depending on the geometric characteristics (slope angle, discontinuity inclination, discontinuity length/persistence) and the mechanical characteristics (discontinuity friction angle and cohesion, intact rock resistance). The results of the simulation will then be failure probability versus slope height curves as shown in Figure 53. An important aspect is the mechanisms of failure through the intact rock bridges. This has been considered through application of Lajtai's (1969) approach in which failure at low normal stresses occurs through interaction of tensile cracks and through shearing at high normal stresses.

O'Reilly's (1980) (see also Einstein *et al.* 1983) approach is limited to a single set of parallel discontinuities. This was expanded by Shair (1981) to include two sets of discontinuities. Lee (Lee 1989, Lee *et al.* 1990) developed an approach which is not limited to joint sets consisting of parallel discontinuities. Figure 54 shows the dynamic process by which kinematically unstable bodies are determined.

Figure 54 is again a single realization of a stochastic model simulation. The kinematically unstable bodies are then kinetically checked comparing resistance distribution to the critical resistance. Failure probabilities in dependence of geometric and mechanical characteristic can again be produced (see Figure 55). So far this is simply done using friction angle and cohesion distributions to represent the mechanical properties of discontinuities, and not the more sophisticated rock bridge resistance consideration of O'Reilly

(1980). To the authors' knowledge, the O'Reilly and Lee approaches are still the most advanced probabilistic stability methods besides the reliability based approaches, which will be discussed below. The mechanism by which existing discontinuities interact is very complex, representing a research problem which will require a lot of work (see e.g. Bobet & Einstein 2004).

Naturally, the numerical methods discussed earlier can be extended to include the distribution of geometric parameters.

5.7 *Reliability type approaches*

The reliability index has been introduced and discussed earlier in Section 2. Low (1979, 1996, 1996, 1997) over the years has developed a very efficient approach using the Hasofer & Lind (1974) reliability index with spreadsheet calculation to determine the reliability index of tetrahedral rock wedges sliding along one or two joint (discontinuity) planes. The procedure minimizes the reliability index by changing the shape of the multidimensional dispersion ellipsoid representing the influencing parameters in the ellipsoid is tangential to the failure surface (see Fig. 4). Figure 56 shows the spreadsheet and results for obtaining the reliability index of a wedge described by seven parameters (strike and dip of the two discontinuity planes, water pres-sure, friction angle and cohesion) sliding in the biplanar mode.

Christian & Urzua (1998) extended Low's approach to obtain probabilities of failure of single plane sliding bodies subject to earthquake effects.

90
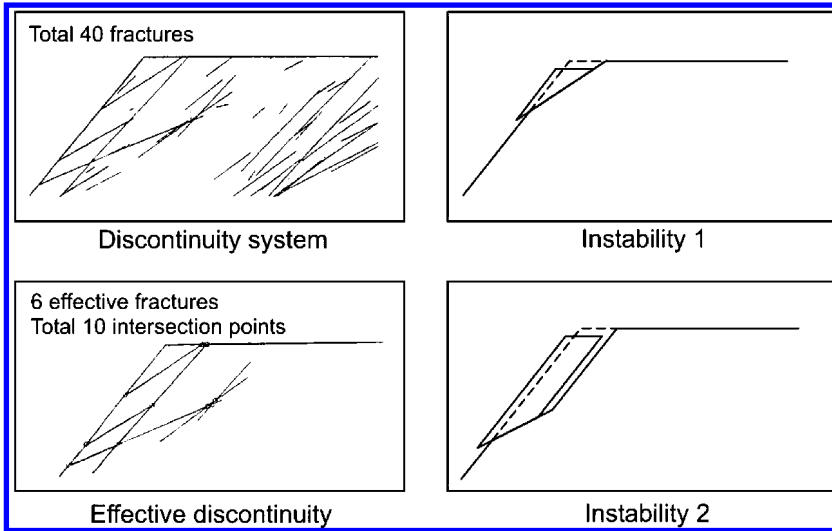
Figure 54. Probabilistic stability analysis with stochastic discontinuity models.
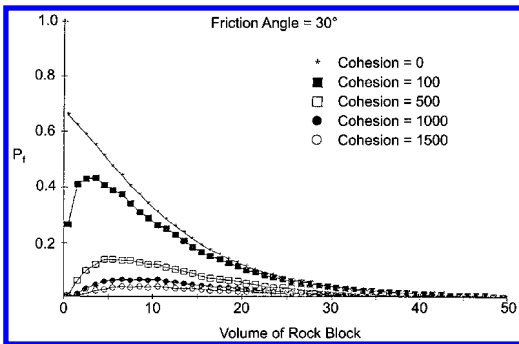
Figure 55. Probability of instability for different block volumes (blocks formed by discontinuities).

Duzgun *et al.* (2003) outlined a methodology for reliability-based design of rock slopes based on FORM (see Section 2.1.2).

5.8 *Statistical approaches for rockfall*

The probabilistic analyses discussed so far involve detachment and initial movement by sliding or toppling. The latter was not specifically discussed above but can be described analogously. The initial phases of rockfalls can thus also be handled with these methods.

As discussed earlier, there is also the "large movement" and runout aspect of rockfalls. Rockfall results in blocks/boulders either coming to rest naturally or stopped by an artificial barrier. This lends itself to statistical data evaluation relating, for instance, slope
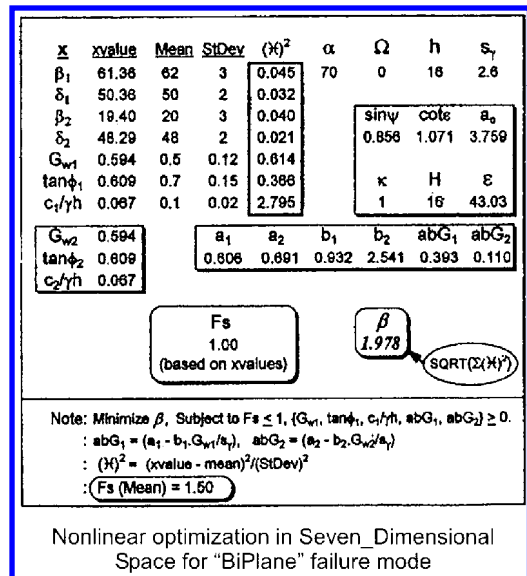
Figure 56. Example of nonlinear optimization in seven-dimensional space (for "bi-plane" failure mode, from Low & Einstein 1992).

geometry and block size to final location. Ritchie's (1963) study falls into this category as do the work by ISMES (Broili 1977) and the more recent results reported in the Oregon Rockfall Study report (Pierson *et al.* 1990). Most of these cases involve some human artificial action such as starting the rock movement and the observation of the final location as well as

91

velocity measurements (this together with rock size provides information on the energy). The Oregon Rock Fall study which also involved the evaluation of different catchment trench geometries, led to recommended trench design criteria. Similar in concept are the Colorado and California rockfall studies in which arresting walls and nets were studied.

An analytical extension of the statistical rockfall studies are several rockfall simulation models. One can use them with parameter distributions to produce e.g. statistical results for the final location and possibly also trajectory and energy information. The Colorado Rockfall Simulation Program (CRSP) (Pfeiffer & Boven 1990) uses information on slope geometry (inclination, length, roughness, lateral variability, slope material i.e., coefficients of restitution, rock geometry, i.e. size and shape, rock material, i.e. durability and mass) which can be varied to obtain the final location, energy and bounce height. The procedure is, however, essentially two-dimensional, projecting different simulated paths into one plane. More advanced simulation programs are those by Zimmermann *et al.* (1987) and by Geotest (1995). The former, which is truly three-dimensional, is a finite element based approach in which both the slope geometry and the differently shaped/sized rocks are discretized. All relevant mechanical aspects regarding the rock block movement can be included.

5.9 *Hazard rating systems*

Although hazard rating systems are applicable to any type of slope instability (or any natural hazard for that matter) they are mentioned in the context of discontinua and follow the section on statistical rockfall approaches since this is the domain in which hazard rating systems are most frequently used. The reader is asked to recall that "hazard" is defined as the "probability that a threat (danger) materializes".

The probabilistic analyses discussed so far, both for continua and discontinua, all produce such an expression. Rockfall hazard rating systems, however, are not based on detailed analyses of rock body movements but arrive at hazard through empirical or semi-empirical approaches. Most importantly, the hazards are not expressed as absolute probabilities but as relative values, usually the highest value representing the greatest relative hazard. Such hazard rating systems allow one to prioritize rock slopes with regard to mitigation or the need for protective measures. These systems have therefore been mainly developed for rockfall/rockslide hazards along highways. Good, practically implemented systems, are for instance: Méthode de cartographie pour éboulements et chutes de pierres sur les routes (LPC 1978); Oregon Rockfall Rating System (Pierson *et al.* 1990); New York State Rock Slope Hazard Rating Procedure (NY State DOT 1993).

All three systems consist of a mix of subjective and objective assessments to rank the rockslope stability on the basis of factors such as slope geometry, geologic structure, climate, vegetation and also the chance that a moving rock block is arrested before reaching the roadway (ditch geometry, vegetation). The two US systems then go a step further and also assess the probability that a rock block falling onto, or already lying on the road, hits or is hit by a vehicle. This latter aspect is actually already a part of risk analysis. Probably the most highly developed hazard/risk rating procedures are those used in Hong Kong (see e.g. Wong *et al.* 1997). Since they involve detailed risk rating and are treated elsewhere in these proceedings, no further explanations are given here.

5.10 *Summary of probabilistic approaches for analyzing the stability of individual rock slopes*

This section summarizes what has been discussed in Sections 5.6 through 5.9 in order to provide the practitioner with a guide as to how to proceed.

Probabilistic analysis is based on collecting data on the following characteristics: discontinuity geometry, discontinuity resistance, slope geometry, water pressure, etc. As a minimum, distributions of discontinuity orientation, of discontinuity trace lengths and of resistance should be collected and used while the other characteristics can be modeled as deterministic. It is desirable, however, to also collect statistical information on the other characteristics.

The simplest probabilistic analysis is to consider wedges/blocks defined by discontinuities with varying orientation and variable resistance. The orientation distributions will lead to a distribution of the kinematic probability of failure as shown in Figure 51, while the resistance distribution can be used directly to obtain the probability of kinetic failure. The two probabilities are combined as shown in Equation 10. Note that the resistance distribution can be obtained from distributions of friction angles. Information on typical friction angles is e.g. listed in Einstein & Dowding (1981). However, due to large variations from site to site, it is strongly recommended to actually conduct tests for the specific case. It is also possible to include, in a simplified manner, the effect of persistence through a distribution of cohesion on the basis of Jennings' relation (Fig. 40).

The derivation of the resulting failure probability can be done either with Monte Carlo simulation or by using the spreadsheet-based reliability method shown in Figure 56. Both approaches allow one to consider also other factors probabilistically, such as pore water pressure and slope geometry. It is important to finally note that all this leads to the probability of failure of a single wedge in a slope. If failure by multiple wedge

failures is possible, one can divide a slope into different sections or use the encompassing methods below.

A more complete treatment of the probabilities of failure of individual rock slopes is through the use of stochastic discontinuity models combined with a more realistic method of consideration of rock bridge failure (persistence effect). For input, it is now possible to not only consider distribution of discontinuity orientation but also of spacing and trace length. Also, since the failure of intact rock bridges is considered, information (deterministic or probabilistic) on intact rock strength is required. The other data (pore pressures, slope geometry, etc.) can also be considered. The discontinuity geometry is computed with stochastic models for which commercial and academic computer programs are available. The results of such stochastic models can be used to obtain distributions of kinematically unstable wedges or blocks, and combined with characteristic resistance distributions. This assumes independence of the geometric and resistance characteristics, thus diminishing the value of using the stochastic approach. Alternatively, the stochastic geometric models can be combined with the dynamic procedure outlined in Section 5.6.2 (Fig. 54) and, most importantly, considering the actual intact rock bridge failure as also described in Section 5.6.2 (Fig. 52). Computer programs for the latter two processes are either academic or proprietary. It is, however, possible to use existing finite element or discrete element codes in conjunction with the stochastic discontinuity geometry programs.

Finally, considering rockfalls, it is possible to use methods based on statistical field observation or simulation programs as discussed in Section 5.8. A logical extension of these approaches are the hazard rating systems mentioned in Section 5.9, which allow one to use field observation on geology and topography together with road traffic and geometry information to arrive at hazard/risk.

6 CALCULATED PROBABILITY OF FAILURE VS FREQUENCY OF SLOPE FAILURE

It was mentioned earlier that there is a significant difference between evaluating the probability of failure, which was the main of this paper, and risk analysis which associates probability of failure with the consequences. The calculated probability of failure and/or reliability index for a slope convey more information about the uncertainties than the conventional deterministic safety factor. However, in most cases it would be wrong to interpret the calculated probabilities in a statistical/frequentist sense (i.e. objective probability), which is what is needed for risk analysis. A physical interpretation of the static probability of failure of a natural slope is particularly problematic, as the slope

is obviously standing at the moment, and if nothing changes (a strict interpretation of the term "static"), then there is no reason for it to become unstable. In such cases the calculated probability of failure is merely an index expressing the degree of our lack of knowledge (i.e. subjective probability or degree of belief).

Whether a particular mode of slope failure occurs will be a function of a variety of factors. Most of these factors change with time to varying degrees and time scales. Some factors can change rapidly and/or fluctuate, e.g.:

– pore pressure changes due to precipitation or leaky services, rapid drawdown, changes in hydraulic properties due to loss of vegetation due to fire, etc.
– ice wedging due to freeze-thaw cycles
– dynamic loads due to earthquakes, construction or transportation
– other load/resistance changes due to rapid erosion, surcharges, fire, etc.

Other factors tend to change much more slowly, often in one direction, e.g., consolidation, weathering, creep, gradual erosion, corrosion of supports, etc. In any case, it is typically one or more of these changes that cause instability. To estimate the frequency of slope failure, some information about variation of parameters with time must be available. This information could be a frequency model for potential triggering mechanisms (e.g. expected peak acceleration of the strongest earthquake in a year, expected extreme daily precipitation in the rainy season, etc.), statistics of slide events for similar slopes in the area, time since the last major slide event at the location, etc.

A (conceptually) straightforward method of estimating the annual frequency of failure would be to evaluate the failure probability for all possible scenarios that could lead to slope instability, estimate the annual probability of occurrence of each scenario, and calculate the annual failure probability by summing up the products of the calculated failure probabilities and the associated scenario probabilities. However, this approach may require so many calculations that simpler approximations would be needed. For example, for earthquake loading, the analysis should cover the full range of loadings and their annual expected probability, not just a few particular loads. The same applies of course to rain- and snowmelt-induced pore pressures. In practice, the slope stability is analyzed for a few key situations and the annual failure probability is estimated on the basis of the few discrete calculations (see e.g. Nadim *et al.* 2005).

Sometimes, the critical values of various triggers (i.e., the values that will cause slope failure) can be identified. The frequency at which such triggers occur (e.g., greater than the 500-year seismic event) determines the "frequency" at which failure occurs (although for an

93

individual slope that can only fail once, frequency is an abstraction). The probability of exceeding the critical values, and thus of failure, can be expressed as a function of the frequency of their occurrence and the time period of interest. Clearly, the larger the event must be to cause failure (i.e., be "critical"), the lower the frequency and thus the lower the probability of failure over any particular time period. Also, the longer the time period of interest, the higher the probability of failure. It should be noted that this approach is often applied in a semi-deterministic manner in which only the uncertainty in the trigger is considered. Obviously, this is a good approximation when the load (trigger) uncertainty is the dominant source of uncertainty. However, it may lead to erroneous results if the uncertainty in resistance, geometry and modeling is of the same order as the load uncertainty.

Sometimes, the annual probability of slope failure could be estimated directly based on the statistical evidence, e.g. frequency of slide events for similar slopes in the area of interest, elapsed time since the last major slide in the area, etc., without doing any probabilistic calculations. The purely statistical approaches, however, do not convey any information or insight about the particular slope in question.

Nadim *et al.* (2003) provided an example of how, despite the interpretation problems, the calculated static failure probabilities could still be used in estimating the annual failure probability. Their example was from the offshore geohazards study performed for a site in the Gulf of Mexico. The deterministic and probabilistic analyses of the critical slope at the site yielded respectively a static factor of safety of 1.22 and a corresponding probability of failure of 0.1. To perform the risk evaluation for the site, it was essential to establish a model of the slide frequency, i.e. the annual probability of slope failure. Clearly, computing a relatively large probability of static failure begs the question about the annual probability of failure and its acceptability. Nadim *et al.* (2003) employed different statistical (based on dating of sediments and estimating the elapsed time since the last major sliding event) and theoretical (based on deterioration of safety margin for the estimated sedimentation rate) approaches for estimating the annual failure probability. They showed that the relatively high static failure probability estimated for the slope in question ($P_f = 0.1$) translated into acceptably low annual failure probability (10^{-6} to 10^{-4}).

Further discussion of estimating the annual probability of slope failure is provided by Nadim (2002) and in Section 4.1 of the State of the Art Paper 5 in this volume.

7 CONCLUSIONS

Probabilistic approaches to analyze the stability of slopes both in soil (continua) and rock (discontinua) allow one to rationally consider uncertainties affecting stability.

The paper tried to show through a number of reasonably complex cases that soil slope stability can be expressed probabilistically through the use of first-order, second-moment (FOSM) approach, first- or second-order reliability methods (FORM/SORM), and Monte Carlo simulations (with or without stratified sampling). The FOSM approach can be done with an effort similar to standard, deterministic analyses but provides much more useful information in that the results are not simply factors/ margins of safety, but allow one to get an idea on the uncertainty of slope performance. With FORM/ SORM and Monte Carlo simulations more information on the uncertainty of the underlying parameters than for FOSM needs to be gathered, requiring an additional effort but also providing more meaningful information on the uncertainty of slope performance.

All these approaches are also applicable, albeit with different underlying mechanisms to probabilistic rock slope analysis. What is interesting, however, is the fact that many of the early applications were in mining where consideration of slope instability in economic terms was and is standard, and where evaluating the cost consequences of preventing slope failure on a probabilistic basis fits well into the overall mine economics assessments, which are probabilistic. Probabilistic approaches in civil engineering applications regarding rock slopes are mostly applications in conjunction with rockfalls and, again, have a reasonably long history with some recent applications particularly through rockfall rating systems. The statistical nature of rockfalls and the fact that the hazard rating procedures produce priorities and not "probabilities of failure" makes such approaches well suited and widely accepted.

It appears, however, that probabilistic stability analyses of both soil- and rock slopes are only reluctantly accepted in civil engineering and engineering geology with the exception of cases involving very large failures or failures with potentially grave consequences.

Another point, which needs to be brought up in these conclusions, relates to the sources of uncertainty. Recall that the probabilistic approaches mainly deal with the inherent spatial and temporal variability of geometric and mechanical properties. It has been shown that this can be done at least adequately. Model uncertainty, unfortunately, is a somewhat different story, both in soil and rock. A variety of models exist to represent failure. So far one does not have a good idea on which models are adequate and, in rock slopes, some of the underlying failure mechanisms are not yet known.

Finally to bring everything together: reliability analyses do not reduce the uncertainties but they provide a rational framework to handle uncertainties explicitly and rationally.

REFERENCES

Alonzo, E.E. & Krizek, R.J. 1975. Stochastic formulation of soil properties, *Proc. 2nd Conf. on Application of Probability and Statistics to Soil and Structural Eng, Aachen, Germany* II: 9–32.

Ang, A.H-S. & Tang, W.H. 1984. *Probability Concepts in Engineering Planning and Design* I & II, John Wiley & Sons, New York.

Archambault, G., Flamand, R., Gentier, J., Riss, J. & Sirieix, C. 1996a. Joint Shear Behavior Revised on the Basis of Morphology 3D Modeling and Shear Displacement. *Proc. of 2nd North American Rock Mech. Symp.,* 1222–1230.

Baecher, G.B. & Lanney, N.A. 1978. Trace Length Biases in Joint Surveys, *Proc. of the 19th U.S. Symposium on Rock Mechanics* 1: 56–65.

Bagnold, R.A. 1956. The Flow of Cohesionless Grains in Fluids. *Proc. of the Royal Society of London* A: 249.

Barton, N. & Bandis, S. 1990. Review of predictive capabilities of JRC-JCS model in engineering practice. *Proc. Int. Symp. on Rock Joints, Loen,* Norway, 1990, 603–610.

Benjelloun, Z.H., Boulon, M. & Billaux, D. 1990. Experimental and Numerical Investigation on Rock Joints. *Proc. of Rock Joints Symp*. 171–178.

Bjerrum, L. & Jørstad, F.A. 1968. Stability of rock slopes in Norway. *Norwegian Geotechnical Institute Publication* 79: 1–11, Oslo, Norway.

Bobet, A. & Einstein, H.H. 2004. Crack Coalescence in Brittle Materials: An Overview, *Proc. EUROCK 2004 and 53rd Geomechanics Colloquium*.

Breitung, K. 1984. Asymptotic approximations for multi-normal integrals, *Journal of Engineering Mechanics, ASCE* 110(3): 357–366.

Broili, L. 1977. Relation Between Scree Slope Morphometry and Dynamics of Accumulation Processes. ISMES Report.

Call, R.D., Savely, J. & Nicholas, D.E. 1976. Estimation of Joint Set Characteristics from Surface Mapping Data, *Proc. 17th U.S. Symposium on Rock Mechanics:* 2B2-1–2B2-9.

Call, R.D. & Nicholas, D.E. 1978. Prediction of Step Path Failure Geometry for Slope Stability Analysis. *Proc. 19th U.S. Symp. on Rock Mechanics*.

CANMET (Coates, D.F. ed.) 1976. *Pitslope Manual*, Canada Centre for Mineral and Engineering Technology.

Chan, H.C. & Einstein, H.H. 1981. Approach to Complete Limit Analysis of Rock Wedges – The Method of "Artificial Supports", *Rock Mechanics* 14.

Chan, L.-Y. & Goodman, R.E. 1983. Prediction of support requirements for hard rock excavations using keyblock theory and joint statistics. *Proc. 24th U.S. Symp. on Rock Mech*.

Chen, G., Ke, J., Jia, Z & Wang, W. 1998. Probabilistic Analysis of Slope Stability with First-Order Approximation. *Int. J. of Surface Mining, Reclamation and Env.* 12: 11–17.

Chiasson, P., Lafleur, J., Soulié, M. & Law, K.T. 1995. Characterizing spatial variability of a clay by geostatistics. *Canadian Geotechnical Journal* 32(1): 1–10.

Christian, J.T. & Urzua, A. 1998. Probabilistic Evaluation of Earthquake – Induced Slope Failure. *ASCE Journal of the Geotechnical and Geoenvironmental Eng.* 124(11).

Christian, J.T., Ladd, C.C. & Baecher, G.B. 1994. Reliability applied to slope stability analysis, *J. Geotech. Engrg., ASCE* 120(12): 2180–2207.

Cundall, P. 1971. A Computer Model for Simulating Progressive, Large Scale Movements in Blocky Rock Systems. *Proc. Int'l. Symp. On Rock Fractures, Nancy*.

Davis, R.O & Salt, G.A. 1986. Strength of Undulating Shear Surfaces in Rock. *Geotechnique* 36(4): 503–509.

Dershowitz, W.S., Lee, G., Geier, J., Hitchcock, S. & LaPointe, P. 1993. *FracMan user Documentation*. Golder Associates Inc., Seattle, WA.

Desai, C.S. & Fishman, K.L. 1987. Constitutive Models for Rocks and Discontinuities. *Proc. of 28th US. Symp. on Rock Mechanics*, 609–619.

Dight, P.M. & Chiu, H.K. 1981. Prediction of Shear Behavior of Joints Using Profiles. *Int. J. Rock Mech. Min. Sci. & Geomech. Abstr*: 18: 386–396.

Dong, J.J. & Pan, Y.W. 1996. A Hierarchical Model of Rough Rock Joints Based on Micromechanics. *Int. J. Rock Mech. Min. Sci. & Geomech. Abstr*. 33(2): 111–123.

Duncan, J.M. 1992. State-of-the-art: Static stability and deformation analysis. *Stability and performance of slopes and embankments-II*, 1: 223–266.

Duncan, J.M. 1996. Soil slope stability analysis. *Landslides: investigation and mitigation*. Ed. By Turner & Schuster. Washington 1996 TRB Report 247.

Duncan, J.M. 2000. Factors of safety and reliability in geotechnical engineering, *J. of Geotechnical and Geoenvironmental Engineering* 126(4): 307–316.

Duncan, J.M, Navin, M. & Wolff, T.F. 2003. Discussion – Probabilistic slope stability analysis for practice. *Canadian Geotechnical Journal* 40: 848–850, reply, 40: 851–855.

Duzgun, H.S.B., Yucemen M.S. & Karpuz, C. 2002. A Probabilistic Model for the Assessment of Uncertainties in Shear Strength of Rock Discontinuities. *International Journal of Rock Mechanics Mining Sciences and Geomechanics Abstracts*. 39: 743–754.

Duzgun, H.S.B., Yucemen, M.S. & Karpuz, C. 2003. A Methodology for Reliability-Based Design of Rock Slopes. *Rock Mechanics and Rock Engineering* 36: 95–120.

Einstein, H.H. & Dowding, C.H. 1981. Shear Resistance and Deformability of Rock Discontinuities. In Touloukían *et al.*, *Physical Properties of Rocks and Minerals*, McGraw Hill.

Einstein, H.H. 1996. Risk and risk analysis in rock engineering. *Tunneling and Underground Space Technology* 11(2): 141–155.

Einstein, H.H. 1997. Landslide Risk – Systematic Approaches to Assessment and Management, *Landslide Risk Assessment*, Cruden & Fell, eds., Balkema.

Einstein, H.H., Baecher, G.B. & Veneziano, D. 1980. Risk Analysis for Rock Slopes in Open Pit Mines – Final Technical Report, *Publication No. R80-17*, Order No. 669, Dept. of Civil Engineering, Massachusetts Institute of Technology, Cambridge, Massachusetts.

Einstein, H.H. & Dershowitz, W.S. 1988. Characterizing Rock Joint Geometry with Joint System Models, *Rock Mechanics and Rock Engineering* 21(1).

95

Einstein, H.H., Veneziano, D., Baecher, G.B. & O'Reilly, K.J. 1983. The Effect of Discontinuity Persistence on Rock Slope Stability, *International Journal of Rock Mechanics and Mining Sciences* 20(5): 227–236.

El-Ramly, H., Morgenstern, N.R. & Cruden, D.M. 2002. Probabilistic slope stability analysis for practice. *Can. Geotech. J.* 39: 665–683.

El-Ramly, H., Morgenstern, N.R. & Cruden, D.M. 2003. Probabilistic stability analysis of a tailings dyke on pres-heared clay-shale. *Can. Geotech. J.* 40: 192–208.

El-Ramly, H., Morgenstern, N.R. & Cruden, D.M. 2004. Probabilistic stability analysis of an embankment on soft clay. In *Proc. 57th Canadian Geotechnical Conf., Quebec City*.

Esterhuizen, G.S. 1990. Combined Point Estimate and Monte Carlo Techniques for the Analysis of Wedge Failure in Rock Slopes. *Proc. of Static and Dynamic Considerations in Rock Engineering Symp.*, 125–132.

Federal Highway Administration. 1989. Rock Slopes Design, Excavation and Stabilization, *Report FHWA, TS-89-045.*

Gauer, P. & Lunne, T. 2002. Statistical analyses of CPTU data from Onsøy, *NGI report 20001099-2*, 25 Feb. 2002.

Genske, D.D. & Walz, B. 1991. Probabilistic Assessment of the Stability of Rock Slopes. *Structural Safety* 9: 179–195.

Geo-Slope International 2003. *SLOPE/W for slope stability analysis, User's guide*, Version 4.23, Calgary, AB, Canada.

Geotest. 1995. Steinschlagmodell.

Glynn, E.F. 1979. A Probabilistic Approach to the Stability of Rock Slopes. *Ph.D. Dissertation* MIT.

Glynn, E.F. 1979b. Probability of Finite Instability in Rock Slopes – A Numerical Approach. *Proc. 10th U.S. Symp. on Rock Mechanics*.

Goldstein, V., Goosev, B., Dyrogovsky, N., Tulinov, R. & Turovskaya, A. 1966. *Proc. 1st Int. Cong. of the ISRM, Lisbon.*

Goodman, R.E. & Bray, J.W. 1977. Toppling of Rock Slopes. *Specialty Conference on Rock Engineering for Foundations on Slopes*. 2, ASCE.

Goodman, R.E. & Shi, G. 1985. *Block Theory and Its Applications to Rock Engineering*. Prentice Hall.

Goodman, R.E. 1970. The Deformability of Joints. Determiniation of the In-Situ Modulus of Deformation of Rock, *ASTM STP 477.*

Hack, H.R.G.H. & Price, D.G. 1995. Description of Discontinuity Friction by Rock Mass Classification. *Proc. of 8th ISRM Congress on Rock Mechanics*, 23–27.

Handanyan, J.M., Danek, E.R., D'Andrea, R.A. & Sage, J.D. 1990. The Role of Tension in Failure of Jointed Rock. *Proc. of Rock Joints Symp*. 195–202.

Hasofer, A.M. & Lind, N.C. 1974. An exact and invariant first order reliability format. *Journal of Engineering Mechanics Division, ASCE*, 100(EM1): 111–121.

Hasover, A.M. & Lind, N.C. 1974. Exact and Invariant Second Moment Code Format, *J. of Eng. Mechanics, ASCE* 100(EMI).

Hendron, A.J., Cording, E.J. & Ayer, A.K. 1971. Analytical and Graphical Methods for the Analysis for Slopes in Rock Masses. *NCG Technical Report*, No. 36.

Heuzé, F.E. & Goodman, R.E. 1972. Three Dimensional Approach for Design of Cuts in Jointed Rock. *Proc. 12th. U.S. Symp. For Rock Mechanics*.

Høeg, K. & Tang, W. 1976. Probabilistic considerations in the foundation engineering of offshore structures, *Proc. 2nd ICOSSAR, Aachen, Germany*, 29 p.

Hoek, E. & Bray, J. 1981. *Rock Slope Engineering*. Revised Third Ed. Inst. Min. Metal. London. 358 pp.

Hsu-Jun, K. 1979. Non-Linear Analysis of the Mechanical Properties of Joints and Weak Intercalation in Rock. *Proc. of 3rd Int. Conf. on Numerical Methods in Geomechanics*, 523–532.

Hudson, J.A., Brown, E.T., Fairhurst, C. & Hoek, E. 1993. *Comprehensive Rock Engineering*, Pergamon Press 1 & 2.

Iman, R.L. & Conover, W.J. 1982. A distribution-free approach to inducing rank correlation among input variables, *Communications in Statistics*, B11, 311–334.

Ivanova, V., Yu, X., Veneziano, D. & Einstein, H. 1995. Development of Stochastic Models for Fracture Systems, *Proc. 35th U.S. Symp. On Rock Mechanics*.

Ivanova, V.M. & Einstein, H.H. 2004. Three-Dimensional Hierarchical Stochastic Modeling of Fracture Systems – An Example from the Yates Field, *Proc. NARMS/ Gulfrock (40th U.S. Symp. On Rock Mech.).*

Ivanova, V.M. 1998. Geologic and Stochastic Modeling of Fracture Systems in Rocks, Massachusetts Institute of Technology, *Ph.D. Dissertation*.

Jaeger, J.C. 1971. Friction of Rocks and Stability of Rock Slopes. *Geotechnique* 21(2): 97–134, 11th Rankine Lecture.

Jennings, J.E. 1970. A Mathematical Theory For The Calculation Of The Stability Of Open Case Mines. *Proc. Symp. on the Theoretical Background to the Planning of Open Pit Mines:* 87–102, Johannesburg.

Jing, L. 2003. A review of techniques, advances and outstanding issues in numerical modeling for rock mechanics and rock engineering. *International Journal of Rock Mechanics & Mining Sciences* 40: 283–353.

Kafritsas, J.C. & Einstein, H.H. 1987. Coupled Flow/ Deformation Analysis of a Dam Foundation with the Distinct Element Method. *Proc. 28th U.S. Symp. on Rock Mechanics*.

Kafritsas, J.C. 1987. Coupled Flow Deformation Analysis of Fractured Rock with the Distinct-Element Method, *Ph.D. Dissertation*, Massachusetts Institute of Technology, Cambridge, Massachusetts.

Kafritsas, J.C., Gencer, M. & Einstein, H.H. 1984. Coupled Deformation/Flow Analysis with the Distinct Element Method. *Proc. 25th U.S. Symp. On Rock Mechanics*.

Kane, F.W. & Drum, E.C. 1987. A Modified Cap Model for Rock Joints. *Proc. of 28th US. Symp. On Rock Mechanics,* 699–705.

Keaveny, J., Nadim, F. & Lacasse, S. 1989. Autocorrelation functions for offshore geotechnical data, *Proc. 5th ICOSSAR,* San Francisco, USA: 263–270.

Kim, H.S., Major, G. & Ross-Brown, D. 1978a. A General Analysis for 3 Dimensional Wedge Failures. *Proc. of 19th US. Symp. on Rock Mechanics*, 51–58.

Kim, H.S., Major, G. & Ross-Brown, D. 1978b. Application of Monte Carlo Techniques to Slope Stability Analyses. *Proc. of 19th US. Symp. on Rock Mechanics*, 28–39.

Kimmance, J.P. & Howe, J.H. 1991. A Combined Geostatistical and First Order Second Moment Reliability Analysis of Slopes in Kaolinsed Granite. *Proc. of 7th ISRM Congress on Rock Mechanics*, 905–911.

Kowalski, H.H. 1989. Numerical Simulation of Rock Falls, MIT, *M.Sc. Thesis*.

Kulatilake, P.H.W. 1988. Minimum Rock Bolt Force and Minimum static Acceleration in Tetrahedral Wedge Stability: A Probabilistic Study. *International Journal of Surface Mining* 2: 19–25.

Kulhawy, F.H. 1975. Stress Deformation Properties of Rock and Rock Discontinuities. *Eng. Geology* 9.

Lacasse, S. & de Lamballerie, J.Y. 1995. Statistical treatment of CPT Data, *Proc. CPT'95*. Linkøping, Sweden.

Lacasse, S. & Nadim, F. 1999. Risk analysis in geo-engineering, *Rocksite 1999: Intern. Conf. on Rock Engineering Techniques for Site Characterization*, Bangalore, India, 6–7 December.

Ladd, C.C., Dascal, O., Law, K.T., Lefebvre, G., Lessard, G., Mesri, G. & Tavenas, F. 1983. *Report of the embankment stability subcommittee*. SEBJ, Montreal, Canada.

Lajtai, E.Z. 1969. Strength of Discontinuous Rocks in Shear. *Geotechnique* 19(2).

Lee, J.-S. 1989. Stochastic Models of Joint Rock. MIT *Eng. Thesis*.

Lee, J.-S., Veneziano, D. & Einstein, H.H. 1990. Hierarchical Fracture Trace Model, *Proc. 31st. U.S. Symp. on Rock Mechanics*.

Li, K.S. & Lumb, P. 1987. Probabilistic design of slopes. *Can. Geotechn. J.* 24: 520–535.

Low, B.K. & Einstein, H.H. 1992. Simplified Reliability Analysis for Wedge Mechanisms in Rock Slopes. *Proc. 6th Int'l. Symp. On Landslides*. A.A. Balkema.

Low, B.K. & Tang, W.H. 1997. Efficient Reliability Evaluation Using Spreadsheet, *ASCE J. Engrg. Mech.* 123(7).

Low, B.K. 1979. Reliability Of Rock Slopes With Wedge Mechanisms, *M.S. Thesis*, MIT, Cambridge, MA.

Low, B.K. 1996. Practical Probabilistic Approach Using Spreadsheet, *Proc. Pub. No. 58, Uncertainty in Geologic Environment from Theory to Practice, ASCE Spec. Conf.*

Low, B.K. 2003. Practical probabilistic slope stability analysis, PanAm Conference, SARA, Cambridge, Mass, June 2003.

Low, J. 1997. Reliability Analysis of Rock Wedges, *ASCE J. of Geotechnical and Geoenvironmental Engineering* 123.

LPC 1978. Eboulements et chutes de pierres sur les routes. Méthode de Cartographie. Groupe d'Etudes des Falaises (GEF) Laboratoire Central des Ponts et Chaussées. *Rapport de Recherche LPC* 80.

Mahtab, M. & Goodman, R.E. 1970. Three-dimensional Analysis of Jointed Rock Slopes. *Proc. 2nd Int'l. Cong. of the ISRM*.

Maksimovic, M. 1996. The Shear Strength Components of a Rough Rock Joint. *Int. J. Rock Mech. Min. Sci & Geomech. Abstr.* 33(8): 769–783.

McCracken, G. 1983. Probabilistic Analysis of Slope Stability at a Large Quartzite Quarry. *Proc. of 2nd Int. Surface Mining and Quarrying Symp.*, 13–20.

McMahon, B. 1971. A Statistical Method for the Design of Rock Slopes.

McMahon, B. 1974. Design of Rock Slopes Against Sliding on Pre-Existing Failures. *Proc. 3rd Int'l. Congress of the ISRM*.

McPhail, G.I. & Fourie, A.B. 1980. A Practical Application of Probabilistic Slope Stability Analysis Methods. *Proc. of The South African Geotechnical Conf.*, 65–77.

Morriss, P. & Stoter, H.J. 1983. Open-Cut Design Using Probabilistic Methods. *Proc. of 5th ISRM Congress on Rock Mechanics,* 1: C107–C113.

Muralha, J. & Trunk, U. 1993. Stability of Rock Slopes-Evaluation of Failure Probabilities by the Monte Carlo and First Order Reliability Methods. *Proc. of Assessment and Prevention of Failure Phenomena in Rock Engineering*, 759–765.

Muralha, J. 1991. A Probabilistic Approach to the Stability of Rock Slopes. *Proc. of 7th ISRM Congress on Rock Mechanics*, 905–911.

Muralha, J. 1991. A Probabilistic Approach to the Stability of Rock Slopes. *Proc. of 7th ISRM Congress on Rock Mechanics*, 905–911.

Nadim, F. 2002. Probabilistic methods for geohazard problems: State-of-the-Art, *Probabilistics in GeoTechnics: Technical and Economic Risk Estimation, Graz, Austria*, September 15–19.

Nadim, F., Krunic, D. & Jeanjean, P. 2003. Probabilistic slope stability analyses of the Sigsbee Escarpment. *Procs, OTC 15203, Offshore Technology Conference '03, Houston*, Texas, May 2003.

Nadim, F., Kvalstad, T.J. & Guttermsen, T. 2005. Quantification of risks associated with seabed instability at Ormen Lange. *Special issue of Marine and Petroleum Geology on Ormen Lange*.

Nadim, F. & Lacasse, S. 1999. Probabilistic slope stability evaluation, *Proc. 18th Annual Seminar on Geotechnical Risk Management, Hong Kong,* 177–186, 14 May.

Nemat-Nasser, S. & Horii, H. 1982. Compression-Induced Nonplanar Crack Extension with Application to Splitting, Exfoliation and Rockburst, *J. Geophys. Res.* 87(B8).

New York State DOT. 1990. *Rockslope Hazard Rating Procedure*, Working Draft.

O'Reilly, K.J. 1980. The Effect of Joint Persistence on Slope Reliability. MIT, *M.S. Thesis*.

Oregon DOT. 2002. *Rockfall Report* (Federal and State DOT – Pool Study).

Özgenoğlu, A. & Fotoohi, K. 1991. Analysis of Stepped-Path Sliding with three Joint Sets. *Mining Science and Technology* 13: 359–367.

Patton, F. 1966. Multiple Modes of Shear Failure in Rock and Related Materials, *Ph.D. Thesis*. U. of Illinois.

Pfeiffer, T.J. & Bowen, T. 1989. Computer Simulation of Rock Faults. *Bulletin of the Association of Engineering Geologists* 26(1).

Phoon, K.K. & Nadim, F. 2004. Modeling non-Gaussian random vectors for FORM: State-of-the-Art Review, *Workshop on Risk assessment and Geohazards*, Indian Institute of Science, Bangalore, India, 26 November.

Phoon, K.K. & Kulhawy, F.H. 2003. Evaluation of Model Uncertainties for Reliability-based Foundation Design, *Proceedings, Ninth International Conference on Applications of Statistics and Probability in Civil Engineering, San Francisco, July 6–9 2003* 2: 1351–135.

Pierson, L.A., Davis, S.H. & VonVickle, R. 1990. The Rockfall Hazard Rating System *Implementation Manual*, Oregon State Highway Division.

Piteau, D.R. & Martin, D.C. 1977. Slope Stability Analysis and Design Based on Probability Techniques at Cassiar Mine. *Bulletin of Canadian Institution of Mining and Metallurgy* 70: 139–150.

Piteau, R.D. 1970. Geological Factors Significant to the Stability of Slopes Set in Rock, *Proc. Open Pit Mine Symposium*.

97

Plesha, M.E. 1987. Constitutive Models for Rock Discontinuities with Dilatancy and Surface Degradation. *Int. J. for Numerical and Analytical Meth. in Geomech.* 11: 345–362.

Poschmann, A.S., Klassen, K.E., Klugman, M.A. & Goodings, D. 1983. Slope stability study of the South Nation Rover and portions of the Ottawa River. *Ontario Geological Survey, Misc. Paper 112.* Accompanied by Geotechn. Series Maps 2486 and 2487, scale 1:50 000.

Power, C.M. & Hencher, S.R. 1996. A New Experimental Method for the Study of Real Area of Contact Between Joint Walls During Shear. *Proc. of 2nd North American Rock Mech. Symp., NARMS'96*, 1217–1222.

Priest, S.D. & Brown. E.T. 1983. Probabilistic Stability Analysis of Variable Rock Slopes. *Trans. Inst. Mining Metall, A.* 92: 1–12.

Priest, S.D. & Hudson, J. 1976. Discontinuity Spacings in Rock, *International Journal of Rock Mechanics and Mining Sciences* 13.

Quek, S.T. & Leung, C.F. 1995. Reliability-Based Stability Analysis of Rock Excavations. *Int. J. Rock. Mech. Min. Sci. & Geomech. Abstr.* 32(6): 617–620.

Rahhal, M.E. & Germani, M. 2003. Risk assessment of water effect in slope stability, PanAm Conference, SARA, Cambridge, Mass, June 2003.

Ritchie, A.M. 1963. The Evaluation of Rockfall and Its Control. *Highway Research Record.*

Roberds, W.J. & Ho, K.S. 1997. A quantitative risk assessment and risk management methodology for natural terrain in Hong Kong. *ASCE's First Int. Conf. on debris-Flow Hazards Mitigation: Mechanics, Prediction and Assessment, San Francisco*, USA, August.

Roberds, W.J. 2001. Quantitative landslide risk assessment and management. *Proc. Int. Conf. on Landslides: Causes, Impacts and Countermeasures, Davos, Switzerland.*

Roberds, W.J., Ho, K.S. & Leroi, E. 2002. Quantitative risk assessment for landslides. *Transportation Research Record*, No. 1786, Paper No. 02–3900.

Rosenbaum, M.S. & Jarvis, J. 1985. Probabilistic Slope Stability Analysis Using a Microcomputer. *Q. J. Eng. Geol.* 18: 353–356.

Schmidt, W. 1932. Tektonik und Verformungslehre Bornträger, Berlin.

Shair, A.K. 1981. The Effect of Two Sets of Joints on Rock Slope Reliability. MIT, *M.Sc. Thesis.*

Skempton, A.W. & Brown, J.D. 1961. A landslide in Boulder Clay at Selset, Yorkshire. *Géotechnique*, 11: 280–293.

Snow, D.T. 1965. A Parallel Plate Model of Fractured Permable Media, *Ph.D. Dissertation*, Univ. of California, Berkeley, California.

Snow, D.T. 1968. Anisotropic Permeability of Fractured Rocks. In: R.J.M. DeWiest (ed.) *Hydrology and Flow Through Porous Media*. Academic Press, New York.

St. John, C. 1971. Three Dimensional Analysis of Jointed Rock Slopes. *Proc. Int'l. Symp. on Rock Fractures, Nancy.*

Steiner, W. 1977. Three Dimensional Stability of Frictional Slopes. MIT, *M.Sc. Thesis.*

Swan, G. & Zongqi, S. 1985. Prediction of Shear Behavior of Joints Using Profiles. *Rock Mechanics and Rock Engineering* 18: 183–212.

Swan, G. 1981. Tribology and the Characterization of Rock Joints. *Proc. of 22nd US. Symp. on Rock Mech.*, 402–407.

To, A., Ernst, H. & Einstein, H.H. 2003. Lateral Load Capacity of Drilled Shafts in Rock. *ASCE Journal of Geotechnical and Geoenvironmental Engineering* 129(8).

Trunk, U. 1993. Probabilistic Stability Analysis of Rock Wedges. *Proc. of Safety and Environmental Issues on Rock Engineering, Eurock'93 Symp.* 227–231.

Vanmarcke, E. 1977. Probabilistic modeling of soil profiles, *ASCE Journal of Geotechnical Engineering Division* 103(GT11): 1227–1246.

Vanmarcke, E. 1984. *Random fields*, MIT Press, Cambridge, Mass, USA, 382 p.

Veneziano, D. 1979. Probabilistic Model of Joints in Rock, *Internal Report*, M.I.T.

Vick, S.G. 2002. *Subjective Probability and Engineering Judgement – Expert Thinking in Geotechnical Engineering and Related Earth Sciences*, ASCE Press.

Warburton, P.M. 1981. Vector Stability Analysis of Arbitrary Polyhedral Rock Block with any Number Of Free Faces. *Int. J. Rock Mech. Min Sci*. 18.

Wittke, W. 1965. Verfahren zur Berechung der Standsicherheit belasteter und unbelasteter Felsbäschungen, *Rock Mech. and Eng. Geol.*, Supplementum II: 57–79.

Wong, H.N., Ho, K.K.S. & Chan, Y.C. 1997. Hierarchy of Consequences of Landslides, *Landslide Risk Assessment*, Cruden & Fell, eds., Balkema.

Zimmermann, Th., Rebora, B., Duvalle, E. & Descoeudres, F. 1987. *A Three-Dimensional Numerical Simulation Model for Rock Falls*. Institut d'économie et aménagements énergétiques to EPFL.

Estimating landslide motion mechanism, travel distance and velocity

O. Hungr
Earth and Oceans Sciences, University of British Columbia, Vancouver

J. Corominas
Department of Geotechnical Engineering and Geosciences, Technical University of Catalonia, Spain

E. Eherhardt
Earth and Oceans Sciences, University of British Columbia, Vancouver

ABSTRACT: An essential part of any landslide hazard or risk assessment is the prediction of the character of failure and a quantitative estimate of post-failure motion ("runout") including travel distance and velocity. The tools available for these tasks are reviewed. At first, phenomenological and analytical methods for predicting the failure character and timing are shown. The second part of the paper covers empirical methods of runout prediction and the third part, analytical methods of runout modelling. Although the various methodologies are now highly developed, they are not free of potential for error. It is recommended that multiple methods be used simultaneously and combined with experienced judgement. Each of the analytical techniques also require careful verification and calibration against field data.

1 INTRODUCTION

Since the early work of Heim (1932) and Terzaghi (1950), landslide researchers have striven to better understand and predict catastrophic slope failure. Despite considerable advances in understanding landslide mechanisms and being able to simulate them using numerical models, prediction of the onset of extremely rapid motion and the resulting propagation (runout) of the slide mass is still exceedingly difficult. This paper attempts to list and critically review the main existing techniques and quantitative models. Given the explosion of literature dealing with this subject in recent years, our treatment is necessarily selective.

The first section summarizes methods of recognizing and modelling failure behaviour, with emphasis on recognition of phenomena that may lead to extremely rapid failure. The second section deals with the key empirical techniques for runout prediction, and the third with quantitative modelling of landslide runout. Both landslides originating in soil and rock are treated. The landslide terminology used derives from Varnes (1978), Cruden & Varnes (1996) and Hungr et al. (2001).

2 PREDICTION OF FAILURE BEHAVIOUR

2.1 *Prediction methodologies*

The fundamental question connected with landslide hazard assessment is "what will be the character of failure?" Some landslides are slow and ductile, moving in a continuous or intermittent manner. They may cover long distances (e.g. earth flows), but the low velocity permits risk reduction action such as stabilization or evacuation to be taken. Others are brittle, meaning that after a certain prelude of slow deformation, or as a result of sudden loading (e.g. during an earthquake), they accelerate and attain extremely rapid velocities of the order of 5 m/s or faster, exceeding the speed of a running person. Such landslides are sometimes referred to as "catastrophic".

How do we recognize whether a given potential landslide can become extremely rapid? The three possible means of answering the question include judgmental approach, based on experience and comparison with precedents, experimental approach based on monitoring, and analytical approach based on limit equilibrium or stress–strain analysis. Neither approach is error-proof, and in most cases, specialists attempt to apply all three.

2.2 Judgmental approach, based on landslide typology

From experience, we know that certain types of landslides behave in a brittle manner, while others tend to be ductile. Unfortunately, there is also a large transitional group that may exhibit either behaviour, or both in sequence. Nevertheless, a well-designed typological classification of landslides permits certain distinctions to be made, at least on a preliminary basis. The following description of typical soil slide trends is based on Hungr et al. (2001).

Extra-sensitive ("quick") clay flow slides are always extremely rapid events, both at initiation, retrogression and during flow-like travel. The same can be said about *flow slides in loose saturated sands*, often subaqueous. In fact the term *flow slide* was coined by Casagrande (1976) to signify a slide accompanied by liquefaction of a zone of saturated soil at the rupture surface, which invariably leads to catastrophic acceleration. Speculations periodically appear in the literature that certain loose, dry fine-grained soils can liquefy due to air pressure in the pores. However, this process has yet to be conclusively demonstrated (e.g. Crosta 2005). Most truly *dry granular flows* are slow. Many extremely rapid flow slides appear to consist largely of dry or moist soil, with liquefaction affecting only a thin saturated layer at the base. Such behaviour is observed in well-graded mine waste (Hungr et al. 2002) and loess. It is possible that the largest landslide disaster in history, the 1921 series of loess flow slides in the Loess Plateau, with 280,000 victims, was due largely to this mechanism (Close & McCormick 1922). Hunter & Fell (2003) summarize conditions where rapid sliding of soil slopes can be expected. They show that, based on case studies, soils susceptible to spontaneous liquefaction and extremely rapid flow sliding span a very wide range of gradations in the silt, sand and gravel classes. To be rapid, they show that the soils must be contractive.

Sassa (2002) suggested that liquefaction of soil at the rupture surface may occur as a result of grain crushing during long-displacement sliding, as the modified grain size distribution of the crushed soil allows closer packing, accompanied by pore-pressure increase. This could explain the spectacular mobility of many moderately deep-seated flow slides in residual soil, which probably begin by sliding on relict joints.

Rotational, translational or compound slides in non – sensitive clay are usually rapid or slower. They may transform into *earth flows* and continue moving at moderate speeds for hundreds of metres. The highest recorded speed of an earth flow is about 0.1 m/sec (Hutchinson 1974), although speeds in the order of metres per minute or per hour are more common, even within the course of surging.

In stiff overconsolidated clays and silts, care must be taken to account for physical changes caused by soil disturbance. A striking example of this is the Attachie Slide on the Peace River, British Columbia, described by Fletcher et al. (2002). The slope, composed of glacio-lacustrine clays and silts compacted by an ice sheet and covered by till, had been slowly failing by compound sliding for many decades. Suddenly, following a period of heavy rain, 7 million m^3 of the disturbed mass liquefied, descended a bedrock scarp at the foot of the slope and flowed across the kilometer wide floodplain of the Peace River with enough speed to raise a violent wave on the opposite shore (Fig. 1). This is an example where clay softening produced a material that is very sensitive in its bulk behaviour.

Most shallow slides occurring on steep slopes are extremely rapid, simply as a result of cohesion loss necessary to start failure (Hungr 2003). They usually involve loose granular veneer overlying stable substrate. Such failures nearly always begin during heavy rain, ensuring perched saturation of the loose layer. As fast movement occurs, soil situated downslope of the initial failure is over-ridden, liquefied by rapid undrained loading and incorporated in a growing *debris avalanche* (Sassa 1985). When debris avalanches enter established steep stream channels or gullies, they become channelized, incorporate further material as well as water and turn into surging, extremely rapid *debris flows*.

Rock slides in stronger rock, usually with a high degree of structural control, are extremely rapid due

Figure 1. The Attachie Slide, Peace River, B.C., Canada. The disturbed slope of clay and silt failed suddenly during a rain storm. The base of the photo is approximately 1800 m wide (Fletcher et al. 2002).

to sudden loss of cohesion. Many become fragmented and flow-like, forming extremely rapid *rock avalanches* (sturzstroms). Of these, *rock collapses* are especially sudden and rapid, and involve failure of strong rock controlled by a combination of non-systematic joints and intact rock bridges (Hungr & Evans 2004b). In contrast, rotational *rock slumps* and some non-rotational *compound slides* in very weak rock are slow, or at best rapid. Block topples, in stronger rock and deriving stability from block equilibrium, are sudden and extremely rapid. Flexural topples, often involving large slopes in weak, highly anisotropic foliated rocks, rely on their stability through interlayer friction and tend to be slow.

A general assessment of typical failure behaviour for various types of landslides is given in Table 1. Of course, such generalizations must be treated with caution. The best means of assessing a landslide's potential for catastrophic motion is to compare it with similar case histories whose failure stage has already taken place.

2.3 *Empirical approach based on monitoring*

Prediction of time to failure can be based on measurements of surface displacements, repeated over time. Unlike most numerical analyses, time is explicitly incorporated into the analysis and the question of when a given slope might fail is directly addressed. Such empirical approaches however, are phenomenological (i.e. "holistic") and disregard details of the underlying mechanisms while concentrating on the overall performance of the system. Whether the displacement measurements are made using crack extensometers across individual tension cracks or a system of geodetic monuments covering an entire slope, the empirical technique is applied in the same way; surface displacement measurements are recorded over time, which are then analyzed for accelerations in order to predict catastrophic/impending failure. As such, empirical methods generally overlook the kinematics and causes of failure, relying instead on the surface manifestation of the instability (e.g. surface displacements).

In describing the dynamics of a landslide, Terzaghi (1950) suggested that many landslides are preceded by a gradual decrease in the ratio of shearing resistance to shearing strength (defined by the factor of safety) which, in turn, involves downward slope deformations (Fig. 2). Once the factor of safety reaches unity, slope movements begin to sharply accelerate and catastrophic failure occurs. For Terzaghi, the amount of downslope displacement accommodated through slope creep prior to failure ($D_{failure}$ in Fig. 2) was related to the thickness of the basal shear zone, i.e. the zone

Table 1. A simple classification of landslides, showing typical ranges of velocities (classification adapted from Varnes 1978, Hungr et al. 2001, Hungr & Evans 2004b).

TYPE	VELOCITY CLASS*							COMMENT
	ES	VS	S	M	R	VR	ER	
SLIDES IN ROCK								
Translational (or Wedge) Rock Slide							▓	May be slow in very weak rocks
Rotational Rock Slide(Slump)	▓	▓	▓	▓	▓			Very weak rock mass
Compound Rock Slide	▓	▓	▓	▓	▓	▓	▓	Various types of mechanisms
Rock Collapse							▓	Strong rock, joints, rock bridges
FALLS AND TOPPLES								
Rock (Debris) Fall							▓	Fragmental fall, small scale
Rock Block Topple							▓	Single or multiple blocks
Rock Flexural Topple	▓	▓	▓	▓	▓			Very weak rock mass
SLIDES IN SOIL								
Clay Slump (Rotational)	▓	▓	▓	▓				Non- sensitive
Clay Slide (Compound)	▓	▓	▓	▓				Non- sensitive
Sand (Gravel, Talus, Debris) Slide					▓	▓	▓	Usually shallow
FLOW-LIKE LANDSIDES								
Dry Sand (Silt, Gravel, Talus Debris) Flow	▓	▓	▓	▓	▓			No cohesion
Sand (Silt, Debris, Peat) Flow Slide							▓	Liquefaction involved
Sensitive Clay Flow Slide							▓	Quick clay
Debris Avalanche							▓	Non-channelized
Debris (Mud) Flow						▓		Channelized
Debris Flood						▓		High water content
Earth Flow	▓	▓	▓	▓				Plastic clay
Rock Avalanche							▓	Begins in bedrock
Rock Slide-Debris Avalanche							▓	Entrains debris

* Extremely Slow, Very Slow, Slow, Moderate, Rapid, Very Rapid, Extremely Rapid (>5 m/sec; Cruden & Varnes 1996).

101
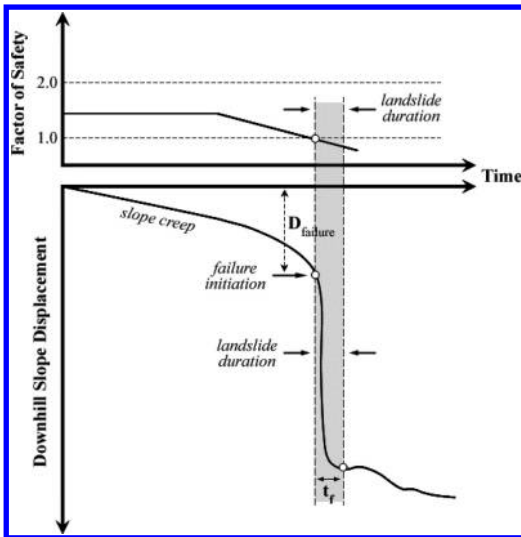
Figure 2. Illustration of ground movements that precede a landslide, shown as a function of the factor of safety (after Terzaghi 1950).

within which the state of stress approaches the state of failure. If the zone is very thin, the slope displacements preceding failure may be on the scale of millimetres. If the potential sliding surface involves a thicker zone within a homogeneous soil material, like clay, then the slope may experience displacements on the scale of metres before catastrophic failure can occurs.

Indeed, the monitoring of slope movements had already become standard practice on most mining and geotechnical projects. In a move towards failure prediction, focus shifted to the creep behaviour of materials and the projection of time to failure during tertiary creep. Saito (1965) proposed that through the continuous measurement of relative slope displacements, a constant strain rate may be calculated and compared to the estimated creep rupture life for that strain rate as determined through laboratory testing. Voight (1989) and Fukuzono (1990) followed with observations of a linear relation between the logarithms of the first and second derivatives of slope displacement (i.e. creep velocity and acceleration). Fukuzono (1990) used this linear relation to propose a simple means for predicting catastrophic failure using the inverse mean velocity (Fig. 3). Several rheological models have since been forwarded (linear, exponential, power law), with further differences between proposed models arising due to the subjective nature of what constitutes failure (e.g. Bhandari 1988). Comprehensive reviews of these methods are provided by Bhandari (1988), Federico et al. (2002) and Crosta & Agliardi (2003).

The practical application of these methods to failure prediction requires that warning thresholds be set with
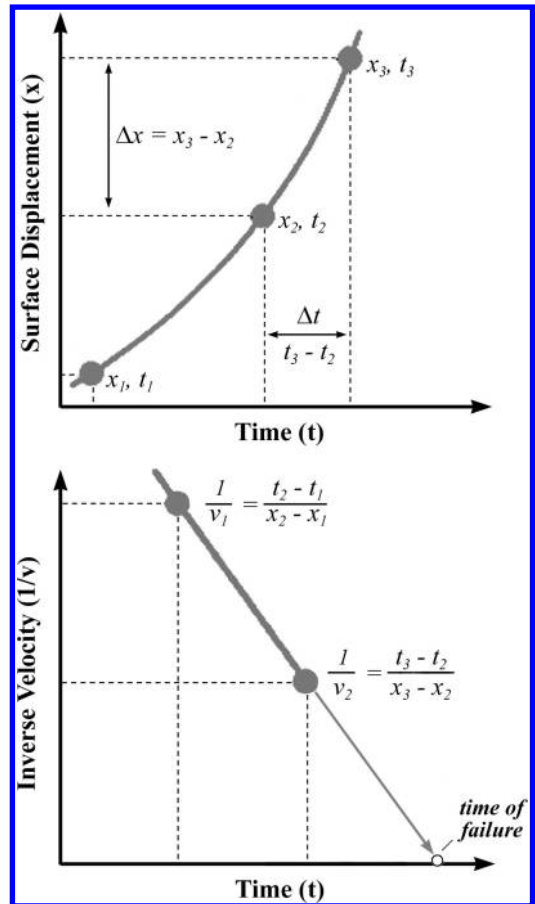
Figure 3. Method for temporal prediction of slope failure based on inverse mean velocity as calculated from surface displacements (after Fukuzono 1990).

respect to the magnitudes of velocity, or acceleration, for a given unstable slope. Salt (1988) proposed a set of empirical alarm levels for large New Zealand slides in schist, citing downslope velocities of 50 mm/day (or accelerations of 5 mm/day^2). Based on the case histories used, the cited alert threshold amounted to a forewarning of approximately 10 days. Crosta & Agliardi (2003) proposed a modified version of Voight's semi-empirical time-dependent failure criterion to provide velocity thresholds across time spans of 30, 15 and 7 days (i.e. defining pre-alert, alert and emergency standings, respectively). The case histories used involved large deep-seated, creeping-type rockslides, with velocity threshold values differing by an order of magnitude for the different cases (e.g. for the 7-day emergency alert: 2–12 mm/day for Val Pola, 74–77 mm/day for Vaiont, 207–923 mm/day for Chuquicamata). Given the complexity and differences in the geological and

102
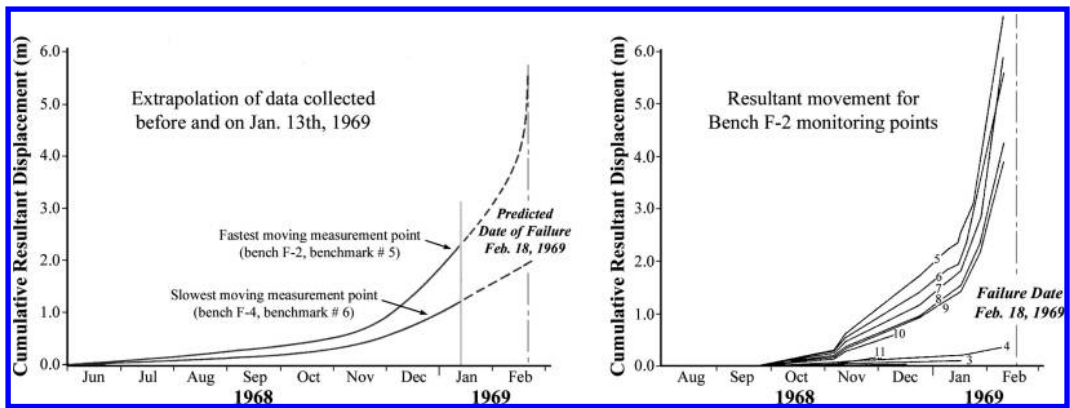
Figure 4. Extrapolation of displacement vs. time data used to predict a major rock slope failure at the Chuquicamata mine in the Chilean Andes, and the corresponding record subsequent to the prediction (after Kennedy & Niermeyer 1970).

environmental factors contributing to rock slope failure, Crosta & Agliardi (2003) note that as a predictor, such empirical methods only give an order of magnitude prediction of the failure time. Judgement should be exercised as to the prevailing external conditions involved in each individual case, including factors relating to the reliability of the monitoring network, the complexity of the displacement pattern, and the contributing influence of precipitation and/or other loading conditions.

It should be noted that the previously mentioned studies all involved back analyses (i.e. hindsight). Reported cases of successful forward prediction are few. In one of the better documented cases involving the Chuquicamata mine in Chile, Kennedy & Niermeyer (1970) report the successful extrapolation of displacement *vs.* time plots, based on open pit bench movements (of the F-2 bench), to predict the correct date of catastrophic collapse – five weeks in advance of failure. The collapse criterion used in this prediction was 6 m of displacement (Fig. 4), a value based on engineering judgement, displacement data, rock mass quality and lessons learned from two previous minor failures (Voight & Kennedy 1979). In this sense, the adopted methodology relied heavily on experience gained over time. Similar successes in forward prediction have likewise been documented by Zvelebil (1984) for a toppling failure in sandstone, Azimi et al. (1988) for a rockslide in gypsum, Suwa (1991) for a rockslide in tuff, and Hungr & Kent (1995) for coal mine waste dump failures.

The complexity of the measured displacement pattern, and thus the subjectivity and ambiguity involved in its subsequent interpretation, makes defining critical thresholds extremely difficult with respect to forward prediction. For example, Petley et al. (2002) maintain that since the linear inverse velocity relationship used by Fukuzono can be attributed to stress-induced brittle fracture processes (e.g. Main et al. 1993), it is only applicable to landslides that develop through the generation of a shear plane in previously un-failed rock. For failures involving ductile deformation processes or sliding on existing planes of weakness, they found that the inverse velocity follows an asymptotic trend. Crosta & Agliardi (2003) found that the linear inverse velocity trend was only applicable to data characterized by continuous acceleration and invariant to external conditions. Their experiences were that such empirical models fail when deviations induced by seasonal variations in temperature and rainfall take place.

In many displacement-time records, these seasonal fluctuations, which give rise to changing pore pressure conditions, produce a "stick-slip" or episodic creep behaviour (e.g. Bonzanigo et al. 2001). Heim (1932) encountered these difficulties in his early attempts to interpret accelerating slope movements for failure prediction, incorrectly predicting catastrophic failure for a rock slope above the town of Kilchenstock in the Swiss Alps – twice! Following a first incorrect prediction based on slope accelerations of 5–10 mm/day, which led to the evacuation of the town (Fig. 5a), Heim (1932) reported that "*lack of experience*" was the reason for being misled. Associating the accelerating slope movements with the wetter Fall and their deceleration with the dryer Winter, two years later when velocities increased to 20–40 mm/day during the dryer July and August months, Heim again predicted catastrophic failure followed by a second evacuation of the town, and again, a second unexpected cessation in slope movements (Löw 1997).

The case of Kilchenstock may have occurred 75 years ago, but today, the same difficulties in interpreting and predicting landslide failure from slope displacement records arise. In summer 2001, near Innertkirchen in the Swiss Alps, accelerations observed through surface displacement measurements of a

103
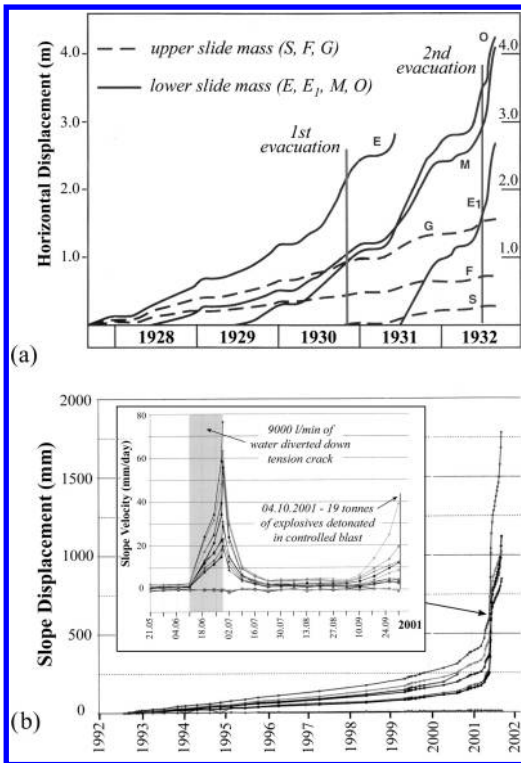
Figure 5. Extrapolation of displacement vs. time data used to incorrectly predict major rock slope failures in the Swiss Alps: (a) at Kilchenstock (after Heim 1932); (b) at Innertkirchen with inset showing velocity *vs.* time plot and response to different attempts to induce failure (after Gruner 2001).

250,000 m^3 unstable rock mass were interpreted as reaching a critical level (Fig. 5b) thereby requiring the closure of the only highway leading through the mountain pass (the Grimsel Pass). While the road remained closed and with failure believed to be imminent, a nearby stream with a flow rate of 9000 litres/minute was diverted down the tension crack for a period of 18 days to accelerate and induce failure (Gruner 2001).

Through this action, slope accelerations increased but failure did not occur (inset Fig. 5b). A decision was then taken to use 19 tonnes of explosives to bring down approximately 150,000 m^3 of unstable rock in what would be the largest controlled blast in Switzerland. Following the blast, official figures were not released but inspection of before and after photos suggested that maybe only 50% of the (supposedly critical) unstable mass was brought down. A second blasting campaign was subsequently carried out in August 2002 to bring down the remaining mass (Gruner 2003).

Such examples of failed prediction should not be interpreted as a criticism of those involved in the decision making process. Instead, they demonstrate the inherent difficulty in relying solely on phenomenological-based analyses in which the underlying kinematics, controlling processes and failure mechanisms are largely ignored. The prevalent use of surface displacement measurements obviously addresses certain economic realities in terms of what may be feasible for on-site monitoring of a given slope. Yet it must also be asserted that only so much can be inferred at surface when the problem itself takes place at depth. Moreover, the time span of displacement monitoring on which the predictive analysis is based (1–5 years in many cases) is only a small snapshot in time with respect to the natural processes driving the slope to failure. In the case of an engineered slope, the time over which failure develops closely corresponds to that over which the measurements are made. In the case of a natural slope however, creep deformations and slope movements have been in action for thousands of years, and have likely encompassed numerous cycles of acceleration and deceleration. From this, it is difficult to say whether slope accelerations observed in a short time period are those indicating imminent failure, or are only a short-term slip interval and second-order acceleration (like hundreds before it), which with time may eventually lead to a first-order tertiary creep acceleration and catastrophic failure. The answer to such questions likely lies in the mechanism of failure, the extent of basal shear plane development and how much deformation/strain a given slope can accommodate. As Bhandari (1988) notes, criteria for failure prediction based on the rate of slope movement will eventually require that they be related to the state of a slope prior to failure.

2.4 *Numerical approach*

Mechanistic approaches try to break the problem down into its constituent parts to understand the cause and effect relationships (and their evolution), which govern the behaviour of a system. In this sense, numerical techniques are commonly employed to study the balance between driving forces and resisting forces within a given slope, and the interaction between the soil/rock mass and external environmental factors (e.g. pore pressures, seismic loading, etc.). However, this requires tighter controls on boundary conditions, material properties and soil/rock mass constitutive relationships. Still, through the use of elasto-plastic yield criteria, numerical methods have been applied to determine/predict the location of a potential failure (for example around an open pit mine), the stability state of a slope as a function of changing environmental factors, the mode of failure, and/or the potential depth/volume of failure. Although time-dependent constitutive relationships are available (e.g. creep models), numerical methods are rarely directed towards

104
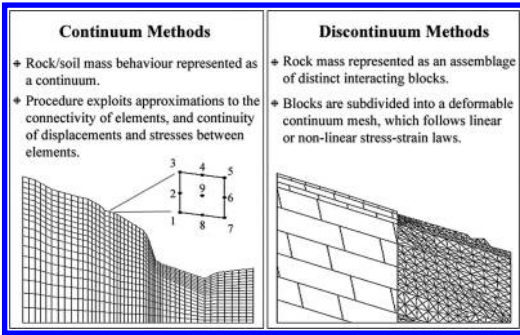
Figure 6. Overview of continuum and discontinuum numerical methods, with discontinuum model showing cut-away of interacting blocks discretized into deformable elements.

temporal prediction given the complexity and detailed data requirements such predictions would require.

Numerical approaches provide a means to analyze factors relating to landslide behaviour, including extent, depth and volume of a potential failure, mode of failure and stability state as a function of changing environmental factors. In their simplest form, limit equilibrium techniques examine static stability, where a simple balance of disturbing and resisting forces is used, for example, to search for the most likely depth of failure (i.e. most critical slip surface). A comparison of the different solutions employed to achieve a determinate solution is given by Fredlund & Krahn (1977). These methods, however, do not take into account the stress–strain behaviour of the slope mass. Numerical methods on the other hand, do utilize stress–strain constitutive relationships to calculate the stresses and deformations in a slope, as well as the evolution of these deformations as the slope mass strength degrades and failure localizes and initiates.

Numerical methods are generally divided into continuum and discontinuum techniques (Fig. 6). Hybrid codes, involving the coupling of these two techniques, have also been introduced to maximize their respective key advantages. Coggan et al. (1998) and Stead et al. (2001) summarize the advantages and limitations inherent in these different methodologies. The technique(s) chosen depends on both the site conditions and the potential mode of failure, with careful consideration being given to the varying strengths, weaknesses and limitations inherent in each methodology. Chiriotti et al. (1999) suggest that the objectives of a numerical analysis should be directed towards providing a reasonable understanding of the current conditions of the slope, making it possible afterwards to predict possible evolution scenarios of the instability (with attention paid to triggering mechanisms which may lead to catastrophic failure). The degree to which these objectives can be achieved depends on the quality of the

input data. High quality data enables the objectives to focus more on prediction (i.e. forward modelling of a potential instability), whereas limited data may restrict the analysis to establishing and understanding the dominant mechanisms that may affect the behaviour of the system (Fig. 7).

Working from a continuum assumption, the application of a finite-element (or finite-difference) analysis does not require any pre-definition of the failure surface. Instead, a yield criterion (e.g. Mohr-Coulomb, Hoek-Brown, etc.) can be employed to model and forward-predict the shape and location of the failure surface by following the elasto-plastic transition of groups of elements as they pass from an initial linear elastic state to an ultimate state of plastic yield. No commitment is required in the analysis as to any particular form of the failure mechanism *a priori* (Griffiths & Lane 1999). Figure 8 provides an example for a rock slope in southern Switzerland, for which a prediction of potential rockslide volume was required to perform a runout analysis to assess the risk to sensitive industry infrastructure in the valley below. The model was solved using a strain softening elasto-plastic constitutive model (decreasing strength as a function of increasing plastic strain; e.g. Lo & Lee 1973). The data available for the assessment were limited to those collected through geological mapping and field observations. Through this, the surface topography and geology were used to construct the model, and the location of tension cracks at the top of the slope was used to constrain the model results. The assumption of a continuum, although discounting the importance of discontinuities in controlling the path of the rupture surface, provides a clear picture of strain localization and the development of a displacement/velocity discontinuity delimiting the depth of failure (Fig. 8). As suggested by Griffiths & Lane (1999), failure occurs "naturally" within the zones of the slope mass where the shear strength is insufficient to resist the shear stresses, with yielding stresses being redistributed to neighbouring zones. Recent examples involving these techniques applied to case histories of massive unstable/failed slopes include Benko & Stead (1998),
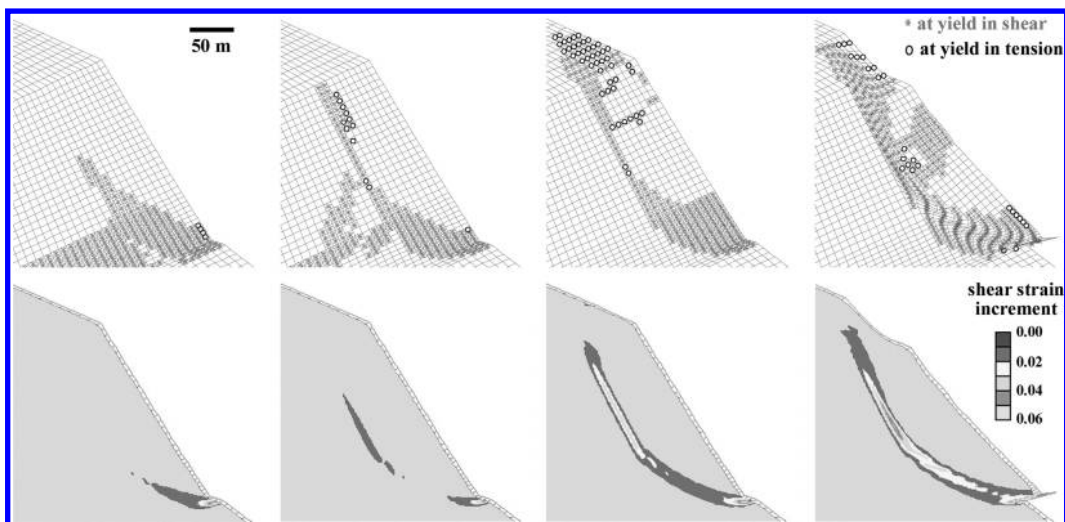
Figure 8. Forward prediction of the shape and location of a rock slope failure surface using an elasto-plastic continuum analysis. Model results show the plasticity indicators for several stages in the progressive development of the failure surface, and below, the corresponding localization of plastic shear strains.

Agliardi et al. (2001), Hajiabdolmajid & Kaiser (2002) and Eberhardt et al. (2004). More advanced numerical methods for modelling shear face localization in conjunction with adaptive remeshing (i.e. mesh refinement) techniques is discussed by Zienkiewicz & Huang (1995).

Where the slope instability mechanism is largely influenced by discontinuities (e.g. joints, faults, bedding planes, etc.), as is the case for many rock slopes, discontinuum methods provide a more suitable alternative for analyzing landslide behaviour.

Discontinuum methods, like the distinct-element method (Hart 1993), treat the problem domain as an assemblage of deformable blocks for which complex non-linear interaction between blocks are solved (i.e. slip and/or opening/closing along discontinuities). The method is also capable of modelling the deformation and elasto-plastic yielding of the joint-bounded intact rock blocks, similar to that discussed for the continuum techniques. Distinct-element modelling has been used to investigate a wide variety of rock slope failure mechanisms including those ranging from simpler planar/translational mechanisms (Costa et al. 1999, Eberhardt et al. 2005a), to complex deep-seated sliding/rotation (Chryssan-thakis & Grimstad 1996, Bhasin & Kaynia 2004), toppling (Board et al. 1996, Nichol et al. 2002) and buckling (Stead & Eberhardt 1997). These authors illustrate the need to consider both intact rock and joint-controlled displacements in the analysis of complex rock slope instabilities.

Figure 9 provides an example of a distinct-element analysis performed for a thinly bedded rock slope at a western Canadian coal mine, examining the potential
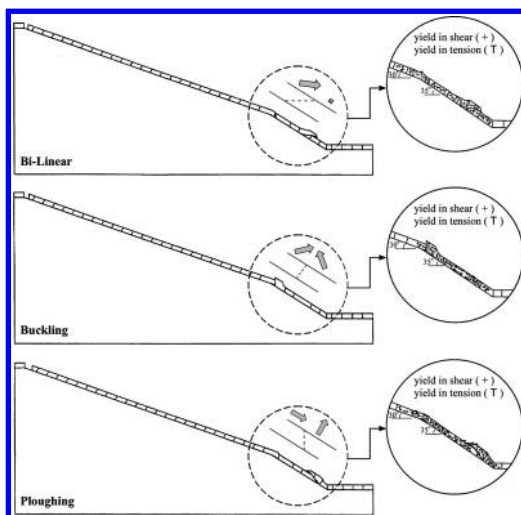
Figure 9. Distinct-element modelling of complex modes of slope failure in thinly bedded weak rock, showing plasticity indicators and movement of movement vectors of driving and passive slabs (after Stead & Eberhardt 1997).

modes of failure taken as a function of the orientation of an undetected cross-cutting discontinuity. The major failure mechanisms recognized include bilinear, ploughing and buckling slab failures, each involving some form of shear or tensile failure near the toe of the slope followed by planar sliding of the driving slab (Stead & Eberhardt 1997). By comparing the modelled displacement vectors for each failure mode

106
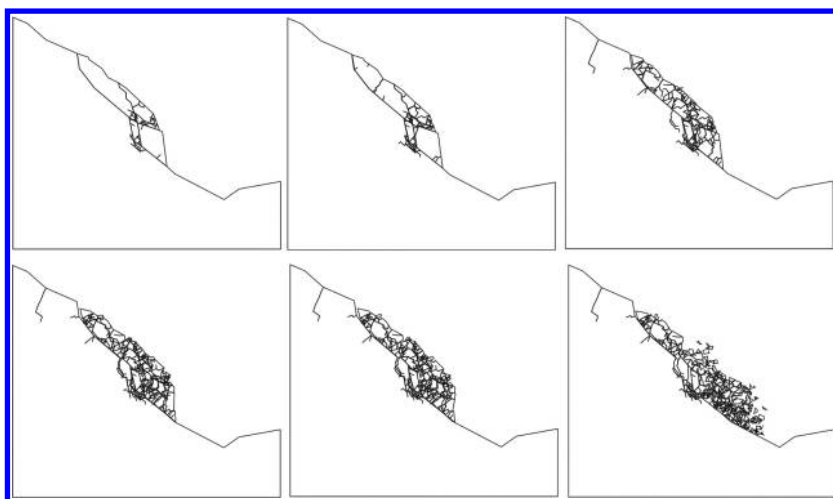
Figure 10.   Hybrid finite-/discrete-element analysis of the 1991 Randa rockslide showing several stages of progressive brittle failure (after Eberhardt et al. 2002).

to pit wall slope measurements, a prognosis of the mode of failure and therefore the best way to remediate the slope may be gained.

Further extensions of these methods have worked to combine both continuum and discontinuum techniques to model intact behaviour, interactions along existing discontinuities and the generation of new fractures (i.e. the transition from a continuum to a discontinuum). The simulation of softening and damage leading to brittle fracturing is accomplished using adaptive remeshing techniques, contact search algorithms and a fracture energy approach controlled by a designated constitutive fracture criterion (Munjiza et al. 1995). Such methods provide a means to model the degree of internal fracturing and coherency of a failed slope mass, a key consideration in any related runout analysis. If the moving mass fails coherently, higher velocities may accompany failure, whereas if the moving mass is ruptured internally, it will fail block by block, one after the other, and the travel distance and area covered would be much more limited (Eberhardt et al. 2004a). Figure 10 shows a series of model snapshots of the breakdown of a large rockslide mass, subsequent to failure initiation, based on Stead & Coggan's (2005) "Total Slope Failure" approach.

Through a better understanding of the mode of failure, numerical methods have also been extended to the problem of predicting the stability state for a given slope. In general, this has taken two forms: the use of strength reduction techniques to determine a factor of safety, and the use of coupled models to test a slope's sensitivity to various triggering mechanisms. Strength reduction techniques implement a procedure whereby the shear strength of the soil/rock is reduced until collapse occurs, from which a factor of safety is produced by comparing the actual shear strength of the material to the reduced shear strength at failure. This technique has the advantage over limit equilibrium solutions of automatically finding the critical slip surface as a function of the stress state and elasto-plastic yielding (Dawson et al. 1999). In addition, the coupled influence of pore pressures and/or dynamic loading on material yield, and therefore the factor of safety, can be more accurately represented. The modelling of nonlinear stress–strain behaviour together with one or more coupled process also allows for deeper insights to be gained into slope instability mechanisms and their sensitivity to different landslide triggers (e.g. intense rainfall, earthquakes, etc.). When combined with precipitation and infiltration records, thresholds may be determined through which predictions of depth and relative time of failure can be made. Collins & Znidarcic (2004) outline a methodology combining numerical analysis (for seepage infiltration) and limit equilibrium analysis (for stability state) to quantify failure depth and time in relation to soil, slope and rainfall parameters. Shou & Wang (2003) performed a similar threshold/sensitivity analysis in relation to dynamic loading of a landslide failure triggered by the 1999 Chi Chi earthquake in Taiwan.

The value of understanding such coupled processes also extends to decisions regarding mitigation measures to be undertaken and prediction of the response of an unstable slope to such measures. Bonzanigo et al. (2001) report the case of a massive 800 million m^3 deep-seated creeping landslide in the southern Swiss Alps, which threatened a local community located on the foot of the unstable slide mass (Campo

107
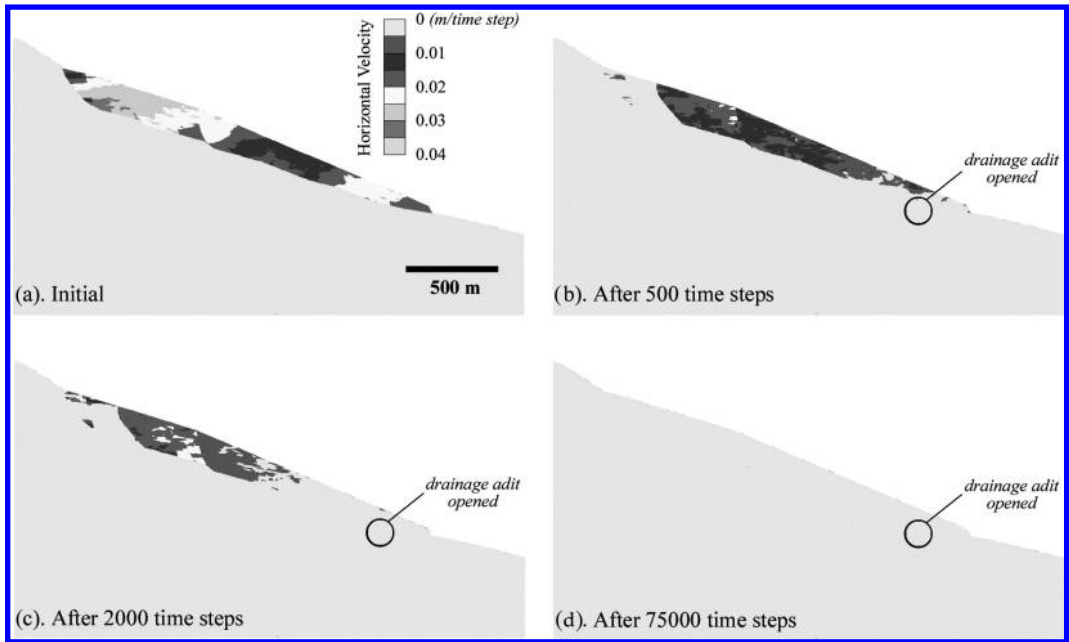
Figure 11. Coupled hydro-mechanical distinct-element model of Campo Vallemaggia, showing: (a–d) slope velocities prior to and after simulated opening of the drainage adit (after Eberhardt et al. 2005b).

Vallemaggia). Several different mitigation measures were proposed based on competing arguments as to the underlying factors causing the instability. Bonzanigo et al. (2001) used instrumentation records to show that sudden accelerations of the slide mass closely corresponded to pore water pressure increases exceeding an apparent threshold value. Subsequent modelling results showed that between the different mitigation measures implemented, deep drainage through the construction of a drainage adit provided the only significant benefit, resulting in a near immediate reduction in water head of 150 m and the almost complete cessation of downslope movement (Fig. 11). The coupled hydro-mechanical modelling procedure involved solving for the steady state pore pressure conditions (reproducing those recorded in boreholes), reduction in shear strength properties along the basal sliding surface (to initiate movements comparable to those recorded in the field), and activation of deep drainage through the modelled opening of the drainage adit. The modelling results showed that in terms of fracture permeability, where storativities are low, large water inflows through drainage are not necessary to achieve significant reductions in head, thereby explaining the relatively small water outflows measured from the drainage gallery that led to scepticism as to the effectiveness of the deep drainage solution (Eberhardt et al. 2005b).

In presenting these methods, it should be emphasized that elements of field mapping and monitoring,

in situ measurements and laboratory testing must also be included if the overall state-of-the-art is to move towards the total assessment or prediction of the rock slope stability state. Currently, an integrated network of displacement, pore pressure and microseismic monitoring devices has been installed at a site in southern Switzerland (the Randa Rockslide Laboratory), to help in quantifying the spatial and temporal evolution of such processes and to constrain complex numerical models (Willenberg et al. 2002, Eberhardt et al. 2004b). Yet it must always be emphasized that numerical modelling is only a tool and not a substitute for critical thinking and engineering judgement. Still, the potential exists to use numerical modelling to build upon empirical methodologies to improve the visualization and comprehension of the coupled processes and complex mechanisms driving such instabilities.

3 EMPIRICAL METHODS FOR ESTIMATING TRAVEL DISTANCE

Several empirical methods for assessing landslide travel distance and velocity have been developed based on field observations and on the analysis of the relationship between parameters characterizing both the landslide (i.e. the volume of the landslide mass) and the path (i.e. local morphology, presence of obstructions), and the distance travelled by the landslide debris. The

108
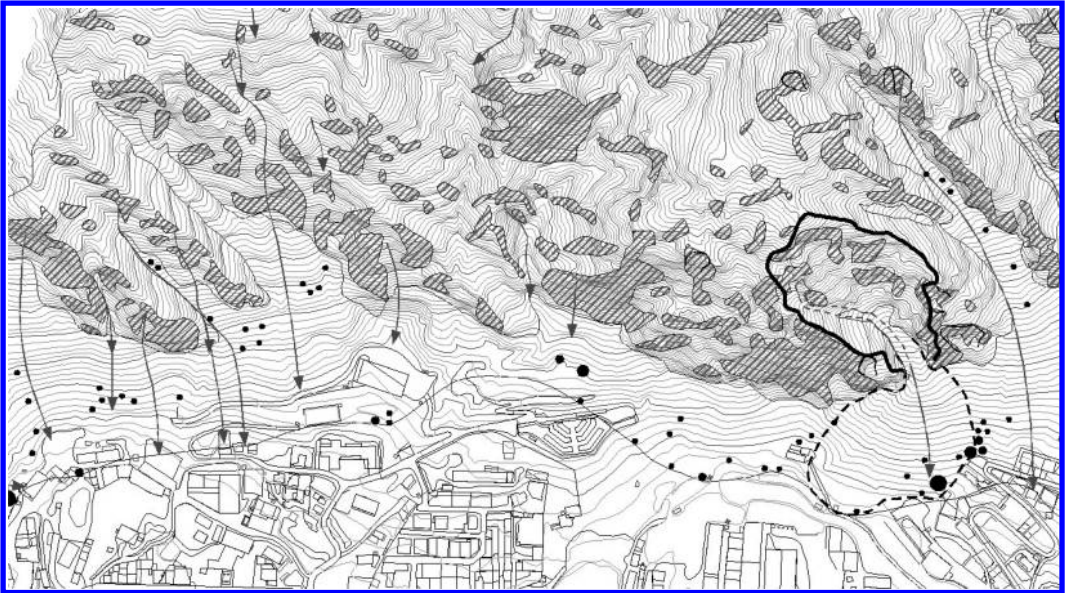
Figure 12. Boundary of the potential rockfall runout area in Santa Coloma (Principality of Andorra), defined by the line that links the farthest fallen blocks observed in the field (Copons 2004). Arrows indicate historical rockfall paths and solid circles are large fallen boulders.

availability of landslide data sets has encouraged the performance of simple statistical analyses (bivariate and multivariate analyses) which have produced indexes that are directly or indirectly related to the landslide mobility. As will be later shown, empirical indexes are based on simplified assumptions and, consequently, they might not have an evident interpretation. Because of this, the lack of agreement among researchers is not unusual.

Methods for predicting landslide runout can be classified as geomorphologically-based, geometrical approaches and volume change methods.

3.1 *Geomorphological assessement of landslide runout*

Field work and photo interpretation are the main sources of the geomorphological analysis for determining the travel distance of landslides. The assessment of the extent of both ancient and recent landslide deposits is the basis for defining future travel distances. The outer margin of the landslide deposits give an appraisal of the maximum distances that landslides have been able to reach during the present landscape, for a span of time that may last for several thousands of years (Fig. 12).

The first constraint that this approach has to overcome is the proper identification of the landslide deposits. Thus, in mountain regions, steep slopes of formerly glaciated valleys are the source of periodical

rock fall events. Isolated boulders of glacial origin (erratic boulders) scattered on the valley floor might be mistakenly attributed to rockfall events. Some features, like the lithological nature of the boulder, the presence of scratches, rounded edges and other erosive features, may help to discriminate the gravitational from glacial origin. In alluvial fans, debris flow deposits are often interbedded with torrential (aqueous) laid deposits. Several authors have provided both morphological and textural criteria to identify debris flows and their extent (Costa 1984, Jackson et al. 1987). Analysis of outcrops of both debris flows and mudflow events have allowed the delineation of catastrophic avalanches. For instance, mapping these types of deposits, which cover an area of about $550\,km^2$ in the Puget Sound lowland close to Seattle, has allowed the delineation of the largest lahar originating from Mount Rainier in the last 10,000 years, which is known as the Osceola Mudflow (Fig. 13). This cohesive lahar, which occurred about 5600 years ago, was at least 10 times larger than any other known lahar from Mount Rainier (Crandell & Mullineaux 1967, Scott & Vallance, 1993, Hoblitt et al. 1998) and delineates the scenario of the maximum extent that similar events might reach.

For these large and ancient landslide events, the limit of the affected zones are well established in the first part of the path but in the far reaches the lack of continuous outcrops makes the delineation of the boundaries more difficult. Because of this, areas

109

located immediately beyond distal hazard zones are not free of risk because the hazard limits can only be approximately located, especially in areas of low relief. Uncertainties relating to the source, size, and mobility of future debris flows preclude precise location of the hazard zone boundaries.

The geomorphological approach does not give any clue of the emplacement mechanism. Furthermore, the slope geometry and the circumstances responsible for past landslides might have changed. Therefore, results obtained in a given place cannot be easily exported to other localities.
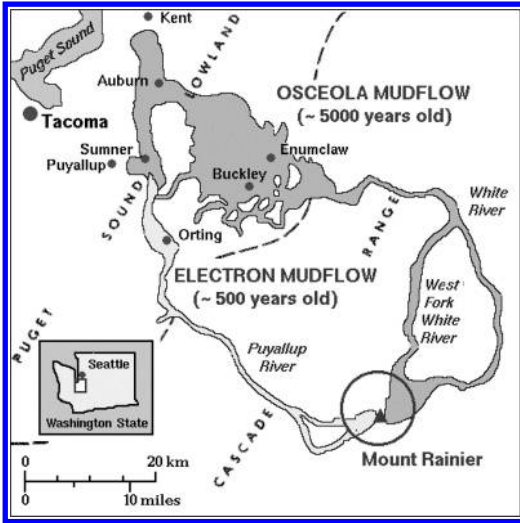
Figure 13.   Extent of two Holocene mudflows from Mount Rainier, WA established from field reconnaissance of the mudflow deposits (modified from Crandell et al. 1979).

3.2   Geometrical approaches

In this section, travel distance (L) is defined as the horizontal projection of the line linking the upper part of the landslide source and the outermost edge of the landslide deposits (Fig. 14). Finlay et al. (1999), using multiple regression analyses obtained several expressions for determining travel distance in cut slopes, fills, retaining walls and boulder falls (Table 2). These models apply only where debris runs onto a nearly horizontal surface below.

Finlay et al.'s (1999) data was a mixture of good and modest quality information which is reflected in the large scatter of the predicted travel distances. Hunter & Fell (2003) revised this work using more selective good quality data and their recommendations are to
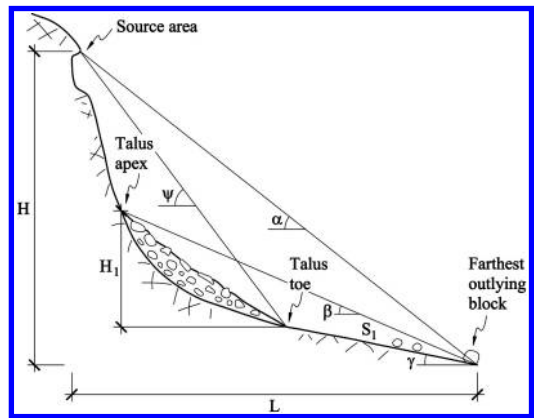
Figure 14.   Geometrical variables: vertical drop (H), travel distance (L), reach angle (α), shadow angle (β), source-talus angle (ψ), substrate angle (γ), and shadow distance (S_1).

Table 2.   Equations for landslide travel distance for Hong Kong slope failures (Finlay et al. 1999).

Dependent variable		Equation
Cut slope	LCI	Log L = 0.062 + 0.965 Log H − 0.558 Log (tan δ)
	Mean	Log L = 0.109 + 1.010 Log H − 0.506 Log (tan δ)
	UCI	Log L = 0.156 + 1.055 Log H − 0.454 Log (tan δ)
Fill slope	LCI	Log L = 0.269 + 0.325 Log H + 0.166 Log (V/W)
	Mean	Log L = 0.453 + 0.547 Log H + 0.305 Log (V/W)
	UCI	Log L = 0.693 + 0.768 Log H + 0.443 Log (V/W)
Retaining wall	LCI	Log L = 0.037 + 0.350 Log H + 0.108 Log (V/W)
	Mean	Log L = 0.178 + 0.587 Log H + 0.309 Log (V/W)
	UCI	Log L = 0.319 + 0.825 Log H + 0.150 Log (V/W)
Boulder fall	LCI	Log L = 0.041 + 0.515 Log H − 0.629 Log (tan δ)
	Mean	Log L = 0.253 + 0.703 Log H − 0.417 Log (tan δ)
	UCI	Log L = 0.466 + 0.891 Log H − 0.206 Log (tan δ)

Note: H is the vertical drop; δ the slope angle; V the landslide volume, and W the landslide width. LCI and UCI are the lower and upper 95% confidence intervals, respectively.

110

be preferred (Fell, personal communication). The slope failures showing the largest travel distance in the data set are fills, followed by retaining walls, cuts and rock falls. The interpretation of this is that many of the fills involved loose, granular materials with contractive behaviour during shearing.

The angle of reach (a) is the angle of the line connecting the highest point of the landslide crown scarp to the distal margin of the displaced mass (Fig. 14). This angle was defined by Heim (1932), who named it the fahrböschung angle. Other names given by various authors include the reach angle (Corominas 1996), travel angle (Hungr 1990, Cruden & Varnes 1996) and travel distance angle (Hunter & Fell 2003).

What the angle of reach represents has numerous interpretations. It has been considered as a measure of the relative mobility of the landslide (Nicoletti & Sorriso-Valvo 1991, Corominas 1996). Shreve (1968) called this angle the equivalent coefficient of friction and Scheidegger (1973) refined this concept, indicating that for a sliding body, the tangent of the reach angle is, in fact, the coefficient of friction of the surface of contact between the sliding mass and the ground, which is also expressed by the ratio between the vertical drop H and the horizontal component of the runout distance L. Several authors suggest, however, that Scheidegger's assumption is only valid in the case of the slope of the line linking the centres of gravity of both the landslide source and deposit (e.g. Hsü 1975, Voight 1978).

From empirical observations, Heim (1932) ascertained the dependence of the travel distance of a rock avalanche upon the initial height, the regularity of the terrain and the volume of the rockslide. A correlation was found between the height of fall and the distance travelled (Li 1983, Nicoletti & Sorriso-Valvo 1991), but this correlation is difficult to apply for practical purposes because the height of fall is not known beforehand except for slopes having a flat lying topographical surface below.

A plot of the tangent of the reach angle (H/L) against the landslide volume shows that large land-slides display lower angles of reach than smaller ones (Scheidegger 1973, Hsü 1975). This is the reason why large landslides have been considered as being more mobile. The reach angle of large landslides and rock avalanches is smaller than the expected friction angle of dry broken rock (about 32°). This greater mobility has been expressed by the "excessive travel distance" (Hsü 1975), which is the length (L_e) of the horizontal projection of the runout distance beyond the point where the line traced from the landslide crown dipping at an angle of 32° intersects with the topographical surface.

$$L_e = L - \frac{H}{\tan 32°} \qquad (1)$$

Large landslides may have L_e values of several kilometres. Corominas (1996) showed that both large and

small landslides had larger mobility that expected using a friction angle of 32°. This angle of 32° is anyway arguable as many landslide materials have frictional parameters much less than 32°. However, different mechanisms have been suggested to explain this higher mobility. The reader will find detailed discussion on these theories in several research papers (Hungr 1990, Van Gassen & Cruden 1989).

The volume dependence of the reach has been questioned by several authors for both large landslides (Hsü 1975, Hungr 1990) and small landslides (Hunter & Fell 2003), and other alternative explanations have been proposed (i.e. Davies et al. 1999). These works show that there is a lack of agreement among researchers, and opposite conclusions have been derived from these simple relations. As a consequence, the use of the reach angle to determine travel distance has to be made with care.

When the landslide source and potential landslide volume are known, the travel distance can be obtained from the following expression:

$$L = \frac{H}{\tan \alpha} \qquad (2)$$

In practice, for a given landslide source, the drop of fall (H) is sometimes not a variable known beforehand, except for slopes having a flat surface below. In such cases, a graphical solution can be obtained by assuming an angle of reach, for which a line can be traced from the source; the intersection with the topographic surface will give both H and L. Consequently, the key point is to assign an appropriate value of angle of reach to the landslide source. However, this is not an evident task.

Many authors have proposed empirical expressions based on the inverse relationship between the tangent of the reach angle (H/L) and the landslide volume. Initial studies assumed that only large land-slides and, particularly, rock avalanches, experienced a reduction of H/L with volume increase (i.e. Scheller 1971, Scheidegger 1973, Li 1983). Further studies with smaller landslides (Hutchinson 1988, Corominas 1996) and rockfall experiments (Okura et al. 2000) found a similar correlation with the following form:

$$Log \ tan \ \alpha = A + B \ Log \ V \qquad (3)$$

where A and B are constants and V, the volume. In Table 3 there are several suggested expressions for this relationship which correspond to the equation of the regression line.

In some of the landslide sets, the correlation coefficients of the relationship between volume and H/L are too weak to be used for runout prediction (Nicoletti & Sorriso-Valvo 1991). Similar attempts using a population of cuts, fills, retaining walls, and boulder falls in Hong Kong also found a weak correlation ($R^2 < 0.2$) and a lot of scatter (Finlay et al. 1999).

111

Table 3. Regression equation of Log H/L = A + B Log V, for different landslide inventories.

Authors	A	B	R
Scheidegger 1973	0.624	0.15666	0.82
Li Tianchi 1983	0.664	−0.1529	0.78
Nicoletti & Sorriso-Valvo 1991	0.527	0.0847*	0.37
Corominas 1996 (mean)	−0.047	−0.085	0.79

(*) Volume is expressed in $10^3 m^3$.

Table 4. Regression equation of H/L versus landslide volume for different landslide types and paths (from Corominas 1996).

Landslide type	Paths	A	B	R^2
Rockfalls	All	0.210	−0.109	0.76
	Obstructed	0.231	−0.091	0.83
	Unobstructed	0.167	−0.119	0.92
Translational slides	All	−0.159	−0.068	0.67
	Obstructed	−0.133	−0.057	0.76
	Unobstructed	−0.143	−0.080	0.80
Debris flows	All	−0.012	−0.105	0.76
	Obstructed	−0.049	−0.108	0.85
	Unobstructed	−0.031	−0.102	0.87
Earthflows	All	−0.214	−0.070	0.65
	Unobstructed	−0.220	−0.138	0.91

In order to improve the regression equations, Corominas (1996) performed an analysis using more homogeneous landslide populations. Landslides were split in different groups according to their predominant mechanism (rock falls and avalanches, translational slides, debris flows and earthflows) and the characteristics of the path (i.e. unobstructed, channelled, forested, obstructed by an opposite wall, etc.). The regression equations show a noticeable improvement (Table 4). However, a re-analysis of these data considering only volumes lesser than $10^6 m^3$, have given poorer correlations (Hunter & Fell 2003). The reasons that explain the scattering are manifold: (i) different motion mechanisms; (ii) different material properties, plus residual strength is not considered; (iii) pore fluid pressures are not accounted for; (iv) simplified morphology and variety of path constraints; (v) presence of obstacles, etc.

Due to the large scattering of the plots, the use of such equations for estimating the expected landslide travel distance needs to be applied with care because the mean values may give optimistic results. Many landslides will travel far beyond the calculated distance. Instead, it is recommended that the lower envelope be used (Fig. 14) and, if enough data is available, the lines that correspond to the different percentiles (98%, 95%, 90%, etc.) of the spatial probability.

Table 5. Regression equation of H/L versus tangent of the downslope angle (α) for landslides from natural slopes with different degree of confinement of the path (Hunter & Fell 2003).

Paths	A	B	R^2	SD
Unconfined	0.77	0.087	0.71	0.095
Partly confined	0.69	0.110	0.52	0.110
Confined	0.54	0.27	0.85	0.027

In many cases it is relatively easy to model the uncertainty in the travel distance in the calculation of the hazard. This can be done by assigning a probability that the travel distance will be in a certain range based on the equations in Tables 4 or 5. The lowest envelope gives the minimum reach angle and that will correspond to the maximum landslide runout (Fig. 15). This seems appropriate for preliminary studies of runout distance assessment (Corominas et al. 1990, Ayala et al. 2003, Corominas et al. 2003). Hunter & Fell (2003) found that the travel reach angle correlates reasonably well with the downslope angle and the degree of confinement of the path (Table 5). However, their data also exhibits the wide scatter typical of such correlations.

Domaas (1994), determined the reach angle from the angle (ψ) of the line linking the rockfall source with the talus toe (Fig. 14), for three intervals of height of vertical drop (H):

H < 200 m	$\alpha = 0.909\,\psi - 8°$
200 < H < 300 m	$\alpha = 0.875\,\psi - 3.7°$
H > 300 m	$\alpha = 0.842\,\psi - 0.7°$

To overcome the constraint of the previous estimate of both drop of fall and volume, other approaches have been proposed (Nicoletti & Sorriso-Valvo 1991) that only require the previous estimation of the elevation difference (this is very appropriate in slopes having flat surfaces below). These authors found that for landslide volumes ranging from 5×10^6 to $1.6 \times 10^9 m^3$ the ratio Le/L is usually contained between 0.5 and 0.8. Solving the equation:

$$L_e = L - H/\tan 32° \qquad (4)$$

for this range of values, L falls between 3.2 H and 8 H.

The rockfall shadow is the area beyond the toe of a talus slope that falling boulders can reach by bouncing and rolling. Hungr & Evans (1988) and Evans & Hungr (1993) have used the concept of shadow angle (β) to determine the maximum travel distance of a rockfall. It is defined by the angle of the line linking the talus apex with the farthest block (Fig. 14). This concept is applied only to fragmental rockfalls, which are defined as those events characterized by a more or

112
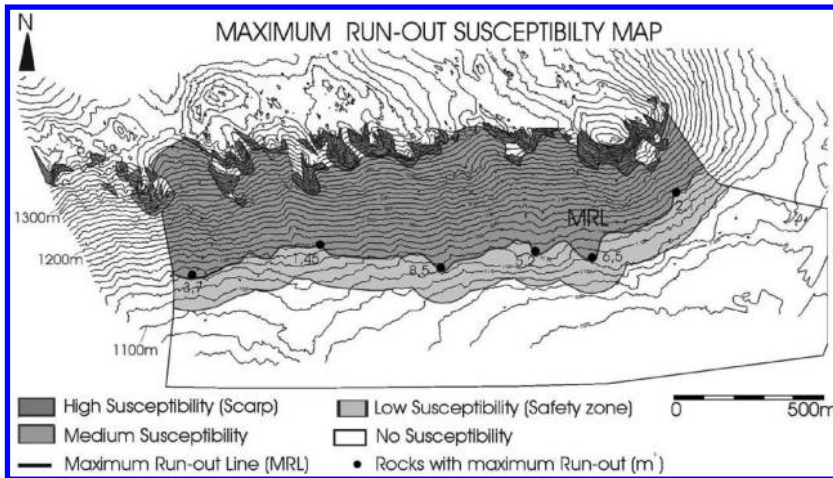
Figure 15. Boundary of the potential rockfall runout area in La Cabrera Sierra (Madrid, Spain), defined by the maximun runout line (MRL) that links the farthest fallen blocks observed in the field. A safety zone of 100 m width has been traced as well (Ayala et al. 2003).

less independent movement of individual particles generally involving less than 105 m^3, although there is no well defined volume limit. The application of this method also requires the presence of a talus slope since the shadow angle in delineated from the talus apex, and the talus toe is used as the reference point beyond which the distance travelled by the fallen blocks is determined.

The basic concept behind the shadow angle is that most of the kinetic energy of a rock fragment is lost in the first impacts on the talus slope and that the final runout is given by the rolling friction angle, which is obtained by projecting the slope of the energy line from the talus apex. An absolute value of 27.5° has been suggested for the minimum shadow angle (Evans & Hungr, 1993), which is a preliminary estimation of the maximum rockfall reach. However, flatter angles sometimes result where the talus and (or) the substrate is relatively smooth, like a glacier or a grass covered surface, with angles eventually reaching 23–24°. Domaas (1994) observed even smaller angles, as low as 17°, and found that the shadow angle is dependent on the height of the talus. The minimum shadow angle is related to the talus height (H$_2$ of the Fig. 14) in the following way:

$$\beta = 0.562 H_2 + 13.7° \qquad (5)$$

For talus slopes heights less than 200 m, the shadow angle obtained was smaller than 25° while for talus slopes lower than 100 m, the shadow angle reduced to as much as 16° (Domaas 1994).

The shadow angle has been used for zoning of hazardous rockfall areas in Andorra la Vella (Copons

2004). The shadow angle (β) has been determined for about one hundred blocks and boulders of recent rockfall events and an inverse relationship has been found between the tangent of this angle and the volume (V) of the individual fragments. The smallest shadow angles observed were about 26°. A lower envelope of the minimum shadow angles for the different volumes has the following shape:

$$\text{Log} \tan \beta = 0.045 \, \text{Log} \, V - 0.233 \qquad (6)$$

Rockfall susceptible zones were defined based on the spatial distribution of the fallen blocks. Several shadow angle boundaries were traced from the different talus apexes, taking into account the probabilities of blocks traveling further. Shadow angles of 33°, 32° and 30° correspond to a probability of 1, 0.1, and 0.01, respectively, while a lower value of 27.5° was taken from Evans & Hungr (1993) due to the small number of available cases. These angles define the boundaries between very high, high, medium, low and very low rockfall susceptibility zones (Fig. 16).

The Norwegian Geotechnical Institute (NGI) has developed a method for estimating the travel distance of rockfalls detached from mountain sides (Domaas 1994). This method like the shadow angle method can be applied only in places where talus slope deposits (screen) have developed. Furthermore, the validity of the NGI analysis is restricted to rockfall cases where the average ground surface slope beyond the talus toe is less than 12°. Under such conditions, a relationship between the total height of fall (H) and the distance travelled (S1) by the rock blocks beyond the talus toe (see Fig. 14) was derived. The greater the height, the

113

Figure 16. Rockfall susceptible zones, from very high (near the slope) to very low (away from the slope), defined from travel distance probabilities using the shadow angle (Copons 2004).

longer S1 will be. Again, a lot of scatter appears in such plots. A lower boundary line including 98% of the cases inventoried can be traced to show the worst-case scenario. The boundary line is expressed by the following equation:

$$S_l = aH + b = 0.3065H + 24.1 \, m \qquad (7)$$

3.3 Prediction of area covered by landslide debris

Another way to express the spatial susceptibility is by considering the area affected by the arrival of landslide debris. A rough proportionality has been found between volume (V) of the landslide debris and the area (A) covered by it. Such relationships have been observed by Davies (1982) and Li (1983), the latter providing the following empirical equation:

$$Log \, A = 1.9 + 0.57 \, Log \, V \qquad (8)$$

3.4 Volume-change method for debris flow runout prediction

The volume change method (Fannin & Wise 2001) estimates the potential travel distance of debris flows by imposing a balance between both the volume of entrained and deposited mass. The path is subdivided into "reaches", for which reach length, width and slope are measured. The model considers confined, transitional and unconfined reaches and imposes no deposition for flow in confined reaches and no entrainment for flow in transitional reaches. Using the initial volume as input and the geometry of consecutive reaches, the model establishes an averaged volume-change formula by dividing the volume of mobilised material by the length of debris trails. The initial mobilized volume is then progressively reduced during downslope flow until the movement stops (i.e. the volume of actively flowing debris becomes negligible). The results give a probability of travel distance exceedance that is compared with travel distances of two observed events.

3.5 Performance of the empirical methods

Geomorphological methods are purely empirical, without the capability of transferring the results to other areas of interest. Boundaries are defined based on the presence of previously deposited landslide material. In areas of low landslide activity, tracing this boundary may be a difficult exercise and subject to a high degree of uncertainty and error. Geometrical methods, however, are applicable in many other environments. All geometrical methods have in common a large scatter in the empirical relationship between parameters. This fact limits their use as a predictive tool for landslide travel distance predictions except where envelopes defining extreme cases (maximum extent) are considered or when the number of cases available in the database allows a probabilistic analysis. Despite these constraints, geometrical methods are useful.

The calculation of the reach angle requires the measurement of both the starting and end points for

114

individual landslides. For rockfalls, this constrains the preparation of a database, as events must be recent enough to allow for the identification of both source location and end point, otherwise the determination of the angle might be subjected to high degree of uncertainty and error.

Prediction of landslide debris travel distances requires knowledge about future detachment locations on the slope. A conservative approach in this circumstance may involve taking a minimum reach angle from the top of the slope which would overestimate the runout at a site (Evans & Hungr 1993). Shadow angle determination does not require the identification of the rockfall source area, only the location of the boulders beyond the talus toe. However, this method can not be applied unless a talus cone has developed at the base of the rock cliff. For slopes partly covered by fallen blocks, alternative procedures must be used.

Using envelopes derived through empirical methods are conservative but not unrealistic because they are based on observed cases. In effect, the travel distance prediction derived corresponds to the most extreme observed events that are attained by only a minority of the landslide cases. The conservative nature of this approach may be very appropriate in preliminary assessments of landslide susceptibility and hazard. However, for detailed studies the uncertainty in travel distance should be modelled as described above. Ideally, travel distance should also be calculated with numerical analyses calibrated for local conditions.

Empirical methods are very simple and travel distances can be obtained very easily. The main advantage is their simplicity and that they can be implemented in GIS to delineate the areal extent of potential slope failures for susceptibility and hazard mapping purposes (Ayala et al. 2003, Michael-Leiba et al. 2003, Copons 2004). However, it should likewise be noted that assumptions implicit in these methods are not precise and their statistical scatter is very large. Also, they do not provide kinematic parameters during the runout process, which are needed for engineering design.

4 ANALYTICAL METHODS

4.1 General

Analytical methods seek to model a moving landslide using the physical rules of solid and fluid dynamics. Most models are solved numerically, using some form of finite difference or finite element solutions. The three main groups of solutions include the block ("lumped mass") models, two-dimensional models looking at a typical profile of the slide and neglecting the width dimension and three-dimensional models treating the flow of a landslide over irregular 3-D

terrain. Most models (but not all) belonging to the latter two categories are simplified by integration of the internal stresses in either vertical or bed-normal directions to obtain a form of St. Venant equations. Hydraulicians tend to refer to integrated 2-D solutions as 1-D and integrated 3-D as 2-D, which may introduce a degree of confusion. Herein we will retain the original definitions.

Certain groups of researchers attempt to derive the required constitutive relationships from first principles, using the theory of frictional grain flow (e.g. Savage & Hutter 1989), or mixture flow (e.g. Iverson 1997). Some attempts have been made recently to model landslide motion as the movement of discrete particles, without pore fluid (e.g. Campbell 1989). Most models use a semi-empirical approach called "equivalent fluid method" (Hungr 1995), assigning simple constitutive relationships judged appropriate for a given material. The validity and parameters of a given rheological model are determined by back-analysis of case histories similar in character to the case under consideration. Most models use a unique, constant constitutive relationship for a given case. Others vary the material properties for different segments of the path or for selected zones within the moving mass such as the front and the body of the landslide.

The processes involved in the movement of rapid landslides are very complex and direct measurements of key variables such as pore-pressure and viscosity are impossible in full-scale examples. Thus, any theoretical solution must necessarily contain major simplifications. As is the case with static stress-deformation analyses in soil and rock mechanics, no analytical solution can be relied on without being calibrated against field observations. Simple models are preferred, as a limited number of parameters can more easily be constrained. Many models that are too complex contain large numbers of changeable parameters that cannot be reliably dimensioned, permitting almost any desired result to be obtained. Preferably, calibration analyses should be applied to more than one test case, to ensure that the analysis is repeatable.

4.2 Sliding-block models

In the first known attempt to analyse landslide movement, the physicist E. Müller-Bernet, working in association with Albert Heim (1932), used the analogy of a block sliding on a curved path, characterised by constant frictional resistance. Figure 17a shows the geometry of a path with local slope angle β and a block with a mass M, moving along the path surface characterized by a Coulomb friction angle, ϕ. From the Work-Energy Theorem, the rate of change of kinetic energy of the block equals the work of the net force acting on the block.

115

$$d(\frac{Mv^2}{2}) = FdL \tag{9}$$

Here, v is the velocity and the net force, F = Mg (sin β − cos β tan ϕ) is the difference between the gravity driving force, S and the frictional resistance, T and L is the curvilinear distance along the path.

The changing kinetic energy of the block can be graphically expressed by plotting the "energy head", $v^2/2$ g as a vertical height above the current centre of gravity of the block. The locus of the resulting points was called by Müller-Bernet "energy line" and is plotted in Figure 17a.

From Equation (9):

$$d(\frac{Mv^2}{2}) = Mg(\sin\beta - \cos\beta\tan\phi)dL \tag{10}$$

From this equation and the geometry of Figure 17b, the differential gradient of the energy line, dE, equals:

$$dE = dz - d(\frac{v^2}{2g}) = (-\tan\phi)dx \tag{11}$$

Thus, as Müller-Bernet had shown, the energy line of a block moving against constant frictional resistance is a line, inclined at an angle equal to the applicable friction angle. This result formed the theoretical basis of Heim's fahrböschung method, as described in
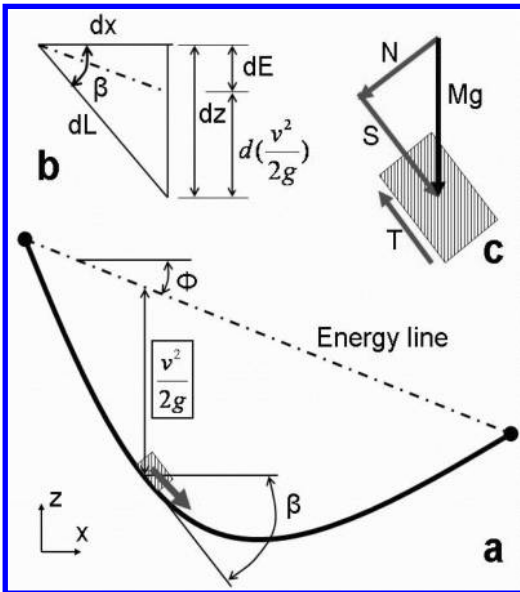
Figure 17. Derivation of the sliding block dynamic equations. (a) Path profile; (b) Local slope geometry relationships; (c) Force diagram.

Paragraph 3.2 above. The theory also provides a simple means of estimating the velocity of a frictional slide, from the vertical separation between the energy line and the ground.

Of course, representing the mass of a moving landslide by a dimensionless block is a major simplification. In particular, the important effect of lateral and longitudinal spreading of the slide mass cannot be accounted for. It should also be pointed out that the Work-Energy Theorem of Equation (9) should be applied with reference to the centre of gravity of the sliding mass, not between the crown of the source area and the toe of the deposit. Physically, therefore, the block theory and the fahrböschung concept are only crude approximations of the flow process for most types of landslides.

4.3 Rheological relationships

Körner (1976) demonstrated a useful application of the simple block model that helps to clarify the influence of various constant and changing rheological relationships on the dynamic behaviour of landslides. He noted that the height of the frictional energy line resulting from typical snow avalanche and rock avalanche path profiles often implies unrealistically high velocities. He then introduced a two-parameter frictional-turbulent resistance relationship proposed for snow avalanches by Voellmy (1955). The resisting stress on the base of a flowing sheet of fluid material is given by the sum of a Coulomb frictional and Chézy turbulent term (see also Hungr 1995):

$$\tau = \rho g h \cos\beta \tan\phi_b + \rho g \frac{V^2}{\xi} \tag{12}$$

Here, h is the normal thickness of the flow, ρ is density and ξ is a turbulence parameter similar to the Chézy coefficient, with dimensions of L/T^2. Dry cohesionless granular materials appear always to be frictional (e.g. Hungr & Morgenstern 1984). Therefore, the turbulent term is needed only in the presence of a pore-fluid. In the presence of a pore-fluid, the friction angle ϕ_b is mediated by a pore-fluid pressure according to the principle of effective stress and can thus be much lower than the dry friction angle of the material, ϕ:

$$\tan\phi_b = (1 - r_u)\tan\phi \tag{13}$$

The pore-pressure coefficient, r_u is the ratio between the pore fluid pressure and the total normal stress, as commonly used in soil mechanics. Provided that r_u can be assumed constant for the soil mass under consideration, the right hand side of Equation (13) remains of a frictional character, i.e. the shear strength component represented by it is proportional to the total

116

normal stress (Hungr 1995), even though it represents both material friction and pore pressure.

Körner (1976) showed that the energy line resulting from the Voellmy rheology is curved and concave. Thus, for a given overall displacement of the block on a path profile, the two-parameter model predicts lower maximum velocity. This result can be shown by a re-derivation of the energy line differential equation. Equation (10) is modified by assuming that the "block" is of a constant thickness, h and by introducing the Voellmy rheology from Equation (12) as:

$$d(\frac{Mv^2}{2}) = Mg(\sin\beta - \cos\beta\tan\phi - Mg\frac{v^2}{gh\xi})dL \quad (14)$$

Then from Figure 17b:

$$dE = dz - d(\frac{v^2}{2g}) = (-\tan\phi - \frac{v^2}{gh\xi})dx \quad (15)$$

With two parameters instead of one, the Voellmy solution is no longer unique for a given landslide displacement profile. Many different pairs of the bulk friction angle and turbulence coefficient can produce the same displacement. A unique pair of ϕ_b and ξ must be selected so as to match any available data on movement velocity. The largest velocity will be predicted for the frictional rheology, when the turbulence coefficient ξ is very large and the second term in Equation (12) can be neglected.

An example back-analysis of a real landslide profile, produced by a numerical solution of Equation (15),

is shown in Figure 18. This is a rock slide – debris avalanche with a final volume of over 700,000 m³ that occurred in 1999 in the valley of the Nomash River, Vancouver Island, Canada and was described by Hungr & Evans (2004a). As shown on the profile in Figure 18a, the landslide descended a steep 600 m high slope, turned 90° in azimuth and flowed for more than 1.5 km along a gently sloping valley bottom. Field observations of superelevation in bends along the path allowed the true velocity to be estimated at three points along the path, as described in Hungr & Evans (2004a). Figure 18b shows three block model solutions. The frictional solution was run with a ϕ_b equal to the fahrböschung angle (13.8°), neglecting the turbulent term. Two Voellmy solutions are also shown, one with a $\tan(\phi_b)$ of 0.05 and ξ of 400 m/sec², the second with 0.04 and 200 m/sec². All three solutions produce approximately the same overall displacement of the block, but they differ in their velocity profiles (Fig. 18b). As found by Körner, 1976, the frictional rheology overestimates the speed, while the Voellmy model provides a much closer fit.

Other rheologies have been proposed in the context of the block model. The so-called sliding-consolidation model (Hutchinson 1986) assumes that high pore pressure forms during failure in the source area, as a result of undrained pore-pressure response or liquefaction. As the slide flows down the path, the excess pore pressure acting on the rupture surface dissipates through consolidation. Eventually, the effective stress acting on the sliding surface recovers sufficiently to cause the slide to stop. This process is illustrated by the short-dashed line in Figure 19. The solution was obtained using the frictional model controlled by a ϕ_b as
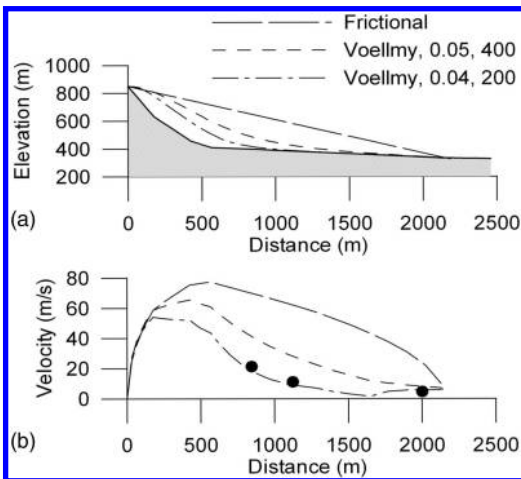
Figure 18. Example block model analysis of the Nomash Slide, using frictional and Voellmy rheologies. (a) Path profile and energy lines. (b) Velocity profiles. The black dots indicate field estimates of velocity by Hungr & Evans (2004a).
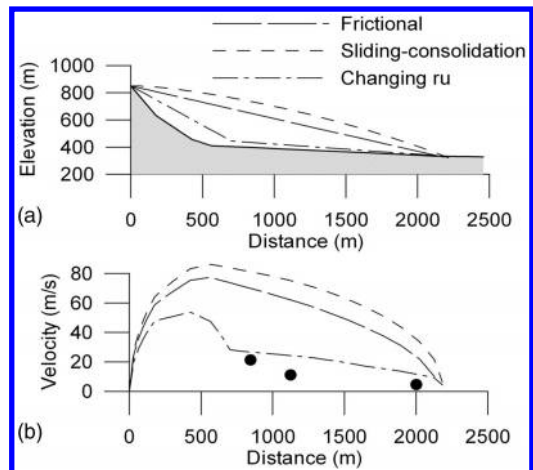
Figure 19. Alternative block model analyses of the Nomash Slide, using frictional, sliding-consolidation and r_u-controlled frictional solutions.

117

for the frictional solution. However, the pore-pressure ratio in Equation (13) was allowed to dissipate as an inverse exponential function of the elapsed time of travel, approximating pore-pressure diffusion. In the solution shown in Figure 19, the initial ru was 1.0 (geostatic value), but the ratio fell to 0.3 during the 50 seconds of travel. The energy line is convex upwards, so that the velocity required to reach a given displacement is greater than that predicted by the frictional model. Thus, the sliding-consolidation models will tend to over-estimate movement velocities to an even greater extent than frictional models. It is also unclear whether unhindered consolidation can exist in a rapidly shearing mixture of grains and fluid and, if it does, whether the short time interval occupied by extremely rapid flow slides allows sufficient time for significant consolidation to occur (e.g. Hungr & Evans 2004a).

Another configuration of the block model was used by Sassa (1988) to show the influence of pore-pressure that changes during the flow as a result of over-riding and undrained loading of saturated soil found in the path of the landslide. The model shown by the dash-dot line in Figure 4.19 is frictional, based on the assumption of an initial pore-pressure ratio of 0.0 (dry sliding), changing to a value of 0.87 at the foot of the steep slope, where saturated valley deposits may be over-ridden. The pore-pressure change appears as a sudden reduction in the slope of the energy line. The resulting velocity profile falls close to the values estimated in the field.

Sassa's undrained loading model can simulate the limited velocities of real landslides, provided that an appropriate sequence of ru's is chosen. Whether rate-dependent (turbulent) flow resistance is also involved in the same process is a question that remains unanswered. Possibly, the development of flow resistance in a slide moving over saturated soil involves both changes of pore-pressure and the appearance of turbulent effects. This can be modelled by a combination of a frictional model in the steep proximal part of the path, followed by a Voellmy segment with a relatively low ϕ_b combined with a turbulent term. Such configurations have been tried using 2-D and 3-D flow models (e.g. Hungr & Evans 2004a, McDougall & Hungr 2005).

One piece of evidence in favour of rate-dependent resistance is the behaviour of debris flows. Debris flow surges, although fronted by frictional boulder accumulations often move for a number kilometres at moderate speeds, implying the existence of a normal depth – and rate-dependent rheology – in the liquefied granular mass behind the front (e.g. Takahashi 1991, Hungr 2000).

4.4 *True 2-D models based on the Bingham rheology*

The first analytical models dedicated to the dynamics of landslides were two-dimensional and based on the Bingham rheology, in which the resisting stress is determined by the flow depth, h, a constant yield strength, τ_y and a linear viscous term with Bingham viscosity η. An explicit formula for the resisting stress, τ like Equation (12) cannot be given but the stress can be related to mean velocity, v, through a third-order equation (e.g. Hungr 1995):

$$v = \frac{h}{6\eta}(2\tau - 3\tau_y + \frac{\tau_y^3}{\tau^2}) \qquad (16)$$

Trunk et al. (1986) modified an existing true two-dimensional finite-difference laminar flow code to accept two viscosities, one applied up to the level of the yield stress and a smaller one above, to approximate Bingham rheology. The same code, called BVSMAC, was used by Sousa & Voight (1991) and Voight & Sousa (1994) to model rock avalanches. The advantage of the true 2-D formulation is the ability to derive the vertical velocity distribution and the stratigraphy of the deposits. On the other hand, there is no direct justification for using the Bingham model with materials other than clayey debris (e.g. Johnson 1970). Voight & Sousa (1994), as well as Hungr & Evans (1996) both concluded that the Bingham model used for rock avalanches tends to overestimate velocities and predict excessive longitudinal spreading of deposits. Recently, however, it was found that a small rock avalanche mobilizing and entraining large quantities of plastic clayey colluvium could only be modelled realistically using the Bingham model, in order to duplicate a thin, even spreading of the deposits (Geertsema et al. 2005).

4.5 *Integrated 2-D models*

Two-dimensional solutions of landslide motion can be derived from the momentum equation for unsteady fluid flow. The basic equation can be derived phenomenologically by considering the dynamic equilibrium of a column isolated from the flowing sheet, as shown in Figure 20.

The stresses acting on the column are integrated in the bed-normal direction, assuming that flow lines are parallel with the base, so that there are no shear stresses on the sides of the column and the normal stress increases linearly with depth. In hydraulics, these are known as the shallow water assumptions. The classic, Eulerian form of the governing equation of motion is then:

$$\chi v\frac{dv}{dx} + \frac{dv}{dt} = g\sin\beta - \frac{\tau}{\rho h} - gk\cos\beta\frac{dh}{dx} \qquad (17)$$

This is a simple re-statement of Newton's Second Law, divided by material density, ρ and flow thickness, h. The left hand side is the acceleration, consisting of a convective and local part. v is the mean flow velocity.

118
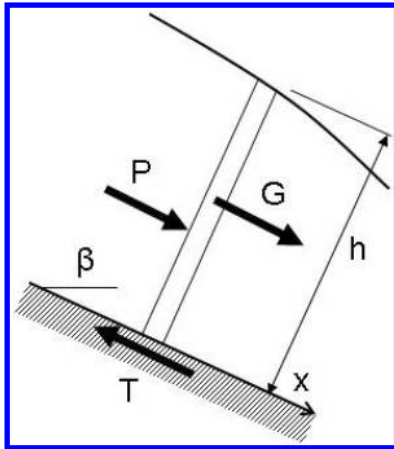
Figure 20. A reference column used in deriving the equation of motion for the 2D flow.

Figure 21. Framework for the numerical solution of the St. Venant Equation in the Lagrangien form (Equation 10). After Hungr (1995).

The coefficient X is a correction factor, required because the convective part of acceleration is non-linear with depth. The first term on the right-hand side is the gravity component, G. The second term is the basal shear resistance, T and the third is the pressure gradient, P. In fluid, the constant k in the pressure term would equal 1.0, consistent with hydrostatic conditions. In a frictional mass, it may be a lateral pressure coefficient depending on the internal strain of the flowing mass as discussed below.

Equation (17) is derived with reference to bed-normal thickness. A similar equation could be used with reference to vertical column boundaries, as is common in hydraulics (e.g. Iverson 2005). However, the force diagrams used in solving the equilibrium of the vertical column become severely distorted on steep slopes and this may affect the performance of the model.

Given the highly unsteady nature of landslide motion, as well as the need to monitor internal strain and entrainment of material, it is convenient to re-state Equation (17) in its Lagrangian form, where the reference coordinate x is not fixed in space, but travels with the flow. Physically, the Eulerian form could be imagined as a set of observations made by an observer stationed on the bank of a flowing stream. The Lagrangian form results from measurements made by an observer floating on top of the flow. Mathematically, the Lagrangian assumption makes the convective acceleration part disappear:

$$\frac{dv}{dt} = g\sin\beta - \frac{\tau}{\rho h} - gk\cos\beta \frac{dh}{dx} - \frac{dhv}{h} \qquad (18)$$

The last term added on the right hand side of Equation (18) is an adjustment for the entrainment of

material from the path during the flow. Such material must be accelerated to the reference frame velocity v, consuming some momentum (Hungr 1995).

A Lagrangian solution of Equation (18) (without the entrainment term) was developed by Savage & Hutter (1989) for the frictional rheology. The numerical solution is based on the framework illustrated in Figure 21. Narrow reference columns, as depicted in Figure 21 and numbered i = 1 to n, separate wider "mass blocks", numbered j = 1 to n − 1. The mass blocks remain of constant volume, unless entrainment is specified, thus implicitly satisfying the continuity equation. The solution is explicit. In each time step, Equation (18) is applied to each reference column and the column is displaced forward. When all the columns have assumed new positions, the mass blocks are re-dimensioned by interpolation to obtain new estimates of flow depth.

The Savage-Hutter model introduced non-hydrostatic internal tangential stress, based on the assumption that the flowing mass is frictional, controlled by an internal friction angle ϕ_i and undergoing plastic deformation according to the Rankine theory. As a result, the coefficient k in the last term of Equation (18) varies typically between approximately 0.5 in zones where the flowing mass is stretching on convex path segments and about 4 when it is being compressed, corresponding to Rankine's active and passive conditions respectively. The ability to model non-hydrostatic internal stress is perhaps not essential for fluid-like, fully saturated flows such as debris floods or fully-liquefied flow slides. But it is important for the large group of flow-like landslides that involve relatively strong frictional masses, moving on a basal liquefied or otherwise weakened layer. Thus, it is especially important for rock avalanches, as without it, the motion of the slide front cannot be properly predicted (e.g. Hungr 1995). It is also important for any dry granular flows, in nature or the laboratory, that exhibit frictional internal strength.

Hungr (1995) added the possibility to change the width of the flow according to a user-defined path-width function. This allows the flow depth to reflect

119

narrowing or spreading of the flow according to the anticipated degree of confinement, producing a pseudo-3D solution. This approach neglects momentum expenditure in the direction perpendicular to the flow direction. However, comparisons with 3-D solutions and real cases indicate that the effects of this simplification are not significant, except in the case of very abrupt changes of confinement (e.g. McDougall & Hungr 2005). Figure 22 shows an example of a Voellmy analysis of a rock avalanche carried out using the model DAN ("dynamic analysis"). The case illustrated in this analysis is the right-hand streamline of a T-shaped constrained rock avalanche shown in Figure 23. Both the pseudo-3D analysis and the true integrated 3-D analyses produced very similar results in terms of runout distance, debris distribution and velocity.

The frictional Savage-Hutter (1989) model was verified against controlled small-scale laboratory experiments involving the flow of sand. Hungr (1995) added an open rheological kernel, allowing the resisting stress, τ, to be determined by a number of alternative rheological formulas, while the internal shearing of the flowing mass remains frictional. This allows the user to search for the optimal type of rheology, as required by the "equivalent fluid" approach. The resisting stress can thus be determined from Equation (12) for frictional or Voellmy rheology with pore pressure, from Equation (16) for Bingham rheology, or using viscous, plastic and other relationships. The model was verified against laboratory experiments for the dry frictional, frictional with pore pressure and viscous rheologies.

Verification against the BVSMAC model was made for the Bingham rheology (Hungr 1995). More recently, the DAN model was calibrated against multiple case histories of flow slides in mine waste and a specific type of natural debris avalanches (Hungr et al. 2002, Revellino et al. 2003). The DAN algorithm has been coded into a spreadsheet form and as a GIS macro by the Geotechnical Engineering Office in Hong Kong (H.N. Wong, pers. comm. 2003). A feature allowing entrainment of path material at a user-prescribed rate was described by Hungr & Evans (2004a).

Iverson (1997) extended the Savage-Hutter model to simulate the behaviour of debris flow surges fronted by coarse debris accumulations. In his modification, the bouldery front was simulated by a frictional mass of a given volume, whose pore-pressure ratio was assumed to increase linearly from the leading edge backwards. The front was followed by inviscid fluid flow. The model results compared favourably with experimental debris flows observed in a large-scale
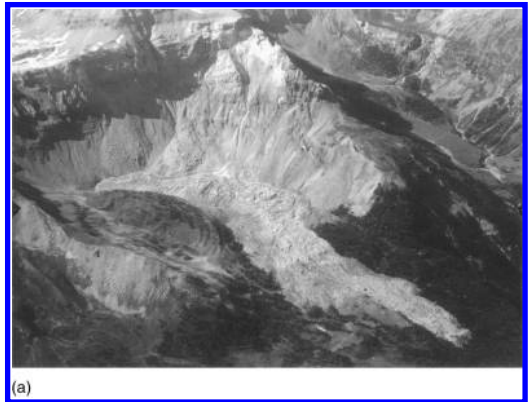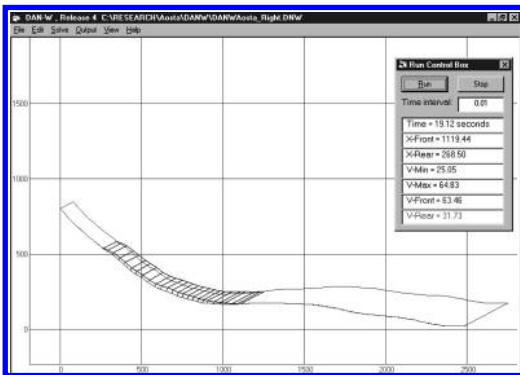
Figure 22. An example of a pseudo-3D analysis using the model DAN (Hungr 1995). The picture represents an instantaneous position of the landslide in an isometric view. This analysis is of the right-hand streamline of the Eaux Froides rock avalanche shown in Figure 23. Voellmy rheology, $\phi_b = 12°$, $\xi = 200\,\text{m/sec}^2$. (Data courtesy Dr. J-D Rouiller, CREALP, Switzerland)
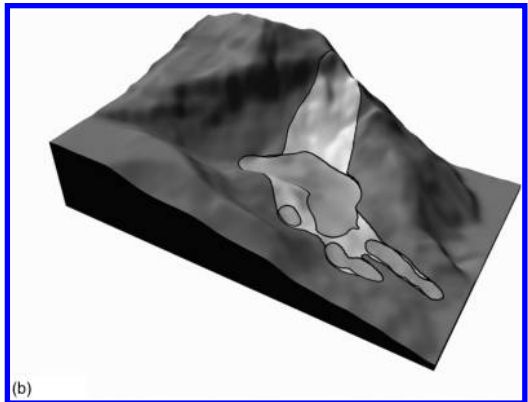
Figure 23. A 3-D analysis of the Eaux Froides rock avalanche in Switzerland, using the method of McDougall & Hungr (2004a). (a) Aerial photo of the landslide, (b) Deposit calculated by the model. Voellmy rheology, $\phi_b = 12°$, $\xi = 200\,\text{m/sec}^2$. (Data and photo courtesy Dr. J-D Rouiller, CREALP, Switzerland).

120

flume, but to date no comparison with natural debris flow surges has been made. As shown by Hungr (2000), the flow profile is such compound models is strongly influenced by the volume of the frontal accumulation, which is a function of the granulometry of the debris and the maturity of the longitudinal sorting of a given surge.

4.6   *Three-dimensional fluid dynamics models*

Several three-dimensional models have been developed using the standard Eulerian form of the equations of motion configured as a 3-D extension of Equation 17. These solutions are implemented on a fixed rectangular grid. Besides the local acceleration of the fluid, the models also need to keep track of fluid discharge across the fixed grid boundaries and the associated momentum fluxes.

"FLOW-2D" (O'Brien et al. 1993) is one of the few existing models actually used for practical work (it is a 3-D integrated Eulerian model). It is designed for analysis of the behaviour of debris flows and debris floods on colluvial fans. A good example of its use is illustrated by García et al. (2003). The flow resistance in the model is determined using an empirical rheological relationship similar to the Voellmy formula (Equation 12), but with the addition of an additional ("viscous") term, linear with velocity. Some attempts to calibrate the rheological formula through laboratory viscometer testing have been described in the literature, but in practice, the three resistance parameters must be dimensioned through back-analysis. The model does not simulate the motion of the landslide from the source area along the path. Instead, the input is in the form of a flow hydrograph at the head of a depositional debris fan. From there, the model determines the distribution of debris over the fan surface, allowing for obstructions and pathways such as buildings, roads, channels and bridges. These features make the model relevant to the determination of flow patterns on the surface of a fan, subject to debris flow or debris flood. No allowance is made for frictional boulder fronts and this may limit the ability of the model to predict hazard intensity in the channel upstream of the fan, or near the fan apex. The model is not suitable for other types of landslides, such as rock or debris avalanches, or flow slides. Similar models, based on dilatant rheology, have been described by Takahashi (1991).

Sassa (1988) developed a 3-D Eulerian model based on his approach of frictional flow resistance, combined with variable pore-pressure coefficient r_u. The pore-pressure coefficient must be mapped over the path area beforehand, as an input function and this largely determines the behaviour of the model. Sassa recommends the use of undrained ring shear tests to determine the r_u coefficients applicable to various substrate material

types found along the path. The model limitations include the inability to simulate non-hydrostatic lateral pressure, or other types of rheology than frictional.

4.7   *Three-dimensional models with non-hydrostatic lateral stress*

All three of the 2-D models reviewed in Paragraph 3.4 and including non-hydrostatic internal stress, have now been extended into three-dimensions. Gray et al. (1999) extended the Savage-Hutter theory of dry, frictional flow, calibrating it against small-scale laboratory experiments. Iverson & Denlinger (2001) also extended the mixture-theory-based model of Iverson (1997) to 3-D and obtained reasonable simulation of results from debris flow flume experiments. As in the 2-D case, the debris flow front is modelled as a frictional mass with pore-pressure, followed by a viscous flow. Interactions between the fluid phase and solid grains are accounted for using Darcian drag rules, with the implicit assumption that any turbulent drag can be neglected. The model has not yet been tested against natural debris flow examples.

Both Chen & Lee (2000) and McDougall & Hungr (2004a) extended the DAN model, using an open rheological kernel in the context of the "Equivalent Fluid approach".

All of the above models take the Lagrangian approach similar to the original Savage-Hutter method, resulting from a 3-D extension of Equation (18). The reference slices shown schematically on Figure 20 become columns, subject to bed-parallel fluid thrust both in the direction of motion and perpendicular to it. The main difference between the various models lies in the assumptions used to derive the magnitude and direction of the internal stresses. The McDougall & Hungr (2004a) model takes advantage of the Lagrangian framework to keep account of the bed-parallel strain in the moving mass. This provides realistic simulation of the internal stress state, while improving the stability of the solution.

The second major difference is in the way the model interpolates flow depth to re-establish the free surface of the flow at the end of each time step. The flow surface interpolation method used by Chen & Lee (2000) was based on the finite element method. The finite element mesh is subject to distortion with large displacements. McDougall & Hungr (2004a) based the interpolation on the smooth particle hydrodynamics theory, that permits unlimited distortion as well as separation and joining of flowing masses. An example analysis of a rock avalanche in the Swiss Alps is shown in Figure 23.

An important feature of up-to-date dynamic models is the ability to entrain material from the path of the landslide. Many rock avalanches, although starting as dry granular flows, override and erode saturated

surficial soils on the flow path, such as colluvial and alluvial or even organic deposits. This increases their volume, but may also change the basal rheology from that of dry frictional sliding to viscous or turbulent slurry flow. In case of debris flows and debris avalanches, the major part of the volume in motion may result from entrainment. Hungr & Evans (2004a) analysed two "rockslide-debris avalanches", in which entrainment of saturated debris amounted to as much as 50% of the volume. They showed that the process could be simulated successfully using Hungr's (1995) pseudo-3D model DAN, together with user-specified quantity of entrainment, referred to as "erosion depth". McDougall & Hungr (2005) repeated the back-analysis with a 3-D model based on Smooth Particle Hydrodynamics and obtained similar results, using the same rheological parameters and entrainment quantities. Revellino et al. (2003) calibrated DAN for 19 debris avalanches in pyroclastic veneer of the Campanian Region, Italy, using constant entrainment depth of 1.5 m. More than 80% of the volume of these landslides resulted from entrainment. One of the cases was re-analysed with a 3-D entraining model by McDougall & Hungr, (2004b). From these studies it is clear that the entrainment feature is crucial for successful modelling of many landslides.

4.8 *Simplified models*

A number of 2-D and 3-D dynamic models are based on simplifications of the Equation of Motion, based on Kinematic Wave theory that neglects local acceleration (Arattano & Savage 1992) or Cellular Automata (e.g. Segre & DeAngeli 1995). The latter models update the state of a landslide mass in a gridwork of cells over series of time steps. The updating controls transfer of mass and momentum between adjacent cells on the basis of pre-determined rules, which are a simplification of the physical concepts discussed previously in connection with the physical models. Since physically-based integrated 3-D dynamic models have now been developed to a high degree and computing power is easy to obtain, there would seem to be less reason at present to use or continue developing simplified models. They are beneficial for analysis of sediment transport, where the constitutive relationships are very complex (e.g. Pitman et al. 2003).

4.9 *Verification and calibration of models*

Verification testing serves to demonstrate that a given model is physically correct, consistent with the assumptions of a given method. The best way to achieve this is to compare the model results to controlled laboratory experiments utilizing materials with known constitutive relationships. Real landslide cases are not as useful for model verification since neither the constitutive

laws nor the details of motion are sufficiently well known for them.

Many researchers conduct specially designed experiments for this purpose, or adopt detailed experimental results reported by others (e.g. Hutter & Savage 1989, Hungr 1995, Iverson 1997, Denlinger & Iverson 2001, Iverson et al. 2004, Gray et al. 1999). For example, Figure 24 shows the analysis by Hungr (1995) of a dam-break experiment involving the viscous laminar flow of oil. The laboratory experiment was carried out and reported on by Jeyapalan (1981). Figure 25 shows the results of a simple verification experiment on "deflected flow" of dry sand, carried out by McDougall & Hungr (2004a). These experiments show the model's ability to steer the flowing mass along a curving path and also to simulate lateral spreading, controlled by strain-dependent internal stresses. Iverson et al. (2004) used laser devices to produce
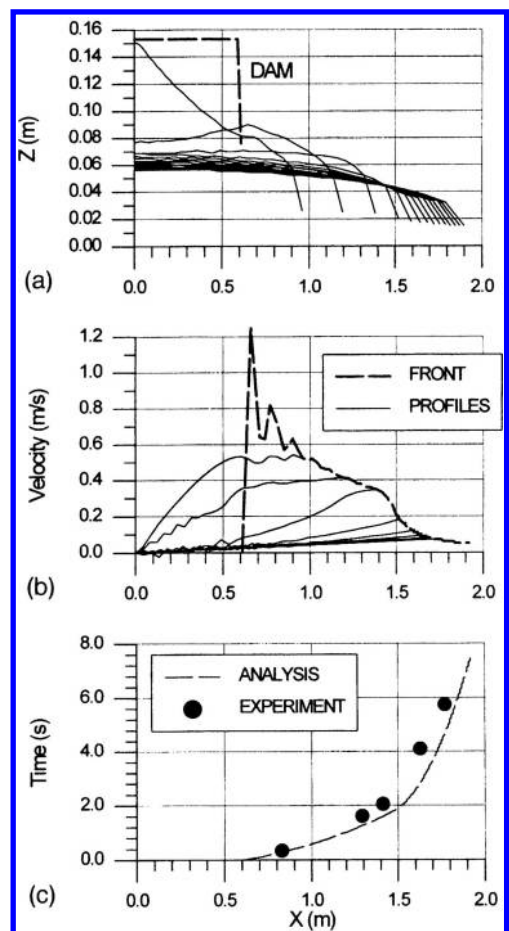
Figure 24. A flume test with the laminar flow of oil by Jeyapalan (1981), back-analysed by Hungr (1995).

122

contour maps of moving sand masses, to better compare with calculated dimensions.

It is important that each analytical model should be similarly compared with controlled experiments to confirm the validity of the numerical code, before attempting calibration against real landslide cases or use for prediction.

Any dynamic analysis of a landslide necessarily incorporates important simplifications in terms of material and pore-pressure spatial heterogeneity as well as variability of key parameters with time. As is the case with static analysis of stress in soil or rock, to be practically useful, models must be calibrated by comparison with full-scale behaviour of real events. Provided that a model is correct and verified, calibration is needed to (1) select the appropriate rheological kernel and (2) dimension the controlling resistance parameters. The goal of calibration is to compare certain control parameters calculated by the model with their equivalents available from observations. The control parameters may include total displacement ("runout") of the landslide toe, length and width of the deposit (for 3-D models), travel duration, spot velocities and spot measurements of the flow depth or of the thickness of deposits at certain locations. Each calibration study should use more than one landslide of a given type, in order to properly constrain the model.

Spot velocities are often estimated using hydraulic formulas for superelevation in bends, or runup against adverse segments of the path (e.g. Hungr & Evans 2004a). At other times, eyewitness estimates or film/video recordings can be used. Velocities have also been back-calculated from observed damage to structures along the path (e.g. Faella & Nigro (2001)). During such back-calculation, care must be taken to correctly specify the mechanism causing the structural damage. For example, much lower velocities are needed to damage structures through boulder impact, then through fluid thrust alone (Revellino et al. 2003).

In order to make the maximum use of available observations, the calibration needs to be carried out opportunistically using model results wherever field numbers are available. As an example, Hungr & Evans (1996) reported back-analyses of 23 well-known large rock avalanches, using Hungr's model DAN (1995) with three alternative rheological kernels: frictional, Voellmy and Bingham. The model parameters were adjusted in each case so as to obtain a perfect fit in terms total runout distance and the best possible fit in terms of velocities. As shown in Figure 26, a good fit could only be obtained with the Voellmy rheology. Both frictional and Bingham consistently overestimated the velocities. The same study found that the Voellmy rheology produces the best approximation of deposit length and thickness; it tends to concentrate the deposits forward into the distal zone. In contrast, the frictional rheology predicts thin tapering fronts
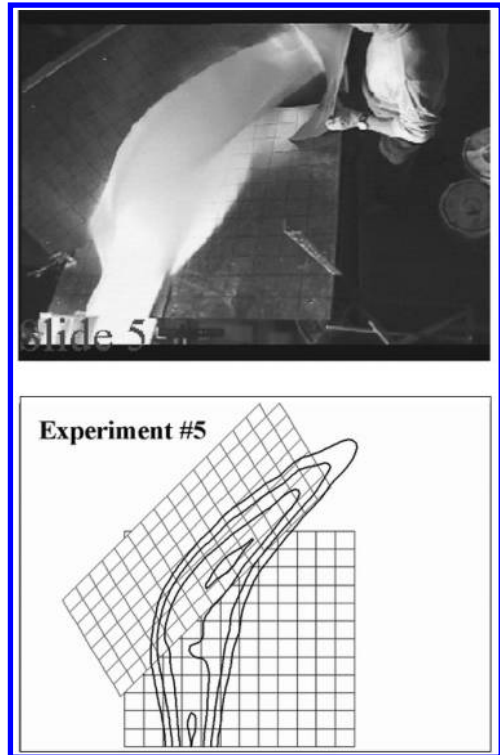
Figure 25. Comparison of actual and predicted flow in a deflected flow experiment using polystyrene beads (McDougall & Hungr 2004a).

(Fig. 27). This is appropriate only for dry, granular landslides and model tests.

Only a few systematic calibration studies, using multiple events have been published. Hungr et al. (2002) found that large flow slides in coal mine waste usually conform to the frictional model (Equation 13), with a bulk friction coefficient averaging 21°, with a standard deviation of about 3°. An exception occurs in locations where the slide is able to entrain saturated material from the path, in which case Voellmy analysis is needed and much longer travel distances occur. Hungr & Evans (1996) found that 70% of cases of large rock avalanches conform reasonably well to the Voellmy model, with a tan (ϕ_b) of 0.1 and a ξ of 500 m/sec^2. Of the remaining 30% some were relatively dry rock avalanches, behaving as frictional fluids. The remainder were more mobile due to major entrainment of snow, ice or loose saturated soil and were analysed by the Voellmy model with lower bulk friction angles.

Revellino et al. (2001) found that 19 of the large debris flows and debris avalanches derived from pyroclastic soils in the Campanian region of Italy behaved

123
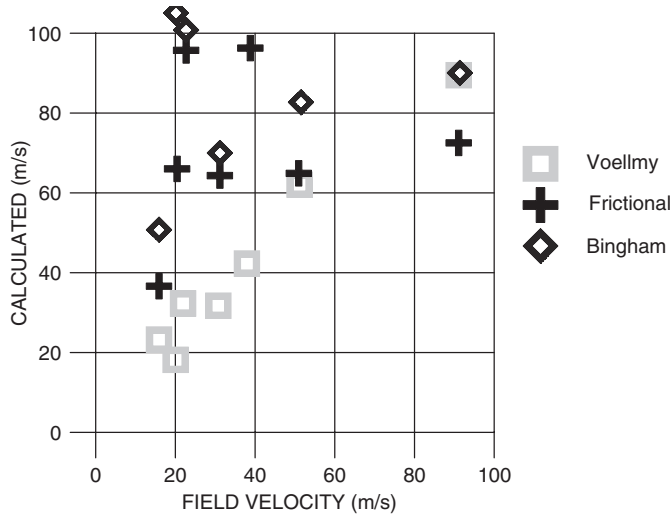
Figure 26. Comparison between calculated and observed flow velocities at various locations on the paths of 23 rock avalanches back-analysed by Hungr & Evans (1996).
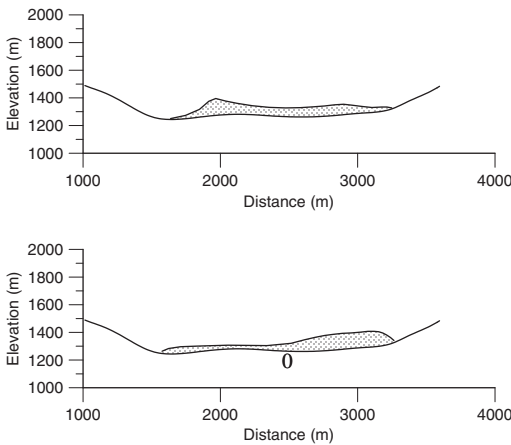
Figure 27. Longitudinal debris distribution of the Frank Slide, Alberta, Canada, calculated by (a) frictional and (b) Voellmy rheology (Hungr 2005).

as Voellmy fluids, with a tan (ϕ_b) of 0.07 and a ξ of 200 m/sec[2]. Ayotte & Hungr (2001) found that many debris avalanches in Hong Kong, involving both natural and filled slopes, could be simulated with the frictional model, with a bulk friction angle in the range of 20° to 30°. For those events smaller than 1000 m[3], the angle increased to as much as 43° and was inversely related to volume. Debris flows in the same region conformed better to the Voellmy model. The Bingham model appears suitable only for landslides containing plastic material (Johnson 1970, Geertsema et al. 2005).

However, much more work is required before we can generalize the optimal selection of rheological parameters for prediction. For the time being, it is necessary to conduct focused calibration for each given case, by systematically back-analysing examples similar in scale and geological character, concentrating on the nature of the substrate in the flow path. Recently, attempts have been made to calibrate entraining models, where the rheology of the landslide changes along the path (e.g. Hungr & Evans 2004a). Such models are more difficult to constrain, as the point of the beginning of entrainment, where the rheology changes, and the entrainment depth, become additional input parameters. Fortunately, surficial geological observations can be used to estimate these parameters, but much more work is required in this aspect.

In general, reological relationships defining the equivalent fluid should be simple with few changeable parameters that can be easily constrained. The recommended maximum number of parameters in the basal resistance equation is two. The success of calibration runs must be judged on the basis of a sufficient number of control quantities (e.g. runout distance, velocities, depths) to securely constrain the changeable input parameters as well as the overall design of the model. Wherever possible, calibration should use more than one event. An example of a successful calibration was presented by Revellino et al. (2003), who showed that successful back-analysis of 19 similar debris avalanches could be made with a single set of Voellmy parameters. A model thus calibrated is ready for forward predictions.

124

5 CONCLUSION

Thanks to intensive research by many groups over the last 20 years, numerous powerful tools now exist for prediction of the failure behaviour of extremely rapid landslides. What is most urgently needed, however, is to establish a connection between field observations and analysis. We must try to bridge the frequent gap between model developers, many of whom are trained mainly in theoretical sciences, and field geologists and engineers who understand earth structures, materials and processes. Development of focused typological classification of landslide and systematic, quantitative back-analysis using various models is important. Rules must be established for using sophisticated models and judging their reliability. Different types of models should be compared against each other. Above all, we must exercise healthy skepticism regarding the results of any model, no matter how complex and impressive.

REFERENCES

Agliardi, F., Crosta, G. & Zanchi, A. 2001. Structural constraints on deep-seated slope deformation kinematics. *Engineering Geology* 59(1–2): 83–102.

Aratano, M. & Savage, W.Z. 1992. Kinematic wave theory for debris flows. USGS Open File Report 92–290, Denver, Colorado.

Ayala, F.J., Cubillo, S., Álvarez, A., Domínguez, M.J., Laín, L., Laín, R. & Ortíz, G. 2003. Large scale rockfall reach susceptibility maps in La Cabrera Sierra (Madrid) performed with GIS and dynamic analysis at 1:5,000. *Natural Hazards*, 30: 325–340.

Azimi, C., Biarez, J., Desvarreux, P. & Keime, F. 1988. Forecasting time of failure for a rockslide in gypsum. In Bonnard (ed.), Proceedings of the Fifth International Symposium on Landslides, Lausanne. A.A. Balkema, Rotterdam, v.1, 531–536.

Benko, B. & Stead, D. 1998. The Frank slide: A reexamination of the failure mechanism. *Canadian Geotechnical Journal* 35(2): 299–311.

Bhandari, R.K. 1988. Special lecture: Some practical lessons in the investigation and field monitoring of landslides. In Bonnard (ed.), Proceedings of the Fifth International Symposium on Landslides, Lausanne. A.A. Balkema, Rotterdam, v.3, 1435–1457.

Bhasin, R. & Kaynia, A.M. 2004. Static and dynamic simulation of a 700-m high rock slope in western Norway. *Engineering Geology* 71(3–4): 213–226.

Board, M., Chacon, E., Varona, P. & Lorig, L. 1996. Comparative analysis of toppling behaviour at Chuquicamata open-pit mine, Chile. *Transactions of the Institution of Mining and Metallurgy – Section A: Mining Industry* 105: A11–A21.

Bonzanigo, L., Eberhardt, E. & Loew, S. 2001. Hydromechanical factors controlling the creeping Campo Vallemaggia landslide. In Kühne et al. (eds), UEF International Conference on Landslides – Causes, Impacts and Countermeasures, Davos. Verlag Glückauf GmbH, Essen, 13–22.

Campbell, C.S. 1989. Self-lubrication for long runout landslides. *Journal of Geology* 97: 653–665.

Casagrande, A. 1976. Liquefaction and cyclic deformation of sands: a critical review. Harvard Soil Mechanics Series, No. 88, Cambridge, Massachussetts, 26 p.

Chen, H. & Lee, C.F. 2000. Numerical simulation of debris flows. *Canadian Geotechnical Journal* 37:146–160.

Chiriotti, E., Mahtab, A., Xu, S. & Kendorski, F. 1999. Methodology for characterizing very large rock masses: An illustrative example. In Amadei et al. (eds), Rock Mechanics for Industry, Proceedings of the 37th U.S. Rock Mechanics Symposium, Vail. A.A. Balkema, Rotterdam, v.1, 263–270.

Chryssanthakis, P. & Grimstad, E. 1996. Landslide simulation by using the distinct element method. In Aubertin et al. (eds), Rock Mechanics: Tools and Techniques, Proceedings of the 2nd North American Rock Mechanics Symposium (NARMS '96), Montréal. A.A. Balkema, Rotterdam, v.2, 1921–1928.

Close, U. & McCormick, E. 1922. Where the mountains walked. *National Geographic Magazine* 41(5): 445–464.

Coggan, J.S., Stead, D. & Eyre, J.M. 1998. Evaluation of techniques for quarry slope stability assessment. *Transactions of the Institution of Mining and Metallurgy, Section B* 107: B139–B147.

Collins, B.D. & Znidarcic, D. 2004. Stability analyses of rainfall induced landslides. *Journal of Geotechnical and Geoenvironmental Engineering* 130(4): 362–372.

Copons, R. 2004. Avaluació de la perillositat de caiguda de blocs a Andorra la Vella (Principat d'Andorra). PhD Thesis. Universitat de Barcelona. Unpublished. 244 pp.

Corominas, J. 1996. The angle of reach as a mobility index for small and large landslides. *Canadian Geotechnical Journal* 33: 260–271.

Corominas, J., Esgleas, J. Baeza, C. 1990. Risk mapping in the Pyrenees area: a case study. Hydrology in Mountainous Regions II. IAHS Publication 194: 425–428.

Corominas, J., Copons, R., Vilaplana, J.M., Altimir, J. & Amigó, J. 2003b. Integrated landslide susceptibility analysis and hazard assessment in the Principality of Andorra. *Natural Hazards* 30: 421–435.

Costa, J.E. 1984. Physical geomorphology of debris flows. In Costa & Fleisher (eds). Developments and Applications of Geomorphology. Springer Verlag. pp. 268–317.

Costa, M., Coggan, J.S. & Eyre, J.M. 1999. Numerical modelling of slope behaviour at Delabole slate quarry. *International Journal of Surface Mining, Reclamation and Environment* 13(1): 11–18.

125

Crandell, D.R. & Mullineaux, D.R. 1967. Volcanic Hazards at Mount Rainier, Washington. USGS Bulletin 1238, 26, pp.

Crandell, D.R., Mullineaux, D.R. & Miller, C.D. 1979. Volcanic-hazards studies in the Cascade Range of the western United States. In Sheets & Grayson (eds.), Volcanic Activity and Human Ecology. Academic Press, pp. 195–219.

Crosta, G.B. & Agliardi, F. 2003. Failure forecast for large rock slides by surface displacement measurements. *Canadian Geotechnical Journal* 40(1): 176–191.

Crosta, G. B., Imposimato, S., Roddeman, D., Chiesa, S. & Moia, F. 2005. Small fast moving flow-like landslides in volcanic deposits: the 2001 Las Colinas Landslide (El Salvador). *Geotechnique*: In press.

Cruden, D.M. & Varnes, D.J. 1996. Landslide types and processes. In Turner & Schuster (eds), Landslide Investigation and Mitigation. TRB Special Report 247. National Academy Press, Washington D.C. pp. 36–75.

Davies, T.R.H. 1982. Spreading of rock avalanche debris by mechanical fluidization. *Rock Mechanics* 15: 9–24.

Davies, T.R., McSaveney, M.J. & Hodgson, K.A. 1999. A fragmentation-spreading model for long-runout rock avalanches. *Canadian Geotechnical Journal* 36: 1096–1110.

Dawson, E.M., Roth, W.H. & Drescher, A. 1999. Slope stability analysis by strength reduction. *Geotechnique* 49(6): 835–840.

Denlinger, R.P. & Iverson, R.M. 2001. Flow of variably fluidized granular masses across three-dimensional terrain. 1. Numerical predictions and experimental tests. *Journal of Geophysical Research* 106:553–566.

Domaas, U. 1994. Geometrical methods of calculating rockfall range. Norwegian Geotechnical Institute. Report 585910–1. 21 pp. Unpublished.

Eberhardt, E., Bonzanigo, L. & Loew, S. 2005b. Long-term investigation of a deep-seated creeping landslide in crystalline rock – Part 2: Mitigation measures and numerical modelling of deep drainage at Campo Vallemaggia. *Canadian Geotechnical Journal*: In preparation.

Eberhardt, E., Spillmann, T., Maurer, H., Willenberg, H., Loew, S. & Stead, D. 2004b. The Randa Rockslide Laboratory: Establishing brittle and ductile instability mechanisms using numerical modelling and microseismicity. In Lacerda et al. (eds), Proceedings of the 9th International Symposium on Landslides, Rio de Janeiro. A.A. Balkema, Leiden, v.1, 481–487.

Eberhardt, E., Stead, D., Coggan, J. & Willenberg, H. 2002. An integrated numerical analysis approach to the Randa rockslide. In Rybár et al. (eds), Proceedings of the 1st European Conference on Landslides, Prague. A.A. Balkema, Lisse, 355–362.

Eberhardt, E., Stead, D. & Coggan, J.S. 2004a. Numerical analysis of initiation and progressive failure in natural rock slopes – the 1991 Randa rockslide. *International Journal of Rock Mechanics and Mining Sciences* 41(1): 69–87.

Eberhardt, E., Thuro, K. & Luginbuehl, M. 2005a. Slope instability mechanisms in dipping interbedded conglomerates and weathered marls – the 1999 Rufi landslide, Switzerland. *Engineering Geology* 77(1–2): 35–56.

Evans, S.G. & Hungr, O. 1993. The assessment of rockfall hazard at the base of talus slopes. *Canadian Geotechnical Journal* 30: 620–636.

Faella, C. & Nigro, E. 2001. Effetti delle colate rapide sulle costruzioni. Parte Prima: Descrizione del danno. Forum per il Rischio Idrogeologico "Fenomeni di colata rapida di fango nel Maggio '98", Naples, June 22 giugno 2001: 105–112.

Fannin, R.J. & Wise, M.P. 2001. An empirical-statistical model for debris flow travel distance. *Canadian Geotechnical Journal* 38: 982–994.

Federico, A., Fidelibus, C. & Interno, G. 2002. The prediction of landslide time to failure – A state of the art. In Proceedings of the 3rd International Conference on Landslides, Slope Stability and the Safety of Infra-Structures, Singapore, 167–180.

Finlay, P.J., Mostyn, G.R. & Fell, R. 1999. Landslide risk assessment: prediction of travel distance. *Canadian Geotechnical Journal* 36: 556–562.

Fletcher, L., Hungr, O. & Evans, S.G. 2002. Contrasting failure behaviour of two large landslides in clay and silt. *Canadian Geotechnical Journal* 39: 46–62.

Fredlund, D.G. & Krahn, J. 1977. Comparison of slope stability methods of analysis. *Canadian Geotechnical Journal* 14(3): 429–439.

Fukuzono, T. 1990. Recent studies on time prediction of slope failure. *Landslide News* 4: 9–12.

García, J.L., López, J.L., Noya, M., Bello, M.E., Bello, M.T., Gonzájez, N., Paredes, G. & Vivas, M.I. 2003. Hazard mapping for debris flow events in the alluvial fans of northern Venezuela. In Rickenmann & Chen (eds.), Debris Flow Hazards Mitigation: Mechanics, Prediction and Assessment. Millpress, Rotterdam, 1: 589–600.

Geertsema, M., Hungr, O., Schwab, J.W. & Evans, S.G. 2004. A large rock slide – debris avalanche at Pink Mountain, northeastern British Columbia, Canada. *Engineering Geology*: In press.

Gray, J.M.N.T., Wieland, M. & Hutter, K. 1999. Gravity driven free surface flow of granular avalanches over complex basal topography. *Proceedings, Royal Society of London, Ser. A* 455: 1841–1874.

Griffiths, D.V. & Lane, P.A. 1999. Slope stability analysis by finite elements. *Geotechnique* 49(3): 387–403.

Gruner, U. 2001. Felssturzgefahr Chapf – Üssri Urweid (Gemeinde Innertkirchen): Angaben zur Geologie und zu den Bewegungen. Bern, Kellerhaus + Haefeli AG, 6 pp.

Gruner, U. 2003. Zweite Sicherheitssprengung am Chapf bei Innertkirchen vom 20. August 2002. *Bulletin für Angewandte Geologie* 8(1): 17–25.

Hajiabdolmajid, V. & Kaiser, P.K. 2002. Modelling slopes in brittle rock. In Hammah et al. (eds.), Proceedings of the 5th Northern American Rock Mechanics Symposium (NARMS-TAC), Toronto. University of Toronto Press, Toronto, v.1, 331–338.

Hart, R.D. 1993. An introduction to distinct element modelling for rock engineering. In Hudson (eds), Comprehensive Rock Engineering: Principles, Practice & Projects. Oxford: Pergamon Press, v.2, 245–261.

Heim, A. 1932, Landslides and human lives (Bergsturz and menschenleben): Translated by N. Skermer, vancouver, British Columbia, Bi-Tech Publishers, 195 p.

Hoblitt, R.P., Walder, J.S., Driedger, C.L., Scott, K.M., Pringle, P.T. & Vallance, J.W. 1998. Volcano Hazards from Mount Rainier, Washington, Revised 1998. USGS Open-File Report 98–428.

Hsü, K.J. 1975. Catastrophic debris stream (sturzstroms) generated by rockfalls. *Geological Society of America Bulletin* 86: 129–140.

Hungr, O. 1990. Mobility of rock avalanches. Report of the National Institute for Earth Science and Disaster Prevention, 46: 11–20.

Hungr, O. 1995. A model for the runout analysis of rapid flow slides, debris flows and avalanches. *Canadian Geotechnical Journal* 32: 610–623.

Hungr, O. 2000. Analysis of debris flow surges using the theory of uniformly progressive flow. *Earth Surface Processes and Landforms* 25: 1–13.

Hungr, O. 2003. Flow slides and flows in granular soils. Keynote Paper. In Picarelli (ed.), Proc., FLOWS 2003, International Workshop, Sorrento, Italy, Kluwer Publishers.

Hungr, O. 2004. Prospects for prediction of landslide dam geometry using dynamic models. Proceedings, NATO conference on Landslide dams, Bishkek, Kyrghistan, July, 2004, In review.

Hungr, O. 2005. Rock avalanche occurrence, process and modelling. Keynote Paper, NATO Advanced Workshop on Massive Slope Failure, Celano, Italy. Kluwer NATO Science Series, In press.

Hungr, O., Dawson, R., Kent, A., Campbell, D. & Morgenstern, N.R. 2002. Rapid flow slides of coal mine waste in British Columbia, Canada. In Catastrophic Landslides Geological Society of America Reviews in Engineering Geology No. 14.

Hungr, O. & Evans, S.G. 1988. Engineering evaluation of fragmental rockfall hazards. In Bonnard (ed.), 5th International Symposium on Landslides, Lausanne, Switzerland. A.A. Balkema, vol. 1: 685–690.

Hungr, O. & Evans, S.G. 1996. Rock avalanche runout prediction using a dynamic model. Proceedings, 7th International Symposium on Landslides, Trondheim, Norway, 1: 233–238.

Hungr, O. & Evans, S.G. 2004a. Entrainment of debris in rock avalanches; an analysis of a long runout mechanism. *Bulletin, Geological Society of America*, In press.

Hungr, O. & Evans, S.G. 2004b. The occurrence and classification of massive rock slope failure. *Felsbau* 22: 16–23.

Hungr, O., Evans, S.G., Bovis, M. & Hutchinson, J.N. 2001. Review of the classification of landslides of the flow type. *Environmental and Engineering Geoscience* VII: 221–238.

Hunter, G. & Fell, R. 2003. Travel distance angle for rapid-landslides in constructed and natural soil slopes. *Canadian Geotechnical Journal* 40(6): 1123–1141.

Hutchinson, J.N. 1988. Morphological and geotechnical parameters of landslides in relation to geology and hydrogeology. In Bonnard (ed.), 5th International Symposium on Landslides, Lausanne, Switzerland. A.A. Balkema, vol. 1: 3–35.

Hungr, O. & Kent, A. 1995. Coal mine waste dump failures in British Columbia, Canada. *Landslide News* 9: 26–28.

Hungr, O. & Morgenstern, N.R. 1984. Experiments in high velocity open channel flow of granular materials. *Géotechnique* 34: 405–413. Discussion and Reply, 35: 383–385.

Hutchinson, J.N. 1986. A sliding-consolidation model for flow slides. *Canadian Geotechnical Journal* 23: 115–126.

Hutchinson, J.N., Prior, D.B. & Stephens, N. 1974, Potentially dangerous surges in an Antrim mudslide. *Quarterly Journal of Engineering Geology* 7: 363–376.

Itasca 2000. UDEC – Universal Distinct Element Code. Itasca Consulting Group, Inc., Minneapolis.

Iverson, R.M. 1997. The physics of debris flows. *Reviews of Geophysics* 35(3): 245–296.

Iverson, R.M. 2005. Debris flow mechanics. Chapter 7 in Jakob & Hungr (eds.), Debris Flows and Related Phenomena. Praxis, Springer, Heidelberg, In press.

Iverson, R.M. & Denlinger, R.P. 2001. Flow of variably fluidized granular masses across three-dimensional terrain. 1. Coulomb mixture theory. *Journal of Geophysical Research* 106: 537–552.

Iverson, R.M., Logan, M. & Denlinger, R.P. 2004. Granular avalanches across irregular three-dimensional terrain: 2. Experimental tests. *Journal of Geophysical Research* 109: 16 pp.

Jackson, L.E., Kostashuk, R.A. & MacDonald, G.M. 1987. Identification of debris flow hazard on alluvial fans in the Canadian Rocky mountains. *Geological Society of America. Reviews in Engineering Geology* VII: 155–124.

Jeyapalan, K. 1981. Analysis of flow failures of mine tailings impoundments. Ph.D. Thesis, University of California, Berkeley.

Johnson, A.M. 1970. Physical Processes in Geology. W.H. Freeman, New York, 577 pp.

Kennedy, B.A. & Niermeyer, K.E. 1970. Slope monitoring systems used in the prediction of a major slope failure at the Chuquicamata Mine, Chile. In Van Rensburg (ed.), Planning Open Pit Mines, Proceedings, Johannesburg. A.A. Balkema, Cape Town, 215–225.

Körner, H.J. 1976. Reichweite und Geschwindigkeit von Bergsturzen und fleisschnee-lawinen. *Rock Mechanics* 8: 225–256.

Li, T. 1983. A mathematical model for predicting the extent of a major rockfall. *Zeitschrift für Geomorphologie* 24: 473–482.

Lo, K.Y. & Lee, C.F. 1973. Stress analysis and slope stability in strain-softening materials. *Geotechnique* 23(1): 1–11.

Löw, S. 1997. Wie sicher sind geologische Prognosen? *Bulletin für Angewandte Geologie* 2(2): 83–97.

Main, I.G., Sammonds, P.R. & Meredith, P.G. 1993. Application of a modified Griffith criterion to the evolution of fractal damage during compressional rock failure. *Geophysical Journal International* 115(2): 367–380.

McDougall, S. & Hungr, O. 2004a. A model for the analysis of rapid landslide runout motion across three-dimensional terrain. *Canadian Geotechnical Journal* 41(6): 1084–1097.

McDougall, S. & Hungr, O. 2004b. A universal model for 3-D runout analysis of landslides. Proceedings, 9th International Symposium on Landslides, Rio de Janeiro, Brazil.

McDougall, S. & Hungr, O. 2005. A dynamic model for rapid landslides that entrain material from the path. *Canadian Geotechnical Journal*: In review.

Michael-Leiba, M., Baynes, F., Scott, G. & Granger, K. 2003. Regional landslide risk to the Cairns community. *Natural Hazards* 30: 233–249.

Munjiza, A., Owen, D.R.J. & Bicanic, N. 1995. A combined finite-discrete element method in transient dynamics of fracturing solids. *Engineering Computations* 12: 145–174.

Nichol, S.L., Hungr, O. & Evans, S.G. 2002. Large scale brittle and ductile toppling of rock slopes. *Canadian Geotechnical Journal* 39(4): 773–788.

Nicoletti, P.G. & Sorriso-Valvo, M. 1991. Geomorphic controls of the shape and mobility of rock avalanches. *Geological Society of America Bulletin* 103: 1365–1373.

127

O'Brien, J.S., Julien, P.Y. & Fullerton, W.T. 1993. Two-dimensional water flood and mudflow simulation. *Journal of the Hydraulics Division, ASCE* 119(HY2): 244–261.

Okura, Y., Kitahara, H., Sammori, T. & Kawanami, A. 2000. The effects of rockfall volume on runout distance. *Engineering Geology* 58: 109–124.

Petley, D.N., Bulmer, M.H. & Murphy, W. 2002. Patterns of movement in rotational and translational landslides. *Geology* 30(8): 719–722.

Pitman, E.B., Nichita, E.B., Patra, A.K., Bauer, A.C., Bursik M. & Webb, A. 2003. A model of granular flows over an erodible surface. *Discrete and Continuous Dynamical Systems–Series B* 3: 589–599.

Revellino, P., Hungr, O., Guadagno, F.M. & Evans, S.G. 2003. Velocity and runout prediction of destructive debris flows and debris avalanches in pyroclastic deposits, Campania Region, Italy. *Environmental Geology* 45: 295–311.

Saito, M. 1965. Forecasting the time of occurrence of a slope failure. In Proceedings of the 6 International Conference on Soil Mechanics and Foundation Engineering, Montreal. University of Toronto Press, Toronto, v.2, 537–541.

Salt, G. 1988. Landslide mobility and remedial measures. In Bonnard (ed.), Proceedings of the 5 International Symposium on Landslides, Lausanne. A.A. Balkema, Rotterdam, v.1, 757–762.

Sassa, K. 1985. The mechanism of debris flows. Proceedings, 11th International Conference on Soil Mechanics and Foundation Engineering, San Francisco, v. 1, pp. 1173–1176.

Sassa, K. 1988. Geotechnical model for the motion of landslides. In Bonnard (ed.), 5th International Symposium on Landslides, Lausanne, Switzerland. A.A. Balkema, v. 1: 37–55.

Sassa, K., 2002. Mechanism of rapid and long traveling flow phenomena in granular soils. Proceedings, International Symposium on Landslide Mitigation and Protection of Cultural and Natural Heritage. Kyoto University, Kyoto, Japan, 11–30.

Savage, S.B. & Hutter, K. 1989. The motion of a finite mass of granular material down a rough incline. *Journal of Fluid Mechanics* 199: 177–215.

Scheidegger, A. 1973. On the prediction of the reach and velocity of catastrophic landslides. *Rock Mechanics* 5: 231–236.

Scheller, E. 1971. Beitrag zum bewegungsverhalten grosser bergstürze. *Eclogae Geologicae Helvetiae* 64: 195–202.

Scott, K.M. & Vallance, J.W. 1993. History of Landslides and Debris Flows at Mount Rainier: Water Fact Sheet. USGS Open-File Report 93–111.

Segre, A. & DeAngeli, C. 1995. Cellular automaton for realistic modelling of landslides. European Geophysical Society, Non-linear Processes in Geophysics.

Shou, K.-J. & Wang, C.-F. 2003. Analysis of the Chiufengershan landslide triggered by the 1999 Chi-Chi earthquake in Taiwan. *Engineering Geology* 68(3–4): 237–250.

Shreve, R.L. 1968. The Blackhawk landslide. Geological Society of America, Special Paper 108.

Soussa, J. & Voight, B. 1991. Continuum simulation of flow failures. *Geotechnique* 41: 515–538.

Stead, D. & Coggan, J.S. 2005. Numerical modelling of rock slopes using a total slope failure approach. In Evans et al. (eds), Massive Rock Slope Failure: New Models for Hazard Assessment, Proceedings of the NATO Advanced Research Workshop, Celano, Italy. Kluwer Academic Publishers, Dordrecht, In Press.

Stead, D. & Eberhardt, E. 1997. Developments in the analysis of footwall slopes in surface coal mining. *Engineering Geology* 46(1): 41–61.

Stead, D., Eberhardt, E., Coggan, J. & Benko, B. 2001. Advanced numerical techniques in rock slope stability analysis – Applications and limitations. In Kühne et al. (eds.), International Conference on Landslides – Causes, Impacts and Countermeasures, Davos. Verlag Glückauf Essen, Essen, 615–624.

Suwa, H. 1991. Visually observed failure of a rock slope in Japan. *Landslide News* 5: 8–10.

Takahashi, T. 1991. Debris flow. IAHR Monograph, A.A. Balkema, Rotterdam, 165 pp.

Terzaghi, K. 1950. Mechanism of landslides. In Paige (ed.), Application of Geology to Engineering Practice (Berkey Volume). New York: Geological Society of America, 83–123.

Trunk, F.J., Dent, J.D. & Lang, T.E. 1986. Computer modelling of large rockslides. *Journal of the Geotechnical Division, ASCE* 112(GE3): 348–360.

Van Gassen, W. & Cruden, D. 1989. Momentum transfer and friction in the debris rock avalanches. *Canadian Geotechnical Journal* 26: 623–628.

Varnes, D.J. 1978. Slope movement types and processes. In Schuster & Krizek (eds), Landslides, Analysis and Control: Transportation Research Board, National Academy of Sciences, Washington, DC., Special Report 176: 11–33.

Voellmy, A. 1955. Über die Zerstorungskraft von Lawinen. *Schweiz. Bauzeitung* 73: 212–285.

Voight, B. 1978. The Lower Gros Ventre slide, Wyoming, U.S.A. In Voight (ed.), Rockslides and avalanches. Elsevier, Amsterdam. v. 1: 113–166.

Voight, B. 1989. A relation to describe rate-dependent material failure. *Science* 243: 200–203.

Voight, B. & Kennedy, B.A. 1979. Slope failure of 1967–1969, Chuquicamata Mine, Chile. In Voight (ed.), Rockslides and Avalanches. Amsterdam: Elsevier Scientific Publishing Company, 595–632.

Voight, B. & Sousa, J. 1994. Lessons from Ontakesan: A comparative analysis of debris avalanche dynamics. *Engineering Geology* 38: 261–297.

Willenberg, H., Spillmann, T., Eberhardt, E., Evans, K., Loew, S. & Maurer, H. 2002. Multidisciplinary monitoring of progressive failure processes in brittle rock slopes – Concepts and system design. In Rybár et al. (eds), Proceedings of the 1st European Conference on Landslides, Prague. A.A. Balkema, Lisse, 477–483.

Zienkiewicz, O.C. & Huang, M. 1995. Localization problems in plasticity using finite elements with adaptive remeshing. *International Journal for Numerical and Analytical Methods in Geomechanics* 19(2): 127–148.

Zvelebil, J. 1984. Time prediction of a rockfall from a sandstone rock slope. In Proceedings of the 4 International Symposium on Landslides, Toronto. University of Toronto Press, Downsfield, v.3, 93–95.

Estimating temporal and spatial variability and vulnerability

W. Roberds

Golder Associates, Seattle, USA

ABSTRACT: The state-of-the-art in assessing the consequences of landslides, such as casualties and financial costs is reviewed. Such consequences are a function of the landslide hazard characteristics , such as the probability or frequency of occurrence and type, volume, velocity, and extent of movement, which are reviewed in companion state-of-the-art papers. In consequence assessments, it is necessary to consider the uncertainties in both the "vulnerability" and in the "hazard", including the significant temporal effects on landslide initiation and subsequent movement (which were not considered in detail in the companion state-of-the-art papers), as well as the temporal effects on vulnerability. It is demonstrated that, although not perfect and often requiring significant effort and not often used, various methods are currently available to adequately assess the risk (including probable consequences) associated with potential landslides for better decision making regarding those slopes and potentially affected areas for a wide range of applications (from detailed design of individual slopes to regional evaluations).

1 INTRODUCTION

Landslides cause an average of more than 25 fatalities and more than US$1 billion in damages each year in the United States alone, and thousands of deaths and injuries and many billions of US dollars in direct and indirect damages around the world each year. Figure 1 shows a recent landslide at La Conchita, California, which resulted in 10 fatalities and destroyed 15 expensive (on the order of US$600,000 each) homes and damaged another 16, as well as disrupted life and caused nearby property values to plummet. Figure 2 shows a landslide that happened *at the same location* about 10 years earlier, which resulted in 9 homes being destroyed, as well as life disruption and significant property value decreases (which eventually recovered as memory faded), but no fatalities. On the other hand, most landslides have no significant impact, simply rearranging the topography. The primary questions that need to be addressed are:

- Why do landslides occur when they do, how can we predict them, and what should we do to prevent or at least control them?
- What are the consequences of landslides, how can we predict them, and what should we do to avoid them (in addition to preventing landslides from occurring in the first place or controlling them)?

This paper addresses the state-of-the-art in assessing the consequences of landslides (e.g., casualties, financial costs, etc.), as a function of landslide hazard characteristics. The general framework for such risk assessment and management is presented in companion

(a) Post-landslide looking seaward.

(b) Pre-landslide looking landward with outline of landslide debris

Figure 1. La Conchita CA Landslide 2005 (by UCSB) [see colour plate I].
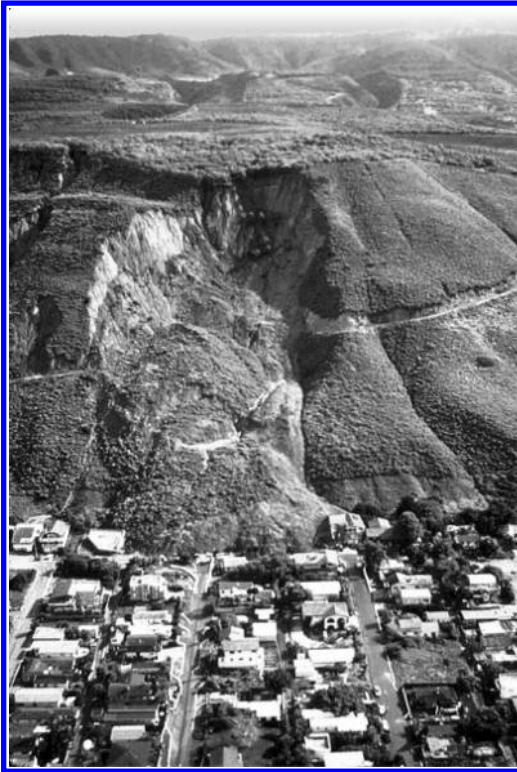
Figure 2. La Conchita CA Landslide 1995 (by USGS) [see colour plates].

State-of-the-Art Paper 1. The assessment of relevant landslide hazard characteristics (i.e., probability or frequency of occurrence and type, volume, velocity and extent of movement) are reviewed in companion State-of-the-Art Papers 2 through 4.

In landslide consequence assessments, it is necessary to consider the uncertainties in both the "vulnerability" and in the "hazard", which combine to give uncertainty in the consequences ("risk"). Some of the uncertainties relate to the significant temporal effects on landslide initiation and subsequent movement (which were not considered in detail in the companion state-of-the-art papers), as well as the temporal effects on vulnerability.

Hence, the first section of this paper briefly restates the risk framework, to provide the context for vulnerability assessment and how it is used. The second section discusses landslide vulnerability assessments, and provides some simple illustrative examples. The third section expands the discussion of vulnerability, as well as of landslide hazards, to consider their significant temporal aspects, as well as ways to reduce risk through reducing vulnerability. The fourth section

presents several case studies, which are expanded on in an appendix.

2 RISK FRAMEWORK

As discussed in the companion State-of-the-Art Paper 1 (A framework for landslide risk assessment and management – Fell et al. 2005), *risk assessment is the assessment of possible "losses" or undesirable consequences associated with some particular plan*, including the status quo in some cases. These risks can be compared to specified criteria (e.g., re public safety) to determine acceptability or, if assessed for different plans, can be used to compare alternatives.

Although qualitative risk assessments, in which specific risks associated with different types of events are rated high, medium or low based on similar ratings of hazard and vulnerability, are often used for screening purposes, they are generally inadequate for definitive evaluations.

The most complete description of the possible losses (risk) is quantitatively in terms of a "probability distribution", which presents the relative likelihood of any particular loss value or the probability of losses being less than any particular value. Alternatively, the "expected value" (i.e., the probability weighted average value) of loss can be determined as a single measure of risk. A general "scenario"-based risk formulation is given (in integral form for "continuous" distributions or in summation form for "discrete" distributions) by:

$$E[\underline{C}] = \int_{all \ \underline{C}} \underline{C} \, p[\underline{C}] \, d\underline{C} = \sum_{all \ \underline{C}} \underline{C} \, p[\underline{C}] \ if \ discrete \qquad (1)$$

$$P_{\leq}[\underline{C}^*] = \int_{all \ \underline{C} \leq \underline{C}^*} p[\underline{C}] \, d\underline{C} = \sum_{all \ \underline{C} \leq \underline{C}^*} p[\underline{C}] \ if \ discrete \qquad (2)$$

$$p[\underline{C}^*] = \sum_{all \ S} p[\underline{C}^* \,|\, S] \, p[S] \qquad (3)$$

where *C* is particular set of undesirable consequences (of comprehensive and mutually exclusive set of possible consequences, either infinite or discrete), S is particular scenario (of comprehensive and mutually exclusive discrete set of possible scenarios), p[x] is probability distribution of x (i.e., relative likelihood of being exactly x), p[x|y] is "conditional" probability distribution of x for a particular value of y, E[x] is "expected value" of x, P ≤ [x] is "cumulative" probability of x (i.e., probability of being less than or equal to x).

For the case of landslides, the simplest formulation is where there are only two scenarios: a) landslide occurs; or b) landslide does not occur. In this case, there would be uncertain consequences if the

130
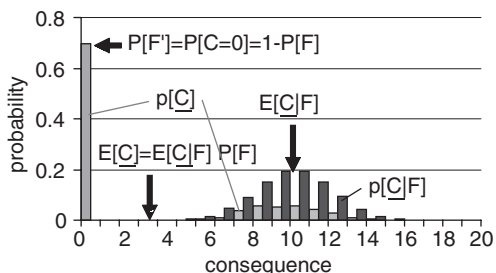
Figure 3. Simple two-scenario based risk formulation.

landslide occurs, but no consequences if the landslide does not occur (Fig. 3):

$$p[\underline{C}^*{=}0] = P[F'] = 1 - P[F] \qquad (4)$$

$$p[\underline{C}^*{=}\underline{C}] = p[\underline{C}|F]\, P[F] \qquad (5)$$

$$E[\underline{C}] = E[\underline{C}|F]\, P[F] \qquad (6)$$

where F is where landslide occurs, F′ is where landslide does not occur, p[C|F] is probability distribution of set of undesirable consequences if landslide occurs, E[C|F] is expected value of set of undesirable consequences if landslide occurs.

In the above simple formulation, there might be great uncertainty in the set of consequences if a landslide occurs, due at least in part to the large uncertainty in landslide hazard characteristics (including possibly the number of landslide events for a regional evaluation). A more complicated formulation divides the landslide occurrence scenario F in equations 4 through 6 and Figure 3 into various sub-scenarios that account for the different possible hazard characteristics. As will be discussed subsequently, there is significant latitude in how this might be done. In this case (which is still covered by equations 1 through 3), there will generally be much less uncertainty in the consequences for a particular set of hazard characteristics, but the uncertainty in those hazard characteristics needs to be assessed (see companion State-of-the-Art Papers 3 and 4).

For example, a modular risk assessment framework was developed for natural slopes in Hong Kong (Roberds & Ho 1997). The overall framework consists of three components: detachment, movement and vulnerability. Various versions of each component were developed, ranging from simple analyses (e.g., for regional studies) to complex analyses (e.g., for detailed critical slope design). These different versions are interchangeable and can be "slotted" into the framework as appropriate; e.g., a simple detachment module can be replaced with a more complex one if desired.

As another example, Hungr (1997) reasonably proposed combining detachment and subsequent ground movement characteristics into a single spatial function called "hazard intensity", which can then be combined directly with a spatial "vulnerability" function to determine a spatial risk function. These various spatial functions can be presented as maps and, as will be discussed later, developed using Geographic Information Systems (GIS). The overall risk can then be determined by integrating the spatial risk function over the potentially affected area.

Risk management consists of identifying and evaluating ways to "manage" risks, e.g., by minimizing them to acceptable levels, or further if cost-effective, or by accepting them, possibly after minimization to the extent practical. In addition to reducing the hazard (e.g., by reducing the probability of detachment through stabilization, and/or by reducing subsequent ground movement through barriers or containment), risk can also be reduced by reducing vulnerability (i.e., reducing the consequences of failure). This will be discussed later in the paper (also see State-of-the-Art Papers 1 and 6).

3 VULNERABILITY

As noted above, to assess risks, not just hazards, requires that the "consequences" associated with any particular set of landslide characteristics be assessed, and then be combined with the likelihood of those various sets of landslide characteristics. Such an *assessment of "vulnerability" can be done in various ways and to various levels of detail and approximation*, depending on the particular application. For example, there is no point in assessing vulnerability in great accuracy and detail if the hazards are not assessed in similar accuracy and detail. Conversely, if the hazards are assessed accurately and in detail, then the vulnerability should also be. However, *consequences are not often assessed for landslides and well-established methods are not generally available*. Possible methods are discussed below.

3.1 *Consequences*

The *types of "damages" of interest* generally include casualties (injuries and fatalities), property damage/cleanup/repair/litigation (financial cost), loss of service (time, which can be translated to financial cost), and possibly environmental and social impacts (including community relations and politics). For example, as noted in the companion State-of-the-Art Paper 1, a primary concern with respect to landslides is often public safety. As will subsequently be discussed in more detail, public safety is often expressed in terms of both: a) individual protection, so that no one person

131
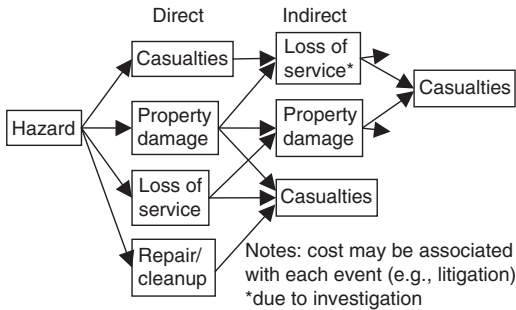
Figure 4.   Direct and indirect consequences.

Figure 5.   Loss of service due to landslide at McClure Pass Colorado (note car on landslide) (by USGS).

Figure 6.   Property damage on large slow moving landslide in Kelso WA (by NW Geoscience).

has a significant incremental probability of being seriously injured or killed; and b) society protection, so that the incremental probability of one or more fatalities among the population (collective risk) is not significant. Typically, societal risk governs for large exposed populations, whereas individual risk governs for small exposed populations. Different types of casualties (not just fatalities) can also be considered, e.g., casualties of various types (such as age at fatality and injuries of varying severity and duration) can be translated into similar terms (such as "years lost"), which can in turn be combined and translated back into "equivalent" fatalities. As another example, major pit or dump slope failures can significantly affect open pit mining cost and progress (and thus revenues), as well as cause casualties and other damages.

Van Westen et al. (2005) discuss various landslide damage scenarios. Such "damages" can be direct or follow-on (Fig. 4):

- *direct* damages occur when so-called "vulnerable elements" (people, structures, services, etc.), which are sometimes called "elements at risk", are impacted by ground movement; e.g.,
  – ground movement below structures or services causes property damage and/or loss of service (Figs 5–6)
  – ground movement directly impacts structures/ vehicles (causing property damage), people (causing casualties), or services (causing loss of service) (Figs 1–2, 7–8)
- follow-on or *indirect* damages occur as a result of direct damages of ground movement; e.g.,
  – structural/vehicle damage or loss of service resulting from ground movement causes casualties or additional structural/vehicle damage or loss of service, and so forth. For example, people are in a vehicle that is crushed or in a building that collapses, a gas pipeline is damaged causing a fire, property values in area decrease, lack of necessary services lead to unnecessary

illness, detours result in additional accidents, construction accidents occur during repair, etc.
  – a moving vehicle impacts debris or structural/ vehicle damage (e.g., road damage) resulting from ground movement, causing property damage (and so forth) and possibly casualties; similarly, a pedestrian can fall and be injured due to structural damage resulting from ground movement
  – ground movement dams a stream, which overtops and floods downstream, causing property damage, loss of service (and so forth) and possibly casualties
  – investigation of direct damages (e.g., casualties or property damage) may result in loss of service
  – any damages may result in litigation and associated costs

Such direct and indirect consequences can be identified through "event tree" analyses, in which the possible sequences of events after the hazard occurs are identified (Fig. 4); conversely, "fault tree" analyses, in which the various ways that a failure can occur, are often used to evaluate hazards (especially landslide initiation).

Ultimately, both direct and indirect consequences are important and should be assessed. For convenience,

132

Figure 7. Casualties (four fatalities) and property damage due to landslide in Bainbridge WA 1997 (by WSDOE).
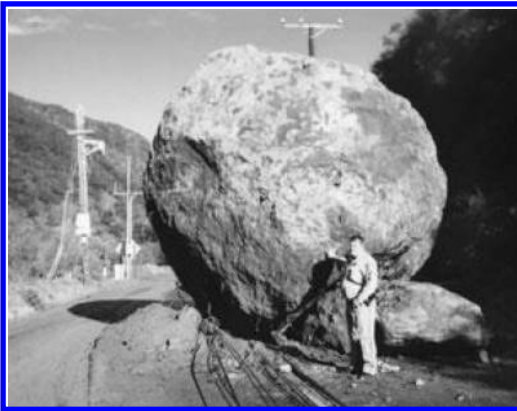
Figure 8. Loss of service (luckily no casualties or property damage) due to rock fall in Malibu CA 2005 (by The Malibu Times).

Table 1. PLL for Reference Landslide (*PLL for ref LS*) for various land uses in Hong Kong (Roberds et al 2002).

Facility group no.	Example description (see Ho et al. 2000 for more examples)	PLL for ref LS
1	Buildings (densely used) or roads (very high traffic density)	3–6
2	Buildings (lightly used) or roads (high traffic density)	1–2
3	Open space (densely used) or roads (moderate traffic density)	0.25
4	Open space (lightly used) or roads (low traffic density)	0.03
5	Country parks or roads (very low traffic density)	0.001

as will subsequently be discussed, they are often combined.

For decision making, it is often convenient to combine the different types of consequences (e.g., financial costs, loss of services, etc.) into a single measure. This requires the assessment of "tradeoffs" amongst the various types of consequences, typically expressed in terms of equivalent costs (or willingness to pay to change the consequence). For example, an amount of about US$4 million has often been used recently as the amount decision makers would be willing to pay to reduce public casualties by one equivalent fatality (Roberds et al. 2002). However, clearly, *this is a policy, rather than a technical, issue*. Other tradeoffs, such as the cost of delays or loss of service, may be easier to establish. For example, the equivalent cost of a road closure is sometimes quantified in terms of the average number of hours of "lost" time per affected person (e.g., 2 hrs per day for detour times 100 days of detour) times their average "value" per hour (e.g., US$20/hr) times the expected number of affected people (e.g., 1000); the

equivalent cost for this example would be US$4 million; not including administrative "headaches".

In some cases, such as regional landslide evaluations where there are numerous potential landslides and large variabilities/uncertainties in their characteristics, using statistically-based average consequences per event of a particular type of landslide may be adequate. For example, in Hong Kong, the "expected" or average number of fatalities if a cut slope fails has been determined to be about 0.012 (Roberds et al. 2002). This estimate can be improved, for example, by determining the average consequences as a function of some simple, general vulnerability characteristics (such as down-slope land use category).

For example, in Hong Kong, the potential loss of life (*PLL*, which is the mean of the probability distribution of the number of public fatalities) for various landslide cases was determined based on probabilistic modeling (Roberds et al. 2002):

$$PLL = \{PLL\ for\ ref\ LS\} \times \{SF\} \times \{PF\} \qquad (7)$$

where *PLL for ref LS* is PLL for reference landslide (defined as 10 m wide failure of 50 m^3 in volume, based on past landslide data in Hong Kong), which has been determined for various land uses (see Table 1), *SF* (for *scale factor*) is ratio of width of debris in landslide of interest to that of reference landslide (10 m), *PF* (for *proximity factor*) is function of debris mobility (run-out) vs. facility location.

Consequence rating systems are also sometimes used, in conjunction with hazard rating systems, to approximately determine risks of a particular landslide type, especially for comparative purposes. For example, in Hong Kong, a consequence rating system (NPCS) is used that involves estimating about a dozen parameters for a particular slope, and produces

133

a score that can be converted into a rough approximation of the expected number of fatalities if that slope fails (Roberds et al. 2002).

For other cases, more detail may be required, as discussed below. Individual and population (or societal) risk involves temporal issues, which will be discussed later.

3.2 Vulnerable elements

"Vulnerable elements" (or "elements at risk") are those *objects that can be affected by landslides, resulting in the damages* discussed above. They can be categorized as "stationary" (e.g., property, structures, services, environment) or "non-stationary" (e.g., vehicles, people). Such vulnerable elements have particular characteristics, such as value, dimensions, location, etc. Moreover, different vulnerable elements can coexist; for example, people might be inside structures or vehicles, vehicles might be inside structures, etc.

For detailed analyses, it is important to identify *all* the vulnerable elements that could be affected by a particular landslide scenario, including those that could be indirectly affected (Figure 4). If potentially vulnerable elements are ignored (e.g., because they are outside the area of ground movement and thus will not be directly affected), the consequences may be underestimated. If consequences of each type are additive among the vulnerable elements, which is reasonable and generally assumed, then the collective consequences are simply the sums of the consequences for each vulnerable element (many of which might have no consequence). This can be greatly simplified, without loss of accuracy, in terms of average consequences for each type of vulnerable element and the number of vulnerable elements of each type:

$$\underline{C}^* = \sum_{\text{all VE}} \underline{C}^*(VE) \\ = \sum_{\text{all VE types}} avg\underline{C}^*(VE\ type)\ N(VE\ type) \tag{8}$$

$$p[\underline{C}^* \mid S] = f\{p[\underline{C}^*(VE) \mid S]_{all\ VE}\} \\ = f\{p[avg\underline{C}^*(VE\ type), N(VE\ type) \mid S]_{\text{all VE types}}\} \tag{9}$$

where $C^*(VE)$ is set of consequences for each individual vulnerable element, $avgC^*(VE\ type)$ is average set of consequences for each type of VE, $N(VE\ type)$ is number of individual vulnerable elements of each type.

Probability distributions of average consequences for each *type* of vulnerable element and the number of vulnerable elements of each type are much simpler to assess than probability distributions of consequences for each *individual* vulnerable unit, which within any

one type may have great variability and strong correlation with other individual elements.

The type, number and, to some extent, characteristics (specific location, value, strength, etc.) of vulnerable elements in any particular area can generally be determined by current maps and airphotos, corroborated by visual observation. However, as will subsequently be discussed, such characteristics can change with time (e.g., due to development), so it is necessary to consider *what will be there when the landslide occurs*. Such information can be stored in GIS, which facilitates subsequent analysis, as discussed below.

3.3 Spatial intersection

Generally for *direct* consequences to occur, the physical locations of vulnerable elements must at least in part intersect with the locations of landslide ground movement; although the magnitude of consequences may be affected by the degree of intersection, this is typically ignored, assuming that any encroachment will be significant. Such spatial intersection is not necessary for indirect consequences.

For a particular location and lateral dimensions of a vulnerable unit, and for a particular location and lateral dimensions of ground movement, spatial intersection can clearly be determined geometrically, i.e., either they overlap or they do not. For example, a vulnerable element on a landslide clearly intersects. However, if there is uncertainty in the geometry of the ground movement (which there typically is), even if there is none in the geometry of the vulnerable unit, there may be uncertainty in spatial intersection (from equation 3):

$$P[\text{int}(VE)] = \sum_{\text{all S}} P[\text{int}(VE) \mid S]\, p[S] \tag{10}$$

where P[int(VE)] is probability of spatial intersection (overlap), P[int(VE)|S] is probability of spatial intersection (overlap) given the characteristics of ground movement, and p[S] is uncertainty in the characteristics of ground movement.

The probability of spatial intersection, *given the geometry of the vulnerable element, can be determined as a function of probability distributions for the path, width, and distance of ground movement, relative to the spatial characteristics of the vulnerable element. The probability of overlap (i.e., spatial intersection) equals a) the probability that the potential debris path will laterally overlap the vulnerable element, times b) the probability that the debris will travel as far distally as the vulnerable element*:

$$P[\text{int}(VE)|S] = P[L(VE)|S]\, P[D(VE)|S] \tag{11}$$

where P[int(VE)|S] is probability of spatial intersection (overlap) given the characteristics of ground

134

movement, P[L(VE)|S] is probability of lateral (perpendicular to direction of ground movement) intersection given the characteristics of ground movement, and P[D(VE)|S] is probability of distal (parallel to direction of ground movement) intersection given the characteristics of ground movement.

For example, if a downstream vulnerable element is clearly in the path of landslide debris (e.g., in the throat of a valley), then the probability of intersection is simply the probability that the landslide debris will travel that far. The probability of distal intersection can be determined simply as follows:

$$P[D(VE)|S] = P[D(S)>D(VE)] \qquad (12a)$$

$$= P[\alpha(S)<\theta(VE)] \qquad (12b)$$

where D(S) is distance to distal end of ground movement, D(VE) is shortest distance to any point of vulnerable element, $\alpha(S)$ is run-out angle from slope crest to distal end of ground movement, $\theta(VE)$ is angle from slope crest to nearest point on vulnerable element.

Obviously, the larger the landslide event (in terms of both lateral and distal extent of ground movement), the more likely that it will spatially intersect vulnerable elements.

As noted above, the location of vulnerable elements can be determined from maps and plans. Developing probability distributions for the geometry of ground movement (e.g., distance traveled or run-out angle) is discussed in companion State-of-the-Art Paper 4 (Estimating landslide movement distance and velocity – Hungr et al. 2005). A simple example will subsequently be presented demonstrating equation 12.

General equations for determining the probability of *any* intersection (however minor) given the probability distribution of ground movement are discussed in Roberds et al. (1997); a simple example is subsequently provided to illustrate such an analysis. If the degree of intersection is important, this can be determined in a similar but more detailed way.

Such probabilistic analyses can also be done by simulation and/or in GIS. For example, as subsequently discussed, the paths of debris from any location can be modeled automatically in GIS (based on maximum gradients), with the probability of intersecting specific locations (cells) determined by the specified probability distribution for run-out angle compared to the actual gradient to that cell, even considering humps in between (Roberds 2001). Combining such movement uncertainties with detachment uncertainties could be used to produce a "hazard intensity" map, as proposed by Hungr (1997).

The ground movement and vulnerable elements must also intersect temporally. This is generally not an issue for stationary vulnerable elements, but is an issue for non-stationary vulnerable elements. Temporal aspects of vulnerability will subsequently be discussed.

3.4 *Damage function*

"Damage functions" express each type of consequence (both direct and indirect) for each vulnerable element affected by the landslide. Damage functions for direct consequences can range from simple expressions (% of value lost if intersected or as a function of "hazard intensity", combined with initial value) to detailed analyses that are a function of the specific landslide characteristics (depth, viscosity, velocity, impact energy, etc.) and the vulnerable element characteristics (resistance/strength, protection, value, etc.). For example, widely-used damage functions have been developed by the United States Bureau of Reclamation (USBR) that express the probability of fatality for each individual for particular flood characteristics (depth and velocity), and property damage (in terms of % of value) as a function of flood depth. Similarly, the United States Geological Survey (USGS) has developed damage functions for homes (specifically in the Los Angeles area) in terms of % of property value lost as a function of peak acceleration rates due to an earthquake, based on statistical analysis of insurance records of actual losses correlated to estimated peak acceleration at those locations. Widely used approximate damage functions (in terms of % of value) have also been established for structures as a function of ground subsidence. It should be noted that, although using a % (or 0.0 to 1.0 scale) of value lost, combined with each vulnerable element's value, works for some consequences (e.g., property damage), it is generally not sufficient for all types of consequences (e.g., loss of service). In any case, however, unfortunately, *damage functions have generally not been developed for landslide intersections*.

Typically, in the absence of such established damage functions, *reasonable assumptions must be used in developing damage functions for landslide intersections*. For property damage, it is often somewhat conservatively assumed that a moderate amount of damage (which in many cases would occur with virtually any intersection) requires that the element be replaced (i.e., full replacement value); for example, see Figures 1–2, 5–7. However, some structures are strong enough to survive a landslide intersection with repairable damage, so that a lower damage function should be used for those vulnerable elements. For these, structural analysis of the particular structure considering the anticipated dynamic impact loading of the landslide is sometimes used. For casualties, it is often somewhat conservatively assumed that, if hit by a landslide and unprotected, that person will die (i.e.,

probability of fatality is 100%). However, not everyone who is hit by a landslide dies, so that a lower probability of fatality can be used. For example, Wong et al. (1997) suggested a probability of 0.3 that any particular person in a car that was hit (but not crushed) by a landslide would die. However, this probability (as are many consequences) is clearly a function of the magnitude of the event (e.g., see Bunce et al. 1997, 1998, Hungr & Beckie 1998). Similarly, repairs and loss of service can typically be estimated relatively well for a wide range of landslide movement scenarios. Methods for developing defensible subjective assessments are presented in Roberds (1990).

As previously noted, damage functions can be established for *types* of vulnerable elements, which express the average consequence amongst the various individual vulnerable elements of that type. However, the uncertainty in the average is a function of the number of individuals averaged over (i.e., $\sigma_{avg(x)} = \sigma_x / \sqrt{n}$, where σ_x is the standard deviation of x and n is the number of x's averaged over, if they are independent). Whereas the uncertainty in the average is small for a large number of individual elements, it may be large for a small number of individual elements or if they are correlated. Such damage functions for types of vulnerable elements can be used, along with landslide initiation, movement and landuse, in GIS to determine the landslide risks, at least for direct consequences (Roberds 2001).

Damage functions also need to account for *indirect* consequences (Fig. 4). This can be done for those vulnerable elements that are not intersected by the landslide as a function of the direct damage to those vulnerable elements that are intersected by the landslide. Hence, the damage functions can be divided into direct damage functions and indirect damage functions:

$$p[\underline{C}(VE_i)_{direct}|S]$$
$$= p[\underline{C}(VE_i)|\{int(VE_i) \text{ and } S\}] \, P[int(VE_i)|S] \quad (13)$$
$$p[\underline{C}(VE_j)_{indirect} | S]$$

$$= \sum_{all \, i} \int_{all \, C(VE_i)_{direct}} p[\underline{C}(VE_j) | \underline{C}(VE_i)_{direct}] \, p[\underline{C}(VE_i)_{direct} | S] \quad (14)$$

where $int(VE_i)$ is intersection of landslide with particular vulnerable element VE_i.

As may be obvious from equation 14, while direct consequences are relatively straightforward, indirect consequences can get very complicated. However, when integrated over all vulnerable elements, the indirect consequences often result in a simple "inflation" of the direct damage functions for landslide intersections, as discussed above. For example, property damage might simply be increased by 10% to account for indirect (follow-on) property damage.

3.5 Simple examples

Several simple examples are presented below to illustrate the above concepts. Please note that temporal aspects will be discussed later.

3.5.1 Example A

Consider an area that would be covered by a landslide (if it occurred) and that any people there when the landslide occurred would each have a 50% probability of being killed. For example, if there were 3 people there when the landslide occurred, the expected number of fatalities (societal risk) would be 1.5. The actual probability distribution of the number of fatalities (if the landslide occurred) would depend on the correlation amongst those fatalities:

- if *independent*, then $p[N_F|F]$ is a binomial distribution

$$p[N_F | F] = \frac{N!}{N_F!(N - N_F)!} P^{N_F} (1 - P)^{N - N_F} \quad (15)$$

where N_F is number of fatalities, N is total number of people exposed, P is probability of fatality for each person (if the landslide occurs)

so that for N = 3 and P = 0.5
$$p[N_F|F] = 12.5\% \text{ for } N_F = 0$$
$$= 37.5\% \text{ for } N_F = 1$$
$$= 37.5\% \text{ for } N_F = 2$$
$$= 12.5\% \text{ for } N_F = 3$$
$$P \leqslant [N_F|F] = 12.5\% \text{ for } N_F = 0$$
$$= 50.0\% \text{ for } N_F = 1$$
$$= 87.5\% \text{ for } N_F = 2$$
$$= 100\% \text{ for } N_F = 3$$

- if *perfectly positively correlated* (i.e., nobody or everybody), then

$$p[N_F|F] = 50\% \text{ for } N_F = 0$$
$$= 50\% \text{ for } N_F = 3$$
$$P \leqslant [N_F|F] = 50\% \text{ for } N_F = 0$$
$$= 50\% \text{ for } N_F = 1$$
$$= 50\% \text{ for } N_F = 2$$
$$= 100\% \text{ for } N_F = 3$$

If the number of people exposed were uncertain, then this uncertainty would be considered as follows:

$$p[N_F] = \sum_{all \, N} p[N_F | N] \, p[N] \quad (16)$$

where $p[N_F|N]$ would be determined as above.

If the expected number of exposed people were still 3, then the expected number of fatalities (if the landslide occurs) would still be 1.5, regardless of correlations amongst those fatalities, although the range in the number of possible fatalities would obviously increase.

136

3.5.2 *Example B*

Consider a power line tower (with a base width of 40 ft) near the toe of a relatively steep slope (Fig. 9). A landslide could occur anywhere along the crest of this slope, with a 50 ft wide debris trail of significant depth coming anywhere (equally likely) over a 1000 ft wide area that contains the power pole. The run-out angle for the landslide (defined as the angle from horizontal from the top of the landslide to the distal end of debris where there is enough remaining energy to cause significant damage) is uncertain, and has been assessed to be a normal distribution with a mean of 20 degrees and a standard deviation of 5 degrees. The leading edge of the tower is at a 15 degree angle (below horizontal) from the crest of the slope.

The probability of intersection can be determined from equations 11 and 12 as follows:

$$P[int(VE)|S] = P[L(VE)|S]\ P[D(VE)|S] \qquad (11)$$

where from Figure 9a

$$P[L(VE)|S] = (40\ ft + 25\ ft + 25\ ft)\ /\ 950\ ft$$
$$\approx 10\%$$
$$P[D(VE)|S] = P[\alpha(S) < \theta(VE)] \qquad (12b)$$

1000 ft (possible debris area)

possible CL location

CL

50 ft

25 ft   25 ft   40 ft   25 ft   25 ft

debris

tower

centerline (CL) locations that miss tower
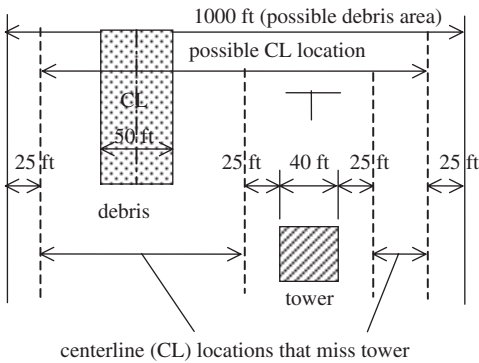
(a) Lateral (plan view)

α   θ   tower

tower hit if α < θ

$P[\alpha < \theta]$

$p[\alpha]$

θ   run-out angle
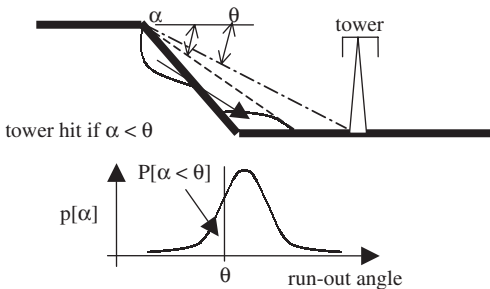
(b) Distal (section view)

Figure 9. Simple example of spatial intersection.

where for normal distribution of $\alpha(S)$

$$P[\alpha(S) < \theta(VE)] = \phi[\ \{m[\alpha(S)] - \theta(VE)\}\ /\ s[\alpha(S)]]$$
$$= \phi[(20^\circ - 15^\circ)\ /\ 5^\circ] = 16\%$$

so that

$$P[int(VE)|S] \approx 10\% \times 16\% \approx 1.6\%$$

If the tower is hit by the landslide, it will cost about US\$100,000 and take about 10 days to repair it, during which time power service to 1000 customers has been reduced by 20%. The amount that the power company would be willing to pay to have prevented that service reduction is US\$100/day per person (considering actual costs and poor press). Hence, loss of service is more significant than repair costs, and the total equivalent cost of such damage would be US\$1.1 million. However, there is only a 1.6% probability of such damage, so that the expected equivalent cost associated with a landslide is about US\$18,000. Logically, no more than US\$18,000 should be spent on landslide mitigation, even less if such mitigation is less than 100% effective.

In the above example, the width of the landslide, as well as the consequences if the tower is hit, could be uncertain and treated as such by expansion. This would increase the uncertainty in the conditional consequences, although the expected values would remain the same.

3.5.3 *Example C*

Consider extensive rock slopes above a highway. Rocks can loosen and fall onto the roadway, and then either stay in the roadway or pass through and possibly travel far down-slope. The frequency-magnitude relationship of rock falls for each of these hazards can be assessed for each zone along the highway, as documented in Table 2 (e.g., see Bunce et al. 1997, 1998, Hungr & Beckie 1998, Hungr et al. 1999). As will subsequently be discussed, the hazard frequency can be used to determine the probability of each hazard occurring during a particular time period.

The consequences of interest in this case include:

- casualties
- property damage

Table 2. Simple example of rock fall hazard (frequency–magnitude) for each zone.

Hazard/magnitude	Small ($<1\,m^3$)	Medium ($1–10\,m^3$)	Large ($>10\,m^3$)
Rock falls passing through road			
Rock falls staying in road			
Rock falls impacting down-slope			

137

Table 3. Simple example of vulnerability (direct and indirect consequences) to each rock fall hazard for each zone

Consequences of *each* occurrence (direct and indirect) Direct consequences	Rock falls passing through road			Rock falls staying in road			Rock falls impacting downslope		
	Small ($<1\,m^3$)	Medium ($1\text{–}10\,m^3$)	Large ($>10\,m^3$)	Small ($<1\,m^3$)	Medium ($1\text{–}10\,m^3$)	Large ($>10\,m^3$)	Small ($<1\,m^3$)	Medium ($1\text{–}10\,m^3$)	Large ($>10\,m^3$)
Expected value of casualties									
Expected value of property damage									
Direct delay / road closure	NA	NA	NA				NA	NA	NA
Direct cost	NA	NA	NA				NA	NA	NA

Indirect consequences	Expected value
Indirect delay/road closure per fatal event	
Indirect delay/road closure per property damage	
Indirect cost per fatality	
Indirect cost per property damage	
Indirect cost per delay/road closure (direct or indirect)	

- delays/road closures
  - direct for cleanup and repair (excluding for casualties and/or property damage)
  - indirect due to casualties and/or property damage (for investigation)
- costs
  - direct for cleanup and repair (excluding for casualties, property damage and/or delays/road closures)
  - indirect due to casualties, property damage and/or delays/road closures

The vulnerability (i.e., consequences if a hazard occurs) can be assessed for each type of hazard in each zone (if it varies by zone), as documented in Table 3. However, both casualties and property damage resulting from a rock fall in or through the road are a function of many other factors, which combine to determine the probability and nature of a resulting accident with casualties and property damage (e.g., see Bunce et al. 1997, 1998, Hungr & Beckie 1998). These will be discussed further in additional detail in a subsequent case study.

The hazard and vulnerability can be combined using equations 13 and 14 to determine the direct and then indirect consequences (i.e., the risks) in each zone (for a particular time period), which in turn can be combined over all zones to determine the risks for the entire roadway (for a particular time period).

3.6 *Future developments*

As previously noted, landslide hazard and risk maps can be automatically and efficiently developed using GIS (e.g., Hungr 1997, Roberds et al. 2002,

van Westen et al. 2005) adequately considering: a) the uncertainty of various types and sizes of slope detachment modes occurring throughout an area (during a particular time period); b) the uncertainty in the debris run-out characteristics for each such detachment; and c) the uncertainty in the consequences of such detachments and subsequent debris run-outs. In particular:

a) the likely debris paths and their critical attributes (path angles along that path) from each potential slope detachment area throughout an area are automatically estimated, based solely on a digital terrain map of that area;

b) this debris path information, in conjunction with other assessments regarding the uncertainties in whether various failure modes will occur in an area (during a particular time period) and the uncertainties in the run-out angles if they do (assessed separately, based on geologic conditions), appropriately considering convergence and overlap of debris paths (e.g., due to large detachment areas), are used to determine the hazards throughout a mapped area, where hazard is expressed in terms of the probability (over a specified time period) of significant ground movement (possibly of varying "intensity") at that location;

c) the uncertainties in what the consequences will be if such ground movement occurs in an area ("vulnerability") are assessed separately, based automatically on detected land use (e.g., from air photos and maps), and established damage functions; and

d) the hazard and vulnerability assessments are combined to determine the risks throughout a mapped

138

area, where the risk is generally expressed in terms of the "expected" (probability-weighted average) values of various types of consequences (over a specified time period) at that location:

$$p[\underline{C}_j] = \sum_{all\ i} p[\underline{C}_j \,|\, D_j]\, P[D_j \,|\, F_i]\, P[F_i] \qquad (17)$$

$$E[\underline{C}_j] = \sum_{all\ i} E[\underline{C}_j \,|\, D_j]\, P[D_j \,|\, F_i]\, P[F_i] \qquad (18)$$

where C_j is set of consequences at "cell" j due to ground movement, D_j is whether cell j experiences ground movement, F_i is whether cell i experiences detachment.

This can be done for current slope and development conditions or for proposed future development. However, the vulnerability assessment (especially identifying all the vulnerable elements and specifying their damage functions) is currently time consuming and, especially for current conditions that need to be periodically updated, could someday be done automatically (e.g., through air photos, maps and records).

4 TEMPORAL ASPECTS

As previously discussed, risk associated with slopes is a combination of: a) "hazard", i.e., uncertain slope instability and subsequent ground movement, in one or more events; and b) "vulnerability", i.e., uncertain damages associated with any particular ground movement event. The uncertainties in hazard and vulnerability are due to uncertainties in the various factors that determine hazard and vulnerability. Although not previously discussed, however, *some of these factors are not static, but actually change with time, so that both hazard and vulnerability (and thus risk) change with time*; part of their uncertainty is due to this temporal variability (i.e., not knowing how the factors will change with time and when failure will occur).

As summarized in Figure 10, for risk assessment, it is necessary to assess *ground movement characteristics and vulnerability for the time at which landslide initiation occurs*, not at some random time (unless they are independent). For example, if a landslide initiates due to heavy rainfall, then movement will tend to be more extensive than usual (due to the low viscosity of debris associated with surface and ground water) and people will tend to be indoors more than usual (to avoid the rain).

Another important temporal consideration in risk assessment is the time period of interest. For example, if multiple failures can occur over time, they can be expressed in terms of a frequency of occurrence. The likelihood of at least one failure occurring, and the expected value of the number of failures
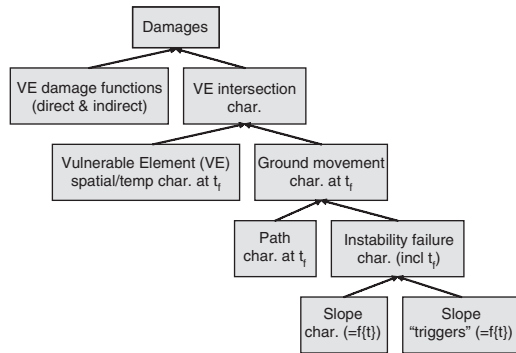
Figure 10. Temporal effects on risk (simultaneous factors).

occurring, during a particular time period increases with the length of that time period. For example, if the occurrences reflect a "stationary" random and independent process, they can be expressed as a Poisson distribution:

$$p[N] = \frac{e^{-\lambda t}\lambda t^N}{N!} \qquad (19)$$

$$E[N] = \lambda t \qquad (20a)$$

$$p[N=0] = e^{-\lambda t} \qquad (20b)$$

$$P[N>0] = 1 - e^{-\lambda t} \qquad (20c)$$

where N is number of failures, λ is average frequency of failures, and t is duration of time period of interest.

It should be noted that if landslide initiation is a Poisson process, and adequate movement given a landslide is simply a probability and consequences given adequate movement are simply expected values, then consequences can also be expressed as frequencies (albeit different frequencies than landslide initiation). For example, if ten rock falls occur on average each year along a particular stretch of road, and 10% of those on average make it to the roadway, and 10% of those that make it to the roadway on average result in a fatality (i.e., there is a 1% probability of fatality associated with each rock fall), then the average frequency of fatalities due to rock falls on this stretch of road is once every ten years. From equation 19, the probability of at least one fatality in this road section over a time period of 5 years is about 39%, rising to about 63% for a time period of 10 years. From equation 20, the expected value of the number of fatalities in this road section over a time period of 5 years is about 0.5, rising to about 1.0 for a time period of 10 years.

4.1 Temporal aspects of hazards

Although the assessment of hazards has been discussed in companion State-of-the-Art Papers 2 through 4 as

139

functions of uncertain variables, the temporal aspects of this uncertainty were generally not discussed.

The temporal aspects of hazards can be assessed in one of two ways, either:

- assess the temporal aspects of each slope instability mode and ground movement mode separately (considering correlations, including temporal aspects), and then mathematically combine; or
- assess the temporal aspects of each combination of slope instability mode and ground movement mode directly – e.g., frequency of rock falls in roadway based on statistics of past rock falls in roadway (e.g., see Bunce et al. 1998 regarding mapping rock fall impacts in asphalt).

The second approach is relatively straight forward; the first approach is discussed in more detail below.

4.1.1 *Temporal aspects of instability*

As discussed in companion State-of-the-Art Paper 3 (Probabilistic stability analysis for individual slopes in soil and rock – Nadim et al. 2005), there are various types (or modes) of slope instability, e.g., slide (continuum or discontinuum). Each failure will have a particular set of characteristics, e.g., volume, depth, area, location, brittle vs. ductile, etc.

Whether a particular failure mode occurs, and if it does the characteristics of that failure, will be a function of a variety of factors. *Most of these factors change with time to varying degrees and time scales*. Some factors can change rapidly and dramatically, and may fluctuate (Fig. 11); e.g.:

- pore pressure changes due to precipitation or leaky services, rapid draw-down, changes in hydraulic properties due to loss of vegetation due to fire, etc.
- ice wedging due to freeze-thaw cycles
- dynamic loads due to earthquakes, construction or transportation
- other load/resistance changes due to rapid erosion, progressive failure, surcharges, fire, etc.

Other factors tend to change much more slowly, often in one direction (trends); e.g., consolidation, weathering, creep, gradual erosion, corrosion of supports, etc. In any case, it is typically one or more of these changes that cause instability, i.e., the conditions change from a stable set of conditions to an unstable set.

The probability of failure (for a particular mode) during a particular time period $t_1 \rightarrow t_2$ is a function of the uncertainty (including consideration of temporal variability) and correlation (including temporal) of specific factors x during that time period:

$$P[F(t_1 \rightarrow t_2)] = P[\min FS(t_1 \rightarrow t_2) < 1.0] \quad (21a)$$

$$= \int_{all\ \underline{x}} P[F\,|\,\underline{x}]\,p[\underline{x}(t_1 \rightarrow t_2)]\,d\underline{x} \quad (21b)$$
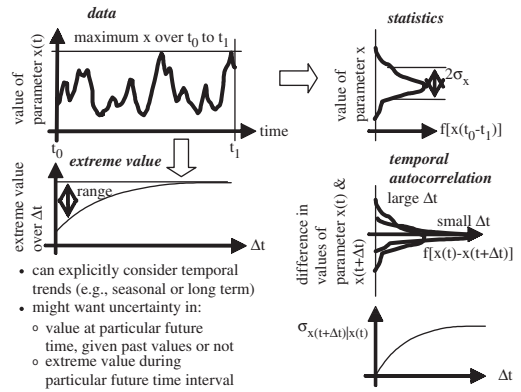
Figure 11. Temporal variability in factors.

where $FS(t) = f\{x(t)\}$, $x(t_1 \rightarrow t_2)$ is "worst" set of x over time period $t_1 \rightarrow t_2$, $P[F|x]$ is either 0.0 or 1.0 (unless there is model uncertainty).

Hence, due to temporal variability: a) *the worst combination of factors occurring over a time period will determine whether failure will occur*; b) the longer the time period, the more extreme the worst combination of factors is likely to become; and therefore c) the longer the time period of interest, the more likely failure will occur during that time period. The assessment of the probability distribution for the worst combination of factors occurring during a particular time period can be expressed in terms of probability distributions for each factor independently and correlations among them. For example, a probability distribution for maximum seismic loading can be derived from a statistically-derived (from an historical data base) frequency – magnitude relationship (Fig. 12). In the absence of adequate data for statistical analysis (e.g., for maximum pore pressure in newly constructed slopes), this may have to be done through judgment (Roberds 1990) supplemented by analyses (e.g., analyze pore pressure in the proposed slope as a function of precipitation, and use a statistically-derived frequency–magnitude relationship for precipitation).

Equation 21 can often be simplified in terms of a particular critical factor or "trigger" (e.g., seismic loading or pore pressure) (Fig. 12):

$$P[F(t_1 \rightarrow t_2)] = \int_{all\ x} P[F\,|\,x]\,p[x(t_1 \rightarrow t_2)]dx \quad (22)$$

where x might be maximum seismic load (with random pore pressure) or maximum pore pressure (with random seismic load), $P[F|x]$ includes uncertainties in model and in all other parameters.

140
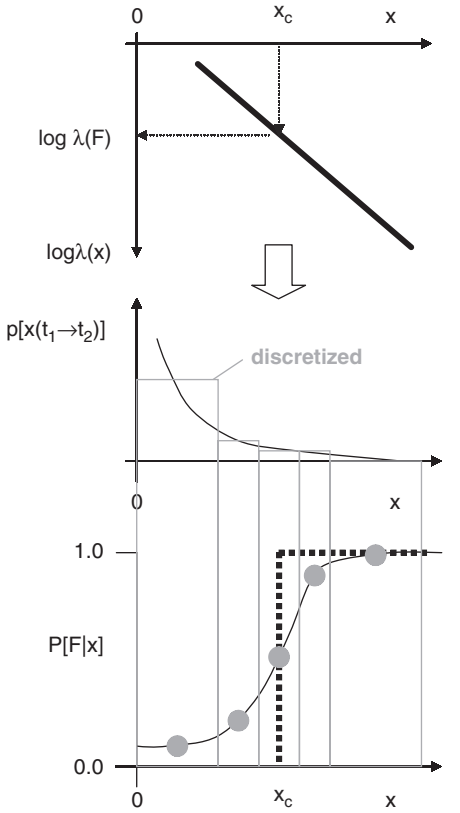
x is "trigger" parameter (e.g., max seismic load)

$\lambda(x)$ is frequency of exceeding particular value of x

Figure 12.   Triggers.

This in turn can be approximated by a discrete distribution (Fig. 12):

$$P[F(t_1 \to t_2)] \approx \sum_{all\ x} P[F \mid x]\, p[x(t_1 \to t_2)] \qquad (23)$$

Finally, if the uncertainty in other factors is insignificant, so that:

$P[F|x] \approx 0.0$ for $x \leqslant x_c$
$\qquad \approx 1.0$ for $x > x_c$

then equation 23 simplifies to (Fig. 12):

$$P[F(t_1 \to t_2)] = P[x(t_1 \to t_2) > x_c] \qquad (24)$$

This can also be expressed in terms of frequency of failure simply as a function of the frequency of exceeding the critical factor value:

$$\lambda[F] = \lambda[x_c] \qquad (25)$$

Note: For design, equation 25 is sometimes inverted, so that the frequency of a critical event (e.g., 500-year seismic load) can be specified for design to achieve a particular reliability.

The probability of failure over a particular time period can then be determined from the frequency of failure, e.g., assuming a Poisson distribution (equation 20c) with $\lambda = \lambda[F]$ and $t = t_2 - t_1$. For small probabilities of failure, this can be approximated (equation 20a):

$$P[F(t_1 \to t_2)] = \lambda[F] \times (t_2 - t_1) \qquad (26)$$

For multiple possible triggers (e.g., pore pressure or seismic loading) (not showing the time period, which is implied):

$$P[F_{a\ or\ b}] = P[F_a] + P[F_b] - P[F_a]\, P[F_b] \qquad (27a)$$

$$\approx P[F_a] + P[F_b] \text{ for small } P[F_{a\ or\ b}] \qquad (27b)$$

where $P[F_{a\ or\ b}]$ is probability of failure due to *either* a (seismic load) or b (pore pressure), $P[F_a]$ is probability of failure due to seismic load only, $P[F_b]$ is probability of failure due to pore pressure only.

Similarly, in terms of frequency of failure:

$$\lambda[F_{a\ or\ b}] = \lambda[F_a] + \lambda[F_b] \text{ if independent} \qquad (28a)$$

if $P[F|x_a]$ and $P[F|x_b]$ are simply 0 or 1, then

$$\lambda[F_{a\ or\ b}] \approx \lambda[x_{ac}] + \lambda[x_{bc}] \qquad (28b)$$

where $\lambda[F_{a\ or\ b}]$ is frequency of failure due to *either* a (seismic load) or b (pore pressure), $\lambda[F_a]$ is frequency of failure due to seismic load only, $\lambda[F_b]$ is frequency of failure due to pore pressure only, $\lambda[x_a]$ is frequency of critical seismic load, $\lambda[x_b]$ is frequency of critical pore pressure, $P[F|x_a]$ is the probability of failure given seismic load x_a, and $P[F|x_b]$ is the probability of failure given pore pressure x_b.

Clearly, a major change in parameter values occurs during slope construction; often, separate analyses are conducted for initial construction and for long-term post-construction. For example, for a cut slope in free draining material, if failure is going to occur it typically occurs at this time, but if it does not occur then, it probably will not occur afterward because the changes in parameters will generally not be large enough to go from stable to unstable conditions. Similarly, if an existing slope has been stable for an extended period, during which some triggers have been experienced, it is unlikely that smaller triggers would cause failure. Hence, the *probability of failure given a particular load should be modified to reflect this previous stability*. A more general way to conduct such "updating" of the probability of future failure of an existing slope, to

141

account for previous stability of that slope, is to: a) analyze the slope using Monte Carlo simulation, first for the previous time period $t_0 \rightarrow t_1$ and then, if the simulated properties are valid (i.e., they show stability during $t_0 \rightarrow t_1$), for the future time period $t_1 \rightarrow t_2$; and b) recognize that failure F will occur only if FS < 1.0, where FS = f{x}, and failure F will occur during $t_1 \rightarrow t_2$ only if min{FS($t_1 \rightarrow t_2$)} < 1.0. The steps are as follows:

1. assess p[$x(t_0 \rightarrow t_1)$] and p[$x(t_1 \rightarrow t_2)|x(t_0 \rightarrow t_1)$]
2. simulate $x(t_0 \rightarrow t_1)$ and thereby FS($t_0 \rightarrow t_1$) = f{$x(t_0 \rightarrow t_1)$}
3. a) if FS($t_0 \rightarrow t_1$) < 1.0, then invalid sample, ignore result and go back to step 2
   b) if FS($t_0 \rightarrow t_1$) > 1.0, then valid sample, simulate $x(t_1 \rightarrow t_2)$ and thereby FS($t_1 \rightarrow t_2$) = f{$x(t_1 \rightarrow t_2)$} and go back to step 2
4. after a large number of valid samples, calculate statistics of all valid results

p[FS($t_1 \rightarrow t_2$)|FS($t_0 \rightarrow t_1$) > 1.0]

P[F($t_1 \rightarrow t_2$)|F'($t_0 \rightarrow t_1$)]

Note: P[F($t_1 \rightarrow t_2$)|F'($t_0 \rightarrow t_1$)] will be less than P[F($t_1 \rightarrow t_2$)] if previous stability is ignored, and much less if P[F($t_1 \rightarrow t_2$)] is high.

4.1.2 *Temporal aspects of ground movement*

As discussed in the companion State-of-the-Art Paper 4 (Estimating landslide movement distance and velocity – Hungr et al. 2005), there are various types (modes) of ground movement, which are tied to the type of instability, e.g., slide, flow, rolling/bouncing, etc. Each ground movement event will have a particular set of characteristics, e.g., volume, depth, energy/velocity, path/location, maximum distance, viscosity/integrity, etc., relevant to risk assessment. The characteristics of ground movement will be a function of a variety of factors. Similar to instability factors, most of these *factors change with time to varying degrees and time scales*. Some factors can change rapidly and dramatically, and may fluctuate (e.g., debris "viscosity" is a function of water content and surface water drainage, which in turn will be affected by precipitation), whereas other factors tend to change much more slowly (e.g., path characteristics are a function of vegetation, erosion, barriers, containment capacity, etc., which in turn are affected by development, previous failures, etc.).

As previously noted (Fig. 10), the *various path factors must be assessed for the specific time of failure*, and not for a random time, unless they are independent. There will be uncertainty in relevant ground movement characteristics at the time of failure:

$$p[\underline{g}(t_f)] = f\{p[\underline{y}(t_f)]\} \tag{29}$$

where g is set of ground movement characteristics, y is set of factors that determine the ground movement characteristics, and t_f is time when the landslide occurs.

For some slope failure modes (e.g., seismically triggered), most of the important factors affecting ground movement are probably independent of landslide occurrence, so that the probability distribution for a random time would be appropriate. However, for other slope failure modes (e.g., precipitation triggered), some of the important factors affecting ground movement might be correlated with landslide occurrence (e.g., due to a common factor such as high precipitation), so that the probability distribution is different from that for a random time.

For convenience, the uncertainty in the relevant factors and thus in the ground movement characteristics can generally be adequately expressed in terms of a *comprehensive and mutually exclusive set of "scenarios" and their relative likelihood of occurring simultaneously with landslide initiation*. Unlike instability, the issue is not what the worst set of factors with respect to ground movement will be over the time period of interest, but what the set of factors will be when instability occurs. In the absence of adequate data for statistical analysis, this will often be based on judgment supplemented by analyses (Roberds 1990).

4.2 *Temporal aspects of vulnerability*

As previously discussed, vulnerability is a function of a variety of factors. Similar to instability and subsequent ground movement factors, some of these *factors change with time to varying degrees and time scales*. Some factors can change rapidly and may fluctuate (e.g., the number and location of non-stationary vulnerable elements (e.g., people and vehicles), whereas other factors tend to change more slowly (e.g., buildings, services, etc.). In fact, if a hazard is detected, non-stationary vulnerable elements can sometimes move out of the way to avoid spatial intersection. Clearly, for example, vulnerability parameters are very different during construction (of slope or development) than after construction.

Vulnerability must be assessed for the time when ground movement occurs, not for a random time, unless they are independent. Similar to ground movement characteristics, there will be uncertainty in relevant vulnerability characteristics at the time of failure (analogous to equation 29):

$$p[\underline{v}(t_f)] = f\{p[\underline{z}(t_f)]\} \tag{30}$$

where v is set of vulnerability characteristics, z is set of factors that determine the vulnerability characteristics, and t_f is time when ground movement occurs.

Where the important factors affecting vulnerability are independent of landslide occurrence, the probability

142

distribution for a random time would be appropriate. Otherwise, the probability distribution is different from that for a random time. For example, for precipitation triggered landslides, people might tend to be indoors to avoid the rain, or the rain might tend to occur at night when people tend to be indoors anyway.

Besides major changes associated with changes in land use, as previously noted, there are more rapid changes, i.e., over the course of a day (e.g., due to working hours), a week (e.g., due to working days), and seasons (e.g., due to weather). Any particular non-stationary vulnerable element will move around, sometimes out of the area; this is sometimes called "temporal spatial variability". The question is, "What is the probability they will be in a particular location when ground movement occurs?" This defines "temporal intersection", which is sometimes called "encounter probability" (LaChapelle 1966, Smith & McClung 1997, McClung 1999). For a random occurrence of ground movement, the probability that they will be there when it happens simply equals the average fraction of the time that they are there. For example, someone who works an average of 10 hours per day, 200 days per year in an office building spends about 23% of their time in that building, so that the probability that they will be there at some random time (e.g., when a seismically-triggered landslide occurs) is 0.23.

Temporal variability can also affect the uncertainty in consequences. For example, if no vulnerable elements are exposed half of the time, and a large number are exposed the other half of the time, then there would be a 50% probability of no consequences and a 50% probability of high consequences if a landslide occurs randomly. Although the expected value would be the same, the range in consequences would be much narrower if a moderate number of vulnerable elements were always exposed.

As previously noted, if a hazard is detected early enough (considering the hazard's velocity), a non-stationary vulnerable element that would otherwise spatially and temporally intersect ground movement could move out of harm's way if mobile enough. For example, someone in the eventual path of landslide debris sees the debris coming and runs out of the way. Clearly, they must be aware of the hazard and detect it, and then be mobile enough to avoid it (considering how far away it is when detected, how fast it's moving, how extensive it is relative to their location, and how fast they can run). Hence, equation 11 can be expanded:

$$P[int(VE)|S]$$
$$= P[A'(VE)|S]\, P[T(VE)|S]\, P[S(VE)|S] \qquad (31)$$

where $P[A'(VE)|S]$ is probability that the vulnerable element does not detect the hazard and/or is not mobile

enough to avoid the hazard even if detected, $P[T(VE)|S]$ is probability of temporal intersection (i.e., the vulnerable element is there when the ground movement occurs), $P[S(VE)|S]$ is probability of spatial intersection (i.e., if the vulnerable element is there when the ground movement occurs, they overlap spatially).

For example, a particular person spends 10% of their time in a location that has a 10% probability of being affected by a particular ground movement, and they have a 50% probability that they will not be able to avoid the ground movement if they are there when it happens (e.g., because they are asleep some of that time). That person has a ½% probability of intersecting both spatially and temporally with the ground movement. For a stationary vulnerable element, the probability of not avoiding the ground movement and the probability of temporal intersection are both 100%, so that the probability of intersection is simply the probability of spatial intersection.

Based on the above, public safety can be evaluated with respect to (Roberds et al. 2002): a) *societal safety criteria*, which is collective over the potentially affected population in terms of "F-N" curves (i.e., the frequency of exceeding any particular number of fatalities, or the cumulative probability of the number of fatalities per year) or, if integrated, in terms of the expected value of the number of fatalities per year; and b) *individual safety criteria*, which is for the maximum exposed individual in terms of their incremental probability of fatality per year. For example, in the example above, where a particular person has a ½% probability of intersecting ground movement (if it occurs):

- If they have a 100% probability of fatality if intersected and if there is a 1% probability of ground movement per year, then that person's incremental risk with respect to landslide is 0.00005 per year. Note: this example risk would generally be considered unacceptable under most current public safety criteria (i.e., each person must have less than 10^{-5} probability of being killed in this way in any year). For individual public safety criteria, generally only the most vulnerable (typically the most exposed) individual is evaluated and compared to the criteria.

- If the person above represented the *average* member of the potentially affected population (instead of the most exposed individual), and if that population consisted of 100 independent individuals, then the probability distribution of the number of fatalities per year (from which the F-N curve could be derived) would be given by a binomial distribution (equation 15) with N = 100 and P = 0.00005. The expected value of the number of fatalities per year would simply be 0.005. Note: this example risk would generally be considered acceptable under most current public safety criteria (i.e., the expected value of the number of people killed in this way must be less

143

than 0.01 per year) If a larger population had been considered, their average probability of fatality would have been lower.

Hence, temporal intersection of a vulnerable element with specific ground movement can be determined as a function of:

- for stationary vulnerable elements, simply whether or not they exist at the time of ground movement (e.g., considering future development)
- for non-stationary vulnerable elements, temporal characteristics of the vulnerable elements (occupancy, awareness/warning, mobility/velocity) and of that ground movement event (timing, extent and velocity of ground movement), and correlations among them

These various factors must be assessed for the individual vulnerable elements or for types of vulnerable elements. Although occupancy can typically be relatively well estimated through surveys, the other factors will typically have to be assessed based on judgment (Roberds 1990).

4.3 *Vulnerability reduction*

As discussed in companion State-of-the-Art Papers 1 (A framework for landslide risk assessment and management – Fell et al. 2005) and 6 (Risk criteria assessment and management – Leroi et al. 2005), risk can be reduced by reducing the hazards and/or the vulnerability. Reducing vulnerability is briefly described below; reducing hazards (e.g., by preventing instability or controlling subsequent ground movement) is discussed in companion State-of-the-Art Paper 6 and elsewhere (e.g., Tse et al. 1999).

As previously discussed, vulnerability is a function of: a) the number of vulnerable elements potentially affected by a particular landslide; b) the probability that they will intersect the landslide ground movement, both spatially and temporally; and c) their damage functions with respect to ground movement. Hence, *vulnerability can be reduced in the following ways*:

- decrease the number of vulnerable elements potentially affected by a particular landslide, e.g., by
  – zoning to prevent development in hazardous areas or removing existing development from hazardous areas (exclusionary zones)
  – traffic restrictions (reduce number of vehicles)
- decrease the probability that vulnerable elements will both spatially and temporally intersect ground movement, e.g., by
  – moving non-stationary vulnerable elements to less hazardous locations
  – increasing awareness, detection, and warning of hazards (either detected movement or trigger

conditions), and subsequent avoidance (evacuation or temporary exclusion, followed by inspection before resuming normal use)
- decrease damage functions for vulnerable elements with respect to ground movement, e.g., by
  – strengthening or increasing resistance to ground movement
  – emergency plan for once initial (direct) damage has occurred to prevent follow-on consequences
  – insurance

The *optimal* vulnerability reduction program depends on the application, and is a function of the cost (including financial and socioeconomic) and effectiveness of implementing the various possible approaches. Such costs can typically be reasonably estimated directly, whereas the effectiveness (or benefit) typically must be evaluated in terms of subjectively assessed specific changes in particular vulnerability factors and then an analysis of how those changes reduce risks (e.g., using the same risk model).

5 CASE STUDIES

Several case studies are described below. Each case study involves the assessment and implementation of vulnerability, as well as of landslide hazards, in risk assessment and subsequent risk management.

5.1 *Italy (Roberds 2001)*

A narrow 2-lane uncontrolled roadway (la Gardesana) that serves an important tourist area (Lago di Garda) in northern Italy lies at the base of steep rock slopes, up to 1000 m high (Fig. 13). Over many years, numerous rock falls and landslides have occurred on this road, occasionally resulting in fatalities. Although sheds have been built over some of the roadway, and support and fences have been installed above some of the remaining 2.4 km that is exposed, a landslide on the roadway in 2001 resulted in a fatality and the road was closed for safety reasons. The local province (Brescia) needed to know what actions it should take to safely reopen the road as quickly as possible and thus save its tourist industry.

A quantitative baseline risk assessment was first conducted for the current conditions and for unrestricted traffic. This was done separately and then collectively for each of 13 exposed roadway sections. For each section:

- The *hazard* (i.e., average frequencies of various magnitudes of debris landing and then remaining in the road) was based on estimates of:
  – the average frequency of various sizes of detachments for each of three zones above the road, which was in turn based on geology, stabilization

Figure 13. Two-lane roadway at base of 1000 m high cliffs in Italy (note road and tunnel at base of cliff).

effectiveness and historical evidence specifically for that road section; and
– the likelihoods of various debris magnitudes landing and then remaining in the road for each detachment magnitude and height, which was in turn based on topography, barrier effectiveness and historical evidence specifically for that road section.

• The *vulnerability* (i.e., number of casualties for each magnitude of debris that lands or remains in the road) was based on (see Appendix):
– the likelihoods of each of six types of accidents caused by debris of a specific magnitude that lands or remains in the road, which was in turn based on roadway and traffic conditions (e.g., sight and braking distance and frequency of different types of vehicles) specifically for that road section; and
– the expected value of the number of casualties associated with each type of accident, which was in turn also based on roadway and traffic conditions (e.g., average number of occupants per vehicle, vehicle protection, and impact velocity for different types of vehicles) specifically for that road section.

• The *risk* (i.e., the expected number of casualties per year) was determined by mathematically combining the hazards and the vulnerability for that road section.

The risk (i.e., the expected number of casualties per year) for the entire roadway was then determined by summing the risks for each of the thirteen road sections.

As noted above, vulnerability regarding casualties was assessed in terms of: a) the likelihood of falling debris of a specific magnitude impacting a vehicle (either a bus, an automobile, a motorcycle or a truck) and/or causing an accident (due to driver distraction or because a vehicle runs into a previous accident), and, in either case, if so the likely number of casualties; or b) the likelihood of debris of a specific magnitude remaining in the road either being run into by a vehicle and/or causing an accident (due to driver avoidance or because a vehicle runs into a previous accident), and, in either case, if so the likely number of casualties. This in turn was appropriately based on estimated vehicle and road characteristics (e.g., reaction times, braking coefficients, sight distances at various times, vehicle speed, number of vehicles per hour for various times, number of lanes, number of vehicle occupants and their protection, etc.). This previously unpublished vulnerability assessment is presented in detail in the appendix.

Consistent with historical data, the baseline risk assessment indicated that the risks associated with reopening the road without additional mitigation were too high, compared to typical public safety criteria (such as used in Hong Kong). Hence, various potential mitigation activities were identified and evaluated, including traffic restrictions and additional debris retention and slope stabilization. Nine combinations of activities were evaluated by:

• assessing the expected changes in the various hazard or vulnerability factors if those activities were carried out; and then
• determining the residual risks, in the same way as described above for the baseline (status quo) case, based on those changes.

It was found that the risks could be reduced (by a factor of more than eight) to acceptable levels by one specific combination of activities (consisting primarily of traffic restrictions/control and slope/roadway inspections, especially during and immediately after inclement weather), which could be implemented relatively quickly. The long term solution was to build a tunnel behind the slope and close the exposed roadway.

5.2 *Hong Kong (Roberds 2001, Pine & Roberds 2005)*

A major highway (Tuen Mun Road) below and immediately adjacent to large and potentially unstable slopes in Hong Kong needed to be widened while keeping all six lanes of the road open (Fig. 14). A previous attempt by others to widen the road under these

145

conditions was unsuccessful, resulting in a slope failure and a casualty as well as extensive traffic delays. In response, two phases of risk assessment/ management were conducted for the Hong Kong Highway Department.

In the first "feasibility" phase, various alternate basic design options (e.g., realignment, tunnels, slope excavation), which were intended to minimize hazards during construction as well as minimize cost, schedule and traffic disruptions, were identified and evaluated. The evaluation adequately considered the following: a) all the various consequences of interest (e.g., cost, safety, schedule, traffic delays) and trade-offs amongst them; and b) all the various ways that adverse consequences could occur (e.g., slope failures of various types, traffic accidents, construction accidents), and their likelihood of occurrence and consequences if they did occur for each slope and option. On this basis, a different option than had previously been selected was found to be best (by several tens of millions of US dollars), and was thus selected for design.

In the second "design" phase, the slope support and debris barriers for the option selected in the first phase were designed to achieve acceptable levels of risk along the alignment at the lowest possible cost, where the acceptable level of risk was specified in terms of public safety by the Hong Kong government. This, in turn, was done by: a) expressing public safety risk for a slope as an explicit function of, among other factors, the frequency of various types of slopes failures, which in turn is a function of the number of potential failures of each type (a function of area) and their probability of failure; b) relating the probability of slope failure to the design factor of safety, including slope support, based on historical evidence in Hong Kong as well as other considerations; c) relating the

design factor of safety to the cost of slope support for each type of failure, each of which would generally have a different type of support system; and d) solving for the set of design factors of safety for each type of failure that produces the acceptable level of risk at minimum cost, while also meeting minimum design factors of safety specified by the government. In this way, an optimal slope support system, which was heavier than normal because of the abnormal risks, was defensibly designed; a normal support system would have been insufficient and an even heavier support system would have been unnecessarily expensive.

5.3 North Carolina (Roberds 2001)

About a dozen major rock slopes, up to 400 feet high and collectively many thousands of feet long, had to be designed by the North Carolina Department of Transportation (NCDOT) for construction of Interstate Highway 26 north of Ashville, NC (USA). One of the primary design variables was the slope angle in the un-weathered rock that comprises the major portion of each cut. As this angle increases, the construction cost decreases but the risks associated with rock falls increase, with various other advantages and disadvantages. The optimum angle for each slope was determined based on: 1) quantifying the risks and all other relevant attributes (e.g., construction costs) for each design alternative; 2) combining those attributes into a single measure for each design alternative using trade-offs elicited from NCDOT management; and 3) comparing the slope design alternatives based on their respective combined measure.

The decision factors included: a) construction and post-construction costs (both routine and non-routine due to wedge failures); b) worker safety during construction, and public safety after construction (including but not limited to accidents due to wedge failures); c) public relations and aesthetics/land use (including but not limited to the impacts of wedge failures); and d) schedule (considering delays and their impacts due in part to wedge failures). The risk assessment explicitly considered: a) the uncertainty in geotechnical parameters (e.g., fracture length, orientation, spacing, and strength; maximum pore pressure and seismic acceleration) affecting wedge failures and how they change with time and space, especially considering changes after construction; and b) the likely consequences of each wedge failure if it occurs during construction or operations, as a function of its size. The risk assessment then quantitatively determined the following separately for short-term (during construction) and long-term (during operation) for each slope alternative: a) the probability of failure for a random wedge (searching for the critical wedge size), considering correlations amongst wedges and between construction and operations; b) the uncertainty in the number and

Figure 14. Steep rock slope to be excavated to accommodate widened expressway in Hong Kong (Pine & Roberds 2005).

146

cumulative volume of wedge failures (considering the number of potential wedges of various sizes in a slope and their overlap); and c) ultimately the uncertainty in the consequences (e.g., clean-up costs, casualties) due to wedge failures.

In this way, the optimal slope angles were defensibly determined for each slope, saving millions of US dollars compared to previous designs.

6 CONCLUSIONS

Adequately quantifying the risks associated with landslides allows for: a) better insight and communication; b) determination of acceptability (by comparison with risk criteria, if they exist); and c) rational cost-benefit decisions to be made on landslide mitigation (e.g., stabilization, zoning, etc.).

It has been demonstrated that, although not perfect and often requiring significant effort, methods are currently available to adequately assess the risk (including probable consequences) associated with potential landslides. This involves assessing and then combining: a) "hazard" (uncertain slope instability and subsequent ground movement, in one or more events); and b) "vulnerability" (uncertain damages associated with any particular ground movement event). This can be done *adequately in various ways to different levels of detail and accuracy*, depending on the application, as shown in particular for vulnerability (Fig. 15). Because hazard and vulnerability, and thus risk, change with time, the *temporal aspects must be considered*.

Although available, such *methods are not well known and not often used*. Particular areas for improvement regarding vulnerability assessment in particular include: a) better damage functions (e.g., derived from case studies or detailed analyses); and b) easier input assessments (e.g., derived automatically from air photos or land use planning maps).
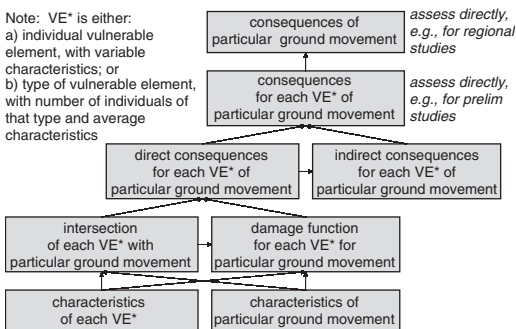
Figure 15. Summary of vulnerability assessment process.

REFERENCES

Bunce, C.M., Cruden, D.M. & Morgenstern, N.R. 1997. Assessment of the hazard from rock fall on a highway. *Canadian Geotechnical Journal* 34: 344–356.

Bunce, C.M., Cruden, D.M. & Morgenstern, N.R. 1998. Assessment of the hazard from rock fall on a highway: Reply. *Canadian Geotechnical Journal* 35(2): 410.

Fell, R. 2005. Hazard identification and quantification. State-of-the-Art Paper 2, *Proceedings of International Conference on Landslide Risk Management*, Vancouver, Canada, 31 May–02 June.

Fell, R., Ho, K., Lacasse, S. & Leroi, E. 2005. A framework for landslide risk assessment and management. State-of-the-Art Paper 1, *Proceedings of International Conference on Landslide Risk Management*, Vancouver, Canada, 31 May–02 June.

Ho, K., Leroi, E. & Roberds, W., 2000. Quantitative risk assessment – application, myths and future direction, *GeoEng2000, Proceedings of International Conference on Geotechnical & Geological Engineering, Melbourne, Australia, November, 2000*, Technomic Publishing Cp., Inc., Lancaster PA (USA).

Hungr, O. 1997. Some methods of landslide intensity mapping. Invited paper. *Landslide Risk Assessment, Proceedings of the International Workshop on Landslides Risk Assessment, Honolulu Hawaii, 19–21 February 1997*, Cruden & Fell (eds), Balkema, Rotterdam.

Hungr, O. & Beckie, R.D. 1998. Assessment of the hazard from rock fall on a highway: Discussion. *Canadian Geotechnical Journal* 35: 409.

Hungr, O., Evans, S.G. & Hazzard, J. 1999. Magnitude and frequency of rock falls and rock slides along the main transportation corridors of south-western British Columbia. *Canadian Geotechnical Journal* 36: 224–238.

Hungr, O., Corominas, J. & Eberhardt, E. 2005. Estimating landslide movement distance and velocity. State-of-the-Art Paper 4, *Proceedings of International Conference on Landslide Risk Management*, Vancouver, Canada, 31 May–02 June.

LaChapelle, E.R. 1966. Encounter probabilities for avalanche damage. *USDA Forest Service, Miscellaneous Report 10*.

Leroi, E., Bonnard, C., Fell, R. & McInnes, R. 2005. Risk criteria assessment and management. State-of-the-Art Paper 6, *Proceedings of International Conference on Landslide Risk Management*, Vancouver, Canada, 31 May–02 June.

McClung, D.M. 1999. The encounter probability for mountain slope hazards. *Canadian Geotechnical Journal* 36: 1195–1196.

Nadim, F., Einstein, H. & Roberds, W. 2005. Probabilistic stability analysis for individual slopes in soil and rock. State-of-the-Art Paper 3, *Proceedings of International Conference on Landslide Risk Management*, Vancouver, Canada, 31 May–02 June.

Pine, R.J. & Roberds, W.J. 2005. A risk-based approach for the design of rock slopes subject to multiple failure modes – illustrated by a case study in Hong Kong. *International Journal of Rock Mechanics and Mining Sciences* 42(2): 261–275.

Roberds, W.J. 1990. Methods for Developing Defensible Subjective Probability Assessments, in *Transportation Research Record No. 1288 Soils, Geological Foundations – Geotechnical Engineering 1990*, pp. 183–190, Transportation Research Board, National Research Council, Washington, D.C., January.

Roberds, W.J. 1991. Methodology for optimizing rock slope preventative maintenance programs. *Proceedings of Geotechnical Engineering Congress 1991, Boulder Colorado, 10–12 June 1991, Special Publication No. 27*, McLean, Campbell & Harris (eds), ASCE, NY

Roberds, W.J., Ho, K.S. & Leung, K.W. 1997. An integrated methodology for risk assessment and risk management for development below potential natural terrain landslides. *Landslide Risk Assessment, Proceedings of the International Workshop on Landslides Risk Assessment, Honolulu Hawaii, 19–21 February 1997*, Cruden & Fell (eds), Balkema, Rotterdam

Roberds, W.J. & Ho, K.S. 1997. A quantitative risk assessment and risk management methodology for natural terrain in Hong Kong. *ASCE's First International Conference on Debris-Flow Hazards Mitigation: Mechanics, Prediction and Assessment*, San Francisco, USA, August.

Roberds, W.J. 2001. Quantitative landslide risk assessment and management. *Proceedings of International Conference on Landslides: Causes, Impacts and Countermeasures,* Davos, Switzerland, 17–21 June.

Roberds, W.J., Ho, K.S. & Leroi, E. 2002. Quantitative risk assessment for landslides. *Transportation Research Record*, No. 1786, Paper No. 02–3900.

Smith, M.J. & McClung, D.M. 1997. Avalanche frequency and terrain characteristics at Rogers' Pass, British Columbia, Canada. *Journal of Glaciology* 14(143): 165–171.

Tse, C.M., Chu, T., Wu, R., Hungr, O. & Li, F.H. 1999. A risk-based approach to landslide hazard mitigation design. *Proceedings of Hong Kong Institution of Engineers, Geotechnical Division Annual Seminar*, May, 35–42.

van Westen, C., van Asch, T. & Soeters, R. 2005. Landslide hazard and risk zonation; why is it so difficult? *Proceedings of International Conference on Landslide Risk Management*, Vancouver, Canada, 31 May–02 June.

Wong, H.N., Ho, K.S. & Chan, Y.C. 1997. Assessment of consequences of landslides. *Landslide Risk Assessment, Proceedings of the International Workshop on Landslides Risk Assessment, Honolulu Hawaii, 19–21 February 1997*, Cruden and Fell (eds), Balkema, Rotterdam.

APPENDIX – DETAILED VULNERABILITY ASSESSMENT CASE STUDY

For the case study presented in Section 5.1, the possible "consequence" of interest of the hazard consists of public casualties, resulting from (see Figure A1a): (a) a rock fall or landslide directly impacting a vehicle; (b) a vehicle directly impacting rock fall or landslide debris remaining in the roadway; or (c) a vehicle accident due to (i) road damage caused by a previous rock fall or landslide, (ii) avoiding a rock fall or landslide into the roadway, (iii) a vehicle in front being affected by a rock fall or landslide into the roadway (chain reaction), or (iv) distractions caused by real or potential rock falls or landslides. Casualties can range from minor injuries to fatalities.

The Conditional Consequence (Vulnerability) Model thus consists of calculating the probability distribution for the number and severity of casualties for each particular hazard, i.e., volume of rock fall or landslide material passing through or remaining in the roadway.

A.1 Conditional consequence model: debris landing in the roadway

The conditional probability distribution for consequence *if* debris of a particular magnitude lands in the roadway can be determined for each roadway section as follows:

$$p[C \mid M_L] = \sum_{all\ V_i} p[C \mid V_i, M_L] \times P[V_i \mid M_L] \qquad (A1a)$$

where:

$p[C/M_L]$ is the conditional probability distribution for consequence C *if* debris of magnitude M_L lands in the roadway

$p[C/V_i, M_L]$ is the conditional probability distribution for consequence C *if* debris of magnitude M_L that lands in the roadway causes event V_i

$P[V_i \mid M_L]$ is the conditional probability that debris of magnitude M_L that lands in the roadway will cause event V_i

V_1 is the event of debris landing in the roadway impacting a vehicle

V_2 is the event of debris landing in the roadway not impacting a vehicle but causing an accident anyway (e.g., due to avoidance, distraction, or road damage)

V_3 is the event of a follow-on accident due to events V_1 or V_2, where V_{3a} is for a vehicle behind in the same lane and V_{3b} is for a vehicle in front in the other lane (if two lanes of traffic).

As shown in Figure A1b:

$P[V_1 \mid M_L] = P4$
$P[V_2 \mid M_L] = (1 - P4)* P6$
$P[V_3 \mid M_L] = P4*P5 + (1 - P4)* P6*P7$

where P4–P7, as subsequently discussed in Section A.3, are a function of: (a) the vehicle(s) involved and their characteristics (e.g., number of occupants and their vulnerability); and (b) M_L.

If only the "expected value" (i.e., probability weighted average) of the conditional consequence,

148
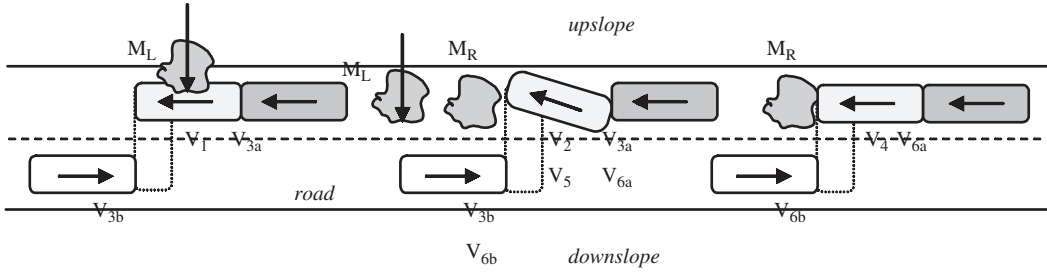
(a) Consequential events
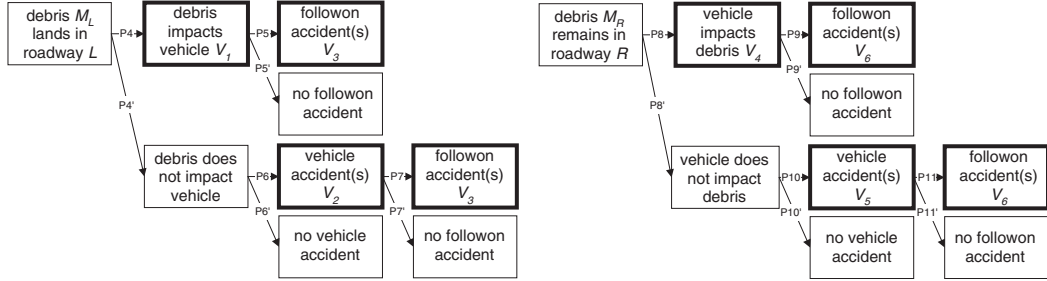
(b) Consequences if debris lands in roadway

(c) Consequences if debris remains in roadway

Note: Consequences (casualties) result from boxes with dark borders. These consequences, as well as *P4-P11*, depend on the vehicle(s) involved and their characteristics (e.g., number of occupants and their vulnerability) and on M_L and M_R. Follow-on accidents V_3 and V_6 are divided into V_{3a} and V_{6a} (for a vehicle behind in the same lane) vs. V_{3b} and V_{6b} (for a vehicle in front in the other lane, if two lanes of traffic).

Figure A1.   Conditional consequence models.

and not the entire probability distribution, is of interest, equation A1a becomes:

$$E[C \mid M_L] = \sum_{all\ V_i} E[C \mid V_i, M_L] \times P[V_i \mid M_L] \qquad (A1b)$$

where:

$E[C/M_L]$ is the expected value of consequence *C if* debris of magnitude M_L lands in the roadway

$E[C/V_i,M_L]]$ is the expected value of consequence *C if* debris of magnitude M_L that lands in the roadway causes event V_i.

A.2   *Conditional consequence model: debris remaining in the roadway*

The conditional probability distribution for consequence *if* debris of a particular magnitude remains in the roadway can be determined for each roadway section as follows:

$$p[C \mid M_R] = \sum_{all\ V_i} p[C \mid V_i, M_R] \times P[V_i \mid M_R] \qquad (A2a)$$

where:

$p[C/M_R]$ is the conditional probability distribution for consequence *C if* debris of magnitude M_R remains in the roadway

$p[C/V_i,M_R]$ is the conditional probability distribution for consequence *C if* debris of magnitude M_R that remains in the roadway causes event V_i

$P[V_i|M_R]$ is the conditional probability that debris of magnitude M_R that remains in the roadway will cause event V_i

V_4 is the event of a vehicle impacting debris remaining in the roadway

V_5 is the event of a vehicle not impacting debris remaining in the roadway but being in an accident anyway (e.g., due to avoidance or distraction)

V_6 is the event of a follow-on accident due to events V_4 or V_5, where V_{6a} is for a vehicle behind in the same lane and V_{6b} is for a vehicle in front in the other lane (if two lanes of traffic).

As shown in Figure A1c:

$P[V_4|M_R] = $ P8
$P[V_5|M_R] = $ (1 – P8)* P10
$P[V_6|M_R] = $ P8*P9 + (1 – P8)* P10*P11

149

where P8–P11, as subsequently discussed in Section A.3, are a function of: (a) the vehicle(s) involved and their characteristics (e.g., number of occupants and their vulnerability); and (b) M_R.

If only the expected value of the conditional consequence, and not the entire probability distribution, is of interest, equation A2a becomes:

$$E[C \mid M_R] = \sum_{all\ V_i} E[C \mid V_i, M_R] \times P[V_i \mid M_R] \qquad (A2b)$$

where:

$E[C/M_R]$ is the expected value of consequence C if debris of magnitude M_R remains in the roadway

$E[C/V_i,M_R]$ is the expected value of consequence C if debris of magnitude M_R that remains in the roadway causes event V_i.

A.3 *Conditional consequence (vulnerability) model inputs*

The various conditional consequence (vulnerability) model input parameters have been assessed for each road section for the base case as follows:

- *The probability that debris of amount M_L landing in the roadway will impact a vehicle, P4*. As shown in Figure A2, this is a function of the characteristics of traffic and of debris. The *probability of debris intersecting a vehicle in one lane* is given by:

$$P4_1 = 1 - \frac{[V_s - (D_L + V_w)\dfrac{V_v}{D_v}] - D_w}{V_s + V_L} \qquad (A3a)$$

where:

V_s is the average spacing (gap) between vehicles V_s, which can be determined as follows:
$V_s = [V_v / \lambda\{V\}] - V_L$
$\lambda\{V\}$ is vehicle frequency
V_v is vehicle speed
V_L is vehicle length
V_w is vehicle width
D_L is debris length (up slope), which can be determined approximately as follows (assuming a cube):
$D_L = (M_L)^{1/3}$
D_w is debris width (along road), which can be determined approximately as follows (assuming a cube):
$D_w = (M_L)^{1/3}$
D_v is debris velocity (down-slope)
M_L is amount of debris landing in road

For example, for a frequency $\lambda\{V\}$ of 1000 vehicles per hour, a vehicle velocity V_v of 50 kph and a
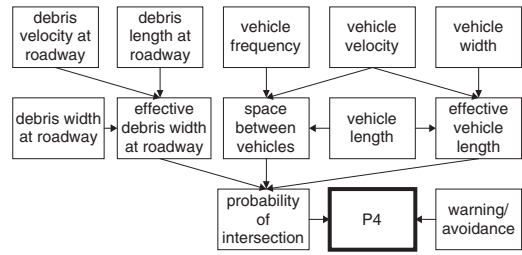
Figure A2.   Derivation of P4.

vehicle length V_L of 10 m, the average vehicle spacing V_s is 40 m. In addition, for a debris volume M_L of 1 m³, a debris velocity D_v of 100 kph, a vehicle width V_w of 3 m, and one lane of traffic, the probability of intersection for one lane $P4_1$ is 26%.

The various vehicle characteristics were estimated based on available information.

For traffic in *both* directions, the probability of intersecting a vehicle in the second lane $P4_2$ would be determined in the same way as for $P4_1$. The probability of intersecting at least one vehicle with two lanes of traffic (i.e., in either lane) is given by:

$$P4 = P4_{1+2} = P4_1 + P4_2 - (P4_1 P4_2) \qquad (A3b)$$

If the conditions are the same in both lanes, this reduces to: $P4 = 2P4_1 - P4_1^2$. For example, if the conditions were the same in both lanes as discussed in the example above, the probability of intersection for two lanes is 45%.

It is assumed that: a) a driver is either unaware of approaching debris or, if aware, cannot avoid it, so that the probability of impact is the same as the probability of intersection; and b) the probability of more than one vehicle being impacted is small enough to ignore.

- *The probability that a follow-on accident will occur after a vehicle has been impacted by debris of amount M_L landing in the roadway, P5*. As shown in Figure A3, this is a function primarily of traffic characteristics. It is assumed that the impacted vehicle immediately stops in the road and blocks both lanes. Hence, the driver in the vehicle behind either sees it immediately (if the vehicle spacing is less than the "maximum sight distance") or not until he comes within sight distance (if the vehicle spacing is more than the "maximum sight distance"). The maximum sight distance is the smaller of the following: a) distance vision, which is a function of the size of the object (assuming adequate illumination); and b) line of sight, which is a function of road curvature and illumination. Once the driver sees the impacted vehicle in the road, it is assumed that he tries to stop and that he will hit the

150
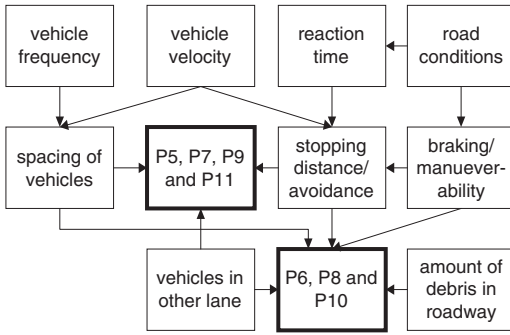
Figure A3. Derivation of P5–P11.

Note: Consequences are expressed in terms of the number of "equivalent" fatalities, which combines different severities of casualties into one measure as follows: 5–10 minor injuries are equivalent to one serious injury, and 5–10 serious injuries are equivalent to one fatality.

Figure A4. Factors affecting consequences of accident.

impacted vehicle or run off the road at that location (i.e., follow-up accident V_3) if his vehicle's "stopping distance" is greater than the available distance, which is the smaller of the vehicle spacing and the maximum sight distance. The vehicle's nominal stopping distance V_d is given by:

$$V_d = V_t \times V_v + V_\alpha \times V_v^2 \qquad (A3c)$$

where:

V_d is the vehicle's nominal stopping distance
V_t is the driver's reaction time, between when he sees the object and when he starts braking, which is a function primarily of driver awareness
V_v is the vehicle velocity
V_α is vehicle's braking coefficient, which is a function primarily of the type and condition of tires and road surface (dry vs. wet)

For example, a vehicle that is going 100 kph on a road for which that vehicle's braking coefficient is 0.01 (m/kph^2), whose driver has a 1.0 second reaction time, will take about 128 m to stop.

The actual stopping distance is assumed to be expressed as a lognormal distribution with a specified mean (which is assumed to be the nominal stopping distance) and "coefficient of variation" (or COV, which equals the standard deviation divided by the mean). Hence, the probability of there not being enough distance to stop is equal to the probability that the actual stopping distance is more than the available distance, which in turn equals:

$$P5_1 = 1.0 - \Phi\{\frac{\ln(V_x) - \ln(m[V_d])}{\ln(COV(V_d) \times m[V_d])}\} \qquad (A3d)$$

where:

$P5_1$ is the probability of a vehicle in one lane hitting a vehicle that had been impacted by debris

V_x is the available stopping distance, which is the minimum of the vehicle spacing and the maximum sight distance
$m[V_d]$ is the nominal stopping distance
$COV[V_d]$ is the coefficient of variation of the stopping distance
$\phi\{\}$ is the standard normal cumulative distribution

If the specified COV is small, then the probability of a follow-on accident is close to 1.0 for available distances slightly less than the nominal stopping distance and close to 0.0 for available distances slightly more than the nominal stopping distance. Conversely, if the specified COV is large, then the probability of a follow-on accident is close to 0.5 for all available distances.

For example, as shown in Figure A5a, if a vehicle has a nominal stopping distance of 50 m (due to its velocity, etc.) with a COV of 0.1 and the available stopping distance is 60 m (due to sight distance and average vehicle spacing), then $P5_1$ equals 45%.

For traffic in *both* directions, the probability of an accident in the second lane $P5_2$ would be determined in the same way as for $P5_1$, except that the available stopping distance may be less (because the distance between vehicles heading in opposite directions is on average half the vehicle spacing). The probability of at least one vehicle being in an accident with two lanes of traffic (i.e., in either lane) is given by:

$$P5 = P5_{1+2} = P5_1 + P5_2 - (P5_1 P5_2) \qquad (A3e)$$

If the conditions are the same in both lanes, this reduces to: $P5 = 2P5_1 - P5_1^2$.

It is assumed that the probability of more than one vehicle being in an accident in this way is small enough to ignore.

The vehicle and driver characteristics that determine the nominal stopping distance, and its COV, were assessed based on available information and judgment.

151
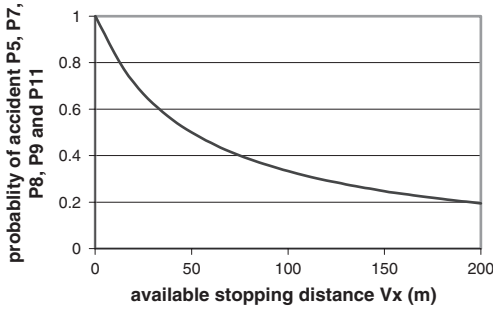
a) for *P5, P7, P8, P9* and *P11*

Note: For specific average vehicle velocity, driver reaction time, and braking coefficient, as well as COV of required stopping distance. The available stopping distance for *P8* (running into debris in the road) and for *P5b, P7b, P9b* and *P11b* (running into a stopped vehicle in the other lane) may be different than for *P5a, P7a, P9a* and *P11a* (running into another vehicle in the same lane).
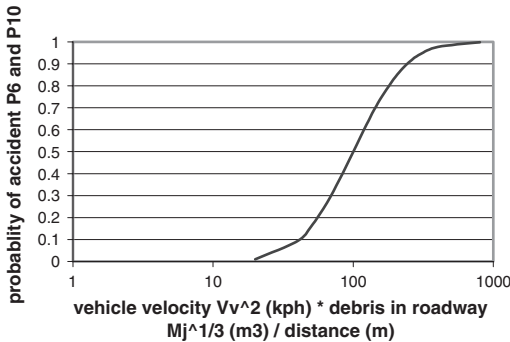
(b) for *P6* and *P10*

Note: For specific assessed combination of values of V_v, M_L or M_R and distance (which equals minimum of $V_s/2$ and maximum debris sight distance) that result in P6 and P10 equaling 50% and 84%. *P6* = 0 if $V_s/2$ > maximum debris sight distance.

Figure A5. Example relationship of probability of accidents to specific factors (varies among vehicles).

• *The probability that a vehicle will have an accident due to debris of amount M_L landing in the roadway (but not due to direct impact), P6.* As shown in Figure A3, this is a function of traffic characteristics and of M_L. If the debris is too far away to be seen (i.e., the "debris sight distance" is less than the distance from the vehicle to the debris, which on average is half the vehicle spacing), then *P6* is zero. Otherwise, *P6* increases with: increasing vehicle velocity V_v^2; decreasing distance to the debris (i.e., vehicle spacing $V_s/2$); and/or increasing debris size

in the roadway $M_L^{1/3}$ It has been assumed that *P6* can be expressed as a function of $\{V_v^2 * M_L^{1/3}/V_s/2\}$:

$$P6_1 = \Phi\{\frac{\ln\{V_v^2 \times M_L^{1/3}/(V_s/2)\} - \ln\{[V_v^2 \times M_L^{1/3}/(V_s/2)]_{50}\}}{\ln\{[V_v^2 \times M_L^{1/3}/(V_s/2)]_{84}\} - \ln\{[V_v^2 \times M_L^{1/3}/(V_s/2)]_{50}\}}\}$$

(A3f)

where:

$P6_1$ is the probability of a vehicle in one lane having an accident due to debris landing in the road (but not due to direct impact)

$[V_v^2 * M_L^{1/3}/(V_s/2)]_{50}$ is the value $[V_v^2 * M_L^{1/3}/(V_s/2)]$ for which $P6_1$ equals 50%

$[V_v^2 * M_L^{1/3}/(V_s/2)]_{84}$ is the value $[V_v^2 * M_L^{1/3}/(V_s/2)]$ for which $P6_1$ equals 84%

For example, if $P6_1$ equals 50% for $V_v = 50$ kph, $M_L = 1$ m^3, and $V_s = 50$ m, then $[V_v^2 * M_L^{1/3}/(V_s/2)]_{50}$ equals 100 (kph^2). As shown in Figure A5b, if a vehicle has specified 50 and 84 percentile values of $[V_v^2 * M_L^{1/3}/(V_s/2)]$ of 100 and 200 (kph^2), respectively, then $P6_1$ equals 16% for $[V_v^2 * M_L^{1/3}/(V_s/2)] = 50$ (kph^2), e.g., if $V_v = 50$ kph, $M_L = 1$ m^3, and $V_s = 100$ m.

For traffic in *both* directions, the probability of an accident in the second lane $P6_2$ would be determined in the same way as for $P6_1$. The probability of at least one vehicle being in an accident with two lanes of traffic (i.e., in either lane) is given by:

$$P6 = P6_{1+2} = P6_1 + P6_2 - (P6_1 P6_2) \qquad (A3g)$$

If the conditions are the same in both lanes, this reduces to: $P6 = 2P6_1 - P6_1^2$.

It is assumed that the probability of more than one vehicle being in an accident in this way is small enough to ignore.

The various traffic characteristics were estimated based on available information.

• *The probability that a follow-on accident will occur after a vehicle has had an accident due to debris of amount M_L landing in the roadway (but not due to direct impact), P7.* As shown in Figure A3, this is a function primarily of traffic characteristics, in a similar way as for *P5*. It has been assumed that *P7 = P5*.

• *The probability that a vehicle will impact debris of amount M_R remaining in the roadway, P8.* As shown in Figure A3, this is a function of traffic characteristics and of M_R, in a similar way as for *P5*, except that: a) the object in the road is debris rather than a stopped vehicle; and b) there is a chance that the debris will not be in the driver's lane (in which case it is assumed that it will not be impacted). It is assumed that the driver in a vehicle either sees the debris in his lane immediately (if the

152

distance to the debris, which on average is half the vehicle spacing, is less than the "maximum sight distance") or not until he comes within sight distance (if the distance to the debris is more than the "maximum sight distance"). Once the driver sees the debris in his lane, it is assumed that he tries to stop and that he will hit the debris (i.e., event V_4) if his vehicle's "stopping distance" is greater than the available distance, which is the smaller of half the vehicle spacing and the maximum sight distance. Hence, similar to P5:

$$P8_1 = P[lane1] \times (1.0 - \Phi\{\frac{\ln(V_x) - \ln(m[V_d])}{\ln(COV(V_d) \times m[V_d])}\}) \quad \text{(A3h)}$$

where:

$P8_1$ is the probability of a vehicle in one lane hitting debris remaining in the road
$P[lane\ 1]$ is the probability that debris in the road will be in the driver's lane, assumed to equal 50% if $M_R < 10\,\text{m}^3$ and 100% if $M_R \geqslant 10\,\text{m}^3$
V_x is the available stopping distance, which is the minimum of half the vehicle spacing (on average) and the maximum sight distance, which in turn is a function of the size of the object, illumination and road curvature
$m[V_d]$ is the nominal stopping distance, which is a function of vehicle velocity
$COV[V_d]$ is the coefficient of variation of the stopping distance
$\phi\{\}$ is the standard normal cumulative distribution

For example, as shown in Figure A5a, if a vehicle has a nominal stopping distance of 50 m (due to its velocity, etc.) with a COV of 0.1 and the available stopping distance is 60 m (due to sight distance and average vehicle spacing), then $P8_1$ equals 45%.

For traffic in *both* directions, the probability of a vehicle impacting debris in the road in the second lane $P8_2$ would be determined in the same way as for $P8_1$. The probability of at least one vehicle impacting debris in the road with two lanes of traffic (i.e., in either lane) is given by:

$$P8 = P8_{1+2} = P8_1 + P8_2 - (P8_1\ P8_2) \quad \text{(A3i)}$$

If the conditions are the same in both lanes, this reduces to: $P8 = 2P8_1 - P8_1^2$.

It is assumed that the probability of more than one vehicle impacting debris in the road is small enough to ignore.

The various traffic characteristics were estimated based on available information.

- *The probability that a follow-on accident will occur after a vehicle has impacted debris of amount M_R*

remaining in the roadway, P9. As shown in Figure A3, this is a function primarily of traffic characteristics, in a similar way as for *P5*. It has been assumed that *P9 = P5*.

- *The probability that a vehicle will have an accident due to debris of amount M_R remaining in the roadway (but not due to direct impact), P10.* As shown in Figure A3, this is a function primarily of traffic characteristics and of M_R, in a similar way as for *P6*, except that: a) unlike debris that falls without being seen, debris that remains in the road will eventually be seen, possibly causing an accident; and b) there is a chance that the debris will not be in the driver's lane (in which case it is assumed it will not cause an accident). Like *P6*, *P10* increases with: increasing vehicle velocity V_v^2; decreasing distance to the debris *d* (i.e., minimum of debris sight distance and half vehicle spacing $V_s/2$); and/or increasing debris size in the roadway $M_R^{1/3}$. Again like *P6*, it has been assumed that *P10* can be expressed as a function of $\{V_v^2 * M_R^{1/3}/d\}$:

$$P10_1 = P[lane1] \times \Phi\{\frac{\ln\{V_v^2 \times M_R^{1/3}/d\} - \ln\{[V_v^2 \times M_R^{1/3}/d]_{50}\}}{\ln\{[V_v^2 \times M_R^{1/3}/d]_{84}\} - \ln\{[V_v^2 \times M_R^{1/3}/d]_{50}\}}\}$$

$$\text{(A3j)}$$

where:

$P10_1$ is the probability of a vehicle in one lane having an accident due to debris landing in the road (but not due to direct impact)
$P[lane\ 1]$ is the probability that debris in the road will be in the driver's lane, assumed to equal 50% if $M_R < 10\,\text{m}^3$ and 100% if $M_R \geqslant 10\,\text{m}^3$.
d is the distance to debris in the road when the driver becomes aware of it
$[V_v^2 * M_R^{1/3}/d]_{50}$ is the value of $[V_v^2 * M_R^{1/3}/d]$ for which $P10_1$ equals 50%
$[V_v^2 * M_R^{1/3}/d]_{84}$ is the value of $[V_v^2 * M_R^{1/3}/d]$ for which $P10_1$ equals 84%

For example, if $P10_1$ equals 50% for $V_v = 50$ kph, $M_R = 1\,\text{m}^3$, and d = 25 m, then $[V_v^2 * M_R^{1/3}/d]_{50}$ equals 100 (kph^2). As shown in Figure A5b, if a vehicle has specified 50 and 84 percentile values of $[V_v^2 * M_R^{1/3}/d]$ of 100 and 200 (kph^2), respectively, then $P10_1$ equals 16% for $[V_v^2 * M_R^{1/3}/d] = 50$ (kph^2), e.g., if $V_v = 50$ kph, $M_R = 1\,\text{m}^3$, and $d = 50$ m.

For traffic in *both* directions, the probability of a vehicle being in an accident in the second lane $P10_2$ would be determined in the same way as for $P10_1$. The probability of at least one vehicle being in an accident with two lanes of traffic (i.e., in either lane) is given by:

$$P10 = P10_{1+2} = P10_1 + P10_2 - (P10_1\ P10_2) \quad \text{(A3k)}$$

153

If the conditions are the same in both lanes, this reduces to: $P10 = 2P10_1 - P10_1^2$.

It is assumed that the probability of more than one vehicle being in accident in this way is small enough to ignore.

The various traffic characteristics were estimated based on available information.

- *The probability that a follow-on accident will occur after a vehicle has had an accident due to debris of amount M_R remaining in the roadway (but not due to direct impact), P11. As shown in* Figure A3, *this is a function primarily of traffic characteristics, in a similar way as for P5. It has been assumed that P11 = P5.*
- *The consequences if debris of amount M_L lands in the roadway and directly impacts a vehicle, $p[C|V_1,M_L]$. As shown in* Figure A4, *this is a function of vehicle characteristics and the remaining kinetic energy of debris at impact. If debris impacts a vehicle, casualties can occur either because the debris hits someone in the vehicle or because debris impact causes the vehicle to have an accident.*

The probability of a random occupant of a vehicle that is hit by debris experiencing a casualty because they are hit by the debris P_x increases with the size of debris M_L. P_x is assumed to be expressed as a function of M_L as follows:

$$P[C\,|\,V_1, M_L]_x = \Phi\{\frac{\ln\{M_L\} - \ln\{[M_L]_{50}\}}{\ln\{[M_L]_{84}\} - \ln\{[M_L]_{50}\}}\} \quad \text{(A3l)}$$

where:

$P[C/V_1,M_L]_x$ is the probability of a random occupant of a vehicle that is impacted by debris (event V_1) experiencing a casualty because they are hit by the debris of size M_L

$[M_L]_{50}$ is the value M_L for which $P[C/V_1,M_L]_x$ equals 50%

$[M_L]_{84}$ is the value M_L for which $P[C/V_1,M_L]_x$ equals 84%

The probability of a random occupant of a vehicle that is hit by debris experiencing a casualty because debris impact caused the vehicle to have an accident P_y increases with the size of debris M_L and with the vehicle velocity at the time of the accident V_i. P_y is assumed to be expressed as a function of M_L and V_i as follows:

$$P[C\,|\,V_1, M_L]_y = \min\{1, \sqrt{M_L}\} \times \Phi\{\frac{\ln\{V_i\} - \ln\{[V_i]_{50}\}}{\ln\{[V_i]_{84}\} - \ln\{[V_i]_{50}\}}\} \quad \text{(A3m)}$$

where

$P[C/V_1,M_L]_y$ is the probability of a random occupant of a vehicle that is impacted by debris (event V_1)

experiencing a casualty because their vehicle is in an accident

V_i is the velocity of the vehicle when the accident occurs, which is assumed to be the initial vehicle velocity V_v

$[V_i]_{50}$ is the value V_i for which $P[C/V_1,M_L]_y$ equals 50% for large M_L

$[V_i]_{84}$ is the value V_i for which $P[C/V_1,M_L]_y$ equals 84% for large M_L

The probability of a random occupant of a vehicle that is hit by debris experiencing a casualty because either they were hit by debris or debris impact caused the vehicle to have an accident is then given by:

$$P[C|V_1,M_L] = P[C|V_1,M_L]_x + P[C|V_1,M_L]_y - P[C|V_1,M_L]_x \times P[C|V_1,M_L]_y$$

$$\text{(A3n)}$$

For example, as shown in Figure A6a, if $[M_L]_{50}$ and $[M_L]_{84}$ equal 1 and 2 m^3, respectively, and $[V_i]_{50}$ and $[V_i]_{84}$ equal 100 and 150 kph, respectively, then $P[C/V_1,M_L]$ equals 18% for $M_L = 0.5$ m^3 and $V_v = 50$ kph.

It is assumed that the uncertainty in the number of casualties for a vehicle that is impacted by falling debris is adequately represented by a binomial distribution, with parameters N equal to the number of occupants in the vehicle and p equal to the probability of an equivalent fatality for any random vehicle occupant. For example, if $N = 4$ and $p = 0.13$, the probability of: zero casualties is 57.3%, one casualty is 34.2%, two casualties is 7.7%, three casualties is 0.76%, and four casualties is 0.03%. The "expected value" of the number of casualties is simply N*p, or 0.5 in this example.

The various traffic characteristics were estimated based on available information.

- *The consequences if an accident occurs due to debris of amount M_L landing in the roadway but not impacting the vehicle directly, $p[C|V_2,M_L]$. As shown in* Figure A4, *this is a function of vehicle characteristics and the energy at impact. It is assumed that the vehicle velocity when such an accident occurs is the same as the initial vehicle velocity (i.e., no significant braking occurs).*

The probability of a random occupant of a vehicle that is in an accident experiencing a casualty increases with the vehicle velocity at the time of the accident V_i. This probability is assumed to be expressed as a function of V_i as follows:

$$P[C\,|\,V_2, M_L] = \Phi\{\frac{\ln\{V_i\} - \ln\{[V_i]_{50}\}}{\ln\{[V_i]_{84}\} - \ln\{[V_i]_{50}\}}\} \quad \text{(A3o)}$$

154
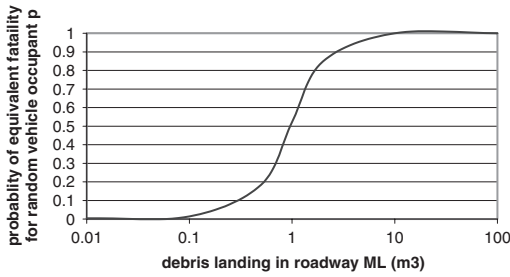
(a) for V_1

Note: For specific assessed combination of values of V_i and M_L that result in $P[C|V_1,M_L]$ equaling 50% and 84%, and for V_v = 50 kph.
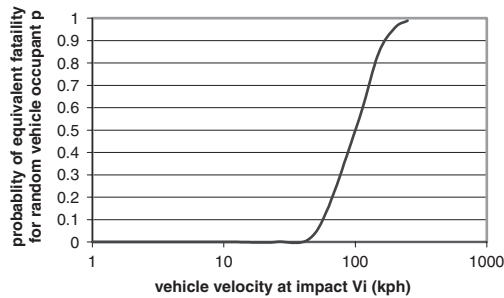
(b) for V_2 - V_6

Note: For specific assessed values of V_i that result in $P[C|V_i,M_L]$ equaling 50% and 84%. For V_2 and V_5 the vehicle velocity at impact is the same as the initial vehicle velocity, whereas for V_3, V_4, and V_6 it may be less. For V_4, this is for $MR > 1\ \text{m}^3$ (will change for smaller MR).

Figure A6. Example relationship of probability of equivalent fatality for random vehicle occupant to specific factors (varies among vehicles).

where:

$P[C/V_2,M_L]$ is the probability of a random occupant of a vehicle that is in an accident (event V_2) experiencing a casualty

V_i is the velocity of the vehicle when the accident occurs, which is assumed to be the initial vehicle velocity V_v

$[V_i]_{50}$ is the value V_i for which $P[C/V_2,M_L]_y$ equals 50%

$[V_i]_{84}$ is the value V_i for which $P[C/V_2,M_L]_y$ equals 84%

For example, as shown in Figure A6b, if $[V_i]_{50}$ and $[V_i]_{84}$ equal 100 and 150 kph, respectively, then $P[C/V_2,M_L]$ equals 4% for V_v = 50 kph.

As for V_1, it is reasonably assumed that the uncertainty in the number of casualties for this event V_2 is also adequately represented by a binomial distribution,

with parameters N equal to the number of occupants in the vehicle and p equal to the probability of an equivalent fatality for any random vehicle occupant. The "expected value" of the number of casualties is simply $N*p$.

The various traffic characteristics were estimated based on available information.

- *The consequences if a follow-on accident occurs due to vehicle impact or other accident from debris of amount M_L landing in the roadway, $p[C|V_3,M_L]$. As shown in Figure A4, this is a function of vehicle characteristics and the energy at impact. In this case, significant braking may occur before impact, so that the velocity at impact may be significantly less than the initial vehicle velocity.*

As for V_2, the probability of a random occupant of a vehicle that is in an accident experiencing a casualty increases with the vehicle velocity at the time of the accident V_i. This probability is assumed to be expressed as a function of V_i as follows:

$$P[C\,|\,V_3,M_L] = \Phi\{\frac{\ln\{V_i\} - \ln\{[V_i]_{50}\}}{\ln\{[V_i]_{84}\} - \ln\{[V_i]_{50}\}}\} \qquad \text{(A3p)}$$

where:

$P[C/V_3,M_L]$ is the probability of a random occupant of a vehicle that is in an accident (event V_3) experiencing a casualty

V_i is the velocity of the vehicle when the accident occurs, which may be less than the initial vehicle velocity V_v

$[V_i]_{50}$ is the value V_i for which $P[C/V_3,M_L]_y$ equals 50%

$[V_i]_{84}$ is the value V_i for which $P[C/V_3,M_L]_y$ equals 84%

The velocity at impact V_i is a function of the required stopping distance (which in turn is a function of reaction time, braking coefficients, and initial vehicle velocity) and the available stopping distance (which is a function of maximum sight distance and vehicle spacing):

- if the available stopping distance is greater than the required stopping distance, then the velocity at impact V_i is 0;
- if the available stopping distance is less than the product of the reaction time and the initial vehicle velocity V_v, then the velocity at impact V_i is the same as the initial vehicle velocity V_v;
- otherwise, the velocity at impact V_I is given by

$$V_i = V_v - \sqrt{\{d_{avail} - (V_t \times V_v)\}/V_\alpha} \qquad \text{(A3q)}$$

where:

d_{avail} is the available stopping distance, which is the minimum of vehicle spacing and sight distance

155

V_t is the driver's reaction time, between when he sees the object and when he starts braking, which is a function primarily of driver awareness

V_α is vehicle's braking coefficient, which is a function primarily of the type and condition of tires and road surface (dry vs. wet)

For example, for a vehicle that is going 100 kph on a road for which that vehicle's braking coefficient is 0.01 (m/kph²), whose driver has a 1.0 second reaction time, will still be going 53 kph if he has only 50 m to stop.

There may be a difference between $P[C/V_{3a},M_L]$ and $P[C/V_{3b},M_L]$ due to a possible difference in V_i for V_{3a} and V_{3b}, which in turn is due to possible different available stopping distances.

As for V_1, it is reasonably assumed that the uncertainty in the number of casualties for this event V_3 is also adequately represented by a binomial distribution, with parameters N equal to the number of occupants in the vehicle and p equal to the probability of an equivalent fatality for any random vehicle occupant. The "expected value" of the number of casualties is simply $N*p$.

The various traffic characteristics were estimated based on available information.

- *The consequences if a vehicle impacts debris of amount M_L remaining in the roadway, $p[C|V_4,M_R]$. As shown in Figure A4, this is a function of vehicle characteristics and the energy at impact. In this case, significant braking may occur prior to impact, so that the velocity at impact may be significantly less than the initial vehicle velocity.*

As for V_2, the probability of a random occupant of a vehicle that is in an accident experiencing a casualty increases with the size of debris M_R and with the vehicle velocity at the time of the accident V_i. This probability is assumed to be expressed as a function of M_R and V_i as follows:

$$P[C \mid V, M_L] = \min\{1, \sqrt{M_r}\} \times \Phi\{\frac{\ln\{V\} - \ln\{[V]_s\}}{\ln\{[V]_s\} - \ln\{[V]_s\}}\} \quad (A3r)$$

where:

$P[C/V_4,M_R]$ is the probability of a random occupant of a vehicle that is in an accident (event V_4) experiencing a casualty

V_i is the velocity of the vehicle when the accident occurs, which may be less than the initial vehicle velocity V_v

$[V_i]_{50}$ is the value V_i for which $P[C/V_4,M_R]_y$ equals 50% for large M_R

$[V_i]_{84}$ is the value V_i for which $P[C/V_4,M_R]_y$ equals 84% for large M_R

Similar to V_3, the velocity at impact V_i is a function of the required stopping distance (which in turn is a

function of reaction time, braking coefficients, and initial vehicle velocity) and the available stopping distance (which is a function of maximum sight distance and *half* the vehicle spacing):

- if the available stopping distance is greater than the required stopping distance, then the velocity at impact V_i is 0;
- if the available stopping distance is less than the product of the reaction time and the initial vehicle velocity V_v, then the velocity at impact V_i is the same as the initial vehicle velocity V_v;
- otherwise, the velocity at impact V_I is given by

$$V_i = V_v - \sqrt{\{d_{avail} - (V_t \times V_v)\}/V_\alpha} \quad (A3s)$$

where:

d_{avail} is the available stopping distance, which is the minimum of half the vehicle spacing and sight distance

V_t is the driver's reaction time, between when he sees the object and when he starts braking, which is a function primarily of driver awareness

V_α is vehicle's braking coefficient, which is a function primarily of the type and condition of tires and road surface (dry vs. wet).

As for V_1, it is reasonably assumed that the uncertainty in the number of casualties for this event V_4 is also adequately represented by a binomial distribution, with parameters N equal to the number of occupants in the vehicle and p equal to the probability of an equivalent fatality for any random vehicle occupant. The "expected value" of the number of casualties is simply $N*p$.

The various traffic characteristics were estimated based on available information.

- *The consequences if a vehicle does not impact debris of amount M_L remaining in the roadway but has an accident anyway, $p[C|V_5,M_R]$. As shown in Figure A4, this is a function of vehicle characteristics and the energy at impact. It is reasonably assumed that this is the same as for V_2.*
- *The consequences if a follow-on accident occurs due to vehicle impact or other accident from debris of amount M_R remaining in the roadway, $p[C|V_6,M_R]$. As shown in Figure A4, this is a function of vehicle characteristics and the energy at impact. It is reasonably assumed that this is the same as for V_3.*

A.4 *Implementation of inputs in conditional consequence models*

When the above inputs were implemented in the Risk Model along with the results of the Hazard Model for a particular road section, the average frequency of

156

casualties due to debris landing in the roadway $\lambda[C(M_L)]$ and due to debris remaining in the road $\lambda[C(M_R)]$ were determined, from which the average frequency of casualties due to either case $\lambda[C]$ was determined, for that road section. For example, based on a specific set of example input parameters, the following might be determined:

- The average frequency of casualties due to debris landing in the roadway $\lambda[C(M_L)]$ is 0.05 per year for a particular road section;
- The average frequency of casualties due to debris remaining in the roadway $\lambda[C(M_R)]$ is 0.01 per year for that particular road section;

- The average frequency of casualties due to either debris landing or remaining in the roadway $\lambda[C]$ is 0.06 per year for that particular road section; and
- The average frequency of casualties (due to either debris landing or remaining in the roadway) per 500 m of slope $\lambda[C/500\,m]$ is 0.03 per year for that particular road section (which is 1000 m long). Note: this would be unacceptably high per Hong Kong public safety criteria.

Risk assessment and management

E. Leroi
Urbater, Roquevaire, France

Ch. Bonnard
Ecole Polytechnique Fédérale de Lausanne, Switzerland

R. Fell
School of Civil and Environmental Engineering, the University of New South Wales, Sydney, Australia

R. McInnes
Isle of Wight Centre for the Coastal Environment, Ventnor, Isle of Wight, UK

ABSTRACT: Over recent decades, most countries have experienced an expansion of their urban areas. The complexity of the technological and human systems have also increased sharply. This concentration and complexity has largely contributed to an increase in global risks to society, albeit occasional individual risks may have decreased thanks to the progress of science and technology. Despite the development of risk prevention, social structures seem paradoxically less prepared to face disasters and alleviate their effects. It is noted that the approaches developed have not managed to successfully reduce the impact of the natural hazards so a better knowledge of the phenomenon is required to mitigate increasing losses. This is due to the fact that risk management has remained for too long concentrated on the strict analysis of the physical processes and favours technical solutions and structural measures rather than more qualitative and more global solutions. It too often focuses on the short term and on the management of the crisis and dismisses local know-how. From now on, risk management policies should adopt an integrated approach, involving all the stakeholders, from global to local, on the basis of a full diagnosis of the area, far beyond the problems of natural risks alone. This should take account of an analysis of the political aspirations for development, and be achieved through sharing research and good practice which is communicated efficiently between practitioners.

1 PREAMBLE

From time immemorial, natural phenomena have surpassed our expectations, and man has tried to protect himself against the outbursts of fury of the forces of nature. Disasters have always had an impact on the imagination and have not been forgotten thanks to witness accounts. For example, letters from Pliny the Younger gave an account of the destruction of Pompeii by Vesuvius. The first examples of risks management are very ancient. However, natural phenomena were, for a very long time, perceived as the expression of divine wrath (until the end of the eighteenth century in Europe).

The Lisbon earthquake on 1st November 1755, represented a first major step towards the awareness of human activity as a component of the risk, on the one hand, and towards the social demand for protection, as understood from correspondence between Voltaire and Rousseau, on the other. The latter has, from then on, never stopped growing.

1.1 *Definition & objectives of risk management*

The assessment of landslide risk is defined as: "The process of making a decision recommendation on whether existing risks are tolerable and present risk control measures are adequate, and if not, whether alternative risk control measures are justified or will be implemented. Risk assessment incorporates the risk analysis and risk evaluation phases."

Risk management of slope instability, whether of natural or anthropic origin, is defined as "The systematic application of management policies, procedures and practices to the tasks of identifying, analysing, assessing, mitigating and monitoring risk".

Insofar as possible, it aims at reducing the risk below the threshold of tolerable or even acceptable risk, by
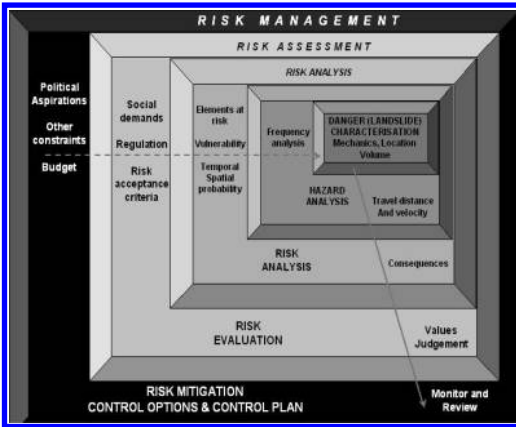
Figure 1. General flow chart of Landslide Risk Management (LRM).
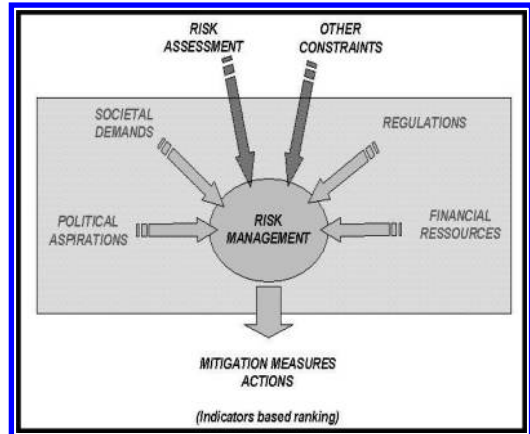
Figure 2. The constraints to be taken into account in Landslide Risk Management.

taking into account the statutory and environmental protection constraints, by integrating the aspirations of societies and individuals to develop within a harmonious and secure environment, and by making sure that viable and economically tolerable solutions are proposed. At best, its aim is not to worsen the existing situation. It therefore contributes to the sustainable development of societies.

In essence, risk management poses the problem of the thresholds of acceptable risk and tolerable risk. If a regulation has been developed, it, therefore, imposes responsibilities on the authorities concerned, and the respect of the objectives falls within a contractual process that can then be met with two distinct logics:

– A logic of means: this is the case when the thresholds have not been legally defined, or in an implicit manner, notably in comparison with the other risks (industrial, health, transport). Such logics are generally found in centralised systems with a strong implication of the responsibility of the State; the effects are multiple, whether at the level of the responsibility, notably penal, or concerning the scientific or technical choices;
– A logic of results: as soon as the thresholds are set by regulations or come under case law, they represent the criteria of respect of the objectives. Such logics are generally met either in decentralized systems, or in the case of private or public managers of properties, networks. The effects are as numerous but have a very different nature from those of the logic of means.

These points will be developed in section 4.

Successfully completed in terms of a global approach, the logic of which is described in Figure 1, landslide risk management should not be envisaged in

a sector-based manner. The choice of measures for reducing risk and the operational actions to be implemented, are made in view of other constraints and risks affecting the area of interest. The ambitions for development, the financial resources available, the needs of society and the regulation (cf. Figure 2) restrict the field of potential solutions, on the basis of economic, social, environmental, cultural, legal, technical, political indicators, in order to reach acceptable solutions.

2 PRELIMINARY ELEMENTS OF RISK ASSESSMENT AND RISK MANAGEMENT

2.1 *Evolution of societies and of social demand for protection*

Whatever its scale, landslide risk management is above all land use planning management. Risk mitigation actions are defined in view of the social demand in term of protection, development, and quality of life – to quote only the main aspirations. However, the needs of society and social demand have, for the past century, evolved strongly regarding natural risks. This evolution is more or less pronounced depending on the countries and the cultures, but its tendency is relatively constant whatever the society. It is noted that:

– The more important the development of the country and the wealth of the gross domestic product, the more the comfort of the population increases, the less risks from natural hazards are accepted.
– Social demand for protection is growing stronger and stronger. This includes natural phenomena despite the fact that, until now, they are mostly imponderable. If rural populations suffered the quirks of nature with a certain fatalism, most of the

160

urban populations do not accept these damages anymore, even to the level of the simple inconvenience generated by hazardous phenomenon. Even more so, as soon as a disaster happens, responsibilities and even culpability are sought with ever increasing requests for compensation. This tendency for society to become more judiciary – which occurs in various ways depending on the civil (Common Law) and penal codes of the countries – has important consequences on risk management, and notably on political decision-making. The principle of precaution has a tendency to apply without distinction and the conflicts of land use multiply.

– The increasing demand for protection is also accompanied by a demand for compensation increasing in importance and speed, via insurance systems. The reduction in purchasing power and the standard of living are difficult to accept, even in the short term. The compensation processes and philosophies adopted are numerous and vary, from mutualistic systems based on national solidarity under the responsibility of the State, to individual private insurance coming under the competitive domain. Numerous countries do not have a compensation system or, if one has been implemented, this system is not within reach of most of the population.

– In order to face this evolution of social demand, legal processes and tools have been set up by the authorities. Their aim is to supervise and manage land development in vulnerable areas, to standardise the risk analysis processes, to manage critical situations and to compensate the victims. Does this approach facilitate risk management? Not always! Individual aspirations may not agree with conflicts of use, of restrictions and the consequences for land or property. This is where one encounters the current limits of highly regulated systems based on constraint.

– One can also note the strong disconnection – conscious or unconscious – within the population between the cost of the damages encountered and the protection desired. In highly protected societies, the demand for protection becomes unreasonable, notably when it must be met by the public authorities. Although it is very difficult to put a price on human life, it is recognised that the cost of protection must be within reasonable limits. The adequacy of the protection solutions, the cost/benefit analysis and the choice of protection level must not only develop, but also be subject to a global and educational discussion with the population. Such discussion can no longer only be restricted to exchanges between risk managers and technicians.

– Civil society now wishes to take part in the discussion and be a stakeholder in the prevention and risk reduction policies. If civil society does not wish to, and indeed cannot interfere in the scientific discussions, this does not mean that the technicians have a free hand. The control happens afterwards, often following a disaster, and the implications are then brutal, irrational, and ruthless for the scientists: "If we can go to the moon, the disaster should have been foreseen and avoided!". Only a rigorous approach, explained and shared prior to the disaster, allows engagement in a balanced discussion. Qualitative approaches and the lack of explicit criteria on acceptable risk level do not however facilitate the task of the scientist, in addition to the fact that good faith and omniscience are no longer a guarantee of immunity.

2.1.1 Urban concentration and modification of the environment

Beyond the evolutions of social demand, strong shifts of land occupancy must be taken into account for landslide risk management.

– Society is more individualistic. This translates notably at the planning level into the development of the "property owner", through private housing, with the quest for a better standard of living; slope areas are more and more "colonised" around towns, with the implementation of road networks and infrastructure. In a similar fashion, the development of outlying areas on sloping sites is found in developing countries, for obviously different reasons, but with identical consequences for the human modification of the environment, the alteration of the drainage and the problems of uncontrolled excavations.

– Urban concentrations are more and more important with, yet again modification of the environment, and a change to the pre-existing equilibriums. Cases of urban extensions carried out within the framework of an integrated development and a preliminary impact analysis – notably concerning the risks – are few and far between; at best, selective geotechnical studies are undertaken. If such analyses have been undertaken they may often be abandoned because of development pressures.

– This urbanisation of the environment also corresponds with a strong shift of activities and lifestyles, with the discontinuation of agricultural practices generally accompanied by a reduction in land maintenance. Water flow management is no longer ensured, whether naturally by vegetation cover or by the implementation and maintenance of collecting devices for drainage and/or irrigation. Water flow and drainage method both on and within the ground and their imbalances can occur at variable frequency. It is important to note that the upgrading of communication routes contributes to an important modification of the flows, and even more so if the rainwater drainage systems have not been constructed or maintained properly.

– Urban civilisation, by leading man away from nature, suppresses the points of reference that verbal or written tradition could offer him regarding natural phenomenon, natural environment in general and the great equilibriums they govern. Land maintenance reflexes lessen, which also contributes to the imbalance of the natural environment. Henceforth, demands aiming at finding best practice for environment management must often be expressed in a statutory manner and are thus felt as constraints, especially when they are not accompanied by sufficient information. Recommendations or obligations are too often expressed in a technocratic fashion without really taking into account local and cultural circumstances.

2.1.2 *From political to politicking risk management*

– Considering the legalisation of society, the precautionary principle is not always used in a reasonable fashion. Preventative protection now aims more at protecting the decision-maker and the decision-making from a possible legal implication rather than anticipating – through an action – too imperfect knowledge. It generally leads to hold-ups and to inactivity, as well as the usual conflicts. These conflicts are furthermore pronounced as the decision-makers do not have to bear the direct financial consequences of their decision. The same applies to the technicians as soon as they perform sector-based risk analysis. The integrated approaches, based on the logic of stakeholders must prevail. This requires risk technicians to open up towards social sciences and towards relevant disciplines, such as town and country planning, architecture, network engineering and political management planning. Multidisciplinary teams – if they are necessary – are not sufficient; in addition to the juxtaposition of the competence, it is necessary to favour multi-competence training and communication.

– Through the impetus given by the media, political management of the area and in turn risk management, except on rare occasions, are more and more focused on the short term and sometimes on the present moment. Societies have this strong tendency and the research actions as the operational actions of risk management and reduction tend to be in line with this approach. However, if policies are modelled on laws, nature is free from these contingencies. Communication, education, experience feedback, as well as the scientists independence, must counterbalance this evolution towards the management of the present moment, and inscribe actions on the long term and for a period of time.

– Finally, and in the continuity of the management of the present moment, there has been a progressive evolution toward the management of what is visible, if not only visual: priority has been given to repairs (it can be seen) rather than prevention (it is less visible if visible at all); this touches on the unrewarding role of prevention as it experiences serious difficulties in 'proving' its action and its efficiency. Even when funds are allocated for prevention they may be spent on more general development measures and are thus diverted from their real purpose.

2.2 *Scientific shortcomings*

The processes leading to slope instability are, from a theoretical viewpoint, fairly well known, whether these are mechanisms, equilibrium models, or behavioural laws or other approaches. The models developed are particularly good. However, some uncertainty remains, notably on the outer conditions, the characteristics of the materials, or the detailed geometry of the environments.

Moreover, the development of personal computers in the past decades has enabled us to now have at our disposal calculation abilities far superior to the demand of the operational users.

Therefore, to date, neither the understanding of the phenomenon, nor the ability to calculate represent the true break to a systematisation of deterministic analysis. The limits are, therefore, imposed by the difficulty to access the parameters of entry of the models (mechanical and hydraulic characteristic of the ground, geometry of the environments), even if major progress has been made for surface data.

The determinist models are most of the time limited to engineering studies on selected and active phenomenon; their support to the planning system is only starting. In many cases, the assessment of the hazards rests on empirical laws and approaches, on the basis of experience feedback and temporal series, using the principle of causality, that is to say that the same causes bring the same effects.

The principle of causality, applied to highly modified «natural» processes, and sometimes controlled by man, is no longer necessarily valid. The strength and the simplicity of this principle rest on the strict similarities of the causality factors that intervene directly in the process. The fact that the rainfall series are constant does not infer that the consequences will be similar; the artificialisation of the environments, notable in urban areas, and the lack of maintenance, mostly regarding water flow control, modify, sometimes radically, the modes of propagation and concentration of the water in the ground. The transfer functions between rainfall in a given place, and the interstitial pressure in another place are modified, and sometimes highly modified. Therefore, the same causes will not bring the same consequences.

This observation is not specific to landslides and identical effects are observed for floods. Climatic

162

changes – regularly forecasted – will reinforce this drift, even if there is no possible comparison between the alterations imposed by man and the alterations inferred by nature itself, whether regarding the intensity or the temporal variations in change.

Few studies have been led to quantify the consequences of human modification of the environment and the drift from agriculture on whole sections of the territory, even with relatively simple approaches bases on the Manning-Strickler coefficient.

The influence of anthropic activities on the triggering of slope instabilities is very significant, including for largescale phenomenon; it is not, however, immediately visible and the alterations can take several years and sometimes several decades. Therefore, beyond man's impact on the assets (urban concentrations on at-risk sectors), he significantly increases the risk by his more or less direct intervention on the triggering of the phenomenon, and on its annual frequency and intensity.

How then can we integrate these alterations in a realistic fashion in the temporal series in order to have at our disposal stable scientific models and be able to continue to apply the causality principle? Is the notion of annual probability generally used to characterise the risk only relevant from the viewpoint of the swift and important fluctuations imposed by man?

Beyond the problems inherent to the anthropic activities for which scientists are only spectators, there are also some shortcomings directly attributable to them, whether concerning the scientific methods themselves, or their relation with the non-scientific world (population, law-makers, risk managers, media…):

– Assumptions and facts are not always clarified or the distinctions are insufficient;
– Uncertainties are not often displayed;
– Solutions are not conceived sufficiently upstream from the risk managers;
– Education and communication are insufficient;
– Information is often considered as communication, but it is very rare to be able to determine whether the messages have been properly received or not.

Finally, few studies really address the risk, notably in management terms. Certain elements are not yet accessible – this is the case for intensity and vulnerability – and development ambitions have not been given sufficient attentions. In many cases, the hierarchical organisation of the risk virtually exclusively rests on the hierarchical organisation of the hazards.

2.3 Interdependency of the environments

An area is the result of the juxtaposition and the more or less harmonious confrontation of three environments:

– Natural

– Human
– Constructed

Each environment is defined by a spatial distribution (number, dimensions, position), a temporal probability (between 0 and 100%) of presence on the site, and by characteristics in term of:

– Frailty (physical, social, psychological, environmental, functional or economic)
– Importance (social, economic, in a normal situation or during a crisis)

Each environment has in addition its own properties. These properties are not exclusive to one environment. That is to say:

– Beauty
– Usefulness
– Destructive ability
– Energy power
– Cultural importance

These environments are in constant interaction with one another, and any action on one environment creates evolutions on all three environments (see Figure 3). Therefore, the mutations of the areas which accompany, for example, a drift from the land, modify the modes of circulation and of concentration of ground water, therefore provoking an increase in the frequency of the landslides, which effectively makes any development established in the area more exposed.

Any area is in constant change, and its state of balance or imbalance results from its past evolution. Landslide risk management rests on the understanding of the phenomenon and their cause, and consequently on a full territorial diagnosis which integrates its past. Risk mitigation solutions must be chosen in relation to the political ambitions for development and protection, within the framework of a stakeholder's logic.
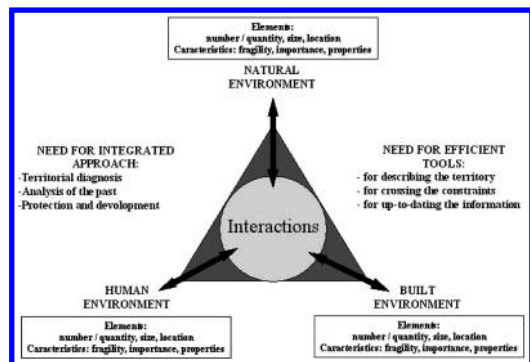
Figure 3. Interdependency of the natural, human and built environments.

163

3 THE DIFFERENT TYPES OF LANDSLIDE RISKS MANAGEMENT

Landslide risk management is not unique in the world; numerous factors lead to modification of the tools used, the approach followed and the objectives to be reached. Some are presented below.

3.1 *The nature of the phenomena and the assets to be taken into account*

It is obvious the risk management varies depending on whether or not it deals with:

– An active landslide or a potential landslide,
– A slow landslide or a fast landslide,
– A phenomenon in rock or soil conditions: the fore-warning of the phenomenon and the reaction time may vary,
– A natural slope, instrumented, shaped by man, or even an artificial slope: the acceptable risk criteria vary,
– An isolated movement, a linear, a village … : the first two come under engineering whereas the latter comes under planning,
– A private property (house, network…) or a public property (forest…): responsibilities and obligations might not necessarily be the same,

The tools, the approach and even the logic used will vary; if the phenomenon is declared and represents an imminent hazard, priority will be given to the technicians who often benefit from important financial means. If the phenomena are potential and concern the entire area, it will be wiser to start the analysis with the development ambitions and the stakes inventory; in this case, the financial means to mobilise will be less and generally will have various order of importance: technical ascending logic (we start from the phenomenon and we analyse whether or not the effects are compatible).

3.2 *Cultural, social and other issues*

Beyond the technical consideration, risk management rests mostly on:

– The culture (notably in term of acceptable risk, of relation to immovable property and property ownership, of history, of religions or beliefs, of experience regarding the risks…);
– The laws, if they exist and if they are specific to natural risks;
– The organisation and the responsibilities of the authorities (notably in term of distribution of power, term and tenure);
– The organisation of the administration, operational relays at various levels of the society of the political power;

– The public and private stakeholders including the organisation of engineering and technical expertise (public engineering, small consultants, major consultants, universities…);
and risk management also rests on:
– The wealth of the country (in term of GDP), the available financial means, the level of technological development…
– The density of population,
– The price of the land and building,
– The need for sustainable development.

The very philosophy of risk management can be radically different, whether in term of prevention, rescue organisation, risk reduction, compensation and information. This point is detailed in the following paragraph as it may affect all the other factors.

3.3 *Dependence on political choices*

Independently from the laws and organisation systems which are, by nature, specific to each country, four fundamental criteria will affect the risk management modes, and their operational implementation:

– Recommendations/Obligations: is the management of risks related to landsliding based on a regulation with prescriptions that are optional (recommendations) or compulsory? In the case of the second assumption, do the prescriptions apply to all, including the State, in which case is it a heavy constraint of public servitude type? If not, do the prescriptions come under land rights or planning? Finally, do they apply retrospectively on existing property or do they only concern the properties and activities which have been set up after the elaboration of the regulatory process?
– Centralised national management/decentralised local management: is the risk management performed under the responsibility of the State and in a centralised fashion, or under the responsibility of the local authority in a decentralised fashion? In the case of the second assumption, do the local decision-makers have full powers on the prescriptions, and have a free hand in the methods to be implemented, or are they obliged to apply a standardized procedure?
– Principle of solidarity or not: is the risk management based on a principle of national or regional solidarity, in which case the financial impacts, notably concerning the insurance, are identical for all, independently from the level of exposure (mutualisation of the risks) or is it directly connected to the risk level? The principle of solidarity prevails notably on reconstruction actions following damages, with the same coverage whatever the level of damage.

164

– Link between prevention and compensation or not: is there a link between prevention and compensation, or more precisely, does the compensation level depend on the actions of risk reduction and prevention? It then raises the question of the role of the insurance companies, of their power and autonomy in relation to the public authority, notably in term of premium rates and compensation level.

Other element than intervene in the analysis of the systems implemented, that is to say:

Information: whose responsibility does it come under? How is it provided? What control and analysis feedback is there on its efficiency?

The control related to the respect of the prescriptions: who provides it? What are the coercive powers of the auditors?

Crisis management and rescue organisation: how is security organised in relation to prevention? Are the operational interventions and responsibilities ensured by a unique authority or are they spread across several structures?

4 ACCEPTABLE RISK: BASIC NOTIONS AND PRINCIPLES

The definition of acceptable risk is a necessary stage in rational landslide risk management. It enables the elaboration of risk analysis and reduction methodologies on the basis of clear and shared objectives. The criteria used can be multiple, and so can their value; acceptable risk can be defined in a qualitative, quantitative or even implicit fashion. It can also be entered in a statutory framework, or be offered as information only as recommendation. The methodological choices, the means used and the responsibilities will vary depending on the method used. But in any case, if it is necessary, the choice of acceptable risk level is not sufficient.

4.1 Some general principles

4.1.1 The need for risk assessment criteria
Risk analysis alone has limited benefits, and it is normal to carry the process to the next stages of risk assessment and risk management. In the risk assessment stage, the calculated risk is evaluated against risk acceptance criteria. These may relate to loss of life, financial and socio-environmental values. Each of these may be considered in several ways:

Loss of life
– individual risk
– societal risk, eg. as f-N or F-N criteria
– annualized potential loss of life
– cost to save a life.

Financial
– cost benefit ratio
– financial capability
– annualized cost
– corporate impact
– accidents per million tones of freight hauled
– frequency of accidents.

The risk assessment process will, or should involve the owner, regulator, other professionals and, in some cases, society as a whole, or at least those affected by the hazard. It is desirable, if not essential, that the risk analyst be involved in the process because the process is often iterative, requiring assessment of the sensitivity of calculations to assumptions, the development proposed, and risk mitigation measures. This involvement, which is often understated, is a key factor in contributing towards a proper risk management strategy.

4.2 Tolerable life loss risk criteria

4.2.1 Concepts and background to tolerable life loss criteria
As defined in the glossary, *tolerable risks* are risks within a range that society can live with so as to secure certain net benefits. It is a range of risk regarded as non-negligible and needing to be kept under review and reduced further of possible.

Acceptable risks are risks which everyone affected is prepared to accept. Action to further reduce such risk is usually not required unless reasonably practicable measures are available at low cost in terms of money, time and effort.

These definitions are consistent with IUGS (1997), HSE (2001), ANCOLD (2003) and ICOLD (2004). It should be noted that there is a significant difference between tolerable and acceptable risk. In most situations the trade-off between risk and net benefits is a factor, so the discussion here will deal mostly with tolerable risk criteria. IUGS (1997) listed some common general principles that can be applied when considering tolerable risk criteria.

(a) The incremental risk from a hazard to an individual should not be significant compared to other risks to which a person is exposed in everyday life.
(b) The incremental risk from a hazard should, wherever reasonably practicable, be reduced, ie. the As Low As Reasonably Practicable (ALARP) principle should apply.
(c) If the possible loss of life from a landslide incident is high, the risk that the incident might actually occur should be low. This accounts for society's particular intolerance to incidents that cause many simultaneous casualties, and is embodied in societal tolerable risk criteria.

165

(d) Persons in society will tolerate higher risks than they regard as acceptable, when they are unable to control or reduce the risk because of financial or other limitations.

(e) Higher risks are likely to be tolerated for existing slopes than for planned projects, and for workers in industries with hazardous slopes, eg. mines, than for society as a whole.

IUGS (1997) noted that these principles are common with other hazards such as Potentially Hazardous Industries (PHI) and dams. They considered there to be other principles that are applicable to risk from slopes and landslides:

(f) Tolerable risks are higher for naturally occurring landslides than those from engineered slopes.

(g) Once a natural slope has been placed under monitoring, or risk mitigation measures have been executed, the tolerable risks approach those of engineered slopes.

(h) Tolerable risks may vary from country to country, and within countries, depending on historic exposure to landslide hazard, and the system of ownership and control of slopes and natural landslide hazards.

It is common to consider individual, societal and total risk when assessing whether risks are tolerable.

Individual risk to life is the increment of risk imposed on a particular individual by the existence of the hazard. This increment of risk is in addition to the background risk to life, which the person would live with on a daily basis if the facility did not exist. Individual risk is usually expressed as the annual probability of the individual being killed as a result of the hazard.

Figure 4 shows the average background risks for males and females in Australia.

HSE (1999, 2001) present similar figures for persons living in the United Kingdom. Such information can be used as the basis upon which to set tolerable risk criteria so they do not significantly increase the risks compared to risks persons normally live with. It is common to consider the individual or group most at risk when assessing whether the individual risks are tolerable (eg. ANCOL 2003).

Societal risk is the risk of widespread or large scale detriment from the realization of a defined risk, the implications being that the consequences would be on such a scale as to provoke socio/political response. Societal risk is usually measured either in terms of a cumulative probability that N or more lives will be lost (ie. an F-N plot) or as total risk. Figure 5 shows an example of an F-N plot.

It is usually accepted that if any part of the data plots above the limit (of tolerability) line, the risks are intolerable. If they plot below the limit line, the
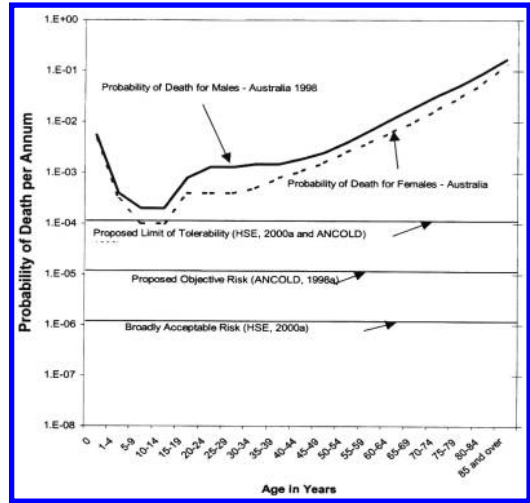
Figure 4. Average background risk for males and females in Australia (ANCOLD 2003).
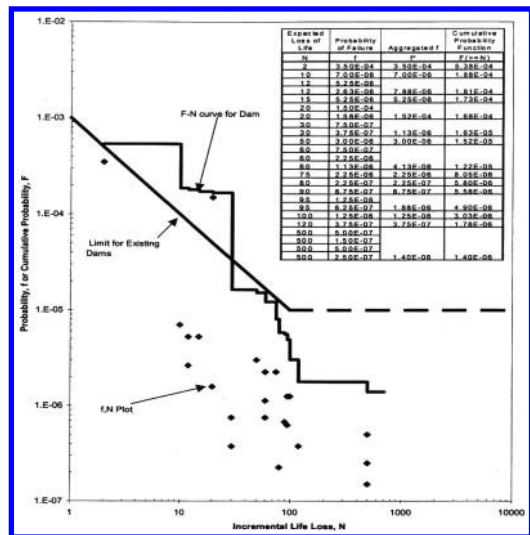
Figure 5. Example of F-N plot of societal risk. Also shown are the frequency – loss of life pans (F-N) (ANCOLD 2003).

ALARP (as Low as Reasonably Practicable) principle applies. The ALARP principle also usually applies for individual risks less than the tolerable limits.

ANCOLD (2003) give a good review of the ALARP Principle. They rely heavily on the Health and Safety Executive of the United Kingdom who state: "Risk is tolerable only if risk reduction is impracticable or if its cost is grossly disproportionate to the improvement gained (HSE 1992)" and "Residual

166

risk is tolerable only if further risk reduction is impracticable or requires action that is grossly disproportionate in time, trouble and effort to the reduction in risk achieved (HSE 1999)". Note the emphasis on disproportionality between the cost and reduction in risk gained. In the Swiss recommendations for the consideration of landslide hazards in land planning (OFAT, OFEE, OFEFP 1997), residual risks are considered as risks still subsisting after all foreseen safety measures have been carried out. They are assessed as acceptable for limited physical damage, but all technical means (eg. rescue by helicopters) must be implemented to save lives.

Determination of whether the ALARP principle has been satisfied is a matter of judgement for the owner, subject to any regulatory requirements that must be met. The cost-to-save-a-statistical-life (CSS) of potential risk reduction measures has been used as a guide or to whether ALARP has been met. As discussed in Bowles (2004) and ANCOLD (2003) there are two variants of CSSL referred to as:

– "unadjusted" CSSL(U)
– "adjusted" CSSL(A)

The "adjusted" CSSL is calculated as follows:

$$CSSL(A) = \frac{C_A - (E[R:e] - E[R:pr]) - ([O:e] - [O:pr])}{E[L:e] - E[L:pr]}$$

where CSSL(A) = adjusted cost-to-save-a-statistical-life, with the proviso that a negative value is taken as zero; C_A = annualized cost of implementing risk reduction measure, dollars per annum; E[R:e] = existing expected value of risk cost (failure probability times monetary losses to the owner) for existing slope, dollars per annum; E[R:pr] = expected value of risk cost post-risk reduction, dollars per annum; E[L:e] = expected value of life loss for existing slope, lives per annum; E[L:pr] = expected value of life loss post risk reduction, lives per annum; O:e = existing operating costs per annum; O:pr = post-risk reduction operating costs per annum.

The "unadjusted" CSSL is calculated as follows:

$$CSSL\ (U) = \frac{C_A}{E[L:e] - E[L:pr]}$$

The "adjusted" form takes account of the extent to which the cost of risk reduction measures is offset by the expected value of the reduction in monetary loss risks and any reduction in annual operating costs.

The total risk, (also called the expected value), can be calculated from:

$$\text{Total risk} = \sum_0^i f_i N_i$$

where f_i and N_i are frequency (annual probability) and number of lives lost.

These are summed over the i f_i, N_i pairs. In Table 1, the total risk is 5.7×10^{-3} lives per annum. Examples of using total risk criteria include USBR (1997) who use it to prioritise risk reduction works on their dams. It is important to report the f-N pairs as well as plotting on F-N curves, or estimating the total risk, so the decision makers are aware of what is contributing to the risk. It is a common principle to tolerate higher risks for existing structures than for new ones. This is embodied in the tolerable individual risks given in HSE (1999, 2001), ANCOLD (2003), and AGS (2000), often individual risks up to an order of magnitude higher are tolerated for existing structures.

It is also common to have higher tolerable individual risks for workers who voluntarily expose themselves to a hazard, than for members of the public upon whom the hazard is involuntarily imposed. This is for example accepted in HSE (1999, 2001), AGS (2000) and ANCOLD (2003). Again the difference is an order of magnitude.

Points (f), (g) and (h) above are more contentious. They were the considered opinion of those who attended the IUGS (1997) workshop. Some information which tends to support those views is described in Section 2.3.

Some detailed issues in assessing tolerable risks for landslides.

There are a number of issues which are particular to risk assessment for landsliding as compared to assessing risks for a single hazard eg. a dam, or a chemical plant.

(a) Summing risks for multiple hazards

When considering risk due to landsliding on a highway or railway, the way risks are summed needs to be carefully considered. Typically highways and railways have a number of types of landslide hazard, and there are usually more than one of each. For example, a highway from Town A to Town B may have:

– "n" cut slopes which are subject to rockfall
– "m" cut slopes which are subject to landsliding
– "o" slopes which are subject to natural small scale landslides which may travel onto the highway
– "p" fills which may be subject to landsliding

Persons travelling between Towns A and B are exposed to all these hazards, so the probability they will be killed is the sum of the probabilities for all the types of landslides, allowing for all the cuts, fills and natural slopes. If the person travels along the road say 100 times in a year, the annual probability of being killed is approximately 100 times that for a single journey (assuming the probability is small for a single journey). (See Section 2.4 for a discussion on how to calculate totals).

167

This is not to say that the probability of being killed for each slope should not be calculated. In most cases some slopes will be more hazardous than others, so there is merit in calculating the probabilities of persons being killed for each slope, so remedial works can be prioritized to reduce the risks most economically and quickly. If the road is owned and managed by one authority, it would seem clear that the tolerable risk criteria should be applied to the summed risks. If however the road is owned and managed by more than one authority the situation is less clear, but is likely that the risks would only be summed for the slopes owned or managed by each authority.

(b) What constitutes an "event" when considering tolerable societal risk?

In risk assessment of a dam, it is reasonably clear what an "event" is, ie. it is the uncontrolled breaching of the dam, which may be due to any one of several causes, eg. flood, earthquake, static loading (piping, slope stability). The picture is not so clear when considering landslides. There would appear to be a least two situations which need to be considered:

– an event being a single landslide. This may have different f-N conditions contributing to the F-N plot depending on the volumes of the landslides and probability of their occurrence and temporal pattern of the elements at risk
– an event being a major rainstorm (or snow melt, or earthquake) which induces a large number of landslides, which collectively result in extensive loss of life.

In both situations, society is likely to be more concerned where there are multiple deaths than a single death – the typical situation where societal risk is applicable. Case (ii) is more likely to be applicable when one authority is responsible for managing all the slopes eg. on a highway, or in a town.

(c) Societal risk may be dominated by the case of one death

When assessing tolerability of risks from landsliding, it will often by the case that the controlling criteria is the societal risk for one (or maybe 2 or 3) deaths. This is quite different to the more normal case, eg. for failure of a dam, where societal risk controls for the potential for large number of lives lost, and individual risk for single life loss.

The reason for this is that a slope may pose an annual probability of death of say 10^{-7} for any individual driving a car below the slope (a low figure, almost certainly tolerable), but if 10,000 persons drive along the road each year, each having the same annual probability of being killed the probability one person is killed will be 10^{-3}/annum – on the limit of tolerability in Figure 4. This also emphasizes how important traffic numbers are on whether risks are tolerable on roads and railways.

4.2.2 Preparation of F-N plots

Table 1 presents the data from which Figure 5 was prepared. The data is for a dam with a number of components which can fail and different consequences depending on the warning time and population at risk which in turn are dependent on seasons and time of the day. To prepare the F-N plot, the f-N pairs are re-ordered to group them into the same N values as shown in Figure 5 and the frequencies then summed for the same N values. The data is then plotted.

Whether the lines between points are drawn as shown in Figure 5 – verticals up from the larger N values, or as lines joining the data points depends on what the f–N pairs represent. If in fact N has uncertainty as is often the case, the latter approach may be reasonable. Usually, it is assumed that if any part of the plot falls above the limit line, the risks are intolerable. It should be noted that the F-N plot is dependent on the way the calculations are partitioned eg. in Table 1, if the life loss for each failure mode was considered as a distribution of possible outcomes rather than discrete values, a different plot would result.

4.2.3 Aggregating individual risk

As discussed in ANCOLD (2003) the guiding principles for aggregating individual risk components are:

(a) It is always acceptable to add results form mutually exclusive states (eg. landsliding caused by rainfall and earthquakes).
(b) For states that are not mutually exclusive, (eg. large, medium and small landslides on one slope all potentially triggered by rainfall) simple addition can give erroneous results unless the estimated conditional probability of slope failing is low (say less than 0.01). What can be calculated are the upper and lower bounds of the overall conditional probability of failure using the theory of uni-model bounds (Ang and Tang 1975), the upper bound conditional probability is

$$P_{uB} = 1 - (1-P_1) \cdot (1-P_2) \cdots\cdots\cdots (1-P_n)$$

where P_{uB} = the estimated upper bound condition probability of failure; P_1 to P_n = the estimates of the several individual mode conditional probability of failure.

The probabilities should be calculated before applying the conditional probability of the loading scenario eg. the rain event. The lower bound estimate is the maximum individual conditional probability.

168

Table 1. Data for the F-N plot in Figure 5 (Fell & Hartford 1997, after D. Bowles).

Failure Mode				Exposure					
Initiating event	Dam component	Failure mechanism	Prob (Failure mode) (A)	Season	Day/ night	Prob- ability (B)	Incremental life loss N(C)	Prob (incremental life loss) f(A × B)	(C) × (D)
Flood	Embankment	Erosion	5.00E-04	Spring	Day	0.7	2	3.50E-04	7.00E-04
				Spring	Night	0.3	20	1.50E-04	3.00E-03
	Stilling basin	Headcut	1.00E-05	Spring	Day	0.7	10	7.00E-06	7.00E-05
				Spring	Night	0.3	50	3.00E-06	1.50E-04
Seismic	Embankment	Liquefaction	1.00E-05	Summer	Day	0.075	60	7.50E-07	4.50E-05
				Summer/open	Day	0.05	500	5.00E-07	2.50E-04
				Summer	Night	0.125	100	1.25E-06	1.25E-04
				Non-summer	Day	0.525	15	5.25E-06	7.88E-05
				Non-summer	Night	0.225	75	2.25E-06	1.69E-04
	Outlet works	Rupture	3.00E-06	Summer	Day	0.075	80	2.25E-07	1.80E-05
				Summer/open	Day	0.05	500	1.50E-07	7.50E-05
				Summer	Night	0.125	120	3.75E-07	4.50E-05
				Non-summer	Day	0.525	20	1.58E-06	3.15E-05
				Non-summer	Night	0.225	90	6.75E-07	6.08E-05
Internal	Embankment	Piping	1.00E-05	Summer	Day	0.075	30	7.50E-07	2.25E-05
				Summer/open	Day	0.05	500	5.00E-07	2.50E-04
				Summer	Night	0.125	95	1.25E-06	1.19E-04
				Non-summer	Day	0.525	12	5.25E-06	6.30E-05
				Non-summer	Night	0.225	60	2.25E-06	1.35E-04
	Outlet works	Piping	5.00E-06	Summer	Day	0.075	30	3.75E-07	1.13E-05
				Summer/open	Day	0.05	500	2.50E-07	1.25E-04
				Summer	Night	0.125	95	6.25E-07	5.94E-05
				Non-summer	Day	0.525	12	2.63E-06	3.15E-05
				Non-summer	Night	0.225	60	1.13E-08	6.75E-05
		Total	5.38E-04				Total	5.38E-04	Total 5.70E-03 Risk

4.3 Review of tolerable life risk criteria

4.3.1 Tolerable life risk criteria in use for landsliding, and other engineering fields

Fell and Hartford (1997) present a review of tolerable life risk in use at that time and the results of a survey of landslide risk perception and acceptance (Finlay 1996, Finlay & Fell 1993). As there were few examples of formally adopted criteria for landslides, there was a reliance on criteria from other fields, such as those for hazardous chemical industries and dams. This is still the situation, and the following discussion considers tolerable risk criteria in these related fields, as well as criteria which have been proposed for landsliding.

(a) Individual risk: Table 2 summarises relevant published tolerable risk criteria: It can be seen that there is broad consistency in tolerable individual risks, between industries. Those few criteria specifically for landsliding are also consistent.

(b) Societal risk: There are fewer published societal risk criteria, and these use different approaches:

– *Health and Safety Executive, United Kingdom*
HSE (2001) propose for limit of tolerability for a chemical industry continuing to operate next to a housing estate (ie. existing installation), the frequency of an accident causing 50 or more deaths should be less than 2×10^{-4}/annum. They do not have specific criteria for new developments, relying on individual risk criteria. HSE (2001) relied on the examination of levels of risk around the Canvey Island industrial installations to develop this criteria. Figure 6 shows the assessed risks for Canvey (HSE 1981) on an F-N plot. The criteria above are on the "local scrutiny line".

– *Hong Kong Special Administrative Region Government*
HKSAR has published interim risk guidelines for natural slopes using F-N curves for societal risk. These are described in ERM (1998), Reeves et al. (1999) and Ho et al. (2000), and shown in Figure 7.

169

The first option involves a 3-tier system which is the conventional approach incorporating an unacceptable region, a broadly acceptable region and an ALARP region. The second option involves a 2-tier system comprising an unacceptable region and an ALARP region. It will be noted that there is a vertical boundary at 5000 lives. This implies that developments which could lead to 5000 lives lost in a single landslide will not be allowed, they will be sited elsewhere.

This vertical truncation is practicable for situations where there are options on siting developments.

– *Australian National Committee on Large Dams* ANCOLD (2003) also use F-N curves for societal risk criteria (Fig. 8a, b), which are the criteria for existing dams, and for new dams and major augmentations respectively. Risks 10 times higher are tolerated for existing dams than for new dams. ANCOLD (2003)

Table 2.   Individual life loss risk criteria.

Organization	Industry	Description	Risk/annum	Reference
Health and Safety Executive, United Kingdom	Land use planning around industries	Broadly acceptable risk. Tolerable limit	10^{-6}/annum, public and workers 10^{-4}/annum public[1] 10^{-3}/annum workers	HSE (2001)
Netherlands Ministry of Housing	Land use planning for industries	Tolerable limit[2]	10^{-5}/annum, existing installation 10^{-6}/annum, proposed installation	Netherlands Ministry of housing (1989), Ale (2001), Vrijling et al. (1998)
Department of Urban Affairs and Planning, NSW, Australia	Land use planning for hazardous industries	"acceptable" (tolerable) limits[2]	5×10^{-7}/annum hospitals, schools, childcare facilities, old age housing 10^{-6}/annum residential, hotels, motels 5×10^{-6}/annum commercial developments 10^{-5}/annum sporting complexes	
Australian National Committee on Large Dams	Dams	Tolerable limit	10^{-4}/annum existing dam, public most at risk subject to ALARP 10^{-5}/annum new dam or major augmentation, public most at risk, subject to ALARP.	ANCOLD (2003)
Australian Geomechanics Society guidelines for landslide risk management	Landslides (from engineered and natural slopes)	Suggested tolerable limit	10^{-4}/annum public most at risk, existing slope 10^{-5}/annum, public most at risk, new slope	AGS (2000)
Hong Kong Special Administrative Region Government	Landslides from natural slopes	Tolerable limit	10^{-4}/annum public most at risk, existing slope. 10^{-5}/annum public most at risk, new slope	Ho et al. (2000), ERM (1998), Reeves et al. (1999)
Iceland ministry for the environment hazard zoning	Avalanches and landslides	"acceptable" (tolerable) limit	3×10^{-5}/annum residential, schools, daycare centres, hospitals, community centres. 10^{-4}/annum commercial buildings 5×10^{-5} recreational homes[3]	Iceland Ministry for the environment (2000), Arnalds et al. (2002)
Roads and Traffic Authority, NSW Australia	Highway landslide risk	Implied tolerable risk	10^{-3}/annum[4]	Stewart et al. (2002), RTA (2001)

Notes: (1) But for new developments HSE (2004). Advises against giving planning permission where individual risks are $> 10^{-5}$/annum. (2) Based on a temporal spatial probability of 1.0. (3) Assumes temporal spatial probability of 0.75 for residential, 0.4 commercial, 0.05 recreational. (4) Best estimate of societal risk for one person killed, top risk ranking. If slope ranks in this range action is taken to reduce risks within a short period. For the second ranking, societal risk is 10^{-4}/annum, and slope is put on priority remediation list.
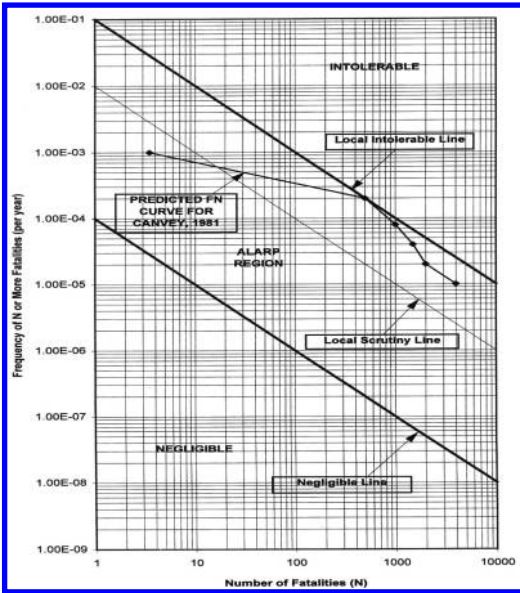
Figure 6. Societal risk F-N plot for Canvey Island with limits of tolerability (ERM 1998).

apply the ALARP principle as described above. ANCOLD (2003) reviewed practice in regards to cost-per-statistical-life saved, tentatively suggest Table 3 for guidance on ALARP justification.

The horizontal truncations in Figure 8 are without precedent, but "represent ANCOLD present judgement of the lowest risk that can be realistically assured in light of: present knowledge and dams technology; methods available to estimate risks (ANCOLD 2003). Note the ALARP principle applies below the horizontal truncation.

Table 3. Tentative guidance on ALARP justification for risks just below the limit of tolerability (ANCOLD 2003).

ALARP justification rating	Range of cost-per-statistical-life saved (A$M/life)	
	Greater than or equal to	Less than
Very strong	Zero	5
Strong	5	20
Moderate	20	100
Poor	100	

Notes :
(1) The above societal risk criteria are to be used in conjunction with a reference toe length of the natural hillside of 500 m (Reeves et al, 1999).
(2) If a development is affected by more than 500 m toe length of natural terrain, an appropriate linear scaling factor should be used to scale up the risk criteria. For example, in the case of a large development affected by natural terrain with a toe length of 5 km, then the above societal risk criteria should be increased by one order of magnitude.
(3) If the development is affected by less than 500 m toe length of natural terrain, then the same criteria as proposed above are taken to apply (i.e. the criteria will not be scaled down).
(4) The societal risk criteria are intended to aid decision-making and not intended to be mandatory.

Figure 7. Interim societal risk criteria for landslides and boulder falls from natural terrain in Hong Kong (Ho et al. 2000).

171

Figure 9. Netherlands societal risk criteria for fixed installations (ERM 1998).

Figure 8. Australian national Committee on Large Dams societal tolerable risk criteria, (a) for existing dams; (b) for new dams and major augmentations.

– *Netherlands Ministry of Housing, physical planning and environment*

ERM (1998) report from Lommers & Bottelberghs (1995) and Pikas & Seaman (1995), Figure 9, applies to existing and proposed developments. This has a gradient minus 2 which shows particularly strong aversion to high consequence events.

4.3.2 *Qualitative tolerable risk criteria*

In many risk analyses the outcome of the analysis will be qualitative. Some examples are given in Einstein

(1997), PIARC (1997), RTA (2001), Stewart et al. (2002), US Department of Transportation (1990), Bonnard et al. (2004). In practice, the tolerability of risks for land use planning is often qualitative, based on descriptive scenarios, and results in zoning where building is forbidden, permitted with some conditions imposed, or permitted without controls.

4.3.3 *Application of quantitative tolerable risk criteria*

The information provided in Section 2 is a selection of quantitative tolerable risk criteria for loss of life. There are no internationally accepted criteria for landsliding. It is necessary therefore to develop tolerable loss of life criteria for each situation, taking account of the legal framework of the country, and regulatory controls in place.

Criteria should be developed in consultation with all the affected parties, including the affective public. Those doing the risk analysis are likely to be most informed about precedents and understand the analyses and their limitations, so it is appropriate they are involved in this process.

All should understand that the criteria are an attempt to quantify societies requirements. In fact society has widely different perceptions of risk (eg. See Finlay (1996), Finlay & Fell (1996). The boundaries should

172

not be regarded as absolute. There are also significant uncertainties in the risk calculation which should be allowed for eg. see Baynes et al. (2002). For further discussion on application of criteria see ANCOLD (2003), Lee & Jones (2004), Bonnard et al. (2004), and Christian (2004). Where there is reliance on the examples in Section 2, account should be taken of the relevance of those examples, e.g. the risk for landsliding from engineering slopes comparable to criteria for (engineered) dams (possibly yes but if the slope was a natural one, possibly higher risks would be tolerated).

Risk reduction actions aim at bringing the risk below the tolerable risk threshold, and if possible below the acceptable risk threshold. The various technical options have been extensively described in international documents. They depend on the conditions of the site, and there is no need to establish a new list. The effort is on the strategies and the policies underlying these actions, on human, social and financial factors controlling them, and not on the technical aspects. The acceptable or tolerable risks thresholds, as presented in the previous paragraphs, will not be discussed either.

5 EXAMPLES OF LANDSLIDE RISK MANAGEMENT

5.1 *Definition of parameters and choice*

The selection of examples concentrates on global risk management, relevant to town and country planning problems, and not on more restrictive management where engineering plays an essential part, because there is a range of parameters that need to be taken into account (e.g. social, economic, political).

There are several reasons for this choice:

– Risk management in the framework of town and country planning includes the other types of management, even if the purpose and the participants may vary;
– It concerns a field for which prospective analysis must be led in the longer term, without, however, neglecting the short term, and with wider possibilities and choices;
– The functions and responsibilities cover both the private and the public domain as well as their interactions and conflicts, and involve a wide variety of stakeholders;
– The components to take into account are more numerous, more complex, notably components outside the landslide domain, or more generally the risk domain. Risk management related to town and country planning is the reflection of civil society in its diversity, its contradictions, its aspirations, its successes and its expectations. It is a good indicator of the public policies for the prevention, and of the investment agreed by the society.

A few examples will be used as an illustration, knowing that virtually each case is «unique» because of the differences previously mentioned. We will endeavour to demonstrate, from these examples, that risk management is not the product of a single method, even if approaches, basic ideas and transitions points can be recommended. In any case, there is no "push-button" or automated method, and the experience of all feed a process based, above all, of help to decision-making. We will also try to show the level of influence of qualitative approaches and the contributions of the quantitative approaches. Each example is organised according to the same structure. That is to say:

– National policy for landslide risk management
  • Laws
  • Responsibilities
  • Project Manager
  • Process
  • Control
– An example of landslide risk management
– Lessons learnt

5.2 *Risk prevention plans – La Désirade, France*

5.2.1 *Risk management general strategy*

RISK MANAGEMENT GENERAL STRATEGY

Prevention		Comments
Specific Regulations (including landslide)	yes	Qualitative approach No acceptable risk criteria
Responsibility	Central Government	Ministère de l'Ecologie (Ministry of Ecology)
Project Manager	State Services	Technical performance by consultants
Process	PPR (Risk Prevention Plan)	Public encumbrance attached to the planning documents

(*Continued*)

173

Prevention		*Comments*
		Prescriptions (obligations and recommendations)
		Applies to the existent
		In conformity within 5 years
		Maximum expenditure threshold for the existent (10% of the value of the properties)
Control	State Services	Rarely performed
Information		
Specific Regulations (including landslide)	yes	
Responsibility	Central Government	Ministère de l'Ecologie (Ministry of Ecology)
Project Manager	Services de l'Etat, Commune	
Process	DCS – DICRIM and information through the mayors every two years	DCS: Document Communal Synthétique (Council Synthesis document) DICRIM: Dossier d'Information communal sur les risques majeurs (Council information document on the major risks)
Control	State Services	Rarely performed
Crisis Management – Relief Organisation		
Specific Regulations (including landslide)	Yes	
Responsibility	State and Commune	Ministère de l'Intérieur (Home Office)
Project Manager	Prefect, Mayor	
Type of process	ORSEC Plan and Plan Communal de Secours (Commune Relief Plan)	
Feedback	State	
Insurance and Compensation		
Insurance specific to natural risks	Yes	
Responsibility	State	Interdepartmental and caisse centrale de reassurance (reassurance central fund)
Project Manager	Insurance	
Process	CAT-NAT: Declaration by the State of natural disaster (State)	Compulsory insurance Principle of solidarity/risk mutualisation
Relation between prevention and compensation	yes	Insurance guaranteed in fine by the Ministère du Budget (Treasury)
Control	State	

5.2.2 *The PPR: Objectives – Content – Process – Limits – Perspectives*
Objectives
The object of the PPR is to analyse the risks on a given territory, and to then infer a delimitation of the exposed areas, and to privilege the development on the risk-free areas, or introduce prescriptions regarding town planning, building and management within the risk areas.

The PPR: a competence of the State
The PPR is financed and developed by the State, at the scale of 1:10000 in urban areas and 1:25000 in rural areas. The objective is to provide the 5000 most exposed Councils with a PPR by the end of 2005 (36000 Councils in France, 21000 of them are at risk).

PPR development: a process in four stages
– prescription: the PPR is prescribed by the Prefect (it is performed under the responsibility of the services of the State)
– town council consultations and public surveys
– approval: once the PPR is approved by the Prefect, it becomes a state-approved constraint, and is appended to the zoning regulations

174

– statutory disclosure: the approval order can only be opposed at the close of the disclosure formalities (in the compendium of the administrative acts of the State in the department, in two local newspapers, display on the town hall board and documents available to the public)

PPR Content: 3 elements
Standardized prevention document, put together with pragmatism from the existing knowledge and on the basis of qualitative studies. It is composed of:

– A presentation note, presenting:
  • the PPR prescription reasons
  • the natural phenomenon known (inventory and cartography)
  • the hazards, allowing for uncertainties (models and cartography)
  • the stakes (qualitative inventory and cartography)
  • the objectives aimed at for risk prevention
  • the choice of zoning and statutory measures.
– A statutory zoning plan with two zones:
  • the red zone where building is not permitted
  • the blue zone where new activities and constructions are welcome, pending the respect of certain prevention measures
  • The rules and regulations

Rules and regulations: they are composed of:
– bans and limits on the new constructions: the basis of the project regulations within the perimeter of the PPR is to put a stop to development in the zones where the risk is highest, and thus the ban on developing or building on the land. In the areas where new constructions are allowed subject to agreement with the local planning plan (PLU), these constructions are subject to compulsory provisions. These planning, building and management regulations must be clearly stated, realistic and proportional to the stakes
– general prevention and protection measures: they include the measures to be taken by the private individuals, and the collective measures of the competence of the project manager
– Measures applicable to existing constructions: they concern the terms of planning, use or operation related to the existing buildings and to any type of planning that may have an influence on the risk. The occupiers of the areas under PPR protection must however retain the possibility to lead a normal life or perform normal activities if these are compatible with the safety objectives. The prevention and protection measures, as well as the measures applicable to the existing constructions can become compulsory within a maximum deadline of 5 years

with automatic enforcement by the State if they have not been performed in time.

Limits
The PPR is a state-approved encumbrance and is imposed to all. Attached to the Zoning Regulations, it represents a heavy constraint in terms of planning and development, notably concerning the granting of building permits. There are three types of constraints:

– Scientific: the scale of 1:25000, qualitative studies based on the existing knowledge and restricted budgets for the studies, often lead to the drawing up of zones that are too pessimistic, under the cover of the precaution principle;
– Strategic: applying to existing buildings, there are important consequences on land and assets value;
– Methodological: the stakes do not take – or insufficiently – into account the local ambitions for development, even if there is a consultation with the Council, and this can lead to important conflicts of interests between the State and the Council.

New tools
Despite the consultation stages planned in the process, the mayors often perceive the PPR as a State interference in local development, and as a constraint blocking planning and development.

The PPR proposes solutions to reduce the risk but not development prospects. This work of integration and taking into account of the risks in planning and development is a necessity. This was the desire of the ministry when implementing PPR accompanying programmes. The example performed in La Désirade shows the relevance of the dual "development and risk" approach. It resulted in mixed protection and development proposals, on the basis of an exhaustive diagnosis of the territory, of a close consultation with the local elected members and the population, of a determination to propose balanced solutions (win/win), and of a determination to offer positive prospects for the future.

5.2.3 *La Désirade: example of integrated risk management*
Context (cf. Fig. 10)
The island of La Désirade looks like a large bar of rock. It is 11 km long and 3 km wide. It forms part of the eastern end of the Guadeloupe archipelago. It is mostly crowned with a chalk plateau with a 200 m overhang over the coast. La Désirade is located on the path of the cyclones and on the zone of confrontation of the Caribbean and Atlantic tectonic plates and has

175
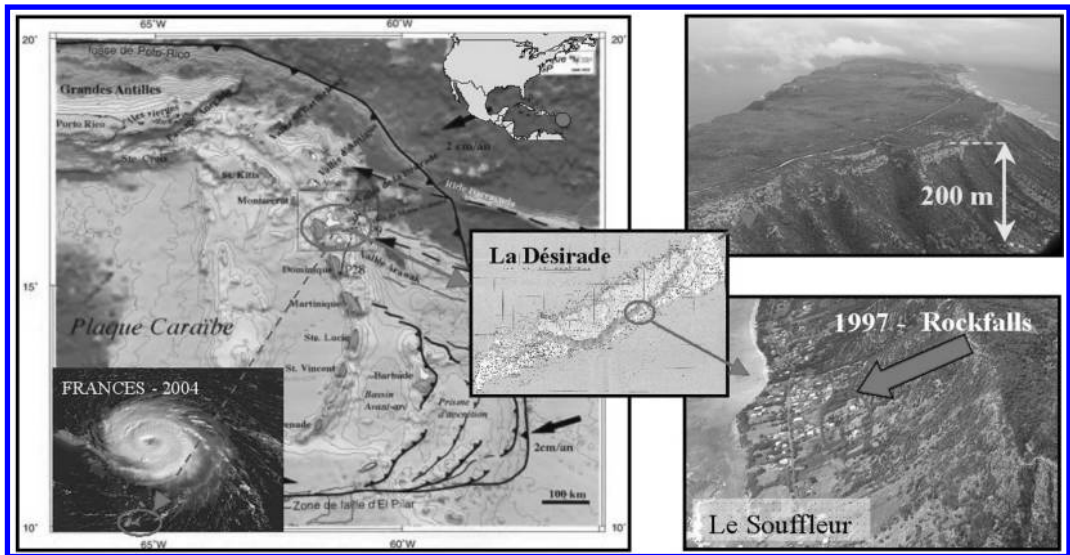
Figure 10. General context of La Désirade island [see Colour Plate III].

therefore a high natural risk exposure (landslides, earthquakes, cyclones).

In 1997, a house was badly damaged by a rock fall (le Souffleur area), two people are slightly injured. Temporary protection nets were fitted and the State appointed a consultant to propose sustainable solutions to secure the site. The State also contemplated to relocate some dwellings if the protection solutions were too costly.

Initial solutions proposed: unbalanced and not accepted
At the end of the first phase, the following points were observed:

– the protection nets recommended (ASM nets) were too costly (FF. 14M) compared to the number of houses protected (2).
– the residents were strongly opposed to the relocation solutions.
– the configuration of the chalk cliff where the damaged houses were located was far from being uncommon.

Approach undertaken: a 4 point study (cf. Fig. 11)
The State then decided to undertake the simultaneous performance of the risk prevention plan for La Désirade, and a planning and development study of the Souffleur area, in order to analyse the land available to accommodate the potentially

highly exposed families. The methodology proposed rested on:

– An exhaustive territorial diagnosis of the island

  • Diagnosis of the natural, human and constructed environments, analysis of the island history and the culture of the population,
  • An inventory of the natural phenomenon, models and cartography of the hazards, on the basis of a three-dimensional trajectory determination of the rock fall on the stake areas, and of a qualitative and naturalistic analysis on the other areas for the other phenomenon,
  • An inventory and an analysis of the development ambitions for la Désirade, as well as the protection constraints, notably the constraints imposed by the State.
– The proposal for a risk reduction solution and a planning and development project based on:
  • An integrated approach of the solutions (protection and environment)
  • A multi-scale approach (local analysis and global analysis)
– The ability to listen, communicate and educate (survey of the population to understand its perception of the risks and identify its aspirations, public meetings to explain the approach and the actions)
– The proposal of a regulatory risk zoning and associated regulations

176
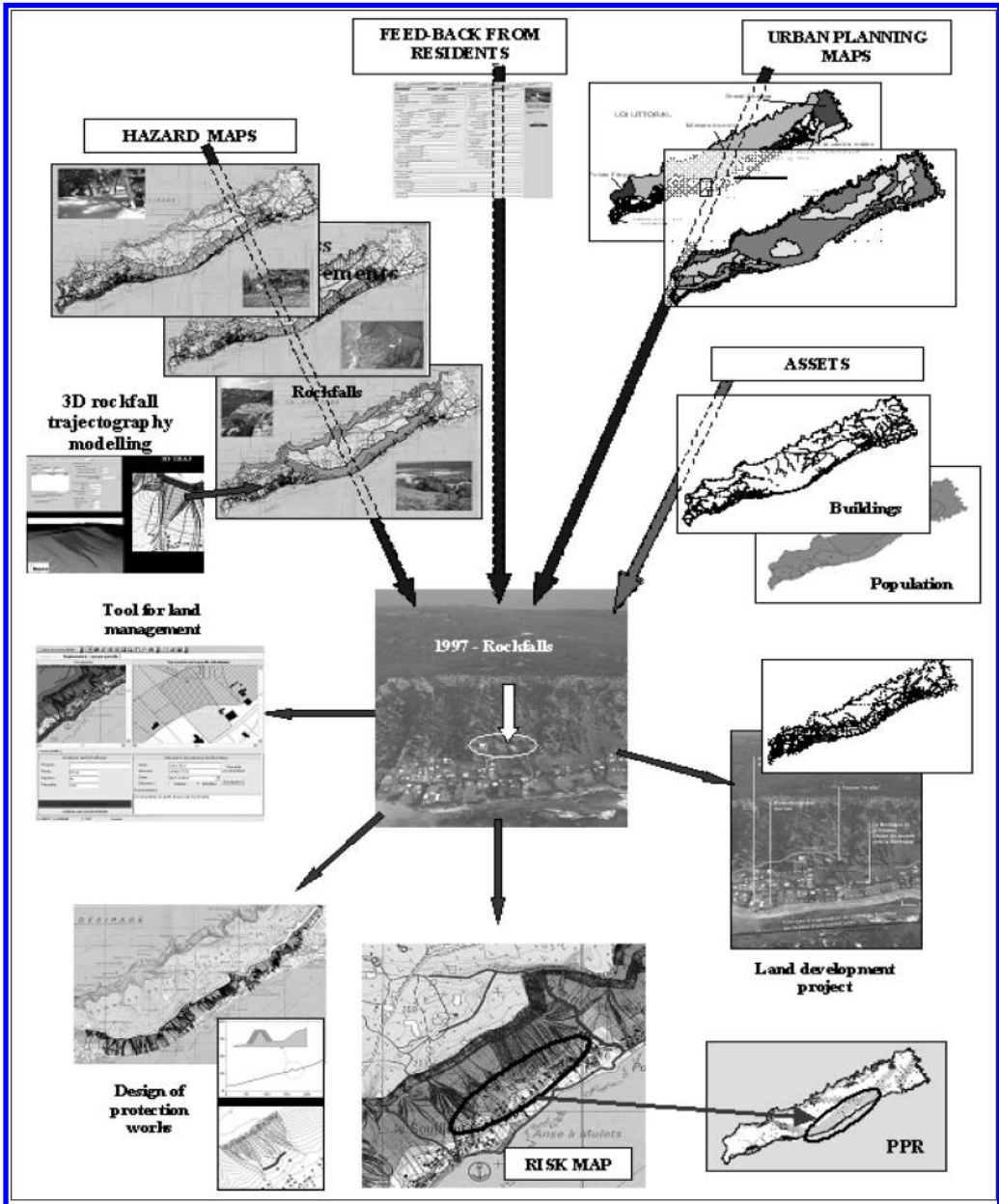
Figure 11. General framework of works carried-out to manage landslides risks in La Désirade island after 1997 rockfall event [see Colour Plate IV].

Results and lessons learnt from the approach proposed for la Désirade:
Following the 1997 events, risk management of rock fall consisted in the performance of a Risk Prevention Plan, the proposal and pre-proportioning of protection structures, the proposal of a planning and

development project, the information of the population and the development of a tool to visualise, analyse and manage the area.

The proposed protection structures (walls) were financially acceptable considering the dwellings proposed (€ 2M for 50 houses protected); they answered

177

the development ambitions of the island (eco-tourism), and could perform the water control and management functions (reduction of the mudslides and gullying, resource available to the population – crop, washing…).

The population has now accepted the zoning and constraints imposed by the PPR. The proposal to transform the intermediate hazard area in an area where building is not permitted resulted from the global analysis of the development potentials of the island, of the land availability on the other areas, and the development ambitions carried by the Council.

Such solution of "freezing" of the intermediate hazard area has also been possible because it has been counterbalanced by an opening and a "re-negotiation" of the other protection constraints imposed by the State (win/win solution), and because of the important communication and education effort made by the risk and planning and development technicians towards the population.

Risk management, performed on the basis of a global, integrated, multi-risk and multi-scale approach has enabled the proposal of a balanced solution, accepted by all the stakeholders (State, Mayor, population), in conformity with the responsibility of each, and financially acceptable.

5.2.4 Synthesis of French risk management strategy

Even if some actions are financed by the European Community (research, development of eurocodes, some attempts to share civil safety actions limited to the management of a crisis), natural risk management remains at the State level, in the name of subsidiarity.

In France, natural risk management is divided into three major poles:

– A risk prevention pole, under the responsibility of the Ministère de l'Ecologie et du Développement Durable (Ministry of Ecology and Sustainable Development), which has the interdepartmental responsibilities in the matter;
– A civil safety pole (intervention in case of a crisis and preparation of the corresponding planning), under the responsibility of the Ministère de L'intérieur, de la Sécurité Intérieure et des Libertés Locales (Home Office);
– A compensation pole which is only truly tackled through the compensation scheme for the properties insured, and the assistance granted in case of a major disaster, for which the Minsitère de l'Economie, des Finances et de l'Industrie (Treasury and the Department of Trade and Industry) play a major role.

The French particularity has enabled to highlight prevention device with a strong Jacobinic approach (centralised). Compensation is slightly managed.

The Risk Prevention Plan (PPR) is a major element of natural risk management in France, it combines land occupancy, information of the population and compensation in the event of a disaster. The aim is to ensure, through its intermediary, the protection of people against exceptional phenomenon (the frequency of appearance of the phenomenon by elementary administrative unit is inferior to 1% per year).

The acceptable risk criterion are not described in term of loss probability, but considering the probability of occurrence of an abnormal phenomenon. This means that for any phenomenon with a probability superior and/or inferior magnitude, the tolerance level will be zero, and the protection will have to be full. This is what is perceived by the population.

The PPR remains essentially based on a technical approach of natural risk prevention, insufficiently integrating the local development ambitions carried by the elected members. The accompanying tools implemented by the Ministère de l'Ecologie et du Développement Durable (Ministry of Ecology and Sustainable Development), and the implementation of a "planning, development and risks" integrated approach, bring more balanced solutions. These solutions are also better accepted by the population and the local elected members.

The study of La Désirade has been performed in this perspective. The aim was not only to protect the residents, but also to propose sustainable local development prospects. The global approach undertaken on the island, at the risk level but also at the planning and development level, enabled the proposal of a solution accepted by all (State, local elected members and the population). The initial scientific approach, solely based on the analysis and the reduction of the risk showed its restrictions and its shortcomings.

Above all, landslide risk management must be integrated in a territorial approach, and this, whatever the scale of the natural phenomenon taken into account. It must rely on the population and propose win/win solutions, whatever the coercive power of the risk manager (i.e. the State); it is the best way to design sustainable, efficient and accepted solutions.

5.3 Landslide hazard maps and risk management processes in Switzerland

5.3.1 Introduction: the Swiss political framework
Switzerland, which is a country exposed to several types of hazard, given that its major part extends in mountainous areas (e.g. more than 6% of the territory is prone to landslides – Noverraz & Bonnard, 1990 –; the location of the main landslides is shown in Fig. 12), is a federal state grouping 26 sovereign cantons. These cantons are responsible for many domains of activity and in particular for elaborating their master plan, whereas the communes or municipal entities are

178

Figure 12. Location of main landslides in Switzerland (according to Swiss Federal Office of Water and Geology). The dark stars correspond to very large slides.

entitled to proceed to local planning. As far as risk management is concerned, especially for special events related to natural hazards, the first responsibility lies in the hands of the communes (except for earthquakes), but the higher cantonal or federal authorities establish legal frameworks and recommendations for prevention actions. This procedure ensures an homogeneity in the consideration of hazards that is required, as the federal authorities take a subsidiary responsibility and also contribute to the cantonal prevention and protection actions through financial subsidies.

This is the reason why it is not really possible to determine a single management policy in Switzerland for landslide hazards, but the federal legal bases and recommendations can be presented as a guideline for the development of risk management processes.

5.3.2 *Legal bases for the landslide risk management at the federal level*

The first law establishing the framework for the consideration of natural hazards in land planning is the federal law for land-use planning, dated 1989 (LAT). In particular this law requires that the cantons designate the areas significantly affected by natural hazards or harmful effects in their master plan.

Two subsequent federal laws on forest (LFo) and water course management (LACE), issued in 1991, stipulate in their objectives that the cantons must ensure a protection of man and properties of a significant value against natural hazards (e.g. snow avalanches, erosion, landslides) in the areas in which it is required; moreover a priority is given to maintenance and planning measures, as regards water courses, with respect to engineered protection works, in order to prevent the development of landslides. To accomplish such objectives, the Federal State provides subsidies for the documentation of past events and for the preparation of hazard maps.

The application ordinances of these two laws, enacted in 1992 and 1994, specify that the federal offices responsible for the management of forests and water courses will set prescriptions concerning the production of hazard maps. The cantonal authorities will have to establish such maps and take them into account in the master plans and the local management plans. They will also update them periodically and register the natural events of a certain magnitude.

5.3.3 *Recommendations for the consideration of landslide hazards in land planning*

An interdisciplinary task force was set up to prepare a document of recommendations, aiming at specifying the process of preparation of landslide hazard maps, fixing criteria for the limit values of the different levels of hazard for each type of landslide (slide, fall and mudflows) and defining the planning measures applicable to each level of hazard. Two similar documents were published in 1997, one concerning landslides and the other concerning floods (OFAT, OFEE, OFEFP 1997). A similarity was maintained in the probability classes with what had been established for snow avalanches in 1984 (30, 100 and 300 year return period, as reference values).

The main intention of this document is to avoid the step of a detailed risk analysis. After the determination of a hazard level ("high", "medium", "low", as well as "very low" for events with a return period exceeding 300 years – see Fig. 13), corresponding planning measures are specified and must apply in the local management plans. In principle, for the high hazard zones (red zones in the map), no building or technical plant housing men and/or animals is allowed and can be enlarged. The destroyed buildings (for any reason) cannot be rebuilt. This zone is thus a prohibition zone for building, mainly justified by the fact that life is in danger event inside the buildings.

For the medium hazard zones (blue zones in the map), buildings are allowed under specific regulations, depending on the types of hazard. Sometimes detailed building prescriptions can be imposed, like the prohibition of a door on the side of the house directly exposed to the landslide hazard. No sensitive buildings, like a hospital for instance, may be located in such a zone. This zone is thus a regulation zone for building, as it is considered that life is not threatened inside the buildings, provided the building criteria are safe enough.

For the low hazard zone (yellow zone in the map), buildings are allowed without restrictions by the authorities, but the owners must be informed of the existing hazards and of the possible protection measures that can be taken. Sensitive objects require special protection measures to ensure that a low residual hazard is tolerable. This is thus a public awareness zone for buildings requiring an open information.

179
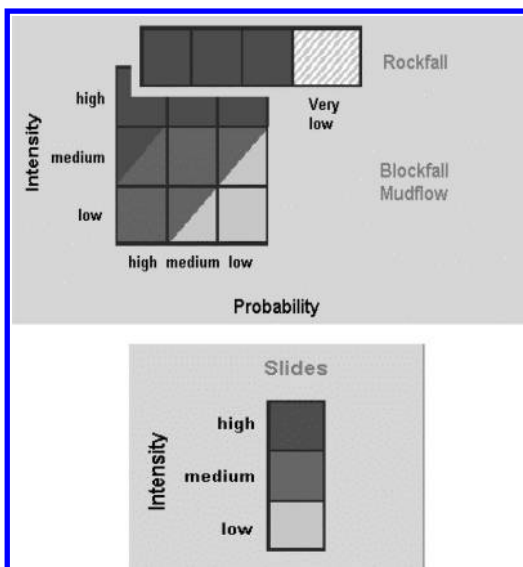
Figure 13. Matrix for the determination of hazard levels, first for occasional events (e.g. rockfall), taking their probability of occurrence into account, then for permanent processes like existing slides with possible important reactivation phases.

These three zones are complemented by a "residual risk" zone (yellow and white stripes in the map) used either in the case of very rare hazards (e.g. rockfall from an intrinsically stable high rock cliff) or to express that a certain risk may be present after the eventual failure of protection works. In this zone the plants that imply a high damage potential must be avoided (e.g. chemical plants).

5.3.4 *Proposed approaches for risk assessment*

In order to assess the importance of the potential impact of a hazard on the different types of exposed objects, all buildings, infrastructure and exploited land can be classified into different categories that deserve a level of protection varying from a weak or negligible value to a high value. In the case of the Canton of Vaud, for instance, Figure 14 specifies 7 categories ranging from A to G related to areal objects (e.g. vineyards, dwelling zones), linear objects (e.g. secondary roads, main electric lines) and pinpoint objects (specific plants require a particular risk analysis, like major town gas tanks in a town). In the first three categories A to C, the expected losses imply nearly only material goods, whereas in the higher categories D to G, potential life losses may also be expected in conjunction with medium to high material losses (EPFL/CADANAV Project 2002).

On the basis of such categorization, the political authorities can elaborate a strategy determining the protection objectives for all types of hazards. For any considered hazardous event with a determined return period (1 to 30 years, 30 to 100 years, 100 to 300 years, or a continuous process), the authorities fix the maximum accepted intensity of a potential danger, with a scale varying from 0 (no damage is accepted) to 3 (a high damage is accepted) (see Fig. 13). Such a matrix for all categories of objects is used in a GIS, in conjunction with the map of deficits of protection, i.e. derived from the presence of objects in hazardous zones. It will then be possible to determine if a specific protection scheme is needed locally and should be designed for a given return period, or if a future building zone must be declassified into an agricultural zone, for example, if the required protection works would be too costly.

Another specific methodology for risk assessment concerning natural hazards has been developed in Switzerland (BUWAL 1999). It proposes a method with three steps, according to the required level of precision. At level 1, the hazard map is simply superimposed on the land-use map to determine the protection deficit zones that are qualified by a specific scale. At level 2, the risk is quantified for exposed areas and linear objects determined at level 1. This implies a global approach based on average statistical values of the exposed objects. Finally, at level 3, a detailed risk analysis of a determined object is carried out, considering its vulnerability, its rate of occupation (e.g. traffic density), its production value and the potential costs required for dismantling it after a disaster. However this last level is only recommended for specific objects of high importance for which the necessary information exists. This very detailed methodology does point out the necessity of having complete data concerning the natural phenomena, their development and their consequences, that often are not available, which justifies a more qualitative approach.

5.3.5 *Responsibilities in the process of working out landslide hazard documents*

Despite the legal federal requirement to produce hazard maps according to the 1997 recommendations, several cantons have not produced such documents yet, or have only carried out the mapping of landslide phenomena, but without incorporating the factors related to their hazard level.

In this respect the canton of Freiburg has been one of the pioneers in this field. After establishing a map of landslide phenomena for the whole canton (i.e. $1600 \, km^2$) between 1993 and 1999, including a specification of the probable rate of movement, it has established a joint methodology for assessing flood, snow avalanche and landslide hazards, respecting the federal recommendations, but including some specificities like the consideration of the depth of a slide as a factor influencing the hazard level. This methodology

180

Rotated left margin: 181

Categories	Areal objects						Linear objects			Pinpoint objects	Potential damage			Protection objectives*			
	"Natural" areas			Built areas or planned for buildings						Specific isolated buildings or plants	Human lives	Material damage	Secondary effects**	Return period (years)			Continuous
	Agriculture (in general)	Forests	Green spaces	Dwelling zones	Socio-economic zones	Industrial zones	Roads	Railways	Electric lines					1 to 30	30 to 100	100 to 300	
A	Pastures	Forests	Natural land								WEAK	WEAK	WEAK	3	3	3	3
B	Agricultural zones		Parks (without cultural objects)								WEAK	MEDIUM	WEAK	2	3	3	2
C	Vineyards						2nd class secondary cantonal roads				WEAK	MEDIUM	MEDIUM	2	2	3	2
D					Public utility, leisure and sport zones (except campgrounds)	Quarries, gravel pits	1st class secondary cantonal roads and main cantonal roads				MEDIUM	MEDIUM	MEDIUM	1	1	2	1
E				Spread dwelling zones			National roads, motorways	Railway lines	High voltage lines		MEDIUM to HIGH	MEDIUM to HIGH	MEDIUM to HIGH	0	1	2	0
F				Urban centers, built-up dwelling zones	Commercial zones (offices, shopping centers), camp grounds	Industrial zones					HIGH	HIGH	HIGH	0	0	1	0
G					Hospitals, hotels, cultural buildings					Specially protected objects ***	Needs a specific analysis			Needs a specific analysis			

Notes :

* For the considered hazardous event, the accepted maximum danger intensity is : nil (0), weak (1), medium (2) or high (3)

** The secondary effects imply the development of hazards of another kind caused by a landslide (e.g. failure of a landslide dam)

*** These objects that imply a certain risk need a specific risk assessment that is not published

Figure 14. Proposed matrix of object categories, potential damage and protection objectives in the Canton of Vaud (EPFL/CADANAV Project, 2002).

has been tested in a small region where all sorts of natural phenomena abound.

After prequalifying a series of consulting engineers and geologists for the production of hazard maps and favouring the constitution of consortia, the elaboration of comprehensive hazard maps has been contracted to several consortia between 2000 and 2004, each one dealing with a limited area varying between 50 an 100 km^2 (6 areas have been established).

The hazard maps require a simplified process in that zones where no exposed objects exist and a detailed approach including field checks in the planned and existing building areas. The existing maps of landslide phenomena have to be considered as an approved basis, which facilitates the process. The works of all the implied specialists of the consortia is controlled by a committee of officers of the different concerned administration offices so as to ensure a high quality in the various contracts.

Finally the cantonal hazard maps are submitted to the Federal Office in charge of water and geology that provides subsidies for their development. This allows a high degree of homogeneity between the cantons and the possibility of requiring improvements if the documents do not comply with the preset rules.

5.3.6 *Implementation of landslide hazard maps in local management plans*

All the communes in Switzerland have established local management plans some 10 to 20 years ago, some of which already take specific natural hazards into account, in general either related to floods or to snow avalanches. The consideration of recently achieved hazard maps concerning landslides for instance is then carried out through the ten yearly revision process of the local management plan that is compulsory. Different actions can be foreseen:

– Inclusion of hazard zones in the plan that will affect these different uses of the land (e.g. prohibition to build in a sector of an existing building zone or declassification of a former building zone, by a reduction of the density of construction).
– Introduction of specific rules in the standard building regulation document, that may either require additional studies to obtain a building permit, like a geotechnical study of the stability of the building, or oblige the owner to adopt special protection measures or for example to limit the weight of fills around the house that might trigger shallow slides.

All the modifications to a local management plan proposed by the authorities are voted in the communal council, so that they receive a popular approval. The revised local management plans are also submitted for approval to the cantonal authorities, which ensures a control of the new restrictions and a homogeneous treatment of the landslide hazards in the whole concerned canton.

In specific cases in which a clear protection deficit is evidenced and cannot be solved by a change in land use, the commune may decide to build protection works whenever possible.

5.3.7 *An example of communal risk management by fostering information*

The small Commune of Belmont near Lausanne that is highly praised for its view on the lake of Geneva is affected by landslides over nearly half of its territory. In 1990, an important accident occurred there, following the widening of a secondary road, and caused the destruction of three houses (Fig. 15), due to a shallow slide (Noverraz et al. 1991).

The Communal Council decided then to proceed to a comprehensive detailed landslide map at a scale 1:2000, as well as a map of unstable zones at a scale 1:1000 on the cadastral map (for the potentially unstable zones) and finally to the preparation of a specific text for each of the approximately 600 affected plots on the communal territory, explaining the phenomenon and the possible protection measures.

Therefore, any person wishing to build a house in the commune is informed of the existence of hazardous zones and is required to produce a geological and geotechnical expert advice with the building permit request form. At the beginning of the works, an official meeting is held on site to check that the necessary precautions are taken to ensure the stability of the

Figure 15. Three houses were destroyed in 1990 in the upper part of the Commune of Belmont s/Lausanne, which induced the local authorities to proceed to a complete inventory of landslides.

excavations that are the cause of most of the recorded incidents. The situation of instability of the plot of land is officially notified to the cantonal insurance company, so that the necessary restrictions of liability are included in the insurance contract. But unfortunately it is not always foreseen that it is necessary to control the efficiency of the temporary or permanent protection works (Noverraz 2002).

This exceptional effort of information to manage the landslide problems properly was initially regarded as a potential cause of loss of value of the plots of land, but the present situation on the market does not seem to show such a trend.

5.3.8 *Lessons learned: the revision of the federal recommendations*

After applying the federal recommendations quoted above during 7 years (OFAT, OFEE, OFEFP 1997), it appears that some prescriptions must be detailed in order to yield a homogenous treatment of specific situations. For instance, the zones in the vicinity of main or secondary scarps require a more severe hazard level, as the differential horizontal or vertical movements observed in theses zones are often the cause of damage. The zones in which a possible severe reactivation may occur must also be affected by a higher hazard level. On the contrary, the very deep slides (i.e. more than 30 to 50 m deep – the final figure is not yet established) deserve a less severe hazard level, especially in the case of large translational slides.

On the other hand, the requirements referring to the necessary investigation methods according to the type of document to be produced (indicative map, hazard map, expert advice) will also be included. The experience gained will finally allow the preparation of guidelines that will have a more compulsory character than the recommendations.

However it is important to encourage all the cantonal authorities which deal with very different situations and economic contexts to collect and process their experiences with respect to the management of landslide zones, so that a better knowledge regarding the risk evaluation and management of landslide-prone areas is gained.

5.4 *Instability management from policy to practice: Isle of Wight, UK*

The Isle of Wight is located off the central south coast of England and is separated from the mainland county of Hampshire by the Solent, a stretch of water ranging from 5–7 km in width. The Isle of Wight is lozenge shaped and is 35 km from east to west and 23 km from north to south.

The south coast of the Isle of Wight comprises an ancient landslide complex known as 'The Undercliff', which is 12 km in length and between 500–1,000 m in width; it forms the largest urban landslide complex in north-western Europe (Fig. 16). The landslide complex developed in Lower and Upper Cretaceous rocks during two main phases of landsliding which took place after the last Ice Age around 8,000–4,500 years ago and 2,500–1,800 years ago. These phases of landslide activity followed significant changes in climate and sea level rise and the resulting impacts of coastal erosion along the Isle of Wight's southern coastline. The Undercliff has been studied in detail by a number of eminent researchers (Hutchinson and Bromhead, 2002) and is of great interest for field visits and instability policy and management practice.

The geology of the area comprises approximately 40 m of Gault Clay (locally known as "Blue Slipper"), which is underlain by sandstones of the Lower Greensand and overlain by the massive Cherty

Figure 16. View of the town of Ventnor form the sea.
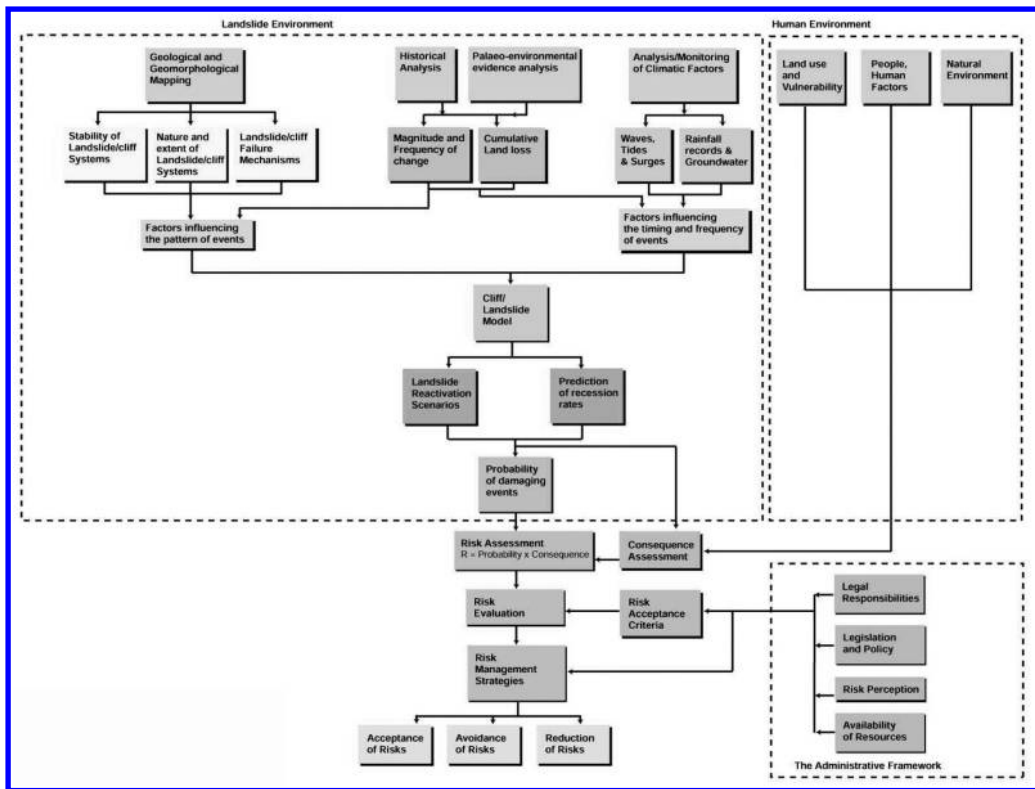
Figure 17.   The risk framework approach adopted on the Isle of Wight (after Lee 2000).

sandstones of the Upper Greensand and the Chalk. A particularly significant feature is the thin clay layers within the Sandrock of the Lower Greensand, which, together with the Gault Clay, have a particular influence on ground stability within the Undercliff.

5.4.1 *Legal and administrative framework for landslide management in the UK (cf Fig. 17)*

Introduction
A basic and longstanding principle of British law is that individuals have the right to protect their own property, under common law (Lee et al. 2000). Hence, the primary responsibility rests with the landowner, not within the State. However, common law rights have been altered and reduced over time by statute law to allow State intervention in the interests of the common good. Individuals do not have to exercise their rights, although case law has indicated that landowners or occupiers have a general duty to their neighbours to take reasonable steps to remove or reduce hazards if they know of the hazard and of the consequences of not reducing or removing it.

In the past, individuals or private businesses have either avoided high risk areas, accepted the losses as the price to pay for living and working in such

areas, or have sought to improve the conditions through engineering works. Maintenance, repair and clean-up are often a central element of most strategies for dealing with natural hazards (Lee et al. 2000). Insurance has become available for mitigating the losses associated with landslip (but excluding landslide losses caused by marine or river erosion).

National government level
Over the last few centuries, the State has gradually acquired a key role in addressing a number of specific problems associated with coastal instability (Lee et al. 2000). These include:

– controlling development in areas at risk and minimising the impact of new development on risks experienced elsewhere, through the land use planning system.
– the provision of publicly funded coast protection works to prevent erosion or encroachment by the sea;
– funding and coordinating the response to major events;

There are, however, no provisions for compensating property owners if protection works are considered too expensive, or not in the national interest.

184

There is also a need to balance the pressures for reducing the risks faced by communities and obligations to take into account the interests of other groups such as conservation bodies. The evolution of Statute law has, therefore, introduced (Lee 2000):

– consenting arrangements which ensure that management measures do not affect other interests or increase the level of risk elsewhere;
– provisions to ensure the conservation and enhancement of landscape and nature conservation features, involving the protection of designated sites and areas of national and international importance;
– consultation arrangements between key interest groups whose interests may be affected by risk management measures.

Regional and local government
Policies concerning instability, coast protection and land use planning developed at a national strategic level in Great Britain are principally implemented at the level of local government. Regional coastal engineering groups also play an important role in reducing the impacts of instability and coastal protection works on adjacent areas of coastline. Implementation of the instability management framework is described below.

Avoidance of natural hazards – the control of development in unstable areas
The Town and Country Planning system is designed to regulate the development and use of land in the public interest. The system is intended to provide:

– guidance – which will assist in planning the use of land in a sensible way and enabling planning authorities to interpret the public interest wisely and consistently.
– an incentive with local authorities stimulating development by the allocation of land in Statutory Plans.
– development control to ensure that development does not take place against the public interest and to allow people affected by development to have their views considered.

The primary legislation which forms the basis of the planning system is supported by statutory Regulations and by non-statutory Circulars, Planning Policy Guidance and Advice issued in various forms by the government.

An example of central government guidance is: PPG14 – Development on Unstable Land: (together with Annex 1: Landslides and Planning; DoE 1996), which states "*It is important that the stability of the ground is considered at all stages of the planning process. It therefore needs to be given due consideration in development plans as well as in decisions on individual planning applications.*" (DoE 1991). PPG14 confirms that the ultimate responsibility for the safe development and secure occupancy of individual sites rests, not with the local planning authorities, but with landowners and developers. By extension, this responsibility might also extend to technical advisors appointed by landowners or developers and applies equally to any other form of hazard such as flooding or erosion.

5.4.2 *Background to the landslide management strategy*

Until about 1991 ground movement events within the Isle of Wight Undercliff tended to be viewed as 'Acts of God', in other words unpredictable, entirely natural events that could at best only be resolved by avoidance or large scale engineering works (Doornkamp et al. 1991). A fundamental change took place following completion of a study commissioned by the former Department of the Environment (DOE, 1991) which wished to use the coastal town of Ventnor within the Undercliff as a case study for developing national planning policy guidance for development on unstable land.

As part of the DOE study four suites of maps were prepared for the Undercliff comprising land-use, geomorphology, ground behaviour and planning guidance; all of these were prepared on a 1: 2,500 scale. Following completion of the study the local authority, South Wight Borough Council, carried out additional investigations extending the study area westwards along the Undercliff and on local government reorganisation in 1995 the Isle of Wight Council completed the study comprising a total length of approximately 12 km from Luccombe in the east to Blackgang in the west, including the main centre of population, the town of Ventnor (population 7,000).

Ventnor and the nearby villages of Bonchurch, St Lawrence, Niton and Blackgang were developed on the landslide complex, particularly during the reign of Queen Victoria in the 19th Century when the popularity of sea bathing and the beneficial climate of the south coast of the Isle of Wight for health were being promoted. Fortunately the geological setting and the style of landsliding is such that significant movements are often concentrated in a few locations and most of the intervening areas show relatively slight or negligible movement (Lee & Moore 1991, Moore et al. 1995). Of the areas affected by more serious ground movements a number of sites have been acquired by the local authority and transformed into public open space thereby assisting with implementing a policy of 'avoidance'; this approach forms part of a Landslide Management Strategy that has been in place since 1993.

The Undercliff Landslide Management Strategy (Fig. 18) aims to reduce the likelihood of future ground movement by seeking to control the factors that cause ground movement and by limiting the impact of future movement through the adoption of appropriate planning and building controls (Lee et al. 1991). Ground

185

ISLE OF WIGHT COASTAL LANDSLIDE MANAGEMENT STRATEGY

Landslide Management Technical Committee

| PLANNING CONTROLS | BUILDING CONTROL | CIVIL ENGINEERING MEASURES | GROUND MOVEMENT & RAINFALL MONITORING |

Planning Guidance Map

Codes of Practice

Coastal Protection

Landslide Forecasting

Drainage Measures

Early Warning Systems

MITIGATION OF LOSSES

Adapted from High-Point Rendel

Contributions to landslide management

Local Government
- tighter planning controls
- improved building standards
- coast protection
- early warning systems
- monitoring and landslide forecasting
- control of construction activity including walls
- groundwater lowering
- research and investigations

Service Industries
- water supply and drainage issues
- appropriate trench excavations and backfill

Developers, Architects and Builders
- adequate site investigation
- improved design of buildings and structures
- adequate slope treatment measures

Property owners
- repairs and precautionary measures
- maintenance

Estate Agents, Solicitors and Insurers
- awareness of variable ground movement problems
- adaption of a flexible approach

Figure 18.   Isle of Wight Coast Landslide Management Strategy.

instability in the Undercliff has in fact been addressed in a number of ways but the key tasks have been:

– preventing unsuitable development through sound planning controls and building control measures;
– monitoring ground movements and weather conditions using a range of automatic and manual recording instruments and stations;

– seeking to improve ground conditions through a range of measures aimed at controlling water in the ground as well as coast protection schemes which reduce marine erosion at the toe of the landslide;
– a major awareness-raising programme for the benefit of both professionals and the general public living and working in the area.

186

5.4.3 *Implementing landslide management*

To implement the Landslide Management Strategy a Landslide Management Committee comprising key professionals including representatives from the local authority (coastal management, highways, planning and building control), the water authority and other service industries, surveyors, estate agents and insurers meet twice a year to discuss progress on implementation of the Strategy and to hear about new initiatives being led by the local authority, the Isle of Wight Council.

A key element of the Strategy is to try and ensure that future development is compatible with ground conditions and to try and prevent development where the likelihood of ground movement is high. Clearly, the range of maps that are available, now incorporated on a Geographical Information System, form a key resource in this respect. New property located within the Undercliff must be sustainable and be capable of withstanding slight movements, and importantly any new development should not lead to a worsening of ground conditions on the site or affect adjacent properties situated on the steep slopes that exist within many of the developed areas of the Undercliff. These measures are regulated by the Isle of Wight Council through its planning and building control offices but with support from the Isle of Wight Centre for the Coastal Environment, which is based in Ventnor and which provides a coastal management and geotechnical service for the Isle of Wight Council.

5.4.4 *Consultation and information exchange with Undercliff residents*

There has been a long history of discussion and consultations over ground conditions within the under-cliff and, therefore, many residents are aware of the geological situation. The town is extremely attractively located with development on the various landslide benches offering panoramic sea views over the Victorian town, the adjacent spectacular coastline and the English Channel and the property market is healthy.

On completion of the DOE study in 1991 the first of a range of publications were produced to disseminate the findings of the study. In addition, a shop was opened in the town centre where the Council's geotechnical consultants were able to deal with questions from interested or concerned residents and businesses on a one to one basis.

As well as the technical report produced by the DOE and the various maps (described above), a summary non-technical report was published which was aimed particularly at non-specialist professionals including such groupings as local authority staff, politicians, insurance companies, designers and the 'educated layman' (McInnes et al. 2000). A series of presentations were made following the launch of the DOE report, first to the Association of British Insurers'

and then to a range of interest groups in order to try and spread the landslide management message as widely as possible. After two and a half months the geological information centre in the town closed but shortly afterwards the Isle of Wight Centre for the Coastal Environment transferred its staff to Ventnor and opened a coastal interpretive centre and offices in the town, providing a permanent display on ground instability issues, a comprehensive technical library and contact point for local residents.

Political support for improving knowledge and understanding of ground conditions in the under-cliff has been particularly strong. The Centre for the Coastal Environment has aided the process by commissioning or producing a series of information leaflets that have been distributed to every homeowner in the area together with more comprehensive reports which provide a wealth of information on the range of landslide management measures that have been promoted by the Council.

Over the last ten years four different information leaflets have been circulated to all 2,600 property owners (e.g. Fig. 19) and a range of reports and technical information have been provided with financial support from the Council as well as from the European Union through programs such as LIFE Environment (L'Instrument Financier de L' Environnement – European Commission 1997 and 2001).

In particular a study led by the Centre entitled "Coastal change, climate and instability" (1997–2000) allowed the development of the landslide management work on the Isle of Wight Undercliff to be taken forward; the methodology was transferred elsewhere, for example to certain locations in Italy, France and elsewhere.

As part of the Landslide Management Strategy the feedback from local residents is regarded as very important. During the course of the LIFE project a survey was conducted which showed that a high percentage of residents (over 60%) had lived in the Undercliff over ten years and the majority were aware of ground instability issues at the time of moving into the area (82%). It is interesting to note that approximately 50% of those who intended to move to the Undercliff had obtained some kind of professional advice on ground instability and the majority of these had obtained information from surveyors, consulting engineers or estate agents.

The Isle of Wight Council was encouraged to note that of those who sought its advice on ground instability, some 90% found the advice very helpful or helpful and 66% of those who responded to the Council survey had read the key report on ground movement in the Undercliff. It was very pleasing to note that all those who responded had found this report to be either very informative (55%) or informative (45%). It should be noted, however, that over
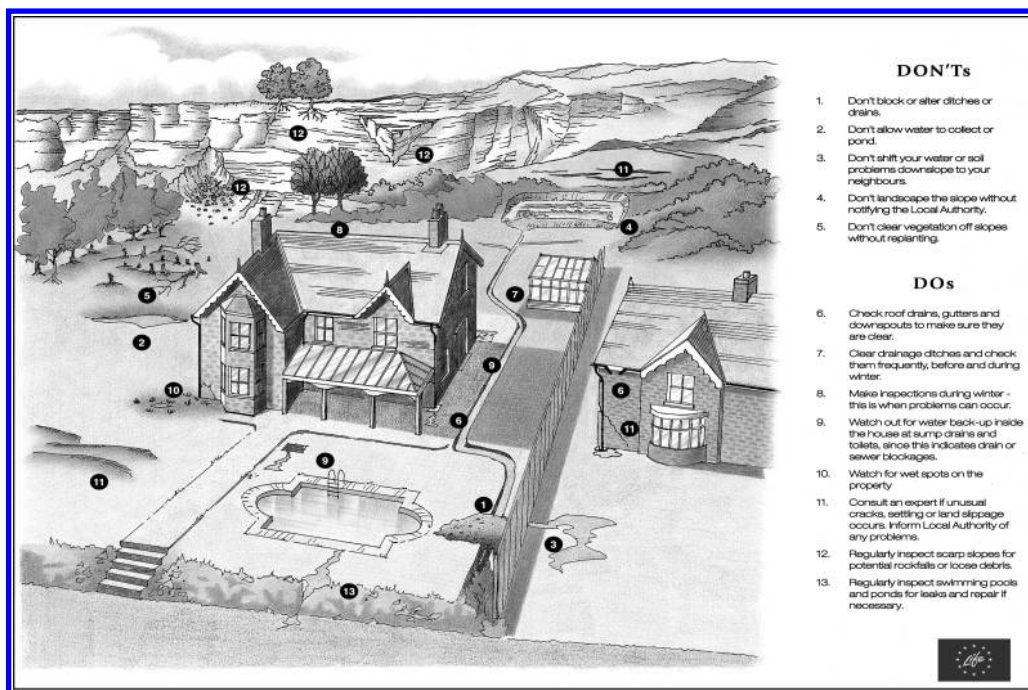
Figure 19.   Advice to homeowners diagram.

the last four years some 25% of those responding had moved into the area, which indicated a significant turnover in occupation of residential properties. As a result this demonstrated the need to continue to provide up to date information for residents on a regular basis.

One particular concern as far as property owners are concerned has been difficulty in obtaining property insurance in certain parts of the Undercliff, often due to a lack of knowledge over the true extent and nature of ground instability conditions. Certainly the DOE study assisted the process by indicating those areas where the risk is greatest. It was encouraging to note, therefore, from the resident's survey that 85% of those questioned had been able to obtain full insurance including subsidence cover. The Centre for the Coastal Environment believes that a significant contributory factor to this statistic has been the availability of better information and guidance for local residents as well as for insurers over the intervening period.

Whilst the results of the residents surveys have proved encouraging it is recognised by the Council that there are significant problems still to address. A ground investigation commenced in 2002 and further works are planned in 2005, which will allow the completion of a Landslide Quantitative Risk Assessment for central Ventnor in order that the Council can plan

how to address increasing levels of risk arising from the predicted impacts of climate change (McInnes et al. 2003).

The good practice set out in a number of publications including "Managing ground instability in urban areas – A guide to best practice" (McInnes 2000), which was published as part of the LIFE Environment project 'Coastal change, climate and instability' (McInnes et al. 2000) has been particularly welcomed. A comprehensive EU LIFE study concluded that development in areas like the Undercliff requires wise decision-making taking full account of past and present ground conditions. The study believed that this could be achieved most effectively by a coordinated approach to instability management, thereby minimising risks to vulnerable communities by:

– identifying and understanding the nature and extent of ground instability in the area;
– aiming to guide development towards the most suitable locations;
– ensuring that existing and future developments are not exposed to unacceptable risks;
– ensuring that development does not increase risks for the rest of the community.

These points underpin the Isle of Wight Landslide Management Strategy. The success of this approach has

188

been tried and tested and now other parts of the Isle of Wight coastline, for example the frontage between Cowes and Gurnard (Moore et al. 2000) and at Seaview (Woodruff 2004) on the Island's northern coast, have also benefited from a similar geomorphological appraisal and landslide strategy being implemented.

The main focus at the present time is further research into the predicted impacts of climate change. A new European Union LIFE Environment project entitled 'Response' (Responding to the risks from climate change) (McInnes et al. 2003) is examining the impacts of different climate change scenarios at five European coast study areas, including the central south coast of England and the Isle of Wight. The impacts of sea level rise, changes in storminess and increased winter rainfall of between 26–30% by the year 2080 are being assessed on a range of coastal landforms within the five study areas. Use will be made of regional climate models in order to test potential impacts on areas such as the Isle of Wight Undercliff in order to provide more informed advice to assist long term planning and management.

6 STAKEHOLDERS AND THEIR ROLE

Considering the impacts on human life, property, individual liberty and legal responsibility, to mention only a few, risk management is above all the outcome of a dialogue between various components of society. Interests are numerous and sometimes antagonistic; the powers of some constraint the powers of others. Therefore risk management comes under a logic of stakeholders who are often unfamiliar with, and even impervious to the scientific and technical aspects proposed. Therefore, beyond the conflicts of interest there are also semantic and dialectic considerations, "co-products" of a communication that is not based on an exchange, but on one way information, and this even more as information is disseminated in a regulatory, constrained, general and theoretical framework. Amongst these "external" stakeholders, the population, the law-maker, the judge, the insurance companies and the media will be presented in the following paragraphs.

6.1 *Population and demand for protection*

The population is a fundamental element to landslide risk management, it is the victim, the stakeholder and the reference criteria of the risk. Its expectations are numerous, sometimes contradictory and even irrational, in most cases, based on sector-based analysis.

Therefore, demand for protection is constantly increasing. But it must be met, most of the time by the public authorities, without infringing on individual freedom, and without a reduction of the buying power. The population wants to be both protected and free, and without any significant additional cost; this requirement is even stronger as the population is ill-informed or not informed at all of the contingencies related to natural risks. When it is informed, it is most of the time through legal, compulsory and often dry documents – when they are not impossible to understand.

Of course, the reaction and the behaviour of the population varies according to:

– The culture of the risk (notably the alarm drills)
– Its exposure to dangerous phenomenon and its experience of disasters
– The relation with property, its living standard, its level of technological development…

Furthermore, the population maintains a certain confusion concerning its expectations, between the risk it accepts at the individual level (very low, if not zero), and the risk it imposes for society, the risk imposed to "the other". Concerning this, its requirements are somehow unbalanced, and are the reflection of the individualism that now prevails in numerous societies.

The population is a stakeholder of the risks through the human alteration of the environment, it must be kept informed, and, if necessary, educated. The regulatory constraints and the interdictions imposed in term of planning and development, land regulations and spatial use cannot bring a satisfactory answer. It is preferable to base risk management on explaining and convincing rather than on constraining; in the latter case, risk management would require disproportionate control systems. Moreover, in order to be sustainable, the solutions must be designed according to a win/win logic.

6.2 *Law-maker and the law*

In order to face the increasing social demand for protection, but also to anticipate potential at risk situations and to protect the decision-maker and the decision-making, the law-maker has implemented a legal and regulatory framework. Even if general principles and international texts have been created over the past decades, the laws are specific to each country. They reflect the organisation of society, its culture, its history and its administrative organisations. The law is above all a political choice, giving priority to the general interest rather than individual or sector-based interests.

In the field of the Law, three fundamental principles are regularly called upon regarding natural risk management. That is to say:

– the principle of precausstion: it defines the attitude to be observed by anybody making a decision

189

concerning the activity which can be reasonably considered as bearing a major danger for health or safety for the current and future generations, or for the environment. The principle of precaution appeared in the International Law related to the environment as early as 1987, and has been recognised in the Rio Declaration of 5th June 1992 (article 4-3). Its objectives are, above all, to forecast, prevent or alleviate the causes of the prejudicial phenomenon and to limit its harmful effects. It stipulates that the absence of absolute scientific certainty should not be used as an excuse to do nothing.

– The principle of preventative action: its objective is to highlight the best available techniques, with an economically acceptable cost, to prevent and if possible suppress the harmful effects that can be generated by a prejudicial phenomenon.
– The principle of participation: it means, on the basis of a dialogue, integrating the populations in the development of the choices and in the definition of projects of development and protection of the environment and of the people.

The organisation of the relief and the crisis management, as well as the principle of post-crisis repair, complement these principles.

The law-maker rarely defines in an explicit manner the criteria of acceptable and tolerable risks. The reasons are numerous, but are above all related to the commitment of responsibility. It would then be on the basis of a logic of result, which is difficult to guarantee, and not on the basis of a logic of means, which is easier to justify.

It is obvious that the exchanges are insufficient between the risk specialists and the law-maker. The latter has an imperfect understanding of the experiences, the operational difficulties on the field, the reality of the risk, the scientific locks and the needs for research… Only a coherent framework and a communication effort will allow to fill this gap.

6.3 Judge and responsibility

When a disaster occurs, the decision-makers as well as the risk specialist are questioned. Responsibilities are sought, on the legal, civil or penal level, and as soon as they are regulatory texts, as soon as criteria have been set, they will determine the rules of the analysis. In addition to the trauma and the pressure on the risk specialist, several fundamental questions are asked:

– Prospective v. retro-analysis: in a field, uncertain by nature, as the field of landslide risk, the specialist makes his choices on the basis of probabilities, possibilities and uncertainties. The field of the possible is enormous. Political decision-making does not accept uncertainties. The necessary balance between protection and development, between

the principle of precaution and risk taking directs the specialist towards a solution he judges as being optimal, suited to the particular case studies, to the means at disposal (financial, human and technical), but in which uncertainty remains. And nature is there to remind it! When a disaster occurs, there is no reference to uncertainty and probability. The fact is known and the probability is 1. The return analysis is no longer scrambled by numerous possibilities, and it is more simple to understand the mechanisms. By focusing the investigations on the event that occurred, its causality factors are quickly understood. It is then difficult to go back to the previous situation, "forgetting" the outcome, and being free from the permanent milestone of the phenomenon that has occurred on modelling. The system of reference of the analysis is modified, sometimes radically, and the confrontation between the analysis before and after the crisis is difficult.

– Qualitative v. quantitative: as soon as there is such a change in the system of reference, only clear, formalised and quantified criteria allow to balance the debates: "were we, yes or no, above the threshold required?". In the case of a qualitative approach, the only possible defence will consist in asserting that the necessary actions or the maximum had been done (proof of means), this will be invariably renounced by the facts. How do you explain or prove that the solution retained was the "best" solution as it was not able to prevent the disaster from occurring? How do you define and calibrate sufficient investments when the protection level to be reached has not been defined? Whatever the professionalism of the specialist, nature will plead against him. In addition, media and population pressure will alter the debate. In the case of a qualitative approach, and as no threshold will have been defined, the judge can only rely on an innermost conviction not only biased, but also influenced.

Considering this situation, the temptation can be strong not to want to commit into the prevention and the choice of solutions. Do nothing, do nothing wrong! True, however if a mistake is unfortunate, inaction is a sin. In any case, if there is no evidence of professional misconduct, the wrong answer to a given problem is always more acceptable than none at all. In an uncertain and complex field as landslide forecast, only a quantified approach and clearly stated criteria will keep the debate at the level it should be, that is to say the field, the decisions and actions, and not at the level of polemics and tribunals.

6.4 Insurance companies, compensation and prevention

Rapid repair following a disaster, to go back if not to normal, at least to an acceptable situation is necessary

190

in order to prevent the addition of a second trauma. This is the role to be played by the insurance companies.

Insurance systems are, regarding natural risks, extremely varied around the world. The variations are numerous, from the absence of insurance (certainly the most frequent situation, and especially in the most exposed poor countries), to the optional private insurance, and to the compulsory insurance through mutualisation.

Disasters cannot come under the sole private system, as the effects go largely beyond the ability to react of the individual. The system implemented in France, is fairly comprehensive, and the description illustrates all the element and problems of insurance. It is organised around:

The principle of equality: whatever the area we are in, exposed or not, the insurance rate is the same and determined by the State, and not by the insurance companies.

The principle of solidarity – mutualisation of the risks: the money thus collected is managed within a single fund (Cat-Nat fund) which will be used to finance the repair work.

Link between prevention and compensation: compensation is conditioned by the respect, within a 5 year deadline, of the recommendations or obligations expressed in the regulations of the risk prevention plan (PPR).

The definition of the insurance activation threshold: the compensation starts as soon as a phenomenon of abnormal intensity is recognised by the State (declaration of state of natural disaster).

This system has a few deficiencies and imperfections, that is to say:

– Efficient control is not implemented to ensure that the prescriptions expressed in the PPR are followed.
– The abnormal intensity of a phenomenon is not clearly established, and it is not necessarily valid considering the fact that the series of hazards are not stationary. Should the abnormal intensity of a phenomenon be considered or should it be the abnormal intensity of the damage? Under the pressure from the population and the media, compensation tends to become the rule, which often leads to taking the responsibility away from the people exposed: "in any case, if I am affected by a natural phenomenon, I will be reimbursed!"

It will be important to balance the necessary principle of solidarity, which sometimes tends to take responsibility away from the populations exposed, with individual incentives, on the basis of profit-sharing. It will also be important to invest more in prevention in order to limit the cost related to the damages. Insurance companies must have a more upstream involvement in the prevention, with a strict control of the public authority on its obligations to reimburse quickly.

6.5 *The media and its implications*

The media play a predominant role in our societies, and have a high influence on the risk, on its reality, on the way it is perceived, as well as on the responsibilities related to it. They have means to investigate that cannot be compared to the means of the technicians, and this even more as they intervene, afterwards, on disasters that have occurred. The questioning and the public "trials" are then unbalanced, to the detriment of the decision-makers and the scientists. The effects of this on decision-making and on the precautionary principle can be very significant.

The media "accuse" very quickly, often without enough knowledge of the complexity of the reasoning underlying the choices made by the specialists. Quick to put on the robe of the judge, they nail the short-comings on the basis of a sector-based reasoning and short term analysis for which solutions are always easier to identify. Once again, the decisions-makers and the scientists must be able to justify themselves, to present a clear and flawless reasoning, and where the uncertainties, considered here as weaknesses of incompetence and not as intrinsic properties of the hazards, must be banished.

Even more now than ever, it is necessary to be able to justify one's choices, on the basis of explicit criteria and an irreproachable method, as, since the Age of Enlightenment, science appeared to bring uncontested truths and constant progress to mankind, these times are now over. The media now have a relation with science and scientists which is at best favourable, but more often suspicious. The demand for justification, the seeking of the responsibility must now lead the scientist towards a greater clarity, increased communication and educational skills, and if possible before the disaster occurs. The difficulty rests yet again at the level of the qualitative approaches, and even more on the approaches for which the acceptable and tolerable risk thresholds have not been defined. On what basis can a sufficient investment be justified? Even more as the situation towards which the media have turned their attention, reminds us how much the investment granted is, by definition, not sufficient!

The media also influence the way the population perceives the risk. Today, the information society informs us virtually instantly about disasters anywhere in the world. The number of event relayed by the media and thus drawn to our attention is greater and greater and develops the feeling of increasing vulnerability of our societies. We live, through the media in a world subject to a pressure for change leading to a global

191

feeling of insecurity for the present and of loss of vision for the future.

7 SYNTHESIS ELEMENTS AND RECOMMENDATIONS

7.1 *Understanding the territory and its evolution to understand the risk*

Whatever the framework defined by the regulations, whatever the administrative and political organisation of the country, whatever the culture, and finally, whatever the type of phenomenon studied, it is necessary to understand the territory, its past evolution and its history to better understand the risk. Sustainable and more balanced solutions to protect the population and the properties can then be proposed.

Beyond the scientific and technical element, understanding the territory from a social, economical and political viewpoint is essential. This is due to several reasons:

– The natural, constructed and human environment constantly interact with one another, and the effect of human activity on natural risks is constantly increasing, sometimes making natural causalities of a secondary importance. This is notably the case of the artificialisation of the environments which can highly modify the flow and concentration of superficial water, and therefore increase the frequency of superficial landslides and mudslides. Understanding the mutations of the territory, in term of land occupancy and activity allows to better understand the evolution of the risk and to establish a more reliable diagnosis of the current situation.
– The population perception of the risks explains certain critical situation, as, if forgetting certain practices – forest maintenance, water and runoff control – can lead to an aggravation of the hazards, certain inherited concepts are sometimes untrue. Tradition does not necessarily mean relevant practices, actions or behaviours. What was thought to be valid in the past, may no longer be valid, or may even have never been valid.
– Risk perception by the population, its experience and its relation to nature and to danger, its knowledge and understanding of the phenomenon allows to know how to efficiently involve it in risk reduction actions. The local appropriation of the risk is the best guarantee of the efficiency and sustainability of the actions.

7.2 *Towards an integrated, participative and positive approach*

If landslide risk management is specific to each country, some base principles can however be expressed.

Landslide risk management must not be a descending technocratic approach, but an integrated approach, that is to say, at the same time:

– Scientific: All the stages (knowledge/understanding of the phenomenon, prediction of the landsliding/surveillance/alarm, prevision of the trajectory, stake analysis and their vulnerability, protection…) of risk assessment must be lead with rigour, while clarifying the facts, the assumptions, the uncertainties and the choices. Insofar as possible, it is preferable to adopt a quantitative approach based on clear acceptable risk threshold.
– Environmental: beyond the efficiency of the risk reduction measures, the efficiency of which will have to be verified (as far as possible) on the long term, the impacts on the environment should be integrated, if the anti-block nets represent for example the only pertinent solutions to reduce the risk of block of rocks falling, their negative visual impact on the environment can lead to choosing excavation solution, which are, in addition, sometimes more efficient and less expensive. The implementation of structures can be accompanied by planting, which will allow the maintenance of the eco-tourism vocation of a region.
– Social: the population is a fundamental element of the management, it is at the same time a stakeholder, a victim and an indirect prescriber of protection orientations. It must be made aware of its responsibilities and involved at the earliest stage in the analysis approach and in the operational choices, and this especially as it knows the territory better than the specialist. The latter must not only immerse himself in the area, with its strengths and weaknesses, but also in its inhabitants with their customs, their aspirations, their fears and their ill-founded ideas. Each inhabitant must have the impression that the analysis is personally dedicated to him or her; it is the cost to pay to mobilise the population, and get it to engage in a positive and not irrational debate.
– Economic: the protection of properties and populations is an urgent necessity, but it bears a cost, and this cost must remain proportionate to the stakes. The solutions envisaged must be expressed on the basis of a cost/profit analysis, but this "profitability" must be assessed for all the parties concerned. The quest for solutions must therefore be designed in the framework of a win/win approach, in order for the population to stop considering the risk only as a constraint. The risk specialists must put a lot of effort downstream from their competence, develop multifunctional solutions, integrate financial and tax incentives, as well as the management of the land assets. Beyond the transfer of the downstream competence, or, at best, beyond

192

the accompanying of the decision-makers, it is a case of encouraging the risk specialist to integrate the socio-economic element as early as the beginning of the risk analysis.

– Societal and political: planning and development, its sustainable, harmonious and secure development, rest on a balance between the protection obligations and the development ambitions. It is the choice of a society, a question of ambition and will-power, a duty and a gamble for future generations. Landslide risk management comes within the scope of this "protection/development" dialectic, with an idiosyncrasy related to the partially uncertain character of the phenomenon considered. The scientific and technical element of risk management is essential: it determines the limits of what is possible, but not the limits of what is acceptable, it is therefore not sufficient. It is sometimes considered as secondary, marginal, or altogether ignored. The technicians as well as the politicians are responsible, and the regulatory constraints counterbalance this imbalance only in appearance. It is fundamental for the risk specialist to widen his analysis and to integrate in his approach the ambitions for the territory, whether individual or collective, whether reasonable or unrealistic. The approach is difficult as the development ambitions are often little or badly formalised. Concerning the protection "ambitions", they are rarely made explicit. There are important consequences on the society and on the individuals, these go beyond the strict limits of the area studied, notably in term of land organisation. Most of the conflicts in landslide risk management, and more generally in natural risk management, come from the development ambitions, the expectations or the fears of the population being taken into account too late, and each time, of a tackling of the problem that is too technocratic and sometimes scientific. It does not come from the technical risk analysis as such. Human, social and political science must be involved in the risk management approach.

Risk management must also integrate strong communication. It is fundamental to ensure that the messages have been understood, by the decision-makers and by the population. Therefore, it is wrong to only give little information at the end of the analysis, but, it is important to define, instead, a true communication strategy, with exchanges, listening and control (feed-back), and this from the start of the study.

Beyond the emergency plan, crisis preparation and management, repair and compensation of the victims of the natural disasters must be performed as soon as possible, if it is not the case, there should be provisional, adequate, and sometimes simplified administrative procedures.

Landslide risks must therefore be considered as a constraint amongst others. Whatever the country, risk assessment and management must be performed on the basis of:

– An exhaustive diagnosis of the three environment: natural, human and constructed,
– The history and the changes to the area,
– The political development ambitions (equilibrium between development and protection).

Risk management must of course take into account the regulations in force, the distribution of the responsibilities, the administrative organisation, and the necessary complementarities between public and private actions. The solutions developed are sustainable:

– If the technical choices turn towards measures for which maintenance is low (for example drain-sump), and the control is fast,
– If the population is part of this choice, if it understands them and takes part in their implementation: to convince rather than to constrain,
– If the system is designed on a "win/win" logic, to therefore change paradigm, and transform the risk into at least an asset and at best a "treasure".

Whatever the phenomenon to be analysed, as soon as human lives are exposed and risk reduction solutions must lead to a partial or total despoilment of the properties (loss of value of the property, preventative evacuation), it is necessary to undertake a broad approach and to integrate risk assessment in a global analysis of the natural risks and the development. The feeling of equity must prevail within the population, and any despoilment of the properties must be defined and explained within a general framework considered as fair for and by the community.

7.3 Qualitative or quantitative approach

The choice between a qualitative and a quantitative risk assessment obviously depends on the data available, the experience of the specialist, and the aims. However, beyond the technical considerations, it is important to know if the qualitative approaches allow, in the framework of a contradictory debate, the analysis of the responsibilities of each concerning the work performed and the objectives.

The qualitative risk assessment approaches allows to organise the problems into a hierarchy, if the analysis is on the same type of phenomenon. If rigorous approaches can be designed on the basis of qualitative approaches, the notions of threshold remain subjective and are the object of controversies. It is difficult to prove the respect of the protection objectives through qualitative approaches even when the tolerable and acceptable risk thresholds have been defined. At most, it allows to explain that the investment granted

193

was important, and that the approach followed the rule book in the matter. However, if it is possible to infer an important investment, it is not possible to prove that this investment was enough.

In the case of legal questioning, following a landslide with damage, and even victims, contradictory debates performed on the basis of qualitative analysis can quickly turn against the risk specialist even if the means implemented were important. The justification of means inherent to qualitative approaches always remains difficult to defend when human lives are taken into account. If the culpability of the specialist is not generally sought insofar as it is rare that professional errors are made intentionally, the responsibility is often involved.

Considering the trauma represented by this questioning, the qualitative analysis tends to increase the constraints in order to protect the prescriber. Therefore, this leads to an excessive principle of precaution, but it is easy to understand why. The risk specialist will prefer to transcribe his uncertainties in precaution demands rather than in responsibility increase, even if the constraints are highly penalising for the development, or if they lead to the depreciation of the goods or properties. He will do even more so as he will not be able to "rest" his analysis on objective criteria without guarantee.

Insofar as possible, it is therefore preferable to perform a quantitative landslide risk assessment. Not only the choices can be more easily explained and defended, but it will also be possible to compare the constraints encountered to reposition the risk problematics at its adequate level within the development of the territory. This approach does not relegate the political choices to a position of second importance, and is no greater constraint for the decision-makers, on the opposite, it provides consolidated elements to assist the decision making on which the decision-maker can base his orientations.

This assumes the risks specialists understand and master the quantitative approach and that it is of quality. The allocation of a numerical value to thresholds defined in a qualitative manner (for example 1, 2 and 3 corresponding to high, average, low) does not transform a qualitative analysis into a quantitative approach. In numerous cases, the quantitative risk assessment will not be possible. The process will then have to be rigorous and reasoned, making sure that the populations exposed are not excessively penalised.

7.4 *Indicators and tools*

7.4.1 *Indicators: for a shared and consensual approach*

Whatever the approach selected, landslide risk management must be performed in an integrated manner, on the basis of a logic of stakeholders. The risk specialist,

integrated to a multidisciplinary team, will be able to elaborate indicators to assess the relevance of the solutions envisaged. These indicators must cover all the interlocutors concerned by the risk studied, and this, in coherence with the regulations in force. For each interlocutor, and for each action envisaged, it will mean verifying the degree of satisfaction compared to the expectations, the needs, the obligations or the responsibilities. The following figure illustrates the case of la Désirade presented earlier. The stakeholders are the States, the local elected members and the population. Simple indicators have been used to compare the various solutions (Table 4).

The optimisation of the indicators enables to develop common and balanced solutions with maximum consensus. In the case presented above, the solutions consisted in proposing:

– Protection structures in mud, less expensive and performing a double function of protection and drainage water collection for the population,
– Partial unblocking (30 metres of the coast remain blocked) of a sector belonging to the State, on which a protection measure related to the environment is currently in force (50 geometric steps),
– Freezing of development (no new constructions) below the protection structures.

If the first meetings between the State, the local authority and the population have been very tense, but the solutions developed within the framework of a global analysis of planning and development and risks have received the support of all concerned.

7.4.2 *The tools*

Risk management cannot be envisaged without effective tools, whether for the hazard models (stability, propagation, impact…), the thematic and spatial management of the data, the understanding of the territory or the information.

– Modelling tools: there are numerous tools from simple models to very sophisticated models, and there is a wealth of material on the subject. Computer means (equipment, object programming, network operation via the Internet…) are extremely powerful and are available to all at a lesser cost. User-friendly interface enables the user to perform scenarios to support his analysis. It is necessary to give priority to the three-dimensional models, even if empiric laws are used, whether for the calculation in itself, for the development of the results or the information.
– Territory management and analysis tools: geographic information systems are now within everyone's reach, even if these basic tools are a closed book to some decision makers. It is now unconceivable to manage a territory without GIS, in addition,

194

Table 4.

Solutions	None	Evacuation	Protection nets and evacuation	Structures (in mud) & evacuation	Structures (in mud) & 50 steps zone made available	Structures (in mud) & 50 steps zone made a vailable & 30 m zone	Structures (in mud) & 50 steps zone made available & 30 m zone & freezing of development below the structures
Satisfaction of the State in term of:							
Responsibility	No	Yes	Yes	Yes	Yes	Yes	Yes
Protection of the natural environment	Yes	Yes	Yes	Yes	No	/	/
Protection of the population	No	Yes	Yes	Yes	No	Yes	Yes
Local Development	/	/	/	/	/	/	/
Global development coherence on the island.	No	Yes	Yes	Yes	No	No	Yes
Satisfaction of the Council in term of:							
Responsibility	No	Yes	Yes	Yes	Yes	Yes	Yes
Protection of the natural environment	Yes	No	No	No	Yes	Yes	Yes
Protection of the population	No	Yes	Yes	Yes	Yes	Yes	Yes
Local Development	Yes	No	No	No	Yes	Yes	Yes
Global development coherence on the island.	Yes	No	No	No	Yes	Yes	Yes
Satisfaction of the population	Yes	No	No	No	Yes	Yes	Yes
Respect of the Law	No	Yes	Yes	Yes	No	Yes	Yes
Acceptable financial cost	Yes	Yes	No	Yes	Yes	Yes	Yes
Strategy/Approach	None	Single risk	Single risk	Single risk	Single risk & local planning and development	Multi-Risk & local planning and development	Multi-Risk & global planning and development
Communication/Exchange	None	Unilateral	Dialogue but imbalance	Dialogue but imbalance	Dialogue & negotiation but imbalance	Dialogue & negotiation but imbalance	Dialogue & negotiation & balance

three-dimensional management tools are starting to become popular. They facilitate knowledge analysis and structuring, but should not be considered as expert systems. They remain at the level of assistance to decision making and require the permanent expertise of risk technicians. The functionalities now available enable to reveal the territory and its risks; they mainly allow to understand the full dimensions and complexity of the territories, thus leading to truly integrated analysis of "development and planning and risks".

– Information and communication tools: the inter-compatibilities of the software and formats allow the development of efficient communication tools; multimedia and access via the Internet are not gadgets. They are the true basis of a dialogue; it is now possible during a public meeting to have dynamic access to maps, photos, regulations, animations and simulations. It is therefore easier to understand the phenomenon, to rapidly identify the obligations and responsibility of each, to display the uncertainties, to present the facts. Discussions between the various parties involved change dimension, and the sterile arguments disappear. They are real exchange and analysis tools for complex issues and allow to focus of searching for solutions, in the framework of a common, positive and flexible approach.

8   CONCLUSIONS

– The problems of landslide risks are increasing worldwide because in many countries insufficient attention is paid to the integration of ground instability in the planning system.

– Increasing pressure for development expansion into marginally stable areas is likely to result in increasing levels of risk; this is likely to be exacerbated as a consequence of the predicted impacts of climate change.

– Landslide risk is one of the constraints to be taken into account in sustainable land development; integrated approaches have to be carried out for defining efficient mitigation measures combining scientific, economic, social and political aspects of the solutions analyzed.

– The quantitative risk assessment (QRA) approach is recommended for addressing landslide risk, even if all the components of the risk are not always well known.

– However, if it is not possible to address a reliable quantitative risk assessment, it is often better and sufficient to combine a good hazard analysis with an accurate analysis of the exposed assets instead of developing a complex approach based on theoretical or sectorial information.

– To compensate for the lack of knowledge or experience in quantitative risk assessment, risk management should involve both the population and the local authority in a constructive dialogue; awareness and local appropriation of the risks by residents will lead to better management of critical situations.

– The definition of acceptable and tolerable risk criteria is the key issue of a balanced, operational and efficient strategy of landslide risk management; without these criteria the responsibility of the specialists might be, furthermore, difficult to justify in case of injuries or fatalities induced by a landslide.

– Ground movement problems may be reduced if the local community, the professionals and the local authority adopt a coordinated approach toward landslide management.

– Individual technical (and often private) actions are to be considered within a global political scheme; such a coordinated action has to be addressed first so that risk is not only modified from one place to another, and so that financial resources are optimised.

– Ground instability is a key consideration in the planning process and must fully be taken into account in relation to development proposals; a balance should be defined jointly by scientists and decision-makers between protection and development.

– Communication is a key aspect of risk management; information should be provided through discussions with the local community, and attention should be paid to ensure the population understands the reasons for the constraints induced by the mitigation measures, as well as their consequences on daily life.

– Human activity is likely to modify largely the risk by increasing the vulnerability as well as by modifying the intensity of the phenomenon; one of the difficulties is that the consequences of urban growth can not necessarily been seen immediately. Once again information has to be disseminated so that people understand the processes; this point will also be tackled in SAO7.

– Research should be encouraged to better assess the components of the risk, and if possible in a quantitative way. Efforts have to be focused mainly on propagation models, intensity of the phenomena and vulnerability. The gaps, uncertainty and lack of knowledge have to be clearly explained to decision-makers, first so that no misunderstanding remains, and second so that they are open to fund research programmes.

– Improvement of models and information through research programmes and open-databases are the key of risk management, as the lack of knowledge generally leads to an excessive principle of precaution which considerably constraint the population and the local authorities.

– Finally, risk management should stay a (courageous) political act supported by rigorous scientific methodology, and should not be a scientific approach as itself.

ACKNOWLEDGMENTS

REFERENCES

AGS 2000. Landslide risk management concepts and guidelines. *Australian Geomechanics* 37(1).

Ale, B.J.M. 2001. *Risk Assessment Practices in The Netherlands, RIVM* (National Institute of Public Health and the Environment), P.O. Box 1, 3720 BA Bilthoven, The Netherlands.

Alexander, D.E. 2002. *Principles of emergency planning and management*. New York, Oxford University Press.

ANCOLD 2003. *Guidelines on Risk Assessment. Australian National Committee on Large Dams Inc*., Melbourne, ISBN 0731 027 620.

Arnalds, P., Sauermoser, S., Jóhannesson, T. & Jensen, E. 2002. *Hazard zoning for Eskifjörõur. Iceland meteorlogical Office Report 02015*. Reykjavík available at IMO website http://www.vedur.is/english/

Baynes, F.J., Lee, I.K. & Stewart, I.E. 2002. A study of the accuracy and precision of some landslide risk analyses. *Australian Geomechanics* 37(2): 149–156.

Bell, F.G. 1999. *Geological Hazards – Their assessment, avoidance and mitigation*. London, New York, E & FN Spon.

Bonnard, C.L., Forlatti, F. & Scana, C. (2004). *Identification and mitigation of large landslide risks in Europe*. Advances in Risk Assessment, Imriland Project. Balkema.

Bowles, D. 2004. ALARP evaluation: using cost effectiveness and disproportionality to justify risk reduction. ANCOLD Bulletin No.127, Australian National Committee on Large Dams, Melbourne, 89–105.

BUWAL, 1999. Risikoanalyse bei gravitativen Naturgefahren. Bundesamt für Umwelt, Wald und Landschaft, Bern. Order No. UM-107/I-D (exists only in German); 115 p.

Christian, J.T. 2004. Geotechnical Engineering Reliability. How well do we know what we are doing? *J. Geotech. and Geoenvironmental Engineering, ASCE* 130(10): 985–1003.

Dai, F.C., Lee, C.F. & Ngai, Y.Y. 2002. Landslide risk assessment and management: an overview. *Engineering Geology* 64: 65–87.

Department of the Environment, 1991. *'PPG14 – Development on unstable land'*. London: HMSO.

Doornkamp, J., Lee, E.M. & Moore, R. 1991. *'Coastal landslip potential assessment: Isle of Wight Undercliff'*. Technical Report by Geomorphological Services Ltd for the Department of the Environment, UK. Research contract PECD/7/1/272. London. Department of the Environment, HMSO.

EPFL/CADANAV, 2002. *Projet CADANAV*. Etablissement d'une méthodologie de mise en oeuvre des cartes de dangers naturels du canton de Vaud. Unpublished report; 200 p.

ERM 1998. *Landslides and Boulder Falls from Natural Terrain: Risk Guidelines.* Report to Geotechnical Engineering Office of Hong Kong. ERM-Hong Kong Ltd.

European Commission, 1997. *'LIFE Environment – Information Package 1997–1999'*. Brussels. European Commission DGXI (XI.B.2).

European Commission, 2001. *'LIFE Environment in action – 56 new success stories for Europe's environment'*. Luxembourg: European Commission.

Fell, R. & Hartford, D. 1997. Landslide Risk Management, in Landslide Risk Assessment, Cruden & Fell (eds.), Balkema, Rotterdam, 51–110.

Fischhoff, B., Lichtensetin, B.S., Slovic, P., Derby, S.L. & Kenney, R.L. 1981 *Acceptable Risk*. Cambridge, Cambridge University Press.

Garrick, BJ. & Willard, CG. (eds.) 1991. *The Analysis, Communication and perception of risk*. New York, Plenium Press.

Glade, T., Anderson, M. & Crozier, M. 2005. *Landslide Hazard and Risk.* John Wiley & Sons Publisher. In press.

Ho, K.K.S., Leroi, E. & Roberds, B. 2000. Quantitative Risk Assessment: Applications, Myths and Future Directions, in GeoEng 2000 Invited Papers. TECHNOMIC, Lancaster PA, 209–312.

HSE (Health and Safety Executive, United Kingdom) 1992. The Tolerability of Risk from Nuclear Power Stations, Her Majesty's Stationery Office, London.

HSE (Health and Safety Executive, United Kingdom) 1999. *Reducing Risks, Protecting People*, Discussion Paper, Risk Assessment Policy Unit, Health and Safety Executive, London.

HSE (Health and Safety Executive, United Kingdom) 2001. *Reducing Risks, Protecting People*, Her Majesty's Stationery Office, London.

Hutchinson, J.N. & Bromhead, E.W. 2002. 'Isle of Wight landslides'. *International Conference 'Instability – Planning and Management'*, Ventnor: Thomas Telford, pp 3–70.

Iceland Ministry for the Environment 2000. 'Regulation on hazard zoning due to snow- and landslides, classification and utilization of hazard zones, and preparation of provisional hazard zoning' 6 July 2000 available at IMO website http://www.vedur.is/english/

ICOLD 2004. Risk assessment in dam safety management. Bulletin No.__, International Commission on Large Dams, Paris. (Draft document).

IUGS 1997. *Quantitative risk assessment for slopes and landslides – the state of the art*. IUGS working group on landslides, committee on risk assessment in Landslide Risk Assessment, Cruden & Fell (eds.), Balkema, Rotterdam, 3–14.

Larrouy-Castera, X. & Ourliac, J-P. 2004. *Risques et urbanisme. Le Moniteur*.

Lee, E.M. & Jones, D.K.C. 2004. *Landslide Risk Assessment.* Thomas Telford, London.

Lee, E.M. & Moore, R. 1991. *'Getting the message across: Ground movement and public perception'*. Birmingham. Report for South Wight Borough Council.

Lee, E.M., Jones, D.K.C. & Brunsden D. 2000. The landslide environment of Great Britain. In Bromhead et al. (eds.), Landslides: In Research, Theory and Practice. Thomas Telford, London.

Lommers, G.C. & Bottelberghs, P.H. 1995. *Dutch Policy on External Safety,* Ministry of Housing, Physical Planning and Environment, External Safety Division (665).

McInnes, R.G. 2000. *'Managing ground instability in urban areas – A guide to best practice'*. Newport, Isle of Wight: Isle of Wight Centre for the Coastal Environment.

McInnes, R.G. & Jakeways, J. (eds.) 2002. 'Instability – Planning and management'. *Proceedings of the International Conference*, Ventnor, Isle of Wight, May 2002. London. Thomas Telford.

McInnes, R.G. & Jakeways, J. 2000. The development of guidance and best practice for urban instability management in coastal and mountainous areas of the European Union. In *'Landslides: Research, theory and practice'*. London: Thomas Telford.

McInnes, R.G., Jakeways, J. & Houghton, H. 2003. EU *'Response'* project information leaflet, Ventnor, Isle of Wight.

McInnes, R.G., Tomalin, D. & Jakeways, J. 2000. *'Coastal change, climate and instability'*. Final report of the EU LIFE Environment demonstration project. Centre for the Coastal Environment, Ventnor, Isle of Wight. 1,736 pps.

Ministère de l'Aménagement du Territoire et de l'Environnement, Ministère de l'Equipement, des transports et du Logement 1999. *Plans de prévention des risques naturels prévisibles* (PPR) – risques de mouvements de terrain: guide méthodologique. La Documentation Française (Eds).

Moore, R., Lee, E.M. and Brundsden, D. 2000 *'Cowes ground stability study'*. Report by Halcrow for Isle of Wight Council.

Moore, R., Lee, E.M. & Clark, A.R. 1995. *'The Undercliff of the Isle of Wight – A review of ground behaviour'*. Report by Rendel Geotechnics for South Wight Borough Council, Ventnor, Isle of Wight.

Netherlands Ministry of Housing 1989. Physical Planning and Environment, Dutch national Environmental Policy Plan – Premises for Risk Management, Second Chamber of the States General, Session 1988–1989, No. 5.

Noverraz, F. & Bonnard, Ch. 1990. Mapping methodology of landslides and rockfalls in Switzerland. Proc. VIth Int. Conf. and Field Workshop on Landslides, Milan, 43–53.

Noverraz, F. 2002. *Stability study relating to the Communal Territory of Belmont s/Lausanne. Instability Planning and Management.* Thomas Telford, London, 747–754.

Noverraz, F., Bonnard, Ch. & Giraud, A. 1991. Environmental impact of a large landslide near Lausanne, Switzerland. Proc. Int. Conf. on Slope Stability Engineering, Shanklin, Isle of Wight. Thomas Telford, London, 101–106.

OFAT, OFEE, OFEFP 1997. *Recommandations, Prise en compte des dangers dus aux mouvements de terrain dans le cadre des activités de l'aménagement du territoire.* Office fédéral de l'aménagement du territoire, Office fédéral de l'économie des eaux, Office fédéral de l'environnement, des forêts et du paysage, Berne. No. de commande OCFIM 310.023f; 42 p.

PIARC 1997. Landslides techniques for evaluating hazard. PIARC Technical Committee on Earth Works, Drainage, Subgrade.

Pikaar, M.J. & Seaman, M.A. 1995. *A Review of Risk Control, VROM*.

Reeves, A., H. K.K.S. & Lo, D.O.K. 1999. Interim risk criteria for landslides and boulder falls from natural terrain. Proc. Seminar on Geotechnical Risk Management. Geotechnical Division, Hong Kong Institution of Engineers, 127–136.

RTA 2001. *Guide to Slope Risk Analysis Version 3.1 Roads and Traffic Authority*, New South Wales, Australia. (www.rta.nsw.gov.au).

Stewart, I.E., Baynes, F.J. & Lee, I.K. 2002. The RTA guide to slope risk analysis version 3.1. *Australian Geomechanics* 37(2): 115–148.

U.S. Department of Transportation 1990. *The rockfall hazard rating system implementation manual*. US Dept. Commerce, National Technical Information Service, Springfield VA.

USBR (United States Bureau of Reclamation) 1997. *Guidelines for Achieving Public Protection in Dam Safety Decision Making*, Denver, Colorado.

Veyret, Y., Garry, G. & Meschinet de Richemond, N. 2004. *Risques Naturels et Aménagement en Europe*.

Vrijling, J.K., van Hengel, W. & Houben, R.J. 1998. *Acceptable Risk as a Basis for Design, Reliability and Engineering Safety,* Apostolakis et al. (eds.), Vol. 59, No.1.

Weichselgartner, J. 2001. *Disaster mitigation: the concept of vulnerability revisited*. Disaster Prevention and Management 10: 85–94.

Woodruff, M. 2004. *'Report on landsliding at Seagrove Bay, Seaview, IW'*. Southampton. Report for IW Council.

Landslide hazard and risk zoning for urban planning and development

L. Cascini
Department of Civil Engineering, University of Salerno, Italy

Ch. Bonnard
Ecole Polytechnique Fédérale de Lausanne, Switzerland

J. Corominas
Department of Geotechnical Engineering and Geosciences, Technical University of Catalonia, Spain

R. Jibson
United States Geological Survey, Golden, Colorado, USA

J. Montero-Olarte
Department of Civil and Agricultural Engineering, National University of Colombia

ABSTRACT: Disasters caused by landslides have continued to increase during the last decades notwithstanding the significant efforts of the United Nations aimed to reduce their consequences. The reason for a risk increase is essentially related to demographic pressures and territory mismanagement. Fortunately, some countries and regions have already progressed in the development of procedures for managing urban and population growth as well as for minimizing the associated risks. The procedures are based on hazard and risk zoning which, however, can imply difficulties because of technical and socio-economic contributing factors. Starting from the valuable experience gained in several countries, the present paper discusses the improvement of urban planning and development by hazard and risk zoning, albeit recognizing the efforts still required for quantifying zoning criteria and adapting them to landslides risk management necessities. Risk mitigation strategies are therefore discussed, also considering the valuable contribution that can be furnished by the skilful use of new technologies and mathematical modeling. However, improvement of both remote sensing and data treatment techniques should not detract from field work and personal judgment since the current use of landslide inventories, which are the key input parameter for hazard assessment and validation, cannot be prepared in a reliable way with automatic data capture techniques exclusively. Uncertainties and errors in landslide zoning restrict the applicability of the hazard and risk maps for practical purposes and can generate conflicts. The validation of both procedures and maps is, therefore, a necessity especially in urban areas.

1 INTRODUCTION

Previous State of the Art papers have introduced numerous landslide typologies that can involve several soil and rock types which fail through complex mechanisms strictly depending on the triggering factors, the stage of slope movements and the mechanical behaviour of the material. The previous SOA have also discussed the available landslide classifications that, starting from the 1863's (Dana 1863), have tried to place such phenomena in a general framework.

Several uses of such classifications are possible. For example, referring to the slope movement stage as introduced by Leroueil et al. (1996), landslides can be separated into two main categories: first-time failures and reactivated landslides.

First-time landslides commonly are characterised by high velocity and can produce fatal consequences. Reactivated landslides commonly cause great economic damage and, sometimes, temporary or permanent evacuation of large zones. Unfortunately, both kinds of movements and their consequences are widespread all over the world (Fig. 1) and often affect urban centres.

Interaction between landslides and many other natural hazards is also a great concern. Earthquakes, tropical cyclones, volcanic eruptions, and tsunamis can trigger or exacerbate landslides, as well as deforestation
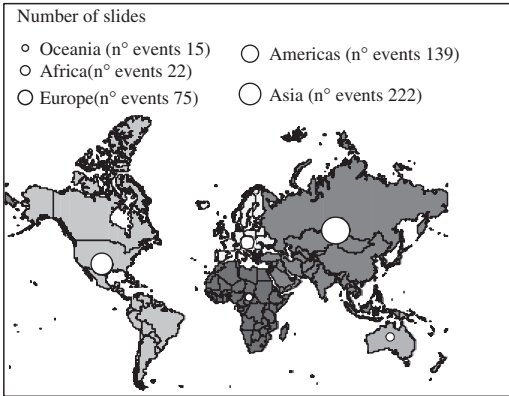
Figure 1. Number of Occurrences of Slide Disasters by Continent (1903–2004) [EM-DAT: OFDA/CRED database].

that is indeed an anthropic hazard. Landslides, in turn, can produce and/or exacerbate floods, volcanic eruptions and tsunamis.

It is interesting to observe that, due to such interactions, landslides are considered the second most significant natural hazard among those identified by the United Nations Development Programme (UNEP 1997) which regards landslides as a type of "geological hazard", even if the term flood is commonly used to describe the consequences of rapid slope movement.

The full awareness of the effects produced by natural hazards led the United Nations, in 1989, to sponsor a resolution that declared the years 1990–2000 the "International Decade for Natural Disaster Reduction" in order "to marshal the political resolve, experience and expertise of each country to reduce loss of life, human sufferings and economic losses caused by natural hazards". Unfortunately, the praiseworthy aim of this resolution has been eclipsed by the large increase, during the end of the last century, in the occurrence of both natural disasters in general and landslides in particular (Fig. 2). The increase of damage has even been worse (Fig. 3).

There are many reasons for this increase, and it is difficult to disagree with the U.N. General Secretary when he observes (Annan 2002) that:

"*Communities will always face natural hazards, but today's disasters are often generated by, or at least exacerbated, by human activities. At the most dramatic level, human activities are changing the natural balance of the earth, interfering as never before with the atmosphere, the oceans, the polar ice caps, the forest cover and the natural pillars that make our world a liveable home. But we are also putting ourselves in harm's way in less visible ways. At no time in human history have so many people lived in cities*
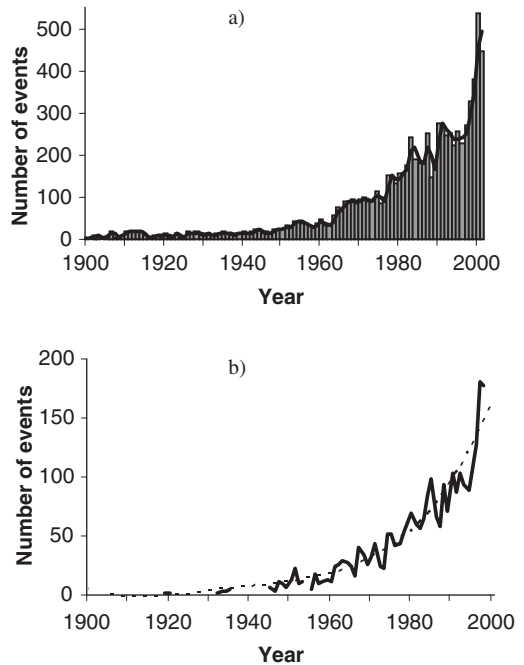
Figure 2. EM-DAT: OFDA/CRED database: a) Natural disasters; b) Landslides and Floods (Cascini 2005).
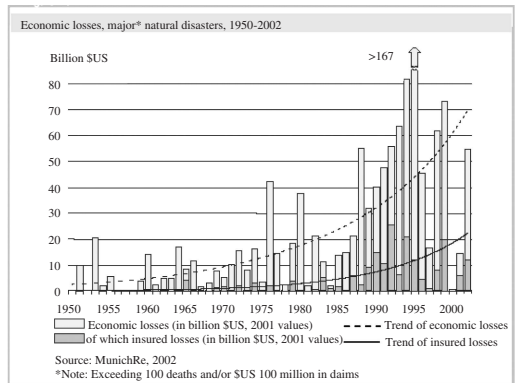
Figure 3. Economic and insured losses caused by natural disasters (MunichRe 2002).

clustered around seismically active areas. Destitution and demographic pressure have led more people than ever before to live in flood plains or in areas prone to landslides. Poor land-use planning, environmental mismanagement and a lack of regulatory mechanism both increase the risk and exacerbate the effects of disasters".

200

Several examples of the negative role played by demographic pressure on the increasing number of disasters can be mentioned (Brand 1988). A reliable hazard and risk zoning for urban planning and development is, therefore, an urgent need, as is clearly stressed by the United Nations (2004). Particularly, hazard zoning should be devoted to prevent further increases of risk, which could produce both an unacceptable number of casualities and economic hardship in many countries. This is, for example, the case of several South American capital cities in which the development of marginal housing in landslide-prone areas is poorly controlled by local planning.

Hazard and risk zoning is not, however, a simple topic because of the many contributing factors: the intrinsic complexity of both landslides and their geological environment; the sector-based approach generally used in many countries, which can produce untimely and, sometimes, misleading answers to societal requests; the lack of understanding and acceptance of concepts of hazard and risk by both the politicians and populations; the absence of data regarding both the existing landslides, even more acute in built-up areas, and urban planning, including the future urban development.

Because of these difficulties, and taking the drastically different conditions in various countries into account, no single approach can be used for land-use planning to manage urban or population growth and to minimize associated risks (Programme Interreg IIC – "Falaises" 2001).

Bearing in mind the addresses of the United Nations, the present paper preliminary discusses typical landslide hazard and risk situations in urban areas as well as the scale of the studies. After a brief review of hazard and risk frameworks, the relevant data for landslide hazard zoning, the criteria used for establishing hazard and risk classes, the validation procedures and how the existing mitigation measures can be taken into account for hazard and risk mapping are therefore examined. Later, risk mitigation strategies based on warning systems are discussed. Finally, several case histories are presented in order to show the usefulness of good policy aimed at risk mitigation.

2   STUDY AIMS AND SCALE

2.1   *Typical situations in urban areas*

Several situations may occur with respect to landslide hazard in which urban areas are concerned:

– in the case of very large dormant landslide zones, or that are generally affected by slow movements that may be permanent or occasional, old villages or new urban areas may extend onto these unstable areas, first because an active landslide zone generally presents a more gentle slope than adjacent stable zones, and thus is assessed as more favourable for settlements; then because the fast development of the suburbs of a city located in a valley may induce inhabitants to occupy unstable slopes in the vicinity of the city center, where stable areas are not available. Well-known examples of South American cities can be mentioned in this respect (Le Paz, Cuzco), but also villages in Italy or Switzerland that have developed on active landslide zones for several centuries (Noverraz et al. 1998);

– parts of towns may be exposed to rock fall hazards either if they are located at the toe of steep rock slopes, like Grenoble (FR) or St-Maurice (CH) or if they are founded at the top of a cliff formed by a rock slab capping a hill like Orvieto (IT) or Laon (FR); in this last case, the development of anthropogenic activities (e.g. mining or sewage pits) may increase the hazard level;

– cities built in debris fans (i.e. Yungay and Ranrahirca affected by the rock avalanche of Nevado Huascarán in Peru) or cities located in the paths of mudflows, lahars (i.e. Mount Rainier volcano, Washington State, USA) and lateral spreading of sensitive clays;

– instability can also be produced by non-conventional land use. Most of the urban development in the city of Manizales (Colombia), settled on an irregular relief, has been built up using a local practice of hydraulic fills: thick fills of volcanic ash are placed in the slopes using water pressure, with a scarce technical control. Several neighborhoods of this city have been affected in the rainy season by erosion, collapse and dis-placement of those fills;

– indirect risks for urban areas may derive from the possible damming of a river by a landslide in the valley upstream of the town, which may cause a flood when the temporary dam fails, as in Grenoble in 1219, or from a mud flow caused by the sudden melting of a snow-capped volcano, as at Armero in Colombia in 1986, or from debris flows caused by catastrophic rainfall events in the nearby mountain range, as at Carmen de Uria or Caraballeda in the northern Venezuela in 1999, or from "seiches" caused by landslides falling into lakes;

– finally, the Colombian town of Restrepo, located in the east flank of the East Andean range, is settled in the left shore of the torrential Upin River, five kilometres downstream of a large landslide. Frequently, the supply of sediments to this river has permitted that the base level of the river has increased by several meters, and now the river bed is higher than the mean level of the town, with a high risk of a flooding.

The previous examples highlight that the major risks in urban areas derive from the unplanned development during centuries as well as from the growth of

marginal housing in landslide-prone areas which imply cut and fill in slopes without appropriate design, construction of leaking sewage and water pipes and a concentration of flow in creeks during rainfall events which accelerate the erosion process and destabilize the slopes along their banks. Due to the dense occupation of such poor urban areas, the risk for life related to a sudden landslide event is more critical every day.

Therefore, landslide hazard and risk studies in such exposed areas imply the assessment of various scenarios according to the type and intensity of the triggering mechanism, in which local and regional developments of landslide mechanisms must be considered, as well as their direct and indirect consequences. Then, such scenarios have to be taken into account in local and general planning, either by prevention actions (like prohibition to build in very exposed areas), mitigation actions (like construction of drainage systems) or preparedness actions (like organization of evacuation plans and installation of warning systems).

2.2 *Study area and scale*

The complexity of the landslide phenomena, and in particular the role of rainfall infiltration and run-off, often require a hazard analysis at the level of the drainage area. A very significant case is that of the valley of Rimac River in Peru, extending over an area of $3,300 \, km^2$ and reaching the Pacific Ocean in the densely populated suburbs of Lima; although the climate at its lower end is nearly dry ($2 \, mm/year$), the intense and sudden rainfall events in its upper reaches (some $800 \, mm/year$) cause devastating debris flows called "huaicos" which may generate damage in extensive flat areas apparently not affected by landslide hazard.

Such extensive investigations first require an analysis at a small scale (1:100,000–1:50,000) in which the hazard is generally expressed in a binomially (yes/no) without any assessment of its intensity. This document is useful for general planning purposes, in which the natural hazards only constitute one of the numerous planning constraints.

Then, in densely populated areas, investigation on landslide hazards have to be improved at an intermediate scale (1:25,000) in order to give more precise delimitations of the exposed zones and to be able to express a reliable gradation of hazard intensity with precise criteria. On the other hand, valuable hazard maps, at this scale, can be useful also in implementing monitoring systems.

Finally, when risk analyses are carried out at the level of plots of land or individual buildings, large scale mapping is required (1:5,000 or larger, depending on the available topographic documents), especially where the value of the land justifies exploiting

any possibility of housing development in safe zones even if they are quite near to landslide zones.

Of course, it is important to adapt the quality of the landslide investigations to both the required scale and the pursued aims. In particular, when large scale landslide maps may severely reduce the value of a plot of land, detailed in-depth data must be gathered by in-situ investigations (boreholes, inclinometers and other techniques) as well as by mathematical modeling which, in turn, can improve the monitoring system at a site scale.

3 FRAMEWORK FOR HAZARD AND RISK ZONING

3.1 *Theoretical background*

In order to be a profitable tool for urban planning and development, landslide hazard and risk zoning must be clearly placed in a "risk management" framework which, referring to Fell et al. (2005), comprises "risk analysis" and "risk assessment".

Risk analysis is based on hazard analysis (landslide or danger characterisation and analysis of frequency) and consequence analysis (characterisation of consequence scenarios, analysis of probability and severity of consequence). Risk estimation is, therefore, obtained by a suggested formula that allows the integration of the hazard identification with the consequence analysis.

Once this process is concluded, risk evaluation calls for policy-maker decisions regarding risk acceptability or treatment and priorities to be set according to a complex and, sometimes, iterative procedure that must consider both technical and socio-economic aspects. At the end of the risk-assessment procedure, and taking the selected option into account (risk acceptance or avoidance, likelihood or consequence reduction), a treatment plan aimed at risk mitigation and control is devised as the final stage of the risk-management process.

Within the framework proposed by Fell et al. (2005), hazard zoning turns out to be a part of both risk analysis and risk assessment since the hazard distribution must be compared with the urban plan. Development can thus be authorised in terms of cost-benefit analysis and taking the available mitigation and protective measures into account. Risk zoning can be related to risk estimation and risk mitigation, highlighting the most threatened areas where remedial, protective, warning and even evacuation measures must be implemented.

With reference to the first stage of the process, identified as risk assessment by Ho et al. (2000), it must be emphasized that, frequently, hazard and risk zoning can imply problems and requires attention for

several reasons, including the absence of a standardized procedure for hazard and risk mapping; the size of the study area and the need of maps at various scales; the political and economic implications; the weakness of the available data and/or, sometimes, the difficulty related to the evaluation of their reliability and so on.

Fortunately, the previous reasons are not pertinent everywhere, as some countries or regions have already progressed in the development of specific procedures that allowed the solution of practical problems. However, the current use of such procedures calls for some considerations due to several open questions, as discussed in the following section.

3.2 *Open questions*

An overview of methods and procedures for hazard and risk zoning is provided by Einstein (1988), who analyzes the landslide risk mapping framework with many examples of danger, hazard, risk and landslide-management maps.

Bonnard et al. (2004a), within the IMIRILAND Project, analyze the consequence of risk studies on land planning procedure as well as the tendency, in the European countries, of risk management policy; moreover they give suggestions for future risk-management studies not disregarding the open questions.

Consideration of hazard and risk mapping for land-use management and development planning are also furnished by Ho et al. (2000) who outline the significant advance made all over the world. After brief comments on the meaning of some maps, they show the relevance of quantitative risk assessment (QRA), which is strongly recommended through detailed key messages.

To deepen the open questions of Bonnard et al. (2004a) and the suggestions of Ho et al. (2000), two relevant experiences are here summarized, regarding the hazard and risk zoning procedures respectively developed in France (Europe) and in Hong Kong (China).

3.2.1 *Experiences in France and Hong Kong*
France is located in Central-Western Europe on a total surface of 544,965 km^2, where 60 million people live. Its territory is systematically affected by several natural hazards among which floods are prevailing but landslides assume a relevant role from a socio-economic point of view.

To deal with these hazards, the technical and scientific communities have been engaged, since the 1970's, in producing landslide-related maps as documented by several authors and discussed by Einstein (1988) who places such maps in the landslide-risk mapping framework. The main contents of the maps are summarized below.

The first maps produced in France are those of the ZERMOS project (*Zones exposées à des risques liés aux mouvements du sol et du sous-sol*), which dates back to the 1970's (Humbert 1972, 1977, Antoine 1978). They have been produced at 1:25,000 scale and cover different terrain instabilities such as subsidence and landslides. Inside these maps three zones are identified to distinguish the absence of movements, the presence of active movements, and the potential for future activity. Lines and figurative symbols are utilized for the existing instability; scarps and run-out zones are also marked inside such maps, which can be classified indeed as "danger maps" according to the glossary definition.

During the summer of 1982, the PER (*Plans d'Exposition au Risque*) were promulgated by law with the aim of increasing risk prevention (DRM 1990). According to these plans, maps should be developed at scales of 1:5,000 and/or 1:10,000 to be compared with urban planning documents. The final goal of the maps was risk mapping at an urban scale and the set up of regulations for land-use planning. However, such maps cannot be classified as "risk map", as they do not strictly consider all the terms (i.e. hazard and vulnerability) necessary for risk assessment.

Due to the enormous cost of the project at a national scale, PPR (*Plans de Prévention des Risques Naturels*) were successively introduced for risk mapping at 1:25,000 scale (Besson et al. 1999, Garry & Graszk 1997, Graszk & Toulemont 1996) having a regulatory function for urban development and, at the same time, connection with urban planning. The meaning of the produced maps can be considered similar to that of the PER maps.

Interesting comments were furnished by Leroi (1996) on problems faced by the technical and scientific communities, the political and cultural choices, the financial arbitrage related to such a difficult topic. Thus, the author introduced risk mapping as a problem at different scales, with each scale having a well defined meaning and aim (Fig. 4).

Concerning Hong Kong, the territory is situated at the mouth of the Pearl river on the south coast of China; its total area is 1,050 km^2, and in 1988, its population was 5,6 million. Due to both the very hilly terrain over a large part of the area and the impressive growth of population during the previous decade, buildings and other structures were built on the mid-slopes and upper slopes of natural hillsides. As a consequence of the intensive land-use, and without a well-defined land-use planning, the territory experienced catastrophic landslides that resulted in fatalities and large economic costs (Vail 1984, Vail & Beattie 1985, Lumb 1975, Brand 1984, 1985, Burnett 1987).

To mitigate the landslide hazard, the Geotechnical Control Office (GCO) was established in 1977; two years later the Geotechnical Area Studies Programme

203
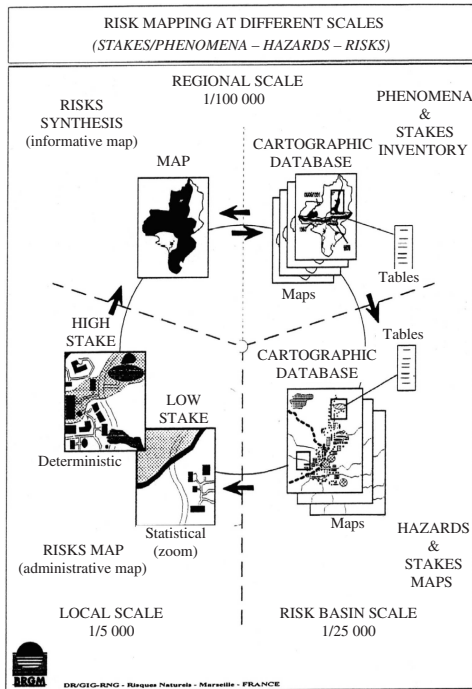
Figure 4. Risk mapping at different scales (Leroi 1997).

Figure 5. Example of individual risk contours obtained by QRA; Lei Yue Mun squatter villages (Atkins Haswell 1995).

(GASP) was initiated and directed towards two aspects: (a) Regional studies (at scale of 1:20,000), (b) District studies (stage 1) and District studies (stage 2) to be both carried out at a scale of 1:2,500.

Regional studies were performed subdividing the territory in eleven sub-areas, 50–100 km² in size, essentially on the basis of photograph investigation, site reconnaissance and existing geotechnical information. The stage 1 of District studies essentially followed the same planning, even though at a more detailed scale, whereas during stage 2 an accurate geotechnical assessment was carried out; both stages 1 and 2 were performed all over the territory within areas having a size of 2–4 km² each.

The results of regional studies were summarized in 7 maps [*Terrain Classification Map, Landform Map, Erosion Map, Engineering Map, Physical Constraints Map, Geotechnical Land use Map (GLUM), Generalised limitations and Engineering Appraisal Map (GLEAM)*], whereas the District studies produced 6 maps [*Terrain Classification Map, Surface Hydrology Map, Vegetation Map, Engineering Data Sheet, Engineering Geology Map, Geotechnical Land use Map (GLUM)*]. These maps are described in detail by Brand (1988) who stresses the relevance of GLUM and GLEAM maps, which can be considered as danger maps for urban planning and development.

Thanks to the high quality of the available data, a wide range of limit-equilibrium slope-stability analyses were completed. The calculated value of the safety factor, in reference to groundwater conditions produced by rainfall with a ten-year return period, was therefore associated with three risk categories respectively defined high, low and negligible concerning both the human life and the economic damage. In the paper of Brand (1988), reference is also made to the use of a probabilistic approach for both risk assessment and acceptability of failure consequence.

Starting from the impressive knowledge and data sets acquired during the time, the risk assessment has been successively developed in Hong Kong using the quantitative risk assessment (QRA) which has been applied to quantify both the global risk failure posed all over the territory by some kind of slopes and the site-specific risk at a given site. Several papers describing such studies are summarized by Ho et al. (2000), who give an overview of case studies involving the use of QRA in landslide risk assessment (Fig. 5).

3.2.2 *General suggestions*

The experience gained in France and Hong Kong, as well as the widely available literature, suggests that – due to the complexity and, sometimes, the extension of the geological context to be analyzed – hazard and risk zoning calls for theory and wide-zoning practice. Moreover, the financial support over a long period of both the Central and Local Authorities as well as the participation of the public are absolutely necessary.

From a technical point of view two different levels of zoning are almost constantly analyzed: at an intermediate scale (1:25,000 or smaller) and at a large scale (1:5,000 or larger).

Concerning the first level (1:25,000), present knowledge suggests that zoning must be produced using a qualitative approach that could be usefully applied even at the largest scales, when a lack of risk culture

204

Figure 6.   Input elements to zoning maps.

and further data sets); the hazard map would take that information and adds frequency of sliding; and the risk map adds the consequences to the elements at risk by the characterisation of consequence scenarios (elements at risk and vulnerability of elements at risk) and temporal probability analyses.

At the intermediate scale (1:25,000), landslide susceptible areas would show as input the classification, location, areal extent and, possibly, other geometric characteristics of each landslide, creeping zone and potential sliding; the activity classes of landslides; the areas onto which the potential sliding may travel with qualitative and/or quantitative information on past events. Landslides intensity should be based on simple parameters describing the destructiveness of landslides or potential sliding as, for instance, the potential post-failure velocity. Whenever possible, other information can be useful to improve the landslides characterisation as those regarding the volume, the qualitative or the quantitative estimation of the actual rate of movement, the data set on geotechnical aspects, triggering factors and so on. Unfortunately, many of such data are difficult to collect in a systematic way at an intermediate scale; however, the danger map can be improved with time provided that the state of the nature maps have been produced according to a high quality standard.

At a large scale (1:5,000 or larger) the above elements, even if implemented in a qualitative risk procedure, must be considerably improved with quantitative data on volumes, the actual rate of movement, more advanced parameters describing the landslides intensity; moreover, advanced geotechnical, triggering factors and further data sets are necessary. If well related such maps, even those at intermediate scale, may allow mathematical and quantitative risk assessment (QRA). Of course the choice of the most suitable model is strictly related to both the scale and the quality of the available data.

The danger map, when carefully realized, can considerably simplify the analysis of sliding frequency and the compilation of the hazard maps that must clearly indicate the likelihood of landslide magnitude (velocity and/or volume). Generally, at 1:25,000 scale, the likelihood is expressed in a qualitatively way on the basis of indicators such as, for instance, some geomorphological factors (i.e. state of activity). On the other hand, at 1:5,000 scale, the quantitative hazard estimation requires the use of advanced mathematical models such those relating, for example, the triggering factors to the landslide mobilization. However, such models need an accurate data set and an appropriate calibration inside sample areas where monitoring and other in-depth investigation are systematically completed.

With respect to consequence analysis, that is necessary to produce the risk maps, different procedures

is clearly recognized. On the contrary, at the second level (1:5,000 or larger, as well as at a site-scale) the quantitative risk assessment (QRA) must be preferred, above all, where good and extensive knowledge is available. Moreover, independently from the utilized approach, all the maps (state of the nature, danger, hazard and risk map) must be clearly addressed and defined since, too often, confusion arises amongst danger, hazard, consequence and risk. Finally, with reference to the input elements to zoning maps, some suggestions can be furnished considering both the terms in the glossary and the available literature.

Passing over the state of the nature maps, the input elements to danger, hazard and risk zoning maps are schematically shown in Figure 6. Particularly, the danger map must include the landslide characterisation (landslide susceptible areas, landslides intensity

must be adopted according to the reference scale. At an intermediate scale, the analysis should be performed by appropriately selecting the reference area, the most relevant elements at risk within, and criteria for an overall qualitative estimation of the consequence. On the contrary, at a large scale, each element at risk, its vulnerability, temporal probability and criteria able to transform the individual into an areal estimation of the consequences, taking potential development programs into account, should be considered.

Finally, for risk zoning maps, risk estimation based on a well-known formula is absolutely necessary, whereas the study is carried out at either intermediate or large scale. A simple formula like that proposed by Varnes (1984) or Einstein (1988) could be better used at 1:25,000 scale, while a more complex equation (Fell 1994, Leroi 1997) should be preferred at 1:5,000 scale.

At the present, the previous described analyses have not been exhaustively developed, at both intermediate and large scale. Therefore, hazard and risk zoning can be considerably improved on condition that a wide range of research is developed with the aim of identifying, testing out and choosing reliable procedures (Bonnard et al. 2004b). These procedures must have a clear meaning from a theoretical point of view and, at the same time, the capacity to simplify the production of maps at various scales, in order to connect the regional and local requests of both risk assessment and mitigation.

Starting from the above considerations, the next chapter discusses in detail the objectives of hazard and risk zoning maps; the most relevant inputs to landslide hazard and risk zoning; the criteria for defining hazard and risk levels and subsequent zoning. Finally, the validation procedures, that are absolutely necessary in order to estimate the reliability of zoning procedures, are illustrated.

4 ZONING FOR HAZARD AND RISK MAPPING

Landslide hazard and risk maps have different objectives within the framework of landslide risk assessment and management.

Landslide risk maps provide a global view of the expected annual damage due to the potential landslide hazard by identifying the most vulnerable elements that are threatened. Based on the information supplied by such maps and cost-benefit analyses, either protective or reinforcement works can be envisioned to minimize the risk level, whereas alert systems can be established in places in order to protect the human lives. Risk maps, however, are documents that are not intended for direct use in urban planning and development because they generally reflect the current situation of potential damage but not the spatial distribution of the hazardous zones. In that respect, non-urbanized areas are often displayed as having low risk level regardless the level of existing hazard which is not quite appropriate.

The spatial distribution of hazard is shown on landslide hazard maps that are used to avoid the development of threatened areas, representing the most efficient and economic way to reduce future damage and loss of lives. On the other hand, such maps provide the appropriate elements of decision for considering the feasibility of the development with or without any stabilisation or protective countermeasures.

Zoning for both landslide hazard and risk mapping introduces the spatial dimension of the landslide hazard management. The purpose of zoning is to divide the studied area into homogeneous compartments (units) in which hazard or risk is expected to attain a similar level. To be profitably used for urban planning and development, the hazard and risk maps must be performed at an appropriate scale in order to avoid controversy in delivering building permits, expropriation and compensating measures (Leroi 1996). However, the most large scale maps (usually 1:5,000 and larger) may create difficulties due to the high level of refinement required by the necessary data (DTM, geological maps, superficial formation maps, landslide inventory, vegetation cover, groundwater regime, soil/rock properties, etc).

Notwithstanding such constraints, in the following sections the attention is essentially devoted to the largest scale, even though suggestions and comments could also be applied to the intermediate scale (1:25,000).

4.1 *Hazard zoning parameters*

Ideally, a landslide hazard map should provide information concerning the spatial probabilities and frequencies of all anticipated landslide types, the expected travel trajectories and the intensities within the mapped area (Hartlén & Viberg 1988).

A significant amount of effort has been made during the last decades in developing procedures for hazard mapping which, however, have to face some important challenges.

Landslides are gravitational processes that display a variety of motion mechanisms and propagate at different velocities, with travel distances strictly dependent on the landslide mechanism, the mobilised volume and the characteristics of the path which cannot always be predicted beforehand. Moreover, the spatial assessment of the magnitude-frequency relationships is not easy to obtain. Finally, the definition of landslide hazard levels and subsequent zoning – no matter whether they are expressed in qualitative or quantitative way – should have a correspondence with the damaging

capability of the phenomena as well as the feasibility of implementing countermeasures.

Despite such constraints, quite often classes of the different landslide hazard components are defined arbitrarily rather than on landslide risk management considerations.

4.1.1 *Defining landslide susceptible areas*

As previously stated, landslides characterisation calls for zoning susceptible areas that can be pursued by many approaches. Early attempts were based on qualitative overlaying of geological and morphological slope-attributes (Nilsen et al. 1979), and soon evolved to more sophisticated assessments involving data treatment and multivariate analyses (Neuland 1976, Carrara 1983). The reader will find comprehensive summaries in Carrara et al. (1995), Van Westen (1994, 2004).

Anyway, to be exhaustive, the zoning of landslide susceptible areas have to include both the potentially unstable slopes (Brabb 1984) and the area affected by the arrival of landslide debris (propagation area). Not considering this area will lead to an underestimation of the risk over the exposed elements (Leroi 1996).

Notwithstanding the availability of several methods for estimating the distances travelled by landslides – respectively based on empirical, deterministic or mathematical models (Sassa 1988, Sassa et al. 2004, Coromins 1996, Pastor et al. 2003) – only a few experiences have been published in which the travel distance of landslide debris has been taken into account in defining susceptible areas (Corominas et al. 2003b, Michael-Leiba et al. 2003).

Ayala et al. (2003) have combined the concept of reach (travel distance) angle with a numerical model for delineating the area affected by rockfalls. The method is based on the intersection of the line of sight dipping according to the angle of reach, from the potential rockfall source, with the ground surface. The line defined by linking all the intersections is the minimum reach angle line (MRAL); the procedure has been implemented in a GIS environment (Fig. 7). Zoning criteria have distinguished between a high susceptibility area (the scarp or rockfall source), a medium susceptibility area (the run-out zone) and a low susceptibility area (a stripe of land of 100 m wide, defined for safety purposes). The zoning criteria can be refined by using boundary lines of expected travel distances determined by using trajectographic analyses (Copons et al. 2004).

4.1.2 *Zoning landslide intensity*

Once the susceptible areas have been defined, intensity (magnitude or severity) of the landslide phenomena is a key parameter in landslide (danger) characterisation, which lack a standardised accepted definition and scale. Nevertheless, it is widely accepted that

MINIMUM REACH ANGLE SUSCEPTIBILITY MAP
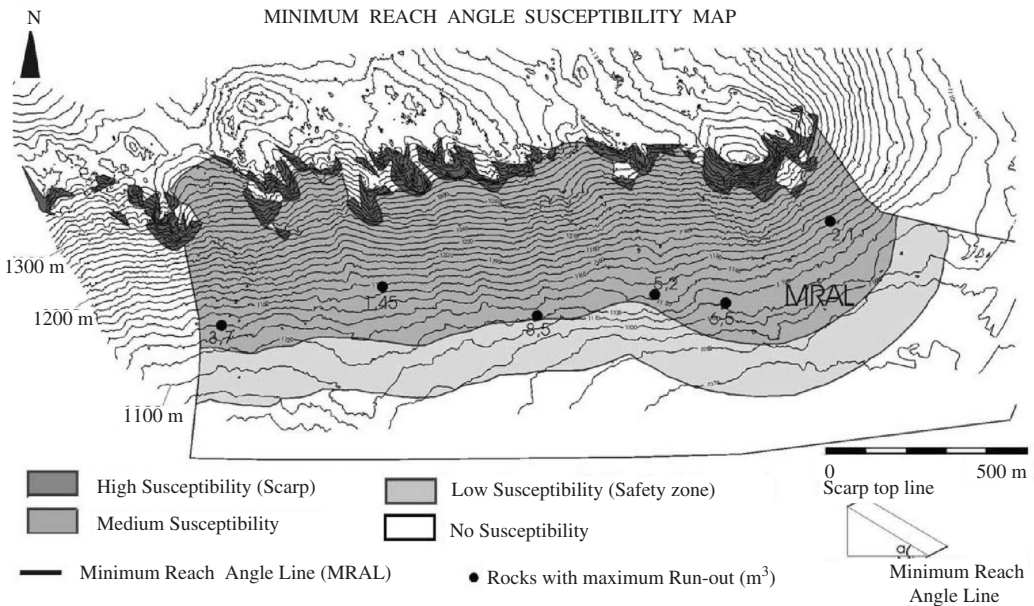
Figure 7. Rockfall susceptibility map of the La Cabrera Sierra (Ayala et al. 2003). Boundary of the susceptible area (MRAL) has been traced using the minimum reach angle for the expected rockfall volume.

207

landslide intensity is the capability to produce damage. Concerning the reactivated landslides, the damage can be related to the slope movement stage, as in the case analysed by Bonnard and Noverraz (1984), who use rate of displacements of the landslide units (>10 cm/yr, 5–10 cm/yr, 1–5 cm/yr and presently stable zone) to select sectors that must be evacuated or continuously monitored. Instead, first time-failures and subsequent rapid movements of large masses generally have catastrophic consequences.

Hungr (1997) defined landslide intensity as a set of spatially distributed parameters describing the destructiveness of the landslide. These parameters are varied, being the maximum movement velocity the most accepted one although total displacement, differential displacement, depth of moving mass, depth of deposited mass, depth of erosion are alternative parameters. Nevertheless, by keeping in mind the design of protective structures, other derived parameters like peak discharge per unit width, kinetic energy per unit area, maximum thrust or impact pressure may be also considered. However, no direct correlation can be established between intensity and both the landslide mechanism and size because intensity is also given by the relative location of the threatened elements with respect to the landslide source, transit or deposition area, as in the case of many rockfall events (Fig. 8).

In conclusion, the establishment of a landslide intensity scale for danger zoning requires first the discussion on how it will affect the definition of hazard levels. In terms of landslide hazard management, intensity could be defined referring to the resistance (resilience) of the exposed elements, or the possibility of occurring fatalities, but thinking on cost-benefit bases it should consider the capability of either stabilization or protective works. These different approaches can be observed, for instance, in the intensity levels defined for Swiss hazard maps which were based on the expected damage on both persons and buildings (Lateltin 1997), while in the case of the Andorra Principality hazard mapping, intensity was defined taking the resistance of the protective structures, particularly for rock falls, and the feasibility of stabilization works into account (Corominas et al. 2003b).

4.1.3 Frequency classes

It is recommended that frequency will be expressed as probability of occurrence or by a return period (Lateltin 1997) based on hazard acceptability criteria.

Frequency of landsliding can be determined from historical data, relation to triggering event frequencies (e.g. rainfall, earthquake) with known annual exceedance probabilities, or relating pore water pressures to rainfall or snowmelt exceedance probabilities, which will produce instability conditions. However, care should be taken in the establishment of landslide frequencies, based on either historical or prehistorical
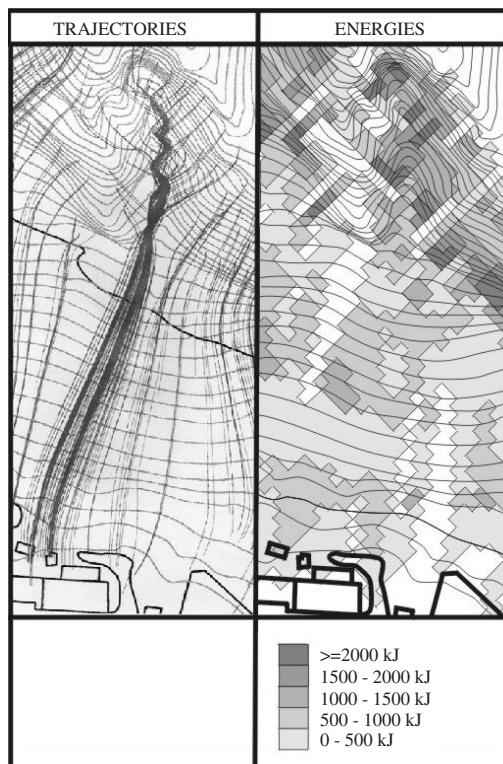
Figure 8. Rockfall trajectories (left) and spatial distribution of the kinetic energy in KJoules (right) for simulated rockfall events in Andorra (Copons et al. 2004).

(silent witnesses, landslide dated series) because the conditions responsible for a given landslide frequency in the past may no longer exist (Lateltin 1997). Similarly, land-use changes like forest logging or forest spreading may change significantly the magnitude (intensity)–frequency relationships.

Several methods have been proposed for defining landslide frequency classes, based on landslide inventories and qualitatively describing landslide activity by a geomorphological assessment. Suggested activity classes (WP/WLI 1993, Cruden & Varnes 1996) include: active, suspended, dormant, relict and stabilized landslides.

Activity classes have also been used to produce landslide hazard maps (Carrara et al. 1991), although these classes require some additional judgement to be translated in recurrence periods or probability of occurrence before the resultant maps could be considered as real hazard maps.

Ideally, landslide hazard maps should also provide some insight on when first-time failures might occur, although this is an unsolved challenge. Frequency and return period are valid concepts for repetitive events

208

but not for unique ones. This issue may be approached by using predictive models. For instance, maps showing safety factor values of the slopes for different rainfall and/or groundwater scenarios are already available in some regions (i.e. Savage et al. 2004). In such cases it is possible to determine the groundwater conditions that may lead a given slope to fail for the first time and the probability of occurrence (which is obtained from annual exceedance probability of the triggering factor). However, other factors such us stress release mechanisms or weathering processes can introduce a great degree of uncertainty in the obtained figures.

4.1.4 *Zoning landslide hazard levels*
Landslide hazard is the result of the interplay of different factors, some of which can be obtained and mapped easily and some not. As previously stated, zoning must include both landslide detachment zones and the deposition areas.

Referring to the detachment zone, it must be considered that changes produced by urban development may induce changes in the behaviour of the slopes. For instance, overloading of the slopes by new constructions or leaks from the sewage system can aggravate the previous stability conditions.

As it concerns the deposition zone, it must be taken into account that progression of the destabilised mass can be impeded by the presence of buildings, producing the stoppage of the movement, the diversion of the moving mass or the thickening, although the case of Las Colinas in Salvador in 2002 proved that the progression of a fast landslide mass could not be limited by small houses.

A particular challenge for landslide hazard maps is predicting the evolution of ongoing instability situations such as the rate and extent of a receding cliff in both coastal and river rain areas which are subjected to erosion and undermining action of streams, or that of landslide head scarps developed in weak and unstable materials, that in the case of sensitive clays can reach several hundreds of meters and even kilometres. Successive landslides and removal of the material by erosion generate new slope geometries that have different stability conditions. It has been observed that development boundaries established for safety beyond the unstable crest may become obsolete in a matter of few decades (Fekner 2002). In such cases it is necessary to integrate the cliff receding rates in the maps, which are often based on the observation of series of aerial photographs or on results of numerical models (Walkden et al. 2002). Similarly, the consequences of future climate change or land-use changes are seldom considered and this fact introduces a degree of uncertainty that must be quantified.

A source of uncertainty can also come from cascading effects such as the temporary blockage of debris flow material by bridges and subsequent breakage.

Finally, in some areas protective and stabilization works have been carried out. The affected slopes must be considered in terms of hazard (residual hazard). According to the type of works, a straightforward consideration of a reduction in hazard level cannot be justified.

4.2 *Risk zoning parameters*

4.2.1 *Vulnerability of the elements at risk*
The characterisation of consequence scenarios is based on elements at risk and vulnerability of elements at risk.

The classifications of elements at risk for landslides are very preliminary compared to other hazards. They range from generic classifications based on the main land uses, namely urban, industrial, infrastructures, or agricultural (Calcaterra et al. 2003, Remondo et al. 2003) to detailed structural analyses of the buildings (Spence et al. 2004) which require specialized expertise. A different approach considers that main damage to the exposed elements is structural, corporal and operational (Leone et al. 1996).

Vulnerability is the degree of loss of an element within the landslide affected area (Fell 1994). Procedures for assessing the resistance and vulnerability to earthquakes and floods are relatively well established and accepted. On the contrary, the assessment of vulnerability of the elements at risk (e.g. buildings, persons) to landslides still requires significant efforts in terms of definition and grading.

First, the main loads that landslides can exert on exposed elements depend on displacements and associated deformation, in particular: tilting; pressure, either lateral or resulting from impact; accumulation due to transport; and ablation or undercutting due to the erosion (Leone et al. 1996).

Moreover, within a large landslide, there exist sensitive areas where damage will be more likely (or higher), no matter the total landslide displacement or the released energy will be. This occurs, for instance, in the landslide boundaries, such as the head, or in local scarps where tensile stresses are developed with the result of tension cracks, surface ground depletion and local rotation. Similarly, large differential deformations are expected in the landslide foot where thrusting and bulging of the ground surface might take place.

Finally, the resistance of a building might be enough to resist the impact of a falling block but it can be insufficient to avoid the development of tension cracks due to differential displacements produced by a translational slide. On the other hand, the vulnerability of lives and properties may be different and, for instance, a house may have a similar high vulnerability to both slow-moving and rapid landslide, while a person living in it may have a low vulnerability in the first case (Fell 1994, Fell & Hartford 1997).

For the above considerations, some specificities must be taken into account in the assessment of the

vulnerability to landslides. For a similar structure or building, the expected damage will depend on three factors: (i) the type of landslide mechanism (rockfall, debris flow, slide, etc); (ii) the intensity (velocity, volume); and (iii) the relative location of the vulnerable element in relation to the landslide trajectory (Table 1) or to the position inside the landslide affected area.

In order to include these relationships, the different landslide types and intensities are faced against the vulnerable elements in Figure 9. In any case, vulnerability assessment with such accuracy can be usually performed, at a very detailed scale, where well-documented landslides are available. This is the case of La Frasse in Switzerland where, after detailed reconnaissance study and systematic monitoring, a map showing different landslide units, moving at different displacement rates could be prepared (DUTI 1983, Noverraz & Bonnard, 1990).

In order to obtain reliable results, the performance of structures during past landslide events is also a suggested criterion, taking also the quality of maintenance works into account. In that respect, the preparation of inventories of the damage caused by past events and back-analyses of impact velocities and performance of the structural elements (Faella & Nigro 2003) are really indispensable.

4.2.2 Risk zoning

Risk cannot always be readily determined because of the difficulty in assessing the elements at risk (in a

Table 1. Vulnerability to destruction of people, buildings and roads by debris flow events in Cairns, Australia (Michael-Leiba 2003).

Unit	People	Buildings	Roads
Hill slopes	0.05	0.25	0.3
Proximal debris fan	0.5	1.0	1.0
Distal debris fan	0.05	0.1	0.3

forward planning situations) and vulnerability of the elements at risk. There is also a need to make some assumption about the temporal probability of the elements at risk. For buildings is not an issue (it is 1.0), but for persons it will be less than 1.0 in most of the cases. In practice for zoning it is common to assume persons are in the area affected by the landsliding 100% of the time. This is conservative but has precedents in other industries.

Risk classes must also take the risk culture into account which is different from one society to another, particularly when comparing non-developed and developed countries. As a consequence, in what concerns landslide risk, there is almost no indication of what is an acceptable, tolerable and unacceptable risk. Therefore, we must first distinguish between risk to life and risk to properties.

Risk to persons is evaluated by the loss of lives. According to the IUGS (1997), the incremental risk from a hazard should not be significant compared to other risks to which a person is exposed in the everyday life. The probability of the individual risk is, therefore, compared with the probability of natural death. A normally accepted order of magnitude of a hazard of death related to a particular activity is around 10^{-4} per annum (Archetti & Lamberti 2003). The Australian Geomechanics Society (AGS 2000) considers as tolerable a value of 10^{-4} per annum for the person most at risk in existing constructed slopes, and 10^{-5} per annum in newly constructed slopes while acceptable risk is considered to be an order of magnitude smaller than the mentioned figures. This criterion is similar to that adopted by Hong Kong for new and existing developments (ERM 1998, Ho et al. 2000). A graphical view of the risk acceptability criteria is given by F–N curves (Fig. 10). These curves represent the relationship between the annual probability of an event causing N or more fatalities and the number of fatalities. The boundaries between acceptable, tolerable (or As

	Buildings at risk				
	SL		M	H	S - Squatter

Landslide characteristics: T, M, S, V, R

S - Squatter
L - Low-rise building
M - Multi-storey building
H - High-rise building

T - Type of failure
M - Mechanism of failure
S - Scale
V - Velocity
R - Runout distance

Location, nature and other properties of low-rise building

Vulnerability		Distance to slide (m)			Nature		...
Scale (m³)		<10	10-50	>50			
	$<10^2$	0.3	0.2	0.1			
	10^2-10^3	0.4	0.3	0.2			
	10^3-10^4	0.6	0.5	0.4			
	$>10^4$	1.0	0.9	0.8			

Figure 9. Example of structural vulnerability matrix (Dai et al. 2002).

210

Low As Reasonably Practicable), and unacceptable may be used as a criteria for risk zoning. A review of criteria used for establishing acceptable and tolerable risk in the industry and several administration offices is found in Fell and Hartford (1997).

The vulnerability matrix method proposed by Leone et al. (1996) gives an example of allowing the consideration of a wide range of situations and reducing the subjectivity in the assessment of landslide risk. It is transparent because it is possible to calculate indexes of economic (direct and indirect), functional and human losses. When multiplying these indexes by the annual probability of occurrence of the landslide and the number of exposed elements, it will provide a quantitative estimation of the risk (Fell et al. 2005).

This type of calculation can easily be carried out for zoning studies based on subareas defined by GIS. However, to the authors' knowledge, there exist no standardised costs that can help in defining risk classes.

Finally, residual risk, that is to say, the risk remaining after mitigation or protective measures have been undertaken, has to be considered in urban areas. At this end, risk maps must be documents easily updatable and any change, either in hazard assessment (i.e. by implementing countermeasures) or in the elements at risk, have to be incorporated (Copons et al. 2004). However, it should be kept in mind that residual risk has different meanings. For instance, in Switzerland (Lateltin 1997), areas with residual risk are those affected by a hazard of high intensity but with very low probability of occurrence.

4.3 *Validation of zoning*

Despite the large amount of work carried out and the availability of landslide hazard assessment methods, they seldom have been validated. Nevertheless, there is a need of checking the predictive capability of future landslides, in both space and time, which strictly depends on the quality of the input data used and, among them, the landslide inventory. Particularly, the latter plays a fundamental role as either dependent variable in statistical analyses or for validation purposes.

An exercise of independent landslide inventory mapping performed by three groups of geomorphologists in the Italian Apennines (Ardizzone et al. 2002) has shown that discrepancies among maps were very high (in the range of 55–65%). When all the maps were overlain, the spatial mismatch of the landslide deposits polygons was over 80%. These authors also analysed how such errors might affect areas with villages and infrastructures, considering a buffer of 100 m width from roads and urban areas. Comparison of the landslide inventory maps (Fig. 11) showed that the disagreement was 58.9% of the mapped landslide area. The mismatch can be strongly reduced up to 20–25% by working with morphologically-meaningful-terrain units and by training the members of the group mapping the area. Similar results were obtained in another hazard mapping exercise by three different teams in Alpago Basin, Italy (Van Westen et al. 1999); the area mapped equally by all three teams is only 35% and landslides inventoried differ in almost an order of magnitude. These results show that we are still far from having reproducible results for landslide hazard assessment.
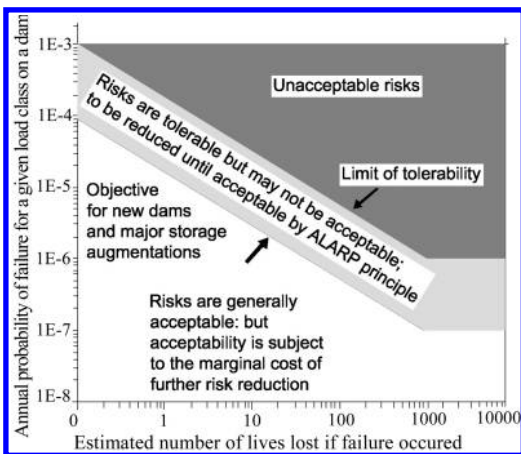
Figure 10. ANCOLD criteria for societal risk (ANCOLD 1998).
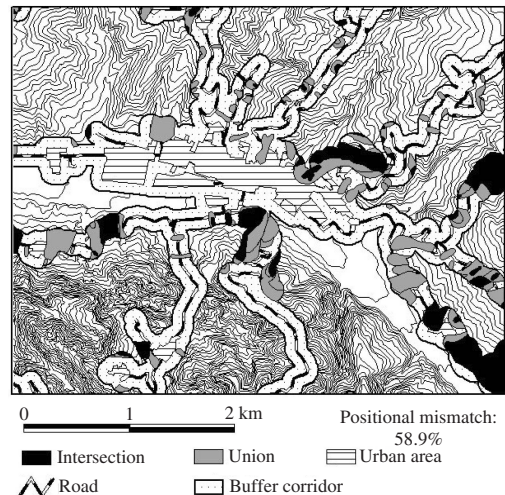
Figure 11. Comparison of the landslide inventory maps prepared by two groups of geomorphologists of Milano and Perugia in an urban area of the Staffora basin, Italy (Ardizzone et al. 2002). Landslide coincidence (intersection) and disagreement (union) is indicated. The position mismatch is 58.9% (Ardizzone et al. 2002).

211

The IUGS Working Group on Landslides understood that the variety of approaches used in assessing the different components of landslide risk can result in significant differences in outcome if the same problem is considered separately by different practitioners (IUGS 1997). However, the objectivity in the assessment of landslide hazard does not necessarily result in an accurate hazard map. For example, if a very simple but verifiable model is used or if only few parameters are taken into account, the procedure may be highly objective but will produce an inaccurate map (Soeters & Van Westen 1996). In such a situation, a key issue is finding a reliable procedure for validating the susceptibility and hazard maps prepared by one or more teams. Validating process is not trivial. A common method for validating is to consider a landslide population independent from that used to assess landslide hazard and calculate the percentage of landslides within each susceptibility or hazard class.

Several strategies have been developed to obtain the landslide control set. The strategies differ basically in the method for obtaining the landslide set (Remondo et al. 2003): (a) the landslide inventory of the study area is split in two groups, one for estimating hazard and another for validation (i.e. Carrara et al. 1991); (b) the hazard assessment analysis is carried out in a part of the study area and the map (model) is tested in another part, obviously with different landslides; and (c) the hazard assessment is carried out using landslides occurring in a certain period and validation is performed with landslides occurring in a different period. The latter is the most adequate to test the validity of the prediction made; it has been performed after the occurrence of extreme events in zones where previous susceptibility or hazard mapping were available (Irigaray et al. 1999).

The results of the exercises performed with different groups of landslide specialists mentioned above and the analysis validity procedures confirm that discrepancies are mostly due to the quality of the input data used in landslide hazard and risk assessment rather than on the methodologies used. In particular, the landslide inventory (type, activity, number and extent of landslides) is the basis for hazard assessment and its validation.

The most frequent technique used for producing landslide inventories is aerial photo-interpretation. Several studies have shown that differences between the interpretations carried out by different observers can be very large (Carrara et al. 1992, Dunoyer & Van Westen 1994).

Powerful computer programs and GIS technology have given the opportunity to solve complex problems requiring large amount of data and computational capabilities. However, it is not always true that computer-generated maps could be more objective, accurate and credible than hand made maps (Carrara et al. 1999).

We still have to rely on field work performed by skilled and experienced professionals for obtaining some key parameters. In any, case, when data available are insufficient for analytical evaluation of failure (or reactivation) probability and its intensity, error bars in deriving magnitude-frequency relationships can be more than two orders of magnitude, and errors in risk may be larger (Michael-Leiba et al. 2003).

5 RISK MITIGATION STRATEGIES

5.1 *Urban planning and emergency plans*

At the end of risk-estimation procedure, acceptance or avoiding of both hazard and risk must be selected and priorities have to be individuated (Fell et al. 2005). Of course, such relevant decisions can be made easier by hazard and risk zoning which can direct the urban planning and development, the emergency plans and the countermeasure planning.

Concerning the first aspect, it can be observed that many cities and towns in developed and developing countries, that are affected by landslide-prone areas, have been applying legal rules for their development for several decades, which are specified in the local planning documents and regularly updated. The most common practice includes the delimitation of zones in which building is either prohibited or restricted to some types of constructions with a low occupation level. Sometimes prescriptions can be imposed with respect to preliminary geotechnical studies or simply information is given to the owners regarding the existence of a low intensity hazard level due to landslides.

The main problem is, however, not the elaboration of local plans or rules for the use of landslide-prone areas, but the long-term applicability of such plans. For instance, in the capital of Honduras, Tegucigalpa, the planning documents elaborated in the seventies excluded any construction on the zone of Berrinche landslide on the left bank of Comayagua River; but after several decades of non-respect of these prescriptions, hundreds of houses built at its toe were destroyed by the sudden reactivation of the slide following Hurricane Mitch.

Another situation in developing countries may occur when marginal housing is suddenly expanding outside of the planned building areas, even despite of the existence of strict limitations or regulations, and implies a high risk situation due to uncontrolled debris flow hazard, as it is the case in the outskirts of Pichincha volcano, west of Quito, the capital city of Ecuador. It is even more difficult to evacuate these zones as the municipal services themselves are supplying electricity and water to these new housing developments.

Due to the previous considerations, emergency plans and remedial measures must be strongly implemented,

within the short time, to limit the consequence of landslides. In the present section a significant example of both emergency plan and subsequent risk mitigation is discussed, whereas the second part of the Chapter is devoted to monitoring systems aimed at the improvement of emergency plans.

5.1.1 *The case of Falli Hölli village management*

The Canton of Freiburg, in the Western part of Switzerland, presents a high percentage of landslide-prone areas, i.e. more than 10% of the whole cantonal area, especially in the Prealps, where Flysch formations are abundant. This canton had been one of the first ones, in 1976, to prepare a preliminary map of landslides at a scale 1:25,000 that included a distinction between active slide zones, probable or substabilized slide zones and stable zones.

In a mountainous area of the Commune of Plasselb, called Falli Hölli (i.e. literally "fall in to hell!"), in which the forest cover had been removed in the XIX century, it was planned to build a small tourist village and the first building permits were already delivered in 1969. When a more extensive local management plan was developed and submitted to the approval of the cantonal authorities, several cantonal administrative offices that were required to give their advice opposed the plan, arguing the presence of an active slide that was clearly delimitated in the preliminary map of landslides, but also the difficulties of access (the road leading to the area was very narrow) and the lack of connections with other tourist areas.

However, these denials were objected by the communal authorities as an unjustified obstacle to economic development. Therefore, the State Council of the Canton of Freiburg, after listening the opinion of an expert who had not seen any signs of active movements at the site of the planned village (which indeed was correct, but did not consider the global slide phenomenon called Chlöwena), finally accepted the project for political reasons in 1977. Most of the 36 chalets were thus built between 1980 and 1990 (Fig. 12).

In 1992, in order to improve the due consideration of natural hazards in the Canton of Freiburg, a special "Natural Danger Committee" was set up by the Government, including representatives of the political authorities, of the planning and forest services, of the cantonal insurance office and of the juridical service. This committee proposed to launch a landslide mapping program at a scale 1:10,000 that was carried out between 1993 and 1999 over an area of 400 km^2 (the plain areas were not mapped).

In March 1994, one of the houses of the village of Falli Hölli began to be seriously affected by movements and was dismantled, after some attempts to divert the sliding mass with 7 m long wooden piles, which later proved to be inefficient as the slip surface was much deeper. The progressive reactivation of the sliding zones

Figure 12. View of the village of Falli Hölli at the beginning of the crisis. These houses moved over more than 200 m. Some drainage ditches are seen in the back of the village.

from the top to the bottom of the slope was observed and monitored from May 1998 on and it clearly appeared to the panel of experts that a major and uncontrollable phenomenon was developing. Therefore, several preparedness actions were set up step by step, between April and June 1994, without any phase of panic:

– prohibition to sleep in the houses of the village;
– prohibition to stay in the houses;
– evacuation of the furniture of all houses;
– auction sale of the furniture and goods of the hotel;
– emptying of gas tanks for domestic heating;
– prohibition to penetrate in the landslide zone.

Between the middle and the end of July 1994, the movement in the zone of the village seriously accelerated from 0.20 m/day to 6.0 m/day, causing indeed few structural damage to the chalets, but major tilting, as the slip surface was some 36 m deep; the building area was somehow compressed, the access roads crushed and sheared, and finally the restaurant located in the lower part of the village was totally destroyed (Fig. 13). At the end of September the crisis was over, with a total displacement of 200 to 250 m, and since then, only residual movements of a few millimeters to 2 cm per year are recorded at Chlöwena landslide (Vulliet & Bonnard 1996).

The owners of the buildings were compensated for their loss by the Cantonal Building Insurance Company at a very short notice (17 million SFr, i.e. 15 million USD), even though the structures were no destroyed; but they could not be repaired. However no compensation is possible for the loss of value of the land (about 99% of loss), which caused the opening of a judicial action; but later the complaint by a group of owners was withdrawn.

Despite of the nearly complete stabilization of the 1,5 km^2 slide, it was decided to destroy the ruins of the chalets, to clear the site and give it back to nature.

213

Figure 13. The restaurant was destroyed at the end of July, 1994, due to a shear movement.

Only one corner of a basement was left, as a memorial of the "disaster".

This local event induced the cantonal State Council to provisionally suspend all building projects in active landslide areas, to require a technical review of all existing building zones in conflict with active landslide areas in 13 communes of the Prealps and finally to state specific planning and building prescriptions for the landslide areas. They were classified in three categories: liable to build, liable to build under determined conditions, not liable to build. It is clear in this case that even though a full risk analysis was not carried out, a detailed qualification of the risk level was produced, allowing the short term management of the landslide areas on which building zones had been legally planned for many years.

The second consequence of Falli Hölli disaster was the elaboration of comprehensive hazard maps for landslides, floods, snow avalanches and debris flows, taking into account the relative intensity and probability of the phenomena, as well as the resulting threats. The mapping of all the zone of the Prealps is now carried out. On the basis of such documents, the local management plans are progressively revised and in specific situations protection works are undertaken.

The third consequence of Falli Hölli disaster was to induce the Swiss federal authorities to publish recommendations for the consideration of landslide hazards in land planning, in 1997, which could contribute to homogenize the elaboration of hazard maps between the 26 cantons of Switzerland that are independently responsible of such a task (see SOA6). This document is presently revised to produce constraining guidelines. Thanks to the risk conscience that developed after Falli Hölli case, most cantons have produced or are producing comparable hazard maps that are coupled with practical building limitations, so that an efficient protection is provided despite of the fact that no thorough quantified risk analysis is carried out.

5.2 *Monitoring systems*

Before analysing the possibilities furnished, at small and large scale, by both the present technology and the mathematical modelling, few considerations are necessary as it concerns: the problem to be faced; the best approach to be used; the test to be systematically carried out in order to improve the confidence on systems devoted to the population safeguard.

As it concerns the first aspect, monitoring systems are directed to the check-in of several elements which can be essentially included among the triggering factors (rainfall, earthquake, anthropogenic factors, etc.), the indicators or revealing factors of slope stability conditions (water content, groundwater and/or pore pressure regime, opening of superficial cracks, etc.) and the effect caused by the triggering factors (soil and/or element at risk displacements). Such elements can be qualitatively and/or quantitatively measured and can be or not related to other elements included in the same or other classes. The selected option strictly depends on the size of the study area, the landslide typology and the available instrumentation.

With reference to the second question, the multidisciplinary approach seems to be the most profitable one, due to the complexity of problems to be faced, above all when wide area must be considered. From this point of view large efforts need to be done as all the scientific communities are, sometimes, reluctant to furnish their contribution not having the control over the whole process.

Finally, all procedures, especially those based on an advanced technology and/or modelling, must be systematically tested in sample areas as, too many times, enthusiasms and initial beliefs are not confirmed by the obtained results.

Notwithstanding the absence of studies that simultaneously respect all these points, summarizing the research able to furnish a significant contribution in the monitoring field is not easy. As a consequence, in the following the attention will be essentially focused on some examples, highlighting the relevant contribution that, in the next future, will be furnished by monitoring systems at both regional and urban scales.

5.2.1 *Regional scale*

The scientific literature does not define techniques, methods of use and aims of monitoring systems over large areas. However, the available proposals indicate that the most promising techniques can be essentially based on remote sensing in order to confine, inside a large area, zones where an emergency will probably occur. To this end and referring to the intermediate – small scale (1:25,000 and smaller), in the following examples or considerations will be furnished stressing, when possible, the role played by hazard and risk maps in order to obtain useful results.

214

The first example refers to a back-analysis devoted to test the meteorological and hydrological maps as possible indicators of imminent instability phenomena inside a portion of the Campania Region (Southern Italy) whose total extension is 13,595 km^2. The study area (of about 3,000 km^2 in size) is covered by pyroclastic soils of volcanic origin which, during the centuries, have been systematically involved in fast slope movements causing victims and huge economic damages (Cascini & Ferlisi 2003).

As discussed in Cascini (2005), the instability phenomena are triggered inside well defined geomorphological units which are accurately indicated in the hazard and risk maps available, since 1999, at 1:25,000 scale all over the region territory and at 1:5,000 scale as it concerns some urban territories. The first stage movements involve soil covers of the geomorphological units according to complex mechanisms generally characterised by slip surfaces not deeper than $1 \div 2$ m. The whole area simultaneously affected by these phenomena can range from some hectares up to 100 km^2 as in the case of the events dated 1954 and 1998 (Cascini & Ferlisi 2003). Consequently, the total destabilized volume can range from few thousands to some million cubic meters which rapidly move downslope where high urbanised areas are located. Finally, rainfall triggers such phenomena although different intensity and duration are necessary passing from autumn to spring; anyway a minimum duration of many hours is necessary to trigger instability phenomena of a significant magnitude.

Taking the characteristics of the analysed phenomena into account, meteorological and hydrological maps have been drawn with reference to the event occurred during the night between the 15th and 16th December 1999, as a consequence of rainfall started about 40 hours before. The instability phenomena, of medium magnitude, threatened the town of Cervinara where 5 casualties were recorded. It is interesting to observe that fast movements were originated inside a geomorphologic unit defined as at high attention level (see Sect. 6.3) by the hazard maps available at 1:25,000 scale.

On the basis of the meteorological maps and by an interpolation of rainfall data, Rossi et al. (2004) reconstructed hydrological maps within an interval of 6 hours. Some of these hydrological maps are furnished in the Figure 14 which highlights two different zones affected by heavy cumulated rainfall: one inside the pyroclastic cover (zone 1) and the second one outside (zone 2). It is interesting to note that, inside zone 1, the cumulated rainfall over 24 hours – computed backwards from the 6.0 p.m. of the 15/12/1999 (i.e. more than 6 hours before the event) – reached values having a return period of 10–20 years; on the other hand, the return period rapidly increased in the following hours (Fig. 14d). Referring to the hazard map and the rainfall

threshold value, at the present in force in some other parts of the Campania Region (Rossi et al. 1998), it can be concluded that the availability of the meteorological and hydrological maps should have activated the emergency plan, some hours before the event occurrence, only with reference to the few little towns located inside the zone 1 (Fig. 14).

Of course this is just a back-analysis, so no definitive conclusion can be drawn; anyway the obtained results strongly encourage a real time experimentation with the aim of further improving the warning systems in force.

The second example deals with the soil moisture detection over large areas using remote sensing (LANSAT-7-ETM) and a digital elevation model. Particularly, Urciuoli (2004) analyzes, at a small scale, the instability phenomena inside a river basin, about 63 km^2 large, of Southern Apennine where landslides involving clayey soils are widespread all over the investigated territory. The author furnishes, first of all, accurate "state of the nature maps" where landslide phenomena are inventoried according to a geomorphological scheme which identifies four different stages of slope movements (Guida & Iaccarino 1991). Each of these stages is, therefore, characterised by velocities ranging from 0.3 m/day to 0.06 mm/year on the basis of data collected in sample areas by inclinometers and topographical survey. Using statistical techniques, MIRI and NDVI indexes are obtained by the remote sensing observations and overlapped to the instability phenomena classified as previously described (Fig. 15a). Observing that different values of MIRI index correspond to the four defined stages of slope movements, the author individuates different hazard levels inside well defined zones of the whole investigated territory (Fig. 15b).

Referring to (Reginato et al. 1976, Quattrochi & Luvall 1999, Scipal et al. 2002, Moeremans & Dautrebande 2000) as it concerns the soil moisture detection by remote sensing, it is evident that this kind of experimentation must be strongly encouraged and, where it is possible, coupled with meteorological and hydrological maps in order to link triggering factors, indicators (revealing factors) of slope instability phenomena and effects produced by the triggering factors.

At this regard, growing attention is worthy to be put on the use of SAR (Curlander & McDonough 1991) interferometry to measure the superficial displacements (Massonet et al. 1994), using two interferograms at different time periods (DInSAR) (Van Westen 2004). However, at the present, the application of DInSAR is restricted to the monitoring of a single landslide phenomenon, notwithstanding the world-wide coverage by single images on area of 10,000 km^2, available since 1992.

Some interesting attempts to overcome the limitations of the DiffSAR are represented by both the new

215
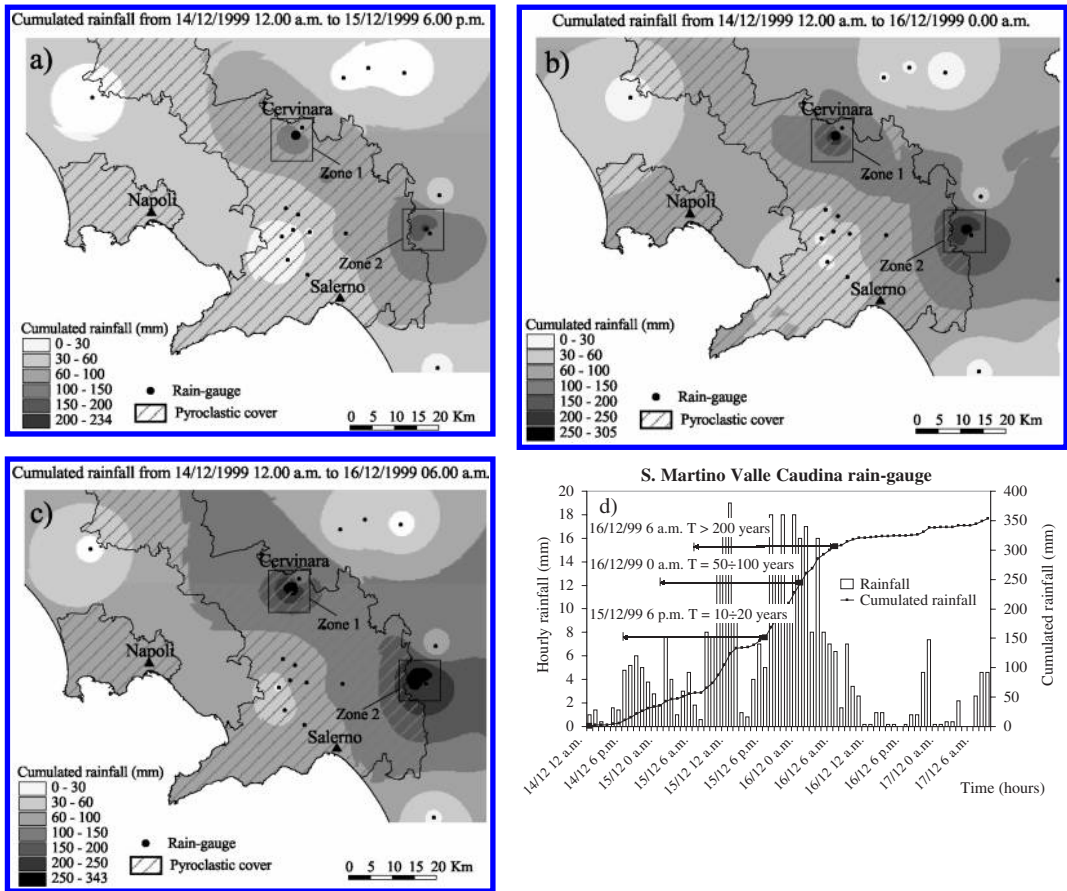
Figure 14. Rainfall event of 15–16 December 1999 in Campania Region (Southern Italy). Areal distribution of cumulated rainfall at different time (a, b, c). Cumulated and hourly rainfall recorded at a rain-gauge inside zone 1, and return period (T) of the backwards cumulated rainfall over 24 h period (d).

algorithm SBAS (Small Baseline Subset) (Berardino et al. 2002), implemented at I.R.E.A. and based on a particular post-processing of a set of interferograms, and the PS technique (Ferretti et al. 1999a, b), developed at POLIMI and patented worldwide (Colesanti & Wasowski 2004). However, up to now, such techniques have been utilised to measure ground displacements characterised by a prevailing vertical component (e.g. subsidence phenomena) as discussed in Allievi et al. 2003, Van der Kooij et al. 1995, Carnec et al. 1995, Worawattanamateekul et al. 2003, Kircher et al. 2003, Galloway et al. 2000, Wegmuller et al. 2000.

At the present, reliable data can be furnished by remote sensing to update the urbanised areas as it is discussed by van Westen (2004). Such information, easily obtained with reference to the elements at risk (Stilla et al. 2003, Priestnall et al. 2000, Fraser et al. 2002), are particularly useful for the Central and Local

Authorities to improve the emergency plans and/or to impose sanctions in the case of buildings located, without permission, inside inhibited areas.

In conclusion, remote sensing seems to be able in furnishing, in the next future, a significant contribution for landslide risk mitigation, at small – intermediate scales, on condition that multidisciplinary studies will be systematically carried out and the obtained results will be rigorously tested in sample areas on the basis of ground monitoring validation and reliable hazard and risk maps.

5.2.2 *Urban scale*
At large scale (1:5,000 or higher), monitoring systems can be based on instruments, techniques and interpretative procedures that can notably improve the landslide risk mitigation. Above all, remote sensing based on satellite techniques begins to furnish significant

216
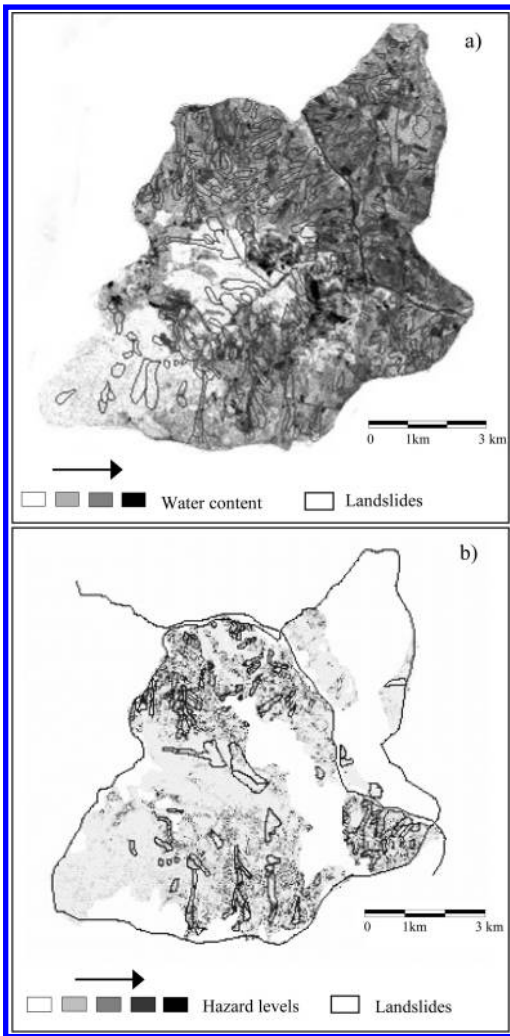
Figure 15. Landslides and Miri index (a) landslides and hazard levels (b) (Urciuoli 2004).

Figure 16. Alert and alarm rainfall thresholds over a 24 h period. PE24: mean value of the cumulated rainfall over 24 h period before the time t; PA24: mean value of the cumulated rainfall from the beginning of the hydrologic year up to 24 hours before the time t (Rossi et al.1998).

features with reference to the displacements of a single landslide phenomenon (Fruneau et al. 1996, Squarzoni et al. 2002, Berardino et al. 2003, Colesanti & Wasowski 2004, Gili et al. 1999, Malet et al. 2001). On the other hand, the reduction in area extent allows measurements of physical quantities, at local and site scale, as well as the use of well-known and powerful engineering models to correlate the experimental data. Such models can be used to define alert threshold which can be based, for a certain landslide typology, on displacement rate, groundwater change, rainfall characteristic and so on. Referring to instability phenomena triggered by rainfall, some examples are furnished in the following.

The first case study refers to an area of about 60 km^2, located in Southern Italy where, in May 1998, fast landslides, originated in pyroclastic deposits covering a dolomitic bedrock, caused 160 victims and large economic damage in 5 small towns (Cascini 2004). Thanks to the real time monitoring of the rainfall intensities over small time intervals (5–10 minutes) measured at 5 rain-gauge stations, Rossi et al. (1998) set up rainfall thresholds (Fig. 16) with the aid of hydrologic models, which were used as an alarm system to safeguard the people living inside the risk area. These hydrologic models use empirical based probabilistic methods capable to furnish relationships between historic records of rainfall and landslide occurrence; the obtained relationships are then utilised to predict the probability of future landslides on the basis of actual rainfall intensities. Hydrologic models, like the previous one or similar, are quite diffuse in the scientific literature and they have furnished significant results in many geo-environmental contexts (i.e. Caine 1980, Crozier & Eyles 1980, Cascini & Versace 1988, Wilson & Wieczorek 1995, Sandersen et al. 1996, Wilson 1997).

The results obtained by these models can be, however, notably improved with the aid of further instruments oriented at the monitoring of physical quantities related to the indicators of slope stability conditions.

For example, considering the superficial in situ water content, a promising procedure has been experienced in a number of sites inside some hydrologic basins of the Australian territory (Woods et al. 2001) by TDR sensors and neutron probes installed in the first 0.6 m of depth and whose data are acquired via remote locations. The above data have been then utilised to link rainfall to the distribution of superficial water content (Western & Grayson 1998). Notwithstanding this procedure has been used for a proper validation of a deterministic model rainfall-runoff, it

217
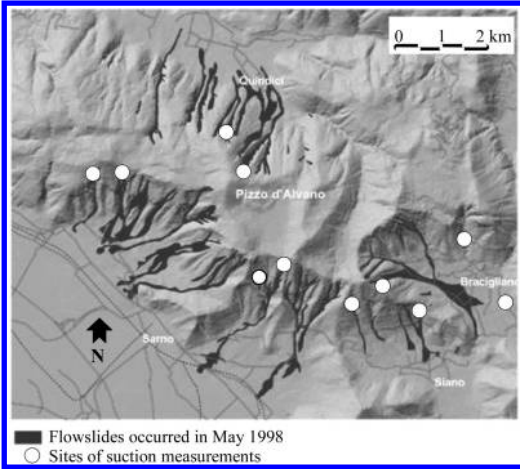
Figure 17. Map of May 1998 flowslides and sites of suction measurements (Cascini et al. 2003).

Figure 18. Comparison among monthly average suction values at depths lower than 1.0 m and the moving average daily rainfall over two-month and three-month period (Cascini & Sorbino 2003).

could be suitable employed in the field of mass movements, in order to individuate, during and before a rainfall event, those areas where considerable aggravating conditions for slope stability could develop. In addition, the availability of these data could notably improve an appropriate calibration of physically-based analytical methods – e.g., SHALSTAB (Pack et al. 1998), SINMAP (Montgomery & Dietrich 1994), DSLAM (Wu & Sidle 1995), TRIGRS (Savage et al. 2003) and other recent methods (Savage et al. 2004) – aimed to estimate potential relative instability of slopes in a GIS setting.

Besides the superficial water content, other indicators can be measured such as the pore water pressure both in saturated (positive pore water pressures) or in unsaturated (negative pore water pressures or suction) conditions.

An example of suction measurements over large areas is furnished by the tensiometers data acquired over the above cited area located in Southern Italy, where unsaturated pyroclastic deposits are susceptible of fast landslides. In this area, investigated sites were mostly situated at medium-high slope levels, nearby and/or inside the triggering areas of 1998 landslides (Fig. 17). The analyses performed by Cascini & Sorbino (2003), on more than 3000 suction data acquired at the investigated sites, have shown that monthly average suction values differ only with respect to depth, but they attain the same values independently of the investigated sites. These findings seem to reveal that the pore pressure in the pyroclastic deposits is affected by analogous time trend all over the area and, consequently, they evidence the possibility to correlate soil suction values to rainfall data. At this respect, Figure 18 compares the average suction values at depths of less
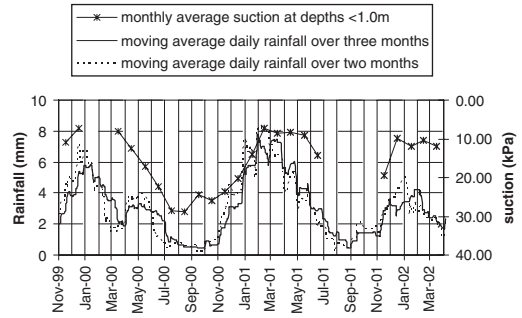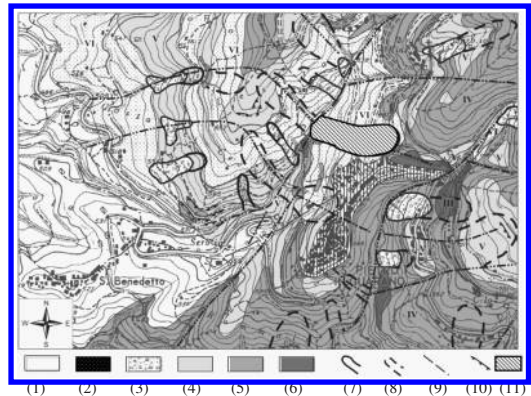
Figure 19. Part of the weathering grade and landslides map of the Western Sila study area (Calabria-Southern Italy): 1) sedimentary soils; 2) colluvial and residual soils (class VI); 3) landslide debris; 4) completely weathered gneiss (class V); 5) highly weathered gneiss (class IV); 6) moderately weathered gneiss (class III); 7) recent landslide scarp; 8) old landslide scarp; 9) fault; 10) rock landslide scarp; 11) analysed landslide (Cascini et al. 1994).

than 1 m, that is the depth generally involved in the flowslide triggering areas, to the daily moving average rainfall values, the latter being calculated over two- and three-months periods. As can be seen, the average suction values are in clear agreement with the moving averages of the rainfall data. These results highlight encouraging perspectives towards an improvement of the alarm system – which, as previously stated, is currently based on rainfall data only – by taking the suction values into account. Further improvements can also derive by the application of geomechanical models inside specific and representative sites (see Sect. 6.3).

As for positive pore pressures, the monitoring performed over an area of about 7.5 km² is briefly

218
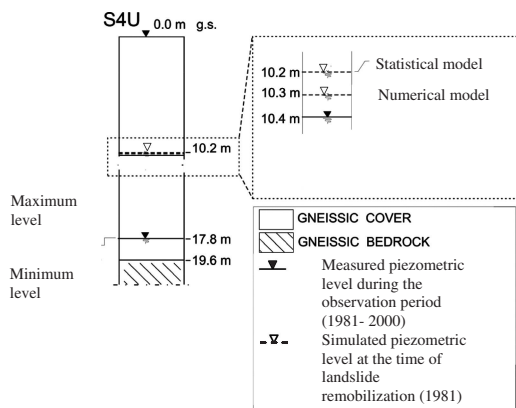
Figure 20. Measures and estimates of the piezometric levels inside the analyzed landslide.

synthesised. The area is located on the western slopes of the Sila Grande massif (Southern Italy), where gneissic lithotypes, generally deeply weathered, crop out (Fig. 19). In the area, the most common forms of instability involve covers (of depths ranging from 10–20 m) composed of colluvial, residual, and saprolitic soils (Cascini et al. 1994), that are characterized by several decades of total quiescence, followed by sudden reactivations in correspondence of particularly wet seasons.

Measurements of pore pressure regime – performed in correspondence of representative landslide phenomena – have systematically revealed (Gullà & Niceforo 2003) the presence of two aquifers with distinct groundwater tables: the first one located in the bedrock and having a quite steady-state character; the second one inside the unstable cover showing a strongly transient character, strictly related to seasonal rainfall events. Notwithstanding the monitoring of groundwater regime – in some sites taken over a long period of time (up to twenty years) – the absence of effects during many decades in all the sites did not allow the individuation of pore pressure values responsible for remobilisation of the landslides (Gullà 2004). For this reason, it was considered worthwhile to analyse in detail a representative landslide phenomenon (of about 20,000 m² in size) whose reactivations, in 1931 and 1981, caused severe damage to many public and private buildings.

The analyses, carried out by three different models, were aimed to predict both the critical rainfall events and the pore pressure able to mobilise the cover. On the basis of the rainfall data, available since 1923, the first hydrologic model highlighted that a five-month cumulated rainfall (900 mm) having a return period of 50 years is capable to reactivate the cover (Cascini & Versace 1988). On the other hand, a statistical analysis

of piezometer measurements (Cascini et al. 1992) taken over twenty years, allowed the estimation of the local groundwater table presumably attained during the recent cover mobilisations (1931, 1981). Finally, through the seepage analyses of the saturated-unsaturated regime (Sorbino 1994, Cascini et al. 1995), the third model furnished the pore pressure corresponding to the mobilisation of the whole cover.

The obtained results (Fig. 20), together with other in-situ measurements, were therefore utilised to define the indicators of the landslides reactivation at both site and local scale, notwithstanding the total absence of movement, during the investigation period, for all the instability phenomena inventoried inside the sample area.

6 CASE HISTORIES

Notwithstanding the absence of a standardized procedure for hazard and risk zoning, several hazard and risk maps have been developed to solve practical problems at small, intermediate and large scales. An overview of the aims pursued, the adopted methods and the obtained results are furnished in Ahmad & McCalpin (1999), Atkins Haswell (1995), Brabb et al. (1999a, b), Corominas et al. (2003a), Dai et al. (2002), Einstein (1997), Hayne et al. (2002), Michael-Leiba et al. (1999, 2002), Turrini & Visintainer (1998).

In the following, five case studies show the way to overcome the difficulties generally faced with hazard and risk zoning, essentially related to reference scale, weakness of the available data and procedures; moreover, they allow to realise the usefulness of the produced maps as it concerns the risk mitigation to be pursued by regional and urban planning, warning systems and stabilisation works.

Particularly, the first example (Colombian cases) shows the usefulness of the small and large scale analysis in function of both the aim pursued and the size of the study area. The second case (Southern California) highlights, at an intermediate scale, the usefulness of back analyses based on reliable input data concerning the triggering factors, in absence of detailed in-situ investigations. The third case (Southern Italian Apennine) discusses the method for hazard and risk assessment, at an intermediate scale and over large areas, which was developed – in absence of either a suggested procedure or risk education – to confront the urgent need requested by the Central Authorities. Finally, the last two cases (Andorra Principality and Icelandic lowlands) highlight the feasibility of both accurate investigations and studies, at large scale, when some conditions are satisfied (risk management process started some years before; availability of advanced data sets; small extension of the analysed area).

219

6.1 *Some Colombian cases*

The geographic location of Colombia, both in the circumpacific region and in the inter-tropical area, the population concentration and the development of main economic activities in the Andean mountainous area, favor the occurrence of landslides and other instability processes, with great detriment for the development of the country. In the last 25 years many investigations had been carried out related with the distribution and effects of mass movements that affect mainly infrastructure works and urban areas.

One of these studies was a landslide inventory along the road country network that was carried out by the Ministry of Public Works and the National University of Colombia (1989).

For hazard assessment, the direct or heuristic method was used (Soeters & van Westen 1996) by combination of geomorphologic criteria with thematic maps on geology, morfo-structural units, climate, seismicity and land-use (Montero & Cortés 1989). On this basis, the whole country was classified into 15 relative hazard provinces, each one distinguished by a particular landslide-related behavior and numbered in descending order of susceptibility to slides, flows and other types of movements. Later, these 15 provinces were regrouped into 5 hazard categories, according to the distribution of the processes in the territory, with density, frequency and recurrence of the movements (INGEOMINAS 2002). This information is presented in Figure 21, with the following conclusions:

– 30% of mass movements are of great magnitude (greater than one million cubic meters and/or causing catastrophic effects).
– 90% of the mass movements are located in geological fault areas being triggered mainly by rainfall (more than 4000 mm/year and intensities frequently ranging from 20 to 30 mm/hour).
– 55% to 60% of the movements are concentrated in provinces I and II (Very High Hazard zones).
– 20% to 25% of movements fall in provinces III and IV of High Hazard.
– 28% of the cities and town are affected by landslides especially the ones located in the Very High and High Hazard zones that correspond to the more developed areas of the country.

It is worth noting that 69% of the large landslides are still active or dormant; most of them are triggered by human activities related with highways construction, deforestation, improper land-use and population settlements in sub-urban areas of the cities and towns (Montero 2003).

In the late 90s, Bogotá, the Colombian Capital city, carried out several studies to identify and quantify the main natural hazards that could affect or affects the urban zone. Studies were done, and three hazard maps
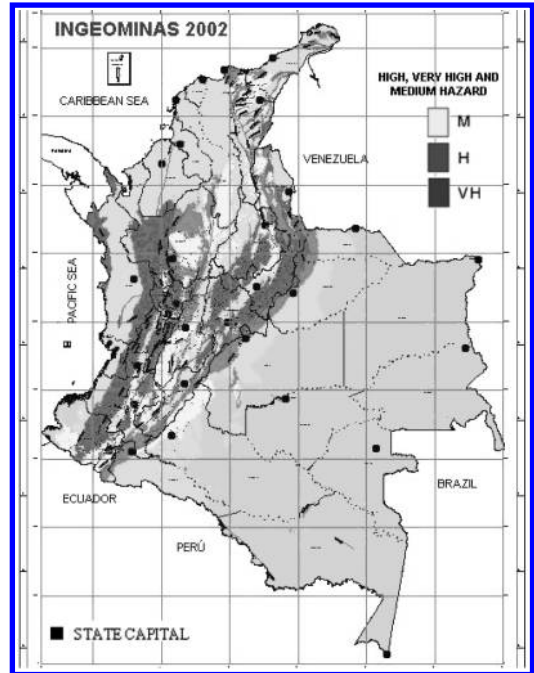
Figure 21. Relative Landslide Hazard Map for Colombia (INGEOMINAS 2002).

were obtained: seismic hazard map, flooding hazard map and landslide hazard map.

The landslide hazard map (Fig. 22) was done in 1998 for a 10-year exposure period and it was obtained by means of three concurrent methods: Semiquantitative Landslide Hazard Index (SCLHI), Natural Slope Methodology (NSM) and Landslide Inventory (LNDI). The first method (SCLHI), developed by Ramirez & Gonzàlez (1989), uses weighted indexes for 4 intrinsic factors (surface materials, relief, drainage density and vegetation) and 4 triggering factors (rainfall, earthquake, erosion and anthropogenic effects). The second method (NSM), by means of surface morphology deconvolution of topographic and geological data (Shuk 1990), allows to find relative factors of safety (Fs) and relative failure probabilities (Pf), including rainfall and earthquake effects, for several exposure periods. Finally, the landslide inventory (LNDI), allowed the calibration of the other two methods and five maps at 1:10,000 scale were produced. Excluding the southern Usme District, studied by other methodologies, 181.2 square kilometers of hillslopes were evaluated with the result listed in Table 2.

6.2 *Southern California*

The 1994 Northridge, California, earthquake (**M** 6.7) triggered more than 11,000 landslides over an area of

220
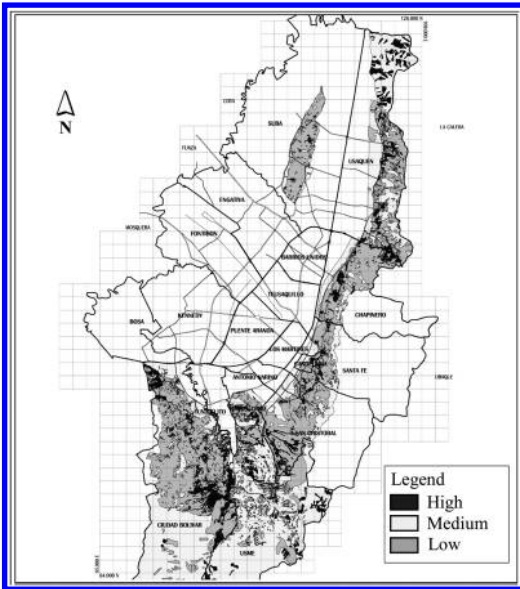
Figure 22. Landslide Hazard Map for Bogotá, Colombia [Dirección de Prevención y Atención de Emergencias (DPAE)].

Table 2. Hillslope evaluation for Bogatá, Columbia.

Landslide hazard	Relative 10 yr – Fs	Relative 10 yr – Pf	Area (km²)	Area (%)
High- H	Fs < 1.1	Pf > 44.3%	19.97	11.0
Med- M	1.1 < Fs < 1.9	12.1% < Pf < 44.3%	111.10	61.3
Low- L	Fs > 1.9	Pf < 12.1%	50.13	27.7
TOTAL	**181.20**	**100.0**		

about 10,000 km² (Harp & Jibson 1995, 1996). This is the first earthquake for which all of the data sets needed to conduct a rigorous, detailed regional analysis of factors related to seismically triggered landsliding are available. The data sets include (1) a comprehensive inventory of triggered landslides (Harp & Jibson 1995, 1996), (2) about 200 strong-motion records of the main shock recorded throughout the region of landsliding, (3) detailed (1:24,000-scale) geologic mapping of the region, (4) extensive data on engineering properties of geologic units, and (5) high-resolution digital elevation models of the topography. All of these data sets were digitized and rasterized at 10-m grid spacing using ARC/INFO geographic information system (GIS) software. Then these data sets were combined in a dynamic model based on Newmark's (1965) permanent-deformation (sliding-block) analysis, which yields estimates of coseismic landslide displacement in each grid cell from the Northridge earthquake
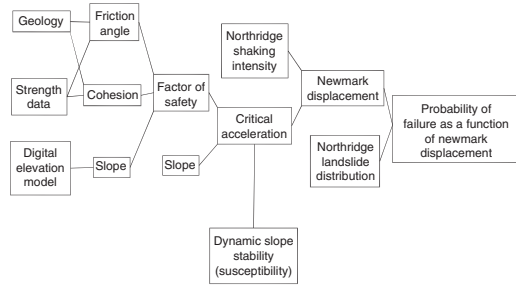
Figure 23. Flow chart showing procedure for producing seismic landslide hazard maps (from Jibson et al. 2000).

(Jibson et al. 1998, 2000). The modeled displacements were then compared with the digital inventory of landslides triggered by the Northridge earthquake to construct a probability curve relating predicted displacement to probability of failure. Once calibrated with Northridge data, the probability function can be applied to predict the spatial variability of failure probability in any ground-shaking scenario of interest in the southern California region. Because the resulting hazard maps are digital, they can be updated and revised with additional data that become available, and custom maps that model any ground-shaking conditions of interest can be produced when needed.

Figure 23 is a flowchart showing the sequential steps involved in the hazard-mapping procedure. Data layers consist of 10-m grids. The sequence is relatively straightforward:

– estimation of the static factor of safety against slope failure (ratio of resisting to driving forces) in each grid cell. To this aim shear-strength data were compiled from local geotechnical engineering firms, and a representative shear strength was associated to each unit on the geologic map, which yields friction (ϕ') and cohesion (c') grids. A digital elevation model (DEM) was analyzed to produce a slope map;

– estimation of the critical acceleration (threshold seismic acceleration needed to initiate slope movement) by combining the factor-of-safety grid with the slope grid to yield the critical acceleration grid, which represents seismic landslide susceptibility (Newmark 1965);

– estimation of Newmark landslide displacements using an empirical regression equation (Jibson et al. 1998, 2000) that requires knowing the critical acceleration of the slopes and the distribution of shaking intensities from the Northridge earthquake. Critical accelerations were estimated as described in step 2. Arias (1970) shaking intensities were contoured throughout the region, as measured by about 200 strong-motion recordings of the mainshock;

221
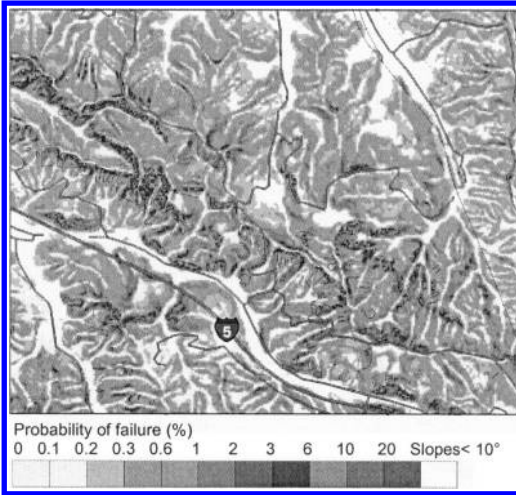
Figure 24. Map showing probability of landsliding during shaking conditions identical to the 1994 Northridge earthquake for a part of southern California (from Jibson et al. 2000). Actual landslides triggered in 1994 shown outlined in black.

– construction of a curve to estimate probability of slope failure as a function of Newmark displacement. The map of landslides triggered by the Northridge earthquake was compared to the Newmark-displacement grid. For sequential intervals of Newmark displacement, the proportion of cells containing landslides was computed and the proportion of failed slopes in each interval as a function of Newmark displacement was plotted. A regression curve based on a Weibull distribution was fit to the data.
– use of the calibrated regression equation to generate maps showing probability of seismic slope failure in any shaking scenario of interest. This is done simply by estimating Newmark displacements by combining a ground-shaking grid of interest with the critical acceleration grid, as in step 3 and then estimating probabilities of failure using the calibrated regression curve from step 4.

Figure 24 shows a sample area from southern California of a seismic landslide hazard map using this procedure. Maps made in southern California using this method are experimental and currently are being used as research tools. A much simplified version of this methodology does, however, form the basis of regulatory maps (scale 1:24,000) produced in 2004 by the State of California. These maps simply define zones of potential seismic landslide hazards; a site is either in a potential hazard zone or not. Any development planned within the hazard zone must then comply with various public policies aimed at insuring that seismic landslide hazards are identified and mitigated as part of the project. Each local municipality (city, county, etc.) is responsible to prescribe its own procedures to be followed for development within a potential hazard zone. Thus, the maps trigger a public-policy process that is tailored to each local government's need.

6.3 *Southern Italian Apennine*

Two landslide disasters, in 1997 and 1998, caused 166 fatalities and huge economic losses in several towns of the Campania Region of Southern Italy (Cascini 2005). As a result of these disasters, the Central Government passed a law requiring the River Basin Authorities to zone the landslide risk using simple and rapid procedures.

Notwithstanding the total absence of hazard and risk maps at the time the Law was passed, risk zoning was obtained at a 1:25,000 scale all over the Italian territory (301,401 km^2) in the following two years. Particularly, the risk zoning was calibrated according to the four risk levels defined by the Central/Government as follows:

- Very high (R4): human life loss and destruction of buildings, infrastructure and environmental as well as interruption of economic activities are expected;
- High (R3): victims, functional damage to buildings and infrastructure, as well as partial interruption of economic activities are possible;
- Medium (R2): limited damage to buildings, infrastructure and environmental may occur;
- Low (R1): social, economic and environmental damage are of marginal relevance.

To assess the risk levels, general instructions were furnished, but no specific technical advice and procedures were suggested. In the present section, the results obtained for the territory of the National Authority of Liri – Garigliano and Volturno river basins (Central-Southern Italy) are summarized (Cascini 2005). Inside this territory (of about 12,000 km^2 in size), undeveloped areas affected by dormant, active or potential landslides were also mapped and classified, although it was not required by the Law. Particularly, referring to the risk levels so far defined and the Cruden & Varnes (1996) suggestions, these areas were considered worthy of different attention levels classified as follows:

- Very high (A4), if the area was inside the source, transport or depositional zone of extremely rapid, very rapid or rapid landslides;
- High (A3), if it was inside a moderate or slow landslide, both active or dormant, potentially triggered by an earthquake;
- Medium (A2), if moderate or slow landslide was inside an aseismic area;
- Low (A1), if the area was involved in a very slow or extremely slow landslide.

222

I ≡ the highest expected velocity	
I	**Landslide type**
High	Flowslides, Debris flow, First Failure in brittle materials
Medium	Occasional reactivation and Active landslides
Low	Deep-Seated Gravitational (Slope) Deformation, Lateral spreads

Figure 25.   Intensity classes of the landslides (Cascini 2005).

To zone the risk and attention areas, detailed and territory-wide state-of-nature maps (geology, geomorphology and soil cover) were preliminarily compiled. Subsequently, with the aid of such maps as well as of aerial photo interpretation and available information, 30,000 landslides together with their surrounding areas, and zones potentially affected by fast slope movements were mapped using Varnes classification (1978), creep evidence, a simplified version of the slope movement stage defined by Leroueil et al. (1996), state of activity, and other simple criteria described in Cascini (2005).

Starting from these elements, susceptibility maps (danger maps in the sense of the present paper) were then obtained by adopting velocity estimates of the dormant or active landslides, as well as of the source and propagation areas potentially affected by first stage movements, using a simplified version of the Cruden and Varnes criterion (1996). Particularly, a maximum movement velocity was associated with each of the mapped landslide according to the nominal scale shown in Figure 25; an example of so obtained danger map is furnished in Figure 26. Finally, on the basis of landslides activity, simplified hazard maps were produced by using the nominal scale of Figure 27.

Inside the analyzed territory, simplified vulnerability maps for all the towns (450) were also produced. These maps also contain the expansion areas in the urban-planning scheme, the essential facilities (hospitals, barracks, schools etc.) and the damaged buildings, scheduled according to the nominal scheme of Figure 28.

Referring to the Varnes' formula, the risk levels (Fig. 29) were obtained by overlapping hazard and vulnerability maps. An example of map containing the attention and risk levels previously defined, is shown in Figure 30. Considering the small extent of risk areas (about 4.6% out of the whole territory) compared to the extent of the attention areas (about 15% out of the whole territory), it can be concluded that an improvement of land-use planning is an urgent need. This is confirmed by an historical analysis (O.U. 2.38 1998) that highlights the increase, in Southern Italy, of victims and damages after the second World War despite
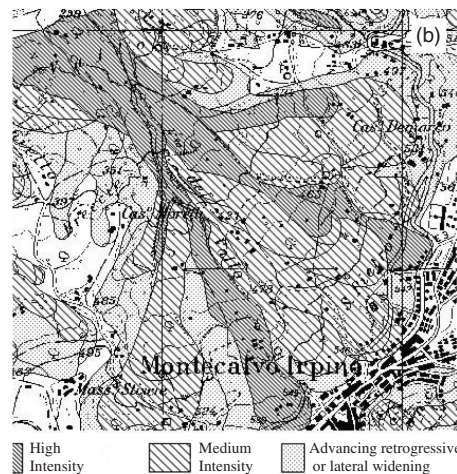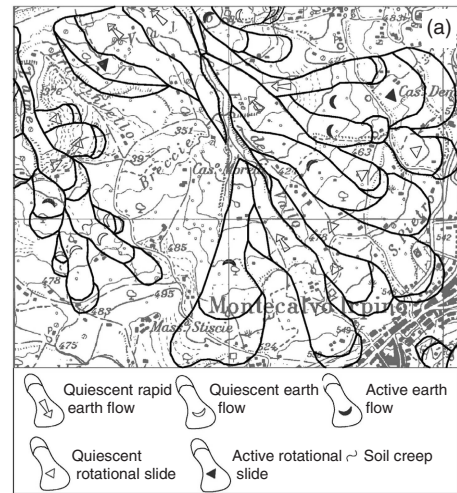
Figure 26.   Example of landslide inventory and danger map, not considering earthquake effects (Cascini 2005).

INTENSITY	HAZARD	Landslide activity
HIGH	HIGH	active
		quiescent
MEDIUM	HIGH	active
	MEDIUM	quiescent
LOW	HIGH	active
	MEDIUM	quiescent

Figure 27.   Hazard nominal scale (Cascini 2005).

the same frequency through time of the most dangerous phenomena.

An improvement of land-use planning calls for in-depth investigation and analysis to be carried out at more detailed scales (1:5,000, 1:2,000) and to be implemented into the quantitative risk assessment (QRA)

223

I	Building tipology	Observed Damages	VULNERABILITY
HIGH	All	Not considered	HIGH
MEDIUM	Strategical building	Not considered	HIGH
	Common building	YES	
	Common building	NOT	MEDIUM
LOW	Strategical building	Not considered	MODERATE
	Common building	YES	
	Common building	NOT	LOW

Figure 28. Nominal scale for vulnerability (Cascini 2005).

I	HIGH		MEDIUM		LOW	
HAZARD	H	H	M	H	M	
Vulnerability high	Hh	Hh	Mh			
medium		Hm	Mm			
modest				Hm	Mm	
low				Hl	Ml	

R4	R3	R2	R1

Figure 29. Nominal scale for risk level evaluation (Cascini 2005).

procedure. As a matter of fact, the current deepening at 1:5,000 scale, by using the previously described procedure, systematically confirms the obtained results at 1:25,000 scale, not allowing the reduction of both the hazard and risk zone, as it is reclaimed by Local Authorities. A further confirmation of the reliability of the official documents is furnished by the fast slope movements triggered after their presentation, which all developed inside the mapped hazard and risk zones.

Investigations and studies at more detailed scale (1:5,000, 1:2,000) are in progress inside an area (3,000 km^2) characterised by widespread high attention (A4) and risk zones (R4) for the presence of pyroclastic covers, potentially threatened by fast slope movements.

Such deepening is strongly based on geotechnical and geomechanical models that are systematically tested by back-analyses of phenomena triggered during the events occurred in 1998's. Such analyses are developed using topographic surveys, detailed in-situ investigations, pore-water-pressure measurements and soil properties estimated both in saturated and unsaturated conditions, since pyroclastic covers are commonly characterized by partial saturation during the triggering stage.

| R4 | R3 | A4 | A3 |

Figure 30. Example of map containing attention and risk zones (Cascini 2005).

An example is furnished in Figure 31 which refers to a sample basin (of about 40,000 m^2 in size) where covers B and C were destabilized during the events dated 1998. As discussed in Cascini (2004), the geomechanical modelling agrees with a hydrogeomorphological model set up at massif scale (1:25,000) extending over an area of about 60 km^2. Similar results, at both basin and massif scale are not obtained using other physically based models that neglect some local conditions (stratigraphy, presence or absence of outlets in the triggering zone, and so on) playing a relevant role in the triggering stage.

Considering the encouraging results furnished by the geomechanical models as well as by the vulnerability analyses carried out in the same area by Faella & Nigro (2003), it can be concluded that a quantitative risk assessment seems to be possible even if improvement of hazard and risk zoning maps requires both time and adequate financial support. Moreover, alarm system and countermeasures design should significantly be improved when investigations and studies at more detailed scale will be completely developed.

However, up to now, in the areas where the disasters occurred, the available maps have allowed the implementation of an alarm system for population safeguard, based on rainfall threshold values, and the countermeasure identification in order to assess the necessary financial cost.

6.4 *Andorra Principality*

The Principality of Andorra is a small country located in the Pyrenees, between France and Spain. In recent

224
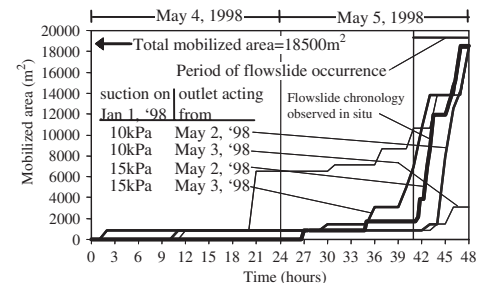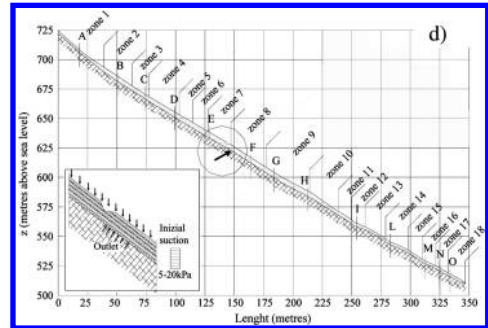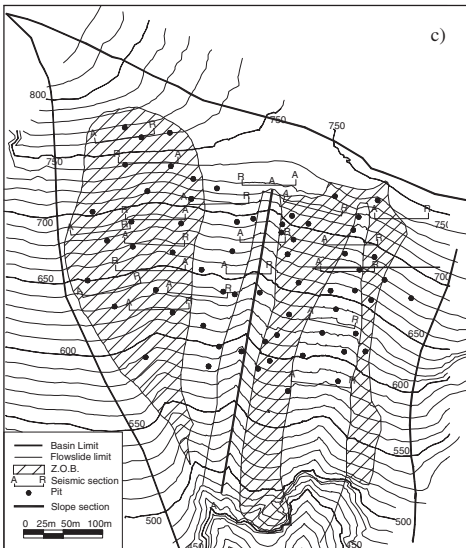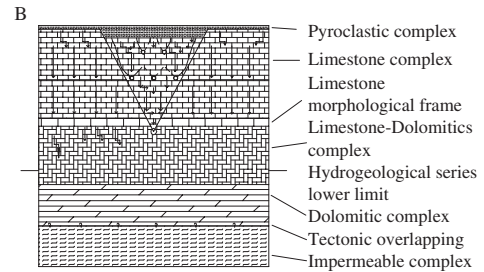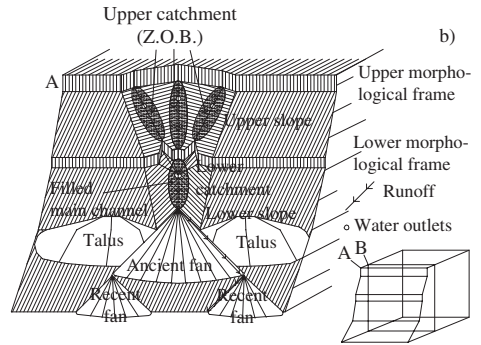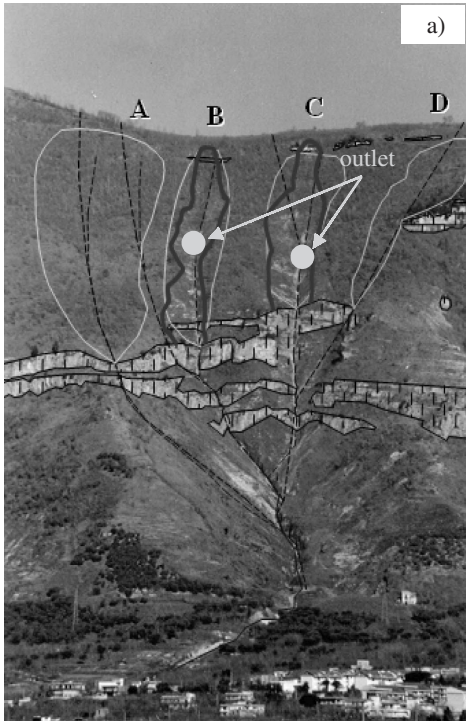
Figure 31. Sample area and Zero Order Basins (Z.O.B.) covered by pyroclastic covers (a) outlets are identified by the hydro-geomorphological model (b) only in correspondence of the Z.O.B. where instability phenomena occurred (B-C). In-situ detailed investigations (c) geomechanical analysis of groundwater regime and slope stability condition, along section A-A, based on recorded rainfall, different unsatured initial condition and considering the outlet presence according to the hydrogeo-morphological model (d). (Cascini et al. 2003, modified).

225

times the country has been hit by large floods and several landslide events. The most intense events occurred in October 1937 and November 1982, producing widespread shallow sliding, debris flow activity, and flooding of the Valira river. In October 1987, rains lasting for several days triggered a rock slide, killing three people, blocking a primary road and isolating for some weeks one of the main valleys. On the other hand, frequent rock falls produce damages and great concern in the highly urbanised areas of Andorra la Vella, the capital of the country, and Santa Coloma (Corominas et al. 2003a).

Actions for landslide risk management started in 1989 after some scattered initiatives. In 1989 the Andorran administration promoted the completion of a landslide and flooding hazard map at 1:25,000 scale for most of the territory (Corominas et al. 1990). The map was prepared based on both geomorphological reconnaissance and expert criteria. The landslide susceptibility was assessed taking into account the presence of instability features, a land-slide inventory and the critical slope angles for different landslide types (Corominas et al. 1990). The probability of occurrence was established only in a qualitative way by considering the presence of field instability features (open scars, tilted trees, cracks, etc.) in large landslides and the degree of preservation or dismantling of existing dormant movements. Frequency of shallow landslides was assumed that of the triggering factors, in this case, heavy rains. Four hazard categories were defined and mapped with different colours: green (no hazardous phenomena have been detected), yellow (presence of either local or small magnitude phenomena), orange (either generalized small magnitude phenomena or dormant large landslides) and red (active large landslides). The map was used by the administration to directly deliver building permits and for the design of protective works. However, for practical landslide management, the map showed important restrictions due to the scale of the map, which was too small for urban planning, and to the simplicity of the method used for the landslide hazard assessment that defined imprecise hazard boundaries.

A great step forward in the control of landslide hazard was given by the Urban and Land-Use Planning Law approved in 1998. This law demands that those zones exposed to natural hazards can not be urbanized and that Urban Plans of the municipalities must take the presence of zones exposed to natural hazards into account. Following this law, the Andorran administration promoted several studies and maps, among them, the landslide hazard map of Andorra at 1:5,000 scale (Corominas et al. 2003a).

The methodology for establishing the hazard categories and zones included the susceptibility assessment, runout distance, expected intensity and the probability of occurrence (Corominas et al. 2003b). All existing large landslides were considered susceptible for reactivation. For small first-time failures (shallow landslides, debris flows, rockfalls), the lithological map was combined with the critical slope angles for each landslide type to define landslide susceptibility. Compared with the previous map of 1989, the availability of a detailed DTM along with a brand new layer of superficial formations has allowed a much precise identification of potential landslide sources. The susceptibility assessment was completed with the definition of the expected travel distances which were delineated based on the extent of the landslide deposits, the empirical relationships between landslide volume and the angle of reach (Corominas 1996) and checked with Eurobloc, a 3-D numerical model (Lopez et al. 1997, Copons et al. 2001). The treatment of these information layers was carried out by means of a GIS (Arc-Info).

In the landslide hazard map of Andorra, intensity classes were defined taking the resistance of the protective structures into account (especially for rock falls) rather than the vulnerability of the threatened elements. In particular, three intensity (energy) classes were considered: low (0 to 2,000 KJ), medium (2,000 to 10,000 KJ) and high (more than 10,000 KJ). Boundaries between classes were established based on the performance of the commercial rock fall fences and earth embankments. Impact energies over 10,000 KJ were considered as non-manageable while existing large landslides were all supposed of high intensity because, even though they often display small displacement rates, remedial works use to be both inefficient and economically unaffordable and catastrophic surges can not be always disregarded. Hazard categories for zoning and planning purposes were based on these intensity classes. Those places where impact energy of rock falls is high, and where either active or dormant large landslides may experience sudden reactivation, have been considered of high hazard, except for those events with low probability of occurrence (Corominas et al. 2003b). When landslide threat can be handled with the appropriate countermeasures, hazard was considered of a moderate (mid) level.

The landslide hazard zoning has been incorporated in the administrative procedure for delivering building permits. The map has been first subjected to public audience. All the land classified as high hazard can not be developed with only a few exceptions (i.e. roads without alternative corridors). In case of moderate hazard, the owner or developer must fill a form of acknowledgement of the type of threat that may affect the property which must be signed by the engineer or architect in charge of the project. Furthermore, they must provide a technical report including explicitly the countermeasures that will be undertaken to avoid or mitigate the potential landslide hazard along with an estimation of the residual risk. In the moderate hazard category sensitive buildings such as schools or hospitals

226

are not allowed. Hazard category of a particular area can be reconsidered in the future if more detailed studies demonstrate that hazard level is lower than previously estimated or new remedial or protective works are feasible. It is thus implicitly accepted, that improvement of engineering protection practices may alter the hazard category of an area (Corominas et al. 2003b).

Parallel to the landslide hazard map, special attention was paid to the rock fall hazard in Andorra la Vella and Santa Coloma (Copons et al. 2004). Frequent rockfall, ranging from about $1 m^3$ to few hundred cubic meters, occur on the steep slopes of the glacial-shaped Valira river valley, made of granodiorite. Fallen block accumulate at the slope foot generating coalescent talus slopes which have been developed during last decades. In December 1983, January 1994, and January 1997, several buildings were hit. In June of 1998, the Andorran Ministry of Public Works started a Rock Fall Master Plan (RFMP) with the purpose of reducing the risk in the area.

The main achievement of the RFMP was the establishment of a boundary line (Fig. 32) above which hazard is considered very high and building is forbidden. The line was defined by taking the impact energy of the falling blocks into account. The boundary line was published in the Official Journal of the Principality in 1998, and since then it has been used by the Andorra Government for authorization of new developments. Rockfall fences were built above the mentioned line to protect building. Nevertheless, when the boundary line was defined, some buildings were already within the exclusion area. For all the cases, the RFMP also considered the design of additional rockfall defences (Copons et al. 2000).
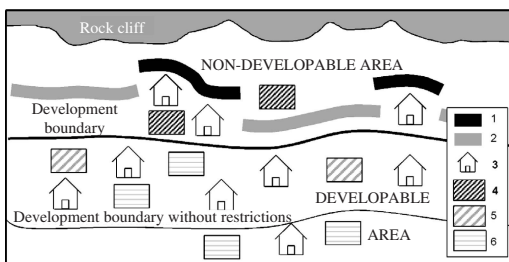
Figure 32. Development zoning at the Andorra la Vella-Santa Coloma based on rockfall hazard. The upper boundary for development is given by the thick continuous line. Above it rockfall protective fences and embankments (1 and 2) are design to protect the existing buildings and the developable area below. There, new buildings (3) are prohibited in the available plots of land (4). Below this boundary, land plots (5) can be developed provided that protective structures exist. A lower development boundary is defined by a thin continuous line. Below it development of plots of land (6) can be made without restrictions (Copons et al. 2004).

The establishment of this line required many trajectographic analyses with a 3-D numerical code (Copons et al. 2001) and the assessment of rockfall frequencies from tree damages (Moya & Corominas 2004). A rockfall flow (events per unit length) was obtained as well (Copons et al. 2004). Results of the numerical simulation of rock fall trajectories were the kinetic energy, height of bounce and rock fall trajectory which were used for the design of the protection fences and to calculate the residual hazard. At any given location, the numerical modelling yielded the percentage of intercepted blocks by the projected fences. The product of the percentage of passing rocks with the rock fall flow, defined above, gives a first estimation of the residual hazard (expressed as a number of events per unit length in a given period of time) existing in the area after protective works were completed. In the RFMP the residual hazard obtained for new development areas below the development boundary is always lower than 10^{-5} to 10^{-6} events per metre and year. By assuming the presence of a person 100% of the time in this one metre wide path with a vulnerability of 1.0, which is a conservative value, this rate is considered in the scientific literature as an acceptable risk (Fell & Hartford 1997).

The administrative procedure for building authorisation has been conceived not as an additional constraint to the developers but as guidance. By means of the GIS and its data base, they may know the type and nature of the hazard, if any, they are confronting with. Furthermore, they know in advance a first estimate of magnitude and frequency of the event, thus allowing a preliminary cost-benefit analysis of the intended development. On the other hand, with this map and the administrative procedure, local authorities are expected to have better tools for land use planning and hazard management.

6.5 *Icelandic lowlands*

Since the coastline of Iceland is highly incised by fjords having steep slopes, villages developed on the few available lowlands below the mountains. Due to location, climate and still active geological processes, the villages are frequently damaged by several typologies of slope movements, snow avalanches and floods.

Following two catastrophic avalanches occurred on 1995, when 34 casualties were recorded inside zone marked "safe" on the official hazard maps, regulations for avalanches and landslides (including debris flows) were completely revised. At the present, hazard and risk zoning must be developed at large scale (1:5,000), on the basis of the quantitative risk assessment (QRA) and by observing a number of constraints among which: preparation and structure of hazard zoning; data collection; risk assessment; acceptable risk; explanation accompanying the hazard maps.

227

Figure 33. Eskifjörður and the names of main landmarks. (Photo: Esther H. Jensen).

Figure 34. The standard path (Jónasson et al. 1999).

Due to the complexity of the phenomena, observance of regulations requires efforts from operative, technical and scientific points of view, as it is highlighted by the IMO (Iceland Meteorological Office) website that offers documents, data, reports and papers on the subject. An overview of both the natural phenomena occurring in Iceland and the approach used for hazard and risk zoning is furnished by Jensen and Sönser (2002), Arnalds et al. (2002), Jónasson et al. (1999).

After a brief introduction about general settings, topographic characteristics and land-use in Iceland, Jensen and Sönser discuss the process oriented to landslide hazard assessment for Eskifjörður (Fig. 33), furnishing data on sites, human settlements, climate and extreme rainfall, geology and bedrock of rivers watershed (about 2–4 km^2 in size) falling through the village, and the loose soils (Andosols) covering the bedrock. Then, the authors analyse flood and geomorphic processes of mass movements (creep slope, slide, rockfall and debris flow) observing that debris flows generally initiate at zone > 25°, travel along the channel (>10°) where erosive phenomena can occur, and stop at flat areas <10°. Floods and debris flows are mainly triggered by intensive rainstorms and/or rapid snow melting, bursting of a dam created by snow or debris blocking the channel.

The hazard assessment for mass movement is, therefore, analysed on the basis of site investigation, literature review and some elements (historical events and frequency map) required by legislation (The Ministry of Environment 2000). Moreover, water runoff in the channels is determined for different return periods of rainfall intensity. Hydrographs for the catchment area are then developed, and the dominating channel process is estimated by using the van Dine's (1985) model, that allows to distinguish among stable condition; bedload transport; debris torrent; infinite slope failure and bedrock sliding. Finally, referring to some phenomena
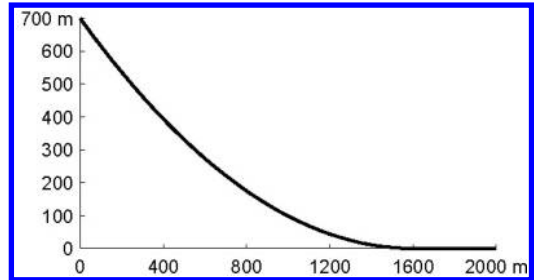
(floods and debris flows) and critical rainfall with different return periods, the authors furnish for some selected sites the waterload, debris volume (erosional processes) and debris volume including slides from the banks.

Further details on hazard assessment and zoning of mass movements can be obtained from Arnalds et al. (2002), who also analyse the avalanche hazard for Eskifjörður. With reference to avalanches, the authors describe the snow depth measurements in starting area together with track and runout zones. Estimation of runout is, therefore, furnished for selected sites with the aid of a method that is not explained in detail. However, the basic concepts of this and similar methods can be obtained by Jónasson et al. (1999), who describe a quantitative procedure for estimation of snow avalanche risk in residential areas, measured as annual probability of being killed.

The procedure is developed on the basis of a data set including 196 Icelandic avalanches, fallen from 81 different paths in 50 different hillsides, threatening 8 towns and villages. The observation history of each path (name, date, stopping position, width, profile, etc.) ranges from 80 to 100 years.

Considering that frequency estimation must regard avalanches expected to fall every 100, 300, 1,000 and 3,000 years (The Ministry of Environment 2000), the authors recognise the impossibility of frequency estimation of long avalanches if limited to local history. Therefore, they suggest to combine the avalanches history of all the paths in data set, so lengthening the observation time. To this aim, they assume an avalanche standard path that is representative of the Icelandic avalanche paths; it is parabola shaped, 700 m high and reaches level ground 1,600 m from the starting point (Fig. 34).

In order to calculate the runout of avalanches along the standard path, a physical transfer method for avalanche flow, based on the Coulomb resistance parameter μ and the mass-to-drag parameter M/D, is used as an alternative to the topographical α/β model developed by Jóhannesson (1998a, b). On the basis of the standard path, the physical transfer method and all the

228
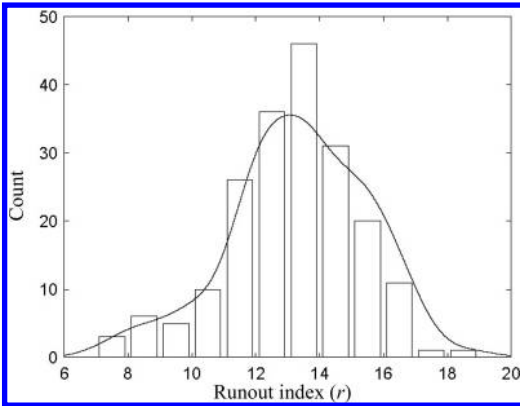
Figure 35. Runout indices of 196 Icelandic avalanches together with kernel estimated data density function (Jónasson et al. 1999).

Figure 36. Risk estimation due to avalanches from Bakkagil, Neskaupstaður. Scale 1:7,500 (Jónasson et al. 1999).

data collected data set, the authors obtain the "runout indices", measured in hectometres (Fig. 35), and estimate, via statistical analysis, the exceedance probability that an avalanche reaches a "runout index (r)" larger than $r = 13$, that is assumed as reference value for the Icelandic avalanches. Therefore, the exceedance probability is used to estimate, on the basis of the local history, the frequency of a single path avalanche at a general runout index.

As it concerns the elements at risk, the authors estimate the probability of surviving an avalanche striking a house on the basis of: the element exposure; the avalanche speed profile obtained by the physical transfer method; recorded data by previous case histories, etc.. Finally, a formula is furnished to calculate the risk of living or working in a building under an avalanche hillside; the formula takes into account the speed and shape (tongue effect) of the avalanche, the frequency of avalanches pasting the building, the probability of death. An example of risk estimation is furnished in Figure 36, where dashed and unbroken lines respectively represent the estimated level of risk and the runout indexes. It is interesting to observe that, in correspondence of the acceptable risk fixed by regulations ($R = 0.3 \times 10^{-4}$ for living house), the calculated return period is approximately $T = 5,700$ years, while $T = 800$ years corresponds to $R = 3 \times 10^{-4}$.

Referring to Jónasson et al. (1999) for more details, it must be stressed that the authors suggest the way to further improve the proposed method that, however, is considered not helpful in identifying starting zones of avalanches and not suitable with reference to: other natural hazards (for instance slush or mudflow); areas where countermeasures have been realised; hillsides where information on avalanche history is not available in data set. In this case, however,
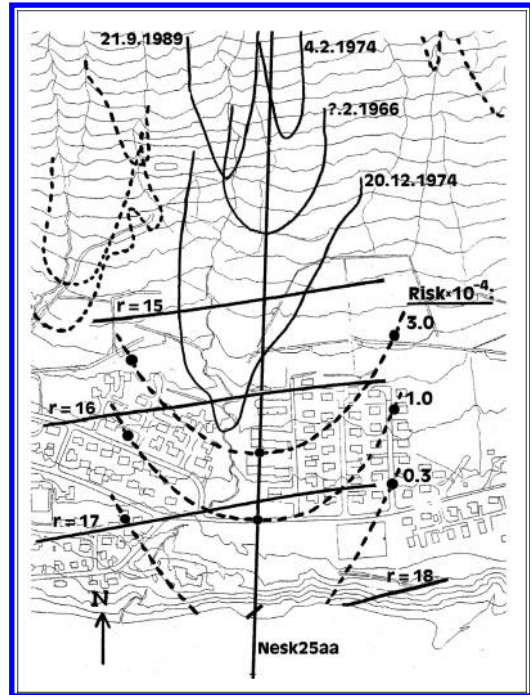
the method could be used to evaluate an upper limit of the risk under the hillsides.

7 CONCLUDING REMARKS

During the last decades several strategies for landslides risk management have been developed to fight against the consequence of such phenomena which threaten all the continents, although with different intensity and recurrence. The strategies include hazard and risk zoning methods, as well as non-structural measures.

As it concerns the first point, the experience gained and the results obtained in several countries encourage the use of hazard and risk zoning to improve the urban planning and development as well as to minimize the associated risk. However, some remarks derive from the scientific literature.

There is a need for standardized and reproducible methods for assessing hazard and risk components, and particularly in what respects to the definition of classes.

Frequency and risk should be quantitatively assessed, as they can improve the reliability of hazard and risk zoning that is the way forward to getting uniformity in planning.

229

Development in automatic data capture techniques should not put aside field work and personal judgement. Exercises of comparing hazard maps performed by different teams show important discrepancies in the results. The main differences are due to the quality of the input data and, particularly, in the completion of the landslide inventories. Despite of the impressive improvement of the remote sensing techniques, the identification and interpretation of landslide features is not evident and the appropriate completion of the landslide inventories still rely on the skill of the specialists.

Both hazard and risk maps must be checked and validated with reliable procedures. Working with large scale maps requires a great deal of accuracy in defining boundaries of the hazardous zones and of the magnitude-frequency of the events. The lack of both complete and reliable data sets in many landslide threatened urban areas is a constraint for the achievement of a minimum level of quality in the documents. This might be a source of future arguments and conflicts.

With reference to the non-structural measures, they include the prohibition or restriction of building in hazardous areas, the establishment of warning systems in location where the hazard cannot be avoided but risk can be minimized by early warning and evacuation plans, and legal measures and economic subsides in case of catastrophe.

Prohibition and restriction to development, if possible, is probably the most efficient way to minimize both hazard and risk. This can be put into practice if landslide hazard maps and hazard zoning are available in a particular area, the last to be integrated in urban planning and regional development analysis. However, the long-term applicability of local plans or rules for the use of landslide-prone area still represents a main problem in several countries.

Evacuation plans and warning systems can represent a valuable safeguard measure for population living inside risk zones, providing that a good educational programme including training has been developed, as in the case of Hong Kong, and an efficient monitoring system has been implemented.

Monitoring systems are generally based on the check-in of selected factors among the triggering ones, the indicators of slope stability conditions and the effects caused by the triggering factors. To be efficiently implemented in warning systems, the experimental observations must be systematically tested in sample areas and elaborated by an advanced mathematical modeling aimed to individuate reliable threshold values of rainfall, displacement, etc. Moreover, the efficiency can be improved by coordinating national, regional and urban systems, working at different scales, and by systematically testing out of the new technologies, not disregarding difficulties and misleading results.

REFERENCES

AGS Subcommittee on Landslide Risk Assessment 2000. Landslide risk management, concepts and guidelines. *Australian Geomechanics* 35: 49–92.

Ahmad, R. & McCalpin, J.P. 1999. Landslide susceptibility maps for the Kingston metropolitan Area. *Jamaica Organisation of America States General Secretariat Unit for Sustainable Development*, *UDS Publication no. 5*. Available at: htpp://www.oas.org/en/cdmp/document/kma/udspub5.htm

Allievi, J., Monsignore, F., Cespa, S., Colesanti, C., Ferretti, A., Morelli, M. & Pistocchi, A. 2003. Analisi di fenomeni di deformazione superficiale sul territorio dell'Autorità dei bacini romagnoli a partire da serie di dati radar satellitari elaborati con la tecnica dei diffusori permanenti. *T.R.E.s.r.l.* Available at: http://www.treuropa.it/

ANCOLD 1998. *Guidelines on Risk Assessment. Position Paper on Revised Criteria for Acceptable Risk to Life*. Working Group on Risk Assessment, August 1998.

Annan, K. 2002. *Disaster reduction and sustainable development: understanding the links between vulnerability and risk related to development and environment*. Open File Report, International Strategy for Disaster Reduction United Nations, UN/ISDR.

Antoine, P. 1978. Glissements de terrains et aménagement de la motagne. *Bulletin de la Société vaudoise des Sciences Naturelles* 74(1): 1–14.

Archetti, R. & Lamberti, A. 2003. Assessment of risk due to debris flow events. *Natural Hazards Review* 4(3): 115–125.

Ardizzone, F., Cardinali, M., Carrara, A., Guzzetti, F. & Reichenbach, P. 2002. Impact of mapping errors on the reliability of landslide hazard maps. *Natural Hazards and Earth System Sciences* 2: 3–14

Arias, A. 1970. A measure of earthquake intensity. In Hansen (ed), *Seismic design for nuclear power plants*. Massachusetts Institute of Technology Press, Cambridge, Mass.: 438–483.California Geological Survey, 2004.

Arnalds, þ., Sauermoser, S., Jóhannesson, T. & Jensen, E. 2002. *Hazard zoning for Eskifjörõur*. Iceland Meteorological Office Report 02015. http://www.vedur.is/english/

Atkins Haswell, A. 1995. *Quantitative landslide risk assessment for the squatter village in Lei Yu Mun*. Report prepared for the Geotechnical Engineering Office (Hong Kong).

Ayala, F.J., Cubillo, S., Álvarez, A., Domínguez, M.J., Laín, L., Laín, R. & Ortíz, G. 2003. Large scale rockfall reach susceptibility maps in La Cabrera Sierra (Madrid) performed with GIS and dynamic analysis at 1:5,000. *Natural Hazards* 30: 325–340.

Berardino, P., Costantini, M., Franceschetti, G., Iodice, A., Pietranera, L. & Rizzo, V. 2003. Use of differential SAR interferometry in monitoring and modelling large slope instability at Maratea (Basilicata, Italy). *Engineering Geology* 68: 31–51.

Berardino, P., Fornaro, G., Lanari, R. & Sansosti, E. 2002. A new Algorithm for Surface Deformation monitoring based on Small Vaseline Differential SAR Interferograms. *IEEE Transactions on Geoscience and Remote Sensing* 40(11): 2375–2383.

Besson, L., Durville, J.L., Garry, G., Graszk, E, Hubert, T. & Toulemont, M. 1999. Plans de prévention des risques naturels (PPR) – Risques de mouvements de terrain. Guide méthologique. *La Documentation Française*, Paris.

Bonnard, Ch., Coraglia, B., Durville, J.L. & Forlati, F. 2004a. Suggestions, guidelines and perspectives of development. In Bonnard et al. (eds.), *Identification and Mitigation of Large Landslide Risks in Europe – IMIRI-LAND Project, European Commission – Fifth Framework Program*: 289–306, A.A. Balkema, Rotterdam.

Bonnard Ch., Forlati F., Scavia C. (eds.) 2004b. *Identification and Mitigation of Large landslide Risks in Europe*. IMIRILAND Project. European Commission – Fifth Framework Program, 317 pp. A.A. Balkema, Rotterdam.

Bonnard, Ch. & Noverraz, F. 1984. Instability risk maps: from the detection to the administration of landslide prone areas. *Proc. of the IV International Symposium on Landslides, Toronto*. Vol. 2: 511–516.

Bonnard, Ch., Noverraz, F., Lateltin, O. & Raetzo, H. 1995. Large landslides and possibilities of sudden reactivation. *Felsbau* 13(6): 401–407.

Brabb, E.E. 1984. Innovative approaches to landslide hazard and risk mapping. *Proc. of the IV International Symposium on Landslides, Toronto*. Vol. 1: 307–323.

Brabb, E.E., Colgan, J.P. & Best, T.C. 1999a. *Map MF-2329 showing inventory and regional susceptibility for Holocene debris flows and related fast moving landslides in the Conterminous United States*. U.S. Geological Survey Map. U.S. Department of the Interior.

Brabb, E.E., Colgan, J.P. & Best, T.C. 1999b. *Pamphlet to accompany Map MF-2329, Map showing inventory and regional susceptibility for Holocene debris flows and related fast moving landslides in the Conterminous United States*. U.S. Geological Survey Map. U.S. Department of the Interior. http://geopubs.wr.usgs.gov/map-mf/mf2329/.

Brand, E. W. 1984. Landslides in Southeast Asia: a state-of-art report. *Proc. 4th Int. Symp. Landslides, Toronto*. Vol. 1: 17–59.

Brand, E.W. 1985. Landslides in Hong Kong. *Proc. 8th S.E. Asian Geotech. Conf., Kuala Lampur* 2: 107–122.

Brand, E.W. 1988. Special Lecture: Landslide risk assessment in Honk Kong. *Proc. V Int. Symp. on Landslides, Lausanne*, Vol. 2: 1059–1074.

Burnett, A.D. 1987. Slope failures in Hong Kong and their mitigation. *Proc. US-Asia Conf. Engineering for Mitigating NaturalHazards Damage, Bangkok*.C4.1-C4.20.

Caine, N. 1980. The rainfall intensity-duration control of shallow landslides and debris-flows. *Geografiska Annaler* 62A: 23–27.

Calcaterra, D., de Riso, R. & Santo, A. 2003. "Landslide hazard and risk mapping: experiences from Campania, Italy". In Picarelli (Editor). Fast Slope Movements,

Prediction and Prevention for Risk Mitigation. Patron Editore, Bologna. Vol. 1: 63–70.

Carnec, C., King, C. & Massonnet, D. 1995. Measurement of land subsidence by means of differential S.A.R. interferometry. In Barends et al. (eds), *Land Subsidence*, Balkema, Rotterdam.

Carrara, A. 1983. Multivariate models for landslide hazard evaluation. *Mathematical Geology* 15(3): 403–426

Carrara, A., Cardinali, M., Detti, R., Guzzetti, F., Pasqui, V. & Reichenbach, P. 1991. GIS techniques and statistical models in evaluating landslide hazard. *Earth Surface Processes and Landforms* 16: 427–445.

Carrara, A., Cardinali, M. & Guzzetti, F. 1992. Uncertainty in assessing landslide hazard and risk. *ITC Journal* 2: 172–183.

Carrara, A., Cardinali, M., Guzzetti, F. & Reichenbach, P. 1995. GIS technology in mapping landslide hazard. In Carrara & Guzzetti (eds.). *Geographical Information Systems in Assessing Natural Hazards*. Kluwer Academic Publishers, pp. 135–175.

Carrara, A., Guzzetti, F., Cardinali, M. & Reichenbach, P. 1999. Use of GIS technology in prediction and monitoring of landslide hazard. *Natural Hazards* 20: 117–135.

Cascini E., Cascini, L. & Gullà, G. 1992. A back-analysis based on piezometers response. In Bell (ed), *Proc. of VI Int. Symp. on landslides, Christchurch*, Vol. 2: 1123–1128.

Cascini, L. 2004. The flowslides of may 1998 in the Campania Region, Italy: the scientific emergency management. *Italian Geotechnical Journal* 2: 11–44.

Cascini, L. 2005. Risk assessment of fast landslides – From theory to practice. General Report. *Proc. of the Int. Conf. on "Fast Slope Movements – Prediction and Prevention for Risk Mitigation", Napoli*. Vol. 2. Pàtron Editore (in press).

Cascini, L., Critelli, S., Di Nocera, S., Gullà, G. & Matano, F. 1994. Grado di alterazione e franosità negli gneiss del massiccio silano: l'area di S. Pietro in Guarano. *Geologia Applicata ed Idrogeologia* XXVII: 49–76. (In Italian).

Cascini, L. & Ferlisi, S. 2003. Occurrence and consequences of flowslides: a case study. *Proc. of the Int. Conf. on "Fast Slope Movements – Prediction and Prevention for Risk Mitigation", Napoli*. Vol. 1: 85–92. Pàtron Editore.

Cascini, L., Gullà, G. & Sorbino, G. 1995. Modellazione delle acque sotterranee di una coltre di detrito in frana: risultati preliminari. *Rivista Italiana di Geotecnica* XXIX(3): 201–223. (In Italian)

Cascini, L. & Sorbino, G. 2003. The contribution of in situ soil suction measurements to the analysis of flowslide triggering. *Proc. of the Int. Workshop "Flows 2003 – Occurrence and Mechanisms of Flows in Natural Slopes and Earthfill"* (Sorrento, Italy),: 77–86, Pàtron Editore.

Cascini, L., Sorbino, G. & Cuomo, S. 2003. Modelling of flowslide triggering in pyroclastic soil. *Proc. of the Int. Conference on "Fast Slope Movements – Prediction and Prevention for Risk Mitigation"*, (ed. Picarelli). Pàtron Editore, Vol. I, 93–100.

Cascini, L. & Versace, P. 1988. Relationship between rainfall and landslide in a gneissic cover. *Proc. 5th Int. Symposium on Landslides, Lausanne*, Vol. 1: 565–570.

Colesanti, C. & Wasowski, J. 2004. Satellite SAR interferometry for wide-area slope hazard detection and site-specific monitoring of slow landslides. *Proc. of the 9th International Symposium on "Landslides: evaluation and stabilization"*. Taylor & Francis Group, London.

Copons, R, Altimir, J., Amigó, J. & Vilaplana, J.M. 2001. Medotología Eurobloc para el estudio y protección de cáidas de bloques rocosos. Principado de Andorra. *Proc. of V Simposio Nacional sobre Taludes y Laderas Inestables. Madrid*. Vol. 2: 665–676.

Copons, R., Vilaplana, J.M., Altimir, J. & Amigó, J. 2000. Estimación de la eficacia de las protecciones contra la caída de bloques. *Revista de Obras Públicas* (3394): 37–48.

Copons, R., Vilaplana, J.M., Corominas, J., Altimir, J. & Amigó, J. 2004. Rockfall risk management in high-density urban areas. The Andorran experience. In Glade et al. (eds), *Landslide Hazard and Risk*. John Wiley and Sons (in press).

Corominas, J. 1996. The reach angle as a mobility index for small and large landslides. *Canadian Geotechnical Journal* 33: 260–271.

Corominas, J., Copons, R., Vilaplana, J.M., Altimir, J. & Amigó, J. 2003a. From landslide hazard assessment to management. The Andorran experience. In Picarelli (ed). *Fast slope movements. Prediction and prevention for risk mitigation.* Vol. 1: 111–118. Patron Editore.

Corominas, J., Copons, R., Vilaplana, J.M., Altimir, J. & Amigó, J. 2003b. Integrated landslide susceptibility analysis and hazard assessment in the Principality of Andorra. *Natural Hazards* 30: 421–435.

Corominas, J., Esgleas, J. & Baeza, C. 1990. Risk mapping in the Pyrenees area: a case study. *In Hydrology of Mountainous Regions II- Artificial Reservoirs, Water and Slopes*. IAHS Publ. 194: 425–428.

Crozier, M.J & Eyles, R.J. 1980. Assessing the probability of rapid mass movement. *3rd Australia-New Zealand Conference on Geomechanics*. Wellington, NZ. Vol. 2: 2.47–2.51.

Cruden, D.M. & Varnes, D.J. 1996. Landslide types and process. *In "Landslides – Investigation and Mitigation", Trasportation Research Board Special Report No. 247*, Turner & Schuster (eds.), National Academy Press, Washington DC: 36–75.

Curlander, J.C. & McDonough, R.N. 1991. *Synthetic Aperture Radar: Systems and Signals Processing*. John Wiley and Sons, New York, 672 pp.

Dai, F.C., Lee, C.F. & Ngai, Y.Y. 2002. Landslide risk assessment and management: an overview. *Engineering Geology* 64: 65–87.

Dana, J.D. 1863. *Manual of geology: treating of the principles of the science with special reference to American geological history, for the use of colleges, academies, and school of science*. Trübner & Co., London: 798 pp.

DRM. 1990. Les études préliminaires à la cartographie réglementaire des risques naturels majeurs. Secreteriat d'État auprès du Premier ministre charge de l'Environnement et de la Prevention des Risques technologiques et naturels majeurs. *La Documentation Française*: 143 p.

Dunoyer, M. & Van Westen, C.J. 1994. Assessing uncertainty in interpreting landslides from air-photos. *ITC Journal* 3.

DUTI. 1983. *Detection et utilisation des terrains instables*. École Polytechnique Féderale de Lausanne, Switzerland. 130 pp.

Einstein, H.H. 1988. Landslide risk assessment procedure. *Proc. of V Int. Symp. on Landslides, Lausanne,* Vol. 2: 1075–1090. Balkema, Rotterdam.

Einstein, H.H. 1997. Landslide risk – Systematic approaches to assessment and management. *Proc. of the Int. Workshop on Landslide Risk Assessment, Honululu*: 25–50.

ERM. 1998. Landslides and boulder falls from natural terrain: interim risk guidelines (GEO report No. 80). Geotechnical Engineering Office, Hong Kong, 183 pp.

Faella, C. & Nigro, E. 2003. Dynamic impact of the debris flows on the constructions during the hydrogeological disaster in Campania-1998: failure mechanical models and evaluation of the impact velocity. *Proc. of the Int. Conf. on "Fast Slope Movements – Prediction and Prevention for Risk Mitigation", Napoli*. Vol. 1: 179–186. Pàtron Editore.

Feckner, S. 2002. Development setbacks from river valley/ravine crests in newly developing areas. In McInnes & Jakeways (eds.). *Instability Planning and Management*: 135–142, Thomas Telford.

Fell, R. 1994. Landslide risk assessment and acceptable risk. *Canadian Geotechnical Journal* 31: 261–272.

Fell, R. & Hartford, D. 1997. Landslide risk management. In Cruden & Fell (eds.). *Landslide Risk Assessment*. A.A. Balkema Publishers: 51–109.

Fell, R., Ho, K.K.S., Lacasse, S. & Leroi, E. 2005. Framework for landslide risk assessment and management. State-of-the-art Lecture (SOA1). *This volume*.

Ferretti, A., Prati, C. & Rocca, F. 1999a. Permanent scatterers in SAR interferometry. *IEEE Trans. Geosc. Remote Sensing*, June.

Ferretti, A., Prati, C. & Rocca, F. 1999b. Non-linear subsidence rate estimation using permanent scatterers in differential SAR interferometry. *IEEE Trans.Geosc. Remote Sensing*, September.

Fraser, C.S. Baltsavias, E. & Gruen, A. 2002. Processing of IKONOS imagery for submetre 3D positioning and building extraction. *ISPRS Journal of Photogrammetry and Remote Sensing* 56(3): 177–194.

Fruneau, B., Delacourt, C. & Achache, J. 1996. Observation and modelling of the Saint-Etienne-de- Tinee landslide using SAR interferometry. *Proceedings of FRINGE 1996 Workshop*.

Galloway, D.L., Burgmann, R., Fielding, E., Amelung, F. & Laczniak, R.J. 2000. Mapping recoverable aquifer-system deformation and land subsidence in Santa Clara Valley, California, USA, using space-borne synthetic aperture radar. *Proc. of the 6th Int. Symposium on Land Subsidence, Ravenna (Italy)*.

Garry, G. & Graszk, Ed. 1997. Plans de prévention des risques naturels (PPR) – Guide général. *La Documentation Française*, Paris.

Gili, J.A., Corominas J. & Rius, J. 1999. Using Global Positioning System techniques in landslide monitoring. *Engineering Geology* 55: 167–192.

Graszk, E. & Toulemont, M. 1996. Plans de prévention des risques naturels et expropriation pour risques majeurs. Les mesures de prèvention des risques naturels de la loi du 2 février 1995. *Bull. Labo. P. & Ch.* 206: 85–94.

Guida, D. & Iaccarino, G. (1991). Fasi evolutive delle frane tipo colata nell'alta valle del F. Basento (Potenza). Studi Trentini di Scienze Naturali, *Acta Geologica* 68: 127–152.

Gullà, G. 2004. *Personal communication*.

Gullà, G. & Niceforo, D. 2003. *Linee guida per interventi di stabilizzazione di pendii in aree urbane da riqualificare*. Regione Calabria – UE – POP 1994/99 Misura 4.4

"Ricerca scientifica e tecnologica", 196 pp., Rubbettino Editore.

Harp, E.L. & Jibson, R.W. 1995. *Inventory of landslides triggered by the 1994 Northridge, California earthquake*, U.S. Geological Survey Open-File Report 95–213, 17 pp., 2 plates.

Harp, E.L. & Jibson, R.W. 1996, Landslides triggered by the 1994 Northridge, California earthquake: *Bulletin of the Seismological Society of America* 86(1B): S319-S332.

Hartlén, J. & Viberg, L. 1988. Evaluation of landslide hazard". *Proc of the 5th International Symposium on Landslides, Lausanne, Switzerland*. In Bonnard (editor), Landslides, vol. 2: 1037–1057, A.A. Balkema Publisher.

Hayne, M., Michael-Leiba, M., Gordon, D., Lacey, R. & Granger, K. 2002. *Geoscience Cities project, Chapter 7: Landslide Risks*. Available at Geoscience Australia website: http://www.AGSO.gov.au

Ho, K., Leroi, E. & Roberds, B. 2000. Quantitative risk assessment: application, myths and future direction. Special Lecture. *Proc. of the Int. Conf. on Geotechnical and Geological Engineering, GeoEng2000, Melbourne:* 269–312. http://www.unisdr.org/eng/about_isdr/bd-lwr-2004-eng.htm

Humbert, M. 1972. Les Mouvements de terains. Principes de réalisation d'une carte previsionelle dans les Alpes. *Bulletin du BRGM.* Section III, n°1: 13–28.

Humbert, M. 1977. La Cartographie ZERMOS. Modalités d'établissement des Cartes des zones exposées à des riques liés aux mouvements du sol et du sous-sol. *Bulletin du BRGM*, Section III, n°1/2: 5–8.

Hungr, O. 1997. Some methods of landslide hazard intensity mapping. In Cruden & Fell (eds.). *Landslide Risk Assessment*: 215–226. Balkema, Rotterdam.

INGEOMINAS. 2002. *Clasificación Regional de Amenaza Relativa de Movimientos en Masa de Colombia* (Colombia).

Irigaray, C., Fernández, T., El Hamdouni, R. & Chacón, J. 1999. Verification of landslide susceptibility mapping: a case study. *Earth Surface Processes and Landforms* 24: 537–544.

IUGS. 1997. Quantitative risk assessment for slopes and landslides- The state of the art. In Cruden & Fell (eds.). *Landslide Risk Assessment*: 3–12. Balkema, Rotterdam.

Jensen, E. & Sönser, T. 2002. *Process orientated landslide hazard assessment for Eskifjörõur*. IMO, Rep. 02014.

Jibson, R.W., Harp, E.L. & Michael, J.A. 1998. A method for producing digital probabilistic seismic landslide hazard maps: An example from southern California. *U.S. Geological Survey Open-File Report 98–113*, 17 pp., 2 pl.

Jibson, R.W., Harp, E.L. & Michael, J.A. 2000, A method for producing digital probabilistic seismic landslide hazard maps: *Engineering Geology* 58: 271–289.

Jóhannesson, T. 1998a. Return period for avalanches on Flateyri. *Greinargerð Veðurstofu Íslands*. Report VÍ-G98008-ÚR07. Reykjavík, 12 pp.

Jóhannesson, T. 1998b. Icelandic avalanche runout models compared with topographical models used in other countries. In: E. Hestnes (editor), 25 years of snow avalanche research, Voss, May 12–16, 1998. *Norwegian Geotechnical Institute Publications* 203: 43–52.

Jónasson, K., Sigurõsson, S.˚. & Arnalds, ˚. 1999. *Estimation of avalanche risk Iceland Mteorological Office*. Reykjavik. Available at http://www.vedur.is/english.

Kircher, M., Hoffmann, J., Roth, A., Kampes, B., Adam, N. & Neugebauer Horst, J. 2003. Application of Permanent Scatterers on mining-induced subsidence. *Proceedings of FRINGE 2003 Workshop, Frascati, Italy*.

Lateltin, O. 1997. *Recommandations: prise en compte des dangers dus aux mouvements de terrain dans le cadres des activités de l'aménagement du territoire*. OFAT, OFEE and OFEFP. Switzerland. 42 pp.

Leone, F., Asté, J.P. & Leroi, E. 1996. Vulnerability assessment of elements exposed to mass moving: working towards a better risk perception. In Senneset (ed.), *Landslides*, Vol. I: 263–269 Balkema, Rotterdam.

Leroi, E. 1996. Landslide hazard-Risk maps at different scales: objectives, tools and developments. In Senneset (ed.) *Landslides*, Vol. I: 35–51. Balkema, Rotterdam.

Leroi, E. 1997. Landslide risk mapping: problems, limitations and developments. In Cruden & Fell (eds.) *Proc. of Int. Workshop on Landslide Risk*: 239–250. Balkema, Rotterdam.

Leroueil, S., Locat, J., Vaunat, J., Picarelli, L. & Faure, R. 1996. Geotechnical characterisation of slope movements. *Proc. of the VII Int. Symp. on Landslides. Trondheim, Norway.* Vol 1: 53–74.

Lopez, C., Ruíz, J., Amigó, J. & Altimir, J. 1997. Aspectos metodológicos del diseño de sistemas de protección frente a las caídas de bloques mediante modelos de simulación cinemáticos. *IV Simposio nacional sobre taludes y laderas inestables*, Granada. Vol. 2: 811–823.

Lumb, P. 1975. Slope failures in Hong Kong. *Quarterly Journal of Engineering Geology* 8: 31–65.

Malet, J.P., Maquaire, O. & Calais, E. 2001. The use of Global Positioning System techniques for the continuous monitoring landslides: application to the Super-Sauze earthflow (Alpes-de-Haute-Provence, France). *Geomorphology* 43: 33–54.

Massonnet, D., Feigl, K., Rossi, M. & Adragna, F. 1994. Radar interferometric mapping of deformation in the year after Landers earthquake. *Nature* 369: 227–230.

Michael-Leiba, M., Baynes, F. & Scott, G. 1999. *Quantitative landslide risk assessment of Cairns*. AGSO Record 1999/36, AGSO Cities Project, Australian Geological Survey Organisation Canberra.

Michael-Leiba, M., Baynes, F. & Scott, G. 2002. Quantitative landslide risk assessment of Cairns. *Australian Geomechanics* 37(3).

Michael-Leiba, M., Baynes, F., Scott, G. & Granger, K. 2003. Regional landslide risk to the Cairns community. *Natural Hazards* 30: 233–249.

Ministry of the Environment (Iceland Nation). 2000. *Regulation on hazard zoning due to snow- and landslides classification and utilisation of hazard zones and preparation of provisional hazard zoning.* July 2000.

Moeremans, B. & Dautrebande, S. 2000. Soil moisture evaluation by means of multitemporal ERS SAR PRI images and interferometric coherence. *Journal of Hydrology* 234: 162–169.

Montero, J. 2003. Deslizamientos en Colombia: Estrategias para reducción de riesgos y costos. *Proc. 12th Panamerican Conference on Soils Mechanics and Geotechnicals Engineering*, Boston USA. Session 5.4: 2819–2826.

Montero, J. & Cortés, R. 1989. Clasificación Regional de Amenaza de Deslizamientos. *Proc. Primer Simposio*

233

Suramericano de Deslizamientos SCG-CSMM, Paipa, Colombia, Vol. 1.

Montgomery, D.R. & Dietrich, W.E. 1994. A physically based model for the topographic control of shallow landsliding. *Water Resources Research* 30: 1153–1171.

Moya, J. & Corominas, J. 2004. Determinación de la frecuencia de desprendimientos mediante la dendrocronología. *In Benito & Díez (eds.). Riesgos Naturales y Antrópicos en Geomorfología*. SEG and CSIC. Madrid: 379–387.

Munich Re, 2002. Topics – Retrospectiva anual catástrofes naturales 2002. Available at: http://www.munichre.com

National University of Colombia. 1989. *Inventario de Deslizamientos en la Red Vial Nacional*.

Neuland, H. 1976. A prediction model of landslips. *Catena* 3: 215–230.

Newmark, N.M., 1965, Effects of earthquakes on dams and embankments. *Geotechnique* 15:139–160.

Nilsen, T.H., Wright, R.H., Vlasic, T.C. & Spangle, W.E. 1979. Relative slope stability and land-use planning in the San Francisco Bay region, California. *U.S. Geological Survey Professional Paper 944*: 96 pp.

Noverraz, F. & Bonnard, Ch. 1990. Mapping methodology of landslides and rockfall in Switzerland. Proc. of 6th International Conference and Field Workshop on Landslides, Milan, 45–53.

Noverraz, F., Bonnard, Ch., Dupraz, H. & Huguenin, L. 1998. Grands glissements de versant et climat. Project VERSINCLIM, Rapport final PNR 31, V/d/f Hochschulverlag AG, Zürich, 314 pp.

O.U. 2.38. 1998. *Ricerca storica sulle colate di fango in terreni piroclastici della Campania*. G.N.D.C.I.-C.N.R., Department of Civil Engineering. University of Salerno (Italy).

Pack, R.T., Tarboton, D.G. & Goodwin, C.N. 1998. The SINMAP approach to terrain stability mapping. *Submitted to 8th Congress of the International Association of Engineering Geology, Vancouver, British Colombia, Canada 21–25 September 1998*.

Pastor, M., Quecedo, M., Gonzales, E., Herreros, M.I., Merodo, J.A.F. & Mira, P. 2003. An eulerian model for soil dynamics: application to fast slope movements. *Revue francaise de génie civil*, Geodynamics and Cycling Modelling, Vol. 7: 1003–1051.

Priestnall, G., Jaafar J. & Duncan, A.(2000). Extracting urban features from LIDAR digital surface models. *Computers, Environment and Urban Systems* 24(2): 65–78.

Programme Interreg IIC – "Falaises". 2001. In K. Karere, S. Ratto & Zanolini F. (eds), *Prévention des mouvements de versants et des instabilités de falaises. Confrontation des méthodes d'étude des éboulements dans l'arc alpin*. Méditerranée occidentale et Alpes latines.

Quattrocchi, D.A. & Luvall, J.C. 1999. Thermal infrared remote sensing for analysis of landscape ecological processes: methods and applications. *Landscape Ecology* 14: 577–598.

Ramírez, F. & González, A.J. 1989. Evaluación de estabilidad para zonas homogéneas. *I Simposio Sudamericano de Deslizamientos*, Sociedad Colombiana de Geotecnia, Paipa (Colombia), vol 1: 174–192.

Reginato, R.J., Idso, S.B., Vedder, J.F., Jackson, R.D., Blanchard, M.B. & Goettelman, R. 1976. Soil water content and evaporation determined by thermal parameters

obtained from ground based and remote measurements. *J. Geophys. Res*. 81(9): 1617–1620.

Remondo, J., González, A., Díaz de Terán, J.R., Cendrero, A., Fabbri, A. & Chung, Ch-J. 2003. Validation of landslide susceptibility maps; examples and applications from a case study in Northern Spain. *Natural Hazards* 30: 437–449.

Rossi, F., Chirico, G. & Ricciardi, F. 1998. *Guida alle soglie pluviometriche d'allarme*. Dep. of the Civil Protection – G.N.D.C.I. – University of Salerno (Italy).

Rossi, F., Villani, P., Tropeano, R., Mastrandrea, G. & Longobardi, A. 2005. *Final report of the Research Line on Hydraulic Risk*. C.E.R.I.U.S.: Centre of Excellence on "Forecasting and Prevention of hydrogeological risk over large areas", University of Salerno, Italy (in press).

Sandersen, F., Bakkehøi, S., Hestnes, E. & Lied, K. 1996. The influence of meteorological factors on the initiation of debris flows, rockfalls, rockslides and rockmass stability. *In Senneset (ed.). Landslides. Proceedings 7th International Symposium on Landslides*. A.A. Balkema. Vol. 1: 97–114.

Sassa, K. 1988. Geotechnical model for the motion of landslides. In Bonnard (ed.), *Proc. of the 5th International Symposium on Landslides*, Lausanne, Switzerland.. Landslides. A.A. Balkema, vol. 1: 37–55.

Sassa, K., Wang, G., Fukuoka, H., Wang, F., Ochiai, T., Sugiyama, M. & Sekiguchi, T. 2004. Landslide risk evaluation and hazard zoning for rapid and long-travel landslides in urban development areas. *Landslides* 1: 221–235.

Savage, W.Z., Godt, J.W. & Baum, R.L. 2003. A model for spatially and temporally distributed shallow landslide initiation by rainfall infiltration. In Rickenmann & Chen (eds). *Proceeding of the Third International Conference on Deris Flow hazard Mitigation: Mechanics, Prediction and Assessment, Davos, Switzerland*: 179–187. Rotterdam: Millpress.

Savage, W.Z., Godt, J.W. & Baum, R.L. 2004. Modeling time dependent areal slope stability. In Lacerda et al. (eds). *Landslides: evaluation and stabilization*. Vol. 1: 23–36. A.A. Balkema Publishers.

Scipal, K., Wagner, W., Trommler, M. & Naumann, K. 2002. The Global Soil Moisture Archive 1992–2000 from ERS Scatterometer Data: first results. *IEEE*.

Shuk, E.T. 1990. La evolución y el estado actual de la metodología basada en taludes naturales para análisis de estabilidad en masas de materiales geológicos. *V Simposio Venezolano de Mecánica de Suelos e Ingeniería de Fundaciones*, Caracas (Venezuela).

Soeters, R. & Van Westen, C.J. 1996. Slope instability recognition, analysis and zonation. In Turner & Schuster (eds.). *Landslide Investigation and Mitigation*. TRB Special Report 247: 129–177, National Academy Press, Washington D.C.

Sorbino, G. 1994. *Il regime delle acque sotterranee nelle rocce metamorfiche alterate*. PhD Thesis, University of Naples "Federico II".

Spence, R.J.S., Zuccaro, G., Petrazzuoli, S. & Baxter, P.J. 2004. Resistance of buildings to pyroclastic flows: analytical and experimental studies and their application to Vesuvius. *Natural Hazards Review* 5: 48–59.

Squarzoni, C., Delacourt, C. & Allemand, P. 2002. Nine years of spatial and temporal evolution of the La Vallette

landslide observed by SAR interferometry. *Engineering Geology* 68: 53–66.

Stilla, U., Sorgel, U. & Thoennessen, U. 2003. Potential and limits of InSAR data for building reconstruction in built-up areas. *ISPRS Journal of Photogrammetry and Remote Sensing* 58(1–2): 113–123.

Turrini, M.C. & Visintainer, P. 1998. Proposal of a method to define areas of landslides hazard and application to an area of the Dolomites, Italy. *Engineering Geology* 50: 255–265.

UNEP. 1997. *Introduction to Hazard. 3rd Edition. United Nation Development Programme.* Department of Humanitarian Affairs.

United Nations. 2004. *Living with Risk. A global review of disaster reduction initiatives.* 2004 version. Inter-Agency Secretariat of the International Strategy for Disaster Reduction (UN/ISDR). Available at:

Urciuoli, G. 2004. *Personal communication*.

Vail, A.J. 1984. Two landslides disasters in Hong Kong. *Proc. 4th int. Symp. Landslides, Toronto.* Vol. 1: 717–722.

Vail, A.J. & Beattie, A.A. 1985. Earthworks in Hong Kong – their failure and stabilization. *Proc. Symp. Failures in Earthworks, London:* 15–28.

Van der Kooij, M.W.A., van Halsema, D., Groenewoud, W., Ambrosius, B.A.C., Mets, G.J., Overgaauw, B. & Visser P.N.A.M. 1995. In Barends et al. (eds.), *Satellite radar measurements for land subsidence detection. Land Subsidence*, Balkema, Rotterdam.

Van Westen, C.J. 1994. GIS in landslide hazard zonation: a review, with examples from the Andes of Colombia. In Price & Heywood. *Mountain Environments and Geographic Information Systems*: 135–165, Taylor and Francis Publishers.

Van Westen, C.J. 2004. Geo-information tools for landslide risk assessment: an overview of recent developments. In Lacerda et al. (eds.). *Landslides: evaluation and stabilization.* Vol. 1: 39–56. A.A. Balkema Publishers.

Van Westen, C.J., Seijmonsbergen, A.C. & Mantovani, F. 1999. Comparing landslide hazard maps. *Natural Hazards* 20: 137–158.

VanDine, D.F. 1985. Debris flows and torrents in the Southern Canadian Cordillera. *Canadian Geotechnical Journal* 22: 44–68.

Varnes, D.J. 1978. Slope movements. Types and processes. In Schuster & Krizker "Landslides: analysis and control", Nat. Acad of Sciences, Trasp. Res. Board, Washington, Special Report 76: 11–35.

Varnes, D.J. 1984. Landslide hazard zonation: a review of principles and practice. *Natural Hazard* 3: 63.

Vulliet, L. & Bonnard, Ch. 1996. The Chlöwena landslide: prediction with a viscous model. In Senneset (ed.), *Landslides*, *Proc. of the 7th Int. Symp. on Landslides, Trondheim*, Vol. I: 397–402. Balkema, Rotterdam.

Walkden, M.J., Hall, J.W. & Lee, E.M. 2002. A modelling tool for predicting coastal cliff recession and analysing cliff management option. In McInnes & Jakeways (eds). *Instability Planning and Management*: 415–422, Thomas Telford.

Wegmuller, U., Strozzi, T. & Tosi, L. 2000. Differential SAR interferometry for land subsidence monitoring: methodology and examples. *Proc. of the 6th Int. Symposium on Land Subsidence. Ravenna (Italy).*

Western, A.W. & Grayson, R.B. 1998. The Tarrawarra dataset: soil moisture patterns, soil characteristics, and hydrological flux measurements. *Water Resources Research* 34(10): 2765–2768.

Wilson, R.C. 1997. Normalizing rainfall/debris flow thresholds along the U.S. Pacific Coast for long-term variations in precipitation climate. *In Chen (ed.), Debris-flow hazards mitigation: mechanics, prediction, and assessment.* ASCE: 32–43.

Wilson, R.C. & Wieczorek, G.F. 1995. Rainfall thresholds for the initiation of debris flows at La Honda, California. *Environmental & Engineering Geoscience* 1: 11–27.

Woods, R.A., Grayson, R.B., Western, A.W., Duncan, M.J., Wilson, D.J., Young, R.I., Ibbitt, R.P., Henderson, R.D. & McMahon, T.A. 2001. Mauranghi River Variability Experiment: MARVEX. In Lakshmi et al. (eds.), *Observation and modelling of land surface hydrological processes*, Water Resources Monograph, AGU.

Worawattanamateekul, J., Hoffmann, J., Adam, N. & Kampes, B. 2003. Urban deformation monitoring in Bangkok metropolitan (Thailand) using permanent scatterers and differential interferometry technics. *Proceedings of FRINGE 2003 Workshop, Frascati, Italy.*

WP/WLI. 1993. A suggested method for describing the activity of a landslide. *Bulleting of the International Association of Engineering Geology* 47: 53–57.

Wu, W. & Sidle, R.C. 1995. A distributed slope stability model for steep forested basins. *Water Resources Research* 31: 2097–2110.

Landslide risk assessment for individual facilities

H.N. Wong
Geotechnical Engineering Office, Civil Engineering and Development Department, HKSAR

ABSTRACT: Geotechnical practice has progressed to the stage that slope engineering is no longer confined to investigation of slope stability. Instead, landslide risk has to be examined and managed in totality. This brings a broad spectrum of landslide-related problems to the agenda of risk assessment. This paper addresses landslide risk assessment that is undertaken at a large scale, in which the facilities at risk are individually recognized and assessed. Selected application cases are presented to illustrate the approaches adopted, their capability and constraints, and the development trends in risk assessment practice. There is a choice between using a qualitative or quantitative approach. There are also significant differences between applying the assessment to a few individual sites and to a large number of slopes. The challenge is for the geotechnical profession to master the diverse range of landslide risk assessment processes, to use the right tools for the right problems, and to become more effective in risk communication with stakeholders.

1 INTRODUCTION

Many practical slope problems are best tackled by a risk-based approach. The key principle is to examine both the likelihood and adverse consequence of slope failure, and thereby address risk in totality. This concept is implicit in our slope design and engineering practice. It has also been explicitly applied in different places, particularly where formal risk assessment is adopted in managing landslide problems.

Different aspects of landslide risk assessment and relevant technological developments are addressed in State of the Art Paper (SOA) 1 to SOA 6. Application of risk assessment is covered in SOA 7 and SOA 8. SOA 7 focuses on landslide hazard and risk zoning, with particular attention given to applications at a smaller scale for urban planning and development.

This paper (SOA 8) deals with landslide risk assessment at a larger scale and its application to risk management. It reviews the methodologies used to assess landslide risk for individual facilities, examines good practice and diagnoses the development trends, with particular attention being given to application and case histories. Selected qualitative risk-based slope rating schemes adopted in various countries are described to illustrate the practice and approaches. Selected examples of qualitative and quantitative risk assessment (QRA) applications are presented to show the range of applications and evolution of techniques.

2 RISK ASSESSMENT FOR INDIVIDUAL FACILITIES

In this paper, 'landslide risk assessment for individual facilities' refers to the assessment that is undertaken at a resolution and scale sufficient for the elements at risk (i.e. the facilities where adverse consequences may occur) to be individually recognized and their landslide risk evaluated, either by qualitative or quantitative means. This is the most common type of landslide risk assessment that is carried out for location-specific risk management purposes. It differs from risk assessment as applied to general landslide hazard and risk zoning (SOA 7) in the following aspects:

(a) It is often carried out at a larger scale, typically 1:2,000 or more detailed, such that both the slopes that pose the risk and the elements at risk can be clearly identified and examined. Landslide hazard and risk zoning is usually carried out at a smaller scale.

(b) The element at risk is known, be it an existing or a planned facility. Hence, not only the likelihood of a landslide but also its consequence can be explicitly evaluated. Landslide hazard and risk zoning would not necessarily involve a comparable level of consequence assessment and may in some cases be carried out without examining in detail the specific facilities at risk.

Table 1. Different types of landslide risk assessment for individual facilities.

Extent of application	Approach	
	Qualitative	Quantitative
A large number of slopes	Qualitative risk rating	Global quantitative risk assessment (QRA)
Individual slopes	Site-specific qualitative risk assessment	Site-specific quantitative risk assessment (QRA)

* This includes semi-quantitative risk assessment.
** This refers to quantification and evaluation of risk using formal quantified risk assessment methodology.

(c) It is often carried out to support or guide risk management decisions affecting specific sites, such as the priority and need for risk mitigation. Its reliability and resolution have to be commensurate with the intended application. The assessment would normally require the use of more detailed data and specific risk analysis techniques.

Depending on the intended application, landslide risk assessment for individual facilities can be carried out in different ways and to different levels of detail. The assessment may be classified according to the analytical approach adopted, i.e. whether it is primarily based on qualitative, semi-quantitative or quantitative methodology. Alternatively, classification may be made in relation to the purpose of the assessment. This typically includes risk rating, screening, prioritization, evaluation of overall risk, formulation of risk management strategy, site-specific risk management action, etc. There is no hard-and-fast rule for classification. It is obvious that the analytical approach must be related to the purpose of the assessment. As a broad categorization to facilitate review and assessment of the current state of practice, a pragmatic classification as summarized in Table 1 is adopted in this paper.

3 QUALITATIVE RISK RATING

Qualitative risk rating is the most common form of application of qualitative landslide risk analysis to a large number of slopes. This is commonly carried out by devising a rating scheme to evaluate the relative likelihood of landslide (i.e. hazard rating) and the relative severity of the consequence of failure (i.e. consequence rating), based on qualitative analysis of the slope attributes and data on the individual facilities affected. The qualitative analysis may be performed by different methods, such as the use of a scoring system, flow charts, qualitative descriptors, a risk matrix, or a combination

of these methods. The rating scheme is then applied to a large number of slopes. Provided that the required slope attributes and facility data are collected, the risks of the slopes can be rated and their relative risk compared. Depending on the complexity of the qualitative risk analysis method adopted, the scheme may be targeted on one or many types of slope (e.g. rock cut slopes and fill embankments), and for one specific type of facility (e.g. roads) or different types of facility.

Qualitative risk rating has been formulated and applied in many different places, some dating back to the late 1970s. It is typically adopted by agencies that are responsible for managing the risk for a large number of existing slopes. The risk rating provided a relatively simple but consistent means to achieve the following objectives:

– to evaluate and rank their relative risk (i.e. 'risk ranking');
– to prioritize the slopes for follow-up study, repair or maintenance (i.e. 'prioritization for action'); and
– to assist in the preliminary assessment of the scope and cost of follow-up action (i.e. 'preliminary estimate').

Selected risk rating schemes are described in Sections 3.1 to 3.8 below to illustrate the practice and approaches adopted in different places. A comparison of the key features of the schemes is summarized in Table 2.

In some cases, the rating process involves a preliminary screening to first identify the more problematic slopes within a large number of slopes, as candidates for risk rating. This is referred to as 'preliminary screening' in Table 2. Some rating systems have also been adopted as a tool and to provide reference data for use in QRA. This is denoted as a 'QRA tool' in Table 2. As explained in Item (g) of Section 3.9.4 below, a rating system may also be characterized depending on whether it is principally an 'expert judgment scheme', or an 'expert formulation scheme', or a 'mixed scheme'.

3.1 Cut slope ranking system, Hong Kong

The dense urban development since the Second World War in Hong Kong has resulted in the formation of a large number of cut slopes, fill slopes and retaining walls. Until about the mid 1970s, cut slopes were generally built empirically to an angle of 10 vertical to 6 horizontal. Fill slopes formed prior to the mid 1970s were generally not compacted to an acceptable standard. These un-engineered man-made slopes were susceptible to landslides. Some resulted in very significant loss of life.

In 1977, upon setting up the Geotechnical Control Office (GCO, which was renamed Geotechnical Engineering Office, GEO, in 1991), the Hong Kong

Table 2. Comparison of different qualitative slope rating systems.

Case No./ Place (Section in SOA8)	Primary application	Type of slope for rating		
		Slope	Facility	Rating method
1/Hong Kong (Section 3.1)	– Risk ranking – Prioritization for action	Un-engineered cut slopes and retaining walls	All types	– Scoring system, with hazard and consequence ratings – Expert formulation scheme
2/Hong Kong (Section 3.2)	– Risk ranking – Prioritization for action	Un-engineered fill slopes	All types	– Scoring system, with consequence rating before hazard rating – Expert formulation scheme
3 to 6/Hong Kong (Section 3.3)	– Risk ranking – Prioritization for action – QRA tool	Un-engineered cut slopes, fill slopes and retaining walls	All types	– Scoring system, with hazard and consequence ratings – Expert formulation scheme
7 & 8/USA (Section 3.4)	– Preliminary screening – Risk ranking – Prioritization for action – Preliminary estimate	Rock cut slopes	Roads	– Scoring system, with emphasis in hazard rating – Mixed scheme
9/Canada (Section 3.5)	– Risk ranking – Prioritization for action	Rock cut slopes	Railway	– Hazard rating system – Mixed scheme
10/Australia (Section 3.6)	– Risk ranking – Prioritization for action	Man-made slopes but primarily rock cut slopes	Primarily Roads	– Risk matrix system, with hazard and consequence ratings – Expert judgment scheme
11/Malaysia (Section 3.7)	– Risk ranking – Prioritization for action	All types including natural slopes	Primarily Roads	– Scoring system, with hazard and consequence ratings – Expert formulation scheme
12/Australia (Section 3.8)	– Risk ranking – Land-use planning	Clay slopes	Different types of land-use	– Scoring system, with simple hazard and consequence ratings – Expert formulation scheme
13/Japan (Section 3.8)	– Risk ranking – Prioritization for action	Rock slopes, deep-seated landslides and debris flows	Roads	– Scoring system, with emphasis in hazard rating – Expert formulation scheme
14/New Zealand (Section 3.8)	– Risk ranking – Prioritization for action	Cut and fill slopes	Roads	– Scoring system; primarily hazard rating – Mixed scheme
15/UK (Section 3.8)	– Risk ranking – Prioritization for action	Rock slopes	Roads	– Scoring system; primarily hazard rating – Mixed scheme

Government embarked on a long-term programme for retro-fitting substandard slopes. A pre-requisite for implementation of this programme was the registration and risk ranking of the existing sizeable man-made slopes in the urban area. This prioritized the slopes, so that the most risky slopes could be stabilized first.

The registration of man-made slopes completed by the GCO at the time identified a total of about 8,500 cut slopes and retaining walls. These were catalogued in a slope inventory (referred to as the 1977/78 Slope Catalogue), which contained the key slope attributes and data on affected facilities. In 1979, the GCO and Binnie & Partners jointly formulated the Cut Slope Ranking System, which was a qualitative risk rating scheme. The system was used by the GCO to calculate a 'Total Score' for each of the 8,500 cut slopes and retaining walls registered in the inventory. Based on the Total Score, which reflected the relative landslide risk, the cut slopes and retaining walls were ranked for follow-up studies to assess whether they met the

239

required safety standard and whether retro-fitting was necessary.

The system was described in Koirala & Watkins (1988). The ranking system was based on an assessment of the potential for failure and the consequence of failure, with numeric weightings assigned to the relevant slope and facility data (Table 3). The weightings were used to calculate an 'Instability Score' and 'Consequence Score' for each slope. The relative risk-to-life of the slope is represented by a Total Score, which is the sum of its Instability Score and Consequence Score.

A plot of the Instability Score vs Consequence Score of the ranked slopes is shown in Figure 1. It is notable that the Consequence Score has a wider spread than the Instability Score. This was consistent with the fact that the consequence of landslide among the slopes varied to a greater extent than the likelihood of landslide that could be differentiated by the scoring methodology used to assess instability.

Experience in using the system indicated that the system performed very satisfactorily in differentiating the 10% to 20% of the slopes with the greatest risk concern, which were subsequently selected by the GCO for investigation and retro-fitting. The calculated Total Score of many of these slopes was dominated by their Consequence Score.

3.2 *Fill Slope Ranking System, Hong Kong*

The Fill Slope Ranking System was formulated in parallel with the development of the Cut Slope Ranking System. The fill slopes constructed before 1977 in Hong Kong were mostly substandard in that the fill material was commonly placed by end-tipping with little, if any, compaction effort applied. Static liquefaction failure, in the form of a fast-moving, mobile flow slide, was known to be the key landslide problem from the fill slopes, as was evident from the 1972 and 1976 Sau Mau Ping landslides, which together resulted in 90 fatalities. It is implicit in the Fill Slope Ranking System that the ranking is based primarily on the relative risk of liquefaction failure.

The system was described in Koirala & Watkins (1988). The Fill Slope Ranking System was applied by the GCO to about 2,000 fill slopes registered in the 1977/78 Slope Catalogue to establish their relative risk ranking and priority for follow-up treatment.

3.3 *New Priority Classification System, Hong Kong*

The GEO has been operating a government-funded Landslip Preventive Measures (LPM) Programme to systematically study old man-made slopes and carry out stabilization works on sub-standard slopes that are under Government's responsibility. The Cut Slope Ranking System and Fill Slope Ranking System

formulated in the late 1970s were applied by the GCO in ranking the priority of the man-made slopes registered in the 1977/78 Slope Catalogue, for treatment under the LPM Programme. The two ranking systems served their intended purposes effectively. By the mid 1990s, about 1,000 top-ranking slopes were selected for detailed studies. Over 630 government-owned slopes that were found to be substandard and of serious consequences in the event of failure were upgraded under the LPM Programme. Engineering inspections were also carried out on about 4,000 slopes in the Catalogue.

As many high ranking slopes were selected for action under the LPM Programme by the mid 1990s, it was evident that a new rating system was required to further improve the effectiveness of prioritizing the remaining slopes. A number of factors contributed to this need:

(a) The old ranking systems were targeted at, and calibrated for, identification of the worst slopes. As a result, many high and sub-standard slopes close to occupied buildings were selected for action under the LPM Programme. By the mid 1990s, landslides affecting roads and other facilities were becoming increasingly important for effective landslide risk reduction. However, the old ranking systems were not tailor-made for differentiating the relative risk of these lower ranking slopes.

(b) Lack of suitable slope data for use in rating was a major constraint faced by the old ranking systems. It was known that a large number of slopes, in particular slopes outside the main urban areas, had not yet been registered in the 1977/78 Slope Catalogue. Hence, in the early 1990s, the GEO commenced compilation of a new Catalogue of Slopes to register all sizeable man-made slopes in Hong Kong. The work included systematic interpretation of the historical aerial photographs and field inspections (Lam et al. 1998). This provided an opportunity to collect new data for use in risk rating. The Catalogue of Slopes now comprises some 57,000 man-made slopes, and about 39,000 of these were formed before 1977.

(c) Improved knowledge of landslides and related technical issues provided a basis for improving the slope rating methodology.

The New Priority Classification System (NPCS) was developed in 1995 and 1996, to replace the old ranking systems as the qualitative risk rating scheme for ranking pre-1977 man-made slopes registered in the new Catalogue of Slopes for treatment under the LPM Programme. There are four main types of man-made slope feature in Hong Kong, viz. soil cut slopes, rock cut slopes, fill slopes and retaining walls. Since the landslide risk of different types of slope feature is affected by different factors, four separate rating schemes have been developed. They combine to form the NPCS.

240

Table 3. Numeric weightings and scoring formulae of Cut Slope Ranking System, Hong Kong (Koirala & Watkins 1988).

Component	Score	Maximum score		Component	Score			Maximum Score
(e) Height, H (metre)	Soil slopes, H × 1 Rock slopes, H × 0.5 Mixed slopes, H × 1	Unlimited	(p)	Channels	None, incomplete = 10 Complete – major cracks = 10 Complete = 0			10

(f) Slope angle	Rock Others
	  90° = 10 ≥60° = 20
	≥80° = 8 ≥55° = 15
	≥70° = 5 ≥50° = 10
	≥60° = 2 ≥45° = 5
	<60° = 0 35° = 3
	            <35° = 0
		20	(q)
			
			(r)
				Water carrying services
				
				Seepage
					Services within "H" of crest
					–Yes = 5
					–No = 0
					            Amount
					Position Heavy Slight
					Mid-height & 15 5
					above
								5
								
								15

(g) Angle of slope above, or presence of roads above	Slope ≥45° = 15 Slope ≥35°, or Major road = 10 Slope ≥20°, or Minor road = 5 Slope <20° = 0	15	(t)	Distance to building, road or playground from toe of slope (metre)	Near toe 10 2 Buildings = actual distance Roadways = distance + 2 metres Playground = greater of actual distance or 1/2H			Unlimited
(i) Associated wall	Height of associated wall (metre) × 2	Unlimited	(u)	Distance to buildings, roads or playgrounds from toe of slope (metre)	As for (t)			
(j) Slope condition	Loose blocks = 10 Signs of distress = 10 Poor = 5 Good = 0	10						
(k) Condition of associated wall	Poor = 10 Fair = 5 Good = 0	10	(v) (w)	Extensive slope at toe or slope Multiplier for type of property at risk at top	Extensive slope at top 0.5 Extensive slope below 20 Hospitals, schools, residential 2 Factories, playgrounds 1.5 Major roads 1.0 Minor roads 0.5 Open space 0			25 2
(l) Adverse jointing	Adverse joints noted = 5	5						
(m) Geology	Colluvium/shattered rock, thin soil mantle = 15 Thick Volcanic soil = 10 Thick Granitic soil = 5 Sound rock (massive) = 0	15	(x)	Multiplier for type of property at risk at top	As above			2
(n) Water access – impermeable surface on and above slope	None = 15 50% (partial) = 8 Complete – poor = 5 Complete – good = 0	15	(y)	Multiplier for risk factor	For densely populated area or where buildings may collapse 1.25 Otherwise 1.0			1.25
(o) Ponding potential at crest	Ponding area at crest = 5	5						

Instability Score = Σ(e,f,g,l,j,k,l,m,n,o,p,q,r)
Consequence Score = y{20w(1.5(e + i) − t 1.5(e + i))} + (40 x)((e + i) − u(e + i)) + (vx) + 2(e + i)}
Total Score = Instability Score + Consequence Score
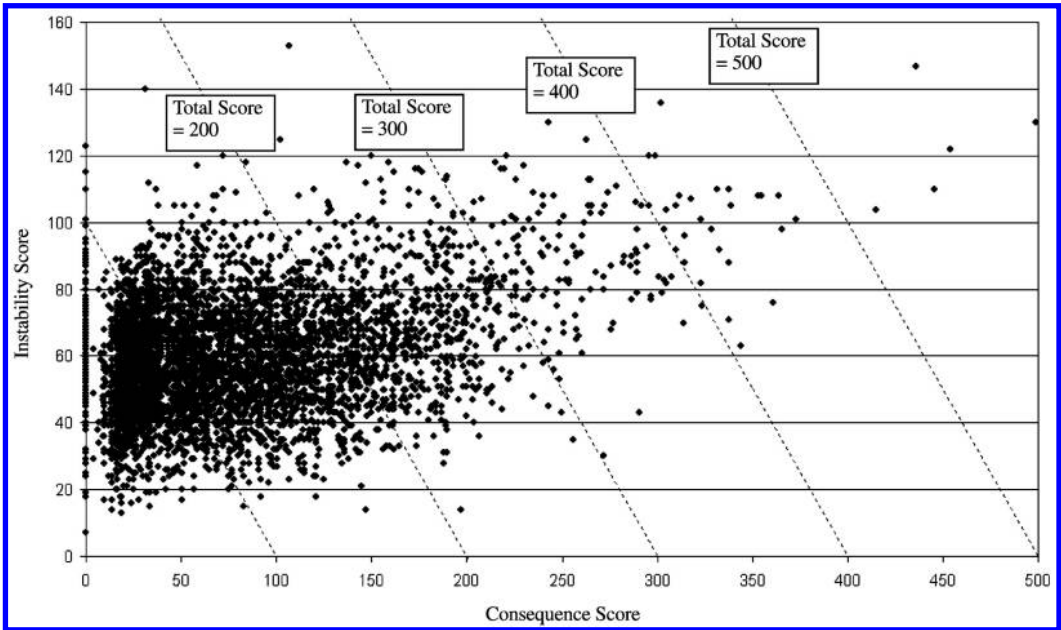
Figure 1. Instability Score vs. Consequence Score of slopes ranked by the Cut Slopes Ranking System, Hong Kong (Wong & Ho 1995).

In each scheme, a Total Score is calculated for each slope, which reflects its relative landslide risk. The Total Score is given by multiplying the Instability Score and Consequence Score of the slope.

3.3.1 *Soil Cut Slope Priority Classification System*

The detailed formulation and calibration of the Soil Cut Slope Priority Classification System are described in Wong & Ho (1995). The scoring scheme is summarized in Figure 2.

A large amount of calibration work was carried out to assist in formulating the numeric weightings and scoring formulae, and to validate the ranking results. For example, the slope geometry classification has been calibrated with the outcome of the detailed stability assessment of 69 slopes under a 10-year groundwater condition (Fig. 3). The worst zone, denoted 'S1', has 80% of cases with a calculated safety factor less than 1.1. Monte Carlo simulation was carried out to validate the boundaries of the geometry zone and to calibrate the landslide probabilistic distributions using typical ranges of soil parameters and groundwater conditions in Hong Kong. There is also an empirical correlation between the Instability Score and the calculated safety factor for the 69 sites (Fig. 4). An Instability Score of less than 80 corresponds to a safety factor of more than 1.2, whereas an Instability Score of more than 120 corresponds to a safety factor less than 1.1. There is a 'grey' zone in between these scores where

the safety factor can be within a large range. Findings from technical development work on assessment of debris mobility and QRA have been incorporated into the formulation of the Consequence Score. Table 4 shows the grouping of different facilities adopted in the NPCS and the corresponding potential loss of life (PLL) in the event of a direct hit by a reference landslide, which is derived by QRA on alignment of the facility grouping using PLL (Wong et al. 1997).

3.3.2 *Formulation of Rock Cut Slopes Priority Classification System*

The detailed formulation and calibration of the Rock Cut Slope Priority Classification System are described in Golder Associates (1996) and summarized in Wong (1998). The system for rock cut slopes is similar, in terms of its rationale and structure, to that for soil cut slopes. However, the parameters and their combinations as adopted in the rating were tailor-made to address the nature of rock slope failures in Hong Kong. Summarized in Table 5 are the key groups of factors considered in the scoring scheme and the range of individual scores that may be assigned.

Four different mechanisms of rock slope failures were examined in the rating: (a) raveling – small scale ($<5\,m^3$) detachment of individual overhanging rock blocks or isolated loose blocks from the slope face; (b) toppling; (c) planar failure; and (d) wedge failure. Their risks were rated separately by multiplying the

242

Slope No. _____ **Section :** ○ 1-1 (Most Severe Consequence) ○ 2-2 (Maximum Feature Height)

(A) GEOMETRY (Figure A1)

		1-1	2-2
(i)	H_c	m	m
(ii)	H_r	m	m
(iii)	H_{cw}	m	m
(iv)	H_{rw}	m	m
(v)	β	°	°
(vi)	θ	°	°
(vii)	α	°	°

· Feature Height, H
$= H_c + H_r + H_{cw} + H_{rw}$ [m]

· $H_w = H_{cw} + H_{rw}$ [m]

· $H_c = H_r + H_r$ [m]

· $H_o = H_r + H_{cw}$ [m]

(Fig. 3)

· $H_e = H_o (1 + 0.35 \tan\beta) + \frac{s}{\gamma_b}$

Feature Type [   ]

For S1 A = 60
S2   40
S3   20
S4   0

(viii) Toe of realistic slip surface within Hs portion — Yes/No* (1-1), Yes/No* (2-2)

· Geometry Classification (Fig. 3) S1/S2/S3/S4* [   ]   A [   ]

(B) EVIDENCE OF INSTABILITY

(B1) Signs of Distress

(i) Severe signs of distress, e.g. large tension cracks behind crest, distortion of channels and berms, severe cracking or bulging ○
(ii) Minor signs of distress, e.g. cracked chunam, damaged channels ○
(iii) Reasonable condition (including minor random cracks on surface cover) ○

For (i) B1 = 40
(ii) 20
(iii) 0

B1 [   ]

(B2) Past Instability

Confirmed Past Instability		B21	Inferred Past Instability		B22
○	Major	40	○	Major	30
○	Multiple Minor	20	○	Multiple Minor	15
○	Minor	10	○	Minor	5
○	None	0	○	None	0

B2 = B21 or B22, whichever is the greater

B2 [   ]

(C) POTENTIAL FOR WATER INGRESS

(C1) Water Ingress through Surface

(i) Soil slope and crest area substantially unprotected ○
(ii) Either soil slope or crest area substantially unprotected ○
(iii) Either soil slope or crest area or both are partially protected but none of them substantially unprotected ○
(iv) Soil slope and crest area substantially protected ○

For (i) C1 = 15
(ii) 10
(iii) 5
(iv) 0

C1 [   ]

(C2) Drainage Provisions for Surface Water

(i) Few or no channels + potential for convergent flow of surface water above crest ○
(ii) Few or no channels ○
(iii) Some channels but insufficient in size or number ○
(iv) Adequate channels ○

For (i) C2 = 15
(ii) 10
(iii) 5
(iv) 0

C2 [   ]

(C3) Water-carrying Services

(i) Presence of potentially leaky services and signs of leakage noted ○
(ii) Presence of potentially leaky services but no signs of leakage noted ○
(iii) No potentially leaky services ○

For (i) C3 = 15
(ii) 10
(iii) 0

C3 [   ]

(C4) Seepage

(i) Heavy seepage at mid-height of H_o or above ○
(ii) Slight to moderate seepage at mid-height of H_o or above, or heavy seepage below mid-height of H_o ○
(iii) Slight to moderate seepage below mid-height of H_o, or signs of seepage at soil slope or crest wall ○
(iv) No signs of seepage ○

For (i) C4 = 15
(ii) 10
(iii) 5
(iv) 0

C4 [   ]

(D) NATURE OF SLOPE-FORMING MATERIAL

Slope-forming Material (Soil Slope)	Weighting Factor, W	Material	Score, D_i
(i) Good - saprolite derived from granitic and volcanic rocks, mainly composed of Grade IV material	[ ]	Good	0
(ii) Uncertain-A - not certain but expected to be between Good and Moderate material	[ ]	Uncertain-A	10
(iii) Moderate - saprolite derived from granitic and volcanic rocks, mainly composed of Grade V material; saprolite of any grade of decomposition derived from rocks other than granite and volcanics; Pleistocene colluvium (Qpd on geological map)	[ ]	Moderate / Uncertain-B	20 / 30
(iv) Uncertain-B - not certain but expected to be between Moderate and Poor Material; not certain and can be any material.	[ ]	Poor	40
(v) Poor - residual soil; all transported soils except Pleistocene colluvium	[ ]		

$D = \Sigma(D_i)(W_i) / \Sigma(W_i)$

D [   ]

Lithology — Typical Granite or Volcanics / Atypical Granite or Volcanics / Other*

Adverse Geological Features — Yes/No*

(E) ENGINEERING JUDGEMENT

Engineering judgement on the likelihood of preventive measures being necessary :

(i) Highly Probable (HP) ○
(ii) Probable (P) ○
(iii) Unlikely (U) ○

For (i) E = 60
(ii) 30
(iii) 0

E [   ]

Figure 2. Scoring scheme of Soil Cut Slope Priority Classification System, Hong Kong (Wong & Ho 1995).

(F) FACILITIES ABOVE CREST OF FEATURE

Type of crest facility
(For roads and footpaths,
give also the name)

Group	1	F1 =	4
	2		2
	3		1
	4		0.5
	5		0.1

Group No.   `F1`

Distance from crest of feature to the facility, F2

m   `F2`

(G) FACILITY BELOW CREST OF FEATURE

Type of toe facility
(for roads and footpaths, give
also the name)

Group	1	G1 =	4
	2		2
	3		1
	4		0.5
	5		0.1

Group No.   `G1`

Distance from the toe of the feature to the facility, G2
(for facility on the feature, G2 = 0)

m   `G2`

(J) UPSLOPE AND DOWNSLOPE TOPOGRAPHY

	For	(i)	J =	0
		(ii)		0.3
		(iii)		0.6
		(iv)		1.2
		(v)		0.9
		(vi)		1.5

(i)   Upslope angle β above crest < 35° & downslope angle α below toe < 15°   ○
(ii)   Upslope angle β above crest $\geq$ 35°   ○
(iii)   Downslope angle α below toe : 15° $\leq \alpha$ < 30°   ○
(iv)   Downslope angle α below toe $\geq$ 30°   ○
(v)   Conditions (ii) & (iii)   ○
(vi)   Conditions (ii) & (iv)   ○

`J`

(K) CONSEQUENCE FACTOR

Priority Group No.
from Stage 1 Study (if available)

Consequence-to-life category
(i)   "1"   ○
(ii)   "2"   ○
(iii)   "3"   ○

Consequence factor is used if a large number of fatalities, say more
than 10, will result from the landslip. The following conditions are
typical for such situation :

(a)   the Consequence-to-life Category of the feature is "1" or "2",   ○
(b)   large volume of failure is expected, and   ○
(c)   occupied buildings may collapse or be covered in the event of   ○
landslip, or mass transportation is seriously affected.

If large number of
casualty will result
in the event of a
failure (e.g.
conditions (a), (b) &
(c) apply),
K = 1.25
Otherwise, K = 1.0

`K`

CALCULATED SCORES AND WARNING MESSAGES

REVISED INSTABILITY SCORE (I.S.)

$$I.S. = A + B1 + B2 + C1 + C2 + C3 + C4 + D + E$$

`I.S.`

REVISED CONSEQUENCE SCORE (C.S.)

$$C.S. = K (F + GJ) V$$

`C.S.`

where :

$$F = F_1 \left[\frac{H_o - F_2}{H_o} \right] \not< 0$$

$$GJ = 2G_1 \left[\frac{(1.5+J)H - G_2}{(1.5+J)H} \right] \not< 0$$

$$V = \gamma H_o$$

Notes: (1) γ = 1.0 for full−scale failure
           = 0.7 for partial failure
           = 0.4 for minor failure

      (2)   If H_o > 30 m, take H_o = 30 m in calculating V

REVISED TOTAL SCORE (T.S.)

$$T.S. = (I.S.)(C.S.) / 100$$

`T.S.`

WARNING MESSAGES

W1 = Warning, if H of Section 1-1 < 75% of H of Section 2-2.   `W1`

W2 = Warning, if Item (A)(viii) is "No".   `W2`

W3 = Warning, if H_{cw} > $H_t/3$.   `W3`

W4 = Warning, if E = 0 and (A + B1 + B2 + C1 + C2 + C3 + C4 + D) $\geq$ 90, or if E = 60 and (A + B1 + B2 + C1 + C2 + C3 + C4 + D) $\leq$ 60.   `W4`

W5 = Warning, if C.S. $\leq$ 20 and Priority Group = 1 or 2, or if C.S. $\leq$ 20 and Consequence-to-life Category = "1".   `W5`

W6 = Warning, if slope reinforcement is present.   `W6`

W7 = Warning, if feature is "post-GCO".   `W7`

W8 = Warning, if lithology is not "Typical Granite or Volcanics" or adverse geological features are observed   `W8`

244

Figure 2(*continued*).   Scoring scheme of Soil Cut Slope Priority Classification System, Hong Kong (Wong & Ho 1995).

Instability Score with the Consequence Score of each mechanism of failure. These were then summed up to give the combined Total Score.

3.3.3 *Fill Slopes Priority Classification System*

Details of the system and the relevant calibration work are described in Wong (1996) and summarized in Wong (1998). Unlike the old Fill Slope Ranking System, which focused on rating the risk of static liquefaction failure, the Fill Slope Priority Classification System rates the total risk arising from three mechanisms of fill slope failure commonly observed in Hong Kong. These included: (1) sliding and minor washout; (2) liquefaction; and (3) major washout.

For each fill slope, a separate Instability Score and Consequence Score were calculated for each of the failure mechanisms. The scoring scheme is shown in Table 6.

The QRA-based consequence model described in Wong et al. (1997) was adopted in calculating the Consequence Score, which gave a direct indication of the potential loss of life in the event of failure. As in the case with the other schemes of the NPCS, the Fill Slope Priority Classification has been benchmarked with case histories to calibrate the scoring methodology and to examine whether the risk rating is reasonable. In addition, trial application of the system was undertaken on sixteen cases, including notable fill slope failures and typical fill slopes in Hong Kong (Wong & Ho 2000). Some of the results of the trial application are extracted and shown in Table 7. The results showed that the relative instability ratings for different mechanisms of failure and the potential number of fatalities (i.e. Consequence Score) were reasonable.

3.3.4 *Retaining Wall Priority Classification System*

The detailed formulation and calibration of the Retaining Wall Priority Classification System are described in Wong (1998). The key groups of factors considered in the scoring scheme and the range of individual scores that may be assigned are summarized in Table 8.

The available landslide data and knowledge of the performance of old retaining walls in Hong Kong have been examined in devising the system. Guidelines on assessment of wall conditions, consolidated from local experience, were prepared to facilitate the use of the system. Typical forms of masonry wall construction were examined and illustrative examples were provided to assist in diagnosing the form of wall construction in field inspections (Chan 1996).
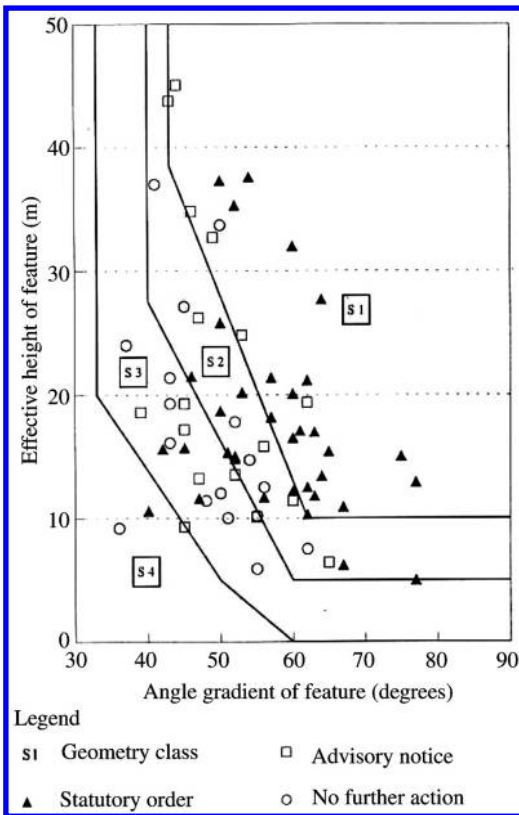
Figure 3. Cut slope geometry classification (Wong & Ho 1995).
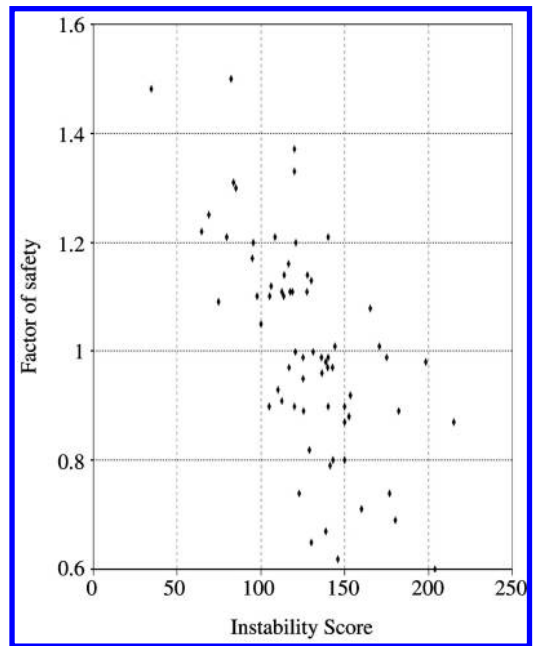
Figure 4. Correlation between Instability Score and calculated factor of safety of soil cut slopes (Wong & Ho 1995).

245

Table 4. Group of facilities adopted in NPCS (based on Wong & Ho 1995).

Group	Facilities	Potential loss of life
1(a)	Buildings – any residential building, commercial office, store and shop, hotel, factory, school, power station, ambulance depot, market, hospital/polyclinic/clinic, welfare centre	3
1(b)	Others – Bus shelter, railway platform and – other sheltered public waiting area – cottage, licensed and squatter area – dangerous goods storage site (e.g. petrol station) – road with very heavy vehicular or pedestrian traffic density	3
2(a)	Buildings – built-up area (e.g. indoor car park, building within barracks, abattoir, incinerator, indoor games' sport hall, sewage treatment plant, refuse transfer station, church, temple, monastery, civic centre, manned substation)	2
2(b)	Others – road with heavy vehicular or pedestrian traffic density – major infrastructure facility (e.g. railway, tramway, flyover, subway, tunnel portal, service reservoir) – construction sites (if future use not certain)	1
3	– densely-used open space and public waiting area (e.g. densely used playground, open car park, densely-used sitting out area, horticulture garden) – quarry – road with moderate vehicular or pedestrian traffic density	0.25
4	– lightly-used open-aired recreation area (e.g. district open space, lightly-used playground, cemetery, columbarium) – non-dangerous goods storage site – road with low vehicular or pedestrian traffic density	0.03
5	– remote area (e.g. country park, undeveloped green belt, abandoned quarry) – road with very low vehicular or pedestrian traffic density	0.001

Notes:
(1) To account for the different types of building structure with different detailing of windows and other perforations, etc, a multiple fatality factor ranging from 1 to 5 is considered appropriate for Group No. 1(a) facilities to account for the possibility that some incidents may result in a disproportionately larger number of fatalities than that envisaged.
(2) 'Potential loss of life' in this Table refers to the average number of fatalities in the event of a direct hit (i.e. 100% vulnerability) by a referenced landslide that is 10 m wide and 50 m^3 in volume, as derived from formal consequence assessment (Wong et al. 1997).

Table 5. Key groups of factors for Rock Cut Slope Priority Classification System, Hong Kong (Golder Associates 1996).

Type of score	Key groups of factors	Range of scores
Instability Score	Slope geometry	10–80
	Mode of slope failure	0.5–5
	Evidence of distress or past instability	0–70
	Potential for water ingress	0–30
	Rock mass condition	0–110
	Engineering judgment	0–30
Consequence Score	Type and proximity of crest facility	0–450
	Type and proximity of toe facility	
	Upslope and downslope topography	
	Likely scale of failure	
	Consequence factor/vulnerability	

3.3.5 *Combined priority ranking*

The four priority classification systems each provided a list of slopes of the respective type, ranked according to their relative landslide risk as reflected by Total Score (TS). The four ranking lists were merged, to allow different types of slope feature to be rated in a single list to establish their priority for treatment under the LPM Programme. The combined system is collectively referred to as the NPCS, and the combined relative risk was denoted by a calculated Risk Score (RS).

The RS was assessed based on the following methodology:

(a) A global QRA was performed to assess the overall distribution of landslide risk among different types of slope feature registered in the Catalogue of Slopes (see Section 6.3). The QRA found that the

246

Table 6.   Scoring scheme of Fill Slope Priority Classification System, Hong Kong (Wong 1996).

Slope Data

Slope No. :	SIFT No. :		SIFT Class :
Slope Height, H = _____ m Slope Angle, θ = _____ °	Crest Wall Height, H_{wc} = _____ m Toe Wall Height, H_{wt} = _____ m		
SIFT Section Profile No.	Part of Larger Fill Body : Yes / No		

Instability Score (IS)

Sliding   (IS_1 = a.b.c.d.e.f.g =   )

(a) Geometry (From Figure C1)
S1 = 32
S2 = 16
S3 = 8
S4 = 4
S5 = 2
S6 = 1

(b) Type of Surface Cover
Bare = 4
Vegetated = 3
Chunam = 1.5
Shotcrete = 1

(c) Surface Drainage Provision
No = 2
Yes = 1

(d) Signs of Seepage
Yes = 2
No = 1

(e) Potential Leaking Services
Leaking = 2
Presence = 1.5
None = 1

(f) Past Instability
Major = 8
Minor = 2
No = 1

(g) Signs of Distress
Yes = 4
No = 1

Liquefaction   (IS_2 = ¼.IS_1.h.i =   )

(h) Slope Height
≥30 m = 4
≥20 - <30 = 3
≥10 - <20 = 1
<10 m = 0.5

(i) Type of Surface Cover
Bare = 1.1
Vegetated = 1.1
Chunam = 0.5
Shotcrete = 0.25

Major Washout   (IS_3 = $(IS_1)^{1/3}$ .j.k.l.m.n.o.p.q =   )

(j) Catchment Characteristics : Topographic Setting and Size of Catchment

Topographic Setting	Size of Catchment (m²)				
	≤100	100 - 500	500 - 1000	1000 - 10000	>10000
Traverse Drainage Line	2	4	8	16	32
Adjacent Drainage Line	2	3	6	12	24
Traverse Topographic Depression	1	2	4	8	16
Adjacent Topographic Depression	1	2	3	6	12
Planar Slope	0.5	1	3	5	10
Spur	0.5	1	2	4	8

(k) Type of Crest Facility

Road	Platform & Urban development	Catch-water	Minor Development eg. Rural Footpath	Natural
1.0	0.5	0.25	0.10	0.05

(l) Volume of Fill Body (m³)

≤100	100 - 500	500 - 1000	1000 - 10000	>10000
0.10	0.25	0.5	1	2

(m) Channelisation of Debris   Yes = 2.0
No = 0.5

(n) Erosion and Entrainment along Debris Trail   Yes = 2.0
No = 1.0

(o) Spread of Debris   Yes = 0.5
No = 1.0

(p) Unstable Terrain   Yes = 2.0
No = 1.0

(q) Masonry Wall at Crest

Wall Height ≥ 3 m	2.0
Wall Height < 3 m	1.5
No Masonry Wall	1.0

Consequence Score (CS)

Facility	Type	Group No.	Proximity			K	L	V			C = H * K * L * V / 10		
								V_1	V_2	V_3	C_1	C_2	C_3
Toe (1)		α =											
Toe (2)		α =											
Crest (1)			<3 m	3 - 6 m	6 - 10 m								
Crest (2)			<3 m	3 - 6 m	6 - 10 m								
										CS = ΣC			

247

Table 7. Results extracted from trial application of Fill Slope Priority Classification System, Hong Kong (Wong & Ho 2000).

Cases (year of failure)	Sliding		Liquefaction		Wash-out		Total score	Description of failure
	IS1	CS1	IS2	CS2	IS3	CS3		
Sau Mau Ping – A (1976)	2304	0.85	2534	10.27	106	3.19	4.45	4,000 m^3 liquefaction failure; 18 fatalities. IS includes consideration of 1972 failure.
Sau Mau Ping – B (1972)	576	1.16	634	18.08	133	6.60	4.11	6,000 m^3 liquefaction failure; 71 fatalities (high fatalities due to flimsy structures completely damaged by landslide debris).
Kennedy Road – A (1992)	3072	1.71	845	3.91	5	3.49	3.93	500 m^3 liquefaction failure; 1 fatality. Slope exhibited signs of distress before failure.
Kennedy Road – B (1989)	96	1.63	36	3.90	1	4.18	2.48	500 m^3 sliding failure; no fatality: a near-miss event.
Baguio Villas (1992)	192	0.32	53	1.32	277	0.60	2.47	3,000 m^3 wash-out failure; 2 fatalities (a child and an engineer on inspection duty).
Waterloo Road (1989)	96	0.43	26	0.67	11	0.43	1.80	50 m^3 liquefaction failure; blockage of 3 lanes of road but no fatality.
Broadcast Drive (1988)	72	0.05	10	0.16	4	0.05	0.73	120 m^3 wash-out failure due to burst of water main; insignificant consequence.
Kung Lok Rd. Park (1988)	24	0.01	3	0.02	46	0.01	−0.02	200 m^3 wash-out failure; insignificant consequence

Notes:
(1) IS = Instability Score, which reflects the likelihood of the respective mechanism of failure.
(2) CS = Consequence Score, which is the potential loss of life (PLL) for the respective mechanism of failure.
(3) Total Score = log (Σ IS * CS).

Table 8. Key groups of factors for Retaining Wall Priority Classification System, Hong Kong (Wong 1998).

Type of score	Key groups of factors	Range of scores
Instability Score	Wall slenderness ratio and nature of retained material	0–100
	Past instability	0–30
	Type of wall	0–30
	Potential for water ingress	0–60
	Wall condition	0–110
	Gradient of terrain below wall	0–60
Consequence Score	Type and proximity of crest facility	0–600
	Type and proximity of toe facility	
	Upslope and downslope topography	

proportion of total risk of the pre-1977 soil and rock cut slopes, fill slopes and retaining wall are 75%, 12% and 13%, respectively. This formed the basis for a risk-based merging of four separate ranking lists.

(b) The risk proportion was distributed to each individual slope to derive the RS, based on the calculation TS and the proportion of total risk of the specific slope type. For soil cut slopes, rock cut slope and retaining walls, RS is given by:

$$RS = (TS \ of \ Individual \ Slope \ / \ \Sigma \ TS \ of \ all \ slopes \ of \ the \ same \ type) \times Proportion \ of \ total \ risk \ for \ the \ slope \ type \times 10^5 \qquad (1)$$

For fill slopes, e^{TS} is used in place of TS, which reflects the nature of the scoring methodology adopted in the ranking system. The resulting scoring formulae of RS for different slope types are given in Table 9. The

248

Table 9. Risk Score adopted in combined ranking using the New Priority Classification System, Hong Kong.

Slope type	Risk score (RS)
Soil cut slopes	$0.19 \times TS$
Rock cut slopes	$0.20 \times TS$
Retaining walls	$0.038 \times TS$
Fill slopes	$0.64 \times e^{TS}$
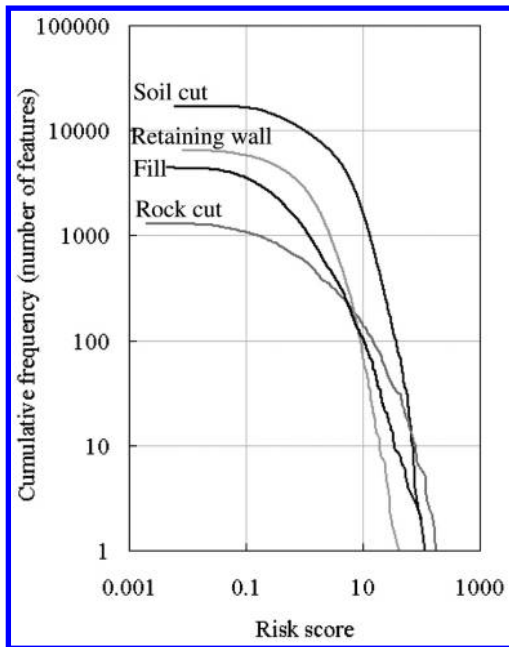
Figure 5. Distribution of Risk Score of different slope types in Hong Kong.

distribution of RS for different slope types as in 1999 is shown in Figure 5.

The NPCS has been adopted by the GEO since the late 1990s in prioritization pre-1977 man-made slopes for action under the LPM Programme. The Government of the HKSAR has pledged that in the 10-year period from 2000 to 2010, detailed studies would be carried out on 5,500 pre-1977 man-made slopes. Among these slopes, 2,500 government slopes would be upgraded to current safety standards. The total capital investment in this 10-year programme is about US$ 1 billion.

The NPCS has also been used as a risk rating tool in connection with slope-related technical development work, including rainfall-landslide correlation and QRA. The NPCS is also serving some other landslide risk management purposes in Hong Kong. For example, it has been estimated that the 'cut-off' value of RS for selection of government-owned slopes into the 10-year

LPM Programme is 8, i.e. slopes with an RS of less than 8 would not become eligible for action under the LPM Programme before 2010. Hence, regular slope maintenance has to play an important role in maintaining the continued stability of these lower ranking slopes.

The calculated RS provides a useful risk-based rating for use by the relevant Government departments in planning their slope maintenance works. The definition of a cut-off value by reference to the calculated RS for each slope has facilitated the planning of landslide risk management action and assessment of resource requirements. This illustrates the benefits offered by qualitative risk rating in landslide risk management. However, it should be noted that the NPCS is primarily developed for priority ranking and its resolution in differentiating the relative risk of the slopes is constrained by the available slope data.

3.4 Rockfall Hazard Rating System, USA

3.4.1 Development and application in Oregon
Pierson et al. (1990) described the Rock Fall Hazard Rating System (RHRS) developed by the Oregon Department of Transport (ODOT) for qualitative rating of the risk of rock falls from existing rock cut slopes alongside transportation routes. Oregon has many miles of highways passing through steep terrain with roadside rock cut slopes, which are prone to failure. In the mid 1980s, ODOT noted the need to develop a procedure, together with the use of a risk rating system, to assist in identifying problematic slopes and prioritizing repair works. Prototype development and trials were carried out from 1985 to 1998. Finalization of the RHRS began in 1989. As at 1990, the RHRS was tested at about 3,000 rock fall sections, and of these, 1,340 were included in Oregon's RHRS database. A 'rock fall section' referred to any uninterrupted slope alongside a highway where the level and occurrence mode of rock fall were deemed to be the same.

Procedures and guidelines for implementation of the system were given in Pierson et al. (1990). The RHRS formed part of a process that helped agencies to rationally manage the landslide risk from rock slopes affecting a highway system. The process involved slope survey, risk rating and preparation for follow-up action, such as cost estimation and preliminary design.

The risk rating comprised two parts, viz. a preliminary rating and a detailed rating. The preliminary rating was a subjective evaluation of the 'estimated potential for rock on roadway' and the historical rock fall activity, to broadly classify the risk into three classes: A (high); B (moderate); and C (low). The 'estimated potential for rock on roadway' was judged by the rater, based on observations on the slope conditions. 'Historical rock fall activity' was assessed based on information provided by the maintenance personnel. Among the approximately 3,000 rock fall

249

Table 10. Rockfall Hazard Rating System, ODOT, USA (Pierson et al. 1990).

Category			Rating criteria and score			
			Points 3	Points 9	Points 27	Points 81
Slope height			25 ft	50 ft	75 ft	100 ft
Ditch effectiveness			Good catchment	Moderate catchment	Limited catchment	No catchment
Average vehicle risk			25% of the time	50% of the time	75% of the time	100% of the time
Percent of decision site distance			Adequate site distance, 100% of low design value	Moderate site distance, 80% of low design value	Limited site distance, 60% of low design value	Very limited site distance, 40% of low design value
Roadway width including paved shoulders			44 ft	46 ft	28 ft	20 ft
Geologic character	Case 1	Structural condition Rock friction	Discontinuous joints, favorable orientation Rough, irregular	Discontinuous joints, random orientation Undulating	Discontinuous joints, adverse orientation Planar	Continuous joints, adverse orientation Clay infilling, or slickensided
	Case 2	Structural condition Difference in erosion rates	Few differential erosion features Small difference	Occasional erosion features Moderate difference	Many erosion features Large difference	Major erosion features Extreme difference
Block size			1 ft	2 ft	3 ft	4 ft
Quantity of rockfall/event			3 cubic yards	6 cubic yards	9 cubic yards	12 cubic yards
Climate and presence of water on slope			Low to moderate precipitation; no freezing periods; no water on slope	Moderate precipitation or short freezing periods or intermittent water on slope	High precipitation or long freezing periods or continual water on slope	High precipitation and long freezing periods or continual water on slope and long freezing periods
Rockfall history			Few falls	Occasional falls	Many falls	Constant falls

sections surveyed in Oregon, 501 were given Class A, and 839 received Class B preliminary ratings. The preliminary rating helped to focus use of resources on the more problematic slopes.

The detailed rating system includes 12 attributes to be evaluated and scored (Table 10). The sum of the scores gives the relative risk rating. Some attributes can be directly measured and scored, e.g. slope height and road width. However, some attributes, e.g. ditch effectiveness and geologic character, require an evaluation by expert judgment. Since the system was devised for use on rock slopes alongside roads, where the consequence setting is fairly uniform, its consequence evaluation is relatively simple.

A preliminary assessment of the rock fall mitigation measures and cost were also made as part of the rating process for the high-ranking sites.

3.4.2 *Development and application in Colorado*
In parallel with the development of the RHRS in Oregon, the Colorado Department of Transport was also devising a system to identify and rank, by milepost, those segments of state highways that had chronic rock fall problems (Stover 1992).

Road segments with rock fall problems were recognized by the occurrence of vehicle accidents caused by

rock fall, or identified by highway maintenance personnel as rock-fall prone areas. Road segments that had a high accident data and frequency ranking by maintenance personnel formed the primary targets for more detailed evaluation. Segments with a high frequency ranking but low accident data were secondary targets. This process of identification of rock fall-prone segments served a similar purpose to that of ODOT's preliminary rating system.

ODOT's RHRS was selected as a risk-rating tool for ranking the identified rock fall-prone segments. Some modifications were made to adapt ODOT's system for use in Colorado (Table 11). New parameters that were considered relevant, including accident data, slope inclination and segment length, were added. However, sight distance, roadway width, average traffic risk and ditch effectiveness were excluded. Their exclusion was noted by Stover (1992) as due to the consideration that their effects were factored in by the accident data and that some of the parameters were difficult to acquire.

3.5 *Rock slope hazard rating, Canada*

Qualitative risk rating systems have been used in Canada for many years in managing the risk of rock falls on transportation routes. Bruce et al. (1997)

250

Table 11. Colorado Rockfall Hazard Rating System (Stover 1992).

Factor			Rank			
			Points 3	Points 9	Points 27	Points 81
Slope profile		Slope height	25 to 50 ft	50 to 75 ft	75 to 100 ft	100 ft
		Segment length	0 to 250 ft	250 to 500 ft	500 to 750 ft	750 ft
		Slope inclination	15° to 25°	25° to 35°	35° to 50°	50°
		Slope continuity	Possible launching features	Some minor launching features	Many launching features	Major rock launching features
Geologic character		Average block or clast size	6 to 12 in	1 to 2 ft	2 to 5 ft	5 ft
		Quantity of rockfall event	1 cu ft to 1 cu yd	1 to 3 cu yds	3 to 10 cu yds	10 cu yds
	Case 1	Structural condition	Discontinuous fractures, favorable orientation	Discontinuous fractures, random orientation	Discontinuous fractures, adverse orientation	Continuous fractures, adverse orientation
		Rock friction	Rough, irregular	Undulating smooth	Planar	Clay, gouge infilling, or slickensided
	Case 2	Structural condition	Few differential erosion features	Occasional erosion features	Many erosion features	Major erosion features
		Difference in erosion rates	Small difference	Moderate difference	Large difference	Extreme difference
Climate and presence of water on slope			Low to moderate precipitation; no freezing periods; no water on slope	Moderate precipitation or short freezing periods or intermittent water on slope	High precipitation or long freezing periods or continual water on slope	High precipitation and long freezing periods or continual water on slope and long freezing periods
Rockfall history			Few falls	Occasional falls	Many falls	Constant falls
Number of accidents reported in mile			0 to 5	5 to 10	10 to 15	15 and over

reported that, prior to the Just incident in 1982 (Cory & Sopinka 1989), the British Columbia Ministry of Transportation and Highways (MOTH) specified locations for rock scaling where resources were available. Subsequently, MOTH developed a comparative method to rank areas by hazard, based on which the limited resources were deployed to reduce the risks posed by the areas with the greatest ranked hazard. Since 1993, the RHRS was adopted by MOTH as the risk rating scheme, which reduced the subjective aspects of the rating.

More recently, a new rock slope hazard rating system was formulated (Hungr et al. 2003), which provided a method of characterizing the relative risk posed by the slopes to Canadian Pacific Railway (CPR) track. This was intended to help to prioritize allocation of mitigation resources for over 1,500 rock slopes alongside over more than 2,100 km of railway track.

The rating system comprised two parts of assessment, viz. 'random rock fall' and 'structurally controlled failure'.

'Random rock fall' referred to small-scale (volume less than 10 m^3) detachment of individual rock blocks from a rock slope. It was rated by a rock mass classification system, with adjustments to cater for effects of any slope stabilization measures that had been provided, recent instability and overburden materials. The rock mass classification system was adapted from the Rock Mass Quality Index (Q) formulated by Barton et al. (1974), and the modified rock mass index was empirically correlated with historical rock fall frequency data. 'Structurally controlled failure' refers to large-scale failure of the rock slope that is controlled by well-defined discontinuities. The degree of hazard for this mode of failure was intended to be assessed by a deterministic approach, based on mapping of dominant discontinuities and supported by simple analysis if necessary. Given the nature of the assessment, subjective rating was made on the relative likelihood of the most likely failure magnitude.

Overall, the system is principally a hazard rating scheme that is independent of the consequence evaluation.

3.6 *Slope Risk Analysis System, Australia*

The Roads and Traffic Authority (RTA) of New South Wales (NSW), Australia, in conjunction with external consultants, has developed a scheme for rating the landslide risk of cut and fill slopes and retaining structures,

251

adjacent to main roads in NSW. The scheme is intended to be used in rating the relative risk of the slopes and thereby setting priorities for further work, such as investigation, monitoring and remediation.

Stewart et al. (2002) described the background of the formulation of this RTA Slope Risk Analysis scheme. The development of a systematic slope risk rating procedure by the RTA first started in the early 1990s. The early procedures were based on weighted scoring of slope attributes and a subjective assessment of consequences, which were grouped via a risk matrix to give the landslide risk level. According to Stewart et al. (2002), the procedures were used in a very limited way prior to 1997, but in late 1997 and early 1998, a revised version (No. 2) was used statewide in NSW to rate about 2,500 slopes. However, review of the results indicated that its reproducibility was poor and that the risk levels derived were not sufficiently accurate for the use in priority setting. Version 3.0 was developed, and tested in late 2000 with about 700 slopes by a panel of consultants. The test identified further revisions to the rating scheme (Baynes et al. 2002). Together with some other changes arising from additional development work, these were incorporated into Version 3.1 of the procedures, which is the scheme described in this Section.

The details of the formulation of the RTA Slope Risk Analysis scheme are given in RTA (2002). Details are summarized in Figure 6. The relative risk of a slope was rated in terms of an Assessed Risk Level, which was given by combining the Likelihood Rating and Consequence Rating. The system was aligned with a QRA framework. The rating was principally assigned by expert judgment combined via qualitative rules and risk matrices, without any quantified risk analyses. The slope unit is generally defined by its physical boundary, but a large slope may be sub-divided based on differences in geological or landform conditions.

This system is a notable development in respect of qualitative slope risk-rating methodology, in view of its attempt to align with the QRA framework and its extensive use of expert judgment in the rating process. The findings of a study on the reproducibility and accuracy of the different versions of the RTA system are given in Baynes et al. (2002). They noted the subjective nature of the rating process and the need for the rating to be carried out by trained personnel to improve the accuracy and precision of the results.

3.7 *Slope Management and Risk Tracking System, Malaysia*

Landslides from slopes alongside roads have resulted in loss of life in Malaysia, as well as major economic consequences due to closures of the road network. A study was carried out on the slopes along the 300 km long Tamparuli-Sandakan Road in Sabah in the early 2000s (TSR 2004). The study comprised collection of data on the slopes along the TSR and formulation of a qualitative slope risk rating scheme to assist in prioritizing remedial and maintenance works on the slopes.

The slope risk rating and management system that has been developed is known as the Slope Management and Risk Tracking System (SMART). Before commencement of the project, little information on the slopes along the TSR was available. The vast majority of the slope data that was used in the risk rating was collected in the project by airborne Light Detection and Ranging (LIDAR) survey and field mapping. Information on a total of 4,740 slopes features was recorded.

SMART rates the risk of slopes through the use of a scoring scheme, which is akin to that adopted by the GEO. The risk rating is represented by a Total Score, which is given by the product of the Instability Score and Consequence Score.

The Instability Score reflects the likelihood of slope failure. The details of its formulation are given in Figure 7. It is calculated by a weighted average of two probabilities of failure, DS and MC. DS is the discriminant probability score, based on a discriminant function obtained from a step-wise discriminant analysis that a slope feature would fall into the failed slope groups. MC is the Monte Carlo probability score, based on findings from Monte Carlo analysis on the probability that the theoretical factor of safety of the slope would fall below 1.0 under a 1 in 100 year rainstorm condition. In applying the scoring scheme to the TSR project, a 90% weighting factor was applied to DS and only 10% was assigned to MC. These reflect the perceived relative reliability of the probability scores obtained from the two approaches.

The Consequence Score was modified from the NPCS of GEO, with the inclusion of a specific term for the road facility because SMART is intended for application to rating landslide risk on roads. The calculated score has been normalized by 480 (maximum value), and hence falls within the range of 0 to 1.

3.8 *Other rating systems*

The systems were selected for a more in-depth description in the above sections in consideration of their more extensive scope of actual or planned application. These are by no means exhaustive. Other systems exist, and each has its own characteristics that serve particular purposes or address specific problems. Selected examples have been incorporated into Table 2. These include:

(a) Rating of Relative Landslide Risk of Clay Slopes, Tasmania, Australia – Stevenson (1977) described a simple method of evaluating the relative landslide risk of clay slopes. This was one of the earliest reported qualitative, risk-based rating schemes. However, compared with current practice, the

(a) Risk Rating

The Assessed Risk Level (ARL) is established based on the following risk matrix:

Likelihood	Consequence Class				
	C5	C4	C3	C2	C1
L1	ARL3	ARL2	ARL1	ARL1	ARL1
L2	ARL4	ARL3	ARL2	ARL1	ARL1
L3	ARL5	ARL4	ARL3	ARL2	ARL1
L4	ARL5	ARL5	ARL4	ARL3	ARL2
L5	ARL5	ARL5	ARL5	ARL4	ARL3
L6	ARL5	ARL5	ARL5	ARL5	ARL4

Notes:

(1) The Likelihood Rating L1 to L6   shown in Figure 6 (b).

(2) The Consequence Rating C1 to C5   shown in Figure 6 (c).

(b) Likelihood Rating

– Likelihood Rating is categorized as follows:

Class	Descriptions
L1	The event may, or is expected to, occur within a short period under average circumstances, or the mechanism is active at present (depending on circumstances the "short" period could be from days to no more than two to three years). Indicative Annual Probability around 0.9.
L2	The event may, or is expected to, occur within a moderate period (from a few years to no more than about 30 years) or within the inspection period under slightly adverse circumstances. Indicative Annual Probability around 10^{-1}.
L3	The event could be expected to occur at some time over about a 100 year period in the normal course of events but would only occur within the next inspection period under adverse circumstances. Indicative Annual Probability around 10^{-2}.
L4	The event would not be expected to occur within about a 100 year period under normal conditions and is unlikely to occur within the next inspection period except under very adverse circumstances. Indicative Annual Probability around 10^{-3}.
L5	The event would not be expected to occur within about a 100 year period and is unlikely to occur within the next inspection period even under very adverse circumstances. Indicative Annual Probability around 10^{-4}.
L6	The event is unlikely to occur even under extreme circumstances. Indicative Annual Probability < around 10^{-5}.

– The likelihood Rating reflects the probability of a landslide occurring and reaching the element at risk. For failures from road-side rock cur slopes, the probability of small rock fall/slide reaching the road may be assessed from the following chart:

Small rock falls/ Rock slides estimating the probability that on detachment the debris will land on the carriageway

For the general case, L = a
Where a catch ditch is present and d > w/3, then
L = a + 2w for slope angles ≤ 65°
L = a + w for slope angles > 65°
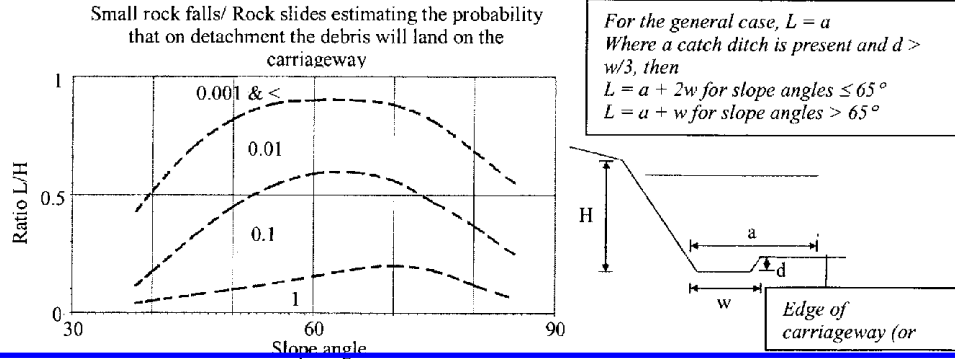
Figure 6.   Formulation of RTA Slope Risk Analysis scheme (extracted from RTA 2002).

(c) Consequence Rating

♦ Consequence Rating for loss of life is categorized as follows:

Vulnerability	Temporal Probability of an Individual Being Present at the Time of Failure				
	T5	T4	T3	T2	T1
V1	C4	C3	C2	C1	C1
V2	C4	C3	C2	C1	C1
V3	C5	C4	C3	C2	C2
V4	C5	C5	C4	C3	C3
V5	C5	C5	C5	C4	C4

Notes:

(1) Temporal probability is classified as follows:

Class	Descriptions
T1	Person usually expected to be present as part of the normal pattern of usage (eg residential buildings, some commercial buildings). Road users in the heaviest of urban traffic conditions. (p > 0.5).
T2	Person often expected to be present as part of the normal pattern of usage (eg many commercial buildings). Road users on major urban arterial roads and the most heavily trafficked rural roads. (p 0.1 – 0.5).
T3	Person may sometimes be present as part of the normal pattern of usage. Road users on many urban arterial roads and most major rural arterial roads. (p 0.01 – 0.1).
T4	Person unlikely to be present even where there is a pattern of usage. Road users on suburban roads and minor rural arterial roads. (p 0.001 – 0.01).
T5	Person is very unlikely to be present. Road users on the most lightly trafficked roads, road shoulders etc. (p < 0.001).

(2) For landslides affecting roads, the following chart may be used in assessing the temporal probability:
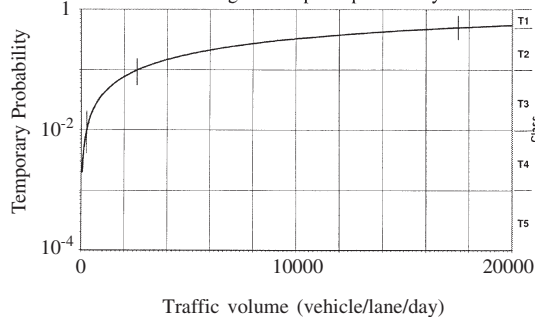
(3) Vulnerability is classified as follows:

Class	Descriptions
V1	Person in the open unable to evade rockfall or other debris (movement very/extremely rapid), or buried, or engulfed in a building collapse. Vehicle impacting a block > 1 m high or lost into a deep, narrow void at highway speeds. (p > 0.5).
V2	Partial building collapse. Person in open may be able to evade debris. Vehicle impacting a 0.5 – 1 m high block at highway speeds or a block > 1 m high at urban speeds or lost into a shallow void. (p 0.1 – 0.5).
V3	Building penetrated, no collapse. Emergency evacuation possible. Most people in open able to evade debris. Vehicle impacting a 0.5 – 1 m high block at urban speeds, or a block > 1 m high at low speeds. Vehicle impacting loose or wet mixed soil/rock debris (or crossing a stepped surface with c 0.1 – 0.2 m steps caused by a developing embankment failure) at highway speeds. (p 0.01 – 0.1).
V4	Building struck, damaged but not penetrated. Vehicle impacting a block around 0.2 m high at highway speeds or a 0.5 – 1 m high block at low speeds. Vehicle impacting loose or wet mixed soil/rock debris (or crossing a stepped surface with c 0.1 – 0.2 m steps caused by a developing embankment failure) at urban speeds. Vehicle interacting with a shallow void/depression where guardfence may prevent a vehicle from leaving the road. (p 0.001 – 0.01).
V5	Building struck, only minor damage etc. Vehicle impacting a block around 0.2 m high at urban speeds or a smaller block at highway speeds. Vehicle impacting loose or wet mixed soil/rock debris at low speeds. Vehicle traversing an irregular surface formed by soil or small (< 100 mm min dimension) rock, or by a developing embankment failure, at highway speeds. (p < 0.001).

♦ Consequence Rating for damage to property and consequential effects is categorized as follows:

Class	Descriptions
C1	Total closure of a Sub-Network Rank 5 or 6 (SN5-6) road for an extended period Major infrastructure or property damage (other than road) Very high disruption cost (other than road users) Very high repair cost (Total direct and indirect costs > $10M)
C2	Total closure of one carriageway of an SN5- 6 road or total closure of an SN3–4 road for an extended period Substantial infrastructure or property damage Large disruption costs High repair cost (Total direct and indirect costs > $2M < $10M)
C3	Partial or total closure of an SN3-4 road for a short period, longer period if reasonable alternatives are available Moderate infrastructure or property damage Moderate disruption costs Moderate repair cost (Total direct and indirect costs > $0.5M < $2M)
C4	Partial or total closure of an SN2 road for a short period Minor infrastructure or property damage Minor disruption costs Low repair cost (Total direct and indirect costs > $0.1M < $0.5M)
C5	Partial or total closure of an SN1 road for a short period Negligible infrastructure or property damage Little or no disruption costs Very low – no repair cost (Total direct and indirect costs < $0.1M)

Figure 6(*continued*).   Formulation of RTA Slope Risk Analysis scheme (extracted from RTA 2002).

Instability Score (IS) = α DS + β MC

where,

α and β are weighting factors, with $\alpha + \beta = 1$

DS = Discriminant Score which is the probability of a slope feature belonging to the failed slope group, ranging from 0 to 1 and based on the following parameters:

Cuts and natural slopes (11 significant variables)	Fill embankment (7 significant variables)
– Vegetation cover condition	– Main cover type
– Height	– Vegetation cover condition
– Presence of corestone boulders	– Slope angle
– Measure of ground saturation	– Geology
– Slope angle	– Plan profile
– Cutting topography relationship	– Presence of structures
– Slope shape	– Upslope / downslope geometry
– Exposed percentage (rock)	
– Rock condition profile	
– Plan profile	
– Surface Drainage rating	

MC = Monte-Carlo probability score which is the probability of the Factor of Safety < 1 for the 1 in 100-year return period 24-hour rain storm, ranging from 0 to 1.

Figure 7. Formulation of Instability Score, SMART (extracted from TSR 2004).

scheme is coarse and may at best be taken as a general zoning system. The method was applied to selected areas in Tasmania.

(b) Stability Evaluation Method, Road Bureau of the Ministry of Construction, Japan – A scoring scheme developed and adopted in Japan for qualitative rating of the relative risk of landslides on roads in Japan was described in Ministry of Construction (1990), and summarized in Escartio et al. (1997).

(c) Slope Condition and Risk Rating, New Zealand – The scheme was intended for rating cut and fill slopes alongside highways, railway and canals, to highlight areas of landslide concern and allow priorities to be set for further investigation and treatment. Sinclair (1991) reported that the method was applied to data obtained for the design of improvement works of a 50 km section of the Kuala Lumpur to Seremban Expressway in Malaysia.

(d) Rock Slope Hazard Index System, Scotland – This scheme was developed in 1996 for use as a first stage assessment of the relative risk of rock slopes affecting roads and determination of the required follow-up actions. Development of the system was supported by the Scottish Office Industrial Department, and the system was tested on 179 rock slopes alongside a 50 km section of Trunk Road in the Scottish Western Highlands (McMillan & Matheson 1997).

(e) Terrain Susceptibility and Risk Zoning – There are a range of methodologies developed for assessing the relative susceptibility and risk of landslides originating from undeveloped hillsides. Qualitative and semi-quantitative risk assessment techniques, together with statistical analyses and expert judgment, are commonly adopted. A detailed review of the methodologies and practice was given in SOA 7. The relevant systems and applications are not further examined in this paper. Most of the applications are couched at a smaller scale, and do not clearly differentiate the individual facilities. Wong (2003) summarizes the practice in compilation and use of susceptibility and risk maps in Hong Kong.

3.9 Observations on state of good practice

A total of fifteen different slope rating schemes are reviewed above. While most of the schemes have certain features in common, the schemes developed in various places differ because of particular circumstances of their formulation and different key issues that they address. There is no hard-and-fast rule as to which particular rating methodology is the best scheme. The best scheme is that which best meets the landslide risk management needs under the particular circumstances. However, some observations can be made on the state of good practice in formulation and application of qualitative slope rating systems, as summarized below.

3.9.1 Objective of rating system

A rating system is designed for specific purposes. The intended objectives of the system and the circumstances of its application should be clearly defined, in order to guide the formulation of the system. This would also help to ensure that the system would be correctly applied. GEO's experience illustrates that even if the intended purposes remain the same, different systems may be required at different times because of changing circumstances in which the systems are applied.

It is evident from the cases reviewed that slope rating systems are typically adopted to provide a relative risk ranking of existing, potentially hazardous slopes. The systems are commonly required by agencies that are responsible for managing the risk of a large stock of slopes, to set out the priority and direct resources for follow-up studies and treatment works. A wealth of experience of successful use of qualitative slope rating in this area is available. There are indications that such applications are receiving increasing attention by many agencies in different countries.

3.9.2 Risk management process

A rating scheme provides a means of relative risk ranking. Although it is a useful tool that plays an important role in the risk management process, it is not the

255

totality of the process. Effective landslide risk management calls not only for the formulation of a slope rating scheme, but also the establishment of a suitable risk management process to which the rating scheme applies. Such a process typically involves systematic collection of landslide and maintenance records, compilation of a comprehensive slope inventory, formulation of a slope rating scheme, collation of data for use in slope rating, establishment of procedures for initiation of follow-up actions, maintenance and dissemination of information, etc. The slope rating scheme would best serve its intended purposes when it is applied in the context of a risk management process. Such applications would in turn provide useful feedback on how the rating scheme should be further improved to achieve better performance.

3.9.3 *Slope inventory*

Compilation of a slope inventory and collation of the relevant slope data are prerequisites for relative slope rating. This work is an important investment for landslide risk management, and it often constitutes the most resource-demanding component of the task. For example, the compilation of the new Catalogue of Slopes in Hong Kong, which comprises about 57,000 man-made slope features, cost about US$ 15 million to produce. In comparison, the NPCS was principally formulated in-house by the GEO and the staff cost was less than US$ 0.1 million, i.e. less than 1% of the cost of compiling the slope inventory. It is therefore essential that in devising a rating scheme, due consideration is given to the practicality of obtaining the required input data. A detailed and sophisticated system may not be the most suitable scheme to adopt if inadequate resources are available to support the data collection.

Where there are major resource constraints, it may be necessary to implement the rating in phases, i.e. the more problematic slopes are first identified with the use of a preliminary rating that is less resource-demanding, and then a more detailed rating is applied to the identified slopes for risk ranking and prioritization. Due consideration should be given to proper demarcation of slope units, which has significant implications for the cost and rating resolution. For example, if a coarse demarcation is adopted, such as one based on the average slope conditions per mile or km along a road, the work would be less costly. However, if individual slopes are registered and rated separately, a much better resolution would be achieved although the cost would also escalate.

To avoid double handling in data collation, it has been good practice adopted by some agencies to develop the rating scheme in advance of compiling the full slope inventory. This is done to ensure that slope parameters required for use in the rating are identified in time, such that the data can be collected when the slope inventory is compiled. In practice, the rating system would inevitably require field trials and calibration, which would often lead to refinements in the rating scheme and changes in either the types or forms of the required slope parameters. Hence, the compilation of the slope inventory and formulation of the rating system have to be carried out in an interactive manner, preferably under the coordination of a dedicated team.

Different methods can be used to assist in identifying the slopes and collating slope data. Advances in digital technology, such as in the use of GIS, remote-sensing, digital photogrammetry and global positioning techniques, have led to improved capability, enhanced efficiency and reduced human error (Wong et al. 2004a). It is also common practice now to operate the slope inventory on a GIS platform that incorporates spatial functionality for retrieval, analysis and web-based dissemination of the data.

3.9.4 *Slope rating methodology*

Although there is no unique methodology for relative slope rating, some good principles that are embodied within many of the more successful systems are notable:

(a) Risk-rating, which accounts for both the relative likelihood and consequence of landslide, is preferred to simply rating the hazard (or the consequence). For slopes affecting a linear facility, e.g. a road or railway track, the type of facility and characteristics of the population at risk are often relatively uniform. Hence, system developed for linear facilities would tend to place more emphasis on hazard rating. However, due account should also be taken of the key factors that affect the likely consequence of a landslide, e.g. proximity of the facility to the slope, any presence of protective ditches or buffer zones and the scale of failure, if the systems are designed for risk rating. For systems that are applied to slopes affecting different types of facility, the consequence rating would warrant considerable attention because it has a very significant contribution to make in assessing the relative risk.

(b) A rating scheme is always subject to constraints associated with data availability, and it should be formulated with due consideration taken of these constraints. The effects are two-fold. Firstly, if the data are not readily available and cannot be made available, the rating scheme cannot incorporate the use of the data irrespective of their relevance to assessing the relative risk. Secondly, even if data on a slope attribute are available and used in the rating scheme, the relative weighting assigned to the slope attribute in the scheme depends not only on the relevance of the attribute to assessing the relative risk, but also on the quality and resolution of the data available. For example, in some

256

schemes where signs of water seepage were included in the rating, a relatively low weighting score was given to this parameter irrespective of the knowledge that groundwater has a significant effect on slope instability. This is appropriate given the relatively poor quality and resolution of the data available for this attribute, e.g. observations being made in different weather conditions and hence not being entirely reliable and consistent. In other cases, subjective judgment is required to be made on, say, the likelihood of landslide. It is fairly common for the rating scheme to involve categorizing the likelihood into different classes that are aligned with notional ranges of probability. These notional ranges of probability typically differ by orders of magnitude. However, the weightings to be assigned to the different classes should not represent a likelihood of failure that differs by such orders of magnitude, if the subjective judgment made by the raters could not support a resolution that could truly differentiate the likelihood of landslide by these orders of magnitude. Otherwise, the significance of this subjective judgment would be mis-represented in the rating scheme, and the overall reliability of the scheme adversely affected.

(c) Separate rating schemes may have to be devised for different types of slope. Many of the existing rating schemes deal with rock slopes alongside transportation routes. In such cases, use of a single rating scheme that is tailor-made for application in a particular place would usually be adequate for use in rating rock slopes of different size and geological condition. In other cases, a system may be required for rating different types of slope, such as cut slopes and fill slopes. It is often necessary to formulate different rating schemes, each tailor-made for a specific type of slope, because the factors that govern the likelihood and consequence of landslides on different types of slope may differ very significantly. A key technical challenge to overcome in these cases is the merging of different schemes into a single rating system. Alignment with the findings of QRA and probabilistic analyses has been adopted as the solution.

(d) Parameters that are often adopted in hazard rating include: slope height; slope gradient; history of instability; signs of distress; type of slope forming material; presence of geological weaknesses or adverse discontinuities; unfavorable groundwater conditions; unfavorable surface water conditions including the type of slope cover; and the effectiveness of any existing slope stabilization measures. To ensure consistency in rating the likelihood of landslide, it is essential that the hazard rating is applied to slopes of a similar class, e.g. un-engineered soil cut slopes should not be mixed in the rating with engineered slopes. It is notable that in a more sophisticated rating system, different mechanisms of failure may be rated separately using different hazard rating methods.

(e) Parameters that are often adopted in consequence rating include: type and proximity of crest facility; type and proximity of crest facility; slope size or volume of landslide; mobility of landslide debris; and effectiveness of any existing provisions for protecting the facility from landslide effects. Consequence rating for slopes affecting a linear facility, e.g. transportation routes, usually involves the use of simpler methods. For slopes that affect a diverse range of facilities under different site settings, a detailed consequence rating may call for the use of a more complicated methodology, and may involve the use of QRA consequence assessment techniques. Loss of life is typically considered in consequence rating. However, the more sophisticated rating systems may include consideration of economic loss and aversion effects associated with multiple fatalities.

(f) Use of a scoring formula appears to be more popular than use of a qualitative risk matrix. They vary in presentation, and have pros and cons. However, in terms of capability as a relative risk rating tool, there is practically little difference between them. The more updated rating systems tend to use qualitative risk descriptors, which are aligned with some standardized categorization (e.g. AGS 2000) or notional ranges of probability figures. This helps to provide a reference point for subjective assessment and communication, and gives the rating schemes a semi-quantitative connotation. However, the probability figures are often loosely defined and the standardized descriptors are not intended to be precise. They would not necessarily improve the reliability of the quality rating, which is to a large extent governed by the rating methodology, quality of the input parameters and reliability of the subjective judgment made.

(g) Two different approaches in formulating the rating methodology are notable: (i) 'expert judgment schemes', which require considerable judgment to be exercised in rating the slopes (e.g. RTA Slope Risk Analysis, Section 3.6 above); and (ii) 'expert formulation schemes', which require the use of relatively simple, factual data (e.g. NPCS, Section 3.3 above). An expert judgment scheme refers to that which requires considerable subjective judgment to be made by the raters in acquiring the input data or in rating the hazard or consequence, e.g. making a subjective rating of 'the likelihood of landslide' or of 'the likelihood that the detached material would reach the downslope facility'. Formulation of an expert judgment scheme may not require much supporting correlation and analytical work to define the effects of different slope

257

data on the likelihood and consequence of landslide. However, its application requires input from experts in exercising subjective judgment. The schemes may be less difficult to formulate, but the demand on data collection is high and their application can be sensitive to reproducibility and consistency issues. An expert formulation scheme adopts relatively simple and factual data as input parameters, and does not require the raters to exercise much subjective judgment in collecting the data and applying the scheme. This is made possible because the relative significance of the various input data and their appropriate weightings have already been assessed, correlated and incorporated into an expert system when the rating scheme is formulated. The work typically involves correlation with historical landslide data, statistical analysis and numerical modeling. These effectively replace the subjective judgment that would otherwise have to be made by the individual raters in applying an expert judgment scheme. An expert formulation scheme is usually more repeatable and less operator-dependent. However, formulating such a scheme is practical only when suitable data and techniques for establishing the correlations are available. The reliability of an expert formulation scheme is governed by that of the correlations established. In some cases, a mixed scheme, i.e. a hybrid of the two approaches, is adopted in a single rating system.

3.9.5 *Testing and calibration*

All rating systems require trial uses for testing and calibrating their performance. The key aspects to be evaluated include:

- Repeatability of data collection, i.e. whether the judgment made by different raters or data collected by different personnel are reasonably consistent.
- Reproducibility of the system, i.e. whether the system can give relatively consistent results for slopes of comparable conditions.
- Performance of the system, i.e. whether the rating given by the system is reliable as compared with the available statistics, actual slope behavior and other indicators (e.g. professional judgment), and whether the system can adequately fulfill its intended purposes.
- Ease of use of the system, i.e. any scope to streamline the system and data collection, without adversely affecting the performance of the system

Systems that are being more extensively applied have all been subject to improvements and refinements after repeated testing and calibration. The testing and calibration work also facilitates the documentation of guidelines on collection of data and use of the systems.

3.9.6 *Maintenance of system*

A rating system would easily become outdated if not properly maintained. There are two key aspects of maintenance. Firstly, the data that are adopted as input parameters should be updated to reflect the latest slope conditions. This may have significant resource implications, which should be duly factored in when designing the risk management process. For example, quality procedures are in place in Hong Kong for checking the key components of the input parameters of each rated slope before it is selected for action under the LPM Programme, and for regularly updating the slope data based on findings from an inspection by a qualified geotechnical professional at least once every five years on each registered slope (GEO 1998a). Secondly, the rating methodology would require enhancement from time to time when new experience in using the system becomes available, or when there are new requirements to be met.

3.9.7 *Public perception of qualitative rating system*

The public perception of landslides and their risk management is affected by many social, economical and political factors, which vary in place and time. There is little published information available on the public perception of use of qualitative risk rating methodology, and this is an area deserving further study and experience sharing. Hong Kong has almost 30 years of experience in using risk ranking methods for prioritizing un-engineered man-made slopes for detailed studies and retro-fitting under the LPM Programme, which involves considerable public works expenditure. Experience shows that application of qualitative risk rating is fairly well received by the public as a rational and pragmatic approach for prioritizing where resources should be used for landslide risk reduction. Challenges, either on the technical or administrative aspects, are rarely received from the public on the rating systems. When a low-ranking slope fails and results in notable consequences, the case would inevitably attract public concern. However, it seems that the public would tend to be more tolerant towards imperfections in the rating methodology due to technical limitations, rather than human errors in collecting the slope data and in exercising professional judgment. In this respect, use of an expert formulation scheme would probably be less prone to criticism than use of an expert judgment scheme. At least, this is the case as far as the raters are concerned.

3.9.8 *Limitations of rating system*

Proper awareness of the capability, as well as the limitations, of a qualitative rating system is fundamental in applying the system successfully. The various systems that have been developed have differing degrees of complexity, with differing resolutions and reliabilities. Overall, it should be recognized that these systems

are, by nature, relative risk rating tools that operate with the use of relatively simple, readily acquired, qualitative parameters and subjective judgment. They may give a useful indication of the relative risk, but cannot provide a sufficiently reliable, absolute risk figure. Even if they have been aligned with some quantitative or semi-quantitative figures, the alignment typically involves subjective judgment and contains significant uncertainties. The rating should only be applied in the circumstances for which it is intended. A rating scheme that has been successfully applied in one place may be entirely inappropriate for use elsewhere, if the nature of slope problems and the risk management objectives are different.

Due care should also be exercised when a system is used for purposes other than relative risk rating, such as risk-screening or risk-based decision making on individual slopes. This is often beyond the capability and reliability of a qualitative rating system, unless it has been specifically calibrated for such applications. Site-specific landslide risk assessment and decision-making would normally call for the use of more detailed data and enhanced risk assessment techniques, such as site-specific qualitative risk assessment and formal QRA as described in the following Sections.

4 SITE-SPECIFIC QUALITATIVE RISK ASSESSMENT

4.1 *Overview*

Site-specific qualitative risk assessment embraces a broad range of qualitative and semi-quantitative processes applied to analyzing and managing the landslide risk at individual sites. The work is carried out with a resolution and reliability that are deemed to be adequate for use in making site-specific risk management decisions, without formally quantifying the risk.

The conventional approach for dealing with landslide problems at individual sites is to provide for a safety margin in slope design based on deterministic stability assessment. This Factor of Safety approach is aimed at reducing the chance of failure. It neither evaluates risk directly, nor manages risk in a holistic manner. For managing landslide problems at specific sites, the following are some typical circumstances that require the use of a risk-based assessment, either supplementary to, or as a replacement of, the conventional factor of safety approach:

(a) where slope stability can be controlled via the provision of a safety margin against failure, but assessment of risk and the uncertainties involved is required to assist in determining the extent of the safety margin to be adopted;
(b) although slope stability can largely be controlled via the use of a design factor of safety, the residual chance of failure has to be considered, typically because of the severity of the failure consequence;
(c) where control of slope stability is not practical (or ineffective) and the landslide risk has to be managed by other means, e.g. mitigating the consequence of failure;
(d) where potential landslide hazards are known, but their risk needs to be evaluated to assist in determining the risk mitigation requirements and the preferred mitigation option; and
(e) where the exact nature of the potential landslide hazards and their possible consequences are not entirely known, and are to be assessed to assist in identifying the hazards and evaluating their risk.

These issues are beyond the scope of conventional slope stability assessment, and can only be tackled from a risk perspective. This often applies to small slopes, natural hillsides and large distressed sites, where detailed characterization of the ground and pore water conditions is not practical, and where prevention of slope failure can be difficult. Depending on the needs of the particular case, the risk assessment process may or may not involve formal quantification of the risk. Qualitative risk analysis had been the principal approach of risk assessment before QRA methodology emerged. Over the years, it has supported sound risk management decisions to be made in many circumstances, without explicitly quantifying the risk.

A variety of qualitative and semi-qualitative risk assessment methods are available, e.g. a summary is given in Lee & Jones (2004). Many examples of site-specific application of qualitative risk assessment have previously been reported in the literature (e.g. Hutchinson 1992, Morgenstern 1995, Vick 2002, Morgenstern 2000). Three cases are described in the following Sections to illustrate its unique role and diverse range of applications in landslide risk management.

4.2 *Design event assessment for natural terrain landslides*

The strategy for dealing with natural terrain landslide risk in Hong Kong has been to avoid, as far as possible, new developments in vulnerable areas (Wong 2003). Where this is not practicable, the conventional approach in the past has been to design the natural hillside to the factors of safety stipulated in GCO (1984). However, in many circumstances, this approach is fraught with inherent difficulties and its use in natural terrain is not practical in that:

(a) As natural hillside is often only marginally stable over a large area, stabilization of the hillside would be expensive and may not be justified. Also, widespread stabilization works on natural hillside are difficult to carry out and could result in considerable impact on the environment.

(b) Preventing failure is not necessarily the most cost-effective engineering solution. Provision of hazard mitigation measures (e.g. debris-resisting barriers) may be the preferred option in reducing the risk of natural terrain landslides.

Two alternative approaches, viz. the QRA approach and the Design Event approach, have been introduced for use in assessment and mitigation of natural terrain landslide risk in Hong Kong (Wong 2001, Ng et al. 2002). The QRA approach would require a detailed assessment of the probability and consequence of natural terrain landslides, together with consideration of the tolerability of the assessed risk level (ERM 1998). Although it may be considered as the most rigorous and comprehensive assessment (see Section 5), it often requires expert input and may be fairly involved and costly.

The Design Event Approach is a qualitative risk assessment and design framework, which is applicable when designers opt for mitigation of natural terrain landslide risk without carrying out a formal QRA. Under this approach, the mitigation measures (e.g. debris-resisting barriers) required to protect a development from natural terrain landslides are determined by reference to an assessment of the design landslide event that may occur on the hillside affecting the development. Uncertainties are generally considered in an implicit and lumped manner through the assessment of the design event (e.g. a landslide of a certain size with a given degree of mobility).

The framework for the Design Event approach takes account of the failure consequence and the susceptibility of the hillside to landsliding in a semi-quantitative manner. Under the framework, the susceptibility of the hillside to failure is categorized into 4 classes (Table 12), based on its historical landslide activity and assessment of geomorphological features and other relevant information. The consequence of failure is categorized into 5 classes based on the types of facilities affected and their proximity to the hillside (Table 13). The design requirements for mitigation measures are given in Table 12. Further studies will not be required if the consequence of failure and the landslide susceptibility of the hillside are insignificant. Otherwise, further studies should be carried out to establish the need for any mitigation measures to deal with the relevant design events. Depending on the consequence and susceptibility classifications of the site, the required design event may be either a 'conservative' event or a 'worst credible' event (Table 12). For the purposes of calibration, the design requirements for the Design Event Approach have been applied to 17 cases where developed areas have been affected by natural terrain landslides or where the landslide hazards have previously been studied.

Applying the Design Event calls for use of geotechnical professional skills to identify the nature of

Table 12. Design requirements for Design Event Approach.

Susceptibility class	Consequence class				
	I	II	III	IV	V
A	WCE	WCE	WCE	CE	N
B	WCE	WCE	CE	CE	N
C	WCE	CE	CE	N	N
D	N	N	N	N	N

Notes:
(1) See Table 13 for definition of Consequence Class.
(2) Susceptibility Class as defined in Wong (2000), where:
  A = Extremely susceptible; notional annual probability ⩾0.1
  B = Highly susceptible; notional annual probability 0.1 to 0.01
  C = Moderately susceptible; notional annual probability 0.01 to 0.001
  D = Low susceptibility; notional annual probability <0.001
(3) WCE = Adopt a 'worst credible' event as the design event. A 'worst credible' event is a very conservative estimate such that the occurrence of a more severe event is sufficiently unlikely. Its notional return period is in the order of 1,000 years.
  CE = Adopt a 'conservative' event as the design event. A 'conservative' event is a reasonably safe estimate of the hazard that may affect the site, with a notional return period in the order of 100 years.
  N = Further study is not required.

Table 13. Consequence class (Wong 2002).

Proximity	Facility Group No.			
	1 & 2	3	4	5
Very close (e.g. if angular elevation from the site is ⩾30°)	I	II	III	IV
Moderately close (e.g. if angular elevation from the site is ⩾25°)	II	III	IV	V
Far (e.g. if angular elevation from the site is <25°)	III	IV	V	V

Notes:
(1) Facility groups are described in Table 4.
(2) For channelized debris flow, if the worst credible event affecting the site is judged to have a volume exceeding 2,000 m^3, the angular elevation given in the above examples should be reduced by 5°.
(3) The above are for general guidance only. Other factors, such as credible debris path, topographical conditions and site-specific historical data, should also be taken into account in assessing the 'proximity' of the natural terrain to the site.

260

the landslide hazards, assess their severity, establish the required design event requirements (i.e. notional return periods) following the design framework, and determine the magnitude of the landslide for risk mitigation (i.e. the design event). This qualitative method of risk assessment is relatively easy to apply. It does not demand formal and rigorous quantification of risk, and is favored by many geotechnical practitioners in Hong Kong.

However, there is always a trade-off between simplicity and versatility. This qualitative risk assessment methodology does not explicitly consider the practicality and cost-effectiveness of risk mitigation. Such consideration is inherent in the QRA approach if the risk level is found to be within the 'As Low As Reasonably Practicable (ALARP)' region.

Observation: The Design Event approach is an illustration of integration of risk assessment and conventional geotechnical practice, to offer a tailor-made methodology for qualitative landslide risk assessment for individual sites.

4.3 Risk analysis for landslides below Wah Yan College

In the morning of 8 May 1992, a $500\,m^3$ landslide occurred on a loose fill slope bordering the building platform of Wah Yan College, Hong Kong. The liquefied fill material ran onto Kennedy Road (Fig. 8). The landslide did not result in any serious consequences at Wah Yan College, but the driver of a car on Kennedy Road was buried and killed by the liquefied debris. The incident highlighted the landslide concern in the area because in 1989, another landslide of similar size had also occurred on an adjoining fill slope bordering Wah Yan College. Fortunately, the debris of this landslide did not liquefy and was deposited on the pedestrian pavement without running onto Kennedy Road (Fig. 9). In 1989, the slope that failed was largely covered by chunam (a 75 mm think cement-soil slope

Figure 8. Liquefied debris of the 1992 Kennedy Road landslide.

cover), which prevented the loose fill from reaching a high degree of saturation, thereby making it less susceptible to liquefaction. An imminent risk management issue to address after the 1992 landslide was whether there were other potentially unstable loose fill slopes bordering Wah Yan College, and if so, what were their liquefaction potential and risk implications.

A qualitative risk assessment was carried out. The development history of the site was reviewed by a detailed interpretation of the old aerial photographs, and the locations and extent of the loose fill bodies bordering Wah Yan College were identified. Apart from the slopes that failed in 1989 and 1992, another sizeable fill slope was present to the north of Wah Yan College overlooking Queen's Road East and the Ruttonjee Clinic (Fig. 9). Detailed ground investigation confirmed that the fill was loose and had comparable susceptibility to liquefaction failure as the 1992 landslide site. The findings provided the technical basis for carrying out stabilization works on the slope. However, as the works would take some time to arrange, further assessment was made, in particular on the consequences of failure.

The consequence assessment involved modeling the mobility of landslide debris. The operating apparent angles of friction along the failure surface and along the debris path in the event of a liquefaction failure were back-analyzed from the 1992 landslide.
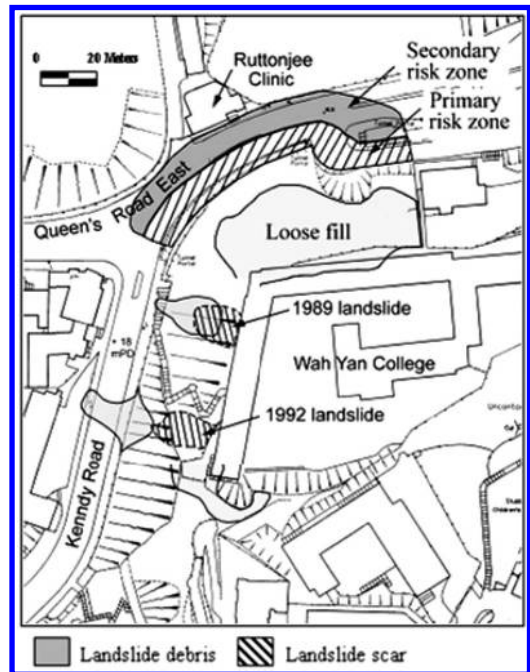

Figure 9. Qualitative risk assessment, Wah Yan College, Hong Kong.

Based on the results, the area that might be affected by the landslide debris was classified into a primary impact zone and a secondary impact zone (Fig. 9). The primary zone was taken to be of high risk, where serious damage would result, as in the case of the 1992 fatal landslide. The secondary zone represented a lower risk region, where serious damage might also occur in case of a larger volume of failure, or more mobile debris than the 1992 landslide. The risk at the Ruttonjee Clinic was also assessed. It was found that the road together with the 1.5 m high retaining wall in front of the clinic would protect the clinic from direct impact from most of the debris.

The risk assessment offered invaluable information on the likely scale of the problem, which was adopted in emergency planning and implementation of precautionary measures. The case may be taken as an example of Consequent Risk Analysis, which was advocated by Morgenstern (2000) as a qualitative risk assessment process to assure geotechnical performance and control risk.

Observation: Landslide study, geotechnical investigation, engineering appraisal and consequence analysis can be combined in a qualitative risk assessment to resolve landslide risk management issues that would otherwise be difficult to handle by conventional means.

4.4 *Failure Modes and Effects Analysis for Shatin Heights*

Over the years, a suite of technical methods have been developed and adopted in qualitative risk assessment. Examples include Failure Modes and Effects Analysis (FMEA), Hazard and Operability Study (HAZOP) and Potential Problem Analysis (PPA). Among these methods, FMEA was fairly commonly adopted in geotechnical risk assessment, e.g. geo-environmental risk management in mining projects (Dushnisky 1996) and dam risk management (Hughes et al. 2000, Stewart 2000). FMEA directs attention towards understanding the behavior of the physical components of a system, the possible modes of their failure, and the influence their failure would have on each other and on the system as a whole. It is usually used in two ways, as noted by (Vick 2002):

(1) to assist in hazard identification and risk screening, typically as a precursor to more detailed risk assessment; and
(2) to serve as a stand-alone preliminary risk assessment procedure.

Table 14 shows an example of applying FMEA to assessing the risk of natural terrain landslides in Shatin Heights, Hong Kong. The FMEA table was devised to address the specific circumstances of the site. The classification schemes that accompanied the FMEA are explained in Figure 10.

The natural hillside at Shatin Heights is bounded by residential buildings at the crest and toe of the hillside (Fig. 11). In 1997, a total of six landslides occurred on the hillside, and three of these developed into debris flows that ran into the buildings at the toe of the hillside. After the failures, the landslides were studied (GEO 1998b) and a Natural Terrain Hazard Study was carried out on the site (FMSW 2001). These provided data, which were incorporated into the FMEA for working out the semi-quantitative hazard and consequence categories in the FMEA table. The case showed the following:

(a) The FMEA has facilitated hazard identification and provided a preliminary assessment of the risk. In this case, out of the 15 possible hazard scenarios, 5 were identified by FMEA as of risk concern and requiring further risk assessment. The likely order of risk of each of the five hazards was also estimated. Although these are not formal QRA figures, they give a preliminary indication of the possible level and severity of the risk. Figure 11. Shatin Height, Hong Kong.

(b) Availability of data and technical understanding of the landslide hazards at the site is a prerequisite for successfully using FMEA in site-specific qualitative risk assessment. Otherwise, the reliability of the assessment and its suitability for supporting site-specific risk management application are in question. In such cases, the FMEA assessment would practically be reduced to at best a relative risk rating process.

(c) The FMEA table can become very long (i.e. with many rows) when applied to a large site. Formulating a suitable FMEA table that addresses the particular circumstances of the site is important to the efficient and effective use of FMEA.

(d) The case also illustrates the use of a risk-matrix (Fig. 10) in evaluating the risk category and thereby providing a basis for risk estimation and hazard identification. The risk matrix combines different classes of the frequency and consequence of landslide, which are aligned with some notional probabilities of failure and descriptions of the severity of landslide consequence respectively. An interesting example of application of risk-matrix to assessing the landslide risk on a proposed house on the western slope of the Warringah Peninsula, Northern Sydney is described in Walker (2002). In this example, the qualitative descriptors given in AGS (2000) were adopted. For each type of landslide that might affect the house, the frequency and consequence classes are determined from judgmental assessment and the corresponding risk level established in a semi-quantitative manner via a risk-matrix.

Observation: Established methods, such as FMEA and risk-matrix analysis, can be used in qualitative landslide

Table 14. FMEA on Shatin Heights Catchment No. 7.

Component	Failure mode (Notes (1))	Effects on K.K. Terrace	Likelihood category			Loss of life		Economic loss & Disruption to community		Risk category (Proceed to detailed assessment?)
			Failure	Effect	Hazard	Consequence category	Risk category	Consequence category	Risk category	
Catchments 7a, 7d & 7h	Shallow landslide resulting in small-scaled open-slope debris slide/avalanche (SH1)	Debris run into and affect 1/F of K.K. Terrace	C to D	z	D to E	2	L to V	III	N	Low (Yes)
	Deep landslide resulting in medium- to large-scaled fast moving debris slide/ avalanche (SH2 to SH3)	Debris run into and affect 1/F of K.K. Terrace	E	x	E	2	V	III	N	Very Low (No)
		Debris hit K.K. Terrance and result in building collapse or major structural damage		z	E-	1	V	II	N	Very Low (No)
	Deep landslide resulting in medium- to large-scaled debris with limited mobility (SH2 to SH3)	Prolonged evacuation of K.K. Terrace	E	y	E-	5	N	II to III	N	Residual (No)
Catchments 7b, 7e, 7f, 7i & 7j	Shallow landslide resulting in small- to medium-scaled debris flow without significant entrainment (TH1 to TH2)	Debris run into and affect 1/F of K.K. Terrace	B	x	B	2	H	III	L	High (Yes)
		Debris hit and affect the entrance to K.K. Terrace		y	B to C	3	M to L	IV	N	Moderate (Yes)
	Shallow landslide resulting in medium- to large-scaled debris flow with significant entrainment (TH2 to TH3)	Debris run into and affect 1/F of K.K. Terrace	D	x	D	2	L	III	N	Low (Yes)
		Debris hit and affect the entrance to K.K. Terrace		y	D to E	3	V to N	IV	N	Very Low (No)
		Debris hit K.K. Terrance and result in building collapse or major structural damage		z	E	1	L	II	N	Low (Yes)
	Shallow landslide resulting in small-scaled debris with limited mobility (TH1)	Temporary evacuation of 1/F of K.K. Terrace	B	y	B to C	5	N	IV	V to N	Very Low (No)
Catchments 7c, 7g & 7k	Shallow landslide resulting in small-scaled open-slope debris slide/avalanche (SH1)	Debris hit and affect the entrance to K.K. Terrace	C to D	z	D to E	3 to 4	V to N	IV	V	Very Low (No)

(*continued*)

Table 14. (*continued*)

Component	Failure mode (Notes (1))	Effects on K.K. Terrace	Likelihood category			Loss of life		Economic loss & Disruption to community		Risk category (Proceed to detailed assessment?)
			Failure	Effect	Hazard	Consequence category	Risk category	Consequence category	Risk category	
	Deep landslide resulting in medium-to-large scaled fast moving debris (SH2 to SH3)	Debris hit and affect the G/F of K.K. Terrace, including the entrance, G/F lobby, car park and drive way	E	x	E	2	V	III	N	Very Low (No)
		Debris hit K.K. Terrance and result in building collapse or major structural damage		z	E-	1	V	II	N	Very Low (No)
	Deep landslide resulting in medium- to large- scaled debris with limited mobility (SH2 to SH3)	Temporary evacuation of K.K. Terrace and the sole vehicular access to K.K. Terrace and Woodcrest	E	x	E	5	N	III	N	Residual (No)
		Prolonged closure of the sole vehicular access to K.K. Terrace and Woodcrest		z	E-	5	N	II	N	Residual (No)

Notes:
(1) See Table 21 for definition of 'SH1' to 'SH4' and 'TH1' to 'TH4'.
(2) See Figure 10 for likelihood, consequence and risk categorization. See Figure 18 for site plan.

264

Risk Category		Risk to Life					Economic Loss				
		Loss of Life Consequence Category					Economic Loss & Disruption to Community Consequence Category				
		1	2	3	4	5	I	II	III	IV	V
Hazard Likelihood Category	A	H	H	H	H	R	H	M	L	R	R
	B	H	H	H	L	R	M	L	V	R	R
	C	H	M	L	V	R	L	V	R	R	R
	D	M	L	R	R	R	V	R	R	R	R
	E	L	V	R	R	R	R	R	R	R	R
	E-	V	R	R	R	R	R	R	R	R	R

Notes: PLL is the average number of fatalities per year. Risk Category is defined as follows:

Class	Descriptions (PLL for risk to life)	Further study
H	High – of major concern (notional PLL > 10^{-3})	This failure mode should be examined with priority attention, to assess/verify the scale of the problem
M	Moderate – of considerable concern (notional PLL 10^{-3} to 10^{-4})	This failure mode should be examined, to assess/verify the scale of the problem
L	Low – of some concern (notional PLL form 10^{-4} to 10^{-5})	It is advisable to examine this failure mode, to assess/ verify the scale of the problem
V	Very Low – practically not a concern (notional PLL less than 10^{-5})	Further study not warranted except in special circumstances
R	Residual risk – no indication of risk problem	Further study not warranted

(a) Risk Category

Class	Failure Likelihood Category
A	Very high (notionally 1 in 10 years)
B	High (notionally 1 in 10 to 100 years)
C	Moderate (notionally 1 in 100 to 1,000 years)
D	Low (notionally 1 in 1,000 to 10,000 years)
E	Very Low (notionally much less than 1 in 10,000 years)

Class	Effect Likelihood Category (likelihood of occurrence of the stated effects given the failure mode)	Adjustment on Failure Likelihood Category
x	Probable (notionally 0.5 or higher)	No change
y	Quite possible (notionally 0.1 to 0.5)	Downgrade by half a category
z	Possible (notionally < 0.1)	Downgrade by one category

(b) Likelihood Category

Class	Loss of Life Consequence Category
1	Very high chance of loss of life (PLL notionally > 1); multiple fatalities may occur
2	High change of loss of life (PLL notionally 0.1 to 1); low chance of multiple fatalities
3	Moderate chance of loss of life (PLL notionally 0.01 to 0.1)
4	Low chance of loss of life (PLL notionally < 0.01)
5	Very low chance of loss of life (PLL much less than 0.01)

Class	Economic Loss & Disruption to Community Consequence Category
I	Very high (severe structural damage to multi-story buildings; prolonged evacuation of multi-story building or a large number of houses; prolonged breakdown of transportation network)
II	High (severe structural damage to within a few flats or individual houses; prolonged evacuation of within a few flats or individual houses; prolonged closure of major road or important access; temporary breakdown of transportation network)
III	Moderate (some damage to properties; temporary evacuation of within a few flats or individual houses; temporary closure of major road or important access)
IV	Low (less serious than above)
V	Very low (much less serious than above)

(c) Consequence Category

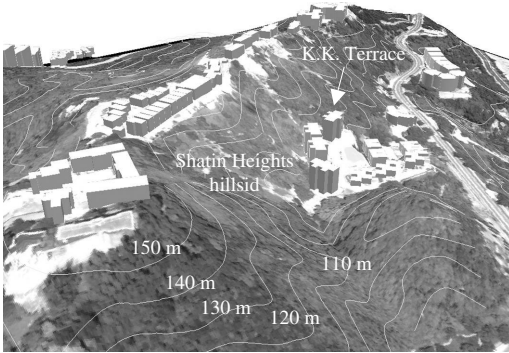Figure 10.   FMEA categorization scheme.

265

Figure 11. Shatin Height, Hong Kong.

risk assessment, to assist in hazard identification, risk screening and evaluation. It may be carried out as a stand-alone qualitative or semi-quantitative risk assessment procedure, or as a precursor to more detailed risk assessment, and in particular QRA.

5 SITE-SPECIFIC QUANTITATIVE RISK ASSESSMENT (QRA)

5.1 Overview

QRA is characterized by quantification of risk, for risk tolerability evaluation and risk management applications. Undertaking landslide QRA at individual sites requires the use of formal risk quantification techniques. It differs from qualitative landslide risk assessment as applied to site-specific level in two key aspects:

(a) the landslide risk, typically in terms of risk-to-life, is explicitly quantified; and

(b) the quantified risk figures are formally compared with the corresponding risk criteria for evaluation of risk management action, based on risk tolerability and risk-cost-benefit considerations.

Geotechnical practice embraces the assessment and management of risk, but the approach taken to handling risk has evolved with time. Qualitative deliberation prevailed in the 1970s and 1980s. Geotechnical application of QRA emerged in the 1990s, particularly in the mining industry, dam management and slope safety (e.g. Fell & Hartford 1997, Wong et al. 1997, Ho et al. 2000). Over the past few years, formal QRA has found a broader and more in-depth application to landslide risk assessment. The methodology and techniques continue to evolve.

There is now a wide spectrum of cases in which QRA was applied at varying degrees of complexity and detail, and conceivably with differing levels of rigor. Selected examples of site-specific QRA applications are summarized in the following Sections.
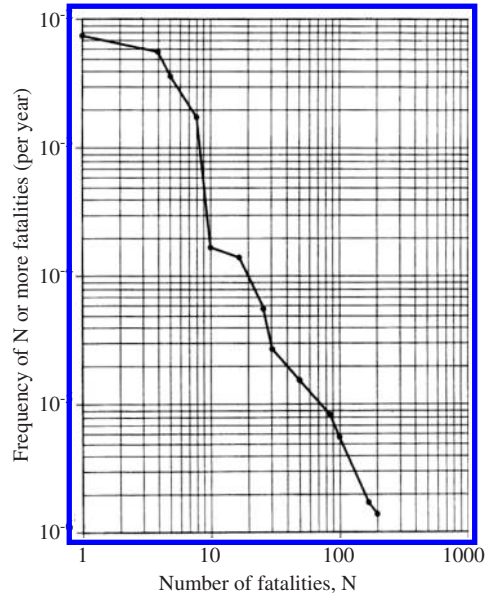
Figure 12. Calculated F-N curve for the Fei Tsui Road landslide (Wong et al. 1997).

While the examples are selected from the more detailed end of the spectrum of QRA cases to illustrate the state of good practice, they also demonstrate the evolution of QRA techniques in recent years.

5.2 QRA of notable landslides

Landslide back-analyses are conventionally undertaken primarily for examining the mechanisms and causes of slope failure. QRA offers another dimension to landslide back-analysis – to assess the landslide risk in retrospect. This provides a basis for a landslide to be evaluated in the light of its theoretic risk, damage potential and consequence scenarios. It also facilitates the interpretation of 'near-miss' events and examination of potential landslide loss figures and risk tolerability. The following are some known examples:

(a) The 1995 Fei Tsui Road landslide, Hong Kong: This landslide, which occurred in mid-night and resulted in one fatality, was a 'near-miss' incident. QRA by Wong et al. (1997) showed that the landslide had a Potential Loss of Life (PLL) of about 4. The F-N curve (Fig. 12) indicated the slope could result in multiple fatalities, e.g. the chance of 10 fatalities or more occurring was 0.015% per year. The back-analysis was also extended to predicting the consequences if the same landslide were to occur alongside a more heavily-used road. The QRA facilitates examination of possible hazard

266

scenarios and risk projections, and provides information for consideration in risk management, including emergency planning.

(b) The 1982 Argillite Cut rock fall, Canada: The rock fall resulted in one fatality and one another person injured. QRA by Bunce et al. (1997) found that the annual PLL was 8×10^{-2}, and annual probabilities of death of a one time user and a daily commuter on the highway were 6×10^{-8} and 3×10^{-5} respectively. Bunce et al. (1997) and Morgenstern (1997) noted that the case set a legal precedent when compensation was awarded because it effectively identified the level of risk at which the judicial system considered the public should be protected, although no QRA results were offered in evidence. This QRA back-analysis, which was carried out after the court case, helped to quantify the likely level of risk posed by the Argillite Cut to road users, and thereby facilitated the interpretation of risk tolerability.

(c) The 1999 Shek Kip Mei landslide, Hong Kong: The landslide caused significant slope movement and resulted in permanent evacuation of about 700 residents from a housing estate. Based on the QRA results by El-Ramly et al. (2003), Wong (2005) assessed that the probability of multiple fatalities (>40 deaths) was about 10^{-2} to 10^{-3} after significant slope movement had occurred. Although there are uncertainties due to the simplified assumptions adopted, the results give a quantified estimate of the likely order of risk perceived at the time when evacuation was recommended on the basis of engineering judgment.

(d) The 1997 Thredbo landslide, NSW, Australia: A fill embankment below the Alpine Way collapsed and the mobile debris destroyed two buildings, which resulted in 18 fatalities. QRA by Mostyn & Sullivan (2002), which was based on consideration of the historical fill embankment failure data in the Alpine Way, debris mobility and consequence analysis, found that the individual risks at the two buildings before the landslide (2.2×10^{-3} and 5.3×10^{-3} per year) exceeded the unacceptable limit (10^{-6} per year) suggested by the NSW Department of Planning for tourist resorts. The societal risk was also found to be high, and was within the unacceptable zone according to the societal risk criteria reviewed by Fell & Hartford (1997). The QRA findings were presented to the Coroner Inquest, and the Coroner took the view that the community would regard the individual risk as 'totally unacceptable' (Hand 2000).

5.3 *Lei Yue Mun squatter area QRA*

QRA has been used in Hong Kong for about a decade in formally assessing landslide risk for evaluating

Figure 13. Landslides in August 1995 affecting the Lei Yue Mun Squatter Area.

site-specific risk management strategy. The QRA of the Lei Yue Mun squatter area (Hardingham et al. 1998) was an early application. The QRA methodology adopted at the time was relatively simplistic. However, all the essential components of a formal QRA, e.g. quantification of individual and societal risks and evaluation in comparison with risk criteria, were in place.

The abandoned quarry faces of the slopes flanking the Lei Yue Mun squatter villages in Hong Kong were between 20 m and 40 m high, and typically sloping at 65° to 80° (Fig. 13). The slopes had a history of instability. QRA was adopted to quantify the landslide risk and to assist in decision-making with regard to the extent of re-housing of the squatter residents.

(a) Hazard identification
This was carried out through a comprehensive geotechnical study. The principal hazards threatening the squatter village included rock falls and debris slides arising from failure of the un-engineered cut and fill slopes. The hazards were categorized according to the volume of failure.

(b) Frequency assessment
Interpretation of aerial photographs, which dated back to 1945 at this site, identified a total of 115 landslides. 'Recognition factors' of 30% and 90% were adopted for small and medium landslides, respectively. This factor represented the proportion of landslides that could be recognized, to address the problem that some of the smaller failures could have been missed by aerial photograph interpretation. The base-line annual landslide frequencies for the site were found to be 3.3 for small (<50 m^3), 1.3 for medium (50–500 m^3), 0.24 for large (500–1,000 m^3), 2.4×10^{-3} for very large (1,000–5,000 m^3), and 2.4×10^{-4} for extremely large failures (>5,000 m^3). The frequency was spatially apportioned to different 20-m wide slope segments via an empirical slope rating scheme.

267
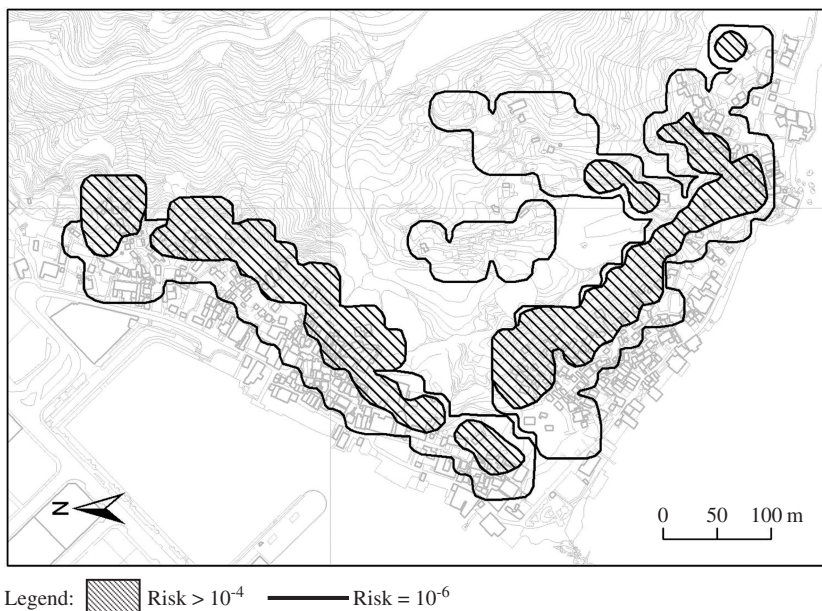
Figure 14. Individual Risk contours for the Lei Yue Mun Squatter Area (Hardingham et al. 1998).

(c) Consequence assessment

Consequence was defined in terms of three different groupings, each with its own level of associated casualties. The groupings took into account the type of landslides and debris travel distance, as well as the proximity of the dwellings. Site surveys were carried out on about 10% of the population and 45 dwellings, to identify the numbers of people at risk and their temporal distributions at different types of facility.

(e) Risk calculation and evaluation

The dwellings were grouped into 20 m by 20 m grid cells. The number of people and the temporal presence in each grid were determined from a population survey. An Event Tree was generated for each of the reference grids, which traced the different credible scenarios by combining the hazard grouping, timing of failure, responses to landslip warning, level of emergency services, secondary hazards, etc.

The site-specific risk acceptance criteria were determined through a review of different safety acceptance criteria and consideration of the situation involving squatters at Lei Yue Mun. The proposed individual risk criteria ranged from an upper boundary (unacceptable) of 10^{-4} to a lower boundary (acceptable) of 10^{-6}. The risk criteria that are currently adopted in Hong Kong (ERM 1998) had not been developed at the time.

The results of the QRA indicated that a large area of the squatter area fell within the unacceptable region in terms of individual risk (Fig. 14). The assessed societal risk was also found to be unacceptable (Fig. 15). Risk
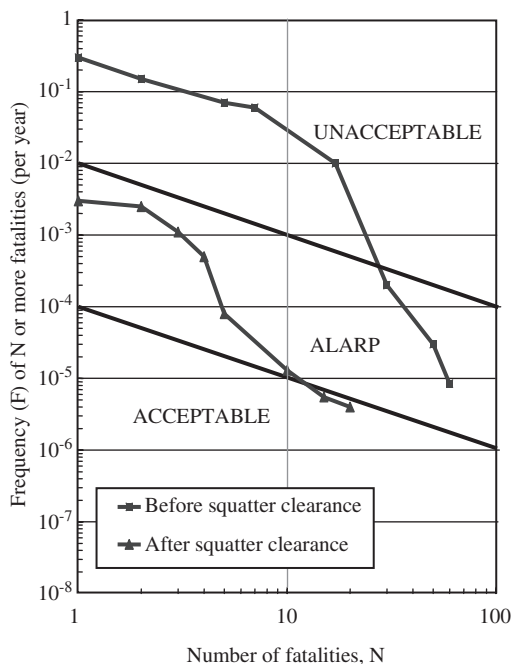

Figure 15. Societal Risk for the Lei Yue Mun squatter area (Hardingham et al. 1998).

268

calculations further showed that if the squatter residents within the area recommended for clearance were re-housed, the societal risk would reduce to the ALARP region. Cost-benefit calculations indicated that the residents in areas where the landslide risk was within the ALARP region did not justify immediate re-housing. Quantification of risk provided a rational basis for decisions to be made on risk mitigation and squatter clearance in this case.

5.4 *Shatin heights QRA*

Hong Kong's natural terrain is susceptible to shallow, small-to-medium-sized landslides (Fig. 16), which can develop into debris flows after entering drainage lines. Should the debris reach densely developed areas, serious consequences may occur, even if the volume of the landslide is relatively small (Fig. 17). The strategy that is being adopted in Hong Kong for management of natural terrain landslide risk entails two principles (Chan 2003):

– For existing developments, deal with natural terrain landslide risk following a 'react-to-known-hazard'

Figure 16.   Landslide-prone natural terrain in Hong Kong.

Figure 17.   A 20 m^3 landslide in 1998 resulted in damage to property.

principle, i.e. to carry out studies and mitigation actions where significant risk becomes evident.

– For new developments, contain the increase in overall risk through studying and undertaking any necessary mitigation actions on sites subject to natural terrain landslide hazards.

Use of QRA as an accepted approach for studying natural terrain landslide risk and determining the required mitigation actions was formally introduced in Hong Kong in 2000.

The natural terrain landslide problem at the Shatin Heights site is described in Section 4.4 above. The QRA of the site, which is documented in FMSW (2001), is one of the earliest QRA applications to natural terrain landslide risk in Hong Kong. The GEO selected the case for risk assessment based on the 'react-to-known-hazard' principle, following six natural terrain landslides that occurred on the hillside in 1997.

The study area (Fig. 18) was sub-divided into seven catchments and a total of 45 segments, based on topographic conditions. The QRA included the following key tasks:

(a) Hazard identification
This was carried out with a desk review of the available data, interpretation of historical aerial photographs, study of the 1997 landslides, ground investigations, geological mapping, geotechnical appraisal and use of engineering judgment. The landslide hazards were classified according to two types of mechanism (open hillslope landslide and channelized debris flow) and three failure scales ('small' for volumes within 50 m^3, 'medium' for between 50 m^3 and 200 m^3, and 'large' for between 200 m^3 and 1,000 m^3).

(b) Frequency assessment
The base-line landslide frequency was assessed from historical landslide data collated from detailed interpretation of aerial photographs dating back to 1963,
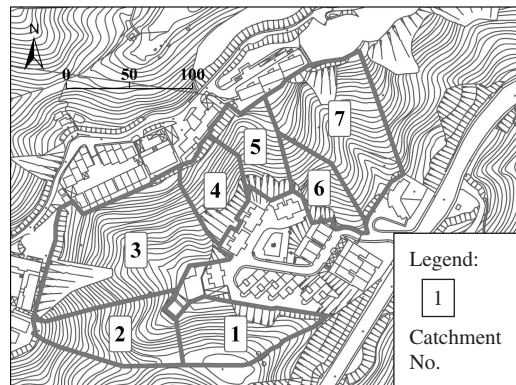

Figure 18.   Natural terrain catchments in Shatin Heights, Hong Kong.

269

with allowance being made for 'recognition factors'. Volume-frequency relationship was established from the landslide data, together with a consideration of the data available from elsewhere in Hong Kong (Wong & Lam 1998, Franks 1998). Probabilistic slope stability analyses were carried out to provide a basis for spatial distribution of the landslide frequency to the different segments. The distributed landslide frequency was further adjusted by a Bayesian approach to take account of any historical landslide frequencies occurring in the segment.

(c) Consequence assessment

A site-specific consequence model was formulated, based on the generalized model developed by Wong et al. (1997). This modified consequence model entailed the use of site-specific data on debris mobility, an empirical runout model, and vulnerability factors for different types of facility at different proximity zones. Scaling factors were applied for adjusting the vulnerability factors under different circumstances. Landslide consequence was quantified by multiplying the expected number of people with the relevant vulnerability factor.

(d) Risk calculation and evaluation

The distribution of the calculated Personal Individual Risk (PIR) at Shatin Heights is shown in Figure 19. PIR adopted in Hong Kong refers to the frequency of harm to a theoretical individual who is exposed to the hazard with account being taken of the temporal factors which expose the individual to the hazard. Parts of the site had an unacceptable PIR, i.e. exceeding 10^{-4} per year for an existing facility (ERM 1998). The societal risk in terms of potential loss of life (PLL) was found to be 5.7×10^{-3} PLL per year. The corresponding F-N curve is shown in Figure 20. The societal risk criteria apply to a consultation zone that is equivalent to a maximum 500 m long segment of natural hillside. The societal risk was within the ALARP region except for the single-fatality portion which was in the unacceptable zone (ERM 1998).

(e) Risk mitigation strategy

The mitigation strategy that was adopted included a qualitative assessment of the design hazard, which was followed by risk-cost-benefit analysis based on the ALARP principle. The design hazard was established with the use of the Design Event Approach (as described in Section 4.2 above), which indicated that a worst credible event (i.e. notionally a 1,000-year event) was to be mitigated. From analysis of the magnitude-frequency data, the design landslide volumes were estimated to be 600 m^3 for catchment No. 3, and 500 m^3 for catchments No. 5 and No. 7. Possible risk mitigation schemes, including use of debris-resisting barriers and local slope stabilization, were examined. The cost of risk mitigation was found to be about US$ 0.7 million, which would result in mitigation of about

(a) Before risk mitigation

(b) After risk mitigation

Legend:

 Risk > 10^{-4} Risk>10^{-5} to <10^{-4} – – – Risk = 10^{-6}
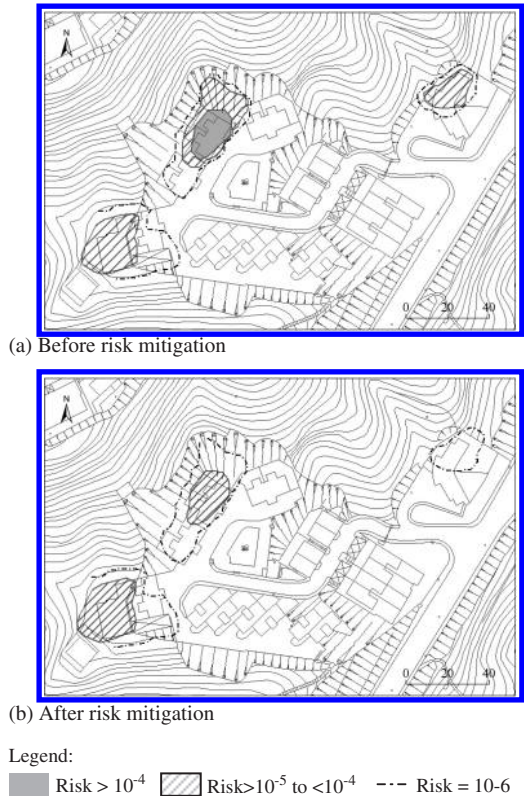
Figure 19. Personal Individual Risk at Shatin Heights (FMSW 2001).

80% of the societal risk. After risk mitigation, the PIR distribution (Fig. 19) and F-N curve (Fig. 20) would be well below the unacceptable zone. The risk mitigation was found to be justified from risk-cost-benefit analysis, based on consideration of an equivalent value of life of US$ 3 to 4 million and an aversion factor of unity. The risk mitigation works were implemented in close liaison with the local residents in 2004.

5.5 *Pat Heung QRA*

In August 1999, two landslides occurred on the natural hillside above No. 92 to 94 Ta Shek Wu Kiu Tau, Pat Heung, Hong Kong (Fig. 21). Based on the 'react-to-known-hazard' principle, the GEO arranged a QRA of the natural terrain landslide risk on the existing developments at the site. The study was documented by OAP (2003).

The QRA at Pat Heung followed methodology that was similar to those developed and adopted in the Shatin Heights study. Use of GIS techniques enabled a more refined sub-division of the hillside into regular 10-m grid cells, which facilitated spatial analysis.

270
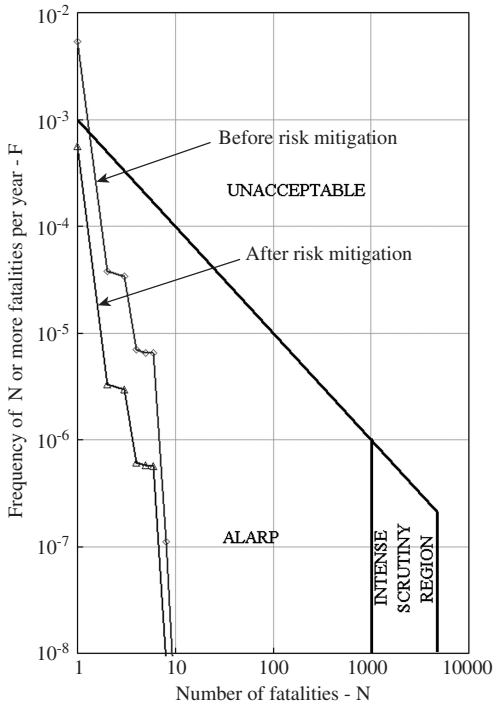
Figure 20. Calculated F-N curves for Shatin Heights (FMSW 2001).
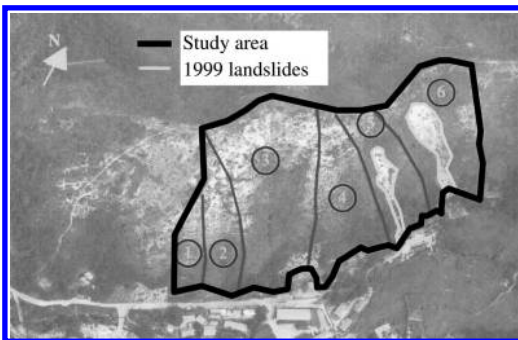
Figure 21. The August 1999 landslides at Pat Heung, Hong Kong.

(a) Hazard identification

The landslide history, geology, geomorphology and hydrogeology were evaluated by aerial photograph interpretation, field mapping, and ground investigation comprising boreholes, trial pits and gravity surveys. The landslides occurred mainly in the surface layer of colluvium, and occasionally with part of the slip surface extending into the underlying weathered volcanic tuff. The landslide hazards were identified as shallow landslides, either in the form of an open hillslope failure or channelized debris flow. Landslide volume was categorized into different ranges.

(b) Frequency assessment

The base-line landslide frequency was established from the historical landslide data, with allowance for 'recognition factors'. The relevant terrain attributes, including slope gradient, slope aspect and regolith type, were analyzed to examine their correlation with the historical landslide distribution. A grid-based landslide susceptibility analysis was carried out to distribute the landslide frequency to each grid cell (Fig. 22). The landslide volume-frequency distribution was established from historical landslides (Fig. 23). The worst credible volumes (i.e. notional 1,000-year event) for open hillslope failure and channelized debris flow were assessed as of $400 \, m^3$ and $550 \, m^3$, respectively.

(c) Consequence assessment

Historical debris runout data at the site were analyzed to establish the mean and standard deviation relationships of debris runout for open hillslope failures and for channelized debris flows (Fig. 24). Runout distance was adopted as an empirical indicator of the probabilistic distribution of debris mobility, whereas the mean travel angle minus two standard deviations was taken as the upper limit of debris runout.

For houses including dwellings and industrial buildings, the expected number of vulnerable people and their temporal distribution were identified from field surveys and interviews. For roads and footpaths, it was estimated from vehicle and pedestrian densities. The vulnerability factor was calculated as the product of a base-line factor, a volume factor and a protection factor (Fig. 25).

(d) Risk calculation and evaluation

The risk arising from landslides originating from each grid cell was calculated and summed. The PIR at houses No. 92 and 93 ranged from 1.2×10^{-4} to 2×10^{-4} per year, which was unacceptable. The societal risk was found to be 2.1×10^{-3} PLL per year. About 77% of this came from people in buildings, 18% from pedestrians and 5% from vehicle occupants. The derived F-N curve (Fig. 26) showed that the single-fatality portion was within the unacceptable zone.

(e) Risk mitigation strategy

Possible risk mitigation options were examined. The recommended option comprised debris deflector walls together with local soil nailing to protect the houses. These would reduce the societal risk to about 5×10^{-4} PLL per year, i.e. by over 80% (Fig. 26). The cost of the mitigation works was about US 1 million. The maximum justifiable expenditure was assessed to be US$ 0.6 to 1.5 million, based on use of 120-year design life, an equivalent value of life of US$ 3 to 4 million (ERM 1998) and aversion factor of 1 to 2. The mitigation measures were being constructed in 2004/05.

271

Figure 22.   Annual landslide frequency (OAP 2003). [see Colour Plate V].
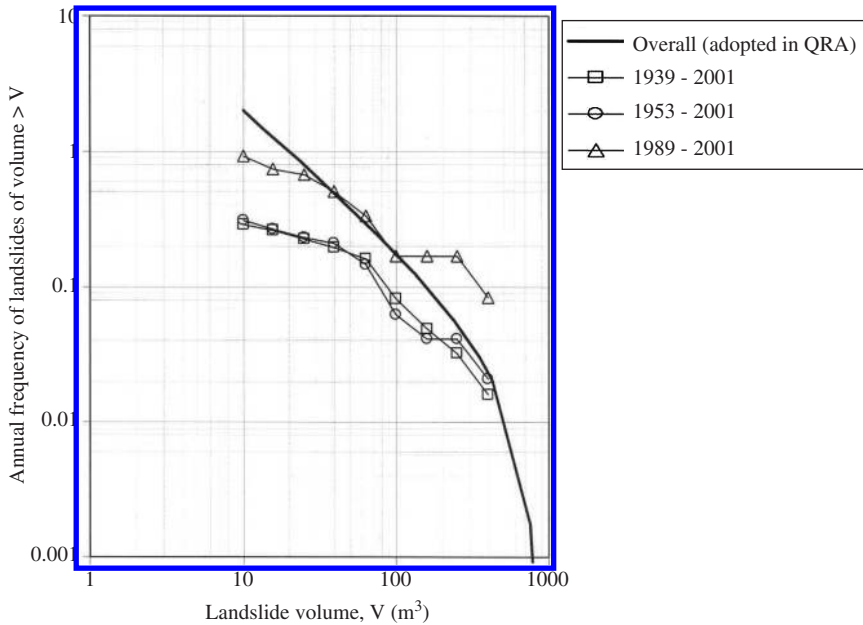
Figure 23.   Volume – frequency distribution for landslides at Pat Heung (OAP 2003).

5.6   *North Lantau Expressway QRA*

The North Lantau Expressway is the sole vehicular access to the Hong Kong International Airport and the adjacent Tung Chung New Town, Lantau, Hong Kong. The road is a two-way highway with 3 lanes each way. It runs for about 20 km along the toe of the steep natural hillside of north Lantau. The hillside has numerous records of historical natural terrain failures, and some of these have reached the present position of the highway.

272
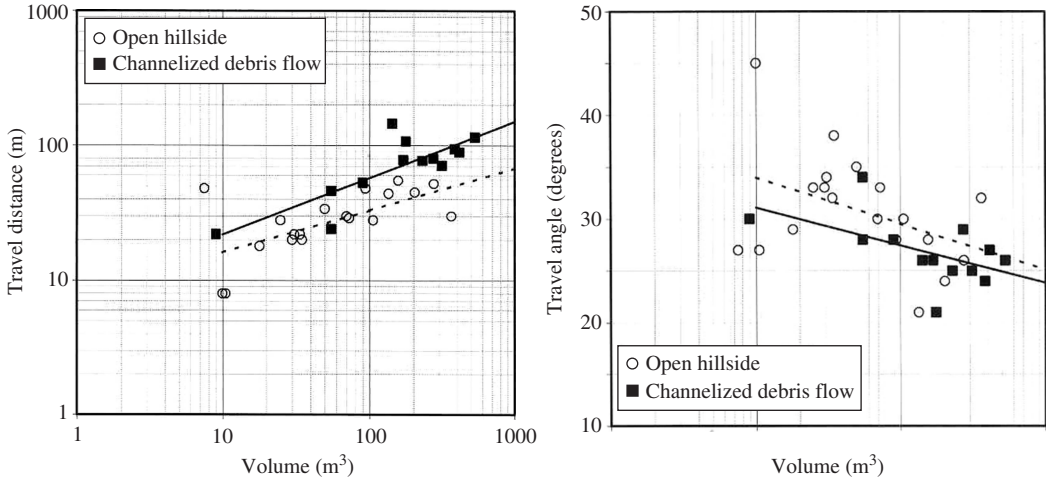
Figure 24. Mobility of landslides in Pat Heung (based on OAP 2003).

(a) Base-line factor

(b) Volume factor and protection factor

```
··· ♦ ···  Building Protection      ··· ■ ···  Vehicle Protection      ──▲──  Volume
            Factor                            Factor                           Factor
```
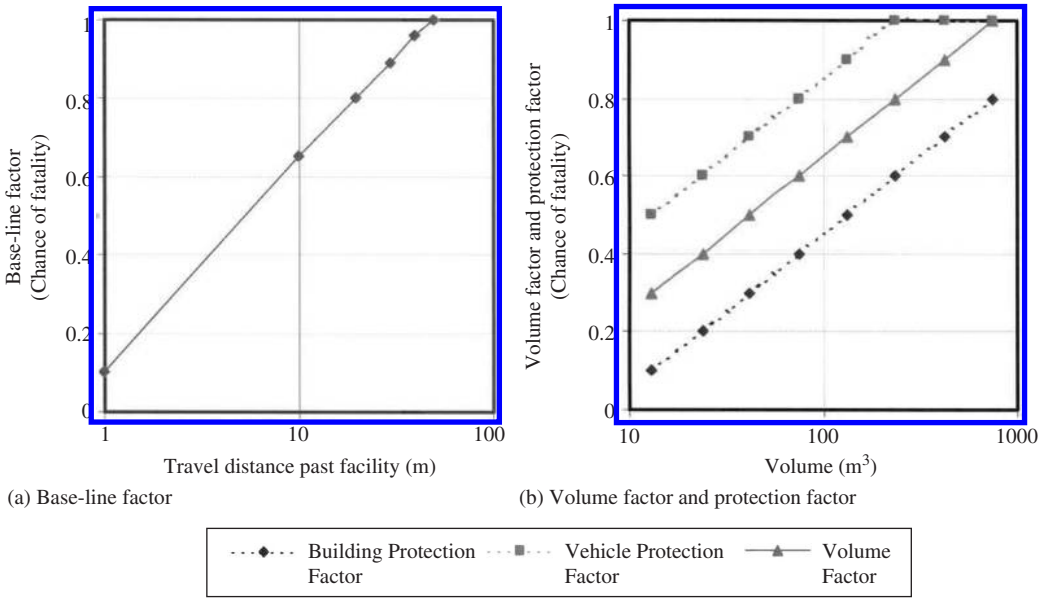
Notes: (1) The base-line factor is applied to a facility located at a given distance from the distal end of the debris runout
        (2) Vulnerability factor = Base-line factor × Volume factor × Protection factor

Figure 25. Vulnerability factor adopted in Pat Heung QRA (based on OAP 2003).

A qualitative hazard assessment was carried out (Ng & Wong 2002). The assessment included a review of the historical landslide records and the geological and terrain conditions, consideration of the historical landslide activity, proximity of the highway to the hillside and empirical debris runout criteria, a 4 km long section of the highway near the Tung Chung New Town (Fig. 27) was found to require a QRA. The QRA findings were documented in OAP (2005).

273
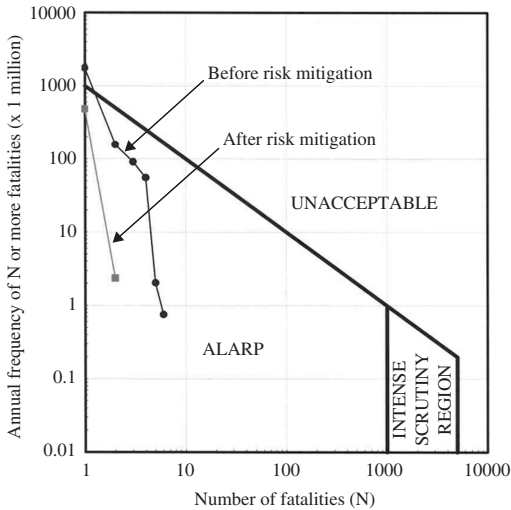
Figure 26. Calculated F-N curve for Pat Heung (OAP 2003).
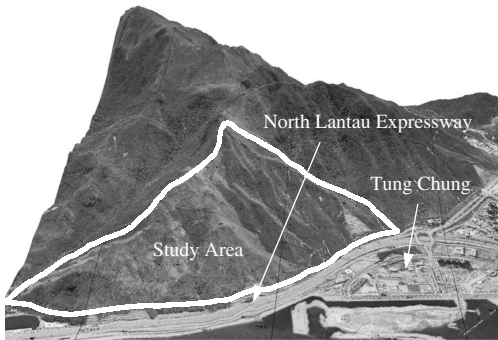
Figure 27. Natural hillside overlooking North Lantau Expressway, Hong Kong.

The QRA followed the procedures and techniques developed and adopted in previous QRA in Hong Kong. Three aspects of this QRA deserve attention:

(a) The natural hillside to be assessed covered a large area, and involved more variable geological conditions and landslide types. Hence, in this QRA, particular attention was given to geological assessment of the terrain morphology and landslide process, which formed an integral part of hazard identification and frequency assessment. The information was synthesized into detailed morphology-based regolith maps and landslide process models (Fig. 28).

(b) The highway was located at some distance from the steep natural hillside and was partly protected by buffer zones, which included open spaces, road reserves and drainage ditches and chambers. The QRA showed that both the PIR and societal risk in terms of risk-to-life were not in the unacceptable zone. The PIR for the most affected people (i.e. bus drivers) was found to be 1.7×10^{-7} per year, which is well within the acceptable limit of 10^{-4} for an existing facility. For societal risk, the total calculated PLL is 6.8×10^{-3} per year, which comes from channelized debris flows. The F-N curves for the eight sections (each 500 m long) of the highway are all within the ALARP region (Fig. 29).

(c) While risk-to-life was found to be in the ALARP region, it was perceivable that the potential economic loss arising from landslides could be significant. This was confirmed by quantifying the risk in respect of different types of economic loss (Table 15). The total potential economic loss was found to be about US$ 54 million in 120 years.

The preferred risk mitigation scheme comprised provision of check dam basins at six vulnerable debris flow channels (Fig. 30). The cost of the mitigation works was about US$ 3.5 million. Based on the ALARP principle, the maximum justifiable expenditure for mitigating loss of life alone was found to be within US$ 3 million, which was less than the cost of the preferred scheme. However, with account also taken of the significant potential economic loss, risk mitigation was considered justified. This case illustrates that for major highways and infrastructures, economic loss can be substantial and may have significant effects on the risk-cost-benefit analysis.

5.7 Ling Pei QRA

In 2004, a land-use concept plan was drafted by the Government of the Hong Kong Special Administrative Region (HKSAR) to guide the development of the Ling Pei area, Tung Chung, Hong Kong. The planned development comprised construction of 76 nos. of 3-storey houses at the toe of the hillside that overlooks the existing village in Ling Pei (Fig. 31). Wong et al. (2004c) carried out a QRA to quantify and evaluate the risk. The case was a notable development in the application of landslide QRA in Hong Kong in the following respects:

– This is a case that extends the application of formal landslide QRA to land-use and development planning at a specific site in Hong Kong.
– As an attempt to standardize the QRA process and further improve practice of QRA on natural terrain landslides, a recent review on the use of QRA has identified 16 key modules of work, as listed in Table 16. The Ling Pei QRA served as a reference

274

Legend:

Distressed ground (with tension cracks and slow moving landslides).

Area of landslide clustering.

Alluvium, channelized debris flow dposit, colluvium and taluvium boulder accumulate along the drainage channels.

Shallow landslides deposit colluvium on gully side slopes. Many landslides.

Taluvial lobes downslope from intermittent rock outcrops.

Rockfall debris at the toe of rock outcrops.

Accumulation of colluvium in topographic depressions.

Landslides occur on former steep coastal slopes.

Open hillslope colluvium accumulates on relatively shallow hillslopes. In feldsparphyric rhyolite/ porphyritic microgranite terrain. Very few landslides.

Open hillslope colluvium on relatively shallow hillslopes (younger terrain) in the rhyolite lava/ tuff terrain as a result of creep. Few landslides.

Relatively steep hillslopes in the upper portion of the rhyolite lava/ tuff terrain (older terrain). Drainage channels generally have well defined convex breaks of slope at their heads but very few recent landslides.

Incised and degraded — Younger — Debris fans, comprising coalescing bodies of colluvium/ alluvium, have developed at the hillslope toe.

Study area boundary

Former shoreline

Former cliffline

Areas of saprolite along hillside spurs. Very few landslides.

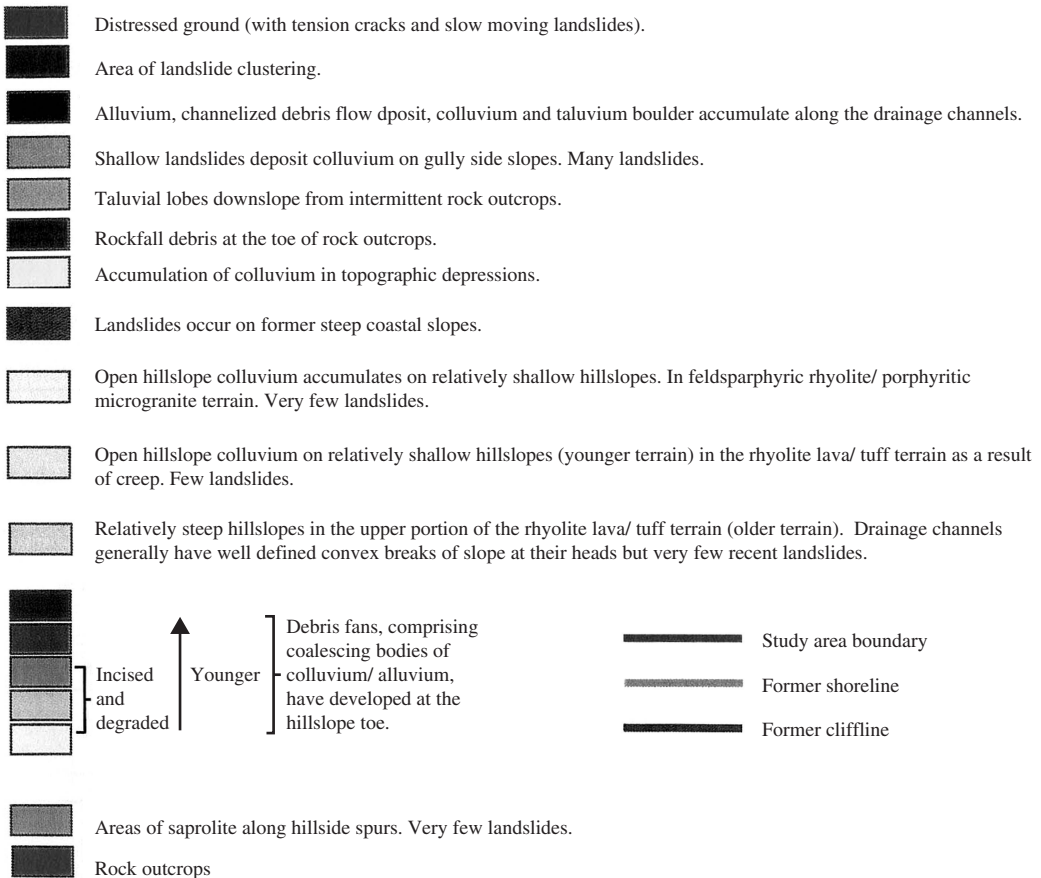Rock outcrops

Figure 28.   Landslide process model (OAP 2005) [see Colour Plate VI].

case that was undertaken in alignment with the 16 key modules of work.
– As part of the work, further enhancements of site-specific QRA techniques were made. The enhancements helped to improve the rigor of the assessment and to overcome some known technical problems that have been encountered in previous QRA.

275

Figure 29. Calculated F-N curves for North Lantau Expressway (OAP 2005).
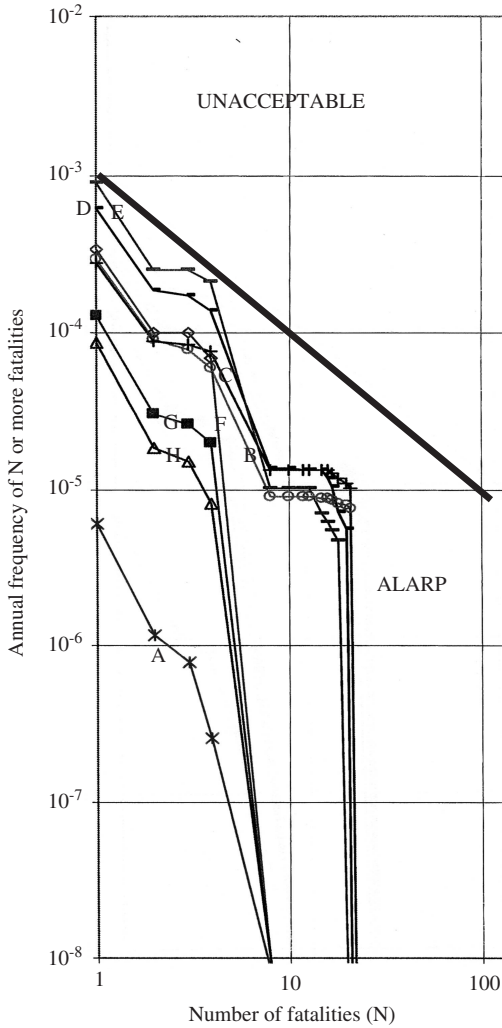
Legend:

A - Chainage 0-500 m   E - Chainage 2001-2500 m
B - Chainage 501-1000 m   F - Chainage 2501-3000 m
C - Chainage 1001-1500 m   G - Chainage 3001-3500 m
D - Chainage 1501-2000 m   H - Chainage 3501-4000 m

Table 15. Potential 120-year economic loss for North Lantau Expressway (extracted from OAP 2005).

Type	Scope	Potential economic loss
Damage to vehicles	Economic loss associated with direct damage to vehicle on North Lantau Expressway due to debris impact	US$0.2 million
Air travel passengers delay	Economic loss associated with potential delays to air travel passengers due to temporary closure of the expressway and thereby causing delayed traffic access the Hong Kong International Airport	US$12 million
Air cargo delay	Economic loss associated with potential delay to air cargo due to temporary closure of the expressway and thereby causing delay to good vehicles' access the Hong Kong International Airport	US$42 million
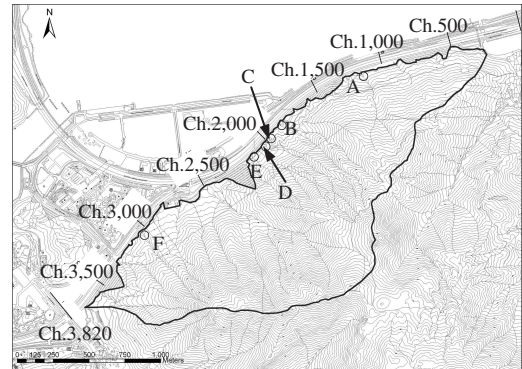
Design requirement for risk mitigation			
Location	Debris volume (m³)	Debris velocity (m/s)	Debris height (m)
A	500	13	2.5
B	500	13	2.5
C	1,000	15	3.0
D	1,000	15	3.0
E	1,000	15	3.0
F	1,700	16	3.5

Figure 30. Mitigation strategy (OAP 2005).

The procedures for the QRA and the key findings are summarized below, under the headings of the relevant modules of work:

(a) Study objectives, approach and area (Module Nos. 1 & 2)
The study served to assess the risk on the planned development and to guide the development strategy. The hillside that overlooked the planned buildings is denoted as Area B in Figure 32. As good practice in site-specific QRA on natural terrain landslides, a larger region was studied for thorough examination of the landslide process and characteristics (Areas A to D, Fig. 32).

276

Figure 31. Catchments and Sub-catchments in Area B, Ling Pei, Hong Kong (Wong et al. 2004c).

(b) Landslide history and rainfall effects (Module Nos. 3 & 4)

Historical landslide activities and characteristics in the region were evaluated from an interpretation of aerial photographs, field inspections and geomorphological mapping. A total of 91 recent natural terrain landslides and five large relict landslide-related morphological features were identified (Fig. 32). The correlations of natural terrain landslide density with normalized rainfall intensity in Hong Kong established by Ko (2003) and Wong et al. (2004c) were applied to the site. The landslide and rainfall histories at the site were found to be broadly consistent with the Hong Kong-wide trend, and the available historical landslide data gave a reasonably conservative base-line landslide density for use in frequency assessment.

(c) Catchment and facility identification (Module Nos. 5 & 6)

The topographic conditions of the hillside was assessed with the use of a 2-m grid digital elevation model (DEM), together with terrain evaluation based on field mapping and interpretation of aerial photographs. This resulted in demarcating the hillside in Area B into a total 21 sub-catchments (Fig. 31). The sub-catchments were classified into three types according to the mechanisms of debris movement (Table 17).

(d) Geological assessment and hazard identification (Module Nos. 7 & 8)

The geological assessment comprised geological mapping, investigation and appraisal to establish the landslide processes at the site, examine the landslide mechanisms, classify the terrain, formulate geological models, diagnose possible hazards, etc. The work provided a technical basis for formulating terrain and hazard models.

(e) Debris runout path and influence zone (Module No. 9)

There are two main aspects of evaluation of debris runout for use in consequence assessment. Firstly, the mobility of the landslide debris has to be assessed. In the Ling Pei site, this was done by statistical analysis of the historical runout data. Secondly, the debris runout path has to be predicted. To do so, sub-catchments in Area B were further divided into small hillside units (Fig. 33). Each hillside unit should have practically the same landslide susceptibility and debris runout path. Based on 3-D GIS analysis and terrain evaluation, the possible debris paths originating from each hillside unit were determined. Each unit was then matched with the segments of the lower boundary of the catchments, and with the existing and planned houses. A Fault Tree methodology was adopted in the matching

277

Table 16. Key modules of work in natural terrain landslide QRA (based on Wong 2005).

Module of Work	Scope
(1) Determine study objectives and approach	– Identify the background and purposes of the study, and any special requirements – Determine the objectives and the level of details required – Select the approaches to be adopted
(2) Delineate study area	– Identify the extent of the site that may be at risk from landslide hazards – Set out the extent of the study area
(3) Validate historical landslides	– Collate information on historical landslides based on documentary records, aerial photograph interpretation, and findings from field mapping and geomorphological assessment – Validate the data and compile a dataset of landslides and related attributes
(4) Examine rainfall records and effects	– Collate information on the rainfall history – Examine any relevant rainfall-landslide pattern/correlation – Establish any need to adjust figures on the historical landslide activity to account for rainfall effects
(5) Demarcate boundaries and types of catchments	– Delineate the boundaries of catchments – Sub-divide the catchments where necessary, e.g. based on topographic conditions and mechanism of debris movement – Match the catchments with the facilities at risk
(6) Identify facilities and population at risk, and their degree of proximity	– Identify the types and locations of the facilities at risk – Establish degree of usage and temporal distribution of population at risk – Examine degree of proximity with reference to GEO's screening criteria, empirical models, relevant historical runout data, etc.
(7) Geological assessment	– Carry out field mapping to establish the engineering geological and geomorphological conditions – Examine landslide processes and mechanisms, regolith type and distribution, signs of distress, and other relevant terrain attributes – Classify terrain, and develop geological and landslide process models
(8) Formulate hazard and hazard models	– Identify potential landslide hazards and the relevant hazard scenarios that require risk quantification – Formulate hazard models for use in QRA and in assessment of Design Events
(9) Identify possible debris runout paths and influence zones	– Divide potential landslide sources into cells – Identify possible debris runout paths for each cell – Match the cells with the facilities at risk – Assess the degree of proximity and the degree of damage to the facilities at risk
(10) Carry out frequency assessment	– Formulate frequency model – Establish the frequencies of occurrence of different types of hazard – Assess the spatial distribution of the landslide frequency, together with the use of susceptibility analysis and Bayesian methodology as appropriate – Assess the frequency of occurrence of special hazard scenarios, e.g. building collapse and events with knock-on effects
(11) Carry out consequence assessment	– Formulate consequence model – Assess the consequence of occurrence of different types of hazards – Assess the consequence of occurrence of special hazard scenarios, e.g. building collapse and events with knock-on effects
(12) Analyze risk	– Calculate the risk by integrating frequency and consequence – Evaluate the distribution of risk – Carry out sensitivity analysis and examine the reliability of the findings of the risk assessment
(13) Assess design events	– Assess the magnitudes of Design Events
(14) Evaluate risk management strategy	– Compare risk results with risk criteria – Formulate possible risk management options – Evaluate the pros and cons of different risk management options and identify the preferred risk management strategy – Interact with and obtain feedback from stakeholders
(15) Draw conclusion and recommendation	– Conclude the findings of the study – Recommend risk management strategy and follow-up actions
(16) Document findings	– Document the findings of the study – File the relevant information, data and calculations – Update the relevant documentary and digital records

Figure 32.   Historical landslides in Ling Pei (Wong et al. 2004c).

Table 17.   Hazard classification (Wong et al. 2004c).

Hazard	Classification	Definition
Mechanism of debris movement (which was related to catchment characteristics)	C	Channelized debris flow
	T	Mixed debris flow/avalanche at topographic depression
	S	Open hillslope debris slide/avalanche
Scale of landslide (which was established from volume-frequency relationships for different classes of catchment)	H1a	$30\,m^3$ notional ($20\,m^3$ to $60\,m^3$)
	H1b	$100\,m^3$ notional ($60\,m^3$ to $200\,m^3$)
	H2a	$300\,m^3$ notional ($200\,m^3$ to $600\,m^3$)
	H2b	$1,000\,m^3$ notional ($600\,m^3$ to $2,000\,m^3$)

to cater for the uncertainties in predicting the debris flow paths.

(f) Frequency assessment (Module No. 10)
This followed standard volume-frequency correlation and spatial distribution of the base-line landslide densities to each hillside unit via susceptibility analysis (Fig. 34). In this QRA, different susceptibility models

were adopted for different terrain types, to cater for the fact that their landslide processes were different.

(g) Consequence assessment (Module No. 11)
An enhanced consequence model, which incorporated consideration of the hazard type, runout mechanism, runout path, debris mobility and vulnerability formulation, was developed for use in this QRA. Vulnerability factors for the buildings were derived from integrating the probabilistic function of debris runout distance and a model for the degree of damage (Fig. 35).

(h) Risk analysis and evaluation (Module Nos. 12 & 13)
The assessments and risk integration were carried out on a GIS platform. The calculated PIR of an individual in the planned buildings ranged from 3.3×10^{-7} to 8.9×10^{-6} per year (Fig. 36), which was within the maximum permissible level of 10^{-5} per year for new developments (ERM 1998). The societal risk for the planned houses was 1.8×10^{-4} per year. The corresponding F-N curve (Fig. 37) was within the ALARP zone.

The PIR on the existing houses was also assessed and found to be within the maximum permissible level. The societal risk on the existing houses was 4.3×10^{-4} per year. Hence, the planned development would result in more than 60% increase in societal risk. The F-N curve of the total societal risk for both the existing and planned houses was within the ALARP zone (Fig. 37).

279
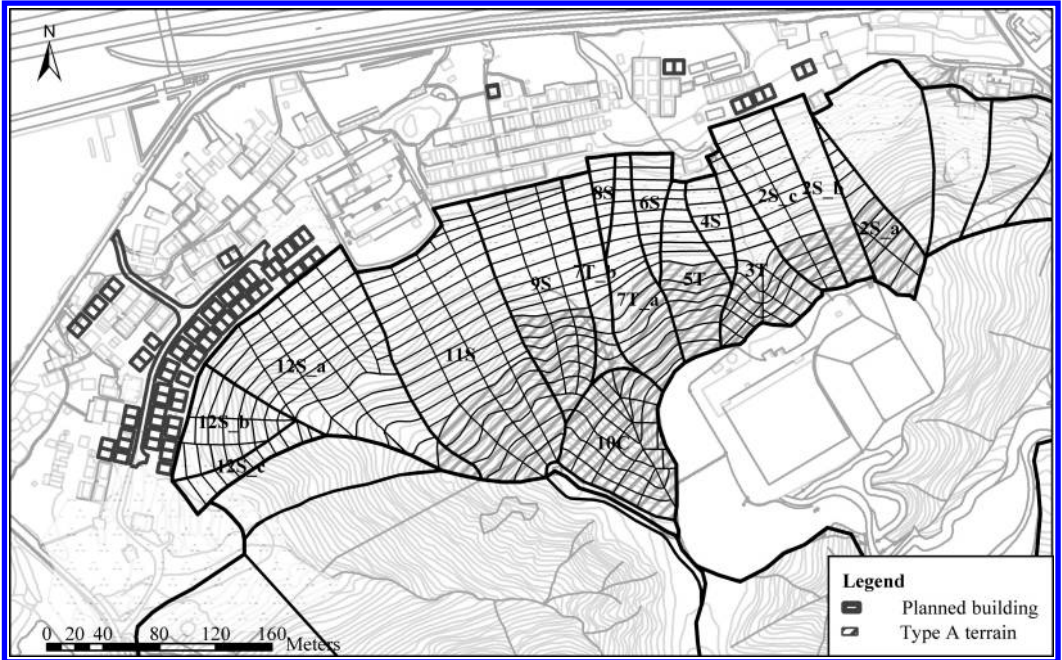
Figure 33.   Hillside units (Wong et al. 2004c).
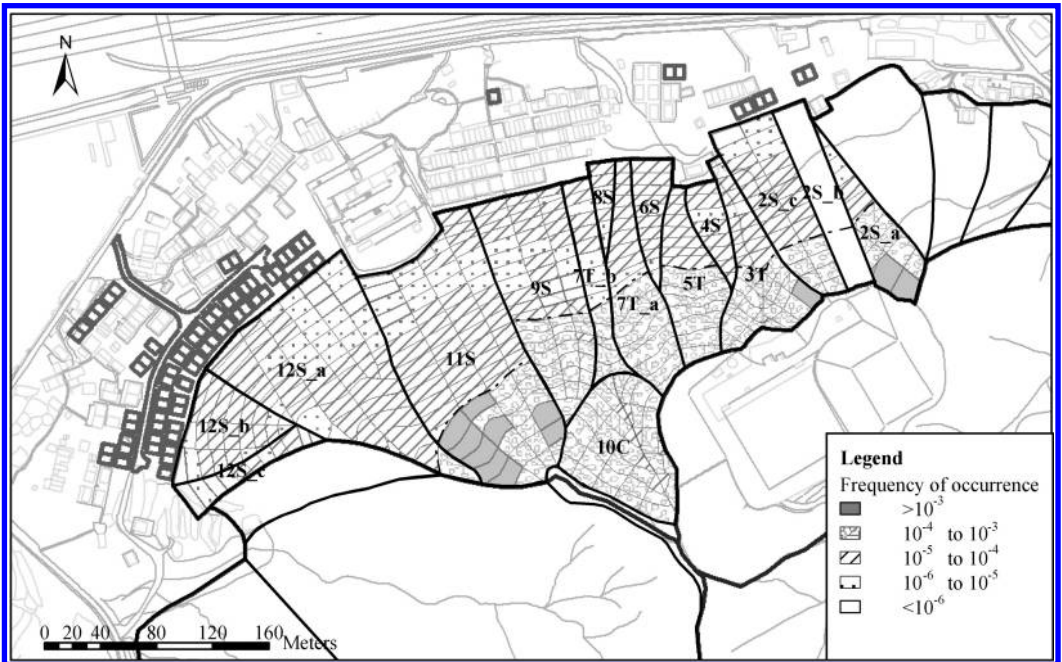
Figure 34.   Calculated annual frequency of landslide hazard H1a ($20\,m^3$ to $60\,m^3$) (Wong et al. 2004c).

280

(i) Risk management strategy (Module No. 13)
The maximum justifiable expenditure calculated from the ALARP principle was found to be about US $ 0.1 million. At this order of maximum expenditure, adopting extensive slope stabilization measures (e.g. soil nailing) and provision of heavy debris-retaining structures would not be practical. Two possible risk mitigation options were evaluated (Fig. 38). Both schemes were within the order of the maximum justifiable expenditure. The total cost of the planned houses was assessed to be about US$ 30 million. Hence, provision of the landslide mitigation measures would only amount to about 0.3% of the total cost.

(j) Risk communication and documentation (Module Nos. 14, 15 & 16)
The QRA findings were presented to the stakeholders and the two possible risk mitigation options provide a guide for formulating the development strategy at the site.

5.8 Commentary on site-specific QRA

5.8.1 Application
QRA has been applied to many sites in Hong Kong to quantify and evaluate natural terrain landslide risk. The F-N curves derived from some the sites, which are representative of the Hong Kong conditions, are shown in Figure 39. From the wealth of experience and QRA results available, some observations on the current state of applications can be made:

(a) The QRAs are carried out by geotechnical professionals as an integral part of geotechnical assessment. The geotechnical practitioners have acquired the skills, and input from risk analysts and QRA specialists is generally not required. QRA is becoming part of local professional practice in slope engineering and landslide risk mitigation.

(b) The QRA results have been taken as a sufficiently reliable estimate of the landslide risk, to support

Note: SH1a, etc. as defined in Table 17.

Figure 35.   Degree of damage to ground floor of building (Wong et al. 2004c).
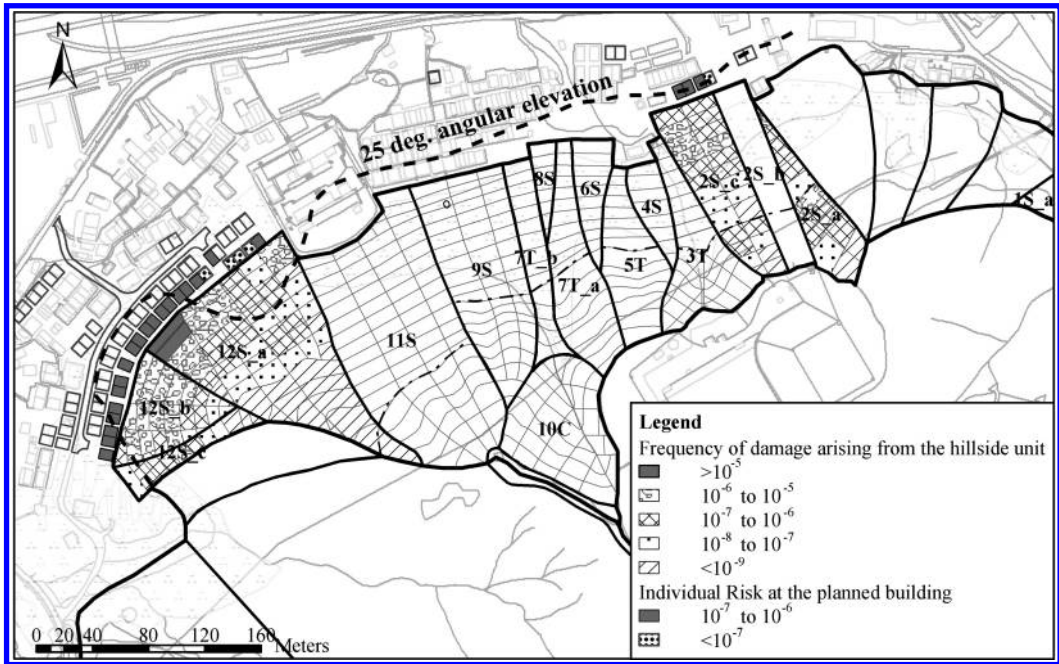
Figure 36.   Individual risk at planned buildings (Wong et al. 2004c).

281
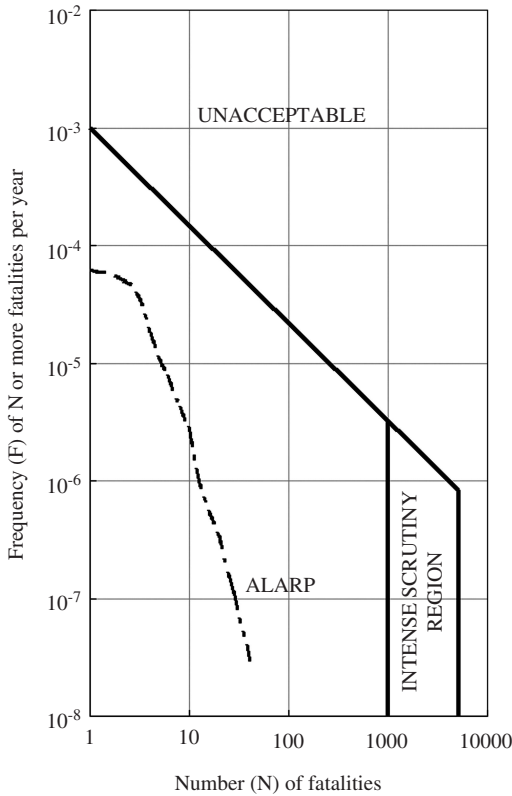
(a) For planned buildings   (b) For existing and planned buildings
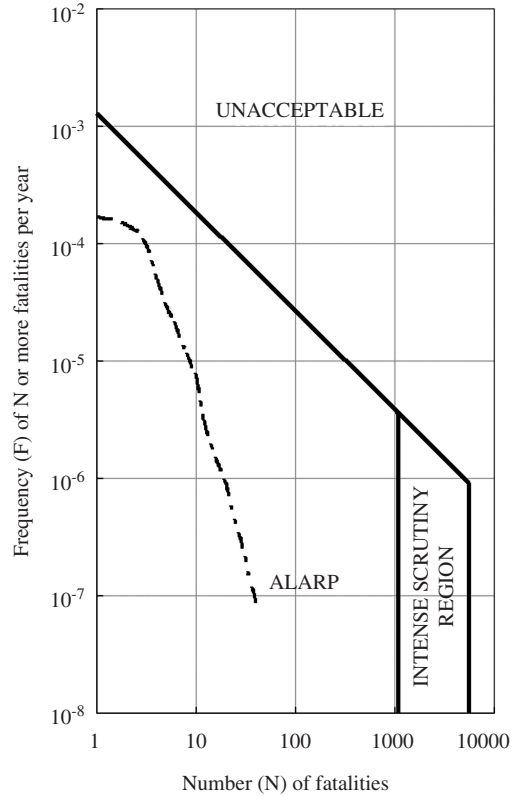
(Note: Risk criteria scaled up according to consultation boundary length = 560 m)

Figure 37.   Calculated F-N curves for Ling Pei (Wong et al. 2004c).
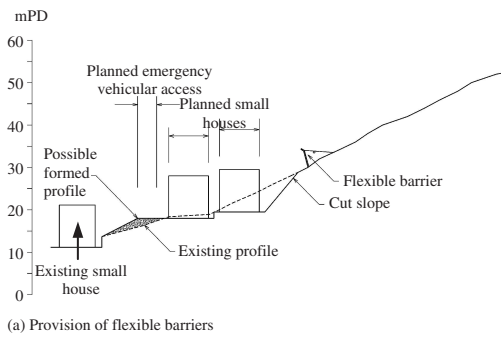
(a) Provision of flexible barriers   (b) Provision of raised building platform
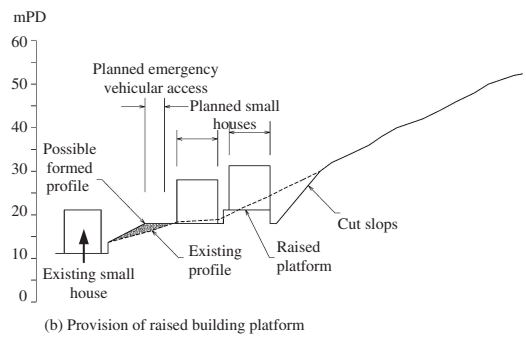
Figure 38.   Evaluation of risk mitigation options (Wong et al. 2004c).

risk management decisions to be made at individual sites. This reflects a general recognition among the geotechnical profession that the risk levels assessed by QRA are consistent with professional judgment of the scale of the problem, and that the risk mitigation actions found necessary by QRA are reasonable and practical to implement. This also shows the practicality of use of the risk criteria.

282
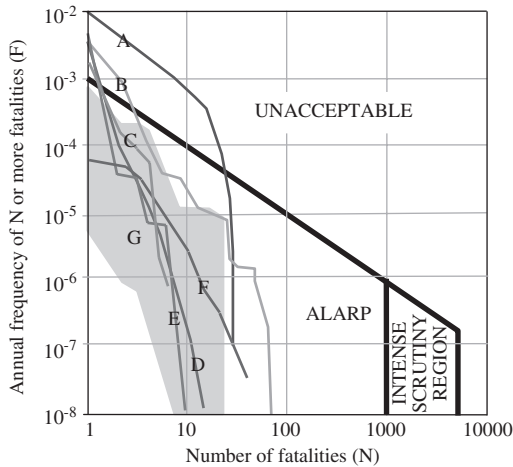
Legend:
    A - Luk Keng (OAP 2004)
    B - Lei Pui (Halcrow 2005)
    C - Pat Heung (OAP 2003)
    D - Victoria Road (Halcrow 2004)
    E - Shatin Heights (FMSW 2001)
    F - Ling Pei (Wong et al 2004)
    G - North Lantau Expressway (OAP 2005)
       (different 500 m sections)

Figure 39. F-N curves of selected natural terrain landslide QRA in Hong Kong.

(c) The calculated risk levels for the sites cover a broad range, which spans from the unacceptable zone to well within the ALARP region. Comparison of the site-specific QRA results with those of the global QRA (Section 6.5.1) shows that they are in reasonable agreement. This gives reassurance that the site-specific QRA results are of the right order of magnitude.

(d) Most of the QRA cases were triggered by the 'react-to-known-hazard' principle adopted in Hong Kong for managing natural terrain landslide risk for existing developments. The QRA results reveal that the PIR and the societal risk for these cases fall into the unacceptable zone. Substantial risk mitigation (typically reducing about 80% of the risk) has been found to be justified by the ALARP principle. These cases indicate that the 'react-to-known-hazard' principle has been exercised with consistent professional judgment in identifying sites with a genuine risk concern. Also, QRA can provide an effective and practical means for assessing and managing their natural terrain landslide risk.

(e) QRA has been applied to a lesser number of new development sites affected by natural terrain landslide risk. Some new development sites in Hong Kong are known to be subject to significant

natural terrain landslide risk. For these sites, use of QRA should be as effective as the 'react-to-known-hazard' cases. However, many other new development sites may only be marginally affected by natural terrain landslide hazards. The Ling Pei site is an example, with the risk found to be well within the ALARP zone. At Ling Pei, relatively minor risk mitigation provisions were found to be justified from the ALARP consideration. It is not entirely clear as to whether the use of a simplistic risk-cost-benefit evaluation to formulate the risk mitigation strategy is defensible and prudent in such cases, where the calculated risk-to-life is low. The North Lantau Expressway QRA has demonstrated that for strategic roads and major infrastructures, the requirements for risk mitigation may be governed by socio-economic factors.

(f) A number of factors have been essential to the progress made in natural terrain landslide QRA in Hong Kong. These include:
   – The public's high expectation of slope safety and the landslide-prone setting of Hong Kong call for vigilant risk management in order to meet the public's expectation.
   – Good quality data are more readily available, in particular historical landslide data and other geotechnical and geological information that are required for use in QRA.
   – QRA has already been formally used in assessing and managing the risk of Potentially Hazardous Installations.
   – Guidelines on natural terrain landslide risk tolerability criteria have been formulated.
   – Other approaches cannot deal with the natural terrain landslide problems more effectively.
   – Continued development and enhancement of techniques during QRA applications

(g) Despite the significant progress in using QRA to deal with natural terrain landslide problems, there have only been limited site-specific QRA applications to man-made slopes in Hong Kong. The availability of other established and effective approaches (factor of safety approach and other qualitative methodologies) is a key factor. The lack of agreed risk criteria for landslide risk from man-made slopes is also relevant.

(h) There is less experience in quantification of the potential landslide socio-economic loss. The techniques are not very well developed.

5.8.2 *Practice*

The distinct advantages of QRA over qualitative assessment rest on the ability to quantify risk instead of analyzing risk in relative terms, and on the explicit consideration of risk tolerability and the ALARP principle to provide a rational basis for evaluating the risk mitigation strategy. To realize the full benefits,

the following two fundamental conditions must be fulfilled:

(1) The relevant quantified risk criteria must be available (and endorsed for use in QRA). Otherwise, a common basis for risk evaluation is lacking. Hence, for places without any agreed risk criteria, or where there is strong objection to using quantified risk criteria, QRA application would be significantly constrained.

(2) The quantified risk levels must be sufficiently reliable. The quantified risk levels should never be taken as precise numbers. However, the figures should at least be adequately representative to ensure that their use in risk evaluation and formulation of risk mitigation strategy is meaningful and would not be misleading. Sensitivity analysis would help to assess the reliability of the risk results. Achievement of reasonable accuracy is critically dependent on the availability of reliable data to support the required risk quantification work and on the use of rigorous risk assessment methods. While the rigor of the risk analysis is typically a matter methodology and skill, lack of data is critical and difficult to overcome.

Detailed discussions about each of the key components of QRA are given in the relevant SOA. Experience gained from QRA applications reveals some noteworthy developments:

(a) Hazard identification
Hazard identification may be regarded as the most important component of landslide QRA. It is not only concerned with classifying the hazards for risk quantification, but also a thorough assessment of the available data and site conditions, landslide processes and mechanisms, and potential hazards. Such work is not new to the geotechnical profession. It has long been undertaken in geotechnical assessments, although in the past, the assessments would not normally proceed as far as risk quantification. Integration of the good practice in geotechnical assessments with QRA, particularly in hazard identification, is essential to the success of a QRA. However, if the landslide process and the nature of the potential hazards are not understood, there is little hope that their risk can be reliably quantified.

In Hong Kong, progress has been made in recent years in improving geotechnical assessment techniques for use in QRA. Examples include landslide investigations, regolith and process-based geomorphological mapping (GEO 2004), age-dating of landslide and debris (Sewell & Campbell 2004), rainfall-landslide correlations (Ko 2003), and applications of remote sensing and GIS technology (Wong et al. 2004a).

(b) Frequency assessment
Use of historical landslide data, if available, in frequency assessment is the most common and probably most reliable. However, properly assessing landslide frequency would often require attention to the following area:

– Consideration should be given as to whether the historical landslide data are complete and sufficiently representative for use in frequency assessment. In a more detailed QRA, addressing this issue could involve assessing the extent of depletion at the potential landslide sources, rainfall history and historical landslide activity, effects of 'recognition factors', etc.
– Where the site that is being assessed is relatively small in size, it may have to study a larger area with a similar geological setting in the geotechnical assessment. This would provide more data for statistical analysis and for assessment of the relevant landslide processes and mechanisms.
– Where only limited or incomplete historical data are available, use of other methods (e.g. probabilistic analysis and expert judgment) becomes more important. However, their reliability should be considered.
– The potential hazards should be properly classified, typically based on the scale and mechanisms of failure. It should avoid lumping frequency data of different types of hazard, which would adversely affect the resolution and accuracy of the frequency assessment. Proper classification also supports a more refined consequence assessment.
– Spatially apportioning the base-line frequency to different parts of the slope/hillside would often involve the use of susceptibility analysis. It is preferable to perform the susceptibility analysis using site-specific data, instead of adopting general susceptibility correlations that may be of limited direct relevance to the site. In addition, use of Bayesian methodology may help to give a balanced consideration of the theoretical susceptibility correlation and historical slope performance.
– The base-line landslide frequency is often spatially distributed before applying the volume-frequency relationship. This simplifies the frequency assessment, but the rationale may be questionable. There are technical merits in applying the volume-frequency split first, followed by spatial distribution of landslides of different volumes. However, this would require separate susceptibility analyses be carried out for landslides of different volumes, which may not be practical for sites with few data available.
– Frequency assessment for low-frequency large magnitude events is more difficult. Use of expert judgment based on findings from geotechnical assessment of the relevant relict events, geomorphology, rainfall-landslide correlation and worst credible failure volume, is a possible approach. Benchmarking with regional data and results of modeling may provide useful information.

(c) Consequence assessment

Models for consequence assessment are available. These models typically follow a standard framework, which includes consideration of the proximity of the element at risk, the average number of vulnerable people, their temporal distribution and vulnerability factors. Experience in formulating and applying consequence models suggests the need to give heed to following:

– Landslides with different mechanisms and scales would affect an element at risk to differing degrees, and should be analyzed separately in consequence assessment. The methodology adopted in consequence assessment should duly cater for the effects of landslide mechanism and scale, and particularly on the average number of people at risk and the vulnerability factors adopted in the assessment.
– Sub-dividing the potential landslide sources into small units is preferable. Previously, the sub-division was primarily aimed at improving the frequency assessment by separating the slope or hillside into cells according to their landslide susceptibility. More recently, the sub-division is also aimed at a more rational consequence assessment, particularly in respect of the debris runout path and influence zone. This may necessitate the use of irregular cells, instead of grid cells with a standard size. It would also require that the consequence model be set up as early as the frequency assessment stage, to ensure that the sub-division would produce cells that meet the requirements of both the frequency and consequence assessments.
– Consideration of debris mobility is a key component of consequence assessment. However, attention should be given not only to assessing the runout distance, but also the potential runout paths. The latter was often not very well addressed in many landslide QRA, and this could lead to gross mistakes. Predicting the potential debris runout paths requires reliable topographic information (e.g. a high resolution DEM), which may be difficult to obtain. For instance, presence of thick vegetation may hinder detailed topographic survey and terrain mapping. The available topographic maps may not be entirely reliable and sufficiently accurate. Remote-sensing technology, in particular multi-return air-borne Light Detection and Ranging (LIDAR), has shown promising results in producing high resolution DEMs that can 'see through' vegetation (e.g. NRC 2004).
– In addition, landslide debris would not always travel downslope along the steepest path. Other factors, such as the orientation of the sliding surface at the landslide source, momentum of fast-moving debris, presence of drainage channels and building platforms, etc, would affect the debris runout path. The example of a bifurcated debris flow in Figure 40 illustrates the uncertainties in predicting the debris

runout path. Event-tree analysis has been adopted, together with a cell-facility matching procedure, as a tool in consequence assessment to cater for such uncertainties.

– The assessment of the width of a landslide and its effects on the average number of people at risk, vulnerability factors, etc. is coarse in many of the existing consequence models. Further work is required to improve the assessment and its integration with the consequence model.
– Less experience is available in quantification of the consequence of building collapse and socio-economic loss. This is an area where input from specialists in the relevant field would be useful.

(d) Risk calculation and evaluation

Risk calculation in QRA is relatively straight-forward. Integration of QRA with GIS techniques, which significantly enhances the capability and efficiency of analysis of spatial data in QRA, is the trend.

Sensitivity analysis has been carried out in many QRAs to examine the effects of the assumptions made and uncertainties involved on the calculated risk results. There is scope for further improving the practice in that many of the sensitive analyses that have been carried out only cover selected aspects of the QRA, and not a complete assessment of the likely order of accuracy of the calculated risk figures.

Furthermore, no provisions are available in the existing risk criteria for formally addressing uncertainties in QRA. The current practice of not using the calculated risk figures and risk criteria in absolute terms is a preferred approach (IUGS 1997). QRA is only one input to the risk management process. Apart from the uncertainties in the risk quantification, other

Figure 40. The Tsing Shan debris flow in 2000.

socio-economic and political factors can play a key role in making risk decisions. The practicality and credibility of the use of risk criteria are to be tested with time. There is no established practice in evaluating economic loss, which requires further attention to ensure that the full range of risk is adequately addressed by QRA.

6 GLOBAL QUANTITATIVE RISK ASSESSMENT (QRA)

6.1 *Overview*

The advantages of QRA are evident when it is used to guide risk management decisions at individual sites. However, QRA is not confined to site-specific applications. QRA can be applied to a large group of slopes for quantifying and evaluating the overall risk. This is referred to as 'global' QRA (Wong et al. 1997, Wong & Ho 2000, Ho et al. 2000). It typically serves to examine the overall scale of a problem and to identify the relative contributions from different components.

Global QRA has been used fairly extensively in Hong Kong, and has proven to be crucial to landslide risk management, particularly in formulating risk management strategy. However, it has not been as popular elsewhere, where landslide-related issues are conventionally addressed by qualitative means.

Global QRA differs from site-specific QRA in a number of aspects:

(a) Unlike site-specific QRA, global QRA is not aimed at quantifying the risk on individual site basis, nor evaluating site-specific risk management actions. Global QRA quantifies risk for the purposes of formulating risk management strategy and identifying risk-based actions that affect a large number of sites. Site-specific QRA is of interest to designers and slope owners. Global QRA, if carried out properly, would provide quantified risk results that are of interest to policy makers and organizations tasked with an overall landslide risk management mission. However, site-specific QRA and global QRA are not entirely independent of one another. They often provide a benchmark for calibrating each other's results.

(b) As a large number of slopes are assessed in a global QRA, carrying out detailed investigations and geotechnical appraisals at each slope in the QRA is normally not practical. This limits the types and quality of data that may be used in global QRA. Hence, simplified frequency and consequence models, which are less data-demanding, are typically adopted in global QRA.

(c) Use of simplified models and less detailed data would not necessarily degrade the reliability and useful functions of global QRA. As global QRA is intended for quantifying and evaluating overall

risk, the QRA results are less sensitive to the models, data and assumptions adopted, as compared with site-specific QRA.

Several applications of global QRA are described in the following Sections to illustrate how it has contributed to strategic landslide risk management.

6.2 *Assessment and application of quantified overall landslide risk*

6.2.1 *Background*

As noted in Section 3.3.1 above, the mid 1990s was a time of major development of landslide risk management in Hong Kong. After many years of investment in retrofitting sub-standard slopes, there was a need to consolidate the practice and review progress. The compilation of a new and comprehensive Catalogue of Slopes, with the number of identified old, un-engineered man-made slopes increasing from about 12,000 to over 35,000 (subsequently known to be 39,000, Fig. 41), showed that potential landslide problems could be of a much larger scale than previously envisaged. Also, an increasing slope safety expectation among the public was evident from the strong public reaction to the fatal landslides that occurred in the early 1990s. Improved awareness and capability in risk assessment also brought about an impetus to use formal risk assessment in landslide risk management. In this context, and as a pioneer application at the time, QRA was formally adopted in a global framework to quantify the overall risk of the old, un-engineered man-made slopes in Hong Kong. The work was described in Wong et al. (1997) and Wong & Ho (1998).

6.2.2 *Methodology of the global QRA*

The hazard model (Fig. 42) adopted reflected the different types of hazard assessed in the QRA. The frequency of occurrence of each type of hazard was calculated from a detailed analysis of the historical landslide data collected systematically in Hong Kong since 1985. The analysis included matching the landslides with the slopes, evaluating the base-line frequency for each category and spatially distributing the
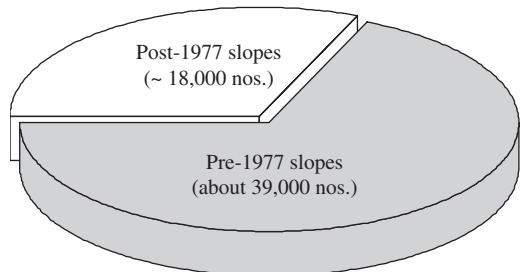

Figure 41. Catalogue of Slopes comprising 57,000 nos. sizeable man-slopes in Hong Kong.

286

frequency to each slope via a frequency model. The large body of information on over 5,000 landslides in Hong Kong was essential to the use of this approach.

A generalized consequence model was developed and this was described in Wong et al (1997). The consequence model included consideration of the categorization of the facility at risk (Table 5), the expected number of fatalities for each category of facility, size of failure, landslide mechanism, proximity of the facility, vulnerability factor and any aversion effects due to multiple fatalities. The consequence in terms of PLL was evaluated for each type of hazard on each slope. The relevant slope attributes and data on the facilities were obtained from the Catalogue of Slope.

6.2.3 Findings and application of the global QRA

The global QRA assessed a total of 35,000 un-engineered man-made slopes that were registered in the Catalogue of Slopes at the time. The calculated PLL figures for different classes of slope are shown in Table

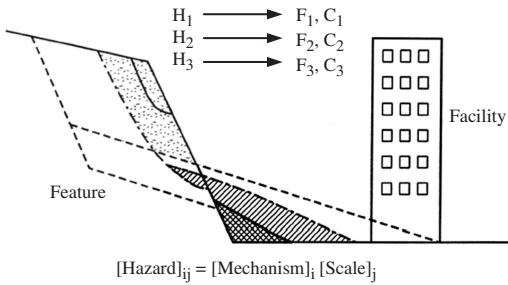$$[Hazard]_{ij} = [Mechanism]_i [Scale]_j$$

Figure 42. Hazard and frequency model (Wong et al. 1997).

18. The total PLL of the slopes (as at 1997) was estimated to be about 11 per year. By projection, it was estimated that the risk of all un-engineered (i.e. pre-1977) slopes should have been over 20 per year as at 1977.

Type of Slope feature	– Cut
	– Fill
	– Retaining wall
Mechanism of failure	– Sliding
	– Wash-out
	– Liquefaction
Scale of failure	– $<20 \, m^3$
	– 20–$50 \, m^3$
	– 50–$200 \, m^3$
	– 200–$1,000 \, m^3$
	– $1,000$–$10,000 \, m^3$
	– $>10,000 \, m^3$

Apart from giving an estimate of the over risk level, the global QRA also provided invaluable information on the risk distribution and characteristics. Examples of applying the information to formulating the risk management strategy for the LPM Programme include:

(a) Application of the calculated risk distribution to priority ranking – The global distribution of the quantified risk from cut slopes, fill slopes and retaining walls is in the ratio of 6:1:1 (Table 19). In terms of average risk per slope feature, the corresponding ratios were about 3:1:1. Experience from the LPM Programme suggested that the stabilization costs of a cut slope, fill slope and retaining wall were comparable. Hence, the ratio of risk per feature reflected the relative proportions of different slope types to be retro-fitted under the LPM Programme, as an optimal risk-cost-benefit

Table 18. Results of global QRA of unengineered man-made slopes in Hong Kong (Wong & Ho 1998).

Group no.	1	1	2	2	3	4	5		
Type of facility	Buildings	Roads	Buildings	Roads	Roads & open space	Roads & open space	Roads & open space	Building colleagues	Total
(a) *PLL for cut slopes (per year)*									
Slope height									
$<10 \, m$	1.53	0.43	0.51	1.07	0.86	0.215	4.66×10^{-3}	0	4.62
10–$20 \, m$	0.61	0.23	0.20	0.58	0.46	0.111	2.36×10^{-3}	0	2.20
$>20 \, m$	0.26	0.20	8.60×10^{-2}	0.49	0.39	6.88×10^{-2}	1.15×10^{-3}	0.171	1.67
Total	2.40	0.86	0.80	2.14	1.72	0.395	8.17×10^{-3}	0.171	8.49
(b) *PLL for fill slopes (per year)*									
Slope height									
$<10 \, m$	0.14	0.05	0.05	0.13	0.10	1.81×10^{-2}	3.03×10^{-4}		0.49
10–$20 \, m$	0.12	0.03	0.04	0.07	0.06	1.00×10^{-2}	1.71×10^{-4}		0.32
$>20 \, m$	0.31	2.38×10^{-2}	1.03×10^{-1}	5.95×10^{-2}	4.76×10^{-2}	9.00×10^{-3}	1.61×10^{-4}		0.55
Total	0.57	0.10	0.19	0.26	0.21	3.71×10^{-2}	6.35×10^{-4}		1.36
(c) *PLL for retaining walls (per year)*									
Wall height									
$\leqslant 5 \, m$	3.76×10^{-1}	2.21×10^{-2}	1.25×10^{-1}	5.53×10^{-2}	4.42×10^{-2}	7.31×10^{-3}	1.15×10^{-4}		0.63
$>5 \, m$	4.44×10^{-1}	6.32×10^{-3}	1.48×10^{-1}	1.58×10^{-2}	1.26×10^{-2}	1.93×10^{-3}	2.74×10^{-5}		0.63
Total	8.20×10^{-1}	2.84×10^{-2}	2.73×10^{-1}	7.11×10^{-2}	5.69×10^{-2}	9.24×10^{-3}	1.42×10^{-4}		1.26

Table 19. Risk distribution according to type of slope (Wong & Ho 1998).

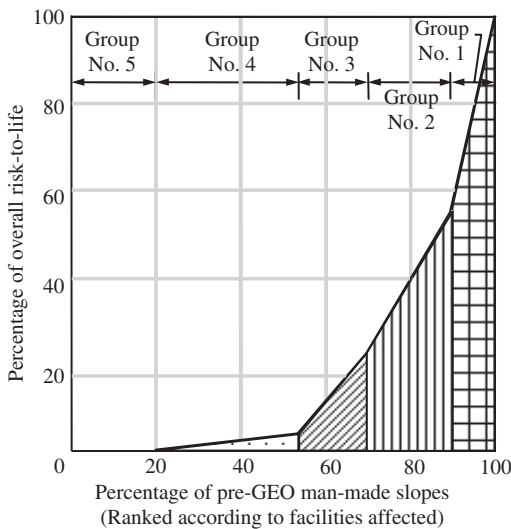| Slope type | Unengineered man-made slopes | | |
	Cut slopes	Fill slopes	Retaining walls
Number of slopes	19,100	9,500	8,100
Global failure frequency (per year)	1 in 100	1 in 500	1 in 350
Proportion of total risk [Risk Ratio]	75% [6]	12% [1]	13% [1]
Average ratio of risk per feature	3.2	1	1.3

Figure 43. Risk profile of un-engineered man-made slopes in Hong Kong in 1997 (Wong & Ho 1998).

strategy for effective reduction of the landslide risks associated with different slope types. This has formed the basis for allocation of retro-fitting resources to different slope types under the LPM Programme since the mid 1990s.

(b) Application of the calculated risk profile to formulating quantified risk reduction targets – The risk profile in Figure 43 shows the overall risk distribution among slopes in different groups, based on the categorization of the facilities at risk. About half of the overall risk came from approximately 10% of the slope population that had the highest potential risk. This indicated that upgrading of a relatively small proportion of the old slopes that posed the highest potential risk would result in a major global risk reduction. This risk reduction ratio (i.e. reduction of 50% risk by retro-fitting the

worst 10% slopes) reflected the likely order of the beneficial return of the retro-fitting programme, which could be achieved by implementing a risk-based slope rating system. This has been formally adopted as quantified risk reduction targets pledged by the HKSAR Government. The LPM Programme was tasked to upgrade about 10% of the pre-1977 slopes by year 2000, and another 10% by 2010. The pledged risk reduction targets entailed: (a) by the year 2000, the overall landslide risk from the pre-1977 man-made slopes would be reduced to 50% of the level in 1977; and (b) by 2010, the risk would be further reduced to 25% of the level in 1977 (Works Bureau 1998).

(c) Application to cost-benefit evaluation and risk communication – Using the global QRA methodology, the overall theoretical annual fatalities can be predicted with some confidence to determine longer-term trends and project future performance, as well as to quantify the effectiveness of the risk mitigating actions over time. Cost-benefit calculations were performed to evaluate the investment made relative to the projected number of lives saved as a result of the efforts of the LPM Programme. It was found that for the 10-year period from 2000 to 2010, the LPM Programme would be operating at about US$ 2 million per statistical life saved. This figure was within the limit of maximum justifiable expenditure as derived from the ALARP principle using the risk guidelines (ERM 1998).

There has been strong and unanimous public option that the GEO should implement the 2000 to 2010 LPM Programme. Hence, the findings of the global QRA provided a means of quantifying and benchmarking the expectation of the public in terms of landslide risk tolerability and ALARP deliberation.

6.3 *Evaluation of risk mitigation performance*

6.3.1 *Performance from 1977 to 2000*
The global QRA described in Section 6.2 above was updated in year 2000. The update was aimed at assessing whether the pledged 50% landslide risk reduction target from 1977 to 2000 was achieved by the LPM Programme. The methodology adopted in the update followed that of Wong & Ho (1998), and the findings were presented in Cheung & Shiu (2000).

In this update, the overall landslide risk of all registered pre-1977 slopes in 2000 was quantified. This included the risk of the remaining pre-1977 slopes that had not yet been upgraded by 2000 and the residual risk of the pre-1977 slopes that had been upgraded by 2000. The total PLL in 2000 of all pre-1977 slopes was found to be 10.3 per year. The PLL of all the pre-1977 man-made slopes as at 1977 was back-analyzed, and was assessed to be 21.8 per year. These indicated that the risk reduction from 1977 to 2000 as a result of the

288

Table 20. Landslide risk reduction from 1977 to 2000 by the LPM Programme (Cheung & Shiu 2000).

| Slope type | Landslide risk (PLL per year) | | |
	As at 1977	As at 2002	Risk reduction from 1997 to 2000
Soil cut slopes	18.52	8.51	10.01 (55%)
Rock cut slopes	1.18	0.74	0.44 (37%)
Retaining walls	0.62	0.41	0.21 (34%)
Fill slopes	1.51	0.61	0.90 (60%)
Total	21.8	10.3	11.5 (53%)

LPM Programme was 53% (Table 20), which met the pledged risk reduction target.

6.3.2 *Performance from 2000 to 2004*

The 10-year LPM Programme from 2000 to 2010 is currently in progress. A global QRA was completed in 2004 by the GEO as an interim review of the progress made in the overall landslide risk reduction.

The methodology adopted in the previous global QRA was adopted, with enhancement made in expressing the landslide frequency in terms of the number of landslides per year per unit slope area, instead of the number of landslides per year per slope. This refinement improved the reliability of applying the frequency model to slopes of different sizes. In addition, systematic landslide investigations carried out by the GEO on failures of engineered slopes provided improved data for estimating the landslide frequencies of different types of engineered slopes (Wong & Ho 2000). This improved the assessment of the residual risk of engineered slopes, i.e. slopes formed or upgraded to the required geotechnical standards after 1977.

The QRA findings are presented in Lo & Cheung (2004). It was found that by 2010, the risk of all the pre-1977 registered man-made slopes, based on a projection from the progress made in the current LPM Programme, would be reduced to about 25% of the risk in 2000 (Fig. 44). This indicated that the pledged risk reduction for the 2000 to 2010 LPM Programme was achievable, and that the LPM Programme was making satisfactory progress towards achieving this target.

The overall risk level of all of the 57,000 registered man-made slopes in 2010, including pre- and post-1977 slopes, was also assessed in this global QRA. The risk was found to be about 5 PLL per year. The numbers and risks of different classes of slope are shown in Figure 45.

6.4 *Development of risk management strategy*

6.4.1 *Global risk from natural terrain landslides*

Hong Kong has about 650 km² area of natural hillsides that have not been significantly modified by man-made activities. The natural hillsides were not registered in
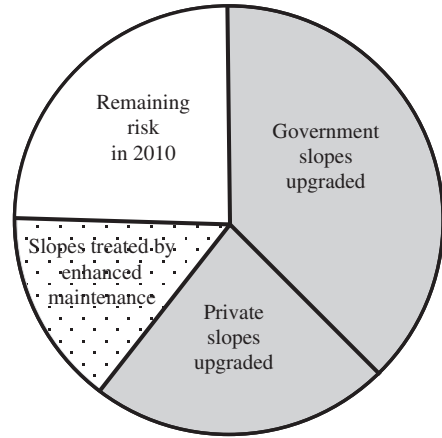
Note: Remaining risk of un-engineered slopes in 2010 is about 25% of the risk in 2000

Figure 44. Reduction of risk of un-engineered man-made slopes from 2000 to 2010 (based on Lo & Cheung 2004).
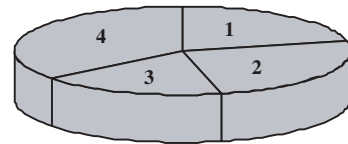
(a) Proportion by slope number (total 57,000 nos)
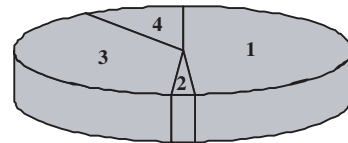
(b) Proportion by risk (total 5 PLL per year)

Legend:

1 = Un-engineered slopes affecting Groups
    No. 2(b) & 3 facilities and unplanned structures
2 = Un-engineered slopes affecting Groups
    No. 4 & 5 facilities
3 = Engineered slopes treated by old technology
    (see Note (4) of Table 25)
4 = Engineered slopes treated by robust technology
    (see Note (4) of Table 25)

Figure 45. Breakdown of risk of 57,000 man-made slopes in the Catalogue of Slopes by 2010 (based on Lo & Cheung 2004).

the Catalogue of Slopes, but they posed a landslide risk too the community. Previously, the landslide risk in Hong Kong was predominantly associated with the large stock of un-engineered man-made slopes that

289
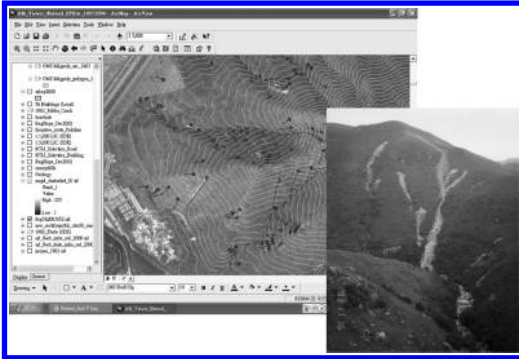
Figure 46. Natural terrain landslide Inventory, Hong Kong (comprising over 30,000 historical natural terrain landslides).

existed within the developed areas. Following years of landslide risk reduction efforts, landslide risk from the un-engineered man-made slopes is reducing. This highlights the need to assess the risk of other types of landslide hazards, in particular natural terrain landslides, for formulating the post-2010 risk management strategy.

Wong et al. (2004b) completed a global QRA of the overall risk of natural terrain landslides in Hong Kong. The key components of the global QRA are described below to illustrate the work involved in a task of this kind:

(a) Review of natural terrain landslides and data compilation and analysis – An inventory of over 30,000 natural terrain landslides (Fig. 46) from interpretation of historical aerial photographs was compiled (King 1999). Rainfall-natural terrain landslide correlation was established by Ko (2003) and Wong et al. (2004c) from spatial analysis of the 5-minute rainfall data available since 1985 (Fig. 47). Susceptibility analysis was carried out (Evans & King 1998) to establish the base-line landslide density for terrains with different characteristics.

(b) Identification of vulnerable catchments – While many of the natural hillsides adjoin developed areas, not all of them would pose a significant risk. As part of the global QRA, a search of vulnerable catchments was carried out. This included identification of the following two types of catchments:

– Historical landslide catchments – these refer to catchments with known historical natural terrain landslides occurring close to existing important facilities, including buildings, major roads and mass transportation facilities. With the use of GIS spatial analysis supplementary by field validation, a total of 453 historical landslide catchments were identified. These 453 catchments had a total area of about 5 km^2, i.e. within about 1% of the natural terrain in Hong Kong.
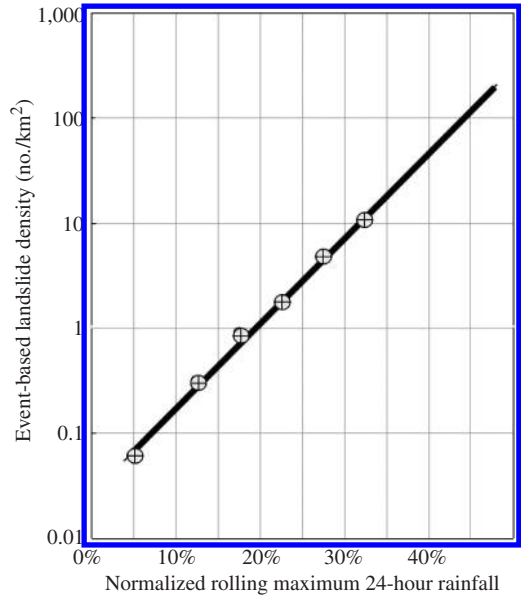
Figure 47. Rainfall-natural terrain landslide correlation (based on Ko 2003, Wong et al. 2004b).
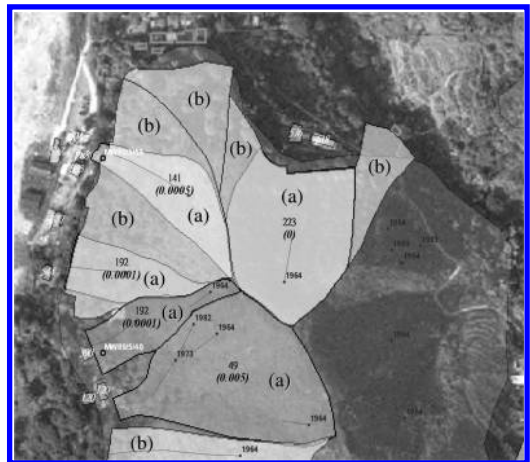
Figure 48. GIS inventory of (a) historical landslide catchments and (b) supplementary catchments.

– Supplementary catchments – these refer to catchments without any known historical natural terrain landslides occurring close to existing important facilities (Fig. 48). It was estimated that more than 10,000 of such catchments are present in Hong Kong, bordering the development boundaries. It was not practical to record and evaluate all these catchments in the global QRA. Hence, only samples of supplementary

290

Table 21. Hazard classification (Wong et al. 2004b).

Hazard combination	Classification	Definition
Mechanism of debris movement (which was related with catchment characteristics)	C	Channelized debris flow
	T	Mixed debris flow/ avalanche at topographic depression
	S	Open hillslope debris slide/ avalanche
Scale of landslide (which was established from volume-frequency relationships for different classes of catchment)	H1	50 m^3 notional (20 m^3 to 200 m^3)
	H2	500 m^3 notional (200 m^3 to 2,000 m^3)
	H3	5,000 m^3 notional (2,000 m^3 to 20,000 m^3)
	H4	20,000 + m^3 notional ($<$ 20,000 m^3)

Table 22. Rainfall scenario (Wong et al. 2004b).

Rainfall scenario	Normalized maximum rolling 24-hour Rainfall	Landslide density (no./km^2)	Annual frequency of occurrence
A	≤10%	0.0593	0.8130
B	>10–20%	0.4387	0.4785
C	>20–30%	2.3354	0.0608
D	>30–35%	10.6811	0.0035

Note: An extreme Rainfall Scenario E, with normalized 24-hour rainfall >35% at 500-year return period, was assessed by extrapolation of the QRA results.

catchments were recorded and analyzed in the QRA. A total of 1,018 supplementary catchments (about 23 km^2) in five selected regions were compiled. In addition, 43 catchments (about 1.5 km^2) in six selected areas, where site-specific natural terrain landslide QRA had been carried out, were also registered for benchmarking purposes.

(c) Hazard identification – A total of 12 types of hazard were analyzed in the QRA, based on a combination of the scale of failure and mechanism of debris movement (Table 21). Four rainfall scenarios, with normalized maximum rolling 24-hour rainfall up to 35%, were explicitly considered in the analysis (Table 22).

In view of the significant uncertainties involved and the lack of reference data, the risk arising from extreme rainfall events with normalized rainfall exceeding 35% was assessed separately by extrapolation of the QRA results.
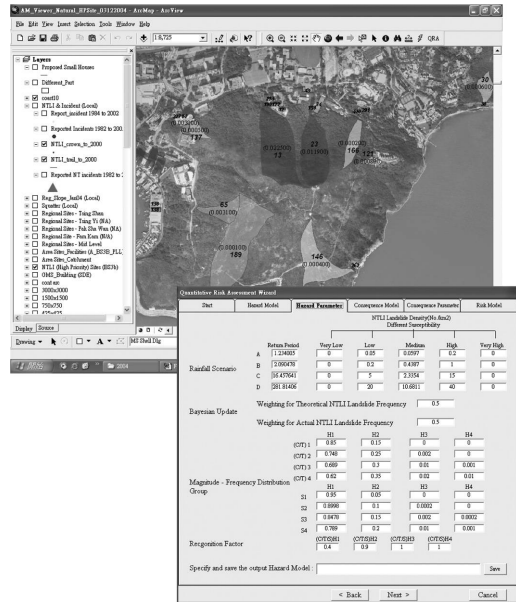
Figure 49. Global QRA undertaken on a GIS platform.

(d) Risk assessment – The frequency model and consequence model adopted, which were enhanced from the previously developed global models, were described in Wong et al. (2004b). Integration of the frequency and consequence models gave the landslide risk of each catchment and for each of the affected facilities. The calculation involved a large volume of work on spatial analysis, and was performed by GIS (Fig. 49). To ensure performance, the global QRA was calibrated with results from sites where detailed site-specific QRA were carried out.

The overall risk of natural terrain landslides in Hong Kong, based on the state of development at 2004, was assessed to be about 5 PLL per year. As shown by the breakdown of risk (Table 23), the total PLL of the 453 historical landslide catchments was 1.8 per year. This included a contribution of 0.4 PLL per year (i.e. 22%) from the extreme rainfall scenario based on extrapolation. The risk results showed that the 453 historical landslide catchments constituted about one-third of the overall risk, i.e. the other two-thirds of the overall risk would come from supplementary catchments. The risk of the supplementary catchments was projected from analysis of the samples of supplementary catchments in the global QRA using the risk model (Fig. 50). This two-thirds of the overall risk was dispersed among a large number of supplementary catchments. Neither the exact locations of these supplementary catchments nor the risk distribution among them were known.

291

Table 23. Summary of results of global QRA (based on Wong et al. 2004b).

Component		Method of quantification	Risk (PLL per year)
453 historical landslide catchments	Rainfall Scenarios A to D (≤35% normalized rainfall)	Global QRA on the historical catchments using the QRA models	1.4
	Rainfall Scenario E (>35% normalized rainfall)	~30% increase, from extrapolation of QRA results using rainfall-landslide correlation	0.4
Supplementary catchments		~200% increase, from projection based on global QRA using the risk model (Fig. 50)	3.2
Total			5.0

Notes:
(1) Other consequences, e.g. economic loss, disruption to community and public aversion to multiple fatalities, not reflected in the calculated PLL.
(2) No. of historical landslide catchments would increase at about 10 no. per year. Risk could increase with more developments taking place near steep hillsides.
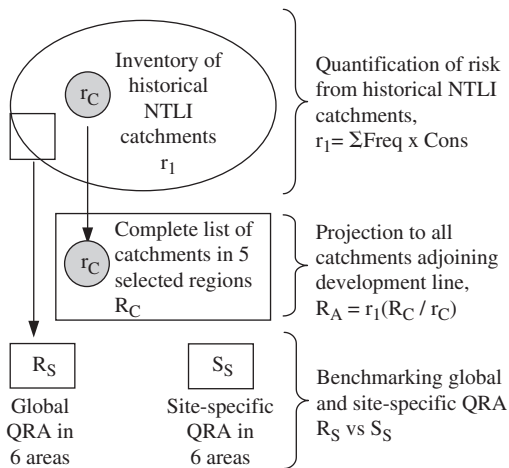
Figure 50. Risk model of global QRA for natural terrain landslides in Hong Kong.

Table 24. Risk distribution according to scale of landslide (Wong et al. 2004b).

	Percentage of total risk value			
	H1	H2	H3	H4
Sensitive routes and mass transportation facilities	21.2%	74.1%	3.4%	1.3%
Building structures including collapse	13.1%	75.5%	8.3%	3.1%
Collapse of building structures only	0.0%	4.1%	4.7%	1.3%
Total risk	13.7%	75.4%	7.9%	3.0%

A series of sensitivity analyses were carried out to examine the reliability of the quantified risk results and their sensitivity to the assumptions made in the frequency, consequence and risk models. It was established that the overall risk might range from about 1 to 10 PLL per year, with 5 PLL per year as the best estimate. The range reflected the uncertainties in the assessment.

6.4.2 *Risk management strategy*

The global QRA on natural terrain landslides revealed the nature and distribution of natural terrain landslide hazards in Hong Kong. The risk distribution according to the scale of landslide showed that H2 (200 m³ to 2,000 m³, see Table 21) constituted about 75% of the overall risk (Table 24). This is consistent with the fact that the risk mitigation works undertaken by the GEO in recent years based on the 'react-to-known-hazard' principle has primarily been dealing with natural terrain landslide hazards at such a scale.

The distribution of the calculated risk for the historical landslide catchments is shown in Figure 51. Also shown in the Figure are the PLLs assessed from some recently completed site-specific QRA on sites that met the 'react-to-known-hazard' principle.

The results showed that the historical landslide catchments were of comparable risk-to-life level as those of the 'react-to-known-hazard' cases. In particular, about 75% of the historical landslide catchments were within the range of risk for the 'react-to-known-hazard' cases that were found to require substantial landslide risk mitigation from risk tolerability and ALARP considerations. The remaining 25% of the historical landslide catchments would probably fall within the ALARP region, and the extent of any necessary risk mitigation might be affected by other factors. These included aversion effects due to multiple fatalities, social-economic factors and political considerations, as is illustrated by the North Lantau Expressway case (Section 5.6).

The quantified natural terrain landslide risk has been compared with the risk of other types of landslides quantified from the global QRA on man-made slopes.

292
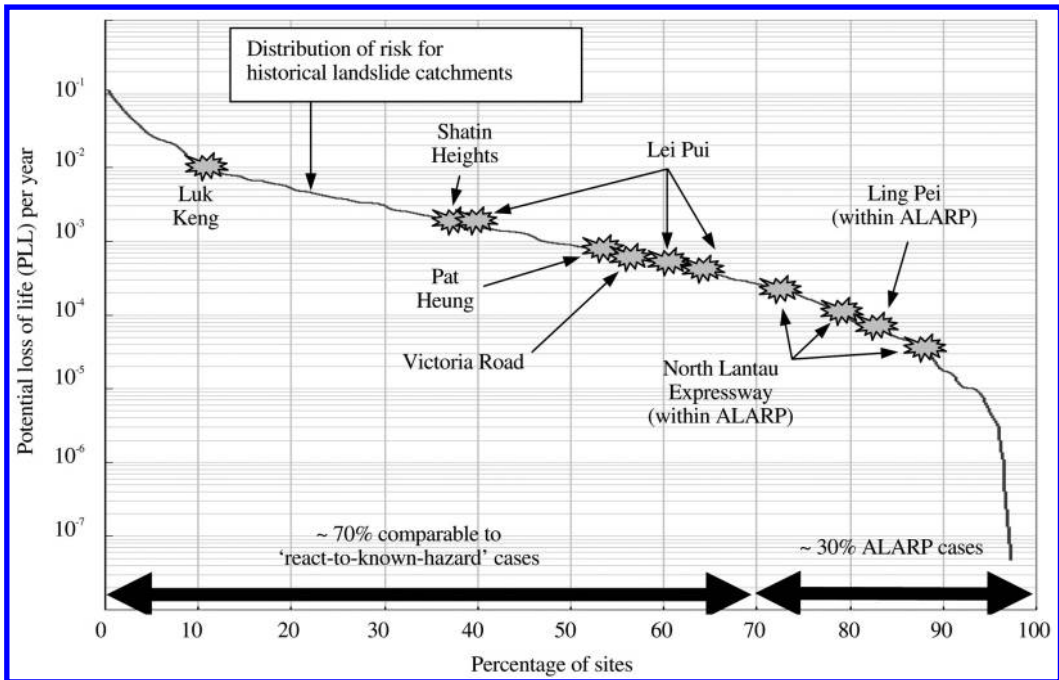
Figure 51. Risk profile of historical landslide catchments.

Table 25. Landslide risk profile in year 2010 (based on Wong et al. 2004b, Lo & Cheung 2004).

	Type of slope	Approximate no.	Proportion of risk	Average PLL per no.	Relative risk-cost ratio
Natural hillside	Historical landslide catchments	450 catchments	~15%	3.3×10^{-2}	10
	Supplementary catchments	Many (exact no. not known)	~35%	Not known	Not known
Unengineered man-made slopes	Affecting Groups No. 2(b) & 3 facilities and unplanned structures	12,000 slopes	~25%	2.1×10^{-4}	1
	Affecting Groups No. 4 & 5 facilities	14,000 slopes	<1%	$<7 \times 10^{-6}$	0.03
Engineered man-made slopes	by old technology	10,000 slopes	~20%	2.0×10^{-4}	1
	by robust technology	20,000 slopes	~5%	2.5×10^{-5}	0.13

Notes:
(1) See Table 4 for definitions of Facility Groups.
(2) Un-engineered man-made slopes affecting Groups No. 1 & 2(a) facilities would have been retro-fitted by year 2010, i.e. they become engineered slopes.
(3) In calculating the relative risk-cost ratio, it is conservatively assumed that the average cost of risk mitigating for a natural terrain catchment is 10 times as that for a man-made slope.
(4) 'Old technology' slopes refer to slopes treated in the early years of setting up Hong Kong's Slope Safety System (typically in late 1970s to mid 1980s) based on the geotechnical knowledge and skills at the time. These are less robust than those treated using structural support or reinforcement, such as soil nails.

The estimated profile of different types of landslide risk in year 2010 is shown in Table 25. The overall risk of natural terrain landslides and man-made slope failures in Hong Kong would be at comparable levels by 2010. By that time, the historical landslide catchments would be a distinct batch with the highest average risk-to-life per feature, as well as the highest risk-cost ratio per feature. This batch would deserve priority for allocation

293

of resources for risk mitigation. This would be followed by un-engineered man-made slopes affecting Groups No. 2(b) and 3 facilities (see Table 4) and engineered slopes treated by old technology. Un-engineered man-made slopes affecting Groups No. 4 and 5 facilities have a much lower risk per feature because of the negligible failure consequences. Although these slopes are susceptible to landslides, they should be given the lowest priority for retro-fitting based on risk-to-life consideration. The global QRA findings provided a rational and consistent basis for formulating risk management strategy.

7 CONCLUDING REMARKS

Landslide risk assessment that is undertaken at a large scale, in which the facilities at risk are individually recognized and assessed, is described in this paper. Selected applications cases are presented to illustrate the approaches adopted and the developing trend in risk assessment practice.

Risk assessment at this scale may be regarded as the most detailed form of landslide risk assessment. The professional practice has clearly evolved to the stage that landslide and slope engineering is no longer confined to an investigation of slope stability. The consequence of landslides has to be examined, and landslide risk has to be assessed and evaluated in totality. This risk-based perspective is fundamental to addressing and managing landslide problems, and it aligns the geotechnical profession with many other fields that explicitly practice risk management.

There is a broad spectrum of landslide risk assessments, in terms of the objectives, methodologies and levels of detail of the assessment. In particular, there is a choice between using a qualitative or quantitative approach. There are also significant differences between applying the assessment to a few individual sites and to a large number of sites. The trend of increasing use of a quantitative approach is evident, and will continue. The available cases of QRA applications have demonstrated the advantages of QRA. They have also helped to refute misunderstandings and misconceptions about QRA. However, this should not detract from the importance also of qualitative assessments. The level of complexity of the analysis should be compatible with the nature of the problem to be solved, as well as with the resources available for solving the problem. Qualitative risk assessment will continue to be the most appropriate solution for some types of problem (e.g. slope risk rating), and it can also be complementary to, or be used in combination with, a detailed QRA.

With the increasing awareness that landslide risk has to be managed, slope owners, regulators and the public as a whole, have become more ready to consider the balance between risk and cost, and less tolerant of any perceived risk that can be reduced without excessive cost. This brings a diverse range of landslide problems to the agenda of risk assessment. The challenge is for the geotechnical profession to master the diverse range of landslide risk assessment techniques and to choose the right tools for the right problems.

While use of QRA is fashionable, the profession must not lose sight of the fact that quantification does not necessarily improve accuracy and reliability. When risk is expressed in subjective and relative terms, it is by nature qualitative and intended to be indefinite. When risk is quantified, it can be expressed and communicated as exact figures, even though these may be far from accurate. The quantitative framework can provide quantified figures, but it cannot guarantee that the QRA will give reliable results. The accuracy and reliability of QRA come only with the rigor of the assessment and with the use of data, techniques and procedures that are appropriate to the specific problem being analyzed. In many practical cases, the resources available for QRA are less than satisfactory, so rendering the results unreliable, potentially misleading, and likely to do more harm than good. In such circumstances, it is imperative that the assessor should maintain good professional discipline in clearly communicating the limitations of the assessment and not overselling the QRA results. This is not at all an impediment to use of QRA. Instead, it forms part of the momentum for the geotechnical profession to further improve the skills and practice in quantified risk assessment, and to become more effective in risk communication with stakeholders.

REFERENCES

Australian Geomechanics Society 2000. *Landslide risk management concepts and guidelines*. Australian Geomechanics Society, Sub-Committee on Landslide Risk Management, *Australian Geomechanics* 35: 49–92.
Barton, N., Lien, R. & Lunde, J. 1974. Engineering classification of rock masses for the design of tunnel support. *Rock Mechanics* 6(2): 189–239.

Baynes, F.J., Lee, I.K. & Stewart, I.E. 2002. A study of the accuracy and precision of some landslide risk analyses. *Australian Geomechanics* 37(2): 149–156.

Bunce, C., Cruden, D.M. & Morgenstern, N.R. 1997. Assessment of the hazard from rock fall on a highway. *Canadian Geotechnical Journal* 34: 344–356.

Chan, Y.C. 1996. *Study of old masonry retaining walls in Hong Kong*. GEO Report No. 31, Geotechnical Engineering Office, Hong Kong, 225 p.

Chan, R.K.S. 2003. 10-year overview on advancement of slope engineering practice in Hong Kong. *Proceedings of the International Conference on Slope Engineering*, University of Hong Kong, Vol. 1, pp. 96–121.

Cheung, W.M. & Shiu, Y.K. 2000. *Assessment of global landslide risk posed by pre-1978 man-made slope features: Risk reduction from 1977 to 2000 achieved by the LPM Programme*. GEO Report No. 125, Geotechnical Engineering Office, Hong Kong, 61 p.

Cory, J. & Sopinka, J. 1989. John Just verses Her Majesty The Queen in right of the Province of British Columbia. *Supreme Court Report*, Vol. 2, pp. 1228–1258.

Dushnisky, K. & Vick, S.G. 1996. Evaluating risk to the environment from mining using failure modes and effects analysis. *Uncertainty in the Geologic Environment*, Geotechnical Special publication No. 58, ASCE, Vol. 2, pp. 848–865.

El-Ramly, H., Morgenstern, N.R. & Cruden, D.M. 2003. Quantitative risk analysis for a cut slope. *Geohazards 2003*, Edmonton, pp. 162–169.

ERM 1998. *Landslides and boulder falls from natural terrain: Interim risk guidelines*. GEO Report No. 75. Report prepared for the Geotechnical Engineering Office, Hong Kong, 183 p.

Escartio, M.V., George, L., Cheney, R.S. & Yamamura, K. 1997. *Landslides – Techniques for evaluating hazard*. PIARC Technical Committee on Earthworks, Drainage and Subgrade, 117 p.

Evans, N.C. & King, J.P. 1998. *The natural terrain landslide study: Debris avalanche susceptibility*. Technical Note No. TN 1/98, Geotechnical Engineering Office, Hong Kong, 96 p.

Fell, R. & Hartford, D. 1997. Landslide risk management. *Proceedings of the International Workshop on Landslide Risk Assessment*, Honolulu, Hawaii, USA, pp. 51–110.

Franks, C.A.M. 1998. *Study of rainfall induced landslides on natural slopes in the vicinity of Tung Chung New town, Lantau Island*. GEO Report No. 57. Geotechnical Engineering Office, Hong Kong, 102 p.

Fugro Maunsell Scott Wilson Joint Venture 2001. *Detailed study of the hillside area below Shatin Heights Road*. Landslide Study Report No. LSR 4/1001. Reported prepared for the Geotechnical Engineering Office, Hong Kong, 204 p.

Geotechnical Control Office 1984. *Geotechnical manual for slopes. (Second edition)*. Geotechnical Control Office, Hong Kong, 295 p.

Geotechnical Engineering Office 1998a. *Guide to slope maintenance (Geoguide 5). (Second edition)*. Geotechnical Engineering Office, Hong Kong, 91 p.

Geotechnical Engineering Office 1998b. *Investigation of some selected landslide incidents in 1997*. GEO Report No. 79, Vol. 2, Geotechnical Control Office, Hong Kong, 142 p.

Geotechnical Engineering Office 2004. *Guidelines on geomorphological mapping for natural terrain hazard studies*. Technical Guidance Note No. 22. Geotechnical Engineering Office, 8 p.

Golder Associates 1996. *New Priority Classification System for rock cut slopes*. Report to Geotechnical Engineering Office, 15 p.

Hand, D. 2000. *Report of the inquest into the deaths arising from the Thredbo Landslide*, 208 p.

Hardingham, A.D., Ho, K.K.S., Smallwood, A.R.H. & Ditchfield, C.S. 1998. Quantitative risk assessment of landslides – a case history from Hong Kong. *Proceedings of the Seminar on Geotechnical Risk Management*, Geotechnical Division, Hong Kong Institution of Engineers, pp. 145–152.

Ho, K.K.S., Leroi, E. & Roberds, B. 2000. Quantitative risk assessment – application, myths and future direction. *Proceedings of the International Conference on Geotechnical and Geological Engineering GeoEng2000*, Melbourne, Vol. 1, pp. 269–312.

Hughes, A., Hewlett, H.W.M., Samuels, P.G., Morris, M., Sayers, P., Moffat, I., Harding, A. & Tedd, P. 2000. *Risk management for UK reservoirs. CIRIA C542*, Construction Industry Research and Information Association, 213 p.

Hutchinson, J.N. 1992. Landslide hazard assessment. *Proceedings of the 6th International Symposium on Landslides*, Christchurch, Australia, Vol. 3, pp. 1805–1841.

Hungr, O., Fletcher, L., Jakob, M., MacKay, C. & Evans, S.G. 2003. A system of rock fall and rock slide hazard rating for a railway. *Geohazard 2003*, Edmonton, pp. 277–283.

IUGS 1997. Quantitative risk assessment for slopes and landslides – the State of the Art. IUGS Working Group on Landslides, Committee on Risk Assessment, *Proceedings of the International Workshop on Landslide Risk Assessment*, Honolulu, Hawaii, USA, pp. 3–12.

King, J.P. 1999. *Natural terrain landslide study – the Natural Terrain Landslide Inventory*. GEO Report No. 74, Geotechnical Engineering Office, Hong Kong, 127 p.

Ko, F.W.Y. 2003. *Correlation between rainfall and natural terrain landslide occurrence in Hong Kong*. Special Project Report No. SPR 7/2003. Geotechnical Engineering Office, Hong Kong, 74 p.

Koiralla, N.P. & Watkins, A.T. 1988. Bulk appraisal of slopes in Hong Kong. *Proceedings of the 5th International Symposium on Landslides*, Lausanne, Switzerland, Vol. 2, pp. 1191–1186.

Lam, C.C.L., Mak, S.H. & Wong, A.H.T 1998. A new slope catalogue for Hong Kong. *Proceedings of the Seminar on Slope Engineering in Hong Kong*, Hong Kong, A.A. Balkema Publisher, pp. 235–242.

Lee, E.M. & Jones, D.K.C. 2004. *Landslide risk assessment.* Thomas Telford Publishing, London, 454 p.

Lo, D.O.K. & Cheung, W.M. 2004. *Assessment of landslide risk of man-made slopes in Hong Kong*. Advisory Report No. 4/2004, Geotechnical Engineering Office, Hong Kong, 82 p.

McMillan, P. & Matheson, G.D. 1997. A two stage system for highway rock slope risk assessment. *International Journal of Rock Mechanics and Mining Science* 34(3/4): Paper No. 196.

Ministry of Construction 1990. *Survey of road hazard (in Japanese)*. Road Bureau, Ministry of Construction, Japan.

295

Morgenstern, N.R. 1995. Managing risk in geotechnical engineering. The 3rd Casagrande Lecture. *Proceedings of the 10th Pan American Conference on Soil Mechanics and Foundation Engineering,* Guadalajara, Vol.4, pp. 102–126.

Morgenstern, N.R. 1997. Towards landslide risk assessment in practice. *Proceedings of the International Workshop on Landslide Risk Assessment*, Honolulu, Hawaii, USA, pp. 15–23.

Morgenstern, N.R. 2000. Performance in geotechnical practice. Inaugural Lumb Lecture, *Transactions of the Hong Kong Institution of Engineers*.

Mostyn, G.R. & Sullivan, T.D. 2002. Quantitative risk assessment of the Thredbo landslide. *Australian Geomechanics* 37(2): 169–182.

National Research Council 2004. *Partnership for reducing landslide risk – Assessment of the national landslide hazards mitigation strategy*. National Academies Press, Washington, D.C., 131 p.

Ng, K.C., Parry, S., King, J.P., Franks, C.A.M. & Shaw, R. 2002. *Guidelines for natural terrain hazard studies*. Special Project Report No. SPR 1/2002, Geotechnical Engineering Office, 136 p.

Ng, S.K.C. & Wong, H.N. 2002. *Review of natural terrain hazards affecting North Lantau Expressway*. Geotechnical Engineering Office, 12 p. (unpublished).

Ove Arup and Partners Hong Kong Limited 2003. *Natural terrain hazard study at Pat Heung, Yuen Long*. Advisory Report No. 1/2003, Geotechnical Engineering Office, Hong Kong, 266 p.

Ove Arup and Partners Hong Kong Limited 2005. *Natural terrain hazard study at North Lantau Expressway*. Report to Geotechnical Engineering Office, Hong Kong (in print).

Pierson, L.A., Davis, S.A. & Van Vickle, R. 1990. *Rockfall hazard rating system implementation manual*. United State Department of Transport, Federal Highway Administration Report No. FHWA-OR-EG-90-01.

Roads and Traffic Authority 2002. *Guide to slope risk analysis Version 3.1*. Roads and Traffic Authority, New South Wales, Australia.

Sewell, R.J. & Campbell, S.D.G. 2004. *Report on the dating of natural terrain landslides in Hong Kong*. Special Project Report No. 1/2004. Geotechnical Engineering Office, Hong Kong, 149 p.

Sinclair, T.J.E. 1991. SCARR: A slope condition and risk rating. *Proceedings of the 6th International Symposium on Landslides*, Christchurch, New Zealand, Vol. 2, pp. 1057–1064.

Stewart, R.A. 2000. Dam risk management. *Proceedings of the International Conference on Geotechnical and Geological Engineering GeoEng2000*, Melbourne, Vol. 1, pp. 721–748.

Stewart, I.E., Baynes, F.J. & Lee, I.K. 2002. *The RTA guide to slope risk analysis version 3.1*. *Australian Geomechanics* 37(2): 115–147.

Stevenson, P.C. 1977. An empirical method for the evaluation of relative landslide risk. *Bulletin of the International Association of Engineering Geology* 16: 69–72.

Stover, B.K. 1992. *Highway rockfall*. Special Publication 37, Colorado Geological Survey, Department of Natural Resources, Colorado, 27 p.

TSR 2004. *SMART system – Tampuruli Sandakan road slope study project*. (Personal communication).

Vick, S.G. 2002. *Degree of belief*. ASCE Press, Virginia, 455 p.

Walker, B.F. 2002. An example of semi-quantitative landslide risk management for an individual lot in northern Sydney. *Australian Geomechanics* 37(2): 89–100.

Wong, C.K.L. 1998. *The new priority classification systems for slopes and retaining walls*. GEO Report No. 68. Geotechnical Engineering Office, Hong Kong, 117 p.

Wong, H.N. 1996. *Fill slope priority classification system*. Geotechnical Engineering Office, 22 p. (unpublished).

Wong, H.N. 2001. Recent advances in slope engineering in Hong Kong. *Proceedings of the 14th Southeast Asian Geotechnical Conference*, Hong Kong, Vol. 1, pp. 641–659.

Wong, H.N. 2003. Natural terrain management criteria – Hong Kong practice and experience. *Proceedings of the International Conference on Fast Slope Movements: Prediction and Prevention for Risk Mitigation*, Naples, Italy.

Wong, H.N. 2005. *Development and application of landslide risk assessment*. Special Project Report. Geotechnical Engineering Office, Hong Kong. (In print).

Wong, H.N., Chan, V.M.C. & Mak, S.H. 2004a. Regional report – development and application of geo-informatics in Hong Kong. *Case Histories of Urban Geo-informatics, Asian Regional Technical Committee No. 10*, International Society of Soil Mechanics and Geotechnical Engineering.

Wong, H.N. & Ho, K.K.S. 1995. *New priority classification system for soil cut slopes*. Special Project Report No. SPR 6/95, Geotechnical Engineering Office, 57 p.

Wong, H.N. & Ho, K.K.S. 1998. Overview of risk of old man-made slopes and retaining walls in Hong Kong. *Proceedings of the Seminar on Slope Engineering in Hong Kong*, Hong Kong, A.A. Balkema Publisher, pp. 193–200.

Wong, H.N. & Ho, K.K.S. 2000. Learning from slope failures in Hong Kong. *Proceedings of the 8th International Symposium on Landslides*, Cardiff.

Wong, H.N., Ho, K.K.S. & Chan, Y.C. 1997. Assessment of consequence of landslides. *Proceedings of the International Workshop on Landslide Risk Assessment*, Honolulu, Hawaii, USA, pp. 111–149.

Wong, H.N., Ko, F.W.Y. & Hui, T.H.H. 2004b. *Assessment of landslide risk of natural hillsides in Hong Kong*. Special Project Report No. SPR 5/2004, Geotechnical Engineering Office, Hong Kong, 115 p.

Wong, H.N. & Lam, K.C. 1998. The November 1993 natural terrain landslides on Lantau Island, Hong Kong. *Proceedings of Seminar on Slope Engineering in Hong Kong*, Hong Kong, A.A. Balkema Publisher, pp. 51–57.

Wong, H.N., Shum, W.W.L. & Ko, F.W.Y. 2004c. *Assessment of natural terrain landslide risk on the planned development in Ling Pei, Lantau*. Geotechnical Engineering Office, Hong Kong, 174 p.

Works Bureau 1998. Slope safety for all – Policy objective for Works Bureau. *1999 Policy Address*, Works Bureau, 17 p.

Invited papers

Landslide risk management in forest practices

R.J. Fannin
University of British Columbia, Vancouver, B.C., Canada

G.D. Moore
B.C. Ministry of Forests, Resource Tenures and Engineering Branch, Victoria, B.C., Canada

J.W. Schwab
B.C. Ministry of Forests, Northern Interior Forest Region, Smithers, B.C., Canada

D.F. VanDine
VanDine Geological Engineering Ltd., Victoria, B.C., Canada

ABSTRACT: Forest development planning is guided by codes of practice, intended to provide for safe, productive and environmentally sound operations. On landslide-prone terrain, risk management offers an effective approach to planning for forest road access and timber harvesting on steep ground. The evolution of landslide risk management in British Columbia is described, from voluntary guidelines through to legislated requirements, with reference to management policies, procedures and practices used to identify and assess landslide hazard and risk. The companion development of methods for landslide hazard mapping is reported, at both a reconnaissance and detailed level, together with the role for terrain stability assessments in the field, and a determination of the consequence for down-slope resources. An extensive body of research has contributed significantly to the confidence with which these methods are applied in professional practice. Experience shows the initiation and travel distance of debris flows is strongly influenced by terrain attributes, both qualitative and quantitative, that can be evaluated with relative ease. Two case studies are reported, which serve to illustrate the value to society of landslide risk management in the forest sector.

1 INTRODUCTION

A critical issue to the advance of environmentally sound forest practices, especially in mountainous terrain, is an appropriate system for the planning, control and evaluation of harvesting operations. The objective is simple, namely to ensure practices that are safe, productive and environmentally sound. Yet, at the international level, forestry is at a critical juncture in the sustainable provision of economic, social and environmental services to society. Policy-makers must develop national codes of practice with reference to regional and local considerations and, above all, establish a coherent framework for decision analysis. To this effect, codes of practice must address recommendations that are compiled with reference to the basic sciences, sound engineering practices, socio-economic constraints, and a critical evaluation of field experience from case studies. Nowhere is this more profoundly evident than in mountainous regions,

where the impact of improper forest operations is so immediately apparent (Fannin 2003).

In this paper we describe the role of codes of practice in forestry management, with reference to landslide risk in mountainous terrain. We then provide a summary of the risk-based approach to resource management that has evolved in BC. Thereafter, we review selected field investigations and research studies that have contributed to the understanding, directly or indirectly, of landslide risk in the BC forest sector. Two case studies are then reported, which serve to illustrate the role for landslide risk management in forest practices.

2 FOREST PRACTICES – REGIONAL AND NATIONAL CODES

Implementing sustainable forest management practices in mountain environments is challenging. Areas to be harvested must be identified as part of a comprehensive

forest and land-use policy framework. Accordingly, there is increasing global support for national and regional codes that provide guidance on improvements to forest practices.

Notable examples of national codes of practice, either published or in draft, include those of Australia, China, Fiji, New Zealand, Papua New Guinea, Solomon Islands, South Africa, Tasmania, and Vanuatu. More recently, 29 member countries of the Asia-Pacific Forestry Commission and various partner organizations developed a regional code of practice for forest harvesting, with support from the UN Food and Agriculture Organization (UNFAO 1999). Although broad-ranging in scope, it does recognize the general need for planning guidelines on "harvest exclusion areas" in terrain that is prone to landslide activity, and the use of buffer zones identified through field inspection. However, no specific advice is given, in this regional code, on appropriate methods to identify landslide-prone terrain. In contrast, and more specifically, the Tasmania code requires slopes that exceed a threshold criterion, or those exhibiting unusual landform features, be assessed for landslide hazard by a geotechnical specialist. In a yet more comprehensive approach, forest practices in the Province of British Columbia, Canada, have evolved to incorporate a risk-based management of landslide-prone terrain.

3 FOREST PRACTICES CODE – BRITISH COLUMBIA

The evolution of forest practices in British Columbia, as they relate to landslide risk arising from timber harvesting and forest road access on steep ground, can be conveniently described with reference to three timeframes: a pre-code period (prior to 15 June 1995); the BC Forest Practices Code (15 June 1995 to pre-31 Jan. 2004); and the BC Forest and Range Practices Act (31 Jan. 2004 to present). The following review is written primarily as a comparative reference for UNFAO member countries with interest in the implementation of landslide risk management in forest resources management.

3.1 *Pre-code forest practices in British Columbia*

In contrast to many jurisdictions, some 95% of the BC forest land base is public land. It provides for timber harvesting, wildlife and fisheries habitat, recreation opportunities, range lands, clean drinking water and other related environmental, social and economic values to its citizens. The BC Ministry of Forests (BCMOF) is the steward of the public forests, and its stewardship function has changed remarkably in the last 20 years, as has forest management on landslide-prone terrain.

Research and technical guidelines, in the 1970s, focused primarily on harvesting techniques to access
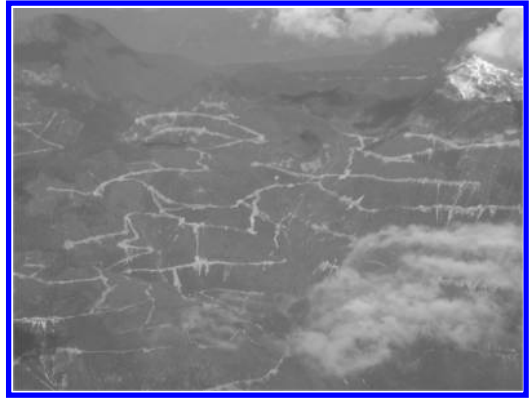
Figure 1. Logging-related slope instability, British Columbia.

and remove old-growth timber in the most economic way possible, without regard to potential adverse effects on other resource values. Indeed, "any values lost were, at the time, either unknown or not considered worthy of preservation" (Forest Resources Commission 1991). Roads were poorly located, poorly constructed, poorly drained with inadequate culverts, and poorly maintained. They were built with bulldozers, and conventional practice called for excavated material from the upslope side of the centerline to be "side-cast" on its down-slope side, thereby forming the road prism. Typically, cut and fill slopes, culverts and ditches were left unattended for many years. The integrity of provisions for road drainage, and related stability of the road cut and fill slopes, were compromised as a result (see Fig. 1). Awareness developed, through the 1970s and 1980s, of the causal link between forest operations and adverse impacts on water supply, fish and fish habitat, landscape aesthetics, soil productivity, and private property (Schwab 1988, Tripp 1994, Slaney & Martin 1997). The first integrated research on impacts to fish habitat was initiated, in 1970, at the Carnation Creek watershed on the west coast of Vancouver Island (Hartman & Shrivener 1990): it has continued to the present (Toews & Hetherington 2004).

A second major initiative, the "Fish-Forestry Interaction Program (FFIP)", began in 1981 on the Queen Charlotte Islands in the aftermath of a historic jurisdictional dispute between the BC government and the Federal Government of Canada over the harvesting of timber on an unstable slope above a salmon stream (Chatwin & Smith 1993). The source of the dispute followed a significant storm that hit the Queen Charlotte Islands in 1978 and triggered many landslides, most from within clearcuts and from roads (Schwab 1983). The Federal Department of Fisheries and Oceans issued a notice to the forest company to suspend logging of the slope that was approved for

300

harvesting. Logging continued, however, leading to the arrest of loggers and charging of forest company officials. A major impasse resulted, with senior politicians including the BC Premier, the Prime Minister of Canada, and the Federal Fisheries Minister becoming involved (Toews & Hetherington 2004). The resulting FFIP program, funded by the BC Ministry of Forests, BC Ministry of Environment and the Federal Department of Fisheries and Oceans, significantly advanced our understanding of logging-related landslides (Hogan et al. 1998).

These inter-governmental research programs, and other related projects, led to a much improved understanding of forestry activities on the complex biological, hydrological, and geomorphologic processes in a watershed. Importantly, a desire to apply these findings led to development of "voluntary" guidelines, by specialists in the BC government through consultation with industry experts. They were primarily "prescriptive" rules aimed at helping foresters, engineers, biologists, and resource managers select timber harvesting and road construction practices that address the importance of all forest resources, and thereby promote a common objective of integrated and sustainable forest management. A workshop, in 1983, led to the Coastal Fish/Forestry Guidelines (CFFG), later revised in 1988 (BCMOF et al. 1988, 1992, 1993). A stream reach classification system was introduced, which identified a range of fisheries habitat values ranging from Class I (highest value) to Class IV (lowest value). Also introduced was the concept of a Streamside Management Zone (SMZ), on all Class I and II streams. These were intended to restrict forest companies from harvesting too close to fish-bearing streams.

Subsequent revisions to the CFFG, in 1992 and 1993, resulted in a series of timber harvesting and forest road development planning and operating guidelines for all major forestry activities, to be implemented in accordance with stream reach class objectives. The guidelines were "process-based", insomuch as they sought to manage risk to the fisheries resource by promoting the adoption of forestry practices that should result in a desired outcome. They also provided the preliminary basis for landslide risk management in environmentally sensitive areas: a CFFG appendix, "Forest Road and Logging Trail Engineering Practices and Instructions for its Implementation" (BCMOF 1993), provided standards for improved forest road planning, design, construction, maintenance and deactivation.

In a parallel initiative, some of the FFIP observations were incorporated in a field-oriented handbook, "A Guide for the Management of Landslide-Prone Terrain in the Pacific Northwest" that addressed four topics: slope movement processes and characteristics; techniques for recognizing landslide-prone terrain; measures to manage unstable terrain, and hillslope rehabilitation (Chatwin et al. 1991, 1994). In the early

1990s, the BCMOF introduced additional guidelines for coastal terrain, intended to prevent harvesting and road-related landslides and erosion. Affected forest companies were required to carry out the following changes to their operations:

- *Terrain mapping and terrain stability mapping*: All coastal timber land was to be mapped to identify landslide-prone terrain and estimate the likelihood of landslide occurrence following conventional timber harvesting or conventional (sidecast) road construction methods using a five class terrain hazard system (Terrain Stability Classes I to V, discussed later in section 4.0).

- *Improved harvesting and road location planning*: All cut-blocks and new road locations were to be carefully reviewed within areas mapped as Terrain Stability Class IV (moderate to high likelihood of slope failures after conventional road construction, and moderate likelihood of failure in logged areas) and Terrain Stability Class V (high likelihood of slope failures after conventional road construction or logging), or environmentally sensitive areas (ESAs) mapped as ES1 (similar to Class V) and ES2 (similar to Class IV). Before any development could be considered on these areas, a professional geotechnical engineer or geoscientist was required to conduct a "terrain stability field inspection."

- *Reductions in the annual allowable cut*: Forest land that could not be developed because of concerns for slope instability was to be removed from the operable timber harvesting land base.

- *Changes to harvesting systems*: Forest companies were required to consider alternative harvesting systems (e.g., skylines or helicopters) if a terrain stability field inspection revealed a moderate to high likelihood of landslide occurrence.

- *Improvements to road construction and deactivation practices*: Existing roads that showed signs of instability (e.g., tension cracks) were required to be stabilized by pulling back unstable fills, or by applying water management techniques or other measures. Where unstable slopes had to be crossed by new roads, techniques such as full-benching and end-hauling were to be implemented to limit any potential road failure. Full-bench refers to 100% construction in cut (no road fill) with removal of excavated material to a stable location (end-haul).

During this period, forest practices were regulated by contracts (e.g., forest licences, timber sale licences, tree farm licences) as depicted in Figure 2(a), and contractual obligations were backed up by statutory obligations (e.g., cut control, basic silviculture obligations) (BCMOF 1994, 1999). Accordingly, voluntary guidelines such as the CFFG and companion coastal guidelines for harvesting and forest roads on potential

Legislation to backup contracts

Forest practices regulated primarily by contracts and guided by non-binding voluntary guidelines outside of contracts and legislation

(a) ***Old Contractual Framework: Pre-Forest Practices Code****. For over eighty-five years, the planning of forest development operations and forest practice standards in British Columbia were based on a combination of contractual requirements and non-binding (i.e., voluntary) forest "industry" guidelines, with statutory backup. "In this regard, some of the most critical components of the management regime were based on a kind of "honour system" (BCMOF 1999).*
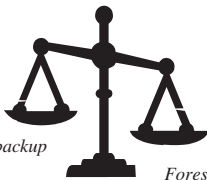
Contracts to backup legislation

Forest practices regulated primarily by "process-based" legislation and guided by very prescriptive mandatory practices, with little emphasis placed on professional reliance to support the policy framework

(b) ***BC Forest Practices Code****: Statutory Framework 15 July 1995 – Pre-31 January 2004. The code of practices during this period was based on legislative mandates with a process-based (prescriptive) approach to risk management, with contractual backup.*

Contracts to backup legislation

Forest practices regulated primarily by "results-based" legislation and guided by less prescriptive mandatory practices, with heavy emphasis placed on professional reliance to support the policy framework

(c) ***Forest and Range Practices Act****: Statutory Framework 31 January 2004 – to Present. This code of forest practices currently in effect is based on legislative mandates with a results-based (non-prescriptive) approach to risk management, with contractual backup.*

Figure 2. Schematic representations of the evolution of British Columbia's legal framework for forest practices (modified from BCMOF 1994).

landslide-prone terrain were unenforceable, unless specifically incorporated as contractual requirements in the tenure documents, which was seldom done. Monitoring of industry compliance with the CFFG was left to industry itself, because of insufficient government resources. Public concern grew, in part as a result of an independent audit on "The Use and Effectiveness of the Coastal Fisheries Forestry Guidelines in Selected Forest Districts of Coastal British Columbia" (Tripp, 1994), which identified a lack of compliance and associated impacts to fish-bearing streams as a result of logging practices.

This finding, coupled with new socio-economic expectations of the forest sector (Forest Resources Commission 1991), led to demand for a more integrated approach to forest management (accounting for non-timber values such as recreation, wilderness, wildlife, fish and fish habitat, water quality and quantity, and landscape aesthetics). Clearly the existing contractual framework, which relied on an honour system, was not achieving the desired results of sustainable forest management. The contractual framework did not mandate specific forestry practices and, given the prevailing attitude of industry to objectives of voluntary guidelines, it was no longer strategically aligned with the public expectations for environmentally, socially, and economically sustainable forest conservation. The BC government then moved to introduce a statutory requirement.

3.2 *Forest practices code of British Columbia Act*

On 15 June 1995 the BC government enacted a new "world class" model for forest management, the "Forest Practices Code" (FPC). It was a mandatory code of forest practices and, although not unique, it was far more comprehensive than similar codes of forest practice in other countries and jurisdictions. In the preceding contractual framework, information governing and guiding forest practices was contained in a multitude of policies, procedures, and guidelines; under the FPC, those sources of information were assembled into a legal framework that consisted of a plan and process-based *Forest Practices Code of British Columbia Act* and supporting regulations, including many content requirements for plans, and methods for how to carry out practices. It consisted of 19 regulations, 7 legally binding guidebooks, and 35 guidebooks in the non-legal realm that specified non-binding management practices (Fig. 3). The vision behind the FPC was the sustainable use of the province's public forests. Five major principles underpinned the term "sustainable use" in the FPC:

- managing the forests to meet the present needs of British Columbians without compromising the needs of future generations;
- providing stewardship of forests based on an ethic of respect for the land;

FPC
"Process-based Code"

Act

Regulations

Cited Guidebooks

Legal Realm Focus on Process: how to conduct forest practices

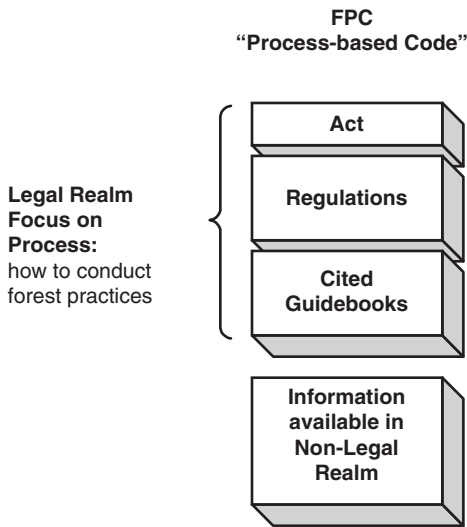Information available in Non-Legal Realm

Figure 3. The FPC consists of a plan and process-based Act and regulations, including 7 legally binding guidebooks, and 35 guidebooks in the non-legal realm that specify non-binding management practices.

- balancing productive, spiritual, ecological and recreational values of forests to meet the economic and cultural needs of peoples and communities, including First Nations;
- conserving biological diversity, soil, water, fish, wildlife, scenic diversity and other forest resources; and,
- restoring damaged ecologies.

Under the FPC, practices were regulated primarily by statute, the Act, and statutory obligations backed up by contractual obligations (see Fig. 2b). Statutory enforcement tools included stop work orders, remediation orders, and punitive fines or imprisonment for practices causing damage to the environment. Failure to comply with the operational plan resulted in administrative penalties. Operational plans included long term (five or more years) forest development plans, access management plans (i.e., road construction, maintenance and deactivation), logging plans, cutblock specific silviculture prescriptions, and range use plans. The staff of BCMOF approved operational plans and the cutting and road permits related to timber harvesting and road construction.

Transition to the legal framework of the FPC established new rules of engagement for the two major stakeholders: the Ministry of Forests was held responsible for administering and enforcing the FPC, and the forest tenure holders (forest companies) were legally required to comply with the new forest practices. The incentive for forest companies to comply with the FPC included: avoidance of penalties and imprisonment; avoidance

of "negative press" from public results of audits conducted by a newly-formed Forest Practices Board of BC; avoidance of civil liability; and, in the latter years of the FPC, a desire to obtain ISO (International Standards Organization) certification of their forest management practices to ensure that they had both access to world markets and consumer acceptance of their products.

The approach was extremely "prescriptive" (Vold 2003). It sought to improve on many of the aspects of the "process-based" CFFG and coastal guidelines for harvesting and forest roads on landslide-prone terrain, by making them legally binding. Forest companies were required to invest, in advance, in the collection of information on every aspect of their timber harvesting and forest road construction operations, in order to facilitate the detailed planning process. Under this approach to overall risk management, the expectation of the FPC was that practices conforming to the prescriptive-based planning requirements would achieve outcomes on the ground that would meet the principles of sustainable forest management. Accordingly, if forest companies followed plans approved under the FPC, they were normally able to transfer some or all of the liability for damage that might occur to forest resources as a result of those practices. Instead, the BC government, in specifying, reviewing and approving mandatory practices, assumed some or all of this liability whenever the practices had been correctly followed.

3.2.1 *Landslide risk management*
The approach used to manage landslide risk, following road construction and timber harvesting, placed most emphasis on landslide hazard identification and the likelihood of landslide occurrence, P, P(SL) or P(H), rather than on landslide risk, P(HA), R(S), or R(SV), in which the spatial effects of a landslide event are considered (see Wise et al., 2004 for definitions). Where potential existed for landslide activity as a result of forest development, FPC regulations (see Fig. 4) called for landslide hazard mapping (Terrain Stability Mapping, or TSM), on-site assessments of terrain stability (Terrain Stability Field Assessment, or TSFA), and professional prescriptions for road construction and deactivation (with professional sign-off) in areas proposed for road construction and timber harvesting. All planning documents, including site-level assessments and any significant changes made in the field, required a review and approval by government.

The FPC legislation required forest companies to first describe where landslide hazards might exist. Companies were required to prepare a "Forest Development Plan" to show the approximate size, shape and location of cutblocks, and the approximate location of roads, including bridges or major culverts. Additionally, they were required to identify areas of potential slope instability to ensure that planned

harvesting and road building activities would not cause landslides and erosion. This also served to bring potential environmental problems to the attention of the public and government agencies. Companies could identify these areas in the Forest Development Plan by one of the three methods described below. Where mapping was undertaken, terrain survey intensity levels were guided by advice from the Resources Inventory Committee (RIC, now called Resources Information Standards Committee), together with additional insights on interpretation of slope stability classifications (RIC 1996a, b).

(1) Detailed terrain stability mapping (DTSM), typically at a scale of 1:20,000, whereby an estimate is made of the likelihood of occurrence of any landslide of any type, size and character, without considering its effects on any identified elements at risk of loss or damage (referred to as P in Wise et al. 2004). Therefore, this type of analysis is a
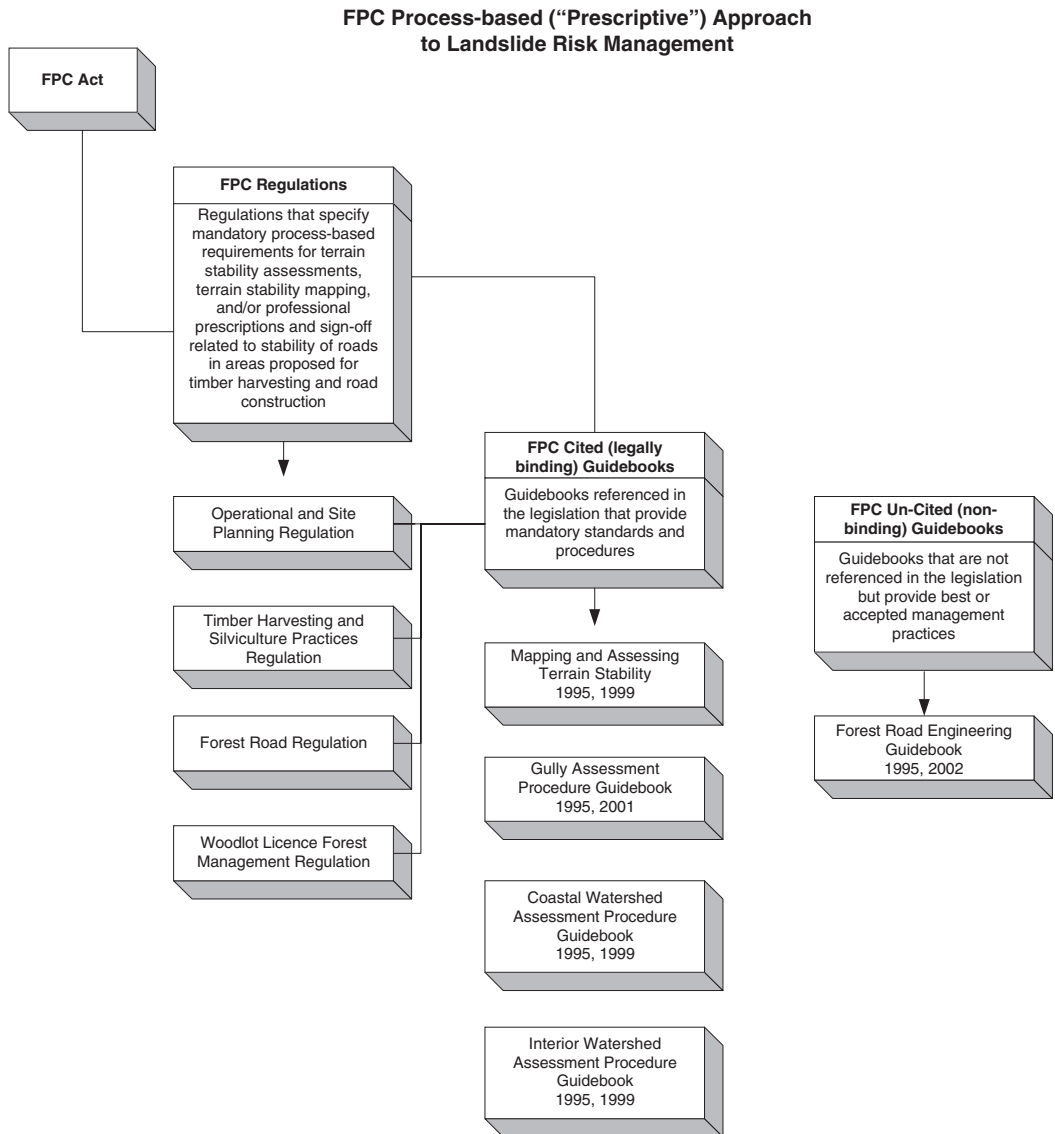

Figure 4. FPC regulations, cited guidebooks, and non-binding guidebooks related to landslide risk management.

304

measure of landslide hazard and not landslide risk. If detailed terrain stability mapping had been completed for an area, there was a mandatory requirement to show those areas designated as Terrain Stability Class IV (moderate to high likelihood of slope failures after conventional road construction and moderate likelihood of failure in logged areas) and Terrain Stability Class V (high likelihood of slope failures after conventional road construction or logging). In a detailed terrain stability mapping project, terrain polygons are mapped and then interpreted to show the relative stability of slope polygons following road construction and timber harvesting (BCMOF et al. 1999a);

(2) Alternatively, if reconnaissance terrain stability mapping (RTSM) was available, typically at a scale of 1:20,000 to 1:50,000, there was a mandatory requirement to show those areas designated as having either potentially unstable or unstable terrain; and,

(3) In the absence of any terrain stability mapping (detailed or reconnaissance), there was a mandatory requirement to indicate areas of slope gradient greater than 60%.

The existence of any one of these three terrain indicators, namely (1) a moderate to high likelihood of landslides, (2) unstable terrain or (3) slope gradients greater than 60%, triggered the requirement to conduct a TSFA. This on-site assessment, made to a higher level of confidence than terrain stability mapping, refined the estimated likelihood of landslide occurrence following timber harvesting or road construction. The TSFA had to be carried out by a qualified terrain stability professional, who provided a subjective probability estimate of the likelihood of landslide activity. Results of the TSFA provided guidance on whether or not to proceed with development in the area. If yes, the findings were used to modify preliminary designs for road construction and harvesting, or to prepare road deactivation prescriptions in the case of existing roads, in order to mitigate the potential for landslide activity. Accordingly, the TSFA is an example of a hazard analysis, P(H), if it estimates the likelihood of a specific hazardous landslide, or an example of partial risk analysis, P(HA), if it estimates the likelihood of a specific hazardous and affecting landslide (Wise et al. 2004).

In addition to RTSM, DTSM and a TSFA, the FPC specified other mandatory forest practices related to landslide hazard and risk management, including:

- No harvesting of an area within a community watershed if the result of the TSFA indicated that the area was subject to a high likelihood of landslide occurrence;

- No clearcut harvesting of an area within a community watershed if the result of the TSFA indicated that the area was subject to a moderate likelihood of landslide occurrence with a high likelihood of landslide debris (given an event occurred) entering directly into streams, unless the site assessment suggested clearcutting the area would not significantly increase the likelihood of landslide occurrence;

- No clearcut harvesting of an area outside a community watershed if the result of the TSFA indicated that the area was subject to a high likelihood of landslide occurrence, unless the assessment suggested clearcutting the area would not significantly increase the likelihood of landslide occurrence and that there was a low likelihood of landslide debris (given an event occurred) (1) entering into a fish stream or a perennial stream that is a direct tributary to a fish stream, or (2) causing damage to private property or public utilities, including but not limited to roads, bridges, transmission lines, pipelines, recreation sites or any other similar structures;

- Assessment of a gully in a cutblock located on coastal areas, carried out in accordance with the "Gully Assessment Procedure" if timber harvesting or road construction was proposed across or near the gully;

- A watershed assessment was required for forest development proposed within a community watershed, and within a watershed that had significant downstream fisheries values or licensed domestic water users and significant watershed sensitivity as determined by a designated environment official, and carried out in accordance with the procedures in the "Coastal Watershed Assessment Procedure" for coastal areas of the province and in accordance with the "Interior Watershed Assessment Procedure" for interior areas of the province;

- A terrain stability professional had to prepare a prescription for road deactivation work to reduce the likelihood of landslides if the terrain had one of the three terrain indicators of potentially unstable terrain mentioned above (i.e., moderate to high likelihood of landslides, unstable terrain, and slope gradients greater than 60%);

- Road layout and design had to incorporate measures to reduce the likelihood of landslide occurrence, or measures to reduce the likelihood of that landslide (given an event occurred) affecting forest resources, if a TSFA was required and indicated that those measures were needed to achieve that reduction.

Some of these mandatory forest practices are specific to community watersheds, defined by water use that is for human consumption. In total, 42 guidebooks were developed to support the FPC regulations.

305

Portions of the guidebooks cited in legislation are, de facto, part of the legislation. Landslide risk management was directly addressed in the following (see Fig. 4):

- "Mapping and Assessing Terrain Stability Guidebook" (BCMOF et al. 1995, 1999a)
- "Gully Assessment Procedure Guidebook" (BCMOF et al. 1995b, c, d, BCMOF 2001)
- "Coastal Watershed Assessment Procedure Guidebook" (BCMOF et al. 1995e, 1999b)
- "Interior Watershed Assessment Procedure Guidebook" (BCMOF et al. 1995f, 1999b)

A "Forest Road Engineering Guidebook" (BCMOF et al. 1995g, BCMOF 2002b), although not cited in legislation, contained many prescriptive procedures or best management practices (acceptable practices) for forest road planning, design, construction and deactivation, which, if followed, would likely result in forest companies meeting their legal responsibilities for landslide prevention under the FPC.

Revisions made to these guidebooks demonstrated the acceptance of a growing science-based knowledge that supported implementation of the 1995 FPC in all areas of forestry development, including landslide risk management. Additionally, much was learned about the effects of post-logging landslides and methods of landslide prevention with implementation, in 1994, of the BC Watershed Restoration Program. It was designed to provide "… an opportunity for diverse and stakeholder partnerships to accelerate the recovery of watersheds impacted by logging practices of the past" (Slaney & Martin 1997). It further contributed to a refinement of new techniques and guidance to better manage landslide hazards and risks. Specifically, its publications were another source of guidance for the FPC to build on, including:

- "Resource road rehabilitation handbook: planning and implementation guidelines (interim methods)" (Moore 1994), supplemented and updated by Best Management Practices Handbook: Hillslope Restoration in British Columbia (BCMOF 2001); and,
- "Guidelines for planning watershed restoration projects" (Johnston & Moore 1995)

Generally, the FPC met its objectives of engaging all forest companies in a common manner, improving environmental protection, increasing consistency in enforcement, and building public confidence in forest management. However, its framework was complex, and resulted in increased costs both for government and the forest industry. As a result, from 1998 onwards, the FPC began to evolve into a "results-based" mandatory code of forest practice. A number of amendments were made to the FPC (Act and regulations), to reduce costs, by placing less emphasis on plan approvals and more on results. For example:

- The FPC's complexity was reduced by limiting the required number of operational planning documents;
- There was a shift to a "results-based" rather than "prescriptive" approach to risk management, by focusing on the goals of forest management; and,
- Greater reliance was placed on professional foresters, engineers, geoscientists and other professionals to manage risk and uncertainty in preparing plans.

This evolution was driven by concern that the FPC had "… stifled innovation by requiring adherence to practices that were not always the most cost effective nor efficient in delivering outcomes needed to meet the broad public outcome" (BCMOF 2002a). "The best codes of forest practice are those that provide a firm foundation for decision making and assessment but also permit sufficient flexibility so that guidelines can be amended as more is learned about ecosystem function and silvicultural requirements, or as the socioeconomic situation in a country or region evolves" Dykstra & Heinrich (1996).

3.3 BC Forest and Range Practices Act (FRPA)

The transition to a new mandatory "results-based code" of forest practice formally began on 31 January 2004, with enactment of the *Forest and Range Practices Act* (FRPA). The FRPA will replace, by 31 December 2006, all parts of the FPC. At that point in time, British Columbia will be one of the "… few jurisdictions in the world to move to results-based forest practices legislation" (Vold 2003).

As before, forest practices under the FRPA are regulated primarily by statute, and statutory obligations are backed up by contractual obligations as depicted in Fig. 2(c). The transition from a plan and process-based regime under the FPC, to a results-based regime under FRPA, is accompanied by a shift in the balance between the requirements in the legal framework versus information available in the non-legal realm (see Fig. 5). It introduces subtle, yet important changes, including:

- A simplified policy framework, with only 12 regulations (instead of 19 under the FPC) and no legally binding guidebooks (there were 7 guidebooks cited in legislation under the FPC);
- The only approval required from government will be that for a Forest Stewardship Plan, and it is expected that professional foresters will have an important role in preparing those plans;
- In the Forest Planning and Practices Regulation under the FRPA, government has set measurable, auditable, and enforceable goals (called government objectives) for managing and protecting forest and
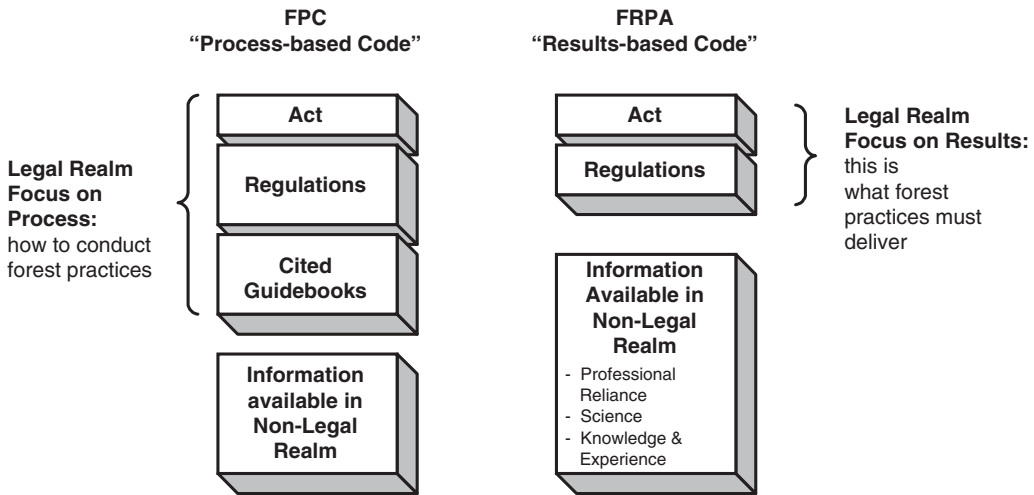
306

Figure 5.   The transition from a plan and process-based regime under the FPC to a results-based regime under FRPA.

range resources (called FRPA values): there are 11 FRPA values, namely soils, visual quality, timber, forage and associated plant communities, water, fish, wildlife, biodiversity, recreation resources, resource features, and cultural heritage resources;

- In contrast to requirements of the FPC, there will be no requirement for forest companies to submit site-level plans for government review and approval (e.g., TSFA reports, prescriptions to maintain slope stability along forest roads, road deactivation prescriptions, road layout and design, silviculture prescriptions);

- Guidebooks are not cited in FRPA legislation, but will become part of the non-legal realm to support the standard of due diligence for professional conduct (see APEGBC 2003).

- Under the past prescriptive approach of the FPC, practitioners were expected to primarily comply with mandatory detailed procedures and guidelines. Since many of the process-based requirements that used to be in the FPC have been replaced by an approach that focuses on achieving defined and measurable results with less direct government intervention, more emphasis is placed on professional reliance to support the policy framework (Fig. 6). Typically, reliance will be placed on the judgment of professionals (foresters, engineers, geoscientists, agrologists, and biologists) to achieve the required outcomes for which they are accountable to their employers or clients (BCMOF et al. 2004);

- As time goes on, government will conduct scientifically valid effectiveness evaluations to assess if forest and range policies and practices in BC are achieving government's objectives for the 11 FRPA values, with a priority on environmental outcomes

and consideration for social and economic parameters, where appropriate. In other words, it will compile scientific data on whether or not the FRPA is accomplishing sustainable forestry in BC, and make adjustments to the legislation as necessary.

With the FRPA, a greater emphasis will be placed on landslide risk management. The Forest Practices Board of BC (originally established under the FPC) will continue to act as an independent watchdog for sound forest practices in the province, and its essential mandate remains unchanged. Terrain stability professionals will continue to play an important role in forest operations planning, especially with slope stability for clear cut harvesting, harvesting around gullies and on fans, and forest road construction and deactivation. The expectation is that terrain stability professionals will often have to conduct, at minimum, a partial risk analysis (see Wise et al. 2004) to ensure clients mitigate the potential effects of landslides.

In effect, forest companies building, maintaining, or deactivating a road, or timber harvesting, on steep slopes must not cause a landslide or a gully process, or fan destabilization, that has a material adverse effect on soils, visual quality, timber, forage and associated plant communities, water, fish, wildlife, biodiversity, recreation resources, resource features, or cultural heritage resources. However, and in contrast to the FPC, the FRPA will not specify when terrain stability mapping or field assessments should be conducted, or indeed how they should be conducted. Rather, forest companies will have the ability to decide whether or not to conduct these types of investigation.

307
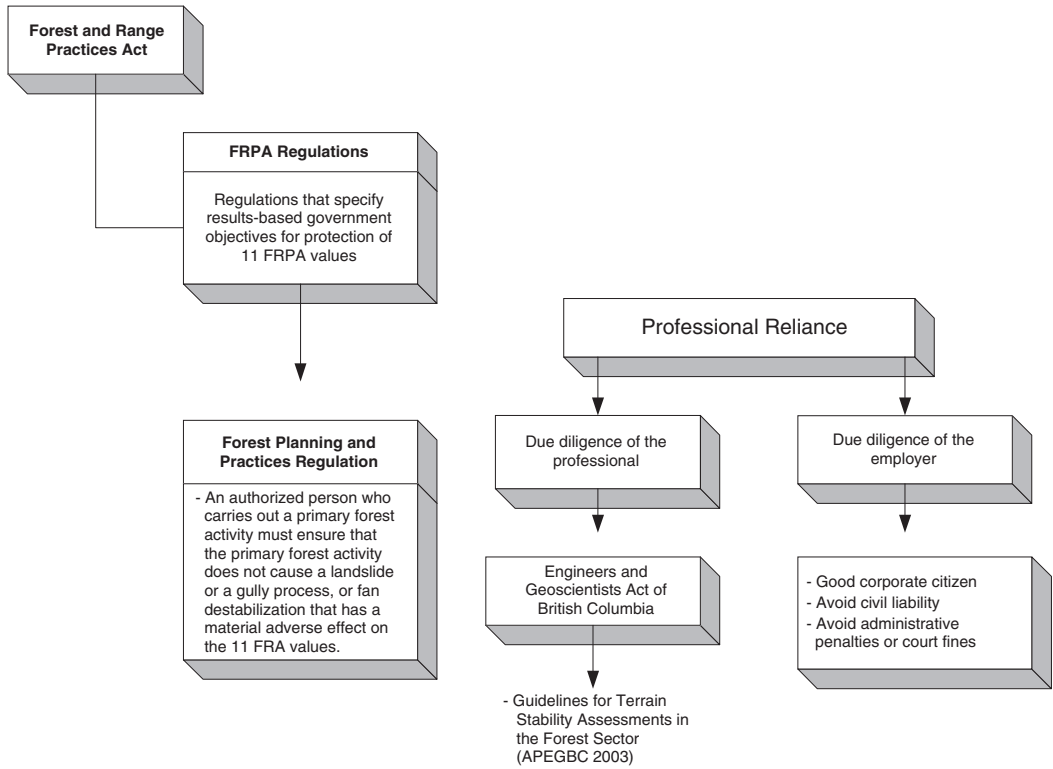
Figure 6. FRPA framework to support landslide risk management.

4 FIELD MONITORING AND RESEARCH

The most widely used methods of assessing terrain stability are those of: (1) field inspection, (2) a ranking based on select criteria, (3) use of landslide inventories to predict future patterns of instability, (4) multivariate analysis of factors associated with instability, and (5) computation of a factor of safety based on a slope stability model (Montgomery & Dietrich 1994). They all make use of terrain attributes that are either qualitative or quantitative. Our understanding of these attributes is primarily based on results of field studies.

4.1 Qualitative attributes: terrain stability maps

Landslide hazard mapping in BC forest practices has evolved considerably over the past three decades. Its origins are in a terrain classification system (Environment and Land Use Committee Secretariat 1976) that was based on work of Fulton et al. (1979). The objective is to categorize, describe and delineate characteristics and attributes of surficial materials, landforms and geological processes that have modified the landscape (Howes & Kenk 1988, 1997, Resource Inventory Committee 1996). Ryder (1994) provides a comprehensive description of standards and guidelines for terrain mapping in BC. Experienced specialists (typically a geoscientist) create terrain maps, through air-photo interpretation of landscape features, the presence of geomorphic processes (landslide and erosion), slope and soil characteristics, and judgment based on experience. Terrain stability maps (TSM) are derived from these source maps. They are used to delineate polygons where timber harvesting or road building may cause landslides (BCMOF et al. 1999a).

The first general recognition, and mapping, of potentially unstable terrain for purposes of forest land-use planning was undertaken by the BCMOF in the 1970s. Forest cover polygons that showed evidence of landslides were delineated as environmentally sensitive areas. The productive forest land base was then adjusted accordingly for forest harvesting cut control. This forest inventory based method is described in BCMOF

308

Table 1. Subclasses for mass movement processes[1].

Subclass name	Map symbol
Initiation zone	"
Soil creep	c
Rock creep	g
Tension cracks	k
Rock spread	p
Soil spread	j
Debris fall	f
Rock fall	b
Debris flow	d
Debris torrent	t
Earthflow	e
Rock slump	m
Soil slump	u
Slump-earthflow	x
Debris slide	s
Rock slide	r

[1] Table modified from Howes & Kenk (1997).

Table 2. Detailed terrain stability classification [1].

Terrain stability class	Interpretation[2]
I	• No significant problems exist
II	• Very low likelihood of landslides from timber harvesting or road construction
	• Minor slumping expected in road cuts
III	• Minor instability
	• Low likelihood of landslides from timber harvesting or road construction
IV	• Moderate likelihood of landslides from timber harvesting or road construction
V	• High likelihood of landslides from timber harvesting or road construction

[1] Table modified from BC MOF et al. 1999a.
[2] Modifiers are sometimes added. For example "IVR" to indicate landslide initiation following road construction.

(1992a). Limitations of the approach resulted in no distinction of the type of instability present, and no detailed information in support of the ES1 or ES2 rating. The first operational terrain stability maps were introduced on the Queen Charlotte Islands, in 1974, by W.W.Bourgeois of MacMillan Bloedel Ltd., Land Use Planning Advisory Team (LUPAT), as described by Bourgeois (1975, 1978) and Bourgeois & Townsend (1977). The method was subsequently used by others for forest development planning along the BC coast, in the 1980s, and then extended to the BC interior during the 1990s. The system was refined over time by Schwab (1982, 1993), Howes (1987), and Howes & Swanton (1994). With the BCMOF et al. (1995, 1999a) publications came the introduction of reconnaissance terrain stability mapping (RTSM) and detailed terrain stability mapping (DTSM) with three and five hazard classes, respectively.

The RTSM classes are stable (U), potentially unstable (P), and unstable (U). On the maps, classes P and U include a terrain symbol, geomorphic process (see Table 1) and a slope range. The DTSM classes range from I to V, from stable to the highly unstable (Table 2; Fig. 7). As mentioned above, these terrain classes were created for forestry purposes. DTSM polygons are derived from terrain polygons mapped by the geoscientist. Even though a terrain stability polygon may be in the travel path of a landslide, if the associated terrain symbol does not indicate a landslide initiation zone (Table 1), the stability polygon will likely not be a class IV or V (Table 2).

Terrain stability mapping is now an integral part of forest development planning in BC. APEGBC 2003. Its focus is landslide hazard, and specifically the likelihood of development activity causing a slope failure.

Figure 7. Example terrain stability classes: slope polygons.

Polygons are rated for the likelihood that a landslide might initiate within the polygon, but not on whether a landslide may impact it. Therefore fans, despite their vulnerability to impact by landslides, would have a lower terrain stability class. A separate analysis is sometimes undertaken to evaluate the travel distance of a landslide, and hence the likelihood of sediment entering a stream (Hogan & Wilford 1989, Maynard 1987). Recognizing that the stability classes were created for application to forest development activities, the method of landslide hazard mapping is not suitable for general land use zonation (Hungr et al. 1994) in association with infrastructure or residential development. Furthermore, since the terrain stability classification system was developed for steep terrain, shallow soils and relatively simple landslides (debris flows on open slopes or in a fluvial channels), complex large landslides are not adequately addressed (Geertsema & Schwab 2004). General standards for professional practice by

309

engineers and geoscientists undertaking terrain stability assessments are provided by APEGBC (2003).

4.2 *Qualitative attributes: research studies*

Concurrent with development of the terrain stability classification system, considerable effort was made to characterize and identify unstable terrain that is subject to debris slides and flows. A summary of BC coastal research is given by Hogan et al. (1998), and BC interior research by Jordan & Orban (2002). Early research sought to provide qualitative and semi-quantitative approaches to predict landslide occurrence, and evaluate gully susceptibility to landslide hazard (Wilford & Schwab 1982, Chatwin et al. 1994, Hogan et al. 1995, BCMOF et al. 1995d, h).

Qualitative approaches, to identify terrain subject to high landslide frequencies, sought to correlate landslide frequency with individual landscape attributes and combinations of attributes in mapped terrain polygons (Rollerson & Sondheim 1985, Rollerson et al. 1997, Rollerson et al. 2001a-b, Millard et al. 2002). Recent work, by Rollerson et al. (2004), uses categorical and scale data from terrain and landslide inventories to produce semi-quantitative landslide hazard maps for forest management purposes. Detailed studies by Millard (1999), in BC coastal gullies, address factors associated with debris flow initiation. Wilford et al. (2004) propose a model using watershed (basin) and terrain characteristics to differentiate between watersheds prone to debris flows and debris floods.

In the BC interior, landslide frequency is comparatively lower and more likely attributed to road management practices, making it impractical to contrast attributes of landslide and non-landslide terrain polygons. Hence research has focused on describing terrain attributes of individual landslides (Pack 1995, Jordan 2002, Ward et al. 2002). The objective is to establish whether development related landslides can be determined with reference to terrain attributes that can be mapped, or whether landslide occurrence is essentially independent of such factors. In a recent study, VanBuskirk et al. (2005) compared terrain attributes at sites with landslides to attributes at sites without landslides. The findings enabled the distinguishing of critical terrain attributes from road construction and road drainage.

4.3 *Quantitative attributes: initiation and travel distance*

Shallow landslide activity, such as debris slides and debris flows, is usually governed by topographic controls on shallow groundwater flow convergence. Quantitative attributes that influence the initiation of failure, typically expressed as a deterministic or probabilistic measure of the factor of safety, include site attributes (soil depth and ground slope), material attributes (angle of shearing resistance, soil cohesion, apparent cohesion as a result of a root network) and groundwater attributes (typically an assumed slope-parallel depth of flow). The availability of digital elevation model (DEM) data has led to considerable interest in the development of models that incorporate geographic information system (GIS) technology, thereby quantifying topographic attributes that control slope stability (Montgomery & Dietrich 1994, Wu & Sidle 1995, Pack 1995). A common feature of all methods is the coupling of a hydrologic model that describes the groundwater flow regime, with the infinite slope stability model that describes the factor of safety, in an approach similar to that advocated by Hammond et al. (1992). Uncertainty can be incorporated through use of probability density functions for the input parameters. Such methods require calibration, and are most confidently implemented in conjunction with other terrain stability mapping techniques. Ideally, the methods are suited to calibration against a set of data that capture known landslide activity, with the intent of then applying them to other areas of terrain where data on landslide activity are sparse or unavailable.

Following initiation of an event, the travel distance is defined by the slope distance from point of origin to point of terminal deposition. The travel distance of a debris slide or debris flow is a complex phenomenon governed by properties of the material and attributes of the path of movement. Analytical methods for determining travel distance may be categorized either as empirical or dynamic in nature. Empirical models are typically based on limiting criteria (for example, Benda & Cundy 1990) or on statistical relations (for example, Cannon 1993, Fannin & Wise 2001). Dynamic models may incorporate a rigid body analysis, energy-based approach, or the principle of continuum mechanics (for example, Hungr 1995), with simplifying assumptions often made where input parameters cannot easily be measured. In contrast to dynamic methods of analysis, empirical approaches do not address the material rheology or mechanics of movement. In many situations where our understanding of material properties is limited and the flow path is controlled by subtle changes in terrain, empirical methods offer a practical means for predicting behaviour. However, there is an inherent limitation with empirical techniques, given the dependence of prediction on an adequate database of field observations for model development, and uncertainty in applying them in new areas that may differ from that used in model development.

4.4 *Quantitative attributes: research studies*

Most landslide activity on forested hill-slopes is rainfall-induced. The common model used to describe groundwater flow assumes, for simplicity, an infinite

slope with seepage occurring parallel to the ground surface. None of the reported data, from field studies conducted in BC, support that simplified model (Hetherington 1995, Fannin & Jaakkola 1999, Fannin et al. 2000). More importantly, the occurrence of transient artesian pressures is reported at a site where the bedrock is fractured, from records of the hydrological response of the soils that pre-date timber harvesting at the site. The artesian pressures were noted to last for hours, and exhibit a relatively short return period of 2 to 6 months. The findings confirm the highly spatial response of soils to rainfall, and suggest that GIS models incorporating hydrologic models be diligently calibrated. Of equal importance is a proper attention to the selection of the angle of shearing resistance for the soil. The plane of rupture in these landslides is shallow, typically less than 2 m below the ground surface and, therefore, the effective stress governing mobilization of soil strength at the onset of failure is very low indeed. The mobilized peak strength of a soil can be expected to increase with diminishing effective stress, and this has been confirmed by a comparison of results from in-situ direct shearbox testing at the headscarps of debris slides with similar data at low effective stress obtained in laboratory studies (Fannin et al. 2005). The results of this research support the use of probability density functions, carefully determined, to ensure uncertainty in parameters governing the factor of safety are adequately accounted for in a probabilistic rather than deterministic analysis.

Upon initiation, one the most significant differences between debris slide or flow, and other types of landslide, is the fact that the cumulative volume of the event can change enormously along the path of movement. The changes occur as a result of entrainment and deposition of debris, on a reach-by-reach basis (Fannin & Rollerson 1993). Accordingly, an event that initiates with a relatively small volume at the point of origin, may grow by orders of magnitude. This presents a considerable challenge for methods intended to predict the travel distance of an event, which must properly account for the impact of such changes.

5 ILLUSTRATIVE CASE STUDIES

Two case studies are reported, which serve to illustrate the role of landslide risk management in the forest sector.

5.1 *Philpott road (Belgo Creek) debris flow, B.C.*

Six debris flows occurred in the vicinity of Belgo Creek, 30 km east of Kelowna, B.C., in the period 11–13 June 1990. The most destructive event occurred on 12 June, resulting in the loss of 3 lives, destruction

Figure 8. Debris flow at Philpott Road, B.C.

Figure 9. Deposition zone.

of a private dwelling (Fig. 8) and the burial of 135 m of Philpott Road under 2 m of debris (Fig. 9). A forensic investigation (Schwab et al. 1990) revealed the event initiated progressively, from an explosive outburst of debris in a 3 m by 5 m hillslope depression that projected material up 2.5 m on trees within 10 m of the headscarp (Fig. 10) and traveled less than 60 m. It triggered a companion flow, which traveled over a

311

Figure 10. Point of origin.

Figure 11. Evidence of redirected water down the forest road.

deactivated forest road and into a depressional channel that had been receiving redirected water (Fig. 11). Approximately 80 m below the road, geological conditions changed from deep colluvium to a shallow colluvium overlying dense impervious till. A rapid expansion of the landslide occurred at this point, accompanied by a substantial increase in velocity, evident from observations of mud splashed up to 5 m high on trees. The erosion scar increased, at the widest point, to 134 m. Deposition commenced on the valley flat in four main lobes, spread over a zone approximately 145 m in width and 250 m long. The total distance traveled by the debris flow was 1540 m, over a land area of about 17 ha.

5.1.1 General site characteristics

Belgo creek area is situated on the eastern boundary of the Thompson Plateau (Holland 1964), where elevations range from 825 to 900 m. Drainage is deranged, with very few well-developed streams that source on the plateau surface and extend down into Belgo Creek valley. The area was overridden at various times by

Pleistocene ice, yielding a veneer of colluvium over bedrock along upper valley slopes and a veneer to blanket of colluvium over till on the middle to lower valley slopes. Bedrock exposed along some ridges and steep slopes is a granodiorite and gneiss with banded rhyolite at higher elevations (Tempelman-Kluit 1989). Isolated organic soils have developed in poorly drained depressions and along watercourses. Ice contact, fluvial materials are deposited along the mid elevation and lower valley slopes.

The forest cover of the plateau is primarily lodgepole pine with some Engelmann spruce, subalpine fir and Douglas-fir occupying a transitional area between the Engelmann Spruce-Subalpine Fir and Montane Spruce Biogeoclimatic Zones (Meidinger & Pojar 1991). The steep slopes below the plateau contain Douglas-fir, lodgepole pine, some western larch, ponderosa pine, trembling aspen, western red cedar and paper birch of the Interior Douglas Fir Zone. Pinegrass is a common under story species on drier sites and rocky mountain maple on wetter seepage sites.

Airphotos, from 1963, show extensive selective logging on Crown (public) land above the point of origin of the debris flow, and intensive selective logging and small clearcuts on private land along the subsequent debris flow path. The older roads and trails on private lands were not deactivated. All logging activity on the plateau east of Belgo Creek occurred between 1983 and 1988 creating a clearcut block of 303 ha. Timber harvesting used ground skidders. Most of the cut block was planted except for about 30 ha. The total area was grass seeded for erosion control. Roads and skid roads were all considered deactivated upon completion of harvesting, with the placement of cross-ditches and water bars.

Weather data for May and June 1990 revealed the highest precipitation ever recorded for Kelowna area. A storm at the Kelowna airport on 3 June 1990 exceeded the 100 year: 5 min. event (9.2 mm) and equaled the 15 year: 1 hr. event (14.0 mm). Although storm precipitation immediately preceding the debris flow (1 hour to 3 days) was heavy, it was not exceptional, with return periods estimated at less than 5 years. However, anecdotal evidence, from people in the area suggests an intense convective storm cell may have been situated over the plateau and missed by local weather stations. Similar types of storm cells have triggered debris flows in coastal B.C. (Church & Miles 1987, Couture & Evans 2000).

A conceptual model was developed to account for temperature, contrast snow accumulation in clearcuts with interception and melt in forest stands, and conditions that prevail during rain-on-snow events (Beaudry & Golding 1983). It suggested the peak rate of water delivery to the soil upslope from the debris flow was 15% greater under a clearcut scenario. Detailed field inspection revealed that surface runoff,

312

Figure 12.   Perry Ridge, B.C.

controlled by roads and skid trails, may have caused a 20% increase in the water at the source area of the debris flow. However, the routing and actual delivery of water down slope to the landslide was difficult to determine because of considerable spillage out of poorly defined channels into distinctly different micro basins and channels on the hillslope above the point of origin.

5.1.2   *Landslide risk analysis*

Following the tragic event of June 12, 1990, the BC Provincial Emergency Program commissioned an analysis of landslide risk to individuals in residences situated at the base of the slope along Philpott Road. A specific risk analysis was carried out, and the results of the analysis are presented by Golder Associates Ltd. (1990). The risk, expressed as an annual probability of death of a specific individual exposed to a hazard (PDI), was estimated based on the work of Pack & Morgan (1987). Risk (event) zone maps similar to Morgan et al. (1992) were presented based on PDI and the spatial characteristics of different landslide potential. The event zone maps showed that there was a PDI of about 1:100 to 1:1,000 at four locations situated along the base of the slope and a PDI of 1:1,000 to 1:10,000 for much of the area on the valley flat. An engineered structure (lined channel and levee) was constructed within the vicinity of the June 12 event to control erosion and to mitigate the risk from potential future debris flows onto Philpott Road. In addition, remedial measures were undertaken on the steep slopes and gentle terrain above Philpott Road to control water runoff through the placement of water bars and cross ditches, the installation of culverts, and channeling of water away from sensitive sites.

5.2   *Perry Ridge, B.C.*

Perry Ridge is located in the West Kootenay region of BC, close to the small community of Winlaw. The relatively flat-topped ridge is approximately 25 km long, 9 km wide and ranges in elevation from 500 to 2100 m (Fig. 12). Most of its upland is Crown (public) land. Privately owned land extends along the base of, and part way up, the east side of the ridge. Much of the private land has been cleared for pasture or cultivation, or has been logged, and numerous residences with associated surface water supply intakes, are located along the base of the ridge.

In the 1980s, the BCMOF started the planning process to log a portion of the Crown land on Perry Ridge over the next 100 years. Local residents and land owners were concerned about the potential increase in risk to themselves and their property as a result of logging activities. In the 1990s, MOF began more comprehensive planning for forest development including hazard mapping and overview analyses of *existing risks* to life and limb, property and water supply, and *anticipated risks* from logging activities. This case study briefly describes the method used for those overview risk analyses. For more details, refer to Boyer et al. (1999) and VanDine et al. (2002).

The risk analyses were carried out by a three-member technical review panel, using *consensual qualitative risk analyses* based on available information and

313

empirical evidence, combined with the experience and judgment of the panel. Panel members comprised a geomorphologist, an engineering hydrologist and a geological engineers, all professionals with experience in forest development planning. The consensual aspect of these risk analyses was used to reduced biases and provided a balance of three individual's qualitative judgments.

5.2.1 General site characteristics

The study area covered approximately 76 km^2 along the east side of Perry Ridge: 69 km^2 of Crown land and 7 km^2 of private land. The area has a moist climate and is heavily forested by timber nearing maturity after a large wildfire 80 to 100 years ago. In general, the level of geomorphic activity on most of the ridge is low. Landslides and other sediment sources are scarce. Many creeks, however, are deeply incised in bedrock, and their channels and fans exhibit debris flow deposits. Most creeks flow year-round and are dominated by spring snowmelt. In the valley bottom, there are extensive and deep glacial deposits that are subject to a variety of potentially hazardous processes, including slumps, slides, and sinkholes.

The study area was divided into 16 watershed units and 16 face units between the watersheds, a total of 32 *hydrologic units*. The approximate areas downslope of the hydrologic units that could potentially be affected by surface water, groundwater, and landslide runout were delineated from detailed topographic maps and airphotos and referred to as *zones of influence*. Groundwater flow was inferred from surface contours. The zones of influence between adjacent watershed and face units commonly overlapped.

A hypothetical forest engineering plan (Spencer Forestry Consulting Ltd. 1998) identified over 300 hypothetical cutblocks and over 100 km of potential logging roads. For the purpose of these risk analyses, the study area was divided into 18 *forest development areas*, based primarily on independent access for development.

Equivalent Clearcut Area (ECA) is a forest hydrology concept used to estimate the per cent of a watershed that is equivalent to having been clearcut (BCMOF et al. 1995f). ECA considers the silvicultural system (eg: clearcut, partial cut, selective), watershed elevation, and amount and density of regeneration. For each hydrologic unit, an *ECA Index* was estimated as an indicator of the hydrologic effect of the existing condition and proposed logging, assuming: between 40 and 80% of the private land had already been logged; 30% of the timber on Crown land would be logged during the initial 30 years of development; logging would not be concentrated in any one hydrologic unit; and logging a given volume of timber would have the same effect whether clearcut or selectively logged.

5.2.2 Risk analyses

Existing *hazard* mapping included: a detailed terrain stability map at 1:20,000 scale (Wehr 1985; updated by S. Chatwin Geoscience Ltd. 1998b); stream channel assessments at 1:10,000 scale (S. Chatwin Geoscience Ltd. 1998a); geological hazards mapping on the private land at 1:25,000 scale (Apex 1998); floodplain mapping along the adjacent Slocan River at 1:5,000 scale (Canada-British Columbia, 1990). (The term *hazard* is used for convenience. Not all the geomorphic processes were everywhere estimated as harmful or potentially harmful, and therefore, by definition, are not strictly hazards.) From the existing hazard mapping nine different types of possible events were identified and grouped into three categories:

- primarily water related events: (1) *peak flow/flood;* (2) *sediment yield*
- primarily slope/channel related events: (3) *debris slide into a stream;* (4) *debris flow down a stream;* (5) *debris flood/avulsion along stream channel;* (6) *open slope landslide (any type of landslide that occurs on an open slope above the valley bottom and does not enter a stream);* (7) *snow avalanche*
- primarily valley bottom related events: (8) *valley bottom landslide;* (9) *sinkhole development.*

Each event type was identified by a number (1) through (9). The existing probability (likelihood) of occurrence of a hazard, $P_{existing}$, for each of the 9 event types with each of the 32 hydrologic units was qualitatively and relatively rated *high, moderate, low, very low* or *none* based on the probability of an event anywhere within the hydrologic unit, independent of the magnitude of the event. The qualitative relative ratings were defined by ranges of annual probability of occurrence. One of the challenges of the project was to establish a common rating system that could be applied to all nine quite different event types for all hydrologic units.

The anticipated probability (likelihood) of occurrence of a hazard after logging, $P_{after\ logging}$, for each of the 9 event types with each of the 32 hydrologic units, was based on the existing probability of occurrence of a hazard plus the perceived direct and indirect effects of forest development. The effects were subjectively inferred from: the proposed road system and logging method; estimated ECA Index after logging; and location of roads; and proximity of cutblocks with respect to areas mapped as more hazardous. Effects were qualitatively and relatively rated as *low, moderate* and *high* assuming: 30% removal of timber in development areas as discussed above; good road building and logging standards; and overlapping adjacent zones of influence. The effects of present and/or future land use activities on the private land were not considered.

The *elements potentially at risk* were divided into three groups: life and limb (primarily residences), property (primarily roads, utilities, and agricultural

Table 3. An example risk analysis of the existing condition to the water supply of Watson Creek, Hydrologic Unit 14.

Risk to water supply existing condition		Vulnerability of water supply $V(L:T)_{\text{water supply}}$		
		High	Moderate	Low
Annual probability (likelihood) of a hazardous event affecting the water supply P_{existing}	High	Very high	High	Moderate
	Moderate	High	Moderate (1),(3),(4)	Low
	Low	Moderate	Low (5)	Very low (6)
	Very low	Low	Very low (2)	

Table 4. An example risk analysis of the anticipated condition to the water supply after logging of Watson Creek, Hydrologic Unit 14.

Risk to water supply after logging		Vulnerability of water supply $V(L:T)_{\text{water supply}}$		
		High	Moderate	Low
Annual probability (likelihood) of a hazardous event affecting the Water Supply $P_{\text{after logging}}$	High	Very high	High (1), (3), (4)	Moderate
	Moderate	High	Moderate (2), (5)	Low
	Low	Moderate	Low	Very low (6)
	Very low	Low	Very low	

Notes to Tables 3 and 4:
Event types: *(1) peak flow/flood; (2) sediment yield; (3) debris slide into a stream; (4) debris flow down a stream; (5) debris flood/avulsion along stream channel; (6) open slope landslide (any type of landslide that occurs on an open slope above the valley bottom and does not enter a stream); (7) snow avalanche; (8) valley bottom landslide; (9) sinkhole development.*
Not all event types are present. Event types with vulnerabilities < *Low* were not considered.

land) and water supply (primarily water intake locations). The elements were mapped with the intent to provide a uniform level of information within each zone of influence and across the study area, rather than to accurately map each and every element. Only existing elements potentially at risk were considered.

Because these were overview analyses, it was assumed that if an event occurred anywhere in the hydrologic unit, either before or after logging activities, all elements in that hydrologic unit could potentially be affected by the event. In other words, the spatial probability, P(S:H), and the temporal probability, P(T:S), were both assumed to be certain. Therefore, P_{existing}, and $P_{\text{after logging}}$ were assumed to be equivalent to the probabilities of specific hazardous affecting events for both the existing condition and after logging.

The *vulnerability* of the elements potentially at risk, V(L:T), was estimated in qualitative relative terms as *high, moderate*, and *low* expressed as the proportion of loss or damage to which those elements could potentially be subject. The vulnerability ratings were not intended to be compared among the three different groups of elements. For example a *high* vulnerability

rating for life and limb should not be compared to a *high* vulnerability rating for water supply.

The *existing risk*, R_{existing}, from each of the 9 event types for each of the 32 hydrologic units was estimated with the help of three risk matrices that combined P_{existing} and V(L:T): one relating to life and limb, one relating to property and one relating to water supply. An example risk analysis of the existing condition to the water supply of Watson Creek, Hydrologic Unit 14, is given in Table 3.

It was assumed that the vulnerability of elements potentially at risk would not change after logging activities, only the probability of occurrence of a specific hazardous affecting event. Once $P_{\text{after logging}}$ was estimated, it was combined with the V(L:T) on each of the three risk matrices to estimate the *risk after logging*, $R_{\text{after logging}}$. An example risk analysis of the anticipated condition to the water supply after logging of Watson Creek, Hydrologic Unit 14 is given in Table 4.

Where *very high*, *high*, and *moderate* risks were estimated, either existing or anticipated after logging, and based on the information contained in the background documents and the experience of the panel

315

members, alternatives to the logging or logging road building were suggested and recommendations made to reduce the effects of the proposed forest development. The effects of the alternatives on the feasibility (economic or otherwise) of the forest development plan were not considered.

Examples of recommendations were: extend geological hazard mapping in specific areas; carry out stream channel assessments on specific streams not already assessed; better determine stream courses or watershed boundaries; carry out detailed field assessments to address specific hazards; pay special attention to the location, design and construction of specific logging roads and creek crossings; design and construct specific logging roads to higher drainage control standards; minimize ground disturbance associated with skidding in specific areas. Most recommendations were aimed at doing further geotechnical studies, or carrying out detailed planning, design or operations in excess of minimum requirements, to reduce the probability of a hazard. Examples of suggested alternatives were: eliminate logging in specific forest development areas, limit the ECA in specific forest development areas (equivalent to reducing the rate of cut); add riparian reserve zones; modify road locations; eliminate specific stream crossings; eliminate specific roads and instead consider skyline logging, helicopter logging, or no logging.

The risk analyses carried out by the technical review panel did not address the acceptability of risk. It was thought that thresholds or criteria of risk acceptability should be established by government, which must incorporate appropriate socio-economic and environmental factors into its decision making.

6 SUMMARY REMARKS

A careful evaluation of landslide risk, in any proposed forest development plan, is critical to meeting the objectives of good forest resources management. Guidance on landslide risk management is prepared for one of two reasons. Either it is to interpret mandatory codes of practice arising from legislated regulations or, alternatively, it is to describe voluntary activities that, if adopted, could reasonably be expected to yield improvements to professional practice. Landslide activity, often arising from improper road construction and maintenance, has one the greatest potentials to impact on public safety and impose a lasting environmental impact on the landscape. Risk management is gaining acceptance as a basis for decision analysis on steep, landslide-prone terrain.

ACKNOWLEDGEMENTS

REFERENCES

Apex Geoscience Consultants Ltd. 1998. *Geological hazards mapping of the Slocan Valley, Phase I.* Prepared for MOF Arrow Forest District, Castlegar, B.C.

Association of Professional Engineers and Geoscientists of British Columbia (APEGBC) 2003. *Guidelines for terrain stability assessments in the forest sector*. Burnaby, B.C. October 2003.

B.C. Ministry of Forests (BCMOF) 1992. *Forest inventory manual: forest classification, sampling and environmentally sensitive areas (Volume 2).* B.C. Min. For., Inventory Branch, Victoria, B.C.

B.C. Ministry of Forests (BCMOF) 1993. *Forest road and logging trail engineering practices and instructions for its implementation*. B.C. Min. For., Resource Tenures and Engineering Br., Victoria, B.C.

B.C. Ministry of Forests (BCMOF) 1994. *Forest Practices Code legislation module – resource booklet, version 2.0*. Forest Practices Code of British Columbia, Victoria, B.C.

B.C. Ministry of Forests (BCMOF) 1999. *Managing Risk Within a Statutory Framework*. B.C. Min. For., Compliance and Enforcement Br., Victoria, B.C.

B.C. Ministry of Forests (BCMOF) 2001. *Best management practices handbook: Hillslope restoration in British Columbia*. Res. Ten. & Eng. Br., B.C. Min. For., Victoria, B.C. Watershed Restoration Program.

B. C. Ministry of Forests (BCMOF) 2002a. *A result's-based forest and range practices regime for British Columbia: Discussion paper for public review and comment*. B.C. Min. For., Victoria, B.C.

B.C. Ministry of Forests (BCMOF) 2002b. Forest road engineering guidebook. For. Prac. Br., B.C. Min. For., Victoria, B.C. Forest Practices Code of British Columbia Guidebook.

B.C. Ministry of Forests (BCMOF) B.C. Ministry of Environment Lands and Parks, Federal Department of Fisheries and Oceans & Council of Forest Industries 1988. *Coastal Fisheries/Forestry Guidelines: Second Edition.* Research Branch. B.C. Min. For., Victoria, B.C.

B.C. Ministry of Forests (BCMOF) B.C. Ministry of Environment Lands and Parks, Federal Department of Fisheries and Oceans & Council of Forest Industries 1992. *Coastal Fisheries/Forestry Guidelines: Second Edition*. Research Branch. B.C. Min. For., Victoria, B.C.

B.C. Ministry of Forests (BCMOF) B.C. Ministry of Environment Lands and Parks, Federal Department of Fisheries and Oceans & Council of Forest Industries

1993. *Coastal Fisheries/Forestry Guidelines: Third Edition Revised*. Research Branch. B.C. Min. For., Victoria, B.C.

B.C. Ministry of Forests (BCMOF) & B.C. Ministry of Environment 1995. Mapping and assessing terrain stability guidebook. Forest Practices Code of British Columbia. Victoria, B.C.

B.C. Ministry of Forests (BCMOF) & B.C. Ministry of Environment 1995b. Gully assessment procedure guidebook. Forest Practices Code of British Columbia. Victoria, B.C.

B.C. Ministry of Forests (BCMOF) & B.C. Ministry of Environment 1995c. Gully assessment procedure guidebook. 2nd edition. Forest Practices Code of British Columbia. Victoria, B.C.

B.C. Ministry of Forests (BCMOF) & B.C. Ministry of Environment 1995d. Gully assessment procedure guidebook. 3rd edition. Forest Practices Code of British Columbia. Victoria, B.C.

B.C. Ministry of Forests (BCMOF) & B.C. Ministry of Environment 1995e. Coastal watershed assessment procedure guidebook (CWAP). Forest Practices Code of British Columbia. Victoria, B.C.

B.C. Ministry of Forests (BCMOF) & B.C. Ministry of Environment 1995f. Interior watershed assessment procedure guidebook (IWAP). Forest Practices Code of British Columbia. Victoria, B.C.

B.C. Ministry of Forests (BCMOF) & B.C. Ministry of Environment 1995g. Forest road engineering guidebook. Forest Practices Code of British Columbia. Victoria, B.C.

B.C. Ministry of Forests (BCMOF) & B.C. Ministry of Environment 1995h. Hazard assessment keys for evaluating site sensitivity to soil degradation processes guide book. Forest Practices Code of British Columbia. Victoria, B.C.

B.C. Ministry of Forests (BCMOF) & B.C. Ministry of Environment 1999a. Mapping and assessing terrain stability guidebook. Forest Practices Code of British Columbia. Victoria, B.C.

B.C. Ministry of Forests (BCMOF) & B.C. Ministry of Environment 1999b. Coastal watershed assessment procedure guidebook (CWAP) – Interior watershed assessment procedure guidebook (IWAP), 2nd edition. Forest Practices Code of British Columbia. Victoria, B.C.

B.C. Ministry of Forests (BCMOF) 2001. Gully assessment procedure guidebook. 4th edition. Version 4.1. For., Prac. Br., Min. For., Victoria, B.C. Forest Practices Code of British Columbia Guidebook.

B.C. Ministry of Forests (BCMOF) & B.C. Ministry of Sustainable Resources Management 2004. *BC's New Forest and Range Practices Framework – FRPA Training Companion Guide: Forestry Modules. B.C. Ministry of Forests and B.C.* Ministry of Sustainable Resources Management, Victoria, B.C. Website: http://www.for.gov.bc.ca/code/training/frpa/forestry_modules_companion_guide_download.html

Beaudry, P. & Golding, D.L. 1983. Snowmelt during rain-on-snow in coastal British Columbia, *Proceedings of the 51st Annual Western Snow Conference*.

Benda, L.E. & Cundy, T.W. 1990. Predicting deposition of debris flows in mountain channels. *Can. Geotech. J.* 27: 409–417.

Bourgeois, W.W. 1975. *Geotechnic Inventory of a portion of Louise Island (QCI)*. 60 pp.

Bourgeois, W.W. 1978. Timber harvesting activities on steep Vancouver Island terrain. *Proc. 5th North American Forest Soils Conference, Colorado State Univ., Fort Collins, CO,* pp. 393–409.

Bourgeois, W.W. & Townshend, R.B. 1977. *Geotechnic report, Memkey watershed*. MacMillan Bloedel Ltd., For. Div., Nanaimo, BC Rep. No. 11

Boyer, D., Jordan P. & VanDine, D.F. 1999. *Perry Ridge Risk Assessment*. Prepared for the Perry Ridge Local Resource Use Plan Table, MOF Arrow Forest District, Castlegar, BC, including 3 addenda.

Canada-British Columbia. 1990. Canada-British Columbia Floodplain Mapping Program, Slocan River, Drawing No 88–26, Sheets 1 to 11. Supporting report by Northwest Hydraulic Consultants Ltd. 1989. Floodplain Mapping Study Slocan River British Columbia Design Brief, prepared for Water Management Branch British Columbia Ministry of Environment

Cannon, S.H. 1993. An empirical model for the volume-change behavior of debris flows. In *Proc. Hydraulic Engineering '93*, San Francisco, Vol. 2, pp.1768–1777.

Chatwin, S.C., Howes, D.E., Schwab, J.W. & Swanston, D.N. 1991. *A guide for management of landslide-prone terrain in the Pacific Northwest*, B.C. Min. For., Land Manage. Handb. 18

Chatwin, S.C. & Smith, R.B. 1993. Reducing soil erosion associated with forestry operations through integrated research: an example from coastal British Columbia, Canada. *In*: Walling et al. (*eds.*), *Erosion, debris flows, and environment in mountain regions: Proceedings of the international symposium held at Chengdu, China, 5–9 July 1992. IAHS publication 209.* Wallingford, Oxfordshire, UK.

Chatwin, S.C., Howes, D.E., Schwab, J.W. & Swanston, D.N. 1994. *A guide for management of landslide-prone terrain in the Pacific Northwest (second edition)*, B.C. Min. For., Land Manage. Handb. 18.

Church, M. & Miles, M.J. 1987. Meteorological antecedents to debris flow in South Western British Columbia; some case studies. *Reviews in Engineering Geology, Volume VII*, Geological Society of America.

Couture, R. & Evans, S.G. 2000. *Five-Mile Creek debris flow, Banff National Park, near Banff, Alberta*, August 4, 1999; Geological Survey of Canada, Open File 3876, 57 pp.

Dykstra, D.P. & Heinrich, R. 1996. *FAO model code of forest harvesting practice.* Food and Agriculture Organization of the United Nations, Rome, Italy. Website: http://www.fao.org/documents/show_cdr.asp?url_file = /docrep/v6530e/v6530e00.htm

Environment & Land Use Committee Secretariat 1976. *Terrain Classification System*; B.C. Ministry of Environment, Resource Analysis Branch, 56 pp.

Fannin, R.J & Rollerson, T.P. 1993. Debris flows: physical characteristics and behaviour. *Can. Geotech. J.* 30: 71–81.

Fannin, R.J. & Jaakkola, J. 1999. Hydrological response of hillslope soils above a debris-slide headscarp. *Can. Geotech. J.* 36: 1111–1122.

Fannin, R.J., Jaakkola, J., Wilkinson, J.M.T. & Hetherington, E.D., 2000. Hydrologic response of soils to precipitation at Carnation Creek, British Columbia, Canada. *Water Resources Research* 36(6): 1481–1494.

Fannin, R.J. & Wise, M.P. 2001. An empirical-statistical model for debris flow travel distance. *Can. Geotech. J.* 38: 982–994.

Fannin, R.J. 2003. Forest road construction in mountainous terrain: national codes, land management and development planning. *Proceedings of the International Expert Meeting on the Development and Implementation of National Codes of Practice for Forest Harvesting – Issues and Options, Chiba, Japan, Nov 17–20*, pp. 149–156.

Fannin, R.J., Wilkinson, J.M.T & Eliadorani, A. 2005. Shear strength of cohesionless soils at low stress. *Geotechnique* (in press).

Forest Resources Commission 1991. *The future of our forests*. British Columbia Forest Resources Commission, Victoria, B.C.

Fulton, R.J., Boydell, A.N. Barnett, D.M. Hodgson, D.A. & Rampton, V.A. 1979. Terrain Mapping in Northern Environments. In Romaine & Ironside (eds.), *Proc. of a Technical Workshop – To Develop an Integrated Approach to Base Data Inventories for Canada's Northlands. Ecological Land Classification Series, No. O, Supply and Services Canada, Ottawa: 3–21.*

Geertsema, M. & Schwab , J.W. 2004. Challenges with terrain stability mapping in northern British Columbia – the special case of large complex landslides. *Proc. 57th Canadian Geotechnical Conference 5th Joint CGS/IAH-CNC conference Géo Québec 2004. Session 4C*, pp. 11–18.

Golder & Associates Ltd. 1990. *Report to the Provincial Emergency Program on the Geotechnical study of slide and debris flow potential, Philpot road Kelowna, B.C.* Golder and Associates Ltd., Vancouver, B.C. 148 pp.

Hammond, C.J., Hall, D., Miller, S. & Swetik, P. 1992. Level 1 Stability Analysis (LISA) documentation for version 2.0. Gen. Tech. Rep. INT-285, U.S. Dept. of Ag., Forest Service, Intermountain Res. Station, Ogden, USA.

Hartman, G.F. & Schrivener, J.C. 1990. Impacts of forestry practices on a coastal stream ecosystem, Carantion Creek, British Columbia. *Can. Bull. Fish. Aquat. Sci.* 223: 148 pp.

Hetherington, E. 1995. Subsurface flow rates over bedrock on steep slopes in the Carnation Creek Experimental Watershed. In *Proc. of Mountain Hydrology: Peaks and valleys in Research and Applications*, Vancouver, B.C. Can. Water Resour. Assoc., pp.17–21.

Hogan D.L. & Wilford, D.J. 1989. A sediment transfer hazard classification system: linking erosion to fish habitat. *Proceedings Watershed '89 A conference on the stewartship of soil , air and water resources. Juneau, USDA Forest Service Alaska Region.* pp.143–154

Hogan, D.L., Rollerson T.P. & Chatwin, S. 1995. *Gully assessment procedures for British Columbia forests*. B.C. Min. For., Water Restoration Technical circular. 46 pp.

Hogan, D.L., Tschaplinski, P.J. & Chatwin, S. (eds). 1998 Carnation Creek and Queencharlotte Islands Fish/forestry Workshop: Appling 20 years of Coastal Research to management Solutions. *Land Management Handbook 41*. Res. Br. B.C. Min For. Victoria, B.C. 275 pp.

Holland, S.S. 1964. *Landforms of British Columbia, A Physiographic Outline Bulletin No. 48*. British Columbia Department of Mines and Petroleum Resources. 138 pp.

Howes, D.E. 1987. *A terrain evaluation method for predicting terrain susceptible to post-logging landslide activity – a case study from the southern Coast Mountains of British Columbia.* BC Ministry of Environment and Parks Technical Report 28, 38 pp.

Howes, D.E. & Kenk, E. 1988. *Terrain Classification System for British Columbia (revised Edition)*. B.C. Ministry of Environment, Manual 10, 90 pp.

Howes, D.E. & Swanston, D.N. 1994. A technique for stability hazard assessment. Chap. 2 In *A guide for management of landslide prone terrain in the Pacific Northwest.* Chatwin et al. (eds), BC Min. For. Land Man. Handbook No. 18, pp. 19–84.

Howes, D.E. & Kenk, E. 1997. *Terrain classification system for British Columbia (Version 2).* B.C. Ministry of Environment, Recreational Fisheries Branch, and B.C. Ministry of Crown Lands, Surveys and Resource Mapping Branch, Victoria, B.C.

Hungr, O. Gerath, F. & Van Dine, D.F. 1994. *Landslide hazard mapping guidelines for British Columbia.* Report to The Earth Sciences Task Force, B.C. Government Resources Inventory Committee.

Hungr, O. 1995. A model for the runout analysis of rapid flowslides. *Can. Geotech. J.* 32: 610–623.

Johnston, N.T. & Moore, G.D. 1995. *Guidelines for planning watershed restoration projects.* Province of British Columbia, Ministry of Environment, Lands and Parks and Ministry of Forests. Watershed Restoration Technical Circular No. 1: 52pp. Website: http://srmwww.gov.bc.ca/frco/bookshop/tech.html

Jordan, P. 2002. Landslide frequency and terrain attributes in Arrow and Kootenay lakes forest districts In Jordan & Orban (eds.), *Terrain stability and forest management in the interior of British Columbia: workshop proceeding 23–25 May 2001.* Nelson British Columbia Canada. Res. Br., BC Min. For., Victoria, B.C. Tech Rep. 003. pp. 80–102.

Jordan, P. & Orban, J. (eds.) 2002. *Terrain stability and forest management in the interior of British Columbia: workshop proceeding 23–25 May 2001.* Nelson, B.C. Canada. Res. Br., B.C. Min. For. Victoria, B.C. Tech Rep. 003, 417 pp.

Maynard, D.E 1987. *Terrain Classification, Terrain Stability, and Surface Erosion Potential, Kiteen River Watershed.* Prepared for Skeena Cellulose Inc. Terrace, B.C.

Meidinger D.V. & Pojar, J. 1991. *Ecosystems of British Columbia*. Special Report No 6. B.C. Ministry of Forests Victoria, B.C. 330 pp.

Millard, T. 1999. *Debris flow initiation in coastal British Columbia gullies.* Res. Sec. Van. For., Reg., B.C. Min. For. Nanaimo, TR-02, 22 pp.

Millard, T., Rollerson, T.P. & Thomson, B. 2002. *Post logging landslide rates in the Cascade mountain, southwestern British Columbia. Res. Sec.* Van. For., Reg., B.C. Min. For. Nanaimo, TR-023, 18 pp.

Montgomery, D.R. & Dietrich, W.E. 1994. A physically based model for the topographic control on shallow landsliding. *Water Resources Research* 30(4): 1153–171.

Moore, G.D. 1994. *Resource road rehabilitation handbook: planning and implementation guidelines (interim methods).* Province of British Columbia, Ministry of Environment, Lands and Parks and Ministry of Forests, Watershed Technical Circular No. 3: 115pp. Website: http://srmwww.gov.bc.ca/frco/bookshop/tech.html

Morgan, G.C. Rawlings, G.E. & J.C. Sobkowicz, 1992. Evaluating total risk to communities from large debris flows. In Geotechnique and Natural Hazards. Bitech Publishers Ltd., Richmond, B.C. pp. 225–236.

318

Pack, R.T., Morgan, G.C. & Anderson, L.R. 1987. Philosophy of landslide risk evaluation and acceptance. In Proceedings of 5th International Conference on Application of Statistics and Probability in Soil and Structural Engineering, Vancouver, B.C., 25–29 May 1987, pp. 946–952.

Pack, R.T. 1995. Statistically-based terrain stability mapping methodology for the Kamloops Forest Region, B.C. *Proceedings of the 48th Canadian Geotechnical Conference*, Vancouver, Canada, pp. 617–624.

Resources Inventory Committee 1996. *Guidelines and standards for terrain mapping in British Columbia*. Government of British Columbia, Victoria, B.C.

Resources Inventory Committee 1996a. *Terrain Stability Mapping in British Columbia: A review and suggested methods for landslide hazard and risk mapping – final draft*. Report Prepared for Terrain Geology Task Group, Earth Science Task Force, Resources Inventory Committee, B.C. Web site: http://srmwww.gov.bc.ca/risc

Resources Inventory Committee 1996b. *Guidelines and Standards to Terrain Mapping in British Columbia*. Report Prepared for Terrain Geology Task Group, Earth Science Task Force, Resources Inventory Committee, B.C. Web site: http://srmwww.gov.bc.ca/risc

Rollerson, T.P., Thomson, B. & Millard, T.H. 1997. Identification of Coastal British Columbia terrain susceptible to debris flows. In Proceedings 1st Intl. Conf. on Debris – Flow Hazards Mitigation: Mechanics, Prediction and Assessment, San Francisco, California, 7–9 August 1997, pp. 484–495.

Rollerson, T.P., Millard, T. & Thomson, B. 2001a. Using Terrain Attributes to Predict Post-Logging Landslide Likelihood on Southwestern Vancouver Island. Res. Sec. Van.For., Reg., B.C. Min. For. Nanaimo, TR-015 15 pp.

Rollerson, T., Millard, T., Jones, C., Trainor, K. & Thomson, B. 2001b. *Predicting post-logging landslide activity using terrain attributes: Coast mountains, British Columbia*. Res. Sec. Van.For., Reg., B.C. Min. For., Nanaimo, TR-011 20 pp.

Rollerson, T.P. & Sondheim, M. 1985. Predicting post-logging terrain stability: a statistical-geographic approach. *Proceedings of the IUFRO mountain logging section and sixth pacific northwest skyline logging symposium Improving mountain logging planning, techniques and Hardware. May 1985,* Vancouver, B.C. pp. L25–L31.

Rollerson, T.P., Maynard, D., Higman, S. & Ortmayr, E. 2004 *Klanawa landslide hazard mapping pilot project*. A joint conference IUFRO S3.06.00: Forest operations under mountainous conditions and 12th International Mountain Logging Conference June 13–16 Vancouver, British Columbia, Canada. 24 p.

Ryder, J.M. 1994. *Guidelines and Standards to terrain geology mapping in British Columbia*. Terrain Geology Task Group, Earth Science Task Force. Resource Inventory Committee, British Columbia 1993–1994 pp. 45.

S Chatwin Geoscience Ltd. 1998a. *Perry Ridge stream channel survey*. Prepared for MOF Arrow Forest District, Castlegar, B.C.

S Chatwin Geoscience Ltd. 1998b. *Upgrade of TSIL C mapping and surface soil erosion hazard mapping for the east side of Perry Ridge*. Prepared for MOF Arrow Forest District, Castlegar, B.C.

Schwab, J.W. 1982. *Slope stability mapping workshop*. BC Min. For., Pr. Rupert Forest Region, Smithers, B.C.

Schwab, J.W. 1983. Mass wasting, October–November 1978 storm Rennell Sound, Queen Charlotte Islands, British Columbia. BCMOF, Res. Note No. 91, 23 pp.

Schwab, J.W. 1988. *Mass wasting impacts to forest land: Forest management implications, Queen Charlotte Timber Supply Area*. B.C. Min. For., Res. Br., Victoria, B.C. Land Management. Report No. 56.

Schwab, J.W. 1993. *Interim Terrain and Slope Stability Mapping Standards, Prince Rupert Forest Region; Forest Sciences Section*. B.C. Forest Service, Prince Rupert Forest Region.

Schwab, J.W., Mitchell, W.R., Clark, P., Dobson D.A. & Reimer, R.J. 1990. *Investigation into the cause of the destructive debris flow, Joe Rich – Belgo Creek area, June 12, 1990*. B.C. Ministry of Forests. Penticton Forest District. 57 pp.

Slaney, P.A. & Martin, A.D. 1997. The watershed restoration program of British Columbia: accelerating natural recovery processes. *Water Qual. Res. J. Canada* 32(2): 325–346.

Spencer Forestry Consulting Ltd. 1998. *Engineering plan report, Perry Ridge total chance plan*. Prepared for MOF Arrow Forest District, Castlegar, B.C.

Tempelman-Kluit, D J. 1989. *Geology, Penticton, West of Sixth Meridian, British Columbia*. Geological Survey of Canada, "A" Series Map , 1736A.

Toews, D. & Hetherington, E. 2004. A brief history of forest hydrology in British Columbia. *Streamline – Watershed Management Bulletin* 8(1): 1–5.

Tripp, D. 1994. *The use and effectiveness of the Coastal Fisheries/Forestry Guidelines in selected forest districts of British Columbia*. Consultant's Report. Prepared for the B.C. Min. For., Integrated Resources Branch, Victoria, B.C.

UNFAO 1999. *Code of Practice for Forest Harvesting in Asia-Pacific*. FAO Regional Office for Asia and the Pacific, Bangkok, Thailand. 133 pp.

VanBuskirk, C.D., Neden, R.J. & Schwab, J.W. 2005. Attributes of forest road-fill landslides (These proceedings).

VanDine, D.F., Jordan, P. & Boyer, D.C. 2002. An example of risk assessment from British Columbia, Canada. In McInnes & Jakeways (eds.), *Proceedings Instability, Planning and Management*, Isle of Wight, UK. Thomas Telford Publishing, London, pp. 399–406.

Vold, T. 2003. Experience developing a results-based forest practices code for British Columbia, Canada. *In XII World Forestry Congress in Quebec City, 2003*. Web site: http://www.for.gov.bc.ca/hfp/WFC%20RBC%20Paper.pdf

Ward, B., Rollerson, T. & Tsang, S. 2002. Terrain attribute study in the Prince George Forest Region, British Columbia. In Jordan, P. & J. Orban (ed.), *Proceedings Terrain stability and forest management in the interior of British Columbia: workshop proceeding 23–25, May 2001* Nelson, British Columbia Canada. Res. Br., BC Min. For., Victoria, B.C. Tech Rep. 003. pp. 208–209.

Wehr, R. 1985. *Terrain survey: Perry Ridge, preliminary assessment*. Report and maps prepared for Slocan Forest Products, Slocan, B.C.

Wilford, D.J. & Schwab, J.W. 1982. Soil mass movement in the Rennell Sound area, Queen Charlotte Islands, British Columbia. *Proc. Canadian Hydrology Symposium 82*. Natl. Res. Counc. Can. Fredricton N.B. pp. 521–541.

Wilford, D.J., Sakals, M.E., Innes, J.L., Sidle, R.C. & Bergerud, W.A. 2004. Recognition of debris flow, debris flood and flood hazard through watershed morphometrics. *Landslides* 1: 61–66.

Wise, M.P., Moore, G.D. & VanDine, D.F. (eds). 2004. *Landslide risk case studies in forest development planning and operations.* B.C. Min. For., Res. Br., Victoria, B.C. Land Manage. Handb. No. 56. Web site: (http://www.for.gov.bc.ca/hfd/pubs/Docs/Lmh/Lmh56.htm)

Wu, W. & Sidle, R.C. 1995. A distributed slope stability model for steep forested watersheds. *Water Resources Research* 31(8): 2097–2110.

Risk assessment for submarine slides

F. Nadim
International Centre for Geohazards/NGI, Oslo, Norway

J. Locat
Université Laval, Département de géologie et de génie géologique, Québec, Canada

ABSTRACT: The state-of-the-art in understanding offshore geohazards, in particular seafloor mass movements, has advanced significantly in the past decade. The paper reviews the major recent contributions in risk assessment for submarine slides and recommends a stage-wise approach for performing the risk assessment.

1 INTRODUCTION

Exploitation of offshore resources, development of communication and transport corridors, fishing habitat protection, and the protection of coastal communities, have contributed to a growing interest in improved understanding of offshore geohazards, in particular seafloor mass movements and their consequences. Figure 1 shows the main offshore geohazards that might pose a threat to offshore installations and people and infrastructure along the coastlines. This figure shows the complexity of submarine mass movements risk assessment studies, which are far from the more simplistic view put forward in one of the first approaches to risk assessment by Favre *et al.* (1992).

Submarine slides are common and very effective mechanisms of sediment transfer from the shelf and upper slope to deep-sea basins (Hampton *et al.* 1996,

Figure 1. Potential geohazards on deepwater margins.

Locat & Lee 2002, Syvitsky *et al.* 1987). During one single event enormous sediment volumes can be transported on very gentle slopes with inclination in the range 0.5–3°, over distances exceeding hundreds of kilometers. Typically such events last from less than an hour to several days and can severely damage fixed platforms, pipelines, submarine cables and other seafloor installations. Research on understanding the mechanisms behind and the risks posed by submarine slides has intensified in the past decade, mainly because of the increasing number of deep-water petroleum fields that have been discovered and in some cases developed (Locat & Mienert 2003). Production from offshore fields in areas with earlier sliding activity is ongoing in the Norwegian margin, Gulf of Mexico, offshore Brazil, the Caspian Sea and West Africa.

Submarine landslides occur frequently on both passive and active continental margins, especially on the continental slopes. Despite the generally low slope angles, these are areas of sloping stratigraphy, often with more active and vigorous geological processes, including seismicity, than those found in the shallow, sub-horizontal continental shelf areas. The shelf edge and slope area contain the most recently deposited materials, and in areas with high deposition rate, underconsolidation/excess pore pressure may exist. The excess pore pressure often plays a major role in destabilization of submarine slopes. The expenses of finding and developing new fields in deep water are very high, and this greatly increases the economic consequence part of the risk aspect connected to submarine slides in the continental margin settings.

Large submarine slides may also generate tsunamis with potential for severe damage along the coastline. The tsunami generated by the earthquake-triggered Grand Banks slide in 1929 killed 27 people in
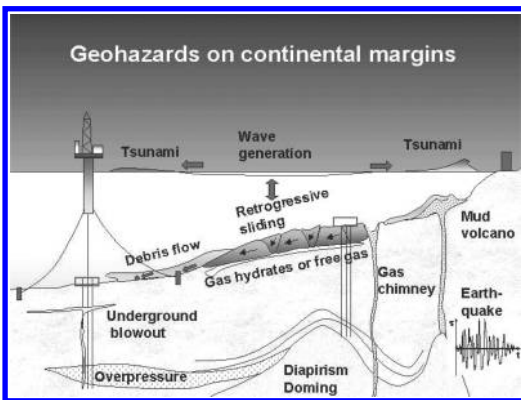
Newfoundland. The 15-m tsunami that killed more than 2000 people in Papua New Guinea in 1998 was also a result of an earthquake-triggered submarine slide. The catastrophic tsunami that was triggered by the magnitude 9.0 earthquake off the coast of Sumatra on 26 December 2004 killed over 200,000 people. It is still not known if the large sea floor movements that caused the tsunami were only the result of fault displacement, or an earthquake-triggered submarine slide was also involved.

The assessment of the risk associated with submarine mass movements is thus not just a matter related to commercial interests of oil companies. The societal and environmental consequences of such events could also be enormous for coastal communities.

2 ISSUES THAT SHOULD BE CONSIDERED IN RISK ASSESSMENT

Assessment of the risk posed by a potential submarine slide requires identification and analysis of the relevant failure scenarios, *i.e.* failure modes, triggering sources and related failure consequences, which have a significant contribution to the total risk. The triggering mechanisms could be natural, such as earthquake, tectonic faulting, temperature increase caused by climate change, excess pore pressure due to rapid sedimentation and gas hydrate melting due to climate change with increased sea water temperature after glacial periods; or man-made, such as anchor forces from ships or floating platforms, rockfilling for pipeline supports, temperature change around oil and gas wells in the offshore field development area, underground blow-out, and reservoir depletion and subsidence (including induced seismicity). The key issue in the slide risk assessment is the identification of potential triggers and their probability of occurrence, the associated failure modes and their consequences.

Evaluation of the stability of natural or man-made slopes has traditionally been based on a deterministic approach where the margin of safety is quantified by the safety factor. Many of the parameters that are used in a stability analysis, in particular the soil shear strength and the earthquake load effects (for seismic stability evaluation), are inherently uncertain. The uncertainties involved in assessment of site and soil conditions are in many cases amplified by the spatial extent and depth of the sediments and geological units involved, the presence of gas in sediments, and the practical and economical limitation of the site investigations. In a deterministic stability evaluation, the geotechnical engineer tries to deal with the uncertainties by choosing reasonably conservative parameters through the use of partial load and material coefficients. The deterministic approach, however, fails to address the problem of dealing with uncertainties properly.

Reliability theory and probabilistic analyses provide a rational framework for estimating the probability of slope failure and are powerful tools for quantitative risk assessment. However, reliability methods require more data and estimates of the variances in significant parameters. This can be expensive and it will also require expert judgment. The cost and judgment are part of the price paid for a better answer. This tends to make the reliability methods more useful for major projects than for routine work. For this reason, application of reliability methods for evaluation of stability of soil slopes is more common in offshore geohazards studies than in traditional land-based geotechnical engineering.

Risk quantification has to be based on site investigations with mapping of topography and local gradients, identification of different geological/geotechnical units, assessment of soil and/or rock properties and *in situ* stresses, pore pressure and temperature conditions. An understanding of the regional and local geology, ongoing geological processes, and type, locations and extent of anomalies is required to quantify the potential impact and rate or frequency of ongoing natural processes (see also Leroueil *et al.* 2003 and Locat 2001). This element is significant since one must be able to answer the question about whether or not a given process is active and in which direction it is going (Locat 2001).

If we look at a given natural slope, an important question to ask ourselves is whether or not the processes responsible for the formation of the slope are still active (Fig. 2), *i.e.* how is the hazard evolving? If the answer is yes, then we can assume that the long term factor of safety, defined as the ratio between the resisting forces to the gravitational forces, is about one, i.e. the slope, on the long term, is responding (or adjusting) to the ongoing slope process(es). If the answer is no, then there are two other options related to the evolution of the geological processes which can either improve the stability situation or deteriorate it. For example, if we look at a submarine canyon slope and have indications that it had been created at the time of lower-than-today sea levels, then the actual condition may be that the stability is improving, since erosion has more-or-less ceased and partial filling may have started to take place. As another example, consider slopes which have been destabilized by gas hydrates at times of low sea levels. The slopes may be more stable now, but local reservoir exploitation could change the confining stresses conditions or fluid movements. These could in turn influence the gas hydrate stability and decrease the factor of safety, so as to re-activate or generate some slides (Kayen & Lee 1991). In the case of the Eel River Margin (Fig. 2), the actual slope processes are still very active: high sedimentation rate (potential for overloading the slope) and seismic activity (Lee *et al.* 1999) so that the

322
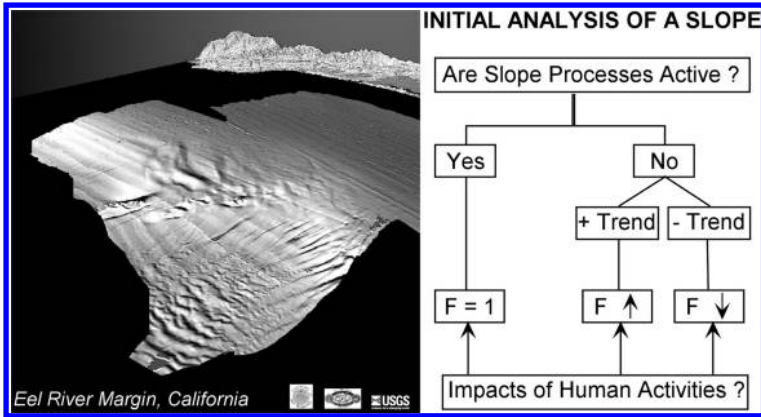
Figure 2. The initial analysis of the safety factor of a slope (F = Resisting Forces/Gravitational Forces) illustrated with a multibeam 3D view of the Eel River Margin off Eureka, California (multibeam image is from USGS, Locat 2001).
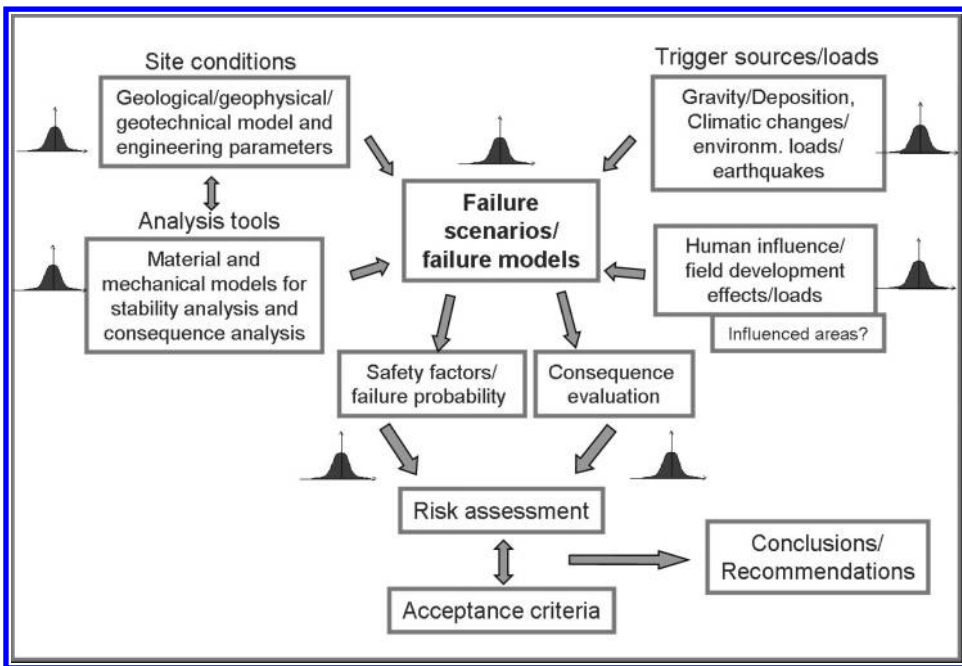
Figure 3. General framework for risk assessment for submarine slides.

estimated long term factor of safety must be close to unity.

Going from hazard to risk requires other considerations as shown by the general framework for risk assessment for submarine slides provided in Figure 3.

Detailed mapping and extensive studies of submarine slides in recent years have increased our knowledge immensely regarding slide morphology, extent and volume. However, there are still many unknowns concerning the triggering, development and dynamics of submarine slides and how various mechanisms relate to the geological setting.

The state-of-the-art in quantitative risk assessment for submarine slides is represented by the recent site-specific geohazards studies performed for the Storegga slide in the Norwegian Sea in connection with the

323

Ormen Lange gas field development, the Mad Dog and Atlantis licenses in the Sigsbee Escarpment in the Gulf of Mexico, the ACG and Shah Deniz licenses in the Caspian Sea, and several studies off the west coast of Africa. Furthermore, the large research programmes initiated by the European Commission (ENAM-I and -II, COSTA, EuroSTRATAFORM), European Science Foundation (Euromargins), and in North America (COSTA-Canada, STRATAFORM) have contributed greatly to enhancing our understanding of the processes involved in submarine mass movements. The methodologies adopted in some of these studies are reviewed below.

3 EXAMPLES OF RECENT SUBMARINE SLIDE RISK ASSESSMENT STUDIES

3.1 *Major research efforts*

One of the first steps in developing an approach to submarine slide risk assessment is to develop an understanding of the hazard itself, *i.e.* where, why and how submarine slides occur and what are their geomorphological and sedimentological signatures. This can only be achieved through major projects aiming at understanding submarine mass movements and their consequences. Since the early eighties, significant steps were taken as part of major national and international projects which have been directly related to the study of submarine mass movements. These projects have various acronyms: ADFEX (Arctic Delta Failure Experiment, 1989–1992), GLORIA (1984–1991, a sidescan survey of US Exclusive Economic Zone), STEAM (Sediment Transport on European Atlantic Margins, 1993–1996), ENAM II (1996–1999, European North Atlantic Margin), STRATAFORM (1995–2001, Nittrouer 1999), Seabed Slope Process in Deep Water Continental Margin (Northwest Gulf of Mexico, 1996–2004) and COSTA (Continental slope Stability) in Europe (2000–2004) and Canada (2000–2005). These various projects have clearly shown the extent and significance of submarine mass movements in all types of environments, as illustrated in the proceedings of the 1st International Symposium on Submarine Mass Movements and their Consequences (Locat & Mienert 2003).

As an example of such an inventory two maps are shown in Figures 4 and 5 showing the distribution of
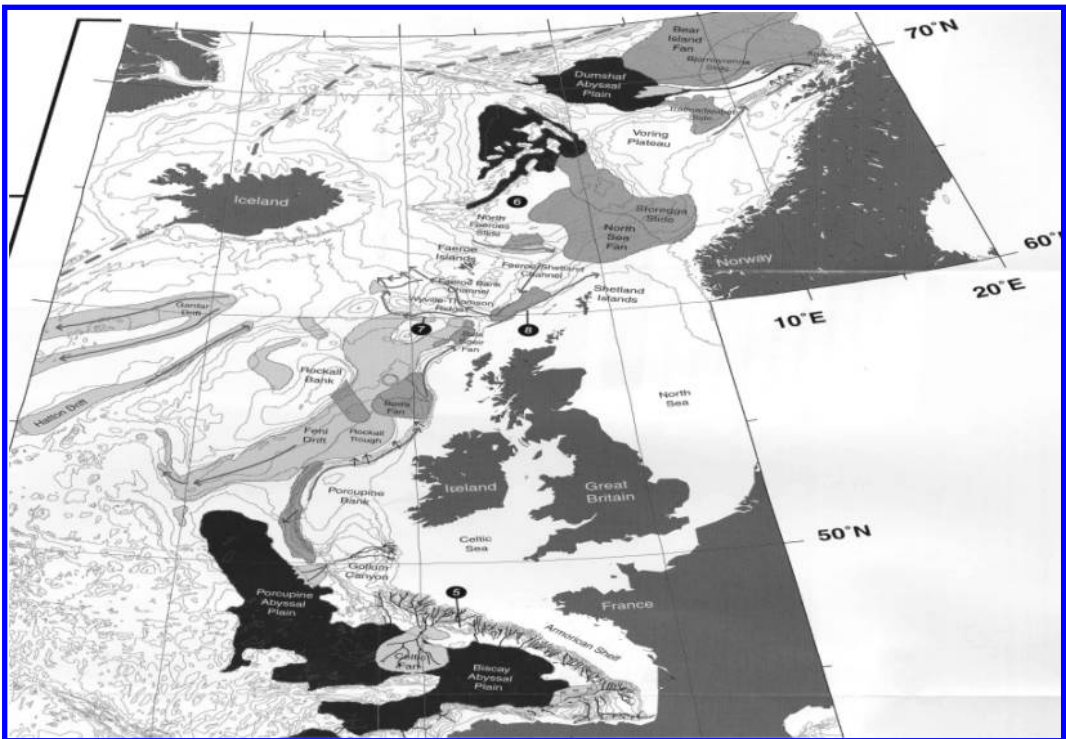

Figure 4. Distribution of various types of mass movements along the northern part of the Atlantic European margin (Weaver & Mienert 2003).

various types of mass movement deposits along the European margin.

In the same region, but also including the Mediterranean and Adriatic Sea, Canals *et al.* (2004) have presented a detailed picture of the various types of mass movements that have occurred from about 17,000 years ago (e.g. Canary Islands) until recently (Finneidfjord in 1996). As part of COSTA-Canada, Piper & McCall (2003) have produced an inventory of submarine mass movements along the Canadian Atlantic margin and St. Lawrence River System. The inventory includes the historical Grand Banks slide mass movements of 1929, which generated a tsunami killing 27 people in southern Newfoundland.

In the case of recent slides, like the Grand Banks (Canada 1929), Finneidfjord (Norway 1996) and in Nice (France 1979), consequences (e.g. coastal destruction of infrastructure and loss of lives due by tsunamis) can be quantified. For older events such as the Storegga slide, the consequences can be deduced from back-calculation of their size and slide dynamics, and the information could be used to estimate the potential consequences of such slides were they to take place today.

The on-going project Slope Stability of Europe's PAssive COntinental MArgins (SPACOMA) forms a part of the program EUROMARGINS, which was initiated by the European Science Foundation (ESF) and funded by the individual national research councils. The SPACOMA project is organized as cooperation among organizations from Norway, Germany, UK and Spain. The project has the following main research themes: (1) slide headwall development on upper continental slopes, (2) slope stability of river-influenced margins, (3) slope stability of glaciated margins, (4) geo-mechanical controls on slope stability and trigger mechanisms of submarine landslides, (5) numerical modeling of sediment break up, mobility and run out, and (6) slide frequencies in regions of long-term instability in relation to sea level change. A close link to global climatic change is expressed particularly in the last theme. The comparison between river-fed margins in the Mediterranean and glacial margins along NW Europe, with regards to sliding mechanisms is also an important part of the research. The project involves field studies and a huge slide north of Svalbard, the Norwegian Arctic, which was poorly known, has recently been mapped in detail with swath bathymetry systems.
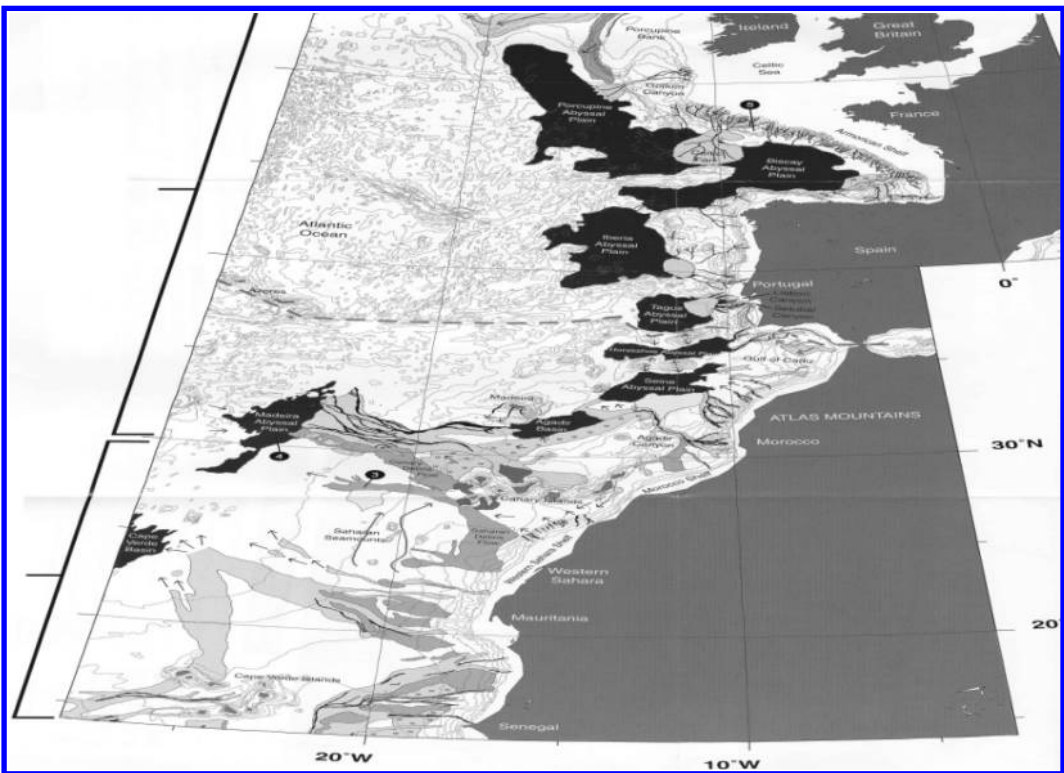

Figure 5.   Distribution of various types of mass movements along the southern part of the Atlantic European margin (Weaver & Mienert 2003).

325

Amongst all of these studies, only a few address directly the topic of risk assessment. As part of the COSTA Project, Leynaud & Mienert included reliability methods and Monte Carlo simulation to back-calculate the slide hazard for the Trænadjupet slide (Leynaud & Mienert 2003). Leroueil *et al.* (2003) have also developed the use of the geotechnical characterization of mass movement method as part of a risk assessment protocol (see section below about Saguenay Fjord).

3.2 *Probabilistic slope stability analyses for the Sigsbee Escarpment*

The development of the Mad Dog and Atlantis prospects in Gulf of Mexico included an integrated geohazard study which covered a variety of geological, geophysical and geotechnical subjects. Both prospect areas are located at the main geological feature in the area, the Sigsbee Escarpment. The challenges faced by the decision-makers in siting facilities along the Sigsbee Escarpment are described by Jeanjean *et al.* (2003). To assist the decision-making process probabilistic slope stability evaluations were performed for the Atlantis and Mad Dog prospects (Nadim *et al.* 2003).

The probabilistic slope stability analyses were performed for the most critical slopes in each area, for example Slump E in the Atlantis prospect. The starting point of the analyses was the critical failure mechanism identified in the deterministic slope stability calculations. For Slump E, this mechanism had a static safety factor of 1.52 (see Fig. 6). In the probabilistic analyses, the limit equilibrium model used in the deterministic analyses was coupled with the first-order reliability method (FORM) (Gollwitzer *et al.* 1988).

The following parameters were considered random in the analyses: submerged unit weight in each layer (total of 6 distinct soil layers with total thickness of 105 m were involved in the critical failure mechanism shown on Fig. 6), undrained shear strength parameters in each layer, removed overburden in each layer, removed overburden at toe of the slope, shear strength anisotropy and modeling uncertainty.

The probabilistic stability analyses gave a reliability index of $\beta = 3.34$ and a corresponding failure probability of $P_f = 4.2 \cdot 10^{-4}$ for the critical failure mechanism in Slump E. The variables contributing most to the total uncertainty were (in the order of importance):

1 Shear strength parameter in the deepest layer
2 Modeling uncertainty parameter
3 Strength anisotropy factor
4 Shear strength parameters in other layers (deep layers more important than shallow layers)
5 Removed overburden in deeper layers and at toe of slope
6 Submerged unit weights
7 Parameters describing the geometry of critical failure surface.

Probabilistic analysis of the critical slump at the Mad Dog prospect yielded a static factor of safety of 1.22 and a corresponding probability of failure of 0.1. This "static" probability of failure, however, must not be confused with the annual failure probability. To perform the risk evaluation for an offshore site, where the main hazard to the facilities is submarine slides, it is essential to establish a model of the slide frequency (i.e. the annual probability of slope failure). Clearly, computing a relatively large probability of static failure
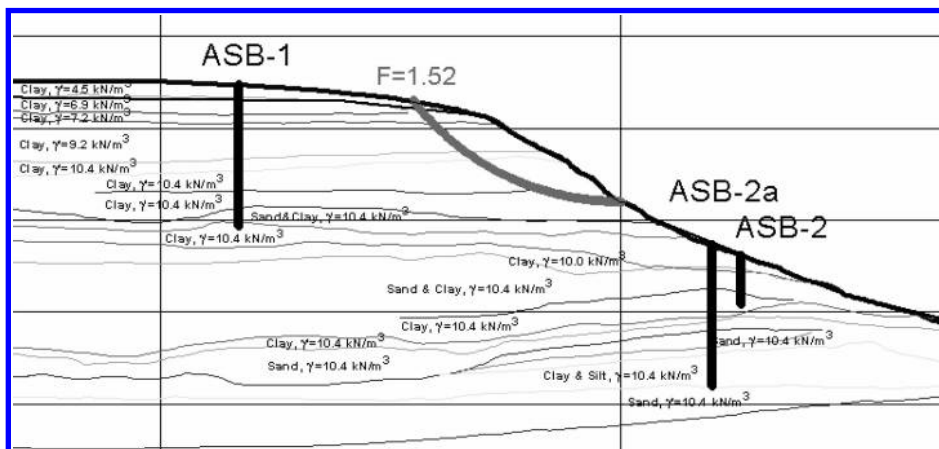

Figure 6. Soil layering, geotechnical boreholes and critical failure mechanism for Slump E in Atlantis prospect (Nadim *et al.* 2003).

begs the question about the annual probability of failure and its acceptability.

Nadim *et al.* (2003) employed different statistical (based on dating of sediments and estimating the elapsed time since the last major sliding event) and theoretical approaches (based on deterioration of safety margin for the estimated sedimentation rate) for estimating the annual failure probability. They showed that even the relatively high static failure probabilities estimated by FORM ($P_f = 0.1$) for the Mad Dog prospect translated into acceptably low annual failure probabilities ($P_{f,annual} = 10^{-4}$ to 10^{-6}).

For offshore sites, defining the acceptable level of failure probability is usually done by the "problem owners", i.e. the operating oil companies, certifying agencies and government authorities. Typically, an annual probability of failure of 10^{-4} or lower is considered acceptable as long as the consequences of failure are local. When there is potential for significant damage to 3rd parties as a result of slope failure, stricter acceptance criteria may be established by the authorities (see following example for slides in Storegga area).

3.3 *New slides in Storegga area*

The Ormen Lange field is the largest undeveloped gas field on the Norwegian Continental Shelf. The field is located in the Norwegian Sea in water depths of about 800–1,100 m. The field is situated approximately 120 km from the coastline, within the scar of the prehistoric Storegga slide (Fig. 7). The Storegga slide, which took place 8,200 years ago, is one of the world's largest known submarine slides with an estimated slide volume in excess of 3,000 km^3. Evidence of a major tsunami generated by the Storegga slide has been found along the coasts of Norway, Scotland and the Faeroe Islands.

Considering the enormity of the Storegga slide and the potentially catastrophic consequences of a similar event today, it was essential to clarify and quantify the risks associated with submarine slides in the area to obtain approval for field development from the authorities. A major effort was therefore undertaken to evaluate the stability situation of the slopes in the Ormen Lange area today, identify the areas/volumes that might be negatively affected by slope instability, and quantify the 1st party and 3rd party risks. The risk assessment study was a multi-disciplinary project and the following key activities were performed in connection with the slide risk evaluation (Bryn *et al.* 2004):

– Establishing a regional and local geological model
– Establishing an explanation model for the Storegga Slide
– Evaluation of static stability of the escarpments in the vicinity of the development area
– Evaluation of natural slide triggering mechanisms and their relevance for slide risk, based on:
  • Earthquake analyses
  • Gas hydrate studies and gas hydrate dissociation modeling
  • Pore pressure measurements and modeling
  • Evaluation of reservoir subsidence and its possible influence on the slope stability
  • Evaluation of the possible effect of an underground blow-out on the present day stability
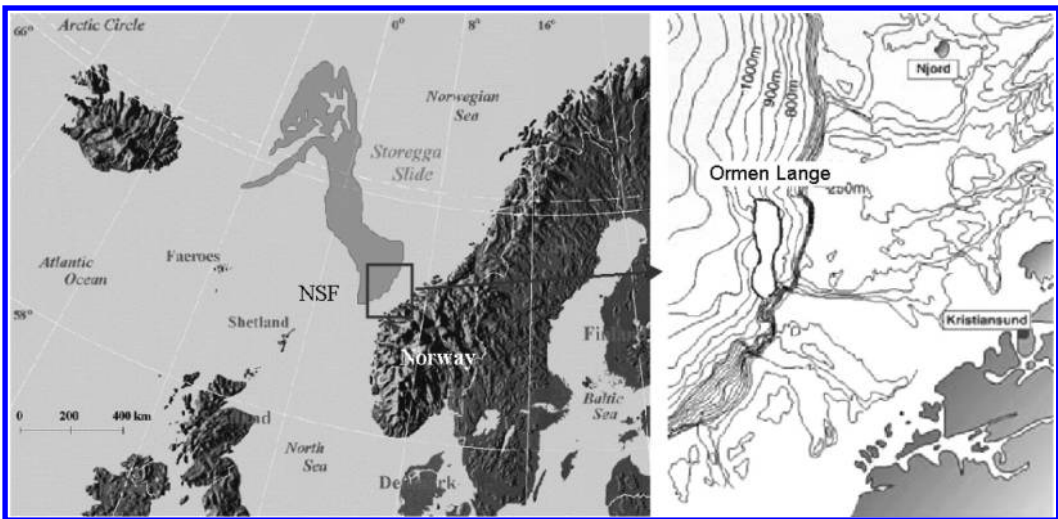

Figure 7. Location maps of the Storegga slide and the Ormen Lange field.

327

- Evaluation of the possible effect of the development activity on the local slope stability
- Dating the Storegga Slide and possible younger slide events in the area
- Evaluation of possible consequences of a new slide on the Ormen Lange field installations and for 3rd party (including run-out distances and tsunami analyses)
- Mapping of tsunami sediments onshore and in the fjords in Western Norway
- Establishing risk acceptance criteria and performing quantitative risk assessment
- External verification of work program and results.

Acceptance criteria for first party risk and environmental risk are mandatory for all offshore installations on the Norwegian Continental Shelf (NORSOK Standard Z-013: Risk and Emergency Preparedness Analysis, www.olf.no/norsok). The Ormen Lange field development is no exception in this context and conventional risk acceptance criteria were applied (Lund *et al.* 2004), i.e.

- The Group Individual Risk (GIR) shall not exceed 10^{-3} per year when at work. GIR shall be calculated for all defined personnel groups.
- The environmental risk acceptance criteria are based on the principle that the duration of environmental damage shall be insignificant compared to the expected time between such damages.

The main challenge for the Ormen Lange operator and partners was to formulate acceptance criteria related to risk to third party (i.e. the general public). Third party risk is normally not an issue for offshore activities. However, for the Ormen Lange field development the slide risk called for acceptance criteria limiting the risk exposure of the people living along the coastline from the potential Ormen Lange generated slide events.

Third party risk acceptance criteria are normally expressed as limitations on the risk to most exposed person and societal risk. This concept, however, is not well suited for evaluation of consequences of a tsunami generated by a submarine slide. The local variations in wave run-up along the coast and the general model uncertainties made it impossible to identify the most exposed person and predict (with any confidence) the consequences expressed as fatalities. The chosen criterion defined the risk as intolerable if the frequency of a slide with "significant damage potential" generated by Ormen Lange activities exceeds 10^{-7} per year. Significant damage potential was defined as a tsunami with vertical run-up exceeding 1.5 m in representative coastal areas. Risk-reducing measures must be considered if the frequency is greater than 10^{-7} per year.

The potential triggering mechanisms for inducing a submarine slide in the Ormen Lange area were extensively evaluated. Both natural and man-made triggers were considered, and only a strong earthquake was shown to be capable of triggering a new slide. The assessment of risks associated with slope instability consisted of the following steps (Nadim *et al.* 2005):

1. Evaluate the potential triggering mechanisms for initiating a new slide.
2. Identify the critical slopes along the upper and lower headwalls of the Storegga slide where new slides could be initiated.
3. Quantify the uncertainty in the soil shear strength in different soil units, the earthquake load effects.
4. Compute the probability of static slope failure and slope failure after a major earthquake.
5. Based on the evidence that the slopes have adequate static stability, update the computed failure probabilities.
6. Evaluate the annual probability of an earthquake-induced slide for the critical sections of the headwalls.
7. Evaluate the total probability of an earthquake-induced slide happening anywhere along the headwalls.
8. Evaluate the conditions required for a slide to generate a significant tsunami and estimate the probability for such conditions to be present.
9. Evaluate the annual probability of occurrence of a slide with 1st and/or 3rd party consequence based on the results obtained in Steps 6 and 7.

Steps 1 through 3 are described in Kvalstad *et al.* (2005), Steps 4 through 7 and Step 9 are described in Nadim *et al.* (2005), and Step 8 is described in Løvholt *et al.* (2005).

The potential slides were categorized into three consequence classes:

(a) **Major consequence slide**: A slide that could cause 3rd party damage. The sliding scenario of concern in this context is a tsunami generated by slide that causes wave impact in inhabited areas along the coast.
(b) **Medium consequence slide**: A slide with potential damaging effect in the development area. Either a deep cut outside the development area or run-out from a slide in the upper head wall may typically give medium consequences.
(c) **Small consequence slide**: The effect of a slide is local and only equipment and structures in the vicinity of the slide, for example a pipeline in the steep headwall would be affected.

The results of the risk assessment studies for the Ormen Lange field are provided in Lund *et al.* (2004), Bryn *et al.* (2004) and Nadim *et al.* (2005), and are summarized in Table 1 (after Guttormsen *et al.* 2003).

Table 1. Results of the risk assessment for new slides in Storegga area (Guttormsen *et al.* 2003).

Consequence class	Volume	Description	1st party consequence	3rd party consequence	Results of risk analyses ($P_{f,annual}$)
Major	100–3000 km^3	Regional mega-slides that related to glaciation – de-glaciation periods	Damage to structures, wells, pipelines and control cables	Tsunami wave that causes damage along the coast	Natural causes: None No project-generated risk
	5–100 km^3	Slide initiating from upper headwall of Storegga slide	Damage to structures, wells, pipelines and control cables	Tsunami wave that could cause damage along the coast	Natural causes: $<4 \cdot 10^{-8}$ No project-generated risk
Medium	<5 km^3	Slide initiating from upper headwall of Storegga slide	Severe damage to pipelines and control cables	None	Natural causes: $<2 \cdot 10^{-8}$ No project-generated risk
	<0.3 km^3	Shallow slide at upper headwall of Storegga slide	Local damage to pipelines and control cables	None	Natural causes: $\sim 10^{-5}$ No project-generated risk
Small	<0.02 km^3	Surficial slide at upper headwall of Storegga slide	Minor local damage to pipelines and control cables	None	Natural causes: $<<10^{-2}$ Choose best technical solutions to minimize project-generated risk

3.4 *Saguenay Fjord*

The Saguenay Fjord is located about 250 km to the north-east of Québec City. It has been carved by successive glaciers in an elongated shape about 90 km long, 2–5 km wide and up the 275 m deep (Fig. 8a). A major earthquake shook this area in 1663 and has left many landslide scars, both on land and on the sea floor (Urgeles *et al*. 2002, Locat *et al.* 2003). The overall approach for the risk assessment is described in Figure 9. This effort has, thus far, been focused on evaluating the hazard component of the risk assessment. Although this has not been studied in any detail, one could speculate that the actual consequences of submarine mass movements in the Saguenay Fjord are limited mostly to the western end, where the industrial zone is developed and where there are more people living along the coast.

Some examples of these landslides are shown in a segment of the Saguenay Fjord in Figure 8b. The figure shows the intense degree of mass wasting which, most likely, took place as a result of the 1663 earthquake (except may be for one case indicated by the letter 'A' in Fig. 8b). The intensity of the shaking was such that most of the failed material was remolded and flowed in the central part of the basin. The high anisotropy created by a strong layering (*i.e.* thin sand layers sandwiched in clayey layers) has, most likely, favored an almost complete remolding of the failed material. Syvitski & Schafer (1996) use the term "basin collapse" for this situation with many slides scars to illustrate the large extent of landsliding as a result of the earthquake.

The detailed mapping of the landslides (partly shown in Fig. 8) has revealed that more than 30 landslide scars were created as a result of the 1663 earthquake. The submarine slides along the Saguenay Fjord are mostly concentrated in the upper part, which is shown in detail in Figure 8b. The slide hazard assessment has required the inventory of submarine mass movements (shape, size), identification of the slide mechanism, and analysis of the variability of the geotechnical properties in both failed and unfailed areas (Levesque 2005). The overall risk assessment approach is described in Figure 9. This effort has, thus far, been focused on the hazard component of the risk assessment. The approach is comprised of three components. The first one is related to the geo-investigations, which are needed to establish both the geological and the geotechnical models. The next component illustrates the use of the "Geotechnical Characterization of Mass Movements" methodology (Leroueil *et al.* 1996) as an integrated part of the hazard assessment, which is done as the third component.

3.5 *Other studies*

Many of the recent advances in risk assessment for offshore slopes have been achieved through consulting projects financed by oil and/or energy companies. The results of these studies have not been published, except in confidential reports, but the knowledge gained by the consultants involved in the projects has been extremely valuable for the advancement of the state-of-the-art.

Examples are studies carried out by IFREMER and NGI offshore Angola, Congo and Nigeria; offshore geohazards studies for oil companies active in Gulf of Mexico, Caspian Sea, Black Sea, Mediterranean Sea,
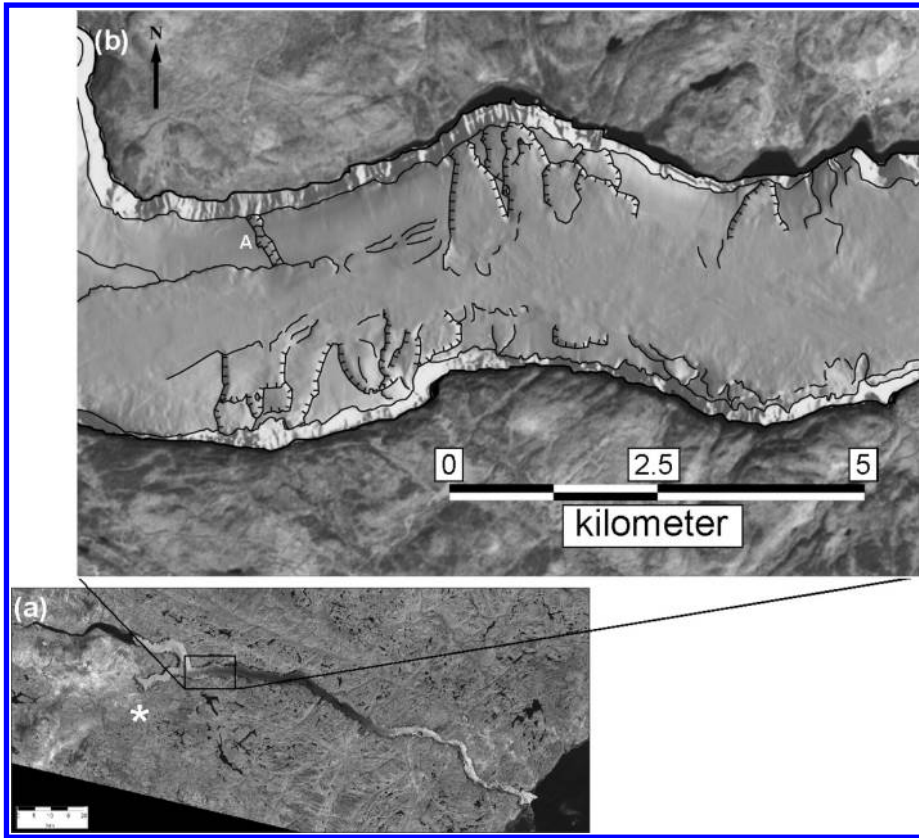
Figure 8. Distribution of submarine mass movements in the Upper Saguenay Fjord. The slide scar in 'A' may have been formed by the 1988 magnitude 5.7 earthquake with the epicenter at about the location shown by '*' in (a) (modified after Levesque *et al.* 2004).

offshore Indonesia, and Gulf of Bengal; and the recent seabed stability evaluation performed by Golder Associates for BC Hydro in connection with new submarine cables from Vancouver to Vancouver Island.

4 RECOMMENDED PRACTICE FOR RISK ASSESSMENT FOR SUBMARINE SLIDES

The approach adopted for risk assessment for submarine slides and other offshore geohazards depends on the elements at risk and consequences of sliding. A general approach that could be applied in all situations is neither logical nor desirable.

Typically, offshore geohazards evaluation requires a staged approach. In the first phase a close cooperation among geologist, geotechnical engineers, geophysicists, and seismologists is required to:

– Establish the geological model of region (age and source of sediments)

– Evaluate in-line and cross-line shallow and deep seismics in region
– Identify main stratigraphy and buried features
– Identify signs of slide activity. Are the slides recent, or older buried features?
– Identify active faults in the area of interest
– Evaluate bathymetric information and seabed inclination and morphology
– Identify recent slide scars, fluid escape features, pock marks, mud volcanoes
– Look for signs of seabed instability, special features etc. upslope and downslope of the area of interest
– Establish whether there is earthquake activity in area.

The first assessment of geohazard situation is done on the basis of above evaluations and should address the following questions:

– Are there elements at risk, locally or regionally, from submarine mass movements?
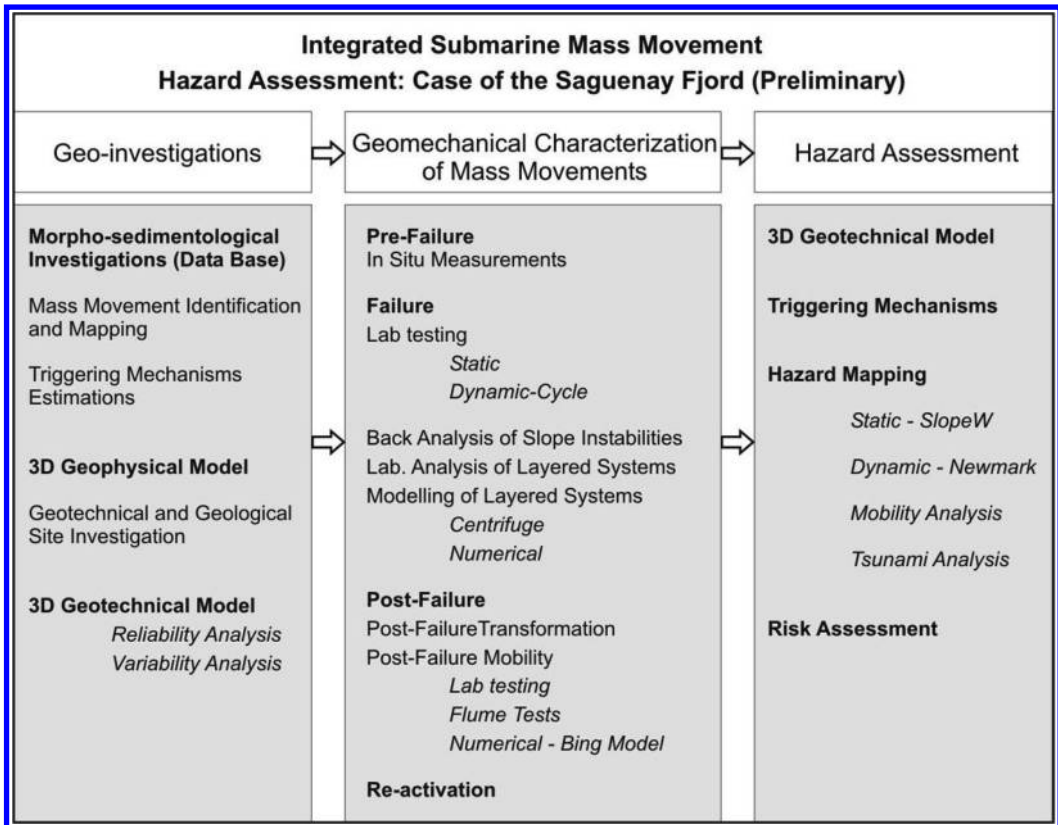
330

Figure 9.   Overall approach for hazards assessment in the Saguenay Fjord region.

– What are the potential triggering mechanisms for seabed instability?
– What is slope stability situation in high gradient areas?
– Is there need for better information? i.e.
  • Should one obtain more information outside the main region of interest, for example detailed bathymetric maps upslope and downslope?
  • Are additional/extended seismic profiles required?
  • Is there need for high quality geotechnical data and pore pressure measurements?

The second phase of evaluations typically includes:

– Evaluation of 3D seismics, well logs, detailed shallow seismics, detailed bathymetry and side scan sonar
– Re-interpretation of seabed morphology and potential signs of instability and slide mechanisms
– Evaluation of pore pressure conditions, signs of overpressure
– Planning and drilling geo-borings to acquire site-specific soil data. Focus should be on shear strength and brittleness (sensitivity) of soils

– Assessment of deposition rate and potential for excess pore pressure
– Establish occurrence frequency vs. magnitude of earthquakes, mud volcano eruptions etc
– Establish whether other ongoing natural processes, such as erosion and diapir displacements, are present.

The second assessment of geohazards situation for petroleum exploitation projects typically involves the following steps:

– Study the field development plans and associated geohazard failure scenarios
– Evaluate heat flow through wells and its potential for gas hydrate melting
– Evaluate the potential for underground blow-outs
– Evaluate reservoir subsidence and potential for induced earthquakes
– Is there human influence on the geohazards situation, e.g. installation of structures, anchors, pipeline supports etc
– Is there need for quantification of failure probability and risk? If yes, is sufficient information available?

331

– Identify final site investigation program if sufficient information is not available, e.g. locations of geo-borings, field and laboratory testing and interpretation, need for pore pressure measurements, local bathymetric surveys/pipeline corridors.

Depending on the outcome of the second geohazards assessment, a final geohazard evaluation may be required. This involves the following steps:

– Select relevant failure scenarios and associated trigger mechanisms
– Identify, describe and quantify relevant trigger sources; magnitude and frequency
– Develop geo-model of the area: stratigraphy, bathymetry, relevant soil data and their uncertainty
– Apply geomechanical models for analysis of failure scenarios (stability analyses, finite element analysis, fluid flow, heat flow, slide run-out, etc.) and assess model uncertainty
– Evaluate annual probability of failure
– Evaluate physical consequences of failure (loss of support, slide run-out and impact, tsunami generation and impact, etc.) and associated damage
– Calculate risk contribution of all geohazard failure scenarios
– Are the calculated probabilities and risk within clients' and authorities' acceptance criteria? If not, what actions could be taken to mitigate the risk?

The main challenges that face us today are related to risk assessment for deep and ultra-deep sites. Our knowledge, technology and tools required for deep and ultra-deep water site investigations have improved significantly in the past decade. However, further improvements in the following areas are needed to reduce the uncertainties:

– Geophysical/geological and geotechnical site investigation techniques
– Control on possible deepwater effects on soil behavior in situ and effect of sample disturbance
– Location and quantification of gas hydrates
– Tools and methodology for prediction and measurement of pore pressures
– Interpretation of sediment rate, stress conditions, pore pressure conditions
– Field measurements, monitoring, and early warning
– Analysis tools for assessment of seabed instability and failure probability
– Material models, mechanical models and analysis tools for stability assessment
– Slope stability and dynamic slide mechanisms (progressive and retrogressive failure)
– Effect of earthquake loading on soil strength and post-earthquake stability
– Gas hydrates effects on soil behavior
– Probabilistic methods and quantification of uncertainty

– Analysis tools and methods for evaluation of consequences, e.g.
  • slide dynamics and run-out
  • slide velocity and impact
  • tsunami generation, impact and run-up.

ACKNOWLEDGEMENTS

REFERENCES

Bryn, P., Kvalstad, T.J., Guttormsen, T.R., Kjærnes, P.A., Lund, J.K., Nadim, F. & Olsen, J. 2004. Storegga slide risk assessment. *OTC 16560, Offshore Technology Conference '04, Houston*, Texas, 3–6 May.

Canals, M., Lastras, G., Urgeles, R., Casamor, J.L., Mienert, J., Cattaneo, A., De Batist, M., Haflidason, H., Imbo, Y., Laberg, J.S., Locat, J., Long, D., Longva, O., Masson, D.G., Sultan, N., Trincardi, F. & Bryn, P. 2004. Slope failure dynamics and impacts from seafloor and shallow subseafloor geophysical data: case studies from COSTA project. *Marine Geology*, 213: 9–72.

Favre, J.L., Barakat, B., Yoon, S.H. & Franchomme, O. 1992. Modèle de risque de glissements de fonds marins. *6th International Symposium on Landslides*, Bell (ed.), Balkema: 937–942.

Gollwitzer, S., Abdo, T. & Rackwitz, R. 1988. FORM (First-Order Reliability Method) *Manual*, RCP GmbH, Munich, Germany.

Guttormsen, T.R., Bryn, P., Berg, K. & T.J. Kvalstad 2003. Ormen Lange Field Development. *Fjellsprengningsteknikk-Bergmekanikk/Geoteknikk 2003*, Oslo, Norway (in Norwegian).

Hampton, M.A., Lee, H.J. & Locat, J. 1996. Submarine landslides. *Reviews of Geophysics* 34: 33–59.

Jeanjean, P., Hill, A. & Taylor, S. 2003. The challenges of confidently siting facilities along the Sigsbee Escarpment in the Southern Green Canyon area of the Gulf of Mexico – Framework for integrated studies. *OTC 15156, Offshore Technology Conference '03, Houston*, Texas, 5–8 May.

Kayen, R.E. & Lee, H.J. 1991. Pleistocene slope instability of gas hydrate-laden sediment on the Beaufort sea margin, *Marine Geotechnology* 10: 125–141.

Kvalstad, T.J., Berg, K., Bryn, P., Wangen, M., Nadim, F., Forsberg, C.F. & Gauer, P. 2005. The Storegga slide: Evaluation of triggering sources and slide mechanics. *Special issue of Marine and Petroleum Geology on Ormen Lange.*

Lee, H.J., Locat, J., Dartnell, P., Israel, K. & Wong, F. 1999. Regional variability of slope stability, application to the Eel Margin, California. *Marine Geology* 154: 305–321.

Leroueil, S., Locat, J., Levesque, C. & Lee, H.J. 2003. Towards an approach for the assessment of risk associated with submarine mass movements. In: *Submarine Mass Movements and Their Consequences*, Locat & Mienert (eds.), Kluwer Academic Publisher, pp. 59–67.

Leroueil, S., Vaunat, J., Picarelli, L., Locat, J., Lee, H. & Faure, R. 1996. Geotechnical characterization of slope movements, *Proceedings of the 7th International Symposium on Landslides*, Trondheim, Balkema, Rotterdam, 1: 53–74.

Levesque, C. 2005. Contributions to the risk assessment evaluation of submarine mass movements in the Saguenay Fjord, Québec, Canada. *Ph.D. Thesis*, Laval University, in prep.

Levesque, C., Locat, J., Leroueil, S. & Urgeles, R. 2004. Preliminary overview of the morphology of the Saguenay Fjord with a particular look at mass movements. *Proceedings of the 57th Canadian Geotechnical Conference*, Québec City, Session 6G, 23–30.

Leynaud, D. & Mienert, J. 2003. Slope stability assessment of the Trænadjupet slide area offshore the mid-norwegian margin. In: *Submarine Mass Movements and Their Consequences*, Locat & Mienert (eds.), Kluwer Academic Publisher: 255–265.

Locat, J. 2001. Instabilities along Ocean Margins: A Geomorphological and Geotechnical Perspective. *Marine and Petroleum Geology* 18: 503–512.

Locat, J. & Lee, H.J. 2002. Submarine landslides: advances and challenges. *Canadian Geotechnical Journal* 39: 193–212.

Locat, J., Martin, F., Locat, P., Leroueil, S., Levesque, C., Konrad, J.-M., Urgeles, R., Canals, M. & Duchesne, M.J. 2003. Submarine mass movements in the Upper Saguenay Fjord (Québec, Canada), triggered by the 1663 earthquake. In: *Submarine Mass Movements and Their Consequences*, Locat & Mienert (eds.), Kluwer series on Natural and Technological Hazards 19: 497–508.

Locat, J. & Mienert J. 2003. *Submarine Mass Movements and Their Consequences. 1st International Symposium*. Kluwer Academic Publishers, 540 p.

Løvholt, F., Harbitz, C.B., Haugen, K.B. & Bondevik, S. 2005. A parametric study of tsunamis generated by submarine slides in the Ormen Lange/Storegga area off western Norway. *Special issue of Marine and Petroleum Geology on Ormen Lange*.

Lund, J.K., Olsen, J., Bryn, P., Brekke, G., Guttormsen, T.R., Kvalstad, T.J. & Nadim, F. 2004. Slide risk assessment in the Ormen Lange Field development area. *The Seventh SPE International Conference on Health, Safety, and Environment in Oil and Gas Exploration and Production*.

Nadim, F., Krunic, D. & Jeanjean, P. 2003. Probabilistic slope stability analyses of the Sigsbee Escarpment. *Procs, OTC 15203, Offshore Technology Conference '03, Houston*, Texas, May 2003.

Nadim, F., Kvalstad, T.J. & Guttermsen, T. 2005. Quantification of risks associated with seabed instability at Ormen Lange. *Special issue of Marine and Petroleum Geology on Ormen Lange*.

Piper, D.J.W. & McCall, C. 2003. A synthesis of the distribution of submarine mass movements on the eastern Canadian margin. In: *Submarine Mass Movements and Their Consequences*, Locat & Mienert (eds.), Kluwer Academic Publisher: 291–298.

Syvitski, J.P.M., Burrell, D.C. & Skei, J.M. 1987. *Fjords: Processes and Products*. Springer-Verlag, New York, 379 p.

Syvitski, J.P.M. & Schafer, C.T. 1996. Evidence for an earthquake-triggered basin collapse in Saguenay Fjord, Canada. *Sedimentary Geology* 104(1–4): 127–153.

Urgeles, R., Locat, J., Lee, H. & Martin, F. 2002a. The Saguenay Fjord, Québec, Canada: integrating marine geotechnical and geophysical data for spatial seismic slope stability and hazard assessment. *Marine Geology* 185: 319–340.

Weaver, P.P.W. & Mienert, J. 2003. *European Margin Sediment Dynamics Side-Scan Sonar and Seismic Images*, Springer, New York, 310 p.

333

Risk assessment for very large natural rock slopes

Ch. Bonnard
Ecole Polytechnique Fédérale de Lausanne, Switzerland

J. Glastonbury
Parsons Brinckerhoff, Godalming, Surrey, England

ABSTRACT: The risk posed by mass movements from large natural rock slopes is inherently related to the deformation behaviour prior to, at and following failure, as movement may impact on persons and/or property on or close to the toe of the slope. This paper examines the characteristics of large natural rock slope failures and discusses those attributes identified to be of influence on the deformation behaviour. A risk framework considering these factors is introduced. The discussion on characteristics and behaviour of large natural landslides is then considered against current practice for landslide risk assessment in various communities. The aspects of risk management in such cases are also addressed.

1   INTRODUCTION

1.1   *Background and context*

The mortality rate associated with landslides in Italy over the course of 1999 was calculated to be 0.14 deaths per 100,000 people (Guzzetti 2000) – a figure not dissimilar to the rate for workplace accidents (0.70). These figures emphasise the need for improved methods of landslide risk assessment, especially as tourism development is intensively extending on or at the toe of large landslide zones, especially in the Alps.

The assessment of risk associated with failure of any slope must necessarily involve an examination of the probability and consequences associated with that failure. The consequences associated with failure of large rock slopes are inherently a function of (amongst other things) the:

- Extent of warning related to slope deformations prior to failure;
- Volume of the failed mass;
- Deformation behaviour at failure;
- Post-failure travel distance and velocity.

However, there are several attributes, chiefly relating to the physical characteristics and deformation behaviour, which are particular to large natural rock slopes. It is these attributes that form the focus of the first part of this paper and they are considered in light of current risk management practices adopted in various communities.

This paper deals in particular with the examination of the characteristics and behaviour of large volume landslides (typically in excess of 1 million cubic metres and often 10 to 100 million cubic metres) derived from rock slopes, and with the possible management strategies in the potentially affected zones.

1.2   *Specific aspects of risk from large natural rock slopes*

The risk posed by landslides from large natural rock slopes is distinct from that of other mass movements in many ways including:

1 Typically much larger slide volumes;
2 Variability in character due to size and interlocked mechanisms;
3 Often extremely mobile debris movement as evidenced by extremely long travel distances.

The large size of these landslides is such that there is often a direct development or habitation on the slide mass or in close proximity to the slide mass and consequently a high temporal exposure of persons. For instance, eight villages are located on the Lugnez landslide in Switzerland implying a high tourism potential (Noverraz et al. 1998).

Their size also means that there is often substantial spatial variation in characteristics, typically illustrated in terms of distinct differential internal movement, even in the case of translational slides such as

335

the case quoted above. This spatial variability also often results in a high level of epistemic uncertainty due to limits on investigation and analysis.

Further compounding the risk presented by large rock slope failures, there are innumerable cases through history of long run-out of debris from specific classes of mass movement. The potential for long travel distances from various classes of rock landslide results in increased spatial exposure of elements at risk.

Arguably the most effective approach to management of this risk first involves development of an understanding of the characteristics and behaviour of the various types of large rock landslide, requiring one to analyse several scenarios of possible failure mechanisms and run-out with different probabilities of occurrence.

1.3 *Current practice, challenges and limitations*

Will a landslide fail in a rapid, brittle manner or will it deform in a slow, ductile manner? What warning signs can be expected prior to collapse?

Current industry or engineering practice is such that significant time and resources are spent investigating and understanding the behaviour of features that show very apparent geomorphological signs of mass movement, mainly because they worry the population. In many instances this effort is warranted, however in some cases the distinct geomorphological signs of movement may also indicate a reduced brittleness within the slide mass. Consequently, this well-investigated feature may no longer present the highest risk to surrounding communities.

Many authors, including Heim (1932), Varnes (1978), Hutchinson (1988) and Hungr et al. (2001) have developed classification schemes for mass movements, with general velocity ranges for various types of movement. It is generally accepted that the class of mass movement or mechanism (eg: translational rock slide) is a primary determinant in the behaviour of a slide mass at failure. However, this alone must be considered an inadequate basis for predicting the deformation behaviour of a landslide mass, as proved by many well studied cases like La Frasse Landslide (Noverraz & Bonnard 1990, Laloui et al. 2004).

1.4 *Approach*

The diverse characteristics and relatively infrequent occurrence of large landslides derived from natural rock slopes are such that probabilistic methods for predicting their behaviour are generally of limited value.

Perhaps the most reliable, if not precise, method for predicting the behaviour of a landslide, before trying to model its movement, is by recognition of the

general characteristics and relating these to deformation behaviour based on precedence (e.g. Hungr & Evans 2004).

It is this approach that has formed the basis for much of the work presented in this paper. The following sections summarise the results of examination of a very large database of landslides, divided into general categories based on maximum velocity immediately following failure. These characteristics are then used as a basis for formulation of a risk assessment framework.

2 LARGE SLOW NATURAL LANDSLIDES

2.1 *General characteristics*

In the development of a landslide risk assessment framework, Glastonbury & Fell (2002a) examined a large database of rock slope failures recognised to have exhibited velocities in the slow, very slow and extremely slow ranges – collectively referred to in this study as "slow" (ie: velocity immediately following failure less than 13 metres per month according to the velocity system presented in IUGS 1995).

Classification was based on geomorphological evidence of a long history of slide movement without evidence of "rapid" movement. Many of the slides also had a long history of deformation monitoring, extending sometimes to more than a century.

Five classes of slow landslide derived from rock slopes were identified in this study, with their general characteristics summarised in Table 1. Diagrammatic illustrations of three particularly well-represented classes of slow landslide, namely debris slides, earth-flows and complex slides, are presented in Figures 1, 2 and 3.

Common features across the dataset of "slow" landslides include:

1 Pre-sheared (residual strength) basal surfaces of rupture;
2 Inclination of the basal surface of rupture less than the laboratory measured residual friction angle;
3 Translational movement with varying degrees of internal deformation, hence little change in shear stress with displacement;
4 Slide masses of low rock mass strength with varying degrees of disaggregation;
5 Minimal influence of lateral margins either because of slide disaggregation or geometry;
6 With the exception of one slide, all "slow" cases were either reactivated or long-term active slides. The exception was a first-time failure on a pre-sheared rupture surface; and
7 Slide movement was largely controlled by fluctuations in piezometric pressures with varying levels of sensitivity.

336

Table 1. Observed characteristics of "slow" rock landslide classes.

Characteristic	Earthflows	Debris Slides	Translational Block Slides	Complex (Internally Sheared) Slides	Rotational Slides
General geology	Argillaceous sedimentary strata	Highly anisotropic rock with faulting/folding	Sedimentary – horizontally bedded	Sedimentary – horizontally bedded	Massive cap-rock over argillaceous strata
Slide mass characteristics	Highly disaggregated, low P-wave velocity Clay fraction = 30–40%	Highly disaggregated, low P-wave velocity GP/GM	Predominantly intact	Variable – some intact, some disaggregated	Variable disaggregation dependent on age
Surface of rupture characteristics	Rotational at rear, then planar. CI/CH infill	Foliation shears/crush zones with CL/CI infill	Follow argillaceous layers	Horizontal bedding in argillaceous layers	Rotational mass failure in argillaceous layer
Surface of rupture inclination, α	Parallel to ground surface – 10–20°	Parallel to ground surface – 15–30°	Sub-horizontal (0–5°)	Basal surface = 0–5° Rear surface = 50–70°	Variable – rotational Vertical in cap-rock
α versus ϕ_r*	ϕ_r approx 1–3° > α	ϕ_r approx 1–3° > α	ϕ_r approx 3–4° > α	ϕ_r approx 5° > α	Rock mass failure
Lateral margin influence	Minimal	Minimal	Variable but low influence	Variable but low influence	Unknown – likely minimal
Water influence	Higher influence in track & accumulation zones	Greater influence on scarp slope failures	Significant for intact faster slides. Minimal for disaggregated slides.	Significant – seasonal reactivations	Minor
Slide history	Reactivated/Active	Reactivated/Active	Reactivated/Active	Reactivated/Active	Active
Internal deformation	Minor $$80% of movement on basal surface	Multiple internal shears 60–70% on base	Minor – retrogressive behaviour	Major – bi-planar and rotational	Not apparent
Typical velocity range	0.1–100 mm/day	0.01–20 mm/day	0.01–20 mm/day	0.1–30 mm/day	0.03–5 mm/day
Other comments	General compression trend	Slide expansion related to valley development. General extension trend	Retrogressive behaviour common	Variable nature of internal shearing. Small graben wedges (<25%)	Commonly associated with progressive valley development.

* α = Inclination of basal surface of rupture; ϕ_r = residual friction angle on basal surface of rupture
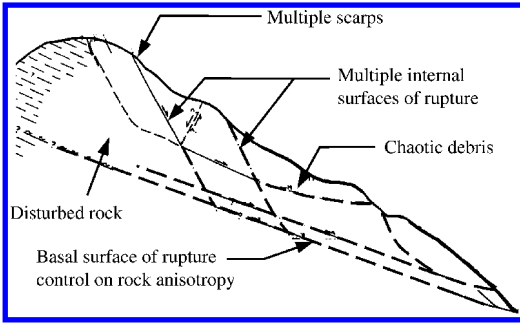
337

Figure 1. Cross-section through typical debris slide showing general geomorphological features.
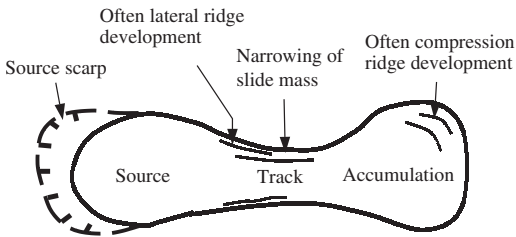

Figure 2. Diagrammatic plan view illustration of earthflow showing general geomorphological features.
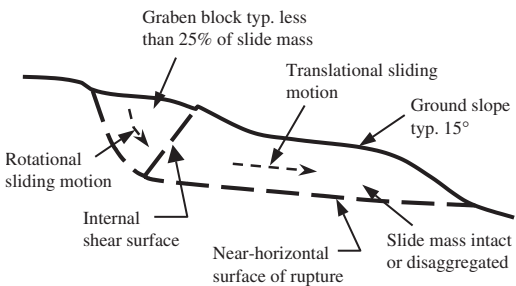

Figure 3. Typical observed characteristics of "slow" complex (internally sheared) slide.

Class specific factors of influence on "slow" slide behaviour include:

1 Low rock mass strength in complex (internally sheared) slides or the presence of suitably oriented pre-sheared defects such that internal shearing was of a ductile nature;
2 Geometry of complex (internally sheared) slides such that internal shearing occurs towards the rear of the slide mass and graben wedges are small in relation to total slide volume (<25%);

3 Low rock mass strength in relation to normal stress levels resulting in ductile yielding of low strength argillaceous strata beneath cap-rock in translational block slides; and
4 The rate of natural development of a slope appears to influence the rate of movement of some slow slides. This was observed in debris slides and is likely of influence in translational block slides.

Some of the identified characteristics may perhaps be unexpected but they are reflective of a carefully assembled and analysed database.

2.2 Deformation behaviour of slow slides

2.2.1 Earthflows

Surface and subsurface displacement monitoring data were examined particularly for the earthflow and debris slide cases. This monitoring data was considered alongside geomorphological evidence of past movement.

In the case of earthflows, it was observed that typically 80–95% of maximum surface movement was measured as shear on lateral margins and 70–85% on the basal rupture surface indicating that earthflows typically show minimal internal deformation. This would suggest a general translational sliding behaviour, despite geomorphological indications of possible flow behaviour (such as hourglass slide shapes and ridges suggesting wave like movement).

The behaviour of earthflows, as with other classes of slow slides, was found to be closely linked to fluctuations in groundwater level. Glastonbury & Fell (2002a) examined published data for several earthflow cases and observed that the relative sensitivity of the slide to fluctuations in groundwater level was possibly related to velocity of movement of the earthflow (amongst other things).

Using an infinite slope analysis approach, various factors of safety were calculated for the range of groundwater levels recorded in the slide. These factors of safety were then related to the measured displacement rates at the time of groundwater measurement. Faster moving earthflows showed an apparently reduced sensitivity to groundwater changes as illustrated in Figure 4, possibly as a result of undrained or rate dependent strength effects or as a result of slide mass properties. Original source reference details for each of the cases included in Figure 4 are presented in Glastonbury and Fell (2002a).

Figure 4 illustrates that 10-fold changes in earthflow velocity were observed to occur in response to changes in factor of safety ranging from as little as 1.3% (La Chenaula) up to 16.3% (La Mure). La Chenaula slide had typical velocities in the range of 0.01 to 0.5 mm/day compared to La Mure with 0.1 to 7 mm/day, with intermediate velocities for other slides.
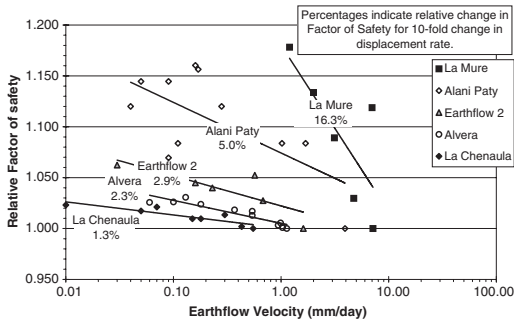
338

Figure 4. Relative factor of safety versus velocity for earthflow database cases.
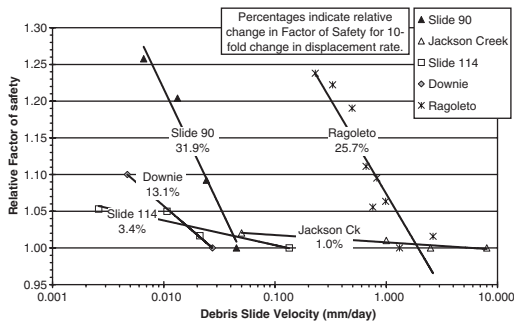

Figure 5. Relative factor of safety versus velocity for debris slide database cases.

2.2.2 Debris slides

Debris slides were observed to exhibit maximum velocities typically between 0.1 and 10 mm/day. Comparisons of surface and subsurface monitoring reveal that velocity typically decreases with depth and shear across the basal surface of rupture accounts for approximately 50–90% of total measured surface movement. Distinct variations in behaviour were also noted across the surface of debris slides, with decreases in velocity and total displacement moving towards the slide head and towards the lateral margins. This monitored deformation behaviour of translational debris slides clearly indicates that internal deformation is a distinct component of movement in this particular class of slide.

Stability analyses were conducted for the debris slides, again using an infinite slope model and relating measured groundwater levels to the various observed slide velocities. A selection of results is presented in Figure 5, with more detailed results presented in Glastonbury & Fell (2002a). Original data source details for each of the cases included in Figure 5 are also presented in this reference. It should be noted that data in some cases was provided under a confidentiality

agreement, hence a slide numbering system was adopted rather than naming in these instances.

It was observed that the sensitivity of debris slides to fluctuations in groundwater level varied considerably. Several slides within the debris slide database exhibited 10-fold changes in velocity associated with changes in factor of safety of less than 1%. While others showed a reduced sensitivity to groundwater fluctuations sometimes exhibiting 10-fold changes in velocity due to change in factor of safety of 20% or more.

Further discussion on the possible reasons for this range of sensitivities is presented in Glastonbury & Fell (2002a). One apparent factor separating relatively high sensitivity and low sensitivity slides appears to lie in the relationship between surface of rupture and rock mass anisotropy.

Typically, those cases of sliding parallel to rock mass anisotropy (including Ragoleto, Slide 90 and Downie) required in excess of 10% change in factor of safety to induce a 10-fold change in velocity. In contrast, cases involving basal sliding at an angle to rock mass anisotropy required less than 5% (and often less than 1%) change in factor of safety to induce a 10-fold change in displacement rate (including Jackson Creek and Slide 114). This apparent difference in sensitivity is possibly related to differences in the influence of field scale asperities on the surface of rupture. Many debris slides have a brittle character and produce extremely rapid movements.

3 LARGE RAPID NATURAL LANDSLIDES

3.1 General characteristics

The characteristics of rock slope failures that attained "extremely rapid" velocities during failure (ie: velocities greater than 1.8 m/sec) were determined based on examination of a large dataset of cases.

The vast majority of these cases (82%) were classified either as translational slides or complex (internally sheared) slides. Differences in behaviour and characteristics were observed within each of these categories, resulting in a need to further discretise these general mechanism classes. Diagrammatic illustrations of the identified subset classes are presented in Figure 6. Summary characteristics of these and the other "rapid" slide classes are presented in Table 2.

Characteristics identified within this dataset that suggest an increased likelihood of "rapid" post-failure velocity include:

1 Shear movement on peak strength basal (eg: rough translational slides) or lateral (eg: large rock glides) surfaces or brittle failure of high strength buttress elements (eg: toe buckling translational).

339

Table 2. Observed characteristics of "rapid" rock landslide classes.

Slide Characteristics	Translational Slide Classes				Complex (internally sheared) Slide Classes				Rock Falls
	Large Rock Glide	Rough Translational	Planar Translational	Toe Buckling	Bi-Planar Complex	Curved Complex	Toe Buttress Complex	Irregular Complex	
General geology	Sedimentary (esp. carbonate)	Anisotropic rock mass	Sedimentary (esp. carbonate)	Sedimentary	Variable – anisotropic	Folded sedimentary terrains	Anisotropic rock mass	Irregular – disturbed rock mass	Brittle cap rock over argillaceous strata
Slide mass characteristics	Very thick (several hundreds of metres), generally intact	Some disaggregation	Intact	Intact	Often highly fractured	Structure parallel to slope	Often highly fractured	Often partly fractured	Intact
Characteristics of surface of rupture	Pre-sheared, bedding defined	Stress relief joints	Pre-sheared, bedding defined	Pre-sheared, bedding defined	Bi-planar, pre-sheared	Curved, pre-sheared	Upper surface pre-sheared	Irregular geometry	Rotational geometry in low strength rock
Surface of rupture inclination, α*	Very low (10–20°)	40°+	Typ 20–30°	Typ 30–40°	$\alpha_L = 20–30°$	$\alpha_L = <30°$	$\alpha_L = 10–25°$	$\alpha_{av} = 5–50°+$	Variable – rotational
Surface of rupture inclination versus ϕ_r	$\alpha \approx \phi_r$	α typ 10–30° greater than ϕ_r	α typ within 5° of ϕ_r	α typ within 5° of ϕ_r	$\alpha_L \approx \phi_r$	α_L typ 2–3° less than ϕ_r	α_L typ 5° less than ϕ_r	α typ within 5° of ϕ_r	Variable
Surface of rupture asperity influence	Minimal	High	Minimal	Minimal	Some	Minimal	Minimal	High	Likely some
Lateral margins	High influence	Moderate influence	Moderate influence	Low influence	Variable	Unknown	Unknown	Unknown	Moderate
Water influence	Unknown	Some	Common	Some	Some	Some	Limited	Unknown	Some
First time/ reactivated	First-time	Predominantly first-time	Both	First-time	Both	Both	Both	Both	First-time
Slope history (dominant cause)	Glacial debuttressing	Fluvial & glacial	Fluvial erosion	Fluvial erosion	Glacial	Fluvial & glacial	Fluvial & glacial	Fluvial & glacial	Fluvial
Pre-collapse signs	Very Limited	Limited	Limited	Limited	Unknown	Some	Common	Limited	Common

* α = Inclination of basal surface of rupture; α_L = Inclination of lower or basal surface of rupture in complex slide (as opposed to rear surface of rupture)
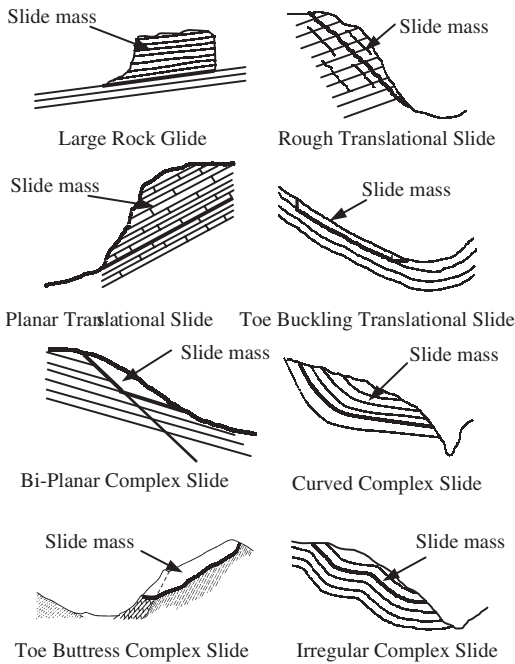ϕ_r = residual friction angle on basal surface of rupture

Figure 6. Recognised sub-classes of translational and complex (internally sheared) rockslides in database.

2 Brittle internal shearing in "rapid" complex slides typically occurred at a high angle (approaching perpendicular) to rock mass anisotropy;

3 Little disaggregation of slide masses in both translational and complex slides;

4 Graben wedges of "rapid" complex slides were typically in excess of 50% of the total slide volume (in contrast to the slow slides with less than 25%); and

5 Basal rupture surface inclination (α) was observed to be typically 0–10° higher than laboratory measured residual friction angles (considered to be equivalent to an effective basic friction angle on the surface of rupture). This would suggest additional restraint for these slides through asperities on rupture surfaces and/or buttress restraint by rock masses.

Other general characteristics observed from the database of rapid slide cases are presented in Table 2.

3.2 *Lessons from studies on excavated and natural rock slopes*

Observations of the deformation behaviour of large natural landslides prior to collapse include audible rock noise, local cracking, slumping and rockfalls and changes in the hydrological regime surrounding the slide. Such observations were recorded by Heim (1932), Hadley (1978) and Hendron & Patton (1985).

The management of risk from the failure of large rock slopes must necessarily involve consideration of the deformation behaviour prior to collapse. Sufficient warning of impending slope collapse provides opportunity to remove vulnerable persons and facilities from the potential runout path.

It is widely accepted that prediction of time of collapse of a rock slope is only possible when the slope reaches a stage of accelerating displacement (Saito 1965, Voight et al. 1989, Fukuzono 1985) as depicted in Figure 7.

Various attempts have been made to predict the time of collapse of a rock slope based on extrapolation of monitoring data, with limited success (Zavodni & Broadbent 1980, Kennedy & Niermeyer 1970), but in some specific cases with a good success such as at Randa for the second stage of the rockfall in May 1991 (Noverraz & Bonnard 1992).

Most prediction methods are based on acceleration, velocity or displacement criteria and extrapolation of displacement-time curves by fitting suitable functions. However, the use of displacement-defined criteria is considered limited in that larger landslides are expected to undergo greater movement prior to collapse than small landslides (assuming all other things are equal).

In a study of the pre-collapse behaviour of excavated rock slopes, undertaken by Glastonbury and Fell (2002b), strain (where displacement is normalised against the downslope length from slide crown to tip) was found to be a more appropriate parameter for comparison of slope behaviour. However, variations in the commencement and duration of monitoring meant that direct comparison of measured strain was limited. Conversion of displacement rates to strain rates provided a direct means of comparison of deformation behaviour leading to collapse.

Pre-collapse monitoring data for several rock slides (of varying failure mechanism) were examined in this study. Data relating to translational and toppling failures is presented in Figures 8 and 9, while data on other mechanisms is provided in Glastonbury and Fell (2002b). Source reference details for each of the cases denoted in Figures 8 and 9 are presented in Glastonbury & Fell (2002b).

The data presented in Figures 8 and 9 is considered alongside the relationship proposed by Saito (1965) based on tests on failure of laboratory samples and observed failures in soil slopes. It is apparent from the data presented in Figures 8 and 9 that differences in pre-collapse behaviour exist between mechanisms, with toppling failures (Fig. 9) lying closer to the Saito range when compared to translational failures (Fig. 8).

Glastonbury & Fell (2002b) concluded that a single mathematical form of equation (eg: power or exponential function) could not adequately model all types
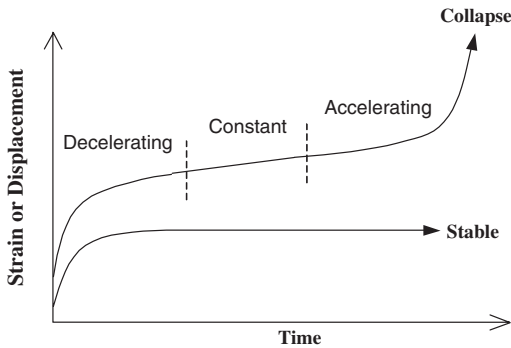
341

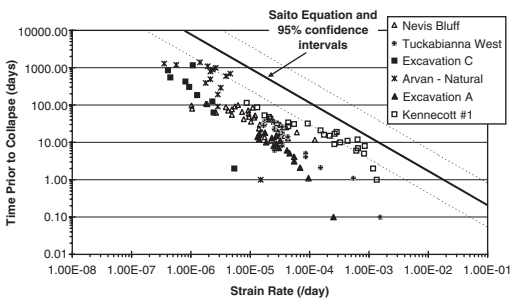Figure 7. Recognised displacement – time stages for landslides.

Figure 8. Relationship between strain rate and time prior to collapse for translational slides in excavated rock slopes.
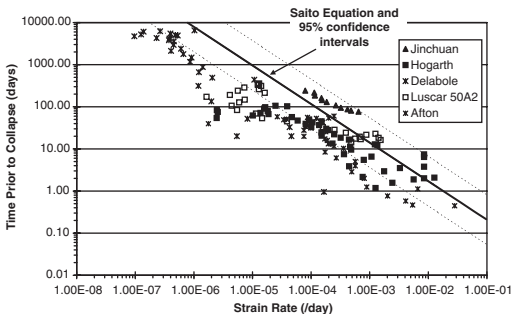
Figure 9. Relationship between strain rate and time prior to collapse for toppling failures in excavated rock slopes.

of failure mechanism due to fundamental differences in the mechanics of deformation.

Rotational failures have a general tendency towards a more stable geometry with increasing displacement. Hence, it would be expected that the strain rate behaviour leading up to collapse would reflect this. In contrast, toppling failures move towards a less stable geometry with displacement and would therefore be
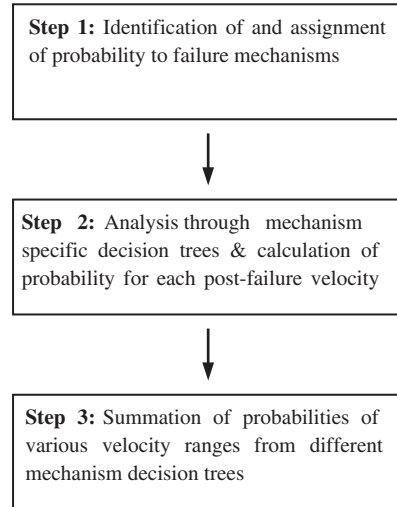
Figure 10. General structure of decision analysis framework.

expected to show a greater increase in strain rate immediately prior to collapse than other failure mechanisms. Translational and complex (internally sheared) failures undergo comparatively little change in stress with displacement and hence the relationship between strain rate and time to collapse is expected to be intermediate between that observed in toppling and rotational failures.

Glastonbury & Fell (2002b) also observed that accumulated strain prior to collapse (calculated by integration of the function between time and strain rate) varies depending on slide characteristics. More ductile slides (including those on pre-sheared rupture surfaces) were observed to exhibit generally larger pre-collapse strains than similar cases on peak strength rupture surfaces. Also, differences in behaviour were observed for translational slides with argillaceous rupture surfaces, possibly as a result of strain rate effects.

4 RISK FRAMEWORKS

The assignment of probability to a complex event, such as the prediction of post-failure velocity of a landslide, is arguably most readily achieved by decomposition of the problem into smaller, simpler events, using a decision tree system. This approach allows the ability to incorporate the inherent uncertainty in some input parameters and also the level of confidence in input data (reflecting methods of measurement). The general structure of the framework is summarised in Figure 10.

342

The decision framework developed in this study for post failure velocity prediction has two essential components:

1. Matrices for assisting in calculation of probability of a particular failure mechanism; and
2. Mechanism specific decision trees and supporting matrices for each node within the decision trees.

It is evident from the earlier study of "slow" and "rapid" slides that the post-failure velocity of a landslide is primarily related to the source, magnitude and rate of strain weakening. The framework structure is reflective of this observation, with fundamental differences in deformation behaviour between and within failure mechanisms derived from differences in rupture surface characteristics, slides mass characteristics, lateral and toe restraints and triggering factors. This framework presents a systematic method for assessment of this strain weakening in the absence of detailed quantifiable data.

Initial investigations in this work indicated that failure mechanism is a primary determinant in the pre- and post-failure deformation behaviour of a rock slope. The first step in this framework therefore involves identification of the failure mechanism, based on:

1. Analysis of monitored displacement behaviour;
2. Geomorphology of the slide mass within the regional context;
3. Surface and subsurface geology;
4. Past-performance indicators, such as similar slides in close proximity.

The probability calculated for each failure mechanism should reflect the amount and quality of available data. For instance, a failure mechanism determined purely on the basis of geomorphological indicators would naturally have a higher uncertainty associated with it than a case determined on the basis of detailed surface and subsurface geotechnical investigations.

Separate decision trees have been developed for each of the main failure mechanisms observed within this study. The structure of each of these trees is reflective of observations and conclusions drawn from the initial rock slope database study. The decision tree for the case of translational rock slides is presented in Figure 11, while other mechanism specific decision trees and their supporting matrices are presented in Glastonbury & Fell (2002c).

Calculated mechanism probabilities are then applied to each of the relevant mechanism decision trees. Within each tree, probabilities are then assigned to various decisions such as:

- Is the basal rupture surface at residual strength?
- Are geological conditions such that high piezometric pressures will be sustained on sliding?
- Are lateral or toe buttress restraints present?

Probabilities are assigned to these "yes" or "no" decisions with the help of information matrices, and again the value reflects the confidence or uncertainty based on available data and method of assessment.

Probabilities (conditional on failure of the landslide occurring) are presented at the end of each decision tree branch for each of four general velocity classes based on the IUGS system (IUGS 1995). These probabilities have been determined based on analysis of the historic performance of more than 200 rock slope failures and also on the understanding of each of the failure mechanisms examined and judgement of the relative importance of various factors.

Various "anchor" points (in terms of slide characteristics) were established through the studies of rapid and slow slides. These anchors were used as starting points at the uppermost and lowermost branches of the decision trees and high probabilities of rapid or slow movements were attributed to these branches. Some range in behaviour existed within these rapid and slow slide datasets and assessment of the relative importance of various factors could be established, enabling the identification of various intermediate anchor points.

The probabilities determined along each branch of the decision trees are multiplied with the conditional velocity probabilities at the end of each branch to give four calculated post-failure velocity probabilities.

Finally, the probabilities for each velocity range are summed across all identified possible failure mechanisms or scenarios to give a total probability for each velocity range.

In current engineering practice much effort is concentrated on the investigation and analysis of slides that have obvious geomorphological signs. However, it is apparent from this study that these slides are inherently more likely to move slowly compared to first-time slides. This framework allows comparison between first-time and reactivated slides and particularly highlights those characteristics that suggest an increased probability of a high post-failure velocity.

The system allows the user to identify landslide characteristics of particular influence, identify areas of uncertainty within the knowledge of a particular landslide, quickly reassess cases as knowledge improves and finally establish a relative ranking of landslides in terms of risk, thereby enabling better allocation of limited resources for investigation and stabilisation.

It has to be noted that the probability values given in Figure 11 are conditional on failure of the landslide occurring and these are not temporal probabilities so their value does not depend on the time period considered.
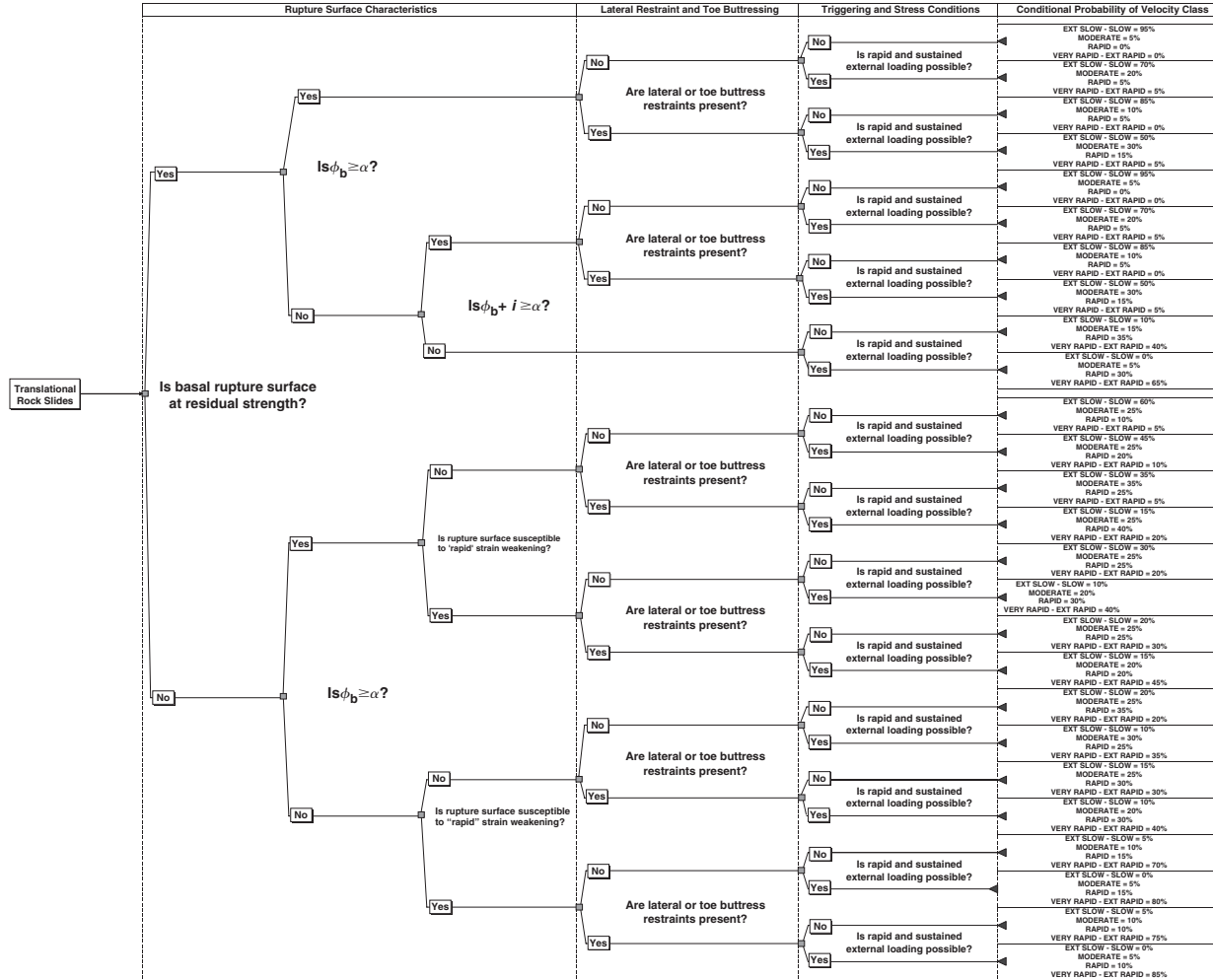
343

Figure 11. Decision tree for translational rock slides (ϕ_b = basic friction angle on surface of rupture, i = relevant field scale dilation angle on surface of rupture, α = inclination of basal surface of rupture).

5 COMMUNITY RISK MANAGEMENT PRACTICE

5.1 Meaning of risk related to large landslides for mountain communities

It has to be recollected that large landslides tend to have very low probability of critical global movement, whereas the potential consequences of such movement may be catastrophic (Bonnard et al. 2004).

Moreover several extreme scenarios may be possible with various consequences. Therefore the population of the potentially affected mountain communities and their authorities tend to react either in a too optimistic way (the risk is nearly denied) or in a too pessimistic way (a prohibition to build is declared in extensive areas, or a part of the population decides to leave the exposed areas after the occurrence of a minor threat). It is therefore difficult to measure the real impact of a proper risk assessment process on the local development of an exposed community, mainly because the practical or political measures adopted by the authorities are not founded on a transparent and systematic approach.

The lack of objective information or the growth of an uncontrolled feeling of panic may then lead to the execution of protection works which rarely do control the stability problems or really reduce the hazard levels in some parts of the exposed zones, but allow the local authorities to preserve a good conscience thanks to visible actions. Another perception of the risks involved may imply a clear minimization of the risk by the inhabitants, referring to the fact that their ancestors have never been confronted by such a threat. This case often occurs when another type of hazard, like snow avalanche, is much more pronounced, so that the landslide risks are ignored.

5.2 Possible attitudes when facing large landslide risks

The population of mountain communities and their local authorities may basically adopt three different attitudes whenever they accept to recognize the existence of a potential landslide risk:

- They may judge the situation with fatalism, taking the very low probability of the landslide phenomenon into account, and decide to carry out no specific action. Such an attitude is perceived as unacceptable in developed societies, but may exist in communities that feel submitted to the power of nature.
- They may express a clear will to oppose the risks and take practical protection measures to limit their intensity or reduce their impact. When facing large landslides, that headstrong attitude is generally unrealistic, except maybe in a few cases where

the protection of land against natural hazards is assessed as a first priority, like in Japan.
- Between the two attitudes mentioned above, the correct way to manage landslide risks implies to take their possible occurrence into account in local planning, by a delimitation of the potentially exposed zones according to different scenarios, by the adoption of appropriate measures depending on the vulnerability of the threatened properties and by organizing mitigation actions. This responsible attitude is the only sensible one, but requires good information to the population and their active participation.

5.3 Consideration of direct and indirect impacts in land planning

When facing a situation of large landslide risk, communities may suffer direct or indirect potential impacts that will affect them locally or at a regional scale. Under direct consequences are of course included physical damage to buildings, infrastructure and equipment, leading either to destruction, partial failure of even excessive deformation, like the tilting of a house. The social impacts, i.e. fatalities, injured persons, families affected by the loss of their houses, are also obvious direct consequences. But environmental impacts also have to be taken into account, such as the damage to protection forests that play a major role in reducing snow avalanche risks. All these direct potential impacts need to be analysed separately as independent risk components at a local scale, not only because it is not appropriate to add their intrinsic values (expressed in terms of monetary value, number of lives and environmental resource), but also because the possible management actions that can be carried out to mitigate each type of impact are clearly different.

The fourth aspect of risks, i.e. the economic impacts related to the indirect consequences of a large landslide event, implies an assessment not only at a local scale, but also at a regional scale. Indeed the occurrence of a major landslide damming a valley causes considerable economic consequences even if the implied sources of production are not directly affected by the disaster. An interruption of communication lines, a threat on tourism activities, the possibility of extreme flooding in the valley downstream of the landslide following overflow, imply real impacts that need to be assessed in the master plans of the concerned regions or cantons even though they may be analysed as a rare event. In such a case an appropriate management policy at the level of the exposed communities requires a global view and evaluation of all the possible consequences that may affect the region upstream and downstream of the landslide site. It has to be remembered, with respect to other hazards such as snow avalanches, that the indirect economic

consequences may represent a global value exceeding 2 to 3 times the cost of the direct damage, on the basis of an assessment following the disaster of the winter 1999 in Switzerland (SLF 2000).

5.4 *Typical actions to manage large landslide risks at the level of the commune*

5.4.1 *Large slides*

In the case of large slides with perpetual movement on which villages have been located for several centuries, it appears that the initial positioning of the most ancient houses was quite adapted, in zones that do not display differential movements corresponding to the limits of secondary landslide mechanisms (DUTI 1984). However the large growth of these villages due to the tourism activity, combined with a lack of long-term observation of the behaviour of the ground and with a wish to select building sites more for their view of the mountains than for their quality, has caused several critical situations leading to major damage to buildings inappropriately built (large masonry structures, cuts in slope causing reactivations of surface movements).

The first appropriate local planning measure consists in the production of a detailed landslide map indicating all the secondary scarps and the potential reactivation mechanisms, in order to discriminate low, medium and high level hazard zones. A provision for an increased hazard level zone some 20 m wide along the localized scarps is appropriate.

A second measure calls for the requirement of rigid raft foundations for the buildings that may bear horizontal movements without displaying major cracks in the walls, if they are well built and of limited size.

A third measure must require flexible connections for the water and sewage pipes, especially near the buildings and the secondary scarp zones. These requirements imply to accept the risks related to the regular movements of the slide mass, which of course need to be regularly monitored, so as to detect an eventual acceleration phase early enough.

The possibility of a critical acceleration of the whole slide mass may exist, but generally with such a low probability that the local planning does not take this risk explicitly into account, as it would induce the evacuation of the village. The eventual residual risks related to a major crisis, that will certainly be anticipated in due time by the monitoring program, are dealt with in the framework of emergency measures (evacuation of the population). However it is important that the population and the persons investing in the area are aware of such a situation, which is indeed rarely the case (Bonnard et al. 2004a).

5.4.2 *Large rapid rock slides*

When a large rock slide zone poses a threat to an existing village at the toe of a slope, but with a very small probability of occurrence, the village should not necessarily be evacuated, but the various potential scenarios must be studied in detail, as it is often observed that limited falls of rock blocks may be triggered at a significant return period (e.g. below 100 years), whereas a major rock slide scenario will imply a much larger return period (e.g. above 1,000 years). In such a case it is clear that a prohibition zone for building development may be introduced in the local management plan to control the risks related to falls of rock blocks, and will be accepted by the population. It may consider either the maximum limit reached by the simulated block trajectories, which ensures the safety of any person outside the buildings, or the limit corresponding to a low value of energy (e.g. 30 kJ) that a simple wooden chalet may support without damage (OFAT, OFEE, OFEFP 1997).

When such limited rock block fall phenomena are concerned, it may be possible to install fairly efficient protection measures, by earth dams or nets, but these works will not protect the community against larger rock slope failures and thus tend to develop a false feeling of safety.

For scenarios implying large rock slide masses, no efficient protection works can be carried out and the only possible solutions are either the evacuation of endangered houses or the building of a tunnel to protect a road (Amatruda et al. 2004). In such cases it is generally not possible to rely on alarm systems to mitigate the risk.

Major difficulty arises when a rockfall zone implies a progressively increasing risk with time due to the slow evolution of the mechanism, like at Sedrun village in Switzerland (Bonnard et al. 2004a) (Fig. 12). The population below cannot rely on its past experience to judge the risk as negligible and the local

Figure 12. View on the Cuolm da Vi landslide (the whole mountain behind the creek is moving) posing a threat to the village of Sedrun in Switzerland. The uncertain mechanism of development of the phenomenon and the absence of preliminary rockfall events or debris flow events lowers the perception of risk among the population.

346

authorities cannot take any serious precaution measures without severely affecting the development of the area. In such cases, besides a monitoring program that is indispensable, some protection works might delay the impact of the phenomenon on the village and leave some more time for evacuation. But again, such works may give an inappropriate feeling of safety to the population.

In some cases for which the risk is assessed as high enough, an evacuation of the exposed zone may be decided, but it is always difficult to enforce such a decision in a permanent way.

5.5 *Differences in risk management policies between several alpine countries*

Within the IMIRILAND Project (Bonnard et al. 2004), a comparison has been established between the tendencies observed in risk management policy in several European countries. Indeed, it is not possible to state that each country has formulated a specific risk management policy regarding landslides, as the consideration of these phenomena in town and country planning rather depends on the regional or cantonal authorities, in particular in Italy and Switzerland. However some major trends may be mentioned.

In Italy, the regions are entitled to deal with landslide risk problems and dispense the necessary technical know-how, but a homogeneous way to define risk levels does not exist yet. Within a new project called IFFI, an inventory of landslide hazards has been carried out at the national level and principles for landslide management in land-use planning are proposed. However the real management mainly depends on local authorities that do not always dispose of the required technical capabilities (Ramasco 2005).

In Austria, a fairly homogenous classification of landslide hazard zones, similar to the types of zones used for snow avalanches, has been adopted. However, in terms of local management, the system proposed is not yet applied everywhere and implies only qualitative levels.

In Switzerland the landslide hazards are classified in a homogeneous way (see SOA6) and the consideration of hazards in land planning is progressing at the cantonal level following the requirements of federal laws. But the Swiss recommendations for the consideration of landslide hazards in the land-use planning framework do not specify the explicit use of the notion of risk, except for some specific objects for which a detailed risk assessment is required (OFAT, OFEE, OFEFP 1997). They only establish a link between the three main hazard levels and the corresponding recommended planning measures. The concept of risk is nevertheless present, as for the existing buildings located in hazard zones that present a deficit of protection, the rate of accepted potential damage for various return periods depends on their value and importance.

Finally, in France, the PPR hazard mapping including the consideration of all types of hazard and the corresponding potential of damage is underway and should be completed in a few years. The principles of such action are established at the national level, but its application depends on the regional and local authorities. It has to be observed that the notion of acceptable risk, when facing a clearly identified hazard, is not legally recognized, as it is required to take all necessary measures to mitigate the risks involved.

5.6 *Importance of cultural background in large landslide risk management*

Beyond the different techniques and concepts used in landslide risk assessment and management that can always be discussed (Fell & Hartford 1997), it is important to remember that one of the main aspects controlling the reaction of the population to the related restrictions of freedom in land-use planning rules is the physical experience of any type of hazard that the inhabitants may have had. Persons who have actually been confronted by a risk situation are more inclined to accept the necessities of prevention and mitigation measures, whereas the inexperienced persons, like the tourists coming from "landslide-free" countries, often oppose the safety measures imposed by the local authorities. In the same way, the local authorities that do not have a proper perception of potential landslide risks may oppose the requirements imposed by the regional or cantonal authorities to apply strict prevention measures in case of low probability events.

On the other hand, a distinction in landslide risk management may be made between "void" countries or regions, qualified as such because they dispose of a large reserve of open undeveloped land, and "full" countries or regions, in which the development of human and economic activities has reached such a level that the resources of open land are quite scarce. In the first category, it is easy to achieve a higher level of safety by evacuating buildings or villages exposed even to a low risk, because it is possible to find other safer places for a new development; Canada is one example of such a type of country. In the second category, a higher level of risk is accepted for existing villages, because it is generally not possible to find an alternative place to create a new settlement; Italy is one example of such a type of country. The experience of the new village created after the Vajont disaster, far from its original mountainous setting, is a sad illustration of what should not be done to prevent landslide risks, by depriving the population of its roots and its socio-cultural background.

347

6 CONCLUSIONS

This paper illustrates some unique aspects of landslide risk posed by large natural rock slopes that may affect the safety of people, properties and the environment, as they often imply volumes of some tens to hundreds of million cubic meters. It highlights the importance of understanding and recognising several factors which influence the level of risk from this class of landslide. These factors first include the characterization of the failure mechanism and its influence on rates of movement at and following failure. Then an appropriate identification of the pre-failure deformation behaviour is essential, especially in the perspective of long term risk management of the communities exposed.

An appreciation of these aspects of the behaviour, based on a detailed understanding of numerous precedent cases, selected all over the world and divided into two "slow" and "rapid" categories, provides a way forward for effective management of risk from large natural rock slopes. This first step includes the elaboration of decision trees allowing the quantified expression of different possible behaviours or scenarios that will be considered in the risk management strategies.

This approach is useful as in many cases, the population tends to minimize the risks involved, preferring to promote tourism development that is not easily compatible with a clear information on risks. The selection of different scenarios that are more or less likely to occur allows an objective assessment of the respective potential consequences and the adoption of prevention measures for the most probable hazards. A clear understanding of the potential mechanisms also insures the development of appropriate monitoring systems that will be the basis for mitigation actions (warning systems and evacuation plans) in case of an extreme potential event.

It has to be remembered that the attitude of the population, when facing large landslide risks, is not homogeneous and depends on the political systems and on the cultural background. It is thus important that strategies of risk management correspond not only to the characteristics of the landslides but also to the expectations of the citizens.

ACKNOWLEDGEMENTS

REFERENCES

Amatruda, G., Castelli, M., Forlatti, F., Hürlimann, M., Ledesma, A., Morelli, M., Paro, L., Piana, F., Pirulli, M., Polino R., Prat, P., Ramasco, M., Scavia, C. & Troisi, C., 2004. The Ceppo Morelli rockslide. In: Identification and mitigation of large landslide risks in Europe. Advances in Risk Assessment. Imriland Project. Balkema, Leiden, pp. 181–225.

Bonnard, Ch., Forlatti, F. & Scavia, C. (eds.) 2004. Identification and mitigation of large landslide risks in Europe. Advances in Risk Assessment. Imriland Project. Balkema, Leiden, 317p.

Bonnard, Ch., Dewarrat, X. & Noverraz, F. 2004a. The Sedrun Landslide. In: Identification and mitigation of large landslide risks in Europe. Advances in Risk Assessment. Imriland Project. Balkema, Leiden, pp. 227–252.

DUTI 1984. Projet d'Ecole Détection et Utilisation des Terrains Instables, rapport d'activité à fin 1983. Chapitre 7 sur les glissements de la region d'Hérémence (Valais). Ecole Polytechnique Fédérale de Lausanne, pp. 39–84.

Fell, R. & Hartford, D. (1997). Landslide Risk Management, in Landslide Risk Assessment, Cruden & Fell (eds.), Balkema, Rotterdam, pp. 51–110.

Fukuzono, T. 1985. A new method for predicting the failure time of a slope. Proceedings, Fourth International Conference and Field Workshop on Landslides, Tokyo, pp. 145–150.

Glastonbury, J. & Fell, R. 2000. Report on the analysis of "rapid" natural rock slope failures. UNICIV Report No. R-390, The University of New South Wales, Sydney. ISBN 85841 357 4.

Glastonbury, J. & Fell, R. 2002a. Report on the analysis of slow, very slow and extremely slow natural landslides. UNICIV Report No. R-402, The University of New South Wales, Sydney. ISBN 85841 369 8.

Glastonbury, J. & Fell, R. 2002b. Report on the analysis of the deformation behaviour of excavated rock slopes. UNICIV Report No. R-403, The University of New South Wales, Sydney. ISBN 85841 370 1.

Glastonbury, J. & Fell, R. 2002c. A decision analysis framework for assessing post-failure velocity of natural rock slopes. UNICIV Report No. R-409, The University of New South Wales, Sydney. ISBN 85841 376 0.

Guzzetti, F. 2000. Landslide fatalities and the evaluation of landslide risk in Italy. *Engineering Geology* 58(2): 89–107.

Hadley, J.B. 1978. Madison Canyon Rockslide. Montana, USA. In Voight (ed.), Rockslides and Avalanches, Elsevier, Amsterdam, pp. 167–180.

Heim, A. 1932. Bergsturz und Menschenleben (Landslides and Human Lives). Translation by N. Skermer. BiTech Publishers Ltd, Vancouver, Canada.

Hendron, A.J. & Patton, F.D. 1985. The Vaiont Slide, A geotechnical analysis based on new geologic observations of the failure surface. US Army Corps of Engineers Technical Report GL-85–5.

Hungr, O. & Evans, S.G. 2004. The occurrence and classification of massive rock slope failure. *Felsbau* 22: 16–23.

Hungr, O., Evans, S.G., Bovis, M. & Hutchinson, J.N. 2001. Review of the classification of landslides of the flow type. *Environmental and Engineering Geoscience* VII: 221–238.

Hutchinson, J.N. 1988. General Report: Morphological and geotechnical parameters of landslides in relation to geology and hydrogeology. In Bonnard (ed.) Proceedings, Fifth International Symposium on Landslides, Lausanne, Switzerland, Balkema. Vol. 1, pp. 3–35.

IUGS – International Working Group, Landslides 1995. A suggested method for describing the rate of movement of a landslide. Bulletin of the International Association of Engineering Geology 52: 75–78.

Kennedy, B.A. & Niermeyer, K.E. 1970. Slope monitoring systems used in the prediction of a major slope failure at the Chuquicamata Mine, Chile. Proceedings of the Symposium on Planning Open Pit Mines, Johannesburg, South Africa. Balkema, pp. 215–225.

Laloui, L, Tacher, L., Moreni, M. & Bonnard, Ch. 2004. Hydro-mechanical modelling of crises of large landslides: application to the La Frasse Landslide. Proceedings, Ninth International Symposium on Landslides, Rio de Janeiro, Vol. 2, pp. 1103–1108. Taylor & Francis, London.

Noverraz, F. & Bonnard, Ch. 1992. L'écroulement rocheux de Randa, près de Zermatt. In Bell (ed.) Proceedings, Sixth International Symposium on Landslides, Christchurch. Vol. 1, pp. 165–170. Balkema, Rotterdam.

Noverraz, F., Bonnard, Ch., Dupraz, H. & Huguenin, L., 1988. Grands glissements de versants et climat. Rapport final PNR 31. v/d/f Zurich, 314 p.

OFAT, OFEE, OFEFP 1997. Recommandations. Prise en compte des dangers dus aux mouvements de terrain dans le cadre des activités de l'aménagement du territoire. Office Fédéral de l'Aménagement du Territoire, Office Fédéral de l'Economie des Eaux, Office Fédéral de l'Environnement, des Forêts et du Paysage, Berne, 42 p.

Ramasco, M. 2005. Pers. Comm.

Saito, M. 1965. Forecasting the time of occurrence of a slope failure. Proceedings, Sixth International Conference on Soil Mechanics and Foundation Engineering, Montreal, Canada. Vol. 2 pp. 537–541.

SLF Davos 2000. Der Lawinenwinter 1999. Ereignisanalyse. 588 p.

Varnes, D.J. 1978. Slope movement – types and processes. In Schuster & Krizek (eds.) Landslides – Analysis and Control, Transportation Research Board Special Report 176, National Academy of Sciences, Washington, pp. 11–33.

Voight, B., Orkan, N. & Young, K. 1989. Deformation and failure time prediction in rock mechanics. In Khair (ed.), Rock Mechanics as a Guide for Efficient Utilisation of Natural Resources, Balkema, Rotterdam, pp. 919–929.

Zavodni, Z.M. & Broadbent, C.D. 1980. Slope failure kinematics. *CIM Bulletin* (April, 1980): 69–74.

Landslide risk assessment in Canada; a review of recent developments

S.G. Evans
Department of Earth Sciences, University of Waterloo, Waterloo, Ontario, Canada

D.M. Cruden
Department of Civil and Environmental Engineering, University of Alberta, Edmonton, Alberta, Canada

P.T. Bobrowsky
Geological Survey of Canada, Natural Resources Canada, Ottawa, Ontario, Canada

R.H. Guthrie
British Columbia Ministry of Water, Land and Air Protection, Nanaimo, British Columbia, Canada

T.R. Keegan
Canadian National Railways, Edmonton, Alberta

D.G.E. Liverman
Geological Survey, Dept. of Natural Resources Newfoundland & Labrador, St. John's, NFLD, Canada

D. Perret
Geological Survey of Canada, Natural Resources Canada, Quebec City, Quebec, Canada

ABSTRACT: Recent developments have added considerably to our understanding of landslide risk in Canada and has led to the implementation of formal risk reduction methods in selected jurisdictions. New knowledge of historical landslides in Newfoundland and the Maritime Provinces has given insight into the most damaging landslide types in that region which has formed the basis for more accurate landslide hazard assessment. In the St. Lawrence Lowlands, land-use zoning guidelines, especially setbacks, in areas of potential landslide hazard underlain by Champlain Sea sediments, are designed to reduce future landslide losses, especially with respect to rapid earth flows. In the Prairie Provinces, the application of similar methodologies, coupled with an enhanced understanding of landslide mechanisms, presents the possibility of mitigating landslide risk. In the Canadian Cordillera, landslide losses have been extensively analysed and the most damaging landslide types identified. The results of this analysis form the basis for a greater understanding of regional landslide hazard particularly when used in conjunction with volume and frequency data. Volume and frequency analysis has proved useful in quantifying landslide hazard at regional and site scales in the Cordillera. With respect to landslide risk and infrastructure, substantial progress, based largely on the analysis of comprehensive event inventories, has been made in the quantification of landslide hazard along highways and railways. From a national perspective, it is suggested that the understanding of landslide hazard is sufficiently well developed that it now provides an entry to quantitative risk assessment at the regional level and the design of robust risk-reduction measures in the most landslide-prone areas.

1   INTRODUCTION

The understanding of landslide risk in Canada has evolved considerably in the sixteen years since the publication of the first attempt at a broad national landslide hazard assessment in 1989 (Cruden et al. 1989). Evans (2001, 2003) and Hungr (2004a, b) have recently reviewed some of this progress. In these papers the regions most susceptible to landslide hazard have been defined (the Canadian Cordillera and the Eastern Canada Lowlands of Quebec and Ontario), the most damaging landslides have been identified, and national and regional assessments of damage both in terms of loss of life and economic impact have been attempted.

In this paper we highlight significant recent regional and thematic developments in the assessment of landslide risk in Canada. These include a greater understanding of the distribution of landslide hazard at regional (e.g., Canada's Atlantic and Prairie Provinces) and national scales (e.g., the Canada Landslide Inventory), a greater understanding of the damaging landslide types in the regions subject to highest landslide hazard (e.g., the St. Lawrence Lowlands and the Canadian Cordillera), and new approaches to quantitative hazard assessment (the development and use of magnitude and frequency relations) and the evaluation and management of landslide risk along linear infrastructure (e.g, the Canadian National railway system).

2 LANDSLIDE HAZARD IN CANADA'S ATLANTIC PROVINCES

Landslides and other slope movements have not generally been thought to be a major hazard in Atlantic Canada (cf., Cruden et al. 1989). Examination of the distribution of Canadian landslide disasters (a disaster is defined as a landslide causing three or more fatalities) supports this belief in that only two such events out of forty-three listed by Evans (2001) occurred in the region. It is misleading to assume, however, that landslides are insignificant in the region. For example, there may have been up to 68 fatalities in Newfoundland alone from landslides (Liverman et al. 2001); and although no deaths are known from the other Atlantic Provinces, landslides have a significant impact on transportation, forestry and other activities. The worst landslide disaster in the Atlantic Provinces is the poorly substantiated Ferryland disaster of circa 1823, when 42 fisherman apparently were killed by rockfall when a cave roof collapsed onto them (White 1902). In addition 27 deaths resulted from the tsunami that struck the Burin Peninsula of Newfoundland in 1929, caused by a large submarine landslide triggered by an earthquake.

Newfoundland and Labrador – A variety of slope movement are found in Newfoundland and Labrador, including debris avalanches, rotational slumps, and rockfalls. Debris avalanches are the most hazardous to life, generally being triggered by high rainfall events. They are widespread in the province and frequently pose problems for highway engineering. Typically failure involves a thin cover of till which overlies a steeply sloping bedrock substrate. When failure occurs, the resulting debris avalanche incorporates surface vegetation, large boulders, as well as the till. Other examples involve the mobilization of fluvial sediments overlying till. Such landslides have caused deaths at Harbour Breton (Liverman et al. 2001), in St. John's, and elsewhere. Rotational slumps are mostly found in the major river valleys of coastal Labrador, where a stratigraphy of outwash overlying thick glaciomarine clays is common.

High cut-banks of the river frequently fail, giving rise to large rotational slumps. These failures have had little effect on human activities to date, but will be an important consideration in hydroelectric development of the lower Churchill River. Rockfalls are common occurrences, but rarely fatal or destructive (with the notable exception of the Ferryland disaster noted above). Several fatalities have occurred when victims have been working at the base of coastal cliffs, or climbing on unstable slopes. Although damage to property is frequent, no fatalities are known from residences, and only a single serious injury. Protective rockfall fences have been installed in three locations in recent years to protect houses from rockfall (Springdale, St. John's, and Upper Island Cove).

Nova Scotia – Nova Scotia suffers from frequent landslides, but there is at present no record of fatalities resulting from them (apart from several deaths caused by slope failure in quarries and other excavations). Although found throughout the province, the most susceptible area is Cape Breton. Finck (1992), Grant (1994) and Wahl (2003) identified numerous landslide scars in the Cape Breton highlands. These are complex failures involving rock topple, rotational slip, translational sliding and flow. The deep glacially cut gorges of the region contain steep rock cliffs from which rockfall is a frequent event (as shown by extensive talus slopes). In terms of impact, the largest landslide consisted of a series of slope failures that caused almost complete destruction of part of the road at Kelly's Mountain in 1982. Other smaller landslides frequently affect transportation routes, and most commonly occur during the spring, as thawing of frozen ground leaves slopes saturated.

New Brunswick and Prince Edward Island – Carboniferous and Permian clastic redbeds along the Gulf of St. Lawrence coastlines of New Brunswick and Prince Edward Island are subject to incremental slope failures resulting from a combination of marine undercutting and frost action. Locally, saturation of the bedrock and overlying Quaternary deposits resulting from agricultural practices has contributed to debris flow and creep failures. Quaternary bluffs along the Bay of Fundy in New Brunswick, notably at Red Head near Saint John, show suffered slope failure involving debris flow, frost creep, and slumping. Block failures resulting from frost action have affected coastal cliffs along the Bay of Fundy and Baie des Chaleurs. Rotational sliding has accompanied frost heave in the Precambrian units at Saint John, Saint Martins, and Fundy National Park (Ruitenberg et al. 1976). Rockfall has been noted in the Campbellton area.

Risk management for landslides is still in its infancy in the Atlantic provinces. Slope stability is taken into account to some extent in road planning and engineering, perhaps due to the frequency of minor events affecting transportation routes. Before steps are taken to

manage risks, the presence of slope hazard must be recognized. Research on the historical record has helped define landslide hazard, particularly in Newfoundland and Labrador. Identification of the main types of landslide, along with understanding the controls on their development and occurrence may lead to a more systematic identification of areas at risk. Awareness of landslide hazard in Newfoundland and Labrador has led to increased consultation and referral by planners, but no formal hazard mapping exists for communities.

3 LANDSLIDES ON CANADA'S INTERIOR PLAINS

The Interior Plains of Canada extend from the U.S.A. border north to the Arctic Ocean and from the Foothills of the Rockies and the Mackenzies in the west, to the Canadian Shield in the east. This update focuses where economic activity and risk are concentrated, within a few hundred kilometres of the U.S.A. border. Future reviews might include risks to the oil and gas exploration and production on the Plains in north eastern British Columbia, the south western corner of the Northwest Territories and the pipeline corridor down the Mackenzie Valley. The impacts of global warming there have been reviewed by Couture et al. (2003).

In an earlier review, Scott (1989) commented "The common locus for slope failures in the Prairie region is along the valleys of large present-day rivers such as the Peace, the North and South Saskatchewan, and the Red and along the slopes of proglacial meltwater channels. The geological settings for slope failures can be grouped into 3 broad categories: (1) clay shale of Cretaceous age, which may be locally disturbed by glacial tectonics……. (2) discontinuities at stratigraphic contacts within the drift…….. (3) surficial stratified drift overlying till deposits….."

Cruden et al. (1989) provided examples of typical landslides in these settings and commented "…..the strata most prone to slope movements are clay shales of marine origin, then mudstones deposited in a shallow, near shore environment. …….the rapid down cutting of valleys during deglaciation resulted in … rebound … and the weakness thus generated along the flat-lying bedding resulted in a planar rupture surface for slope movement." These strata have continued to provide examples of the impacts of landslides. Slow movements on the west bank of the Assiniboine River, Manitoba in the Pierre Shale have disrupted the Canadian Pacific Railway line (Yong et al. 2003); a rapid translational slide on the east bank of the North Saskatchewan River in the local Edmonton Group rocks destroyed 3 houses in Edmonton, Alberta in 1999 (Barlow et al. 2002)

In this paper, the list of geological settings is expanded to include pre-glacial Pleistocene lake sediments in buried valleys. The largest historic landslides on the Interior Plains, tens of millions of cubic metres in volume, have occurred in the hundred metre and more thick sediment fills of the pre-glacial channels of the Peace River and its tributaries. The massive 1973 Attachie landslide temporarily blocked the Peace River in British Columbia (Evans et al. 1996, Fletcher et al. 2002). Landslides on the Saddle (Cruden et al. 1993), Spirit (Miller & Cruden 2001), Montagneuse (Cruden et al. 1997) and Eureka Rivers (Miller & Cruden 2002) and on Hines (Lu & Cruden 2000) and Dunvegan Creeks have dammed river flows to form landslide lakes which are sufficiently long-lived to destroy kilometres of valley-bottom timber. Slope movements have caused tens of metres uplift in the thalwegs of some of these rivers.

The landslides in these silty clays are typically retrogressions of reactivated translational slides. Sub-horizontal surfaces of rupture in the thick, fine-grained tills of the Peace River Lowland produce relatively short-lived dams. In contrast, movements within the pre-glacial sediments elevate stream beds to form longer lasting dams. Land clearing for agriculture has preceded the large landslides in the Peace River Lowlands but the landslides do not appear to have resulted from increased runoff and erosion (Cruden & Miller 2001).

In the southern half of Alberta, the pre-glacial drainage rose on the eastern slopes of the Rockies and infilled the pre-glacial valleys with Saskatchewan Sands and Gravels, sediments coarse enough to draw down water tables and stabilize river banks. Fine grained sediments within these fluvial sequences may be the loci of occasional slope movements (Sabourin et al. 1998). However on the shoulders of these valleys, groundwater flow and prolonged weathering soften the underlying Cretaceous rocks (Cruden et al. 1995).

A landslide in the Cretaceous rocks typically begins with the formation of a gaping main scarp on the crest of the valley. This is induced by translational movement along a weak horizontal layer, usually a bentonite seam. Translation promotes the growth of a minor, uphill-facing counter scarp within the displaced material. Rupture along the counter scarp creates an active block whose subsidence into a graben drives the down-slope passive block into the river valley. Movement of the displaced material is limited by the downward movement of the active block onto the horizontal surface of rupture (Cruden et al. 1991, Cruden et al. 2003).

After the rapid rock slide, the displaced material may continue to soften and flow. Rotational slides may occur on the surface of separation as the toe of the displaced material is eroded and removed by the river. When displaced material no longer protects the toe of the slope, further rapid erosion may reinitiate the cycle of slope movement (Cruden et al. 2002, Dewar & Cruden 1998). Another scenario saw the displaced material load earlier

353

colluvial deposits on the slope sufficiently to allow the advance of the slide down the slope as a slow earth flow (Cruden et al. 1995).

Cruden et al. (1989) attributed landslides in the cities of the Interior Plains to rises in groundwater tables following urbanization. Conservative planning would suggest setbacks from actively-eroded river banks which would sum the erosion by the river over (Cruden et al. 1989, De Lugt et al. 1993). Construction within these setbacks has been preceded by bank stabilization (Martin et al. 1998) and by berming the toes of the slopes (Thomson & Townsend 1979). It is possible to design structures such as oil wells and bridges to accommodate the very slow movements of the slopes supporting them (Brooker & Peck 1993). Where the mechanics of the movements are closely monitored and better understood, more sophisticated analyses of structures on slopes are possible (El Ramly et al. 2003) and more precise calculations of the risks of unsatisfactory performance become credible.

Losses from landsliding on the Interior Plains still take place (Barlow et al. 2002) even where the hazards have been identified. Owners have accepted the risks of construction they perceive. These risks and others less well understood are then shared with local authorities and others who may not have knowingly consented to them all (Fekner 2002). A more formal insurance scheme would be appropriate.

4 LANDSLIDE RISK ASSESSMENT IN THE SOUTH-EAST CANADA LOWLANDS

Due to historical and economic factors, most of the population in Quebec and Eastern Ontario is concentrated in lowlands along the St. Lawrence River system and its tributaries. The limits of these lowlands (the south east Canada lowlands (SECL)), which cover an area of about 70,000 km^2, approximately correspond to the maximum extension of former post-glacial seas. Around 6 million people live in SECL (ca. 20% of Canada's population), for an average population density of 85 persons/km^2.

South-eastern Canada lowlands are extensively covered with marine clays which were deposited between 12,000 to 8,000 years ago during the wanning of the Wisconsin ice sheet. Landslides in these clay deposits are widespread and occur along river valleys, lake and sea shores, margins of marine terraces, and escarpments of old quick-clay slide scars.

Comprehensive reviews of landslide processes in the south-east Canada lowlands were presented in the 1970s and 1980s (e.g., Mitchell & Markell 1974, Lebuis et al. 1983, Tavenas 1984, Lefebvre 1986). The reader is referred to these reviews for additional information on the geology, geomorphology, hydrogeology, and mechanical behaviour of slopes in SECL marine clays.

For the last ten years or so, an important effort has been devoted to organise this type of knowledge and provide the practitioner with a coherent and structured framework for analysing landslides, assessing hazards, and eventually estimating risk the lifetime of the affected structures and the flattening of the valley wall to its ultimate angle of stability (Vaunat et al. 1994, Leroueil et al. 1996, Leroueil & Locat 1998, Leroueil 2001). While it is noted that this framework has not been developed exclusively for landslides in sensitive clays, its application to landslide analysis and risk assessment in these materials has been beneficial in developing risk mitigation strategies (see discussion below). Vaunat et al. (1994) and Leroueil et al. (1996) propose a formal geotechnical approach to characterise slope movements, in which the landslide, actual or potential, is analysed by considering three elements: the type of the movement, the materials involved, and the different stages of the movement, from pre-failure to post-failure. For all relevant combinations of these three elements, a characterization sheet can be prepared for a slope movement with information on the controlling laws and parameters, predisposing factors, triggering or aggravating factors, revealing factors, and consequences. Figure 1 shows an example of a characterization sheet for the post-failure stage of retrogressive slides in sensitive clays. Leroueil & Locat (1998) and Demers et al. (1999) discussed how this approach can help to evaluate landslide hazard and risk, and determine more efficient mitigation measures.

In parallel with the development of this general framework, a number of detailed site surveys have been done to better document landslide processes. Systematic use of the piezocone (CPTU) has allowed the identification of soil weakening in slopes of marginal stability (Demers et al. 1999, Delisle & Leroueil 2000). Demers et al. (1999) showed that if softening of the clay in slopes can be identified with the piezocone, it could provide an approach for detecting slopes in a state of marginal stability. This approach could be used for landslide hazard assessment in areas at high risk where an accurate determination of the stability reserve of a slope may contribute to the selection of the appropriate mitigation strategy. The respective role of the two main triggering factors for deep rotational landslides – toe erosion and pore water pressure fluctuation – has been investigated in slopes along the Lac Saint-Jean shore line, Quebec. Results provide valuable information for dimensioning setback zones at the rear of slopes that have been protected against toe erosion by rip-rap.

Other site investigations were aimed at studying geological and geotechnical factors controlling the spatial occurrence of earthflows. Of interest is the observation that the location of the failure surface during retrogression may be controlled by a layer, or a series of layers, with lower shear strength (Demers et al. 2000, Potvin 2001). The reappraisal of the 1971 St-Jean-Vianney
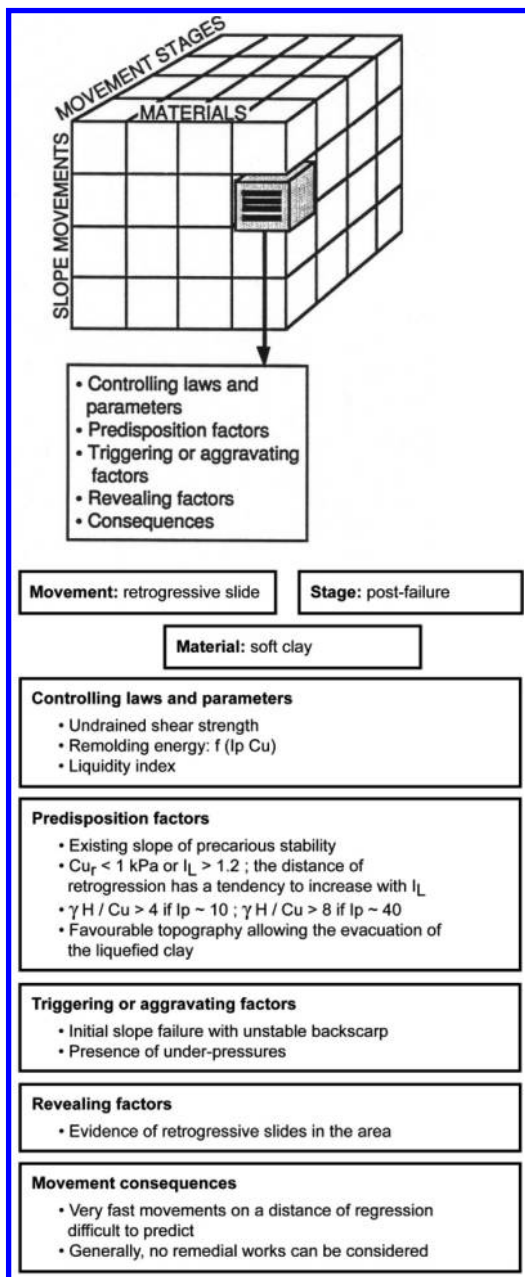
Figure 1. Schematic slope movement characterization sheet for a retrogressive slide in soft clays (after Vaunat et al. 1994, Leroueil et al. 1996).

landslide (one of the two most destructive and expensive landslides that has occurred in SECL since 1840; cf. Evans 2003) has shown that an earthflow may develop entirely in the debris of an old earthflow, even if the clay mobilised is already in a remoulded state. This new fact has major implications for landslide hazard mapping in sensitive clay areas, as the possibility that an earth-flow may occur under similar conditions must now be carefully evaluated. At a more regional scale, different reconnaissance surveys were conducted to evaluate the potential of geophysical techniques for mapping critical geological factors related to land sliding (e.g., Aylsworth & Hunter 2004). Electrical methods appear to be promising for detecting non-saline sediments and thus for inferring the 3-D extension of sensitive clay deposits.

These recent developments have contributed to shape a new procedure for assessing regional landslide hazards in the Saguenay/Lac Saint-Jean region, Quebec (Robitaille et al. 2002). This procedure, which is build on the pioneering work done during the seventies by the Geotechnical Division of the former Quebec Ministry of Energy and Resources (Lebuis et al. 1983), leads to the preparation of a final cartographic document displaying the different constraints to land-use that must be implemented or considered in a given area. This is a true land-use management map tailored to match the needs of land-use planners and municipal engineers in local communities. These maps are presented at very large scales, 1:5,000 in rural settings and 1:2,000 in urban areas, and are provided with guidelines detailing allowed and forbidden practices. Setback zones, either at the top or at the base of slopes (or both), depending on the potential landslide types and the geomorphological environment, are dimensioned from regional and local inventories of landslides (e.g., Perret & Bégin 1997). Hazard levels within setback zones are estimated by considering predisposing, aggravating and triggering factors (including human bad practices), and the overall frequency of occurrence of the different types of landslides.

5 LANDSLIDES IN THE CANADIAN CORDILLERA

Evans (2001, 2003) identified the Canadian Cordillera as the region most susceptible to the impact of landslides in Canada. Landslide hazard in the region is the highest in Canada and the region has experienced the most severe impact of landslides in historical time. Large landslides including rock avalanches, debris avalanches, and landslides in Quaternary sediments continue to occur with measurable frequency (Geertsema et al. In Press).

Historical landslides and their geological framework have been studied along major transportation corridors (e.g., Clague & Evans 2003). Further understanding of background landslide hazard has resulted from recent studies of prehistoric landslides which have been constrained by the dating of landslide events (e.g., Clague et al. 2003, Orwin et al. 2004). In the case of the

Table 1. Costs of landslide damage in western Canada – 1880 to 2001 (after Hungr 2004a).

Sector and landslide types	Estimated annualized losses ($ M/y)	
	Direct damage	Prevention
Residential (debris flows, slides)	2.5–3.5	1–2
Roads and bridges (debris flows, rockfalls, slides)	4	5.5
Railways (debris flows, rockfall, slides)	2.5–3.5	2–4
Hydro power network (rock slides)	1	4
Pipelines (earth and rock slides)	1–2	2–4
Forestry (debris avalanches and flows)	2–3	1
Subtotal	12–16	16–21
Residential land sterilisation		10–50
Forest harvestable land loss	16–48	
Total	28–64	26–71

Cheam rock avalanche, landslide debris covers part of the populated lower Fraser Valley, 125 km east of Vancouver; the event has been dated as having occurred 5,000–5,300 calendar years ago (Orwin et al. 2004).

Landslides associated with heavy rainfall form an important element of regional landslide hazard in the Cordillera (see references in Evans 2003). In January 2005, for example, a heavy rainfall-induced debris slide destroyed homes in North Vancouver resulting in the death of one person. In a recent review, Hungr (2004a) estimates the impact of landslides on the Province of British Columbia (Table 1). He argues that despite the existence of a high landslide hazard in the province's mountainous terrain, the relative impact of landslides in terms of life loss and material costs is relatively modest. This is rationalized on the basis of a low density of population, the scouring of the landscape by glacial erosion by Pleistocene glaciers, and rational and safety-conscious government policy concerning urban development. Hungr (2004a) estimates annual direct and indirect material losses in the period 1880–2001 to be in the order of $28–37 M/y (Table 1) excluding the cost of land sterilization and forest harvest losses. In Table 1 the cost of prevention appears to roughly equal the cost of direct damage excluding life loss.

6 MAGNITUDE AND FREQUENCY RELATIONS AND REGIONAL LANDSLIDE HAZARD ASSESSMENT

Recent progress has been made in the use of magnitude and frequency (m/f) relations for both regional

(e.g., Hungr et al. 1999) and site landslide risk analysis (e.g., Hungr 2004b). This has been made possible by the developing understanding of m/f relations for many types of landslides for datasets that span historical time scales (Malamud et al. 2004, Guthrie & Evans 2004a) as well as those for individual trigger events, such as earthquakes (Pelletier, et al. 1997) and heavy rains (Guthrie & Evans 2004b). In these studies magnitude can be taken as initial landslide area (or scar area), initial landslide source volume, landslide debris area, landslide debris volume, or the area of both scar and debris. M/f relations can be used to quantitatively estimate the hazard component of the risk equation (e.g., Hungr et al. 1999, Singh & Vick 2003).

Studies of rockfall magnitude and frequency and their application to risk assessment were initiated by Hungr et al. (1999) and followed by a number of authors (e.g., Singh & Vick 2003, Guzzetti et al. 2004). These analyses express landslide magnitude in terms of volume and include estimation of frequency distributions for single stones as small as $0.01 \, \text{m}^3$ to larger events that can span 7 orders of magnitude (Hungr et al. 1999). Hungr et al. (1999), showed a steep power law relation for rock falls greater than about $1 \, \text{m}^3$, with a slope of about -0.64 in the Canadian Cordillera. Most of the data gathered by Hungr et al. (1999) exhibited a rollover, or flattening, of the data at volumes below $1 \, \text{m}^3$. The rollover effect for rock falls may be a consequence of undercounting the smaller events (often events on highways are counted by impact marks); however, it may also reflect a real physical effect that limits the occurrence of rockfall.

M/F analyses have also been carried out on datasets of other landslide types (e.g., shallow debris slides, debris avalanches, debris flows). Most of these studies have expressed landslide magnitude as landslide area, which can be acquired quite accurately from remote sensing methods such as air photograph analysis. Landslides of medium to large size typically exhibit power law relations with a steep negative slope (e.g., Pelletier et al. 1997, Hovius et al. 1997, Stark & Hovius 2001, Guzzetti et al. 2002, Brardinoni et al. 2003, 2004, Guthrie & Evans 2004a, b, In Press), with a flattening of the slope, or rollover, for smaller sizes. Figure 2 shows the conceptual distribution of landslide frequencies and magnitudes. At very small landslide sizes (e.g., $<650 \, \text{m}^2$, the threshold determined by Brardinoni et al. 2003) a substantial portion of the rollover might be explained by data censoring. That is to say, the mappers inability to consistently count all landslides approaching a minimum resolvable size. However, there is substantial evidence to show that the rollover represents a real physical phenomenon (Hovius et al. 2000, Guzzetti et al. 2002, Martin et al. 2002, Guthrie & Evans 2004 a, b, this volume, Malamud et al. 2004). In particular, Guthrie & Evans (2004a, b) propose that for coastal British
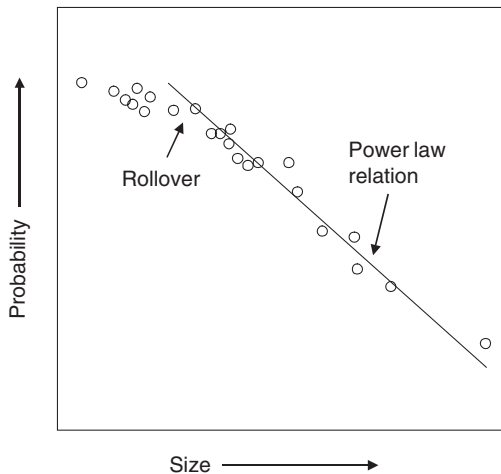
356

Figure 2. The conceptual relationship between landslide magnitude and frequency. Typically a power law relation is observed for medium and large landslides (the power law relation is a straight line with a negative slope on log-log scale axes), but for smaller landslides a flattening of actual data is common. Smaller landslides are often well described by an exponential curve, and probably relate to physical processes in the landscape.
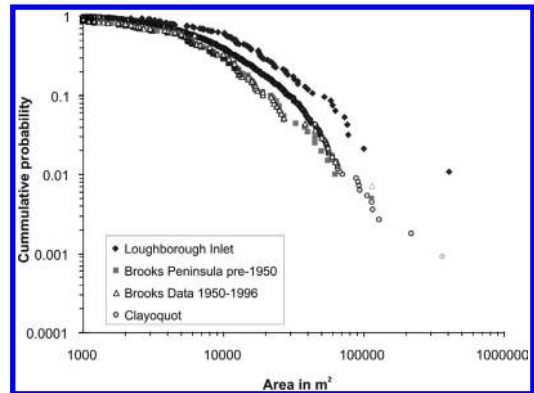

Figure 3. A family of magnitude-frequency curves from coastal British Columbia (after Guthrie & Evans 2004a). Note that the rollover occurs at magnitudes greater than 10,000 m^2. The curves suggest some degree of process similarity and therefore indicate that a total hazard model for the region is achievable.

Columbia, landslides tend to a larger size based on their landscape position. They argue that landslides often occur in mid and upper slopes where there is the right combination of erodible sediment and slope for sliding; slides then tend to travel to a baseline marked by the stream or gully thalweg, rather than stopping at mid-slope. As the geometry of the landscape becomes more and more limiting, the power law relation comes into effect. Figure 3 shows a family of curves from coastal British Columbia showing magnitude/frequency magnitude. Note that the power law relation (a straight line on log-log scales) could only be drawn for landslides ≥10,000 m^2. Malamud et al. (2004), report similar results, of increasing landslide volumes to a maximum distribution value.

The issue of the precise form of the m/f relation is especially relevant as we attempt to calculate risk. If we have reliable magnitude-frequency curves then we should be able to plot the total hazard of an area by fitting the resolvable landslides on the curve and extrapolating the remainder. Stark & Hovius (2001) proposed a distribution model using the double Pareto distribution. Based on data from coastal British Columbia, this curve predicted the bulk of the landslide distribution well, including the rollover, however, it predicted the small and very large landslides less well (Guthrie & Evans 2004b). Figure 4 shows 1107 landslides from Clayoquot sound in coastal British Columbia fit onto a double Pareto curve, as well as a quantile probability

plot of the fit. Note that the curve, in this example, slightly under predicts small landslides as well as landslides greater than about 100,000 m^2. Malamud et al. (2004), proposed an inverse gamma distribution for the same reason. Malamud et al. (2004), claim a good fit over the range of data, including landslides up to 1,000,000 m^2, for large datasets worldwide. They propose that the equation is universal and generate a series of curves against which incomplete inventories may be calibrated. While the data presented appears to fit their universal curves well, based on experience in coastal British Columbia, it seems likely that landscape physiography could affect both the slope of the curve and the maximum probability (the inflection point of the distribution curve). In either case, both distribution models attempt to accurately characterize the total landslide hazard over a region.

It is from the analysis of magnitude frequency curves that we are able to predict the influence of other specific aspects of the hazard including differences in terrain vulnerability and human impacts (see Guthrie and Evans, this volume).

Zhou et al. (2002), Guthrie & Evans (2004a, b) and Malamud (2004) among others, observed that landslides occur unevenly in time and space. We propose that the term landslide clusters be used to describe landslides that occur following the occurrence of a particular triggering mechanism (c.f. Evans & Guthrie 2004a). Attempts to rank landslide event clusters began with Keefer (1984) when he discussed an event magnitude scale related to earthquake-triggered landslide clusters. In this approach, 100–1,000 landslides (triggered by an earthquake) was accorded a magnitude of 2, 1,000–10,000 a magnitude of 3 and so on. Malamud et al.
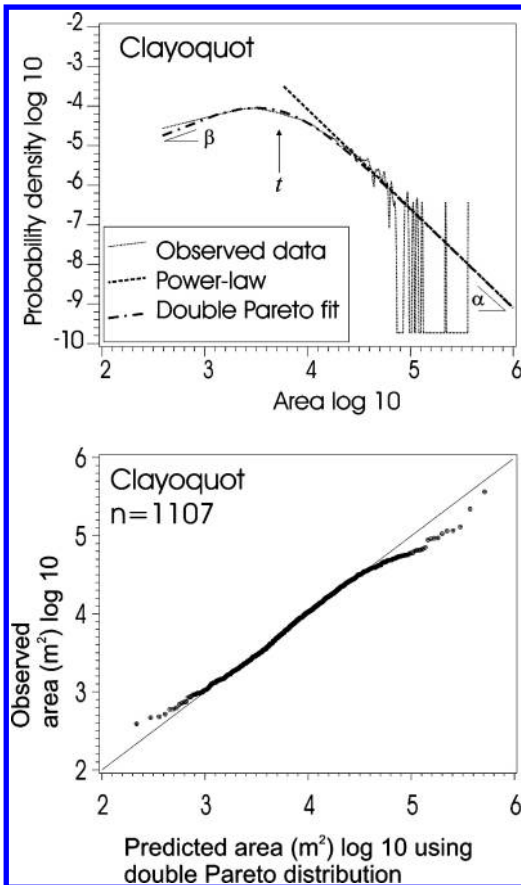
357

Figure 4. Landslides from Clayoquot, Vancouver Island, British Columbia, plotted against a Double Pareto curve using maximum likelihood estimation. The quantile probability plot below indicates that the Double Pareto distribution predicts the bulk of the data well, but less well at the extremes.

(2004) more precisely proposed that $M_L = \log N_{LT}$ where M_L is landslide event magnitude and N_{LT} is the total number of landslides recorded. They propose another, probably more relevant equation that incorporates landslide area, however, is preliminary and based on the universality of their landslide equation above. In Canada, Evans (2003) has assigned event magnitudes to landslides by considering fatal events and proposing a landslide destructiveness index. The landslide destructiveness index dealt primarily with consequence, however, it appears a suitable companion to the work of Malamud et al. (2004) to determine ultimate risk. Both Malamud et al. (2004) and Evans (2003) propose magnitude envelopes of impact. Currently, this aspect of landslide hazard and risk analysis is in its infancy; however, we suggest that further development of the notion of landslide cluster magnitude is both relevant and
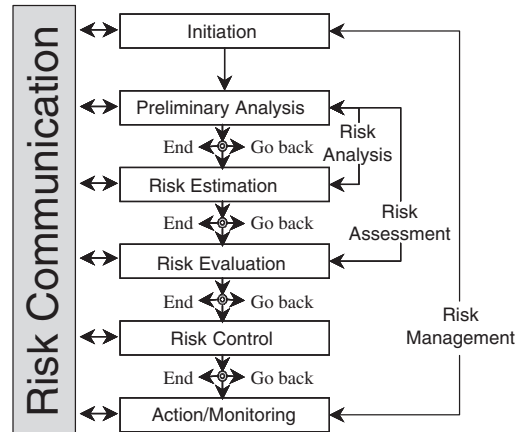
Figure 5. Simple Model (CSA Standard "Risk Management: Guidelines for Decision Makers", CAN/CSA Q850–97).

necessary for estimates of regional landslide hazard and thus regional landslide risk.

7 MANAGING THE RISK FROM RAILWAY GROUND HAZARDS

Ground hazards, broadly categorized as either geotechnical, of which landslides are a significant subset, or snow and ice related, are known to represent a significant exposure to accidental losses or risk to Canadian railways. Linear facilities are inherently more exposed to a wider variety and higher frequency of ground hazards than single site facilities. Furthermore, in comparison to other linear features, railways tend to have higher exposure to ground hazards because of their grade limitations. Canadian railways, for example, have to deal with (a) a great diversity of soil and rock conditions, (b) extensive and deep ground freezing conditions and related peat terrain, (c) active geomorphologic processes associated with the relative youth of the terrain since glaciation, and (d) climate extremes in both temperature and precipitation.

Recognizing this exposure, the two class one railways in Canada, namely Canadian National Railway (CN) and Canadian Pacific Railway (CPR), are working on a number of initiatives within the framework of systematic risk management of Railway Ground Hazards.

7.1 The risk management framework

The general risk management framework adopted by CN and CPR is consistent with CAN/CSA-Q850–97: Risk Management: A Guideline for decision makers, (Canadian Standards Association 1997), which outlines a six-step process as illustrated in Figure 5. CN's

358

Railway Geotechnical Hazard Classification				
Level I	Level II	Level III	Level IV	Abbrev.
Geotechnical (rock, soil & water)	Landslides	Rock landslides	Rock fall	RF
			Rock topple-rock fall	RT-RF
			Rock topple…rock slide…rock fall	RT-RSl-RF
			Rock slide-rock fall	RSl-RF
			Rock topple	RT
			Rock slide	RSl
			Rock topple-rock slide.	RT-RSl
		Debris landslides	Debris fall	DF
			Debris slide-debris fall	DSl-DF
			Debris slide	DSl
			Debris flow	DFw
			Rock slide-debris flow	RSl-DFw
		Earth landslides	Earth fall	EF
			Earth slide-earth fall	ESl-EF
			Earth slide	ESl
			Earth flow-earth slide	EF-ESl
			Earth spread-earth slide	ESp-ESl
			Earth flow	EFw
			Earth slide-earth flow	ESl-EFw
			Earth spread	ESp
	Subsidence	Settlement	Consolidation	Cn
			Compression	Cm
			Sub grade plastic deformation	SPD
			Sub grade dynamic liquefaction	SDL
		Collapse	Piping or dissolution voids	PD
			Culvert failure	CF
			Timber deterioration	TD
			Voids in rock fill	VRF
			Liquefaction	L
			Other (animal borrowing, mining,etc.)	O(specify)

Railway Geotechnical Hazard Classification (cont'd)					
Level I	Level II	Level III	Level IV	Level V	Abbrev.
Geotechnical (rock, soil & water)	Hydraulic Erosion	Overland flow erosion	Slope wash		SW
			Gully erosion		GE
		Through flow erosion	Seepage erosion		SE
			Piping		P
			Dissolution		D
		Sub aqueous flow erosion	Channelized flow erosion	Channel aggradation	ChA
				Channel degradation	ChD
			River Erosion	Local scour	LS
				General scour	GS
				Ice & log jams	(I or L)J
				Encroachment	En
				Bank erosion	BE
				Avulsion	Av
			Wave erosion		WE

Railway Ice & Snow Hazard Classification			
Level I	Level II	Level III	Abbrev.
Ice and snow (ice)	Snow avalanche	Slab avalanche	SA
		Loose snow avalanche	LSA
		Dry snow avalanche	DSA
		Wet snow avalanche	WSA
		Slush flow	SF
	Icing	Frost heaves	FH
		Surface ilcing	SIc

Figure 6.   Draft Railway Ground Hazard Classification System (after Keegan 2004).

approach to applying this process to railway ground hazards is documented in Keegan et al. (2000).

7.2 *Railway Ground Hazard Classification System (RGHCS)*

Essential to effective risk management of railway ground hazards is the development and use of an appropriate classification system. CN and CPR have adopted a system developed by Keegan (2004) to classify railway ground hazards that affect their networks.

The intent of the classification system is to provide a means to practically categorize relevant railway ground hazards for avoidance, control, or remediation. The RGHCS enables a structured framework for the risk management of railway ground hazards by providing (a) a means to systematically identify and characterize railway ground hazards, (b) a consistent and systematic organization of ground hazard information for use in both qualitative and quantitative risk analysis, (c) a means to correlate between a ground hazard type and the appropriate risk control measure, and (d) the systematic sharing and organization of experience and understanding gained by a variety of geotechnical practitioners.

As illustrated in Figure 6, the system accounts for two main factors: (1) Material type (e.g., water, soil and rock, and snow and ice), and (2) Process (e.g., hydraulic erosion, slides, falls, avalanches, etc.). It is essential that the name given to a particular railway ground hazard incorporate the entire risk scenario that may result in loss. Commonly the chain of events that ultimately results in track failure involves more than one type of railway ground hazard.

For instance, river erosion often results in undercutting of a railway embankment that often leads to a landslide and track failure. These types of railway ground hazards are referred to as complex railway ground hazards consistent with the terminology introduced by Cruden & Varnes (1996) for complex landslides. Similarly, complex ground hazards are named using the sequence of ground hazards that may lead to track failure.

The system has been used to organize the railway ground hazard loss records and to classify railway ground hazards identified in the field.

7.3 *CN Rockfall Hazard and Risk Assessment (CNRHRA) system*

The CNRHRA system is an established quantitative risk analysis system developed and used by CN since 1996 to systematically manage the derailment risk associated with rock falls (Abbott et al. 1998a, b). CNRHRA assessment culminates in a derailment risk (DR) score that takes the following into account:

Derailment Hazard (DH): The likelihood a particular rock slope with specific characteristics will generate a rock fall that will lead to a derailment given a certain train speed and the presence or absence of a detection system.

359

Frequency (F): The frequency of rock falls from a given rock slope determined either subjectively or using the incident record for the site.

Derailment Consequence (DC): The severity of the potential derailment determined subjectively from location specific characteristics such as steepness of down hill slope, proximity to a water coarse or structure (bridges or tunnels).

The system facilitates a rational prioritization of monitoring and mitigation activities.

7.4 *CN River Attack Track Risk Assessment System (RATRAS)*

A review of CN's loss records has demonstrated that River Erosion (RE) and the compound mechanism River Erosion – Earth Slide (RE-ESl) are among the leading mechanisms of loss. Keegan et al. (2003) have previously described the (RE-ESl) hazard. CN is currently developing a quantitative risk assessment system entitled the River Attack Track Risk Assessment System (RATRAS) modeled after the CNRHRA system. It is intended that the RATRAS will become an effective tool to guide the allocation of resources for proactive site inspection, monitoring, risk control assessment and mitigation work.

CP Rail, CN, Transport Canada, The University of Alberta and Queens University have collaborated in forming the Railway Ground Hazard Research Program (RGHRP) to facilitate directed research to assist in the risk management of Railway Ground Hazards. The program is currently entering the second of a planned five-year initiative.

Ultimately, this research will enhance railway safety and facilitate a more effective prioritization of mitigative efforts. The frequency and severity of loss from ground hazard incidents should be reduced through a more rational risk management approach. The railways can look for break-throughs in (a) methodologies and technologies for assessing and predicting hazards, (b) technologies available for detecting and monitoring ground hazards, (c) response criteria for natural hazard triggers such as inclement weather, and (d) techniques for managing relevant information.

Encouraged by tangible results the Canadian railways will continue to focus on a risk management approach as the standard of practice for the management of railway ground hazards.

8 THE CANADA LANDSLIDE INVENTORY

The qualitative and quantitative assessment of risk associated with a geohazard requires an adequate understanding and clear identification of those areas that are actually and not just potentially under threat. One needs to know the type of hazard, the likelihood of occurrence, the potential level of impact and what aspects are actually under risk. To this end, for landslides, a clear indication of where landslides have occurred in the past is a basic parameter necessary in subsequent steps to evaluate potential risk and future threats.

In regard to landslide hazard in Canada, the threat from landslide varies across the country depending on a variety of conditions. Ironically, our knowledge of landslide mechanisms and processes for different types of landslides far exceeds our current knowledge of exactly where these events have occurred in the past and where they are likely to occur in the future. In response to this knowledge gap, the Geological Survey of Canada (GSC) has embarked on a program to compile and document the historic and prehistoric record of landslides across Canada. The aim of this activity is to provide a database record of landslide occurrences for use in the analysis of landslide risk for particular areas and regions of the country. To be useful, the national inventory is designed to be readily accessible; hence an internet-based system was adopted.

During the past few years the actual inventory of Canadian landslides documented by the Geological Survey of Canada program has increased dramatically to >23,000 in 2004. Over the next few years the inventory will flatten as most known events become recorded in the database and the number of new additions added annually are proportionately low in comparison to the total.

An interactive web-based tool allows users to select an area in Canada (at any scale) and view the record of landslides recorded for that region. Alternatively, users can activate a landslide type differentiation in the area under question. For the purposes of the GSC database, landslide type follows the classification of Cruden & Varnes (1996).

The interactive database provides the research scientist a variety of options. For instance, the right side of the web page provides access to the various features that can be activated or deactivated as necessary by the individual users. One or more of the features can be illustrated in relation to the landslides within a targeted area of study. Two other images illustrate the ancillary information that can be gleaned from the inventory structure. Figure 5 shows an example from Alberta/British Columbia of the online surficial geology data that can be overlayed with the inventory. The current database indicates that landslides are known to occur across the country. But equally apparent is the current bias in the records, clusters are not necessarily real and the bias for our records to parallel populated regions in the southern part of the country is an indication of the lack of attention given to largely uninhabited areas of the country. The viability of the inventory will increase gradually as individual researchers contribute their own data to the national database. Moreover, our own efforts to compile northern landslides will help populate these regions.

360

9 CONCLUSIONS

Significant new knowledge has emerged concerning landslide hazard in Canada since 1989. Regional developments have included data on damaging landslides in Newfoundland and Labrador, more information concerning the geologic framework of landslides in Canada's Prairie Provinces and the Canadian Cordillera, and the enhancement of the knowledge of landslide mechanisms in sensitive clays in Canada's south-east lowlands. Despite high levels of landslide hazard in some regions of Canada, the analysis of historical landslide loss/damage data shows that vulnerability at a national and regional scale remains relatively low. Approaches to risk assessment have recently been developed and includes the use of landslide magnitude and frequency relations in regional landslide risk assessment and a formalised risk management framework custom designed for the management of ground hazard risk along linear infrastructure. The ongoing Canada Landslide Inventory is gradually filling gaps in our knowledge of the distribution of landslide hazard in Canada. However, from a national perspective, it is suggested that the understanding of landslide hazard is sufficiently well developed that it now provides an entry to quantitative risk assessment at the regional level and the design of robust risk-reduction measures in the most landslide-prone areas.

REFERENCES

Abbott, B., Bruce, I., Keegan, T., Oboni, F. & Savigny, W. 1998a. A methodology for assessment of rockfall hazard and risk along linear transportation corridors. *Proceedings* 8th Congress of the International Association for Engineering Geology and the Environment, Vol. II: 1195–1200.

Abbott, B., Bruce, I., Keegan, T., Oboni, F. & Savigny, W. 1998b. Application of a new methodology for the management of rockfall risk along a railway. *Proceedings*, 8th Congress of the International Association for Engineering Geology and the Environment, Vol. II: 1201–1208.

Aylsworth, J.M. & Hunter, J.A. 2004. A geophysical investigation of the geological controls on landsliding and soft deformation in sensitive marine clay near Ottawa. Proceedings, 57th Canadian Geotechnical Conference, Quebec City, Session 1C, p. 30–37.

Barlow, P., Cazes, P., Cruden, D. & Lewycky, D. 2002. Setbacks in Edmonton, Alberta, Canada. Proceedings, International Conference on *Instability – Planning and Management*, Ventnor, 19–23 May, Thomas Telford, London, UK, pp 73–80.

Brardinoni, F. & Church, M. 2004. Representing the landslide magnitude-frequency relation: Capilano River Basin, British Columbia. *Earth Surface Processes and Landforms* 29: 115–124.

Brardinoni, F., Slaymaker HO. & Hassan, M.A. 2003. Landslide inventory in a rugged forested watershed: a comparison between air-photo and field survey data. *Geomorphology* 54: 179–196.

Brooker, E.W. & Peck, H.B. 1993. Rational Design Treatments of Slides in Overconsolidated Clays and Clay Shales. *Canadian Geotechnical Journal* 30: 526–544.

Canadian Standards Association 1997. *Risk management: Guidelines for decision makers.* CAN/CSA-Q850–97, 1997., Canadian Standards Association, Etobicoke, Ontario, Canada.

Clague, J.J. & Evans, S.G. 2003. *Environmental and Engineering Geoscience*, Clague, J.J. and Evans, S.G. 2003. Geologic framework of large historic landslides in Thompson River Valley, British Columbia. *Environmental and Engineering Geoscience* 9: 201–212.

Clague, J.J., Friele, P.A. & Hutchinson, I. 2003. Chronology and hazards of large debris flows in the Cheekye river basin, British Columbia, Canada. *Environmental and Engineering Geoscience* 9: 99–115.

Couture, R., Smith, S., Robinson, S.D., Burgess, M.M. & Solomon, S. 2003. On the Hazards to Infrastructure in the Canadian North Associated With Thawing of Permafrost. Proceedings, 3rd Canadian Conference on Geotechnique and Natural Hazards, Edmonton, June 9–10, pp 125–132.

Cruden, D.M. & Miller, B.G.N. 2001. Land Clearing and Landslides Along Tributaries of the Peace River, Western Alberta, Canada. *Proceedings*, International Conference, Landslides – Causes Impacts and Counter Measures, Davos, Switzerland, pp 377–385.

Cruden, D.M. & Varnes, D.J. 1996. Landslide types and processes. *Landslides investigation and mitigation*, Special report 247, Transportation Research Board, National Research Council, National Academy Press, Washington, D.C., 36–71.

Cruden, D.M., Keegan, T.R. & Thomson, S. 1993. The Landslide Dam on the Saddle River Near Rycoft, Alberta. *Canadian Geotechnical Journal* 30: 1003–1015.

Cruden, D.M., Lu, Z.Y. & Thomson, S. 1997. The 1939 Montagneuse River Landslide, Alberta. *Canadian Geotechnical Journal* 34: 799–810.

Cruden, D.M., Martin, C.D. & Soe Moe, K.W. 2003. Stages in the Translational Sliding of 2 Inclined Blocks: Observations From Edmonton. Proceedings, 56th Canadian Geotechnical Conference, Winnipeg, Vol. 1, pp 823–830.

Cruden, D.M., Peterson, A., Thomson, S. & Zabeti, P. 2002. 35 Years Activity at the Lesueur Landslide, Edmonton, Alberta. *Canadian Geotechnical Journal* 39: 266–278.

Cruden, D.M., Tedder, K.H. & Thomson, S. 1989. Setbacks From the Crests of Slopes Along the North Saskatchewan River Valley. *Canadian Geotechnical Journal* 26: 64–74.

Cruden, D.M., Thomson, S. & Hoffman, B.A. 1991. Observations of Graben Geometry in Landslides, in Proceedings, *International Conference on Slope Stability*, Isle of Wight. Thomas Telford London, pp 33–36.

Cruden, D.M., Thomson, S., Kim, H.J. & Peterson, A. 1995. The Edgerton Landslides, *Canadian Geotechnical Journal* 32: 989–1001.

Cruden, D.M., Bornhold, B.D., Chagnon, J.Y., Evans, S.G., Heginbottom, J.A., Locat, J., Moran, K., Piper, D.J.W., Powell, R. Prior, D.B., Quigley, R.M. & Thomson, S. 1989. In Brabb & Harrod (eds.), Landslides; Extent and Economic Significance in Canada: in *Landslides; Extent and Economic Significance*: 1–24, Rotterdam, A.A. Balkema.

Delisle, M.-C. & Leroueil, S. 2000. Détection, à l'aide du piézocône, de zones ramollies dans des pentes argileuses et évaluation de leur comportement mécanique. Université Laval, Report GCT-98–23 prepared for the Ministère des transports du Québec.

De Lugt, J., Cruden, D.M. & Thomson, S. 1993. A Suggested Method for Estimating Setbacks From the Crests of Slopes on the Interior Plains in Alberta. *Canadian Geotechnical Journal* 30: 863–875.

Demers, D., Leroueil, S. & d'Astous, J. 1999. Investigation of a landslide in Maskinongé, Québec. *Canadian Geotechnical Journal* 36: 1001–1014.

Demers, D. Robitaille, D. & Drolet, A. 1999. Exemples de gestion du risque de glissements de terrain. *Bulletin d'information technique, Direction du laboratoire des chaussées, Ministère des transports, Québec*, Vol. 4, No. 11.

Demers, D., Robitaille, D. & Perret, D. 2000. The St. Boniface landslide of April 1996: a large retrogressive landslide in sensitive clay with little flow component. *Proceedings*, 8th International Symposium on Landslides, Cardiff.

Demers, D., Potvin, J., Robitaille, D. & Ouellet, D. 2002. Stabilité des berges du Lac Saint-Jean, région de Desbiens, Québec. *Proceedings*, 55th Canadian Geotechnical Conference and 3rd Joint IAH-CNC and CGS Groundwater Specialty Conference, Niagara Falls, p. 1169–1176.

Dewar, D. & Cruden, D.M. 1998. The Largest Historic Landslide in the Mackay River Valley, Northeast Alberta. *Proceedings*, 51 Canadian Geotechnical Conference, Edmonton, Vol. 1:73–80.

El Ramly, H., Morgenstern N.R. & Cruden, D.M. 2003. Probabilistic Stability Analysis of a Tailings Dyke on Presheared Clay Shale. *Canadian Geotechnical Journal* 40: 192–208.

Evans, S.G. 2001. Landslides. In: *A Synthesis of geological hazards in Canada*. Geological Survey of Canada Bulletin 548, Brooks (ed.), p 43–80.

Evans, S.G. 2003. Characterizing landslide risk in Canada. *Proceedings 3rd Canadian Conference on Geotechnique and Natural Hazards*, Canadian Geotechnical Society, Edmonton Canada: 19–34.

Evans, S.G., Hu, X-Q. & Enegren, E.G. 1996. The 1973 Attachie Slide, Peace River Valley, near Fort St. John, British Columbia, Canada : a landslide with a high velocity flowslide component, in Pleistocene sediments. *Proceedings*, 7th International Symposium on Landslides, Trondheim, Norway, v. 2, p. 715–720.

Fekner, S. 2002. Development Setbacks From River Valley and Ravine Crests in Newly Developing Areas, *Proceedings, International Conference on Instability – Planning and Mangement*, Ventnor, 19–23 May, Thomas Telford, London, UK, pp 135–142.

Finck, P.W. 1993. An Evaluation of Debris Avalanches in the Central Cape Breton Highlands, Nova Scotia, Mines and Energy Branch, Nova Scotia Department of Natural Resources, Paper 93–1, 65 pages.

Fletcher, L., Hungr, O. & Evans, S.G. 2002. Contrasting failure behaviour of two large landslides in clay and silt. *Canadian Geotechnical Journal* 39: 46–62.

Geertsema, M., Clague, J.J., Schwab, J.W. & Evans, S.G. In Press. An overview of recent large catastrophic landslides in northern British Columbia. Engineering Geology.

Grant, D.G. 1994. Quaternary Geology, Cape Breton Island, Nova Scotia. Geological Survey of Canada Bulletin 482, 159 p.

Guthrie, R.H. & Evans, S.G. 2004a. Analysis of landslide frequencies and characteristics in a natural system, Coastal British Columbia. *Earth Surface Processes and Landforms* 29: 1321–1339.

Guthrie, R.H. & Evans, S.G. 2004b. Magnitude and frequency of landslides triggered by a storm event, Loughborough Inlet, British Columbia. *Natural Hazards and Earth System Sciences* 4: 475–783.

Guzzetti, F., Malamud, B.D., Turcotte, D.L. & Reichenbach, P. 2002. Power-law correlations of landslide areas in central Italy. *Earth and Planetary Science Letters* 195: 169–183.

Guzzetti, F., Reichenbach, P. & Ghigi, S. 2004. Rockfall hazard and risk assessment along a transportation corridor in the Nera Valley, Central Italy. *Environmental Management* 34:191–208.

Hungr, O. 2004a. Landslide hazards in BC: achieving balance in risk assessment. *Innovation* 8: 12–15.

Hungr, O. 2004b. Geotechnique and the management of landslide hazards. *Proceedings*, 57th Canadian Geotechnical Conference, Quebec City, Session 4C, 10 p. Conference CD.

Hungr, O., Evans, S.G. & Hazzard, J. 1999. Magnitude and frequency of rock falls and rock slides along the main transportation corridors of southwestern British Columbia. *Canadian Geotechnical Journal* 36: 224–238.

Hovius, N., Stark, C.P. & Allen, P.A. 1997. Sediment flux from a mountain belt derived by landslide mapping. *Geology* 25: 231–234.

Jakob, M. & Weatherly, H. 2003. A hydroclimatic threshold for landslide initiation on the North Shore Mountains of Vancouver, British Columbia. *Geomorphology* 54:137–156.

Keegan, T. 2004. Railway Ground Hazard Classification System, Unpublished.

Keegan,T., Abbott, B. & Ruel, M. 2000. A risk management framework for ground hazards along Canadian National Railways, Paper presented at the 53rd Canadian Geotechnical Conference, Montreal, Quebec, October 15 2000 Volume 2, P. 809.

Keegan, T., Abbott, B., Cruden, D., Bruce, I. & Pritchard, M. 2003. "Railway Ground Hazard Risk Scenario: River Erosion: Earth Slide", *Proceedings* of the 3rd Canadian Conference on Geotechnique and Natural Hazards, Edmonton, June 2003.

Keefer, D.K. 1984. Landslides caused by earthquakes. *Geological Society of America Bulletin* 95: 406–421.

Lawrence, D.E., Morey, C.R. & Aylsworth, J.A. 1997. Landslides in sensitive marine clays, South Nation River valley: The role of ravines in limiting retrogression. *Proceedings*, 50th Canadian Geotechnical Conference, Ottawa, p. 815–822.

Lebuis, J., Robert, J.M. & Rissmann, P. 1983. Regional mapping of landslide hazard in Quebec. *Symposium on soft clay slopes*. Linköping, Sweden, Report No. 17, Swedish Geotechnical Institute, p. 205–262.

Lefebvre, G. 1986. Slope instability and valley formation in Canadian soft clay deposits. *Canadian Geotechnical Journal* 23: 261–270.

Leroueil, S. 2001. Natural slopes and cuts: movement and failure mechanisms. *Géotechnique* 51: 197–243.

Leroueil, S. & Locat, J. 1998. Slope movements: geotechnical characterization, risk assessment and mitigation. *Proceedings*, 8th Congress of the International Association of Engineering Geology, Vancouver, p. 933–944.

Leroueil, S., Vaunat, J., Picarelli, L., Locat, J., Faure, R. & Lee, H. 1996. A geotechnical characterization of slope movements. *Proceedings*, 7th International Symposium on Landslides, Trondheim, vol. 1, p. 53–74.

Liverman, D.G.E., Batterson, M.J., Taylor, D. & Ryan, J. 2001. Geological hazards and disasters in Newfoundland. *Canadian Geotechnical Journal* 38: 936–956.

Lu, Z.Y. & Cruden, D.M. 2000. Interaction Between Fluvial Processes and Landslide Activity in the Western Peace River Lowland, Alberta, *Proceedings*, 8th International Symposium on Landslides, Cardiff, UK, Volume 2:955–960.

Malamud, B.C., Turcotte, D.L., Guzzetti, F. & Reichenbach, P. 2004. Landslide inventories and their statistical properties. *Earth Surface Processes and Landforms* 29: 687–711.

Martin, L.R., Lewycky, D.M. & Ruban, A.F. 1998. Long Term Movement Rates in a Large Translational Landslide, Proceedings, 51st Canadian Geotechnical Conference, Edmonton, Volume 1, pp 23–30.

Martin, Y., Rood, K., Schwab. J.W. & Church, M. 2002. Sediment transfer by shallow landsliding in the Queen Charlotte Islands, British Columbia. *Canadian Journal of Earth Sciences* 39: 189–205.

Miller, B.G.N. & Cruden, D.M., 2001, Major Landslides in the Pre-Glacial Valleys of the Peace River Lowlands, *Proceedings*, 54th Canadian Geotechnical Conference, Calgary, Volume 1, pp 363–370.

Miller, B.G.N. & Cruden, D.M., 2002, The Eureka River landslide and Dam Peace River Lowlands Alberta. *Canadian Geotechnical Journal* 39: 863–878.

Mitchell, R.J & Markell, A.R. 1974. Flowsliding in sensitive soils. *Canadian Geotechnical Journal* 11: 11–31.

Orwin, J.F., Clague, J.J., & Gerath, R.F. 2004. The Cheam rock avalanche, Fraser Valley, British Columbia, Canada. *Landslides* 1: 289–298.

Pelletier, J.D., Malamud, B.D., Blodgett, T. & Turcotte, D.L. 1997. Scale-invariance of soil moisture variability and its implications for the frequency-size distribution of landslides. *Engineering Geology* 48: 255–268.

Perret, D. & Bégin, C. 1997. Inventaire documenté des glissements de terrain associés aux fortes pluies de la mi-juillet 1996, région du Saguenay–Lac Saint-Jean. Institut national de la recherche scientifique (INRS-Géoressources). Report presented to the Bureau de reconstruction et de relance du Saguenay–Lac-St-Jean.

Potvin, J., Pellerin, F., Demers, D., Robitaille, D., La Rochelle, P. & Chagnon, J.-Y. 2001. Revue et investigation supplémentaire du site du glissement de Saint-Jean-Vianney. *Proceedings,* 54th Canadian Geotechnical Conference, Calgary, vol. 2, p. 792–800.

Robitaille, D., Demers, D., Potvin, J. & Pellerin, F. 2002. Mapping of landslide-prone areas in the Saguenay region, Québec, Canada. *Instability – Planning and Management*, Thomas Telford, London, p. 161–168.

Ruitenberg, A.A., McCutcheon, S.R. & Venugopal D.V. 1976. Recent gravity sliding and coastal erosion, Devils Half Acre, Fundy Park, New Brunswick: geological explanation of an old legend. *Geoscience Canada* 3: 237–239.

Sabourin, M.T., Patrick, R.A. & Ruban, A.F. 1998. A Landslide in an Urban Setting, *Proceedings*, 51st Canadian Geotechnical Conference, Edmonton, Volume 1, pp 39–46.

Scott, J.S. 1989. Engineering Geology and Land Use Planning in the Prairie Region of Canada, In Fulton (ed.) *Quaternary Geology of Canada and Greenland*, 713–723 Geological Survey of Canada, Ottawa.

Singh, N.K. & Vick, S.G. 2003. Probabilistic rockfall hazard assessment for roadways in mountainous terrain. *Proceedings, 3rd Canadian Conference on Geotechnique and Natural Hazards,* Canadian Geotechnical Society, Edmonton, p. 253–260.

Stark, C.P. & Hovius N. 2001. The characterization of landslide size distributions. *Geophysical Research Letters* 28: 1091–1094.

Tavenas, F. 1984. Landslides in Canadian sensitive clays – A state-of-the-art. *Proceedings*, 4th International Symposium on Landslides, Toronto, vol. 1, p. 141–154.

Thomson, S. & Townsend, D.L. 1979. River erosion and Bank Stabilization, North Saskatchewan River, Edmonton, Alberta. *Canadian Geotechnical Journal* 16: 567–576.

Vaunat, J., Leroueil, S. & Faure, R.M. 1994. Slopes movement: a geotechnical perspective. Proceedings, 7th Congress of the International Association of Engineering Geology, Lisbon, p. 1637–1646.

Wahl, K. 2003. A GIS based landslide hazards assessment for Cape Breton Highlands National Park, Nova Scotia. M.Sc thesis, Department of Geology, Acadia University.

White, J.W. 1902. Ferryland – what doth not appear in history. *Newfoundland Quarterly*, March 1902.

Yong, S., Martin, C.D., Sego, D.C. & Bunce, C., 2003, The Harrowby Hill Slides, *Proceedings*, 3rd Canadian Conferences on Geotechnique and Natural Hazards, Edmonton, pp 219–226.

National landslide risk strategies

The analysis of global landslide risk through the creation of a database of worldwide landslide fatalities

D.N. Petley, S.A. Dunning & N.J. Rosser
International Landslide Centre, Department of Geography, University of Durham, Durham, UK

ABSTRACT: There is little doubt that most global datasets on fatalities caused by landslides greatly under-estimate the impact of landslides. The reasons for this are varied, and include a tendency to classify disasters by trigger rather than mechanism (so a landslide triggered by a seismic event will be recorded as an earthquake disaster); the occurrence of landslides in remote locations in less economically developed countries; and the frequency of large numbers of relatively small landslides involving less than ten fatalities, which do not get reported widely. In consequence, investment into the prevention of landslide disasters, especially in mountainous, less developed countries has lagged behind that of other, actually less significant hazards such as volcanic eruptions. To counter this, the International Landslide Centre has embarked upon the generation of a worldwide landslide database, initially concentrating on events that cause fatalities. The analysis of the initial landslide database has generated some surprising results. It is clear that in terms of fatalities landslide disasters are focused upon less economically developed countries, especially in mountainous regions that are subject to precipitation extremes such as tropical cyclones or the monsoon. Excluding rare, very large events, in most years the majority of rainfall-induced landslide fatalities of occur in China and South Asia during the northern hemisphere summer. A second peak occurs in the annual cycle during the December and January, as heavy rains along the Indonesian archipelago induce extensive landsliding. Interestingly, the data suggests that the number of fatalities each year caused by rainfall induced landslides is closely correlated with the global temperature anomaly, which may account for a clear increase in landslide occurrence worldwide over the past twenty years. The implications of these data, and the trends of increasing landslide occurrence, are analyzed in terms of landslide hazard and risk assessment, and suggestions are made for future research directions in the context of the distribution of landslide fatalities.

1 INTRODUCTION

Whilst there is little doubt that the impact of landslides worldwide is substantial, the quantification of this impact remains surprisingly poor. Estimates of the costs of landslides in human terms vary hugely. For example, Alexander (1993) suggested that the global cost of landslides in the period 1900–1976 was 17 000 'people affected'. On the other hand, Brabb (1991) estimated that the global death toll from landslides has increased from 600 per year in the early 1970's through to several thousand per year by the early 1990's. The economic costs of landslides are equally difficult to quantify, but estimates have included $1.6–3.2 billion per annum for the USA, >$1 billion per year for Japan, and $62 million for Venezuela (Schuster & Highland 2001) (Table 1). However, these statistics are rather general and are difficult to compare.

Whilst local and national databases of landslide events have been created, most notably for Italy (Guzzetti 2000), global databases of landslide fatalities have proven difficult to initiate, despite the obvious advantages of so-doing. The usefulness of such a database is clear: it should allow quantification of the actual level of impact of landslide events; it should allow the determination of the major controls upon landslide occurrence (e.g. El Nino cycles, the Asian monsoon); it should permit estimations of the degree to which landslide occurrence is increasing against time; it should permit comparison of the impact of landslides with other disasters for which similar databases exist; and it should allow spatial analysis of the occurrence of landslides at the continental and national level at least.

This paper examines the initial results achieved from the compilation of such a database, the global landslide fatality database at the International Landslide Centre, University of Durham, UK.

Table 1. Socio-economic costs of landslides for selected countries in the Western hemisphere (after Schuster & Highland 2001).

Country	Estimated fatalities per annum	Estimated economic cost per annum US$	Selected notable large landslide events and estimated death toll
Canada	5	50 million to 1 billion	1903: Frank: 70 deaths 1971: Quebec: 31 deaths
USA	25–50	1.6–3.2 billion	1970: Virginia: c. 150 deaths 1985: Puerto Rico: 129 deaths
Mexico	–	–	1920: Orizaba Peak: c. 600 deaths
Honduras	–	–	1998: Hurricane Mitch: c. 1000 deaths
El Salvador	–	–	1986: El Salvador earthquake: 200 deaths 2001: El Slvadir earthquake: 1000 deaths
Nicaragua	–	–	1998: Casita Volcano: 2500 deaths
Costa Rica	–	–	1963: Rio Reventado: >20 deaths
Venezuela	–	62 million	1987: Rio Limon: 210 deaths 1999: Vargas: up to 30,000 deaths
Colombia	–	–	1985: Nevado del Ruiz: >22,000 deaths 1987: Villa Tina: 217 deaths
Ecuador	–	–	1983: Chunchi: c. 150 deaths 1993: La Josepfina: 35 deaths
Peru	–	–	1941: Huaraz: 4–6000 deaths 1970: Huascaran: c. 18,000 deaths
Chile	–	–	1991: Antofogosto: c. 150 deaths
Brazil	–	–	1966–7: Rio de Janeiro: c. 2000 deaths 1988: Rio de Janeiro and Petropolis: 320 deaths
Argentina	–	–	1976: Rio Escoipe: unknown

2 THE ILC DATABASE

Since September 2002, we have been collating a database of landslide events worldwide on a daily basis. The creation of such a database is fraught with difficulties and it has to be acknowledged that the data that we are collecting does not provide a 100% representation of global landslide events. However, the initiation of such a project, with subsequent improvements through time, will greatly improve our knowledge of landslide occurrence. In this first phase of this long term project, our data is centered around landslide fatalities. The reasons for selecting fatality data are simple – our pilot project suggested that this the one set of information regarding landslides that is reasonably reliably reported, even in remote areas and in less developed countries. We hope in the future to be able to expand our data collection beyond just fatal events, but such a move would inevitably lead to a much more spatially-inconsistent dataset. The data sources are a mixture of personal communications, newswire reports, academic papers, government data, and aid agency reports. Data are collated on a daily basis. The key information collected are:

- Date
- Location (national, regional and local)
- Type
- Size
- Trigger
- Number of fatalities
- Number of people injured
- Number of people reported missing
- Notes on landslide impact
- Source

In general, it is straight-forward to collate information pertaining to date, location, trigger, number of fatalities and of course the information source. Collating data on the type of landslide, the size and the socio-economic impact is usually rather more difficult. An attempt is made for all events to monitor post-event activity, including the recovery of bodies, and the impact of secondary events such as, for example, flood waves resulting from the collapse of landslide dams. It is likely that for many large events the recorded number of fatalities under-estimates the actual number for two reasons: 1. A proportion of the people reported as missing will in fact have been fatally injured, but often it is difficult to validate what proportion this actually is; and 2. a (usually) unknown proportion of the people reported as being injured will eventually succumb to their injuries. Again,
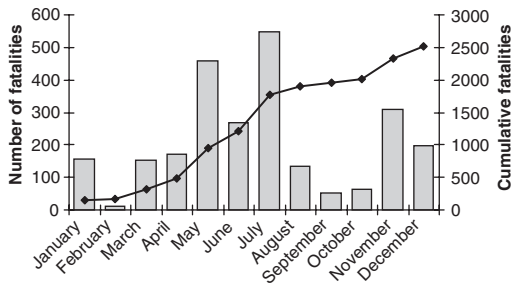
368

Figure 1. The temporal occurrence of landslide fatalities in 2003, based upon the ILC database. The bar graph represents the monthly totals; the line graph is the cumulative frequency.

Figure 2. The geographical occurrence of landslide fatalities in 2003, based upon the ILC database.

reporting of this after the event is extremely erratic, especially in less developed countries and rural areas.

In compiling the database, a decision has to be made about which events to consider, and also the criteria for including a fatality within the database. For the former, we have tried to include all soil/rock failures, including slides, flows and falls. Debris flows are included where the movement can be clearly differentiated from a flood, though we readily accept that this is a grey area that inevitably incorporates some ambiguity/error. We also include physical processes directly associated with a landslide event. The criterion used is generally a conceptual one – if it had been possible to prevent the landslide, would the fatality have been avoided? If yes then the event is included in the database.

3 EXAMPLE OF RESULTS – LANDSLIDE EVENTS IN 2003

To illustrate the results of this study, we analyze here the data collected for the year 2003. Although some collation of the data is still ongoing, this dataset is essentially now complete. The dataset includes 193 fatal landslides, plus a further seven large magnitude trigger events that led to multiple landslide fatalities. In total, we recorded 2536 fatalities from landslides, which we judge to be significantly below average (by comparison, the total number of recorded fatalities for 2004 at the time of writing (mid December 2004) was nearly 7,000). An analysis of the temporal occurrence of the landslides (Fig. 1) indicates that they show an essentially bimodal distribution, with a substantial concentration of events in May, June and July, and a second peak in November and December.

The reasons behind this distribution are clearly shown in an analysis of the geographical location of the fatality data (Fig. 2) by broad continental area, focusing on landslide fatalities in Asia. It is clear that the majority of landslide fatalities recorded in 2003 occurred in Asia, with South Asia (i.e. the Indian subcontinent) bearing the brunt (c. 35%), whilst South-East Asia
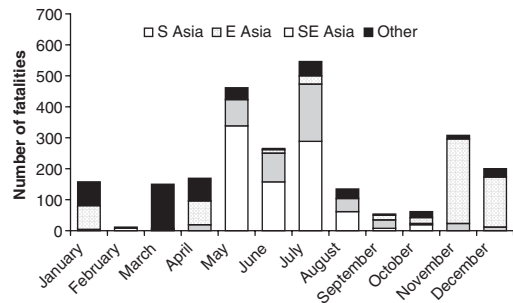
represented c. 20% of the total and East Asia (taken here to include China, Taiwan, Korea and Japan) represented c. 26%, most of which occurred in China. Thus, in total Asia suffered over 81% of the recorded landslide fatalities worldwide in 2003. Surprisingly, both Central and South America carries only a small part of the burden in the study year (though our preliminary data suggest that a rather different picture will emerge for 2004).

These data suggest that the peak in the northern hemisphere summer is the result primarily of landslides occurring in the South Asia area, with a smaller but nonetheless significant contribution from East Asia. However, outside of this three month period landslide fatalities in these two areas were relatively rare. On the other hand, South–East Asia suffered landslide fatalities throughout the year, with a notable peak in November and December.

The explanation lies for this pattern lies in the large-scale weather systems that dominate precipitation patterns as 98% of recorded landslide fatalities in 2003 were associated with rainfall events. The South Asia area is strongly influenced by the Asian monsoon, which brings intense rainfall across the northern part of the Indian subcontinent in the northern hemisphere summer months. It is this rainfall that triggered the majority of fatal landslides in 2003. This monsoonal rainfall also affects southern and southeast China, causing many of the landslides seen in East Asia during the same period. On the other hand, South–East Asia is affected by seasonal rainy seasons that are quite varied spatially, not least because part of this area straddles the Equator. Thus, it should be expected that this area will see landslides in association with the NW Pacific tropical cyclone (typhoon) season, which occurs in the mid to late part of the northern hemisphere summer, extending through much of the autumn with a lower intensity, and the summer rains in the southern hemisphere part of this area, which peak in December. The latter process is clearly evident, with most of the landslides recorded during this time being recorded in deforested areas of

369

Indonesia. However, in 2003 the NW Pacific typhoon season was comparatively weak, with in particular a low number of landfalling typhoons in the South China Sea area. For this reason, the occurrence of fatal landslides in the SE Asia during the northern hemisphere summer months is probably much lower than would normally be expected.

4 THE OCCURRENCE OF LANDSLIDES IN 2003 IN COMPARISON WITH OTHER YEARS

A key question is the degree to which 2003 represents a typical year for landslides. At this point it is difficult to give a definitive indication of this, but some impression can be gained by comparing this dataset with the results from other studies, and by considering the occurrence of triggering events. Brabb (1991) estimated that the global death toll from landslides was several thousand per year in the early 1990's. This suggests that the toll in 2003 was lower than normal. There is some logic in this suggestion as the magnitude-frequency graph suggests (Fig. 3). This shows that the largest single event had less than 320 fatalities associated with it, whilst the greatest contribution to the total number of fatalities came from the large number of small events. However, it is well established that much larger landslide events do occur, sometimes causing thousands or even tens of thousands of deaths. The lack of such an event in 2003 suggests that the total landslide related death toll was probably lower than average.

Examination of the occurrence of triggering events supports this view. First, there were no major landslide-triggering seismic events in populated areas. Climatically, the global precipitation level was below the 1961–1990 average in 2003. The South Asian monsoon was however slightly above average (c. 2% above normal) (Lawrimore & Levinson 2004). This is reflected by the comparatively large number of landslide fatalities in South Asia and southwest China. On the other hand, the NW Pacific tropical cyclone season, which historically is associated with substantial landslide occurrence in SE and East Asia, was slightly weaker than average (Chan 2004). Interestingly, typhoon activity over the South China Sea was notably lower than average (Fig. 4). The N. Atlantic hurricane season was stronger than average (16 named storms), but the incidence of landfalling events, especially within the Caribbean, was low, meaning that landslide triggering was modest. Tropical cyclone induced rainfall was considerably higher than for the average year, but few fatal landslides occurred – probably reflecting the resilience of this environment to intense precipitation.

Hence, it would appear that the major climatic and tectonic controls on landslide occurrence in 2003 would indicate a comparatively low number of fatal landslides, which appears to agree with the database.
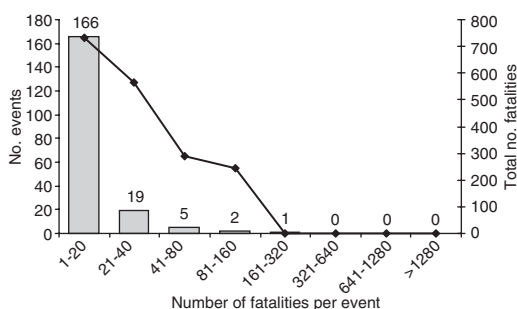

Figure 3. Magnitude – frequency relationship for the 2003 landslide events, based upon the ILC database. The bar graph (left axis) shows the total number of events of each size class (the actual number of events is indicated), whilst the line graph (right axis) shows the total number of fatalities for each class.
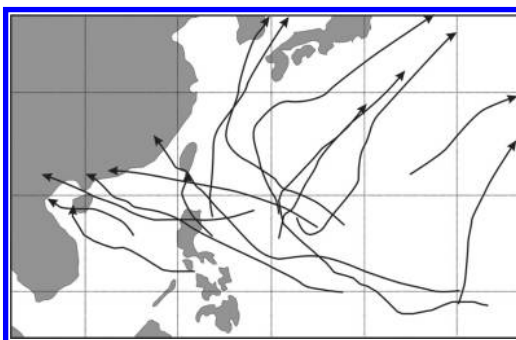

Figure 4. Indicative tracks of typhoon strength tropical cyclones in the NW Pacific in 2003. Notable is the relatively low number of tracks crossing the Philippines, Taiwan and Eastern China.

5 LONG TERM TRENDS IN LANDSLIDE OCCURRENCE

In addition to the annual database, we are also in the early process of developing a long term database of fatal landslide events, with the aim of extending this back to 1900. It is clear that this dataset will never be complete, and it is likely that there will be a decay effect back through time as information on landslide events becomes increasingly difficult to obtain. Despite these problems, the dataset is already generating some interesting results in terms of the long term averages of landslide occurrence. Based on this database, the average number of landslide fatalities during the period 1980–2002 was 3984 p.a., although this figure is almost certainly an under-estimate as it is likely that most of the smaller landslide events are currently missing from the database. During this period, three very large events were recorded – the Nevado del Ruiz disaster in Colombia in 1985 the
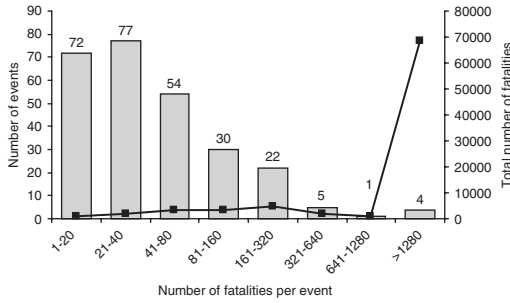
370

Figure 5. The magnitude frequency plot for the l980–2002 landslide dataset, which shows a markedly different distribution to that of the 1983 dataset.

Figure 6. The corrected magnitude frequency plot for the l980–2002 landslide dataset, amended on the basis of the 2003 dataset to allow for the poor records for the smaller events.

landslides associated with the passage of Hurricane Mitch in 1998 across much of Central America, and the landslides in Vargas, Venezuela in 1989. These three events combined represent approx. 67,000 of the 91,600 recorded fatalities during this time.

The magnitude frequency relationship for this period shows a distinctly different pattern to that of the 2003 (high resolution) dataset, with the largest number of events being seen in the 21–40 fatalities per event range, rather than for the 1–29 fatalities as for 2003 (Fig. 5). It is also clear that the rare, very large events cause the vast majority of the fatalities. This different pattern of occurrence is almost certainly a consequence of the failure to capture the smaller events. If it is assumed that all events in the range 81–160 fatalities per event are captured by this dataset (and it is likely that these large events are quite reliably reported), and that the ratio between the number of events of this size, and the number of events of each of the smaller events is constant, then an estimate of the number of fatalities from all events can be made. This estimate uses the number of fatalities per event data for 2003 for the three smaller fatality classes. The results are shown in Figure 6. The resulting estimated annual fatality rate is 4928 people per annum, or nearly half a million people per century. Again, this is probably an under-estimate as it excludes occasional massive landslide events, such as the flowslides triggered by the 1920 Kansu earthquake in China, in which perhaps as many as 250,000 people died. If it is arbitrarily assumed that such events might occur once a century, then the average fatality rate is probably in the order of 7–8000 people per annum.

A particularly interesting aspect of this longer term dataset is the change in the occurrence of landslide fatalities with time. Figure 7 depicts the occurrence of climatically-triggered landslide fatalities for events with more than five deaths but less than 1500. The data have been clipped in this way to allow for the difficulty in collecting information about the small scale events, especially when compiling a database retrospectively,
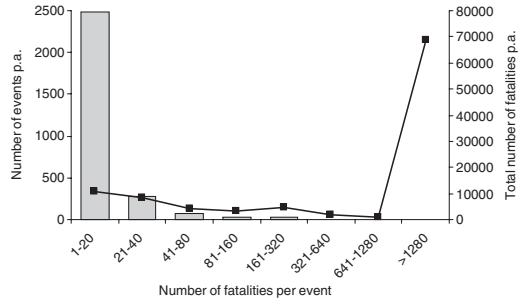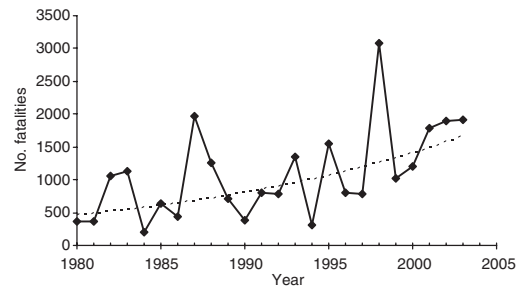

Figure 7. The trend in recorded landslide fatalities for moderately-sized events, 1980–2003.

and to allow for the fact that the very large events occur so infrequently that they represent outliers on a dataset of this duration. The data are shown accompanied by an exponential trend line to show the rising trend. This increasing trend has been reported elsewhere (e.g. Brabb 1991), but is powerfully evident here. An element of this is almost certainly the result of the increasing availability of data on landslide events in more recent years, but the trend is unlikely to be caused by this alone. These data suggest that there is a genuine rising trend in fatalities caused by landslides. This rising trend is usually attributed to a range of factors including environmental degradation; rural to urban migration, and in particular the growth of slum areas on marginally-stable land around megacities; increasing population pressures; and deforestation. All of these factors are undoubtedly important.

However, a rather different perspective on this issue can be gained by examining this provisional landslide dataset in the context of global temperature anomaly data. The temperature anomaly dataset used is that derived for the University of East Anglia – full details of its derivation can be found within Jones and Moburg (2003) and Parker et al. (2004). The dataset provides an indication of the difference between surface
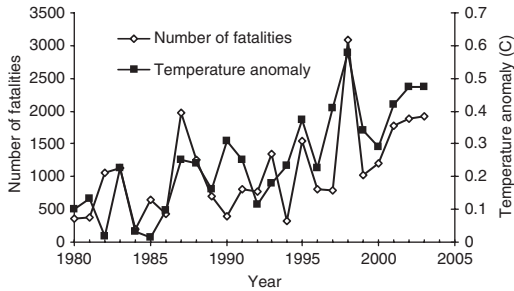
371

Figure 8. The trend in recorded landslide fatalities for moderately-sized events (left axis) plotted with global surface temperature anomaly (right axis) (data from Jones & Moburg 2003).
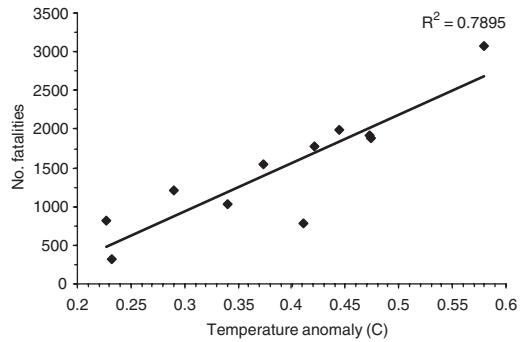

Figure 9. The regression between the recorded landslide fatalities for moderately-sized events (and global surface temperature anomaly (temperature data from Jones & Moburg 2003) for the period 1994–2004. The R^2 value for the regression is noted on the graph.

temperature across both the continents and the oceans in any given year in comparison with the average global surface temperature for the period 1864 to 2004. The estimate of global temperature anomaly is considered to be accurate to about $\pm 0.05°C$ (Jones & Moburg 2003).

The plot of global temperature anomaly and landslide fatalities as per Figure 8 are provided in Figure 9. It must be stressed at this point that this dataset is provisional and requires further development. However, the indication from these data are that there is a surprisingly close relationship between the number of landslide fatalities in any given year and the global temperature anomaly. Interestingly, the relationship between the two datasets becomes stronger in the latter part of the period, most notably from 1994 onwards. This may well be because the landslide fatality data become increasingly reliable in this period. An examination of the regression between the two datasets (Fig. 9), taking the more reliable data from 1994 to 2004, shows that a simple linear relationship appears to define the relationship between the two datasets, with an R^2 value of close to 0.8. This is a remarkably close correlation.

The causes of this relationship are unclear, given that there would appear to be so much complexity in the system. The simplest argument is that global temperature anomaly causes changes in global precipitation totals, that are then reflected in landslide occurrence. However, the relationship between global temperature anomaly and global precipitation anomaly is generally considered to be weak (Jones & Moburg 2003). A more likely explanation may lie in the possible relationship between temperature anomaly and precipitation intensity – perhaps years with high temperature anomalies are associated with higher rainfall intensities (possibly associated with more convective rainfall systems), and this is then mirrored in the occurrence of fatal landslides.
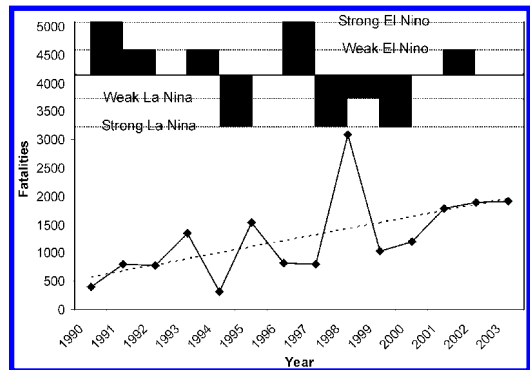
Figure 10. The annual trend in landslide fatalities in comparison with the occurrence of weak/strong El Nino and weak/strong La Nina events. It is clear that no strong correlation is evident.

It is also possible that the two datasets are both showing a response to some other external stimulus. So, for example, perhaps global temperature anomaly and intense rainfall events are both controlled by sunspot cycles (Parker et al. 2004), explaining the correlation. Clearly further research is needed. It is also possible, though less likely, that some socio-economic factor is driving both. Finally, it is of course also possible that the relationship between the two is coincidental.

It is commonly stated that landslide occurrence is controlled at least in part by the occurrence of El Nino Southern Oscillation events (Gabet & Dunne 2002, Negecu & Mathu 1999). However, this dataset shows no evidence that El Nino and La Nina events play a substantial role in the occurrence of global landslide fatalities (Fig. 10).

372

Table 2. Landslide fatality data for the period 1980–2000 for the main continental areas.

Continent	Deaths	Pop. density	Total pop. ($\times 10^6$)	Deaths/ 10^6 people/ year
N. America	62	16	307	0.01
Europe	535	30	795	0.03
Africa	612	26	860	0.03
S Asia	2596	305	1300	0.10
E&SE Asia	5125	193	2205	0.11
Australasia	119	4	33	0.17
C. Asia	1958	9	80	1.17
S. America	57365	19.5	351	7.78
C. America	38250	64	174	10.47

6 IMPLICATIONS FOR GLOBAL LANDSLIDE RISK

The data presented here are enlightening in terms of understanding global landslide risk. The key findings are:

1. The average number of annual fatalities from landslides is probably in excess of 5000 per annum;
2. The majority of fatalities occur in less developed countries;
3. There appears to be a close correlation between global climate change and the number of fatalities from landslide events;
4. There does not however seem to be a correlation between fatal landslides and the occurrence of El Nino/La Nina events.

The landslide data can be used to examine the occurrence of landslide fatalities over the study period in terms of total population and population density (Table 2). This preliminary dataset shows that North America has the lowest number of per capita deaths, closely followed by Europe and Africa. The per capita landslide death rate is more than 1000 times higher for Central Asia, and a thousand times higher for Central America. The variations in landslide risk are probably a combination of socio-economic factors (e.g. N. America and Europe are the two richest areas in the world, whilst Central America is one of the poorest), physical (i.e. Africa has a low density of landslides due to a mostly stable tectonic setting and a lack of monsoonal type rainfall events), and structural (it may well be that the dataset for Africa is seriously under-representing the occurrence of landslides there for example.

7 CONCLUSIONS

The research presented in this paper represents part of a large, ongoing project to examine landslide risk through the compilation of a database of landslide events. The results are not at this stage definitive, and further work is needed. However, the resulting analyses are proving to be immensely interesting for a variety of reasons. First, it is shedding new light on the occurrence of landslides both temporally and spatially. Perhaps more importantly, the data appear to be showing that the major factor driving the occurrence of landslide fatalities worldwide is global temperature anomaly. Depressingly, the data show that despite all the efforts of scientists and engineers, the occurrence of landslide fatalities is still increasing essentially unchecked, especially in less developed countries. There is still clearly a great deal to do to reduce the global disaster burden associated with landslides.

REFERENCES

Alexander, D. 1993. *Natural disasters*. Chapman & Hall, New York. 632 pp.

Bell, G., Goldenberg, S., Landsea, C., Blake, E., Chelliah, M., Mo, K. & Pasch, R. 2004. *The 2003 North Atlantic hurricane season – a climate perspective.* National Weather Center Climate Prediction Report. 9 pp.

Brabb, E.E. 1991. The world landslide problem. *Episodes* 14: 52–61.

Chan, C.L. 2004. *Verification of Forecasts of Tropical Cyclone Activity over the Western North Pacific in 2003*. Laboratory for Atmospheric Research Report, City University of Hong Kong.

Gabet, E.J. & Dunne, T. 2002. Landslides on coastal sage-scrub and grassland hillslopes in a severe El Nino winter; the effects of vegetation. *Geological Society of America Bulletin* 114: 983–990.

Guzzetti, F. 2000. Landslide fatalities and the evaluation of landslide risk in Italy. *Engineering Geology* 58: 89–107.

Jones, P.D. & Moberg, A. 2003. Hemispheric and large-scale surface air temperature variations: An extensive revision and an update to 2001. *Journal of Climate* 16: 206–223.

Lawrimore, J. & Levinson, D. 2004. *Climate of 2003 Annual Review.* National Oceanic and Atmospheric Administration, National Climatic Data Center Report.

Negecu, W.M. & Mathu, E.M. 1999. The El Nino triggered landslides and their socio-economic impacts on Kenya. *Episodes* 22: 284–288.

Parker, D.E., Alexander, L.V. & Kennedy, J. 2004. Global and regional climate in 2003. *Weather* 59: 145–152.

Schuster, R.L. & Highland, L.M. 2001. Socioeconomic and environmental impacts of landslides in the western hemisphere, *USGS Open-File Report*, 01–276.

The role of magnitude-frequency relations in regional landslide risk analysis

R.H. Guthrie
Ministry of Water, Land and Air Protection, Nanaimo, British Columbia, Canada

S.G. Evans
University of Waterloo, Waterloo, Ontario, Canada

ABSTRACT: Correct characterization of landslide magnitude and frequency is necessary to adequately resolve the hazard component of the risk equation. Recent work across several watersheds in coastal British Columbia has lead to new insights into magnitude-frequency relationships. These insights include probabilistic data that support the notion that landslides in coastal British Columbia tend to a larger size until limited by the landscape (valley bottoms, streams other landslides). Beyond about $10,000\,m^2$, the probability of successively larger landslides decreases rapidly in a relation typically described as a power law. We elucidate the relative importance of reliable regional inventories, data robustness and resolution (in both space and time), and temporal variation including human activity and climate change. We argue that probabilistic regional hazard analysis is a logical outcome of magnitude frequency analysis and related to the sensitivity of the landscape to the hazard. To this end we have mapped the regional mass movement hazard for Vancouver Island and present the generalized probabilistic result across four major hazard zones.

1 INTRODUCTION

Risk is commonly used as both a scientific term and a colloquialism. In general it is philosophically easy to comprehend. Risk is typically defined as some variation of the hazard times the consequence of that hazard occurring (Lee & Jones 2004). Recently, there has been considerable progress in the quantification of landslide hazard through the use of a characteristic magnitude and frequency (m/f) relation. The m/f relation is a type of hazard model (Lee & Jones 2004).

Analysis of risk takes geoscientists and engineers away from simply determining whether a landslide will occur in a specific area and asks the pivotal questions (1) with what probability? and (2) with what consequence? While it is generally recognized that the probability of a hazard occurring is a critical component of the risk equation, there is perhaps the notion that we already fully understand hazard analysis or that we are at the very least competent in assessing hazard. To a certain extent this notion is probably true; quantitative hazard analysis is well documented, particularly for site specific hazards (see Turner & Schuster 1996) for detailed examples of landslide hazard analysis techniques.

Significant recent progress has been made on the quantification of regional landslide hazard (see recent review by Malamud et al. 2004).

The application of landslide m/f relations to hazard and quantitative risk assessment has been most successfully demonstrated with respect to rockfall hazard along linear transportation corridors. Following Hungr et al. (1999) work by Guzzetti et al. (2003, 2004), and Singh & Vick (2003) has demonstrated the utility of the methodology.

However, this progress has used a very limited number of landslide data sets. In addition, a dearth of natural landslide data sets, complete inventories, time series analysis and available terrain data, combined with qualitative and inconsistent classification of hazard, have resulted in, at best, inconsistent understanding of regional landslide hazard from one practitioner to another.

Our objectives in this paper are fourfold. We argue that the correct characterization of landslide magnitude and frequency is critical to adequately resolve the hazard component of the risk equation. We show that useful magnitude frequency relationships can be established as a result of complete landslide inventories and present recent data from British Columbia.

We briefly discuss the implications for the general understanding of landslide hazard. Lastly, We argue that probabilistic regional hazard analysis is a logical outcome of magnitude-frequency analysis and related to the sensitivity of the landscape to landslide hazard.

2 LANDSLIDE HAZARD MAPPING IN BRITISH COLUMBIA

2.1 *Qualitative regional hazard analysis*

In 1995 British Columbia introduced the Forest Practices Code to govern its largest resource extractor: the forest industry. Terrain hazard mapping was required for all areas proposed for harvest or road construction (alternatively a conservative series of defaults were applied that led to detailed assessments of potentially unstable ground at the site level).

Knowledge of the landslide processes and terrain features generally resulted in a "traffic light" system of hazard rating for landscape units at a given scale. The rating scheme was typically qualitative, with predictive descriptors and/or harvest and construction limitations attached to it (Table 1).

The result was typically a landslide hazard map (often at a scale of 1:20,000, however, hundreds of block specific maps have also been produced) codified to represent the range in hazard.

Despite a relatively consistent methodology for determining hazard, there is, in practice, little consistency in the meaning of each of the categories. Second there is a somewhat inconsistent application of decisions based on the hazard score. In effect, prior to formal risk analysis, risk was implicitly incorporated by practitioners based on incomplete understanding

Table 1. Landslide hazard classification scheme adapted from the Mapping and Assessing Terrain Stability Guidebook (British Columbia Ministry of Forests and Ministry of Environment 1999).

Terrain stability class	Interpretation
I	No significant stability problems
II	Very Low likelihood of landslides following forestry activities; minor slumping at road cuts
III	Low likelihood of landslides following forestry activities; minor stability problems can develop
IV_R	Moderate likelihood of landslides following road construction, low to very low following harvesting
IV	Moderate likelihood of landslides following forestry activities
V	High likelihood of landslides following forestry activities

of the hazard and incomplete consideration of the consequences.

New legislation passed in 2004 obligates forest companies to "… *ensure that the primary forest activity does not cause a landslide that has a material adverse effect …*" (Government of British Columbia 2004). Consequence is now written into law.

Despite this, or rather because of it, we argue that accurate hazard analysis is more important than ever.

2.2 *Quantifying regional hazard analysis*

In the regional context, quantifying the landslide hazard depends on an accurate and complete inventory. There are several types of landslide inventories including:

- Total count of landslides within an area from a point in time (air photograph analysis or a geomorphological map for example).
- Total count of landslides within an area through several points in time (time series analysis, including air photographs, archived maps, reports, dendrochronology and so forth).
- Total count of landslides within a sampled subset of the area of interest (through time or not)
- Partial or stratified count of landslides (by landslide type or size for example) through any of the above.
- Various incomplete inventories.

In each case, the power of the inventory is dictated by the constraints that bound it, and the completeness of the inventory within those constraints.

Landslides that are spatially constrained from a point in time give us an indication of landslide density rather than frequency, or more exactly, landslides per unit area rather than landslides per unit area per unit time. Such an inventory provides substantial data that is amenable to probabilistic analyses; however, it incorporates several temporal biases that make comparisons between natural and altered landscapes difficult. Landslide inventories are by nature a retrospective exercise, and the natural conditions have existed for substantially longer than the conditions consequent of humans altering the landscape (in our previous examples, by logging and building roads).

In general this serves to increase the natural landslide count as compared to, for example, the landslide count related to logging activity. Jakob (2000) recognized the problem in a complete inventory of landslides in Clayoquot Sound, British Columbia, and applied a correction factor to allow for an analysis of how landslides changed in time.

The correction factor, while overemphasizing strong differences in landslide density and underemphasizing weak differences, gives reasonably comparable results to the more recent time series analyses (Guthrie & Evans 2004a, Guthrie 2002, in prep.).

376

This is by far the most common type of inventory with several notable examples from coastal British Columbia (Rood 1984, Sauder et al. 1987, Thomson 1987, Gimbarzevsky 1988, Rollerson et al. 1997, 1998, Jakob 2000, Guthrie & Evans 2004a).

The second example, while less common in the literature, offers the additional ability clearly understand the hazard through time (Guthrie 2002, Guthrie & Evans 2004a) and the return interval of a particular hazard or series of hazards. Time series analysis can be used to calibrate the spatial inventories, thereby increasing their analytical power (Guthrie, in prep.).

Incomplete inventories are somewhat like case studies in that they help to define, recognize and characterize landslide hazard, however, they tell us little in the way of predictive results or allow us to accurately assign risk. Unfortunately many decisions are made as the result of incomplete inventories, beginning with our mental maps of landslide hazard through to analysis of only those landslides reported for a region and the biases inherent within.

The inaccuracy of mental maps is demonstrated in the following example. In any given year, an employee takes (for example) two weeks off work for summer vacation. In year x 10 of 14 days he is on vacation are rainy and gray. In year y all 14 days are hot and sunny. Upon reflection the summer of year x is remembered as relatively cool and wet, while the summer of year y is remembered as hot and dry. In either case, the mental map may or may not be related to the actual conditions of a summer that occurs over 90 days. Similarly, an incomplete data set may or may not be a reflection of the whole. This is even more evident (in our example) if the vacation occurs in a place that is unfamiliar to the employee. His frame of reference is reduced further. In landslide-speak, this occurs when someone estimates landslide hazard in a watershed (or a given area) based on an incomplete inventory, and is compounded when that watershed is unfamiliar.

2.3 Magnitude and frequency

Complete inventories allow for the probabilistic analysis of landslide data, which in turn, allows for the accurate characterization of the landslide hazard: How big, how likely and if calibrated against time, how often?

Guthrie & Evans (2004a, b) examined several complete inventories for coastal British Columbia (Fig. 1). Magnitude frequency relations were compared between data sets that differed in location and study design. Clayoquot data was bound spatially while the Brooks Peninsula study incorporated a time series analysis, and the Loughborough Inlet study was the result of a single storm.

The resultant magnitude frequency curves were remarkably self similar (Fig. 2). In all cases landslides

tended to a larger size until about 10,000 m² where probability of occurrence dropped substantially as the landscape became the primary limiter.

Insights gained from these analyses included a renewed understanding of the rollover effect and on the potential run-out distance of coastal British Columbian debris slides and flows. Specifically, for coastal BC, landslides have a tendency to initiate on mid and upper slopes between about 31 and 45 degrees (generalized somewhat for this discussion), and travel to or beyond a topographic baseline of streams or the valley floor. The notion that landslides in coastal BC
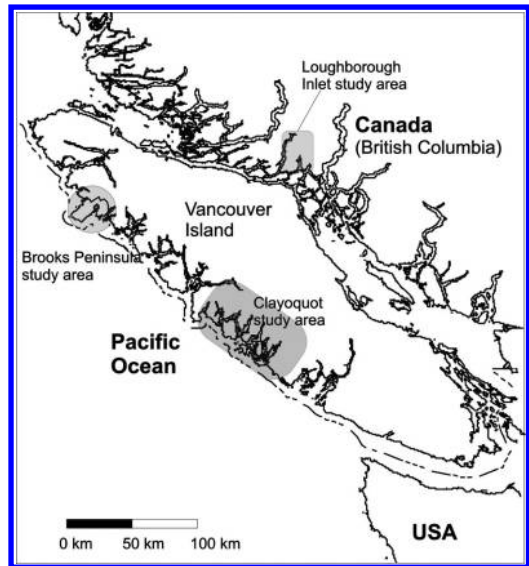

Figure 1.   Locations of complete inventories for coastal BC analyzed by Guthrie & Evans (2004a).
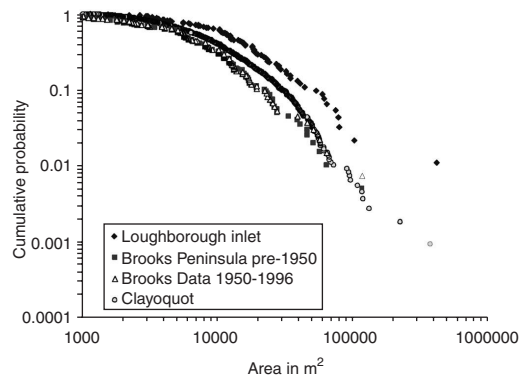

Figure 2.   Cumulative magnitude frequency curves for some coastal BC watersheds (from Guthrie & Evans 2004a).

377

will stop at a "bench" on the slope is a common misconception that, while possible, remains improbable.

The inventories have also allowed us to begin to characterize the actual impact of human effects on the natural landslide rate. While there is substantial local variability, the regional impact that has resulted from logging and road building in coastal BC appears to be in the order of a 10 times increase in landslides per unit area per unit time (Jakob 2000, Guthrie 2002, in prep., Guthrie & Evans 2004a). A complete inventory and subsequent analysis for the Nelson forest region (interior British Columbia) yielded similar results (Jordan 2003).

Additional analysis successfully applied from complete landslide inventories in coastal British Columbia include: relating landslide to terrain attributes and geology (Rollerson et al. 1997, 1998, 2002, Sterling 1997, Guthrie & Evans 2004a, Guthrie, in prep.), determination of landscape denudation (Martin et al. 2002, Guthrie & Evans 2004a, b) and establishing a relationship between high intensity storm cells within regional precipitation events and landslide distribution patterns (Guthrie & Evans 2004a, b)

In another example, complete inventories recently conducted by Weyerhaeuser suggest that there is a discernable improvement in road related landslides following the Forest Practices Code in 1995 (Higman, personal communication).

In each case the analysis requires an understanding of the frequency characteristics of landslides for that region, and in all cases denoting impact (landscape denudation for example) magnitude is also critical.

2.4 *A probabilistic regional hazard map: The next step*

The next step has begun on Vancouver Island British Columbia where a regional map showing mass movement potential was derived at a scale of 1:100,000. The map was based on the compilation of the research of several authors referred to above, and on the digitally available data on terrain, geology, climate, physiography and so forth. Guthrie (in prep.) subsequently developed an inventory based on stratified randomly sampled sites across the island to further establish the magnitude frequency relationships.

The result divides Vancouver Island into four major zones:

- Zone I – The wet west coast; characterized by steep fjords, densely vegetated terrain and high precipitation falling as rain in winter months ($>2.6\,\mathrm{m\cdot y^{-1}}$). Landslides are typically debris slides and flows.
- Zone II – The moderately wet central island; characterized by steep terrain, densely vegetated with exposed small outcrops, precipitation between 1.6–$2.6\,\mathrm{m\cdot y^{-1}}$ falling mostly in winter months.
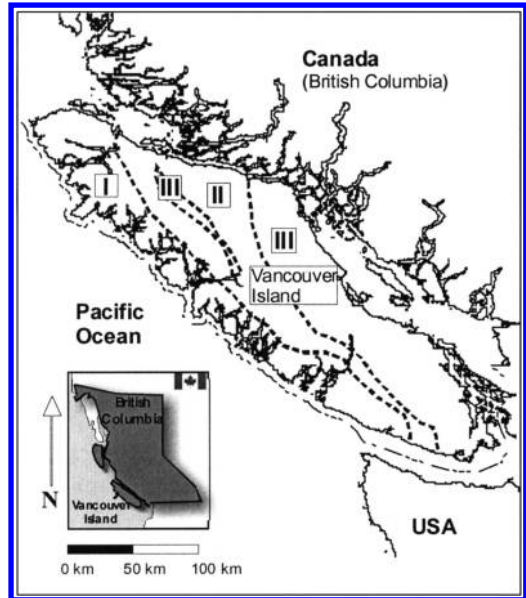

Figure 3. Simplified mass wasting potential zones for Vancouver Island, British Columbia. Zones I–III are described in Table 2. Note that the Alpine zone (IV) is not shown and spans the higher elevation portions of all three zones on this map. The Alpine zone is at least four times more active than Zone I.

Landslides are typically debris slides and flows with some rock falls.
- Zone III – The moderately dry east coast; characterized by more exposed bedrock lower rainfall ($<1.6\,\mathrm{m\cdot y^{-1}}$), increased urbanization and rural development and shallower slope gradients. One quarter of landslides identified were rock falls.
- Zone IV – The alpine zone; characterized by high elevation steep cliffs and plateaus, exposed bedrock, ponded water, steep gorges and sparse vegetation, most of the precipitation falling as snow in the winter months. Landslides commonly include rock falls, snow avalanches, debris slides and debris flows.

The approximate locations of three of the major zones are shown in Figure 3. The alpine zone spans the high elevation components of all three zones and was not included in the figure. Please note that the figure is greatly simplified for discussion purposes.

Additional sub zones were also determined based on the effects of geology, however, for that discussion the reader is referred to Guthrie (in prep.).

The natural landslide frequency was determined for zones I–III and compared to previous research. The results mapped onto Figure 3 give a first ever approximation of the actual failure rates for those zones across Vancouver Island (Table 2).

378

Table 2. Natural landslide frequency tables for zones I–III. Logging related landslide frequencies were also calculated and were about 10–13 times greater than the natural frequencies for all zones (see Guthrie, in prep.). Note that the frequency relates to a long term average, the actual failures are typically clustered in both time and space (Guthrie & Evans 2004a, b).

Zone	Natural landslide frequency ($\# \cdot km^{-2} \cdot y^{-1}$)	Area required for 1 landslide per year (km^2)
I	0.012	83
II	0.007	143
III	0.004	250

While local variability is expected to be large, the map attempts to quantify the regional hazard and examines the difference in landscape sensitivity across the island. Differences in landscape sensitivity were already part of the mental maps for several slope specialists with local experience, however, the extent to which this is in fact the case, is finally being explored.

The analysis can be taken still further by incorporating frequency magnitude curves such as those in Figure 2 to predict over a defined period, not only how many, but how large the landslides will be. This leads to additional insights into overall landscape denudation and begins to contribute to the consequence component of risk analysis, again, at a regional level.

3 CONCLUSIONS

Accurate landslide hazard assessment is a critical component of the risk equation. A dearth of natural landslide data sets, complete inventories, time series analysis and available terrain data, combined with qualitative and inconsistent classification of landslide hazard have resulted in, at best, inconsistent understanding of regional landslide hazard between practitioners. Complete inventories are becoming available, or can be acquired, that allow the user to place hazard within a quantifiable regional context. Analysis of these inventories yields answers to the all important questions: How big, how likely and how often? With sufficient data analyzed, differences in landscape sensitivity are revealed and can be handled accordingly.

Regional hazard mapping of Vancouver Island resulted in the generation of four major zones of mass movement potential, and subsequent frequency magnitude characteristics. Differences in landslide type and frequency for each of the four zones are caused primarily by differences in climate. Natural landslides are three times more common on the wet west coast of Vancouver Island, than the eastern zone at, on average, one landslide per 83 km^2 per year. Distribution of

landslide size can be derived from the magnitude frequency relation for the west coast watersheds.

Once the landslide hazard is accurately characterized, the question of consequence takes on new relevance, and the risk assessment increases in value and accuracy.

REFERENCES

British Columbia Ministry of Forests & Ministry of Environment 1999. *Forest Practices Code of British Columbia, Mapping and Assessing Terrain Stability Guidebook*, Second Edition. Government of British Columbia, Victoria, BC.

Government of British Columbia 2004. Forest Planning and Practices Regulation, Forest and Range Practices Act.

Gimbarzevsky, P. 1988. Mass wasting on the Queen Charlotte Islands – a regional inventory. *British Columbia Ministry of Forests Land Management Report* 29, Victoria, BC.

Guthrie, R.H. 2002. The effects of logging on frequency and distribution of landslides in three watersheds on Vancouver Island, British Columbia. *Geomorphology* 43: 273–292.

Guthrie, R.H. in prep. Geomorphology of Vancouver Island: Mass movement potential. *Ministry of Water, Land and Air Protection technical report*. Ministry of Water, Land and Air Protection, Victoria, BC.

Guthrie, R.H. & Evans, S.G. 2004a. Analysis of landslide frequencies and characteristics in a natural system, Coastal British Columbia. *Earth Surface Processes and Landforms* 29: 1321–1339.

Guthrie, R.H. & Evans, S.G. 2004b. Magnitude and frequency of landslides triggered by a storm event, Loughborough Inlet, British Columbia. *Natural Hazards and Earth System Sciences* 4: 475–783.

Guzzetti, F., Reichenbach, P. & Ghigi, S. 2004. Rockfall hazard and risk assessment along a transportation corridor in the Nera Valley, Central Italy. *Environmental Management* 34:191–208.

Guzzetti, F., Reichenbach, P. & Wieczorek, G.F. 2003. Rockfall hazard and risk assessment in the Yosemite valley, California, USA. *Natural Hazards and Earth System Sciences* 3: 491–503.

Hungr, O., Evans, S.G. & Hazzard, J. 1999. Magnitude and frequency of rock falls and rock slides along the main transportation corridors of southwestern British Columbia. *Canadian Geotechnical Journal* 36: 224–238.

Jakob, M. 2000. The impacts of logging on landslide activity at Clayoquot Sound, British Columbia. *Catena* 38: 279–300.

Jordon, P. 2003. Landslide and terrain attribute study in the Nelson forest region. *Final report to Ministry of Forests Research Branch*, Nelson, BC.

Lee, E.M. & Jones, D.K.C. 2004. *Landslide Risk Assessment*. Thomas Telford, London. 454 p.

Malamud, B.D., Turcotte, D.L., Guzzetti, F. & Reichenbach, P. 2004. Landslide inventories and their statistical properties. *Earth Surface Processes and Landforms* 29: 687–711.

Martin, Y., Rood, K., Schwab, J.W. & Church, M. 2002. Sediment transfer by shallow landsliding in the Queen

Charlotte Islands, British Columbia. *Canadian Journal of Earth Science* 39: 189–205.

Rollerson, T.P., Thomson, B. & Millard, T. 1997. Identification of Coastal British Columbia terrain susceptible to debris flows. In *Proceedings of the 1st International Symposium on Debris Flows, August 7–9, San Francisco*. United States Geological Survey and the American Society of Civil Engineers: San Francisco, CA.

Rollerson, T.P., Jones, C., Trainor, K. & Thomson, B. 1998. Linking post-logging landslides to terrain variables: Coast Mountains, British Columbia – preliminary analyses. In *Proceedings of the 8th International Congress of the International Association for Engineering Geology and the Environment*. Balkema Rotterdam; 3: 1973–1979.

Rollerson, T.P., Millard, T. & Thomson, B. 2002. *Using terrain attributes to predict post-logging landslide likelihood on southwestern Vancouver Island*. Forest Research Technical Report TR-015. Research Section, Vancouver Forest Region, BC Ministry of Forests: Nanaimo, BC.

Rood, K.M. 1984. An aerial photograph inventory of the frequency and yield of mass wasting on the Queen Charlotte Islands, British Columbia. *Ministry of Forests Lands Management Report* 34, Victoria, BC.

Sauder, E.A., Krag, R.K. & Welburn, G.V. 1987. Logging and mass wasting in the Pacific Northwest with application to the Queen Charlotte Islands, B.C. *British Columbia Ministry of Forests Land Management Report* 53, Victoria, BC.

Singh, N.K. & Vick, S.G. 2003. Probabilistic rockfall hazard assessment for roadways in mountainous terrain. *Proceedings, 3rd Canadian Conference on Geotechnique and Natural Hazards*, Canadian Geotechnical Society, Edmonton, p. 253–260.

Sterling, S.M. 1997. *The influence of bedrock type on magnitude, frequency and spatial distribution of debris torrents on northern Vancouver Island*. M.Sc. Thesis, University of British Columbia, Vancouver, BC.

Thomson, B. 1987. Chapman Creek landslide inventory. 1:20,000 scale map with legend. *British Columbia Ministry of Environment, Lands and Parks technical report*, Victoria BC.

Turner, K.A & Schuster, R.L. (eds) 1996. *Landslides, Investigation and Mitigation.* Transportation Research Board Special Report 247, National Research Council, Washington, D.C.: National Academy Press.

Evaluation of risk to the population posed by natural hazards in Italy

F. Guzzetti & P. Salvati
IRPI CNR, Perugia, Italy

C.P. Stark
Lamont-Doherty Earth Observatory, Columbia University, Palisades, NY, USA

ABSTRACT: In Italy, people's lives are put at risk by a variety of natural hazards. We use historical catalogues of landslides, floods, earthquakes and volcanic events to estimate and compare, in a quantitative fashion, those levels of risk. We reveal the temporal distribution of harmful events, and we estimate the completeness of the available catalogues. Next, we evaluate individual and societal risk levels posed by the damaging events. We determine individual risk by computing mortality rates, which we compare with the death rates of societal and technological hazards and of the leading medical causes of death in Italy. We further quantify the societal risk by analyzing the frequency of damaging events versus their consequences, measured by the total number of fatalities in each event. To accomplish this we used a Bayesian model that describes the probability of lethal landslide, flood, earthquake and volcanic events in Italy.

1   INTRODUCTION

Landslides, floods, earthquakes and volcanic eruptions are common events in Italy that cause damage every year. Systematic information exists on the consequences of landslides and floods for the population of this country (Guzzetti 2000, Salvati et al. 2003). For this paper, we have revised and updated the catalogues of landslides and floods with human consequences compiled by Guzzetti (2000) and Salvati et al. (2003), and we have prepared a new catalogue of earthquakes and a list of volcanic events that have caused deaths, missing persons, injured people and homelessness in Italy. We use this information on historical damaging events to evaluate the risk posed by different natural hazards to the Italian population, and to compare it with levels of societal and technological hazards and of the leading medical causes of death in Italy.

1.1   *Glossary*

In this work, we use the term *fatalities* to indicate the sum of the deaths and the missing persons caused by a damaging event. *Casualties* indicate the sum of fatalities and injured people. *Evacuees* were people forced to abandon their homes temporarily, while the *homeless* were people that lost their homes. *Human consequences* encompass casualties, homeless people and the evacuees. A *fatal event* is an event that resulted in fatalities. *Individual* risk is the risk imposed by a hazard to any unidentified individual. *Societal* risk is the risk imposed by a hazard on society as a whole (Cruden & Fell 1997, Guzzetti 2000, ISSMGE TC32 2004).

2   AVAILABLE DATA

To evaluate levels of risk posed by natural hazards in Italy we use four catalogues of damaging natural events, namely: (i) the catalogue of landslides with human consequences originally prepared by Guzzetti (2000) and revised by Salvati et al. (2003); (ii) the catalogue of floods with human consequences prepared by Salvati et al. (2003); (iii) a new catalogue of earthquakes with human consequences; and (iv) a new list of volcanic events that resulted in casualties.

Details on the sources of information and on the problems encountered in compiling the catalogues of landslide and of flood events with human consequences are given in Guzzetti (2000) and Guzzetti et al. (2005). For this work, we have updated these catalogues to cover the period from 91 BC to 2004 and the period from 1195 to 2004, respectively. To complete the update we searched newspapers for the recent period, and we conducted a specific library and archive search for the period 1800 to 1900.

We compiled the new catalogue of earthquakes with human consequences by systematically searching the "Catalogue of the Strongest Italian Earthquakes", 3rd edition (Boschi et al. 2000), which covers the period

from 461 BC to 1997. In this catalogue, information on events that caused damage to the population spans the period from 51 AD to 1997. Additional information on damage caused by recent earthquakes in Italy in the period from 1997 to 2004 was obtained by searching newspapers and the sparse technical literature.

No systematic information is available in Italy for volcanic eruptions and associated phenomena resulting in damage to the population. To compile the list of damaging volcanic events we used the work of Catenacci (1992) who reported natural disasters in Italy, including eruptions for the period from 1945 to 1990. In addition, we searched the Internet and the archives of local newspapers, the latter for the period between 1990 and 2004. The list of harmful volcanic events covers unsystematically the period from 79 AD (i.e., the famous eruption of Mount Vesuvius that destroyed Herculaneum and Pompeii) until 2004. Table 1 lists the characteristics of the four historical catalogues, and Figure 1 shows box plots portraying descriptive statistics for the catalogues.

2.1 Historical distribution of events with casualties

Figure 2 shows the historical distribution of events with casualties in Italy, for the period from 1500 to 2004. In the graphs black squares indicate the number of fatalities in each event, and black triangles the number of the injured people. Open squares indicate schematically events for which casualties are know to have occurred but for which the exact, or even an approximate number, is unknown.

Inspection of Figure 2 indicates that between 1500 and 2004, the worst year for landslides was 1963 with

1950 casualties, 1921 of which occurred at Vajont. The second worst year was 1618, when 1200 people were killed by the Piuro rockslide-avalanche (Lombardy), followed by 1765 with about 600 deaths at Roccamontepiano (Abruzzo). Between 1500 and 2002, the worst year for floods was 1705 with as many as 15,000 flood casualties in the Po plain. The second worst year was 1557, with as many as 7000 estimated flood casualties in Palermo (Sicily). Particularly severe events occurred in 1610, with 4034 deaths in Piedmont, and in 1530 and 1598, with 3000 estimated flood casualties in Rome. For earthquakes, the worst year in the record was 1908, with as many as 80,000 casualties caused by the December 28, Messina-Reggio Calabria earthquake (7.1 Me) and associated tsunami. The second worst year was 1693, with 54,000 casualties caused by the January 1, Eastern Sicily earthquake (7.4 Me). In the same period, the worst year for volcanic eruptions was 1631, with 4000 estimated casualties caused by an eruption of Mount Vesuvius (Campania). The same volcano killed 16,000 in 79 AD.

In the period between 1900 and 2004, the years in which more than one hundred people were killed by landslides were: 1910 (255 deaths), 1924 (118 deaths), 1951 (167 fatalities), 1954 (336 deaths), 1963 (1950 fatalities), 1985 (300 fatalities) and 1998 (171 fatalities). In the same period, the years with more than one hundred fatalities caused by floods were: 1902 (113 deaths), 1915 (131 deaths), 1923 (359 deaths), 1935 (157 deaths), 1951 (178 fatalities), 1953 (114 deaths) and 1985 (271 fatalities). Guzzetti et al. (2005) noted that the three most catastrophic landslide and flood events in the 20th century were all caused by or were associated with the presence or the failure of dam or a man-made embankment, indicating the potentially destructive effect of artificial structures. From 1900 to 2004, 7 earthquakes killed more than 100 people, and

Table 1. Characteristics of four historical catalogues of damaging natural events. L, landslides; F, floods; E, earthquakes; V, volcanic events.

|	L	F	E	V
From	91 BC	1195	51 AD	79 AD
To	2004	2004	2004	2004
Number of events with casualties	1275	955	182	26
Fatalities				
Total	11,546	37,167	394,791	35,340
Mean	11.4	41.9	2530.7	2078.8
Standard dev.	83.0	588.2	756.8	5145.3
Maximum	1921	15,000	80,000	16,000
Injured people				
Total	2295	2483	38,077	193
Mean	4.6	10.1	624.2	19.3
Standard dev.	17.0	40.4	219.1	43.5
Maximum	300	529	9000	142
Events with homeless	1335	1278	134	–
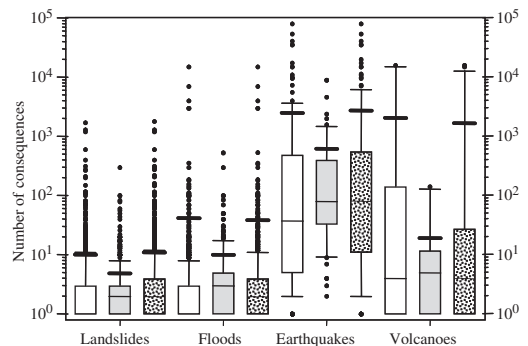
Figure 1. Box plots showing statistics for the four catalogues of natural events with human consequences in Italy. White boxes show fatalities, gray boxes injured persons, and dotted boxes casualties. Horizontal thick lines show mean values.

3 earthquakes killed more than 1000 people, including the Messina-Reggio Calabria earthquake (80,000 deaths, 2000 of which were caused by a tsunami (Boschi et al. 2000)), the Marsica earthquake of 13 January 1915 (7.0 Me, 35,610 deaths), and the 23 November 1980 Irpinia-Basilicata earthquake (6.7 Me, 2483 deaths). From 1900, only one eruption, of Mount Vesuvius on 4 April 1906, caused more than 100 fatalities (227 deaths in the villages near Naples).
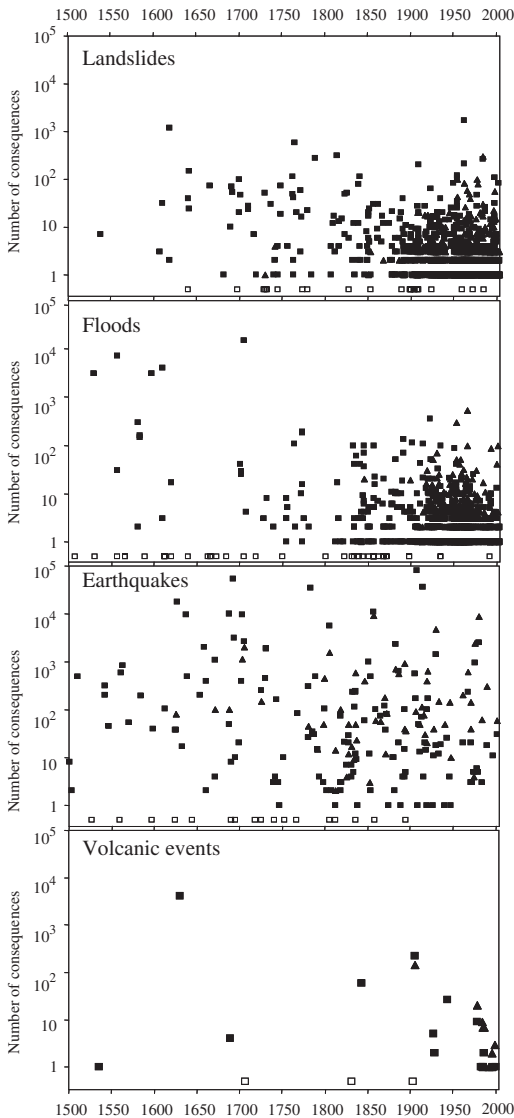

Figure 2. Historical distribution of damaging events in Italy, form 1500 to 2004. Black squares, fatalities; black triangles, injured people; open squares, events for which casualties occurred in unknown number.

Inspection of Figure 2 reveals different historical patterns of the damaging events. For earthquakes, events of all intensities are – almost – equally distributed in time, with a certain increase of low to medium intensity events after about 1800. Landslides and floods show a much larger number of damaging events (Table 1) than earthquakes, particularly for low to medium intensity events. This is due to the higher frequency of the meteorological events that cause landslides and floods when compared to the frequency of the damaging earthquakes. Landslides and floods exhibit an increase in the number of events (for all intensities) starting from 1800 and more manifestly after 1900. This is due to incompleteness of the landslide and flood records in the early years of the catalogues. The record of volcanic events with fatalities and injured people is small when compared to the other catalogues. This is largely a result of the incompleteness of the historical record, and of the low frequency of volcanic events with large human consequences, when compared to other natural hazards.

3 COMPLETENESS OF THE CATALOGUES

Historical catalogues are non-instrumental records of past events. Estimating the completeness of a historical catalogue is not an easy task. In a historical database, the absence of recorded events in any given period may be due either to database incompleteness or to variation in the conditions that led to hazardous events. Causes for the variations include differences in the frequency and magnitude of the natural phenomena that result in damage, including the triggering causes and changes in the abundance, distribution, vulnerability and values of the elements at risk, including the population. Most often, both variations exist and affect (in an unknown form) completion of the historical record.

We estimate the completeness of the historical catalogues using the empirical approach of Guzzetti (2000). The approach is based on the visual comparison of the cumulative curves of damaging events of increasing intensity, from very low (1–2 fatalities) to very high (≥100 fatalities, ≥1000 fatalities for earthquakes). Our results are summarized in Figure 3. Inspection of the figure reveals that the (apparent) rate of fatalities (i.e., the slope of the curves) has increased significantly since the beginning of the record, largely as a result of variations in the completeness of the historical catalogue. The more remote the period considered, the larger the number of events that probably remained unrecorded.

In the historical catalogues, low intensity events, i.e., events that caused fewer than three fatalities (Evans 1997), rarely appear before 1800 (32 flood events, 29 landslide events, 5 earthquake events and

1 volcanic event), but after 1800 they represent 30.5% of the total number of landslides, 27.5% of the total number of floods, 15.6% of the total number of earthquakes, and 58.3% of the total number of volcanic events. The percentages are still larger after 1900. Even considering the increase in population that has occurred, there is no reason for the distribution of less catastrophic events to be so skewed, except as a result of incompleteness of the database.

Inspection of Figure 3 reveals different degrees of completeness for the different hazards. For landslides and floods, the slope of the cumulative curves of all

Figure 3. Cumulative distributions of events that resulted in fatalities in Italy.

the events that resulted in one or more fatalities (D) increases sharply after about 1900, indicating incompleteness in the catalogues before the 20th century for low intensity events. For earthquakes, the slope of the cumulative curve of all the events that resulted in one or more fatalities (D) increases after about 1700, indicating incompleteness in the catalogues before the 18th century for low intensity events. The cumulative curves for high and very intensity events (A and B) are about constant after 1600 for landslides, after 1750 for floods, and after 1350 for earthquakes. For floods, Figure 3 shows a distinct lack of information for the 15th and 16th centuries. The lack of high intensity events in the 20th century is possibly due to the remedial measures taken in large cities and flood plains at the end of the 19th century (Guzzetti et al. 2005). For volcanic events, Figure 3 shows that the record is deficient and incomplete before 1920.

The completeness of the catalogues varies with the intensity of the events. For very large intensity events (≥100 fatalities) the landslide catalogue is probably complete for the period 1600–2004, the flood catalogue for the period 1750–2004, and the earthquake catalogue for the period 1500–2004. If all events are taken into account, the landslide and the flood catalogues can be considered substantially complete for statistical purposes starting in 1900 and complete after 1950 (Guzzetti et al. 1995). The earthquake catalogue can be considered substantially complete starting in 1600 and complete after 1850. The catalogue for volcanic events is complete for statistical purposes starting in 1950.

4 RISK TO THE POPULATION OF ITALY

We now attempt to evaluate the levels of risk posed by the considered natural hazards, and to compare them. We first discuss individual risk levels, and we then illustrate societal risk.

4.1 *Individual risk*

Individual risk criteria are most commonly expressed using mortality rates, which are given by the number (or average number) of deaths per 100,000 of any given population over a pre-defined period. In Italy, nationwide information on population is available from 1861 to 2001 from censuses carried out every ten years by the *Istituto Nazionale di Statistica* (the Italian census bureau, http://www.istat.it). For the period from 2002 to 2004 we used estimates. By combining this information with the annual number of fatalities caused by natural hazards, we estimated the average death rates for landslides, floods, earthquakes and volcanic eruptions in Italy in the 145-year period between 1861 and 2004. Table 2 summarizes the results.

384

If one considers the period 1861–2004, average mortality was largest for earthquakes (2.42), followed by landslides (0.09), floods (0.05) and volcanic events (0.005). Similarly, for the period between 1900 and 2004, the average death rates are 3.22 for earthquakes, 0.11 for landslides, 0.06 for floods, and 0.007 for volcanic events. The ranking of the most destructive hazards changes in the post World War II period, when the average landslide mortality was 0.14, a value similar to the mortality for earthquakes (0.12), and more that three times larger than the mortality for floods (0.04). In the period, the death rate for volcanic events was 0.007. The change in the ranking of the most destructive hazards is largely due to the Vajont landslide event (1921 fatalities) and to the lack of

Table 2. Mortality rates for natural, technological and human-induced hazards in Italy, for different periods.

Hazard	min	max	mean	stdv
1861–2004				
Landslides	0.0	3.80	0.09	0.33
Floods	0.0	0.90	0.05	0.11
Earthquakes	0.0	228.9	2.42	20.55
Volcanoes	0.0	0.60	0.005	0.05
1900–2004				
Landslides	0.0	3.80	0.11	0.38
Floods	0.0	0.90	0.06	0.11
Earthquakes	0.0	228.9	3.22	24.12
Volcanoes	0.0	0.60	0.007	0.05
1950–2004				
Landslides	0.002	3.80	0.14	0.52
Floods	0.0	0.38	0.04	0.07
Earthquakes	0.0	4.41	0.12	0.64
Volcanoes	0.0	0.60	0.007	0.05
1990–2004				
Landslides	0.002	0.34	0.05	0.08
Floods	0.0	0.11	0.02	0.03
Earthquakes	0.0	0.05	0.007	0.02
Volcanoes	0.0	0.002	0.0003	0.0007
Snow avalanches[1]	0.016	0.065	0.032	0.017
Airplane accidents[2]	0.00	0.20	0.02	0.06
Road accidents[3]	10.29	13.21	11.61	0.87
Workplace accidents[4]	2.06	2.52	2.48	0.16
Homicides[5]	1.10	3.19	1.83	0.61
Drug overdose[6]	1.48	2.45	2.02	0.38
All types of disease[6]	955.1	983.7	967.5	9.03
Heart diseases[6]	127.8	134.2	129.4	2.88
Cancer[6]	260.6	276.1	270.3	5.31
Diabetes[6]	28.58	34.12	31.40	1.96
AIDS[6]	2.18	8.31	5.54	2.18
Influenza[6]	0.73	2.00	1.38	0.48

Sources: of information: [1] Italian Alpine Club (1986–2001); [2] Aviation Safety Network (1990–2003); [3] ISTAT (1990–2000); [4] ISPSEL (1995–2002); [5] EuRES (1991–2002); [6] Istituto Superiore di Sanità (1990–2003). Modified after Guzzetti et al. (2005).

earthquakes that resulted in several thousands of fatalities. However, it should be noted that in the period the single event that caused the largest number of fatalities was the Irpinia-Basilicata earthquake (2483 deaths).

In the period 1990–2004, landslides were the primary cause of fatalities due to natural hazards (0.048), followed by floods (0.025), earthquakes (0.007) and by volcanic events (0.0003). Since 1990, the landslide mortality has been about twice the flood mortality, confirming that in Italy slope movements are more dangerous than floods.

A limitation of the mortality criteria lies in the fact that they depend on the size and the distribution of the population with which they are associated, which change with time. Figure 4 shows that the population of Italy increased from 22.16 million in 1861 to 57.88 million in 2003, an increase of 161.2%. In the investigated period, the average number of fatalities per year (i.e., the total number of fatalities in the period divided by the length of the period) was: 865.8 for earthquakes, 39.2 for landslides, 21.9 for floods, and 1.9 for volcanic eruptions. Thus, the average mortality (the risk to any individual) decreased, from 3.91 to 1.50 for earthquakes, from 0.18 to 0.07 for landslides, from 0.10 to 0.04 for floods, and from 0.01 to 0.003 for volcanic events.

The latter figures may lead to the conclusion that risk imposed by natural hazards has halved over the last 145 years. If the average mortality has decreased (because the population has increased), the abundance and geographical distribution of the population have changed. Figure 4 shows that the population of Italy increased differently in various physiographical regions. The increase was largest in the "plains" (300.8%), moderate in the "hills" (117.9%), and least in
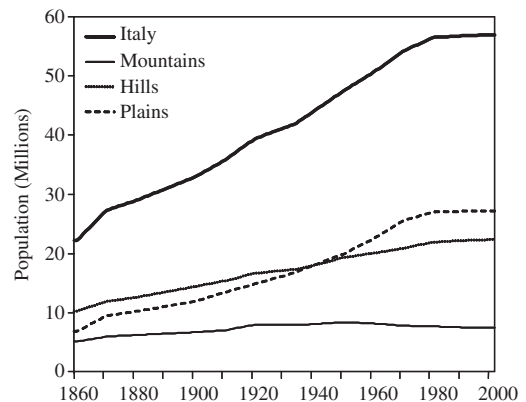

Figure 4. Historical variation of the population in Italy, from 1861 to 2004. Population for the entire Country and for three physiographical subdivisions is shown.

the "mountains" (44.6%). Starting in the 1920s, and more substantially in the second half of the 20th century, there has been a migration from mountainous areas into urban areas that are generally located in the plains or lowland hills. Consequently, the increase in the urban population has been larger than that in rural and mountain areas, some of which have suffered net losses in the number of inhabitants (Guzzetti et al. 2005).

Considering these changes, Guzzetti et al. (2005) showed that landslide and flood mortality rates for the entire country decreased significantly in the period 1861 to 1920, decreased less distinctly in the period 1920–1970, and remained roughly constant in the period 1970–2004. In mountain areas, the death rate for floods is higher and that of landslides is considerably higher than the rates in other physiographic regions. In the mountains, death rates decreased significantly in the period 1861–1920, remained about constant in the period 1920–1950, and increased noticeably in the period 1950–2004. In mountain areas, where tourist resorts were developed, seasonal residency may increase the size of the population exposed to flood and landslide risk. Flood mortality also increased in rural areas in the period 1960–2004. In the plains, flood mortality halved over the period 1861–2004, to the large increase of population and to the effect of remedial measures and warning systems.

For volcanic events, the risk is for the population directly exposed to the hazard, i.e., living on or close to a volcano. In Italy, two provinces are particularly exposed to volcanic risk, i.e., Naples, from the Mount Vesuvius, and Catania, from Mount Etna. In the period from 1861 to 2001 the population of Naples has grown from 951,026 to 3,059,196, and the population of Catania has grown from 369,361 to 1,054,778. Hence, the size of the population at risk has tripled, even if average mortality rates have decreased substantially.

4.1.1 Comparison with other hazards

Information on fatalities caused by other natural and human related hazards is available in Italy. Guzzetti et al. (2005) searched the historical archive of Italian landslides and flood events (Guzzetti et al. 1994, Guzzetti & Tonelli 2004, http://sici.irpi.cnr.it), which lists non-systematic information on snow avalanches. Analysis of the database indicates that snow avalanches caused at least 796 deaths and 273 injured people in the period from 1706 to 1988, 330 of which (178 deaths and 152 injured people) since 1990, and 88 (74 deaths and 14 injured people) since 1950. These figures are underestimates. In the 15-year period from winter 1986 to spring 2001, detailed statistics of the Italian Alpine Club (*http://www.cai-svi.it*) indicate that 511 avalanche-related accidents resulted in 303 deaths, 85% of which during sport activities.

Mortality rates are available for a variety of medical, technological and human-induced risks, including technological hazards (i.e., car and airplane accidents), societal hazards (i.e., homicides, work place accidents, drug overdoses), and the leading medical causes of deaths (heart diseases, cancer, diabetes, AIDS, influenza) (Table 2).

Inspection of Table 2 reveals that mortality rates for natural hazards are, on average, much lower than the leading medical causes of death, and lower than or comparable to the rates of many voluntary risks. Interestingly, the death rate for airplane accidents is less than half of the mortality of landslides, in the period 1990–2003. We argue that the economic and technological investments made for aviation safety is not comparable to what is spent for preventing mass movements.

4.2 Societal risk

Societal risk is the risk posed by a hazard on society. It is established by analyzing the relationship between the frequency of the damaging events and the magnitude of their consequences. The relationship between the frequency of the harmful events and their consequences is commonly shown on cumulative (F-N) or non-cumulative (f-N) plots (Cruden & Fell 1997, Evans 1997, Guzzetti 2000). To model these relationships, we use the Bayesian method proposed by Guzzetti et al. (2005), which we summarize below.

4.2.1 Bayesian model of fatalities

The probability distribution of fatalities caused by natural hazards is known to be power-law distributed (Cruden & Fell 1997, Evans 1997, Woo 1999, Guzzetti 2000). When data samples appear to be power-law distributed, there are two probability distributions that statisticians use to model them. The Pareto distribution is the better known: it prescribes a power-law probability for the size of a random event, given that the size can take any fractional value above a given minimum value. The zeta distribution is less well known: it also prescribes a power-law probability for the size of a random event that takes an integer value of at least one. Numbers of fatalities are integer values. So, if we are to treat the frequency distributions of such data as power-laws, we must assume a zeta distribution model, in which the number of fatalities N_F has a Probability Mass Function (PMF):

$$P(N_F) = \frac{N_F^{-(\alpha+1)}}{\zeta(\alpha+1)} \tag{1}$$

where $P(N_F)$ is the probability that N_F fatalities will occur in a single random event, α is the power-law exponent, and ζ is the Riemann zeta function. In this

model, there is no upper limit to the number of fatalities that can occur in a single event.

We use a Bayesian method to model the fatalities data. Each harmful event is treated as an independent and uncorrelated stochastic event, and the number of fatalities N_F is modeled as a zeta random variate. The inventory of harmful events is combined into a likelihood, which is the relative probability that all the harmful events would cause the observed number of fatalities. It is obtained by multiplying together, for all N_e events, the probability that each harmful event should have caused the reported number of fatalities:

$$L(a \mid \{N_F\}) = P(N_F[1]) \times P(N_F[2]) \times \ldots \times P(N_F[N_e]) \quad (2)$$

Since each N_F is a zeta variate,

$$L(a \mid \{N_F\}) = \frac{\{N_F[1] \times N_F[2] \times \ldots \times N_F[N_e]\}^{-(a+1)}}{\{\zeta(\alpha+1)\}^{N_e}} \quad (3)$$

We would like to estimate the value of the power-law scaling exponent α. Bayes' theorem allows us to infer the probability distribution of α given the data $\{N_F\}$. This is called the posterior distribution of α:

$$\begin{aligned} \text{posterior probability} &(\alpha \mid \{N_F\}) \propto \\ &\text{likelihood} (\alpha \mid \{N_F\}) \times \text{prior probability} (\alpha) \end{aligned} \quad (4)$$

The difficulty of a Bayesian analysis lies in the concept implicit in this equation: that we have some *a priori* idea of the likely value of the scaling exponent α, and that this idea is revised when we look at the data $\{N_F\}$. The way in which the idea is revised depends on our model understanding of how likely a certain value of α is, given the observations $\{N_F\}$: hence the term "likelihood". The likelihood moulds our prior probabilistic description of the scaling exponent α into a posterior probability distribution for α.

Ideally, in a Bayesian analysis the prior distribution has only a very weak effect on the posterior inference, and most of the information comes from the likelihood. Many Bayesian treatments use what are called "non-informative" priors, which are designed to be as vague a statement as possible about the model parameters, so as not to bias the inference unduly. We use a "weakly informative" prior in the form of a uniform distribution for the zeta scaling exponent α:

$$\text{prior probability} (\alpha) = U(0,2) \quad (5)$$

i.e., *a priori* we consider any value of α between zero and two as equally likely. The steepness of the power law $\alpha - 1$ is therefore considered to range anywhere between -1 and -3.

The challenge in Bayesian modeling is to turn the proportionality in equation 4 into an equality, i.e. to normalize the right hand side of the equation so that it becomes a true probability. For most Bayesian models, normalization is only possible through numerical integration. A popular method of numerical integration is Markov chain Monte Carlo (MCMC) sampling, in which (pseudo)random samples are generated on a computer in such a way that their distribution obeys (asymptotically) the posterior distribution. We have implemented an MCMC solution of the zeta power-law distribution model for fatalities caused by natural hazard using software called WinBUGS (http://www.mrc-bsu.cam.ac.uk/bugs).

4.2.2 *Assessment of societal risk*

The results of our Bayesian MCMC analysis are shown in Figure 5. The figure shows the Probability Mass Function (PMF, upper graph) and the yearly frequency of events with fatalities (frequency, lower graph), versus the magnitude of the consequences, measured by the number of fatalities in each event. To perform the analysis we used the section of the catalogues deemed substantially complete, i.e., the period from 1900 to 2004.

Inspection of Figure 5 indicates that the predicted probability for low intensity events (fewer than 5 fatalities) is larger for flood and landslides, followed by earthquakes and by volcanic events. For events having 5 or more fatalities, the probability is larger for earthquakes. The predicted yearly frequency of landslide and flood events with fatalities is considerably larger than that for the earthquakes and the volcanic events, at least up to event with 180–200 fatalities. Mass movements are second only to earthquakes in the frequency of very large intensity events ($>$200 fatalities).

Comparison of the curves shown in Figure 5 with the historical distribution of the damaging events (Fig. 2) reveals that the frequencies of the very high intensity events are underestimated. For landslides, events with 1000 or more fatalities have an estimated yearly frequency smaller than 7×10^{-6}. From 1410 to 2004, at least twice (in 1618, at Piuro, and in 1963, at Vajont) individual landslides killed more than 1000 people. For earthquakes, events with 10,000 fatalities have an estimated frequency of $\sim 2 \times 10^{-6}$. In the available record, 10 events caused more than 10,000 fatalities. Even considering the confidence intervals for our probabilistic estimates (not shown in Figure 5), mismatch exists between the predicted and the observed frequencies for very large intensity events. This may indicate one of the following: (i) the relationship between fatal events and their consequences is not power-law distributed over the entire range of fatalities – violating a fundamental assumption of our model; (ii) fatalities
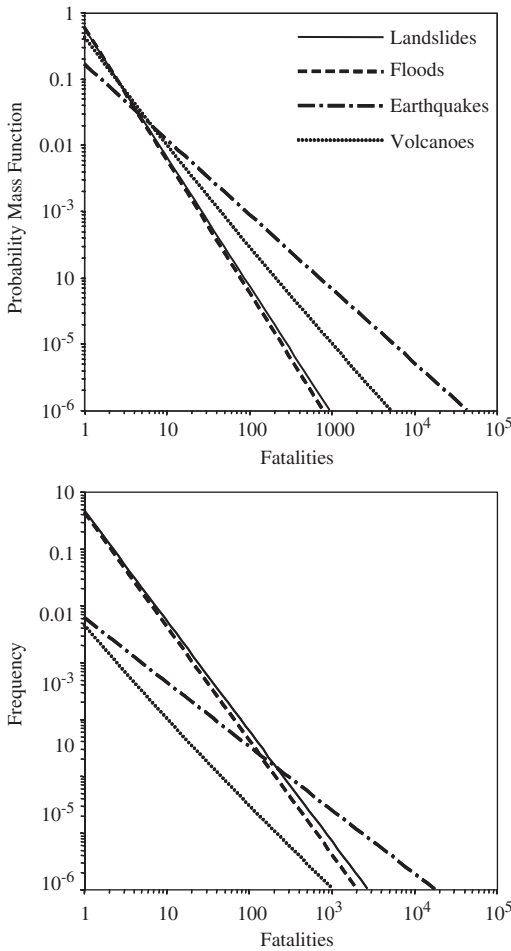
Figure 5. Societal risk due to landslides, floods, earthquakes and volcanic events in Italy. Upper graph shows the Probability Mass Function, PMF. Lower graph shows frequency of events per year. Data to construct the curves span the period from 1900 to 2004.

in population density has affected the rate of the most catastrophic events significantly in the 20th century – the record of fatal events for the most recent part of the catalogue (1900–2004) cannot be used to explain the frequency of events in the entire historical record.

5   CONCLUDING REMARKS

Using four historical catalogues of the consequences to the population of landslides, floods, earthquakes and volcanic events, we have assessed the levels of individual and societal risk in Italy. We estimated levels of individual risk by computing mortality rates, which we compared with the death rates produced by technological and social hazards and the leading medical causes of deaths. The comparison puts in the proper social perspective the harmful effects of natural hazards on the Italian population. We established societal risk levels by studying the frequency-consequence relationship of the known historical events. For this purpose, we assumed that fatalities are power-law (zeta) distributed and we applied a Bayesian method to infer the parameters of these distributions. Our results show that landslide events are most frequent for low and medium intensity events, and that earthquake events are most frequent for high and very high intensity events.

In recent years, the Italian Government and the national Department of Civil Protection have repeatedly attempted to establish a compulsory national insurance against natural hazards. The attempts have failed. Among the reasons for the inability to establish the mandatory insurance was the lack of a credible rationale for establishing such insurance. Our work, despite its uncertainties, provides the data, the rationale and an analysis of the risk posed by natural hazards, and it may contribute to the establishment of compulsory insurance. It may also help decision makers and civil defence authorities to better focus resources for the mitigation and prevention of natural hazards.

are power-law distributed, but the rate of occurrence of small to medium intensity events differs from that of high and very high intensity events (a higher rate) – two power-law models are required, one for small events and one for large events; (iii) human induced events that caused fatalities in very large numbers (e.g., Vajont) bias the statistics; (iv) the uncertainty in the exact number of fatalities for some of the events affects the statistics; (v) uncertainty in establishing the exact cause of fatalities when multiple hazards are present in the same event – e.g., deaths caused by an earthquake and an associated tsunami, or by a flood induced by a landslide (e.g., Vajont); (vi) the increase

REFERENCES

Boschi, E., Guidoboni, E., Ferrari, G., Mariotti, D., Valenise, G. & Gasperini, P. 2000. Catalogue of strong Italian earthquakes from 461 BC. to 1997. *Annali di Geofisica* 43(4): 868 p., with CD-ROM.
Cruden, D.M. & Fell, R. (eds.) 1997. Landslide risk assessment. Balkema, Rotterdam, 371 p.
Catenacci, V. 1992. Il dissesto geologico e geoambientale in Italia dal dopoguerra al 1990. *Memorie Descrittive della Carta Geologica d'Italia, Servizio Geologico Nazionale* 47: 301 p. (in Italian).
Evans, S.G. 1997. Fatal landslides and landslide risk in Canada. In: Cruden, D. & Fell, R. (eds.), *Landslide risk assessment* Balkema, Rotterdam, 185–196.

Guzzetti, F. 2000. Landslide fatalities and evaluation of landslide risk in Italy. *Engineering Geology* 58: 89–107.

Guzzetti, F., Cardinali, M. & Reichenbach, P. 1994. The AVI Project: A bibliographical and archive inventory of landslides and floods in Italy. *Environmental Management* 18: 623–633.

Guzzetti, F., Stark, C.P. & Salvati, P. 2005. Evaluation of flood and landslide risk to the population of Italy. *Environmental Management* (in press).

Guzzetti, F. & Tonelli, G. 2004. SICI: an information system on historical landslides and floods in Italy. *Natural Hazards and Earth System Sciences* 4(2): 213–232.

ISSMGE TC32 2004. Glossary of Risk Assessment Terms. Version 1. International Society of Soil Mechanics and Geotechnical Engineering, Technical Committee on Risk Assessment and Management, 7 p., available at *http://www.engmath.dal.ca/tc32/2004Glossary_Draft1.pdf*.

Salvati, P., Guzzetti F., Reichenbach P., Cardinali M. & Stark C.P. 2003. Map of landslides and floods with human consequences in Italy. CNR GNDCI Publication n. 2822, Perugia, scale 1:1,200,000.

Woo, G. 1999. The mathematics of natural catastrophes. Imperial College Press, London, 292 p.

Business decision-making and utility economics of large landslides within national forest system lands in the United States

T.E. Koler

Koler Geology, Placerville, CA, USA

ABSTRACT: Decision-making by federal managers follows direction from the U.S. government. Therefore, decisions are heavily influence by federal policy, which ebbs and flows in response to societal needs and desires. This doctoral research evaluates the effects of society's economic values associated with natural resource management of large landslides. This economic valuation indicates a trend towards positive benefits of landslide mitigation programs to the general public as measured by their willingness to contribute money to support such programs. This research also indicates that U.S. Forest Service district rangers assign positive benefits to landslide mitigation programs as measured by their willingness to allocate a portion of management budgets to such programs. The general public apparently is not resistant to having business decisions made by federal land managers and these line officers are willing to take measured risks in the management of large landslides.

1 INTRODUCTION

Public forests, private and industrial timberlands are factories that produce raw materials for a variety of commodities and services (Gregory 1987, Constanza et al. 1997). Raw materials include: logs for milling into lumber; woody material for paper-making; clean water for municipality water supplies; water for hydro-electric and geothermal power generation; wood waste products for co-generator electrical plants; floral materials (i.e., ferns, flowers, moss, etc.) for floral products; mushrooms, firewood and Christmas trees for commercial and domestic uses; Native American cultural and religious materials (i.e., bark, herbs, and other materials); and other raw organic materials. Non-organic commodities are coal, fossil fuels, landscaping materials (i.e., flagstones, cinder rock, etc.), metallic and non-metallic minerals, common variety gravel and sand, and other geological materials. Services that these factories provide comprise aquatic and terrestrial habitats; recreational areas for camping, hiking, vehicle trails and roads; hunting and fishing locations; and points of interest (e.g., archeological, panoramic, and historical sites, etc.). These commodities and services are components of what economists refer to as the total economic value.

Over the past 100 years American society has had shifts in attitudes towards the utility (value) of services and commodities of our national forests. These changes in collective thought and national perspective resulted in the enactment of a variety of laws (e.g., U.S. Congress 1966, 1969, 1972, 1973, and 1976) affecting commodity production and delivery as well as services, the motivation being the protection of species. The protection of species appears to be a high value of American society.

In particular the existence values make this economically important. Existence values are those economically positive values associated with an economic service that provides satisfaction by its existence. For example, a pretty lake in a wilderness located in a western state has certain existence values for a person living outside of the western U.S.

Societal values and subsequent legislation have resulted in significant changes in how organic and inorganic commodities and services are managed on national forests as well as on private and industrial timberlands. An example of this significance is the economists' view that these changes are removing the timber industry from a perfect competitive market to a market comprised of niche markets (e.g., Maurice and Thomas 1995). Clearly the *status quo* in business decision-making for managing these lands has changed.

2 RESEARCH PURPOSE

This research focuses on how societal values in general, and the individual values of federal decision-makers in particular, influence the decision-making process of managing commodities and services associated with large landslides in national forests. Parallel to this

focus is an evaluation of how this decision-making influences strategic business management within the U.S. Forest Service.

The over-riding societal view towards risk appears to be to avoid it completely when it comes to protecting wildlife and aquatic species. Intuitively this also includes the management of large landslides because geomorphic landforms have the potential to adversely affect habitats. This mandate from the American public has resulted, through legislation, in the closure of several national forests for the collection of raw materials for commodity production and some changes in services. Over the past decade this viewpoint has also resulted in restrictions of timber harvesting on private and industrial timberlands. The reduction of public, private and industrial lands for timber harvesting severely effects the sustainability of commodity resources: less land for harvesting means less available raw material that can be replenished for future harvests. This conundrum has been elevated to the level of policy makers; for example the U.S. Forest Service Chief addressed it in his speeches on forest health (Stelljes 2003) and in his plenary speech at the recent XII World Forestry Congress in Canada (Knudson 2003).

> We in the United States consume far more timber than we produce. Over the next 50 years, we expect imports to supply a third to half of our total softwood lumber consumption. We're concerned about undermining the health of the world's forest ecosystems through consumption patterns that are out of balance with production. Our habits raise questions of both equity and sustainability.

It is this reduction of the land base that forest economists view as changing the market from perfectly competitive to a variety of niche markets. Another outcome of this risk-aversion is that the reduction in production of wood products in the U.S. will result in the increase of imports that will negatively affect our balance of trade. Also important is that the decrease in domestic timber harvesting will increase foreign timber harvesting in locations where weak environmental laws and regulations can result in increases in habitat degradation. By avoiding risk the American public is forcing natural resource managers into either a Hobbesian or a Hobson's choice in their business decision-making. Investigating how this risk-aversion influences the decision-making process was a goal of this research.

3 PUBLIC CHOICE THEORY

Hobbes and Hobson were early advocates of what was to later become public choice theory. Government behavior and in particular the behavior of individuals with respect to government is analyzed scientifically through public choice (Tullock et al. 2002). An obvious predecessor to Hobbes and Hobson thinking was the Renaissance master of politics, Niccolo Machiavelli who authored the premier primer in political machinations, *The Prince* (1532). Machiavelli influenced Hobbes' and Hobson's thinking and all three were burdened with political and cultural environments that dictated that businessmen, civil servants, politicians, and royalty must make decisions rooted in morality. These three broke this mode of rationalization and were subsequently marked by their contemporaries as baneful thinkers for arguing against morality instead of producing a scientific system that in essence was amoral.

David Hume (1711–1776) breached this monolithic moral thinking by stating what is now obvious to the modern observer: people are interested in self-preservation rather than broadly based public interest (Hume 1741). Hume's work was the first to present a logic based in economics and his contemporary and colleague, Adam Smith, also produced a view that individuals are largely self-interested economically. In his work, *An Inquiry into the Nature and Causes of the Wealth of Nations*, Smith presented his interpretation of economics within governments (1776). Smith is, of course, the father of modern economics.

As economists turned to a systematic process of evaluating choice, political scientists remained tied to choice based in morality. This continued through the 19th and 20th centuries reaching a crescendo in the mid-20th century with seminal work by Buchanan and Tullock (1962) and Downs (1967). Buchanan was awarded the Nobel Prize in Economics for his contribution to the theory of economic and political decision-making. Buchanan and Tullock presented convincing arguments that non-market decision-making within political science has an economic basis founded in self-interest and preservation. Downs provided the Downsian model that presents government as an institution comprised of individuals with their own set of objectives and constraints. From their pioneering work modern public choice theory has provided economists and political scientists with the tools for observing how economics plays in public decision-making. Determining how public choice theory influences the decision-making process was, therefore, a goal of this research.

4 LANDSLIDE RISK AND DECISION-MAKING

A common reason presented for removing land from timber production is the view that some geomorphic processes are deleterious to a variety of wildlife and aquatic habitats. The most common process that has

Figure 1. The Pollock Landslide complex in central Idaho.

this "smoking gun" reputation is the landslide. The focus of this research is the examination of the role of large landslides in the decision-making process as influenced by the economic utility (i.e., economic value) of the American public and federal natural resource managers.

Large landslides are usually several hundred hectares in size and have an average depth of 20 meters or more such as in Figure 1, a large landslide on the Little Salmon River in central Idaho. The Pollock Landslide is not typical for many large landslides within National Forest System Lands due to its lack of timber. It is provided here to aid the unfamiliar eye with what a large landslide looks like.

Many productive timber-producing landscapes are on geologically disturbed ground and some of the highest quality timber stands are located on large landslides (Burroughs 1985). Some visionaries have developed new equipment and harvesting methods that may help mitigate landslide reactivation resulting from timber removal. Helicopters are recognized as one example of being "gentle on the terrain." Another example is the feller-buncher, a machine that was developed in Europe and has been used in the U.S. since the mid-1980s. Shelterwood and selection harvesting techniques are slowly replacing clear-cut harvesting by leaving viable trees for stabilizing landslides. Large landslides will continue to be highly productive sites for commodity production and managers are constantly looking for new and better ways to make decisions in managing these landforms. Determining how these decisions are made and how the decision making process can be improved were also goals of this research.

Modern risk assessments were first developed in the health industry (e.g., Liegey 1991) where "risk" was defined as the product of multiplying the incident probability by its magnitude. Engineers and geologists

similarly view risk as a function of probabilities and consequences when evaluating landslides (Varnes 1984, Wu et al. 1996, Koler 1998). Some large landslides may have a high probability of reactivation or acceleration but because they may not adversely affect wildlife habitat (i.e., a consequence) the landslide risk may be assumed to be low or moderate. The opposite of this scenario is also true. A low probability of landslide movement immediately adjacent to an endangered species habitat may be considered a high risk because the consequence of movement (degradation of critical habitat) is high. Landslide risk assessments are therefore dynamic and need to be repeated over time in environmentally sensitive areas.

Some economists also view risk as a function of probability and consequence, however there is a dearth of information that shows the economic effects of managing wildland resources in concert with the integration of landslide and economic risk assessments. Modeling and developing the methodology for this integration was a goal of this research.

Decision-making in organizations has reached new paradigms for business managers that today include assessments of risk and uncertainty in strategic management planning (Goldoff 2000, Feiock and Stream 2001, Kriebel et al. 2001). In addition, more women are entering decision-making management positions (approximately a quarter of the district rangers in the U.S. Forest Service are female) and they are contributing to this paradigm with alternative perspectives towards risk and planning (Kirchmeyer 1996, Clay 2003). Investigating this shift in developing and implementing a business strategy as it pertains to the resource management of large landslides was a goal of this research.

5 ECOLOGICAL ECONOMIC VALUES

Ecological economic values are the contribution of an action or object to user specified goals, objectives or conditions (Costanza 2000). A specified value of that action or object is tightly coupled with a user's value system and determines the relative importance of an action or object to others within the perceived world (Farber et al. 2002). In a valuation process the value of a particular object or action is expressed. Therefore, an ecosystem valuation represents the process of expressing a value for ecosystem goods or services (i.e., biodiversity, flood protection, recreational opportunity), thereby providing the opportunity for scientific observation and measurement.

Bergstrom & Loomis (1999) provide a summary of ecosystem economic values that are based on broad philosophical/ethical notions of value. The value of an individual agent towards intrinsic goods is intrinsic value; for example, the enjoyment of good health.

393

Functions within an ecosystem contribute to the enjoyment of good health; for example, clean air and water. Clean air and water are extrinsic goods that the ecosystem provides, contributing to the intrinsic good of enjoyment of good health. Bergstrom and Loomis note that both humans and animals can experience intrinsic values – both enjoy good health when not injured or sick. The value of an extrinsic good as an input into the generation of intrinsic goods and values is an instrumental value. Again using the enjoyment of good health (the intrinsic good) as an example, this enjoyment is dependent on eating food (the extrinsic good) of sufficient quantity and quality to sustain good health. Both human and non-human agents can experience instrumental values. Meat has an instrumental value to a carnivore or omnivore, but not to an herbivore. Therefore, Bergstrom and Loomis argue that one role of ecosystems is to provide services that are of instrumental value to humans and animals.

Similarly, Golder et al. (1997) describe a value system in which an ecosystem or species have intrinsic rights to a healthy sustaining condition that is on a par with human rights to satisfaction. The value of any action or object is measured by its contribution to maintaining the health and integrity of an ecosystem or species, per se, irrespective of human satisfaction. This definition differs from Bergstrom's and Loomis' in that Golder et al. view an intrinsic value being separate from human needs. Instrumental values, according to Golder et al., reflect human needs. Therefore, these authors argue that environmental policies will always be based on a mix of intrinsic and instrumental values – that is a point on which Bergstrom and Loomis also agree.

The question of which values count arises in ecosystem management decisions because both humans and animals can experience the extrinsic goods of the ecosystem (Bergstrom & Loomis 1999). The ecosystem management definition proposed by Chief Dale Robertson (1992) clearly shows that the U.S. Forest Service considers that these values do count for both. The human values include both non-economic (e.g., spiritual or cultural) and economic values. For non-human agents a biocentric means of counting values is accomplished through legislation such as the Endangered Species Act. This Act gives much greater weight to the intrinsic values of threatened and endangered species than to humans. The higher values of threatened and endangered species arise from their scarcity. The balance between which values count and how much they count is not always straightforward.

6 CONTINGENT VALUATION METHOD

The contingent valuation method (CVM) has undergone a great deal of scrutiny over the past decade and is considered a well-tested method for evaluating environmental economic utility (Haab & McConnell 2002). The steps in coming to this conclusion have been incremental (e.g., Smith 1996, Boyle et al. 1996, Ready et al. 1996, Carson 1997) as authors showed the validity of CVM when applying discrete survey questions. Loomis (2002) describes the CVM as follows:

> The contingent valuation method is a survey technique that constructs a hypothetical market or referenda to measure willingness to pay (WTP) or accept compensation for different levels of non-marketed natural and environmental resources. The method involves in-person or telephone interviews or a mail questionnaire. The CVM not only is capable of measuring the value of outdoor recreation under alternative levels of wildlife and fish abundance, crowding, instream flow, and so on, but is the only method currently available to measure other resource values, such as the benefits that the general public receives from the continued existence and services of unique natural environments, species, or entire ecosystems.

In the seminal work by Mitchell & Carson (1993) several biases were explained as creating problems with the CVM and these authors proposed the referendum approach as being less troublesome than other approaches such as elicitation, bidding, payment card, and take-it-or-leave techniques. The referendum approach is today recognized as a preferred method (Champ et al. 2002).

7 MEASURING RISK

Hazard and risk are two nouns that many people assume are synonymous. In fact, most if not all dictionaries define these as "danger, risk, and peril" (e.g., Stein 1994). In daily life these words can be interchanged easily with little or no confusion. However, in the sciences these words are actually very different. For example, in the geological and engineering sciences hazard is defined in conjunction with effects as a function that categorizes risk:

$$\text{Risk} = f \text{ (Hazards, Effects)} \qquad (1)$$

This relationship is documented in the literature and has been recognized for two decades (e.g., Varnes 1984, Wu et al. 1996, Koler 1998). Landslides are considered to be geological hazards. Active fault zones, where recent seismic activity (within the last 10,000 years) has occurred, are considered to also be geological hazards. Low strength engineering soils are considered to be an engineering hazard. The word hazard is recognized as a condition.

In the business world hazard is not as clearly defined as it is in the physical sciences. Frequently hazard and risk are conjoined within benefit-cost analyses (e.g., Tietenberg 2000, Koller 1999). As such the analyst is encouraged to find the most beneficial alternative (less risk or hazard) at the least cost. Cost is usually a monetary value but it can also be an intangible such as aesthetics. The utility of what people are willing to pay makes this topic cumbersome and muddled in relation to geological processes. For a large majority of economical analyses it really doesn't matter if the analyst uses the words hazard and risk inclusively or exclusively. For example there are several computer decision models available to the manager. In sales and services the manager can apply computer models for identifying root causes of problems based on observed symptoms. These models include signal detection techniques, diagnostic methods, fault tree analyses, and discriminate and classification analyses (McDonald 1999). These models provide the manager with the ability to problem solve from the top down or bottom up within a risk analysis framework. In environmental economics, however, it is critical to differentiate between hazard and risk so that the utility of the analysis becomes clearer.

Hazard in this study is the probability that a landslide will move. Movement is controlled by a combination of forces acting on a hillside (Koler 1998). Slope gradient and groundwater conditions are the two most influential parameters. A variety of engineering models can be used to calculate the probability of movement. In this study the hazard rating is quantitative based on a modeling approach and the hazard ratings range from very low (0.0% to 2.9% probability) to low (3.0% to 7.9% probability), to moderate (8.0% to 15.9% probability), to high (16.0% to 24.9% probability) to very high (25.0 + % probability) as delineated by U.S. Forest Service geotechnical specialists (Wooten 1988). In this research the probabilistic hazard ratings were explained to the surveyed decision-makers by way of a working example. Other subjects surveyed were only questioned on their individual values towards adverse effects on natural resources.

Effect is less confusing than risk and is defined as the potential or existing consequences to a resource if a landslide moves. Monetarily it is the cost of degradation or loss of a resource; however, this cost is linked to the values of the decision-maker and society. The scale applied is qualitative: low (no adverse degradation occurs), moderate (short-term, reversible degradation occurs), high and very high (long-term, irreversible degradation occurs). All subjects were surveyed for their individual values associated with effects. Risk-averse individuals are those who will accept only low effects (i.e., any degradation activity is unacceptable).

Table 1. Landslide risk rating.

| Effects | Landslide hazard rating | | | | |
	Very low	Low	Moderate	High	Very high
Low	VL	L	L	M	M-H
Moderate	L	L	M	M-H	H
High	L	M	M-H	H	VH

VL = very low; L = low; M = moderate; H = high; VH = very high.

In economics risk is determined in terms of positive option values. For example, if a person is indifferent to two options – one being given a certain $50 and the other being given a lottery ticket with a 50% probability of wining $100 – s/he is risk-neutral (Tietenberg 2000). If this person views the lottery as being more attractive, then s/he would be exhibiting risk-loving behavior. And if the preference is to take the $50 the individual is showing risk-averse behavior. Although this definition is slightly different than the concept of landslide risk it is similar in the sense that a risk-averse person will only select the "sure thing." A risk-averse manager will probably select only the very low or perhaps the low landslide risk option.

Risk in this research is therefore parsed by these two types of hazard and effect (i.e., quantitative versus qualitative). Risk was presented visually to the decision-maker survey using a classification matrix (Table 1). Within the surveying process the decision-makers were asked to "vote" by referendum, which risk rating they are willing to pay (WTP) for and at what maximum dollar amount within the concept of public good utility. Because risk-averse persons are only willing to accept low effects, it follows that they are only willing to accept a very low to moderate hazard probability. Therefore, risk-averse people are only willing to take a very low to low risk.

8 HYPOTHESES AND DATA COLLECTION

Two survey instruments were used to collect data to test three hypotheses. The three hypotheses were:

1. U.S. society is risk-averse toward all commodity production and services related to large landslides on National Forest Service System Lands.
2. A majority of U.S. Forest Service district rangers are not risk-averse towards commodity production and services related to large landslides.
3. An improvement in economic utility (i.e. well being) occurs for society and U.S. Forest Service decision-makers when business risk decisions include hazard and consequence assessment when producing

395

raw material for commodities or providing services on large landslides.

A survey comprised of a sample of the U.S. public and a survey comprised of a sample of Forest Service district rangers followed criteria for CVM that were reviewed and approved by the dissertation committee as well as the university ethics committee. Ten percent the U.S. public survey responded out of a total of 3,000 telephone calls. Ninety-five percent of the 110 district rangers responded to the district ranger survey. The goals of this work included the testing of the three hypotheses and estimation of the economic utility of the two survey samples. Economic utility was described as the positive benefits that the two types of survey respondents showed as a WTP for the total economic value associated with large landslides in National Forest System Lands.

9 STATISTICAL ANALYSIS

Within the general public survey were three open-ended questions on the amount of one-time tax dollars that members of the general public are WTP ($1 to $5), household income, and age. Eight discrete questions in this survey addressed whether or not the participants were agreeable to pay a one-time tax, education (college educated or not), location (east or west of the Mississippi River), active voter or not, member of conservation group or not, urban or rural home, prefer all resources to be protected or not, and whether or not the participants preferred that large landslides are managed to replicate natural conditions.

Questions in the district ranger survey were two open-ended questions: years of district ranger experience, and maximum amount they were WTP for mitigating large landslides on their districts. Nine discrete questions in this survey are: whether or not they are agreeable to allocate money from a hypothetical $1,000,000 budget, there are resource concerns on the district associated with sedimentation (i.e., aquatic and wildlife habitats and water quality), maximum landslide risk they are willing to take, whether or not the district ranger's staff complete professional landslide risk assessments, whether or not the ranger is influenced by societal values associated with landslides, and whether or not the ranger uses decision tools. Decision tools include U.S. Forest Service applications that have been developed and used internally. Goodness-of-fit and statistical significance were completed by logistic regression modeling.

Logistic regression for this study included either the logit, probit or both methods depending on the data distribution from surveys. Logistic regression is a multivariate approach used to discriminate dependent and independent variables for predicting outcomes. Logit regression is completed for lognormal

Table 2. Code sheet for the general public (household) survey.

Name	Codes/Values
Identification code	ID number
Pay	1 if respondent agrees to a one-time payment in federal taxes, 0 otherwise
Tax	Amount of tax in dollars ranging from $0 to $5
Loc	Location relative to the Mississippi River; 0 = west and 1 = East
Age	Years
Ed	1 if participant has a baccalaureate degree, 0 otherwise
Consv	1 if the participant is a member of a conservation group, 0 otherwise
Vote	1 if the participant is an active voter, 0 otherwise
Urb	1 if participant lives in a city with a population greater than 5000, 0 otherwise
Inc	Household income. 1 = Less than $25 K; 2 = $25 K to $40 K; 3 = $41 K to $60 K; 4 = $61 K to $80 K; 5 = $81 K to $100 K; 6 = Greater than $100 K
Averse	1 if participants prefer that all resources do need to be protected in all cases with no exception, 0 if not
Natural	1 if participants prefer that large landslides are managed to replicate natural conditions, 0 if not

distributions and normal distributions are analyzed with probit regression. Each survey in this study has several discrete variables (i.e., binary) as displayed in Tables 2 and 3. The logistic regression models were completed with version 8.0 of the Stata software (Stata Corporation 2003), a commercial statistical product.

10 FINDINGS

A summary of the research findings is provided in Table 4. Risk-averse, by definition in this manuscript, is a citizen or manager who is unwilling to take a higher landslide risk level greater than low. The testing of the first hypothesis utilized the dichotomous nature of the risk-averse survey question (i.e., 0 = no, 1 = yes). Therefore the null hypothesis stated that the mean of the averse question is greater than 0.50 (or in other words greater than 50% of the answers were 1). The mean however was 0.40 and therefore the null hypothesis was rejected at the 5% significance level. The low response rate for the household survey, however, shows significant differences from the general population that may negate this hypothesis test.

396

Table 3. Code sheet for the district ranger survey.	
Name	Codes/Values
Identification code	ID number
Aquatic	1 if respondent has aquatic habitat problems associated with large landslides on their district, 0 otherwise
Wildlife	1 if respondent has wildlife habitat problems associated with large landslides on their district, 0 otherwise
Waterqual	1 if participant has water quality problems associated with large landslides on their district, 0 otherwise
Risk	Maximum landslide risk. $0 =$ Very Low, $1 =$ Low, $2 =$ Moderate, $3 =$ High, $4 =$ Very High
Pay	1 if respondent agrees to allocate money from an hypothetical \$1 million budget for large landslide mitigation work, 0 otherwise
Allocation	Amount of budget allocation in dollars
LS	1 if the participant's staff complete landslide hazard/risk assessments, 0 otherwise
Socval	1 if the participant's decisions related to large landslides is influenced by societal values, 0 otherwise
Tools	1 if the participant uses decision tools, 0 otherwise
Years	Years of district ranger experience
Gender	1 if respondent is male, 0 if female

Table 4. Research study statistical results.	
Hypotheses	Test statistics
1. U.S. society is risk-averse towards all commodity production and services related to large landslides on National Forest Service Lands	H_O: $\mu > 0.5$ H_A: $\mu < 0.5$ z-value > 1.96 "Null hypothesis is rejected"
2. A majority of U.S. National Forest Service district rangers are not risk-averse in commodity production and services related to large landslides.	H_O: $\mu_{risk} > 1.0$ H_A: $\mu_{risk} < 1.0$ z-value < 1.96 "Null hypothesis is accepted"
3. An improvement in economic utility occurs for society and U.S. Forest Service decision-makers when business risk decisions include hazard and consequences when producing raw material for commodities and providing services on large landslides.	"True by inference"

The author, attempted to adjust for the differences by applying logistic regression modeling. The goal in this process was to see what could be gleaned from the survey with the observation that the age variable had the same mean as the mean age recorded within the 2000 U.S. census. The results from logit modeling show that geographical location by itself (east or west of the Mississippi River) has little influence on risk-aversion. Citizens in the western part of our country are risk-averse 39.1% of the time as compared to their eastern cousins who have a 41.5% probability of being risk-averse. However, stratifying by location and then by other variables the author found four discriminators. The four discriminating variables were then ranked by how much difference each was from the sample mean, which in descending order are: age, tax amount, desire for managers to replicate natural conditions of resources on large landslides (labeled as NATURAL in the code), and active voters. Several iterations of logit regression modeling were completed to remove the variables, which are statistically

significant predictors for the risk-averse variable. From these model runs we now know that age, location and natural mitigation are, in reduced logit model form, accurate predictors. An apparent paradox revealed by the analyses was the observation that the older a person is; the less probable that person will be risk-averse towards landslide mitigation. This runs contrary to the conventional wisdom, albeit anecdotal, that older people are more conservative and hence have a tendency to not take on higher risk values. Perhaps the answer to this paradox is simply that older people recognize that natural processes occur and that they need to be dealt with in a pragmatic way. Another answer, of course, is that there may be data biases within the location and natural mitigation variables collected in this survey.

Similarly the natural mitigation variable was evaluated for predictors via the logit modeling. From this work the author discovered that location and whether or not a person is risk-averse would predict the preference for someone to have resource managers practice ecosystem management by replicating natural conditions as much as possible. This is not surprising and makes sense: folks who live in areas where there are landslides and who are not very risk-tolerant will want to have repairs made in a holistic or ecosystem fashion.

Future work in testing the first hypothesis may need a different approach in the logistic regression analyses. What became apparent to the author *post facto* to the collection of the household survey data was a need to evaluate the interaction between variables. Of particular interest is the interaction between the variables for age, geographical location and the

397

preference of respondents to have land managers make decisions that replicate natural conditions. This was not possible because of the binary nature of the geographical location and replication of nature variables in the survey data. Perhaps future researchers will be able to examine this further.

The next step in this process was to determine if the survey sample showed a positive economic value by measuring WTP. Again the logit modeling process was applied to identify the statistically significant predictor variables for whether or not someone is willing to pay a one-time tax for landslide repair. The predictor variables that were found to be significant at the 95% level are: tax bid and active voter. Therefore a reduced logit regression equation with these variables and a constant provides an estimate of the pay tax variable. Interestingly, membership in a conservation group was a marginal predictor (p = 0.052). It may be that if the sample size were larger this variable may become more meaningful. Finally WTP was measured using methods described by Hannemann (1989) for finding the mean and median WTP. These were $0.42 and $0.41, which are small but given our political climate of tax reductions the amounts may be important. It is important here to acknowledge that the WTP calculated might be erroneous due to the low response rate of the household survey, which may have resulted in biases for the predictor variables of tax bid, membership to a conservation group and voting history. Insufficient data were available to test if these biases exist. A key indicator of the erroneous nature of the WTP is the positive value assigned to the tax bid coefficient, which in a majority of CVM studies has a negative sign (J. Loomis, personal communication, March 22, 2004). Future work in this area may be difficult at best because of the reluctance of respondents to participate in a research telephone survey.

Identical methods were applied for testing the second hypothesis, which explored the possibility that district rangers are not risk averse. In the process the author found that the sample mean value for risk-tolerance is 1.70, in the western regions the mean is 1.74 and in the eastern regions it is 1.62. All of these values are above the low risk value of 1.0, which is the threshold of risk-aversion.

Ancillary information to the risk hypothesis included the observation that there is little difference between genders in the decision-making process. The one exception to this is that females are less likely to use decision tools such as decision trees and matrices in making their decisions. Most respondents who stated a "no" response to this question also offered that they depended on a recommendation in a landslide specialist report to aid them in their decision-making. Data from the length of experience as a ranger showed that rangers with less than two years tenure had a statistically significant higher risk-tolerance than the senior rangers with the significance measured at the 5% level.

Conventional wisdom that holds the axiom – if you have a landslide you have ecological problems as well – turned out to be true in this research. Aquatic habitat problems occurred the most often but surprisingly water quality problems were rarely associated with aquatic habitat problems. Wildlife problems were only associated with large landslides by rangers with 17 years or more experience. This may simply be serendipity in the data or it may tell us that wildlife problems are more difficult to recognize and manage. In all cases where there were landslides on a district there were aquatic and/or wildlife habitat problems, water quality problems, or some combination.

In a majority of the cases where landslides are present within a district, the ranger showed sensitivity towards societal values. In cases where the district ranger was not influenced by societal values s/he offered the comment that many times the information made available was very complicated and not available to every citizen; and therefore s/he was indifferent to societal values. This was an important finding when compared with the allocation bids that the rangers made in the survey.

Allocation bids were made by rangers with large landslides and in all but 11 responses the bid amounts were well below the maximum $1 million. The bid amounts for the 11 responses were for the maximum amount of $1 million. This finding coupled with the sensitivity to societal values show that rangers are not, in most cases, rent-seekers. Economists describe individuals who maximize their values at the expense of others as rent-seekers. These decision-makers are clearly attempting to provide the greater good to the largest group possible. Total economic values for both the rangers and the American public coincide.

The positive economic value that rangers showed towards the management of large landslide commodities and services was measured as WTP. As with the public survey WTP, this was accomplished by using Hannemann's methods (1989) for the mean and median WTP, which were $527,192 and $489,378 respectively. Coefficients for these calculations were obtained through logit modeling iterations. This was a process of finding a reduced regression model that had statistically significant predictors for the aquatic variable (i.e., water quality and allocation variables are good predictors). The aquatic variable is predicted by the allocation variable with statistical significance (p = 0.001); and, all large landslides needing allocation for mitigation have a combination of aquatic, wildlife, or water quality problems. However, the allocation variable is not a good predictor solely for the wildlife and water quality problems.

The third hypothesis, that economic utility is improved for large landslide management when risk

assessments are included in the decision-making process was determined to be true at the 5% significance level due to the positive economic value placed in this process by the measured WTP of the decision-makers, and a generally positive trend exhibited in data collected for the household survey. If and when the publics' WTP can be measured, the next step will be a benefit-cost analysis including measuring and forecasting the present net value (PNV) of the resources. Currently there is no inventory of large landslides (or landslides period) in the agency; therefore this may be the first place to start in this future work. Also, the cost might be reduced by other means such as offsetting costs by timber harvesting or other revenue-generating process, which will need to be included in the PNV work.

11 CONCLUSIONS

In summary, the American public survey data show a generally positive trend towards accepting some risk in managing natural resources on large landslides. This positive trend is shown in the publics' WTP a one-time tax for funding a Forest Service landslide mitigation program. Decision-makers at the district ranger level show sensitivity towards the American publics' total economic value for non-market goods and services associated with large landslides. Rangers in general are not economically maximizing their individual economic values at the expense of the American publics' values pertaining to landslide natural resource management.

ACKNOWLEDGEMENTS

REFERENCES

Bergstrom, J.C. & Loomis, J.B. 1999. Economic dimensions of ecosystem management. In: H.K. Crodell & J.C. Bergstrom, eds. Integrating social sciences with ecosystem management: human dimensions in assessment, policy, and management. Sagamore Publishing, Champaign, IL: 181–193.

Boyle, K.J., Johnson, F.R. & McCollum, D.W. 1996. Valuing public goods: discrete versus continuous contingent valuation responses. *Land Economics*, 72: 381–396.

Buchanan, J. & Tullock, G. 1962. The Calculus of Consent Logical Foundations of Constitutional Democracy. Ann Arbor Paperbacks, Ann Arbor, MI. 361 p.

Burroughs, E.J. 1985. Survey of slope stability problems on forestlands in the west. Moscow, Idaho: U.S. Department of Agriculture Forest Service, Pacific Northwest Forestry and Range Experimental Station, General Technical Report 180: 5–16.

Carson, R.T. 1997. Contingent valuation: theoretical advances and empirical tests since the NOAA panel. *American Journal of Agricultural Economics* 79 (5): 1501–1507.

Champ, P.A., Flores, N.E., Brown, T.C. & Chivers, J. 2002. Contingent valuation and incentives. *Land Economics* 78 (4): 591–604.

Clay, R. 2003. Speaking up: women's voices in environmental decision-making. *Environmental Health Perspectives* 111(1): A34–A37.

Costanza, R. 2000. Social goals and valuation of ecosystem services. *Ecosystem* 3: 4–10.

Costanza, R., d'Arge, R., de Groot, R., Farber, S., Gasso, M., Hannon, B., Limburg, K., Naeem, S., O'Neil, R.V., Parulo, J., Raskin, G.G., Sutton, P. & van den Bolt, M. 1997. The value of the world's ecosystem services and natural capital. *Nature* 387: 253–260.

Downs, A. 1967. Inside Bureaucracy: Little, Brown and Company, Boston. 292 p.

Farber, S.C., Costanza, R. & Wilson, M.A. 2002. Economic and ecological concepts for valuing ecosystem services. *Ecological Economics* 41: 375–392.

Feiock, R.C. & Stream, C. 2001. Environmental protection versus economic development: a false trade-off? *Public Administration Review* 61(3): 272–280.

Golder, Litti & Donald, K. 1997. Valuing ecosystem services, philosophical bases and empirical methods. In G.C. Daily, ed. Nature's services: societal dependence on natural ecosystems. Land Press, Washington DC: 23–48.

Goldoff, A.C. 2000. Decision-making in the organizations: the new paradigm. *International Journal of Public Administration* 23(11): 2017–2044.

Gregory, G.R. 1987. Resource Economics for Foresters. John Wiley and Sons, New York. 477 p.

Haab, T.C. & McConnell, K.E. 2002. Valuing Environmental and Natural Resources. Edward Elgar, North Hampton, MA. 326 p.

Hannemann, W.M. 1989. Welfare evaluations in contingent valuation experiments with discrete response data: reply. *American Agricultural Economics Association* 71: 1057–1061.

Hume, D. 1741. Essays Moral and Political. Liberty Fund, Indianapolis. 684 p.

Kirchmeyer, C. 1996. Gender roles and decision-making in demographically diverse groups: a case for reviving

androgyny. *Sex Roles: A Journal of Research* 34: 9–10, 649–665.

Knudson, T. 2003. World's other forests feed state's appetite for timber. The Sacramento Bee, 291, 278, A1 & A18.

Koler, T.E. 1998. Evaluating slope stability in forest uplands with deterministic and probabilistic models. *Environmental and Engineering Geoscience* 4: 185–194.

Koller, G. 1999. Risk assessment and decision-making in business and industry – a practical guide. CRC Press New York. 239 p.

Kriebel, D., Tickner, J., Epstein, P., Lemons, J., Levins, R., Loechler, E. L., Quinn, M., Rudel, R., Schettler, T. & Stoto, M. 2001. The precautionary principle in environmental science. *Environmental Health Perspectives* 109 (9): 871–876.

Liegey, M. 1991. Risk. *Chemical Times & Trends* 31: 31–33.

Loomis, J.J. 2002. Integrated public lands management. Columbia University Press, New York. 594 p.

Machiavelli, N. 1532. The Prince. Bantam Press, New York. 176 p.

Maurice, S.C. & Thomas, C.R. 1995. Managerial economics. Irwin Press, New York. 784 p.

McDonald, G. 1999. Shaping statistics for success in the 21st century: the needs of industry. *The American Statistician* 53 (3): 203–211.

Mitchell, R.C. & Carson, R.T. 1993. Using surveys to value public goods, the contingent valuation method. Resources for the Future Publishing, Washington D.C. 488 p.

Ready, R.C., Buzby, J.C. & Hu, D. 1996. Differences between continuous and discrete contingent value estimates. *Land Economics* 72: 397–411.

Robertson, F.D. (1992, June 4). Ecosystem management of the national forests and grasslands. Memo to regional foresters and station directors, Washington Office. Washington DC: USDA Forest Service.

Smith, A. 1776. An Inquiry into the Nature and Causes of the Wealth of Nations. Kessinger Publishing, White Fish, MT. 356 p.

Smith, V.K. 1996. Can contingent valuation distinguish economic values for different public goods? *Land Economics* 72: 139–151.

Stata Corporation. 2003. Stata Statistical Software user's guide for version 3. Stata Corporation, College Station, TX.

Stelljes, K. 2003. Forest health, not timber and roads, is the key issue, nation's chief forester says. UC Berkeley News. Retrieved 10/16/03 from www.berkeley.edu/news/media/releases-/_bosworth.shtml.

Tietenberg, T. 2000. Environmental and natural resource economics. Addison Wesley Longman, Inc., Menlo Park, CA. 656 p.

Tullock, G. 1965. The Politics of Bureaucracy. *Public Affairs Press*, Washington D.C.

U.S. Congress. 1966. Endangered Species Preservation Act. Washington D.C.

U.S. Congress. 1969. Endangered Species Conservation Act. Washington D.C.

U.S. Congress. 1969. National Environmental Policy Act. Washington D.C.

U.S. Congress. 1972. Endangered and Threatened Species Act. Washington D.C.

U.S. Congress. 1973. Endangered Species Act. Washington D.C.

U.S. Congress. 1976. National Forest Management Act. Washington D.C.

Varnes, D.J. 1984. Landslide hazard zonation: a review of principles and practice. UNESCO Press, Paris.

Wooten, R.M. 1988. Level I stability analysis validation report. Vancouver, WA: US Department of Agriculture Forest Service, Gifford Pinchot National Forest.

Wu, T.H., Tang, W.H. & Einstein, H.H. 1996. Landslide hazard and risk assessment. In A.K. Turner, R.L. Schuster eds, Landslide investigation and mitigation. National Research Council Transportation Research Board, Washington D.C.: 106–120.

Risky business – Development and implementation of a national landslide risk management system

A.R. Leventhal
GHD-LongMac, Sydney, Australia

B.F. Walker
Jeffery and Katauskas Pty Ltd, Sydney, Australia

ABSTRACT: In the year 2000, the Australian Geomechanics Society (AGS) published a benchmark technical paper "Landslide Risk Management Concepts and Guidelines". This was a continued recognition by AGS of the benefits of the concept of risk in potential landslide situations. The following paper discusses the subsequent strategies adopted for implementation of the principles of AGS (2000) into the legislative framework of Australian governments at National, State and Local levels.

1   INTRODUCTION

Slope instability occurs in many parts of urban and rural Australia. Indeed, it has been estimated that virtually every Local Government Area (LGA) in Australia has landslide hazards of one form or another. The continuing need for residential development in all major cities and the coastal areas such as those of NSW, means that increasingly such development will occur in areas previously considered too hazardous for development. Hence, there is an increased likelihood for damage to property and loss of life from landslide.

2   HISTORICAL CONTEXT OF DEVELOPMENT OF LANDSLIDE RISK ASSESSMENT IN AUSTRALIA

Prior to about 1970, there were relatively few areas where development had been affected by landslides. Many LGAs, particularly in proximity to the larger metropolitan areas, required geotechnical "stability" assessments to be provided as part of the development application process for residential housing approvals. This was predominantly the case for those Councils that recognised landslide hazard or had experienced demolition of residential housing within their area as a result of landsliding – for example: in Warringah Shire (now Pittwater Council) at Newport in 1972 (Burgess 1987), which is in Sydney's northern beaches; in Wollongong (a regional industrial city in the Illawarra region of New South Wales) where the nexus of steep terrain, coal seam aquifers and colluvial materials meet with the pressures of urban expansion; and Baulkham Hills (north-western area of Sydney) where existing landslides in high plasticity, low shear strength, residual clays are present in moderately steep terrain.

At that time, the stability assessments were frequently required by LGAs to confirm that the area for the proposed development was "stable" and hence suitable for development. A series of court cases highlighted the legal concept that "stable" meant "not given or subject to change". Clearly, it becomes technically difficult to state with any certainty that a site will be "stable" over any reasonable design life, and by logical extension, all hillside slopes would become unsuitable for development.

As a consequence of this, in 1985 a sub-committee of the Australian Geomechanics Society developed, over a relatively short timeframe, a technical paper dealing with the assessment of individual house blocks in an urban setting. That paper was titled "Geotechnical Risk associated with Hillside Development" (Walker et al. 1985). This was the first time that the concept of risk associated with hillside development was formally introduced to the Australian geotechnical community in an urban planning context. It is recognised that the concept of probability of failure, in contrast to a conventional factor of safety approach, was in the technical domain for mining slopes (e.g. McMahon 1985). However, Walker et al. (1985) was the first introduction of the concept of risk to the scale of residential development. By expressing the stability assessment

in terms of risk, the practitioners were able to avoid the black-and-white requirements associated with "stable", and recognise that there would be uncertainty associated with the limited knowledge frequently associated with development sites. However the level of uncertainty could be relatively small, such that many sites could reasonably be developed.

Pleasingly, many LGAs incorporated the concept developed in Walker et al. (1985), and thereby the concept of risk, into their planning process. The ready acceptance by many local governments was somewhat unexpected by the AGS sub-committee, though clearly was welcomed. Geotechnical consultants also frequently used the concept of risk for sub-divisional scale landslide assessments (e.g. Moon et al. 1992).

3   AGS (2000)

By the mid 1990's, it was recognised by members of the AGS Sub-Committee who drafted it that Walker et al. (1985) had technical shortcomings. In addition, there had been advances internationally in the concepts of risk management, and Australian/New Zealand Standard AS4360, Risk Management (initially 1996, but 1999 being the current version), had been presented.

In recognition of the challenge between development pressures and landslide hazard, in the year 2000, the Australian Geomechanics Society (AGS) published "Landslide Risk Management Concepts and Guidelines" (AGS 2000) – a benchmark technical paper, as recognised for example by US NRC (2004). AGS (2000) superseded the earlier publication of 1985 and was a continued recognition by AGS of the pragmatic benefits of incorporation of the concept of risk for assessment of potential landslides, particularly in planning and management situations. AGS (2000) was the culmination of a seven-year review that was in response to increased appreciation in Australia and internationally of the benefit of a risk management approach to landslide assessment and management.

The purpose of AGS (2000) was to: establish uniform terminology; define a general framework; provide guidance on risk analysis methods; and provide information on acceptable and tolerable risks for loss of life. A copy of the paper can be downloaded from the AGS website www.australiangeomechanics.org. The essence of the risk management process covered by AGS (2000) is presented in Figure 1. Each of the elements in the flowchart was addressed.

In risk analysis, the use of partial probabilities was encouraged. This means that estimates of likelihood (annual probability) of an event are modified by consideration of partial probabilities for spatial impact (including travel distance), temporal probability of occupancy, and vulnerability.

In regard to risk to life, acceptable individual risk for the person most at risk was suggested as 1E-6 per annum for new slopes, and 1E-5 per annum for existing slopes. By way of comparison, Planning NSW (1992) nominated 1E-6 per annum for residential development. AGS (2000) identified tolerable risk as one order of magnitude greater.

In regard to risk to property, an example of qualitative terminology for risk to property was provided in Appendix G to AGS (2000).

AGS (2000) has been accepted as an industry reference paper in legislation in both the Australian states of NSW and Victoria. This introduction into legislation provides methods for all parties (owner, occupier, regulator and also insurer) to be aware of the risks involved in construction of all manner of development – from residential development to infrastructure to critical community safety – and to manage such risks.

4   LANDSLIDE TASKFORCE

On the evening of 30 July 1997, a landslide occurred within the NSW alpine resort of Thredbo in the Koscuiszko National Park. The landslide caused the destruction of 2 ski lodges and the loss of the lives of 18 of their occupants. It was determined as an outcome of a Coronial Inquiry that the deaths were the result of a "mobile" failure of a fill supporting the Alpine Way, the main access roadway to the resort, and that this was the result of breakage of a water supply pipeline situated within a creeping roadway fill constructed of loose granitic material (in the late 1950s and early 1960s, the Alpine Way had been constructed as a temporary haul road for the Snowy Mountains Hydroelectric Scheme).

It is fair to say that, though the volume of the landslide was relatively small, the loss of lives has had far reaching effects. Not surprisingly, the quality of Australian Standards and relevant codes on landslides and hillside construction became an issue of major concern for governments, engineers and the community. Engineers Australia and AGS formed the "Taskforce on the Review of Landslides and Hillside Construction Standards" (the Landslide Taskforce) to review the adequacy of Australian Standards, relevant codes and local government requirements in relation to landslides and hillside construction, and to recommend improvements to them.

The Landslide Taskforce concluded that the existing Australian Standards and relevant codes on landslides and hillside construction were inadequate and recommended producing four guidelines on the subject as a method to rectify this situation. The guidelines identified included: landslide hazard zoning for urban areas, roads and railways; slope management;

LANDSLIDE RISK ASSESSMENT & MANAGEMENT
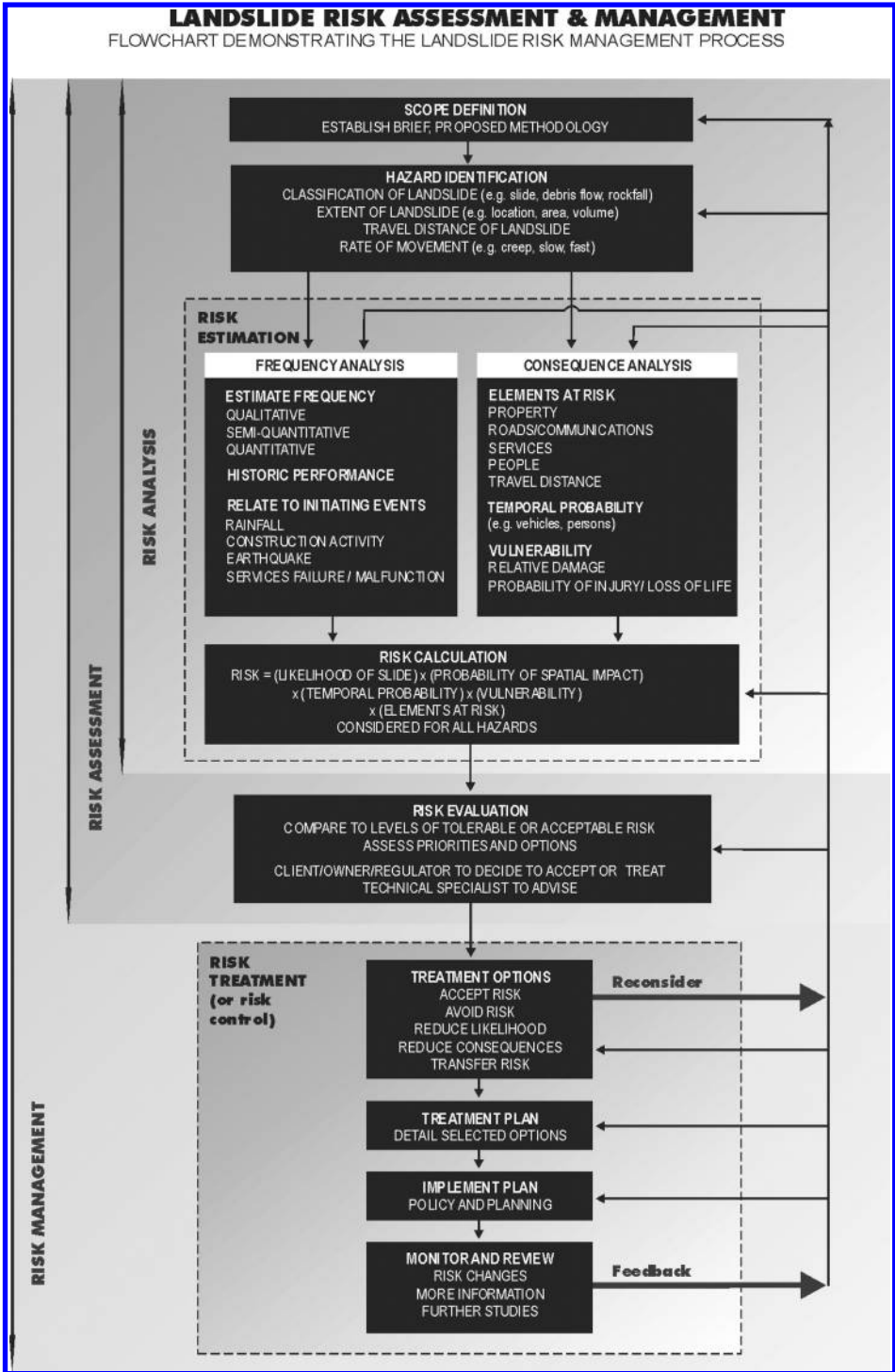### FLOWCHART DEMONSTRATING THE LANDSLIDE RISK MANAGEMENT PROCESS

Figure 1.   Flowchart for landslide risk management (after AGS 2000).

site investigation, design, construction and maintenance (technical edition for geotechnical practitioners and a simplified version to inform the public); and landslide risk assessment.

Funding for these was sought in November 1997, without success. The later development of AGS (2000), again through voluntarily contribution of AGS members, satisfied the need for the technical edition for practitioners covering investigation, risk analysis and assessment, and guidance on risk management.

5 INFLUENCE OF THE THREDBO LANDSLIDE

In the coronial report of 2000 on the Thredbo Landslide, Coroner Hand recorded that he had been provided with a copy of newly published AGS (2000) and he recommended *inter alia* that:

917. .... as urban development increasingly encroaches into steep environment, issues of instability of slopes will become increasingly apparent. It is essential that the local government community generally be fully conversant with those issues.

918. On the last day of the Inquest I was provided with a report on *Landslide Risk Management Concepts and Guidelines* prepared by the Australian Geomechanics Society's Sub-Committee on Landslide Risk Management. The purpose of the report was to establish new guidelines for assessing the geotechnical risk associated with hillside development. The guidelines were said to have a role in explaining to the public, regulators and the legal profession the process and limitations of Landslide Risk Management.

919. I recommend that the Building Code of Australia and any local code dealing with planning, development and building approval procedures, be reviewed and, if necessary, amended to include directions which require relevant consent authorities to take into account and to consider the application of proper hillside building practices and geotechnical considerations when assessing and planning urban communities in hillside environments.

920. I further recommend that the report on "Landslide Risk Management Concepts and Guidelines" be taken into account in undertaking this exercise.

6 BUILDING CODE OF AUSTRALIA

In recognition of the recommendations of Coroner Hand, the Australian Building Codes Board (ABCB)

has engaged Engineers Australia (managed by AGS) for the development of a guideline on landslide risk management (LRM). This guideline is for reference by the Building Code of Australia (BCA) and is in final draft stage, being under review at present by the representatives of the States and Territories on the Building Codes Committee of the ABCB.

The BCA Guideline, Coroner Hand's report on his inquiry into the Thredbo Landslide, and AGS (2000) are linked documents. The guidelines proposed by the Landslide Taskforce, together with AGS (2000) and the BCA Guideline, will provide a means of undertaking LRM with confidence as to quality and will provide a means for uniformity throughout Australia.

In the development of the BCA Guideline, the ABCB is seeking to determine technical solutions to protect buildings against damage from landslide, i.e. it is directed towards risk to property rather than risk to life. Given that the Building Codes Committee contains representatives of the states and territories throughout Australia, the AGS developed a position paper and in January 2004 sought response from that committee as to their opinion of acceptable qualitative risk to property. This position was developed through evaluation of relative annualised costs represented by the various risk levels when considering landslide hazard in relation to a single residence. At the time of preparation of this paper, a response has not been received. The acceptable level of risk to property developed in the position paper was "moderate" risk, as defined in Appendix G of AGS (2000).

7 THE CHALLENGE

The combined effect of the shortcomings identified by the Landslide Taskforce and Coroner Hand's recommendations was identification of the need to

- Prepare guidelines for practitioners and regulators.
- Carry out the required education and training of practitioners and regulators. (usually staff within each LGA responsible for development approvals)
- Gain acceptance by government at all levels Australia wide.
- Have the requirements of LRM incorporated into legislation.
- Provide a means of demonstrating that individual practitioners have the required knowledge and skills to reliably prepare LRM reports.

8 THE "RISKY ROADSHOW" AND EMERGENCY MANAGEMENT AUSTRALIA

With funding assistance from Emergency Management Australia, an Australian Government agency, AGS

presented a nation-wide "Roadshow" explaining the concepts of LRM and their application within the Australian context. In mid-2002, the Roadshow was presented to 561 geotechnical practitioners and officers of government agencies in all Australian capital cities, together with Newcastle and Wollongong. The proceedings of the Roadshow were published in *Australian Geomechanics*, v.37(2), in May 2002, which included a re-print of AGS (2000).

AGS (2000) has been incorporated by Emergency Management Australia as part of their national emergency planning and management strategy.

9 GOVERNMENT IMPLEMENTATION

Since 1997, the production of AGS(2000), Coroner Hand's report on his inquiry into the Thredbo Landslide, the NSW Dept of Infrastructure, Planning and Natural Resources (DIPNR) Koscuiszko Geotechnical Policy, the Victorian Dept of Sustainability and Environment (DSE) Erosion Management Overlay (EMO) for the Victorian Alpine Resorts, the NSW Roads & Traffic Authority slope management system (Stewart et al. 2002), the Pittwater Council Geotechnical Policy (2003) and a similar policy for Colac Otway in Victoria (Dahlhaus & Miner 2002), and the development of the draft of the BCA Guideline have altered the technical and legislative setting.

The requirement for all these policies is for the landslide risk assessment to be conducted by experienced engineering geologists or geotechnical engineers, and a means to demonstrate these competencies will be through the National Professional Engineers Register (see below).

10 SYDNEY COASTAL COUNCILS GROUP

In recognition of the challenges faced by all coastal councils, but particularly those in Sydney because of the density of coastal development, AGS contributed to a Geotechnical Forum and field trip conducted under the auspices of the Sydney Coastal Councils Group (SCCG) on 4 September 2003. The achievement of the forum was to bring together Councillors, Council Officers and state agency representatives involved in areas where coastal lands, including cliff lines or bluffs, have landslide hazards. A key element was recognition of the obligation of duty of care by Councils towards residents in landslide and cliffline hazard situations.

The SCCG and AGS have formed an informal alliance due to the mutual interests in adoption of LRM in the footprint covered by the 15 Councils which form the SCCG. The SCCG has sponsored funding applications under the Australian Government's NDMP

(see below) and have garnered support for the applications from the Local Government Association. AGS provides representation to the Geotechnical Expert Panel of the SCCG, which will provide overview to the funded tasks.

11 NATIONAL DISASTER MITIGATION PROGRAM

The Australian Government has introduced the National Disaster Mitigation Program (NDMP) to fund disaster mitigation, addressing hazards such as flooding, bushfire and landslides. AGS has been successful recently in obtaining funding under the NDMP for three projects.

11.1 *Landslide likelihood research*

Under the 2003–2004 funding round, basic research is being undertaken into landslide likelihood on a focused basis in a residential setting. The objective of this research is to develop base probability estimates for landslide hazards within the study area, which can then be the starting point for conducting quantitative risk assessments. Pittwater Council is situated within a geotechnical setting prone to landsliding, and several significant house-block-sized landslides have demolished and damaged houses in this LGA. Records held by Pittwater Council, which are public documents, are being used as base data for the study. The outcomes of this research will be published in *Australian Geomechanics* as the means of distribution to the profession.

11.2 *Landslide Taskforce guidelines*

In the second project (under the 2004–2005 funding round), the development of two guidelines identified by the Landslide Taskforce is being funded under another successful application, sponsored by the SCCG. Mosman Council, a northern Sydney Council, is the lead agency representing the SCCG in this project.

The first guideline will provide guidance to government regulators (officers of local government and state government instrumentalities) and geotechnical practitioners in the methods of Landslide Hazard Zoning. Such zoning will provide input to the planning process in areas of landslide hazard. The second guideline, on slope management, will provide owners and occupiers, and therefore the public in the broader sense, with guidance on management and maintenance of properties subject to landslide hazard. These two guidelines are important contributions at each end of the process – initial identification of landslide hazard in the planning process, and management of properties prone to landslide hazard by the end-user.

The guidelines proposed will benefit the general community through achieving more sustainable communities in relation to their exposure to landslide risk, and will reduce risk to the community through improved planning and slope management practices. These guidelines will link with the risk management practices presented in AGS(2000) and the BCA Guideline, and will provide long-term natural disaster mitigation benefits to housing and infrastructure.

The output from the studies will be nationally endorsed guidelines.

11.3 *Practice Note*

In the third project (which is also under the 2004–2005 funding round) is a "Practice Note" to be developed by AGS. The Practice Note will provide guidance to practitioners in the performance of project specific landslide risk assessment and management, and to government officers in interpretation of the reports they receive. The Practice Note is to complement the recognised industry "standard" on LRM in Australia – AGS (2000).

It is envisaged that the Practice Note will have application nation-wide and will be integral to the various legislative measures outlined above. The aim is to provide practitioners with the guidance to achieve uniformity in the quality of assessment and reporting, and so promote confidence in the planning and risk management process in regard to landslide hazards.

The Practice Note will provide guidance of a technical nature to the geotechnical practitioner on:

- Minimum field investigation requirements for landslide hazard identification.
- Appropriate risk assessment techniques and methods applicable to selected scenarios and when to change from one method to another.
- Minimum reporting standards and presentation methods.
- Appropriate acceptable levels of risk for both property and life.
- Risk minimisation principles.
- Typical risk minimisation measures and the protocols to be stipulated for implementation and long term management (such as through a management plan).

12 JOINT TECHNICAL COMMITTEE, JTC-1

AGS is the sponsoring society for the first Joint Technical Committee of the three "Sister Societies", IAEG, ISRM and ISSMGE. Joint Technical Committee, JTC-1, under the chairmanship of Prof Robin Fell has the task to support international symposia on landslides and to foster desirable areas of landslide research.

The chairmanship and committee membership is a demonstration of the contribution to international geotechnics by Australians as a professional commitment.

13 NATIONAL PROFESSIONAL ENGINEERS REGISTER – SPECIFIC AREA OF PRACTICE

Engineers Australia operates a scheme of registration of specific areas of practice under the National Professional Engineers Register (NPER) which is an adjunct to Chartered Professional Engineer (CPEng) status within Engineers Australia. CPEng relies upon adherence by members to the tenets of Continuing Professional Development and the Code of Ethics. Auditing provides rigour to the system. Specific areas of practice under NPER are developed to provide recognition of competent personnel for hazardous areas or to satisfy a legislative requirement. AGS and Engineers Australia are proactively introducing a specific area of practice for LRM in recognition of the need for identification of competence in this area, particularly for professionals working in the area of local government.

It is recognised that landslide risk assessments must be undertaken either by experienced personnel or under the direct supervision and involvement of those same experienced people. The NPER category will provide the means of their recognition. Chartered professional status is recognised as the prerequisite for personnel who are competent to conduct LRM within the structure of NPER, be it under the auspices of Engineers Australia, or other kindred professional bodies – such as the Australasian Institute of Mining & Metallurgy (AusIMM) and the Australian Institute of Geoscientists, that provide comparable chartered professional status, being Chartered Professional Geologist (CPGeo) and Registered Professional Geoscientist (RPGeo) respectively.

Figure 2 provides an outline of the proposed mechanics of the NPER process for LRM. Naturally, Code of Ethics obligations underlie the process, with an over-riding requirement that professionals practice only in their areas of competence. It is noted that membership of NPER is not restricted to members of Engineers Australia, it is open to those of the engineering profession who can satisfy the criteria of registration.

There are several important facets of the proposed registration process:

1. It is not intended that gaining NPER LRM registration will be easy.
2. The process will require a clear demonstration of relevant experience and an understanding of slope forming processes and slope mechanics.
3. A field assignment is seen as an essential part of the process since the capability required is very
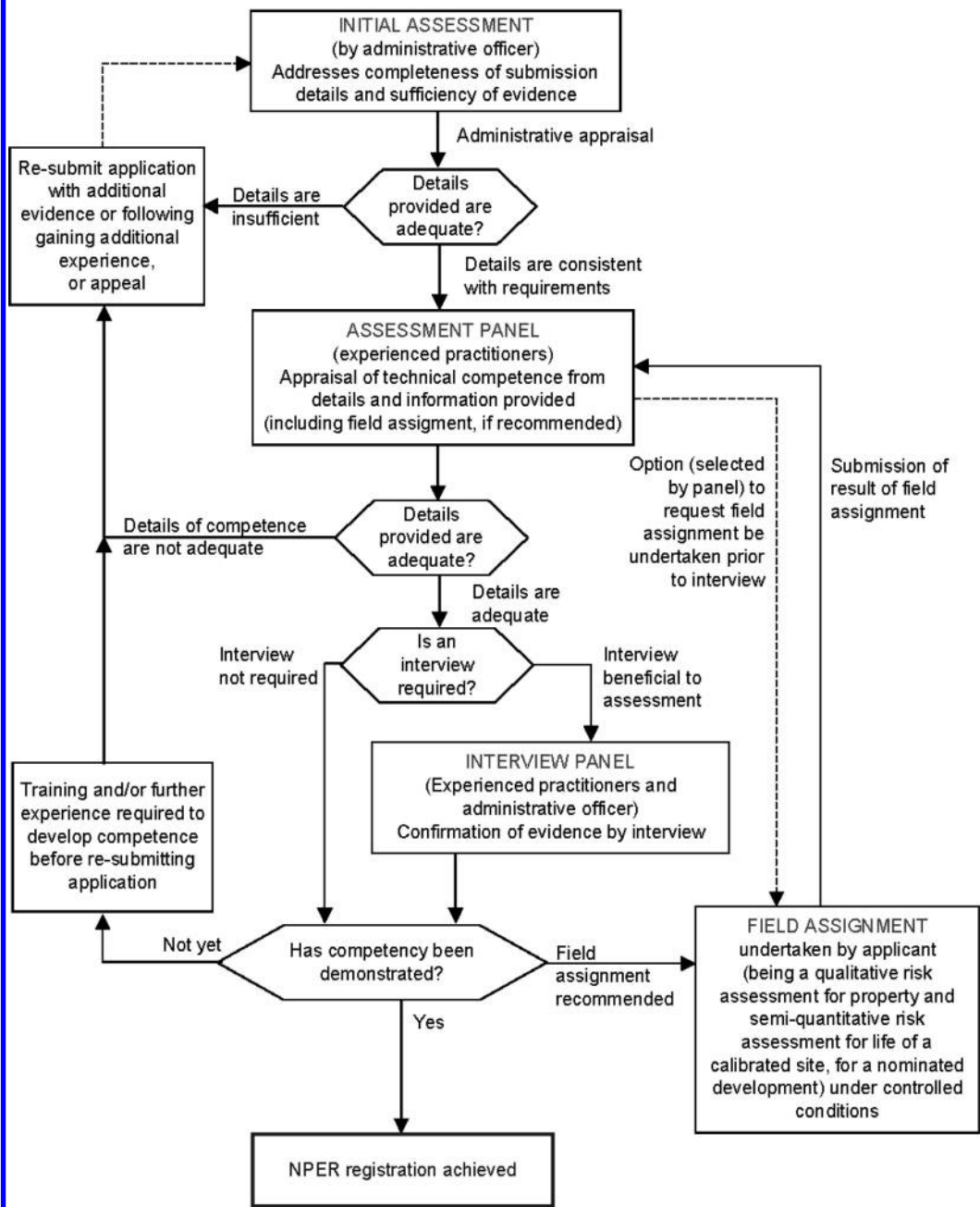
Figure 2.   Flowchart demonstrating the mechanics of NPER LRM registration.
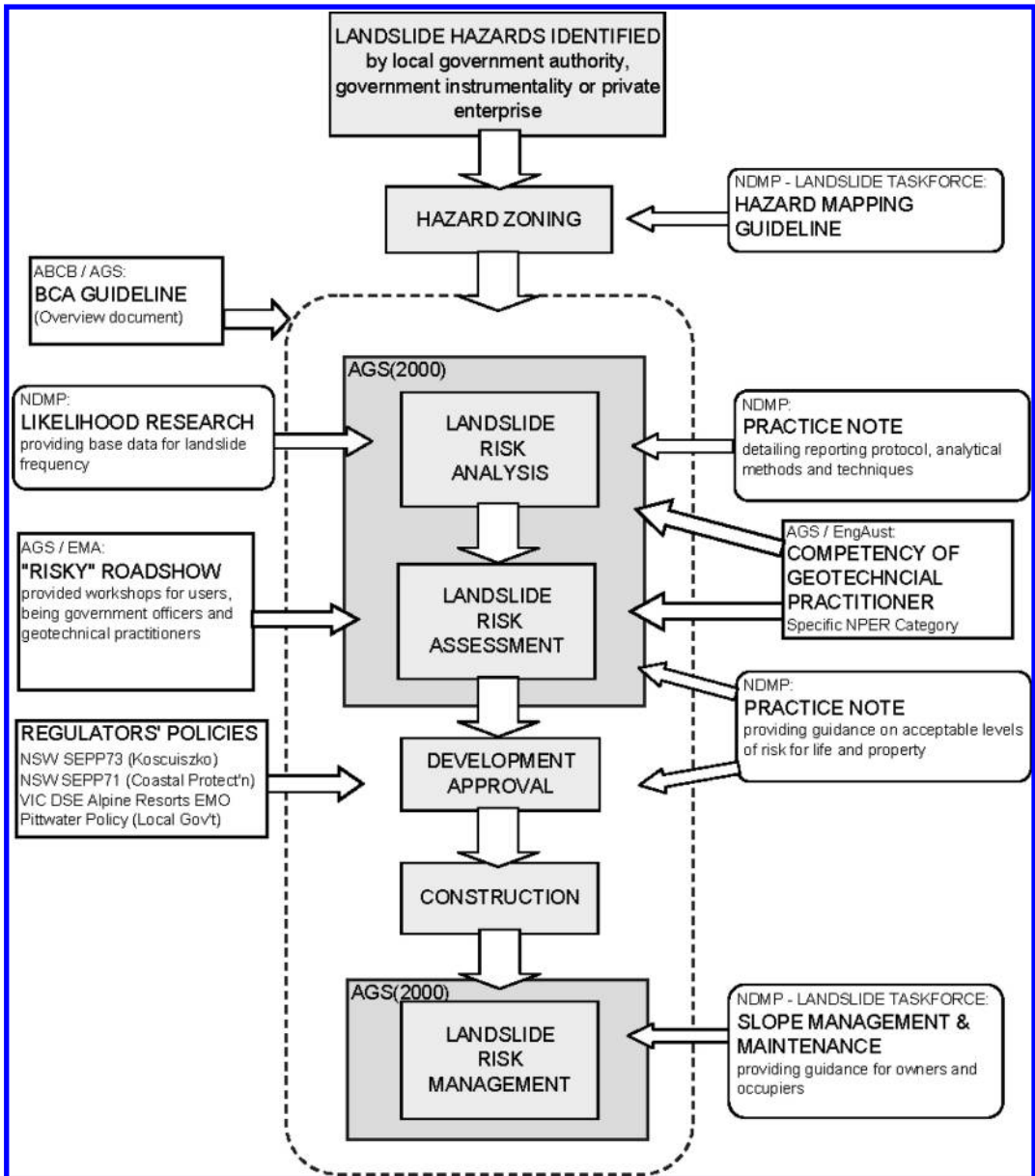
Figure 3. Flowchart demonstrating the LRM framework.

much field related and is unlikely to be assessable solely on the basis of written submissions (unless the candidate has well known and accepted ability). The use of a field assignment means that test sites will need to be established.

4. There is an obligation by members of the profession to be involved in review of applicants, both in the review and interview committees.

14 HOW DOES THIS ALL FIT TOGETHER?

As the LRM research, volunteer commitments and funding have come together over the last decade, this has meant that a nation-wide framework for landslide risk management has become feasible. It is fair to say that the pieces of the jigsaw are now close to fitting together.

408

Figure 3 shows how the pieces of the process are coming together. The essence of this is:

1. The technical basis is provided by AGS (2000).
2. The Building Code of Australia provides an over-arching legislative requirement.
3. Implementation of universal and uniform policies at state and local government levels is fundamental.
4. Hazard zoning guidelines for legislators is provided by a taskforce guideline.
5. Landslide likelihood research is to provide some fundamental data as a starting point for semi-quantitative or quantitative assessments.
6. The Practice Note provides guidance on the process and minimum requirements for conducting a landslide risk assessment, and augments AGS (2000).
7. Slope management principles are provided for the owner and occupier through a taskforce guideline.
8. Technical competence of the practitioner responsible is demonstrated through the NPER.

The flow diagram in Figure 3 shows the inter-relationship between each of those elements, and the need for them in their entirety to complete a systematic and defensible risk management process throughout Australia. The process is not complete, however we are well down the path. Lee & Jones (2004) present lengthy discussion of LRM and give many examples. However if LRM is to be adopted on a wide scale, there needs to be clear guidance to the practitioner and to the regulator and a consistent approach. The proposed guideline and Practice Note will achieve this.

Following completion of the currently funded tasks, the remaining task is to convince (with the assistance of the SCCG) the Australian Government to launch the process nationally.

15 WHAT ARE THE BENEFITS INTERNATIONALLY?

The Australian Geomechanics Society is being instrumental in establishing a framework for the completion of LRM within a defensible and rigorous set of guidelines and legislative requirements.

Clearly, there will be different drivers and various planning schemes internationally. However, if the experience of AGS is of use to others it is in demonstrating that proactive interaction by a professional group can achieve results, given sufficient perseverance. The AGS believes it has made a contribution to the wellbeing of the Australian people, and perhaps to the broader international community.

REFERENCES

AS/NZS 4360. 1999. Risk management, Australian/New Zealand standard, Standards Australia, Standards New Zealand.
Australian Geomechanics Society. 2000. Landslide risk management concepts and guidelines. *Australian Geomechanics* 35(1), reprinted 37(2).
Burgess, P.J. 1987. Urban slope instability in the Warringah Shire of Sydney. In B.F. Walker & R. Fell (eds), *Soil Slope Instability and Stabilisation*: 289–298. Balkema.
Dahlhaus, P.G. & Miner, A.S. 2002. Implementing the AGS landslide risk management guidelines in a municipal planning scheme – a case study in the Colac Otway Shire, Victoria. *Australian Geomechanics* 37(2).
Hand, D. 2000. Report of the inquest into the deaths arising from the Thredbo landslide. Coroner's report, 29 June 2000.
Lee, E.M. & Jones, D.K.C. 2004. *Landslide risk assessment.* London: Thomas Telford.
McMahon, B.K. 1985 Geotechnical design in the face of uncertainty. *Australian Geomechanics News* 10: 7–19.
Moon, A.T., Olds, R.J., Wilson, R.A. and Burman, B.C. 1992. Debris flow zoning at Montrose, Victoria. In D.H. Bell (ed), *Proc Sixth Intl Symp on Landslides, Christchurch, NZ, February 1992.* Balkema.
Pittwater Council. 2003. Interim geotechnical policy. [A copy can be downloaded from the Building & Development section of the Council's website: www.pittwaterlga,.com.au]
Planning NSW. 1992. Risk criteria for land use safety planning. Hazardous Industry Planning advisory Paper No 4, second edition. (Planning NSW is now Department of Infrastructure, Planning and Natural Resources, DIPNR).
Stewart, I.E., Baynes, F.J. & Lee, I.K. 2002. The RTA guide to slope risk analysis, version 3.1. *Australian Geomechanics* 37(2) – the proceedings of the "Risky Roadshow".
U.S. National Research Council. 2004. Partnerships for reducing landslide risk. Assessment of the National Landslide Hazards Mitigation Strategy, Board on Earth Sciences and Resources, Division of Earth and Life Studies., Washington, DC.: National Academies Press.
Walker, B.F., Dale, M., Fell, R., Jeffery, R., Leventhal, A., McMahon, M., Mostyn, G. and Phillips, A. 1985. Geotechnical risk associated with hillside development. *Australian Geomechanics News*, 10: 29–35 – acting as a Sub-Committee of the Australian Geomechanics Society.

A preliminary landslide risk assessment of road network in mountainous region of Nepal

L. Sunuwar & M.B. Karkee
Akita Prefectural University, Honjo City, Akita, Japan

D. Shrestha
Department of Roads, His Majesty's Government of Nepal, Babarmahal, Kathmandu, Nepal

ABSTRACT: The problem of landslides in hill roads is potentially acute in Nepal where about eighty percent of land area is in the hilly and mountainous terrain. The major roads connecting administrative and business centers, including the capital city Kathmandu, pass through mountainous terrain. The problem is compounded by the fact that the annual precipitation is concentrated during the four months (June to September) resulting in frequent floods and landslides. Landslides are also associated with the fragile mountain geology of Nepal Himalayas combined with the concentrated rainfall. Rain induced landslides are frequent in the major highways of Nepal blocking the traffic for several times annually. This study starts by analyzing the present situation of landslides in major highways of Nepal running through mountainous regions. The annual average daily traffic (AADT) volume and the length of hill roads are considered in the qualitative risk assessment of individual routes. The trend observed in road closure data collected by Department of Roads (DOR) in Nepal for the recent four years is summarized. This study is expected to contribute to the disaster mitigation planning by the decision makers of road agencies in relation to the following aspects: (1) developing pre-monsoon road maintenance plan; (2) developing the strategy for swift response to the occurrence of road closure due to landslide; and (3) contribute to better design and construction of hill roads in fragile mountain region of Nepal.

1 INTRODUCTION

Frequent landslide occurrences are encountered during rainy season in the roads of Nepal due to hazardous nature of terrain, stratigraphy and geology. About eighty percent of the land area of Nepal is in either hilly or mountainous region with steep cross slopes. The altitude varies from about 60 m from average mean sea level (amsl) in the southern plain to about 8000 m amsl in the north where the highest peaks of the world are located. This drastic change in altitude occurs over a width of about 120 km. The rivulets, torrents and rivers form the base of hills or mountains. Most of the roads in Nepal thus constitute hill roads, mostly cut section in steep cross-slopes. Landslides are therefore a regular phenomenon in most roads of Nepal.

The importance of road network is overwhelming in the sense that the no other means of land transportation like railways is available in Nepal. Almost all transportation of goods and services depends upon the road network. For example, the distribution of petroleum products transported from neighbouring country India to different part of the country depends

totally upon the road network. As a result, extreme hardship is faced by people when roads are blocked by landslide. In the capital city of Kathmandu, essential goods become scarce when the highway remains blocked for a week. Figure 1 shows the situation in the

Figure 1.   Condition during blockage due to landslide in Narayangadh-Mugling Road (27 July 2004).

month of July last year (2004) along the Narayangadh-Mugling road (H05), which is the main highway connecting the southern pains with the capital city Kathmandu.

Road construction in Nepal started only from 1950 and about 16,800 km of road has been developed in the period of about 50 years. When road construction started around 1950, there was little knowledge about the fragile and hazardous geology of Nepal Himalayas. Significant work by geologists from various countries concerning the geology of Nepal came into fruition only after 1970 (Upreti 1999). The very first instance of the application of the knowledge of engineering geology was perhaps in the planning and construction of Lamosangu-Jiri road in 1980s. This road constructed under grant aid of government of Switzerland is considered as an environment friendly road in Nepal at present. This was achieved by extensive involvement of engineering geologists in the planning and construction phases of the road. Furthermore, when a section of the road in Charnawati watershed area failed in 1987 flood, the rehabilitation also involved extensive involvement of engineering geologists. Based on this experience, the knowledge of engineering geology and geotechnical engineering is normally accepted as required in planning and construction of roads at present. Dhital (2003) mentions following roads for which detailed landslide hazard mapping was carried out: (1) Tulsipur-Salyan road, (2) Ghorahi-Libang road, (3) Baitadi-Darchula road, and (4) Sagarmatha highway (Gaighat-Diktel-Okhaldhunga). However, roads constructed before 1980, which include, major highways and feeder roads, were constructed without detailed landslide hazard mapping.

This paper is concerned with the landslide problems present in the highways constituting strategic road network of Nepal with a view to evaluate the qualitative risk involved. Starting with the discussion of primary factors causing landslides, such as rainfall, tectonic settings and physiographic variations, the paper describes the highway network of Nepal in relation to the stratigraphic and geological conditions. The most recent attempt of the DOR in collecting road closure data is included and discussed. The study aims to provide the basis for identification slope instabilities that can be utilized in planning for pre-monsoon maintenance strategy so that the road closure due to landslides may be ameliorated or dealt with swiftly.

2 GEOLOGY AND TECTONIC SETTING OF NEPAL HIMALAYA

Nepal Himalayas occupy about one third of total length of Himalaya range. Being a boundary of Indian and Eurasian tectonic plates, Himalayas are known to be fragile mountains. Several thrust faults are identified to be prominent in the foothill of Himalayas in Nepal. There are three major faults recognized to constitute the tectonic boundary of Nepal Himalayas. Main frontal thrust (MFT) is identified as the fault in the southernmost part of Nepal, forming the boundary between the plain area called Terai and the Siwalik hills. The main boundary thrust (MBT) is to the north of MFT and marks the starting of middle mountains. Main central thrust (MCT) marking the boundary between middle mountains and higher mountains in the Himalayas, mostly above the snow line. Figure 2 shows the schematic north-south cross section of Nepal showing the locations of thrust faults described above. The regions between these thrust faults, which are locations of geological discontinuities, are designated
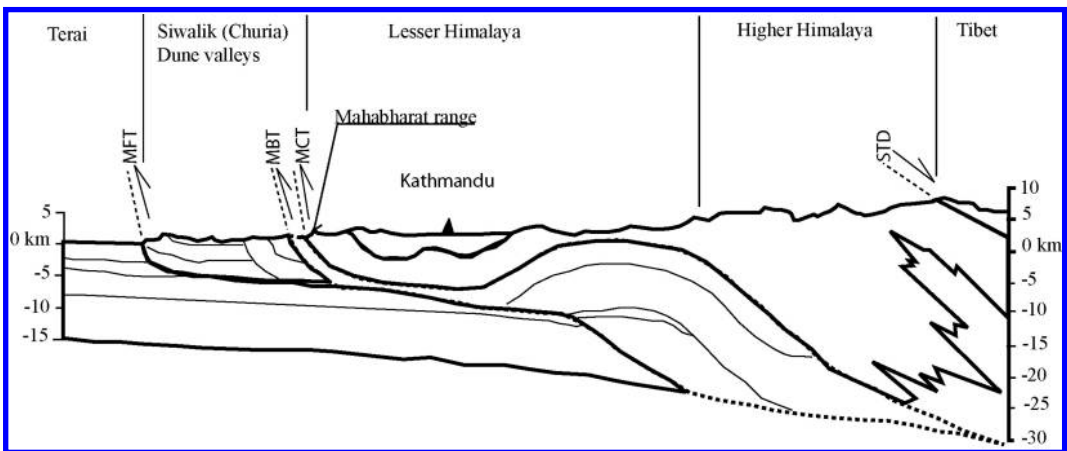

Figure 2. North-south cross section of Nepal Himalaya (Based on Pandey *et al*. 1999 and Upreti 1999).

to be major types of geological units of Nepal. The distribution of geology and location of thrust faults are shown in Figure 3 (Upreti 2001). Almost all major roads pass through these thrust faults of geological discontinuities. The monsoon rainfall can easily trigger landslides in the stretch of roads crossing these geological boundaries. For example, the debris flow frequently blocks the Tribhuwan Highway crossing the Churia range to the south of Hetauda.

Table 1 shows the main stratigraphic divisions of Nepal based on the altitude and terrain structure. The distributions of these stratigraphics are shown in
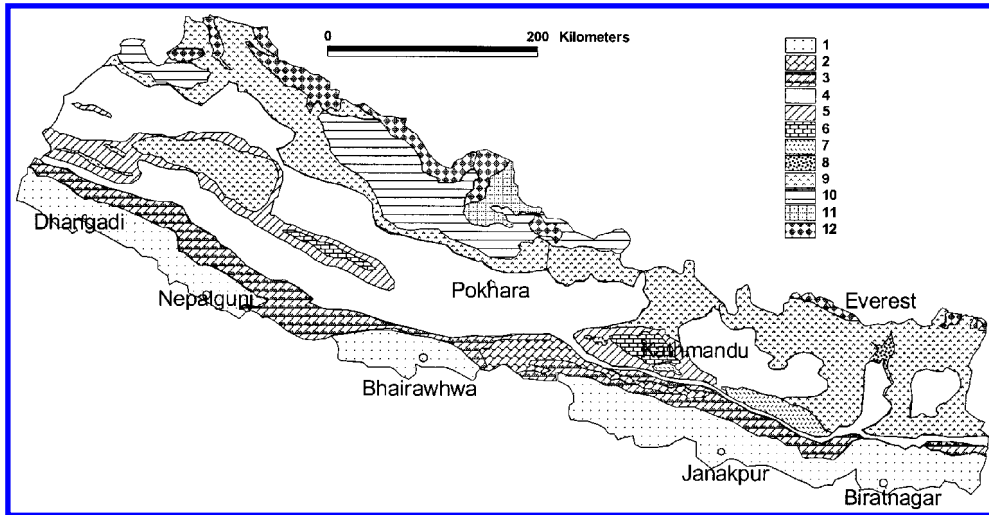

Figure 3. Geology of Nepal (based on Upreti 1999, with the permission from Elsevier Science). 1. Terai, 2. Dunes and recent fillings, 3. Churia group (Siwaliks), 4. Lesser Himalayan (LH) Zone, 5. LH crystalline nappe, 6. LH Paleozoic, 7. LH Granite, 8. LH Augen gneiss, 9. Higher Himalaya (HH) Crystalline nappe, 10. Tibetan Tethys Sediment (TTS) Palezoic, 11. TTS Mesozoic, 12. HH Leucogranite.

Table 1. Stratigraphic units of Nepal (Upreti 1999, with the permission from Elsevier Science).

S. No.	Stratigraphic unit	Width (km)	Altitudes (m)	Main rock types	Age
1	Terai (northern edge of Gangetic plain)	20–50	100–200	Alluvium: coarse gravel in the north near the foot of Churia, gradually becoming finer southward	Recent
2	Churia hills	10–50	200–1000	Molasse deposits: Sandstone, mudstone, shale, conglomerate	Mid-Miocene to Pleistocene
3	Dun valleys	5–30	200–300	Coarse to fine alluvial sediments	Recent
4	Mahabharat range	10–35	1000–2500	Schist, phyllite, gneiss, quartzite, granite and limestone	Precambrian and Paleozoic
5	Midland	40–60	200–2000	Schist, phyllite, gneiss, quartzite, granite, limestone	Precambrian and Paleozoic to Mesozoic
6	Fore Himalaya	20–70	2000–5000	Gneiss, schist and marbles	Precambrian
7	Higher Himalaya	10–60	>5000	Gneiss, schist and marbles	Precambrian
8	Inner and Trans Himalayan Valley		2500–5000	Gneiss, schist and marbles of the Higher Himalayan Zone and Tethyan sediments	Precambrian to Cambrian to Cretaceous

413

Figure 4. Among the stratigraphic units, Churia hill, Mahabharat range, Midland and Fore Himalayas consist of fragile slopes with high degree of hazard from landslides during rainfall. These stratigraphic units contain highly heterogeneous materials on the surface with numerous local instabilities. It can be partly understood from the main rock types prevalent in these units. The stratigraphic feature bears important implications for road construction and maintenance. Most proportion of the road network of Nepal lies within the first five stratigraphic regions. Only Arniko Highway (H03) passes through Fore-Himalayas and encounters several unstable areas near Nepal-China border (Upreti 2001). There are no road access to Higher Himalayas and Inner and Trans Himalayan valleys.

3   RAINFALL PATTERN

The annual rainfall in Nepal is due to monsoon cloud originating from the Bay of Bengal in Indian Ocean and is concentrated during the four months (June–September). The actual amount of rainfall varies depending upon the location in macro and meso scale. Sometimes the local cloudburst phenomenon causes very concentrated rainfall within few days, causing extensive erosion and landslide problems.

The most important feature of monsoon rainfall in triggering numerous landslides is its concentration during four months. Figure 5 shows the monthly rainfall

for Arughat Bazar station (near Prithvi Highway, H04) for the year 2000 compared with the monthly mean precipitation of Kathmandu valley for 50 years. The mean monthly rainfall of Kathmandu is taken from Chalise (2001). It shows that more than 80% of the annual rainfall happens within the period of June–September. Normally eastern part of Nepal gets higher annual precipitation than that of western part, but there are some locations where the annual precipitation is high due to other reasons like topography and presence of water bodies.
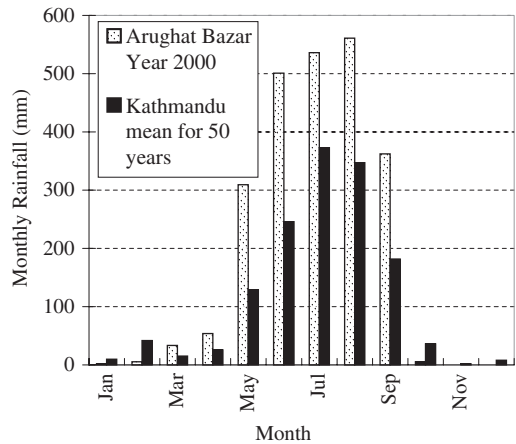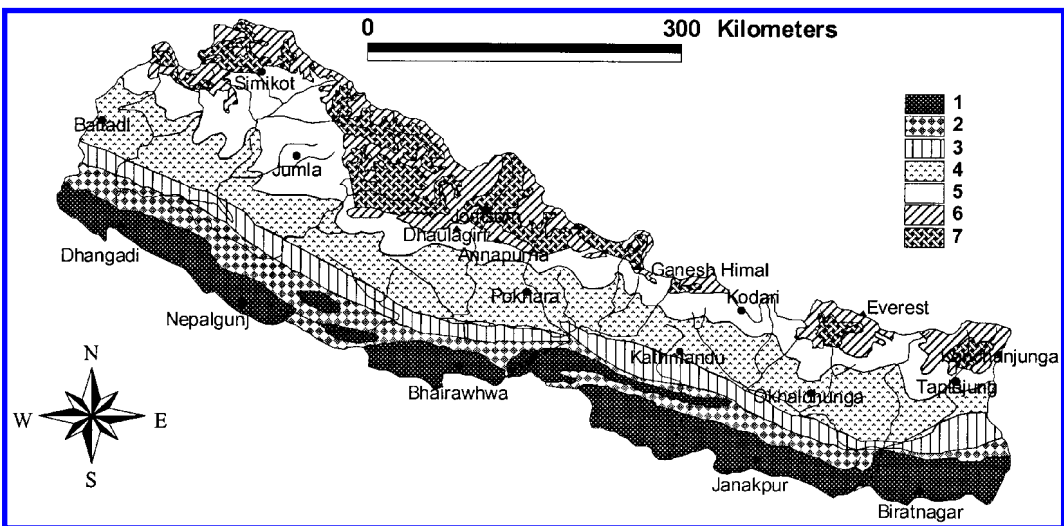

Figure 5.   Monthly rainfall pattern in Nepal.

Figure 4.   Stratigraphic variation of Nepal (based on Upreti 1999, with the permission from Elsevier Science). 1. Terai and Dune valleys, 2. Churia range, 3. Mahabharat range, 4. Lesser Himalaya (midlands), 5. Fore Himalaya, 6. Higher Himalaya, 7. Inner valleys.

414

4 FACTORS TRIGGERING LANDSLIDES

Two main triggering factors for landslides are normally recognized in Nepal: rainfall and earthquakes. Rainfall is the major triggering factor for frequent landslides in Nepal, due to which numerous landslides occur every year. As described in the previous section, monsoon rainfall is normally concentrated during June to September. The rainfall sometimes is intensely concentrated in certain part of the country, resulting in landslide as well as flood disaster in certain interval. Examples are the 1987 flood and landslide disaster in Eastern and Central Nepal (Adhikary 2001), 1993 flood and landslide disaster in Central Nepal (Thapa 2001), 2002 flood and landslide disaster in Eastern and Central Nepal (Wagley 2003). Bhandary *et al.* (2004) give details of landslides along two highways of central Nepal triggered mainly by monsoon rainfall.

The highest rainfall recorded in 24-hour period was at Kulekhani, where 540 mm rain was recorded on July 19–20, 1993. This amounts to average an hourly precipitation of 22.5 mm/hr. In California, USA, it is said that shallow landslides are triggered by rainfall threshold of 6.4 mm/hr (Wieczorec 1996). In addition to rainfall, earthquake induced landslides occur over long stretches of hill roads. For example, numerous landslides were triggered by the 1988 Udayapur earthquake along the Dharan-Dhankuta road (H08). Being located at the boundary between Indian and Eurasian tectonic plates, frequent occurrences of earthquakes constitute serious hazard for the road network of Nepal from earthquake-induced landslides. The hazard level of earthquake in Nepal is comparable with the most seismic prone cities of the world like Los Angeles of USA and Sendai of Japan (Sunuwar *et al.* 2005). Pandey *et al.* (1999) state that the big earthquake events repeat in every century in Nepal at least affecting Kathmandu valley.

In addition to the two major factors, there are other factors that may trigger landslides: (1) toe cutting by river; (2) unsafe cultivation practice including deforestation; (3) unauthorized and improper quarrying practice; (4) improper construction practice for hill roads and irrigation canals; and (5) glacial lake outburst flood (GLOF). Toe cutting by river is related to flood caused by concentrated precipitation and is common in most of the highways that follow alignments adjacent to rivers. GLOF events are not so frequent but it is believed to be a threat about once every decade on the average. Adhikary (2001) mentions two GLOF events in 1964 and 1981 along Arniko Highway (H03).

5 ROAD NETWORK OF NEPAL

Starting from 1950, about 16,800 km load road system has been developed in Nepal during the period of about 50 years. Figure 6 shows major roads under the jurisdiction of DOR. Of the 16,800 km of roads,
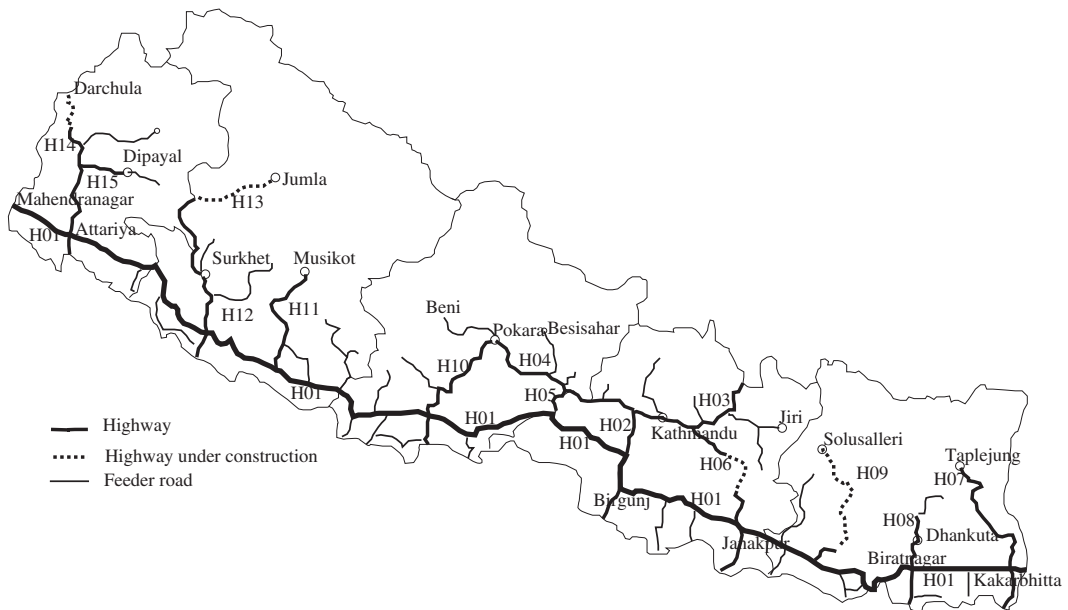

Figure 6.   Road Network of Nepal showing major highways and feeder roads (Source: NRS 2002).

415

Table 2. Major highways of Nepal and thrust faults associated.

S. No.	Desig-nation	Road name	Total length (km)	Hill section (km)	Direction	Construction year	Main faults crossed
1	H01	Mahendra Rajmarg (MRM)	1037	40	East–West	1967–2000	MFT, MBT
2	H02	Tribhuwan Rajpath (TRP)	160	77	North–South	1953–1962	MFT, MBT, MCT
3	H03	Arniko Rajmarg (ARM)	113	73	North–south	1963–1972	MCT
4	H04	Prithvi Rajmarg (PRM)	173	158	East–West	1967–1974	MBT, MCT
5	H05	Narayangadh-Mugling Rajmarg (NMRM)	36	31	North–south	1978–1982	MFT, MBT, MCT
6	H06	Dhulikhel-Sindhuli Rajmarg (DSRM)*	201	101	North–South	1996–	MFT, MBT, MCT
7	H07	Mechi Rajmarg (MERM)	268	213	North–South	1980–	MFT, MBT, MCT
8	H08	Koshi Rajmarg (KRM)	111	58	North–South	1976–	MFT, MBT, MCT
9	H09	Sagarmatha Rajmarg (SARM)**	158	138	North–South	1980–	MFT, MBT, MCT
10	H10	Siddartha Rajmarg (SRM)	181	138	North–South	1964–1972	MFT, MBT, MCT
11	H11	Rapti Rajmarg (RPRM)	169	149	North–South		MFT, MBT, MCT
12	H12	Ratna Rajmarg (RRM)	113	78	North–South	1957–1987	MFT, MBT, MCT
13	H13	Karnali Rajmarg (KARM)	220	220	North–South	1992–	MFT, MBT, MCT
14	H14	Mahakali Rajmarg (MKRM)	326	266	North–South	1967–	MFT, MBT, MCT
15	H15	Seti Rajmarg (SERM)	66	66	East–West		MFT, MBT, MCT

* About 30 km still under construction
** Most part still under construction

about 3,000 km is classified as constituting highways connecting important service centers. The remaining roads are designated variously as feeder roads, district roads, city roads and rural roads (NRS 2002). The main jurisdiction of DOR falls into highways and feeder roads which is about 8000 km at present.

Table 2 shows the details of 15 highways consisting of total length, length in hill section and main directions. These highways are shown in Figure 6 with designations. From this table it is evident that more than 50% of the length of major highways lies in hill sections, where a high degree of hazard from landslide blockage is to be expected. Table 2 also gives the main tectonic thrusts crossed by the highways and construction years. These faults were unrecognized when most of these highways were being constructed and naturally the instabilities were not dealt with in rational ways in many instances. These locations later became bottleneck positions hindering smooth traffic flows. The common measure adopted was to clear the debris from frequent landslides triggered by intense monsoon rain. It is obvious that all roads running north south cross three main faults. Highways running east west also cross these unstable areas at several places.

6 ROAD CLOSURE STATISTICS

Until 2000, DOR did not adopt the recording of road closure data in a systematic manner. The maintenance work was carried out in a responsive basis whenever the closure occurred. However, with the increase in road length and traffic density, a systematic way of allotting emergency funds to carry out maintenance due to flood and landslide was felt in 2000 and the deputy director general (DDG) responsible for maintenance of road network initiated the process of collecting road closure data. The data mainly contains division office name and location, name of road closed and the length of load affected, date and time of closure and opening, and resources (manpower and equipment) used in opening the road. The expenditure incurred is also recorded whenever possible. Accordingly, road closure report form was prepared and all the road maintenance offices were requested to report the closure data. The incentive for reporting was provided by allocating sufficient emergency funds for the following fiscal year to maintenance offices that submitted closure reports.

The road closure reports of DOR for four years starting from the fiscal year of 2001/2002 have been summarized in Table 3. The number of closures for each highway and number of hours of closures are shown. Of course, this includes only the events of closure occurring in highways reported by the road maintenance offices. The number of unreported closure events may exceed by far the reported ones.

Figure 7 shows the road closure time and the cumulative rainfall from the start of monsoon for highway ARM (Table 3) for the year 2001. This is a typical example of the effect of monsoon rainfall in

416

Table 3. Reported road closure events and duration for the years 2001–2004.

S. No	Highway designation	2001/2002		2002/2003		2003/2004		2004/2005	
		Events	Closure	Events	Closure	Events	Closure	Events	Closure
1	MRM (H01)	–	–	1	197.25	4	44	1	–
2	TRP (H02)	–	–	1	62	–	–	–	–
3	ARM (H03)	7	24	2	21	13	1315	2	32
4	PRM (H04)	8	41.75	16	155	4	21.25	5	32.75
5	NMRM (H05)	6	48.75	2	16.25	2	15	6	27
6	DSRM (H06)	–	–	3	321	–	–	2	168
7	MERM (H07)	–	–	–	–	3	69	1	27
8	KRM (H08)	1	6	–	–	–	–	3	26.25
9	SARM (H09)	–	–	1	8	–	–	–	0
10	SRM (H10)	2	43	1	25.5	5	41	3	49.75
11	RPRM (H11)	–	–	–	–	–	–	1	29
12	RRM (H12)	–	–	6	55	6	68.5	2	26
13	KARM (H13)	–	–	–	–	–	–	–	–
14	MKRM (H14)	–	–	2	7	–	–	–	–
15	SERM (H15)	–	–	2	9	–	–	–	–
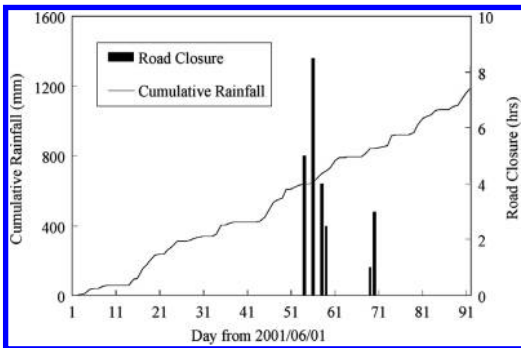
Figure 7. Reported road closure of highway ARM versus cumulative rainfall in 2001.

Figure 8. Rainfall and road closure of PRM (H04) due to Krishna Bhir landslide in the year 2000.

road closures. It shows that the closure is reported in the mid of monsoon after several days of start of the monsoon. It is indicative of the rainfall saturating the soil in hill slopes over a period of time such that the landslides are triggered as the rainfall continues to accumulate. All the road closure reported is in the period of monsoon i. e. in between the month of June to September.

7 CASE OF KRISHNA-BHIR LANDSLIDE

This case study is presented here to show the potential risk of one major landslide occurring in a major highway (H04 in Table 3 and Fig. 6). Krishna-Bhir landslide is probably the most critical event b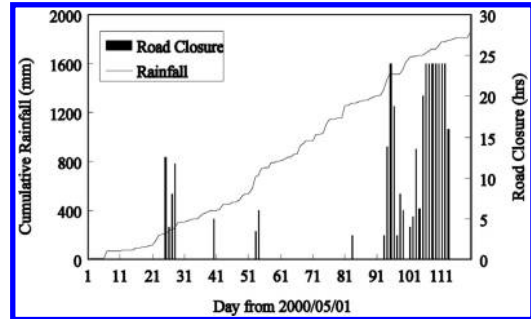locking major traffic connection to Kathmandu for several days during monsoon season year after year. It lies in the 57 + 500 km of highway PRM (H04), at a distance of 83 km west from Kathmandu. It was first triggered in July 1999 and the landslide became worst in the monsoon of 2000 causing about 362 hours of road closure. The longest duration of blockage extended to 11 days starting from 2000/8/13. Figure 8 shows the cumulative rainfall from the start of monsoon and the road closure in hours. The road was blocked for 24 hours for consecutive 9 days. Again, it can be seen that the landslide blockage became eminent as the monsoon rain accumulated. A 10 m high breast wall consisting of gabion filled with stones was erected after the initial minor slide. The breast wall was completely swept away by the landslide in 2000.

The photograph in Figure 9 shows the condition after landslide in 2001, where about 200,000 cubic m of landslide debris had to be cleared during the monsoon of year 2000. The closure data of 2000 and expenditures
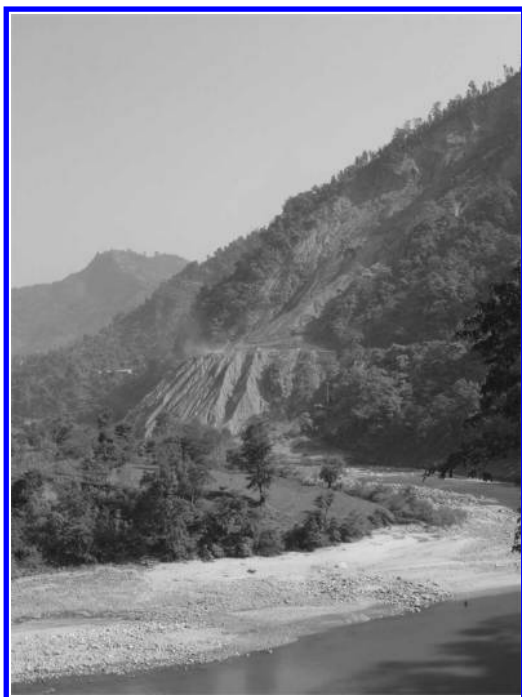
417

Figure 9. Krishna-Bhir landslide during August 2001.

Figure 10. Krishna-Bhir landslide in 2004 November after stabilization by countermeasures.

Table 4. Road closure and expenditure in Krishna Bhir landslide.

Fiscal year	Road closure (hours)	Budget spent ('000 NRs)		
		Emergency	Structures	Total
2000/2001	162	6550	3000	9,550
2001/2002	22	2100	2155	4,255
2002/2003	106	2000	11255	13,255
2003/2004	13	–	–	–
2004/2005	0	–	–	–
Total	303	–		27,060

incurred are taken from Regmi & Sitaula (2003) who were responsible for countermeasure planning and supervising the work to open the road after blockage. By the year 2004, this landslide is believed to have stabilized to certain extent through countermeasures consisting of a combination of retaining structures, drainage and bioengineering. Figure 10 shows the condition of this slide in November 2004. The retaining structure and drainage along with the bioengineering work can be seen in the photograph. The base width and maximum slant length are 200 m and 300 m respectively. The final slope angle is about 30° reduced from 35° in the initial condition.

This landslide created a sense of panic within DOR as well as among the public for three years. The total expenditure for debris clearing and countermeasures for three years is reported to be about 27 million Nepali Rupees (NRs), which comes out to be about US$387,000 (Regmi & Sitaula 2003, in Table 4). This amount is almost equivalent to annual toll fee collected for one year for this road with nominal level of toll tax to maintain the highway. The road closure received high media attention, as the landslide was located in the major highway connecting southern plain to the capital city of Kathmandu. According to the reported closure data, this landslide caused problems of road blockage in the year 2000, 2001 and 2002. In 2004 the road closure data shows there was road closure due to this slide. Table 4 gives the summary of road closure and expenditure.

8 QUALITATIVE RISK ASSESSMENT OF LANDSLIDES IN HIGHWAYS

The road closure due to landslide involves cost to DOR as well as to road users and general public. The emergency maintenance cost is very high in the country like Nepal where government fund is always scarce. Since there are a number of possible landslide sites along highways, it is important to prioritize the instable slopes for proper maintenance and emergency measures. This fact is now realized by DOR and recently efforts are made to prepare a guideline for slope protection work (Eto *et al.* 2003). This section gives brief outline of the main approaches considered in the draft guideline for prioritization of slope instabilities based on potential risk levels.

It should be noted here that majority of slope failures occur in heterogeneous materials consisting mainly of coarse grained soils or rocks in the hill

418

Table 5. Hazard matrix as per the slope failure type.

Hazard level	High (A)	Medium (B)	Low (C)
Landslide	Obvious clear deformations and visible movements of cracks	Obvious landslide topography but no visible movement	Landslide suspected but no visible evidence of deformation
Debris flow	Frequency within every two years	Frequency of over three years	Occurrence is rare
Embankment failure	Visible deformations and disturbing traffic conditions	Visible deformations but traffic flow is normal	No deformations but need of repair of structures and drainage

Table 6. Road vulnerability matrix.

Evaluation item	High (a)	Medium (b)	Low (c)
AADT	$\geq 1{,}000$	$1000 > A \geq 500$	<500
Public assets	Important	Medium	Low
Number of private houses	≥ 10	$10 > H \geq 3$	$H < 3$
Time required for temporary opening of traffic	$P \geq 3$ days	$3 > P \geq 1$	$P < 1$ days

Table 7. Risk levels and possible solutions.

Combination	Risk level	Solution
Aa, Ab, Ba	I	Immediate implementation of countermeasures
Ac, Bb, Ca	II	Frequent monitoring (inspection frequency once a month)
Bc, Cb	III	Periodic inspection (before and after monsoon)
Cc	IV	No more follow up until some changes noticed

roads. The fine-grained soil is always present mixed with gravel and cobbles. Furthermore, most of landslides along roads occur in the geologically unstable locations like faults, thrusts and folds. If we follow the classification given by Cruden & Varnes (1996) majority of slope failures fall into limited categories of rock slides, translational slides, rotational slides and debris flow. Among these slides rotational slides normally covers large area so it is most important to mitigate this type of landslide. There are many landslide events termed as debris flow, but not necessarily following the criteria of debris flow given by Hungr *et al.* (2001). Normally any landslide material flowing through channel irrespective of source materials and movement rate are termed as debris flow in the context of Nepal.

By definition, the risk of slope instability is considered as the combination of hazard and vulnerability. In the DOR guideline, the hazard is identified for three types of slope failures: landslide, debris flow and embankment failure. Again the debris flow mentioned in this context may not necessarily follow the criteria given by Hungr *et al.* (2001). The landslide is considered as the most serious hazard that normally occurs in hill sections of highways which includes here all types of slope failures occurring along the road. Table 5 shows the criteria to decide the hazard level for individual slope instabilities. For landslide, it is the topography and the movement rate. For debris flow, it is the frequency of occurrence. Table 6 gives the consequences of slope failure according to importance of roads and properties if any. The main factor

depicting importance of a road is obviously AADT. The elements of Table 6 can be considered as vulnerability of roads to slope failures. They are assessed in three levels 'a, b and c' as per importance of the road, public assets, number private houses likely to be affected and time required for temporary opening of traffic.

Combining the level of hazard and vulnerability, subjective indices of risk associated with the slope failure are given in Table 7. Four levels of risks are introduced in the guideline so that prioritization for measures against slope failures can be adopted conveniently. The risk of landslide comes either in level I or II depending upon the vulnerability level. The possible solutions for each risk levels are also shown in Table 7. The scenarios for likely potential risks are developed for highways judging the AADT data of 2001 in Table 8. Most of the major highways with AADT >500 come with maximum risk level I, while others fall in risk level II. All four important highways H01 to H04 and H10 have maximum risk of level I due to high AADT. The countermeasures in these highways naturally get first priority because highways H02, H03, and H04 connect the capital city Kathmandu with other part of the country. However, this risk assessment is preliminary in its nature and case-wise risk assessment is needed in future to deal with road landslide problem.

419

Table 8. Landslide risk levels of major highways.

S. No.	High-way	Maxi-mum AADT (2001)	AADT in hill section	Worst combina-tion	Maxi-mum risk level
1	H01	3011	625	Ab	I
2	H02	4333	4333	Aa	I
3	H03	13844	978	Ab	I
4	H04	3416	3416	Aa	I
5	H05	3228	3228	Ac	II
6	H06	1214	173	Ac	II
7	H07	426	426	Ac	II
8	H08	329	329	Ac	II
9	H09	287	287	Ac	II
10	H10	3383	1052	Aa	I
11	H11	256	63	Ac	II
12	H12	1567	402	Ac	II
13	H13	179	179	Ac	II
14	H14	992	116	Ac	II
15	H15	51	51	Ac	II

9 SECONDARY RISK FACTORS TO ROAD NETWORK DUE TO LANDSLIDE

In addition to direct effect of road blockage, landslide causes temporary damming of river which may be very hazardous to downstream roads and habitations if the dam gets burst. The effect will be similar to that of the GLOF. In addition to complete wash out of road sections very near to the river, the bursting of landslide dam or GLOF may also erode or damage cross drainage structures like bridges. Such hazards, though comparatively infrequent, do exist in the hill roads of Nepal. Sharma (1990) gives an account of landslide dam in August 1968 in the Central Nepal. The landslide damming occurred for 29 hours and burst causing wash out of many houses and properties of Arughat Bazar, Central Nepal. The roads H04 and H05 in the likely affected area of landslide dam were not yet constructed.

The roads may also be affected by initiation of toe cutting at stretches adjacent to rivers due to landslide dam outburst. Such hazards are prevalent in the roads following river alignment such as H03, H04, H05, and H06 in Table 3. Other highway following ridge alignment also faces the hazard due to wash out of bridges by the bursting of landslide dams or GLOF.

10 CONCLUSIONS

This study summarizes the potential risk of landslides in highways of Nepal considering the triggering factors and geological and stratigraphic factors involved. Road closure data of recent four years is summarized to show the effect of landslides. Finally, considering the AADT data of highways, the qualitative preliminary risk assessment is carried for road closure due to landslide. This study is expected to contribute awareness and preparedness of road maintenance agency through rational collection and presentation of data in future to develop strategies for swift action in the event of closure along roads due to landslide blockages. In addition, the study is expected to contribute indirectly to rational design and construction of roads in view of the landslide risks associated with fragile geology and concentrated precipitation in Nepal.

REFERENCES

Adhikary, T.L. 2001. Landslide control and stabilization measures for mountain roads: A case study of the Arniko highway, Central Nepal. In: Tianchi *et al*. (Editors), *Landslide Hazard Mitigation in the Hindu-Kush Himalayas*, ICIMOD, Kathmandu, Nepal.

Bhandary, N.P., Yatabe, R., Takahashi, J., Hasegawa, S., Kitagawa, R. & Otsuka, S. 2004. Major roadside slope failures along Kathmandu-Pokhara highway and Narayanghat-Mugling Highway in Nepal. *Proceedings of Second International Seminar on Disaster Mitigation in Nepal*, Organized by Nepal Engineering College, Nepal and Ehime University, Japan.

Chalise, S.R. 2001. An introduction to climate, hydrology, and landslide hazards in the Hindu Kush Himalayan region. In: Tianchi et al. (Editors), *Landslide Hazard Mitigation in the Hindu-Kush Himalayas*, ICIMOD, Kathmandu, Nepal.

Cruden, D.M. & Varnes, D.J. 1996. Landslide types and processes. In: *Landslides Investigations and Mitigation, Special Report 247*, Transportation Research Board, National Research Council, Washington D. C.

Dhital, M.R. 2003. Landslide hazard assessment in hill roads of Nepal. In: *Seminar Papers of International*

Seminar on Sustainable Slope Risk Management 2003 organized jointly by Department of Roads (DOR) and Permanent International Associations of Roads Congress (PIARC) in March 25–28, 2003, Kathmandu, Nepal.

Eto, M., Regmi, D.R. & Shrestha, P.M. 2003. Proposed slope disaster management procedure for strategic roads in Nepal. In: *Seminar Papers of International Seminar on Sustainable Slope Risk Management 2003* organized jointly by Department of Roads (DOR) and Permanent International Associations of Roads Congress (PIARC) in March 25–28, 2003, Kathmandu, Nepal.

Hungr, O., Evans, S.G., Bovis, M.J. & Hutchinson J.N. 2001. A review of the classification of landslides of flow types. *Environmental & Engineering Geoscience* III(3): 221–238.

Nepal Road Statistics (NRS) 2002. *Nepal Road Statistics 2002.* Department of Roads, His Majesty's Government of Nepal, Kathmandu, Nepal.

Pandey, M.R., Tandukar, R.P., Avouac, J.P., Vergne, J. & Heritier, T. 1999. Seismotectonics of the Nepal Himalaya from a local seismic network. *Journal of Asian Earth Sciences* 17: 703–712.

Regmi, S.R. & Sitaula, T.P. 2003. Krishna Bhir slide: A case study. In: *Seminar Papers of International Seminar on Sustainable Slope Risk Management* 2003 organized jointly by Department of Roads (DOR) and Permanent International Associations of Roads Congress (PIARC) in March 25–28, 2003, Kathmandu, Nepal.

Sharma, C.K. 1990. *Geology of Nepal Himalaya and adjacent countries.* Sangeeta Sharma, Kathmandu, Nepal.

Sunuwar, L., Karkee, M.B., Pokharel, G. & Lohani, T.N. 2005. Comparative study of seismic hazard of Kathmandu valley, Nepal with other seismic prone cities. *Paper submitted to 16th International Conference of International Society of Soil Mechanics and Geotechnical Engineering (16ICSMGE)* to be held in September 2005 in Osaka, Japan.

Thapa, K.B. 2001. Water-Induced disasters in the Himalaya: A case study of an extreme weather event in central Nepal. In: Tianchi *et al*. (Editors), *Landslide Hazard Mitigation in the Hindu-Kush Himalayas*, ICIMOD, Kathmandu, Nepal.

Upreti, B.N. 1999. An overview of stratigraphy and tectonics of the Nepal Himalaya. *Journal of Asian Earth Sciences* 17: 577–606.

Upreti, B.N. 2001. The physiography and geology of Nepal and their bearing on the landslide problem. In: Tianchi, L. et al. (Editors), *Landslide Hazard Mitigation in the Hindu-Kush Himalayas*, ICIMOD, Kathmandu, Nepal.

Wagley, K.P. 2003. Landslide and flood disaster appraisal. In: *Seminar Papers of International Seminar on Sustainable Slope Risk Management 2003* organized jointly by Department of Roads (DOR) and Permanent International Associations of Roads Congress (PIARC) in March 25–28, 2003, Kathmandu, Nepal.

Wieczorek, G.F. 1996. Landslide triggering mechanisms. In: Landslides Investigations and Mitigation, Special Report 247, Transportation Research Board, National Research Council, Washington D. C.

Landslide hazard reduction strategy and action in China

Y. Yin
China Geological Survey, Beijing, PR China

S. Wang
Institute of Geology and Geophysics, Chinese Academy of Sciences, Beijing, PR China

ABSTRACT: On the basis of a landslide survey that covered 700 counties of landslide-prone regions, the risk microzonation of landslide hazard is being conducted that will be a basic standard in legal management. A system of citizen monitoring and prevention against landslide hazards has been established from state to province, to county, to village. A weather-forecast-based warning system is running during rainy season combined with geologist and meteorologist advice. A warning TV program in CCTV and local TV shows are shown when landslide potential risk level is greater than 3(5 grades divided). A comprehensive loss reduction plan of landslide hazards is put into force on important infrastructures. Through the effect of risk management of landslide hazards, the rate of losses will be obviously decreasing during present years from above 1000 persons deaths and 10 billions RMB losses to below 300 persons by 2020, i.e., expected rate of losses will be reduced by 50%.

1 INTRODUCTION

China has conducted a large number of projects on landslide prevention during the IDNDR from 1990 to 2000 sponsored by United Nations, and the capability to disaster reduction is obviously rising. Within recent years, the warning system of geo-hazards covering the mainland of China is being established, in response to the International Strategy for Disaster Reduction (ISDR) from A/C. 2/54/L.44 resolution of UN.

1.1 *Nation-wide landslide investigation and risk zoning*

China suffers severe landslide hazards every year. Landslides threaten lives and property in near 30 provinces in the Nation, resulting in an estimated 800 to 1000 deaths and damage exceeding $100 billion RMB (Chinese Dollar) annually (Fig. 1). Although most landslide hazards occur during the rainy season, human activity is increasingly triggering hazards because of large scale construction activity over a wide area.

Since 1990, China has completed a mapping program of geo-hazards at scale of 1:500 000, that shows 55 000 landslides, 13 000 rockfalls and 17 000 mudflows. The map shows the location of landslides and the relations with geologic conditions, and delineates the landslide-prone area. The mapping program provides much information for province zoning of landslide prevention, and is applied to oil & gas pipelines, railways, hydro- power stations and other key projects.
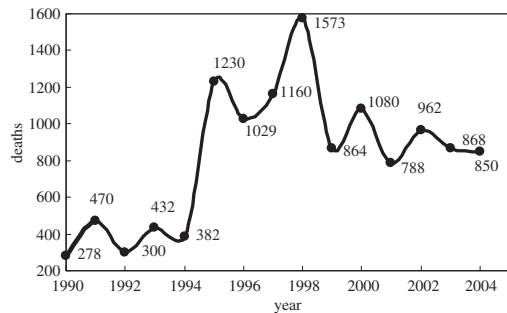

Figure 1. 1990–2004 landslide deaths in China.

More detailed mapping and risk zoning of landslides is ongoing since 1999 involving about 1000 landslide-prone counties. The key task of this investigation is to indicate the potential zones of landslides, to formulate emergency preparedness, and to establish warning systems. About 79 000 potential landslides are being probed, and 400 000 of landslide warnings are followed, in the framework of a complete monitoring system from state to province, to county, to village. The program brings together experts and citizens, mainly through citizen monitoring and prevention.

The successful rate of landslide prediction and warning is obviously rising in China since the mapping and risk zoning program has begun. In 2002, about 700 landslides were predicted and warned about and

this avoided 19 000 deaths; in 2003, 695 landslides were predicted and warned about and that avoided 29 600 deaths; and in 2004, 720 landslides were predicted and warned about that avoided 47 600 deaths.

2 STABILIZATION AND MITIGATION ON MAJOR LANDSLIDE HAZARDS

Since the IDNDR started in 1990, more than 200 major landslides have been stabilized that severely threatened cities, main courses of rivers, and key public facilities. The typical case is from Lianziya dangerous rockmass on the south bank of the Yangtze River in Zigui County, Hubei Province, facing to Xintan landslide across the Yangtze River, 27 km to the Three Gorges Dam site, where the hazard existed since 500 years ago and where navigation was once stopped for 82 years. It could cause a huge disaster if the dangerous rockmass fell into the Three Gorges Reservoir. A comprehensive measurement to control the rockmass has been applied, including pre-stressed cable anchoring, reinforced concrete filling, surface drainage, and a defensive buttress since 1992 (Fig. 2). The monitoring results show the stabilization is successful and prevents the rockmass from falling into the Three Gorges Reservoir.

The Three Gorges Hydraulic Project is the largest power plant in the world. The resettled population of the Three Gorges Reservoir of the Yangtze River is about 1.2 million. During the first period of the project from 1993 to 1997, 82 thousands of people were resettled, and 550 thousands were resettled during the second period project from 1997 to 2003, over 600 thousands are being resettled during the third period project by 2009. The population resettlement is a great challenge, since in the area of the reservoir flat land to suit construction is rare and landslide hazards are quite often encountered. Landslide hazards in the Three Gorges Reservoir could be divided into three periods: 1. the first period is before 1993, when the dam project began, mainly natural geologic hazards, of course, some caused by human activity; 2. the second period is from 1993 to 2003, geologic hazards mainly caused as toe-cut landslides and waste rock material storage; 3. the third period is after 2003, especially, from 2003 to 2009, geologic hazards will be caused by water level fluctuation, and during the third period, when over 600 thousands of people will be relocated, there will be a surge of geologic hazards. The third period of landslide hazards will extend to 2020. Many problems with landslides will have to be met, such as protection, remedy and utilization of landslide and rockfall deposits, "large-scale excavating and large-scale filling" for the construction and relocation. Since 2001, a systematic prevention project on landslides has been carried out at the Three Gorges Reservoir.
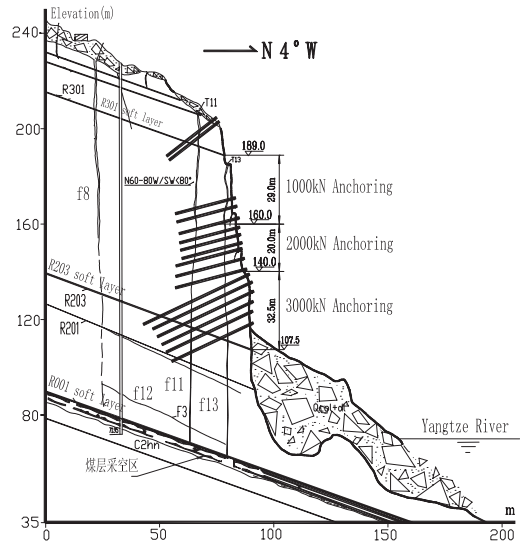

Figure 2.   Anchoring for Lianziya Danderous rockmass.

On April 9 of 2000, a high-speed gigantic landslide occurred in Yigong, Tibet, 2500 m wide and 2500 m long, 280–300 millions cubic meters in volume, that is the largest one in the world in recent time. It caused an ecologic catastrophe to Yaluzangbu River (Fig. 3). The Yigong landslide began to slide at 5200 m elevation and deposited at 2200 m elevation, lasted 10 minutes and the sliding distance is 8000 m. The huge landslide dam that occurred is 60–100 m thick. The landslide-dammed reservoir water level rose 2.37 m per day on average, and the max depth is 62 m. The reservoir stored 3 billions cubic meters of water, and the lake area expanded from 15 km^2 to 50 km^2. If no remedial action was taken, two month later, the lake would overflow and the dam would break out. 2000 persons who lived near the reservoir would be drowned and a severe ecologic catastrophe would occur in the lower reaches of the Yaluzangbu River. An emergency trench was excavated in the middle of the landslide dam to lower the water level as reducing the losses as much as possible. Within 33 days before the dam had broken out, 1.36 million cubic meters of landslide mass was removed and the water level was reduced 24.1 m.

On June 10, the dam burst and within several hours the water level decreased 40 to 50 m. In the lower reaches, the maximum current discharge was 120 000 cubic meters per second. No people died on the China side due to the successful warning and evacuation, but thousands of secondary landslides were triggered by the flooding. But unfortunately, on the India side, when the flood went through "Yaluzangbu Grand Canyon" and arrived at a plain, about 30 deaths, 100 lost, and 50 000 homeless were reported.
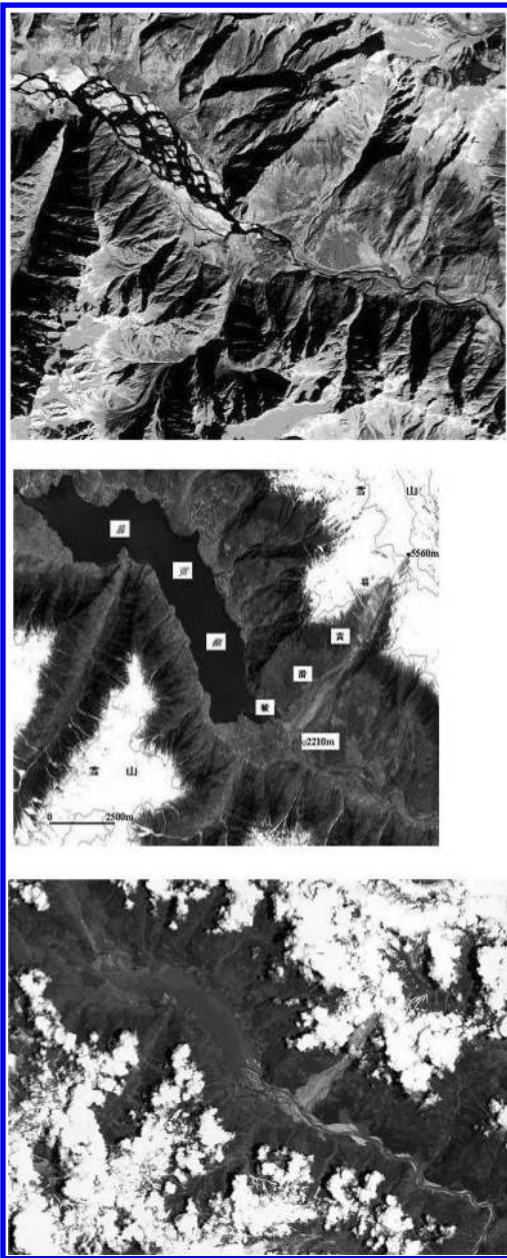
Figure 4. Land slide warning on CCTV.

Figure 3. Yigong landslide RS image showing from top to bottom: (a) Before landslide on 2000.4.9; (b) Landslide dammed the River; and (c) Landslide dam bursting.

3 WEATHER-BASED REGIONAL LANDSLIDE HAZARD WARNING

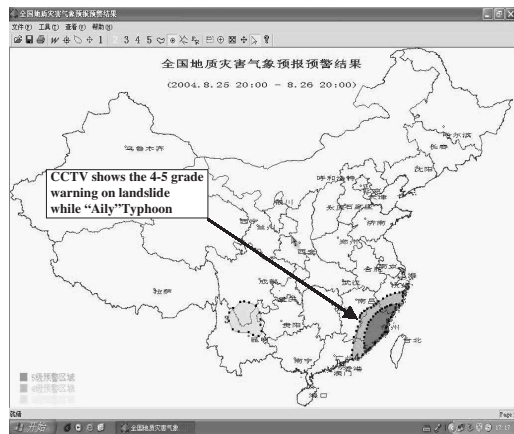In 2003, the Ministry of Land Resources (MLR) and China Meteorological Administration (CMA) signed a cooperative agreement on weather-based geo-hazards warning, by which during the rainy season every year, CMA provides rainfall data to MLR, and then MLR predicts the geo-hazard probability, and releases a warning grade to China Central Television (CCTV) so every citizen can know the landslide news around the clock on the TV program.

Following the same pattern, local cooperative agreements have also been signed. Landslide prevention is very obvious since the weather-based warning is combined with "citizen monitoring and prevention". According to incomplete statistics in 2004, 707 landslides were successfully predicted and warned about, 46 000 persons withdrew from the risk areas. On August 24 of 2004, MRL and CMA jointed to warn that 4–5 grade of landslide hazard would occur in the Zhejiang and Fujian Province coastal area during the "Aily" Typhoon coming on August 25–26. Two days later, the "Aily" brought 400–600 mm of heavy rainfall that triggered hundreds of landslides. No people were injured or died since tens of thousand of people removed from the risk zones of landslide in time, but 260 houses were destroyed.

4 GEO-HAZARD RISK ASSESSMENT REGARDING LAND USE

China is at the surge of engineering construction, especially, in the west mountainous areas, numbers of highway and railway projects are being built and urbanization exploded. That is inducing severe geo-hazards. According to statistical data, among landslide hazards, 60–70% is induced by ill-advised human construction activity. In 1999, Ministry of Land Resources issued an act on geo-hazard prevention administration which specified that geo-hazard risk assessment must be carried out for various

425

Table 1. Classification on importance of constructions.

Importance	Construction type
High	Developing zone; new site of town; key facilities; grade 2 or higher highway, railway, airport, major hydraulic power plant, thermal power plant, harbor, large water supplied field, industry and civil construction, etc.
Middle	New village; grade 3 or lower highway, middle hydraulic power plant, thermal power plant, harbor, mining area, water-supply field, industry and civil construction, garbage disposal site, etc.
Low	Small hydraulic power plant, thermal power plant, harbor, mining area, industry and civil construction, garbage disposal site, etc.

purposes of land use before the application of land use for construction. The assessment includes in (1) possible hazards induced or intensified by construction and (2) risk of hazards to engineering construction in nature.

The largest project on landslide risk assessment in China is concerned with a pipeline carrying natural gas from Xinjiang (the Western China) to Shanghai (the Eastern China). The pipeline, 4200 km long, extends across various complicated geologic and geomorphologic provinces that will limit the engineering construction and operation. The detailed landslide and other geo-hazards potential are zoned and that avoids major hazards.

5 MAIN ACTIONS RELATED TO LANDSLIDE HAZARD REDUCTION

Special teams have been established for survey, assessment, design, stabilization, and emergency response to landslides, and the administration system has been completed from state level to local, and is extending to village level in China since 1990's. A framework for landslide hazard reduction is suggested within next decade.

- A perfect system of laws and regulations, and technical standards will be set up by 2010, and in the main zones the landslide risk zoning is required on the national level by a mandatory rule. The human-induced landslide hazard will be restricted through rational construction and risk management. The hazard reduction strategy and planning for urbanization, Western boom-type development and mega-lifeline projects that will promote Chinese modernization processes must be specially formulated.
- Weather-based regional landslide warning will be completed in 31 provinces and about 1 000 landslide-prone counties. In the key regions, such as

the Three Gorges Reservoir, the GPS-based real-time monitoring system for landslides will be established. Since landslides are widely distributed in China and the landslide volumes are getting smaller and smaller, but hazard degree is more and more severe, the "citizen monitoring and prevention" is still a main and efficient way during the next decades.

- The ability of landslide emergency response teams nationwide is going to be improved and advanced professional teams are being established from state to local level. Development occurs of public awareness, training and education programs involving land use planning, design, landslide hazard curriculums, landslide hazard safety programs, and community risk reduction. The engineer is required to be trained to get the special qualifications needed for taking the geotechnical job in landslide-prone area.
- Landslide occurrence and losses is expected to reduce by 2020 so that death will be reduced by 70%, i.e., from 1000 deaths now to 300 deaths in the future, and expected losses will be reduced from 10 billions now to 5 billions Chinese dollars.
- On the basis of nationwide landslide investigation at the small or middle scale, the more detailed landslide survey will be carried out at large scale within next 5 years that covers the Sichuan-Yunnan, Qinlin-Dabashan and Hubei-Hunan landslide-prone zones where landslide hazards account for seventy-eighty per cent in total. The nationwide landslide hazard risk zoning will be carried out at large scale that can be applied to the risk management as mandatory technical standard.
- By 2010, the network of "citizen monitoring and prevention" will be perfected further and the professional monitoring system equipped with advanced and automatic technology will be established. The real-time monitoring and warning system of the key zones, such as the Three Gorges Reservoir will be completed while the water level rises up to the design level.

6 CONCLUSIONS

Landslide hazards prevention in China has been reviewed during the International Decade of Natural Disaster Reduction since 1990. Especially, with the economic rapid development in recent years, the landslide hazard is increasing. Several main problems have been addressed in the paper: nation-wide landslide investigation and risk zoning; stabilization and mitigation of major landslides; weather-based regional landslide hazard warning; geo-hazard risk assessment of land-use and main actions concerned with landslide hazard reduction.

Recent landslide disasters in China and lessons learned for landslide risk management

B.P. Wen
Department of Hydraulic Engineering, Tsinghua University, Beijing, China

Z.Y. Han
Institute of Hydrogeology and Engineering Geology Techniques, China Geological Survey, Baoding, Hebei

S.J. Wang, E.Z. Wang & J.M. Zhang
Department of Hydraulic Engineering, Tsinghua University, Beijing, China

ABSTRACT: Major characteristics of the fatal landslides in China between 2001 and 2004 were analyzed in terms of their distributions, sizes, prone materials, and triggering factors. Destructiveness of these landslides was estimated in terms of disaster intensity on the basis of their fatalities. It was found that overall characteristics of the landslides were very similar to those of the landslides before 2001. Of different types of the landslides, both their characteristics and destructiveness were much different. It was further found that the areas often affected by the landslides had different vulnerabilities to the disasters. Accordingly, lessons learnt from the fatal landslides in the last four years were advised with respect to landslide risk management in China.

1 INSTRUCTIONS

In China, landslide disasters are widespread and occur most frequently because of its vast mountainous areas and hilly terrains, which are about 69% of the total land area, a wide range of physical conditions, and intense construction activities. It was estimated that at least 10 million people in China are exposed to landslide risk, and landslides result in more than 500 deaths and missing each year (DGEM 2003). Since 2001, more than 400 fatal landslide events have been reported (MLR 2002, 2003, 2004, CIGEM 2005). These fatal landslides caused at least 3000 people dead and missing, and more than $100 billions in property damage (MLR 2002, 2003, 2004, CIGEM 2005).

Based on the classification system proposed by Varnes (1978), the fatal landslides in China can be divided into four types of slope movements: slide, fall, debris flow, and slide-debris flow or slide flow. On the other hand, these fatal landslide events can also be classified into single and regional events in terms of their occurrence nature, the latter of which is composed of a cluster of individual slides, falls, debris flows, and slide-flows (shortened as S-F-DF/R in the figures below). This paper described preliminary analyses on major characteristics of the fatal landslide disasters in China between 2001 and 2004 based on factual data of 147 fatal landslide events, which were relatively well-documented in varying sources. The 147 fatal events include 75 single slides, 21 falls, 7 slide-debris flows and 39 regional landslides, total of which caused 1632 people dead and missing. Subsequently, disaster risk of each type of the landslides was estimated in terms of disaster intensity, and lessons learnt from these fatal events were advised. Data of the 147 fatal events were collected mainly from four sources available: (a) a series of open-file reports of communiqués on geo-environment in China (MLR 2002, 2003, 2004), and annual report on geological disasters in China (CIGEM 2005); (b) open-file reports on geological disasters in some provinces, e.g., YCGEM (2002, 2003, 2004, 2005), HCGEM (2002, 2003, 2004), and SCGEM (2002, 2003, 2004); (c) site inspection reports of some severe fatal events by individual researchers and institutions, e.g., Yin (2001), Xu et al. (2004), Yang & Zhao (2003), Liu & Tang (2002); and (d) online rainfall data reported by China Meteorological Administrations (CMA 2004). Although substantial number of the fatal events between 2001 and 2004 has not been collected due to various reasons, complete records of the fatal events causing more 10 people dead or missing were included in this study.

2 MAJOR CHARACTERISTICS OF THE FATAL LANDSLIDES

2.1 *Spatial distribution*

Fatal landslides between 2001 and 2004 are largely concentrated in the mountainous areas of south-western China and hilly terrains of the south, infrequently in the northwest, and dispersedly in other mountainous areas and hilly terrains (Figs. 1–2).

Of the provinces affected by the fatal landslides, Chongqing, Sichuan, Yunnan and Hunan suffered the disasters most frequently, followed by Guizhou, Guangxi, Hubei, Shannxi, Guangdong, Fujian, Zhejiang, Xinjiang, and Gansu (Figs. 1–2). Distribution pattern of the recent fatal landslides showed little difference from that of the landslides before 2001 (DGEM 2003). Extensive studies have found that landform configuration of China controls distribution of landslides (Duan et al. 1993, DGEM 2003), which shows three distinctive steps from eastern to western China with various gradients, relief of mountains and rolling hills. The mountainous regions and hilly terrains between the second and first steps, where the southwestern, southern and northwestern western China are located, are steepest and most rugged in China. Thus, these areas are most prone to landslides.

Of the common types of the fatal landslides in China, slides were the most widespread, which were about 51% of total fatal landslides in the last four years, while debris flows (5%) and slide flows (3%) were relatively sparse (Fig. 3). With respect to landslide occurrence, the single fatal events occurred much more frequent than the regional events (Fig. 3). Both the single and regional events were very prevalent in southwestern and southern China, whereas the regional events rarely occurred in the other parts of China.

2.2 *Seasonal distribution*

Overall, monthly distribution of the fatal landslides showed a bell-shaped pattern, with the greatest frequency in July, the least in the months of dry seasons (Fig. 4). Accordingly, more than 75% of total landslides occurred in summer season between May and September in the last four years, the rainy season in China. Again, seasonal distribution pattern of the fatal landslides was similar with that of the landslides in the past (Wen 1994) showing close association with the rainfall patterns in landslide prone areas of China (Wen 1994). However, variation of monthly frequency of each type of the fatal landslides was different (Fig. 4). Present data showed that the regional landslide events only concentrated in the rainy season, and hardly occurred in other seasons, whereas frequencies of the single slides in March, and falls in December were significantly high, and even higher than those in some months of the rainy season. This is probably associated with their different sensitivities to rainfall. It is suspected that to some extent, deterioration of slope stability by rainfall in rainy season should have been responsible for high frequencies of the fatal slides and falls in post rainy seasons. For example, the areas of two catastrophic falls in December 2004 at Nayong of Guizhou and Yongtai of Zhejiang, which caused 44 and 7 deaths, respectively, suffered abnormally intense rainstorms in the rainy season (116 mm/24 hrs in early September in Nayong, 916 mm/36 hrs in middle August in Yongtai) with return periods of 50 and 100 years, respectively.

2.3 *Landslide sizes and materials*

Present data showed that for all types of the fatal landslides between 2001 and 2004 in China, small size landslides with volume less than $10^4 m^3$ were the most frequent, medium size landslides with volume of between 10^4 and $10^6 m^3$ were much less common, whereas the large and giant landslides, with volume greater than $10^6 m^3$, were the most infrequent (Fig. 5). Only two giant fatal landslides moved in form of slide in 2003 and 2004, respectively, and few debris flows and regional landslides were large than $10^6 m^3$. In addition, 80% of the fatal slides were shallower than 3 m, only 3% of the slides were deeper than 10 m (Fig. 6). Moreover, it was noted that all the deep-seated fatal landslides (deeper than 10 m) were larger than $2 \times 10^5 m^3$.

In terms of the materials involved, the fatal landslides in the last four years were often found in four types of soils and three types of rocks: colluviums and residual soils (C + R), loess (Loe), alluvium (Al), artificial fill (fill); sandstone and mudstone (S + M), limestone (L), and gneiss and marble (Gn + Ma). A few fatal landslides were also seen in other types of rocks, e.g., granite and basalt. Generally, the soil type landslides (62%) were more often than the rock type (38%) (Fig. 7). Among the seven types of landslide materials, colluvium and residual soils, which were mainly derived from granite, sandstone and mudstone in the landslide prone areas, were most prone to all types of the fatal landslides, except the falls (Fig. 7). The falls occurred more common in rocks than in soils, particularly, the rocks of sandstone and mudstone, and limestone. This may be probably due to both the widest exposure of these rocks in the landslide prone areas, compared with other types of rocks, and generally much steeper occurrence of the slopes comprising these rocks. Notably, the two giant landslides were found in the rocks of sandstone and mudstone.

2.4 *Triggering factors of the landslides*

Corresponding to their seasonal distribution (Fig. 4), the greatest abundance of the fatal landslides (70%)
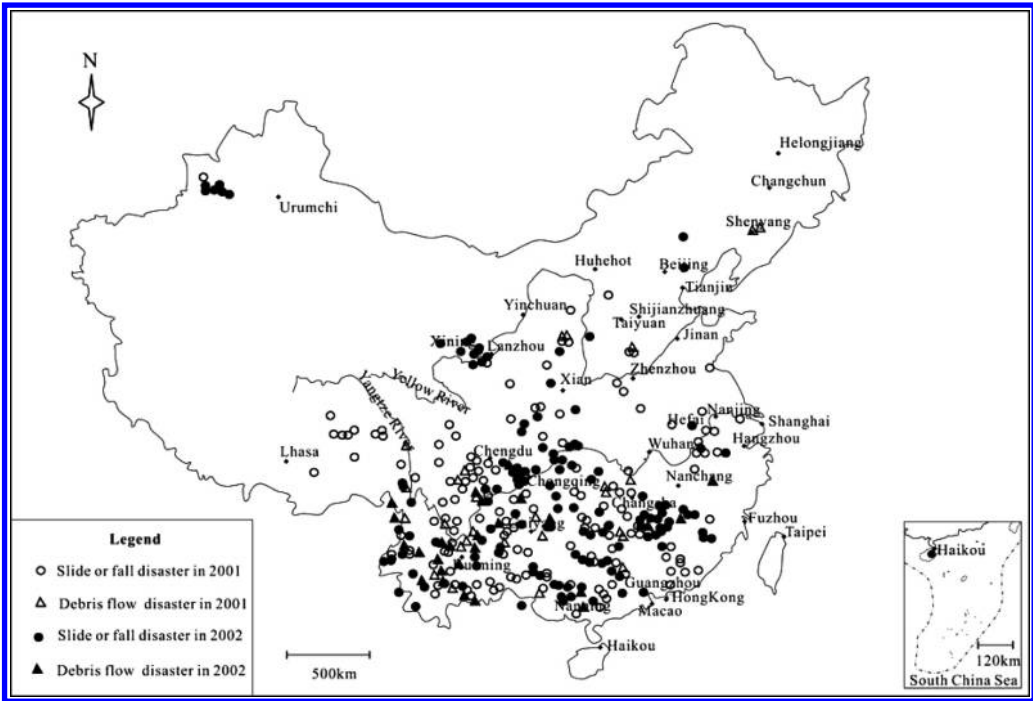
428

Figure 1. Distribution of the fatal landslides in China between 2001 and 2002 (after MLS 2002, 2003).
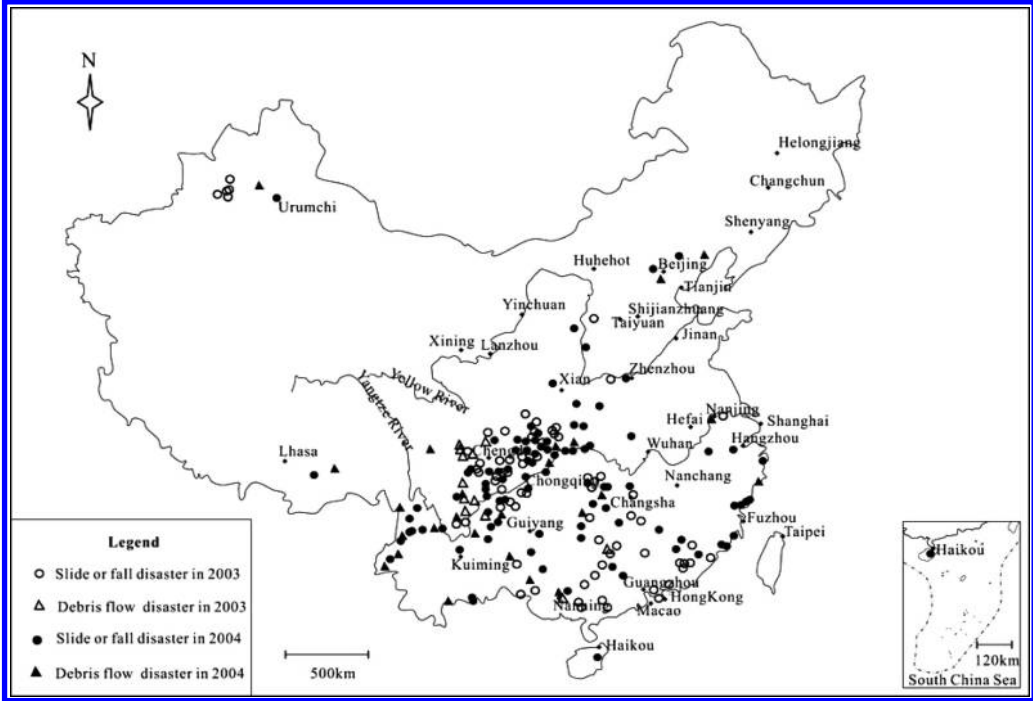

Figure 2. Distribution of the fatal landslides in China between 2003 and 2004 (after MLS 2004, CIGEM 2005).
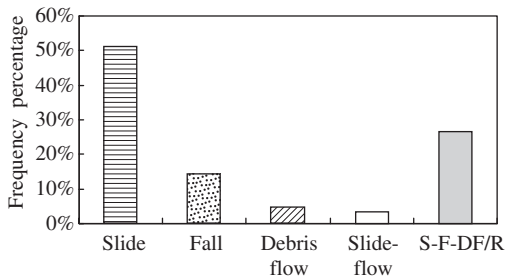
429

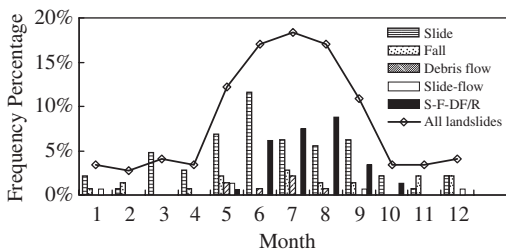Figure 3. Frequency variations of the landslide types.
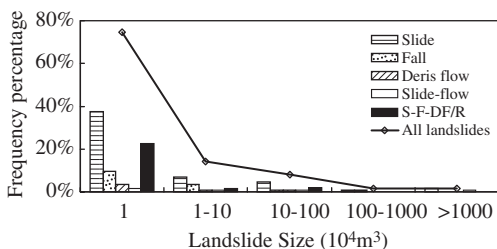

Figure 4. Monthly distribution of the landslides.

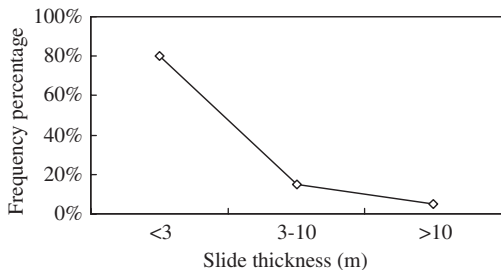Figure 5. Size distribution of the landslides.

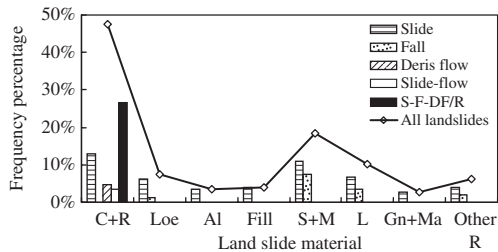Figure 6. Thickness variation of all slides.

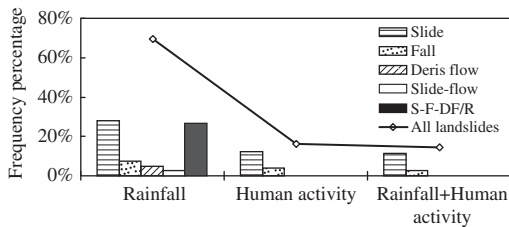Figure 7. Landslide frequency in different materials.

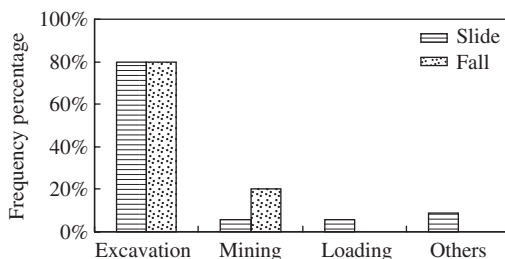Figure 8. Frequency variation of the landslides triggered by different factors.

Figure 9. Frequency of the slides and falls triggered by different types of human activities.

was triggered by varying rainfalls (Fig. 8), which were mostly resulted from monsoon and hurricane in summer season in the landslide prone areas. Besides, about 17% of the landslides were induced by various types of human activities, and 13% of them were associated with both rainfall and human activities. However, present data showed that the fatal debris flows, slide-flows and the regional landslides seemed to be mainly associated with rainfall (Fig. 8). Of various human activities in landslide prone areas, excavation induced most frequently the fatal slides and falls, followed by mining, improper loading (Fig. 9).

On the other hand, rainfall intensity inducing the fatal landslides varied greatly, ranging from extremely intense rainstorm of 35 mm in 30 minutes to prolonged rainfall of 160 mm in 10 days (Fig. 10). The data available showed that there was no identifiable correlation between the rainfall intensity and the landslide occurrence in the last four years (Fig. 10), and also between the rainfall intensity and the landslide sizes (Fig. 11). This should be attributed to great variation of the landslide materials and their properties, slope topography, complex occurrence of water
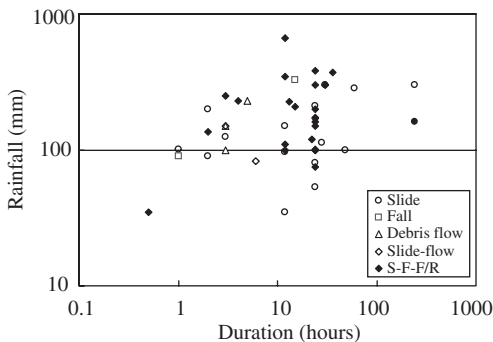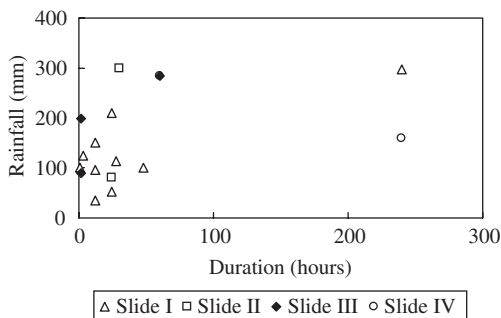
430

Figure 10. Rainfall intensities of the landslides.

Figure 11. Rainfall intensities of the slides of different sizes. (Slide I refers to that less than $10^4 m^3$; slide II denotes that of 10^4–$10^5 m^3$; slide III indicates that of 10^5–$10^6 m^3$; and slide IV is that larger than $10^7 m^3$).

within landslides, as well as many other conditions in the vast landslide prone areas of China. Although the authors have no attempt to establish any relationship between the rainfall intensity and the landslides in China, when comparing the common types of the fatal landslides between 2001 and 2004, it is noted that: (a) the debris flows and slide-debris flows seemed to be most sensitive to the intense rainstorm between 83 mm in 3 hours and 228 mm in 6 hours; (b) the regional landslides appeared to be susceptible to a wider range of rainstorm between 35 mm in 30 minutes and 661 mm in 36 hours; and (c) occurrence of the slides seemed to be associated with the widest range of rainfall intensity between 100 mm in 1 hour and 160 mm in 10 days, particularly the prolonged rainfall lasted for more than one day. This implies that there may be certain ranges of rainfall intensity for different types of landslides. Certainly, sensitivity of each type of the landslides to rainfall intensity is related not only to their failure mechanisms, but also to many other factors, e.g., sizes, materials properties, slope topography, deterioration degree of the slope

before failure, etc. It is thus a very difficult task to define reasonable thresholds of rainfall intensity for landslides.

3 DESTRUCTIVENESS OF THE LANDSLIDES DISASTERS

Present data showed that in the landslide prone areas of China, rural areas (RA), urban areas (UA), various construction sites (CS) (e.g., highway, building and railways), roadways (Rd), mining areas (MA), and quarries were often hit by the fatal landslides. Of these areas, rural areas were affected most frequently by most types of the landslides, particularly the regional landslides, which were only seen in the rural areas (Fig. 12). But, the falls most often hit various roadways. To some extent, this gives an indication that rural areas are most vulnerable to landslides, followed by the roadways and construction sites.

Same as other kinds of disasters in the earth, loss of life is also the severest and most direct consequence among landslide damages. Fatality is thus considered as one of the most important proxies for measuring consequence of landslide disasters. In terms of total fatalities caused by each type of the landslides, more than 50% of them were caused by the regional landslides, about 30% were resulted from the slides, and about 10% were from the falls, whereas less than 10% were the consequence of the debris flows and slide-debris flows (Fig. 13). Fatality distribution of each type of the landslides was different from their abundance distribution, particularly the regional landslides and slides (Fig. 3), indicating that destructiveness of each type of the landslides was different.

To evaluate destructiveness of the fatal landslides in China between 2001 and 2004 in terms of their fatalities, disaster intensity or landslide intensity (Latter 1967) is employed, which has been widely adopted for evaluating landslide risk levels (Fell & Hartford 1997, Evans 1997, Guzzetti 2000). Disaster intensity (DI) is defined as landslide fatality normalized by its frequency. Considering incomplete data of the landslides causing people death and missing less than 10 in this study, overall disaster intensity of the landslides in China in the last four years was less than 11.1, the disaster intensity of the landslides causing more than 10 fatalities was 24.1. With respect to disaster intensity of each type of the landslides, the regional landslides were the most destructive (DI = 20.6), followed by the debris flows (DI = 14.4), slide-debris flow (DI = 7.8), whereas the falls (DI = 7.3) and slides (DI = 7.1) were the much less destructive (Fig. 14). Evidently, the differences of disaster intensities among each type of the landslides were related to many factors and their combinations, particularly their movement velocity, sizes and the areas affected.
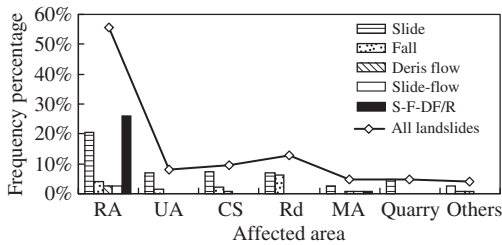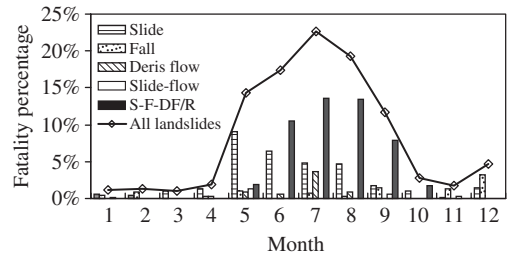
431

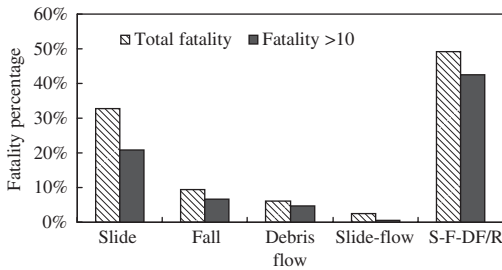Figure 12. Landslide frequency in different areas.

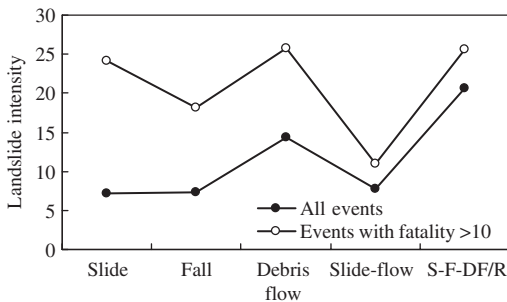Figure 13. Fatality distribution with respect to landslide types.

Figure 14. Disaster intensity variation of the landslides.

Because cluster occurrence of the regional landslides, and generally fast-moving nature of debris flows and slide-debris flows, their disaster intensities were greater than the slides and falls. Less destructiveness of the fatal slides and falls may be associated with their overwhelming occurrence in small sizes. Moreover, although the falls were also fast moving landslides, the areas most often hit by the fall, i.e., the roadways, were generally sparsely populated, the falls were therefore less destructive than other types of the fast moving landslides, i.e., the debris flows and slide-debris flows. When considering the disaster intensity of the landslides causing massive fatalities, say more than 10 people dead and missing, the debris flows was the most destructive (DI = 25.7), followed by the regional landslides (DI = 25.6), slides (DI = 24.1),

Figure 15. Monthly distribution of the landslide fatalities.

falls (DI = 18.2), and the slide-debris flows (DI = 11) (Fig. 14). The reasons leading to variation of the disaster intensity of different landslide types with massive fatalities should be similar to those for overall disaster intensity of these landslides. Additionally, it was found that monthly variations of the landslides' fatalities were about consistent with the monthly distribution of the landslides' abundances, showing that summer was the most destructive season for most landslides. However, December was the most destructive month for the fatal falls (Fig. 15).

4 LESSONS LEARNT FOR LANDSLIDE RISK MANAGEMENT

Reducing disaster fatalities as low as possible is always the most important purpose of landslide risk management at all levels, and is also the primary aim of studying the disasters from all aspects. Based on the characteristics of the fatal landslides in China between 2001 and 2004, and their destructive nature, several lessons could be learnt from these disasters. These lessons should be greatly helpful for landslide risk management in China in the future, and may be also helpful for the disaster risk management elsewhere in the world.

Although the landslides induced by rainfall were inevitable, at least 20% of the total landslide fatalities should have been reduced if there had been no improper human activities in the landslide prone areas, or sufficient preparedness measures for possible landslides had been made before construction activities on the slope susceptible to landslides. Slope protection in residential areas, construction sites, roadways, quarries and mining areas should be one of the most effective strategies in reducing landslide fatalities.

As realizing the abundance and destructiveness of the rainfall-induced landslides, China has launched a national-wide early warning system of landslide disaster during rainy season since June of 2003. The warning was issued based on rainfall intensity thresholds

432

defined for general landslides in the landslide prone areas. The authors believe that the system would have been more effective and applicable if the rainfall thresholds had been defined considering landslide types, since each type has different sensitivity to rainfall, including single landslide event and the regional events. Hence, the rainfall thresholds for the early warning system should be refined in the future.

Considering deterioration of slope stability by rainfall, great attention should be also paid to the landslide prone areas that suffer abnormally intense rainfall during summer after summer season. Single slides and falls are apt to occur then.

If the vulnerability to landslide disasters in rural areas of China had been lowered, the disaster fatalities would have been substantially reduced. Thus, there is an urgent need to strengthen the resistance to landslide disasters in these rural areas by implementing preparedness countermeasures.

5   CONCLUSIONS

Of the fatal landslides in China between 2001 and 2004, four types of slope movement, slides, falls, debris flows, and slide-debris flows commonly occurred with different frequencies. In addition, both single and regional landslide events, the latter being a cluster of individual landslides of different types, were frequent. Major characteristics of the fatal landslides showed: (a) much greater abundance in the southwestern and southern China than in the other parts of China; (b) the most frequent occurrence in summer season between May and September; (c) an overwhelming occurrence in small sizes (less than $10^4 \, m^3$); (d) colluvium and residual soils, and the rocks of sandstone and mudstone are the most susceptible materials; and (e) the landslides were often induced by rainfall and human activities, particularly the former. However, characteristics of each type of the landslides were different, showing that: (a) the slides were favorable to the widest ranges of the disaster prone conditions in every aspect; (b) the falls were more often seen post summer and more susceptible to various rocks; (c) the debris flows and regional landslides rarely occurred in non-summer seasons, and more abundance in small sizes. In terms of relationship between rainfall intensity and the landslide occurrences, there seemed certain rainfall intensity ranges for different types of the landslides. With respect to vulnerability to the landslide disasters among the areas often affected, the rural areas were the most vulnerable, followed by the roadways, construction sites, quarries, mining and urban areas. In light of the disaster intensity, defined as fatalities per landslide event, the regional landslides were the most destructive, then the debris flows, slide-debris flows, falls and slides. For the landslides resulting in massive fatalities (fatality > 10), the debris flows were the most destructive. On the basis of characteristics of the fatal landslides and their destructiveness, at least four lessons could be learnt for landslide risk management in China, including those from human activities, slope protection, refinement of landslide warning system and disaster preparedness in the rural areas.

REFERENCES

China Institute of Geo-Environment Monitoring (CIGEM), Ministry of Land and Resources (MLS) 2005. Open file report: *Preliminary annual report on Geological disasters in China in 2004.*

China Meteorological Administration (CMA) 2004. Historical rainfall data. In: www.tq121.com.cn and www.t7online.com.

Department of Geo-Environmental Management (DGEM), Ministry of Land Resources 2003. *Geological hazards and their control in China.* Beijing: Geological publishing house.

Duan, Y.H., Luo, Y.H. & Liu, Y. 1993. *Geological hazards in China.* Beijing: Architectural Press of China.

Evans, S.G. 1997. Fatal landslides and landslide risk in Canada. In: Cruden & Fell (eds.), *Landslide risk assessment.* Balkema, Rotterdam, 185–196.

Fell, R. & Hartford, D. 1997. Landslide risk management. In: Cruden & Fell (eds.), *Landslide risk assessment.* Balkema, Rotterdam, 51–109.

Guzzetti, F. 2000. Landslide fatalities and evaluation of landslide risk in Italy. *Engineering Geology* 58: 89–107.

Hunan Center of Geo-Environment Monitoring (HCGEM) 2002. Open file report: *Annual report on geological disasters in Hunan province in 2001.*

Hunan Center of Geo-Environment Monitoring (HCGEM) 2003. Open file report: *Annual report on geological disasters in Hunan province in 2002.*

Hunan Center of Geo-Environment Monitoring (HCGEM) 2004. Open file report: *Annual report on geological disasters in Hunan province in 2003.*

Latter, J.H. 1967. Natural disasters. *Advancement of Science* 23: 362–380.

Liu, Y.F. & Tang, D.M. 2002. Some thoughts about flood and landslide disasters in Ankang, Shaanxi. *Shaanxi Hydro & Power* 4: 1–6.

Ministry of Land and Resources (MLS) 2002. Open file report: *Communiqué of Geo-Environment in China in 2001.*

Ministry of Land and Resources (MLS) 2003. Open file report: *Communiqué of Geo-Environment in China in 2002.*

Ministry of Land and Resources (MLS) 2004. Open file report: *Communiqué of Geo-Environment in China in 2003.*

Sichuan Center of Geo-Environment Monitoring (SCGEM) 2002. Open-file report: *Annual report on Geological Disasters in Sichuan province in 2001*.

Sichuan Center of Geo-Environment Monitoring (SCGEM) 2003. Open-file report: *Annual report on Geological Disasters in Sichuan province in 2002*.

Sichuan Center of Geo-Environment Monitoring (SCGEM) 2004. Open-file report: *Annual report on Geological Disasters in Sichuan province in 2003*.

Varnes, D.J. 1978. Slope movement types and processes. *In: Landslides, Analysis and Control. National Academy of Sciences, National Research Council, Washington, DC., Special Report* 176:11–33.

Wen, B.P. 1994. The feature of landslide, rockfall and debris flow in China. In: *Proceedings of 7th International Congress of International Association of Engineering Geology*. Rotterdam: Balkema. 1459–1464.

Xu, Y.N., Cao, W.H., Zhou, X.F. & Wang, L. 2004. Flood and landslide disasters and their countermeasures. *Hunan Hydro and Power* 4: 15–21.

Yang, S.Q. & Zhao, S.H. 2003. Flood and landslide disaster mitigation: a case study of flood and landslide disasters in Suining, Hunan. *Hunan Hydro and Power* 2: 7–12.

Yin, Y.P. 2001. Inspection of disastrous landslide in Wulong, Chongqing in May of 2001. In: CIGEM, *Open file reports on geological disasters of China*.

Yunnan Center of Geo-Environment Monitoring (YCGEM), 2002. Open file report: *Preparedness on the strategies against geological disaster in Yunnan in 2001*.

Yunnan Center of Geo-Environment Monitoring (YCGEM) 2003. Open file report: *Preparedness on the strategies against geological disaster in Yunnan in 2002*.

Yunnan Center of Geo-Environment Monitoring (YCGEM) 2004. Open file report: *Preparedness on the strategies against geological disaster in Yunnan in 2003*.

Yunnan Center of Geo-Environment Monitoring (YCGEM) 2005. Open file report: *Geological disasters in western Yunana in 2004*.

Case histories: hazard characterization

Landslides in the Thompson River valley between Ashcroft and Spences Bridge, British Columbia

A. Eshraghian, C.D. Martin & D.M. Cruden
Dept. Civil & Environmental Engineering, University of Alberta, Edmonton, Alberta, Canada

ABSTRACT: Eight large landslides have occurred along 10 kilometres of the Thompson River valley between the communities of Ashcroft and Spences Bridge in south-central British Columbia, Canada since 1880. The Thompson River flows south through the Thompson Plateau, part of the Interior Plateau of British Columbia. The river has cut down through 120 metres of glacial sediments during the Holocene. Eight units have been distinguished in these Quaternary sediments that fill the Thompson Valley. Unit 2, which may be as much as a million years old, consists of up to 45 metres of rhythmically bedded silt and clay glaciolacustrine sediments. The highly plastic, overconsolidated clays within this unit are believed to contain substantial portions of the rupture surfaces of seven of the landslides. These landslides are now reactivated, retrogressive, multiple, slow to extremely slow, translational earth slides. Most of the recorded slide movements happen in the late summer and early fall. The Ashcroft area, with about 200 mm precipitation per year, has a semi arid climate. In the past, irrigation of the river terraces has been thought to trigger slope movements. The movement rates appear to respond to drops in the level of the Thompson River after high flows and perhaps to rainfall. This paper synthesizes previous individual site investigations into a single geographic information system. The results of current investigations are being added. This synthesis has facilitated the identification of both the triggers and stratigraphy common to the seven landslides.

1 INTRODUCTION

Thompson River valley is a vital section of the strategic national transportation corridor that runs through southern British Columbia. Main rail lines of the Canadian Pacific Railway (CPR), completed in 1885, and the Canadian National Railway (CN), completed about 30 years later, are located in this corridor (Clague & Evans 2003). The study area is located between Ashcroft town and Spences Bridge (50° 10′ to 50° 20′ N and 121° 15′ to 121° 20′ W) just south of Ashcroft town. This area has a history of landsliding which has created problems for both CPR and CN. When the landslides were rapid, they blocked the river, disrupted rail traffic and caused fatalities. When they move slowly, the rails need repairing every few years. Some of the slides created short-lived upstream reservoirs. Figure 1 shows the locations and names of the landslides in Thompson River valley. Table 1 gives the areas and volumes of few of the landslides in this area.

The slides in this area are retrogressive, translational earthslides which have been moving very slowly since the first time sliding happened. According to Christiansen & Sauer (1984) retrogressive landslides in the Canadian Great Plains occur mainly in overconsolidated marine, Upper Cretaceous clay shales or in normally consolidated Quaternary glacial lake sediments. In this case they are moving on a rhythmically bedded silt and high plastic clay layer.

2 GEOLOGY OF THE ASHCROFT AREA

The Ashcroft area is part of the Thompson Plateau, a subdivision of the Interior Plateau. It is characterized by rolling uplands separated from each other by deep valleys. The Thompson River flows south and has down cut through thick glacial sediments and is relatively immature (Porter et al. 2002).

Most of the Quaternary landforms and surficial materials can be related to the last glaciation and thus late-Pleistocene. A variety of Quaternary sediments occur in the area, especially within the major valleys where a deep valley fill has been dissected and terraced by postglacial down-cutting of the trunk rivers (Duffell & McTaggart 1952).

The landslides occurred in a 10-km reach of Thompson valley, within a thick Quaternary valley fill dominated by glaciolacustrine sediments. Failure occurred on the steep walls of an inner valley that formed during the Holocene when Quaternary sediments filling the broader Thompson River valley
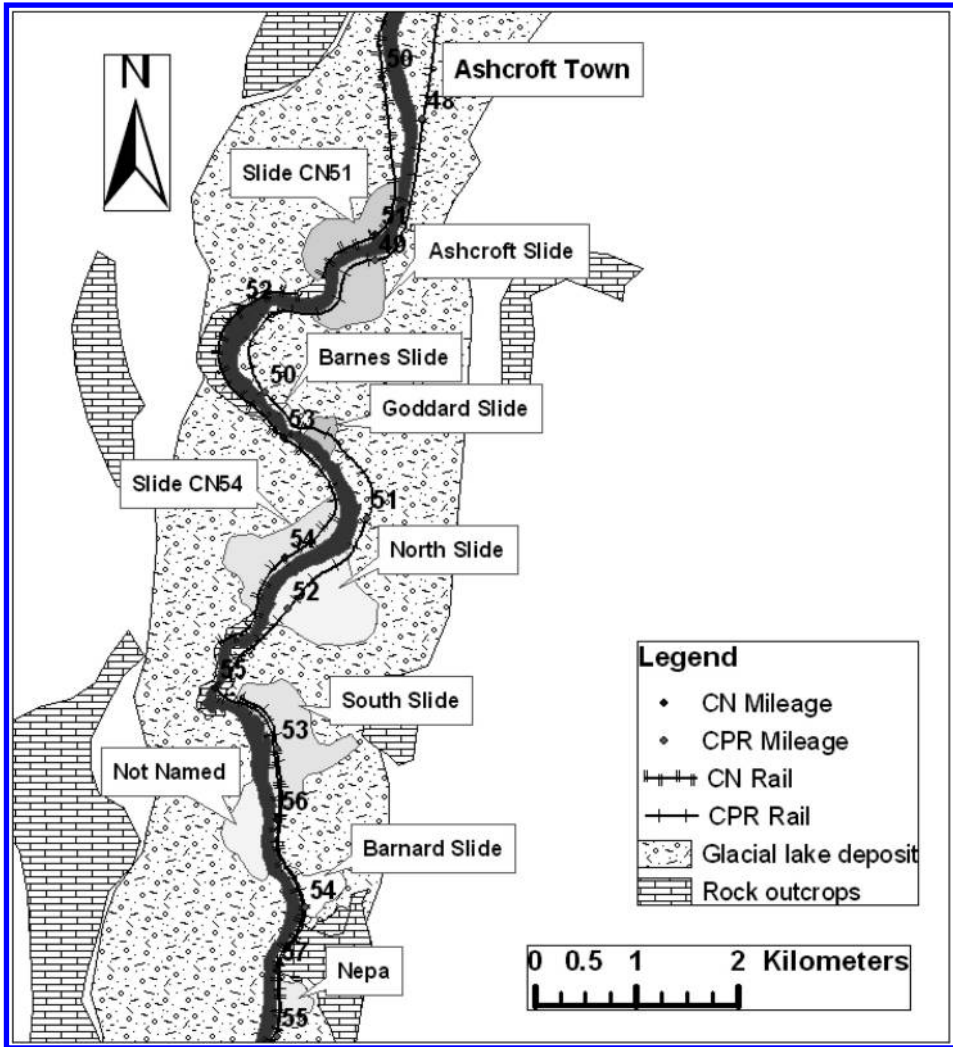
Figure 1. Landslides in the area south of Ashcroft, BC, between 50° 10′ to 50° 20′ N and 121° 15′ to 121° 20′ W. (Slide CN51, Goddard Slide, North Slide, South Slide, and Nepa Slide are discussed in this paper).

Table 1. Volumes and areas of four of the landslides in the Ashcroft area.

Slide name	Area × 10⁴ (m²)	Volume × 10⁶ (m³)
Slide CN51	15.06	3.27
Goddard	9.71	1.95
North slide	58.67	21.36
South slide	27.46	9.03

were incised. The valley fill sequence consists dominantly of permeable sediments, the exception being a unit of rhythmically bedded silt and clay near the base of the Pleistocene sequence (Clague & Evans 2003).

Hodge & Freeze (1977) and also Clague & Evans (2003) mentioned that groundwater flow systems in southern British Columbia show the possibility of generation of high pore pressures in less permeable sediments in discharge zones at the base of terraces underlain by a succession of Pleistocene deposits similar to that in Thompson Valley at Ashcroft.

2.1 Surficial geology of the study area

The surficial materials in the area are tills, fluvial, fluvioglacial, lacustrine and colluvium deposits. The surficial geology map is produced by Geological Survey of Canada (Ryder 1976).

438

Surficial till dates from the last glaciation (Armstrong et al. 1965). Most of the areas mapped as drift (between Ashcroft and the Ashcroft Slide and also beside the Goddard Slide) are probably till, but may include small areas of fluvioglacial gravels, glaciolacustrine sediments, and recent alluvium (Ryder 1976).

2.2 *Quaternary history of the Ashcroft area*

Most of the Quaternary landforms and surficial materials of the Ashcroft map-area can be related to the last Fraser Glaciation (Armstrong et al. 1965). Ice covered all but the highest peaks of the Coast Mountains in the area and generally flowed from the east and west into the Thompson Valley. In the Thompson River Valley ice flow was from north to south. Deglaciation occurred by the thinning and stagnation of ice over most of the Ashcroft area. Several phases of deglaciation may be identified, each represented by characteristic landforms and surficial deposits (Fulton 1969).

Johnsen & Brennand (2004) distinguished development of two late-glacial, ice-dammed lakes within the Thompson Basin: Glacial Lake Thompson and Glacial Lake Deadman. The lakes were narrow (width to length ratio of ~3:100). Glacial Lake Thompson was 140 m deep and Glacial Lake Deadman about 50 m. They had higher elevations at Ashcroft and lower elevation near Spences Bridge with tilting about 1.7 m/km. According to Johnsen & Brennand (2004), these lakes were more extensive than previously thought and they lengthened and lowered as ice decayed. There was an ice dam south of Spences Bridge. Also they estimated the lake bottom at approximate elevation 420 m asl. (Johnsen & Brennand 2004).

Figure 1 shows the extent of the highest terrace of the Thompson (at 420 m asl.) which is perhaps formed by the bottom of glacial lake Deadman (glacial lake deposit in Fig. 1). Fulton (1969), Ryder (1976), Clague & Evans (2003) and Johnsen & Brennand (2004) described the glacial history of the area in more detail.

2.3 *Geological units*

The Quaternary sediment fill in Thompson Valley near Ashcroft consists of deposits of three glaciations. Figure 2 shows the Quaternary sediments of the valley similar to one produced by Clague & Evans (2003). The elevations of the boundaries between the units are the elevations found in the boreholes in Slide CN51 near Ashcroft (see Figure 1 for location). The sediment boundaries should have tilts similar to the Glacial Lakes (1.7 m/km) so the boundary elevations in the other slides can be lower than shown in Figure 2.
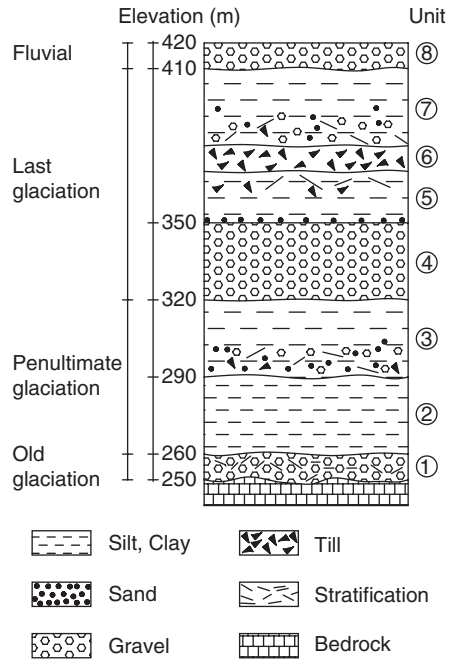
Figure 2. Stratigraphy of Quaternary sediment fill in Thompson River Valley at Ashcroft and their approximate elevations.

The three glacial sequences are separated by unconformities produced by erosion and mass wasting during intervening interglaciations. The oldest exposed sediments are cemented, oxidized, folded and faulted sand and gravel with minor lenses of diamicton (unit 1, Fig. 2). These sediments are interpreted by Clague & Evans (2003) to be ice-contact materials, deposited against decaying masses of glacier ice at the end of a Pleistocene glaciation but their age is uncertain (Clague & Evans 2003).

At sites south of Ashcroft, the till and the oxidized sand and gravel are overlain by rhythmically bedded silt and clay of lacustrine or glaciolacustrine origin (unit 2 in Fig. 2). Figure 3 shows the silt-clay layer at the toe of the Goddard Slide. The darker layers in the picture have more clay content. It is up to 45 m thick and consists of silt and clay couplets, ranging from less than 1 cm to several tens of centimetres thick. Previous study of the samples from this layer suggested that these sediments are at least several hundred thousand years old and thus of Middle or Early Pleistocene age (Clague & Evans 2003).

A second glacial sequence (unit 3, Fig. 2) overlies the Middle or Early Pleistocene. It consists of poorly sorted, intertonguing silt, sand, gravel, and diamicton. They are interpreted by Clague & Evans (2003) as

439

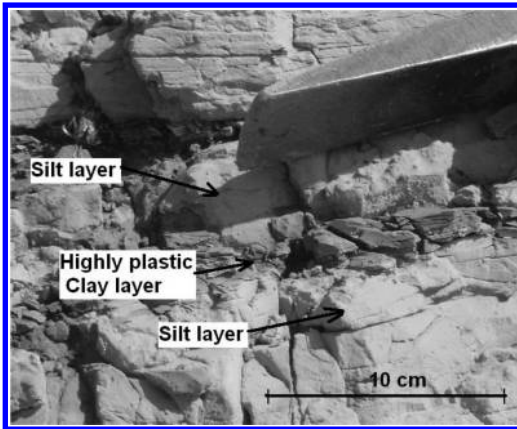Figure 3. Silt clay layers (unit 2, Fig. 4), at the toe of the Goddard Slide, south of Ashcroft.
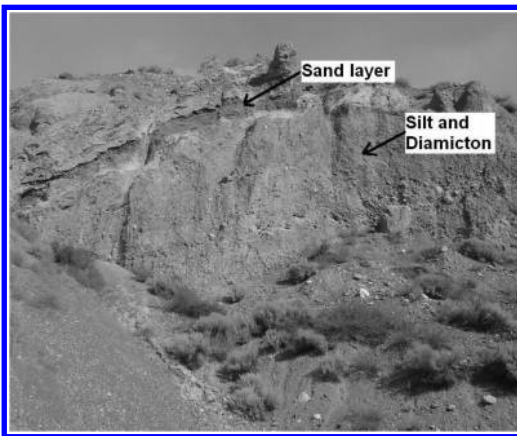

Figure 4. Unit 3, at the scarp of the Goddard Slide, south of Ashcroft (see Fig. 1 for location).

Figure 5. Wisconsin till (unit 6 in Fig. 2) at the main scarp of the South Slide, south of Ashcroft (see Fig. 1 for location).

blocked the regional drainage and impounded a lake in this part of Thompson Valley.

Unit 6 is matrix-supported diamicton. This unit is till dating to the time of Late Wisconsin glacier occupation of the area. Figure 5 shows this unit at the main scarp of the South Slide.

Unit 7 is poorly sorted, weakly stratified gravel, grading up into sand and silt. This unit is glaciolacustrine sediments laid down during deglaciation when the regional drainage was again blocked by glacier ice.

At most sections in the study area, the Fraser Glaciation sequence is incomplete, consisting of only one or two of the four units described above. The Fraser Glaciation sediment sequence described above is locally overlain by horizontally bedded, pebble-cobble gravel (unit 8, Fig. 2) deposited by Thompson River and its tributaries. These sediments date to the Pleistocene-Holocene transition, immediately after the lakes in Thompson Valley drained about 10,000 years ago (Clague & Evans 2003).

glaciolacustrine. This unit, unlike units 1 and 2, is not significantly weathered. Figure 4 shows this unit at the scarp of the Goddard Slide.

Sediments deposited during the last (Late Wisconsin or Fraser) glaciation (units 4–7, Fig. 2) overlie unit 3. Clague & Evans (2003) defined the Fraser glacial sequence in the Ashcroft area as being comprised of, from bottom to top, units 4 to 7, defined below.

Unit 4 is a thick unit of horizontally bedded, pebble-cobble gravel. This unit is braided-river channel gravels deposited by melt-water streams during the initial advance of glaciers into the area early during the Fraser Glaciation.

Unit 5 is horizontally bedded silt and sand containing some isolated stones. This unit is probably glaciolacustrine sediments that were deposited when glaciers

3 GEOTECHNICAL CHARACTERISTICS OF THE SLIDES

3.1 *Movement characteristics*

According to Leroueil (2001) in order to have a complete geotechnical characterization of slope movements the information about type of movement, type of material and stage of movement are required. Types of movements are those proposed in the geomorphological classifications of slides suggested by Cruden & Varnes (1996). They linked geology and landslide activity. The slides in Ashcroft area are moving on a surface of rupture which is planar so they are translational slides. They are very slow moving slides with movement rates in the order of 2 to 10 cm per year. There is evidence that the surfaces of rupture of the slides are extending upslope while the

440

movement is downslope, therefore the slides are retrogressive. The movement repeated following the enlargement of the slip surface therefore those slides are multiple landslides.

These slides have moved rapidly in the past, which in some cases caused transportation problems and also damming of the Thompson River, but now they are moving very slowly. As they are moving along the pre-existing slip surface they are reactivated slides. Therefore, for this kind of slides the soil is not likely to display strain softening and movement rate will be generally small (Leroueil 2001). Movement rate in these landslides varies with the seasonal changes in pore water pressure as discussed below. Therefore they are active slides in post failure stage of movement.

In summary, the slides in the Ashcroft area are reactivated retrogressive multiple translational earth slides that are very slow to extremely slow moving.

3.2 *Controlling laws and parameters*

As the slides are in post-failure stage and moving along pre-existing surfaces of rupture, the controlling Mohr-Coulomb parameters are residual parameters. Due to possible rate effects on shear resistance, parameters should be obtained with laboratory tests at the same shear rates as in the field.

Clay beds in unit 2 (see Fig. 2), which are the main part of the surfaces of rupture in those slides, are highly plastic; plasticity indices of most samples range from about 15% to 55%, and liquid limits range from 45% to almost 90% (Porter et al. 2002). Residual friction angles, estimated using the empirical correlation of Stark & Eid (1994), are 10–12°. Keegan et al. (2003) used similar residual friction angle for this material in their analyses.

The samples around the surfaces of rupture show activities in the range of 0.6 to 0.9. Perhaps the real activity of the clay material responsible for the slides is even higher. If it was possible to take the sample only from the clay layer in the rhythmically bedded clay-silt layer, a higher activity might be detected. Figure 6 shows a sample from this unit. The darker layer has more clay content.

Skempton (1969) found a correlation between the liquidity index and effective overburden pressure (or overburden material height) for normally consolidated clay sediments. This correlation can be used for estimating the overburden material height of overconsolidated clays. Table 2 shows the result using Skempton's approach on the samples from different slides in the Ashcroft area. The samples were taken from the undisturbed part of the rhythmically bedded silt and clay layer (unit 2) (CPR and CN reports). The results show this unit is overconsolidated.

Figure 6. Sample of rhythmically bedded glaciolacustrine silt and clay sediments (unit 2), sample from South Slide (see Figure 1 for location).

Table 2. Estimated overburden pressure and previous deposit height in the Ashcroft area (based on Skempton 1969).

Slide name	Equivalent deposit height (m)	Equivalent deposit elev. (m) asl.	Current ground elev. (m) asl.
Goddard	337.5	607.2	296.7
North slide	400	660.3	300.3
Nepa slide	412.5	668.7	272.2

3.3 *Predisposal factors*

The stratigraphy of the valley fill predisposes it to failure. The role of clayey glaciolacustrine sediments older than the Fraser Glaciation is significant for the stability of slopes in many valleys in central British Columbia. Clague (1988) found that similar units control landsliding in a complex Pleistocene sediment sequence in the Fraser River valley. The disturbance by overriding ice or early slope movements may create pre-sheared discontinuities that predispose these units to failure (Clague & Evans 2003).

By importing all the information from slide inclinometers, borehole logs, geological study of the area and site visit information to a geographical information system, it became clear that all the studied slides are sliding on two surfaces of rupture. Both of these surfaces of rupture are in the rhythmically bedded glaciolacustrine silt and clay unit (unit 2 in Fig. 2).

The surfaces of rupture are at different elevations in different landslides but their elevation differences are about 6.5 metres in average. Table 3 shows the elevations of the slip surfaces for the slides studied.

As shown in Table 3 the elevations for rupture surface decrease toward the South. This is in agreement with the tilting of the Glacial Lakes found by Johnsen & Brennand (2004). Figure 7 shows the shape Goddard Slide lower rupture surface.

The slides in the Thompson River valley have side slopes between 9° to 16°. The places with higher slope angles are controlled by bedrock.

3.4 *Triggering factors*

A trigger is an external stimulus that causes a near-immediate response in the form of a landslide by rapidly increasing the stresses or by reducing the strength of the slope materials. It can be intense rainfall, earthquake shaking, volcanic eruption, storm waves, or rapid stream erosion (Wieczorek 1996).

The rainfall in the area has been increasing since the 1920s. Despite this rainfall increase the area is

Table 3. Surfaces of rupture elevation of the studied slides in the Ashcroft area.

	River elevation (m)	Surface elevation (m)	
Slide name		Slip surface 1	Slip surface 2
Slide CN51	282.6	275.7	280.9
Goddard slide	275.8	270.6	278.1
North slide	273.2	264.2	269.4
South slide	269.0	263.7	272.7
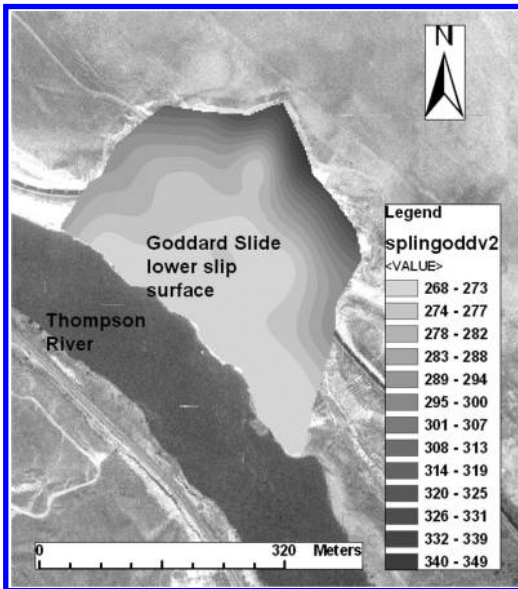
Figure 7. Typical slip surface shape for the slides in the Ashcroft area (Goddard Slide lower slip surface in this case).

quite dry and efforts to find some correlation with slide movements were not promising.

But the situation is different for the Thompson River level. For example the Thompson River level for two different years (1981 and 1982) and the average Thompson River level from Kamloops station are shown in Figure 8. During 1982, some slide activities occured in the Thompson corridor, among them was the Goddard Slide which disrupted the CPR operations at the end of September (CPR reports). As can be seen in Figure 8, the Thompson River level during 1982 (active year) was significantly above normal. Similar situations can be seen in other years when slide movements occur.

Figure 9 shows the differences between the average Thompson River level and the daily Thompson River level from 1980 to 1986. As can be seen in this figure during 1982, the difference was positive and stayed positive for a while. The other interesting point is that although during 1985 the river level was even higher than river level during 1982, no slides occurred so it is

Figure 8. Comparing the Thompson River level in an active year (1982) and non-active year (1981) (data from Kamloops station).

Figure 9. Daily difference between daily Thompson River level and average Thompson River level (Kamloops station).

442

not only the river level that affects slide activities but the area under this differential graph is also important (the period of time they stayed high).
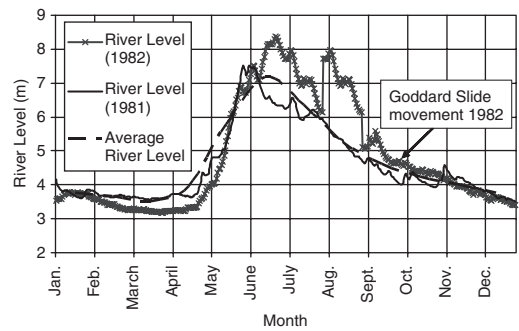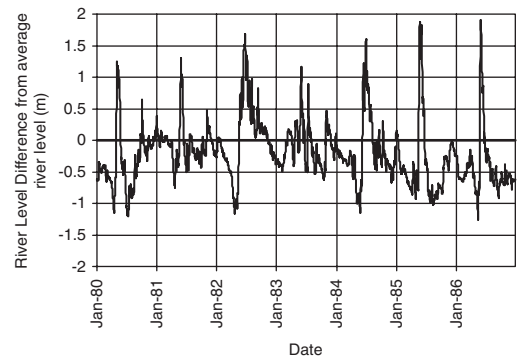
In order to have a quantitative number for comparing the years in this way the cumulative river level difference from average river level (CRLD) was calculated (Fig. 10) for 1980 to 1986. As shown in this figure the only year in this period with a positive (CRLD) is 1982 which was the only year with slide activity in the area during this period.

Similar behaviour is seen for other years. If the pick point of the cumulative river level difference from average river level (CRLD) for each year is selected as a quantitative number for that year and compared with the number of slides activities in the study area a close correlation can be found (Fig. 11). Figure 11 shows that the years with positive maximum cumulative river level difference from average river level difference are active years. Similar results can be found by using data from Spences Bridge station (south of study area). Data prior to 1970 is sparse and no conclusions related to slide movements can be drawn.

3.5 *Mechanism of failure*

Clague & Evans (2003) mentioned some possibilities of increasing pore water pressures in the landslides in this area which would cause failures of the slides. There is a silty gravel layer (unit 1 in Fig. 2) just above bedrock and under the rhythmically bedded silt and clay layer (unit 2 in Fig. 2). As this unit has higher permeability than unit 2 it can act as an aquifer. Piezometers at the toe of Slide CN51 and South Slide show an artesian pressure in this unit. It is believed that this artesian pressure may affect the slide activity in the area.

Figure 12 shows the locations of the piezometers at the toe of Slide CN51 and Figure 13 shows the cross-section A-B of the toe part of the slide. Figure 14 shows the measurement results of piezometers installed at the toe of Slide CN51 (borehole P1) and shows the deeper piezometers have higher heads. All piezometers respond to changes in the river level but the shallower the piezometer, the more the response.

Figure 10.   Cumulative Thompson River level difference form its average river level (Kamloops station).
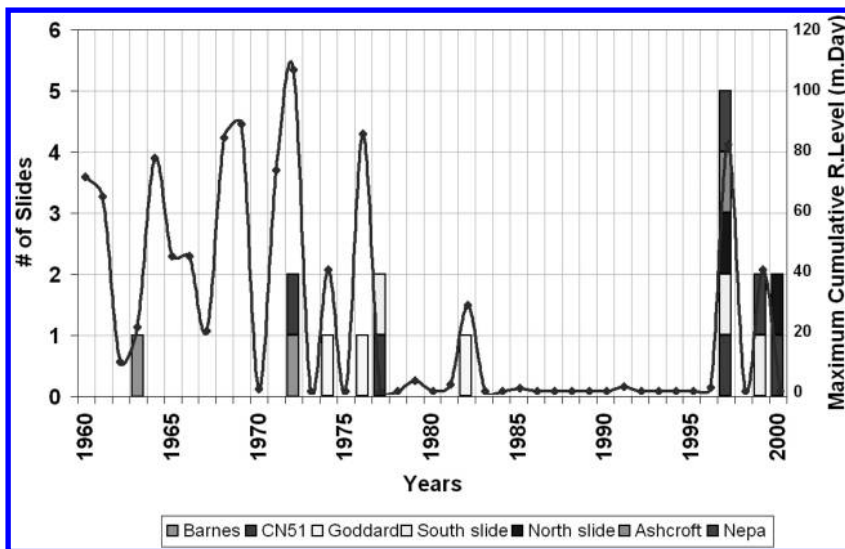
Figure 11.   Slide activity versus maximum cumulative Thompson River level difference from average Thompson River level (river data from Kamloops station).

443

It takes some time for the piezometers to equalize after the river level peaks. Similar behaviour can be seen in other peizometers.

Comparing the piezometers installed in different boreholes showed the piezometers near to the toe of the slide respond more quickly to the river level changes than piezometers near the back scarp.

The readings from piezometers installed near to the back scarp show no artesian pressures at that part of the slide.

From these results it can be said that the scarp is generally a recharge area and the toe is a discharge area most of the time. Because of the higher permeability of unit 1, water from the scarp moves through this unit and then comes up near to the toe. It results in an artesian pressure at the toe. On the other hand, when the Thompson River level starts rising the water from the river seeps toward the slide mass and may offset the artesian conditions but the river does not stay at this high level for sufficient time to let the system reach equilibrium. Therefore, the top part of the rhythmically bedded silt and clay layer (unit 2) may be more affected by the river level changes than the lower part. In the years that the Thompson River level stays at the higher level for a longer time the piezometers show the greatest increase in pore water pressures.

Figure 15 shows the ground water surface for slip surface 2 for Slide CN51. Due to the complexity of the ground water system in this area the ground water surface for slip surface 1 (deeper slip surface) is different from the ground water surface for slip surface

Figure 12. Slide CN51 plan, the location of the piezometers, and section A–B shown in Figure 13.

Figure 14. Sample responses of piezometers installed at the toe of the slides (Bh1, toe of slide CN51, see Figs 12–13).

Figure 13. Piezometers locations at cross-section A–B at the toe of Slide CN51 (see Fig. 12 for location).

444

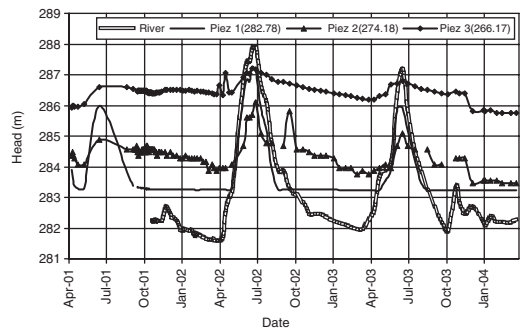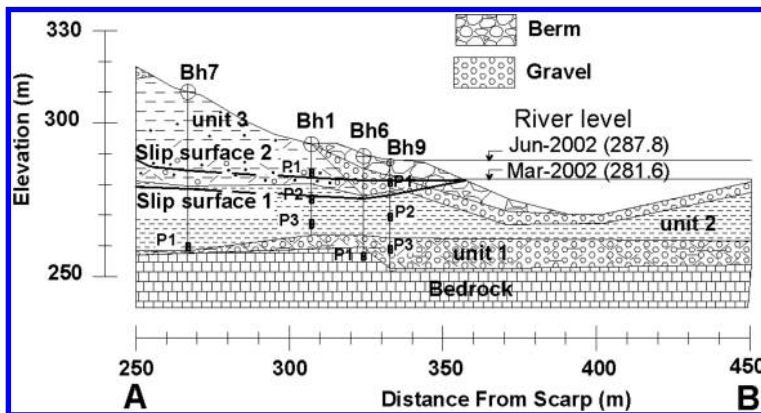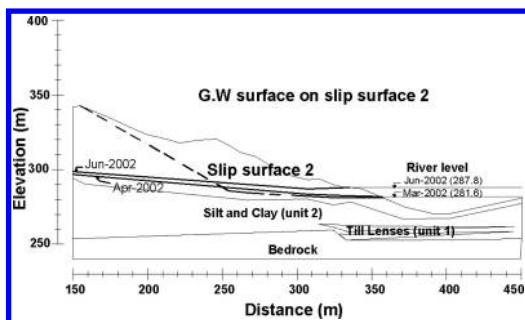Figure 15. Ground water surfaces for slip surface 2 (shallower slip surface) at the toe of Slide CN51 (see Fig. 1 for slide location and Fig. 13 for slip surface location).

2 (shallower slip surface). For the study period (year 2002 and 2003) the maximum river level and ground water surface happened in June 2002 but the minimum river level happened in March 2002 while the minimum ground water surface belongs to the April 2002. Figure 15 shows that the change in ground water level is greatest for the portion of the slide near to the river. The pore water pressure on slip surface 2 at the toe is very low during the low river level periods while during high river level periods it is quite high. The pore water change on this slip surface is more than 180% compare to the minimum pore water pressure on this surface. This change for slip surface 1 (deep slip surface) is about 80%.

The other interesting point is the location of the slip surfaces. While slip surface 2 is almost at the minimum river level, slip surface 1 is located in the river bed (similar situation can be seen in other slides in the area). The river level changes can have some stabilization effects during its high level period while during its low level period, this stabilization force is removed. In this study period the calculated minimum factor of safety for the shallow slide was about 1.06 while for the deep slide it was about 1.2. Therefore the mechanism of increased movement may be a rapid drawdown mechanism due to change of the Thompson River level in the late summer and early fall. Similar instability caused by a drop in river level has been documented along riverbanks in Winnipeg, Manitoba, by Tutkaluk et al. (1998).

4 CONCLUSIONS

The slides in the Ashcroft area are reactivated retrogressive multiple very slow to extremely slow moist translational earth slides which are moving on presheared surfaces. Understanding the geological stratigraphy of the valley fill is essential before undertaking a geotechnical analysis of those slides. The stratigraphy of the area is complex which can cause complex underground water seepage through the slide bodies. The sliding occurs through the rhythmically bedded silt and clay layer (unit 2) and contact of this unit with unit 3 on two rupture surfaces. Those two rupture surfaces can be the locations of weak layers in Unit 2 and 3. Preliminary findings suggest that all the slides may be moving on the same geological layer but proving this idea still needs more study.

The main trigger event for recent slide movements appears to be related to the river water level changes. If the river has a higher than average level for a significant duration the pore water pressure on the rupture surfaces increases. When the river level falls back to its traditional seasonal lower levels the pore water pressure is not equalized and the supporting load at the toe applied by river water is removed. Therefore it is believed that a rapid drawdown mechanism may significantly contribute to the slide movements.

REFERENCES

Armstrong, J.E., Crandell, D.R., Easterbrook, D.J. & Noble, J.B. 1965. Late Pleistocene stratigraphy and chronology in southwestern British Columbia and western Washington. *Geological Society America Bulletin* 76: 321–330.

Christiansen, E.A. & Sauer, E.K. 1984. Landslide styles in the Saskatchewan River Plain: a geological appraisal. *37th Canadian Geotechnical Conference, Toronto.* C. G. Society.1: 35–48.

Clague, J.J. 1988. Quaternary stratigraphy and history, Quesnel. British Columbia. *Geographie Physique Quaternaire* 42: 279–288.

Clague, J.J. & Evans, S.G. 2003. Geological framework of large historic landslides in Thompson River Valley, British Columbia. *Environmental and Engineering Geoscience* IX(3): 201–212.

Cruden, D.M. & Varnes, D.J. 1996. Landslide types and processes. *Special report 247.* Transportation Research Board, No. 247: 36–75.

Duffell, S. & McTaggart, K.C. 1952. *Ashcroft map-area, British Columbia.* Geological Survey of Canada. Memo 262 p.122.

Flint, R.F. & lrwin, W.H. 1939. Glacial geology of Grand Coulee Dam, Washington. *Geological Society America Bulletin* 50: 661–680.

Fulton, R.J. 1969. *Glacial Lake History, Southern Interior Plateau, British Columbia*. Geological Survey of Canada Paper 69–37: p.14.

Hodge, R.A.L. & Freeze, R.A. 1977. Groundwater flow systems and slope stability. *Canadian Geotechnical Journal* 14: 466–476.

Johnsen, T.F. & Brennand, T.A. 2004. Late-glacial lakes in the Thompson Basin, British Columbia: paleogeography and evolution. *Canadian Journal of Earth Science* 41: 1367–1383.

Keegan, T., Abbott, B., Cruden, D., Bruce, L. & Pritchard, M. 2003. Railway ground hazard risk scenario: River erosion: Earth-slide. *3rd Canadian Conference on Geotechnique and Natural Hazards, Edmonton, Alberta*. The Canadian Geotechnical Society: 269–277.

Leroueil, S. 2001. Natural slopes and cuts: movement and failure mechanisms. *Geotechnique* 51(3): 197–243.

Porter, M.J., Savigny, K.W., Keegan, T.R., Bunce, C.M. & MacKay, C. 2002. Controls on stability of the Thompson River landslides. *Proceeding of the 55th Canadian Geotechnical Conference, Niagara*. Southern Ontario Section of the Canadian Geotechnical Society.

Ryder, J.M. 1976. *Terrain inventory and quaternary geology Ashcroft, British Columbia*. Geological Survey of Canada Paper 74–49.

Skempton, A.W. 1969. The consolidation of clays by gravitational compaction. *Journal of the Geological Society* 125: 373–411.

Stark, T.D. & Eid, H.T. 1994. Drained residual strength of cohesive soils. *Journal of Geotechnical Engineering* 120(5): 856–871.

Tutkaluk, J., Graham, J. & Kenyon, R. 1998. Effects of riverbank hydrology on riverbank stability. *Proceeding of the 51st Canadian Geotechnical Conference, Edmonton, Alberta*. Canadian Geotechnical Society.

Wieczorec, G.F. 1996. Landslide triggering mechanisms. In *Special Report 247*. Transportation Research Board, No. 247: 76–90.

446

Phillips River landslide hazard mapping project

T. Rollerson
Golder Associates Ltd., Gabriola, BC, Canada

D. Maynard
Denny Maynard and Associates Ltd., North Vancouver, BC, Canada

S. Higman
Weyerhaeuser Company, Nanaimo, BC, Canada

E. Ortmayr
Chartwell Consultants Ltd., North Vancouver, BC, Canada

ABSTRACT: The Phillips River landslide hazard mapping project utilizes categorical and scale data from terrain and landslide inventories to produce semi-quantitative landside hazard maps for forest management purposes. This project is part of a larger study that includes watersheds in the Vancouver Island Ranges and southern Coast Mountains of British Columbia. The spatial landslide density values developed by this approach are considered an "index" of landslide hazard. They provide an objective way to rank landslide hazards. These indices represent mean values for different categories of terrain. The landslide rate that occurs within a specific map unit can vary from the mean value for that category of terrain.

1 INTRODUCTION

Weyerhaeuser Company Ltd is involved in a long-term program of upgrading the landslide hazard mapping used within its coastal operations. The Phillips River project is part of a larger initiative that includes watersheds in the Vancouver Island Ranges and the southern Coast Mountains.

This paper discusses the methodology and results of a mapping project in the Phillips River in the southern Coast Mountains of British Columbia. The objectives of the project were to carry out detailed terrain mapping, inventory historical landslide activity and then to integrate this information to produce empirical landslide hazard maps for forest management purposes.

2 STUDY AREA

The study area is typical of the Southern Fiord Ranges (Pacific Ranges) of the Coast Mountains (Mathews 1986). Topography is rugged, elevations range from sea level to higher than 1800 m.

Regional bedrock is dominated by hard, coarse-grained granitic rocks of the Coast Plutonic Complex with isolated inclusions of older and younger metamorphic rock types.

Geomorphology of the region is mainly a product of geological events that occurred in the Tertiary and Quaternary Periods. This physiographic evolution initiated with uplift of the Coast Mountains followed by dissection of the uplifted surface. Recurrent glacial erosion and deposition during the Pleistocene Epoch, further modified the major valleys, creating classic U-shaped forms, particularly along the main Phillips River valley which drains southwest into the major trough of Phillips Arm. Topography is largely bedrock controlled and surficial materials are usually thin on the middle to upper valley walls. Deposition of surficial deposits is most extensive along valley floors and lower slopes, often resulting in thick accumulations of pre-glacial, glacial, and/or post-glacial sediments. Glacial erosion increased local relief and ruggedness. Upper elevations are characterized by large areas of bare bedrock, glacial ice and thin surficial materials, with landscapes ranging from smooth rounded glacial surfaces to extremely rugged cliffs and ridges sculpted by valley and alpine glaciers.

The dominant mass movement processes in the study area are snow avalanches, debris flows confined in steep, valley-wall channels; and rock fall and

occasional rockslides from bedrock-dominated, valley sides. Colluvial cones and fans, and blocky talus slopes, common along the base of the valley sides, provide depositional evidence of recurrent up-slope activity. Mass-movement activity also concentrates on the steeper slopes along the valley floors and lower valley sides. Deeply incised, lower slope gullies, stream or river gorges and river and stream escarpments are common sites of landslide activity.

Most of the operable forest occurs within the Coastal Western Hemlock Biogeoclimatic Zone described by Krajina (1973), giving way at higher elevations to the Mountain Hemlock Zone. Alpine ecosystems are found at higher elevations. Mean annual precipitation (Farley 1979) ranges from about 2000 mm near the head of Phillips Arm to upwards of 3500 mm at the northern limit of the valley. Localized orographic effects can produce dramatic short-duration, high-intensity rainstorms. Seasonal precipitation patterns are typical of coastal British Columbia, with most precipitation occurring between October and March, typically as rain near sea-level and snow at higher elevations.

3 METHODS

The terrain mapping process involved inventorying surficial materials, topographic features, soil drainage, and slope processes by map and air photo analyses, augmented with field observations. The study followed provincial and federal mapping standards (Resources Inventory Committee 1996b, Province of BC 1999, Howes & Kenk 1997, Agriculture Canada 1987). Additional terrain-attribute criteria previously identified as being statistically relevant with respect to post-logging landslide activity in the Coast Mountains (Rollerson et al. 2001) were also recorded.

Terrain units were stereoscopically delineated on 1994, 1:20,000-scale colour air photos. These map units subdivide the land surface according to the origin and texture of surficial materials, landform morphology and the presence of geomorphic processes that modify the landscape. Drainage classes are based on landscape characteristics and vegetation patterns; slope gradients were determined by a combination of field and contour-map measurements and air photo interpretation.

Spatial map data was created by digitally transferring terrain polygon boundaries and symbols from the typed air photos to a digital topographic base (British Columbia Terrain Resource Information Mapping – TRIM) and entering the polygon data into a GIS database.

The terrain polygons were transferred directly from the typed air photos using a process called monorestitution (MAPS-3D). This process allows map features to be digitized and transferred from the air photos using the MAPS-3D program which runs simultaneously with Microstation. Ground control points picked from the air photos are tied to the planimetric map base. This orientation is then draped over a three dimensional Triangulated Irregular Network (TIN) surface and a photogrammetric-mathematical model is formed to transform photo locations into X, Y and Z coordinates. The technique solves for the vertical displacement that occurs on a single air photo.

Attribute data for the terrain polygons, including morphologic terrain attributes commonly related to landslide activity, are entered into a database and linked with the numbered map polygons. The database files, digital map layers, and map legends are transferred into ArcInfo format according to specifications described by the Resources Inventory Committee, 1998.

The terrain mapping relied heavily on thorough and detailed interpretation of the air photos, using relevant site data described in the various terrain stability field assessments that have been carried out in the map area in recent years, field data from a research study within the map area (Rollerson et al. 2001), and on the considerable local experience of the terrain mapper. Only a very limited amount of additional fieldwork was done specifically for this project.

4 PHOTOGRAPHS AND FIGURES

We utilize categorical and some scale data from terrain maps and landslide location data to produce semi-quantitative landslide hazard maps. We term these maps "semi-quantitative" because although statistical methods are used to generate landslide density values, the terrain map and landslide inventories used to generate the basic data are qualitative products based on air photo interpretation, limited field validation and professional judgment.

The mapping approach depends on statistical inference based on landslide frequencies (densities) determined across a watershed. The process involves five steps: (1) Map and database creation, involving terrain mapping and landslide inventories in a series of logged and unlogged areas viewed as representative of the entire watershed. (2) Overlay of landform, landslide and other geographic data (e.g., geology, slope angle, geomorphic process) using a geographic information system (GIS). (3) Analysis of the data using univariate and multi-variate statistics to identify relationships between predictor variables (terrain attributes) and landslide frequency. (4) Development of simple algorithms or queries based on the statistical analysis to generate harvest area landslide hazard maps (Fig. 1) that portray expected hazard as landslide density rates or ranges for the project area. (5) Quality assurance and quality control based on professional judgment and review.

448

Figure 1. Landslide hazard map, Phillips River.

449

We assume that most landslides related to forest harvesting and forest road construction occur in the first 5 to 15 years after harvest. The data collection focuses on areas of logging ranging from 5 to 50 years after harvest, consequently most if not all of the shallow landslides related to harvesting or road building will have occurred. We also make the assumption that relationships developed in "recently" logged areas can be extrapolated to "geologically" similar natural forests or areas of older second-growth timber in the remainder of the map area. What is not known is if the landslides rates that followed the original harvest will reflect those that may occur following second-growth harvesting.

It is possible that some sites that experienced landslide activity following the original harvest will not experience similar activity following the second-growth harvest because they have not yet weathered deeply enough or accumulated a sufficient depth of colluvial material to fail again.

The landslide density values developed by this approach are considered an "index" of landslide hazard. That is, they provide an objective and defensible way to rank logging-related landslide hazards. These studies provide only a snapshot-in-time; smaller landslides will not be detected (i.e., <0.05 ha); the natural landscape is highly variable and storms may miss parts of an area, so these studies do not necessarily provide absolute long-term landslide rates. The term "rate" is used because the data reflect landslide densities or frequencies generated by landslides occurring over a 5- to 50-year period after logging. The calculated landslide rates are mean values for different generalized categories of terrain. The landslide rate that occurs within a specific terrain polygon within a generalized terrain category will likely vary from the mean value reported for that category of terrain.

Terrain mapping is carried out as described above. We use recent air photos that show extensive, recently logged areas as these facilitate more precise terrain mapping. Extensive forest cover on older air photos can mask terrain conditions and thereby limits the accuracy of the map product.

Shallow landslides are inventoried using sequenced historical air photos to provide a clear picture of landslide occurrence in logged and natural areas over time. As noted above, most harvest-related landslides are believed to occur in the first 5- to 15-years after harvest. Consequently, inspecting a series of air photos, going back 35- to 40-years, generally provides a sufficiently large sample of logged areas and different terrain types as well as an adequate sample (number) of landslides for data analysis purposes. In this particular case, historical air photos dating from 1961 through 2001 were used to generate the landslide inventory. Albers projection x and y coordinates for landslide initiation points were derived from a year 2001,

1:30,000 scale digital orthophoto image using MrSid Geoviewer software.

Forest cover maps currently in the Weyerhaeuser GIS were used to define logged areas and age of logging.

Recently logged areas not yet plotted on the current GIS forest cover layer were excluded from the study, as well as areas logged between 1996 and 2001. This was done because landslide frequencies in areas of very recent logging tend to underestimate longer-term landslide rates because there may not have been sufficient opportunity for intense, long-duration rainstorms to affect the area. Obviously, if an area has not been exposed to heavy rain or severe rain-on-snow events after logging, it is less likely to exhibit post-harvest landslide activity.

4.1 Data requirements

The main data elements consist of:

- A 1:20,000 scale terrain map.
- A terrain database.
- A landslide inventory map.
- A forest cover map and database.
- A bedrock geology map.

The terrain database contains:

- Surficial material types.
- Polygon area (ha).
- Geomorphic processes.
- Surface morphology.
- Lateral slope curvature.
- Estimated maximum, minimum and average slope classes.
- Soil drainage class estimates.
- Estimated gully depths and escarpment heights (<6 m and >6 m).

4.2 GIS analysis

Terrain, forest cover, bedrock geology and landslide location data layers are used to create and populate resultant "child" polygon and landslide layers. Data is combined and modified using ArcGIS and Microsoft Access. All data are converted to ArcInfo coverages and projected to a common NAD83 Albers projection. The terrain and forest cover data are overlaid to produce a child polygon layer. Bedrock geology attributes are added by overlaying the geology layer with the child polygon layer. The database from this overlay is then joined back to the original child polygon database and populated based on the largest geological polygon within each child polygon.

Landslide data is then intersected with the child polygon data. Landslide locations that lie within twenty metres of a terrain polygon boundary are identified and compared with the typed aerial photos to ensure that the

450

landslides are in the correct terrain polygon. If the landslide is in the wrong polygon, it is moved to the correct polygon and the landslide database is corrected accordingly. After summarising the resultant landslide/terrain/forest cover database, the summary is joined back to the child polygon database and the total number of landslides for each landslide type in every child polygon are added to the landslide type fields.

The revised landslide locations and the updated child polygon database are exported to Microsoft Excel in preparation for statistical analysis. After the analysis is completed, a spreadsheet containing colour-themed hazard polygon codes is used to create the final landslide hazard map.

4.3 *Data analysis approach*

Data analysis includes tabular and graphical analysis as appropriate to investigate one-on-one relationships between potential predictor variables and landslide rate (density). Based on the preliminary graphical analysis, secondary variables or terrain attributes may be generated from the primary variables. For example, primary and secondary surficial material code fields can be combined to create composite surficial material categories. Decision-tree analysis is then used to identify relationships among the various combinations of potential predictor variables and landslide activity. The results of the decision-tree analysis are then used, by way of a series of database queries to generate summary data files. These data files contain each unique child polygon number and the mean harvest landslide density values for each terrain category. These data files are then used in the GIS to generate the final landslide hazard map (Fig.1).

The sample element for this analysis is based on the landform/terrain child polygons created when the primary terrain polygons are intersected with geologic unit and forest cover layer polygons and then overlaid with the landslide location data. These child polygons have a wide range of sizes but are considered to be geological/ecological (biophysical) entities that should not be split in an arbitrary fashion (i.e., they should not be converted to an abstract grid or cell format). Because each child polygon is treated as a single sample, smaller polygons and larger polygons can weigh equally in the analysis. To offset this factor the polygon samples are weighted in the statistical analysis using an area-based weighting factor generated by dividing each polygon area by a nominal minimum polygon area (e.g., 0.1 ha) and then incrementing the number of records for each sample (polygon) by the quotient value.

Landslide density distributions tend to be highly skewed, that is, a substantial number of map polygons have either zero or very low landslide density values. Smaller polygons will influence the mean value to the same degree as larger polygons, even though larger polygons frequently have lower landslide density values. Consequently, mean landslide density values calculated by decision tree analysis or any other statistical procedure using un-weighted individual sample data will tend to overestimate the central tendency of the population. Weighting the sample population acts to correct this problem.

The primary map product is a landslide hazard (density) map for harvesting related landslides (ls/ha). To ensure the most effective use of the project data, the landslide initiation points for logging-related and natural landslides are also displayed on the hazard map. All landslides that initiate below roads are tabulated as harvest-related even though some are likely linked to road drainage.

5 RESULTS AND DISCUSSION

The analysis is restricted to areas where the date of plantation establishment was recorded as occurring between 1950 and 1995. There are some areas in the data set that were logged prior to 1950 but we felt that landslides that had occurred on areas harvested prior to 1950 would have been vegetated to the point that they would not have been visible on the earliest set of air photos used for the landslide inventory (i.e., 1961). The period of record for landslide occurrence is about 50 years and includes landslides visible on the 1961 air photos to landslides visible on the 2001 air photos. The air photo-based approach results in a slight underestimate of management associated landslide rates as there may be a few smaller landslides in plantations that occurred in the early 1950's that are vegetated to the point were they not visible on the 1961 air photos and landslides may not yet have occurred in some of the younger plantations. In general landslides smaller than 0.05 ha are not recorded as it is difficult to consistently identify smaller landslides on the air photo scales utilized for the study (i.e., 1:15,000 to 1:30,000 scale). Many areas on the BC coast were subject to one or more intense rainstorms during the 1996–97 winter and possibly again during the 1997–98 winter, so it is reasonable to assume that most areas of 1995 or earlier logging will have experienced one or more large rainstorms.

5.1 *Harvest-related landslide densities*

A number of relationships between potential predictor variables and harvest landslide rates are revealed by inspection of Table 1.

There is a general increase in harvest-related landslide rates as slope angle increases (see Table 1 for predictor variable-landslide rate relationships). The rate of increase is steeper above slope angles of about 30° and decreases for slope angles steeper than about 40°. This

451

Table 1. Post-harvest landslide rates by attribute.

Attribute	Mean	Std. Dev.	Attribute	Mean	Std. Dev.
Average slope class (°)			**Primary drainage class**		
<20	0.000	0.000	Unclassified	0.000	0.000
20–25	0.003	0.012	Imperfectly	–	–
25–30	0.006	0.080	Moderately	0.026	0.160
30–33	0.039	0.191	Rapidly	0.042	0.193
33–35	0.042	0.177	Well	0.035	0.233
35–40	0.091	0.235	Total	0.024	0.190
40–50	0.068	0.687			
>50	0.000	0.000	**Geologic unit**		
Total	0.024	0.190	Coast Plutonic – average slope class		
			<20	0.000	0.000
Natural landslide types			20–25	0.003	0.012
Absent	0.021	0.127	25–30	0.007	0.085
Debris landslides	0.297	1.206	30–33	0.040	0.194
Debris and rock	0.000	0.000	33–35	0.050	0.195
Rockfall	0.000	0.000	35–40	0.088	0.236
Rockslides	0.000	0.000	40–50	0.073	0.712
Total			>50	0.000	0.000
			Total	0.026	0.200
Slope morphology			Gambier Group – average slope class		
Unclassified	0.000	0.000	<20	0.000	0.000
Benchy	0.005	0.018	20–25	0.000	0.000
Dissected	0.114	0.313	25–30	0.000	0.000
Single gully	0.127	0.342	30–33	0.000	0.000
Headwater basin	0.000	0.000	33–35	0.015	0.068
Irregular	0.009	0.060	35–40	0.115	0.218
Escarpment	0.162	0.740	40–50	0.000	0.000
Uniform	0.023	0.133	>50	0.014	0.079
Total	0.024	0.190	Total	0.000	0.000
Primary surficial material			**Gully/scarp height**		
Unclassified	0.000	0.000	Unclassified	0.000	0.000
Colluvium	0.026	0.150	Absent	0.018	0.116
Fluvial	0.000	0.000	Gully < 6 m	0.053	0.220
Glaciofluvial	0.054	0.207	Gully > 6 m	0.179	0.382
Glaciolacustrine	0.421	0.590	Scarp > 6 m	0.162	0.740
Morainal	0.045	0.337	Subdominant < 6 m	0.036	0.158
Organic [follisols]	–	–	Subdominant > 6 m	0.000	0.000
Bedrock	0.000	0.000	Total	0.024	0.190
Total	0.024	0.190			
Lateral curvature					
Unclassified	0.000	0.000			
Concave	0.074	0.222			
Complex	0.051	0.339			
Convex	0.000	0.000			
Planar	0.027	0.139			
Total					

decrease in landslide density values is likely due to the dominance of exposed, irregular bedrock surfaces on these steeper slopes.

The presence of natural debris slides and debris flows is strongly related to post-harvest landslide rates. Post-harvest landslide densities are high in areas where natural debris slide and debris flow activity was identified or inferred. Rates for terrain with no visible pre-harvest natural landslide activity may be slightly higher than those for areas with rockfall and rockslide activity.

Harvest-related landslide rates vary with changes in slope morphology. Irregular and bench-shaped (often bedrock dominated) slopes tend to have relatively low landslide rates. Landslide rates are low, 0.02 ls/ha, on uniform slopes (relatively smooth often planar slopes)
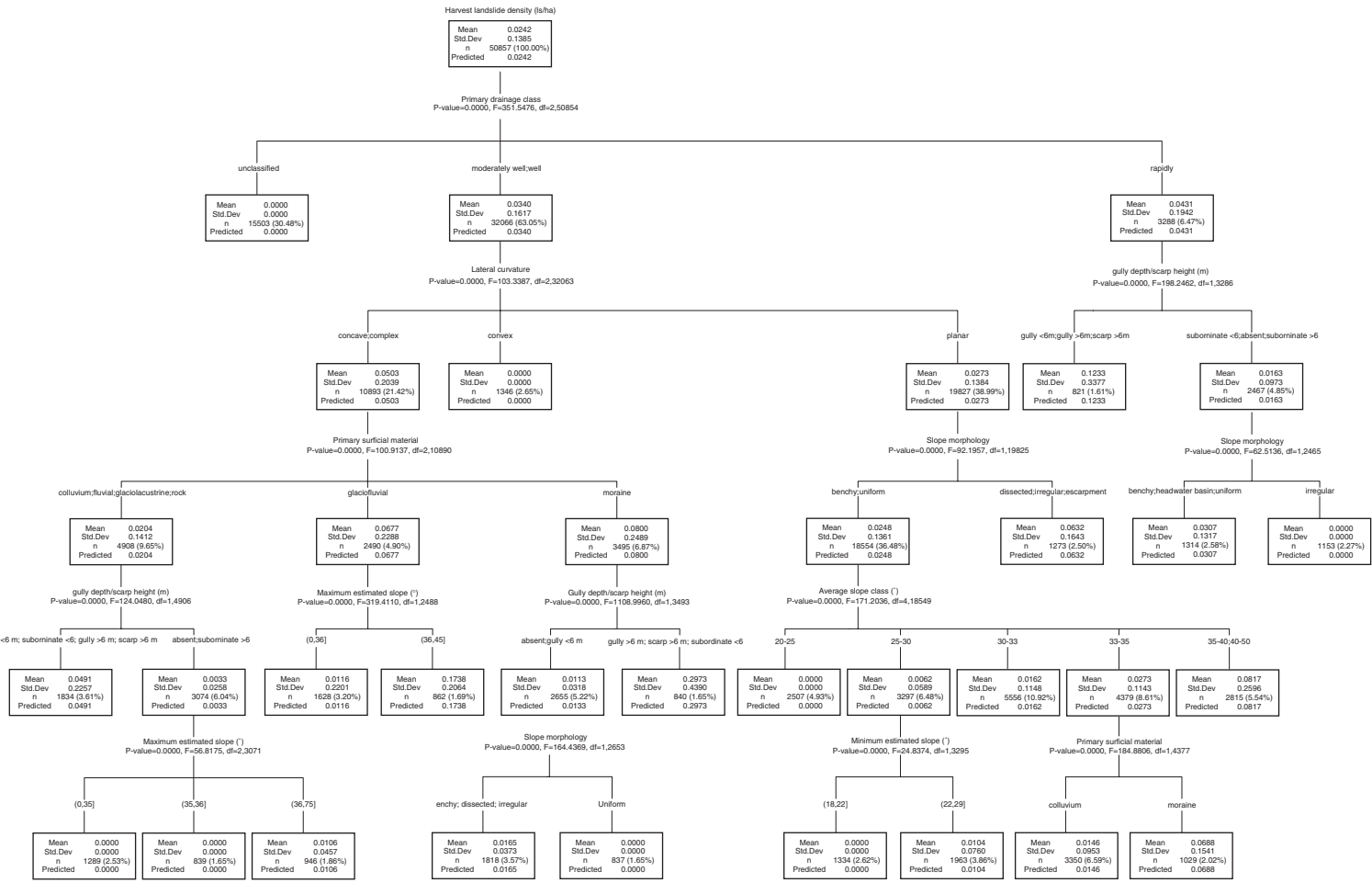
452

453

Figure 2.   Harvest area landslide density decision-tree, Phillips River.

and are quite low in concave headwater basins. Higher rates are associated with dissected slopes (0.11 ls/ha); these are slopes with shallow (generally <3 m deep) gullies spaced intermittently or frequently across the slope. Landslide rates are highest in larger, single gullies (0.13 ls/ha) and along valley floor stream escarpments (0.16 ls/ha). Gently sloping terrain units where slope morphology and surficial materials are not differentiated have the lowest landslide rates.

Laterally concave (convergent) slopes have the highest landslide rates (0.07 ls/ha) with complex and planar slopes having intermediate to low landslide rates. The lowest landslide rates are associated with convex (divergent) slopes and gently sloping areas where no differentiation was made for slope curvature.

Landslide rates are highest for terrain units dominated by glaciolacustrine materials (0.42 ls/ha), and low-moderate rates are associated with morainal, colluvial and glaciolfluvial materials. The rates for fluvial, undifferentiated, and bedrock dominated units are low. The undifferentiated surficial material designation is applied to slopes that are generally less than 20°.

There is relatively little differentiation among the mapped soil drainage classes. Slightly higher landslide rates (0.04 ls/ha) are associated with rapidly drained slopes, and slightly lower rates (0.03 ls/ha) with moderately well drained slopes. Typically, rapidly drained areas are associated with thin soils on steeper slopes, so this particular relationship likely co-varies with slope gradient and possibly the depth of surficial materials. Unclassified areas have the lowest rates.

There may be some very slight differences in landslide rates between the two dominant bedrock types in the area (Coast Plutonic granitic rocks and the Gambier Group meta-volcanics). This relationship varies with slope class.

There is a fairly clear relationship associated with the presence or absence of gullies and escarpments and post-harvest landslide rates. These relationships tend to vary with gully depth and escarpment height. The lowest landslide rates are associated with terrain where these features are not present or are only subordinate features in the landscape. Gullies deeper than six metres and scarps higher than six metres have higher landslide rates than gullies less than six metres deep.

The relationships among these various variables and post-harvest landslide rates are further defined and explored by the decision-tree analysis (Fig. 2). The first predictor variable used to define post-harvest landslide rates is the primary drainage class. This variable is an interpretation that combines both slope steepness and surficial material depth so may be used for this reason. The secondary predictor variables used in the decision-tree analysis are lateral curvature and gully depth/scarp height. Tertiary splits in the decision tree are made using the primary surficial material or slope morphology. The fourth level of the tree is generated by the

variables: maximum estimated slope angle, average slope class and gully depth/scarp height, and the branches for the fifth level are made on the basis of maximum estimated slope, slope morphology, minimum estimated slope and primary surficial material. The landslide densities in each node of the tree represent the weighted mean for all samples in that particular terrain category. As noted above, these terrain categories define a series of database queries used to populate the hazard classes listed in Figure 1. Because of the relatively small number of terrain polygons subject to natural debris slide and debris flow activity, the presence or absence of these features was not used by the decision tree analysis as a predictor variable. At the time of hazard class designation, because of the high post-harvest landslide rates associated with these features identified during the univariate analysis (Table 1), we arbitrarily allocated those terrain polygons exhibiting natural debris slides or debris flow activity that did not fall into the two highest hazard classes to the highest hazard class. Similarly, because a few rare types or combinations of terrain in the Phillips River watershed have not yet been logged, they were not addressed by the decision tree or univariate analysis, consequently, we made a limited number of arbitrary but logical allocations to accommodate these terrain types when assigning hazard classes.

6 CONCLUSIONS

Univariate analysis successfully identifies a series of air photo and terrain-based variables and relationships that when refined through multi-variate decision-tree analysis can be used to generate semi-quantitative landslide hazard maps. The terrain relationships identified and the landslide density values developed from the air photo-based terrain analysis are quite similar to those identified by earlier, more intensive, field-based terrain and landslide studies in the Southern Coast Mountains (Rollerson et al. 2001) and in the nearby Cascade Mountains (Millard et al. 2002).

REFERENCES

Agriculture Canada Expert Committee on Soil Survey. 1987. *The Canadian System of Soil Classification*.

Farley, A.L. 1979. *Atlas of British Columbia: People, Environment, and Resource Use*. University of BC Press, Vancouver, BC.

Howes, D.E. & Kenk, E. (eds.) 1997. *Terrain Classification System for British Columbia: Version 2*, 1997. MoE Manual 10. Resource Inventory Branch, BC Ministry of Environment, Lands, and Parks.

Krajina, V.I. 1973. *Biogeoclimatic Zones of British Columbia*. BC Ecological Reserves Committee, Victoria, BC.

Mathews, W.H. (compiler) 1986. *Physiography of the Canadian Cordillera*. Geological Survey of Canada Map 1701A, scale 1:5,000,000.

Millard, T., Rollerson, T. & Thomson, B. 2002. *Post-logging Landslide Rates in the Cascade Mountains, Southwestern British Columbia*. Technical Report TR-023. Research Section, Vancouver Forest Region, BC Forest Service.

Province of British Columbia. 1995. *Mapping and Assessing Terrain Stability Guidebook* (Forest Practices Code of BC).

Province of British Columbia. 1999. *Mapping and assessing terrain stability guidebook* (Forest Practices Code of BC). Second edition.

Resources Inventory Committee (D. Van Dine, O. Hungr, & W. Gerath) 1996a. *Terrain Stability Mapping in British Columbia: A Review and Suggested Methods for Landslide Hazard and Risk Mapping*. Victoria, BC.

Resources Inventory Committee 1996b. *Guidelines and Standards for Terrain Mapping in British Columbia*. Victoria, BC.

Resources Inventory Committee 1998. *Standards for Digital Terrain Data Capture in British Columbia; Terrain Technical Standard and Database Manual, Version 1*.

Roddick, J.A. & Woodsworth, G.J. 1978. *Geology of Bute Inlet Map Area (92K)*. Geological Survey of Canada Open File 480.

Rollerson, T., Millard, T., Jones, C., Trainor, K. & Thomson, B. 2001. *Predicting Post-Logging Landslide Activity Using Terrain Attributes: Coast Mountains, British Columbia*. Technical Report TR-011. Vancouver Forest Region, BC Forest Service.

Guidelines for the geologic evaluation of debris-flow hazards on alluvial fans in Utah, USA

R.E. Giraud

Utah Geological Survey, Salt Lake City, USA

ABSTRACT: The Utah Geological Survey (UGS) has developed these guidelines to help geologists evaluate debris-flow hazards on alluvial fans to ensure safe development. The purpose of a debris-flow-hazard evaluation is to characterize the hazard and provide design parameters for risk reduction. These guidelines use the characteristics of alluvial-fan deposits as well as drainage-basin and feeder-channel sediment-supply conditions to evaluate debris-flow hazards. Analysis of alluvial-fan deposits provides the geologic basis for estimating frequency and potential volume of debris flows and describing debris-flow behavior. Drainage-basin and feeder-channel characteristics determine potential debris-flow susceptibility and the volume of stored channel sediment available for sediment bulking in future flows. Hazard zones may also be outlined on the alluvial fan to understand potential effects of debris flows and determine appropriate risk-reduction measures. Geologic estimates of debris-flow design parameters are necessary for the engineering design of risk-reduction structures.

1 INTRODUCTION

1.1 *Overview*

Debris flows and related sediment flows are fast-moving flow-type landslides composed of a slurry of rock, mud, organic matter, and water that move down drainage-basin channels onto alluvial fans (Fig. 1). Debris flows generally initiate on steep slopes or in channels by the addition of water from intense rainfall or rapid snowmelt. Flows typically incorporate additional sediment and vegetation as they travel down-channel. When flows reach an alluvial fan and lose channel confinement, they spread laterally and deposit the entrained sediment. In addition to being debris-flow-deposition sites, alluvial fans are also favored sites for urban development; therefore, a debris-flow-hazard evaluation is necessary when developing on alluvial fans. A debris-flow-hazard evaluation requires an understanding of the debris-flow processes that govern sediment supply, sediment bulking, flow volume, flow frequency, and deposition. This paper is a shorter version of debris-flow hazard guidelines developed by the UGS to assist geologists in hazard evaluation, engineers in designing risk-reduction measures, and land-use planners and technical reviewers in reviewing debris-flow-hazard reports.

Large-volume debris flows are low-frequency events, and the time between large flows is typically a period of deceptive tranquility. Debris flows pose a

Figure 1. Example of a drainage basin and alluvial fan at Kotter Canyon, north of Brigham City, Utah.

hazard very different from other types of landslides and floods due to their rapid movement and destructive power. Debris flows can occur with little warning. Fifteen people have been killed by debris flows in Utah. Thirteen of these victims were killed in two different events at night as fast-moving debris flows allowed little chance of escape. In addition to threatening lives, debris flows can damage buildings and infrastructure by sediment burial, erosion, direct impact, and associated water flooding. The 1983 Rudd Canyon debris flow in Farmington deposited approximately 69,000 m^3 of sediment on the alluvial fan, damaged 35 houses and caused an estimated \$3 million in property damage (Deng et al. 1992).

Variations in sediment-water concentrations produce a continuum of sediment-water flow types that build alluvial fans. Beverage & Culbertson (1964), Pierson & Costa (1987), and Costa (1988) describe the following flow types based on generalized sediment-water concentrations and resulting flow behavior: stream flow (less than 20% sediment by volume), hyperconcentrated flow (20 to 60% sediment by volume), and debris flow (greater than 60% sediment by volume). These categories are approximate because the exact sediment-water concentration and flow type depend on the grain-size distribution and physical-chemical composition of the flows. Also, field observations and video recordings of poorly sorted water-saturated sediment provide evidence that no unique flow type adequately describes the range of mechanical behaviors exhibited by these sediment flows (Iverson 2003). All three flow types can occur during a single event. The National Research Council (1996) report on *Alluvial-Fan Flooding* considers stream, hyperconcentrated, and debris-flow types of alluvial-fan flooding.

These guidelines address only hazards associated with hyperconcentrated- and debris-flow sediment-water concentrations and not stream-flow flooding on alluvial fans. The term debris flow is used here in a general way to include all flows within the hyperconcentrated- and debris-flow sediment-water concentration range. These are the most destructive flows, and it can be difficult to distinguish between hyperconcentrated and debris flows based on their deposits.

The purpose of a geologic evaluation of debris-flow hazards on alluvial fans is to determine whether or not a hazard exists, describe the hazard, and if needed, provide geologic parameters necessary for hydrologists and engineers to design risk-reduction measures. The objective is to determine active depositional areas, frequency and magnitude (volume) of previous flows, and likely impacts of future sedimentation events.

1.2 *Limitations*

These guidelines identify important issues and general methods for evaluating debris-flow hazards; they do not discuss all methods and are not a step-by-step primer for hazard evaluation. The level of detail appropriate for a particular evaluation depends on several factors, including the type, nature, and location of proposed development; the geology and physical characteristics of the drainage basin, feeder channel, and alluvial fan; the record of previous debris flows; and the level of risk acceptable to property owners and land-use regulators. A uniform level of acceptable risk for debris flows based on recurrence or frequency/volume relationships, such as the 100-year flood or the 2% in 50-year exceedance probability for earthquake ground shaking, has not been established in Utah.

Historical records of sedimentation events in Utah indicate that debris flows are highly variable in terms of size, material properties, and travel and depositional behavior; therefore, a high level of precision for debris-flow design parameters cannot yet be attained. Consequently, prudent design parameters and engineering designs must be used where risk reduction is necessary. Appropriate disclosure of the debris-flow-hazard evaluation to future property owners is also advisable.

The "state-of-the-art" of debris-flow-hazard evaluation continues to evolve as our knowledge of sediment-flow processes advances. As new techniques become available and generally accepted they should be used in future hazard evaluations. Ranges for debris-flow bulking rates, flow volumes, runout distances, deposit areas, and deposit thicknesses have not been established and further research is necessary to quantify the physical characteristics of debris flows in Utah. The methods outlined in these guidelines are considered to be practical and reasonable methods for obtaining planning, design, and risk-reduction information, but these methods may not apply in all cases. The user is responsible for understanding the appropriateness of the various methods and where they apply.

2 DEBRIS-FLOW-HAZARD EVALUATION

A debris-flow-hazard evaluation is necessary when developing on alluvial fans. The evaluation requires application of quantitative and objective procedures to estimate the location and recurrence of flows, assess their impacts, and provide recommendations for risk-reduction measures if necessary. The hazard evaluation must state the intended land use because site usage has a direct bearing on the degree of risk to people and structures.

To evaluate the hazard on active alluvial fans, the frequency, volume (deposit area and thickness), and runout distance of past debris flows must be determined. The geologic methods presented here rely on using the geologic characteristics of existing alluvial-fan

458

deposits as well as drainage basin and feeder-channel sediment-supply conditions to estimate the characteristics of past debris flows. Historical records can provide direct evidence of debris-flow volume, frequency, and depositional area. The observation period in Utah is short, and debris flows either haven't occurred or haven't been documented on many alluvial fans. Therefore, geologic methods provide the principal means of determining the history of debris-flow activity on alluvial fans. Multiple geologic methods should be used whenever possible to compare results of different methods to understand the appropriateness, validity, and limitations of each method and increase confidence in the hazard evaluation.

2.1 *Alluvial-fan evaluation*

Alluvial fans are landforms composed of a complex assemblage of debris-, hyperconcentrated-, and stream-flow deposits. Alluvial-fan geomorphology, sedimentology, and stratigraphy provide a long-term depositional history of the frequency, volume, and depositional behavior of past flows, and provide a geologic basis for estimating debris-flow hazards.

2.1.1 *Defining the active-fan area*

The first step in an alluvial-fan evaluation is determining the active-fan area using mapping and alluvial-fan dating techniques. The active-fan area is where relatively recent deposition, erosion, and alluvial-fan flooding have occurred (Fig. 2). In general, sites of sediment deposition during Holocene time (past 10,000 years; post-Lake Bonneville in northern Utah) are considered active unless proven otherwise. Aerial photographs, detailed topographic maps, and field verification of the extent, type, character, and age of alluvial-fan deposits are used to map active fan areas. The youngest debris-flow deposits are generally indicative of debris flows produced during the modern climate regime and are important for estimating the likely volume and runout for future flows. The National Research Council (1996) report on *Alluvial-Fan Flooding* provides criteria for differentiating active and inactive alluvial fans.

2.1.2 *Mapping alluvial-fan and debris-flow deposits*

Geologic mapping is critical for identifying and describing the active areas of alluvial fans. Mapping of debris-flow and other deposits generally focuses on landforms; the extent, type, character, and age of geologic deposits, specifically individual debris flows; and stratigraphic relations between deposits. Peterson (1981), Christenson & Purcell (1985), Wells & Harvey (1987), Bull (1991), Whipple & Dunne (1992), Doelling & Willis (1995), Hereford et al. (1996), and Webb et al. (1999) provide examples and suggestions for mapping alluvial-fan deposits.
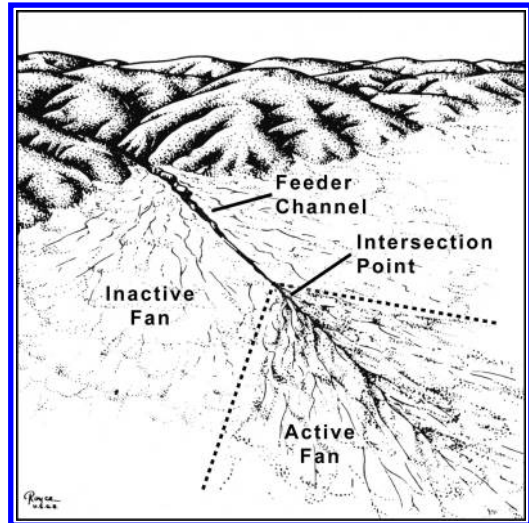
Figure 2. Active and inactive alluvial fans, feeder channel, and intersection point. Modified from Bull (1977). Reproduced with permission by Edward Arnold (Publishers) Ltd., London.
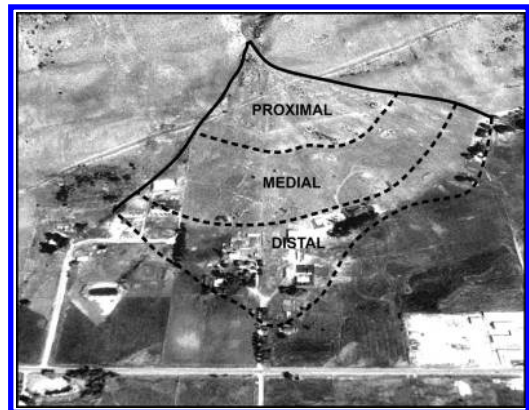
Figure 3. Approximate proximal, medial, and distal fan areas on the Kotter Canyon alluvial fan.

The geomorphic, sedimentologic, and stratigraphic relations recognized during mapping of alluvial-fan deposits provide insight into debris-flow recurrence, volumes, depositional behavior, and therefore debris-flow hazard in the proximal, medial, and distal fan areas (Fig. 3). The intersection point or apex of the active fan is where the feeder channel ends and sediment flows lose confinement and can spread laterally, thin, and deposit sediment (Fig. 2; Blair & McPherson 1994). Most feeder channels lose confinement on the upper fan, but others may incise the inactive upper fan and

459

convey sediment and flood flows farther downfan via a fanhead trench or channel (Fig. 2).

In proximal fan areas, debris flows generally have the highest velocity and greatest flow depth and deposit thickness, and are therefore the most destructive. In distal fan areas, debris flows generally have lower velocities and shallower flow depths and deposits, and therefore are less destructive. Often, distal fan areas are dominated by stream-flow processes only. However, some debris flows may create their own channels by producing levees on the fan and convey sediment farther downfan, or block the active channel and avulse to create new channels. Unpredictable flow behavior is typical of debris flows and must be considered when addressing debris-flow depositional areas, runout distances, and depositional behavior on alluvial fans.

The proximal part of an alluvial fan is generally made up of vertically stacked debris-flow lobes and levees that result in thick and coarse deposits that exhibit the roughest surface on the fan (Fig. 3). Hyperconcentrated flows may be interbedded with debris flows in the proximal fan area, but are generally thinner and have smoother surfaces due to their higher initial water content. Proximal fan deposits generally transition to thinner and finer grained deposits downfan, resulting in smoother fan surfaces in medial and distal fan areas (Fig. 3). Coarser grained sedimentary facies grade downfan into finer grained facies deposited by more dilute sediment flows.

2.1.3 *Determining the age of debris-flow deposits*

Both relative and numerical techniques (Noller et al. 2000) are useful for dating debris-flow deposits and determining the frequency of past debris flows on a fan. Relative dating methods include boulder weathering, rock varnish, soil-profile development (including pedogenic carbonate accumulation), lichen growth, and vegetation age and pattern. The amount of soil development on a buried debris-flow surface is an indicator of the relative amount of time between debris flows at that particular location. Numerical dating techniques include sequential photographs, historical records, dating the age of vegetation, and isotopic dating, principally radiocarbon. Radiocarbon ages of paleosols buried by debris flows can provide closely limiting maximum ages of the overlying flow (Forman & Miller 1989). Radiocarbon ages of detrital charcoal within a debris-flow deposit provide a general limiting maximum age. The applicability and effectiveness of radiocarbon dating of debris-flow events is governed by the presence and type of datable material and available financial resources (Lettis & Kelson 2000).

2.1.4 *Subsurface exploration*

Subsurface exploration using test pits, trenches, and natural exposures is useful in obtaining sedimentologic and stratigraphic information regarding previous debris flows. Test-pit and trench excavations can provide information on flow type, thickness, the across- and down-fan extent of individual flows, and volume based on thickness and area. The type, number, and spacing of excavations depend on the purpose and scale of the hazard investigation, geologic complexity, rate of downfan and across-fan transitions in flow type and thickness, and anticipated risk-reduction measures.

Mulvey (1993) used subsurface stratigraphic data from seven test pits to estimate flow types, deposit thicknesses, the across- and downfan extent of deposits, deposit volumes, and age of deposits to interpret the depositional history of a 2-acre post-Bonneville fan in Centerville. Blair & McPherson (1994) used across- and downfan stratigraphic cross sections to display, analyze, and interpret the surface and subsurface interrelationships of fan slope, deposit levees and lobes, deposit and sediment facies, and grain size. However some stratigraphic data can be problematic. Debris-flow deposits in a sedimentary sequence that have similar grain sizes and lack an intervening paleosol or other distinct layer can be difficult to distinguish. The lack of distinction between individual debris-flow deposits can lead to underestimating debris-flow recurrence and overestimating debris-flow magnitude (Major 1997).

2.2 *Drainage-basin and channel evaluation*

Drainage-basin and channel evaluations determine the conditions and processes that govern sediment supply and transport to the fan surface, and provide an independent check of alluvial-fan evaluations. Drainage-basin and channel evaluation involves estimating the erosion potential of the basin and feeder channel and the volume, grain size, and gradation of sediment that could be incorporated into a debris flow. The evaluation also considers different debris-flow initiation mechanisms. The results of the drainage-basin and channel evaluation are used to estimate the probability of occurrence and design volumes of future debris flows.

2.2.1 *Debris-flow initiation*

Debris flows initiate in the drainage basin and generally require a hydrologic trigger such as intense or prolonged rainfall, rapid snowmelt, and/or groundwater discharge. Intense thunderstorm rainfall, often referred to as cloudburst storms by early debris-flow investigators in Utah (Woolley 1946; Butler & Marsell 1972), has generated numerous debris flows. Conditions in the drainage basin important in initiating debris flows are the basin relief, channel gradient, bedrock and surficial geology, vegetation and wildfire, and land use.

460

In Utah, above-normal precipitation from 1980 through 1986 produced numerous snowmelt-generated landslides (mostly debris slides) that transformed into debris flows and then traveled down channels (Harty 1991). Many of these debris flows occurred during periods of rapid snowmelt and high stream flows, when saturated channel sediment is more easily entrained into debris flows (Santi 1988).

In contrast to wet climate conditions, dry conditions often lead to wildfires that partially or completely burn drainage-basin vegetation, creating conditions for increased runoff and erosion. Wells (1987), Florsheim et al. (1991), Cannon et al. (1995), Meyer et al. (1995), Cannon & Reneau (2000), Kirkham et al. (2000), Robichaud et al. (2000), and Cannon (2001) discuss post-burn conditions and debris-flow susceptibility following wildfires.

2.2.2 *Debris-flow susceptibility of the basin*

Debris-flow susceptibility is related to the erosion and landslide potential of drainage-basin slopes and the volume of erodible sediment stored in drainage-basin channels. Characterizing drainage-basin morphologic parameters, mapping bedrock and surficial geology, and estimating the volume of erodible channel sediment provides information on the likelihood and volume of future debris flows.

Both surficial and bedrock geology play a role in the susceptibility of drainage basins to produce flows. Some bedrock weathers rapidly and provides an abundant sediment supply, whereas resistant bedrock supplies sediment at a slower rate. Exposed cliff-forming bedrock greatly increases runoff.

Surficial geologic deposits that influence the sediment supply include (1) colluvium on steep slopes susceptible to forming debris slides, (2) partially detached shallow landslides, (3) foot-slope colluvium filling the drainage basin channel that may contribute sediment by bank erosion and sloughing, and (4) stream-channel alluvium.

Drainage basins that experience rapid snowmelt events have an increased debris-flow hazard. Pack (1985), Mathewson et al. (1990), and Eblen (1995) determined that in the 1983 and 1984 Davis County debris flows, water infiltration into fractured bedrock aquifers from rapid snowmelt contributed to increased pore-water pressure in steep colluvial slopes that triggered localized colluvial landslides (debris slides) that transformed into debris flows. Santi (1988) suggested that sediment bulking is more likely when passage of a debris flow occurs during periods of stream flow and associated saturated channel sediment, and will result in larger debris-flow volumes.

Wieczorek et al. (1983, 1989) used ground-water levels, the presence of partially detached landslide masses, and estimates of channel sediment bulking to evaluate debris-flow potential along the Wasatch Front between Salt Lake City and Willard. Super-elevated levees, mud lines, and trim lines along channels are evidence of peak discharge. Measurements from these features are useful in estimating velocity and peak flow (Johnson & Rodine 1984). Determining the age of vegetation growing on the levees provides a minimum age of past debris-flow activity.

2.2.3 *Channel sediment bulking and flow-volume estimation*

Sediment supply, erosion conditions, and hydrologic conditions of the drainage basin and channel determine the sediment and water concentration (flow type) and flow volume that reaches an alluvial fan. Estimating channel sediment volume available for entrainment or bulking is critical because study of historical debris flows indicates 80 to 90% of the debris-flow volume comes from the channel (Croft 1967, Santi 1988, Keaton & Lowe 1998). Most estimates of potential sediment bulking are based on a unit-volume analysis of erodible sediment stored in the channel, generally expressed in cubic meters per linear meter of channel (Hungr et al. 1984, VanDine 1985, Williams & Lowe 1990). The sediment volume stored in individual relatively homogeneous channel reaches is estimated, and then the channel-reach volumes are summed to obtain a total volume. The total channel volume is an upper bound volume and needs to be compared to historical (VanDine 1996) and mapped alluvial-fan flow volumes to derive a design volume. If easily eroded soils and slopes prone to landsliding are present, then appropriate volumes for landslide and hillslope contributions determined from other drainage basin landslide volumes should be added to the channel volume.

Estimating a potential sediment-bulking rate requires field inspection of the drainage basin and channels. Measuring cross-channel profiles and estimating the erodible depth of channel sediment is necessary to estimate the sediment volume available for bulking (Fig. 4). Even though a great deal of geologic judgment may be required to make the volume estimate, this is probably the most reliable and practical method for bedrock-floored channels. The design volume should not be based solely on empirical bulking of specific flood flows (for example, bulking a 100-year flood with sediment) because empirical bulking does not consider shallow landslide-generated debris flows (National Research Council 1996), channel bedrock reaches with no stored sediment, and the typically longer recurrence period of debris flows. The channel inspection should also provide a description of the character and gradation of sediment and wood debris that could be incorporated into future debris flows.

Hungr et al. (1984), VanDine (1985), and Williams & Lowe (1990) use historical flow volumes and channel
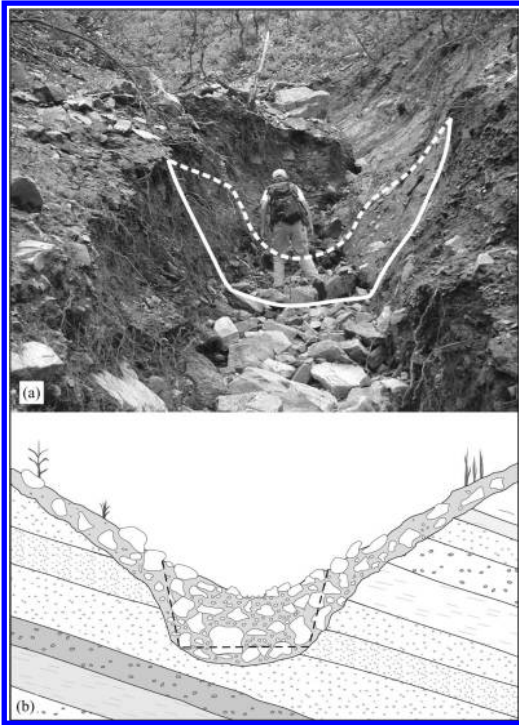
Figure 4. Channel sediment and cross section used to estimate sediment volume available for bulking. (a) Channel erosion and sediment bulking from the September 10, 2002, fire-related debris flow on Dry Mountain east of Santaquin, Utah. The solid line shows the eroded channel after the debris flow, the dashed line shows the estimated channel prior to debris flow passage. (b) Sketch of channel cross-section showing stored channel sediment above bedrock. The dashed line shows the estimated upper-bound width and depth of channel sediment available for sediment bulking.

sediment bulking rates to estimate potential debris-flow volumes. Williams & Lowe (1990), following the 1983 debris flows in Davis County, compared cross-channel profiles of drainages that had discharged historical debris flows with those that had not to estimate the amount of channel sediment bulked by historical flows. They estimated an average bulking rate of 30 cubic meters per linear meter (m^3/m) of channel for historical debris flows and used it to estimate flow volumes for drainage basins without historical debris flows, but recommended using this estimate for perennial streams in Davis County only. Bulking rates for intermittent and ephemeral streams are generally lower. For example, Mulvey & Lowe (1992) estimated a bulking rate of $13\,m^3/m$ for the 1991 Cameron Cove debris flow in Davis County. Some of the fire-related debris flows at the 2002 Dry

Mountain/Santaquin event (McDonald & Giraud 2002) have estimated bulking rates of $4\,m^3/m$ of ephemeral channel. Hungr et al. (1984), VanDine (1985, 1996), and Williams & Lowe (1990) all concluded that channel length and channel sediment storage are the most important factors in estimating future debris-flow volumes.

3 DEBRIS-FLOW-RISK REDUCTION

Eisbacher & Clague (1984), Hungr et al. (1987), and VanDine (1996) group debris-flow-risk reduction into two categories: passive and active. Passive methods involve avoiding debris-flow-hazard areas either permanently or at times of imminent danger. Passive methods do not prevent, control, or modify debris flows. Active methods modify the hazard using debris-flow-control structures to prevent or reduce the risk. These debris-flow-control structures require engineering design using appropriate geologic inputs. In terms of development on alluvial fans, active risk-reduction measures with control structures generally attempt to maximize the buildable space and provide a reasonable level of protection.

Hungr et al. (1987) and VanDine (1996) divide debris-flow-control structures along lower channel reaches and on alluvial fans into two basic types: open structures (which constrain flow) and closed structures (which contain debris). Examples of open debris-flow-control structures include unconfined deposition areas, impediments to flow (baffles), check dams, lined channels, lateral walls or berms, deflection walls or berms, and terminal walls, berms, or barriers. Examples of closed debris-flow-control structures include debris racks, or other forms of debris-straining structures located in the channel, and debris barriers and associated storage basins with a debris-straining structure (outlet) incorporated into the design.

4 DESIGN CONSIDERATIONS FOR RISK REDUCTION

The debris-flow hazard at a particular site depends on the site's location on the alluvial fan. Both debris-flow impact and sediment burial are more likely and of greater magnitude in proximal fan areas than in medial and distal fan areas (Fig. 3). Decisions regarding acceptable risk and appropriate control-structure design involve weighing the probability of occurrence in relation to the consequences of a debris flow and the residual risk level after implementing risk-reduction measures. Therefore, hazard evaluations estimate the likely size, frequency, and depositional

462

area of debris flows on an alluvial fan as accurately as possible.

4.1 *Considering frequency in design*

The frequency of past debris flows on an alluvial fan is a fundamental indicator of future debris-flow activity. To address the past frequency of debris flows, detailed geologic studies involving geochronology are generally required. Little or nothing is known about the past frequency of debris flows on most alluvial fans in Utah. Studies by Keaton (1988), Lips (1993), and Mulvey (1993) indicate that large, destructive debris flows on the alluvial fans they studied have return periods of a few hundred to thousands of years. However, return periods vary widely among alluvial fans and few data exist to quantify debris-flow frequency-volume relations. Generally accepted return periods for design of debris-flow risk-reduction measures based on probabilistic models do not exist, unlike for earthquake ground shaking and flooding, which have established design return periods of 2,500 years (International Building Code) and 100 years (Federal Emergency Management Agency, National Flood Insurance Program), respectively. Although Keaton (1988) and Keaton et al. (1991) developed a probabilistic model for debris flows in Davis County where a relatively complete record of historical debris flows exists, the high degree of irregularity and uncertainty in return periods limited their results and the practical application of their model. In some cases rather than assigning an absolute probability of debris-flow occurrence, many debris-flow practitioners assign a relative probability of occurrence (VanDine 1996) based on frequencies in similar basins and fans in the geographic areas that have experienced historical debris flows.

4.2 *Debris-flow-hazard zones*

Debris-flow-hazard zones identify potential impacts and associated risks, help determine appropriate risk-reduction measures, and aid in land-use planning decisions. Hungr et al. (1987) outline three debris-flow-hazard zones: (1) a direct impact zone where high-energy flows increase the risk of impact damage due to flow velocity, flow thickness, and the maximum clast size; (2) an indirect impact zone where impact risk is lower, but where damage from sediment burial and debris-flow and water transport is high; and (3) a flood zone potentially exposed to flooding due to channel blockage and water draining from debris deposits. These zones roughly equate to proximal, medial, and distal fan areas (Fig. 3). Historical debris-flow records, deposit characteristics, and detailed topography are required to outline these hazard zones. Site-specific studies are required

to define which zone applies to a particular site and to determine the most appropriate land use and risk-reduction techniques to employ.

4.3 *Estimating geologic parameters for engineering design*

Geologic estimates of debris-flow design parameters are necessary for engineering design of risk-reduction structures. The most appropriate data often come from historical or late Holocene debris flows that can be mapped on the fan surface.

Geologic parameters required for engineering design vary depending on the risk-reduction structure proposed. Engineering designs for debris-flow risk-reduction structures are site specific (VanDine et al. 1997), and generally involve quantifying specific fan, feeder channel, deposit, and flow parameters. Geomorphic fan parameters include areas of active deposition, surface gradients, surface roughness (channels, levees, lobes), and topography. Feeder channel parameters include channel gradient, channel capacity, and indications of previous flows. Deposit parameters include area, surface gradient, thickness, gradation, and largest clast size. Flow parameters are difficult to determine unless measured immediately after an event, and are often inferred from deposit characteristics or evidence from the feeder channel. The flow parameters include estimates of flow type(s), volume, frequency, depth, velocity, peak discharge, and runout distance.

Debris flows can have significantly higher peak discharge than stream-flow flooding. Estimation of peak discharge is critical because it is related to maximum velocity and flow depth, impact forces, ability to overrun protective barriers, and runout distance (Hungr 2000). VanDine (1996) states that debris-flow discharges can be up to 40 times greater than a 200-year flood, which shows the importance of carefully estimating peak discharge when designing protective structures.

Estimating debris-flow volume is necessary where debris storage basins are planned. Because debris-flow behavior is difficult to predict and flows difficult to route, debris storage basins and deflection walls or berms are common methods of debris-flow risk reduction. For debris basin capacity, the thickness and area of individual flows on the alluvial fan and erodible channel sediment volumes are needed to estimate design debris volumes. Estimates of sediment stored in channels are usually maximum or "worst-case" volumes that represent an upper volume limit. Channel estimates may exceed the alluvial-fan estimates because typically all channel sediment is not eroded and deposited on the fan, and the channel estimate includes suspended sediment transported off the fan by stream flows. Conversely, the alluvial-fan estimate may exceed the channel estimate if a recent large

flow has removed most channel sediment. VanDine (1996) considers the design volume to be the reasonable upper limit of material that will ultimately reach the fan.

Geologic design parameters are also needed for the design of other types of engineered risk-reduction structures. For deflection walls and berms or for foundation reinforcement, fan gradient, flow type (debris versus hyperconcentrated versus stream), flow depth, peak flow, flow velocity, and debris size and gradation are important to ensure that the structure has the appropriate height, side slope, and curvature to account for runup and impact forces. For design of debris barriers, flow volume, depth, deposition area, and gradient are needed to determine the appropriate storage volume. The size and gradation of debris, and the anticipated flow type are important in the design of debris-straining structures. Flow types are important to help estimate associated water volumes. Baldwin et al. (1987), VanDine (1996), Deng (1997), and VanDine et al. (1997) describe other design considerations for debris-flow-control structures.

5 SUMMARY

These guidelines provide methods for evaluating debris-flow hazards on alluvial fans in Utah. Analysis of alluvial-fan deposits provides the geologic basis for estimating frequency and potential volume of debris flows and describing debris-flow behavior. Surficial geologic mapping, dating, and subsurface exploration can provide data to determine deposit thicknesses, flow volumes, flow types, and flow frequency. Analysis of the erosion and landslide potential of drainage basin slopes and the volume of erodible sediment stored in drainage basin channels provides data to estimate the volume and likelihood of future debris flows. Measuring cross-channel profiles and estimating the erodible depth of channel sediment provides data to estimate the available sediment volume. Hazard zones may be outlined on the alluvial fan to understand potential effects of debris flows based on flow velocity, flow thickness, and flooding, and to determine appropriate risk-reduction measures. Geologic estimates of debris-flow-design parameters are necessary for the engineering design of risk-reduction structures.

Even though geologic methods outlined in these guidelines use quantitative and objective procedures, estimating design parameters for risk-reduction structures has practical limits. Many debris-flow design-parameter estimates have high levels of uncertainty and often represent a best approximation of a complex natural process; therefore, appropriate limitations and engineering factors of safety must be incorporated in risk-reduction-structure design. Investigators must clearly state the limitations of the evaluation methods employed and the uncertainties associated with design-parameter estimates.

REFERENCES

Baldwin, J.E., Donley, H.J. & Howard T.R. 1987. On debris flow/avalanche mitigation and control, San Francisco Bay area, California. In Costa & Wieczorek (eds), *Geol. Soc. of America Reviews in Eng. Geol.* 12: 223–236.

Beverage, J.P. & Culbertson, J.K. 1964. Hyperconcentrations of suspended sediment. *ASCE, J. of the Hydraulics Div.* 90(HY6): 117–126.

Blair, T.C. & McPherson, J.G. 1994. Alluvial fan processes and forms. In Abrahams & Parsons (eds), *Geomorph. of Desert Environments*: 355–402. London: Chapman & Hall.

Bull, W.B. 1977. The alluvial fan environment. *Progress in Physical Geography* 1(2): 222–270.

Bull, W.B. 1991. *Geomorphic responses to climatic change.* New York: Oxford University Press.

Butler, E. & Marsell R.E. 1972. Developing a state water plan, cloudburst floods in Utah, 1939–69. *Utah Department of Natural Resources Division of Water Resources Cooperative-Investigations Report* 11.

Cannon, S.H. 2001. Debris-flow generation from recently burned watersheds. *Env. and Eng. Geosci.* 12(4): 321–341.

Cannon, S.H., Powers, P.S., Pihl, R.A. & Rogers W.P. 1995. Preliminary evaluation of the fire-related debris flows on Storm King Mountain, Glenwood Springs, Colorado. *USGS Open-File Report* 95–508.

Cannon, S.H. & Reneau, S.L. 2000. Conditions for generation of fire-related debris flows, Capulin Canyon, New Mexico. *Earth Surface Processes and Landforms* 25: 1103–1121.

Christenson, G.E. & Purcell, C. 1985. Correlation and age of Quaternary alluvial-fan sequences, Basin and Range Province, southwestern United States. In Weide (ed), *Soils and Quaternary geology of the southwestern United States, Geological Society of America Special Paper* 203: 115–122.

Costa, J.E. 1988. Rheologic, morphologic, and sedimentologic differentiation of water floods, hyperconcentrated flows, and debris flows. In Baker et al. (eds), *Flood Geomorphology*: 113–122. New York: John Wiley and Sons.

Croft, A.R. 1967. Rainstorm debris floods, a problem in public welfare. *University of Arizona, Agricultural Experiment Station Report* 248.

Deng, Z. 1997. Impact of debris flows on structures and its mitigation. *Ph.D. dissertation*, University of Utah.

Deng, Z., Lawton, E.C., May, F.E., Smith, S.W. & Williams, S.R. 1992. Estimated impact forces on houses caused by the 1983 Rudd Creek debris flow. In *Conference on Arid West Floodplain Management Issues, Las Vegas, Nevada, Proc. Assoc. of State Floodplain Managers Inc.*: 103–115.

Doelling, H.H. & Willis, G.C. 1995. Guide to authors of geological maps and text booklets of the Utah Geological Survey. *Utah Geol. Survey Circular* 89.

Eblen, J.S. 1995. A probabilistic investigation of slope stability in the Wasatch Range, Davis County, Utah. *Utah Geological Survey Contract Report* 95–3.

Eisbacher, G.H. & Clague, J.J. 1984. Destructive mass movements in high mountains – hazard and management. *Geological Survey of Canada Paper* 84–16.

Florsheim, J.L., Keller, E.A. & Best, D.W. 1991. Fluvial sediment transport in response to moderate storm flows following chaparral wildfire, Ventura County, southern California. *Geol. Soc. of America Bull.* 103(4): 504–511.

Forman, S.L. & Miller, G.H. 1989. Radiocarbon dating of terrestrial organic material. In Forman (ed), *Dating methods applicable to Quaternary geologic studies in the western United States, Utah Geological and Mineral Survey Miscellaneous Publication* 89–7: 2–9.

Harty, K.M. 1991. Landslide map of Utah. *Utah Geological and Mineral Survey Map* 133.

Hereford, R., Thompson, K.S., Burke, K.J. & Fairley, H.C. 1996. Tributary debris fans and the late Holocene alluvial chronology of the Colorado River, eastern Grand Canyon, Arizona. *Geol. Soc. of America Bull.* 108(1): 3–19.

Hungr, O. 2000. Analysis of debris flow surges using the theory of uniformly progressive flow. *Earth Surface Process and Landforms* 25: 483–495.

Hungr, O., Morgan, G.C. & Kellerhals, R. 1984. Quantitative analysis of debris torrent hazards for design of remedial measures. *Can. Geotech. J.* 21: 663–677.

Hungr, O., Morgan, G.C., VanDine, D.F. & Lister, D.R. 1987. Debris flow defenses in British Columbia. In Costa & Wieczorek (eds), *Geol. Soc. of America Reviews in Eng. Geol.* 7: 201–222.

Iverson, R.M. 2003. The debris-flow rheology myth. In Rickenmann & Chen (eds), *Proc. of the Third Int. Conf. on Debris-Flow Hazards Mitigation – Mechanics, Prediction, and Assessment, Davos*: 303–314. Rotterdam: Millpress.

Johnson, A.M. & Rodine, J.R. 1984. Debris flow. In Brunsden & Prior (eds), *Slope Instability*: 257–361. New York: John Wiley & Sons.

Keaton, J.R. 1988. A probabilistic model for hazards related to sedimentation processes on alluvial fans in Davis County, Utah. *Ph.D. dissertation*, Texas A & M University.

Keaton, J.R., Anderson, L.R. & Mathewson, C.C. 1991. Assessing debris flow hazards on alluvial fans in Davis County, Utah. *Utah Geol. Survey Contract Report* 91–11.

Keaton, J.R. & Lowe, M. 1998. Evaluating debris-flow hazards in Davis County, Utah – engineering versus geological approaches. In Welby & Gowan (eds), *Geol. Soc. of America Reviews in Eng. Geol.* 12: 97–121.

Kirkham, R.M., Parise, M. & Cannon, S.H. 2000. Geology of the 1994 South Canyon fire area, and a geomorphic analysis of the September 1, 1994 debris flows, South Flank Storm King Mountain, Glenwood Springs, Colorado. *Colorado Geol. Survey Special Publication* 46.

Lettis, W.R. & Kelson, K.I. 2000. Applying geochronology in paleoseismology. In Noller et al. (eds), *Quaternary Geochronology*: 479–495. Washington, D.C.: AGU.

Lips, E.W. 1993. Characteristics of debris flows in central Utah, 1983. *Utah Geol. Survey Contract Report* 93–3.

Major, J.J. 1997. Depositional processes in large-scale debris-flow experiments. *J. of Geol.* 105: 345–366.

Mathewson, C.C., Keaton, J.R. & Santi, P.M. 1990. Role of bedrock ground water in the initiation of debris flows and sustained post-flow stream discharge. *Bull. of the Assoc. of Eng. Geol.* 27(1): 73–83.

McDonald, G.N. & Giraud, R.E. 2002. September 12, 2002 fire-related debris flows east of Santaquin and Spring Lake, Utah County, Utah. *Utah Geol. Survey Tech. Rep.* 02–09.

Meyer, G.A., Wells, S.G. & Jull, A.J.T. 1995. Fire and alluvial chronology in Yellowstone National Park – climatic and intrinsic controls on Holocene geomorphic processes. *Geol. Soc. of America Bull.* 107(10): 1211–1230.

Mulvey, W.E. 1993. Debris-flood and debris-flow hazard from Lone Pine Canyon near Centerville, Davis County, Utah. *Utah Geol. Survey Report of Investigation* 223.

Mulvey, W.E. & Lowe, M. 1992. Cameron Cove subdivision debris flow, North Ogden, Utah. *Technical reports for 1990–91, Utah Geol. Survey Report of Investigation* 222: 186–191.

National Research Council, 1996. *Alluvial fan flooding*. Washington D.C.: National Academy Press.

Noller, J.S., Sowers, J.M., Colman, S.M. & Pierce, K.L. 2000. Introduction to Quaternary geochronology. In Noller et al. (eds), *Quaternary Geochronology*: 1–10. Washington D.C.: AGU.

Pack, R.T. 1985. Multivariate analysis of relative landslide susceptibility in Davis County, Utah. *Ph.D. dissertation*. Utah State University.

Peterson, F.F. 1981. Landforms of the Basin and Range Province defined for soil survey. *Nevada Agricultural Experiment Station Technical Bulletin* 28.

Pierson, T.C. & Costa, J.E. 1987. A rheologic classification of subaerial sediment-water flows. In Costa & Wieczorek (eds), *Geol. Soc. of America Reviews in Eng. Geol.* 7: 1–12.

Robichaud, P.R., Beyers, J.L. & Neary, D.G. 2000. Evaluating the effectiveness of postfire rehabilitation treatments. *U.S. Dept. of Agri. Forest Service General Tech. Report* RMRS-GTR-63.

Santi, P.M. 1988. The kinematics of debris flow transport down a canyon. *Masters thesis*. Texas A&M University.

VanDine, D.F. 1985. Debris flows and debris torrents in the southern Canadian Cordillera. *Can. Geotech. J.* 22: 44–68.

VanDine, D.F. 1996. Debris flow control structures for forest engineering. *British Columbia Ministry of Forests Research Program Working Paper* 22.

VanDine, D.F., Hungr, O., Lister, D.R. & Chatwin, S.C. 1997. Channelized debris flow mitigative structures in British Columbia, Canada. In Chen (ed), *Debris-Flow Hazards Mitigation, Proc. of First Int. Conf., San Francisco*: 606–615. ASCE.

Webb, R.H., Melis, T.S., Griffiths, P.G., Elliott, J.G., Cerling, T.E., Poreda, R.J., Wise, T.W. & Pizzuto, J.E. 1999. Lava Falls rapid in the Grand Canyon – effects of late Holocene debris flows on Colorado River. *USGS Professional Paper* 1591.

Wells, W.G. 1987. The effects of fire on the generation of debris flows in southern California. In Costa & Wieczorek (eds), *Geol. Soc. of America Reviews in Eng. Geol.* 7: 101–114.

Wells, S.G. & Harvey, A.M. 1987. Sedimentologic and geomorphic variations in storm-generated alluvial fans,

Howgill Fells, northwest England. *Geol. Soc. of America Bull.* 98(2): 182–198.

Whipple, K.X. & Dunne, T. 1992. The influence of debris-flow rheology on fan morphology, Owens Valley, California. *Geol. Soc. of America Bull.* 104(7): 887–900.

Wieczorek, G.F., Ellen, S., Lips, E.W., Cannon, S.H. & Short, D.N. 1983, Potential for debris flow and debris flood along the Wasatch Front between Salt Lake City and Willard, Utah, and measures for their mitigation. *USGS Open-File Report* 83–635.

Wieczorek, G.F., Lips, E.W. & Ellen, S. 1989. Debris flows and hyperconcentrated floods along the Wasatch Front, Utah, 1983 and 1984. *Bull. of the Assoc. of Eng. Geol.* 26(2): 191–208.

Williams, S.R. & Lowe, M. 1990. Process-based debris-flow prediction method. In French (ed), *Proceedings of Hydraulics/Hydrology of Arid Lands, San Diego*: 66–71. ASCE.

Woolley, R.R. 1946. Cloudburst floods in Utah, 1850–1938. *USGS Water Supply Paper* 994.

Investigation of the origin and magnitude of debris flows from the Payhua Creek basin, Matucana area, Huarochirí Province, Perú

L. Fídel Smoll, A. Guzman Martinez, J. Zegarra Loo & M. Vilchez Mata
Instituto Geológico Minero y Metalúrgico, Direccion de Geológia Ambiental, San Borja, Lima, Perú

J. Colque Tula
Sociedad Científica Peruana Arqueología, Lima, Perú

L.E. Jackson, Jr.
Geological Survey of Canada, Terrain Sciences Division, Vancouver, BC, Canada

ABSTRACT: The small city of Matucana (population 5800), Province of Huarochirí, Perú is located on the flood plain of Rimac River in Andes Occidental, approximately 75 km east of Lima at an elevation of 2390 m (area of 11° 50.489' S, 76° 22.857' W). Adjacent ridges and mountain peaks rise to 5000 m. Matucana shares a 300 m wide valley bottom with two transportation arteries: Carretera Central, the only highway in Perú connecting the Amazon basin to the Pacific Coast and Ferrocarril Central, the highest standard gauge railway in the world which services mines and communities in the Andes. The present course of Rimac River is controlled by a dike and fill for the highway and railroad. These structures confine it to the northern portion of its flood plain. Consequently, parts of Matucana are lower in elevation than the bed of Rimac River. Payhua Creek (PC), a steep, debris-flow-prone tributary to Rimac River, has built an extensive fan at the upstream end of the city. Debris flows from PC has dammed Rimac River and diverted it into Matucana. This type of disaster occurred 1959 and 1983 when heavy precipitation occurred in the normally arid Andes Occidental. The 1959 event was particularly notable as it destroyed 90% of Matucana with loss of life. Although these events were not well documented, investigation of the PC fan and documentation of 1983 deposits on the fan indicate that the 1983 debris flow had a volume in the 0.12×10^6 to 10^6 m^3 range. Investigation of surficial and bedrock geology including mapping of all landslides in PC basin was carried out in 2004. A landslide complex immediately west of Payhua village is the most significant source of debris flow sediment in the basin. Incision of an unfavourable succession of andesite flows overlying a pervasively fractured tuff is responsible for the concentration of landslides in the Payhua village area. The area affected by landsliding in this area has increased by a factor of five since 1951. The PC basin upstream from Payhua has been a relatively small source of debris flows during the past 600 to 800 years based upon archaeological evidence. Exposures of debris flow deposits in the PC fan indicate that debris flow events larger than those of 1959 and 1983 have occurred in the recent geologic past. Matucana has also grown significantly since 1983 and has further encroached on the Rimac River flood plain and the PC fan. As a result, if debris flows of the magnitude of those in 1959 and 1983 occur, direct burial of the upstream area of Matucana by debris flows is likely.

1 INTRODUCTION

1.1 *Geoscience for Andean Communities*

The Multinational Andean Project: Geoscience for Andean Communities (MAP:GAC) began June 28, 2002 and includes Argentina, Bolivia, Canada, Colombia, Chile, Ecuador, Peru, and Venezuela. The project goal is to contribute to improving the quality of life for the people of the Andes by reducing the negative impact of natural hazards (earthquakes, landslides, and volcanoes). Through the project, updated and integrated geoscience and geospatial information on natural hazards will be provided for land use planning and, natural hazard mitigation. As a part of this project, one or more pilot study areas were selected in each country. These areas contain natural hazards that are typical of those that face Andean peoples in their respective countries. Investigations of hazards within the pilot areas develop geotechnical skills, methodologies and insights that are easily applied in similar environments throughout the Andes of the participating country. Inundation by channelized debris flows and

467

debris-flow-induced hydrological flooding in the small city of Matucana in Andes Occidental are typical of hazards faced by communities throughout this region. Debris flows from the adjacent small mountainous drainage basin of Payhua Creek (*Quebrada Payhua*), diverted Rimac River (*Río Rimac*) through. Matucana in 1959 and 1983. They present a continuing hazard to the community. On this basis, Matucana and Payhua Creek basin were chosen as a pilot study area as a part of MAP:GAC. This paper reports the results of field-work and accumulation of documentary evidence in the project area up to December 2004.

2 PHYSIOGRAPHY AND SETTING

2.1 *Matucana area*

Matucana (population 5800) is located in Huarochirí Province, Perú (Fig. 1) approximately 75 km east of Lima at an elevation of 2390 m above sea level (a.s.l.) (area of 11° 50.489' S, 76° 22.857' W). Matucana is situated on a 300 m wide flood plain along the floor of the deep and steep-sided Rimac River (RR) canyon in Andes Occidental. Adjacent ridges and mountain peaks rise to 5000 m within ten kilometres of Matucana. It shares the valley bottom with two strategic transportation arteries: Carreterra Central, the only highway in Perú connecting the Amazon basin to the Pacific Coast and Ferrocarril Central, the highest standard gauge railway in the world which services mines and communities in the Andes to the east. The present course of Rimac River is controlled by a dyke and fills for the highway and railroad. These structures confine the river to the northern portion of its flood plain. Consequently, parts of Matucana are lower in elevation than the bed of RR.

2.2 *Payhua Creek basin*

Payhua Creek (PC) basin lies immediately to the north of Matucana. It is an elongate basin 6.1 km in length and less than 3 km in width at the widest point with a total area of 14.9 km^2. It rises to 4760 m a.s.l. PC lies within a narrow to gorge-like valley. Its overall gradient is 21°. However, its profile is marked by numerous waterfalls along nearly vertical reaches of the channel, particularly along the lower 2 km. Slopes along the gorge are commonly 50°–70°. The basin is underlain by andesitic to rhyolitic flows, breccias and pyroclastic complexes of Cenozoic age (Instituto Geologico Minero y Metalurgico 1995). The basin is asymmetric from west to east reflecting a general dip of flow complexes to the east and south. Scarp slopes along the east side of the basin average around 50° to 60° over elevation-changes of 1000 m. Dip slopes along the western margin of the basin are in the 35° to 40° range over elevation-changes of about 1000 m. However, nearly vertical outcrops of 50 to 100 m can be found
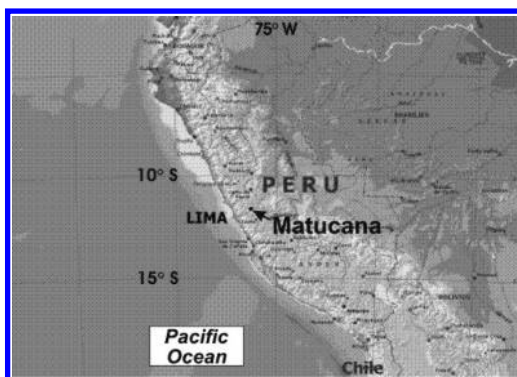

Figure 1. Location of Matucana/Payhua Creek project area.

throughout the basin and rockfall is a problem along the bases of many slopes.

2.2.1 *Neotectonism and surficial geology*
Andes Occidental is a tectonically active mountain belt. It is experiencing rapid uplift and fluvial incision. Incised relict alluvial fans are present in the basin hundreds of m above the floor of RR valley. Although there are no quantitative estimates of uplift rates for the study area, uplift rates in the order of 0.2 to 0.3 mm/yr since the Miocene have been determined for the adjacent central Andes (Gregory-Wodzicki 2000).

2.2.2 *Land use in Payhua*
Mountainsides in PC basin have been extensively terraced for farming and grazing for more than 1000 years. These terraces extend to ridge-tops in many parts of the basin. The terraced fields are irrigated up to about 3500 m and support a variety of crops. Terraced fields above the limits of irrigation presently serve as small pastures.

2.2.3 *Climate and debris flow activity*
Climate at the elevation of Matucana is temperate and dry: average temperature ranges from 27°C during the summer (mid December to March) to 19°C during the winter (mid June to September). Temperature decreases progressively with altitude: below-freezing temperatures occur every night at elevations above about 4200 m. Total annual rainfall averages 239 mm at Matucana. About 70 percent of it falls between January and March. Rainfall patterns are disrupted by El Niño climatic events in the equatorial Pacific Ocean and atmosphere. These events have occurred roughly four years apart in recent years. They bring intense rains to the RR basin and commonly trigger debris flows in the region (Kuoiwa 2002).

2.2.4 *Payhua Creek fan*
PC has built an extensive fan at the upstream end of Matucana where PC joins RR (Fig. 2). It is about 400 m
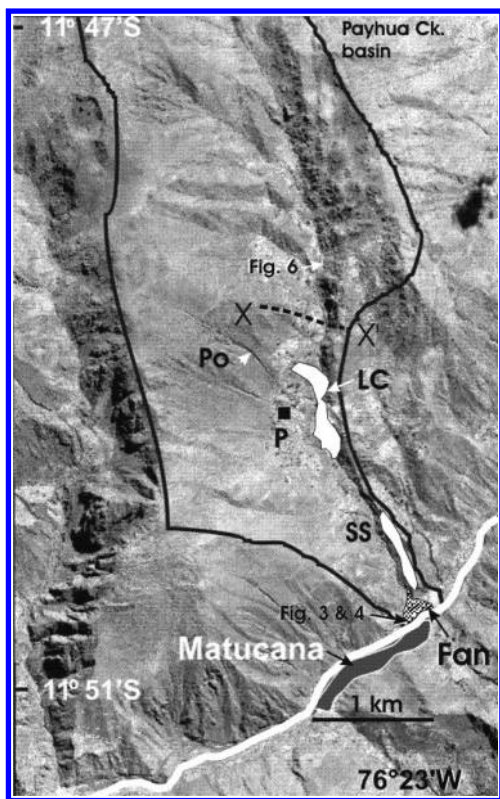
468

Figure 2. A Quickbird satellite image of the Payhua Creek area, Aug. 13, 2004: X-X′- boundary between upper and lower basin, P- Payhua village, Po- *Patipunco* ravine, LC-Payhua landslide complex, SS-sagging slope block, white line-Rimac River (Ferrocarril Central and Carratera Central). Payhua Creek joins Rimac River and the extreme southwest point of the fan.

Figure 3. Bouldery debris flow diamicton near the confluence of Payhua Creek with Rimac River. Oval indicates a man standing next to a 2 m stadia rod.

Figure 4. Looking up the channel of Payhua Creek in the opposite direction from Fig. 3. The channel is deeply incised into Payhua fan. Circle indicates a 1.5 m tall man. Cross sectional area of the channel is approximately $300 \, m^3$. The 1983 debris flow exceed the capacity of the channel.

in length from apex to its southernmost extent. Its overall surface slope is approximately 9° (it has been extensively modified into terraced fields for agriculture). It terminates in a cliff bank created by incision of the fan by RR. The fan is almost entirely underlain by bouldery debris flow diamicton sediments. Poorly sorted bouldery gravel beds, associated with muddy turbulent stream flow, are locally interstratified with diamictons. Boulders 1 m in diameter are common within the diamictons. Individual boulders up to 3 m are present (Figs. 3–4).

3 PREVIOUS WORK

The physiography, geology, climate and hydrology of the Matucana area including past debris flows and floods from PC, are summarized in a report prepared for District of Matucana in 2000 (Martinez Vargas & Medina Rengito 2000).

4 THIS STUDY

4.1 *Objectives*

Field investigations in Matucana and the PC basin in September, 2004 with the objectives of:

1. Mapping of the distribution of surficial sediments and landslides within QP basin with the ultimate goal of understanding the origin of debris flows in the basin.
2. Determination of the past scale and frequency of debris flows in the basin and estimation of the volume of future events.

469

3. Comparison of the present area of landsliding in the basin with past distributions based upon archival air photo coverage.

A draft terrain inventory map PC basin was completed using a terrain inventory legend scheme modified from Howes & Kenk (1997). This included the location of all active landslides within the basin and an inventory of areas affected by rapid mass movement. A Quickbird satellite image (1 m resolution) of the basin that was taken on Aug. 13, 2004, was used as a base for mapping at a scale of 1:10 000 (fig. 2). The final, digital version of the map will be prepared following the generation of a digital elevation model (DEM) and detailed topographic map of the basin to be completed in 2005. Residents of Matucana and the mountain village of Payhua were interviewed in order to reconstruct debris flow events back to 1959 and arrive at order of magnitude estimates of volumes and maximum discharges of past debris flow events. Archaeological techniques were used to determine the long-term stability of fans and terraced hillsides. These included the use of widespread pottery fragments from the pre-Inca period (pre-1400 AD) and distinctive construction of retaining walls from the same period to document absence of debris flow activity on terraced fields (retaining walls destroyed by debris flows during the post European contact period were rebuilt in a different manner). Major landslides within the basin were investigated in order to determine the geological and geomorphological conditions that led to the failure. Sections of the channel of PC containing sediment were surveyed in order to estimate quantities of sediment contained in the channel and along its margins that could be mobilized into future debris flows following the general methodology of Hungr et al. (1984). Estimates of the magnitude of future debris flows based upon this data will be presented in a future paper.

5 PREVIOUS DEBRIS FLOW EVENTS

5.1 *Historic debris flows*

The knowledge base with respect to previous debris flows from PC largely consists of oral accounts of local residents and limited newspaper coverage. As noted above, debris flows from PC blocked RR diverting it through Matucana in February, 1959 and March, 1983. The 1959 event resulted in several deaths was particularly destructive because adobe brick was extensively used for construction at that time. Many buildings were literally washed away by the flood. A smaller event that only affected terraced agricultural fields on the PC fan occurred in 1941. Reliable records of debris flows prior to 1941 do not exist. Local weather records are not available for the

debris flow events. Consequently, antecedent conditions are not known beyond the 1983 event occurring during an El Niño year. Many debris flow events occurred during that year in the Matucana area. RR is confined to an incised channel with near vertical walls between the PC fan to the north and the fan of Huaripachi Creek (*Quebrada Huaripachi*) immediately to the south. Topography dictates that diversion of RR in both cases took place at the downstream limits of the fans where the deeply incised channel of PC joins in the RR. No part of Matucana, which was considerably smaller in area at the time of those events, was directly buried by debris flows although the Ferrocarril Central tracks were buried. It is reasonable to assume that the railway fill acted as a protective dyke for Matucana to some degree. Investigation of terrace fields on the PC fan determined that retaining walls were reconstructed following the 1983 event. Accounts vary as to the limits of the 1983 and 1959 flows on the fan. Some accounts indicate that the entire 4.8 ha fan was covered.

5.2 *Granulometry and clay mineralogy*

Granulometric analysis, determination of Atterberg limits and clay mineralogy of two debris flow matrix samples from the fan and a third sample from higher in the PC basin indicate them to be low plasticity to a non-plastic silty sands ranging from SC to SM in the Unified Soil Classification scheme. The mineralogy of the small clay-size fraction, as determined by X-ray diffraction, is dominated by clay-size, non-clay minerals such as quartz, plagioclase, augite, calcite, muscovite and hematite. True clay minerals such as chlorite or montmorillonite make up only one or two percent of clay-size particles. The mineralogy reflects rapid erosion and predominance of physical weathering over chemical weathering in a tectonically active and arid drainage basin.

5.3 *Estimates of historic debris flow magnitudes*

An order of magnitude volume estimate for the size of the 1983 debris flow (the 1959 event is assumed to be of similar magnitude because of similar effects) can be made based upon field observations in and around the channel of PC. The channel incises PC fan to a depth of about 14 m over a total distance of approximately 400 m. Its mean cross-sectional area is about 300 m^2. In order for a flow to spill out on to the fan surface, it would fill the channel and would consequently have a minimum volume of about 120,000 m^3. Assuming similar incised channel dimensions, this volume was exceeded during the 1983 event with the burial of adjacent fields on the fan surface. Such a discharge would be sufficient to dam and divert RR. However, filling of the PC fan channel to overflow represents the peak discharge of an event with an

470

extensive discharge of debris into the RR channel prior and subsequent to maximum peak discharge. Numerous authors have demonstrated proportionality relationships between debris flow maximum instantaneous discharge (Q_{max}) in m^3/s and total discharge (Q_{total}) in m^3 so that $Q_{total} \sim n\, Q_{max}$ where n can range from 10 to 80 s or more depending on the study, e.g. Hungr et al. (1984), Jakob & Jordan (2001), and cases cited therein. Unfortunately, there is no data on the velocity of either the 1959 or 1983 debris flows. Consequently, $120,000\, m^3$ is a minimum estimate of the volume of the 1983 debris flow. The maximum volume is likely less than $10^6\, m^3$ because a flow larger than that volume would likely have been large enough to bury parts of Matucana.

5.4 *Magnitudes of pre-historic debris flows*

Any estimates of historic debris flow magnitudes must be tempered by evidence of prehistoric event based upon exposures of sediments comprising the PC fan. Exposures along the channels of PC and RR reveal only massive debris flow diamicton that commonly contain boulders exceeding 1 m in length (Figs. 3–4) and lacking obvious flow boundaries or breaks in sedimentation. Based on these observations, the fan has largely been built by debris flow events that covered parts of the fan to depths of 3 m or more and greatly exceeded the volumes of the historic ones. The lack of buried soils or other indicators of long term breaks in debris flow deposition and the rapid uplift rates in the region suggest that the debris flow deposits that have built the fan are geologically recent i.e. hundreds or thousands of years old. At the regional rate of uplift, deposits tens or hundreds of thousands of years old would likely have been deeply incised and would presently form terraces.

6 GEOLOGY OF PAYHUA CREEK BASIN AND ORIGIN OF DEBRIS FLOWS

6.1 *Division of PC basin based on geology and landslide activity*

The PC basin is divisible into a lower and upper basin based upon the types and density of landslides and landslide activity that occurs within in them. These in turn reflect differences in underlying geology. It will be shown that landslide activity is directly linked to debris flow activity.

6.1.1 *Lower basin*
The lower basin stretches from the area of the mountain village of Payhua to the head of the PC fan. Surficial deposits include erosional remnants of debris flow fans. Assuming uplift rates 0.2 to 0.3 mm/yr, the 400 m elevation of some of these fan remnants would date then

as middle Pleistocene. At the elevation of Payhua village, the bedrock of the basin is overlain by active debris flow fans and rockfall aprons from bedrock ridges north and west of Payhua village (the village lies within an active rockfall fan and it is impacted by large blocks several times a year). Underlying bedrock consists of extensively jointed and fractured andesitic or dacitic flows, breccias and pervasively fractured pyroclastic rocks. Vertical succession of lithologies along the PC canyon suggest that these volcanic rocks dip in the general direction of PC basin drainage.

6.1.2 *Landsliding in the lower basin east of Payhua*
The most active and continuous areas of landsliding in PC basin occur along the reach of the PC canyon adjacent to the village of Payhua about 2.2 km north of and 1000 m in elevation above Matucana. This will subsequently be referred to as the Payhua landslide complex (Fig. 2, LC). Approximately 16 ha of active rock and debris slides, rockfall and complex landslides that include old debris-flow-fan remnants and portions of active debris flow fans border on approximately one kilometre of the channel. This reach contributes the greatest amounts of coarse and fine sediment to the PC channel in the basin. These landslides have locally dammed PC in the past and may have the potential to create breakout floods. Furthermore, several rapidly expanding ravines within talus slope/debris-flow cone complexes above Payhua village have produced debris flows that directly entered PC during the 1959 and 1983 debris flow disasters. A debris flow from the largest of these ravines (*Patipunco*) may have been the ultimate source of the 1959 debris flow according to longtime Payhua village residents (Fig. 2, Po).

6.1.3 *Stratigraphic and structural architecture and slope instability*
The ultimate cause of failure along the approximately 70 m deep canyon of PC is the incision of the inherently unstable configuration of pervasively fractured red tuff that is overlain by more coarsely jointed andesitic lava flows (Fig. 5). The red tuff is approximately 40 m in thickness. Incision of this resistant over recessive succession leads to undermining of the andesite flows and rock falls along near vertical canyon walls or rotational or translational type failures with the failure plane(s) seated within the red tuff. The latter varieties are expanding rapidly into slopes immediately east of Payhua village.

6.1.3.1 Documentation of increasing landslide activity
Comparison of 1951 air photographs with 2004 satellite imagery indicates that landsliding has increased

Figure 5. Dashed line indicates the contact between a coarsely jointed andesitic flow unit and the underlying pervasively fractured red tuff unit. The slope is about 70 m high. The rockfall occurred within the past 20 years and continues to grow as the failure in the red tuff undermines the andesite flow. Bouldery debris from the rock fall blocks the channel of Payhua Creek.

Figure 6. Channel of Payhua Creek near the downstream limit of the upper basin (see Fig. 2). Arrow indicates a bouldery levee marking the upper limit of debris flow deposits. Compare channel cross sectional area to the fan channel in Figure 4. The boulder indicated by the arrow is about 3 m above the floor or the channel.

by a factor of five and *Patipunco* and adjacent ravines have expanded in width and depth over the intervening 54 years. The cause of this acceleration is not known. Fields along both sides of the PC canyon are irrigated. The addition of irrigation water to the slope has been suggested as a contributing factor by some residents. However, a cause and effect relationship cannot be demonstrated with currently available data.

6.1.3.2 Sagging of the east side of the PC canyon

One other area of extensive but presently very slow moving or semi-stable slope failure is present in the lower basin. Below the landslide complex adjacent to Payhua village and immediately upstream of the head of PC fan, a 1 km section of the east side of the PC canyon wall has apparently detached from the adjacent upland and has moved into PC canyon. (Fig. 2, SS). Its movement appears to be slower than the landslides immediately east of Payhua. It shows no evidence of past damming of the canyon. Details of its velocity or other aspects of its movement are not known. It is regarded as a sagging mountainside or slow moving rotational failure and requires further study and monitoring.

6.1.4 *Geology and landslide occurrence in the upper basin*

The upper basin (Fig. 2) is underlain by massive cliff-forming andesite flows or flow complexes that apparently overlie the recessive rocks of the lower basin. Agricultural terracing extends to ridge crests along the east side of the basin. Archaeological evidence

and historical changes coincident with the arrival of the conquistadors in the 1530s date these structures as pre-Columbian and likely pre-Inca (ca. 1200 to 1400 AD or older). The preservation of these terrace structures across slopes and tributary ravines indicates that they have been stable for the past 600 to 800 years. Landslides in the upper basin are confined to rock falls and rock slides where the massive andesite cliffs have failed along jointing planes or flow boundaries. These can be dated to the past 600 to 800 years where they have removed or buried agricultural terraces. Three such major failures dating from this period are present in the upper basin.

6.1.4.1 Agricultural terraces and debris flow activity

Agricultural terraces have been built to within about 5 vertical metres of the channel bottom of PC in the upper basin. The highest debris flow levees are about 3 m above the channel floor in this area. Debris flow deposits are distinctive in the basin because they contain clasts from all lithologies occurring in the basin up-stream from any given point. These polymictic deposits are absent from pre-Inca agricultural terraces immediately above the channel. Therefore, the uppermost levees define the upper limits of the largest debris flow event during at least the last 600 to 800 years in the upper basin. They define a channel cross-section less than one-tenth the area of the cross section of the PC channel across the PC fan. Consequently, more than about 90% of the volume of the 1983 debris flow that reached the PC fan apparently had its origin farther downstream in the PC basin.

472

7   PRELIMINARY CONCLUSIONS

Debris flows from PC basin have been a recurring hazard to Matucana, Peru. These events have dammed RR diverting it into this small city with loss of life and extensive damage. Several conclusions can be reached with respect to historic and future events:

1. A 1 km reach of PC immediately east of Payhua village receives sediment from the greatest density of active landslides in the PC basin. This reach is the greatest source of debris flow sediment in the basin. The upper basin is a minor contributor to debris flow volume by comparison.
2. A minimum volume estimate for the debris flows of 1959 and 1983 is 120,000 m^3. However, evidence from fan stratigraphy suggests that prehistoric events may have greatly exceeded the volumes of the historic events.
3. The Payhua landslide complex has increased fivefold in area during the past 54 years. In addition, the *Patipunco* ravine complex, which contributes debris flows directly to PC, has also enlarged and become more active. Consequently, sediment that could be mobilized into debris flows has become more abundant. Landslides are very active in this area and are capable of blocking PC with the potential to trigger an outburst flood and debris flow. Therefore, future debris flows on the scale of the 1959 and 1983 events or larger should be expected.

4. Matucana was significantly smaller in 1983 and 1959. Although no part of the city was directly impacted by debris flows during those events, newly built areas adjacent to the PC fan are likely to be directly impacted by future debris flows of similar magnitude.

Note: Geological Survey of Canada Earth Sciences Sector contribution number 2004398.

REFERENCES

Gregory-Wodzicki, K.M. 2000. Uplift history of the central and northern Andes: a review. *Geological Society of America Bulletin* 112: 1091–1105.

Howes, D. & Kenk, E. 1997. Terrain Classification System for British Columbia, Version 2 (http:// srmwww.gov.bc.ca/ risc/ pubs/teecolo/terclass/index.html).

Hungr, O., Morgan, G.C. & Kellerhalls, R. 1984. Quantitative analysis of debris torrent hazards for design of remedial measures. *Canadian Geotechnical Jorunal* 21: 663–677.

Jakob, M. & Jordan, P. 2001. Design flood estimates in mountain streams. *Canadian Journal of Civil Engineering* 28: 425–439.

Instituto Geologico Minero y Metalurgico 1995. Geologia del Peru. Ministero de Energia y Minas. 177 p.

Kuroiwa, J. 2002. Reducción de desastres: viviendo en amonía con naturaleza. CECOSAMI, Lima, 429 p.

Martinez Vargas, A. & Medina Rengito, J. 2000. Evaluacíon de la amenaza y vulnerabilidad de Matucana. PREDES, Lima, 18 p.

Landslide hazard evaluation for Bogota, Colombia

A.J. Gonzalez
Colombia National University, Bogota, Colombia

J.A. Millan
Consultant, Bogota, Colombia

ABSTRACT: In 1998, Bogota, capital city of Colombia, with about 7 million people, advanced landslide hazard studies for the mountainous zones which surround the main urban area plain. Studies were contracted by the City Disaster Prevention Office (formerly UPES, now DPAE) with INGEOCIM Ltd: main author acted as Director and second author as Coordinator of the study. Three methods were used: (a) Semiquantitive Stability Evaluation (SSE-Ramirez & Gonzalez, 1989), which uses an index derived from point assigned to intrinsic factors (geomaterials, relief, drainage density and vegetation) and external triggering factors (rainfall, earthquake, erosion and anthropic effects); (b) Natural Slope Methodology (NSM-Shuk, 1968 to1999), which by geomorphometric measurements on topographic maps, allows estimation of relative factors of safety and failure probabilities for several time horizons and (c) Landslide Inventory. The three methods were combined for a 10-year horizon to obtain five 1:10,000 landslide hazard maps, each one with 5 landslide hazard categories.

1 PROBLEM DESCRIPTION

Bogota, capital city of Colombia, with 7 million people, on a lacustrine plain surrounded by mountains, at 2,600 meters above sea level, is in the middle of Colombia's eastern mountain range (Figs. 1–2).

The disorderly and sometimes chaotic process of the accelerated demographic growth of the city, during the last decades, has involved an intense modification of land use due to a massive concentration of human settlements in marginal territory such as steep topography, areas of former mining, borders of creeks and rivers and potentially or actual unstable areas. The development of social nuclei in these areas have resulted in an environmental and social crisis, with most of some areas regarded as hazardous zones, and hence with permanent eventual risks, where erosion and small landslides (rockfalls, slides, earth flows) are common.

The eastern and southeastern mountains of the city (called "cerros") are formed of sedimentary rocks, intensely affected by tectonic events, by weathering and mainly by human activity. They are discordantly covered by hillside deposits, alluvial terraces, fluvioglacial deposits and cones. They show morphological diversity between steep and flat terrain, and are crossed by creeks and gullies that dissect small narrow valleys.

The drainage network suffers a high degree of intervention, erosion, deforestation and slope instability, this
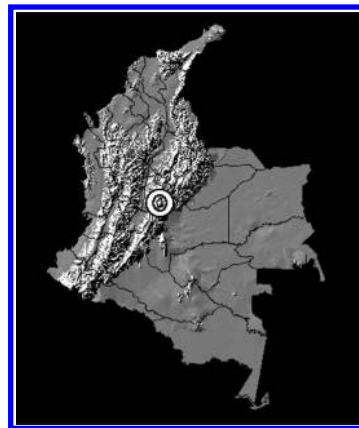
Figure 1. Colombian relief and Bogota location.

last phenomenon favored by domestic waste dumps. The development of mining, to obtain construction materials, has been disordered and often lacking technique, producing instability problems both in the exploitation areas and in the waste disposal zones. These conditions result in the acceleration of the denudative processes, generating constant morphological changes, variations in local stability and increasing hazard, vulnerability and risk levels (Fig. 3).

Figure 2. NW-SE view of Bogota mountains.

Figure 3. Irregular human settlement in Bogota mountains.

In order to evaluate the hazard under which the population was living, the level of risk due to landslides and to legalize some irregular settlements so that they could be provided with basic services, the City Disaster Prevention Office (formerly UPES, now DPAE) contracted with INGEOCIM Ltd., a consulting firm, the study for Hazard, Vulnerability and Risk due to Terrain Instability in Several Localities of Bogota. The study was completed in 1-year (INGEOCIM-UPES 1998).

2 METHODOLOGY

Hazard evaluation is a cumbersome task due to the multiple factors that potentially play an important role in the occurrence of hazardous phenomena. The evaluation thus, requires a great amount of information and the analytical techniques and codes may be expensive and time consuming.

According to the purposes of the study, to the availability of basic and topical information, and specially due to the limitations of financial resources, the scope of the project was determined and two landslide

hazard evaluation models were adopted: (a) the Semiquantitative Stability Evaluation (SSE), as proposed by Ramírez & Gonzalez (1989) (semi-quantitative crossing of maps), which expresses hazard in terms of semiquantitative possibility of landslide occurrence, and (b) the Natural Slope Methodology (NSM) (Shuk1968, 1970, 1990, 1999) which allows to obtain failure probabilities for natural hillslopes, at short, medium and long-term and in addition, geomechanical parameters can be deducted.

Evaluation of map accuracy was analyzed by comparing landslide inventory maps (LIM), with assigned hazard (based on the hypothesis that landslides will take place again in the same place) against maps which had results obtained by SSE and NSM, as well as against maps with results from SSE and NSM, combined with different weights.

2.1 Semiquantitative stability evaluation method

This method (Ramírez & González 1989), basically comprises the evaluation of eight (8) parameters, and each one of them is the result of the addition or superposition of several factors associated with the parameter. Different ranges of variability are assigned to each factor according to its influence on slope stability. The combination of the different factors in each parameter, and in turn the addition of the scores deducted for each parameter, result in a "Stability Qualification" (SQ). Originally, factors and parameters were evaluated for a terrain unit in Grant's PUCE Terrain System (Grant 1976, Cortes 1989) and the method was developed for intermediate scales (1:10.000 to 1:50.000). The 8 original parameters, score ranges and factors are given in Table 1.

Since the model was developed in the late 80's, there were still no clear notions of landslide hazards or risks and also intrinsic and triggering factors were not usually differentiated. As the method was applied, several modifications had been done:

(a) Preserving the score limits and the general SQ range, the parameter F was eliminated (as it represented in part the result which was sought) and was substituted by the parameter A-anthropic effects, specially for urban environments (Lozano & Millán 1995). Also, a new factor f = regional fracture density, was incorporated into the material parameter M, modifying scores for rocks.

(b) With the development of Geographic Information Systems (GIS, i.e. VanWesten 1989), the original Terrain Unit was substituted by the Unique Condition Units, which result from the superposition of different layers in the GIS, and therefore the percentages of area were eliminated.

(c) Due to the above, the Vegetation parameter V was substituted by Land Use parameter L; the concept of critical rain was introduced (i.e.

476

Table 1. SSE parameters and scores.

Parameter	Score	Factors
M – Material.	1–50	Rock: Compressive strength, rock mass fracturing Soil: Origin: residual (parent material); transported (agent) Type: granular (density); fine (consistency) Intermediate – Origin (residual or colluvial) – Matrix erodability. Inherited discontinuities
R – Relief	15–44	Position in slope; gradient; profile convexity
D – Drainage	6–35	Drainage density; average bedstream gradient
V – Vegetation	1–32	Slope gradient; Type; % area with vegetation
F – Instability	7–40	% of area with instability evidence
E – Erosion	2–35	Type (laminar to ravines); % of eroded area
C – Climate	8–40	Mean annual rainfall (low, medium, high)
S – Seismicity	0–24	Material type (S1,S2,S3); 1/475 yr acceleration in rock
SQ	40–300	

Castellanos & González 1997); and surface seismic acceleration was used, including material and topographic amplification.

(d) Parameters were grouped into Intrinsic Parameters (M, R, D, L) and Trigger Parameters (E, C, S and A), and the Instability Parameter F was changed by the Present Mass Movement Processes Map, which is used as a calibration tool for the SSE. Also the addition of the intrinsic parameters was classed as a Susceptibility Index, and the SSE scores, properly manipulated over an area, and treated statistically, lead to a Relative Mass Movement Hazard Index.

2.2 Natural slope methodology

2.2.1 Fundamentals

The Natural Slope Methodology is based on the basic premise that "nature is the best in-situ test", and all the research effort and the results obtained by means of NSM revolve around the best possible quantitative interpretation of the result produced by nature's massive adaptation process, a part of whose observable products at any given moment consist of simple average geometrical parameters of natural slopes. This methodology is thus, a big effort in geomorphological deconvolution and in this paper only a very short

account will be presented, which perhaps does not reflect all the potential and usefulness of it. Therefore the interested reader should read the references at the end of the paper.

This methodology, proposed and developed by the Colombian engineer Tomas Shuk from 1968 to 1999, besides its use to perform stability evaluations on a large scale basis, allows, for the materials of the hillslopes, to estimate their geotechnical parameters. These parameters include density and phase relationships, strength and deformation parameters for both the mass and the elements that constitute such slopes, and also the so called pressurization parameters for the mass, which include, both present and relict, positive, negative and excess fluid pressures.

The basic principle of NSM is that in a family of measurements of the heights H (in meters) and their corresponding lengths L (also in meters) of vertical gradient lines in a natural hillslope of homogeneous composition and origin, are linked by the basic functional relationship:

$$H = AL^b \qquad (1)$$

It is a simple power function named by Shuk (1990) as the Present Envelope that always has a high correlation coefficient ($r > 0.95$), in most of the cases $b < 1$, and represents the average profile of the surface of the hillslope earth mass. Because this surface is the interface of the earthen material with its environment, due to physical and thermodynamic reasons, it should be, on average, in dynamic equilibrium with its surroundings. For these reasons, Shuk postulates (Shuk 1968, 1970, 1990, 1994, 1999) that this function should correspond to an average factor of safety of 1.0 and to a corresponding average probability of failure of 50%.

2.2.2 Stability and Landslide Hazard Evaluation

Therefore, in a hillslope of homogeneous material, and for similar lengths L, the segments with heights larger than the average will tend to be less stable than those with smaller heights, and from this deduction it is possible to obtain relative factors of safety and relative failure probabilities for such segments. Additionally, in all hillslopes, there are maximum values of H and L, termed Limit Values (H_{LD} and L_{LD}), which also determine a limit slope angle β_{LD} ($\tan \beta_{LD} = H_{LD}/L_{LD}$). These values are transformed to made them belong to the Present Envelope, into the values H_{LF}, L_{LF} and β_{LF}, very similar to the original ones.

For a given population of natural slopes (population defined as composed of slopes belonging to the same geological formation) it has been found that the values H_{LF} and L_{LF} (or H_{LD} and L_{LD}) also are related by the basic function (1), but with lower correlation coefficients. But in this case of populations, the stability

477

criterion suffers an inversion, because the hillslopes higher and steeper than the average would be stronger and therefore the more stable ones. Also, if limit values of H_{LD} and L_{LD} of all the slopes in a region (a universe), irrespective of its origin, are examined, they also comply with the basic function (1), a fact that insinuates a fractal nature of this function.

In conclusion, with the measurements of the limit values of hillslopes it is possible to deduct statistically Factors of Safety (F_S) and Failure Probabilities (p_F) of the individual hillslopes, relative to a population or to an universe. As in all statistical methods, the larger the data base, the better the approximation of the relative values to the true ones.

Furthermore, Shuk found that in a single hillslope, the Present Envelope always lied below the results of conventional analyses and that the differences in height were almost constant. This led Shuk to the deduction that the so called Present Envelope should corresponded really to long term stability and that the conventional analyses represented short term stability conditions. Therefore two additional Envelopes emerged, depending on the time span for which the stability was going to be evaluated:

Short Term Envelope: $\quad H = H_{OE} + AL^b \qquad$ (2a)

Medium Term Envelope: $H = H_{OM} + AL^b \qquad$ (2b)

In these envelopes, the Ho parameter is one of the geomechanical strength parameters obtained by means of NSM, and it corresponds to the critical (or maximum) vertical height that can be obtained in a given mass of geologic materials; the results for this parameter correspond very closely to those presented by Terzaghi (1956). The subscript E refers to the hypothetical height of the "element condition" and the subscript M to the "mass condition" (for the long term condition Ho is nil).

With all this background, it is possible to calculate for individual slopes, as referred to an universe, relative factors of safety (Equation 3) and relative failure probabilities by means of a Weibull Type III (Ang & Tang 1984) modified distribution (Equation 4):

$$F_{ST} = \frac{H}{H_{RT}} \qquad (3)$$

$$Ln(p_{FT}) = (F_{ST}^{\;K}) * Ln(0.5) \qquad (4)$$

In which:
F_{ST} = relative factor of safety for time span T
H = limit height of the hillslope under consideration
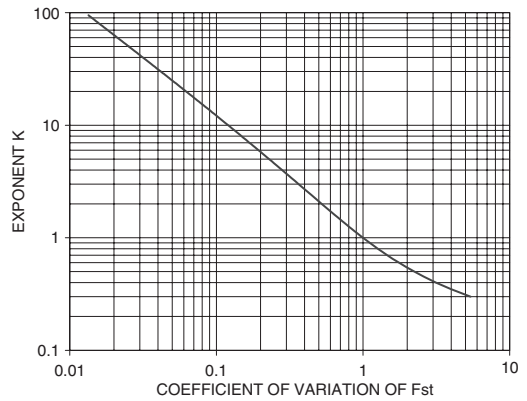H_{RT} = height of the basic function, for the length L of the hillslope and time span T

Figure 4. K-parameter for Weibull modified distribution.

$$\log H_{HT} = \frac{(\log H_{R0})^2}{\log(H_{R0} + H_{0T})} \qquad (5)$$

H_{R0} = height of the basic function (long term) for length L
H_{0T} = critical height of the universe for time span T
p_{FT} = relative failure probability for time span T
K = parameter of the Weibull distribution, which is a function of the coefficient of variation of F_{ST} (Cv_{FST}) (Fig. 4)

$$Cv_{F_{ST}} = \left\{ \frac{\Gamma(1 + \frac{2}{K})}{\Gamma^2(1 + \frac{1}{K})} - 1 \right\}^{0.5} \qquad (6)$$

$\Gamma(x)$=gamma function of x i.e. $\Gamma(1+x) = x!$ (7)

With the values of H_{0M} and H_{0E} for all the slope data, and with correlations among individual reliabilities ($c_F = 1 - p_F$), it is possible to deduct relationships among time spans for the nominal geological time (GT), long term (LT), medium term (MT) and short term (ST) time spans. However, to obtain numerical values of the different time spans, it is necessary to adopt one of them. In the Andean Colombian region the maximum annual rainfall cycle is between 4 and 6 years, very similar to the short cycle of 4.2 years of Denness (1988). Because of that, this period has been usually adopted as the short term time span for this region. For the very rainy zones of Western Piedmont the maximum annual rainfall cycle is between 9 and 14 years, similar to the basic 11.5 year cycle of Denness. For Bogota, the calculated average maximum annual rainfall cycle was 4.22 years (González et al. 1999).

Finally, with critical rain and earthquake data and with the Total Probability Theorem (i.e. González 1992), nominal failure probabilities are calculated for all slopes, and for short, medium and long term time

478

spans, and/or other interpolated time spans. These values, along with their corresponding factors of safety, are worked in the GIS to produce the NSM Landslide Relative Hazard Map for a certain time span.

It should be noted that the reliability of this methodology relies strongly on the accuracy of the topographic maps, and also on the relationship of this accuracy with the relief features. Also, since natural processes are dynamic, it should be remembered that the evaluation is done for the date of the map and that the use of maps of different dates for the same evaluation will distort the results.

3 PROCEDURE

The development of the hazard study was based on the proposal by González (1990a, b), but due to usual restraints in time and budget, it was impossible to develop all the evaluation aspects with maximum detail. Therefore emphasis was put only on the essential aspects considered necessary for landslide hazard evaluation. The stages implemented were:

- Identification
- Model implementation
- Evaluation of Internal factors
- Evaluation of triggering agents
- Landslide Hazard evaluation

3.1 *Identification*

3.1.1 *Available information*
– *Technical Information*: geotechnical studies by governmental institutions and/or private consultants. Information related to environment, social, hydrology, climate, seismic zoning and population data, among others.
– *Cartographic Information*: topographic, geological, geomorphological, hydrological, land use, utilities, other infrastructure and denudational processes drawings and maps with scales ranging from 1:2.000 to 1:50.000.

3.1.2 *Current hazard preliminary identification*
This task had been advanced by UPES by means of concepts and diagnoses issued by its Hazard Group. These documents were consulted, data plotted on the existing urban map and used as a base for field work programming and the making of the Landslide Inventory. Landslide historical record complemented this activity (Millan & Vesga 1999).

3.1.3 *Identification of urgent preventive and corrective measures*
UPES (DPAE) determined and continues to determine the sites that need people relocation and continually contracts detailed studies to carry out mitigation and corrective works in specific places.

3.2 *Model implementation*

3.2.1 *Area delimitation*
Area delimitation started from city political division into wards and taking as a lower altitude limit a minimum land gradient (5%) and as upper limit the basin divide and/or reaching up to areas with dense human settlements. A total area of 181 km^2 was studied.

3.2.2 *Area delimitation*
– *Basic Cartographic Map:* Basic map from the City Cadastral Department was available, (1:5.000), which was complemented by digitizing maps with scales 1:2,000, 1:5,000, 1:10,000 and even a few 1:25.000 documents, from Instituto Geografico Agustin Codazzi (IGAC), to add up nearly 120 km^2. Basic information required to be complemented with additional information, specially related to drainage, streets, roads and wards to be legalized; from the latter the drawings were supplied by Departamento Administrativo de Planeación Distrital [District Planning Department], at 1:1,000 and 1,500 scales.
– *Aerial Photographs*: 1:25,000 photographs of the whole area were acquired and for specific very susceptible zones identified in field work 1:10,000 to 1:5,000 photographs were used.

3.2.3 *Model application*
After defining the hazard evaluation methods, SES and NSM, the following activities were advanced:

– Definition of variables to be evaluated
– Adaptation of the evaluation methods, not developed for urban settings, to an urban area
– Implementation of variables so that they could be managed by a SIG
– Modelling
– Model calibration
– Production of final landslide hazard map

The adaptation of SES and NSM evaluation models to be applied to an urban area, relates mainly to the inclusion of the anthropic factor as a parameter contributing to hillside instability. In this connection, in SES the work of Millan & Lozano (1995) for a preliminary landslide hazard evaluation of a south sector of Bogota was taken as a guideline.

The Landslide Inventory of current processes was used to calibrate the results obtained with the two models used, and the Landslide Hazard Map was the result of the application of overlapping maps and contrasting models.

479

3.3 *Evaluation of internal factors*

3.3.1 *Geology*

Geology work focussed to define lithology and geological structures at 1:10,000 scale. Specifically, the following lithological units were identified:

- *Recent R*: Municipal Solid Waste (Rab), Mining Wastes (Rae), Excavations (Re)
- *Quaternary Q*: Alluvium (Qal), Lacustrine deposits (Qsb), Terraces (Qt), Volcanic ash (Qcv), Debris flows (Qft), Hillside deposits (Talus-Qdlt and Colluvium-Qdlc), Fluvioglacial deposits (Qfg), Cones (Qcd), Tunjuelito Cone (Qct), Residual Soils (Qsr)
- *Tertiary T*: Upper and Lower Usme Formations (mainly argillaceous rocks), Upper and Lower Regadera Formations (mainly sandstones), Bogota (claystones) and Cacho Formations (sandstones)
- *Transition KT* Upper, Medium and Lower *Guaduas Formation (mainly claystones and coal)*
- *Cretaceous K* Soft Sandstone, Labor Sandstone, Plaeners and Hard Sandstone Formations from Guadalupe Group (which form the highest mountains) and Chipaque Group Formations.

For the tectonic features, major fault and fold alignments were identified. Additionally, with information about drainage network, geological units and structures, relationships between drainage and lithological or tectonic control were established.

3.3.2 *Geotechnical characterization of materials*

The SSE model involves three lithological categories: soil, intermediate material and rock. For each category, behavioral features or property indexes are defined, allowing to quantify a score for each category in terms of stability.

Material characterization was made based on: (a) secondary information collection, (b) subsoil investigation, (c) laboratory testing, (d) material properties deduced from Natural Slope Methodology.

By using exploration and tests information, material geotechnical features were obtained for selected zones in the study area, specially those involving landslides, as well as its interaction with meteoric agents, mainly water. Such features were extrapolated to other sites by using NSM data.

3.3.3 *Geomorphology*

The geomorphological work attempted to determine, at a general level, the shape of relief shapes that model the hillsides of eastern and southeastern mountains that border the city. The structural control forms, the denudation produced by relief-destroying agents and the accumulation forms represented by old and recent quaternary deposits were identified.

At morphodynamic level an inventory of current denudative processes was made, resulting in a process map and a database for the major instability problems surveyed in the field.

Morphometrically, a gradient map was produced, whose intervals were discriminated taking into account the average slope of the hillsides making up the surveyed area, obtained from the NSM data and using Dalrymple et al. (1968) hypothetical slope profile, employed in the SSE.

The area was also characterized in function of its drainage network. The basins and microbasins were determined in function of their order and streambed slope in order to determine the drainage density and river bed mean gradients.

3.3.4 *Cover and current land use*

The purpose of land use and cover cartography focussed, on one side, to determine the Anthropic Factor, specifically to determine the urban areas and the mining zones, complementing specific field surveys, and to evaluate the Land Use parameter for SSE.

The units defined in the cover maps were: Forestry Land, Pastures, Agricultural Land, Stubble Ground, Buildings and Land with No Cover. Additionally, these cover maps were used to produce anthropic factor and natural erosion maps.

3.4 *Evaluation of external triggering factors*

Some of these activities are presented after the internal factor evaluation, even though they were made concomitantly or before those already described.

3.4.1 *Climate and hydrology*

Location and Physiography: on the base map 1:10.000 the hydrographic network was drawn, operative pluviometric, meteorological and hydrometric stations were located, and physiographic elements were determined requiring the study of hydrographic basins and stream bed lengths and slopes.

Annual Isohyets: with rainfall series already corrected and complemented, annual mean isohyets were drawn, with care that interpolation gave a satisfactory fit (Fig. 5). Bogota annual rainfall oscillates between 600 mm at the south to 1,100 mm at the east, with average evapotranspiration of 1,000 mm per year and the climate in the city is semi-arid.

Critical Rainfall: for Colombia critical rainfall and duration values had been obtained (Castellanos & González 1997, González & Mayorga 2004). With the same model of critical accumulated rainfall (which is directly proportional to annual rainfall) some historical landslides that occurred in the city were calibrated with rainfall data in order to find out such parameters (González et al. 1999). The equation types are Equations 8 and 9 and the parameter values found are given in Table 2.
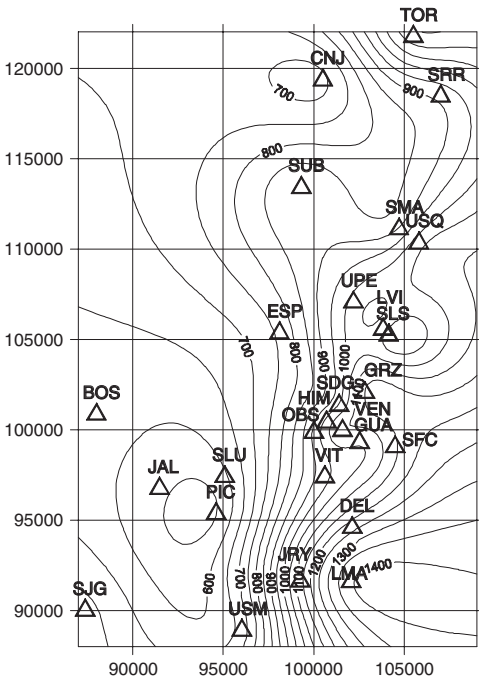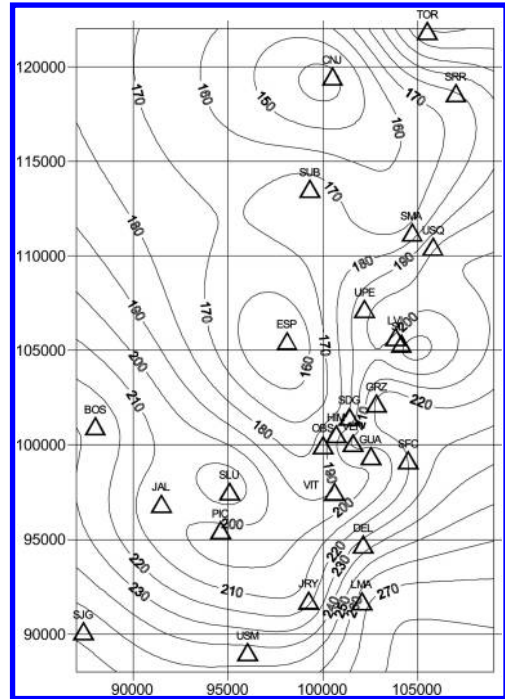
Figure 5.   Mean annual rainfall (mm) for Bogota.

Figure 6.   Critical rainfall (mm) for Bogota.

Table 2.   Critical rainfall parameters.

	M	N	P	Q
Southwestern zone	0.3609	0.0000	3.2829	0.4157
Eastern zone	0.1814	12.6326	0.04923	1.0000

$$LL_{CR} = M (LL_{AN}) + N \qquad (8)$$

$$D = P (LL_{CR})^{Q} \qquad (9)$$

LL_{CR} = critical rainfall (mm)
LL_{AN} = mean annual rainfall (mm)
D = duration of critical rainfall (days)

Zoning: for SSE, the study area was zoned in function of critical rainfall (Fig. 6), duration (Fig. 7) and its returning period in each station (Fig. 8), thus obtaining five zones with different stability scores. For NSM, critical rainfall and return period for each measured slope were obtained.

3.4.2   *Seismic hazard*
Surface accelerations (Am) were used, as obtained from the Seismic Microzoning of Bogota (INGEOM-INAS-UNIANDES 1997) with Am values for a 475-yr

return period (Table 3). Materials were divided into 5 groups and Am values allocated at ground level (Table 4).

Residual and hard soils are associated to Qsr, Qct, Qfg, Qal, medium soils to Qcd, Qdlc, Qdlt, Qcv and soft soils to Qsb, Qt, Qft, Rab and Rae.

3.4.3   *Natural erosion*
Based on geological, geomorphological, vegetal cover and anthropic factor studies, the current erosion grade of the areas under study was assessed and mapped, ranking them according to erosion type, and classifying its intensity from absence of erosion to severe erosion. Areas per type of severe erosion were classified into gullies, deep drains, badland, and stream erosion. In general the method previously used by Millan & Lozano (1996) was adopted.

3.4.4   *Anthropic effects*
Anthropic effects as triggers of landslides are multiple, ranging from the simple fact of standing on a susceptible site (overload) to intensive and extensive mineral resources exploitation (erosion, in the widest sense). Anthropic actions identification and assessment as landslide triggering agents was made in parallel to vulnerability analyses (Millán & González 2001).
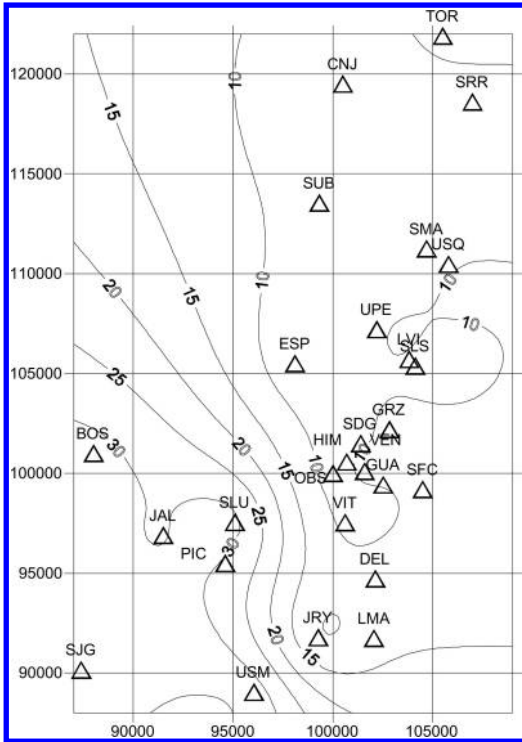
481

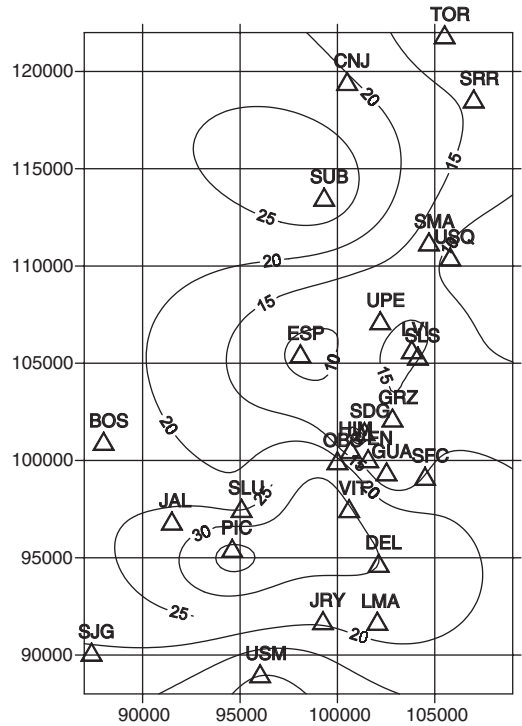Figure 7. Critical rainfall duration (days) for Bogota.

Figure 8. Critical rainfall return periods (yr) for Bogota.

The causes considered were the following: (a) Deforestation, (b) Construction of fills and dwellings, (c) Excavations for mining or civil works and (d) Sewage effluents.

These main human actions impair the physical environment due to the creation of unloaded areas or overloaded (soil stress changes), infiltration (increased piezometric levels and internal erosion), and drainage pattern modifications.

3.5 *Evaluation of landslide hazard*

The general procedure applied to obtain the Final Landslide Hazard, was the following, not necessary in chronological order:

(a) Relative Landslide Hazard Maps with Semi-quantitative Stability Evaluation method (SSE), and the deduced scale (Table 5).
(b) Relative Landslide Hazard Maps with Natural Slope Methodology (NSM), and the deduced scale (Table 6).
(c) Landslide Inventory Maps (LIM) with hazard levels (P_F) that were assigned from qualitative hazard possibilities with diffuse theory and 50% confidence (Table 7).

Table 3. Microzoning surface earthquake accelerations.

Zone 1	Hills	0.24 g
Zone 2	Piedmont	0.30 g
Zone 5	Terraces & Cones	0.20 g

Table 4. Surface earthquake accelerations.

Material	Symbol	Acceleration
Rock	R	0.22 g–0.24 g
Residual and hard soils	M1	0.26 g
Medium soils	M2	0.28 g
Soft soils	M3–M4	0.30 g

Table 5. Hazard scale for SSE method.

Hazard category	Stability qualif. SQ
Very high	SQ < 126
High	126.5 < SQ < 151
Medium	151.5 < SQ < 177
Low	177.5 < SQ < 202
Very low	202.5 < SQ

482

Table 6. Relative hazard scale for NSM method.

Hazard category	Factor of safety F_{ST}
Very high	$F_{ST} \leqslant 0.6$
High	$0.6 < F_{ST} \leqslant 1.1$
Medium	$1.1 < F_{ST} \leqslant 1.9$
Low	$1.9 < F_{ST} \leqslant 3.4$
Very low	$3.4 < F_{ST}$

Table 7. Hazard scale for present landslides.

Slide activity	Possibility	Max P_F	Min P_F
Active	Very high	1.000	0.875
Collapsed	High	0.875	0.625
Incipient	Medium	0.625	0.375
Stabilized	Low	0.375	0.175
	Very low	0.125	0.000

Table 8. Contrasting matrix: SSE and NSM.

		SSE				
	CAT.	VH	H	M	L	VL
NSM	VH	VH	H1	H2	M1	M2
	H	H1	A2	M1	M2	M3
	M	H2	M1	M2	M3	L1
	L	M1	M2	M3	L1	L2
	VL	M2	M3	L1	L2	VL

(d) Contrasting SSE and NSM hazard maps, with each other and with Landslide Inventory Map (LIM), with the following observations:
  – SSQ applies to areal units and has total coverage. These unique condition units have very variable sizes and do not allow previous control.
  – *NSM* produce lines and the extension to area is done with mathematical interpolation procedures, which influence the shape of the hazard zones. Because of the working scale (1,5,000) the minimum measurable slope height is 15 m.
  – LIM covers only the affected areas and does not allow extrapolations. Because of scale (1,5,000) the minimum measurable area is 144 sq. m.
  – Visual contrasting between each pair of hazard maps (SSE vs LIM, NSM vs LIM, SSE vs NSM) is essentially subjective and was accomplished both in the computer screen and with translucid paper copies of the several different maps.
  – It was necessary to obtain a map of hazardous zones of homogeneous behavior, and due to SSE and NSM model characteristics it was not possible to determine which of them could prevail.

Table 9. Contrasting matrix: LIM and SSE + NSM.

		LMI			
	CAT.	VH	H	M	L
CONTR	VH	VH	VH	VH	VH
	H	VH	H	H	H
	M	VH	H	M	M
	L	VH	H	M	L
	VL	VH	H	M	L

Table 10. Hazard probability scale for T = 10 yr.

Hazard category	Failure probability P_{FT}
Very high	$P_{FT} \geqslant 73.1\%$
High	$73.1\% > P_{FT} \geqslant 44.3\%$
Medium	$44.3\% > P_{FT} \geqslant 12.1\%$
Low	$12.1\% > P_{FT} \geqslant 0.4\%$
Very low	$0.4\% > P_{FT}$

What is true is that actual landslide processes, as depicted in the LIM, due to their own nature, prevail over the other two methods.
  – Contrasting matrices used were: (Tables 8–9).
(e) Failure Probabilities Assignment: with five hazard categories, probabilities were assigned, for a 10-year horizon (Table 10), horizon which was agreed with UPES. These categories were subsequently reduced to three levels (low = low + very low, medium, high = high + very high) by DPAE.
(f) Obtaining the Landslide Hazard Final Maps.

4 FINAL RESULTS

The results obtained, in terms of area distribution for each hazard category for the total area under study, are: very high = 1.7%; high = 9.3%; medium = 61.3%; low = 24.2% and very low = 3.4% (Fig. 9).

As a final product the Landslide Hazard Cartography was obtained for the 181 km^2 of the mountains of Bogota, divided into five 1:10.000 maps, (each one for several wards), which were combined by DPAE (Fig. 10).

The final factors of safety and failure probabilities for each hazard level, as adopted by DPAE an as indicated in the map were the following (Table 11).

With this values the area distribution for each hazard category for the total area under study, are finally: high = 11.0%; medium = 61.3%; low = 27.7%.

This map and the hazard values were incorporated, in 2000, into the 10-year City Main Development Plan and also in 2000, the City Disaster Prevention Office (DPAE) issued Resolution 364, in which detailed landslide hazard and risk studies were required to
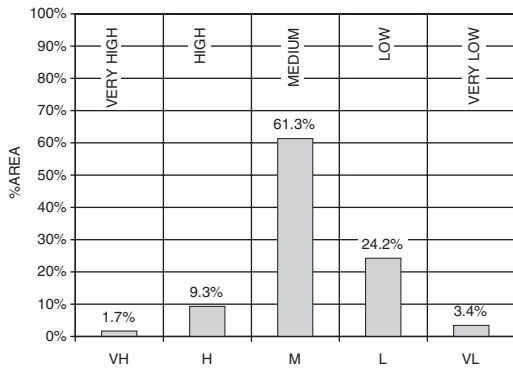
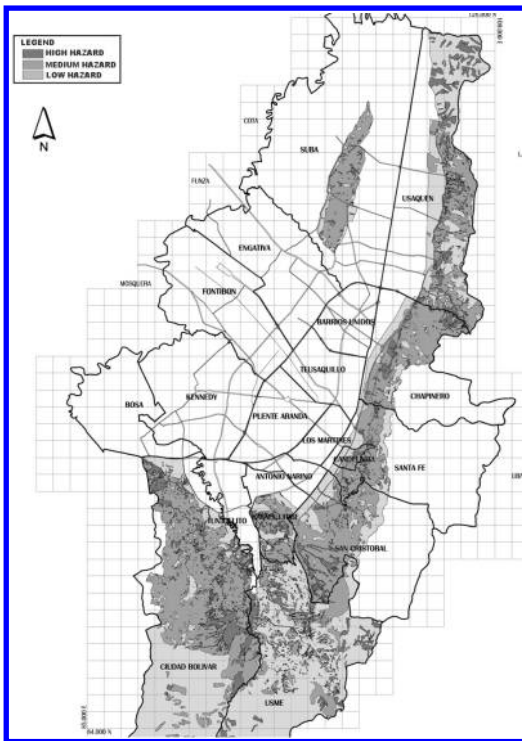Figure 9.   Areal landslide hazard distribution in Bogota.

Figure 10.   Landslide hazard map for Bogota.

Table 11.   Final hazard scale for T = 10-yr time horizon.

Hazard category	Factor of safety F_{S10}	Failure probability P_{FT}
High	$F_{ST} \leqslant 1.1$	$P_{FT} \geqslant 44.3\%$
Medium	$1.1 < F_{ST} \leqslant 1.9$	$44.3\% > P_{FT} \geqslant 12.1\%$
Low	$1.9 < F_{ST}$	$12.1\% > P_{FT}$

housing developers which were interested in advancing projects in zones located in high and medium hazard areas. High hazard areas are normally to be dedicated to parks or to forestry development.

REFERENCES

Ang, A.H.S. & Tang, W.H. 1984. Probability Concepts in Engineering Planning and Design, Vol. II. Decision, Risk and Reliability, 562 pp. John Wiley & Sons.

Caro, P.P. & Garcia, N.J. 1989. Zonificación Geotécnica del Distrito Especial de Bogotá- INGEOMINAS.- I Simposio Suramericano de Deslizamientos- Vol. I, pp. 587–606, Soc. Col. de Geotecnia (SCG)- Paipa, Agosto de 1989. (in Spanish)

Castellanos, R. & González, A.J. 1997. Algunas Relaciones de Precipitación Crítica-Duración que Disparan Movimientos en Masa en Colombia- 2o. Simposio Panam. de Deslizamientos- Vol. 2 pp. 863–878- ABMS-Río de Janeiro, Noviembre 1997. (in Spanish)

Cortés, D.R. 1989. Clasificación de Zonas Geotécnicamente Homogéneas- I Simposio Suramericano de Deslizamientos- Vol. I, pp. 56–75, SCG- Paipa, Agosto de 1989. (in Spanish)

Dalrymple, J.B., Blong, R.J. & Conacher, A.J. 1968. A hypothetical nine-unit landsurface model. Zeit. f. Geomorph. 12: 60–76.

Denness, B. (1988). The variation of the universal gravitational constant and the distribution of earthquakes in China through time and space. Conferencias para la Investigación de Deslizamientos de la Red Vial Nacional – Univ. Nal de Colombia- Fac. de Ingeniería- Nov. 1988.

González, A.J. 1990a. Conceptos sobre la Evaluación de Riesgo por Deslizamientos – VI Jornadas Geotécnicas-Sociedad Colombiana de Ingenieros (SCI) – Tomo I, pp. 153–170, Bogotá, Octubre 1990. (in Spanish)

González, A.J. 1990b. Metodología para Evaluación de Riesgo por Deslizamientos a Nivel Intermedio- VI Jornadas Geotécnicas- SCI -Tomo II- Oct. 1990. (in Spanish)

484

González, A.J. 1992. Avalanche Risk Evaluation at Utica – Colombia – 1er Simposio Internacional sobre Sensores Remotos y Sistemas de Información Geográfica (SIG) – pp. 356–378- Instituto Geográfico Agustín Codazzi – Bogotá, Abril 1992.

González, A.J. & Millán, J. 1999a. Procedimiento para la Evaluación de la Amenaza por Fenómenos de Remoción en Masa en Santafé de Bogotá – Colombia- XI CPMSIF - Vol. 2.- pp. 701–708- ABMS-Foz de Iguazú, Brasil. (in Spanish)

González, A.J. & Millán, J. 1999b. Resultados de la Evaluación de la Amenaza por Fenómenos de Remoción en Masa en Santafé de Bogotá – Colombia- XI CPMSIF – Vol. 2.- pp. 717–723- ABMS – Foz de Iguazú, Brasil. (in Spanish)

González, A.J. & Millán, J. 2001. Evaluación de la acción del hombre en los estudios de amenaza y riesgo por deslizamiento en Bogota. III Simposio Paamericano de Deslizamientos- Vol. I, pp. 163–175, SCG- Cartagena, Agosto de 2001. (in Spanish)

González, A.J., Zamudio, E. & Castellanos, R. 1999. Relaciones de Precipitación Crítica -Duración que Disparan Movimientos en Masa en Santafé de Bogotá - Colombia- XI CPMSIF – Vol. 2.- pp. 709–715- ABMS Foz de Iguazú, Brasil. (in Spanish)

González, A.J. & Mayorga, R. 2004. Thresholds for rainfall events that induce landslides in Colomboia. Landslides- Evaluation & Stabilization- 9th ISL -Rio de Janeiro- Lacerda et al. (eds.), Vol. 1, pp. 349–356. Balkema.

Grant, K. 1976. The PUCE Program for Terrain Evaluation for Engineering Purposes. I: Principles. CSIRO Division of Applied Geomechanics Technical Paper 19, 68 pp., Australia.

INGEOCIM-UPES 1998. Estudio de Amenaza, Vulnerabilidad y Riesgo por Inestabilidad del Terreno para las Localidades de Ciudad Bolívar, Rafael Uribe, San Cristóbal, Santafé, Chapinero, Usaquén y Suba de Santa Fé de Bogota – Octubre 1998. (in Spanish)

INGEOMINAS-UNIANDES 1997. Microzonificación Sísmica de Santafé de Bogotá- 1 Vol. 3 maps-Bogotá, 1997. (in Spanish)

Millán, J. & Lozano, J. 1995. Evaluación de Estabilidad y Análisis de Susceptibilidad Geotécnica a Fenómenos de Remoción en Masa del Sector de Ciudad Bolívar – VIII Jornadas Geotécnicas – pp. 174–201- SCI-SCG- Octubre 1995. (in Spanish)

Millán, J. & Lozano, J. 1996. La Erosión en los Estudios de Zonificación de Areas urbanas por Fenómenos de Remoción en Masa. – VI Congreso Colombiano de Geotecnia, SCG, Bucaramanga. (in Spanish)

Millán, J. & Lozano J. 1997. La Contrastación de Mapas en la Evaluación de la Amenaza por Fenómenos de Remoción en Masa.- IX Jornadas Geotécnicas- SCI- Oct. 1997. (in Spanish)

Millan, J. & Vesga, L.F. 1999. Inventario de Procesos de Remocion en Masa en los Estudios de Amenaza y Riesgo en Santafé de Bogotá – Colombia. XI CPMSIF – Vol. 2.- pp. 673–680- ABMS – Foz de Iguazú, Brasil, August. (in Spanish)

Ramirez, F. & González, A.J. 1989. Evaluación de Estabilidad para Zonas Homogéneas- I Simposio Suramericano de Deslizamientos- Vol. I, pp. 174- 192, SCG.- Paipa, Agosto 1989. (in Spanish)

Shuk, E., T. 1968. – Un Método Sencillo de Diseño para Minimizar el Costo de Taludes en Roca.- 1er Simposio de Ingeniería Geológica, Vol. II, MOPT-SCI, 1968.(in Spanish)

Shuk, E.T. 1970. Optimization of slopes designed in rock. Proceedings 2nd. Intl. Congress on Rock Mechanics, Vol. 3., Paper 7–2, pp. 275–280, ISRM, Beograd.

Shuk, E.T. 1990. La Evolución y el Estado Actual de la Metodología Basada en Taludes Naturales para Análisis de Estabilidad en Masas de Materiales Geológicos- Parte I- III CSMR- SVMSIF, Caracas, Octubre 1990. (in Spanish)

Shuk, E.T. 1994. Key elements and applications of the Natural Slope Methodology with some emphasis on slope stability aspects. ISRM International Symposium- 4th CSMR, Vol. 1, pp. 255–266, SOCHIGE, Santiago.

Shuk, E.T. 1999. Zonificacion geotécnica cuantitativa por medio de la Metodología de Taludes Naturales- State of the Art Paper – XI PCSMGE- Foz de Iguassu, Brasil- Vol. 4. (in Spanish)

Shuk, E.T. & González A.J. 1993. Quantification of slope instability risk and cost parameters for geotechnical applications in a highway project and in a regional study. ICOSSAR'93 (Sixth Intl. Conference on Structural Safety and Reliability), Vol. 3, pp. 2025–2032, Innsbruck, A.A. Balkema.

Terzaghi, K. 1956. Theoretical Soil Mechanics. 8th Edition. John Wiley, New York.

VanWesten, C.J. 1989. ITC-UNESCO Project on G.I.S. for Mountain Hazard Analysis- I Simposio Suramericano de Deslizamientos, Vol. I, pp.214–224, SCG.-Paipa.

Varnes, D.J. 1984. Landslide Hazard Zonation: a Review of Principles and Practice. UNESCO, París.

Failure mode identification and hazard quantification for coastal bluff landslides

B.D. Collins & N. Sitar

Dept. of Civil and Env. Eng., University of California, Berkeley, California, USA

ABSTRACT: Failures of coastal bluffs in marine terrace deposits are a common occurrence owing to their location within an active geologic environment. Along the coastline south of San Francisco, California, USA, bluffs in marine terrace deposits reach heights up to 30 meters and fail periodically during each winter storm season. Along portions of these bluffs, residences and municipal utilities are located sometimes as little as 10 meters from the edge. As a result, there is a significant interest to properly identify and quantify the failure mechanisms and to assess and quantify the landslide hazard. In this paper, we present the results of a study focusing on the failure mode identification and landslide hazard quantification of coastal bluffs composed of *weakly lithified sands*. Specifically, we investigated variably cemented sand units with unconfined compressive strength ranging from 10 kPa (weakly cemented) to over 300 kPa (strongly cemented). Field observations made during the course of the study show that failures occur during winter storms either as a result of wave action or precipitation induced increase in water content and seepage forces, or a combination of both. Correlations between the occurrence of failure and the triggering events are shown to provide a way to quantify the probability of failures in future events. In addition, an improved understanding of the observed failure modes: planar shear failures in the weakly cemented sands, and tensile fractures in the more strongly cemented units, allows for a process-based estimation of the size of the potential failures.

1 INTRODUCTION

Geological hazards associated with coastal bluff landslides are well known (Emery & Kuhn 1982), although in some areas this risk has yet to be quantified and fully understood in terms of the failure mechanics and the prediction of future failures. This has been the case for landslides occurring in young marine terrace deposits composed of weakly lithified sands in numerous settings due in large part, to difficulties in characterizing the failure modes in these materials and in establishing adequate models for slope stability analysis.

In particular, there is an ongoing debate as to what the predominant failure mechanisms are. While it is clear that wave erosion is responsible for maintaining steep slopes along active coastlines, it is not always the immediate trigger for failures. For example, along the San Mateo County coastline in central California, Hampton (2002) found that rainfall infiltration and resulting seepage-induced stresses contribute to landslides in many cases. Similarly, Edil & Vallejo (1980) and Komar & Shih (1993) also found that a combination of wave erosion and seepage-induced loss of stability lead to failure of coastal bluffs along the Pacific

Coast in Oregon and along the shores of the Great Lakes, respectively.

In this paper, we provide evidence that the failure mechanisms and modes in young marine terrace deposits of weakly lithified sand bluffs are linked directly to the strength of the deposits, mainly through the cohesive component of shear strength. We show that wave erosion, rainfall-induced seepage forces, and changes in water content all contribute to failure initiation. Further, we show that separate analyses are required to properly predict the failure hazard in this type of environment whether in weakly or strongly cemented materials.

This paper begins with a discussion of the challenges associated with delineating landslide risk in coastal bluff settings. We then present a summary of the current understanding of soil behavior for weakly lithified sands when exposed in steep outcrops. The expected failure modes and triggering mechanisms are discussed in detail. Using a study area located along the central coast of California, USA (Pacifica), as an example (Figure 1), we then provide quantitative failure analysis using both probabilistic and deterministic methods to obtain predictions of the conditions required for failure.

2 HAZARD AND LANDSLIDE RISK IN WEAKLY LITHIFIED SAND COASTAL BLUFFS

2.1 *Geological hazards of coastal bluff settings*

The slope failure hazards associated with weakly lithified marine terrace are similar to other coastal cliff environments. Structures, utilities, as well as human life are at risk when they are located near either the bluff crest or toe. In general, given the active wave climate at the base of actively eroding coastal bluffs, it is rare for infrastructure to be located here. Rather, most risk is associated with areas located near the crest. Human life on the other hand can be at risk either at the crest or the toe.

Property damage can range from excessive structural settlement and foundation cracking to full destruction and collapse. When utilities such as water and sewer lines are located nearby, these too can be undermined and ruptured, or their drainage alignment compromised.

2.2 *Landslide risk planning*

While landslides in weakly lithified coastal bluffs are a common occurrence, in many cases the risk associated with these failures is ignored based primarily on three reasons. First, in many areas, there is no built infrastructure and no perceived risk to property or life. Some portions of the central California coast fall into
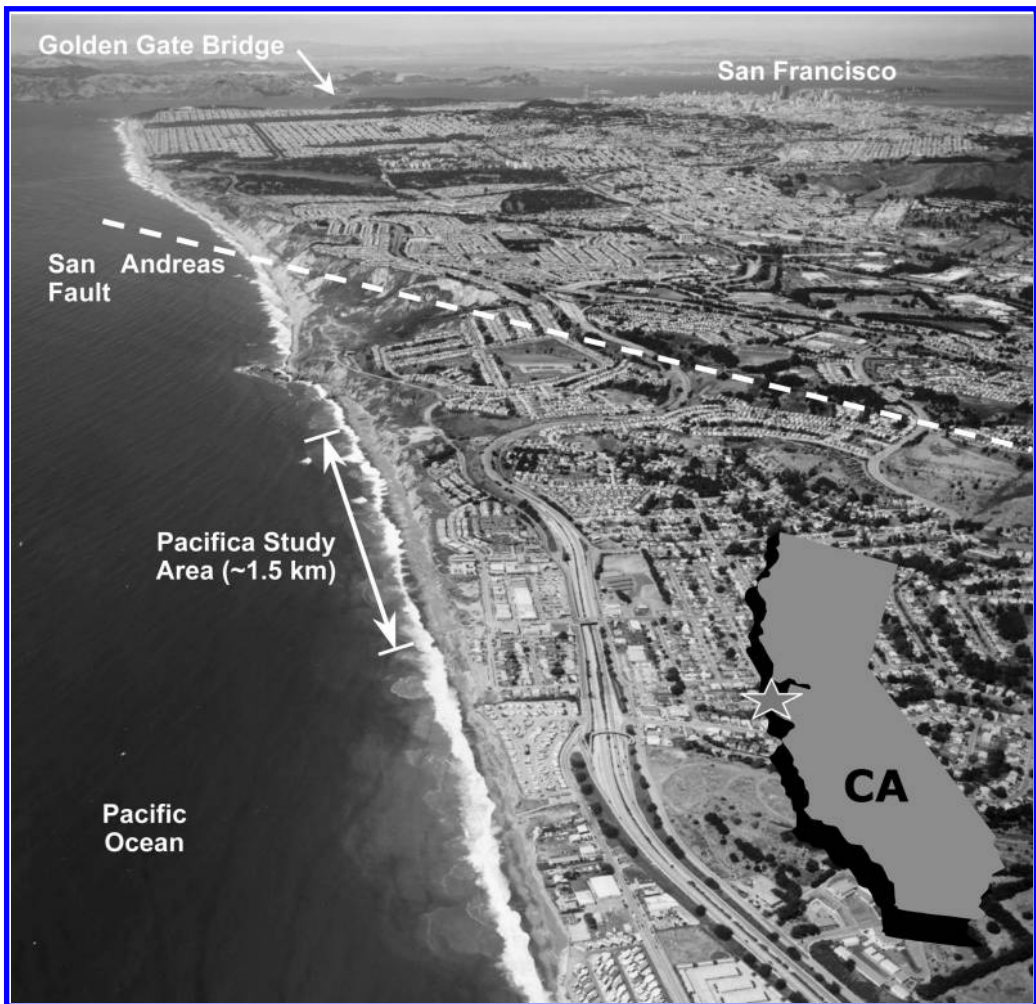

Figure 1.   Overview map of the Pacifica, California study area (Cotton, Shires and Associates photo).

488

this category, in particular, areas associated with parks or nature reserves. Although failures are ongoing, there is no imminent danger as a result of these failures. Second, and perhaps more common, is that failures often appear to be small in size with their cumulative impact unforeseen. The third reason for the lack of perceived risk is that failures occur infrequently, with long intervals of time between subsequent events.

Given that the first and third reasons are at least partially justified by the overall lack of impact to most coastal communities, we focus instead on addressing the second reason concerning the lack of perception of the general size of these failures as significant to public risk. A key element in this view is that it is often assumed that bluff landslides are not important when the failure footprint is small with only decimeters of associated crest retreat. Rather than providing clear evidence of global instability of the bluff face, these types of failures are often ignored as the effects of localized erosion and not of immediate concern. However, we have found that when larger failures do occur, on the order of several meters, it is often too late to react

Figure 2. Removal of homes in Pacifica, California, USA following 1998 bluff failures (USGS photo).

to the established condition and failures may continue over a period of up to several weeks with inevitably dramatic consequences (Figure 2).

In most communities, the long-term risk is often approached with zoning laws established to provide distinct set-back distances from the bluff edge. Based on when a community first established these set-backs, these distances are calculated by forecasting erosion rates based on 20 to 100 years worth of data. However, in many cases, communities such as Pacifica, California, did not have this type of data when land planning commenced, and structures are now very close to the bluff edge (Figure 3). It is now known that the overall retreat rate is approximately 25 centimeters per year for this area (Griggs & Savoy 1985), thus the minimum setback for a structure with a 100-year engineered lifespan would have to be at least 25 meters.

The difficulty with a long term averaging approach is that it fails to recognize the episodic, catastrophic nature of the process. The failures shown in Figure 2 for example, occurred in conjunction with up to 12 meters of crest retreat over a five-day period (Snell et al. 2000). Thus, assuming that the retreat only occurs as small erosional events ignores the reality that the short term crest retreat can be upwards of tens of meters during a given storm event. Consequently, while land planning based on historical crest retreat is warranted, we believe that the maximum credible one-time retreat distance should also be considered to effectively plan for landslide risk.

2.3 *Reactions to landslide hazards and risks*

Given that the landslide hazard in these environments is a known quantity, it is inevitable for most communities to be faced with some form of decision making process to address the landslide risk. In many cases, the hazard is dealt with in a reactive manner, very often after the establishment of a globally unstable condition
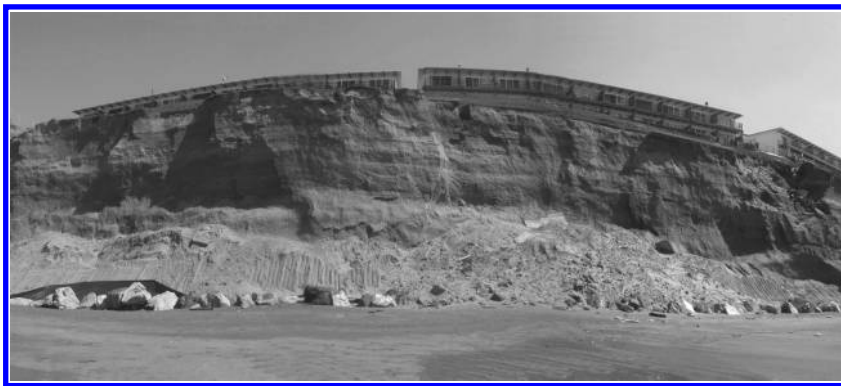

Figure 3. Property in danger of landslide hazard in Pacifica, California, USA. [see Colour Plate VIII]

489

of the bluff. Based on the severity of the hazard and the current distance between structure and bluff edge, the risk may either be ignored or be addressed by means of various passive or active mitigation measures.

Unfortunately, we have found from numerous case studies, that the failure mechanisms and failure modes are not always investigated with the necessary detail. In weakly lithified marine terrace deposits, this is often either due to the lack of knowledge of the material behavior and strength characteristics or due to the assumption that all materials exposed at the beach level and undergoing failures are inherently subject to wave erosion. Rainfall as a triggering mechanism is frequently assigned a minor role in the failure process, despite research that shows otherwise (Nott 1990, Hampton 2002). It is therefore necessary to carefully investigate the failure mechanisms and failure modes for a particular location, especially in the context of the site specific lithology and hydrology.

3 CURRENT UNDERSTANDING OF THE GEOTECHNICAL AND GEOMORPHOLOGIC BEHAVIOR OF COASTAL BLUFFS IN WEAKLY LITHIFIED SANDS

Geotechnical and geomorphologic research has been performed on the soil and slope behavior of weakly lithified sediment coastal bluffs in various locations around the world (e.g. Edil & Vallejo 1980, Sunamura 1982, Arkin & Michaeli 1985, Williams & Davies 1987). In California, this type of research has focused primarily on the weakly lithified sand bluffs near San Francisco (Sitar et al. 1980, Bachus et al. 1981, Shaffii-Rad & Clough 1982, Ashford & Sitar 2002, Hampton 2002, Collins 2004). Much other research has also been performed elsewhere along the California coast focusing on the geomorphologic aspects of beach and cliff erosion (e.g. Kuhn & Osborne 1987, Everts 1991, Lajoie & Mathieson 1998, Benumof & Griggs 1999, Sallenger et al. 2002). In the following sections, we summarize the major conclusions from this body of research.

3.1 Geotechnical behavior of weakly lithified sand coastal bluff deposits

The geotechnical characteristics of weakly lithified sand deposits are in general, typical of sand behavior. In most cases, linear Mohr-Coulomb strength envelopes apply over typical stress ranges, and friction angles are similar to those observed in uncemented materials. Some curvature of the strength envelope has been observed however, and although minor, can affect stability analysis results for soils with very low cohesion (Collins 2004). Strength from cohesion is a function

Table 1. Strength results for variably cemented sands from Pacifica, California (Collins 2004).

Material	UCS (kPa)	φ (deg)	c (kPa)	σ_t (kPa)
Weakly cemented sand	13	39	6	0
Strongly cemented sand	340	46	69	32 6 (wet)

UCS = unconfined compressive strength, σ_t = tensile strength.

of the cementing agent and may span large ranges from less than 10 kPa to over 100 kPa. The unconfined compressive strength (UCS) varies similarly. Tensile strength (σ_t) of these materials is typically only 10% of the UCS and decreases to only 2% of the UCS when wetted. Results from a testing program on over 30 hand-carved block samples from the Pacifica, California area coastal bluffs are summarized in Table 1.

In compression, the initial part of the stress–strain response is essentially linear elastic, with fairly high modulus in the low stress range (Figure 4). Brittle failure occurs at low confining stress with a more ductile response at higher confining stress. In triaxial compression, failure and plastic deformation occurs at low strains on the order of 0.5 to 2%. However, in tests along the field stress path (FSP) in which the confining stress is reduced while the axial stress remains constant, the strain at failure can be much lower, nearer to only 0.1% (Collins 2004). This stress path, implemented specifically for coastal bluffs undergoing a reduction in confinement in the lateral direction (Figure 5), more realistically mimics the stress changes along a retreating bluff slope. Otherwise, Mohr-Coulomb strength parameters remain similar to those obtained using conventional triaxial techniques.

3.2 Geomorphologic behavior of weakly lithified sand coastal bluff deposits

Geomorphologic research on coastal bluff failures has shown that many modes of failure are possible depending on the contributing failure mechanisms Emery & Kuhn (1982). Failures from shear failures, topples, undercutting, stress induced exfoliation, etc. have all been documented and analyzed to some degree. However, there have been relatively few studies correlating the failure mechanisms to lithology and strength of the materials. Among these, analytical studies by Sunamura (1977, 1992) and empirical relationships by Benumof and Griggs (1999) and Budetta et al. (2000) stand out, providing clear evidence of the importance in geotechnical strength characterization for addressing bluff failures.
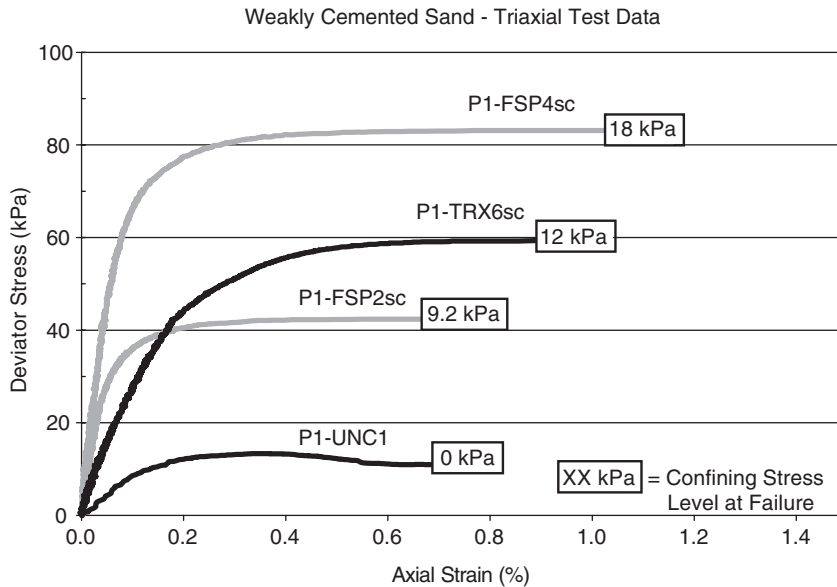
Figure 4. Triaxial test results of weakly cemented sand for both conventional (TRX) and field (FSP) stress paths (Collins 2004).
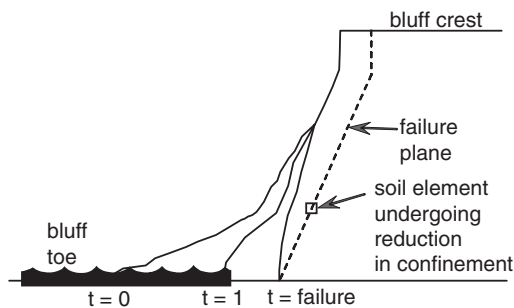

Figure 5. Field Stress Path (FSP) schematic for wave action failure mode (Collins 2004)

In more recent work focusing on the coastal bluffs of Pacifica, California, we have shown that the material strength can be directly related to the failure modes and failure mechanisms through comprehensive empirical and analytical relationships (Collins 2004, Collins & Sitar 2005). Here, the failure mechanisms and failure modes in weakly cemented sands (UCS < 30 kPa) are related to wave action with failure occurring in shear along surfaces inclined parallel to the changing slope surface (Figure 6, Figure 7a). In strongly cemented sands (UCS > 300 kPa), failures occur due to wetting induced tensile strength degradation and tensile failure (Figure 7b, Figure 8).

4 METHODS OF HAZARD ASSESSMENT AND FAILURE PREDICTION

Hazard assessment is typically implemented using either probabilistic techniques or deterministic analyses, depending on the data available and the understanding of the system. In this section, we discuss existing methods for each analysis method and present results from the latest research performed on weakly lithified coastal bluffs. Data from empirical correlations are presented for use in probabilistic analyses while the applicability of limiting equilibrium and finite element techniques is examined for deterministic analysis.

4.1 Probabilistic analysis

Probabilistic analyses for prediction of coastal bluff failures have very often relied on the forecasting of linear crest retreat based on long-term coastal erosion data sets taken from aerial photographs or historic coastline maps (e.g. Griggs & Savoy 1985). Although the problems associated with this method have been highlighted by many researchers, this is still the preferred method for coastal planners, perhaps due to the lack of any other robust method.

An additional technique, adopted from that utilized for landslide prediction from rainfall intensity-duration thresholds (e.g. Wilson & Wieczorek 1995) relies on empirical correlations developed between
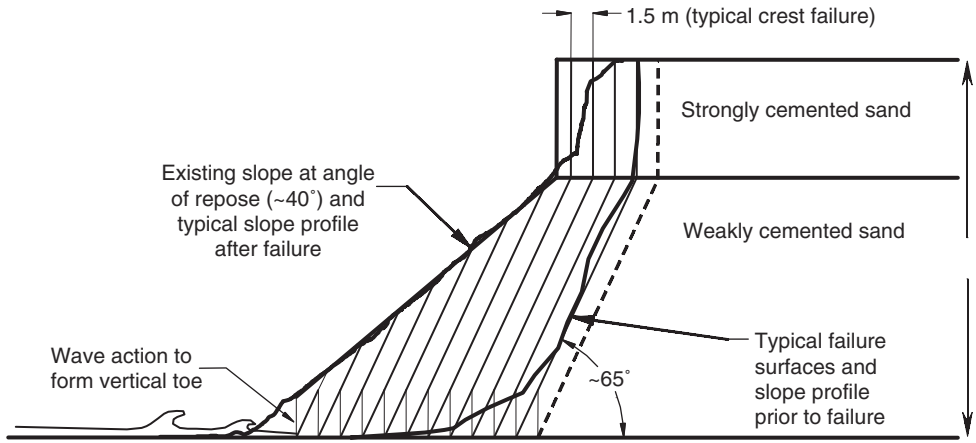
491

Figure 6.   Schematic diagram of wave action failure mode (weakly cemented sand bluffs; Collins 2004).
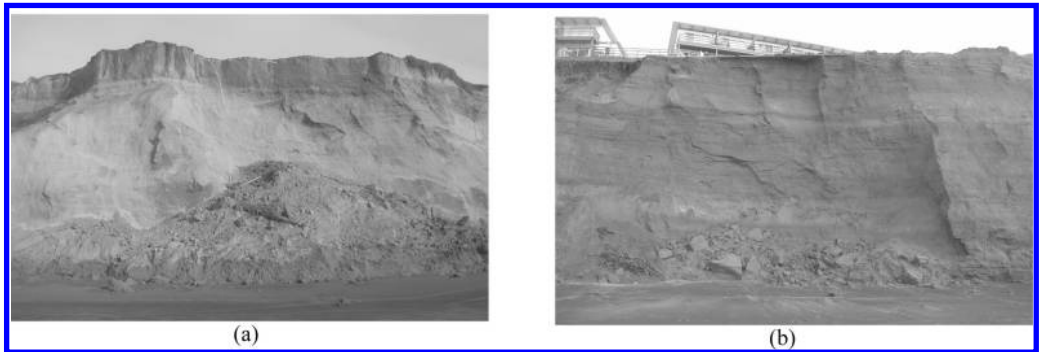

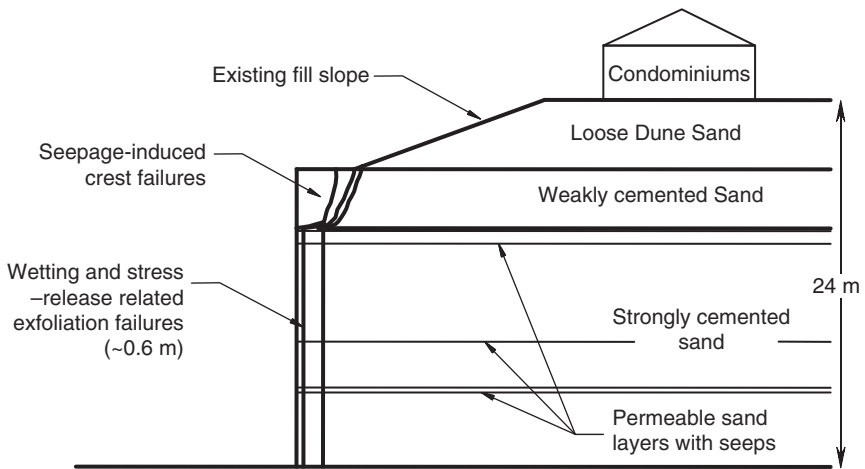Figure 7.   Typical failures in (a) weakly cemented sand bluffs and (b) strongly cemented sand bluffs.

Figure 8.   Schematic diagram of precipitation induced wetting failure mode (strongly cemented sand bluffs; Collins 2004).

492

known triggering events and established data sets of observed failures. For areas of bluff with known causal mechanisms (i.e. rainfall or wave action), future failures can be predicted by forecasting the likelihood of established thresholds that have led to failure in the past. In this manner, the probabilistic analysis is tied much more to the processes rather than just to the effects. This type of analysis can only be performed if an observed failure data set exists that can be correlated to the occurrence of the specific triggering mechanisms.

At the Pacifica study area, baseline empirical correlations have been performed with data collected during a particularly active winter storm season (2002–2003). During this season we made failure observations on a weekly and sometimes daily basis to establish a data set which was correlated with climatological signals for each of the two different lithologic areas of the bluffs.

As discussed, bluffs composed of weakly cemented sands were found to fail due to wave action during periods of high tides. Bluff composed of strongly cemented sands were found to fail due to precipitation-induced seepage and increase in water content causing loss of tensile strength. Thus, correlation was established using the wave action and tide data for the weakly cemented bluffs and cumulative daily precipitation totals for the strongly cemented bluffs.

Correlations for these two data sets are shown in Figures 9–10, which show all observed failures. For the weakly cemented bluffs, a strong correlation can be ascertained with failures generally occurring at a 3.8 meter threshold of combined tide and wave run-up. Similarly, for the strongly cemented bluffs, a correlation signal of 40 mm of cumulative rainfall over any two day period was also found to lead to failures in most cases. Although, this is admittedly a limited data set, we feel that these data are very promising and that this approach could be developed further. For example, a climatological analysis of the past 20 years of wave and tide data could be used to predict how often these types of conditions occur. For failure prediction, these probabilities can be forecasted for a future storm season and the potential magnitude of failure occurrences could be established.

4.2 Deterministic analysis

For most site-specific coastal bluff stability evaluations, deterministic analyses are utilized. These typically employ some form of limiting equilibrium or finite element method analysis, depending on the failure
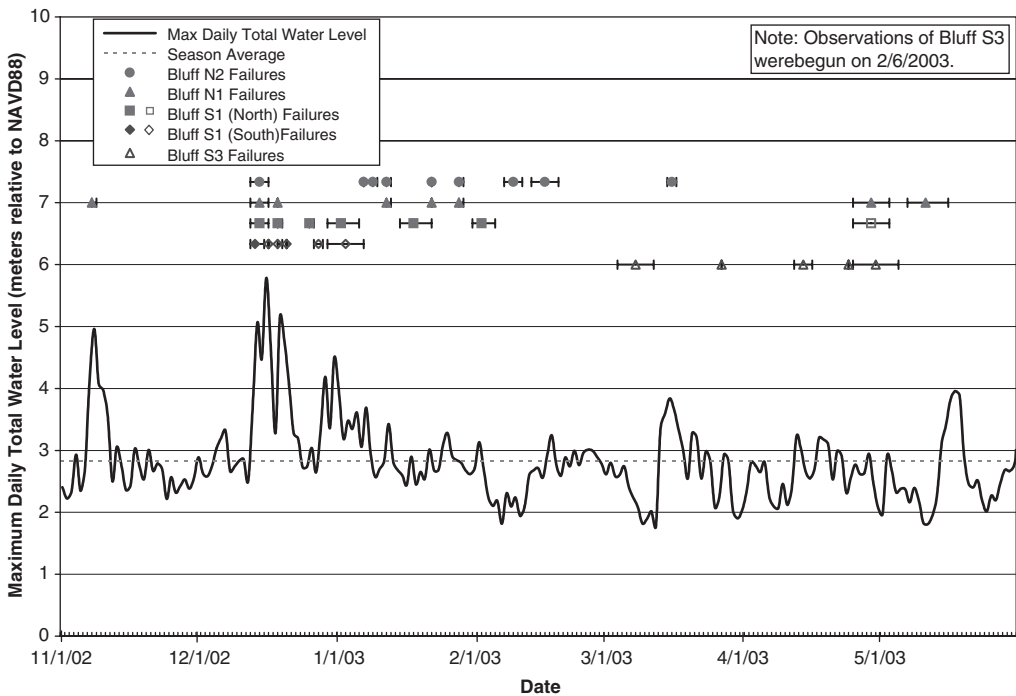

Figure 9. Wave action – bluff failure correlation data. Closed symbols indicate wave action induced failures; open symbols represent precipitation induced failures (Collins 2004).
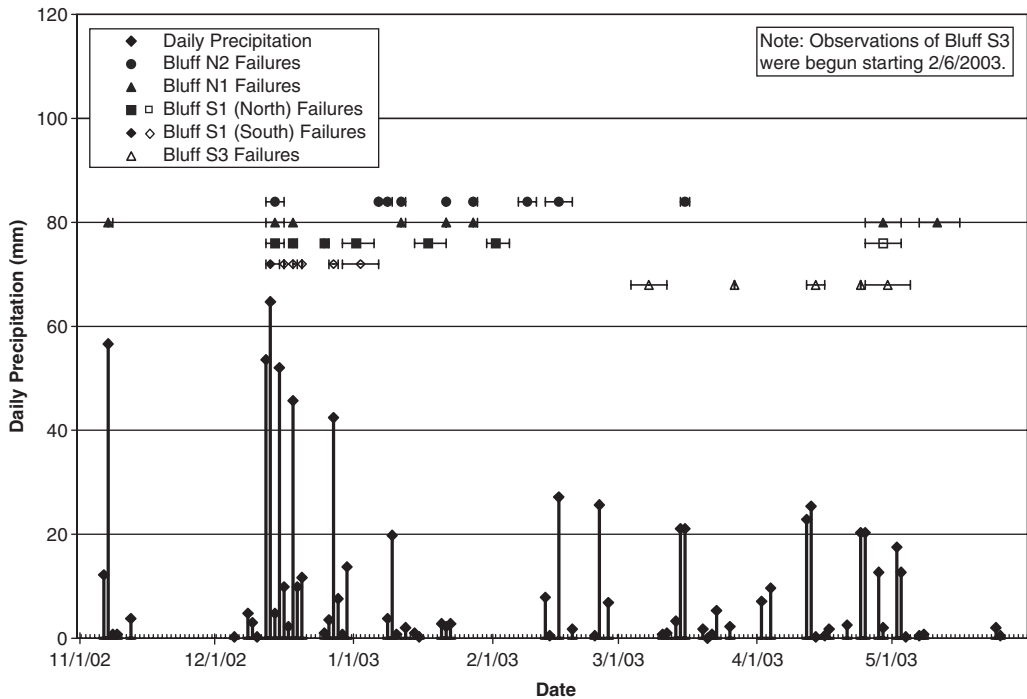
493

Figure 10. Precipitation – bluff failure correlation data. Closed symbols indicate wave action induced failures; open symbols represent precipitation induced failures (Collins 2004).

mode and the degree to which the internal soil behavior affects the stability. For weakly lithified sand coastal bluffs, both methods have been applied with varying degrees of success.

We present here a summary of the analysis techniques developed for use on the weakly and strongly cemented bluffs located in the Pacifica study area (Collins 2004). These techniques, while developed for specific use in this location, should be applicable in other areas as well and can be used as guidelines for implementing analyses in similar environments.

4.2.1 *Geotechnical analysis of weakly cemented sand coastal bluffs*

Because failures in weakly cemented bluffs occur in shear when initiated by wave action, a limiting equilibrium method approach was selected for analysis and evaluation of stability. The formulation relies on the geometry of the slope to be evaluated under changing conditions; identical to what is experienced in the field. A finite slope formulation has been developed to account for changes occurring to the toe, slope, and crest as shown in Figure 11. In this analysis, the height of the toe H_t, the slope inclination β, and the formation of a vertical crest scarp with vertical tension crack H_{tc}, are assigned values consistent with field observations.

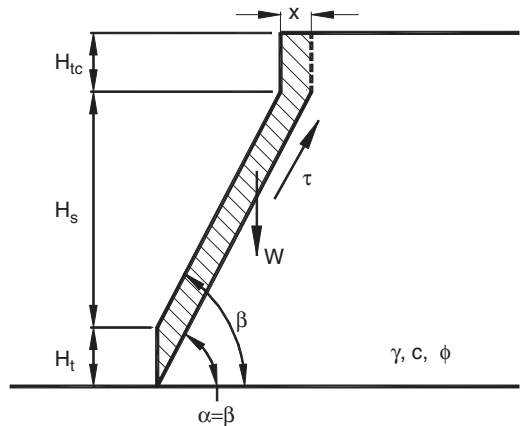Figure 11. Schematic diagram for finite slope formulation with parallel shear plane (Collins 2004).

The key component of this analysis is the assumed geometry of the failure plane which must adopt an inclination that is parallel to the evolving slope surface. Iterations of various forms of both the Culmann method and circular slip surface analysis have been shown to incorrectly predict the failure geometry,

494

whether it be the slope inclination at failure or the predicted crest retreat (delineated "x" in Figure 11) (Collins 2004).

Failure conditions for typical bluffs in the Pacifica area have been evaluated using this analysis method and show that the factor of safety with respect to shear failure for a 24 meter tall bluff decreases from 1.2 when the slope inclination is 45° to 1.0 when the slope inclination reaches the 60° range. Typical geometric conditions consisting of a vertical toe height of 2 meters and a vertical crest and tension crack height of 4 meters were utilized for this analysis and are consistent with observations made in the field.

4.2.2 *Geotechnical analysis of strongly cemented sand coastal bluffs*

The bluff failures in strongly cemented sands occur due to tensile fracture as a result of wetting induced strength degradation. While a full analysis might require an investigation of the infiltration behavior, here we concentrate on the stress analysis assuming that the bluff undergoes sufficient surficial and groundwater seepage to nearly saturate soils in and near the bluff face.

Failures occurring due to tensile fracture cannot be analyzed using limiting equilibrium techniques. Rather, an approach that allows for the development of tensile stresses is required. For this problem, we performed finite element analyses assuming linear elastic behavior to provide insights and to obtain failure predictions. Modeling of typical configurations of strongly cemented sand bluffs performed for the Pacifica study area indicate that a region of tensile stress exists near the bluff face ranging from 5 to 10 kPa (Figure 12).

Given that the tensile strength of the Pacifica strongly cemented sand at its in-situ water content ($\sigma_{t\text{-insitu}}$) is 32 kPa (Table 1), we can deduce that the bluff is stable in this condition:

$$\sigma_{t-insitu} > \sigma_3 \text{ (STABLE)} \quad (1)$$

Upon wetting however, the tensile stress drops dramatically to only 6 kPa (Table 1). Thus, for an identical stress distribution, the slope is now unstable when wetted:

$$\sigma_{t-wetted} < \sigma_3 \text{ (UNSTABLE)} \quad (2)$$

Accordingly, failure will occur along portions of the slope where Equation 2 is valid, near the slope face. The tensile stresses cannot be resisted by the tensile strength of the material and failure occurs in the form of dislodged slabs near the slope face and particularly near the mid-bluff. Tensile strength
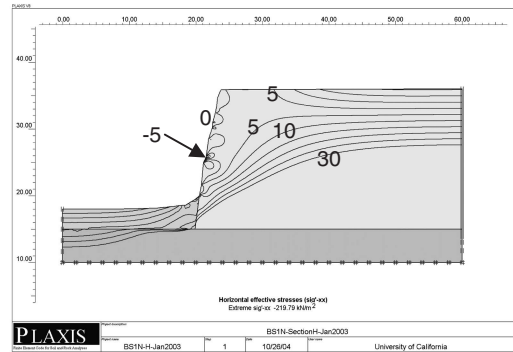

Figure 12. Finite element stress contours for strongly cemented sand bluff configuration (contours in kPa, collins 2004).

degeneration only occurs in areas that are wetted, which coincidentally are typically the bluff face and crest due to heavy, wind-blown precipitation and surficial seepage. It should be noted however, that even under in-situ water content conditions, initial fracture may occur and lead to failure in some cases, since the natural variability of tensile strength within the unit may fall beneath the seemingly stable stress state.

5 CONCLUSIONS

In this paper, we have shown that the landslide hazards in weakly lithified marine terrace deposits can be linked directly to the specific failure mode and failure mechanisms. While the hazards themselves are well known, the ability to appropriately model and predict the stability of bluff configurations and the likelihood of failure is not as well established. Here, we have provided a basis for understanding the geotechnical and geomorphologic behavior of coastal bluff failures in variably cemented sand lithology using results gathered from an investigation of coastal bluffs exposed along the coastline of central California, USA.

Our observations show that the failure mode (shear failure verses tensile fracture) is a function of the failure triggering processes (wave action or precipitation induced seepage) and of the relative strength of the sand deposits, whether weakly cemented (UCS < 30 kPa) or strongly cemented (UCS > 300 kPa).

Probabilistic analyses, comprised of empirical relationships between failure events and quantitative measures of failure triggering processes provide a promising approach to the quantification of the landslide hazard. Predictive analyses based on these methods are in their infancy however, and will require the collection of further empirical data.

495

Deterministic analyses on the other hand are better understood and provide the necessary framework for performing predictive analyses for site-specific bluff configurations. Depending on the type of lithology, and consequently, the compatible failure mode, site specific analyses are necessary. Limiting equilibrium method analyses using a finite slope configuration are recommended for weakly cemented sand slopes subject to wave erosion, while finite element analyses are recommended for strongly cemented sand slopes subject to seepage induced strength degradation and tensile fracture.

REFERENCES

Arkin, Y. & Michaeli, L. 1985. Short- and long-term erosional processes affecting the stability of the Mediterranean coastal cliffs of Israel. *Engineering Geology* 21: 153–174.

Ashford, S.A. & Sitar, N. 2002. Simplified method for evaluating seismic stability of steep slopes. *Journal of Geotechnical and Geoenvironmental Engineering* 128: 119–128.

Bachus, R.C., Clough, G.W., Sitar, N., Shaffii-Rad, N., Crosby, J. & Kaboli, P. 1981. Behavior of Weakly Cemented Soil Slopes Under Static and Seismic Loading Conditions, Volume II, Stanford, California, The John A. Blume Earthquake Engineering Center, Stanford University, p. 247.

Benumof, B.T. & Griggs, G.B. 1999. The dependence of seacliff erosion rates on cliff material properties and physical processes: San Diego County, California. *Shore and Beach* 67: 29–41.

Budetta, P., Galietta, G. & Santo, A. 2000. A methodology for the study of the relation between coastal cliff erosion and the mechanical strength of soils and rock masses. *Engineering Geology* 56: 243–256.

Collins, B.D. 2004. Failure Mechanics of Weakly Lithified Sand Coastal Bluff Deposits: Unpub. Ph.D. Dissertation thesis, University of California, Berkeley 278 p.

Collins, B.D. & Sitar, N. 2005. Monitoring of coastal bluff stability using high resolution 3D laser scanning. *In* Rathje, ed., ASCE Geotechnical Special Publication 138, Geo-Frontiers 2005, Austin, Texas, ASCE.

Edil, T.B. & Vallejo, L.E. 1980. Mechanics of coastal landslides and the influence of slope parameters. *Engineering Geology* 16: 83–96.

Emery, K.O. & Kuhn, G.G. 1982. Sea cliffs: Their processes, profiles, and classification. *Geological Society of America Bulletin* 93: 644–654.

Everts, C.H. 1991. Seacliff retreat and coarse sediment yields in southern California. Quantitative Approaches to Coastal Sediment Processes, p. 1586–1598.

Griggs, G.B. & Savoy, L. 1985. Living with the California Coast: Durham, NC, Duke University Press, 393 p.

Hampton, M. 2002. Gravitational failure of sea cliffs in weakly lithified sediment. *Environmental and Engineering Geoscience* 8: 175–192.

Komar, P.D. & Shih, S.-M. 1993. Cliff erosion along the Oregon coast: A tectonic-sea level imprint plus local controls by beach processes. *Journal of Coastal Research* 9: 747–765.

Kuhn, G.G. & Osborne, R.H. 1987. Sea cliff erosion in San Diego County, California. Advances in Understanding of Coastal Sediment Processes, pp. 1839–1918.

Lajoie, K.R. & Mathieson, S.A. 1998. 1982–83 El Nino Coastal Erosion, San Mateo County, California. Open File Report 98–041, U.S. Dept of the Interior, U.S. Geological Survey, p. 61.

Nott, J.F. 1990. The role of sub-aerial processes in sea cliff retreat – a south east Australian example. *Zeitschrift fur Geomorphologie* 34: 75–85.

Sallenger, A.H., Krabill, W., Brock, J., Swift, R., Manizade, S. & Stockdon, H. 2002. Sea-cliff erosion as a function of beach changes and extreme wave runup during the 1997–1998 El Nino. *Marine Geology* 187: 279–297.

Shaffii-Rad, N. & Clough, G.W. 1982. The Influence of Cementation on the Static and Dynamic Behavior of Sands, Stanford, California, The John A. Blume Earthquake Engineering Center, Stanford University, p. 315.

Sitar, N., Clough, G.W. & Bachus, R.C. 1980. Behavior of Weakly Cemented Soil Slopes Under Static and Seismic Loading Conditions, Stanford, California, The John A. Blume Earthquake Engineering Center, Stanford University.

Snell, C.B., Lajoie, K.R. & Medley, E.W. 2000. Sea-cliff erosion at Pacifica, California caused by the 1997/98 El Nino storms. Geo-Denver: Slope Stability 2000, p. 294–308.

Sunamura, T. 1977. A relationship between wave-induced cliff erosion and erosive force of waves. *Journal of Geology* 85: 613–618.

Sunamura, T. 1982. A predictive model for wave-induced cliff erosion, with application to Pacific coasts of Japan. *Journal of Geology* 90: 167–178.

Sunamura, T. 1992. Geomorphology of Rocky Coasts. New York, John Wiley and Sons, 302 p.

Williams, A.T. & Davies, P. 1987. Rates and mechanisms of coastal cliff erosion in lower Lias rocks. Advances in Understanding of Coastal Sediment Processes, pp. 1855–1870.

Wilson, R.C. & Wieczorek, G.F. 1995. Rainfall thresholds for the initiation of debris flows at La Honda, California. *Environmental and Engineering Geoscience* 1: 11–27.

Risk assessment of deep-seated slope failures in the Czech Republic

J. Stemberk & J. Rybář
Institute of Rock Structure and Mechanics, Czech Academy of Sciences, Prague, Czech Republic

ABSTRACT: This article deals with examples of deep-seated slope failures situated in regions with various geological, morphological and tectonic conditions in the territory of the Czech Republic. The selected examples are situated in the outer western Carpathian flysh zone, Bohemian Cretaceous basin, and Tertiary neovolcanic area. All these regions are characterized by high susceptibility to deep failures. Results of monitoring of recent movement activity and models of slope failures are demonstrated.

1 INTRODUCTION

Slope deformations are a significant geodynamic phenomenon for the Czech Republic territory. They are responsible for considerable damage to technical objects, as well as on the property of the population. Slope deformation studies, as well as practical measures to solve unfavorable effects are of an old tradition.

As early as around 1920 professor Quido Záruba, a founder of the Czechoslovak engineering-geological school, published his first study about landslides. It was the occurrence of landslides destroying a part of the mining town of Handlová in Central Slovakia between 1960 and 1961 that invoked nation-wide systematic registration of dangerous landslide phenomena in economically important regions of former Czechoslovakia between 1962 and 1963. The data were collected and deposited in Central geological archives Geofond in Prague and Bratislava, and they are accessible electronically. Organized updating of Geofond in the Czech Republic was carried out after 1997, in the year of an avalanche-like occurrence of landslides and earth flows in flysh rocks of Western Carpathians (Rybář & Stemberk 2000) of the eastern part of the republic. In the most suffering parts of the republic a detailed mapping of stability conditions at a scale of 1 : 10 000 was carried out. Then, prognostic maps of susceptibility to landsliding were derived and gradually handed over to public administration officials dealing with land use planning (Rybář 2003).

After completing the nation-wide registration of all the dangerous landslide phenomena during the 60's of the last century, a coordinated research into slope movements was organized in Prague and Bratislava. Increased attention has been paid since to deep-seated slope deformations. The majority of cases were considered permanently dormant. Old relict forms of deformations not respected during construction or mining activities may cause a situation when even a minor improper disturbance (e.g. unloading of slope toe, loading of the upper part of the slope, leakage of water from a water supply or sewage line, etc.) may trigger uncontrolled movements and an emergency state.

2 REGIONAL DISTRIBUTION OF DEEP-SEATED SLOPE DEFORMATIONS IN THE CZECH REPUBLIC

The territory of the Czech Republic belongs to two different geological units of quite uneven geotectonic evolution. A major portion of the territory of the Czech Republic is a part of an old Hercynian mountain range, the so-called Variscan province, the geotectonic evolution of which finished at the end of early Paleozoic. This territory is indicated as Bohemian Massif which reaches to Austria in the south, to Bavaria in the west, and to Saxony and Poland in the north. The eastern part of the Czech Republic, considerably smaller, belongs to a younger unit, to a so-called Alpine province. A young mountainous system with a complex nappe de charriage structure originated by the end of the Secondary era and in Tertiary. Engineering-geological conditions between Bohemian Massif and Western Carpathians are substantially different, which results in a serious dissimilarity in slope movement evolution.

Deep-seated slope deformations in Bohemian Massif can be found mainly in the Bohemian Cretaceous Basin, and also in the highland areas of Tertiary volcanites. In Western Carpathians it is mainly flysh rocks of the mountainous relief of the Moravskoslezské Beskydy Mts. that are affected by deep deformations.
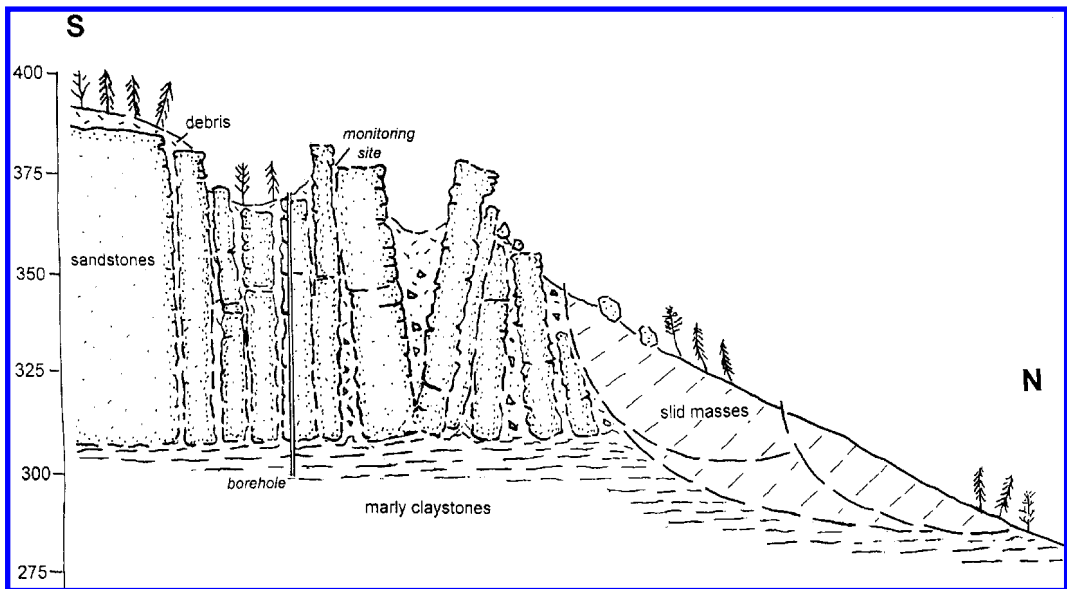
Figure 1. Cross-section through the slope deformation near Olšina Village with position of exploratory borehole and monitoring site.

3 SELECTED TYPES OF DEEP-SEATED SLOPE DEFORMATIONS IN BOHEMIAN MASSIF

Ideal conditions for deep slope failure appear in a situation when the upper part of slopes is built by rigid, brittle and permeable rocks, while the lower part by plastic rocks with low permeability. Then, in the upper parts rigid blocks creep on the plastic bedrock (after classification of Nemčok et al. 1972). After Varnes (1978) it is a "lateral spread". Research into this type of slow and long-range slope movements is of a long tradition in the Czech, as well as in the Slovak Republics (Záruba 1956, Pašek & Košt'ák 1977, Malgot 1977, Nemčok & Baliak 1977).

3.1 Highland region of Bohemian Cretaceous

Classical examples come from the margins of sandstone tabular rock-benches in the region of the Bohemian Cretaceous Plateau (Fencl 1966, Kyrianová 2004). Příhrazy Highland in the watershed of the Jizera River is a typical area. The landslides have been monitored there since 1926 when an extensive landslide originated destroying a substantial part of the village of Dneboh (Záruba 1927; Záruba et al. 1966). The landslide originated in claystones and marlstones overlain by quartzitic thick-bedded sandstones up to 106 m thick. The upper part of the slope built by sandstones was disturbed by intensive gravitational loosening.

As the studies show, these large and complex forms of block-type slope deformations (Fig. 1) resulted from an intensive destruction of the plateau edge under climatic-morphogenic conditions of the Pleistocene and early periods of Holocene. However, under present conditions these forms of block-type deformations have been considered almost constantly inactive or fossil. A long-term stability was, among other considerations, evidenced by the absence of failure of Drábské Světničky Castle ruins, the castle built by the end of the 14th century just above the Dneboh Village.

Since 1989, morphologic signs of a sharp acceleration in slope processes have been observed in the northern slopes of Příhrazy Highland. There appeared subsurface erosion and fresh sinking of ground into fissures without any obvious intervention into the slope. At the beginning of summer 1989 an intensive failure process in a small rock tower at the plateau edge above Olšina Village was found. Considering the geodynamical phenomena indicated above, systematic monitoring of movements in the sandstone massif has started.

Monitoring has confirmed a steady creep process with an average rate of about 2 mm/year. Active block movements can be evidenced with the observation that new fresh sinks in superficial sediments appear up to several tens of meters from the upper edge of the slope (Stemberk & Zvelebil 1999, Stemberk 2003). In an exploratory borehole situated directly into the zone where active block movements had been observed, about 1 m thick layer of marlstones with plastic

498

consistency was detected at the contact sandstones-marlstones. A direct relation between movements at the monitoring place and variations of groundwater level was evidenced by groundwater level monitoring. A sudden block movement by 3 mm occurred at the end 2002, and gradual uplift of groundwater level by about 1,7 m followed. Groundwater level stabilized then by the end of August 2004.

3.2 *Highland regions of neovolcanites*

Engineering-geological region of neovolcanites belongs to the regions in Bohemian Massif that suffered most from deep-seated slope movements. The basic condition for such deep-seated deformations stems from the fact that, as a rule, at least two different rock complexes of uneven strength characteristics are found together. More rigid and more resistant rocks to weathering always represent reinforcement for the slopes. They are found either in subhorizontal positions or cutting less resistant beds through. Slopes in less resistant rocks keep inclinations higher than the critical one, which leads to permanent instability. Deformations reach often even a depth of several tens of meters, in some cases a depth of 100 m and more. Three cases studied in more detail were selected as examples.

The locality of Stadice Village (Fig. 2) is situated on the left bank of the Bílina River in the České Středohoří Highlands. The studies took place within a layout project for Prague-Dresden motorway D-8. The blocks broken off the edge of a basalt lava sheet about 60 m thick, were found sunk into underlying tuffs and tuffites. Numerous undrained depressions and platforms dipping back against the slope were surveyed. Here, in the western part of the separation zone, is the largest compact block 350 m long and 150 m wide is laying. Its surface is inclined about 18 deg against the slope. The lower part of the slope displays landslides with faces reaching the fluvial plain of the Bílina River (Pašek & Demek 1969). The stretch of the motorway D-8 put already into operation is not threatened by slope movements.

Deep-seated deformation of slopes built by a series of lava flows and sheets in alternation with intercalations of clay sediments can be exemplified in the locality of Čeřeniště Village laying on the right bank slope in the valley of the Labe River (Fig. 3). Basanite lavas are often altered here. The upper part of a considerably large landslide area is found here disrupted by creep lateral movements reaching a depth of 100 m, at least. It is separated from the central part of the slope deformation by a conspicuous platform about 500 m long dipping moderately against the slope. Relatively fast sliding movements take place in the central and lower parts of the slope where rocks of the weathered coat are found. Investigations confirmed at least six lava flows up to 30 m thick in the volcanic complex affected by deep
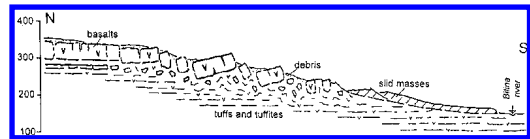
Figure 2. Cross-section through Stadice Village locality in the region of České Středohoří Highlands neovolcanites.
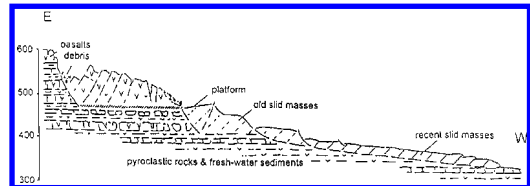
Figure 3. Geological cross-section through the slope deformation of Čeřeniště Village.
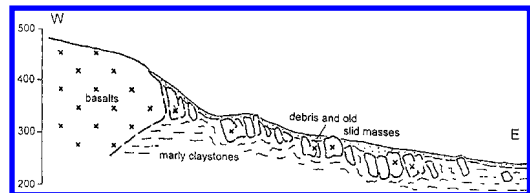
Figure 4. Cross-section through a large landslide area of Prackovice Village on the Labe River left bank.

slope deformations. The lava flows are separated by sedimentary, mainly clayey intercalations. X-ray analysis indicated smectite as the prevailing mineral of all the clayey intercalations. Smectite is very unstable in volume, and brings about weakening of planes and zones characterized of depressed shear strength. These predisposed zones result in gravitational failure of volcanic bodies that can be classified mechanically as lateral-type slides. There was an interdisciplinary research applied here with methods of engineering-geology, Quaternary geology, geomorphology, geomechanics and applied geophysics (Rybář et al. 2000). Monitoring and physical models (Rybář & Košťák 2003) contributed to a closer clarification of the mechanism that produced such complex gravitational slope failure.

On the left bank of the Labe River one finds locality of Prackovice Village where rigid blocks move on plastic beds (Fig. 4). Margins of a volcanic body built partially by basalt, partially by trachytic rocks, that are heavily altered at places, are disrupted. Blocks separated from the mother volcanic body sit on calcareous claystones and marlstones of Upper Cretaceous. Marginal volcanic rocks are displaced and rotated down the slope and form a typical dominant of the local morphology. Their surface often shows a backward tilting,

499

against the slope. It is so even in the case of the largest of the blocks which is about 450 m long and 50 to 60 m wide. Here, crossing this area of Prackovice Village, the route of motorway D-8 was designed. Therefore, engineering-geological, geotechnical and geophysical survey was effected here in several steps.

The layout and size of individual buried basalt blocks was successfully verified with the use of geomagnetic methods. Two blocks were drilled through by core boreholes. At one case the basalt block was found 38,7 m thick and clearly separated from the bedrock of Cretaceous marlstones that were in a zone 1,40 m thick intensively deformed. In the central and lower parts of the slope prospecting verified thickness of the slid material of up to 15 m. All the studies proved that the motorway construction will be demanding but realizable (Pašek & Kudrna 1996).

4 SELECTED TYPES OF DEEP-SEATED SLOPE DEFORMATIONS IN WESTERN CARPATHIANS

Extensive slope deformations in the eastern section of the Czech Republic reached by Western Carpathians developed on the crests and on the slopes of Moravskoslezské Beskydy Mts. Under mountainous conditions of flysh where sandstones alternate with claystones, it is mainly translational slope movements along moderately inclined predisposed planes and zones that occur. They can involve very slow creep at rates of mm per year but also can accelerate and develop into dangerous fast moving character of rock slides.

A long tradition has been the investigation of a mountainous slope under the crest of Mt Lukšinec, a north-western spur of Mt Lysá Hora (1323 m a.s.l.). A group of thick-bedded sandstones, 30 to 70 m thick, is disturbed by block gulches up to several meters wide (Novosad 1966). In one of them covered by debris, a dilatometric instrument TM 71 was installed, and monitoring has proved quasi-continuous rate of about 0, 5 mm per year in block separation (Novosad & Košt'ák 2002). In the bedrock of sandstones one finds a sandstone group of beds intercalated with claystones. Beds are tilted from 10 to 15 deg and the tilt coincides with the slope inclination (Heiland 1998).

Another locality in the Moravskoslezské Beskydy Mts., being monitored for a long time, is a translatory landslide on the right bank of the water reservoir Šance on the Ostravice River. The slide is old and was activated in 1969 by water rise in the reservoir backwater zone. Displacements in total have reached up to 4 m since. Movements were monitored from the very beginning of the reservoir construction and small deceleration of movements was indicated. Monitoring methods were improved radically during the last decade.

The data are registered automatically with remote satellite transmission. Continual monitoring of the rock slide made it possible to handle an emergency situation here when slope movements started to accelerate rapidly during a flood period of July 6, 1997. There was a danger that the reservoir could be partially filled and the dam crown spilled over. An emergency plan allowed for evacuation of the population from the valley under the dam and the notice was bound to monitoring data. Luckily, extreme precipitation stopped after July 9, and landslide movements slowed down rapidly and returned to the original non-catastrophic level (Novosad 2002).

Since 2000 data about gravitational movements have been monitored in the crest area of Moravskoslezské Beskydy Mts. Blocks of rigid sandstones and conglomerates with intercalations of claystones are moving along predisposed planes and zones that are usually bound to bedding and tectonic fault lines (Stemberk & Jánoš 2003). Plan areas of slope deformations reach hundreds of square meters to kilometers. Relief in the crest parts of slopes is usually step-like, and the so-called double crests are frequent. Mapping registered systems of pseudokarst fissure caves in separation zones. These reach considerable depths, e.g. in Kněhyně Cave had a measured depth of 72,5 m.

First results from monitoring in Cyrilka Cave reflect present tectonic movements in the evolution of the cave system (Stemberk 2002). Cyrilka Cave originated on a NNE-SSW fault crossing the main ridge of the Moravskoslezské Beskydy Mts. which is generally oriented to E-W. Sinistral horizontal movements were registered, corresponding to the geologically proven youngest Upper Tertiary movements in the area (Krejčí et al. 2004).

In the eastern part of Hostýnské Vrchy Hills, on SE slope of Křížoý Hill one finds an extensive landslide area up to 800 m long and 375 m wide. Limits of the disrupted area in ground plan show correlation with tectonic fault lines. A separation wall in arcose sandstones is up to 45 m high with fissure caves at its toe that are accessible to a depth of 12 m. A total sink in the upper trench can be estimated up to 65 m. In the uncovered bedrock of sandstones one will find alternating flysh layers of claystones and sandstones. The upper part of the slope deformation displays block-type character while in the lower part passes into a complex of active and temporary stabilized landslides (Fig. 5). Baroň (2004) presents results of dilatometric measurements in pseudokarst of Zbojnická Cave from a period December 2001 – September 2004 and comes to wall separation by about 1,7 mm and to subsidence of cave bottom by about 2,6 mm. Movement reactivation is generally parallel with precipitation, however delayed by 15 to 25 days. Reaction to temperature is considerably smaller.
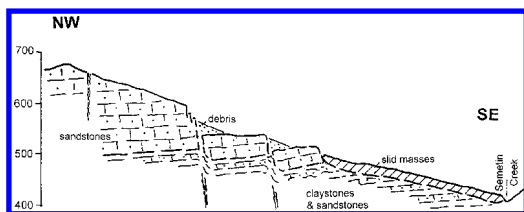
500

Figure 5. A schematic cross-section through the Křížový Hill slope deformation.

5 CONCLUSIONS

The Czech Republic pays an increased attention to deep-seated deformations of creep character. To recognize them in the terrain is often not easy and requires a long experience. In the relief, forms of such deformations are usually most obvious in the upper tensile zone while at the slope toe they are often completely wiped out by denudation processes. In the past such deep slope deformations were considered permanently stabilized. Monitoring with the use of high resolution instruments brought important data showing instability in a series of investigated deformations. Old relict deep-seated deformations not recognized in time may be activated or their low rate movement accelerated in case of an anthropogeneous intervention. A number of examples from Czech Cretaceous Plateau can be named where instability originated during construction of motorways in regions with relict forms of deep-seated slope deformations.

Let us give the example of old deep slope deformations that were underestimated during investigations for dam construction near Žermanice Village in the region of the Carpathian flysh in NE Bohemia in the 50's of the last century. Only after the construction of the concrete gravity dam were the slopes of the valley found to be affected by old deep deformations (Záruba 1956). It was about 30 m thick bedded vein of rigid volcanic rock of Těšínit group of beds that was broken in the Pleistocene into huge blocks sinking in soft Lower Cretaceous marlstones of bedrock. Excavations during dam foundation caused dangerous reactivation of old movements, and a series of measures had to be applied to complete the reservoir. Safe operation called for a monitoring system, and present results give evidence of permanent movements and inclinations of dam blocks at low rates that, however, cannot cause any damage during operation of the water reservoir.

REFERENCES

Baroň, J. 2004. Structure, dynamics and history of deep-seated slope failures. Ph.D. Thesis, Masaryk University, 1–98. Brno.

Fencl, J. 1966. Types of landslides in the Cretaceous Basin of Bohemia (in Czech). *Sbor. geol. Věd, Ř. HIG* 5: 23–36.

Heiland, J. 1998. Translational block-type slope movements-mechanism and examples. *Acta Montana IRSM AS CR*, AB 6 (109): 81–137.

Krejčí, O., Hubatka, F. & Švancara, J. 2004. Gravitational spreading of the elevated mountain ridges in the Moravian-Silesian Beskids. *Acta Geodyn. Geomater*. 1,3(135): 97–109.

Kyrianová, I. 2004. Mapping of geodynamic phenomena in NE parts of the Příhrazy Plateau (in Czech). *Zpr. Geol. Výzk. V r:* 2003: 69–71. Praha.

Malgot, J. 1977. Deep-seated gravitational slope deformations in neovolcanic mountain ranges of Slovakia. *Bull. IAEG* 16: 106–109.

Nemčok, A. & Baliak, F. 1977. Gravitational deformations in Mesozoic rocks of the Carpathian mountain range. *Bull. IAEG* 16: 109–111.

Nemčok, A., Pašek, J. & Rybář, J. 1972. Classification of landslides and other mass movements. *Rock Mech.* 4(2): 71–78.

Novosad, S. 1966. Slope disturbances in the Godula Group of the Moravskoslezské Beskydy Mountains (in Czech). *Sbor. geol. Věd, Ř. HIG* 5: 71–86.

Novosad, S. 2002. Šance dam – "Řečica" landslide. In "*1st ECL Field Trip Guide, Post-Conference Field Trip*", 11–20. Praha, Bratislava.

Novosad, S. & Košt'ák, B. 2002. Lukšinec Hill. In "*1st ECL Field Trip Guide, Post-Conference Field Trip*", 21–23. Prague, Bratislava.

Pašek, J. & Demek, J. 1969. Mass movements near the community of Stadice in north western Bohemia. *Studia Geographica* 3: 1–17.

Pašek, J. & Košt'ák, B. 1977. Block-type slope movements (in Czech). *Rozpr. Čs. Akad. Věd, Ř. mat. přír. Věd* 87(3): 3–58.

Pašek, J. & Kudrna, Z. 1996. Motorway in a landslide area in the České Středohoří Mts. (in Czech). *Zb. 2. Geotechnická konf.*: 97–102. Bratislava.

Rybář, J. 2003. Landslide susceptibility mapping under conditions of the Czech Republic. *Geologisches Jahrbuch*, SC 4: 253–257. Hannover.

Rybář, J. & Kudrna, Z. 2004. Evaluation of dangerous geodynamic phenomena near the town of Mladá Boleslav, Czech Republic. *Zb. ved. konf. "Geológia a životné prostredie"*: 97–101. Bratislava.

Rybář, J. & Košt'ák, B. 2003. Monitoring and physical model simulation of a complex slope deformation in neovolcanics. In Natau, O., Fecker, E., Pimental, E. (eds), *Geotechnical Measurements and Modelling*: 231–237. Lisse, Balkema.

Rybář, J. & Stemberk, J. 2000. Avalanche-like occurrences of slope deformations in the Czech Republic and coping with their consequences. *Landslide News* 13: 28–33.

Rybář, J., Vilímek, V. & Cílek, V. 2000. Process analysis of deep slope failures in České Středohoří neovolcanites. *Acta Montana IRSM AS CR*, AB 8(115): 39–46.

Stemberk, J. 2002. Slope and tectonic movements trial in Moravskoslezské Beskydy Mts. In *1st ECL Field Trip*

Guide, Post Conference Field Trip: 24–27. Praha, Bratislava.

Stemberk, J. 2003. Study of the slope deformations on Příhrazy plateau near Mnichovo Hradiště, map sheet 03-34-01 at a scale of 1:10 000 (in Czech). *Zpr. geol. Výzk. v r. 2002*: 102–103. Praha.

Stemberk, J. & Jánoš, V. 2003. Slope deformations on Radhošt' Ridge, Moravskoslezské Beskydy Mts., map sheets 25-23-09 and 25-23-10 at a scale of 1:10 000 (in Czech). *Zpr. geol. Výzk. v r. 2002*: 104–106. Praha.

Stemberk, J. & Zvelebil, J. 1999. Changes of the slope movements activity along the north-western rim of the Příhrazy plateau (in Czech). *Geotechnika*, 2: 15–20.

Varnes, D.J. 1978. Slope movements types and processes. In R.L. Schuster & R.J. Krizek (eds) "*Landslides Analysis and Control*", 11–33, Special Report 176, Washington D.C.

Záruba, Q. 1927. About sliding of soils in Czechoslovakia (in Czech). *Čs. Vlastivěda,1.díl*: 83–90. *Praha.*

Záruba, Q. 1956. Superficial quasi-plastic deformations of rocks (in Czech). *Rozpr. Čs. Akad. Věd. Ř. Mat. přír. Věd* 66(15): 1–34.

Záruba, Q., Fencl, J., Šimek, J. & Eisenstein, Z. 1966. Analysis of the Dneboh landslide (in Czech). *Sb. geol. Věd, Ř. HIG* 5: 141–160.

Case histories: risk assessment and management

Vulnerability and acceptable risk in integrated risk assessment framework

H.S.B. Düzgün
Middle East Technical University, Ankara, Turkey

S. Lacasse
International Centre for Geohazards, Norwegian Geotechnical Institute, Oslo, Norway

ABSTRACT: Two important aspects of quantitative landslide risk assessment, vulnerability and acceptable risk, are studied as part of a new Integrated Risk Assessment Framework (IRAF). IRAF consists of four steps: data collection, hazard assessment, vulnerability assessment, and risk assessment. Data collection involves obtaining the appropriate data for the hazard, vulnerability and risk assessments. The hazard component integrates the numerical and probabilistic analyses to exploit the added knowledge from the two approaches. A new 3-dimensional framework for quantification of vulnerability is proposed. The fourth component of IRAF is risk assessment, with the computation and evaluation of the risk based on some acceptability criteria. IRAF is implemented for rock slopes. To define an acceptability criterion, published data were collected. Various terminology relating to acceptable risk used in the literature, such as acceptable vs. tolerable, specific vs. total, voluntary vs. involuntary and individual vs. societal, are discussed.

1 INTRODUCTION

The effective mitigation of landslide risk requires analytical approaches. In qualitative risk assessment, the components of risk, which are hazard, elements at risk and vulnerability, are expressed verbally and the final result is in terms of ranked or verbal risk levels (IUGS 1997). Qualitative risk assessment is subjective in nature. Quantitative risk assessment involves quantification of risk components and computation of risk. The purpose of quantitative risk assessment (QRA) is to calculate a value for the risk to enable improved risk communication and decision-making (Lee & Jones 2004). For landslides, the use of quantitative risk assessment procedures is recommended. Several frameworks for QRA have been proposed by many experts and organizations (e.g. Varnes 1984, Whitman 1984, Einstein 1988, Fell 1994, Wu *et al.* 1996, Morgenstern 1997, Fell & Hartford 1997, Einstein 1997, Aleotti & Chowdhury 1999, Ho *et al.* 2000, Roberds 2001, Dai *et al.* 2002, Nadim & Lacasse 2003, Lee & Jones 2004, IUGS 1997, AGS 2000, NRC Transportation Research Board 1996, GEO 1998). The QRA frameworks have common intention to find answers to the following questions (Ho *et al.* 2000, Lee & Jones 2004):

1 What are the probable dangers/problems? [Danger Identification]
2 What would be the magnitude of dangers/problems? [Hazard Assessment]
3 What are the possible consequences and/or elements at risk? [Consequence/Elements at Risk Identification]
4 What might be the degree of damage in elements at risk [Vulnerability Assessment]
5 What is the probability of damage? [Risk Quantification/Estimation]
6 What is the significance of estimated risk? [Risk Evaluation]
7 What should be done? [Risk Management]

Depending on the characteristics of a landslide, available data, scale of investigation and nature of consequences, the QRA frameworks may differ. Hazard assessment for a specific slope usually involves probabilistic analysis of the given slope, while hazard assessment for a region generally requires the computation of frequency of the landslides in the region. The probabilistic models used for a specific slope depend on the failure mechanism (flows, falls or slides) and slope material (soil or rock). Furthermore, the characteristics of a landslide and scale of investigation influence the consequence/elements at risk, vulnerability, risk quantification/assessment, risk evaluation and risk management. Two important aspects of QRA for landslides are the lack of well-established acceptable risk criteria and methods for

vulnerability assessment, which limit the widespread use of QRA.

2 HAZARD ASSESSMENT APPROACHES

Hazard assessment can be viewed from two perspectives (Fig. 1). Under Perspective I, the approaches consider the factors affecting the landslides, susceptibility and trigger. In terms of susceptibility, landslide hazard, or the probability that a particular landslide occurs within a given period of time, is computed from variables such as geology, slope gradient and aspect, elevation, geotechnical properties, vegetation cover, weathering, drainage pattern. In terms of triggers, the analyses focus on triggering factors such as earthquake, rainfall, snowmelt, change in water-level and volcanic activity (Wilson & Wieczorek 1995, Aleotti *et al.* 1996, Polloni *et al.* 1996, Finley *et al.* 1997, Glade *et al.* 2000, Dai & Lee 2001, Wang *et al.* 2003, Alcantara-Ayala 2004). Recent trends are to consider the susceptibility and triggers in a combined manner (e.g. Nadim & Kjekstad 2005).

Under Perspective II, hazard assessment methods consider the scale of investigation either "regional/global" or "specific/local". Regional/global studies use frequency, heuristic, statistical and deterministic approaches. In frequency approaches, the probability of landslide is determined from historical records. Heuristic approaches (Carrara & Merenda 1974, Keinholz 1978, Rupke *et al.* 1988, Moon *et al.* 1992, Kuloshvili & Maisuradze 2000, Tatashidze *et al.* 2000) combine expert opinion with susceptibility and/or trigger factors (Dai *et al.* 2002). The conventional multivariate statistical methods form the basis of statistical approaches (Yin & Yan 1988, Carrara *et al.* 1991, Leroi 1996, Chung & Fabbri 1999). Multiple regression/logistic regression and discriminant analyses determine landslide probability by relating terrain conditions and landslide occurrence

(Lee & Jones 2004). Deterministic approaches (e.g. Ward *et al.* 1982, Okimura & Kawatani 1986) are limit equilibrium models under the assumption of infinite slope. The regional/global approaches require landslide inventory of past landslides. They involve mapping and spatial analyses, which necessitate use of Geographical Information Systems (GIS) and Remote Sensing (RS) (Van Westen 2004). They require the assumptions of one or more of the following (Hearn & Griffiths 2001, Lee & Jones 2004):

1 The locations of past and present landslides are the source of future landslides.
2 Future landslides have the same conditions as the past and present landslides.
3 Only the considered factors determine the distribution of past and present landslides.

The specific/local studies are stability analyses of specific slope based on deterministic (limiting equilibrium, numerical analyses) and probabilistic methods (First Order Reliability Method (FORM), Point Estimate, Monte Carlo Simulation) (Duncan 1996, Tang *et al.* 1999, ICG 2004a, b, Christian 2004). The components in Figure 1 are related to each other. Improved methods of landslide hazard assessment can be developed from new combinations of approaches.

3 INTEGRATED RISK ASSESSMENT FRAMEWORK (IRAF)

The proposed Integrated Risk Assessment Framework (IRAF) is a generic QRA procedure. IRAF (Fig. 2) includes four steps: data collection, hazard assessment, vulnerability assessment and risk assessment. In data collection, the required data for the hazard, vulnerability and risk assessment, are obtained. In hazard assessment the numerical and probabilistic analyses are integrated and exploit the benefits and added knowledge from the two approaches. The vulnerability assessment refers to the degree of loss for elements at risk. Risk assessment includes the calculation and evaluation of the risk based on some acceptability criteria.

3.1 *Data collection*

Data collection involves obtaining the required data for hazard, vulnerability and risk assessment. For specific slopes, required data relate to slope geometry such as height, width, inclination and failure plane (shape and length), strength parameters, namely frictional properties for soil slopes and properties of discontinuities for rock slopes, trigger such as rainfall intensity, water level, earthquake magnitude etc. Data collection is essential and need comprehensive geological and geotechnical investigations in the field and laboratory, and review of existing information.
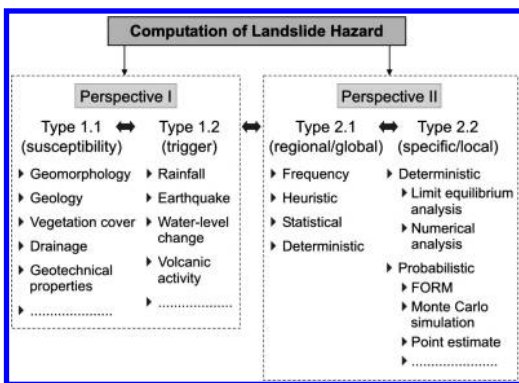

Figure 1. Landslide hazard assessment approaches.

506

3.2 *Hazard assessment*

Hazard assessment for a specific slope in IRAF combines deterministic and probabilistic slope analyses (Fig. 2). Numerical modeling with sensitivity analyses constitutes the deterministic part. The probabilistic part consists of probabilistic modeling with uncertainty analysis. Numerical analysis provides an improved understanding of failure mechanism and failure surface location, thus decreasing the uncertainty related to slope geometry. Combining the procedure with limiting equilibrium analysis is recommended.

There are basically three methods of numerical analysis, namely continuum (e.g. finite element, finite difference), discontinuum (distinct element, discrete element) and hybrid continuum/discontinuum (ICG 2004a). Continuum methods are used for soil and weak rock slopes, discontinuum methods are more appropriate for rock slopes where failure is governed by the rock discontinuities. Numerical analyses are coupled with sensitivity analyses to determine the sensitivity to input parameters.

In IRAF, the probability of slope failure, based on limiting equilibrium models, can be computed based on any probabilistic method (Fig. 1). An uncertainty analysis of the input parameters is essential prior to calculation. Models for quantification of uncertainties are proposed by e.g. Yucemen *et al.* (1973), Ang & Tang (1984), Li & Lumb (1987), El-Ramly *et al.* (2003) and Duzgun *et al.* (2002).

The quantification and analysis of uncertainties play a critical role in risk assessment. Although there are several formulations of risk in the literature (Varnes 1984, Einstein 1988, Fell 1994, Morgan *et al.* 1992, Dai *et al.* 2002, Glade 2003, Lee & Jones 2004), risk is a multiplication of hazard and consequence of the hazard. Both are estimates rather than real values. In a multiplicative function, the uncertainties in the inputs of the model propagate within the model. A careful assessment of the uncertainties helps to control the propagation of uncertainties in the risk estimation process.

3.3 *Vulnerability assessment*

In landslide risk assessment, vulnerability is the degree of loss for a given element at risk, and is expressed by an index ranging between 0 and 1. The assessment of vulnerability for landslides in the literature is usually qualitative and specific to the landslide cases investigated. Reviews of landslide vulnerability are made by Glade (2003) and Lee & Jones (2004). For effective use of QRA in landslides, generalized quantitative models for vulnerability assessment are essential. Risk assessment for multi-hazard situations (e.g. risk due to earthquake, landslide, flood, etc.) requires systematic approaches for vulnerability analyses (ICG 2004c), since in earthquake, flood and hurricane risk assessment, the vulnerability is expressed by probability loss curves, which are mathematical models for vulnerability. Quantitative models for landslide vulnerability provide levels of uncertainty in the consequences (ICG 2004c), which help to assess the uncertainty associated with the risk estimate.

The nature of landslides makes the development of quantitative models difficult. First, landslides are spatially discrete phenomena unlike earthquakes, floods and hurricanes, which have spatially continuous loss measurement parameters such as ground motion, rainfall and wind speed. Second, there is no unique way of computing landslide hazard. Third, the notion of risk in landslides varies according to focus of interest.

Table 1 lists different definitions of risk for landslides. Einstein (1988) gives a generic risk definition for landslides. Definitions by Varnes (1984) and Fell (1994) introduce a distinction between specific and total risk. Specific risk refers to risk for a given element at risk, whereas total risk is the sum of all specific risks computed for lives lost, property damage, loss of economic activity, environmental damage etc. Lee & Jones (2004) also differentiate specific risk from total risk, and introduces a parameter of exposure (proportion of total value of element at risk likely to be present during the landslide and expressed on a scale of 0–1). Exposure reflects the temporal nature
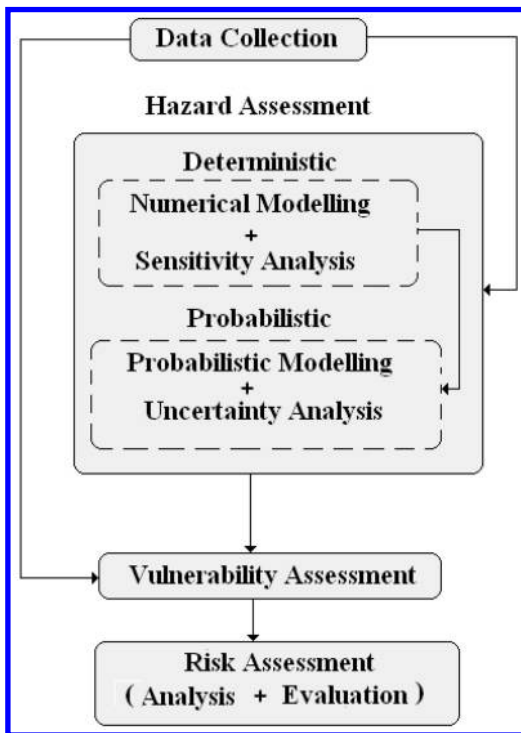

Figure 2. Integrated Risk Assessment Framework (IRAF).

507

Table 1. Various definitions of risk for landslides.

	Risk formulation	Definition	Source
Level of Generalization in Definition of Risk ↑	Risk = Hazard × Consequences Rs = H × V	Consequences: Potential worth of loss Rs: Specific risk, H: Hazard, V: Vulnerability	Einstein (1988) Varnes (1984)
	Rt = Rs × E = (H × V) × E	Rt: Total risk, E: Elements at risk	Varnes (1984)
	Rt = Σ(Rs × E) = Σ(H × V × E)	Rt: Total risk, Rs: Specific risk, V: Vulnerability, E: Elements at risk	Fell (1994)
	Rs = P(Hi) × Σ(E × V × Ex) Rt = Σ Rs(Landslide events 1,…, n)	Rs: Specific risk, Rt: Total risk, P(Hi): Hazard for a particular magnitude of landslide (Hi), E: Total value of elements at risk, V: Vulnerability, Ex: Exposure	Lee & Jones (2004)
	R(DI) = P(H) × P(S\H) × P (T\S) × P(L\T)	R(DI): Individual risk, P(H): Hazard, P(S\H): Probability of spatial impact, P (T\S): Probability of temporal impact, P (L\T): Probability of loss of life for an individual	Morgan *et al.* (1992)
	R(PD) = P(H) × P(S\H) × V(P\S) × E	R (PD): Specific risk (property), P(H): Hazard, P (S\H): Probability that landslide impacts the property, V(P\S): Vulnerability, E: Value of property	Dai *et al.* (2002)

of the vulnerability and hence risk. Morgan *et al.* (1992) and Dai *et al.* (2002) define specific risk for individual and property losses. In the formulations, hazard is defined as conditional probabilities. Variable types of elements at risk lead to decomposition of total risk into specific risk. The total risk is defined as the sum of specific risks. It is difficult to evaluate this sum since the unit of each specific risk is not identical: individual risk has the unit of loss of life/yr, annual property risk has the unit of monetary loss/yr. It is complex, even debatable, to convert loss of life into a monetary value.

Vulnerability assessment for landslides should consider the various ways of hazard computation, the variable nature of elements at risk and the scale of investigation. In IRAF, a 3-D conceptual framework for the assessment of vulnerability is proposed. The magnitude (M) of landslide is the first dimension while scale (S) and elements at risk (E) are the other dimensions (Fig. 3).

The magnitude of a landslide has important effect on the vulnerability value of elements at risk. The magnitude of a landslide is denoted by $M(\underline{x})$ where $\underline{x}$ refers to the vector of parameters for defining the magnitude of the landslide. The parameters for assessing landslide magnitude are (Ojeda-Mocayo *et al.* 2004, Lee & Jones 2004) volume (x_1), velocity (x_2), depth (x_3), run out (x_4) and areal extent (x_5). There are correlations between the parameters of the landslide magnitude (M), which complicates the assessment.

The second dimension Scale (S) refers to the scale of investigation. It is relatively easier to assess
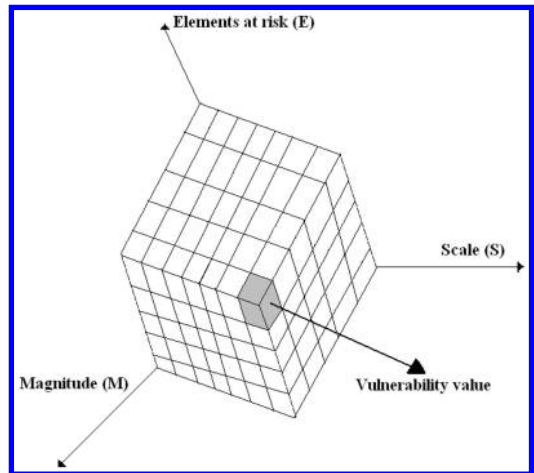
Figure 3. Conceptual 3-D vulnerability framework.

vulnerability of specific slopes than on a regional scale analysis. Elements at risk (E), the third dimension, reflect the specific risk, assessed from attributes such as property, population, environment and economy. The attributes of E can be analyzed within the framework of Multi Attribute Utility Theory (MAUT) to yield a total vulnerability value.

The dimensions E, M and S are statistically correlated. There are also autocorrelations in E and M. The 3 dimensions have a temporal dimension, which can be treated after establishing the framework.

508

3.4 *Risk assessment*

Risk assessment refers to the computation of risk and evaluation of it based on certain acceptability/tolerability criteria. Lack of well-established acceptability criteria for landslide risks is the main handicap of QRA. Some guidance can be found in Whitman (1984), Morgan (1991), Cave (1993), Fell (1994), Morgenstern (1997), Fell & Hartford (1997), IUGS (1997), GEO (1998), AGS (2000), Dai *et al.* (2002), Lee & Jones (2004). The terminology is rather eclectic, and prevents effective risk communication. This paper tries to clarify the acceptable risk terminology.

The nature of risk determines its acceptability, which is associated with for example as (Osei *et al.* 1997):

– Voluntary vs. involuntary
– Controllability vs. uncontrollability
– Familiarity vs. unfamiliarity
– Short- vs. long-term consequences
– Presence of existing alternatives
– Type and nature of consequences
– Derived benefits
– Presentation in the media
– Information availability
– Personal involvement
– Memory of consequences
– Degree of trust in regulatory bodies

Voluntary risks (e.g. cigarette smoking) tend to be higher than involuntary risks (e.g. building a new chemical plant). Once the risk is under personal control (e.g. driving a car), it is more acceptable than the risk controlled by other parties (e.g. traveling as a passenger). For landslides, natural and engineered slopes can be considered as voluntary and involuntary, respectively. People familiar with the risk involved are more willing to accept it. Societies experiencing frequent landslides may have different risk acceptance than those experiencing rare landslide situations. The risk acceptance also depends on for example level of available information. Informed societies can have better preparedness for natural hazards. Societies experiencing frequent natural disasters have fresh memories of consequences.

Acceptable risk refers to the level of risk which requires no further reduction. Tolerable risk refers to the risk level assessment in exchange for certain benefits. It is the society's decision whether to accept or tolerate the risk. When the risk is accepted by the society, no action/expenditure is required for reduction. Tolerated risks require proper control and further risk reduction if possible. Risks above a certain threshold (A) are considered to be unacceptable, while below another threshold (B) are regarded as very small and hence acceptable. If the computed risk lies between A and B (Fig. 4), it should be reduced to an "as low as reasonably practicable" level (ALARP).
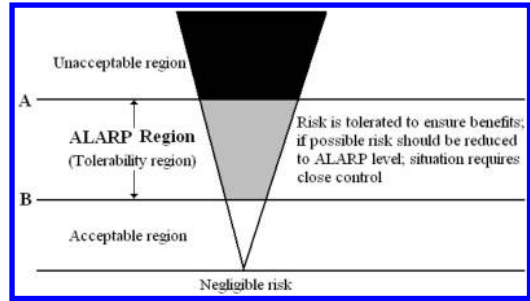
Figure 4. Risk tolerability/acceptability criteria.

Table 2. Suggested individual risk levels for landslides.

Slopes	Individual risk (loss of life/yr)	Reference
Natural slopes	10^{-3}	
Existing engineered slopes	10^{-4}–10^{-6}	Fell & Hartford (1997)
New engineered slopes	10^{-5}–10^{-6}	AGS (2000)
Existing	10^{-4}	ERM-Hong Kong
New	10^{-5}	(1998)

AGS (2000) prepared guidelines for acceptability criteria for landslide risk. The acceptable risk levels for individual risk are well established for the chemical industry, nuclear power and dam safety and are discussed to form a basis for landslide risk by Fell & Hartford (1997). They proposed tolerable risk levels for natural slopes, existing and new-engineered slopes as 10^{-3}, 10^{-4} to 10^{-6} and 10^{-5} to 10^{-6}, respectively. These levels are also suggested by AGS (2000). Lee & Jones (2004) refer to ERM-Hong Kong (1998), Reeves *et al.* (1999) and Ho *et al.* (2000) giving Hong Kong's interim risk guidelines for natural terrain landslide hazard. They used the term "maximum allowable individual risk", which is proposed as 10^{-5} and 10^{-4} for new and existing slopes. Table 2 summarizes the suggested annual individual risk levels.

The society's point of view, called societal risk, is defined as the risk of widespread or large scale detriment from the realization of a defined risk, the implication being that the consequence would be on such a scale as to provoke a socio/political response (definition of the International Society of Soil Mechanics and Geotechnical Engineering Technical Committee 32 on Risk Assessment and Management). In this perspective, risks having low hazard and high consequence are taken into account. For individual and societal risk, the unit of risk is the loss of life/yr. Societal risk is generally expressed by f-N or F-N curves. When the frequency of events causing at least N fatalities is plotted against N on log-log scales, the result is called

509

F-N curves (Bedford 2004). If the frequency scale is replaced by annual probability, the resultant curve is called f-N curve. F-N curves are used for comparing the societal risk due to several risks such as landslides, earthquakes, dams, airplane crashes, etc. (Whitman 1984, Morgan 1991). They are also used to compare the societal risk situation in different countries for landslides (Guzzetti 2000). F-N curves are constructed from historical data on number of landslides and related fatalities. They in fact represent current situation (Christian 2004). F-N curves form the basis for developing societal acceptability and tolerability levels. Currently, the F-N curve proposed by Ho *et al.* (2000) is the most comprehensive one in the literature. The F-N curves can be constructed for various geographical units such as country, province, state etc. Therefore, the number of landslides and related fatalities within the considered geographical unit determines the acceptability and tolerability criteria.

Based on the data collected from the literature and institutional contacts, f-N curves for Canada, China, Colombia, Hong Kong, Italy, Japan, Nepal and Norway were constructed. The annual probability N or more fatalities (f) plotted against N (log–log scale) gives the following linear relation:

$$log\, f = a + b\log N \qquad (1)$$

Figures 5 and 6 illustrate the original data and fitted curves for 8 countries. Table 3 describes the data sets used in Figures 5 and 6.

The data and fitted curves indicate that Japan and China have similar societal risk situations while the Hong Kong and Canada curves agree but show a different trend. When the f-N curves of the 8 countries are compared, the population density and spatial distribution of the hazard should be taken into account. Table 4 gives population density, f-values for different N-values and slope of the best-fit curve. Although Hong Kong has the highest density, the highest N-value is less than 100. The Hong Kong curve presents performance of engineered slopes i.e. the risk imposed to the society by designed slopes. Although Canada has the lowest population density, it has f-values (when N = 10) close to those of Hong Kong. Evans (2003) indicated that although Canada has one of the lowest population densities in the world, 98% of its population lives in 10% of the country, which is equivalent to a population density of 30 persons/km^2. Each country has different f-N curve. If acceptable and tolerable societal risk levels are to be established, each country should probably select different levels.
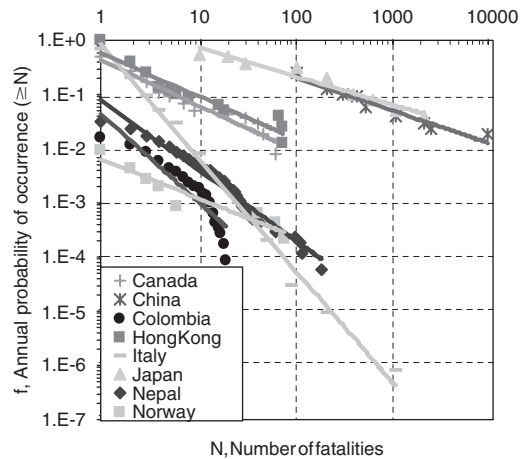
Figure 6.   Fitted curves for f-N plots of Figure 5.

Table 3.   Sources used for construction f-N curves.

Country	Years	Source
Canada	1800–1996	Evans (1997)
China	1900–1987	Tianchi (1989)
Colombia	1936–2000	The Latin American Database DESINVENTAR/ La Red (University of Panama)
Hong Kong	1917–1995	ERM-Hong Kong (1998)
Italy	1900–2002	Guzzetti (2004) http://sici.irpi.cnr.it/danni_ persone.htm
Japan	1948–1996	Morgan (1991)
Nepal	1971–2000	NGI (2004)
Norway	1900–2004	NGU (2004)

Figure 5.   f-N plots for eight countries.

510

Although F-N curves are frequently used for establishing societal risk levels, there are problems associated with F-N curves. The curves are estimates of the current situation as they are constructed from historical data. Data quality and reliability need to be ascertained. To ensure data accuracy, the most recent years can be used but this creates the problem of limited data. Values of F for N = 1 in F-N curves are often used to refer to individual risk, but this is not reliable since they are not determined for a specific person.

When the spatial distribution of hazard for each country is investigated, the landslides are concentrated in only some parts of the considered countries except from Japan. Figures 7 to 10 are obtained for 4

of the 8 countries from the hazard model developed for the Global Landslide and Avalanche Hotspots project (Nadim & Kjekstad 2005). As their model is on a global scale, detailed investigations in each country may also result in different hazard maps. Düzgün & Lacasse (2005) present more details on the

Figure 9.   Landslide hazard map of Japan.

Figure 7.   Landslide hazard map of China.

Figure 8.   Landslide hazard map of Columbia.

Figure 10.   Landslide hazard map of Italy.

511

Table 4. Population density and f-values for eight countries.

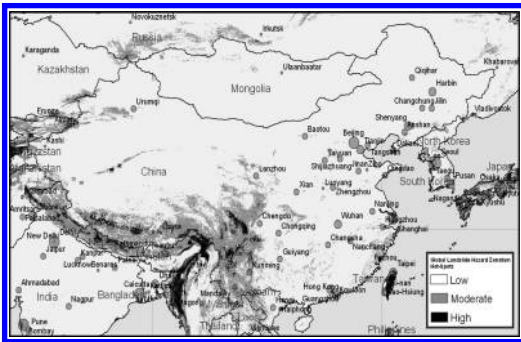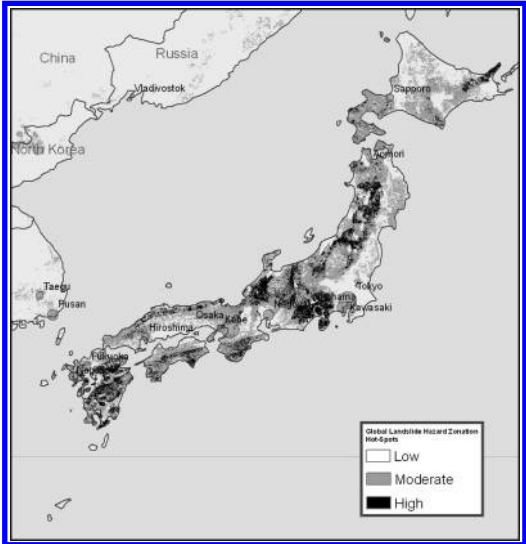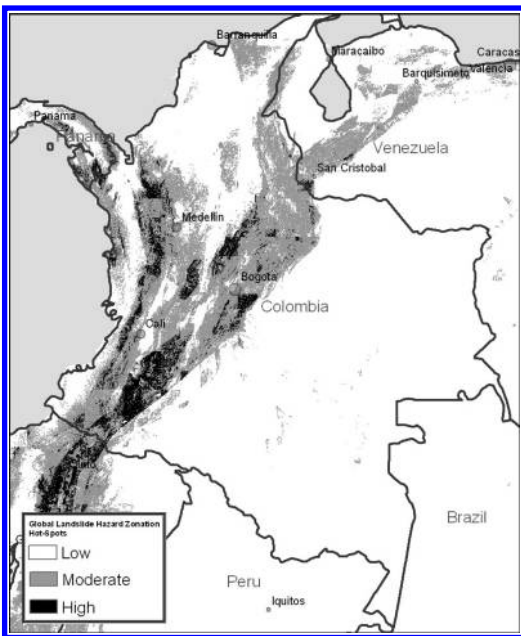| Country	Population density/km²	f-values			Slope (b)
		N = 1	N = 10	N = 100	
Canada	3	0.4	0.07	–	−0.92
China	136	1	1	0.06	−0.61
Colombia	37	0.04	0.001	–	−1.63
Hong Kong	6437	0.6	0.01	–	−0.79
Italy	193	0.9	0.008	5×10^{-5}	−1.99
Japan	336	1	0.8	0.07	−0.53
Nepal	173	0.08	0.004	–	−1.31
Norway	14	0.006	0.001	–	−0.72

maps for the 8 countries in Table 4. Societal risk applies to regional scale hazard analysis (Fig. 1). It is suggested to develop F-N curves for the area of interest whenever possible. If not, it is recommended to choose the most suitable curve from the data in Figures 5 and 6.

For cases with different types of elements at risk, the computation of landslide risk as specific risk leads to introduction of different acceptability and tolerability criteria for the various elements at risk. The societal and individual risk acceptability criteria apply to the human component of element at risk. For property, Fell & Hartford (1997) give the range of 10^{-3} to 10^{-4}/year, or approximately one order of magnitude higher than the individual risk. Up to now, environmental damage is the least considered element at risk and they have no acceptability criteria. Increasing environmental legislation and international commitments may impose new constraints for landslide risk management and acceptability/tolerability criteria (Lee & Jones 2004).

4 IMPLEMENTATION FOR ROCK SLOPES

When IRAF is implemented for rock slopes, it takes the form illustrated in Figure 11. Data collection involves obtaining relevant data for geology, geometry, strength, groundwater condition, dynamic loads and elements at risk.

Hazard assessment is composed of the following stages:

1 Kinematic analysis: Determine discontinuity sets which govern slope instability.
2 Numerical modeling: Understand the failure mechanism and determine failure surface and slope geometry, including volume of rock mass to slide, geometry of slip surface, depth of slide for weak rock, and number of blocks to slide and volume of sliding rock for competent rock.
3 Sensitivity analysis: Evaluate model's sensitivity to input parameters and compare e.g. Mohr-Coulomb and/or Barton-Bandis failure criteria.

4 Uncertainty analysis: Do uncertainty analysis, and quantify the uncertainties associated with most sensitive parameters.
5 Probabilistic modeling: Obtain failure probability for slope based on Monte Carlo Simulation (MCS) or First Order Reliability Method (FORM).
6 Evaluation of slide magnitude: Assess magnitude of the hazard by constructing probability of failure (P_f) versus rock block volumes.

The vulnerability assessment in this case diminishes to 2-dimension as the scale is small. Vulnerability can be assessed in a (n × m) matrix, where n is the type of elements at risk and m is number of rock blocks to slide.

Risk assessment starts with the computation of total and specific risk, in which the total risk can be computed within the MAUT framework. If there are specific risks with inconsistent units such as annual lives lost, number of buildings damaged, number of wild life destroyed, the facts discussed in Section 3.4 should be taken into account.

5 CONCLUSIONS

Quantitative risk assessment (QRA) methods provide a systematic framework for landslide risk assessment. However, the lack of generally accepted models for vulnerability assessment and criteria for risk acceptability and tolerability limit their use. Variable terminology causes misuse, prevents effective risk communication and limits the decision-making process in risk management. This paper contributes to shedding light on the risk terminology.

An Integrated Risk Assessment Framework (IRAF) is proposed to provide a flexible procedure for QRA as well as a new 3-D conceptual framework for vulnerability assessment. The vulnerability framework needs quantification and this can be done by investigating existing databases and publications.
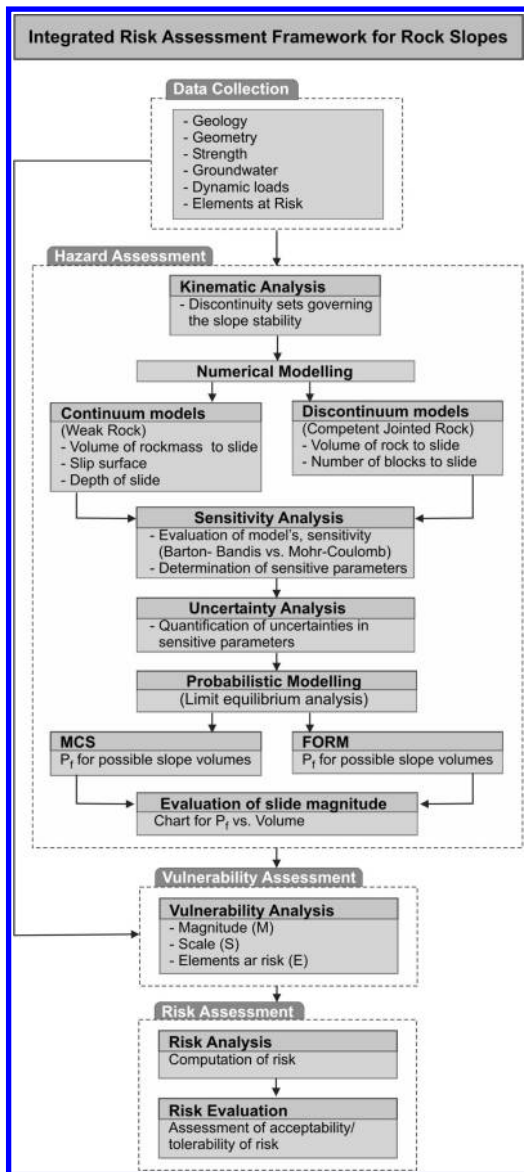
Figure 11.   IRAF for rock slopes.

Although it is difficult to establish a unique acceptability and tolerability criterion for landslides due to the nature of landslide risk, generalizations for various risk types can be made. This requires risk perception research in different countries and societies. It is also equally important to develop acceptability and tolerability criteria for environmental risks due to landslides. As a consequence, establishing risk acceptability for landslides requires interdisciplinary research.

REFERENCES

AGS, Australian Geomechanics Society 2000. Landslide risk management concepts and guidelines. Australian Geomechanics Society, Sub-Committee on Landslide Risk Management, *Australian Geomechanics* 35: 49–92.

Alcantara-Ayala, I. 2004. Hazard assessment of rainfall-induced landsliding in Mexico. *Geomorphology* 61: 19–40.

Aleotti, P, Baldelli, P. & Polloni, G. 1996. Landsliding and flooding event triggered by heavy rains in the Tanarobasin. *Proc. of international congress of Interpraevent*, 435–446.

Aleotti, P. & Chowdhury, R. 1999. Landslide hazard assessment: Summary review and new perspective. *Bulletin of Engineering Geology and Environment* 58: 21–44.

Ang AH-S. & Tang, W.H. 1984. *Probability concepts in engineering planning and design* 2. New York. Wiley, 1984.

Bedford, T. 2004. Risk Acceptance Criteria, FN-curves and Multi-attribute utility theory. *Proceedings of 2nd ASRANET (Network for Integrating Structural Safety, Risk and Reliability) Collequium, Barcelona*, Spain (CD-ROM)

Carrara, A. & Merenda, L. 1974. Landslide inventory in northern Calabria, Southern Italy. *Bulletin of American Geological Society* 87: 1153–1162.

Carrara, A., Cardinali, M., Detti, R., Guzetti, F., Pasqui, V. & Reichenbach, P. 1991. GIS techniques and statistical models in evaluating landslide hazard. *Earth Surface Processes and Landforms* 16: 427–445.

Cave, P.W. 1992. Natural hazards risk assessment and land use planning in British Colombia. In: *Geotechnique and Natural Hazards*, Canadian Geotechnical Society, 1–11.

Christian, J.T. 2004. Geotechnical engineering reliability: how well do we know what we are doing? *Journal Geotechnical and Geoenvironmental Engineering* 130(10): 985–1003.

Chung, C.F. & Fabbri, A.G. 1999. Probabilistic prediction models for landslides hazard mapping. *Photogrammetric Engineering and Remote Sensing* 65: 1389–1399.

Dai, F.C. & Lee, C.F. 2001. Frequency-Volume relation and prediction of rainfall-induced landslides. *Engineering Geology* 43: 27–29.

Dai, F.C., Lee, C.F. & Ngai, Y.Y. 2002. Landslide risk assessment and management: an overview. *Engineering Geology* 64: 64–87.

Duncan, J.M. 1996. Soil slope stability analysis. In *Landslides: Investigation and Mitigation* (eds A.K. Turner & R.L. Schuster). *Transportation Research Board, Special Report* 247: 337–371, National Research Council.

Düzgün, H.S.B. & Lacasse, S. 2005. An integrated landslide risk assessment with special emphasis on vulnerability

513

and acceptable risk. Submitted to *Canadian Geotechnical Journal*, 2005.

Düzgün, H.S.B., Yucemen M.S. & Karpuz, C. 2002. A probabilistic model for the assessment of uncertainties in shear strength of rock discontinuities. *International Journal of Rock Mechanics Mining Sciences and Geomechanics Abstracts* 39: 743–754.

Einstein, H.H. 1988. Special lecture, landslide risk assessment. *Proc. 5th Int. Symp. On Landslides, Lausanne, Switzerland* 2: 1075–1090

Einstein, H.H. 1997. Landslide risk – systematic approaches to assessment and management. In: *Landslide Risk Assessment*, 25–50, Cruden & Fell (eds), Balkema, Rotterdam.

El-Ramly, H., Morgenstern, N.R. & Cruden, D.M. 2003. Probabilistic stability analysis of a tailings dyke on presheared clay-shale. *Canadian Geotechnical Journal* 40: 192–208.

ERM-Hong Kong 1998. Slope failures along BRIL roads: Quantitative Risk Assessment and Ranking. *GEO Report* 81, Hong Kong.

Evans, S.G. 1997. Fatal landslides and landslide risk in Canada. In: *Landslide Risk Assessment*, Cruden & Fell (eds): 185–196.

Evans, S.G. 2003. Characterising landslide risk in Canada. In: *Proceedings of 3rd Canadian Conference on Geotechnique and Natural Hazards*: 19–34.

Fell, R. 1994. Landslide risk assessment and acceptable risk. *Canadian Geotechnical Journal* 31: 261–272.

Fell, R. & Hartford, D. 1997. Landslide risk management. In: *Landslide Risk Assessment*, 51–110, Cruden & Fell (eds), Balkema, Rotterdam.

Finlay, P., Fell, R. & Maguire, P. 1997. The relationship between the probability of landslide occurrence and rainfall. *Canadian Geotechnical Journal* 34: 811–824.

GEO, Geotechnical Engineering Office 1998. Landslides and Boulder Falls from Natural Terrain: Interim Risk Guidelines. *GEO Report*.75, Geotechnical Engineering Office, Government of the Hong Kong SAR.

Glade, T. 2003. Vulnerability assessment in landslide risk analysis. *Die Erde* (Beitrag zur Erdsystemforschung) 134: 123–146.

Glade, T., Crozier, M. & Smith, P. 2000. Applying probability determination to refine landslide-triggering rainfall thresholds using and empirical "Antecedent Daily Rainfall Model". *Pure and Applied Geophysics* 157: 1059–1079.

Guzzetti, F. 2000. Landslide fatalities and the evaluation of landslide risk in Italy. *Engineering Geology* 58: 89–107.

Guzzetti, F. 2004. Sites effected by landslides and floods with human consequences in Italy, http://sici.irpi.cnr.it/ danni_persone.htm.

Hearn, G.J. & Griffiths, J.S. 2001. Landslide hazard mapping and risk assessment. In *Land Surface Evaluation for Engineering Practice* (ed J.S. Griffith), Geological Society, London, Engineering Group Special Publication 18: 43–52.

Ho, K., Leroi, E. & Roberds, B. 2000. Quantitative risk assessment. *Application, myths and future directions*. GeoEng 2000, Technomic Publishing, 269–312.

ICG, International Centre for Geohazards 2004a. Stability analysis of rock slopes. Rock slope failures-models and risk, *ICG report-2004-4-2*, Oslo, Norway, 28p.

ICG, International Centre for Geohazards 2004b. Slope stability analysis for risk assessment. Risk and vulnerability assessment for geohazards, *ICG report-2004-2-5*, Oslo, Norway, 102p.

ICG, International Centre for Geohazards 2004c. Vulnerability in relation to risk management of natural hazards, Risk and vulnerability assessment for geohazards, *ICG report-2004-2-3*, Oslo, Norway, 29p.

IUGS 1997. Quantitative risk assessment for slopes and landslides – the State of the Art. IUGS Working Group on Landsldies, Committee on Risk Assessment, in *Landslide risk assessment*, Cruden & Fell (eds):, 3–12.

Keinholz, H. 1978. Maps of geomorphology and natural hazard of Griendelwald, Switzerlantd scale 1:10 000. *Arctic and Alpine Research* 10: 169–184.

Kuloshvili, S.I. & Maisuradze, G.M. 2000. Geological-geomorphological aspects of landsliding in Georgia (Central and Western Caucasus). In *Landslides: In Research, Theory and Practice* (eds. E.N. Bromheard *et al.*), 861–866.

Lee, E.M. & Jones, D.K.C. 2004. *Landslide Risk Assessment*. Thomas Tilford Publishing, London.

Leroi, E. 1996. Landslide hazard – risk maps at different scales: objectives, tools and developments. In *Landslides Proc. Int. Symp. on Landslides*, Trondheim, 17–21 June, K. Senneset (ed), 35–52.

Li, K. S. & Lumb, P. 1987. Probabilistic design of slopes. *Canadian Geotechnical Journal* 24: 520–535.

Moon, A.T., Olds, R.J., Wilson, R.A. & Burman, B.C. 1992. Debris flow zoning at Montrose, Victoria. In *Landslides* (ed. D.H. Bell) 2: 1015–1022.

Morgan, G.C. 1991. Quantification of risks from slope hazards, *Open File Report* 1992-15, Geological Survey of Canada.

Morgan, G.C., Rawlings, G.E. & Sobkowicz, J.C. 1992. Evaluating total risk to communities from large debris flows. *Proceedings of the 1st Canadian Symposium on Geotechnique and Natural Hazards, Vancouver*: 225–235.

Morgenstern, N.R. 1997. Toward landslide risk assessment in practice. *Landslide Risk Assessment*, Cruden & Fell (eds): 15–23.

Nadim, F. & Lacasse, S. 2003. Review of probabilistic methods for quantification and mapping of geohazards. *Geohazards* 2003, Edmonton: 279–286

Nadim, F. & Kjekstad, O. 2005. Assessment of global landslide hazard and risk hotspots. *Proceedings of 16th Int. Conf. on Soil Mechanics and Geotechnical Engineering, Osaka*, Japan.

NGI, Norwegian Geotechnical Institute 2004. Landslide hazard and risk in Nepal. *NGI report-20041239-1*, Oslo, Norway, 23p.

NGU, Geological Survey of Norway (Furseth, A.) 2004. Personal communication.

NRC, National Research Board, Transportation Research Board 1996. Landslides Investigation and Mitigation. *Special Report* 247, Turner & Schuster (eds.), 673p

Ojeda-Moncayo, J., Locat, J., Couture, R. & Leroueil, S. 2004. The magnitude of landslides: An overview. In *Landslides: Evaluation and Stabilization*, Lacerda et al. (eds), 379–384.

Okimura, T. & Kawatani, T. 1986. Mapping of potential surface failure sites on granite mountain slopes. *International Geomorphology* 1: 121–138.

Osei, E.K., Amoh, G.E.A. & Schandorf, C. 1997. Risk ranking by perception. *Health Physics* 72: 195–203.

Polloni, G., Aleotti, P., Baldelli, P., Nosetto, A. & Casavecchia, K. 1996. Heavy rain triggered landslides in

Alba area during November 1994 flooding event in the Piemonte Region (Italy). *Proc. of 7th International Symposium of Landslides, Throndheim*, 1955–1960

Reeves, A. Ho, K.K.S. & Lo, D.O.K. 1999. Interim risk criteria for landslides and boulder falls from natural terrain. In Geotechnical Risk Management, *18th Annual Seminar Geotechnical Division Hong Kong Institution of Engineers*: 87–96.

Roberds, W.J. 2001. Quantitative landslide risk assessment and management. *Proceeding of International Conference on Landslides – Causes, Impacts and Countermeasures, Davos*, 585–595.

Rupke, J., Cammeraat, E., Seifmonsbergen, A.C. & van Westen, C.J. 1988. Engineering geomorphology of Widentobel Catchment, Appenzell and Sankt Gallen, Switzerland: A geomorphological inventory system applied to geotechnical appraisal of slope stability. *Engineering Geology* 26: 33–68.

Tang W-H, Li, V.K.S. & Cheung, R.W.M. 1999. Some uses and misuses of reliability methods in geotechnical engineering. In *Geotechnical Risk Management, 18th Annual Seminar Geotechnical Div. Hong Kong Institution of Engineers*: 87–96.

Tatashidze, Z.K., Tsereteli, E.D. & Khazaradze, R.D. 2000. Principle hazard factors and mechanisms causing landslides (Georgia an example). In *Landslides: In Research, Theory and Practice* (eds. E.N. Bromheard *et al.*): 1449–1452.

Tianchi, L. 1989. Landslides: Extent and economic significance in China. In *Landslides: Extents and Economic Significance* (Brabb & Harrod, eds): 271–287.

Van Westen, C.J. 2004. Geo-Information tools for landslide risk assessment: An overview of recent developments. In *Landslides: Evaluation and Stabilization*, Lacerda, Ehrlich, Fontoura & Syao (eds): 39–56.

Varnes, D.J. 1984. The International Association of Engineering Geology Commission on Landslides and Other Mass Movements 1984. *Landslide hazard zonation: A review of principles and practice*. Natural Hazards 3: 63. Paris, France. UNESCO.

Wang, W. Chigira, M. & Furuya, T. 2003. Geological and geomorphological precursors of the Chiu-fen-erh-shan landslide triggered by the Chi-chi earthquake in central Taiwan. *Engineering Geology* 69: 1–13.

Ward, T.J., Ruh-Ming, L. & Simons, D.B. 1982. Mapping landslide hazard in forest watershed. *Journal of Geotechnical Engineering, Div. ASCE* 108: 319–324.

Whitman, R.V. 1984. Evaluating calculated risk in geotechnical engineering. *J. Geotech. Eng., ASCE* 110(2): 145–188.

Wilson, R.C. & Wieczorek, G.F. 1995. Rainfall threshold for the initiation of debris flows at La Honda, California. *Environmental and Engineering Geoscience Journal* 1: 11–27.

Wu, T.H., Tang, W.H. & Einstein, H.H. 1996. Landslide hazard and risk assessment in *Landslides Investigations and Mitigation, Transportation Research Board Special Report* 247, National Research Council Washington DC.

Yin, K.L. & Yan, T.Z. 1988. Statistical prediction models for slope stability of metamorphosed rocks. In *Landslides*, Bonnard, C. (ed.): 1269–1272.

Yucemen, M.S., Tang, W.H. & Ang, A.H.-S. 1973. A probabilistic study of safety and design of earth slopes. *Civil Eng Studies SRS* 402, University of Illinois, Urbana, USA.

Cost-benefit analysis for debris avalanche risk management

G.B. Crosta, P. Frattini, F. Fugazza & L. Caluzzi
Dip Scienze Geologiche e Geotecnologie, Università degli Studi di Milano Bicocca, Milano, Italy

J. Chen
Golder Associates Ltd., Calgary, Alberta, Canada

ABSTRACT: Risk management in urban areas forces politicians to make sensible decisions on problems that they normally poorly understand. A decision support from technicians is therefore essential for good management, and should be addressed to the identification of different scenarios in terms of potential damage and probability of events. A 1.2 million m^3 debris avalanche failed in December 2002 on the village of Bindo (Cortenova, Italy), destroying 17 houses and interrupting industrial activities for several weeks. Fortunately, no lives were claimed. A large portion of slope is still active and threatens the remnant part of the village. Considering both the characteristics of the landslide and the socio-economic settings, we identified three possible mitigation strategy: (1) the construction of a large defensive work in front of the potential landslide; (2) the long-term displacement monitoring of the unstable sector of the slope, with a related alarm system; (3) the combination of (1) and (2). The three scenarios have been also compared with a hypothetical zero-scenario, without any mitigation action introduced. In order to provide support to politicians and to identify the mitigation strategy with the lowest cost/benefit ratio, we performed a cost-benefit analysis of the different scenarios. For such analysis, we considered only the direct effects on human life, houses and lifelines. At the same time, we defined levels of social acceptance of landslide risk for the endangered community by means of questionnaires and socio-economic data. Thus, we evaluated the different scenarios on the light of acceptable risk levels and we found that, even with a large uncertainty, the best mitigation strategy would be the combination of the defensive works and the monitoring network.

1 INTRODUCTION

Landslides are highly destructive phenomena, claiming hundreds of lives and causing millions of dollars of property damages throughout the world each year (Committee on Ground Failure Hazards 1985, Schuster & Highland 2001). Their catastrophic nature makes them the most threatening natural hazard in some regions of the world (e.g. Heim 1932, McConnell & Brock 1904, Eisbacher & Clague 1984, Schuster & Highland 2001).

The management of landslide risk in alpine valleys and other mountainous areas where dense population exist is therefore essential (Hungr 1997). Politicians are forced to make sensible decisions on problems that they normally poorly understand, and therefore need a decision support from technicians.

Recently, a large debris avalanche took place in the Central Italian Alps, which involved 1.2 million m^3 of material and destroyed 17 houses and 7 industrial buildings without any casualty thanks to the preventive evacuation. In addition, another landslide happened nearby with 0.1 million m^3 of debris. Fieldwork revealed that the upper part of the slope above the first landslide is unstable and has the potential to fail in the future. The possible failure volume may reach as high as 1.5 million m^3.

In the present paper, we analyze three possible mitigation strategies in terms of risk acceptability and cost-benefit analysis, in order to provide support to politicians and to identify the best mitigation strategy.

2 CASE STUDY

2.1 *Study area*

We present a case history of slope failure that occurred in the Valsassina valley (Central Prealps, Italy; Fig. 1) on December 2002.

The northern sector of the Valsassina area is characterized by the presence of the metamorphic basement of the Southern Alps with the formation of low to medium grade metamorphic rocks, Variscan in age, with post

Figure 1. Geological map of the Prealps to the East of the Lake of Como (Lombardy) 1. Metamorphic basement and quartz dioritic intrusions, 2. Permian – Lower Triassic (Verrucano Lombardo), 3. Middle Triassic (e.g. Esino Limestone), 4. Carnian, 5. Rhaetian – Lower Cretaceous, 6. Fault, 7. Thrust, 8. Axial plane of the Orobic Anticline. The study area of Bindo – Cortenova is delimited by the rectangle in the middle.

Figure 2. Slope instabilities mapped in 2000 through a detailed regional landslide inventory (Crosta et al., 2001) and slope failures (light grey, A to E) occurred on November – December 2002.

Variscan plutonic intrusions (Schonborn 1992, Sciunnach 2001). The study area lies within the Monte Muggio tectono-metamorphic unit (greenschists).

This unit is unconformably overlain by the sedimentary cover represented by the terrigenous Permian-Anisic rocks (Verrucano Lombardo). Basement rocks are meta-pelites (paragneiss, mica schist, phyllites) and orthogneiss (Gneiss Chiari del Corno Stella) pertaining to the Gneiss di Morbegno unit. These basement rocks are intersected by a series of quartz-dioritic intrusions (Val Biandino Granodiorite, Cortabbio Diorite) and a granitic mass outcrops close to the landslide site in Cortenova (Val Biagio Granite). The Verrucano Lombardo (Upper Permian) formation is formed by reddish conglomerates and coarse-grained sandstones. It forms a 100 m thick unit in the Cortenova area with a slight eastward increase in thickness. From a structural point of view, the study area has peculiar features being at the western closure of the E-W trending Orobic Anticline, here locally oriented to the NW (Fig. 1) and placed to the south of the Orobic thrust, and separated from the Grigna unit (Triassic) to the west by the N-W trending Valsassina fault.

The morphology of the area is strongly controlled by the past Pliocene-Quaternary age glaciations and by the subsequent fluvial activity. The Last Glacial Maximum (LGM) is witnessed by the remnants of moraines especially evident along the southern valley flank between Primaluna and Cortenova at an elevation of about 1150 m a.s.l..

A large portion of the valley flank east of the village of Cortenova is occupied by a large prehistoric slope instability (Ambrosi & Crosta 2003, Fig. 2). The unstable area covers 1.2 km^2 and extends between 450 m a.s.l. and 1200 m a.s.l., where a large subvertical rocky scarp up to 80 m high is visible. The old landslide accumulation is limited on the two sides by secondary NE-SW trending valleys (San Biagio and Rossiga valleys) incised into the bedrock. The accumulation presents large blocks of Verrucano Lombardo, opened by NW-SE trending deep and large fractures, immersed in a sandy gravel matrix. The geological controls on the landslide complex include the lithological contact between the metamorphic-igneous rocks and the Permian conglomerates (Verrucano Lombardo), the fracture intensity in the conglomerate, and the dip slope attitude of the tectonic contact at an average angle of 17° to the southwest. The average thickness of the conglomerate debris ranges locally between 35 and 65 m and the piezometric levels lie above these depths (Ambrosi & Crosta 2003).

2.2 *The debris-avalanche event*

On November 2002 an exceptional rainy period triggered numerous large landslides in the Central Italian

Figure 3. Panoramic view of the Bindo debris-avalanche (A in Figure 2), that collapsed on December 1, 2002. The village threaten by the landslide is above accumulation on the photo.

Alps close to the Lake of Como. The sequence of landslide events in the study area started on 27 November 2002, when a small debris flow was observed along the Rossiga valley.

On 29 November 2002, a major landslide of about 80,000 m³ took place along the left-hand side of the relict landslide (landslide E in Fig. 2). Surveys were therefore carried out along the Bindo slope area. Tension cracks were visible all over the area and in continuous evolution. Significant water outflows from the springs were observed at the slope toe. The Mayor of Cortenova decided to evacuate the population in the late afternoon with the help of police forces. A small-scale landslide destroyed a first house at 8:30 PM on November 30. Around 3:00 AM on the next day, an enormous noise was heard. The Bindo landslide landslide A in Fig. 2; Fig. 3) involved about 1 to 1.2 million m³ of debris and disconnected rock mass from the toe of the relict landslide covering a slope sector of about 85,000 m². The mass spreads over an area of about 65,000 m² beyond the slope toe with a thickness of about 5–20 m. The maximum runout distance is estimated as 260 m away from the original slide toe (Fig. 3).

2.3 Socio-economic consequences

The socio-economic consequences of the landslides where extremely heavy: 17 houses and 7 industrial buildings were destroyed, the main road through the valley and the aqueduct interrupted. The main electrical power line passing through the area was cut. Moreover, due to the event 600 people were evacuated and 100 jobs were lost.

Several field checks conducted on the landslide neighboring allowed recognizing a condition of critical stability for a large portion of slope above the landslide crown.

This situation forced the authorities to extend the evacuation for almost 348 people until January 20, 2003, and to arrange an emergency real-time monitoring of the slope displacements using a ground-based SAR device (from December 2002 to March 2003). The authorities started to deploy a permanent network for continuous monitoring of displacements, rainfall and piezometric levels in the potentially unstable zone above the landslide. The monitoring network was operative since June 2003, together with a real-time alert/alarm system based on rainfall and displacements empirical thresholds. Several hydraulic works have been also executed on the Rossiga stream during 2003.

We calculated the costs caused by the landslide event by collecting data from the authorities (Cortenova Municipality, the Consortium of the Municipalities Comunità Montana, in Italian of Valsassina, Val d'Esino e Riviera, and Lombardia Region) and from the companies damaged by the event or involved into the post-event reconstruction.

The direct costs for the authorities amounted to 26,880,000 EUR, including the costs of damaged or destroyed houses (8,135,000 EUR) and the costs for the public works (hydraulic works, reopening of roads to traffic, etc.). The indirect costs supported by the authorities for the evacuation and the monitoring systems (until June 2004) amounted to 1,075,000 EUR.

The factories damaged by the event supported even larger losses. Direct costs, including damages to buildings, industrial machineries, and vehicles, amounted to 28,875,000 EUR. The indirect costs amounted to 33,760,000 EUR. These costs include overheads due to the temporary production rest (i.e. interruption of the electric energy supply, interruption of the roads) or due to the loss of clients, in addition to the costs of the salary paid during the closure period.

Other indirect costs, such as private costs due to interruption of the roads and the detriment of tourism, were not calculated due to the difficulty to collect data for their estimation.

Due to the condition of critical stability of the top of the landslide almost 200 people were still evacuated at July 2003, and the authorities were forced to take a decision on the best long-term strategy to address for the management of the area potentially hit by the landslide. Three main mitigation strategies were considered: the construction of a large defensive work in front of the potential landslide (MS#1); the long-term monitoring of the unstable sector of the slope, with a related alarm system (MS#2); a combination of those strategies (MS#3). Based on qualitative evaluation of risk scenarios and on the expert-knowledge of several consultants, the authorities decided to realize the third strategy, i.e., the construction of a large defensive work together with a long-term monitoring network. The quantitative analysis that is presented in this paper

519

confirms that the choice made by the authorities was the best in terms of cost-benefit analysis.

3 METHODS FOR RISK EVALUATION

The definition of risk in engineering practice needs three things (Kaplan & Garrick 1981): a scenario, a range of consequences, and a probability of the damaging event.

In order to build hazard scenarios, we coupled stability analysis with mobility analysis for different potential landslide masses (Crosta et al., in press).

The stability analysis was performed using a 2-D numerical code, allowing for the code to search the most critical slip surface. The mobility analysis was conducted using the quasi-three-dimensional finite element method of Chen & Lee (2000) in the Lagrangian frame of reference. Both the stability and the mobility analyses are presented in Crosta et al. (in press) and we refer to that paper for discussion of methods and results. From the results of landslide modeling two hazard scenarios have been selected for risk assessment:

- failure volume of 1.5 million m^3 with no countermeasures (Fig. 4);
- failure volume of 1.5 million m^3 with a passive countermeasure at the toe of the slope consisting in two defensive embankments, 25–30 m high; the embankments have been designed for the deviation of the avalanches toward the central part of the valley, where no elements are at risk.

In order to assign a probability to these scenarios we analyzed the historical records of landslides in the Italian Alps and the magnitude-frequency curves of landslides of the Regione Lombardia Inventory (Frattini et al. 2003). We found that the recurrence period of landslides comparable with the one expected in the study area is approximately 250 years. However, the stability conditions of the upper slope are decreased by the occurred landslide to an extent that is difficult to assess. Since this estimation is strongly uncertain, we decided to analyze the acceptability and the cost-benefits accounting for different recurrence periods.

Using the mitigation strategies previously discussed (MS#1, MS#2 and MS#3), we analyzed the residual risks associated with the hazard scenarios (a and b).

For each mitigation strategy, we compared the residual risk with acceptability thresholds that we have developed by means of a questionnaire. This was compiled by 284 inhabitants of Cortenova, representing 27% of the population older than 15 year old.

Finally, we performed a cost-benefit analysis of the different scenarios. For this analysis, we considered only the direct costs (i.e., human life, houses and lifelines) actualized to the present. The cost-benefit
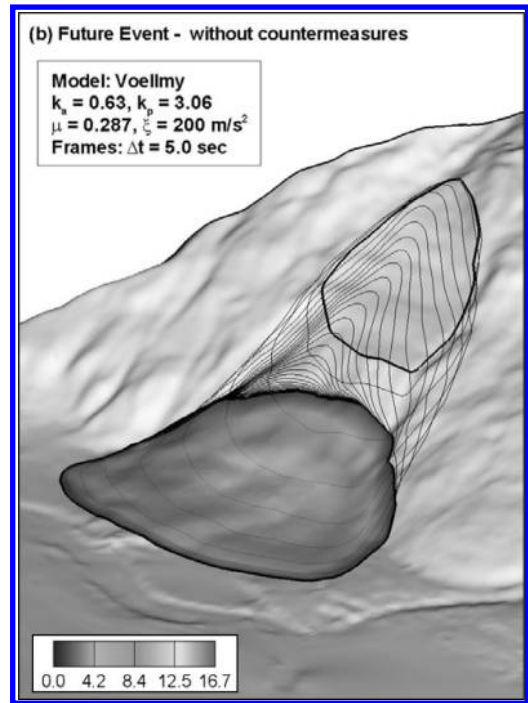
Figure 4. Predicted time sequences of the possible landslide failure without passive countermeasures. The flood contours show the debris depth distribution (in meters) in the final deposition. [see Colour Plate IX]

analysis resulted in the calculation of the Net Present Value (NPV):

$$NPV = \sum_{t=o}^{T} \frac{B_t}{(1+r)^t} - \sum_{t=o}^{T} \frac{C_t}{(1+r)^t} \qquad (1)$$

where B_t = benefit at time t, C_t = cost at time t, and r = discount rate.

The discount rate was fixed to 4.75, being equal to the 50-years swap rate; the inflation rate was fixed to 2% (i.e., the European Central Bank objective), and the rent interest to 6%.

4 ANALYSIS OF MITIGATION STRATEGIES

Starting from the socio-economic situation that was created by the debris avalanche (see Fig. 5), the adoption of one of the mitigation strategies has different socio-economic effects.

1. The construction of two large defensive embankments in front of the potential landslide (MS#1) allows the reoccupation of 19 houses previously

520
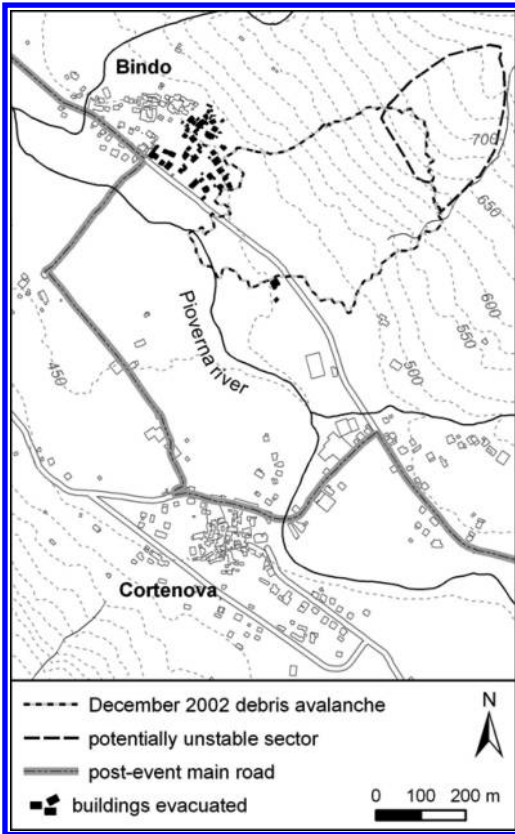
Figure 5. Socio-economic conditions after the debris-avalanche. The main road must cross the village of Cortenova along a narrow passage, causing serious limitation to the traffic and to the handling of goods.

Figure 6. Mitigation strategy # 1: construction of defensive embankments. The main road must be constructed using a new route outside the village of Cortenova, and 19 houses can be reoccupied.

evacuated. Nine houses need to be knocked down to make space available for the work, and the main road must be reconstructed using an alternative route (Fig. 6). In case of landslide reactivation (scenario b), the consequences would be limited to some damages to the embankments, and to the costs for the removal of material accumulated against the embankments.

2. The deployment of a long-term continuous monitoring network, with a related real-time alarm system (MS#2), permits the reoccupation of only 14 houses (13 houses cannot be used), but the main road can be re-opened using the old route below the landslide (Fig. 7). In case of a landslide (scenario a), the only significant consequence would be the destruction of the road.

3. The building of the defensive works together with the monitoring system (MS#3) combines the benefits deriving from the two mitigation approaches. Nineteen houses can be reoccupied, and the main

road can be reconstructed along the old route and passing into a tunnel through the eastern embankment. The consequences of the landslide (scenario b) would be: some damages to the defensive embankments, the costs for the removal of material accumulated against the embankments and within the tunnel, and the destruction of the road.

These three mitigation strategies have been also compared with two hypothetical extreme strategies. The most conservative and expensive strategy (MS# 4) would be the complete relocation of the houses at risk, with the reconstruction of the road following a new route. Conversely, the less conservative approach (MS#5) would be a non-intervention policy, leaving people to reoccupy the evacuated houses without any mitigation.

521
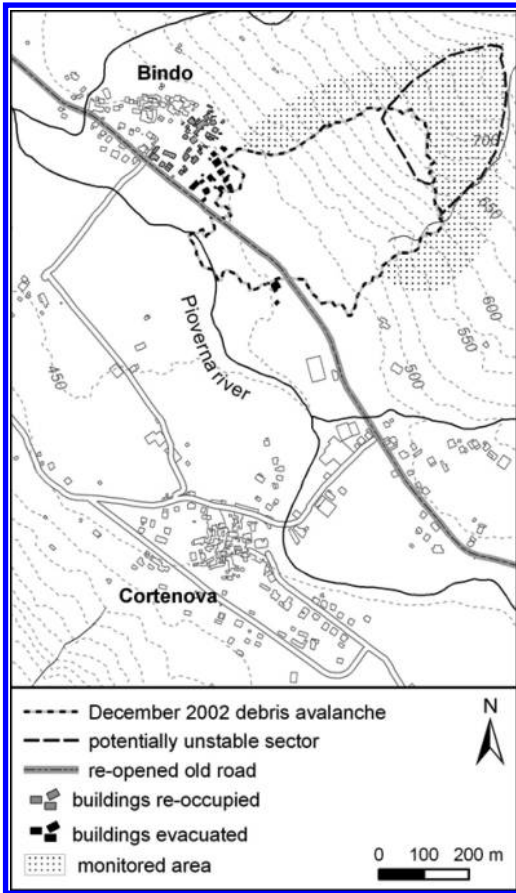
Figure 7. Mitigation strategy # 2: monitoring. The road can be re-opened using the old route; 14 houses can be reoccupied.

Figure 8. Acceptability of the Mitigation Strategies (MS). The vertical lines through the points represent a range of uncertainty from 10^{-3} to 10^{-1} for the event probability.

Table 1. Synthesis of benefit and cost fluxes used in the cost-benefit analysis. MS = mitigation strategy.

MS	Benefits	Costs
# 1	19 old houses 9 new houses	Construction of 9 new houses Construction of the main road along a new route
	Rent interest of houses	Construction of the defensive embankments
# 2	14 old houses 13 new houses	Construction of 13 new houses Re-opening of the main road along the original route
	Rent interest of houses	Evacuations due to false alarm Installation and maintenance of the monitoring system
# 3	19 old houses 9 new houses	Construction of 9 new houses Re-opening of the main road along the original route
	Rent interest of houses	Construction of the defensive embankments Installation and maintenance of the monitoring system
# 4	29 new houses Rent interest of houses	Construction of 29 new houses Construction of the main road along a new route

The comparison of residual risks (Fig. 8) calculated considering only the direct costs (i.e., human life, houses and lifelines) shows that the less conservative approach (MS#5) is socially unacceptable for the community, even assuming a very high recurrence time (higher than 1000 years).

The other strategies lie within the zone that we identified as ALARP (As Low As Reasonable Possible) on the basis of the questionnaire results. In the ALARP zone the social acceptability for the study area ranges from 50% to 90% of the population. Within this zone, the risk is, strictly speaking, "non acceptable" but is tolerated by the population under the condition that a benefit derives from the tolerance of that risk (The Royal Society, 1992, Fell, 1994). Thus, the choice of the best mitigation strategy within the ALARP zone needs the identification of the one that leads to the highest net benefit for the community.

We developed the cost-benefit analysis by accounting for several fluxes of benefits and costs (Table 1), starting from the condition that was created by the 2002 debris avalanche soon after the event (see Fig. 5). We calculated the NPV from one to fifty years (Fig. 9).

The conservative strategy (MS#4), i.e., the one with the higher acceptability, appears to be the most expensive. For short time period its NPV is negative

522
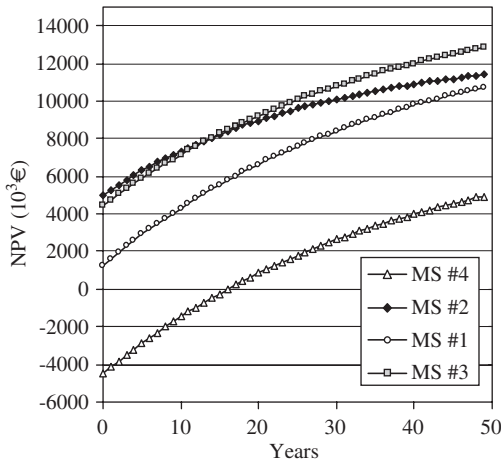
Figure 9. Cost-benefit analysis for the Mitigation Strategies (MS). MS#5 was not considered because not acceptable (see Fig. 7).

and the costs are higher than benefits. After 15 years, the NPV becomes positive, but it remains far smaller than the ones deriving for the other strategies. Among the three realistic mitigation strategies, the second (MS#2) is the best for a period shorter than 15 years. After that period, the best strategy appears to be the third (MS#3), the one that have been chosen by the authorities independently from this study. The fifth strategy, i.e. the non-intervention policy, has not been considered because it was not acceptable (see Fig. 8).

5 DISCUSSION

The analysis of the cost-benefit fluxes (Table 1) is important to understand the differences in the NPV of the analyzed strategies. From the first year on, the NPV increases gradually for all the mitigation strategies. This increase is mainly due to the revaluation of the house value, as represented by the rent interest. This value applies even in case the owner does not rent the house.

The conservative approach (MS#4) results to be the less convenient because it requires the construction of 29 new houses and the complete reconstruction of the main road. The cost flux for the construction of the houses (supported by the authorities) is balanced by the fact that the same flux is a benefit for the owners of the houses. The NPV for the building of the houses is therefore null. Hence, the negative NPV derives entirely from the reconstruction of the road.

For the three more realistic strategies, the NPV is positive from the first year, because the deployment of the mitigation actions allow the reoccupation of houses

(19 for MS#1 and MS#3, 14 for MS#2) that are otherwise unusable. This is considered as a benefit flux.

Among these strategies, the first one (MS#1) is the less convenient, due to the costs related with the construction of the new road and the defensive works. On the other hand, this strategy shows the faster increase of the NPV with time. In fact, it does not include any additional cost flux beyond the ones supported at the beginning. If the cost-benefit analysis were extended for other decades, this strategy would result the more convenient.

Looking at the differences between the second and the third strategy, it appears that the cost for the construction of the defensive embankments (in MS#3) is almost balanced by the benefit deriving from the reoccupation of a larger number of houses (19 against 14). In the long term, the MS#3 becomes more convenient because the presence of the defensive embankments eliminates the costs of evacuations due to false alarms. We assumed an evacuation frequency of one every 5 years. For both MS#2 and MS#3, the costs due to maintenance of the monitoring system are very low when compared to the other fluxes.

We limited the cost-benefit analysis to 50 years for several reasons. It was difficult to account for socio-economic changes within the valley, possibly leading to significant transformations in the land use of the study area. Moreover, the economic parameters that we used for the analysis (i.e., the discount rate, the inflation rate and the rent interest) become more uncertain with time. From this point of view, even a 50 years period appears very long, and the parameters very uncertain. However, this uncertainty is related with the absolute value of each parameter, more than with the proportion of parameters' value. Hence, the uncertainty in the determination of the exact NPV is high, but not so high in comparing the different scenarios and identifying the best strategy.

Another reason that forced us to limit the analysis to 50 years is that it is difficult to account for the efficiency of both the defensive structures and the monitoring network after many years. Moreover, new technologies in monitoring systems can be expected in the next years. It is likely that the monitoring network will be updated with these new technologies, inducing costs that we can hardly quantify today.

6 CONCLUSIONS

This study allowed us to test two important decision-support tools for the management of landslide risk and the choice of the best mitigation strategy: the evaluation of residual risk acceptability and the cost-benefit analysis.

With the first tool we recognized that the risk deriving from a potential instability of the upper slope

523

sector, above the November 2001 landslide, is unacceptable for the population, even assuming a very long recurrence time. Thus, the non-intervention policy is not acceptable for the case study, and the authorities are forced to face the risk with some mitigation. Evaluating the feasible mitigation strategies in terms of acceptability, the most conservative approach (MS#4) appears to be the best one.

With the cost-benefit analysis it was possible to compare the mitigation strategies in term of net benefits that derives from the adoption of a certain strategy. Of course, this analysis is meaningful only for the mitigations that are able to reduce the residual risk to an acceptable level. The result of this analysis shows that the best strategy is not the most conservative, as suggested by the evaluation of residual risks. The third strategy, consisting of the construction of a defensive work together with a monitoring network, is the more convenient. This strategy has also been chosen by the authorities on the basis of qualitative evaluation of risk scenarios and on the expert-knowledge of several consultants.

REFERENCES

Ambrosi, C. & Crosta, G.B. 2003. Rilevamento, modellazione e valutazione della pericolosità di grandi frane nel bacino del Pioverna, Lecco. *Atti I° Convegno Nazionale AIGA*, 31–45. In Italian.

Chen, H. & Lee, C.F. 2000. Numerical simulation of debris flows. *Canadian Geotechnical Journal* 37: 146–160.

Committee on Ground Failure Hazards 1985. *Reducing Losses from Landslides.* In the U.S. Commission on Engineering and Technological Systems, National Research Council, Washington, D.C.

Crosta, G.B., Simonato, T., Bosio, F., Merlo, P., Cucchiaro, S., Sesana, S., Iannaccone, S., Ambrosi, C. & Frattini, P. 2001. *Relazione finale sui lavori di realizzazione della carta inventario delle frane e dei dissesti.* Unpublished Report, IReR 2000C002, Regione Lombardia, Geological Survey. In Italian.

Crosta, G.B., Chen, J. & Frattini, P. (in press). Forecasting hazard scenarios and implications for the evaluation of countermeasure efficiency for large debris avalanches, *Engineering Geology*.

Eisbacher, G.H. & Clague, J.J. 1984. *Destructive mass movements in high mountains: hazard and management*. Geological Survey of Canada, Paper 84–16.

Fell, R. 1994. Landslide risk assessment and acceptable risk. *Canadian Geotechnical Journal* 31: 261–272.

Frattini, P., Crosta, G.B., Ceriani, M. & Fossati, D. 2003. Inventario delle frane e dei dissesti della Regione Lombardia: analisi statistica e probabilistica per una valutazione preliminare delle pericolosità. *Atti I Convegno Nazionale AIGA*, 427–448. In Italian.

Heim, A. 1932. Bergsturz und Menschenleben. *Beiblatt zur Vierteljahrsschrift der Naturforschenden Gesellschaft in Zurich* 77, 1–217. Translated by N. Skermer under the title Landslides and Human Lives, BiTech Publishers, Vancouver, British Columbia, 1989.

Hungr, O. 1997. Some methods of landslide hazard intensity mapping. *Procs. Landslide Risk Workshop*, R.Fell and D.M. Cruden, Eds., Balkema, Rotterdam, 215–226.

Kaplan, S. & Garrick, B.J. 1981. On the quantitative definition of risk. *Risk Analysis* 1(1): 11–27.

McConnell, R.G. & Brock, R.W. 1904. Report on the great landslide at Frank, Alberta. In: *Annual report for 1903*. Department of the Interior, Ottawa, Canada, Part 8.

Schonborn, G. 1992. *Alpine tectonics and kinematic model of the central southern Alps*. Società Cooperativa Tipografica, Padova.

Schuster, R.L. & Highland, L.M. 2001. *Socioeconomic & Environmental Impact of Landslides in the Western Hemisphere*, U.S. Geological Survey Open-File Report 01-0276.

Sciunnach, D. 2001. Early permian palaeofaults at the western boundary of the Collio Basin (Valsassina, Lombardy). *Ann. Mus. Sc. Nat., Brescia*, Monografia 25: 37–43.

The Royal Society 1992. *Risk: analysis, perception and management*. The Royal Society, Report of a Royal Society Study Group, London. U.K.

Landslide risk assessment of coal refuse emplacement

J.P. Hsi
Snowy Mountains Engineering Corporation, Australia

R. Fell
School of Civil and Environmental Engineering, The University of New South Wales, Australia

ABSTRACT: A landslide risk assessment was carried out for the Coal Cliff refuse emplacement, which had experienced downslope movements since cease of placement. A landslide resulting in a debris flow caused by liquefaction of the refuse under static, hydrologic and earthquake loading, was assessed possible. Such a failure would have a substantial impact on the local community, the public at large and the owner of the site. The quantitative risk assessment undertaken for this study indicated an intolerable level of risk to life and costs. Remedial works to improve the stability the emplacement area were subsequently implemented as a result of this assessment.

1 INTRODUCTION

Coal mining at Coal Cliff, New South Wales, Australia commenced in 1909. A coarse fraction of coal refuse was produced from washing the raw coal material and was disposed on site by end tipping into the valley of Stoney creek. About 600,000 tones of refuse were emplaced in the valley between 1909 and 1975. The washery was closed in 1990.

Figure 1 shows a plan view of the site and Figure 2 shows sections through the coal refuse including the geometry, and the underlying talus and sedimentary rocks.
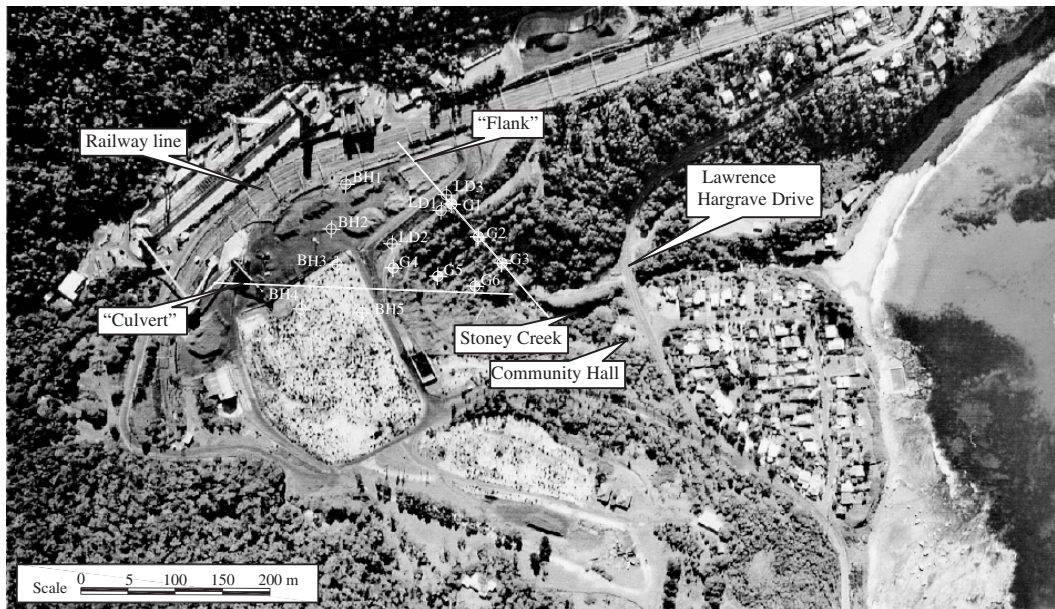
Figure 1. Plan view of emplacement area.

525
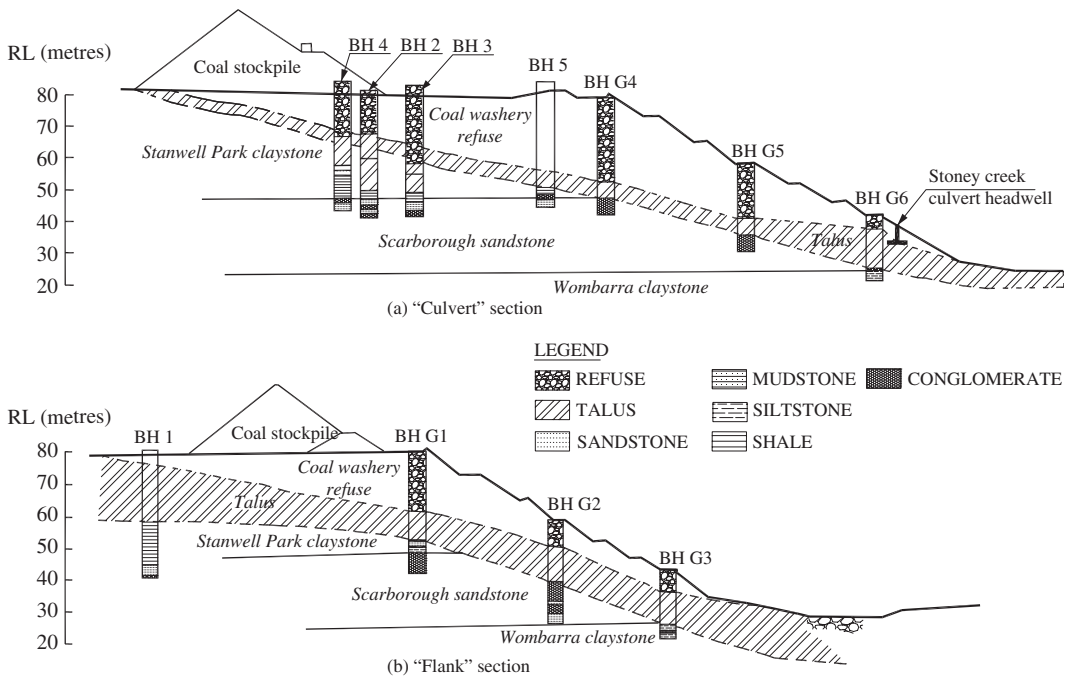
Figure 2. Sections through coal refuse.

Early studies (Longworth & McKenzie Pty. Ltd. 1993, LongMac Associates Pty. Ltd. 1997) of the emplacement involved site investigation, field monitoring of the ground water table and slope displacement, and assessment of slope stability. Slope movements up to 30 mm were measured between 1984 and 1997. These movements probably occurred during periods of high water table.

A further study by SMEC (SMEC Australia Pty. Ltd. 1998) of the stability of the refuse emplacement area was undertaken in response to the measured slope movements. The study involved conventional slope stability analysis, as well as the potential for failure by static liquefaction. Analysis of liquefaction under earthquake loading was also carried out as the refuse was loose silty sandy gravel and the bottom layer was saturated.

These analyses which were based on Standard Penetration Test "N" values, and the assessed earthquake hazard showed that the refuse would liquefy under a 1:1000 AEP event, but would not liquefy under a 1:200 AEP event. Post liquefaction strengths were assessed to be very low, and post liquefaction factors of safety were significantly below 1.0, so rapid sliding, resulting in a debris flow was likely on failure.

Failure could also be triggered by rainfall, and floods exceeding the capacity of a culvert which passed under the emplacement and by leakage of water out of cracks in the culvert.

Travel distances (run-out) were estimated using empirical methods available at the time of the study, and expert judgement. Based on the past static flow failure records for coal mine waste and fills, the maximum runout distance of the Coal Cliff refuse was assessed to be about 200 m from the existing toe of the refuse. This would reach the adjacent Lawrence Hargrave Drive which crossed Stoney Creek about 150 m below the existing toe of the refuse.

A quantitative risk assessment was performed to assess the risks and their tolerability. This was done using event tree methods. The inputs to the risk assessment, although subjective, have been handled rationally and logically. The study reported the estimated annual probability of failure, total risk costs and individual risk for loss of life. These were found to be marginally tolerable and were assessed by the owner as unacceptable.

Based on the findings of the study, remedial work for the refuse emplacement were carried out to improve slope stability and reduce risk of rapid slope failure to an acceptable level.

2 RISK ASSESSMENT

2.1 *Issues*

A quantitative risk assessment of the Coal Cliff refuse fill was carried out. The issues covered in this study included:

- Deciding upon appropriate initiating events
- Choosing a suitable failure mechanism
- Developing an event tree for each type of initiating event
- Carrying out the event tree analyses
- Calculating the annual probability that lives might be lost
- Calculating the annual cost of damages
- Carrying out the life loss and risk-cost evaluation
- Discussing the results and making an appropriate recommendation for consideration by the owner.

2.2 *Initiating events*

The stability assessment concluded that the refuse had a potential to fail or liquefy under both the static and dynamic conditions due to the loose saturated nature of the refuse and the weak talus in its foundation. The loss of material strength associated with liquefaction would cause a slide mass to reach Lawrence Hargrave Drive or other third part property or both.

To cover the full range of events, rainfalls with AEP of 1 in 5 (representing the "normal" long-term condition) to 1 in 1000 were considered for the static and hydrologic load initiating events, and earthquakes below the theoretical liquefaction triggering earthquake as well as above, with a range covering 1 in 10 AEP to 1 in 10,000 AEP event.

2.3 *Failure mechanisms and travel distances*

It was identified that only a flow slide, i.e. one involving liquefaction of the refuse, would endanger third parties and was the major concern. However questions were: is the slide big enough to be potentially damaging and will the slide mass reach the third-party property?

There would seem little doubt that, if the saturated refuse layer liquefied, a large slide mass could move either initially caused by retrogressive failure or a huge mass moving immediately. The effect of either cause would be similar with material moving rapidly downslope. With the depth of saturation at the base of the refuse probably being variable, with the less intense initiating events, whether rainfall or earthquake, small slides would be more likely; whilst the larger slides would be caused by the more intense events.

The assessment of the travel distance (runout) indicated that the slide mass could move down slope in the range of 20 m to 200 m from the toe of the slope The properties under the threat of the landslide were
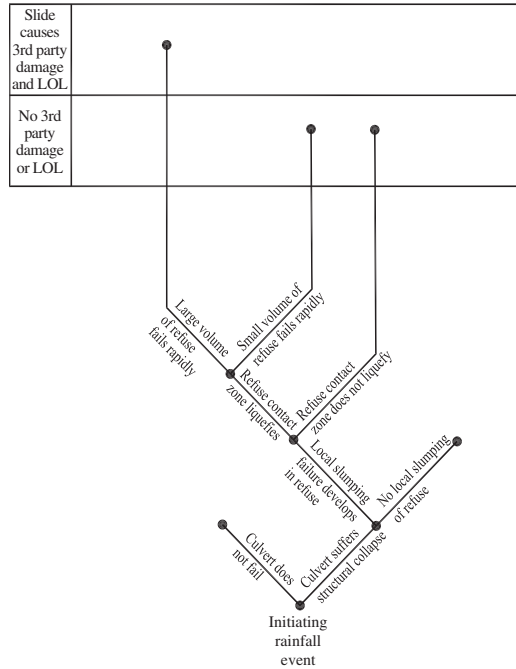
Figure 3. Event tree for static loading.

the Lawrence Hargrave Drive and the community hall which were 50 m and 150 m from the toe of the refuse respectively.

Failure of the culvert would have a substantial impact on the stability of the refuse. Such failure could be caused by a collapse of the culvert due to poor structural conditions or a local toe failure of the fill alongside the culvert causing the culvert to collapse structurally.

2.4 *Development of event tree*

The development of the event tree followed directly from the conclusions of how any flow slide would be initiated and would behave. A series of questions was asked and possible outcomes to each noted so that the event tree began to take shape. Important in the development of the event trees for both static and earthquake events was the culvert, given its existing state.

The event trees developed for the static and earthquake events were drawn up as shown in Figures 3 and 4. The figures show the trees to be a series of nodes where sub-branches or events join. Total branches were made up of lines of sub-branches with either "third-party damage and LOL (loss of life)" or "no third-party damage" representing the outcome.

At any node, conditional probabilities could be assigned to those events coming from that node. The sum of these conditional probabilities must be one.

527

Along each total branch, the various assigned conditional probabilities were multiplied together to give the final conditional probability for the total branch. The sum of these probabilities for all the completed branches must be one. This final sum, because it involved a question of "third party damages and LOL" or "no third party damage" at the end of each branch was conveniently subdivided into these appropriate categories to give an aggregate conditional probability for each.

2.5 Event tree analysis

The analyses in which conditional probabilities were assigned to the individual events were subjective and

Figure 4. Event tree for earthquake loading.

used expert judgement. They reflected the combined efforts of several experienced practicing engineers, whom had experience in risk assessment, and each of whom gave his opinion as to the "best-estimate" of the conditional probability of each sub-branch in the event tree considered. The final value represented a "consensus" figure for each sub-branch.

The event tree analyses gave the aggregate conditional probability of failure for the various selected initiating events. Each of these events was considered as a discrete event. The summary of the initiating events considered and estimated aggregate conditional probabilities are shown in Table 1.

Accepting that the static and earthquake load events were mutually exclusive events, the aggregate conditional probabilities for, firstly, static loading and, secondly, earthquake loading, could be plotted against the appropriate AEP valves. The area under each resulting curve gives the annual probability of failure for the particular class of events, i.e. either static or earthquake. The calculated annual probability values of failure resulting in third party damage or loss of life (LOL) are:

- For rainfall loading: 1.14×10^{-3}
- For earthquake loading: 5.82×10^{-4}

2.6 Lost of life estimate

The loss of life (LOL) is relative to the population at risk (PAR) and the assumed PAR for this study were:

- People in the nearest house on the eastern side of Lawrence Hargrave Drive
- People who use the community hall from time to time
- People in vehicles on Lawrence Hargrave Drive

For this study, given the high percentage of the PAR likely to perish in the large rapid slides, so all of the PAR at the time of failure was assumed to lose their lives if in the area affected by the landslide (i.e. the vulnerability was assumed = 1.0).

Table 1. Summary of initiating events and aggregate conditional probability.

Loading type	Case	Initiating event AEP		Aggregate conditional probability for third party damages and LOL*
Static (rainfall)	1S	1 in 5	(=0.2)	1.47×10^{-3}
	2S	1 in 10	(=0.1)	6.83×10^{-3}
	3S	1 in 100	(=0.01)	2.13×10^{-2}
	4S	1 in 1,000	(=0.001)	6.35×10^{-2}
Dynamic (earthquake)	1E	1 in 10	(=0.1)	5.05×10^{-4}
	2E	1 in 100	(=0.01)	4.03×10^{-3}
	3E	1 in 2,000	(=0.0005)	8.07×10^{-2}
	4E	1 in 10,000	(=0.0001)	3.08×10^{-1}

* These are the probability that given the loading cases, there will be third party damages and loss of life.

The temporal probability of the persons at risk was calculated as follows:

- 1 person in the house on the eastern side of the road for some of the time (8 hours/day): 0.33
- 3 people in the same house at other times (12 hours/day): 0.50
- 15 people in the community hall for some of the time (2 hours/week): 0.012
- 2 people in separate cars/trucks on the 100 m of the road under threat out of 2664 such vehicles each day (assume a travel speed of 40 km/hr): 0.24
- 10 people in a normal service bus out of 32 such buses each day: 0.0033
- 50 people in a school bus out of four such buses each day: 0.00032

2.7 *Economic losses*

The economic losses associated with a potential rapid slide of the refuse fill are the direct third party damages caused to property and infrastructure within the path of the slide and on any other areas affected by slide and the indirect costs associated with disruption to these properties and infrastructure. These third party direct costs are more readily estimated than indirect costs. As well as the damages to third parties, the loss of the owners' property or as in this study, the costs for remedial works must be included.

The total damages were estimated to be $8,500,000 with a breakdown shown below (details not given herein):

- Direct damages $1,500,000
- Indirect damages $2,000,000
- Owner's costs $5,000,000

2.8 *Environmental, social and legal impacts and loss of credibility*

The environmental, social and legal impacts of a rapid slide which engulf some third party property and kill some people were impossible to quantify in monetary terms. To some extent, some of their impacts would come under the indirect costs, for example, for people very closely affected, trauma and litigation had notionally been included in the indirect costs. But the more widespread impact on the community in the nearby towns could not be costed.

One technique used in recent studies is to grade these damages as, high, medium and low on a purely judgemental basis. The suggested descriptions for these terms are:

- Low (L) – Effect on environment mild, with expectation of rapid reestablishment; social impact limited

to small number of people; legal impact due to potential litigation slight.
- Medium (M) – Environmental impact severe with regeneration to occupy say two decades; considerable social impact on farming and town communities affecting some hundreds of people; considerable exposure to litigation from the affected community.
- High (H) – Major environmental impact with devastation of large areas of flora and fauna and regeneration unlikely within 50 years; destruction of social fabric affecting some thousands of people, with imposition of a totally new social framework; extensive litigation due to losses of property, business, land use and social amenity.

Given that most of the environment impact would be confined to the area above Lawrence Hargrave Drive but that because of the road usage the number of people directly affected was significant, a low category is proposed for environmental impact and medium for the social and legal impacts.

Loss of credibility of the owner is very much an organization or company issue. Most organizations and companies would probably place a high "value" on this aspect.

2.9 *Risk evaluation*

Risk is usually evaluated from two points of view. Firstly, and more importantly, is the loss of life risk. Secondly, there is the economic risk.

With no standard acceptance criteria available at the time of the study for the situation at Coal Cliff as far as potential loss of life is concerned, recourse was made to the guidelines of the Australian National Committee on Large Dams (ANCOLD 1994). By so doing, the owner would have an idea of how the risks posed to life by the refuse might be viewed by society, given that the outcome of dam failure and a landslide have some similarities.

There were no standard economic (financial) acceptance criteria with which the Coal Cliff situation could be compared. The financial positions of organizations and companies vary so much that each organization or company must decide on its own what financial risks it is willing to take.

With environmental, social and legal impact and loss of credibility not being quantified, only judgement can be used to assess these associated factors.

With the LOL being based on the assumption that if a person was in the path of the slide that person would be killed, the annual probability is simply the annual probability of the slide occurring times the temporal probability, as shown in Table 2.

The risk cost is the total damages (third party and owner costs estimated to be $8.5 million) multiplied

Table 2. Summary of annual probability of loss of life.

Person(s)			Annual probability of LOL		
Location	No.	Temporal probability	Static event (1.14×10^{-3})	Earthquake event (5.82×10^{-4})	Combined loading events
House on sea side of road	1	0.33	3.8×10^{-4}	1.9×10^{-4}	5.7×10^{-4}
	3	0.50	5.7×10^{-4}	2.9×10^{-4}	8.6×10^{-4}
Community hall	15	0.012	1.4×10^{-5}	6.9×10^{-6}	2.1×10^{-5}
Cars/trucks	2	0.24	2.7×10^{-4}	1.4×10^{-4}	4.1×10^{-4}
Normal service buses	10	0.0033	3.8×10^{-6}	1.9×10^{-6}	5.7×10^{-6}
School buses	50	0.00032	3.7×10^{-7}	1.9×10^{-7}	5.6×10^{-7}
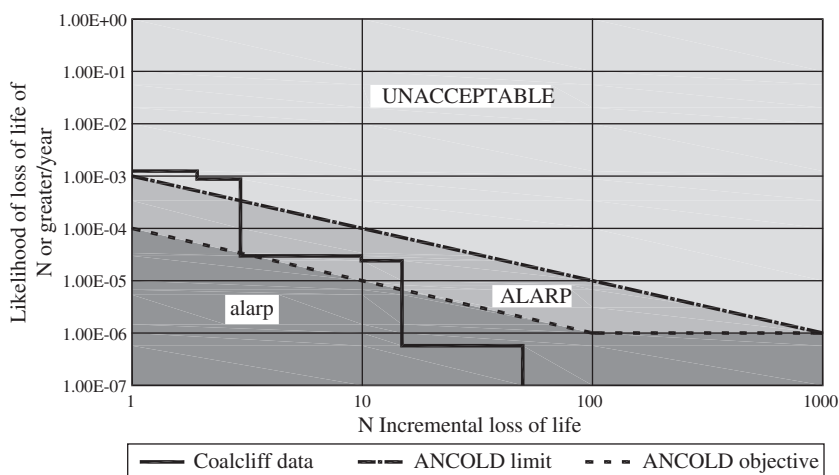
Figure 5. ANCOLD (1994) – Loss of life societal risk acceptance criteria showing the Coal Cliff results.

by the annual probability of the slide. The calculated risk costs are:

- Risk cost for static loading: $9,690/year
- Risk cost for earthquake loading: $4,950/year
- Total risk cost: $14,640/year

2.10 Acceptance of risk

As noted the key test in this risk assessment, as in many others, was almost certainly applied to potential or expected life loss. In Australia, the closest acceptance criteria for Coal Cliff would be the criteria recommended by the Australian National Committee on Large Dams (ANCOLD 1994).

The two measures of socially acceptable risk are individual risk and societal risk, which ANCOLD (1994) defines in its glossary as:

- Individual risk: the socially acceptable level of risk to a particular individual.

- Societal risk: the socially acceptable level of risk in terms of events that impact on society at a community, regional or national level.

When assessing individual risk, ANCOLD (1994) proposed that two situations be examined. The first is the average level of individual risk which considers the risk to an individual when taken as one person in the overall population at risk (PAR). The second is the level of risk to the most exposed person which typically would be the person closest to the dam.

The ANCOLD (1994) risk guidelines recommend an average level of individual risk of 10^{-6}/year for all new dams. For the person at most risk this value is 10 times greater. The average level of risk to particular members of the public for an existing dam is 10^{-5}/year and for a defined or the most exposed person it is 10^{-4}/year, but these limits are subject to the "as-low-as-reasonably-practical" (ALARP) principle.

Figure 5 gives the acceptance criteria for societal risk as suggested by ANCOLD and is called a frequency

530

Table 3.   Average annual individual risk.

Person or Persons		Factor LOL/PAR	Average individual risk/year (=annual probability × factor of PAR)			ANCOLD limit/year	
Location	No.		Static	Earthquake	Total	New dams	Existing dams*
House on sea side of road	1	1/1	3.8×10^{-4}	1.9×10^{-4}	5.7×10^{-4}	10^{-6}	10^{-5}
	3	3/3	5.7×10^{-4}	2.9×10^{-4}	8.6×10^{-4}	10^{-6}	10^{-5}
Community hall	15	15/15	1.4×10^{-5}	6.9×10^{-6}	2.1×10^{-5}	10^{-6}	10^{-5}
Cars/trucks	2	$2/(2 \times 2664)$	1.0×10^{-7}	5.3×10^{-8}	1.5×10^{-7}	10^{-6}	10^{-5}
Normal service buses	10	$10/(10 \times 32)$	1.2×10^{-7}	6.0×10^{-8}	1.8×10^{-7}	10^{-6}	10^{-5}
School buses	50	$50/(50 \times 4)$	9.3×10^{-8}	4.8×10^{-8}	1.4×10^{-7}	10^{-6}	10^{-5}

* Denotes subject to ALARP.

(annual probability of an incremental number of lives or greater than that number being lost) versus incremental number of lives lost chart, which is usually shortened to be described as an F-N chart.

As may be seen on Figure 5, the ANCOLD "F-N" chart, which is log–log chart, has a limit line and an objective line. Above the limit line is unacceptable region; below the limit line is the as-low-as-reasonably-practical region. The latter region has been divided into:

- The "ALARP" region between the limit and objective lines. ALARP here is expressed in the upper case to emphasise the need to aim for the area below the objective line. ANCOLD (1994) requires new dams to achieve the objective line.
- The "ALARP" region below the objective line. The lower case for "alarp" is intended to encourage dam owners to improve their safety position if the costs are not too high.

The ANCOLD "F-N" chart is a cumulative chart which considers the probability of N or greater lives being lost under all loading conditions. N here is the incremental number of lives lost. Beginning at the greatest value of N for a particular loading, the probabilities were added progressively for each value of N and each load type. The result is a line plot which covers the LOL for all load types.

As may be seen, the cumulative plot lies above the ANCOLD (1994) limit line in the "unacceptable" region.

For "average individual", the best approach would seem to be to view the various groups, namely, the people in the house, the people in the hall and the people in vehicles, separately. By so doing, the fact that while, for example, two people in a car may be killed by the slide, they are part of an overall group of 2×2 664 people each day exposed to the risk. On the other hand, the people in the house and the hall are assumed to be killed if the slide occurs. Table 3 summarises the average individual risk for each group of people.

As may be seen from the above table, the level of average individual risk to the people in the house on the sea side of Lawrence Hargrave Drive was significantly outside the ANCOLD (1994) limit. The users of the community hall would also have a level of risk above ANCOLD (1994) limits.

Intuitively, one of the people in the house on the sea side of the road would be the most exposed individual. For this person, a long-term occupancy of 20 hours/24 hours each day would be reasonable. If this temporal probability is used, then the level of risk to the most exposed person is:

- From static loading:
  $1.14 \times 10^{-6} \times 20/24$ $= 9.5 \times 10^{-4}$/year
- From earthquake loading:
  $5.82 \times 10^{-3} \times 20/24$ $= 4.9 \times 10^{-4}$/year
- Total $= 1.4 \times 10^{-3}$/year

This level of risk is more than ten times the ANCOLD (1994) limit of 10^{-4}/year, a limit which is subject to the ALARP principle.

3   RISK MANAGEMENT AND CONSIDERATION OF RISK REDUCTION MEASUREMENTS

From the previous section, on grounds of LOL risks, some form of action would be fully justifiable. The level of risk posed to individuals and the societal risk, both measured in terms of the ANCOLD (1994) requirement for dams, were outside acceptable limits. The nearby permanent residents were particularly exposed.

On financial grounds, the risk costs were high but the total damages were not too severe.

The non-quantifiable factors such as environmental damage, societal impacts, legal costs and particularly loss of credibility did suggest that the existing situation was unacceptable. Whether these concerns were serious enough that they would swing the balance

531

in favour of some action being taken was questionable. All that could be said was that they do not improve the situation.

Remedial works could be implemented to improve the stability of the existing refuse emplacement and hence reduce the risks to acceptable levels. The proposed work included placement of a filter/drainage layer at the toe to control ground water, construction of a stabilisation toe berm to increase FoS against slope instability, installation of a complex drainage system on site to minimise infiltration of surface water into the refuse emplacement, and extension of the major stormwater culvert below the emplacement.

4 CONCLUSIONS

The application of risk analysis methods to problems in civil/geotechnical engineering is steadily evolving. Although it calls for subjective inputs at a number of stages in the analysis, it handles these inputs rationally and logically. Moreover, despite their recognised subjective nature, the inputs to this study represented the collective judgement of a team of practitioners with extensive experience in the relevant areas of expertise necessary to make such judgements.

The risk assessment study showed that the level of risk to life was unacceptable, both on an individual risk basis and from the point of view of societal risk. There was a strong justification to undertake long term measures to lower the risks to life. The risk cost was high, perhaps unacceptably high, but the total damages were not large. Environmental damages, societal impacts, legal costs and loss of credibility, while not quantifiable, did not improve the situation. A reduction in the risks to life and risk costs would best be achieved by implementing remedial measures.

ACKNOWLEDGEMENT

REFERENCES

ANCOLD 1994. Guidelines on Risk Assessment. Australian National Committee on Large Dams Incorporated, Sydney.

Longworth & McKenzie Pty. Ltd. 1993. Geotechnical Investigation of Stoney Creek Emplacement, Coal Cliff Mine, NSW. Report for Coal Development Services Pty. Ltd.

LongMac Associates Pty. Ltd. 1997. Stoney Creek Emplacement Area – Geotechnical Instrumentation. Report for Illawarra Coke Company Pty. Ltd.

SMEC Australia Pty. Ltd. 1998. Coal Cliff – Review of Stability of Refuse Emplacement. Report for Hesketh Mining, Document No. 31816.001.

Debris flow hazard and risk assessment, Jones Creek, Washington

M. Jakob
BGC Engineering Inc., Vancouver, British Columbia, Canada

H. Weatherly
Kerr Wood Leidal Associates, Vancouver, British Columbia, Canada.

ABSTRACT: This study quantifies debris flow hazard and risk on Jones Creek fan. Dating of organic material sampled in eighteen trenches on the fan demonstrated that at least six large ($>$85,000 m^3) debris flows had occurred in the past 7000 years with an average return period of 400 to 600 years. Due to the presence of about 100 buildings on the fan, the local municipality directed that the magnitude of the 500-year return period debris flow be used for land-use zoning. A frequency – magnitude graph was constructed from the data, and used as input to a two-dimensional debris flow runout model. The model results were used to develop hazard intensity zones based on area inundated, maximum flow depth and flow velocity. Quantitative risk analysis was then applied to determine the probability of death of an individual or group for modelled 50, 500 and 5000-year events. The position of the data on an F/N curve suggests that debris flows at Jones Creek pose a risk currently deemed unacceptable by society, and confirms the need to implement mitigation measures.

1 INTRODUCTION

Debris flows are one of the most hazardous landslide processes worldwide. In recent years, some 30,000 people have died through debris flows resulting in hundreds of millions of dollars in damage. While locations with a high frequency of debris flows are easily recognized and can thus be avoided or otherwise mitigated, low frequency debris flows may pose a bigger threat because failure to recognize the process and potential consequences may lead to development along the channel or in the runout zone.

1.1 *Jones Creek*

At Jones Creek, a debris flow causing only minor damage in 1983 alerted regulators that larger events may cause substantial damage to the town of Acme located on the fan. This realization prompted Whatcom County to issue a detailed debris flow study of Jones Creek (Kerr Wood Leidal 2004). The study objectives included: determine the magnitude of the 500-year return period debris flow, assess the potential consequences, and propose risk mitigation alternatives.

An extensive investigation was initiated that included trenching, ^{14}C dating, and debris flow modeling, which are summarized in this paper. With this information at hand, the 50, 500, and 5000-year return period events are modeled to determine likely impacts to houses and infrastructure and probability of death. A graph relating probability of death of an individual or group (N) to the probability of the event (F) is constructed and compared to commonly accepted risk.

1.2 *Regional relevance*

Washington State has hundreds of fans similar to Jones Creek with at least some development in the runout zones of debris flows (Weden & Associates 1983, Fox et al. 1992). Quantification of debris flow hazard and risk is not regulated in North America, and there is no generally accepted approach amongst consultants or local authorities. Unlike flood studies that use the 100-year (USA, Europe) or 200-year (Canada) return period flood for floodplain designation and flood insurance, there is no standard regarding the design return period of debris flows.

Apart from meeting the principal objectives of quantifying hazard and risk, this case study demonstrates the type and considerable effort of study needed to meet these objectives in a scientifically defensible manner. It also underlines the need to create a unified system of hazard and risk assessment that can be applied in a large region, state or province, or even nationally. The alternative would be widely differing quality of work with the consultant or regulator deciding ad hoc as to

hazard and risk quantification, and risk acceptance. This lack of standardization may lead to confusion and legal action in the future.

2 STUDY AREA

Jones Creek drains a 6.8 km^2 watershed in the foothills of the Cascade Mountains in Whatcom County, Washington, USA. The watershed has an eastern aspect and is located about 35 km east of Bellingham. Elevations range from 990 m at the south end of Stewart Mountain to 85 m at the confluence with the broad floodplain of the South Fork Nooksack River. Due to episodic debris flow activity a large composite fan has developed on the valley floor, superimposed on the Nooksack River floodplain and interfingering with fluvial deposits at depth. The town of Acme with approximately 250 residents and some 100 buildings is located on the Jones Creek fan.

Recorded debris flows at Jones Creek include a 25,000 m^3 event in 1983 (Raines et al. 1983) and a smaller event of unknown volume in 1953. The creek channel is about 5 km long with an average channel gradient of 18% above the fan apex. The fan gradient varies between 6% near the apex to 2% at the confluence with the Sooth Fork.

Past disturbances to the watershed include standreplacing wildfires, intensive logging, and landslides. Early development in the watershed was minimal as a large wildfire in 1884 burned much of the forest in the vicinity of Acme (deLaChapelle 2000). Intensive logging of the watershed began in the 1940s with the construction of a sawmill on the fan. Logging has since undergone a couple of cycles during which some 99% of the old growth forest has been removed.

Two geologic formations underlie the Jones Creek watershed (Fig. 1). Bedrock in the upper watershed consists of the Chuckanut Formation, a legacy of an extensive fluvial system in western Washington during the Eocene epoch (Johnson 1984). This formation is characterized by alternating deposits of sandstone, minor conglomerate, mudstone, black shale and coal.

The lower 40% of the watershed is underlain by the Darrington Phyllite, which is separated from the Chuckanut Formation by a northeast trending fault. The Darrington Phyllite is the youngest unit of the Shuksan Metamorphic Suite that forms part of the metamorphic core of the North Cascades (Brown 1987). The highly folded and faulted phyllite is a mechanically weak rock that easily weathers into small chips and clay-rich residues. As a consequence this formation is susceptible to deep-seated rotational failures, creep and block glide (Thorsen 1989). Several of these landslides are shown on Figure 1. The landslides are characterized by a series of scarps with vertical offsets of 1 to 3 m, graben and horst features, and
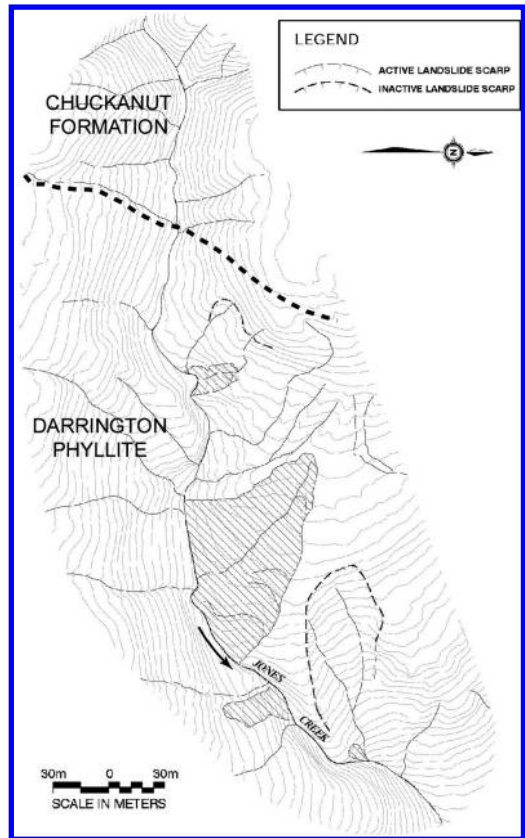

Figure 1. Mid reaches of Jones Creek watershed showing geologic boundary and major landslides.

Figure 2. Large graben that has developed near the toe of the Darrington Slide.

toe slumping and ravelling near the creek (Fig. 2). The largest of these landslide complexes, the Darrington Slide, runs along the north side of the creek for 400 m and extends upslope for a similar distance.

534

The instability of the phyllite is also likely related to the glacial history of the valley. The last of a sequence of Pleistocene glaciations, the Fraser glaciation, lasted from 20,000 to 10,000 years ago and left thick deposits of outwash sediment on the valley floors as well as mantles of till on the hillslopes (Easterbrook 1971). Many tributaries of the South Fork drain hanging valleys that likely developed as a consequence of ice-free conditions in the tributary valleys that drained against a remnant glacier in the Nooksack valley. Subsequent glacial downwasting led to fluvial incision of the lower valleys, which have not yet found an equilibrium slope as indicated by a convex longitudinal creek profile and v-shaped oversteepened slopes. At Jones Creek, this oversteepening likely caused the creep and ultimately landsliding of the Darrington Phyllite, a process linked to the formation of large debris flows by temporary damming of the creek as will be demonstrated in this paper.

3 HAZARD ANALYSIS

The first objective of the study was is to quantify the debris flow hazard at Jones Creek. To analyze hazard, both the probability of the event and its magnitude are determined.

3.1 *Debris flow frequency*

Debris flow frequency or probability at Jones Creek was established by a trenching program. Trenching allowed both radiocarbon dating of individual debris flow deposits and the measurement of deposit thickness, which was used to reconstruct debris flow volumes.

Eighteen trenches up to 5 m in depth were excavated on the fan in July 2003. The trenches were distributed as widely as possible across the fan, though the locations were subject to landowner approval (Fig. 3).

The trenches revealed sequences of debris flow deposits, often separated by paleosols. Figure 4 provides an example of a well-developed sequence of soils and debris flow deposits. The stratigraphy of each trench was recorded and organic material sampled before the hole was back-filled. 23 samples of organic material were sent for radiometric and AMS dating to the radiocarbon dating laboratory of the University of Waikato, New Zealand. The resulting calibrated dates allow the compilation of a debris flow chronology on Jones Creek for the past 7000 years (Table 1).

Table 1 was simplified assuming that overlapping age ranges represent the same event. Depending on the position of the organic sample, a minimum or maximum age was assigned to individual debris flow deposits. This procedure yielded assumed debris flow ages of 400, 900, 2100, 3400, 4200 and 7000 years BP (Table 2).
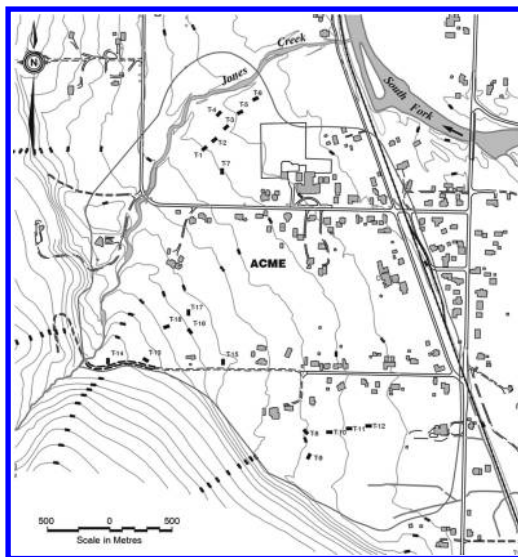
Figure 3. Trench locations on Jones Creek fan.

This analysis implies that eight debris flows can be distinguished over the past 7000 years for an average return period of approximately 900 years. However, two of these events (1953, 1983) are of significantly lower magnitude ($<25,000\,m^3$) than the other events dated. For this reason only six large debris flows are counted (herein defined as a volume in excess of $75,000\,m^3$, see next section), implying a return period of approximately 1200 years.

The above analysis, however, is based on the assumptions that all dated events are debris flows rather than hyperconcentrated flows and that the dated events accurately reflect all large debris flow events that occurred on Jones Creek. The first assumption is reasonable given the stratigraphic information that was logged during the trenching. Furthermore, even if some of the events or their more liquid afterflow may be more appropriately classified as hyperconcentrated flows, differences in terminology do not affect hazard and risk analysis.

The second assumption, however, is probably invalid in that the resolution of debris flow frequency is dependent on the number and depths of trenches, as well as the number of radiocarbon dates obtained. For example, had trench 18 not been excavated (e.g. the landowner may not have given permission), the record would only extend 4200 years and the debris flow return period would be 800 years. It is therefore reasonable to assume that the six large debris flows recorded in the past 7000 years are a minimum rather than the exact number of events. Furthermore, older deposits may be located at a depth outside the reach of the excavator or below the water table.

535
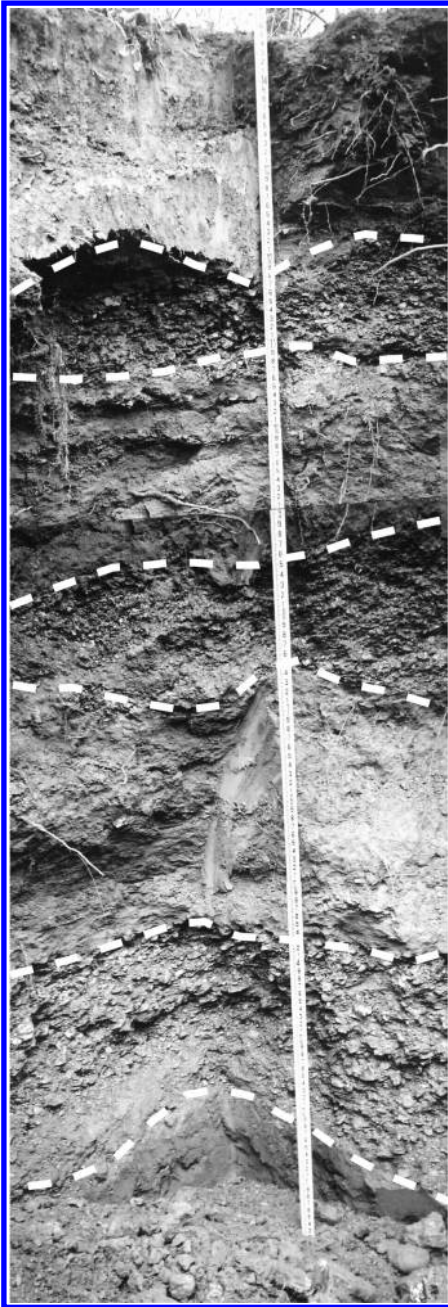
Figure 4. Well developed stratigraphic sequence of debris flow deposits interbedded with paleosols.

Considering the limitations discussed above, it is concluded that large debris flows on Jones Creek occur with a return period of approximately 400 to 600 years.

Table 1. Summary of ^{14}C dates obtained from organic samples in the test trenches.

Calibrated age* (cal yr BP)	Sample	Dated material
1350–1540	1 B	Soil, organics
790–1060	2 B	Soil, organics
550–740	3 A	Wood
310–520	4 A	Charcoal
3160–3470	4 B	Soil, organics
760–930	5 A	Wood
3690–3990	7 B	Soil, organics, charcoal
3360–3580	8 A	Soil, organics
3690–4080	8 B	Soil, organics
450–560	9 A	Wood
300–480	9 B	Wood
3980–4360	9 D	Soil, organics and charcoal
1890–2160	11 A	Soil, organics
−10–290	14 A	Wood
−10–320	14 B	Wood
3160–3450	15 A	Soil, organics and charcoal
1950–2310	16 B	Soil, organics
290–470	17 A	Wood
1510–1780	17 B	Soil, organics and charcoal
Modern	17 C	Wood
6790–7230	18 B	Soil, organics and charcoal

* Calibrated age is reported to two standard deviations

Table 2. Summary of dated debris flow events on Jones Creek.

Calibrated age (cal yr BP)	Assumed age	Sample(s)
0–320	1953 or 1983	14A, 14A, 17C
310–470	400	3A, 4A, 9A, 9B, 17A
790–830	900	1B, 2B, 5A, 17A
1890–2160	2100	11A, 16B
3360–3470	3400	4B, 8A
3690–4360	4200	7B, 8B, 9D
6790–7230	7000	18B

3.1.1 *Regional studies*

The results at Jones Creek are consistent with regional debris flow studies conducted by Orme (1989, 1990) and deLaChapelle (2000). Orme investigated the frequency of debris flows at Mills Creek to the south of Jones Creek and Smith Creek on the western slopes of Stewart Mountain, while deLaChapelle (2000) examined debris flow frequencies at three watersheds located to the north of Jones Creek on the east slopes of Stewart Mountain. Table 3 demonstrates that there is significant overlap of radiocarbon dates for debris flows and Paleosols by deLaChapelle (2000), Orme (1989, 1990) and this study.

536

Table 3. Non-calibrated ^{14}C dates of debris flows and Paleosols at and near Jones Creek.

No.	deLaChapelle (2000)	Orme (1989, 1990)	This study
1	90		
2	370		320, 330, 400,
3		**430**	**470, 730**
4	880, 1055, **1125**		940, 1040
5		1150	
6	**1305, 1520**	**1720**	**1570, 1720**
7	**1930, 2015**		2070, **2130**
8	**2280**		
9	**3045**, 3295	3370	**3090**, 3110, 3240
10	**3750, 3750**		**3570, 3570 3790**
11	4270, **4270**		
12	**4880**		
13	**5225, 5260**		
14			**6120**

Bold values represent dated palesols, the other values represent organic material dated within debris flow deposits.

Table 4. Assumed date, volume and peak discharge of debris flows on Jones Creek fan. All numbers are rounded.

Date (years BP)	V_{med} (m^3)	V_{max} (m^3)	Q_{med} (m^3/s)	Q_{max} (m^3/s)
400	135,000	205,000	420	630
900	100,000	150,000	310	470
2100	170,000	255,000	530	790
3400	90,000	135,000	280	420
4200	170,000	255,000	530	790
7100	85,000	125,000	260	390

3.2 Debris flow magnitude

Debris flow magnitude can be expressed as total volume transported beyond an area of interest or peak discharge at a specific location. Debris flow volume and peak discharge are correlated as demonstrated by Mizuyama et al. (1992) and Jakob & Bovis (1996), and summarized by Rickenmann (1999, 2005).

Debris flow volume was determined by logging the stratigraphy of each trench, dating debris flows or paleosols, and correlating deposits of comparable age with debris flow deposits in other trenches. An important source of error is the lack of trenches in the mid fan area where no trenching permits could be obtained. It is therefore not known if some debris flows deposited a continuous sheet of debris or flowed in separate lobes. Both possibilities were included in the analysis by delineating the deposition area in lobes and by connecting the trench clusters through contour parallel lines. This approach resulted in two different measures of volume that are summarized in Table 4.

Debris flow peak discharge (Q_p) was determined by using an empirical relation between volume (V) and Q derived by Jakob (1996) for muddy debris flows:

$$Q_p = (V/343)^{1.01} \tag{1}$$

A muddy debris flow was assumed based on limited grain size analyses completed for channel, landslide, and trench deposits. Clay content has shown to be very important in explaining debris flow mobility (Scott 1985, Jordan 1994). Debris flows with a clay content exceeding 4% can run out on very low angles and are likely to resist drainage for an extended period. Most samples at Jones Creek exceeded 4% clay, which is consistent with the low average fan gradient (4%) at Jones Creek. Furthermore, fine grained debris flows often do not form coarse bouldery fronts that slow the debris flows through basal friction and encourage early deposition.

3.3 Debris flow initiation mechanism

Debris flows at Jones Creek may be initiated by a number of different processes. The recognition of these processes is important because statistical frequency analysis necessitates that data are homogenous and independent. Homogeneity can only be guaranteed if the same type of initiation mechanism can be associated with debris flows of given return periods.

The most common process of debris flow initiation is the direct transformation of a debris slide or debris avalanche on impact with the main channel (Benda & Cundy 1990). Jones Creek is susceptible to this process as the lower 3 km are confined by steep sideslopes that show evidence of historic shallow landsliding. The lower channel is also characterized by an abundant source of debris due to the presence of phyllite, which weathers rapidly into thick deposits of fine-grained material. The magnitude of these debris flows is a function of the volume of the initiating failure and the amount of material entrained in the channel downstream of the debris flow initiation location. The 1983 debris flow with an estimated volume of 25,000 m^3 is an example of such a debris flow.

However, it is unlikely that the large debris flows summarized in Table 4 were initiated by direct transformation of a debris avalanche. These debris flows were probably initiated following the blockage of Jones Creek by failures from the deep-seated rock slumps in the lower watershed. Two arguments support this hypothesis. First, the debris flow deposits on the fan consist almost exclusively of phyllite, which is found only in the lower half of Jones Creek. Second, the largest reconstructed debris flow had a maximum volume of 255,000 m^3. Assuming a solid concentration of 60% to 75% by volume, the associated water

volume is at least 65,000 m^3. With a 100-year return period peak flow of 8.5 m^3/s, the peak instantaneous discharge would have to be supported over 2 hours to equate the total water volume needed to mobilize the largest debris flow. The most reasonable explanation to achieve a large debris flow is impounded water upstream of a large landslide dam that is released abruptly as the dam breaches. This process has been identified as a commonly occurring event in steep mountain watersheds of the Pacific Northwest (Coho & Burges 1994, Jakob & Jordan 2001). The Darrington Slide has a very active toe scarp and it is conceivable that a deep-seated failure could block Jones Creek to a height in excess of 15 m, which would impound at least 45,000 m^3 of water.

3.4 *Debris flow frequency – magnitude relation*

Having established the presence of large historic debris flows, Whatcom County directed that the magnitude of the 500-year return period debris flow be used for land-use zoning and conceptual design of structural mitigation measures. As a first step, a frequency analysis
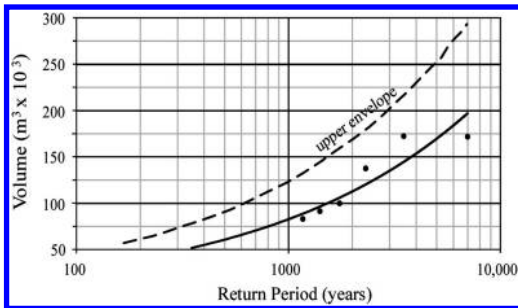

Figure 5. Debris flow frequency – magnitude curve at Jones Creek.

was completed using the data in Table 4. The 1983 and 1953 debris flows were excluded from the analysis because these events stem from a different data population (observed versus reconstructed through stratigraphic information). It is very likely that many more debris flows of the size of the 1983 or 1953 events have occurred in the past, but are not sufficiently recorded in the stratigraphic column.

Debris flow volumes and the corresponding return periods were then plotted on a semi-log scale and a best-fit line was fit through the data (Fig. 5). Figure 5 includes both the best estimate volume (V_{med}) of the known debris flow events and the maximum volume (V_{max}) based on the approximate error analysis of areal extent. The upper envelope of the dataset was used to calculate the magnitude of the 500-year return period debris flow: a volume of 90,000 m^3 and a peak discharge of 280 m^3/s.

Figure 5 is obviously associated with some error in that the dated events probably do not reflect all large debris flow events that occurred on Jones Creek. However, the analysis provides a tool with sufficient detail to approximate the design magnitude.

3.5 *Hazard intensity*

The hydraulic model FLO-2D was used to model maximum debris flow depth and velocity in order to assess the hazard posed by the design event at Jones Creek. FLO-2D is two-dimensional flood routing model that is useful for analyzing unconventional flooding problems, such as unconfined flows over complex topography, debris floods and debris flows. While the model is not particularly well suited for debris flows in the Pacific Northwest, the dataset at Jones Creek allowed for good calibration of input parameters.

The resulting model results for the design event were used to define and map four hazard intensity zones as defined in Table 5:

Table 5. Intensity and qualitative consequence ratings for a 500-year return period debris flow.

Consequence/ impact zone	Likely consequences in developed areas	Intensity terms		
		v (m/s)	z (m)	d (m)
Very high	Direct impact with extensive structural damage.	>7	>3	>1
High	Impact with potential for structural damage along with extensive sediment deposition and damage.	3–7	2–3	0.6–1
Medium	No structural damage but nuisance damage to property from sediment deposition and flooding	2–3	0.3–3	0.3–0.6
Low	Little nuisance flooding	<2	<0.3	<0.3

v = maximum velocity; z = maximum flow depth; and d = maximum sediment size (diameter).

Copyright 2005 by Taylor & Francis Group

4 RISK ANALYSIS

The purpose of risk analysis is to assess whether the hazard under investigation warrants measures to protect human life or property. Risk analysis combines measures of hazards and consequences. Hazard is defined as the combination of event probability and magnitude, which has been established in the previous section. The most commonly used measure for consequence is loss of human life.

4.1 *Qualitative risk*

There are several approaches to quantify risk. One approach uses arbitrary classifications of the severity of consequences and hazard, which are then combined in a risk matrix. At Jones Creek a risk matrix was developed based on hazard intensity, consequence, and debris flow probability (high: <20 year return period; medium: 20 to 100 year return period; and low: <500 year return period). The resulting risk rating is shown in Table 6.

The advantage of this system is its ease of use, while its principal disadvantage is the independency on the number of houses being damaged or people being killed as well as the uncertainty of the objective interpretation of "low, medium, and high" risk.

4.2 *Quantitative risk*

A more objective approach for risk quantification is the F/N curve, which relates the number of fatalities (N) from a single hazard event to the probability of the hazard (P). N can be plotted for several probabilities to obtain a curve that can be plotted on an F/N graph and compared with generally accepted risk.

As a first step, debris flows for 50, 500 and 5000-year return period events were modeled with FLO-2D. The resulting hazard intensity zones were then used to estimate potential deaths. It was assumed that in the high intensity areas the probability of death is one, while in medium and low intensity zones the probability of death is zero. Table 7 summarizes the input parameters for the quantitative risk analysis.

The above analysis indicates that the 500-year return period debris flow will likely kill 7 people,

which results in a probability of death of an individual of approximately 1.4%. The level of acceptable risk as established by ANCOLD (1997) is shown in Figure 6. Therefore, even though the assumptions for the above calculation are simplified (for example, no consideration was made of the number of hours per day buildings are occupied and by how many persons) it shows that debris flow risk at Jones Creek is currently deemed unacceptable by western society.

5 DISCUSSION

Quantitative risk analysis via F/N curves provides a comparable and replicable measure of debris flow

Table 7. Quantitative risk analysis input parameters at Jones Creek.

T_{DF} (years)	N_H	N_R	$P(T_H)$	$P(T_O)$	N_P	$P(T_H T_O)$ (%)
50-years	1	3	0.3	0.1	1.2	2.4
500-years	5	18	0.3	0.1	7.2	1.4
5000-years	10	36	0.3	0.1	14.4	0.3

T_{DF} is the return period of the debris flow; N_H is number of homes likely suffering structural damage leading to injury or death; N_R is no of residents in homes and outside in red and orange hazard zones; $P(T_H)$ is the probability of presence in home at time of debris flow; $P(T_O)$ is the probability of a person being outside at the time of debris flow; N_P is the number of persons likely to die in the debris flow; $N_P = [P(T_H) + P(T_O)] \times N_R$; and $P(T_H T_O)$ is the annual probability of death where $P(T_H T_O) = N_P/T_{DF}$
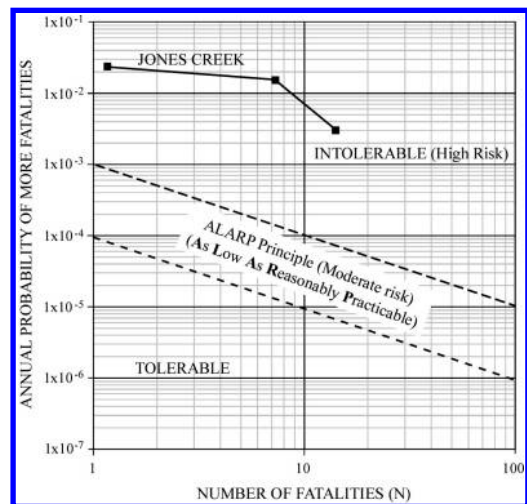
Figure 6. F/N curve for debris flows at Jones Creek (risk definition after ANCOLD, 1997).

Table 6. Qualitative risk matrix for Jones Creek debris flows.

	Hazard probability		
Consequence	High	Medium	Low
Very high	Very high	High	High
High	High	High	Medium
Medium	High	Medium	Medium
Low	Medium	Medium	Low

539

risk, and thus allows objective decisions for life and property protection from debris flow impact. However, psychological and political circumstances can influence the interpretation of F/N analysis results.

An important example has been the US government's reaction to the terror attacks of September 11, 2001 during which approximately 3000 persons died in the Twin Towers of the World Trade Center in New York City.

In the past 500 years, the number of Americans that died on US soil through terrorism is approximately 3200, or 6.4 person per year. There are 260 million US citizens presently living on American soil; consequently the annual probability of death of an American individual by terrorism equals 2.5×10^{-8} compared to the probability of death of an individual on Jones Creek fan (1.4×10^{-2}). Plotted on the F/N curve, the danger of being killed by a terrorist in the US would classify as an acceptable risk, and if applied to an industry or owner of infrastructure, the decision would likely be made that the hazard does not warrant the expenditure of funds. This finding, or course, is in contrast to the billions of dollars currently spent through the newly inaugurated Homeland Defence on fighting terrorism in the US and abroad. This example demonstrates that although F/N curves serve as an objective measure for risk and may support the decision of how to response to the hazard, political considerations and mass psychology may override the desired scientific objectivity.

6 CONCLUSIONS

This study has quantified hazard and risk on Jones Creek fan. The 500-year return period design debris flow frequency and magnitude was determined by dating organic materials and extrapolating deposit thickness on the fan. Peak discharge was determined by correlation with debris flow volume. The design debris flow was estimated to a volume of $90,000\,\text{m}^3$ with a corresponding peak discharge of $320\,\text{m}^3/\text{s}$. Following a debris flow modeling exercise, risk was quantified by plotting the annual probability of fatalities against the number of expected deaths. The F/N curve suggests that the existing risk is unacceptable to current standards of western society and that debris flow mitigation is warranted. Although F/N curves can be used objectively to assess whether a risk is worth the expenditure of funds, psychological or political circumstances can supersede the notion of acceptable risk.

This study, though limited by the number and depth of trenches and radiocarbon dates, has demonstrated the degree of effort needed and the methodologies that can be applied to assess hazard and risk on fans formed by debris flows. Given the vast number of similar populated fans in mountainous regions and the poor predictability of debris flows (as opposed to floods), it may be timely to develop a unified system for hazard and risk quantification and mapping. We hope that this paper contributes towards this goal.

REFERENCES

ANCOLD. 1997. Guidelines for the Design of Dams for Earthquake. Australian National Committee on Large Dams, Melbourne: 98 p.

Benda, L.E. & Cundy, T.W. 1990. Predicting deposition of debris flows in mountain channels. *Canadian Geotechnical Journal* 27: 409–417.

Brown, E.H. 1987. Structural geology and accretionary history of the northwest Cascades system, Washington and British Columbia. *Geological Society of America Bulletin* 99: 201–214.

Coho, C. & Burges, S.J. 1994. Dam-break floods in low order mountain channels of the Pacific Northwest. *Water Resources Series, Technical Report No. 138*. Department of Civil Engineering, University of Washington, Seattle: 70 p.

deLaChapelle, J. 2000. Late Holocene aggradational processes and rates for three alluvial fans, Cascade Foothills, Washington. Unpublished M.Sc. thesis. Western Washington University, Bellingham, Washington.

Easterbrook, D.J. 1971. Geology and geomorphology of western Whatcom County, Washington. Western Washington University, Bellingham, Washington: 68 p.

Fox, S., De Chant, J. & Raines, M. 1992. Alluvial Fan Hazard Areas. *Whatcom County Environmental Resources Report Series*. Whatcom County Planning Department, Bellingham, Washington: 39 p.

Jakob, M. 1996. Morphometric and geotechnical controls on debris flow frequency and magnitude in southwestern British Columbia. Unpublished Ph.D. thesis. University of British Columbia, Vancouver, Canada.

Jakob, M. & Bovis, M.J. 1996. Morphometric and geotechnical controls of debris flow activity, southern Coast Mountains, British Columbia. *Zeitschrift für Geomorphologie, Supplementband* 104: 13–26.

Jakob, M. & Jordan, P. 2001. Design floods in mountain streams – the need for a geomorphic approach. *Canadian Journal of Civil Engineering* 28 (3): 425–439.

Johnson, S.Y. 1984. Stratigraphy, age, and paleogeography of the Eocene Chuckanut Formation, northwest Washington. *Canadian Journal of Earth Sciences* 21: 92–106.

Jordan, P. 1994. Debris flow rheology in the southern B.C. Coast Mountains. Unpublished Ph.D. Thesis. The University of British Columbia, Vancouver, Canada.

Kerr Wood Leidal Associates. 2004. Jones Creek debris flow study. Report for Whatcom County Flood Control Zone District.

Mizuyama, T., Kobashi, S. & Ou, G. 1992. Prediction of debris flow peak discharge, Proceedings of the International Symposium Interpraevent, Bern, Switzerland, 4, 99–108.

Orme, A.R. 1989. The nature and rate of alluvial fan aggradation in a humid temperate environment, northwest Washington. *Physical Geography* 10(2): 131–146.

Orme, A.R. 1990. Recurrence of debris production under coniferous forest, Cascade Foothills, Northwest United States. In: J.B. Thornes (ed), *Vegetation and erosion: process and environments*: 67–84. New York: John Wiley and Sons Ltd.

Raines, M., Hungr, O., Welch, K.F. & Willing, P. 1996. Whatcom County Lower Nooksack River comprehensive flood hazard management plan, alluvial fan hazards: recommended assessment methodology and regulatory approach – final draft. Report for KCM Inc., Seattle, Washington: 27 p.

Rickenmann, D. 1999. Empirical relationships for debris flows. *Natural Hazards* 19: 47–77.

Rickenmann, D. 2005. Runout prediction methods. In: M. Jakob & O. Hungr (eds), *Debris flow hazards and related phenomena*. Springer – Praxis. Heidelberg.

Scott, K.M. 1985. Lahars and lahar-runout flows in the Toutle-Cowlitz River system, Mount St. Helens, Washington – Origins, behavior, and sedimentology. *US Geological Survey Open-File Report* 85–500: 202 p.

Thorsen, G.W. 1989. Splitting and sagging mountains. *Washington Geologic Newsletter, Washington State Department of Natural Resources, Division of Geology and Earth Resources* 17(4): 3–13.

Weden and Associates. 1983. Alluvial fans and deltas flood hazard areas. Report for Whatcom County: 98 p.

Landslide studies and mitigation program: Seattle, Washington, United States

W.T. Laprade
Shannon & Wilson, Inc., Seattle, Washington, United States

C.N. Paston
Seattle Public Utilities, Seattle, Washington, United States

ABSTRACT: Due to geologic, topographic, and climatic factors, much of the steeply sloping land in Seattle, Washington, is susceptible to slope instability each winter. Although Seattle receives only about 86 centimeters (cm) of rain annually, 70 percent of it falls between November and April. The landslide-prone ground occupies only about 1.5 percent of the land within the city; however, much of it is covered with houses, roads, and utilities. In 1997, after the worst spate of landslides and related damage in the city's history, Seattle Public Utilities (SPU) commissioned Shannon & Wilson, Inc. to perform a study of the causes of, locations of, and mitigation for landslides in the city. The records of 1,326 landslides form a valuable geographic information system (GIS)-based database for use by the City engineers. Using proactive policies adopted by the Seattle City Council and the landslide study, SPU established its landslide mitigation program. It includes in-house landslide expertise, funding a long-term capital program, public educational workshops, and increasing maintenance of wastewater and drainage infrastructure. The Landslide Study, the Seattle City Council's actions, and SPU's program have resulted in an increased awareness of the risks that landslides pose to property (public and private) and a reduction in landslide damage in recent storms.

1 INTRODUCTION

During the winter of 1996/97, Seattle, Washington, experienced a devastating landslide spate brought on by a (1) previous wet winter, (2) a rain-on-snow event during the 1996 Christmas and 1997 New Year period, and (3) very heavy rains in March 1997. Signs of a long history of landslides in the Seattle landscape were obvious to the trained eye, and there was institutional knowledge of significant damage due to landsliding in 1933/34, 1971/72, 1973/74, and 1985/86, but nothing could prepare Seattle for the winter of 1996/97. Within the City, more than 300 landslides were recorded and approximately $34 million of damage was sustained due to municipal cleanup and infrastructure repairs. It was estimated that as much as $50 million was lost in private property. More than 300 landslides occurred on the 37-kilometer-long Burlington Northern Santa Fe (BNSF) railroad line between Seattle and Everett.

During a series of four public meetings, Seattle's elected officials and road, building and utility staff heard a tirade of criticism from the public about the City's lack of a proactive and comprehensive approach to dealing with the risks of landslides, both in its policy and practice arenas. In spite of concerns that proactive

practices could make the City more vulnerable to lawsuits, the Council directed the city departments to develop and implement a program to reduce the damaging effects of landslides where the City was liable or responsible. This program is perhaps the most comprehensive landslide mitigation program anywhere in the United States.

A City interdepartmental committee produced a white paper on the direction that it should take to mitigate landslides and their damaging effects. The specifics of the white paper are discussed in subsequent sections of this paper. Because the City did not have a good understanding of the severity of the problems and the necessary remedial courses of action, the first action undertaken was to map landslides and landslide-prone areas (LPAs) in the City.

2 SEATTLE LANDSLIDE STUDY

The first piece of the puzzle was a comprehensive study of landslides in Seattle. For this work, Seattle Public Utilities (SPU) contracted Shannon & Wilson, Inc. (S&W), a geotechnical consulting firm with deep roots in Seattle and a large library of landslide records,

in the fall of 1997 to perform this study (Shannon & Wilson 2000). S&W formed a team of two geologists and two geotechnical engineers. They divided the study into four parts: (1) geology, (2) landslide triggers, (3) engineering toolbox, and (4) potential slide areas and stability improvement areas. This study has promulgated subsequent studies, policies, scientific research, programs, city divisions and public interest since it was completed in February 2000.

2.1 *Geology*

Landslides in Seattle are caused by a combination of steep slopes (topography), glacial stratigraphy, and pronounced wet winter precipitation. The interaction of all three is required to create landsliding in Seattle. The other influence, particularly in the urban setting, is human activity.

Topographically, Seattle is comprised of a series of linear ridges and broad plateaus with intervening river valleys and linear depressions that were most recently shaped during the last glaciation of the central Puget Lowland between about 15,000 and 17,000 years ago. The general trend is north, the same as the glacial movement and outwash channel orientation. The highest hills crest at about 150 to 170 m. As evident on the shaded relief map (Fig. 1), the ridges and plateaus are surrounded on all sides by steep slopes. These slopes range in inclination from about 25 to 90 degrees. In general, the steeper slopes are those that border the shoreline of Puget Sound. The only remaining unprotected shorelines within the city limits are at Discovery Park for about one kilometer. Elsewhere, the shoreline is armored or bulkheaded by individual beach protection or by the BNSF's long, continuous rock embankment in the northwestern corner of the city.

Seattle is underlain by Tertiary bedrock, Pleistocene glacial and nonglacial soil deposits, and Holocene deposits. Although recent geologic studies for transportation routes indicate that many of the Pleistocene deposits are older than previously thought, the soils deposited during the most recent glaciation of the central Puget Lowland (Vashon Stade of Fraser Glaciation) dominate the surface and near surface geologic conditions in Seattle.

Bedrock, primarily sandstone and siltstone, outcrops sporadically in the southern half of the city; to the south of the Seattle Fault. The bedrock provides an impermeable barrier to groundwater flow where it is overlain by younger permeable strata. Pre-Vashon glacial and nonglacial soils include fluvial and lacustrine deposits and glaciolacustrine, glaciomarine, outwash, and till deposits. They underlie all of the ridges and are exposed in the lower parts of the flanks of many of the hills. Figure 2 shows a hypothetical cross-section of a Seattle hill.
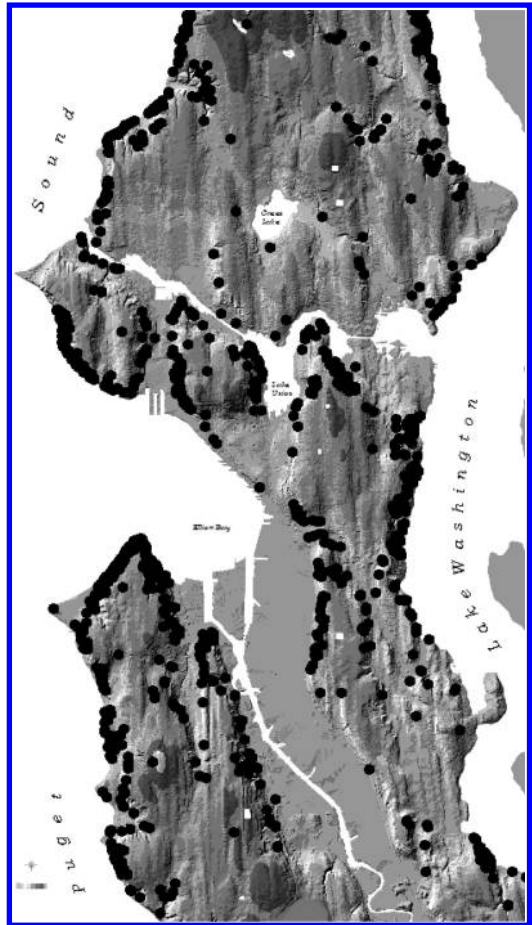
Figure 1. Distribution of reported landslides, Seattle, Washington, 1984 to 1997.

Vashon glacial deposits are composed of four major units: from oldest to youngest, glaciolacustrine clay and silt (locally called Lawton clay), advance outwash sand and gravel (locally called Esperance sand), Vashon Till, and recessional outwash. Most of the hills and ridges are draped with the first three units. Recessional outwash is found in remanent channels on the ridges or in the valleys. Holocene deposits included beach sand and gravel, fine-grained depression fillings, alluvial sand and silt, and colluvium. Colluvium is widespread, covering virtually all of the sloping ground in the Seattle area to a depth of 1 to 3 meters (m).

2.2 *Landslide triggers*

Most deep-seated landsliding (slumps) occurs as the result of penetration of water through pervious strata,
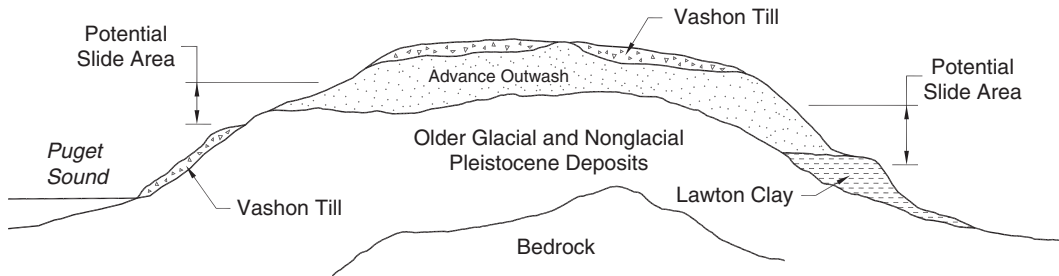
Figure 2. Hypothetical cross-section of Seattle hill.

such as the recessional outwash or advance outwash. This infiltrating water eventually reaches relatively impermeable layers, such as bedrock, older fine-grained deposits, or Lawton clay. The groundwater then travels laterally to springs on the sides of the hills. If pore pressure builds there, slope instability can occur. Surface or subsurface water also penetrates colluvium, engendering debris avalanches, and debris flows.

Without a concentrated wet winter season, landslides would not be much of an issue in Seattle. Although Seattle receives an average of only about 86 cm per year, most of it is concentrated between November and March, and about every eight years there is sufficiently excess rainfall to cause landslides (U.S. Army Corps of Engineers 1997). Every 30 to 40 years, rainfall is elevated to levels that cause widespread slope instability. It is common knowledge that when there is 50 mm in one day or 75 millimeters (mm) in two days, landslides in the region will most likely occur, assuming that there has been sufficient antecedent precipitation to raise groundwater levels. U.S. Geological Survey (USGS) research has produced a table that tracks the relationship between 15-day antecedent precipitation and 3-day precipitation that appears to indicate a very high correlation with the onset of landsliding (Chleborad 2000). This table is posted on the USGS website and updated regularly.

The landslide study also determined that some human influence was reported in about 84 percent of the landslides. This percentage is slightly more, but not significantly different, than two other studies accomplished in Seattle in the 1970s (Tubbs 1974) and for King County in the 1980s (Booth 1990). One implication of this high percentage of human influence is that measures can be taken by the City and private property owners to reduce their exposure to slope instability.

2.3 *Engineering toolbox*

In the Seattle Landslide Study, S&W presented potential remedial measures or approaches that could be applied to each of four landslides types that were identified from the 1,326 historical landslide records. The four types of landslides were, in order of frequency: (1) shallow, colluvial (debris avalanche), (2) deep-seated, (3) earth flow, and (4) earth fall. Strategies and engineering methods were presented for reducing driving forces or increasing resisting forces for each landslide type.

At the request of the City, S&W engineers provided a table of typical costs for landslide mitigation measures. They included surface water improvements; groundwater improvements, such as trench drains, horizontal drains and vertical wells; resisting structures, such as walls and buttresses; soil reinforcement; grading and fills; lightweight fills; and revegetation.

2.4 *Potential slide areas and stability improvement areas*

Since the 1970s, the City of Seattle has regulated potential slide areas (PSAs) by the application of criteria, such as steep slope (steeper than 40 percent gradient) and a combination of geologic factors and slope gradient. An advisory map was used that was based on research by Tubbs (1974) that showed that a preponderance of slope instability occurred within about 60 m of the contact between Esperance Sand and an underlying impervious layer; most commonly Lawton Clay (Fig. 3). During the Seattle Landslide Study, it was recognized that significant areas of landslide-prone ground were not delineated on this map, due to incomplete geologic mapping and cartographic errors. A product of the Seattle Landslide Study was a relining of this map, based on concentrations of landslides, improved geologic information, field observation of landslide scars, and topographic expression of steep slopes.

S&W then delineated 50 Stability Improvement Areas (SIAs), primarily based on concentrations of reported landslides. Within each SIA, individual landslide mitigation projects were identified, engineering remedial measures formulated and cost estimates calculated.
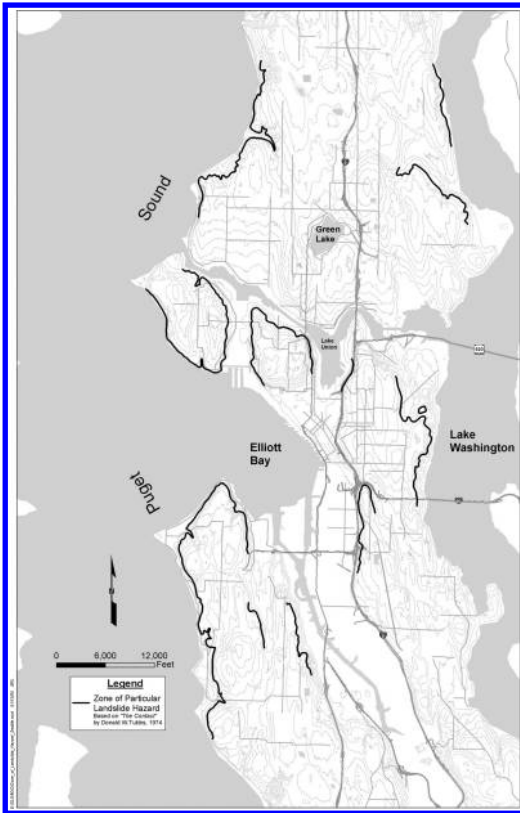
545

Figure 3. Zone of particular landslide hazard, Seattle, Washington (Tubbs 1974).

3 CITY LANDSLIDE POLICIES AND PROGRAMS

The white paper that was produced by the City's interdepartmental team was the result of a number of departments efforts, including staff from the council and mayor's offices, the law and six other operating departments. The team produced a set of policies and thirteen recommendations, which the Council approved in 1998. SPU was tasked with being the lead department responsible for implementing many of the recommendations. The four general areas of policies and actions included:

- Map Landslide Prone Areas
- Educate citizens on the risks of LPAs
- Ensure emergency response and recovery
- Identify, prioritize, fund and fix drainage problems in LPAs

To enable SPU to develop and implement this new program, the Council approved a drainage rate increase and several new staff positions.

3.1 Map LPAs

In order to develop a comprehensive landslide mitigation program, the City needed to better understand the technical and policy challenges of owning facilities and land in LPAs and meeting its mission of protecting public health and safety. The City also did not have the landslide information in a centralized location to even adequately evaluate the scope of the problem. SPU retained S&W to field check and map 1,326 landslides that the City had records of since the 1890s. The geographic information system (GIS) maps as well as other engineering information were produced in the 2000 Seattle Landslide Study, which is described earlier in this paper.

3.2 Public education

The Council recognized that the City had a role in educating owners on their risks and responsibilities of owning property in LPAs. To that end, SPU in partnership with several other City departments and volunteer professional organizations hold free public landslide education annual workshops. These have proven to be very effective and popular with over 1,000 citizens in attendance since 1999. Topics discussed include (1) why landslides are so prevalent in the Seattle area and what triggers them, (2) what steps the City is taking to protect life and health as well as its own facilities from landslides, (3) related regulatory measures the City enforces to minimize the damage and risks from landslides, (4) what property owners can do to protect themselves and their neighbors, and (5) the role of vegetation on steep slopes. Volunteer representatives from several professional organizations and industries including the American Society of Civil Engineers, American Society of Landscape Architects, Associated Builders and Contractors, and the Association of Engineering Geologists have booths to provide additional information and assistance to workshop attendees. These workshops continue to attract first-time attendees with only about 10% who have attended one before.

3.3 Emergency response and recovery

Since Seattle is highly urbanized and has been severely impacted by landslides, it is critical that the City's response to landslide emergencies be coordinated and timely. SPU organizes a workshop with eight other City departments, which is normally held in the fall every 1 to 2 years. Representatives from Emergency Management, Departments of Transportation, Law, Parks, Police, Fire, Planning and Development, Finance, and SPU attend. Each department presents their protocols, staffing capability, and equipment availability for emergency response, including accessing emergency contractor and consultant assistance.

546

The group discusses how to better coordinate and keep each other informed during landslide emergencies. One of the most important documents produced from the workshops is a list of key contact names and their roles.

SPU and Seattle's Department of Transportation both have their field offices staffed 24/7 so there is always some capability for immediate landslide emergency response, even during off hours. The City's building department will also put their building inspectors and geotechnical engineers on an on-call basis if rainfall conditions indicate that slides may occur on off hours.

3.4 *Fix priority drainage problems in LPAs*

An important component of successfully reducing risks and uncertainties in facility maintenance management is to develop and implement an effective maintenance plan. SPU regularly performs closed circuit television (CCTV) inspections of its sewer pipes but rarely did on its storm drain pipes. SPU hired a contractor to conduct CCTV inspections of all its storm drains in LPAs to assess their condition and to provide a baseline for comparison with future inspections. Pipes that are cracked or have separated joints are repaired to prevent exfiltration of water into the surrounding steep slopes or aquifer recharge areas upgradient from deep-seated landslide areas.

The biggest part of SPU's Landslide Mitigation Program in terms of staffing and budget are the projects in the capital improvement program. The projects are intended to reduce the risk of damage to SPU's facilities and to reduce SPU's risk of contributing to a landslide from uncontrolled surface run-off. The highest priority projects identified in the Seattle Landslide Study and a Prioritization Study were implemented first. However, as with all public agencies, there is always more need than available resources. SPU has undertaken an asset management business approach to decide which projects to implement that cost more than $250,000. Projects that are funded must have estimated total life cycle costs of capital, operations and maintenance and benefits gained that are greater than the risk costs of leaving things status quo. Each project must also meet established service levels or address a priority problem.

3.5 *Prioritization process*

Because of the long list of projects that were identified by the Seattle Landslide Study, SPU had to prioritize them, so the program and funding for it could be planned. As a follow-up task to the landslide study, S&W was tasked with the development of a prioritization scheme.

Nineteen criteria were initially considered for the evaluation system. After meetings between S&W and key City personnel, 11 factors were chosen for use in the prioritization system. A scoring system was then needed to evaluate the 50 SIAs in Seattle. Based on experience with the rockfall hazard rating systems used by the Departments of Transportation in Colorado and Oregon, S&W had developed an adaptation for landslides on Andean highways in central Peru and in the western United States in 1997. This was then further revised to fit conditions in Seattle. In the five years since the prioritization matrix was adopted by the City, it has continued to be fine-tuned by SPU. The current version is presented on Figure 4. Criteria considered, but eventually deleted, included:

- construction access
- existing claims against City
- potential losses for City
- type of failure
- equity
- neighborhood plans
- cost to fix
- environmental consequences of slope failure

3.6 *Uses by Seattle department of planning and development*

Regulations for steep slopes and PSAs that were initiated in 1987 and improved in 1993 credited for limiting damage to private properties in the 1996/97 landslide season. The City reported that no dwellings built under those steep slope/PSA rules were damaged during the 1996/97 winter. One of the benefits of the Seattle Landslide Study has been an improved map of PSAs for the Department of Planning and Development, commonly referred to as the building department in other jurisdictions. Its inclusion on a GIS database has made it easier to provide information to the public and to administer the steep slope/PSA rules.

3.7 *Measures of success*

SPU's landslide program is relatively young and the first several years it was in existence were primarily spent collecting data and developing the programmatic components. However, several measures of success have been realized and risks of damage from landslides have been reduced since the program's inception. Key measures of success include:

- Education of the public, department directors and council members on the hazards, risks and responsibilities in landslide-prone areas,
- Education of public officials on how to manage and reduce risks from landslides,
- A prioritization matrix to rank potential landslide mitigation projects, which was developed by four key City departments,
- Completion of a number of medium to large Capital Improvement Program (CIP) projects and dozens

Draft Criterion for Ranking Potential City Landslide Projects						
			Score			
Criteria	Definition or Intent	Weighting Factor	3	9	27	81
Public Safety	Relative risk to the public	4	No people in path of debris	Single person occasionally in path of debris	Few people in path of debris on regular basis	Large concentration or constant presence of people in path of debris
Inconvenience to people, freight and commerce	Length of time before full functionality and services are restored	3	Rarely inconvenient	Blockage of passage for 1-4 hours	Blockage of passage for 5-24 hours	More than one day blockage
Criticality of City Facility	How critical the facility is to delivery or access of public services	3	No city facilities present except for streets w/≤ 1k ADT	Unoccupied facilities and no lifeline services (e.g. 1k< ADT ≤ 5k SD ≤15", SS/CS ≤8")	Facility periodically occupied or slight change in interruption of public services (e.g. W ≤18, 8"< SD ≤36", 15"< SS/CS ≤24", 5k< ADT ≤15k)	Critical facility for lifeline services (e.g. >15k ADT, SD >36", SS/CS >24", W >18)
Vulnerability of City-owned facility	Potential for a City-owned facility to be impacted and protective measures in place	3	Remote chance of impact	Directly in path and adequate protective measures in place	Directly in path and minor protective measures in place	Directly in path and no protective measures in place
	Potential for a City-owned facility to affect the size/potential for failure and the protective measures in place	3	No effect on potential slide	Minor effect on size/potential slide and adequate protective measures in place	Some potential for affecting the size/potential for failure and minor protective measures in place	Likely to affect the size/potential for failure and no protective measures in place
Likelihood of failure	Potential recurrence interval between slide events	3	>100 years	50-99 years	10-49 years	<10 years
Size of failure	Approximate amount of material that may move in an event	2	<5 cu yds	6-99 cu yds	100-999 cu yds	>1,000 cu yds
Existing slope modification by the City	Modification of the slope by the City	2	Undisturbed	Disturbed but engineered	Slightly disturbed and not engineered	Disturbed and not engineered
Potential for cooperation (goodwill, innovation) on projects (public & private)	Potential to leverage funds	1	Single department responsible for repair/mitigation	Two departments willing to repair/mitigate site	Two departments plus private property owners willing to repair/mitigate site	Three departments plus private property owners willing to repair/mitigate site
Maintenance necessary for full functionality	Annual maintenance costs required in response to a slide to restore full functionality	1	≤ $1,500	$1,500-$2,999	$3,000-$14,999	>$15,000
Cost/Benefit Analysis	Evaluation of life cycle costs vs. potential damage costs if not implemented	<1 or >1				

ADT = Average Daily Traffic   W = Watermain   SD = Storm Drain   SS = Sanitary Sewer   CS = Combined Sewer   April 23, 2003

Figure 4. Prioritization matrix used for ranking capital projects for landslide mitigation.

of small drainage projects in LPAs, including structural slope stabilization, controlling surface water runoff or increasing the capacity of storm drains,

- Better coordination among departments responsible for landslide emergency response,
- Developing in-house expertise to plan, manage and implement landslide mitigation projects.

Two example CIP landslide mitigation projects that reduced the City's risks are the Alki/Federal Emergency Management Agency (FEMA) Landslide Mitigation Project and the Atlas Place SW Landslide Mitigation Project. These were ranked as the top two projects to implement according to the priority matrix. The Alki area of West Seattle is notorious for landslides. Residents living below a steep greenbelt owned by the City would call with hundreds of complaints about sloughing and landslides onto their property during a typical winter. The City partnered with the FEMA to construct 425-m-long, 8-m-deep cutoff trench drain and 2,200 m of horizontal drains to control the groundwater. That next winter and subsequent ones after, the number of complaints dropped to only several dozen per year.

The Atlas Place SW area of West Seattle also experienced several large and numerous smaller slides since the early 1900s. A large landslide occurred in 1997; one house was completely destroyed and two others sustained significant damage. The planning level solution was to construct a project similar to the Alki project. The City hired a consultant to conduct a comprehensive geotechnical study of the area and found that the risk of a deep-seated slide was not as great as was initially thought from historical records. All that was necessary was to construct a system that diverted surface water runoff away from the slope to dewater the near surface colluvial soils. This was accomplished by increasing the capacity of storm drainage and street regrading the area.

4 CONCLUSIONS

This program has enabled City officials to develop an effective landslide mitigation program that is based on a rich, world-class database of recorded landslides, a powerful computer GIS mapping tool, coordination among key City departments, valuable consultant

548

technical expertise and solid leadership by public officials. Seattle will always continue to face landslide risks because of its topography, geology and rainfall conditions, but it is hoped that with time and continued focus on implementing and improving the landslide program, damage from slides will be considerably less than in 1997.

REFERENCES

Booth, D.B. 1990. personal communication.

Chleborad, A.F. 2000. Preliminary method for anticipating the occurrence of precipitation-induced landslides in Seattle, Washington. Denver, CO: U.S. Geological Survey Open-File Report 00–0469.

Shannon & Wilson, Inc. 2000. Seattle landslide study, prepared for Seattle Public Utilities.

Tubbs, D.W. 1974. Landslides in Seattle. Olympia, WA: Washington Department of Natural Resources, Information Circular 52.

U.S. Army Corps of Engineers 1997. Post event report: winter storm of 1996–97, federal disaster DR 1159, western Washington summary. Seattle District, prepared for Federal Emergency Management Agency, Region X.

MultiRISK: An innovative concept to model natural risks

T. Glade & K.v. Elverfeldt

Department of Geography, University of Bonn, Germany

ABSTRACT: Analysis of natural risks in arctic and alpine regions includes the study of typical natural processes such as snow avalanches, slush flows, rock falls, shallow landslides, and debris flows. Commonly, the respective processes are modeled individually which might lead to misjudgement of the general natural risks in a specific area. Therefore, fundamental research is needed regarding integrative and multi-processual modeling of natural risks. The aim of this project is to attain a comprehensive, modular risk analysis tool to quantify different natural risks for one area. This software system will be developed in Northwest Iceland and applied to calculate scenarios of global warming and land-use change.

1 INTRODUCTION

In Iceland, natural processes such as snow avalanches, slush flows, rock falls, shallow landslides, and debris flows occur frequently. Although these processes are characterized by varying occurrence in time and space, they result in a constant threat to people and infrastructure. Official statistics denote at least 680 casualties by snow avalanches since 1118, but the real number is estimated to be much higher (Jóhannesson 2001). In 1995, two catastrophic snow avalanches in Súðavik and Flateyri caused 34 casualties. But slush flows, rock falls, and debris flows also endanger lives (Jóhannesson 2001). At the same time, the consequences of global warming and land-use change are completely unknown.

Commonly, the respective processes are modeled individually (Fuchs et al. 2001). Some examples are Aval1-d /2-d and SAMOS for snow avalanches (e.g. Christen et al. 2002, Jóhannesson et al. 2002, Tracy & Jóhanneson 2003), Rocfall, STONE and CRSP for rock falls (e.g. Guzzetti et al. 2002, Jones et al. 2000, respectively), dfwalk and flo-2d for debris flows (e.g. Gamma 2000, O'Brien et al. 1993, respectively), and SINMAP for shallow landslides (e.g. Pack & Tarboton 2004), to name only a few models. In this respect it is of particular importance that the respective processes can not be modeled with the same accuracy regarding their magnitude and frequency as well as location and extent of run-out zones.

Hence, fundamental research is needed regarding integrative and multi-processual modeling of natural risks. A comprehensive, modular risk analysis tool with a high temporal and spatial resolution is of great importance to avoid misjudgement of general natural risks in a specific area.

2 STUDY AREA

The main study area, Bildudalur, is situated in the Westfjords in Northwest Iceland (Fig. 1). Criteria for choosing the study area were: (1) the general threat by snow avalanches, slush flows, rock falls, shallow landslides, and debris flows (Fig. 2); and (2) data availability for risk calculation. Bildudalur is situated
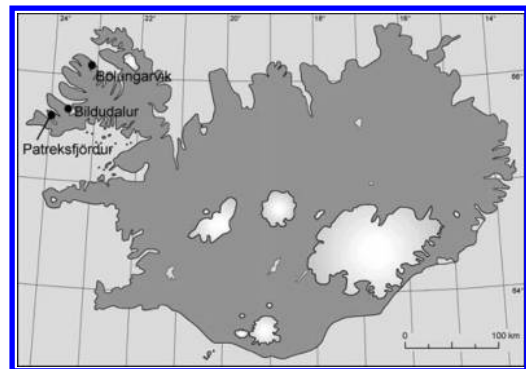

Figure 1. Study area in the Westfjords, Iceland.

along the northern shoreline of Bildudalsvogur within the Arnarfjördur fjord in the southern part of the Westfjords (lat. 65.4°, long. 23.6°) (Bell & Glade 2004) (Fig. 3). Above the village an extensive plateau rises up to 460 m a.s.l. The mountainside is dissected into two large and several smaller gullies (Fig. 3), comprising the respective debris cones. The lithology consists of various basaltic layers with parallel and near-horizontal bedding. Periglacial, gravitational and fluvial processes are dominant (Bell & Glade 2004, Glade & Jensen 2005).

The maritime climate with a mean annual air temperature of 3°C is characterized by cool summers and mild winters. Precipitation amounts to approximately 1250 mm (Glade & Jensen 2005).

In the 18th century, settlement of the area had begun. Today, almost 300 people are living in Bildudalur. Fisheries are the main economic factor.

Two spectacular natural events exemplify the general threat within Bildudalur (Bell & Glade 2004, Glade & Jensen 2005). In February 1939, a slush flow passed through the schoolhouse, trapping the headmaster and

Figure 2. Example for the general threat of rock falls in Bildudalur.

Figure 3. Photography of Bildudalur, view towards northwest.

sweeping him out to sea where he was rescued. In December 1971, a boulder bounced towards a house, moving through the door, rebounding on the floor, finally stopping on a bed. Luckily, the owner was in the kitchen at the time.

The model development and adjustment is carried out in Bíldudalur. For model validation the two villages of Bolungarvik and Patreksfjördur have been chosen (Fig. 1).

3 MULTIRISK: THE CONCEPT

Within risk analyses, processes are commonly modelled and visualised individually in different software systems (e.g. Stötter 1999). Therefore, the aim of this project is to attain a computer-based, modular natural risk model for different processes. GIS-systems such as ArcGIS are especially suitable due to their open structure.

The respective process models will be integrated as separate modules in an open GIS-platform, hence, interfaces have to be programmed as independent scripts. Calculation of the specific processes will take place in the respective modules. This is the specific importance of the project: Due to the modular structure of the GIS-platform a transfer to other regions (potentially including other processes) is possible. Relevant process parameters have to be defined, e.g. height and density of snow cover, lithology, rock shapes and sizes, precipitation, and surface roughness. All calculations are based on a DEM of at least 10 m grid size.

As part of a general natural hazard analysis, the occurrence of single process in space and time has to be determined for specific magnitudes and intensities. Using DEMs and process parameters, hazard run-outs will be calculated and hazard zones derived. Single hazard maps are then joined within GIS resulting in multi-hazard maps. Zonation depends on the magnitude and frequency of the respective process, so that different scenarios are possible.

Data on natural risk due to rock falls, debris flows and snow avalanches is readily available (Bell & Glade 2004). For debris flows and rock falls, risk is calculated following a function of the input parameters hazard (H), vulnerability (of people (V_{pe}), property (V_p), and

Table 1. Damage potential in Bildudalur.

Risk elements	Damage potential
Roads	396 €/m^2
Powerline	36 €/m^2
Buildings	240–1480949 €/building

552

infrastructure (V_{str})), probability of the temporal impact (P_t), probability of the seasonal occurrence (P_{so}), and damage potential (number of people (E_{pe} or E_{ipe}), economic value (E_p)). Snow avalanche risk analysis is based on a preliminary snow avalanche map with two resulting hazard zones (Bell & Glade 2004).

Combining hazard maps with risk elements (e.g. people, houses, roads), their damage potential, and their vulnerabilities to the respective processes, risk maps will be achieved. Risk elements have been classified into three groups: (1) population, (2) property, and (3) infrastructure. Data for the damage potential of properties and infrastructure in Bildudalur was obtained from Icelandic statistics (Table 1).

Vulnerability assessment is crucial within any risk analysis. In general, vulnerability values can only be estimated, which is particularly true for landslide risk analysis (Glade 2003). For Bildudalur, vulnerability values are determined based on the process and its magnitude (debris flow and rock fall) or hazard (snow avalanches). Respective figures are given in Table 2. For detailed discussion of the multi-hazard analysis in Bildudalur refer to Bell & Glade (2004).

The resulting risk maps can be displayed either for a single process or a process group or for a single object at risk or a large region (refer to Bell & Glade 2004 for examples).

The model will be calibrated with the results of a mapping and survey campaign in Bildudalur. Validation will take place in Bolungarvik and Patreksfjördur.

Following the development, calibration and validation of the model risk scenarios of land-use or climate change will be calculated. The calculations will be based on data from global climate models and on scenarios of the study areas, respectively. This results in a quantification of possible future risks.

The general concept is visualized in Figure 4.

4 MULTIRISK: INNOVATIVE ASPECTS

MultiRISK offers several innovations on the conceptual as well as the scientific level. Conceptually, the first innovative aspect is the development of a software system with: (1) modular integration of all process models, (2) risk calculation, and (3) utilization of a joint database. Secondly, the open conceptual structure results in different application levels. Calculation can take place on the level of single processes as well as groups of processes, and on the scale of a specific object as well as on a regional scale.

Scientifically, the challenge is (1) to derive an impartial, repeatable, and comprehensible calculation of multiple natural risks. (2) In particular, MultiRISK offers the opportunity to quantify consequences of land-use and climate change.

The MultiRISK project has just started in October 2004. It is aimed to use existing process models for natural hazard analysis. Currently, negotiations are underway with different developers. First results might be expected by end of 2005.

5 CONCLUSIONS

Commonly, the consequences of global warming and land-use change are estimated. MultiRISK offers the opportunity to quantify present and future risks within a given area. Furthermore, the open, modular structure offers the opportunity to include other process models and thus to transfer MultiRISK to other regions than Iceland.

ACKNOWLEDGEMENTS

Table 2. Vulnerability values used within this study (Note: Vstr = vulnerability of roads and infrastructure, Vp = vulnerability of properties, Vpe = vulnerability of people, and Vpep = vulnerability of people in buildings; high (1) = 10 year event of the high hazard class, high (2) = 150 year event of the high hazard class) (Bell & Glade 2004).

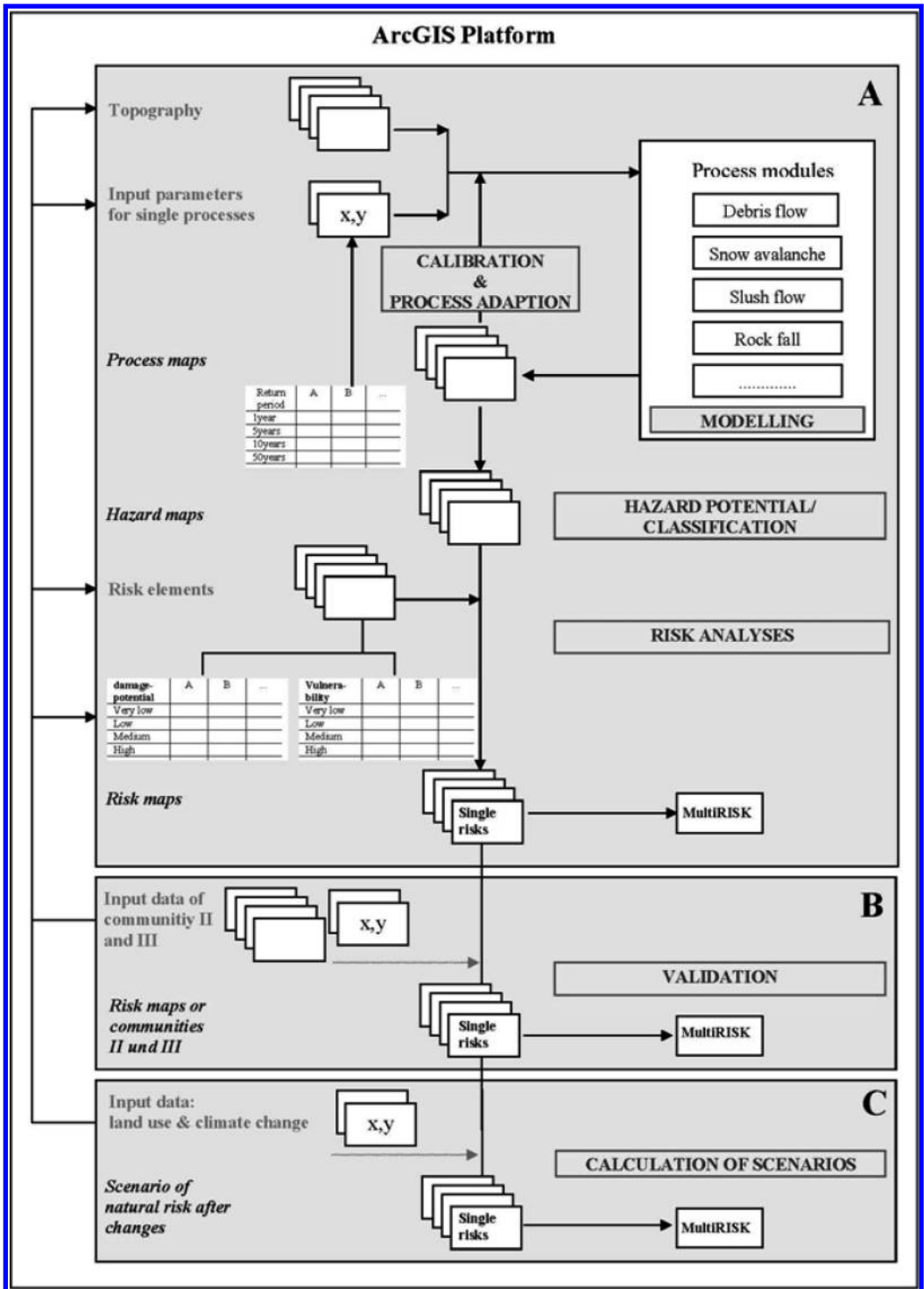| Hazard process	low				medium				high			
	V_{str}	V_p	V_{pe}	V_{pep}	V_{str}	V_p	V_{pe}	V_{pep}	V_{str}	V_p	V_{pe}	V_{pep}
Debris flow	0.2	0.1	0.2	0.02	0.4	0.2	0.3	0.06	0.6	0.5	0.5	0.25
Rock fall	0.1	0.1	0.2	0.02	0.2	0.3	0.4	0.12	0.4	0.5	0.5	0.25
Hazard Process	low				high(1)				high(2)			
	V_{str}	V_p	V_{pe}	V_{pep}	V_{str}	V_p	V_{pe}	V_{pep}	V_{str}	V_p	V_{pe}	V_{pep}
Snow avalanche	0.3	0.3	0.5	0.15	0.1	0.3	0.1	0.03	0.8	1.0	1.0	1.0

Figure 4.   Conceptual flow chart of MultiRISK and procedure.

554

REFERENCES

Bell, R. & Glade, T. 2004. Multi-hazard analysis in natural risk assessments. In: Brebbia, C. (ed.): Proceedings of the International Conference on Computer Simulation in Risk Analysis and Hazard Mitigation (RISK ANALYSIS 2004), Rhodes, Greece, 197–206.

Christen, M., Bartelt, P. & Gruber, U. 2002. AVAL-1D: An avalanche dynamics program for the practice. In: INTERPRAEVENT 2002 in the Pacific Rim – Protection of habitat against floods, debris flows and avalanches, Matsumoto/Japan, 715–725.

Fuchs, S., Keiler, M. & Zischg, A. 2001. Risikoanalyse Oberes Suldental, Vinschgau, Konzepte und Methoden zur Erstellung eines Naturgefahrenhinweis-Informations systems. – Innsbrucker Geographische Studien: Selbstverlag des Instituts für Geographie der Universität Innsbruck, Innsbruck, 249 pp.

Gamma, P. 2000. dfwalk – Ein Murgang-Simulations programm zur Gefahrenzonierung. – Geographica Bernensia: Geographisches Institut der Universität Bern, Bern, 191 pp.

Glade, T. 2003. Vulnerability assessment in landslide risk analysis. Die Erde 134 (2): 121–138.

Glade, T. & Jensen, E.H. 2005. Recommendations for landslide hazard assessments in Bolungarvik and Vesturbyggd, NW-Iceland, Icelandic Metereological Office, Reykjavík.

Guzzetti, F., Crosta, G., Detti, R. & Agliardi, F. 2002. STONE: a computer program for the three-dimensional simulation of rock-falls. Computers and Geosciences 28: 1079–1093.

Jóhannesson, T. & Arnalds, P. 2001. Accidents and economic damage due to snow avalanches and landslides in Iceland. Jökull 50: 81–94.

Jóhannesson, T., Arnalds, P. & Tracy, L. 2002. Results of the 2D avalanche model SAMOS for Bolungarvík and Neskaupstaður. Reykjavík, Veðurstofa Íslands: 35.

Jones, C.L., Higgins, J.D. &. Andrew, R.D. 2000. Colorado rockfall simulation programm. Denver, Colorado Department of Transportation.

O'Brien, J.S., Julien, P.Y. & Fullerton, W.T. 1993. 2-Dimensional water flood and mudflow simulation. Journal of Hydraulic Engineering – ASCE 119 (2): 244–261.

Pack, R. & Tarboton, D. 2004. Stability Index Mapping (SINMAP) applied to the prediction of shallow translational landsliding. Geophysical Research Letters 6.

Stötter, J. 1999. Konzeptvorschlag zum Umgang mit Naturgefahren in der Gefahrenzonenplanung. Herausforderung an Praxis und Wissenschaft zur interdisziplinären Zusammenarbeit. Jahresbericht_1997/98. Innsbrucker Geographische Gesellschaft. Innsbruck**:** 30–59.

Tracy, L. & Jóhanneson, T. 2003. Results of the 2D avalanche model SAMOS for Bíldudalur and Patreksfjördur. Reykjavík, Icelandic Meteorological Office 11.

A comparison of landslide risk terminology

D.F. VanDine
VanDine Geological Engineering Limited, Victoria, British Columbia, Canada

G.D. Moore
BC Ministry of Forests, Engineering Section, Victoria, British Columbia, Canada

M.P. Wise
GeoWise Engineering Ltd, North Vancouver, British Columbia, Canada

ABSTRACT: British Columbia Ministry of Forests' Land Management Handbook 56 (LMH 56) presents a framework for landslide risk management, describes technical terms and methods of landslide risk analysis, and presents eight case studies authored by geotechnical professionals with expertise in forest development. LMH 56 uses consistent landslide risk terminology that is based on terminology presented in recent publications by the Canadian Standards Association, the International Union of Geological Sciences, and the Australian Geomechanics Society. This paper compares the LMH 56 terminology to that of the recently published International Society of Soil Mechanics and Geotechnical Engineering's Glossary of Risk Assessment Terms (ISSMGE). There are many similarities, and some differences, between the LMH 56 and the ISSMGE terminologies. It is important that eventually all geotechnical professionals use the same risk terminology, particularly for situations where different professions or regulators are evaluating risk.

1 INTRODUCTION

In 2004, British Columbia Ministry of Forests published Land Management Handbook 56 (LMH 56) entitled, *Landslide Risk Case Studies in Forest Development Planning and Operations* (Wise et al. 2004a). That handbook presents a framework for landslide risk management, describes technical terms and methods of landslide risk analysis, and presents eight case studies authored by geotechnical professionals with expertise in forest development.

Landslides are relatively common in the steep, mountainous terrain of British Columbia where forest development (road construction and timber harvesting) occurs. Because the legislative framework in British Columbia has changed markedly over the past 10 years, geotechnical professionals are tasked with carrying out landslide risk analyses related to forest development. The results of analyses of existing and future landslide risks are commonly used by professional foresters and biologists, as well as government agencies, to make planning, development and operational decisions.

In the planning stages for LMH 56, it was decided to have all case study authors use consistent landslide risk terminology, and terminology that is consistent with the following three publications:

- *Risk management: guideline for decision-makers,* by the Canadian Standards Association (CSA 1997)
- *Quantitative risk assessment for slopes and landslides – The state of the art,* by the International Union of Geological Sciences' Working Group on Landslides, Committee on Risk Assessment (IUGS 1997)
- *Landslide risk management concepts and guidelines*, by the Australian Geomechanics Society Sub-committee on Landslide Risk Management (AGS 2000).

Chapter 2 of LMH 56 (Wise et al. 2004b) provides some general definitions and presents a framework for landslide risk management. Chapter 3 of LMH 56 (VanDine et al. 2004) further develops the landslide risk terms that were successfully applied to each of the eight case studies in LMH 56. The LMH 56 terminology is being encouraged for use by geotechnical professionals working in the British Columbia forest sector, and is being proposed for use throughout Canada.

Subsequent to the publication of LMH 56, the International Society of Soil Mechanics and Geotechnical Engineering, Technical Committee 32 (Risk Assessment and Management) published its *Glossary of Risk Assessment Terms – Version 1, July 2004* (ISSMGE 2004). The glossary was based, to a large extent, on the CSA (1997), IUGS (1997) and AGS (2000) documents, but is intended for use in all fields of geotechnical engineering, not only those related to landslides.

This paper compares the LMH 56 terminology to that of ISSMGE (2004). For the purpose of this paper, ISSMGE (2004) is simply referred to as ISSMGE and Wise et al. (2004a) is simply referred to as LMH 56.

2 RISK

According to ISSMGE, risk is a "measure of the probability and severity of an adverse effect to life, health, property, or the environment. Quantitatively, Risk = Hazard × Potential Worth of Loss. This can be also expressed as 'Probability of an adverse event times the consequences if the event occurs'."

ISSMGE defines hazard as the *"probability that a particular danger (threat) occurs within a given period of time."* It also uses the term hazard to mean a harmful or potentially harmful danger. Because the double use of the term hazard has led to some confusion in communicating the results of risk analyses, LMH 56 encourages the use of the term hazard only to refer to a harmful or potentially harmful danger (e.g. a landslide), and refers to "*an estimate of the chance for a landslide to occur*" as "probability."

In the above ISSMGE definition of risk, using the symbol P for hazard or probability, and the symbol C for potential worth of loss or consequence, risk can mathematically be expressed as:

$$R = P \times C \qquad (1)$$

LMH 56 defines risk as *"the chance of injury or loss as defined as a measure of the probability and the consequence of an adverse effect to health, property, the environmental and other things of value, (adapted from CSA 1997)."*

Specific risk, R(S) using LMH 56 terminology, is defined as "*the risk of loss or damage to a specific element [potentially at risk], resulting from a specific hazardous affecting landslide.*"

There are two types of specific risk:

- $R(S)_{property}$, specific risk related to property, the environment and other things of value, and
- $R(S)_{human\ life}$, specific risk related to human life.

$R(S)_{human\ life}$ is also known as PDI, annual probability of death to an individual, or PDG, annual probability

of death to a group, where a group is defined as more than one individual.

Mathematically specific risk is expressed as:

$$R(S) = P(H) \times C \qquad (2)$$

Equations 1 and 2 are essentially identical, except that in Equation 2 an (S) modifies R to indicate a risk to a "specific" element, and an (H) modifies P to indicate the probability of occurrence of a "specific hazardous" landslide.

ISSMGE does not have a term similar to specific risk, and neither does CSA (1997), IUGS (1997) or AGS (2000).

3 CONSEQUENCE

According to ISSMGE, consequence is "the outcome or result of a hazard being realized."

LMH 56 defines "consequence" as *"the effect on human well-being, property, the environment, or other things of value, or a combination of these (adapted from CSA 1997). Conceptually, consequence is the change, loss, or damage to the elements caused by the landslide."* LMH 56 further states that consequence is *"the effect to the element, and includes consideration of spatial probability, temporal probability and vulnerability."* That is, it includes:

- the probability that the landslide will reach or otherwise affect the site potentially occupied by the element (spatial probability)
- the probability that the element is at the site when the landslide occurs or reaches the site (temporal probability)
- the vulnerability of the element.

ISSMGE does not have a term similar to spatial probability.

LMH 56 defines spatial probability as the conditional probability, P(S:H), *"the probability that there will be a spatial effect, given that a specific hazardous landslide occurs."* In a quantitative analysis, if it is certain that the landslide will reach or otherwise affect the site potentially occupied by the element, the spatial probability is numerically 1. Otherwise, the spatial probability is between 0 and 1 to account for the possibility that the landslide will reach or otherwise affect the site.

ISSMGE defines temporal probability as *"the probability that the element at risk is in the area affected by the danger (threat) at the time of its occurrence."*

LMH 56 defines temporal probability as the conditional probability, P(T:S), *"the probability that there will be a temporal effect given that there is a spatial effect."* In a quantitative analysis, if the element is a

permanent fixture, such as a bridge, building or a stream, the temporal probability is numerically 1 because it is certain that the element will be at the affected site when the landslide occurs or reaches the site. Otherwise, the temporal probability is between 0 and 1 to account for the fact that a mobile element may not be at the affected site at the time the event occurs. (In the case of a vehicle that drives into a landslide that has recently occurred, temporal probability can also consider a time shortly after an event.)

The ISSMGE and LMH 56 definitions for temporal probability are similar.

ISSMGE defines vulnerability as *"the degree of loss to a given element or set of elements within the area affected by a hazard. It is expressed on a scale of 0 (no loss) to 1 (total loss)."* AGS (2000) extends this definition by stating *"for property, the loss will be the value of the damage relative to the value of the property; for persons, it will be the probability that a particular life (the element at risk) will be lost, given the person(s) is affected by the landslide."*

From LMH 56, vulnerability *"depends upon the type and character of the element. It is a measure of the robustness (or alternatively, the fragility) of the element, and its exposure to (or alternatively, protection from) the landslide."* Quantitatively, vulnerability can be either the estimated "probability of total loss or damage" expressed as between 0 and 1, OR in the case where the probability of some loss or damage is assumed to be certain, it is the estimated "proportion of loss or damage" between 0 (no loss) and 1 (total loss).

The LMH 56 definition for vulnerability is similar to the ISSMGE definition when the AGS (2000) extension is considered.

Using the LMH 56 terminology described above, consequence can mathematically be expressed as:

$$C = P(S:H) \times P(T:S) \times V(L:T) \qquad (3)$$

Consequence can be expressed quantitatively, between 0 and 1, as a "probability" of total loss or damage to the element, OR as a "proportion" of loss or damage to the element, corresponding to the unit of V(L:T) used in the analysis. Note that if it is certain that the landslide debris will reach or otherwise affect the site potentially occupied by the element, then P(S:H) = 1, and if the element is a permanent fixture, then P(T:S) = 1, and consequence and vulnerability are the same.

In general terms, ISSMGE and LMH 56 refer to consequence similarly.

4 CONSEQUENCE VALUE

The ISSMGE quantitative definition of risk is expressed as *"Risk = Hazard × Potential Worth of Loss."* Otherwise that document does not refer to

value or worth. For property, AGS (2000) considers *"the value or the net present value of the property"*, and represents it with the symbol E.

Similarly, LMH 56 uses the symbol E to represent an element's worth. *"An element's worth can include direct and indirect values associated with monetary and qualitative values."* Taking a secondary highway as an example, worth can include:

- direct monetary worth: original or replacement costs, if the highway has to be rebuilt, or cost of clearing landslide debris and making the necessary repairs, if the structure is damaged
- indirect monetary worth: economic loss resulting from the highway being destroyed or blocked by a landslide
- direct qualitative worth: the secondary highway is more valuable to the local population than a nearby highway because the former provides access to a hospital, while the latter does not
- indirect qualitative worth: the highway provides access to a recreational area.

Monetary worth of an element can be the total cost (for example, original, replacement or mitigation), or the total cost annualized (average annual), but should not be a mixture of total cost and annualized cost.

Using the LMH 56 terminology described above, for elements other than human life, consequence can be combined with worth, and a consequence value (CV) of the loss or damage to the property, the environment and other things of value (collectively referred to as property) can be mathematically expressed as either:

$$CV_{property} = P(S:H) \times P(T:S) \times V(L:T)_{property} \times E$$
$$(4)$$

$$CV_{property} = C_{property} \times E \qquad (5)$$

There is no equivalent component $CV_{human\ life}$, because human lives are considered more precious than any direct and indirect, monetary and qualitative, values placed on them.

ISSMGE does not have a term similar to consequence value, but as indicated above does refer to "potential worth of loss" in its risk equation.

5 SPECIFIC RISK VS PARTIAL RISK

Based upon the above discussion of consequence and using the LMH 56 terminology described above, the mathematical equation of specific risk (Equation 2) can also be expressed as either:

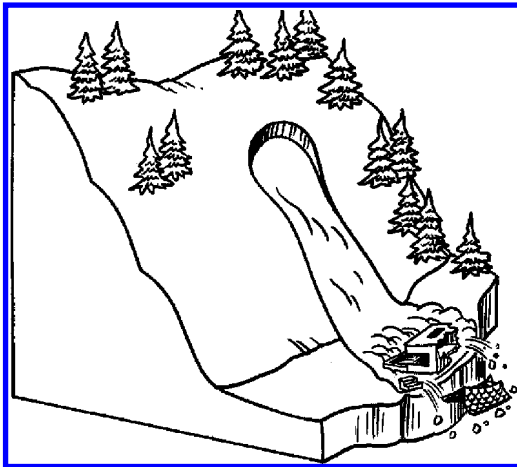$$R(S) = P(H) \times P(S:H) \times P(T:S) \times V(L:T) \qquad (6)$$

Figure 1. Schematic drawing of specific risk, R(S). A specific hazardous affecting landslide and the vulnerability of the element is considered.
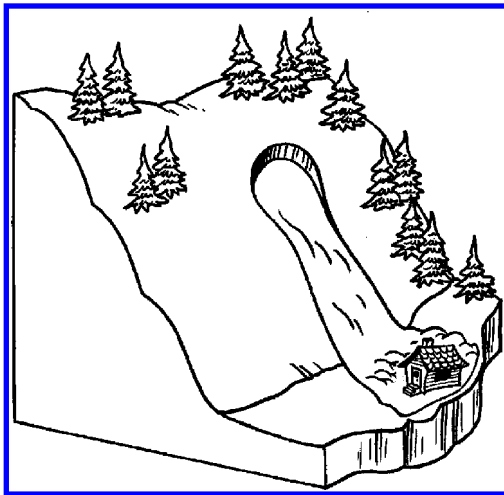

Figure 2. Schematic drawing of partial risk, P(HA). A specific hazardous affecting landslide but the vulnerability of the element is not considered.

$$R(S) = P(HA) \times V(L:T) \tag{7}$$

where

$$P(HA) = P(H) \times P(S:H) \times P(T:S) \tag{8}$$

Specific risk is shown schematically in Figure 1.

In LMH 56, P(HA) in Equations 7 and 8, is defined as "partial risk" – *"the probability of a specific hazardous affecting landslide."* In other words, it
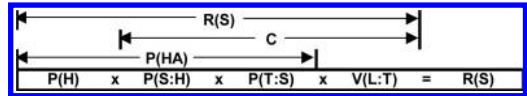

Figure 3. The relationship of P(HA) and C to specific risk, R(S).

is the product of the probability of occurrence of a specific hazardous landslide and the probability of that landslide reaching or otherwise affecting the site occupied by a specific element. Partial risk does not consider the vulnerability of the element, and therefore is not strictly speaking a risk, hence the use of the primary symbol P, as opposed to R, and the qualifier term, "partial." (Fig. 2).

Partial risk is a very useful method of analysis because it can be used to carry out a risk analysis, even when little or nothing is known about the vulnerability of the element – and in practice, for geotechnical professionals, this is quite often the case. In LMH 56, five of the eight case studies used partial risk analysis.

Figure 3 graphically shows the relationship of the risk components for specific risk, and the "mathematical overlap" of partial risk P(HA) and consequence (C).

ISSMGE does not have a term similar to partial risk, and neither does CSA (1997), IUGS (1997) or AGS (2000).

6 SPECIFIC VALUE OF RISK

LMH 56 defines specific value of risk as R(SV) – "the worth of loss or damage to a specific element, excluding human life, resulting from a specific hazardous affecting landslide." Human life is excluded because, as mentioned above, human lives are generally considered more precious than any value placed on them.

The mathematical equation of specific value of risk, using the LMH 56 terminology described above, can be expressed as any of the following:

$$R(SV) = P(H) \times C \times E \tag{9}$$

$$R(SV) = P(H) \times CV \tag{10}$$

$$R(SV) = P(H) \times P(S:H) \times P(T:S) \times V(L:T) \times E \tag{11}$$

$$R(SV) = P(HA) \times V(L:T) \times E \tag{12}$$

$$R(SV) = R(S) \times E \tag{13}$$

Figure 4 graphically shows the relationship of the risk components for specific value of risk, and the "mathematical overlap" of the components.

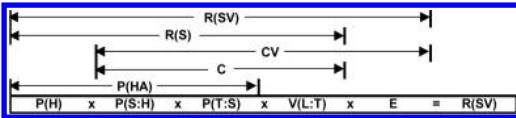ISSMGE does not have a term similar to specific value of risk, and neither does CSA (1997) or IUGS

560

Figure 4. The relationship of the risk components to specific value of risk, R(SV).
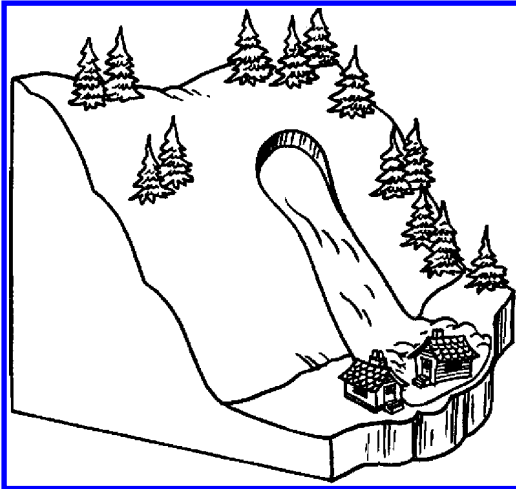

Figure 5a. Multiple risk (one situation). The risk to more than one specific element from a single specific hazardous affecting landslide.
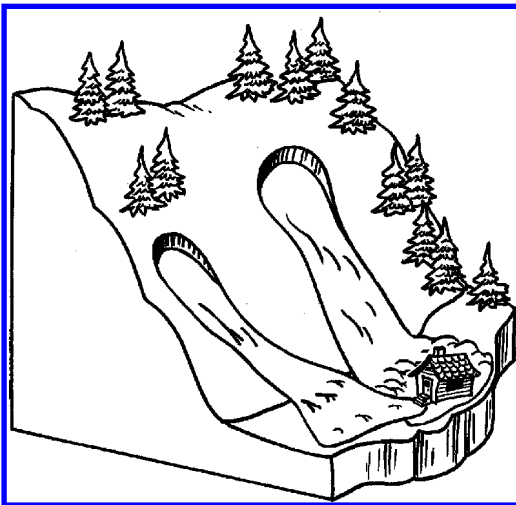
Figure 5b. Multiple risk (another situation). The risk to one specific element from more than one specific hazardous affecting landslide."
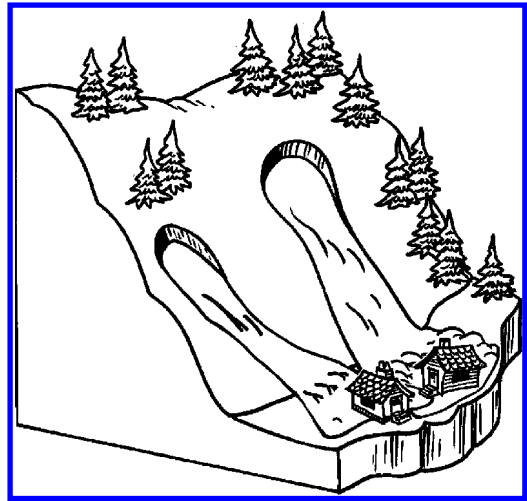
Figure 6. Total risk. The risk to all specific elements from all specific hazardous affecting landslides.

(1997). AGS (2000) does not use the term specific value of risk but, as discussed above, for risk to property it includes the value or net present value of the property.

7 MULTIPLE AND TOTAL RISK

LMH 56 defines multiple risk R(M) – "the risk to more than one specific element from a single specific hazardous affecting landslide, OR the risk to one specific element from more than one specific hazardous affecting landslide." (Figs. 5a–b).

LMH 56 defines total risk R(T) – *"the risk to all specific elements from all specific hazardous affecting landslides."* (Fig. 6)

The estimation of multiple or total partial risk, multiple or total specific risk, or multiple or total specific value of risk are estimated by applying standard probability concepts (for example, Montgomery et al. 2002). In practice, multiple and/or total risks are used much less than partial risk, specific risk or specific value of risk.

ISSMGE does not have any terms similar to multiple risk or total risk, and neither does CSA (1997) or IUGS (1997). AGS (2000) states that "for total risk (whether for property or for life) the risk for each hazard for each element is summed."

8 CONCLUDING REMARKS

Both ISSMGE and LMH 56 are based on CSA (1997), IUGS (1997) and AGS (2000). There are many similarities, and some differences, between ISSMGE and LMH 56 terminologies.

561

To minimize the chance of miscommunication, LMH 56 recommends against the double use of the term hazard, and encourages the term hazard to refer to a harmful or potentially harmful threat (e.g. a landslide). LMH 56 purposely avoids the use of the term hazard in the definition of risk.

The term vulnerability, as used in LMH 56, is not restricted only to mean a "proportion" of loss, where some loss is certain, but it can also be used to estimate "probability" of total loss or damage.

LMH 56 defines the term partial risk – a very useful term for practical risk analysis by geotechnical professionals, particularly for phased land use planning.

Because the components of the risk equation are multiplied, they can be grouped differently for different purposes. LMH 56 graphically shows the relationships of the multiplied components. LMH 56 addresses the inconsistent terminology in CSA (1997), IUGS (1997) and AGS (2000), and promotes better communication of risk terminology between geotechnical professionals and their clients. It is important that eventually all geotechnical professionals agree on and use the same risk terminology. This is particularly important when such professionals carry out studies that will be used by different professions or regulators to evaluate risk. A starting point may be to have all landslide geotechnical professionals agree on and use the same risk terminology.

ACKNOWLEDGEMENTS

REFERENCES

Australian Geomechanics Society (AGS) 2000. Landslide risk management concepts and guidelines; Sub-committee on Landslide Risk Management, Australian Geomechanics, March 2000, 49–92.

Canadian Standards Association (CSA) 1997 Risk management: guideline for decision-makers; Etobicoke, Canada, CAN/CSA-Q850-97, 46p.

International Society of Soil Mechanics and Geotechnical Engineering, Technical Committee 32 (Risk Assessment and Management) 2004. Glossary of Risk Assessment Terms – Version 1, July 2004, electronic copy supplied to authors.

International Union of Geological Sciences' Working Group on Landslides, Committee on Risk Assessment (IUGS) 1997. Quantitative risk assessment for slopes and landslides – The state of the art; in Proceedings of the International Workshop on Landslide Risk Assessment, (eds. Cruden & Fell); Honolulu, Hawaii, USA, pp. 3–12.

Montgomery, D.C., Runger, G.C. & Nairn A.G. 2002. Applied Statistics and Probability for Engineers, 3rd Edition. Wiley & Sons, 2002.

VanDine, D.F., Moore, G.D., Wise, M.P., VanBuskirk, C. & Gerath, B. 2004. Technical Terms and Methods, Chapter 3. In Wise et al. (eds.), Landslide risk case studies in forest development planning and operations, British Columbia Ministry of Forests, Research Branch, Victoria, BC, Land Management Handbook No 56, 13–26.

Wise M.P., Moore, G.D. & VanDine, D.F. (eds.), 2004a. Landslide risk case studies in forest development planning and operations. British Columbia Ministry of Forests, Research Branch, Victoria, BC, Land Management Handbook No 56, 199p, also on the internet at. (http://www.for.gov.bc.ca/hfd/pubs/Docs/Lmh/Lmh56.htm).

Wise M.P., Moore, G.D. & VanDine, D.F., 2004b. Definitions of Terms and Framework for Landslide Risk Management, Chapter 2. In Wise et al. (eds.), Landslide risk case studies in forest development planning and operations, British Columbia Ministry of Forests, Research Branch, Victoria, BC, Land Management Handbook No 56, 5–12.

Hazard and risk assessment: linear projects

Detection and monitoring of complex landslides along the Ashcroft Rail corridor using spaceborne InSAR

C.R. Froese
AMEC Earth & Environmental, Edmonton, Alberta, Canada

T.R. Keegan
CN Rail, Edmonton, Alberta, Canada

D.S. Cavers
AMEC Earth & Environmental, Burnaby, British Columbia, Canada

M. van der Kooij
Atlantis Scientific Inc, Nepean, Ontario, Canada

ABSTRACT: A portion of CN Rail's Ashcroft Subdivision located along the Thompson River in Central British Columbia, traverses an area of complex, slowly moving landslides on the rail line. The rates of movement of these large landslides are such that signs of active movement are often not perceptible to the eye and conventional monitoring with survey and slope inclinometers only provides point source data as to the rate and depth of movement at a specific location. This paper describes the application of Synthetic Aperture Radar Interferometery (InSAR) to assess deformations for five different time frames between 1997 and 2004 in order to map the rates and extents of movement along a seven kilometre section of the railway. As the rates of movement are relatively slow and the ground is dry and has relatively little vegetation, the InSAR technique was very successful in mapping the extents of movements over relatively large time periods that were being monitored by other means and in detecting the rates and extents of landslides where no quantitative movement data previously existed. This new data source will aid in the planning of further investigation and mitigative measures to aid CN in managing risks to their operations associated with landslide hazards.

1 INTRODUCTION

Since the construction of the railways in the Thompson River valley in the late 1800's and early 1900's, there have been many documented large landslides along the Ashcroft Rail corridor. Over this time period there has been a significant amount of work undertaken by both of the main line railway operators, Canadian National Railway (CN) and Canadian Pacific (CP) in mitigating the impacts of the movements on their lines. Recently, there have been a number of papers published reviewing the geological framework for landsliding along the corridor, on the mechanisms of landsliding and on the railway's risk management approach in dealing with landsliding.

In 2001/2002, as part of a project for the European Space Agency, Kosar et al. (2003) undertook a preliminary evaluation of deformations along the rail corridor utilizing spaceborne InSAR. While the results provided interesting additional information on the deformations along the corridor between CN mileages 50 and 57, they were not conclusive in identifying zones of deformation along the valley. Realizing that the InSAR processing capabilities have improved over the two years following the initial study and that additional recent data has been collected over the site, this current study aims to provide a more thorough screening of landslide hazards along the rail corridor utilizing both the re-processed data from the previous study and more recent ascending and descending track data obtained from RADARSAT-1 for a time period between early fall 2003 and early spring 2004.

This paper provides an overview of the process undertaken and the types of information that was derived from the InSAR data.

2 BACKGROUND

Over the past few years, various papers have been published outlining the geology and associated landsliding mechanisms (Clague & Evans 2003), as well

as the detailed observations of the style and contributing factors for movements (Keegan et al. 2003, Porter et al. 2001) along the section of the Thompson River valley considered in this assessment.

The following is a general summary of the main items related to the geology; mechanisms and contributing factors as taken from the above referenced sources:

1 Most of the landslides have occurred within thick Quaternary valley fill dominated by glaciolacustrine sediments and originally formed as part of the rapid degradation of the Thompson River in post-glacial times through extensive glacial lake deposits that filled the preglacial valley.
2 The landslides are retrogressive in nature and the distribution appears to correspond to the presence of a high plastic, laminated clay/silt at the base of the glacial sediments.
3 Back analyses of existing landslides indicate that operational friction angles between 11° and 13° have been mobilized.
4 Due to the retrogressive nature, the stability of the toe blocks adjacent to the river are critical in controlling the overall stability of the displaced masses.
5 Contributing factors to landsliding have been summarised by Porter et al. (2000) as; the presence of high plastic glaciolacustrine clays underlying the younger glacial tills and glaciolacustrine silts; ongoing bank erosion and channel degradation of Thompson River; artesian ground water pressures, possibly influenced by increasing precipitation levels; and a delayed pore pressure response to falling river levels in late summer and early fall.
6 Keegan et al. (2003) indicated a relationship between overall slope angle (crown to tip) and the stage of evolution of landslides along the valley. The authors observed that the overall angles for fully mature compound earth slides are less than 11° to 12°. These mature slides have undergone previous sudden movements and now form an overall more regularly shaped, slow moving mass. Slopes along the valley with steep, uphill facing scarps, overall slope angles greater than 13° and the stratigraphy required for the mechanism to develop have likely not undergone "secondary compound sliding" and have the potential to generate a highly mobile earth slide if the contributing factors and preparatory causes exist. Historic slides of this type are known to have dammed the Thompson River and are therefore of great concern whether they are on the side of the valley that the rail lines occupy or the opposite bank.

Based on the nature of these landslides, CN Rail identified InSAR as a tool that could potentially allow for a high level screening of landslide hazards to
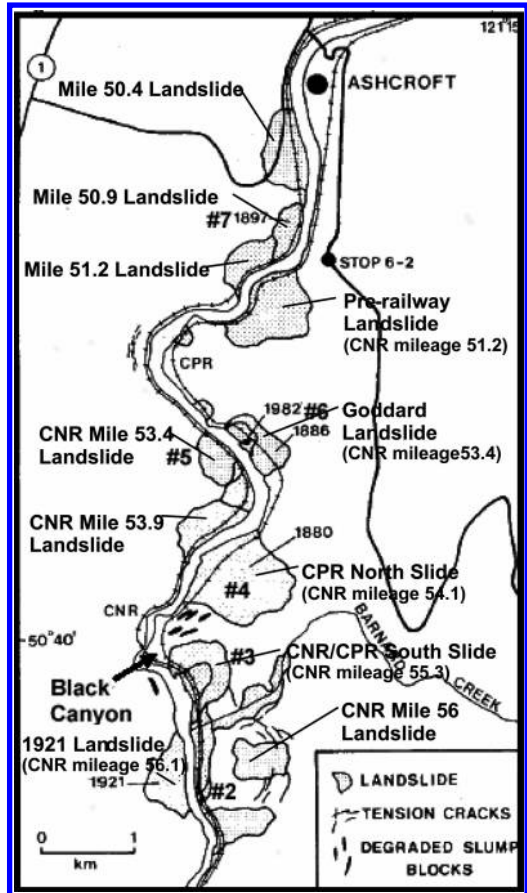
Figure 1. Location plan of Mile 50.9 Landslide and landslides south of Ashcroft (after Porter et al. 2001).

identify zones where the initiation of large catastrophic landslides could occur.

3 TECHNOLOGY

Synthetic aperture radar (SAR) is an active sensor that can be used to measure the distance between the sensor and a point on the earth's surface. A SAR satellite typically orbits the earth at an altitude of approximately 800 km. The satellite constantly emits electromagnetic radiation to the earth's surface in the form of a sine wave. The electromagnetic wave reflects off the earth's surface and returns back to the satellite. This back-scattered microwave signal is used to create a SAR satellite image (a black and white representation of the ground reflectivity).

SAR radar images are made up of pixels. Each pixel has a specific size determined by the SAR satellite

566

resolution, the higher the resolution the smaller the pixel size. The ground reflection is averaged over the pixel area.

To measure differential ground movements over a specified time period, InSAR requires two SAR images of the same area taken from the same flight path, within 500 m laterally. InSAR compares the phase of the echoing signal to a reference wave for each satellite pass. The difference in phase between the two SAR images can be used to determine ground movement in the line of sight of the SAR satellite. For example, if the first pass of the SAR satellite had an echoing wavelength magnitude of fi wavelength and the second pass was $\frac{1}{4}$ wavelength then during the time period between the two passes there has been a $\frac{1}{4}$ wavelength change in the satellite line of sight path length.

The wavelength of the microwave signals emitted by the SAR sensor is typically in the order of a few centimetres. Because InSAR measures the phase difference resulting from the path length change between the sensor and a point on the earth's surface, the magnitude of ground movement between the two satellite passes can be measured to millimetre accuracy.

InSAR has proven highly successful in detecting ground movements in several locations and applications around the world. For example, one of the early users of the technology was the oil sector in the United States, which used spaceborne InSAR to detect very small surface movements above deeply buried reservoirs during hydrocarbon production (Van der Kooij 1997). More recently, examples of successful detection of ground motion for landslides in Canada have been presented by Froese et al. (2004) and Kosar et al. (2003a, b)

Currently there are two agencies operating SAR satellites in the civilian sector, the Canadian Space Agency (CSA) and the European Space Agency (ESA). CSA has had one SAR satellite, RADARSAT-1 in orbit since 1996. ESA recently launched its third SAR satellite, Envisat, in 2002. Its predecessors, ERS-1 and ERS-2 collected SAR images from 1992 to 2000 and from 1995 to 2001, respectively.

The main considerations in choosing and collecting data for the interferometry assessment are as follows:

Satellite Path/Trajectory: One of the main considerations for mapping deformations along slopes is the satellite trajectory. A satellite will pass over the same position on the earth on both an ascending and descending orbit due to the rotation of the earth and the orbit of the satellite. On the ascending orbit, data the satellite sensors are facing approximately to the ENE while the descending orbit will face approximately to the WNW (Fig. 2). For the Ashcroft corridor, the trajectory of the ascending orbit for both ERS and RADARSAT is 344° with a look direction (line of sight) of 074°. The descending orbit has a trajectory of
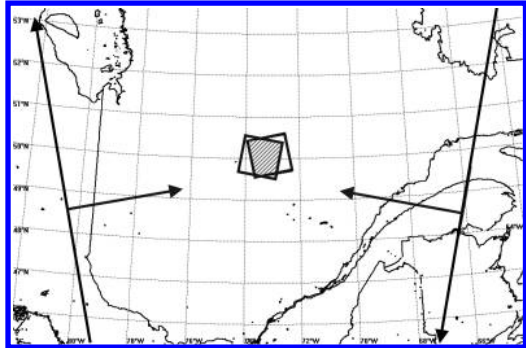

Figure 2.   Schematic showing the acquisition of data from both satellites on an ascending (left) track and a descending (right) track.1

195° with a look direction of 285°. In order to have the best possible chance for success, it is desirable to choose a satellite look angle that is approximately along and parallel to the movement vector of the slope. In general, the slopes along the Thompson River south of Ashcroft face to the east and west, which generally allows movements to be detected using either trajectory, but there are some slope sections where deformations will not be detectable for a certain trajectory as the movements are essentially perpendicular to the line of sight of the satellite.

Figure 3 provides an example showing both ascending and descending scene data for a portion of the left bank at the Goddard Slide. Distinct deformations are observed in the historical ascending data but none on the descending trajectory data as movements are essentially perpendicular to the look direction for a descending trajectory.

Incidence Angle/Slope Geometry: Another important consideration for detecting slope movements is the direction of movement in relation to the angle from vertical that the satellite is looking down at the slope with. This is termed the Incidence Angle and shown on Figure 4. The best case for detecting movements using InSAR is when the movements are parallel to the beam path with the worst case being when the movements are perpendicular to the beam path. This is more of an issue for steep mountainous slopes and less so for the relatively flat slopes present in the landslide topography along the Thompson River.

For relatively flat slopes, the best case is to have the highest incidence angle possible as this correlates to the flattest angle at which the satellite views the earth's surface. Table 1, below, provides a summary of the trajectories, incident angles and look directions for the satellites and various beam modes utilized for the Ashcroft InSAR assessment.

Vegetation/Snow Cover: For the Thompson River valley slope, the climate is semi-arid and therefore the
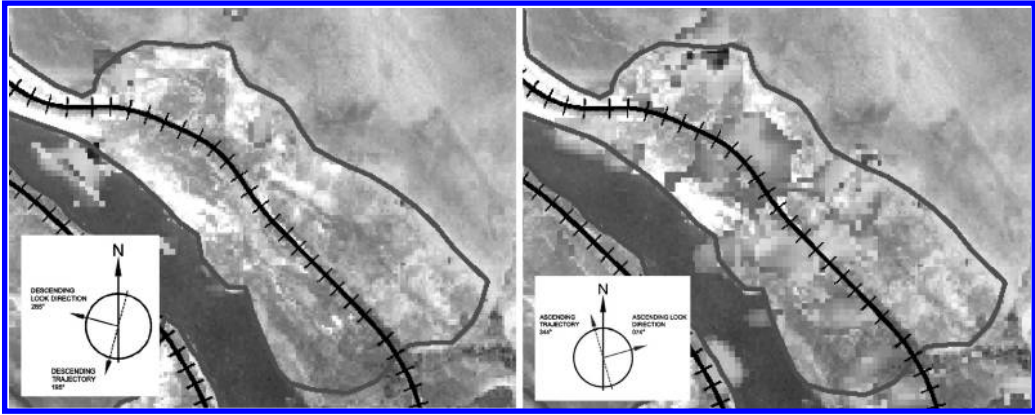
567

Figure 3. Example of motion detected in the ascending trajectory with movement in the line of sight of the satellite (left) and the same site with motion not detected as movement is near perpendicular to the line of site (right). [see Colour Plate X].
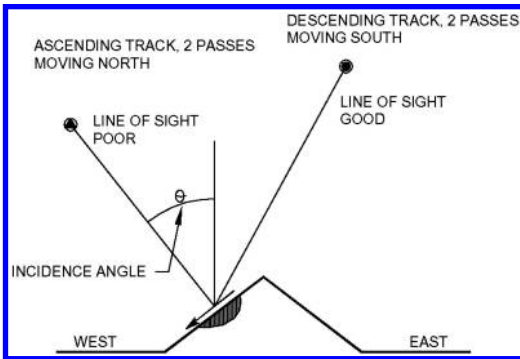
Figure 4. Schematic showing the relation between incidence angle and slope orientation for detection of ground motion.

Table 1. Details of satellite data utilized for the Ashcroft InSAR Assessment.

Satellite (years)	Trajectory	Incidence Angle[°]	Heading[°]
ERS (97–99)	Descending	23.3	195
RSAT(01–02)	Ascending	40.2	344
RSAT(03–04)	Descending	44.7	195.8
RSAT(03–04)	Ascending	40.1	344.3

vegetation cover is relatively sparse and the ground is relatively dry with little to no chance of having snow cover throughout the year. These conditions are ideal for comparing SAR images over longer time periods with less of a chance for temporal decorrelation when compared to ground surfaces that are vegetated and subject to freeze/thaw and various other climatic disturbances which could lead to subtle ground surface changes over time.

Figure 5. Example of data decorrelation in a more active portion of the slope where the movement rate exceeds a full wavelength of phase shift and is therefore represented as black on the slant range data.

Range of Motion: Typically motion ranging between a fraction of a wavelength and a full wavelength can be measured using InSAR. For C-Band satellites (ERS and Radarsat) a 5.6 cm wavelength is utilized. For this assessment a lower bound cut off of 5 mm was utilized to filter out potential atmospheric effects and poor data with a practical upper bound for deformation mapping of 6 cm.

The blacked out portions of the differential interferogram provided on Figure 5 represents slopes that are likely less mature and which may have deformations exceeding a single wavelength of phase change. A more detailed discussion of the application of InSAR to landslide movement detection is provided by Froese et al. (2004).

4 PROCESS

Initial InSAR work on the Ashcroft rail corridor was completed by ASI for ESA and summarized by

568

Kosar et al. (2003). In 2002, as a part of a project for ESA, ASI (2004) undertook InSAR assessments for the following time periods over the Ashcroft Rail corridor:

~ August 8, 1997–August 28, 1998
~ March 19, 1999–October 6, 1999
~ July 29, 2001–April 19, 2002
~ April 19, 2002–May 13, 2002

Due to advances in processing capabilities, it was suggested that as part of the overall Ashcroft InSAR work, ASI reprocess the four data sets originally processed in 2002 for the Ashcroft Corridor between Miles 50 and 57.

The second phase of work included an overall review of the Ashcroft Subdivision between Miles 51 and 57, with additional ascending and descending scene data from September 2003 to April 2004. Both ascending and descending data were chosen for this assessment in order to both aid in the differentiation between shallow and deep seated movement and to provide redundancy and confirm whether movements would be detected from both look directions. These acquisitions were specifically tasked as a follow up to the 2002 work completed under the ESA contract in anticipation of ongoing work in the corridor.

For both the Phase 1 and 2 portions of work, once data processing was completed, the satellite data was projected onto the orthophoto set for the Ashcroft corridor. Two products were produced:

1 Slant Range Maps: These maps depict the raw deformation data as movements either away from or toward the satellite. Positive values refer to movements away (lengthening of wave travel distance) and negative values to movements towards the satellite (shortening of wave travel distance). The slant range data provides important information as to the style of movement and also indications of data decorrelation, which may be indicative of either ground movements that exceed one wavelength ($\sim 6\,cm$) or where the ground surface has changed sufficiently between the satellite passes perhaps due to agricultural activity on the uplands.
2 Horizontal Flow Line Maps: These maps take the slant range data and, for simplicity, resolve it into the direction of the slope surface, assuming that movements are in the direction of the fall line of the slope. These movements are then represented as absolute downslope deformation values. As most movements are not purely in a downslope direction, this assumption will never be totally correct but provides a reasonable depiction to assist in overall zonation of landslide hazards. Figure 6 provides a schematic for the geometric simplification utilized to obtain the flow line data.
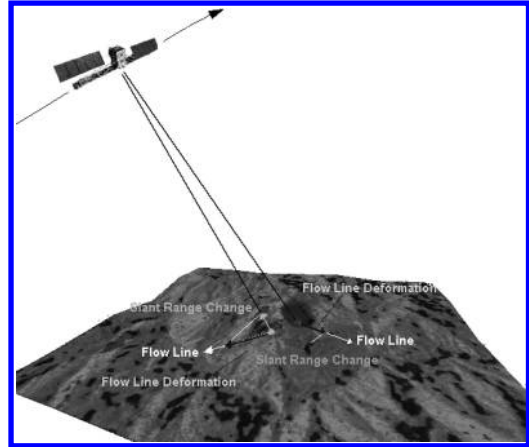
Figure 6. Schematic of the geometric consideration for determination of flow line deformation in relation to slant range deformation.

Although the flow line data have the advantage of providing data resolved into the direction of movement and therefore are more easily compared to conventional means of monitoring there are some limitations to this data. As available satellite digital elevation models (DEM) with a 10 metre resolution are often utilized to generate the flow line data subtle feature on the slope may be averaged out during the flow line calculation. For slowly moving landslides, subtle changes associated with differing zones of movement may then be averaged and not be apparent in the flow line product but show up in the slant range deformation map. Figure 7 provides an example for the Mile 55.3 area of the Ashcroft corridor.

5 CONCLUSIONS

In many of the areas that were reviewed as part of this study, there were ongoing visual observations of deformation, and in some cases, actual deformation data available. In many cases, the InSAR data detected centimetre level movement over the time periods assessed that may not be detectable using visual methods. Kosar et al. (2003) have documented the use of InSAR to detect movements within Central British Columbia along the Fraser River in which deformations associated with a highway and railway alignment that were initially not visually observed were subsequently confirmed after completing a follow up field check. Overall the deformations observed over the seven year time frame were consistent with either physical observations or monitoring data over that time frame.
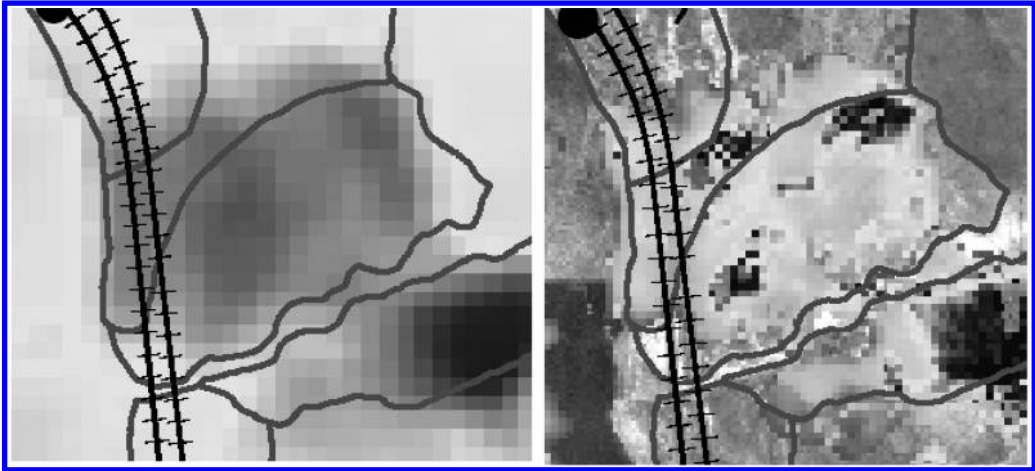
Figure 7. Slant range (left) and flow line (right) data from the Mile 55.3 (left bank) area. The slant range data shows zones of deformation consistent with observations of deep seated retrogressive landsliding while topographic simplifications in the flow line data do not provide the same subtleties as to the style of movement.

The current project involved the application of InSAR as a tool for screening of slope movements along an eight mile transportation corridor in order to provide CN Rail with additional information on which to plan further field assessment and investigation as part of their overall risk management framework to mitigate the impacts of large scale landsliding on their rail line in this area. Caution should be used in utilizing InSAR as a specific monitoring tool to replicate and replace existing slope instrumentation. Rather it should be utilized to supplement existing information to provide a better overall understanding of the extent and style of movements for slow, complex landslides.

For example in the specific case of large high mobility earth slides, such as those encountered along the Ashcroft corridor, although there are limited records of railway losses from these types of ground hazards they are known to have the potential to result in catastrophic failure of the track roadbed and thus warrant attention. Although some research is already underway on the large compound earth slides south of Ashcroft area future work may include researching the utility of using the results of the InSAR surveys to investigate, characterize and monitor these types of complex ground hazards.

REFERENCES

AMEC Earth & Environmental 2004. Ashcroft Subdivision Miles 50–57 InSAR Deformation Assessment, Thompson River Valley, British Columbia. Prepared for CN Rail, dated November 2004. AMEC Project No. EG09133.

Atlantis Scientific Inc. 2004. InSAR Subsidence Monitoring: Deformation Mapping, Ashcroft. Prepared for AMEC Earth & Environmental. June 7, 2004. ASI File 2004-04-0019.

Clague, J.J. & Evans, S.G. 2003. Geologic Framework of Large Historic Landslides in Thompson River Valley, British Columbia. *Environmental and Engineering Geoscience* 9: 201–212.

Froese, C.R., Kosar, K. & van der Kooij, M. 2004. Advances in the Application of InSAR to Complex, Slowly Moving Landslides in Dry and Vegetated Terrain. Invited Lecture. Proceedings of the 9th International Landslide Symposium. Rio de Janeiro, Brazil. Balkema, Netherlands. pp. 1255–1264.

Keegan, T., Abbott, B., Cruden, D.M., Bruce, I. & Pritchard, M. 2003. Railway Ground Hazard Risk Scenario: River Erosion: Earth Slide. Proceedings of the Third Canadian Conference on Geotechnique and Natural Hazards, pp. 234–242.

Kosar, K., Revering, K., Keegan, T., Black, K. & Stewart I. 2003. The Use of Spaceborne InSAR to Characterize Ground Movements Along a Rail Corridor and Open Pit Mine. Proceedings of the 3rd Canadian Conference on Geotechnique and Natural Hazards Edmonton, Alberta.

Porter, M.J., Savigny, KW., Keegan, T.R., Bunce, C.M. & MacKay, C. 2001. Controls on Stability of the Thompson River Landslides. Proceedings of the 55th Canadian Geotechnical Conference, pp. 1393–1400.

Landslide Risk Management – Hungr, Fell, Couture & Eberhardt (eds)
© 2005 Taylor & Francis Group, London, ISBN 04 1538 043 X

Application of a landslide risk management system to the Saskatchewan highway network

A.J. Kelly & A.W. Clifton
Clifton Associates Ltd., Regina, Saskatchewan, Canada

P.J. Antunes & R.A. Widger
Saskatchewan Highways & Transportation, Regina, Saskatchewan, Canada

ABSTRACT: Saskatchewan Highways and Transportation (SHT) required a landslide risk management system to prioritize sites for monitoring and remediation and provide recommended response levels based upon risk level. In 2003, SHT took the first step in landslide management by implementing a landslide risk management system based upon the Alberta Transportation model. Risk in the landslide model was evaluated by defining the likelihood of landslide occurrence or probability factor (PF) and consequences of a landslide or consequent factor (CF). The resultant of the two factors provided a numerical assessment of risk which could be ranked and categorized for response levels and management approach. SHT identified 69 sites in the provincial road network for risk assessment. An expert panel met to assign PF and CF for each site. The sites were assigned a response level of urgent, priority, routine or inactive based upon the risk level. A management approach for inspection, monitoring and investigation was provided for each site based upon the response level. An overview of the risk management system and its application to landslides near Shaunavon and Prince Albert, Saskatchewan are provided. Details of the subsequent slope stability investigations and analysis are included.

1 INTRODUCTION

Saskatchewan Highways and Transportation (SHT) have investigated landslides and their impact upon the transportation network since the 1960's. Early investigations centred around bridge site selection programs on the North Saskatchewan River. The first designed monitoring program was implemented in conjunction with remedial works at the newly opened North Battleford Bridge in 1967. Since that time, the number of unstable sites investigated and monitored has progressively increased. The technical capabilities of investigating and monitoring landslides has increased accordingly; however, the methodologies for assessing the level of hazards and investment strategies has not evolved at the same pace.

2 GEOHAZARD CLASSIFICATION

The interaction of natural forces with the highway system often results in hazards to the motorist or to the physical assets of the transportation system. Hazards can be subdivided into geotechnical hazards and landslide hazards.

SHT routinely deals with a variety of geotechnical hazards during the operation of the highway system.

Erosion, settlement and soil-structure interaction phenomena are examples of geotechnical hazards. Landslide hazards include the mass movement of soil downslope in sufficient volume that it modifies, or may modify the lines and grades of the roadway and may potentially impact motorist safety or operation of the highway. Landslide hazards involve natural and engineered slopes.

SHT was interested in moving towards a comprehensive risk-based system for prioritizing and managing geotechnical and landslide hazards on the Saskatchewan highway transportation network. Partial implementation of this system began in 2003 with the development of a landslide management system, (Clifton Associates Ltd. 2003). This paper discusses the implementation of the landslide management system.

3 LANDSLIDE MANAGEMENT SYSTEM

3.1 *Introduction*

Modern landslide management practices require the ability to:

1 Assess the degree of hazard that may be associated with unstable sites;

571

Table 1. Probability factors (PF).

PF	Natural slope	Engineered slopes
1	Geologically Stable. Very low probability of landslide occurrence.	F > 1.5 on basis of effective stress analysis with calibrated data and model*. Historically stable. Very low probability of landslide.
3	Inactive, apparently stable slope. Low probability of landslide occurrence or remobilization.	1.5 > F > 1.3 on basis of effective stress analysis with calibrated data and model. Historically stable. Low probability of landslide.
5	Inactive landslide with moderate probability of remobilization. Moderate uncertainty level; or, active slope with very slow constant rate of movement; or, indeterminate movement pattern.	1.3 > F > 1.2 on basis of effective stress analysis with calibrated data and model. Minor signs of visible movement. Moderate probability of landslide.
7	Inactive landslide with high probability of remobilization, or additional hazards present. Uncertainty level high. Perceptible movement rate with defined zones of movement.	1.2 > F > 1.1. on basis of effective stress analysis with calibrated data and model. Perceptible signs of movement, or additional hazards present. High probability of landslide.
9	Active landslide with moderate, steady or decreasing rate of movement in defined shear zone.	F < 1.1 on basis of effective stress analysis with calibrated data and model. Obvious signs of ongoing slow to moderate movement.
11	Active landslide with moderate, increasing rate of movement.	Active landslide with moderate, increasing rate of movement.
13	Active landslide with high rate of movement at steady or increasing rate.	Active landslide with high rate of movement at steady or increasing rate.
15	Active landslide with high rate of movement with additional hazards**.	Active landslide with high rate of movement with additional hazards.
20	Catastrophic landslide is occurring.	Catastrophic landslide is occurring.

Notes:
* If the described conditions for slope analysis are unknown or not met, increase the PF by one category, e.g. if quality of data used in analysis is not known, increase PF from 1 to 3. F = Factor of Safety.
** Additional hazards are factors which can greatly increase the rate of movement, e.g. eroding toe, groundwater, etc.

2 Evaluate the need for ongoing monitoring and inspection;
3 Provide for early warning or emergency response where public safety concerns warrant; and,
4 Establish priorities for investment of resources.

The methodology for landslide management incorporates a risk-based approach, mandating expenditures and efforts in proportion to the level of hazard and potential consequences of failure.

3.2 *System selection*

Other agencies are addressing the natural hazard management issue. A well documented, peer reviewed descriptive system suitable for application to Saskatchewan conditions are readily available to support the development of a landslide management system. The Alberta Transportation Landslide Management System was used as an initial template since it was currently in use and could be readily modified for a Saskatchewan application (Alberta Transportation, unpubl).

3.3 *Assessment of risk*

The basis of evaluating risk by Alberta Transportation is defined by:

$$R = PF \times CF \tag{1}$$

where R = risk; PF = probability factor; and CF = consequence factor.

The PF reflects the likelihood of a landslide occurring in the life of the structure as assessed by a qualified geotechnical engineer. The PF is not annualized. A modified 20 point PF scale from Alberta Transportation was used. The main modification was the differentiation of slope instability between natural and engineered slopes. The distinguishing feature between instability in a natural and engineered slope is based on the shear plane. In a natural landslide, the shear plane existed in the subsurface before the engineered construction took place. In an engineered slope, the landslide occurred on constructed slopes in terrain previously assessed to be stable. Table 1 shows the PF factor criteria.

Table 2. Consequence factors (CF).

CF	Typical consequences
1	Shallow cut slopes where slide may spill into ditches or fills where slide does not impact pavement to driver safety, maintenance issue.
2	Moderate fills and cuts, not including bridge approach fill or headslopes, loss of portion of the roadway or slide onto road possible, small volume. Shallow fills where private land, water bodies or structures may be impacted. Slides affecting use of roadways and safety of motorists, but not requiring closure of the roadway. Potential rock fall hazard sites.
4	Fills and cuts associated with bridges, intersectional treatments, culverts and other structures, high fills, deep cuts, historic rock fall hazard areas. Sites where partial closure of the road or significant detours would be a direct and avoidable result of a slide occurrence.
6	Sites where closure of the road would be a direct and unavoidable result of a slide occurrence.
10	Sites where the safety of public and significant loss of infrastructure facilities (such as a bridge abutment) or privately owned structures will occur if a slide occurs. Sites where rapid mobilization of a large-scale slide is possible.
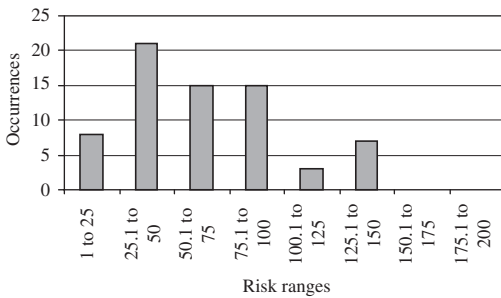
Figure 1. Summary of risk level assessment.

Figure 2. Summary of response levels.

The CF is the consequence of the landslide on transportation infrastructure or driver safety. CF is chosen with public safety, road closure and loss of infrastructure as criteria. Roadway traffic volume and classification is considered as part of the consequence on public safety and infrastructure. The ten point Alberta CF was adopted with only minor modifications. Table 2 shows the CF criteria.

3.4 *Ranking of risk levels*

An expert panel familiar with the 69 sites monitored by SHT met to assign PF and CF for each site. PF and CF were assigned independently by each panel member and the mean Risk Level calculated on the basis of these ratings. The resulting range of risk varied from 1.0 to 160.0 for the 69 sites. The risk values were grouped into six ranges and plotted in Figure 1.

3.5 *Response levels*

Response levels of urgent, priority, routine and inactive were created based upon the risk level. The level of response varies according to the calculated Risk Level for each site. As new sites are added, their response level is classified as urgent, regardless of their calculated risk level, until three years of spring and fall monitoring are completed to characterize the sites. The distribution of sites in the various response levels is indicated in Figure 2. The Risk Level, number of sites, response level and corresponding management approach is included in Table 3.

4 INSPECTION TOUR

Initial inspections of all 69 sites were conducted in Fall 2004 by the expert panel to confirm the risk level for each site. Inspection reports were completed and recommendations for further investigations were provided. Figures 3a,b show an example inspection report with photographs for the Frenchman River Valley south cut, Control Section (CS) 37-02.

The assignment of risk to a site is dependent upon knowledge of the site conditions; therefore, having the expert panel take part in the inspections

Table 3. Recommended response levels and management approach for landslide sites.

Risk level	Number of sites	Response level	Management approach
>125	4	Urgent	Inspect at least once per year. Monitor instrumentation at least twice per year in the spring and fall. Investigate and evaluate mitigation measures.
75 to 125	10	Priority	Inspect once per year. Monitor instrumentation at least once per year.
27.5 to 75	21	Routine	Inspect every 3 years. Monitor instrumentation at least every 3 years with an increased frequency for selected sites as required
<27.5	11	Inactive	No set instrumentation monitoring or inspection schedule. Monitored and inspected as required in response to maintenance requests

provided a more accurate assessment of Risk Level and allowed for a timelier implementation of the appropriate management approaches. Geotechnical hazards such as erosion and seepage were added to the landslide hazard inspections because of the role they play in landslides.

5 APPLICATION OF THE LANDSLIDE RISK MANAGEMENT SYSTEM – CASE STUDIES

5.1 Introduction

Two landslide case studies are presented to show the application of the landslide risk management system. The landslide at the Frenchman River Valley, approximately 35 km south of Shaunavon in southwest Saskatchewan, was the reactivation of a previously unknown landslide while the landslide at Prince Albert. Saskatchewan was a known landslide which was rated as routine with a risk level of 54. The risk level at the Prince Albert landslide was re-assessed after the landslide became more active.

5.2 Frenchman River Valley landslide

In the fall of 2003, a landslide was reactivated during realignment of Highway 37 (CS 37-02) on the south wall of the Frenchman River Valley, Figure 4. A large fill section was placed immediately west of the existing road, resulting in a head scarp which dropped 150 m of the existing highway by 100 mm over a period of a few days.

A risk assessment was conducted to determine the recommended management approach. The PF for the landslide was 15 because of rapid movement and additional hazards from creek toe erosion. The CF was 10 because there was a public safety issue and the

possibility of significant loss of infrastructure. The resulting Risk Level was 150, which fell in the urgent response level category.

Immediate action was taken to detour traffic around the landslide and halt construction of the fill section. An airphoto assessment of the site indicated there were three landslide blocks below the existing road, Figure 4, and a block above the existing road. The existing road was in a cut section between two blocks.

A stratigraphic drilling and instrumentation program was undertaken to determine remedial options. Seven slope inclinometers were installed to depths ranging from 30 m on the lower landslide block to 55 m in the block above the existing road. Four pneumatic piezometer nests with two to three piezometers each were installed adjacent to select slope inclinometers.

Inclinometer readings indicated movement between elevations 885 m to 895 m along a bentonitic rich zone within marine shale. The rate of movement progressively increased from 0.3 mm/day in the lower block (SI6) to 0.9 mm/day in the upper block (SI3/SI203). The block above the road (SI7) did not appear to be moving. The rates of movement indicated the lower and middle blocks were moving independently from the upper block which was loaded with the road fill.

The stratigraphy, porewater pressures, laboratory testing and depth of movement were used in conjunction with a digital terrain model to conduct 2- and 3-D slope stability modelling. Results of stability modelling indicated the location of the landslide toe was very sensitive to minor changes in the stability model, Figures 5 and 6. The stability modelling also showed the extent of the critical failure did not extend back into the road fill which was believed to have reactivated the landslide. The stability model confirmed the upper block was moving independently from the lower and middle blocks.

574

SITE INSPECTION FORM

CONTROL SECTION AND LOCATION 37-02 Frenchman South Cut	PREVIOUS INSPECTION DATE	INSPECTION DATE AND TIME DATE: 20 Sept 2004 FROM:16:40 TO:17:30		
LEGAL DESCRIPTION	NAD 83 COORDINATES Zone:12 N5466761 E687744 H936	RISK ASSESSMENT PF:12 CF:10 TOTAL:120	WEATHER Clear, windy	

	INSPECTED BY:
SUMMARY OF SITE INSTRUMENTATION: SI7: minor movement to the west direction at approximate elevations 886 m and 929 m. SI203: minor movement to the west direction at elevation 922.5 m. SI8: Movement to the west direction at elevation 904 m, decreased rate of movement. SI102: Movement to southwest direction at elevation 899 m. LAST READING DATE: 15 Sept 2004	Jorge Antunes Dennis Klimochko George Put Allen Kelly Hung Vu

PRIMARY SITE ISSUE:

APPROXIMATE DIMENSIONS:

DATE OF REMEDIAL ACTION:

ITEM	CONDITION EXISTS		DESCRIPTION AND LOCATION	NOTICABLE CHANGE FROM LAST INSPECTION	
	YES	NO		YES	NO
Pavement Distress					
Slope Movement					
Erosion	Y		Photos 371, 372, 377.		
Seepage					
Culvert Distress					

OBSERVATIONS AND COMMENTS

18 in. CSP culvert across slope. Armoured south ditch was short on culvert place (Photo 371); erosion has started. Erosion has also started on west ditch, which was not armoured (Photo 372). Erosion channels (0.5 m wide, 0.3 – 0.5 m depth) were found on west ditch (Photo 377).

RECOMMENDATIONS

Provide erosion protection for the above-identified area.

Response level: priority

Figure 3a.   Inspection form.

Remediation considered berming and unloading of the slope. Berming of the toe was believed to be too risky because of the sensitivity of the toe location and the possibility that berming could activate landslides further down the valley wall. The upper block appeared to be moving independently from the other blocks; therefore, the remedial focus was on the upper block. The alignment of the road through the landslide was revisited to shift the highway into further cut above the existing road and off the landslide. In addition the large

HPIM0371 2004-09-20 Missing armoured section at culvert inlet, erosion has started.

HPIM0372 2004-09-20 West ditch at grade point, no armoured ditch, erosion has started.

HPIM0377 2004-09-20 Erosion problem on west embankment face of the fill section.
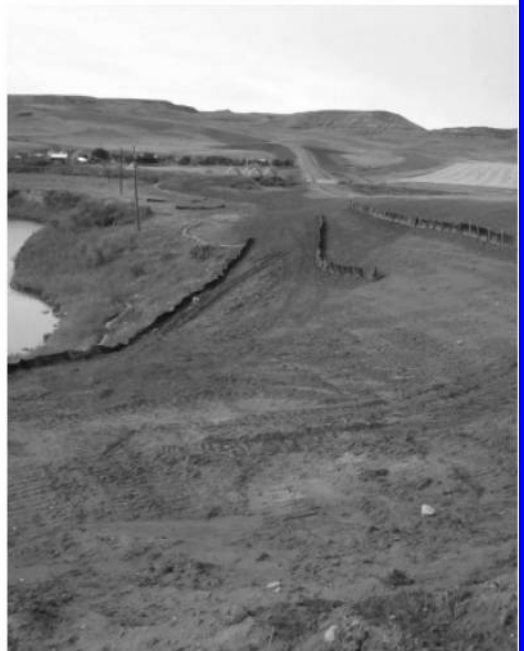
HPIM0381 2004-09-20 Erosion protection on the west fill by the bible camp approach.

Figure 3b.   Inspection photographs.

576

Figure 4.   Approximate location of landslide and slope inclinometers at Frenchman River Valley.
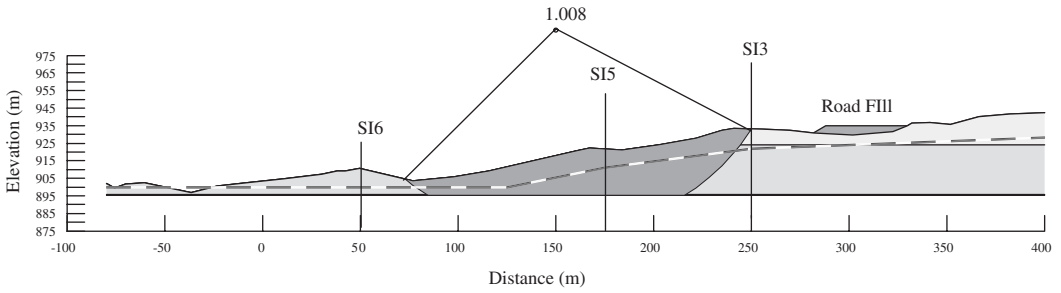
Figure 5.   Slope stability of middle block.
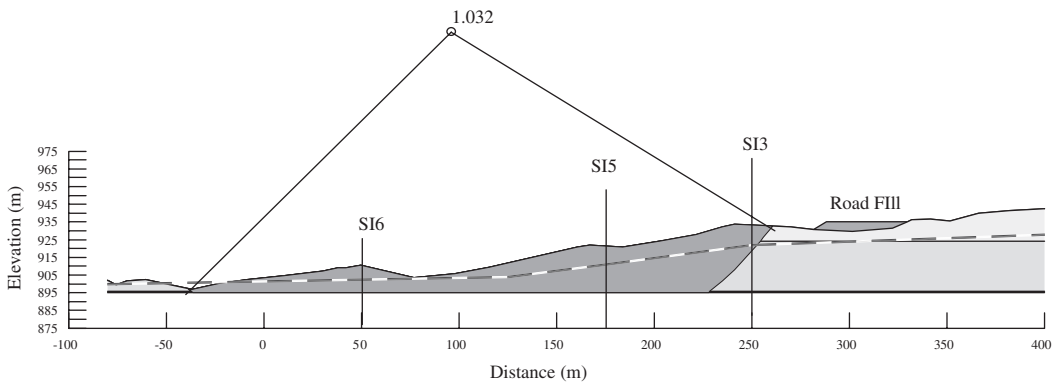
Figure 6.   Slope stability of lower and middle block.

577
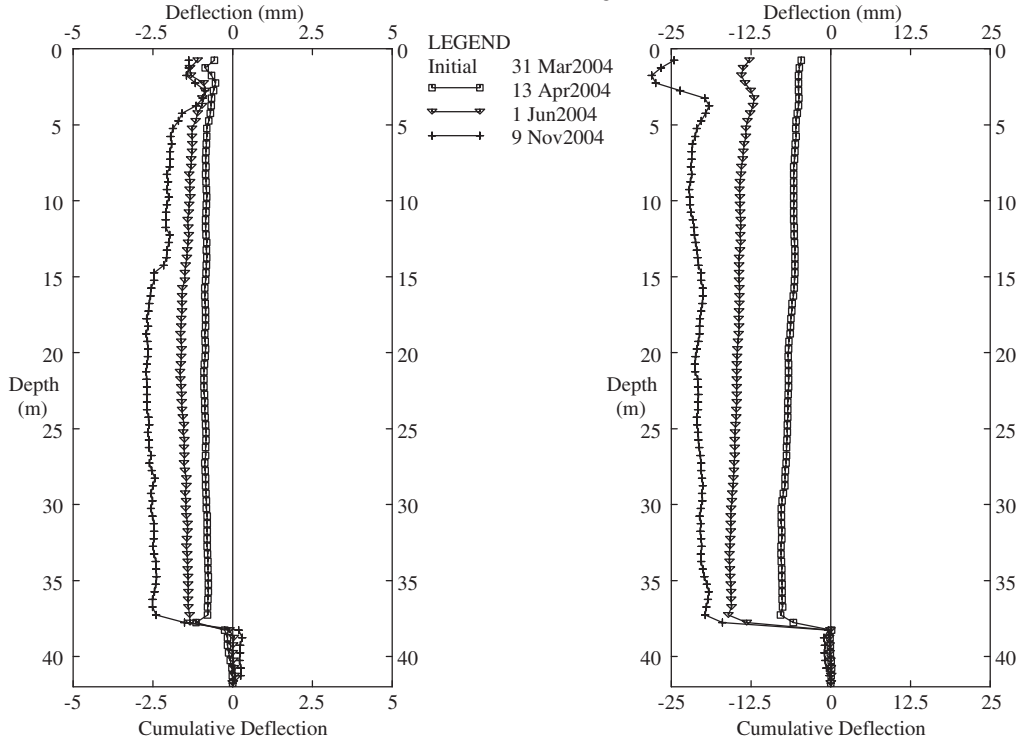
Figure 7. Movement of upper block as indicated by SI203.

fill was removed to return the lower and middle blocks to preconstruction conditions, preventing retrogression of the landslide back into the new highway alignment. Figure 7 shows movement in the upper block (SI203) dropped to minor creep after the large fill was removed between the 06 and 20 May 2004.

5.3 *Prince Albert Penitentiary landslides*

Two landslides approximately 3.5 km and 4.5 km west of the Saskatchewan Penitentiary at Prince Albert are impacting Highway 302 (CS 302-02), Figure 8. The highway is located adjacent the North Saskatchewan River which is actively eroding its river bank, resulting in large retrogressive failures, Figure 9. There are three distinct slump blocks between the highway and the river bank. Locally, there is groundwater discharge along the river bank in the two landslide areas which contributes to the instability of the river bank. The first failure at 3.5 km west has affected the north shoulder, but the west bound lane is in good condition. The length of the failure at the highway right-of-way was 110 m and the vertical displacement in the sideslope of the highway embankment was 230 mm. The highway

at this location is a fill section constructed over the edge of the most southerly landslide block. Erosion of the riverbank has triggered the most recent movement of the fill section.

The second failure at 4.5 km west affects a fill section constructed over a drainage channel. A fourth slump block was forming which crossed the highway into the upslope ditch. The landslide was estimated to be approximately 180 m long along the south shoulder of the highway. A dip in the highway at the west extent of the landslide was evident and signed by SHT.

A risk assessment of the first failure determined the landslide along the north shoulder did not pose an immediate danger to the highway; however, regular inspections and a slope inclinometer were recommended to monitor future movement. The landslide was assigned a PF of 15 because the landslide was active at a high rate of movement with additional hazards such as toe erosion and groundwater discharge on the river bank. A CF of 5 was assigned because a partial road closure may be a result. The risk level was 75 which is at the boundary of a routine and priority site.

A risk assessment of the second failure indicated the failure posed a greater risk to the road and

Figure 8. Prince Albert Highway 302 landslide extents. Landslide at bottom left is 4.5 km from penitentiary.

Figure 9. Active erosion along north saskatchewan river bank.

public safety. A PF of 15 was assigned to the landslide for the aforementioned reasons of the first failure. A CF of 10 was used because of the risk of road closure and a public safety issue in the event of a sudden large movement. The resulting risk level was 150 which classified the landslide as urgent. Daily inspections and additional instrumentation were recommended.

A slope inclinometer was already in place along the east edge of the landslide above the third slump block;

however, another slope inclinometer and a pneumatic piezometer nest were installed in the third slump block immediately below the landslide. The investigation of remedial options is ongoing.

6   CONCLUSIONS

The landslide risk management system was successfully applied to the Saskatchewan highway network. Risk assessments were used to rank 69 sites and allocate appropriate resources for monitoring and investigation.

REFERENCES

Alberta Transportation. Attachment 1 – Risk Level, Project Site Documentation Binder Contents. Alberta Transportation Geotechnical and Erosion Guides, Geotechnical Reference Materials.

Clifton Associates Ltd. 2003. Risk Management System for Landslide Sites in Saskatchewan. Consultants report prepared for SHT, File No. R3392, 12 September 2003.

Computers, cables and collections: digital field data collection for GIS support of landslide mapping along railroad corridors

R. Harrap
Queen's University GIS Laboratory, Kingston, Ontario, Canada

C. Sheriff & J. Hutchinson
Dept. Geological Sciences and Geological Engineering, Queen's University, Kingston, Ontario, Canada

ABSTRACT: Field data collection systems, which incorporate GPS receivers, personal-digital-assistant (PDA) computers, and Geographic Information System (GIS) software, allow field data to be collected in a structured fashion and at a consistent level of detail across a project. Unfortunately, these systems often collect the wrong data in the wrong fashion; this results from software being designed with little attention to the needs and users. Software designers are typically not well versed in GIS, are even less likely to understand geotechnical engineering, and rarely have an appreciation for who will actually use the data and for what purpose. A user-centered design methodology addresses these issues. Herein we discuss the design of systems to support geotechnical mapping along railway corridors. The methods have revealed that understanding workflow, the path that information takes through an organization, is vital to designing a tool that is useable by geotechnical engineers and helps, rather than hinders, their daily work.

1 INTRODUCTION

Geotechnical engineering is rooted in the collection of field data. The advent of mainframe computers in the 1960's, workstations in the 1970's, desktop computers in the 1980's, and notebook computers in the 1990's profoundly changed the laboratory and office component of engineering, bringing numerical simulation methods first into the academic setting and later into many consulting offices. Corresponding advances in computer aided design (CAD) tools led to the widespread use of electronic drafting to prepare site plans, illustrate reports, and analyze field data. The transition to Geographic Information Systems (GIS), computer cartography tools that combine the drawing and illustration power of CAD with the analytical and archiving power of databases, has led to even greater degrees of automation, analytical tool use, and information sharing based on computer technology. This transition is by no means complete; most geotechnical engineers use GIS in at most a limited way, reflecting both the unfortunate complexity of these tools and the relative paucity of specialized geotechnical tool components (often called extensions) for industry-leading GIS software tools.

Since the early 1990's, computers have also become available as hand-held devices that combine the functionality of a notepad and a limited database.

Personal digital assistants, or PDA's, became widespread in the late 1990's and are now virtually ubiquitous in the business world, where they combine the functionality of the rotary index, telephone list, e-mail client, and in some cases, camera and telephone. PDA tools, limited by the screen size, the modest processing power and the limited storage capacity of these devices, have been slow to move into the field support environment, although in fact these devices seem ideally suited for this task. The availability of GIS and related database tools on recent PDA platforms presents an opportunity to move computer support for geotechnical engineering into the field.

In order for this to happen, a number of related issues, which for the most part reflect the underlying structure of the information to be collected, need to be addressed. GIS and PDA tools are open-ended in that far more can be done with these than is needed for geotechnical engineering. There is a danger that field data collection tools based on GIS and PDA technology will not address the actual needs of the user community – namely, geotechnical engineers faced with specific tasks – but instead will reflect the needs *as perceived* by the system designers. This reflects the diversity of skills needed to implement field data collection: most geotechnical engineers lack the specialized programming skills to merge GIS, Global Positioning System

581

tools, and PDA software to build an effective system. Most system designers lack the technical knowledge of geotechnical engineering to understand the foundational issues in field data collection, and essentially all lack the specific, task-oriented focus to understand the context for a specific tool deployment.

In this study, we address this issue of matching the needs of users to the design constraints of system engineers. The context is more specific than geotechnical engineering: we address the collection of field data along railway corridors to constrain hazard mapping, communication of results, and hazard mitigation. Using methods developed in the area of human-computer interaction and usability engineering, we show how iterative, user-centered design can lead to the development of effective handheld field data collection systems for geotechnical engineering.

2 TECHNICAL FOCUS AND BACKGROUND

In brief, there are two domains that provide background to this design study: GIS plus GPS plus PDA, on the one hand, and geotechnical field practice, on the other. We will focus on the first component, assuming the audience for this paper is familiar with geotechnical engineering practice.

2.1 Handheld technology primer

The three hardware and software components of a field data collection system are the PDA itself, the use of a Global Positioning System receiver to determine position, and the GIS software used for data collection, integration, archiving, and communication. These are summarized briefly below.

2.1.1 Personal digital assistant (PDA) units
PDA units, as discussed above, are relatively small handheld computers intended to be used by business executives to manage moment-to-moment information. The context of the design of the hardware and software of these units, then, is that they will be used in an office or other built environment, with relatively easy access to power, other computing devices, and the Internet. Most PDA units are intended to be paired with a notebook or desktop computer; in this process information is mirrored between the PDA and the larger computer in order to move data and programs onto the PDA prior to use, and to move data (notes, addresses, and the like) off of the PDA.

A second common characteristic of PDA units is that most lack a keyboard, and support interaction with a limited number of buttons and a stylus that is used to draw or write onto the touch-sensitive surface of the unit. This form of direct interaction is useful for sketching, filling out forms, and the like.

Most PDA units will operate for between 4 and 12 hours between recharges, and most store between 8Mb and 256Mb of local information. Many have a port that allows additional memory or secondary devices (such as GPS, discussed below) to be added. Finally, most PDA units are neither rugged nor waterproof.

PDA software environments are not strictly compatible with desktop computers; though data may be shared, software for desktop computers will not function on a PDA and vice versa. In many cases, PDA versions of software packages, designed to operate in the limited world of PDA hardware, are available. The process of pairing the PDA to a larger computer both allows such software to be loaded and data to be transferred.

2.1.2 Global Positioning System (GPS)
The Global Positioning System (GPS) uses a collection of satellites in orbit to provide positioning information to mobile units (c.f. El-Rabbany, 2002). The determination of location is based on the highly accurate timing of signals from a number of well-distributed satellites and a ground station. In practice, additional satellites are used to constrain the time at the receiver to avoid incurring the cost of a precise clock in each handheld unit. With most recent systems operating in North America, correction signals for satellite drift and weather effects are transmitted by a second tier of satellites, and as a result 1–3 meter accuracy can be achieved with a unit costing a few hundred dollars. This is sufficient for most geotechnical applications; survey-grade GIS units also exist which are accurate at the centimeter scale.

GPS units are available both as discrete units with an interface and the ability to store a series of locations coded with a textual identifier, and simpler units that can be combined with a PDA or notebook computer to build an integrated system. These components are wired to the PDA or notebook, inserted into an expansion port, or linked via short-distance networking technologies such as the Bluetooth standard. The common limitation of all GPS units is relatively short battery life. Units physically coupled to a PDA have the significant disadvantages that they drain the PDA batteries quickly, and that the cables are prone to damage in realistic field conditions. Wireless units address these problems to a significant degree.

2.1.3 Geographic Information Systems (GIS)
Geographic Information Systems tools (c.f. Laurinin and Thompson 1992), as discussed above, combine tools for drawing, analyzing, communicating, and archiving maps with database technology to make this process efficient. GIS tools use two broad approaches for storing data: the vector approach treats the world as collections of points, lines, or polygons, and the raster approach treats the world as a regular array of cells much like the screen of a television or a digital

582

picture. These approaches reflect their heritage in digital cartography and remote sensing, respectively.

The vector approach is well suited to mapping discrete entities such as roads, utility lines, and rivers. Each unique item on the map is linked to a unique record in the database. In reality, this process operates in the reverse manner: features need to be discrete on the map if they are distinct in the database, and if they are physically distinct. The vector approach results in highly compact datasets, supports analysis such as 'what features are within a specified distance of what other features' and, since features can be drawn to the desired level of detail, typically produces appealing maps.

The raster approach, using regular cells instead of irregular geometric primitives, results in maps that have a fixed granularity. Increasing the granularity of the data by decreasing the cell dimensions dramatically increases the file size; typical raster data sets are orders of magnitude larger than their vector equivalents. Raster data, on the other hand, is much more appropriate for depicting phenomena that vary continuously through a region, such as air temperature, the elevation of a water table, or the distribution of pollutants. Finally, the raster approach is significantly more powerful for analysis where ranking is desired, since the cells can easily contain subjective or objective ranks, and overlaid rasters can be treated algebraically to construct overall expert-knowledge driven rankings that fuse multiple datasets elegantly.

2.1.4 *Integration issues*

From the perspective of PDA, GIS, and GPS integration for geotechnical fieldwork, some key points arise from the technical background:

1. Field data will likely be collected as discrete (vector) points, with the location being derived from GPS readings.
2. GPS readings may not always be available due to satellite geometry or obscuring terrain.
3. The PDA will need to host the GIS tool, showing raster data (such as air photographs) and vector data (such as infrastructure mapping) together. The size of raster images may be a significant issue if the field area is large.
4. GIS uses many datasets that will need to be paired between a host notebook or desktop computer and the PDA, especially if the PDA cannot hold data for an entire field region. Tracking datasets as they are transferred will be necessary.
5. PDA units are not particularly rugged. Destruction or disablement of a device may result in data loss or may interfere with a field project.

There are also issues that arise specifically from the nature of geological mapping – in particular, the nature of certainty, of geological boundary relationships, and of scale issues – but for the most part these affect more regional mapping rather than site reporting. These issues are discussed in detail in Schetselaar et al. (in press).

Over the life of a project, the efficiency garnered by gathering, analyzing, communicating, and archiving digital data warrants addressing these issues. One key observation from this is that field data collection using handheld computers may make little sense *to the individual engineer* while making perfect sense *to the organization*.

As introduced above, a significant problem with many attempts to integrate these tools with field data collection in the earth sciences has been that the persons designing and/or integrating the tool have little or no understanding of the field context, whether from a physical, scientific, or social context. As a result, tools that are poorly matched to the needs of the field engineer are the rule rather than the exception, and this only reinforces the resistance of field engineers to incorporating such devices in their work. Designing a system that not only meets the needs of the field worker but also matches the larger organizational scope of data collection is a significant challenge. We now address overall strategies for achieving this type of design coherence.

3 USER-CENTRED DESIGN PRACTICE

There are a number of software development strategies (c.f. Budgen 2003) that have been used over the last forty years. The most common method, which verges on being informal rather than a fixed process, is the waterfall approach, wherein a development is staged to flow in steps that are in a strict linear sequence. This has the advantage of replicating the natural order of completing a simple task (think – design – build – deploy) but the disadvantage that once a course is taken, no correction is included as part of the process.

A more adaptive method is the spiral approach, wherein a process cycles between reflection, design, building, and trial deployment phases, with the overall product becoming more refined but subject to mid-project corrections as feedback from trials is available. This is of course a far more reasonable process for ensuring that the end result is coherent, but there is still a flaw in the overall approach.

Both the waterfall and spiral approaches to design leave the question of understanding, consulting with, testing, and ultimately addressing the needs of the user to a secondary level at best. Especially in cases where the software developers have a limited grasp of the context of tool use – and field geotechnical engineering is a lot for a software developer in a big-city office to grasp – there is still the danger that the waterfall or spiral will start out so misaligned to what is actually needed that correction will be expensive or impossible.

583

In fact, in many development settings, once software is written, developers are reluctant to back away even if the code doesn't accomplish anything useful (Hunt & Thomas 2000).

An alternative suite of methods has come out of the information architecture (Wurman 2000), usability engineering (Carroll 2000, Cooper & Reimann 2003), and web usability (Krug 2000, Nielsen 2000) communities. These methods form the core of what this project in PDA – GIS integration for geotechnical engineering is about.

3.1 Personas methods

The first problem in designing for a client whose domain is significantly different than one's own is to understand the client. This includes their tasks, their background, their work context, and other technical details, but perhaps more importantly this includes their aspirations, attitudes, personality quirks, and the like. Though this might seem to focus on highly specific details of individuals, personalities and attitudes are sufficiently general that, given some investigation, broad commonalities within a user community appear.

This approach, pioneered by Alan Cooper and documented in Cooper & Reimann (2003), centers on the creation of user *personas*, personality summaries that capture the essential character of an individual or small group of individuals. Personas are captured through an anthropological process – usually, a combination of informal interviews and on-site observation – and refined over time until a coherent set of characteristics is found. In some cases, this will result in a suite of personas that capture different personalities relevant to a task, and in some cases there may be variants on individual task personas. The process may never be completely finished, but even an incomplete process is far better than no conception (in the designer's minds) of the personal context of the tools (for the users).

If personas fix the *people* involved into a framework and offer context for designers to use as part of design, *scenarios* provide the story or process description.

3.2 Scenario methods

Scenarios are stories about the use of a specific artifact (tool, software package, hardware device, and so on) in a specific context by a specific user. In other words, a scenario is a story about a personas using a tool. Scenarios, also known as use-cases, come largely from the work of John Carroll, and are documented in detail in Caroll (2000).

As with personas, scenarios are discovered through interviews, on-site observation, reflection, and refinement. Again, the process is largely human-centered, anthropological, and unlikely to ever be truly complete.

Unlike personas, which have a specific scale (that of the individual), scenarios can cover very large tasks, such as a complete field visit, or a very small task, such as a single measurement with a recording tool. The scale of the scenario is the scale of the tool being designed.

3.3 Integration of personas and scenarios

Together, the anthropologically-based persona and scenario tools provide a framework for understanding the user, the user's context, the physical context of tasks, the physical nature of a task, and how the task relates to other tasks. These together provide field system designers, who in most cases will have no real experience with field-based geotechnical engineering, with both a clear mandate on interviewing engineers and perhaps performing field visits and so capturing at least a portion of the engineering process first hand, and with a framing mechanism for then documenting this experience.

This general approach was used for the development of a field data collection framework for railway ground hazard monitoring. Although this project is ongoing, the remainder of this paper addresses how personas and scenarios have been used, the results to date, and some initial conclusions on the utility of these design and development tools.

4 RAILWAY GROUND HAZARD DESIGN PROCESS

The geotechnical context for this study is the support of field data collection activities along railway corridors by geotechnical engineers. This context includes, or subsumes, an understanding of how geotechnical fieldwork is done, who might be involved both pre- and post-a specific field visit, what infrastructure is available, and the like. The primary context, and the specific tool design context, is the collection of either an initial report of an on- or near-track hazard that might interfere or interact with train traffic.

There exists, in both Canadian National and Canadian Pacific Rail, set procedures for field data collection and reporting. The current practice is paper-based, with some use of later digital reporting. As such, the bounds of what needs to be collected were fairly well defined from the perspective of supporting the field engineers. Since the system would also be used for non-engineers making initial reports of problems, there is a more general tool scope that was less well defined at the start of the project.

4.1 Development of background material

The first step in building a set of personas and scenarios was to establish a base framework for the design. This involved inspection of existing field data collection

584

forms, informal discussions with engineers, and a cursory inspection of the literature on field data collection.

The dialogue between the designers is two-way, and we recognized early on that geotechnical engineers had little understanding of GIS technology, of the key limitations of the existing tools, and of the related GPS and PDA domains. To address this, the first step in the project was to prepare a comprehensive report (Harrap & Sheriff 2004) outlining all aspects of the field data collection domain.

In addition to providing background information, this report included some preliminary observations regarding scenarios and personas established through interviews with railway staff.

4.2 Development of initial personas

Initial personas for the field data collection tool centered on the persons actively involved in recognizing and reporting on railway ground hazards. In the first broad attempt, these included:

- geotechnical engineers
- assistant track maintenance supervisors
- geotechnical consultants and,
- regional managers

Following discussions with the staff, these personas were fleshed-out with supporting details to the point where they read like biographies; each one is approximately a page of text, provides broad technical scope and personal interests, and details personal attitudes towards information technology among other things.

Remember that these personas are generalizations intended to capture the human side of the anticipated human-computer interaction with a field data collection device. Of the personas given, only two (geotechnical engineers and assistant track maintenance supervisors) are supposed to actually use the system. In the case of the engineers, the system would be used for full data collection; in the case of the maintenance supervisors, it would be used for notification of features observed while working along the track. The attitudes of the supervisors to the technology are key, despite the fact that the amount of technical data reported in their case would be far less. This reflects the reality that there are many track maintenance supervisors – many eyes on the job – whereas there are relatively few geotechnical engineers. Bringing the observations of the assistant track maintenance supervisors to the attention of the geotechnical engineers is key, and this is obviously constrained by their willingness to actually *use* the system.

4.3 Development of initial scenarios

Initial scenarios developed, which revolved around the field data collection activities of the assistant track maintenance supervisors and especially the geotechnical engineers, centered on initial reporting and in-depth reporting, respectively. The context for these scenarios, which included both the 'day-scope' scale and the 'individual-observation-scope' scale, was reporting of a rockfall incident on or near the tracks. In principal, any geotechnical hazard could be treated as a broadly similar data collection scenario, though the details of the forms being used would vary.

The 'day-scope' scenarios served to set the overall relationship between the field worker and the field technology, or more properly, to highlight a daunting series of questions about this relationship. Perhaps the most persistent and perplexing was the tradeoff between a field data collection tool being used only as that, and it being also a generic computing and communication device. In other words, could an assistant track maintenance supervisor use a PDA for anything beyond reporting? If not, would it be simply too much to expect to keep it charged, uploaded with current information, downloaded when results exist, and so on? In the case of a field geotechnical engineer, would other tasks, such as report writing, be performed on the same device? What related information would the engineer need to see, such as CAD drawings, regional air photographs, reports, and the like? The tendency in both cases, highlighted when thinking *as the relevant persona* was to push for no device in the case of the track maintenance supervisor, and an unwieldy general purpose laptop in the case of the field engineer.

At the scope of individual data records, the scenarios highlighted the interaction between the data being collected and existing base or framework data, such as tracks (typically vector data) and photographs (raster data). The scenario also highlighted the interactive, richly multimedia nature of fieldwork, where sketching, photography, text capture, and numeric measurements all combine to provide a realistic picture of a setting. Especially in the context of the field geotechnical engineer, this highlights the issue of what physical device is being used: a PDA is easily handled, and can interact with other devices. A notebook computer, on the other hand, is unwieldy to use while walking in the field.

A final, cursory set of scenarios examined how the recorded data from assistant track management supervisors and field geotechnical engineers flowed through the organization. In other words, what happens to the data once it is collected? Who vets it? Who archives it? Initially we intended to downplay this aspect, but we quickly realized that this is in fact the link between the maintenance supervisor and the field engineer: the initial report of the one, results in a call for a field visit by the other.

4.4 Review process

The field data collection report, and the initial personas and scenarios, were circulated to the participating

geotechnical engineering staff at the railways. This process has been iterative, akin to the spiral model of development, in that before the draft field report was circulated we had circulated the broad personas and scenarios for comment, twice. Subsequent to publication of the draft report, we have made minor refinements to the process, but have concentrated on building an actual prototype on a PDA. This prototype is not intended for field use, but is simply a discussion piece to highlight some key issues with system design when working to refine the process with railway staff.

We must emphasize that this kind of prototype development, *with full willingness to abandon any or all of a prototype* is an essential part of the process we are following. As indicated above, a key problem in software development is that often, once code is written, the direction for a project is set. Our prototype was not intended to be a direction-setting exercise. In fact, as discussed above, our reservations about the different needs between assistant track maintenance supervisors and field geotechnical engineers had by this point made the key of the PDA exercise the demonstration that PDA technology might not be right for the field engineers' use for several reasons – chief among these was the issue of screen size. The small screen size of the PDA was simply insufficient to accommodate the suite of tasks and functions required by the geotechnical engineer.

4.5 *Initiation of phase 2 process*

Having built a prototype, a set of scenarios, a set of personas, and made preliminary findings on the field-based needs of the two key personas, we have initiated a second phase process. Based on preliminary findings, the second phase centers on the use of tablet PC computers either alongside or instead of PDAs. Tablet PC computers are transitional between PDA and notebooks: they are interacted with much like a PDA, but are also notebook-like in that they run a desktop operating system, have notebook-like processors, memory, and hard-disk storage, and can be easily used with a keyboard for 'traditional' computer use.

The test implementation of a tablet-based system, unlike the PDA prototype, will be deployed in a test in the field. The current context for this test is the collection of inspection reports on near-track beaver dams in eastern Canada. This work is ongoing at the time of writing.

5 DISCUSSION

The persona and scenario process described above and used in this project appears to be providing real and useful field constraints on the design process. It has been met with enthusiasm from the project partners, who appeared to recognize almost immediately the relevance of using this approach and have provided support, access, and attention to the iterative process of development.

The original scope of the project – to develop a field data collection system – did not explicitly include the office setting as part of the scope of scenarios, although the setting was included in the framing scope. In other words, we recognized that geotechnical engineers have 'lives' when not in the field, but didn't intend to document their activities as scenarios except in the field. However, it quickly became evident that, especially given the very real constraints of GIS discussed above, there is an important transition-to-field process and a transition-from-field process and that these together are vital in the development of a data collection tool. While this seems obvious in retrospect, the actual approach is not obvious: we did not simply expand our framework to include a to-field and from-field scenario.

Scenarios provide cross-sections of activities as stories. As such, they have limited temporal scope. A series of scenarios can be collected into a larger scenario, with larger temporal scope, but this larger scenario will tend to be much more general. In GIS, though, very specific details of data sets, their data model (vector or raster), their use in analysis, and their availability are vital at the longer time scale. These details have the tendency to become subsumed in long-time-scale, broad scenarios. To focus on these, we began to use a third framing mechanism to complement scenarios and personas: workflows. A workflow is a longitudinal (essential, temporal) path that follows a user through the completion of a broad task that may comprise office and field components, involve data collection and analysis, and incorporate decision making in settings such as team meetings. Alternatively, workflows can be constructed to show how data flows through an organization, how transformations happen, and how oversight might be accomplished.

Figure 1 shows an abstract representation of a generic workflow that encompasses the scenarios and
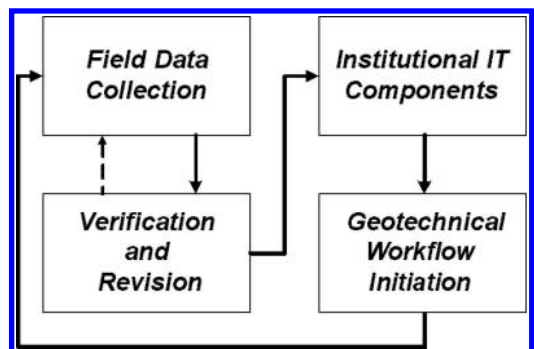

Figure 1. Abstract representation of railway ground hazards geotechnical field data collection.

personas developed in the railway ground hazards field data collection project. The figure is a generalization of a more detailed version that evolved with consultation with the participating railway geotechnical engineers and which we are now using as part of attempts to move the PDA-GPS-GIS system from prototype to field deployable tool, although as noted, using a tablet in place of the PDA.

Figure 2 shows the full workflow model, with individual decision elements identified. This is a highly speculative model, and as part of the current second-phase development cycle we are working with Canadian National Rail to refine this model.

6 CONCLUSIONS

The process of integrating Geographic Information Systems tools, Personal Digital Assistant computers, and Global Positioning System navigation techniques into a field-deployable data collection system involves both system engineering and a strong requirement to understand the field context of geotechnical engineering.

Through the use of techniques from usability engineering, and specifically persona and scenario based design, we have worked in collaboration with field engineers to develop a field data collection tool. We are now refining this design within a specific field context.

A key result of this work is that, given the complexity of GIS data and how it is used in large organizations, a data-flow centered workflow approach is very useful to constrain where data that is carried into the field comes from, and where field results go to, when a field visit is completed. We are refining our work through further development of workflows in consultation with our geotechnical engineering partners.
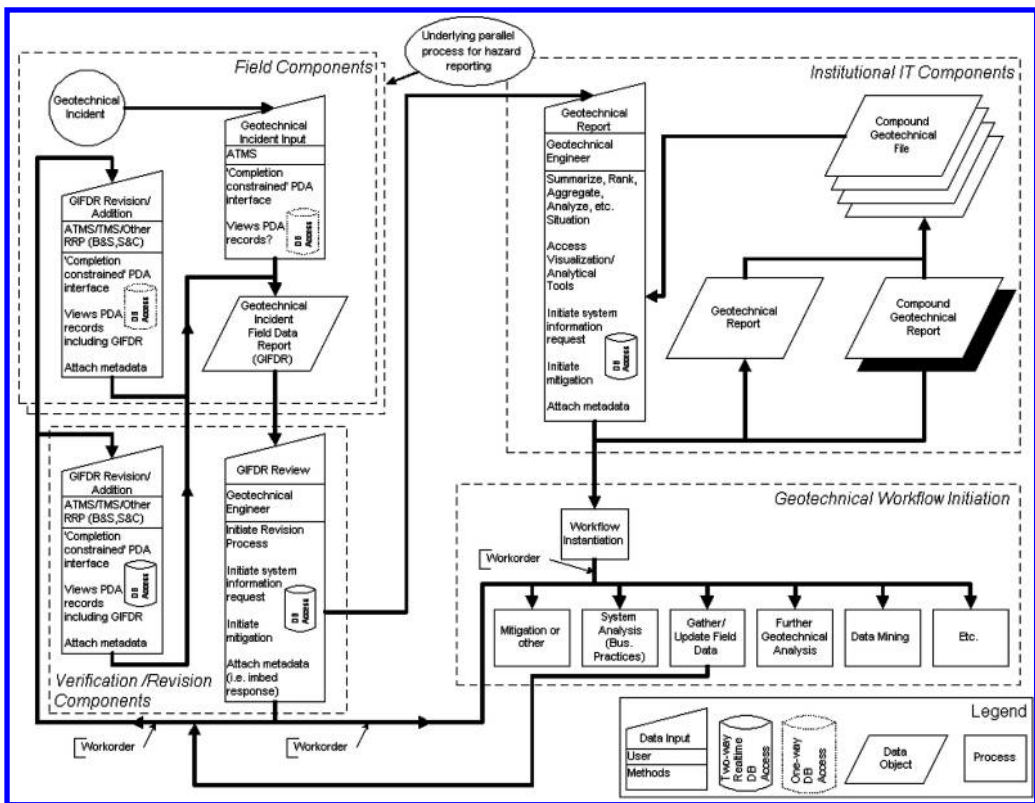
Figure 2. Detailed workflow representation for railway ground hazard geotechnical incident field data collection.

587

REFERENCES

Budgen, D. 2003. Software Design, 2ed. Pearson/Addison-Wesley, Harlowe, U.K., 468pp.

Carroll, J.M. 2000 Making Use: scenario-based design of human-computer interactions. MIT Press, Cambridge, Mass., 368pp.

Cooper, A. & Reimann, R.M. 2003. About Face 2.0: The Essentials of Interaction Design. John Wiley and Sons, New York, N.Y., 504pp.

El-Rabbany, A. 2002. Introduction to GPS: The Global Positioning System. Artech House, Inc., Norwood MA. 196pp.

Harrap, R. & Sheriff, C. 2004. Field Data Collection Systems for Railway Ground Hazard Research. Railway Ground Hazards Research Program – Queen's University GIS Laboratory Report, 106pp.

Hunt, A. & Thomas, D. 2000. The Pragmatic Programmer: From Journeyman to Master. Addison-Wesley, 321pp.

Krug, S. 2000. Don't Make Me Think: A Common Senses Approach to Web Usability. Que Books, Indianapolis, Ind., 195pp.

Laurini, R. & Thompson, D. 1992. Fundamentals of Spatial Information Systems. Academic Press, London, U.K. 680pp.

Nielson, J. 2000. Designing Web Usability. New Riders Press, Berkeley, Cal., 432pp

Rengers, N., Hack, R., Huisman, M., Slob, S. & Zigterman, W. 2002. Information technology applied to engineering geology. Keynote presentation, in J.L van Rooy, C.A. Jermy, eds., Engineering Geology for Developing Countries – Proceedings of the 9th Congress of the International Association for Engineering Geology and the Environment, Durban, South Africa, 16–20 September 2002.

Schetselaar, E.M., Harrap, R. & Brodaric, B. (in press). Digital Capture of Geological Field Data: Bridging the Gap Between a Mapping Heritage and Modern Digital Methods. in Harris, J. ed., Geological Association of Canada Special Volume on Geographic Information Science, to be published 2005.

Wurman, R.S. 2000. Information Anxiety 2. Que Books, Indianapolis, Ind., 350pp.

Application of quantitative risk assessment to the Lawrence Hargrave Drive Project, New South Wales, Australia

R.A.Wilson, A.T. Moon & M. Hendrickx
Coffey Geosciences Pty Ltd, Australia

I.E. Stewart
Road and Traffic Authority, NSW, Australia

ABSTRACT: Lawrence Hargrave Drive between Coalcliff and Clifton, New South Wales has been constructed near the base of a 330 m high coastal escarpment which has been oversteepened by marine erosion. The escarpment, consisting cliffs and intervening steep slopes, is affected by many rock falls, debris slides and debris flows. For safety reasons, the road has been closed and the design solution needs to reduce the annual probability of death from about 10^{-2} to about 10^{-5}. A quantitative risk assessment (QRA) based on landslide process rate models and using an Excel workbook was used to review the slope risks associated with the existing road and to assess the effectiveness of the proposed engineering works. Such approaches allowed the large number and variety of landslide hazards to be addressed, and the component parts of the landslide hazard assessment and the mechanics of the QRA to be explicitly stated and reviewed.

1 INTRODUCTION

Lawrence Hargrave Drive (LHD) is a coastal road that extends between Stanwell Park and Thirroul on the South Coast of New South Wales, about 30 km south of the southern outskirts of Sydney (see locality map on Fig. 1).

The 1350 m section of coastal road between Coalcliff and Clifton had been constructed about 20 to 45 m above sea level through a coastal escarpment environment consisting of steep cliffs that rise to a height of some 300 m above the road (Figs. 1–3). Aggressive marine erosion is taking place at the base of the cliffs causing undercutting of the coastal platform and as a result the road has had a history of severe embankment stability, rockfall and debris flow problems.

On August 29th, 2003, the Minister for Roads closed the road for safety reasons. An Alliance was formed between the Road and Traffic Authority (RTA) (the responsible authority), Barclay Mowlem (civil contractors), Coffey Geosciences Pty Ltd and Maunsell Pty Ltd (consulting engineers) to develop an engineering solution to develop an engineering solution to reduce the risk to "acceptable" levels.

2 LANDFORMS AND GEOLOGY

Over the closed section of the road (the site), there are three headlands separated by two bays. These features
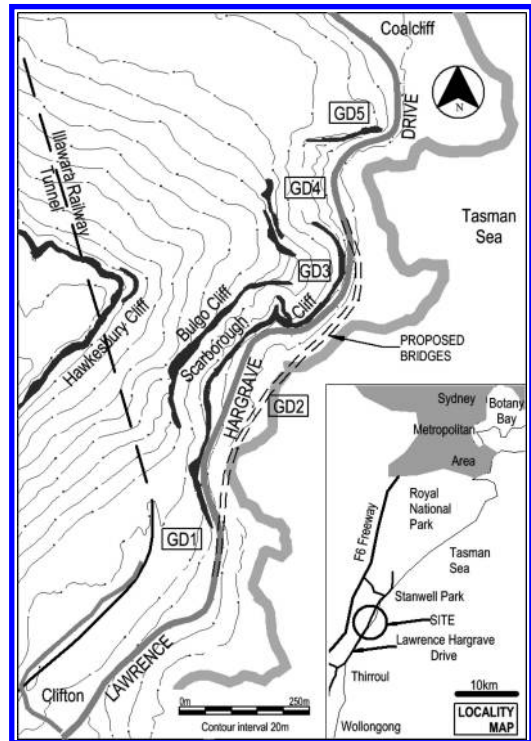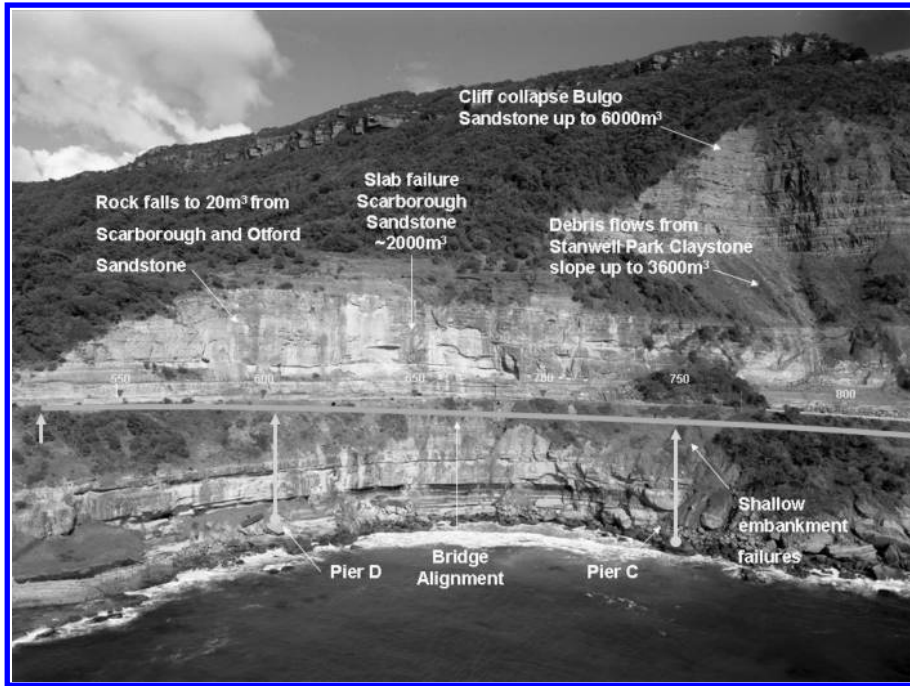

Figure 1. Site plan.

Figure 2. Oblique aerial photograph of Geotechnical Domains GD1 and GD2. The road lies about 40 m above sea level and the skyline cliffs lie about 300 m above sea level.

Figure 3. An oblique aerial photograph of Geotechnical Domain GD3 and part of GD4.
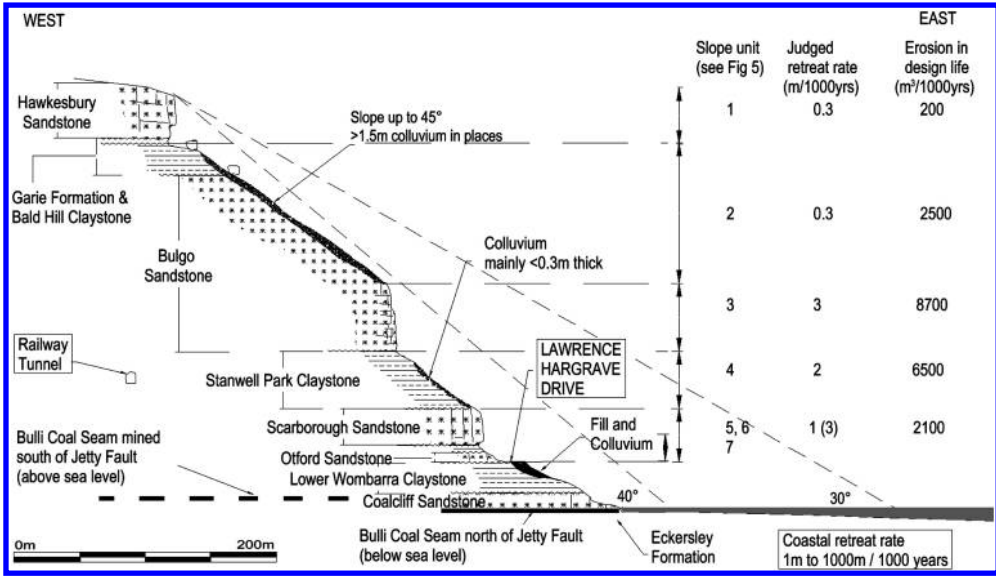
Figure 4. Cross section through GD2 that illustrates the landforms, geology and slope retreat rates.

have been used to separate the site into five geotechnical domains (Fig. 1):

- GD1 – Southern Headland
- GD2 – Southern amphitheatre (Bay)
- GD3 – Middle Headland
- GD4 – Northern Amphitheatre (Bay)
- GD5 – Northern Headland.

The geology of the site is described by Hendrickx et al. (in prep.). In brief, the bedrock geology comprises a thick sequence of sandstone and claystone units of Permian to Triassic age that generally dip between 0° and 5° to the northwest (i.e. obliquely inland). The sandstone units within the succession form prominent, sub-vertical cliffs, whilst the claystones form the intervening slopes. Figure 4 illustrates the relationship between the bedrock geology and these Slope Units.

Superficial deposits of colluvium derived mainly from debris flows and rock falls mantle the lower angled claystone slopes, and form fan-shaped deposits up to 40 m thick in the two amphitheatres (GD2 and GD4).

The most prominent structural features in the area are two well-developed, vertical to sub-vertical joint sets, which strike 040° and 180°–190°. Other important structures are a series of normal faults that affect the stratigraphy.

3 SLOPE HAZARDS

The slope hazards are described by Hendrickx et al. (in prep.). The hazards are distributed over all parts of the escarpment from the crest (up to about 300 m above the existing road) to the coast (Figs. 2–4). Most landslides from the cliffs consist mainly of rock (from single boulders to large masses), whereas most of the landslides from the intervening slopes consist of debris (mixtures of soil and rock).

Typical slope failure mechanisms from the intervening slopes include debris flows and slides. The steeper slopes are also vulnerable to erosion by running water while both cliffs and slopes are vulnerable to coastal erosion at sea level.

The main landslide hazards to road users are:

- *Rock falls/boulder rolls* from the Bulgo and Scarborough Sandstone cliff lines, landing on the road by rolling, directly by falling or subsequently by rolling and falling, when released from talus accumulations on the Stanwell Park Claystone slope. The boulders within the Hawkesbury Sandstone cliff can contribute boulders up to 20 m wide to the hazard profile as well as provide boulders that rest on the steep slope above the Bulgo Sandstone cliff.
- *Debris or Boulder Flows* can be derived from the intervening slopes between the cliff-lines and represent remobilization of talus deposits or failure of in situ material on the Stanwell Park Claystone slope, and also less frequently the Bulgo Slope. Boulder flows can also be derived from the Bulgo cliff where numerous boulders move down slope as a "river of boulders".
- *Road embankment failure by toe erosion by the sea* and loading to embankment crown with man-made fills or through landslide debris accumulation.

591

Whilst most landslides are triggered by intense rainfall (annual rainfall about 1500 mm), the slope processes are being accelerated by marine erosion that is over-steepening the slopes below the escarpment (Hendrickx et al., in prep.). In simple terms, marine erosion is removing the Bulli Coal Seam, which leads to toppling failures of the overlying Coalcliff Sandstone. This in turn leads to oversteepening of the overlying Wombarra Claystone that fails by landsliding. And so the process is repeated up the slope to the Hawkesbury Sandstone forming the cliffs at the crest of the escarpment. The processes are further driven by differential erosion and undercutting of the claystone intervals within the major sandstone units, and these lead to rock falls from the sandstone units. Excavation to form the road has both removed material from the Wombarra Claystone, and resulted in accelerated regression of the Wombarra Claystone, and subsequently the Otford and Scarborough Sandstones.

4 RISK ASSESSMENT FRAMEWORK

4.1 *Project slope risk to life criterion*

The LHD Link Alliance Agreement had a minimum risk to life assessment criterion relating to slope instability of ARL3 as defined in the RTA "Guide to Slope Risk Analysis Version 3.1" (Stewart et al. 2002). Furthermore, the ARL3 criterion applied to the entire project. That is, the sum total of all the slope risks to life on the site must be less than ARL3, not just the slope risks at individual locations. The Assessed Risk Level (ARL) rating for the road prior to remediation was judged to be ARL1.

The ARLs determined using the RTA Guide are derived from "rules" to rate qualitative descriptive phrases describing the likelihood and consequences of slope hazards, which are then combined using matrices to give the Assessed Risk Level. The RTA Guide is based on an underlying quantitative framework and this framework is reflected in the "rules" and the matrices used to assess the risk (Baynes et al. 2002).

There are five ARL levels ranging from ARL1 (highest risk level) to ARL5 (lowest risk level). The median quantitative probability of a fatality implied by the ARL levels have been judged to be roughly one order of magnitude apart with ARL1 roughly equating to an annual probability of death of $>10^{-3}$ and ARL5 roughly equating to an annual probability of death of $<10^{-6}$. ARL3 roughly equates to an annual loss of death of 10^{-5}. The Alliance agreement did not address the risk to property using the ARL criteria. Such risks were addressed as "whole of life costs".

In order to define practical differences between the differing ARL levels, it was agreed at a project QRA

Table 1. Assessed risks levels.

Assessed risk level	Annual probability of death
ARL3	3×10^{-5} to 3×10^{-6}
ARL4	3×10^{-6} to 3×10^{-7}
ARL5	$<3 \times 10^{-7}$

Workshop that the ARLs would be defined for the project as shown in Table 1.

4.2 *Previous quantitative slope risk assessments*

Previously, two quantitative slope risk assessments had been conducted for the site (GHD-Longmac Pty Ltd 2002, URS Australia Pty Ltd 2003).

The GHD-Longmac assessment used the RTA's record of landslide events between March 1996 and November 2001, and selected events in 1988/1989, to conduct quantitative risk assessments of the site in mid-2003 in terms of total (societal) risk, and of individual risk to a bus commuter.

The URS report used the same record of landslide events with a slightly modified event-tree approach to verify the GHD-Longmac results. The URS report also provided separate analyses of the total risk for the individual domains for the site prior to the works in mid 2002 and the site in mid 2003.

The results of these analyses are summarised and discussed in Section 8 of this paper.

4.3 *Adopted risk assessment approach*

This study used a different approach from GHD-Longmac and URS when considering the likelihood of landslides impacting on the road. Specifically, this study used procedures discussed in Moon et al. (in prep.) to develop landslide size frequency models for each of the "slope units".

These models were used to summarise and present judgements, knowledge and evidence on the type, size, frequency and volume of future landslides on site.

5 LANDSLIDES – HOW LIKELY

5.1 *Adopted size frequency distribution of landslides*

The size frequency distribution of landslides from a slope unit depends on the surface form of each slope unit and the underlying geological materials. Figure 5 shows size frequency curves that indicate the adopted number of events for each "order of magnitude" size distributions for hazards emanating from each Slope Unit (Moon et al., in prep.)
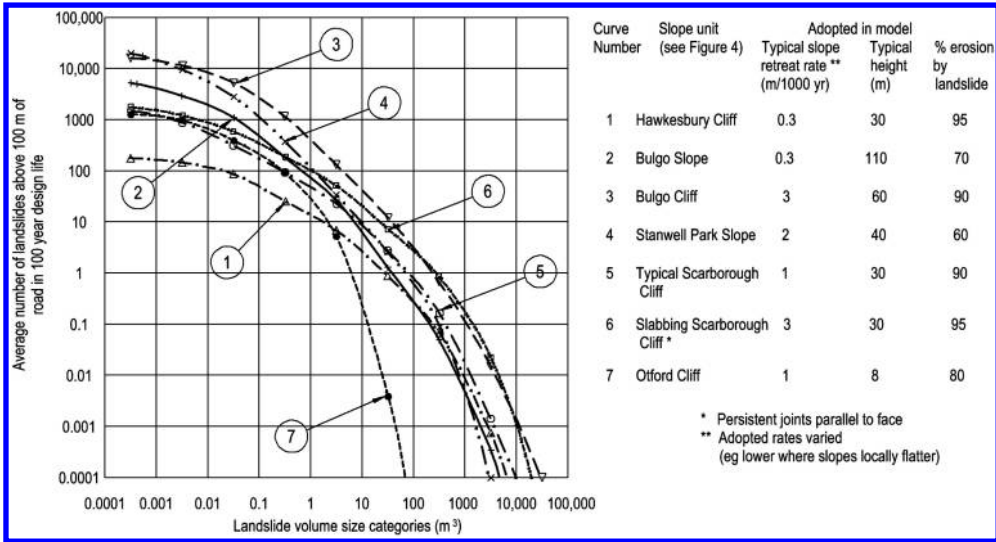
Figure 5.   Adopted size frequency models for the various slope units.

The curves have been normalized to show the size and frequency of landslide debris passing 100 m of road in the design life (100 years). The normalization was done to simplify the data handling in the risk assessment, but had the added advantage that the curves could be directly compared and differences noted. The normalization of the curves involved estimating the design life landslide yield of the slope unit as a proportion of the design life erosion yield, and using this volume to proportionally adjust the raw curve.

The process rate model adopted in this study assumes there is no net deposition on the site. That is, the material eroding from each slope unit will cross the road by landsliding or some other erosion process. But, the model does not assume that all debris from each and every landslide crosses the road each time there is a landslide.

5.2   Percentage of landslides reaching the road

The percentage of landslides (and percentage of debris from individual landslides) reaching the road depends (amongst other factors) on the size and nature of the landslide, the distance and travel angle to the road, and the presence of deposition areas along the flow path. Material that does not pass the road in the first instance locally accumulates on flatter slopes before eventually failing from these slopes.

For example, most landslides (i.e. rock falls) from the roadside cliffs will reach the road, and most of the debris of such landslides will also reach the road (as opposed to depositing on the cliffs). In contrast, many landslides from the other slope units do not directly impact on the road, and of those that do, not all debris reaches the road.

6   ELEMENTS AT RISK AND CONSEQUENCES

6.1   Who could be affected

The annual average daily traffic along LHD in the years from 1986 and 2000 (excluding periods when the road was closed for works) ranged between 2,200 and 3,400 vehicles (mostly cars) per day. This study adopted 4,000 vehicles per day, referred to in the calculations as 2,000 vehicles per lane per day.

Experience in Australia and elsewhere indicate that injuries or deaths could occur on the road as a result of

- Vehicles running into landslides; or
- Vehicles being hit by landslides; or
- Vehicles involved in collisions while swerving to avoid landslides; or
- Vehicles running into the voids created by landslides.

Other events, or combination of events for which it is difficult to predict the likelihood could occur which can result in accidents, injuries or damage. Examples include:

- Rockfall onto people sheltering near a cliff.
- A vehicle hitting a structure damaged by a landslide.
- A vehicle trapped by landslide debris, or otherwise stationary, getting hit by a subsequent landslide event.

593

Historical research (Hendrickx et al., in prep.) indicates that there has been one death probably attributable to a landslide in the project area. This death occurred when a car ran-off the road after probably hitting a developing embankment failure. There have been a number of close calls associated with vehicles being hit by quite large falling rocks, and RTA experience suggest many minor incidents did occur and these went unreported.

6.2 *Vulnerability of persons*

The vulnerability of road users to a landslide depends, amongst other matters, upon the type, speed and size of the landslide, the type and size of the landslide debris, whether the person is in the open or enclosed in a vehicle, and the speed and type of vehicle.

The vulnerabilities adopted for the project were based Stewart et al. (2002) and AGS (2000), modified by the knowledge and experience of the geotechnical team in a workshop.

Two levels of vulnerability were considered, namely:

1) The vulnerability of persons in a car (or similar size vehicle) directly hit by a landslide, which is higher if the landslide debris falls vertically onto a car from the crest of a cliff compared to a landslide moving horizontally and hitting the side of a car.
2) The vulnerability of persons in a car that runs into a landslide.

The underlying assumption in these vulnerabilities is that the landslide reaches the road 40 m or less in front of the car and the driver of the vehicle does not have time to avoid collision. The 40 m distance is based on a 2 second response time at the posted road speed of 60 kph, plus an allowance for braking and avoidance (to avoid death but not necessarily car damage).

Some of the vulnerabilities adopted for this project are given in Table 2.

Table 2. Some adopted vulnerabilities for some landslide events.

Order of magnitude of landslide crossing road (m^3)[1]	Rockfalls from Scarborough Cliff		Debris flows from GD4	
	Landslide hits car	Car hits landslide	Landslide hits car	Car hits landslide
0.03	0.05	0.0006	–	–
0.3	0.1	0.002	–	–
3	0.3	0.03	0.001	–
30	0.7	0.03	0.01	0.001
300	1	0.03	0.1	0.003
3,000	1	0.03	1	0.003

[1] Not all events sizes considered are shown in this table.

7 ASSESSMENT OF THE EFFECTIVENESS OF THE RISK MITIGATION MEASURES

In order to make quantitative judgments about the risk associated with the proposed works, it was necessary to make judgements about the effectiveness of engineering works that have been conducted on the site to date, as well as the effectiveness of those works that are proposed for the site.

7.1 *Existing risk mitigation measures*

There had been an extensive history of construction of risk mitigation measures along the road (Hendrickx et al., in prep.). The last series of works conducted prior to the road closure were conducted in late 2002 and cost about $A3.5 m. These works included substantial enlargement of the catch ditch in the southern half of GD2, the construction of a Geobrugg fence in the southern half of GD3, as well as scaling and the installation of rock bolts in GD1, GD3 and GD5.

Based on field observations of these works and some subsequent computer modelling using the commercially available packages "Rockfall" and "DAN-W", it was judged that the effectiveness of the catch ditch and Geobrugg fence, in terms of the QRA, were as follows:

- The catch ditch in the southern half of GD2 trapped 99.9% of <0.3 m^3 events, 99% of 3 m^3 events, 95% of 30 m^3 events, 70% of larger events.
- In GD3 – Ch1000 to 1150 – The Geobrugg fence and associated works trapped 99% of <0.3 m^3 events, 95% of 3 m^3 events; 90% of 30 m^3 events, 70% of larger events.

The impact of the scaling, the rock bolts and other pre-2002 works were included in judgements about retreat rates for particular slopes.

7.2 *Proposed risk mitigation measures*

In order to reduce the risk to road users to the required level, and to reduce construction risks, it was decided to bypass all of GD2 and GD3, and most of GD1 with two bridges. A 455 m long balanced cantilever bridge will span the area between GD1 and GD3, and a 210 m long incrementally launched bridge will bypass GD3. The bridges largely avoid hazards due to rock falls, debris flows and embankment failures in these zones.

The road returns to the current alignment with minor modification at the southern end of GD4 where slope stabilisation measures are being constructed. A debris containment bund is being built to address the debris flow and rock fall hazards in GD4. Slope

594

stabilization measures including draped mesh, rock anchors and rock fall fences are being built to address rock falls in GD5 and part of GD1.

Where it was judged the slope stabilization measures would intercept almost all events, an effectiveness of 99.9% was adopted for analysis purposes. Also, the analyses assumed that the Armco barrier along the side of the road would be maintained.

The bridge piers are exposed to lesser hazard than the current road because of the differing exposed length (i.e. about 140 m versus 600 m), and their greater distance from the cliff.

The effective exposed length of the piers to each slope unit is greater where the landforms funnel landslide debris towards a pier, and the exposed length is less where the landforms direct debris away from the pier. In the analyses, the effective exposure lengths were estimated by using flow paths from each of the slope units.

The distance of the piers from the cliff have been taken into account by adopting lower percentages of both landslides and debris from each landslide reaching each pier. A conservative vulnerability of 0.1% was assigned for the purposes of estimating the risk of life associated with a large landslide impacting on a pier.

8 RISK ASSESSMENT

8.1 *Mechanics of the risk assessment*

In the study, the calculations were carried out using an Excel workbook composed of 59 linked spreadsheets.

A separate worksheet was prepared for each hazard type in each part of each geotechnical domain and the results from each of these sheets presented on a linked summary spreadsheet. The layout of the worksheets is outlined in Figure 6.

In mathematical terms, the risks to road users were calculated in the spreadsheet models using the following three expressions (adapted from AGS 2000, Reference 5):

$$R_D = P_s \times V_D \tag{1}$$

$$P_s = 1 - (1 - P_{S:H})^{NR} \tag{2}$$

$$P_{S:H} = (N_v \times L \times N_L) / (24 \times 1000 \times V_v) \tag{3}$$

Where:

- R_D = annual probability of death.
- P_S = probability of a car being hit by or hitting a landslide.
- V_D = vulnerability of the individual (probability of death) given the landslide impact on the car.
- $P_{S:H}$ = probability of spatial impact of the landslide on the road given the event.
- NR = annual number of landslides reaching the road.
- N_V = number of cars per day per lane.
- N_L = number of lanes affected by the landslide.
- L = length of the car (assumed to be 5 metres) or the reaction distance (as appropriate). A reaction distance is taken as 40 m allowing some slowing and swerving.
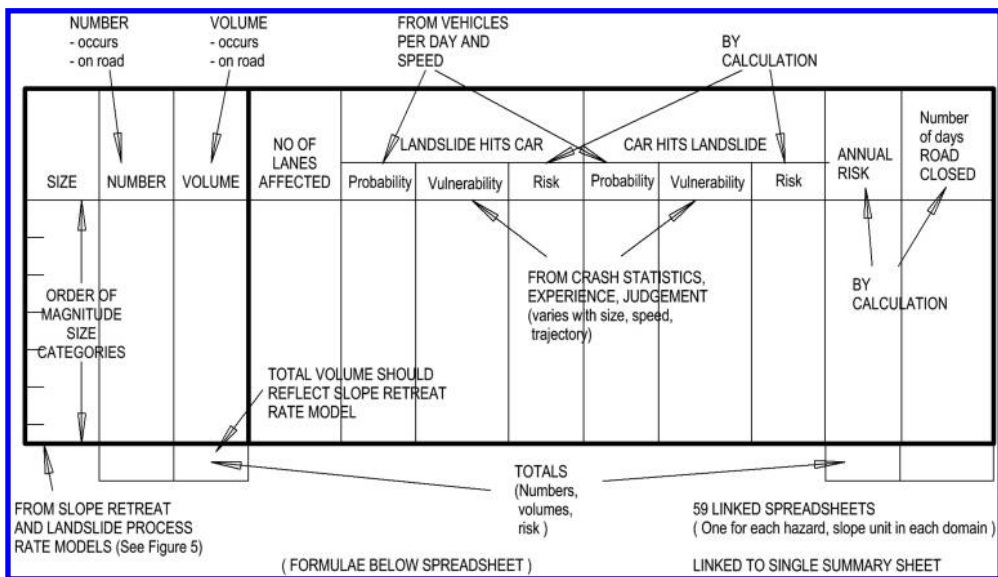

Figure 6. Outline of spreadsheets used for particular hazard, location and slope unit.

595

- V_V = velocity of the car in km/hr (assumed to be the posted speed limit of 60 km/hr).

The four cases considered in this study were:

- *CASE A* for the road prior to mid 2002 without any remedial measures.
- *CASE B* for the site in the period late 2002 to late 2003, including the effect of the Geobrugg fence and the catch ditches in GD2 and GD4.
- *CASE C* for the projected effects of the bridges, but without any other works.
- *CASE D* for the projected effects of the works including the proposed bridges and making assumptions about the effectiveness of the proposed geotechnical works elsewhere.

Cases A and B were analysed to provide a calibration check of the model used. These two cases can be compared to the available historical evidence and the outcomes of the QRAs conducted by GHD-Longmac and URS. Cases C and D were analysed to consider the effectiveness of the engineering works proposed by the Alliance.

8.2 *Summary of the results*

The outcomes of this study are presented graphically in Figure 7, together with the results of the QRAs conducted by GHD-Longmac and URS.

The QRAs showed that:

- The risk profiles tend to be dominated by a few risky hazards at several locations. This is because

the risk is cumulative along the site. For example, the risk for the site prior to the current remedial works was dominated by rockfalls from the northern half of GD2. As the risky hazards were progressively eliminated in the analyses of potential remedial measures, the risk profile shifted to a more uniform pattern that included lower risks at many locations.

- Except for GD4, the results for the base cases and the current cases conducted by GHD-Longmac and URS, and Cases A and B in this study are within about one order of magnitude. In view of the uncertainty and many judgements involved in the analyses they can be considered as effectively the same. It should be noted all of these results indicate a risk level of ARL1.
- The differences in the GD4 results is because this study took into consideration that the road through GD4 lies on the lower half of a debris fan, and adopted reduced percentages of landslide debris interacting with the road and much lower road user vulnerabilities (see Table 2). The GHD-Longmac and URS models did not extend to this level of detail.
- The bridges alone substantially lower the very high risk in GD2 and reduce the total risk by about one order of magnitude. With the bridges alone, much of the remaining risk is in GD1 and GD5.
- The assessment indicated that the bridges and the geotechnical works reduce the risk in all geotechnical domains to either ARL4 or ARL5. The total risk
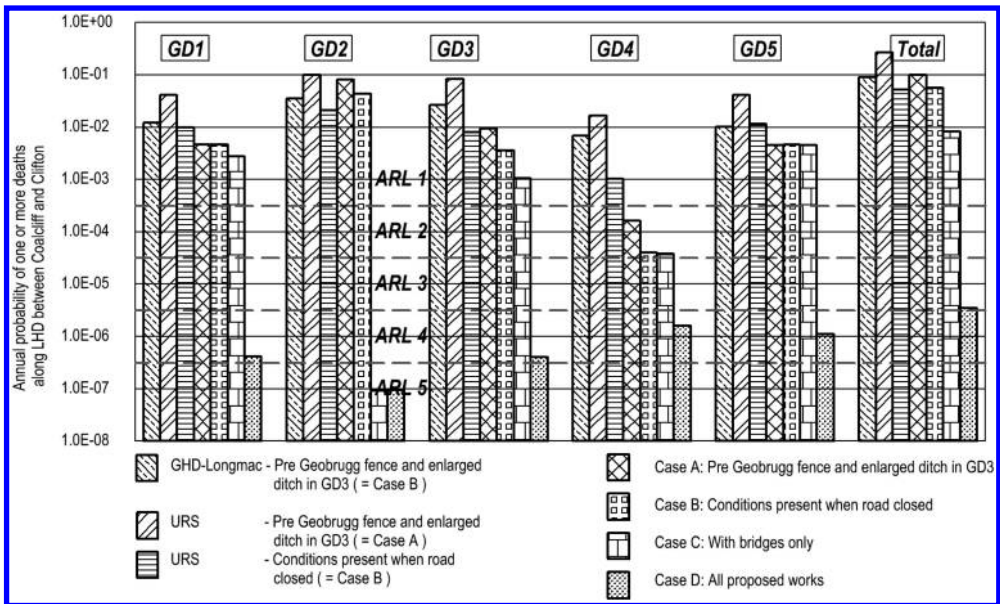

Figure 7.   Summary of the results of the quantitative risk assessment calculations.

596

after completion of the proposed remedial works was judged to be near the ARL3-ARL4 boundary.

8.3 *Simplifications to the numerical analyses*

Many simplifications have to be made when conducting quantified landslide risk assessments given the inherent complexities of landslide behaviour and their resulting interactions with persons/ property at risk.

Those simplifications that have been directly included in the QRA are discussed in Sections 5, 6 and 7. Other simplifications that were not directly included in the QRA included:

- Falling rocks not landing on or staying on the road.
- Variations in the number of vehicles during the day.
- Adopted length of the vehicle and width of the landslide.
- Variations in how the persons in the vehicles are impacted.
- Buses.
- Heavy Vehicles.
- Sight distances.

Based on the results of the earlier QRAs and preliminary work conducted as part of this study it was judged that the effects of these items would produce second order variations in the outcomes of the QRAs for total risk if they were included. That is, individually they may result in variations of less than half an order of magnitude in the outcome of the risk analyses. Furthermore, because some of the effects are conservative and some are non-conservative, it was judged that not including these effects would not significantly alter the outcome of the QRA.

8.4 *Road closures*

The QRA workbooks were also used to assess the number of days of unplanned closures for the road (as opposed to planned road closures for routine maintenance and programmed repairs).

This assessment was conducted by combining the number and size of landslides impacting upon the road from the risk portion of the workbooks with judgements on times the road could remain closed if the events happened.

9 DISCUSSION

9.1 *Advantages of the adopted approach*

The advantages of using the adopted approach included:

a. The quantitative approach reflected the underlying basis of the RTA slope risk system.

b. The large number and variety of landslides throughout the project could be addressed relatively easily.
c. The "sum total of all the slope risks to life" project criterion could be simply addressed by summing the component risks.
d. The component parts of the assessment were stated and hence could be more readily reviewed.
e. The outcomes of the quantification could be interpreted in terms of the project ARL3 criterion (using Table 1), as well as other available risk assessment criterion.

9.2 *Are the results of the QRA credible?*

This study judged that the annual probability of death along the road (Case B) immediately prior to closure was about 1 in 18, and this risk was dominated by the 1 in 23 risk associated with GD2. For this case, the annual probabilities of death for the other domains were less than 1 in 100.

These judged risks were comparable with the history of the site, which suggests only one death potentially attributable to landsliding and a number of close calls. These risks were also comparable with those assessed by GHD-Longmac and URS for the same road conditions, but using differing assumptions.

A further check on the credibility of the results was made by comparing the results for selected hazards across the site with results from a semi-quantitative risk assessment for the same hazards using the procedures described in Stewart, et al, (2002). The results of these checks showed comparable results.

10 WHAT WE LEARNED

1. Whilst the risk calculations were carried out numerically, significant judgments were required to provide many of the input parameters. As a consequence, the reproducibility of the QRAs are typically to an order of magnitude or more regardless of method (Stewart, in prep.).
2. QRAs should be used to facilitate risk decision-making by providing comparisons and those comparisons will always be approximate (Christian 2004). Cut-off points for remediation and management plans have to reflect this reality (Stewart, in prep.) and, as always for ground engineering projects, robust engineering solutions need be adopted.
3. QRA is an indispensable tool to address multiple hazards and multiple consequences such as present on the LHD site because QRA provides a structured framework for collecting and presenting landslide information, and making risk decisions. QRA allows the large number and variety of landslide hazards to be addressed, and it allows the

597

component parts of the QRA to be explicitly stated and reviewed.

4. QRA is a tool to use in conjunction with conventional slope analysis methods, which in the LHD study included rock fall, rock toppling, debris flow, and circular and planar sliding slope modelling and analyses.

5. It is difficult to assess the credibility or otherwise of a QRA because, as stated by Ho et al. (2000), "*much judgement is involved which can be difficult to substantiate and there is considerable room for disagreement.*" Although, as also discussed by Ho et al., similar issues are often faced when using other slope assessment methods.

REFERENCES

AGS Sub-Committee on Landslide Risk Management. 2002. Landslide risk management concepts and guidelines. *Australian Geomechanics* 37(2): 1–44.

Baynes, F., Lee, I. & Stewart, I. 2002. A study of the accuracy and precision of some landslide risk analyses. *Aust Geomechanics* 37(2): 149–156.

Bunce, C., Cruden, D. & Morgenstern, N. 1997. Assessment of the hazard from rock fall on a highway *Can. J. Geotech.* 34(3): 344–356.

Christian, J.T. 2004. Geotechnical engineering reliability: How well do we know what we are doing. *ASCE J. Geotechnical & Geoenvironmental Engineering* 130(10): 985–1003.

GHD-Longmac Pty Ltd. 2002. Report AQ588_1 dated 4 April 2002 titled MR185 Lawrence Hargrave Drive, Clifton to Coalcliff. Assessment of geotechnical risk and risk reduction options. Prepared for RTA Southern Regional Office.

Hendrickx, M., Wilson, R., Moon, A., Stewart, I. & Flentje, P. in prep. Slope hazard assessment on a major road project in NSW, Australia.

Ho, K., Leroi, E. & Roberds, W. 2000. Quantitative risk assessment – application, myths and future direction. Proceedings of the International Conference on Geotechnical Engineering (GeoEng 2000), Melbourne, pp 269–312.

Moon, A., Wilson, R. & Flentje, P. in prep. Developing and using landslide size frequency models.

Stewart, I., Baynes, F. & Lee, I. 2002. The RTA Guide to Slope Risk Analysis Version 3.1. *Aust Geomechanics* 37(2): 115–148.

Stewart, I. in prep. Managing slope risks for a large highway network.

URS Australia Pty Ltd. 2003. Report R005.doc dated 26 August 2003 titled Final report. Independent review of GHD-Longmac Report – Lawrence Hargrave Drive, Wollongong. Prepared for RTA Blacktown.

Managing slope risk for a large highway network

I.E. Stewart & H.G. Buys
Roads and Traffic Authority, NSW, Australia

ABSTRACT: Effective slope risk management for a highway network requires procedures which can provide sufficient accuracy and discriminating power to identify, with confidence, slopes which require management and to set defensible priorities for remediation. The Roads and Traffic Authority NSW has developed such procedures and implemented them on a large number of sites, as part of an ongoing geotechnical risk management programme. A systematic, comprehensive, time- and cost-effective approach to the collection of relevant slope data and subsequent geotechnical risk analysis is described. It has been demonstrated that with the development of suitable analysis methods, effective and defensible risk management is possible within reasonable resource constraints. Experience with the use of the procedures has resulted in the identification and solution of many issues of principle and practice in the use, potential benefits and limitations of geotechnical risk assessment. Some of these issues have wider implications for the practice of risk analysis.

1 INTRODUCTION

New South Wales (NSW) occupies the SE of Australia and extends over an area roughly 1200×1000 km (Fig. 1). Slope risk is concentrated in the area within about 300 km of the east coast, which is dominated by the Great Dividing Range. The range runs parallel to the coast, generally rising to between 1000 and 1300 m above sea level and locally to over 2000 m. The eastern escarpment of the range is steep and deeply dissected by short rivers. The western side falls more gently and grades into a gently sloping, predominantly alluvial plain which extends to the western border.

The range and the slopes immediately to the west consist mainly of highly deformed low grade metasediments and interbedded metavolcanics, with numerous granitic intrusions. Locally these rocks are overlain by slightly deformed to flat-lying sedimentary basins and in some areas by horizontally bedded basalt flows of varying extent.

In NSW, slope risk management is carried out by engineering and geotechnical staff as part of the maintenance function of the Roads and Traffic Authority (RTA). Geotechnical staff within this organisation are distributed at six major locations in the eastern part of the state and have a wide range of responsibilities, which extend to pavement design (for both new construction and maintenance), materials and construction quality, as well as conventional geotechnical functions.

Considerable local knowledge at the professional level is therefore available to assist in the implementation of the slope risk management programme.

2 CHALLENGES IN RISK MANAGEMENT

Risk management for a road network imposes requirements which differ from those appropriate for a single site or a small group of sites. The principal challenges this presents for a road network can be summarized as follows:

- The management system must be able to deal with the widest possible range of conditions, including geology, geomorphology, nature of individual slopes and structures, multiple hazards at a single site, changing geotechnical design standards, road geometry, traffic volumes and vehicle speeds.
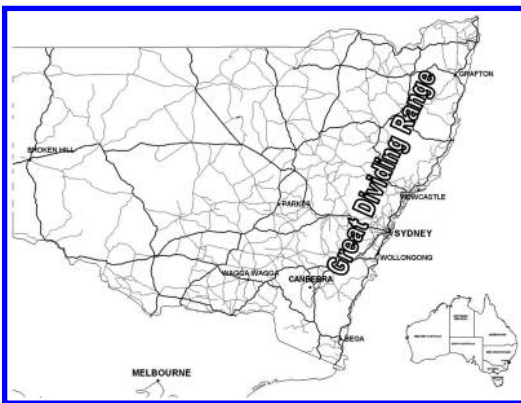

Figure 1. New South Wales main road network (state highways highlighted).

- There are many sites to manage. The NSW state highway network is nearly 20,000 km in overall length, with in excess of 250,000 adjacent slopes (see Fig. 1). Quantitatively, the associated risks vary through many orders of magnitude. The scale of the risk analysis task makes the need for a quick and reliable method imperative.
- Many geotechnical practitioners must be involved, to enable completion of the programme within a reasonable timeframe. To ensure that the programme is managed effectively the outputs have to be consistent between practitioners.
- The situation to be managed is not static. There are continual changes to the inventory of slopes and to conditions at individual sites. Not all of these changes are of a geotechnical nature (e.g. new development on, or adjacent to, a slope).
- The RTA operates in an increasingly litigious environment:
  – Financial liability will follow damage caused, directly or indirectly, by slope instability.
  – There is increasing potential for personal criminal liability, particularly if a risk is known and not addressed.
  – The standard for "duty of care" for the purpose of legal advice is being derived from societal risk criteria, expressed in the form of F-N (frequency of occurrence v expected number of fatalities) diagrams, developed for large dams and other major infrastructure (Fell 1997). These diagrams have now been published and adopted by practitioners in so many areas that they can no longer be regarded as "speculative". In NSW, the interim recommendations from the Australian National Committee on Large Dams (ANCOLD 1997) have been widely used as a basis for societal risk assessment. The appropriateness of adopting these recommendations is open to question, as typical road slope risks involve the potential for small numbers of casualties, rather than the rarer, large scale events that the F-N diagrams were intended to address. As a consequence public authorities are held to a high standard of accountability.
  – Legal considerations tend to promote very conservative management practices as the legal perspective is extremely risk averse and generally considers risk in isolation from other network management considerations.
- A large quantity of data must be processed and held in an accessible form before the programme can be considered to be adequately managed. The data has to be kept alive – it cannot just be an historical snapshot of risk. It must include unambiguous locations and enough descriptive information to allow those unfamiliar with a site to understand the risks associated with it.
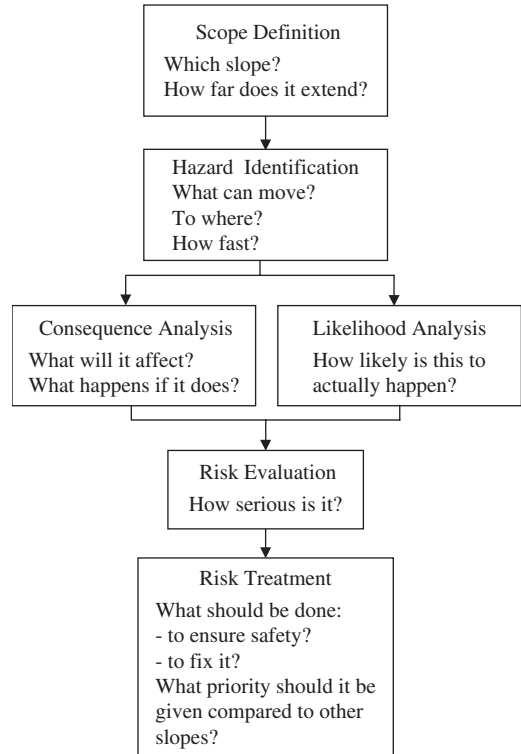
Figure 2. Slope risk management for an individual site.

- The procedures must be compatible with quantitative risk analysis (QRA) studies.

To allow effective management of the slope risks, all of these issues must be addressed effectively.

3 HOW ARE THE ISSUES BEING ADDRESSED IN PRACTICE?

3.1 *What has to be done?*

The general approach to the risk management process for a single site is well understood and can typically be summarized by the flowchart in Figure 2. To implement this process a procedure must first be developed which includes the functions of hazard identification, likelihood and consequence analysis and risk evaluation, i.e. risk analysis. The procedure must be suitable for application over many sites for risk management of a road network. Developing such a procedure takes time and its robustness needs to be established before it can be implemented on a large scale.

A critical requirement is that the risk analysis procedure cannot be allowed to have a conservative bias.

Introducing such a bias may greatly increase the number of ostensibly "high risk" slopes, making it much more difficult to understand the real level of risk to be managed and to set rational priorities.

Once a risk analysis procedure is in place, to successfully extend it to management of the road network, the following need to be determined:

- The absolute scale of the task, including:
  - The numbers and types of slopes.
  - The risk associated with each slope.
  - The slopes that present sufficient risk to require management.
- Priorities for remediation.
- Management plans for those sites which require remediation.

Systems are then required to manage the slopes. The practical steps taken to develop the risk management processes are described in the following sections.

3.2 Risk analysis procedure (2000/2001)

The RTA's earlier risk analysis procedures relied on scoring slope attributes in a checklist. In contrast the RTA's current risk analysis procedure (RTA 2001), developed in its current form, between 1999 and 2001 relies on understanding and interpreting the site.

The current procedure provides a method for quantification of risk to one of five Assessed Risk Levels (ARL1 represents the highest risks, ARL5, the lowest) at individual sites (Stewart et al. 2002, Baynes et al. 2002, Stewart & Buys 2005).

About 700 slopes, assessed as the highest risk slopes in previous assessments or nominated by the RTA's regional staff, were selected for risk analysis. In addition, the 50 slopes previously ranked as the highest risks, together with a selection of others, were reviewed by independent assessors.

The independent review of the 50 sites found the earlier assessments to be unreliable. Many of the supposedly "high risk" sites were found to be low risk ie ARL4 or ARL5. This conclusion was confirmed when the full programme was completed, with about 50% of the 700 analysed sites being ARL4 or ARL5. The nomination process used to select some of the sites was also found to be unreliable. A frequent comment from practitioners was that it was difficult to see why particular sites had been selected for analysis, when many others appeared to present a similar or higher risk.

The current risk analysis procedure was initially found to be insufficiently reproducible and to be conservatively biased. These characteristics were substantially improved in the current procedure (RTA 2001) by modification of some of the details of the procedure, following which the bias was found to be removed and the reproducibility improved to an acceptable level (Baynes et al. 2002).

About 10% of the sites analysed were found to be in the highest risk category (ARL1) with a further 20% in the second highest (ARL2). A programme was initiated to manage and remediate these sites. Efforts were then made to address the question of the many sites which appeared to require analysis, but had not been selected for the programme.

3.3 Inventory collection (2001–2002)

Recognition of the shortcomings of the earlier site selection process raised important questions as to the best method of identifying slopes which warrant formal risk analysis. The issue is critical to the success of the management programme, as a hazardous slope missed at this point will go unmanaged and probably unnoticed until it fails. There are several ways of approaching the task of selecting the inventory of slopes to be analysed:

1 Identify hazardous slopes through past history, local knowledge etc. This approach assumes that slopes not so identified present a low risk. It also requires the least resource for gathering the inventory. However, the RTA's experience, outlined above, shows that this method is unreliable. Records of the performance history of slopes may not be well preserved and where they exist are often difficult to access. Local knowledge, while of great value, is uneven in quality.

2 Analyse all slopes, possibly sorted using a simple filter such as slope height. This approach is very inefficient, as only a small proportion of slopes (estimated at <5% of slopes in NSW) present more than a negligible risk and many more will meet such a simple filter criterion. The filter would have to be set very conservatively to avoid the potential for omitting hazardous slopes. The resources required for risk analysis are enormous and the process, if attempted, would be almost impossible to manage effectively.

3 Given the disadvantages of the first two options, a third was developed – a systematic screening process whereby a full inventory of slopes is gathered, from which sites are selected or culled using more complex criteria which are related to potential for risk. Formal risk analysis would then be undertaken for those slopes that meet the criteria. Every slope will have been inspected, at least briefly, by qualified personnel before the critical decision whether or not to cull the slope is made. This greatly reduces the resources required, while minimizing the possibility of a potentially hazardous slope passing unnoticed.

The third option was adopted and a full inventory of the slopes within the eastern part of the state was collected. This required:

– Defining a "site" or "slope" for a road network in a way that could be simply and consistently applied – essentially based on obvious changes in slope type, supplemented by drainage lines for long cuts and underlying topographic highs for long fills.
– Capturing the location of every slope in eastern NSW (within a defined area, east of the Newell Highway, which runs parallel to the coast, approximately 300 km inland). The capture system was GPS based – in car, with locations captured straight to computer and later converted to chainages and other grid systems as needed.
– Simultaneously with the above, capturing basic slope data (length, type – cut, fill, natural slope going up or down, flat), together with landmark features.

Inventory capture does not require specialist geotechnical personnel and was in fact undertaken by local soils laboratory staff. Some areas had to be covered on foot. Extensive, steep side slopes below a road are not sufficiently visible from a vehicle to allow sites to be defined adequately. In heavily trafficked urban areas conditions often prevent working from a vehicle.

The quality of the data obtained was acceptable with positional accuracy in the typical GPS range of 5 m to 15 m. This is sufficient to define the start and finish of sites unambiguously, even in mountainous terrain where individual sites were often no more that 40 m long, provided that travel speeds were restricted to no more than 30 km/hr. Higher speeds led to unacceptable position errors due to the variable lag time in capturing locations. Overall progress in one direction in rural areas was typically about 15 km/hr, due to the need for stops and to negotiate traffic safely.

The overall cost of the inventory collection was approximately $A300,000 to cover the state main roads network.

3.4 *Slope classification (2002–2004)*

On completion of the inventory in a region, the sites which require risk analysis must be identified, a process referred to as classification. The decision is based on a brief inspection, generally from a vehicle supplemented by a short inspection on foot as needed. These inspections require experienced geotechnical personnel, preferably local, to take advantage of knowledge of the history of the sites.

Predetermined criteria were set to capture risks above mid-ARL4, to ensure that all ARL1, ARL2 and ARL3 sites, which are those requiring management, have their risks analysed. These criteria consider a variety of geotechnical factors in relation to the type of site and non-geotechnical conditions such as traffic volume.

The two-pass system (inventory, then classification) has been found to be more efficient overall. The two-pass system minimises the need for scarce specialist professional resources. Multiple passes, each collecting a single type of data, take less time than one pass, attempting to collect all. The process also greatly reduces the error rate in data collection. Experience has shown that errors (particularly omissions) are much more common when several different forms of data have to be collected simultaneously.

The cost of the classification process in rural areas is similar to that of the inventory, as the process is faster in most areas, but the resources are more costly.

Sydney, where a significant proportion of the network is both in steep terrain and heavily trafficked, requires more resources due to the number of slopes with development below them, much of which is not sufficiently visible from the road. There are also many retaining structures, the relevance of which to the road must be decided. Occupational Health and Safety (OH&S) requirements also dictate that significant lengths must be inspected on foot. Use is being made of other technologies (e.g. Gipsicam, which allows a virtual drive through the network) to pre-plan such inspections, which greatly improves efficiency.

3.5 *Rolling programme for risk analysis (2005 onwards)*

Sampling undertaken during field trails of the classification procedure has indicated that less than 5% of slopes within the inventory would require risk analysis, rising locally to about 10% for the east–west highways which ascend the coastal escarpment, and falling to perhaps 1–2% inland from the great dividing range. It is currently expected that something in the range of 5000–8000 slopes will ultimately require analysis, of which 10–15% have already been completed.

Previous experience has demonstrated that the risk analysis is best managed by packaging the work into groups of about 100 sites. In order to maintain effective control of the process the following procedures have been put in place:

– Only practitioners who have experience in slope stability assessment and who are specifically trained in the RTA's risk analysis procedure would be used. A training programme has been instituted with about 90 practitioners now trained, 65% of these being external to the RTA. To allow resource leveling and to maintain expertise within the local profession, the risk analysis programme is expected to extend over about four years.

602

– Auditing and data validation must be undertaken throughout the programme. This is expected to involve field checks on 10–15% of the sites analysed and desk checks on all sites.

Some sections of road, where geotechnical risk may not be adequately captured on a site-by-site basis, need to be recognised and set aside for separate study. These are often sections where:

– Individual sites cannot sensibly be dealt with separately.
– Large scale hazards encompass multiple sites.
– It is not easy to predict which sites might be affected by a hazard originating well upslope.

These sections are most commonly the mountain passes where width/alignment is a major factor.

OH&S issues associated with the work must also be addressed and kept under review. Specific issues which have proved relevant include working at heights (slope inspections of this type, in NSW, are regarded as construction work and are subject to regulations developed with the building industry in mind), working alone (particularly in remote areas or in steep country) and working adjacent to traffic.

3.6 *Management plans*

ARL1 and ARL2 sites would generally be remediated, although where there is economic risk rather than risk to life, a long term management approach may be considered. Prior to remediation, management of the risk is essential. ARL3 sites, which would not normally be remediated but where the risk could increase over time, and remediated slopes require effective long term management.

Individual management plans are necessary for instrumented or high risk (ARL1 and ARL2) sites. A more generic approach is appropriate for lower risk (ARL3) sites where only an inspection regime is needed.

Development and implementation of risk management plans can be very resource hungry unless care is taken. Plans should therefore be kept simple and cost effective and should only contain essential requirements for site management. A firm grasp of the relationship between the annual probability of a hazard occurring and its probability of occurrence before the next inspection cycle (see Section 3.10, below) is essential. Underlying this is a need to appreciate the way hazards can evolve over time.

3.7 *Data management*

Once risk analysis is complete there is an ongoing need to manage and manipulate the resulting data, to allow risk levels for the sites to be compared and remediation priorities set. Likewise, the ongoing implementation of management plans must be controlled.

For a relatively small number of slopes the management task is not difficult and can be accomplished using simple tools. Once the number of slopes under active management rises into the hundreds or thousands the task requires an effective database system. To this end the RTA has developed its Road Slope Inventory System (RSIS) database, which is in the final stages of implementation at the time of writing and will be the primary programme management tool once the rolling programme starts.

The database stores all of the key information regarding each site, including:

– Location information – GIS based but also incorporating linear referencing (chainage) coordinates.
– A risk analysis summary, which covers all hazards identified at the site, not simply the one giving rise to the highest risk.
– Site sketches – including plan, cross sections, details of identified hazards and the interpreted mechanisms responsible for them.
– Photographs of the site and key features.
– Inspection, monitoring and maintenance requirements.
– Report cross references, if any.

Successive inspections of individual slopes can be added to the database as they become available so that the data eventually provides an easily accessible summary of slope history. The database interfaces with other RTA data sources, including the RAMS (Road Asset Maintenance System) database, which contains extensive maintenance information. RAMS is also expected to be the repository of information from a GPS-based incident recording system, which would include locations of geotechnical events such as rockfalls or embankment failures. Access is also available to the Gipsicam system (photographs of the road system at 10 m intervals in both directions, from which site appearance and road geometry details can be measured directly).

3.8 *Remediation*

For the higher risk slopes (ARL1 and many ARL2) remediation is the obvious choice as a long term management strategy, with the objective of reducing the risk to ARL3 or better and maintaining it at that level. Priorities for remediation are based, as far as possible, on ARL.

Given the time and resources that may be required to remediate a large, complex, high risk site, it can be more effective to remediate a number of simpler, lower risk sites while investigation and planning for the higher risk site is being undertaken. Strict adherence

603

to setting remediation priorities by ARL is therefore not necessarily appropriate.

The RTA will need to remediate some hundreds of sites and given the inevitable limitations on resources, the following need to be kept in view constantly:

– The need to maintain consistency of approach over a wide range of local management.
– Knowing when to stop. The objective is to reduce risk to an acceptable level and maintain it there, not the absolute elimination of geotechnical risk.
– Being aware of the possibility of treating one problem and creating another e.g. narrowing carriageway width in undivided roads, to move traffic away from potential rockfalls, may lead to an increase in collisions between vehicles traveling on opposite directions.
– Design, maintenance requirements and whole of life costs need to be considered for each site. Slopes are now regarded as structures with a 100 year design life. The practicality of proposed measures to maintain acceptable risk levels over this time must be established before a design is accepted.
– OH&S issues are of critical importance when dealing with unstable slopes and must be considered at the design stage, both for constructability and for long term maintenance.

3.9 Decision making process

The decision-making process starts with the fundamental decision of whether to remediate or manage a site in some other way. The decision will be influenced by:

– The nature and magnitude of the risks.
– Time and cost resources required to implement different options.
– Benefits or costs which could include changes to the risk profile of the site, changes to whole of life costs and impacts on road functionality.

There is a degree of uncertainty in all of the above factors and hence in the decision making process. However it is essential that the overall impacts of proposed options are thoroughly understood and that cost estimates for implementing actions are as realistic as possible.

With a large number of sites to be managed, the efficient allocation of resources to making the decisions themselves becomes important. Resources should be concentrated in the areas where the consequences of a poor choice are greatest. This can be understood through a matrix relating risk to cost (Fig. 3). In this concept, resources are concentrated on the highest risk and cost categories. These are the

Risk ⇒ Cost ⇓	L Low ARL3 ARL4 & 5	M ARL2 top ARL3	H Low ARL1	VH Top ARL1
EH >$10M	Do nothing (or manage)	Manage Low priority	Manage Med. priority	Manage?? (or fix??) High priority
VH $2 - 10M	Do nothing (or manage)	Manage Low priority	Manage? (or fix??) Med. priority	Fix (or manage??) High priority
H $0.5 -$2M	Do nothing (or manage)	Manage (or fix?) Low priority	Fix (or manage?) Med. priority	Fix High priority
M $0.1 - 0.5M	Do nothing (or manage)	Manage (or fix) Low priority	Fix Med. priority	Fix High priority
L <$0.1M	Do nothing (or manage)	Fix (or manage) Low priority	Fix Med. priority	Fix High priority

Figure 3. Conceptual matrix for resourcing risk management decision making. Colours relate to degree of difficulty in making the decision (blue easiest, red hardest). "?" – Possible alternative decision, would require justification. "??" – Possible decision or alternative, would require substantial justification. "Fix" means reducing risk to an acceptable level, usually by engineering works. "Manage" for H-VH risk levels means a combination of engineering works (on ALARP principle), traffic management, etc. to lower the risk. Risk may still be in the ARL1/2 range after the measures are instituted. "Manage" for M-L risk levels will normally involve varying levels of traffic management and inspection or monitoring regimes, possibly with limited engineering works. Some of these sites will have been remediated.

cases for which a detailed understanding of the site and the hazards it presents is essential, as is an understanding of the potential management strategies and their impact on the risks. Often, elimination of the risk is impractical and the degree of risk reduction achievable through each option must be estimated and substantiated.

Bias needs to avoided in this process as it prevents resource allocation from being optimized and leads to poor decision-making. By far the most common problem is conservative bias.

Figure 3 shows clearly why this is undesirable, as it forces inappropriate resourcing levels (thus diverting them from more appropriate uses) and influences decisions towards higher cost or higher risk solutions, depending on whether it is risk or cost that is being exaggerated.

Quantitative risk assessment (QRA) is a suitable tool for use in circumstances of high risk and remediation cost and in combination with more traditional geotechnical studies is capable of greatly assisting in option selection. The Lawrence Hargrave Dive project (Hendrickx et al. 2005, Wilson et al. 2005), which was undertaken as part of the RTA's slope remediation programme, well illustrates the ways in which such studies can be used in such a case.

604

3.10 *Keeping the system up to date*

Knowledge of the slope inventory and its risk profile must be kept current for effective ongoing risk management. This is being delivered by:

- The introduction of contractual requirements for new works. These requirements include:
  - Specifications incorporating slope risk targets into design criteria (aiming for ARL4), to be met over the whole of the design life. Batters are treated as structures with a 100 year design life (including any slope support works) with a strategy required to ensure that performance targets are met over that life.
  - Handover requirements for inventory and risk analysis information, using RTA's procedures, before works are commissioned.
- A review of the inventory at regular intervals (of about five years) to cover changes outside RTA control e.g. adjacent development, changes to traffic volumes, small projects which may miss out on the handover requirements, possible changes in the behaviour of previously low risk sites and changes to the appearance of sites due to other activities.
- Maintaining a rolling programme for risk analysis of high/intermediate risk slopes (ARL and higher risk) on about a five year cycle. Additional sites will be introduced to the programme where changes to conditions mean that risk may have increased to significant levels.
- Keeping the risk analysis procedures under review, with enhancements made at regular intervals. As in the past, improvements to the procedure may result from general improvement in knowledge reflected in the literature, attention to specific issues as they arise and through experience and feedback from practitioners.
- Developing guidelines for QRA, in parallel and consistent with the RTA procedure, to make studies more consistent in approach and to ensure compatibility among the results obtained by different approaches.

4 SOME LESSONS FROM EXPERIENCE

4.1 *Critical issues*

The critical issues in developing and implementing the slope risk management programme can be summarized as follows:

- Ensuring that sites presenting significant risks are not omitted. This was addressed through the inventory/classification process.
- Ensuring that site locations are reliable and unambiguous. A GPS-based GIS system is essential. Calibrated odometer-based systems do not provide sufficient accuracy and are generally unreliable.
- Mechanisms and likelihoods for embankments failures. Whilst it is not difficult to propose reasonable failure mechanisms, assigning realistic probabilities to them is problematical in the absence of specific evidence for either active failure or the embankment having reached a state of marginal stability in the past.
- Rare large scale events which may have severe consequences and how to deal with them in risk analysis. The problem is particularly acute in considering the potential for first-time failures in natural slopes. These do not necessarily pose a major risk to life (although they may), but may have serious consequences because of their potential to cause extended closure of major transport routes.
- Complex areas, such as mountain passes, which present a combination of high risks and high remediation costs. These require separate study, as the associated risks are not fully captured on a site-by-site basis. They are often the areas in which large scale natural failures occur.
- Retaining structures, particularly older ones, are not well recorded and require considerable effort to locate. Ownership of the structures is often unclear. The condition of drystone structures, in particular, is often difficult to assess, as they may be prone to brittle failure by toppling or overturning, especially under live loading.
- Preventing conservatism in risk analysis.
- Development of an effective data management system that is responsive to the needs of a variety of users, from mangers to site staff.
- Resourcing the programme to an adequate level, particularly in the development and management phases.
- Setting realistic inspection targets in order to maintain long term commitment by those involved.
- Developing an understanding at senior management level of the meaning of probability and return periods in slope risk analysis. It is important that slope risks be appreciated realistically, and neither exaggerated nor diminished.
- Maintaining consistency in the technical aspects of the programme. This is addressed through training and ongoing technical review and audit of the results.

4.2 *What went well?*

Generally the programme has worked well, which in part reflects the time and resources made available. This has allowed an iterative approach to critical aspects of the technical procedures, eliminating wasted effort. However, some aspects have exceeded initial expectations:

- The level of discrimination provided by the risk analysis procedure is adequate to set priorities and

605

manage the programme. The reproducibility of the results has improved in line with more extended training and now appears to be close to the best that could be expected from theoretical considerations.

- Inventory collection was much easier than was initially expected, with a generally acceptable degree of reliability.

4.3 *What went less well?*

Likewise, some aspects of the programme did not meet initial expectations:

- The classification process was slower than originally anticipated, due to constraints on local resource availability rather than the process itself.
- Defining areas of responsibility for risk, particularly in urban areas. This issue arose due to the complexities of land ownership and the extent of duty of care, when considering hazards which arise from outside the road reserve and therefore outside the control or responsibility of the road authority.

4.4 *How much can really be done?*

An understanding of the limitations of risk analysis is essential for proper management of slope risks. The precision of the outcomes should not be overestimated, for the following reasons:

– The risk analysis procedure adopted by the RTA is subject to the inherent limitations of visual inspection. Knowledge of subsurface conditions and past behaviour is therefore restricted to what can be inferred from observation.
– In the roads context, pavement and shoulder rehabilitation often mask evidence of embankment distress. As a result, evidence of potential hazards can disappear.
– Incidences of slope instability are poorly recorded. This imposes limitation on the accuracy of studies based on such records.
– The evidence from various studies undertaken in conjunction with the programme makes clear the inherent limitations of probabilistic risk analysis. Reproducibility is typically to an order of magnitude, regardless of method (Stewart & Buys 2005).

The inference that can be drawn from these considerations is that the reproducibility of geotechnical risk analyses is in principle unlikely to achieve one significant figure, a conclusion reinforced by consideration of the uncertainties in individual conditional probabilities. This has implications for responsible reporting of risk outcomes, particularly in absolute terms. Relative risk outcomes within a single study are likely to have better reproducibility, as the methodology will ensure that many factors which could vary between studies are held in common. At the least, the issue of reproducibility should be addressed as part of the reporting of risk outcomes.

It follows that priority rankings derived from risk analyses will always be approximate and that cut-off points for the introduction of specific management strategies will generally appear arbitrary when considered in detail. Criteria for determining cut-off points for remediation and formal management plans must reflect this reality.

This last consideration means that a degree of conservatism is inherent in defensible slope risk management practice. This reinforces the need, discussed earlier, to ensure that the risk analyses themselves are as realistic as possible and free from conservative bias. Independent checks should be used whenever possible to verify the results of risk analyses.

Some possible approaches are as follows:

– Use of the historical rate of events, incidents, near misses and fatalities versus the rates implied from the risk analysis. In using historical data, allowance must be made for under-reporting of incidents, short term fluctuations in frequency and possible systematic changes with time.
– Comparison with other sites or studies, or use of different methods, for consistency in outcomes. For QRA studies, the RTA procedure can be used as a check, as it shares the same basis in its underlying conditional probability structure, as most quantitative studies.
– Societal risk is ultimately the sum of individual risks. On a network-wide basis, overall annualised fatality rates can act as an estimator for the sum of societal risks from slope hazards. This can act as a gross check on the overall pattern of risk derived from the study of many individual slopes.

In NSW, less than 100 ARL1 sites have been identified to date. This number is not expected to rise above 200–250 by the time the risk analysis programme is complete. The annualised fatality rate for roads under RTA control, since 1960, is approximately 0.3. This is consistent with the pattern emerging from the risk analysis programme.

5 CONCLUSIONS

Slope risk management for a highway network requires procedures that can be applied to a wide range of conditions, using a large number of practitioners, if the task is to be completed within reasonable time and budget constraints. The procedures must provide sufficient accuracy in risk assessment to provide a sound basis for subsequent management programmes. The overall system must also be comprehensive and able to cope with continuous changes to the network and to individual sites.

RTA NSW has developed a system that addresses these requirements. It is based on a complete inventory of slopes, acquired in GIS format, from which sites are selected for risk analysis, based on a very brief inspection and criteria for quickly identifying the possible presence of significant hazards. Risk analysis is undertaken using a rapid procedure, which gathers critical information about each site. The site information is managed through a database that incorporates the critical information from each site, including sketches and photographs as well as risk analysis results.

Critical issues in applying the procedures have been ensuring that significant sites and hazards affecting them are not missed, reliability in recording locations, maintaining consistency in risk analysis and preventing conservatism in analysis. These are addressed through use of experienced practitioners, an extensive training programme and an intensive auditing programme.

Reproducibility to about an order of magnitude in risk analysis has been found to be an adequate basis for a risk management programme. Supplementary studies may be needed for large or complex areas. Quantitative analysis should be reserved for cases where the risk is high and the cost of remediation is large, requiring the proposed management strategy to be justified in detail.

ACKNOWLEDGEMENTS

REFERENCES

ANCOLD 1997. Guidelines on the design of dams for earthquake. Melbourne, Australian National Committee for Large Dams.

Australian Geomechanics Society 2000. Landslide risk management concepts and guidelines. *Australian Geomechanics 35(1): 49–92*

Baynes, F.J, Lee, I.K. & Stewart, I.E. 2002. A study of the accuracy and precision of some landslide risk analyses. *Australian Geomechanics 37(2): 149–155.*

Fell, R. & Hartford, D. 1997. Landslide risk management. In Cruden, D.M. & Fell, R. (eds), *Landslide risk assessment*. Rotterdam, Balkema.

Hendrickx, M.A., Wilson, R.A., Moon, A.T. & Stewart, I.E. 2005. Slope hazard assessment on a coast road in New South Wales, Australia. *In prep (this volume)*.

Roads and Traffic Authority, NSW 2001. *RTA guide to slope risk analysis Version 3.1.* Sydney, Roads and Traffic Authority.

Stewart, I.E. & Buys, H.G. 2005. Managing slope risk for a large highway network. *In pr*ep.

Stewart, I.E, Baynes, F.J. & Lee, I.K. 2002. The RTA Guide to Slope Risk Analysis Version 3.1. *Australian Geomechanics 37(2): 115–147.*

Wilson, R.A, Moon, A.T, Hendrickx, M.A. & Stewart, I.E. 2005. Application of quantitative risk assessment to the Lawrence Hargrave Drive project, New South Wales, Australia. *In prep (this volume)*.

*Hazard and risk assessment:
individual landslide projects*

InSAR monitoring of the Frank Slide

V. Singhroy
Canada Centre for Remote Sensing, Ottawa, Canada

R. Couture
Geological Survey of Canada, Ottawa, Canada

K. Molch
MIR Télédétection on assignment at the Canada Centre for Remote Sensing, Ottawa, Canada

ABSTRACT: In this study, we used interferometrically derived images, from several radar satellites (RADARSAT, ERS and ENVISAT), to monitor current post slide motion at the Frank Slide, a $30 \times 10^6\,\text{m}^3$ slide-rock avalanche, in the Canadian Rockies. The images cover the period from July 1993 to June 2004. Our results show that the Frank slide is still active and the deformation process is localized and are related to seasonal and local weather conditions. This information is useful in assisting to locate in-situ field monitoring at specific locations, and to plan mitigation strategies. The combination of satellite differential InSAR techniques, covering large areas, and site-specific GPS monitors can produce an integrated monitoring system of active slopes.

1 INTRODUCTION

Remote sensing techniques are increasingly being used in slope stability assessment. (Murphy & Inkpen 1996, Singhroy et al. 1998, Singhroy & Mattar 2000, Singhroy & Molch 2004). Recent research has shown that differential interferometric SAR techniques can be used to monitor landslide motion under specific conditions. (Vietmeier et al. 1999, Rott et al. 1999). Provided coherence is maintained over longer periods, as is possible e.g. in non-vegetated areas, surface displacement of a few centimeters per year can be detected. Using data pairs with short perpendicular baselines, short time intervals between acquisitions, and correcting the effect of topography on the differential interferogram, reliable measurements of surface displacement can be achieved.

Our study focused on the Frank Slide, a $30 \times 10^6\,\text{m}^3$ rock avalanche of Paleozoic limestone, which occurred in 1903 from the east face of Turtle Mountain in the Crowsnest Pass region of southern Alberta, Canada. Seventy fatalities were recorded.

Several investigations have focused on characterizing grain size and distribution of this rock avalanche, in order to understand post-failure mechanism and mobility (Couture et al. 1998, Cruden & Hungr 1986). "Factors contributing to the slide have been identified as the geological structure of the mountain, subsidence from coal mining at the toe of the mountain, blast induced seismicity, above-average precipitation in years prior to the slide, and freeze-thaw cycles" (Alberta Environment 2000). In 2001, 6000 tons of rock fell from the north slope of the Frank Slide, which led to our InSAR investigation. Currently, the Government of Alberta is installing GPS stations to monitor post slide activity at specific locations. Our InSAR results will assist in locating in-situ monitors, as well provide a regional and seasonal view of gravitational mass movement.

2 DATA AND PROCESSING

ERS, ENVISAT and RADARSAT data were used for InSAR analyses. In order to select a set of suitable ERS scenes a thorough baseline analysis of all ascending scenes acquired over the location (track 406, frame 989) during summer between 1992 and 2001 was performed. It was of interest to find as many data pairs as possible during that time period, yet keep the perpendicular baselines ideally below 100 m, thus reducing contributions of topography on the differential phase as much as possible. Ascending orbit was chosen since its look direction corresponds to the aspect of the slope.

Seven ERS scenes, which yielded four data pairs with perpendicular baselines below 100 m (Table 1), were initially selected for processing. The scenes span between 1993 and 1997. Additionally, twenty

Table 1. Data pairs processed to date.

Date master	Date slave	Beam mode	Time between acquisitions days	Perpendicular baseline m
ERS				
24 Jul 93	17 Jul 95	–	723	569
24 Jul 93	21 Aug 95	–	758	693
24 Jul 93	25 Sep 95	–	793	325
17 Jul 95	22 Jul 97	–	736	38
21 Aug 95	22 Jul 97	–	701	86
21 Aug 95	26 Aug 97	–	736	4.5
22 Jul 97	26 Aug 97	–	35	91
RADARSAT				
21 Sep 00	15 Oct 00	F1	24	332
21 Sep 00	08 Nov 00	F1	48	285
15 Oct 00	08 Nov 00	F1	24	174
24 Oct 03	17 Nov 03	F1	24	332
24 Oct 03	09 Apr 04	F1	159	76
ENVISAT				
15 Apr 04	20 May 04	IS-7	35	464
28 Apr 04	02 Jun 04	IS-4	35	351

RADARSAT scenes, acquired between 2000 and 2004, as well as four ENVISAT ASAR image mode pairs (April to June 2004) with different incidence angles (IS-3, IS-4, IS-6, and IS-7) were ordered. The suitable ERS data pairs, as well as – to date – several of the ENVISAT and RADARSAT-1 SLC data were interferometrically processed to geocoded vertical displacement maps using EV-InSAR by Atlantis Scientific Inc. Figure 1 shows selected results of each sensor, displayed over an elevation model.

2.1 *Optimization*

During the processing of the ERS data, the precise orbit data provided by the Delft University of Technology were used (http://www.deos.tudelft.nl/ers/precorbs/). The ENVISAT and RADARSAT data were processed using the ephemeris data provided. Within the differential interferometry processing sequence it was ensured that Master-to-Slave coregistration was precise to a root-mean-square error of better than 0.1 pixels in range and azimuth at the tie points. Employing a simulated SAR image generated from the external DEM, the DEM-to-Master coregistration was refined to below 2 pixels RMS, ensuring the best fit possible. Topographic phase contribution was removed using a CDED 1:50,000 DEM. Azimuth spectral overlap and baseline decorrelation filtering were performed where spectral overlaps fell below 90%.

For all data pairs processed to date, coherence values are generally high on the slide itself, even for temporal baselines of more than 700 days. Values e.g. for the Aug-95/Aug-97 ERS data pair (736 days, $B\perp$ 4.5 m)

are in the range of 0.73 to 0.91. This can be attributed primarily to the lack of vegetation on the slide and indicates a general stability of the individual scatterers on the slope.

Residual topographic phase was removed from the differential interferogram through baseline refinement by iteratively adjusting the slave state vector. This led to an improved differential interferogram, especially for data pairs with longer baselines.

The phase was unwrapped using an iterative disk-masking algorithm. The unwrapped phase was then translated to vertical height change values and subsequently geocoded.

To date the data sets listed in Table 1 have been processed and evaluated. Selected results are presented in Figure 1.

3 DISCUSSION

In this study we analysed the InSAR images from three different types of radar satellites over different time periods. Interpretation of these images are presented below (Fig. 1).

3.1 *ERS-1/ERS-2: August 1995–August 1997*

The InSAR deformation map shows negative vertical surficial deformation between 5 to 20 mm situated above the coal seam and below the regional fault and its splay. The localized slope deformation may be the result of a local surficial slope failure within the colluvium (e.g. old and recent rock fall debris) accumulated
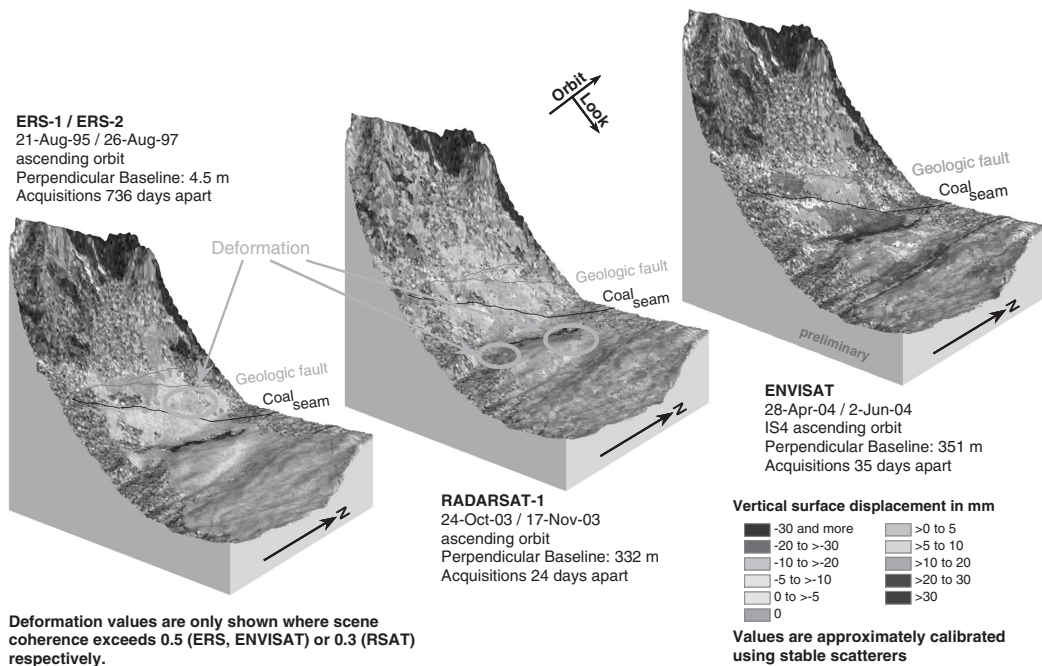
612

Figure 1. Surface deformation maps, interferometrically generated from ERS, RADARSAT-1, and ENVISAT ASAR data.

at the base of the slope. The other most likely scenario is the presence of deformation with the substratum underlying the colluvium, i.e. deformation due to past coal mining activities. Deformation associated to the fault is doubtful, as the measured deformation is localized, well below the fault and not linear, as it would be expected if it were related to the regional fault.

3.2 Radarsat-1: October–November 2003

Significant negative vertical surface displacements up to 30 mm are shown during this 24 day period. This deformation is located within the debris of the 1903 rockslide-rock avalanche and in the alluvium of Crowsnest River. Deformation within the alluvium is probably the result of river erosion associated with peak runoff during intense autumn rainfall events. However, the presence of significant deformation within the debris mass away from the river and the transportation corridor may be due to the removal of granular material from a borrow pit(largest red zone in the debris).

3.3 Envisat: April–June 2004

The surface deformation map produced by ENVISAT images shows numerous zones of significant vertical surface displacement, both positive and negative

vertical displacements. The images used to build the deformation map were taken from April to June, i.e. a critical time of the year for occurrence of gravitational mass movements. Surface deformation situated at the base of the mountain slopes presents a negative value and therefore would be mostly associated with settlement of colluvium and rock avalanche debris; settlement that often occurs following snow melt and ground thaw season. It is difficult to identify which portion of the deformation is associated to gravitational mass movements since there is no positive vertical surface movement in the mountain slope that would be indicative of material transfer from the source area to the deposition area. In addition, the presence of positive vertical displacements within the debris (north and south of the highway) is difficult to explain other than it is either the result of "readjustment" of the particles (e.g. boulders, blocks) due to frozen ground thawing, or less likely, resulting from regional ground displacement. In addition, zones of deformation on both sides of the transportation corridor may be the result of small gravitational mass movements (small localized slumps) along railway and highway cuts. Finally, zones of deformation in the uppermost parts of the slopes are associated to failures in bedrock that had produced rockfalls. This is typical, during springtime, since the higher frequency of

freeze-thaw cycles is responsible for failures along rock fractures.

4 CONCLUSION

Our research has shown that by using different radar satellites, it is possible to continuously monitor large active slopes. Not having to rely on one satellite alone is increasing our InSAR monitoring capability. The series of InSAR images indicate the different level of activity of the slopes (large and small) in the vicinity of Frank with respect to time of year. It is clear, that gravitational mass movements activities are localized and related to weather and seasonal conditions, with springtime being the most active.

ACKNOWLEDGMENTS

REFERENCES

Alberta Environment 2000. *Geotechnical Hazard Assessment – South Flank of Frank Slide*. Edmonton: Alberta Environment.

Couture, R., Locat, J, Drapeau, D., Evans, S. & Hadjigeorgiou, J. 1998. Evaluation de la granulométrie à la surface des débris d'avalanche rocheuse par l'analyse d'images. *Proceedings 8th International IAEG Congress, Vancouver, 21–25 September 1998*: 1383–1390.

Cruden, D. & Hungr, O. 1986. The debris of Frank Slide and theories of rockslide-avalanche mobility, *Can. J. Earth Science* 23: 425–432.

Murphy, W. & Inkpen, R. 1996. Identifying landslide activity using airborne remote sensing data. *GSA Abstracts with Programs* A-408: 28–31.

Rott, H., Scheuchl, B., Siegel, A. & Grasemann, B 1999. Monitoring very slow slope movements by means of SAR interferometry: A case study from a mass waste above a reservoir in the Ötztal Alps, Austria. *Geophysical Research Letters*, 26(11): 1629–1632.

Singhroy, V., Mattar, K. & Gray, L. 1998. Landslide characterization in Canada using interferometric SAR and combined SAR and TM images. *Advances in Space Research* 2(3): 465–476.

Singhroy, V. & Mattar, K. 2000. SAR image techniques for mapping areas of landslides. *Proceedings XIXth ISPRS Congress, Amsterdam, 16–23 July 2000*: 1395–1402.

Singhroy, V. & Molch, K. 2004. Characterizing and monitoring Rockslides from SAR techniques. *Advances in Space Research*. 33(3): 290–95.

Vietmeier, J., Wagner, W. & Dikau, R. 1999. Monitoring moderate slope movements (landslides) in the southern French Alps using differential SAR interferometry. *Advancing ERS SAR Interferometry from Applications towards Operations; Proceedings of Fringe '99 Workshop, Liège, Belgium, 10–12 November 1999*.

Coupling kinematic analysis and sloping local base level criterion for large slope instabilities hazard assessment – a GIS approach

M. Jaboyedoff
Quanterra, Lausanne, Switzerland and Institute of Geomatics and Risk Analysis (IGAR), University of Lausanne, Switzerland

F. Baillifard
Baillifard Géosciences, Bruson, Switzerland

R. Couture
Geological Survey of Canada, Ottawa, Canada

M-H. Derron
Geological Survey of Norway, International Center for Geohazards, Trondheim, Norway

J. Locat & P. Locat
Université Laval, Québec, Canada

ABSTRACT: Based on the concept of the Sloping Local Base Level (SLBL) a method for detection of large rockslides is proposed and illustrated. This method states that if the volume available for erosion is high above the SLBL, the presence of preexisting structures favorable to sliding should increases greatly the creation of instabilities. Because instabilities are viewed as part of larger unstable systems, it implies that pre-existing instabilities exist and recent rockfall may also be detected.

1 INTRODUCTION

The detection of large, potentially unstable rock masses remains a challenge. Often these potential instabilities are not detected, or detected only because of unusual rockfall activities. The widespread availability of digital elevation models (DEM) makes it possible to investigate new detection methods for large rockfalls. Such a method is proposed in this paper using three examples.

Potential for rockfall has been assessed for many years using rock mass rating systems (Romana 1993, Mazzoccola & Hudson 1996). A new tendency is to associate these assessments with Geographical Information Systems (GIS) (Wagner et al. 1988, Rouiller et al. 1998, Jaboyedoff et al. 2004, Gokceoglu et al. 2000, Meentemeyer & Moody 2000, Günther 2003).

For the detection of large rockfalls or deep-seated landslides, most of these researches aimed at identifying the main mechanical principles of slopes stability (Terzaghi 1962, Cruden 1976, 1988, Schmidt & Montgomery 1995, Locat et al. 2000). Some attempts to assess large landslide hazards have used simple mechanical modeling (Miller 1995), and more recently geomorphic analysis (Jaboyedoff et al. 2004a, b, Roering et al. in press)

Some authors (Cruden & Martin 2004, Leroueil 2001, Sartori et al. 2003) have proposed that large landslides are usually the result of a long period (several thousands of years) of destabilization called the pre-failure stage (Leroueil 2001).

Based principally on the analysis of large rockslides, namely Frank (Cruden & Martin 2004, Cruden & Krahn 1973) and Randa (Sartori et al. 2003), important features controlling the stability of rockslopes can be extracted and analyzed with a GIS. These factors are: 1) the slope of the rockslide undercut; 2) unfavorable structural features such as faults, discontinuities or bedding; 3) the volume of rock between ground level and a deep potential sliding surface (Fig. 1).

The first two features are taken into account in the kinematic analysis. The third one, the rock mass volume lying above a potential sliding surface, is estimated with the Sloping Local Base Level (SLBL) concept.
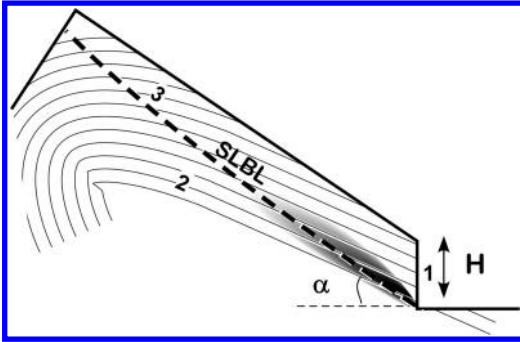
Figure 1. Main features of present deep-seated landslides: (1) undercut slope, (2) preexisting structures and (3) deep potential sliding surface. The grey area indicates the highly stressed zone (Adapted from Terzaghi 1962, Castelli 2000, Eberhardt et al. 2004).

If the possibility of sliding (kinematic analysis) exists simultaneously with the presence of a potential large volume above the SLBL, it can be assumed as a detection criterion. Recent rockfalls and the presence of deposits are additional evidences for potential rockslides. This method has been tested in three well-documented case studies (Jaboyedoff et al. 2004a, b, Baillifard et al. 2004).

2 METHODS

2.1 *Sloping Local Base Level*

Potentially unstable rock volumes can be detected with the Sloping Local Base Level (SLBL) concept, which locates the lowest sliding surface for a slope with a given topography (Fig. 2).

The SLBL can be defined as the surface joining all local minima of altitude of a valley. These can be rivers or other geomorphic features. They are considered fixed during the processing of the SLBL surface. With a DEM, the local topographic minima can be found using stream network generation through GIS (Burrough & McDonnell 1998). Then, computed streams are used as fixed points. The SLBL is calculated using an iterative routine that lowers each point of the DEM located above the average altitude of two opposite points among its four direct neighbors. The procedure is iterated up to convergence (Jaboyedoff et al. 2004b).

The volume defined between the actual topography and the SLBL is the available volume for deep-seated landslides. The SLBL is often physically detectable in the field (Jaboyedoff et al. 2004b, Jaboyedoff et al. in prep.). Comparison of SLBL results with numerical modeling (Eberhardt et al. 2004) shows that the SLBL is located where the extension strain area is maximal (shaded zone in Fig. 1).
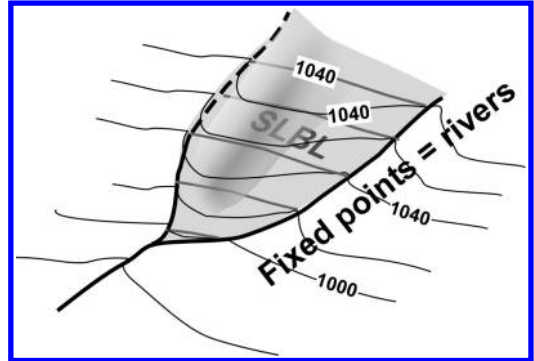

Figure 2. Illustration of the concept of SLBL, i.e. the lowest possible failure surface.
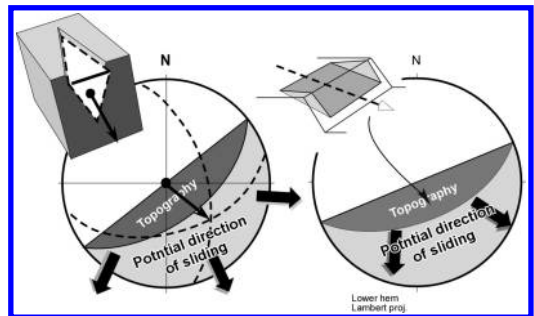
Figure 3. Search of the potential sliding direction for wedge (left) and planar sliding (right). The light grey indicates the potential direction of sliding, which are also indicated by large arrows.

Depending on the order of the streams used to compute the SLBL, different volumes will be obtained, corresponding to erosion/mass wasting processes of different scales.

2.2 *Kinematic analysis*

By comparing the topography orientation with the discontinuity orientations, a kinematic analysis, such as the Markland's test (Hoek & Bray 1981) is possible (Fig. 3). If the mean spacing (L) and the average trace length ($\overline{T}$) of each set of discontinuities are known, it is then possible to quantify the spatial frequencies of hazardous structures (sliding planes or wedges) on a DEM (Gokceoglu et al. 2000, Günther 2003, Jaboyedoff et al. 2004a). If δ is the angle between the pole of a cell of a DEM and the pole of a discontinuity, the apparent surface density of the hazardous structure on the topography is given by:

$$\rho_s = \frac{1}{L\overline{T}\sin\delta} \tag{1}$$

Although if L and $\bar{T}$ are often unknown, this formula permits a relative scale of structure frequency to be calculated. The higher ρ_s, the higher is the probability of finding dangerous structures.

2.3 *Large structural feature mapping or prediction*

Kinematic analysis indicates where slides are geometrically possible but not if these structures exist. Large structural features such as faults or dip slopes can usually be identified on a DEM and/or on aerial and terrestrial photographs. It is also possible to extrapolate the traces of faults on a DEM using the orientation of geomorphic features shaped by regional structures (Jaboyedoff et al. 2004b).

2.4 *Pre-existing instabilities and rockfall activities*

Frequently, pre-existing instabilities are reported within or in the neighborhood of active and past landslides (Govi 1989, Chigira & Kiho 1994, Agliardi et al. 2001, Sartori et al. 2003, Cruden & Martin 2004). The occurrence of pre-existing instabilities is a sign of a long history of destabilization of a slope. They indicate that movements have occurred and therefore imply that nearly continuous failure surfaces have been created. It is usually assumed that the slopes have been moving since the last glacial retreat (Agliardi et al. 2001, Cruden & Martin 2004).

Rockfalls, which are often linked to the presence of preexisting instabilities, appear frequently few days, months or years before a major event (Govi 1989, Sartori et al. 2003, Cruden & Martin 2004). They are the signs of a progressive failure or a reactivation leading to an event (Leroueil 2001, Eberhardt et al. 2004).

2.5 *Proposed criteria*

Assuming that large rockslides occur when large volumes of rocks are potentially erodible and when favorable structural features for sliding are present, a seven-step procedure is proposed:

1. Estimation of the volumes that can be potentially involved in landslides (volumes above the SLBL);
2. Search for large structures (faults) and extrapolations on a DEM;
3. Search for main discontinuity sets (smaller scale than 2), by photo analysis, laser-DEM analysis or rapid field investigations;
4. Identification of the zones where unfavorable structural arrangements (2 and 3) are frequent and can lead to rockslides according to the kinematic test (sliding plane, wedge and toppling);

5. Identification on aerial photographs or from Laser DEMs of old instabilities in the neighborhood of a potential large volume identified with criteria 1 and 2;
6. Identification of rockfalls: blocks or forest destructions;
7. Definition of the zones simultaneously possessing several of the properties of steps 1 to 6, and validated by using aerial photographs.

The 5 criteria of steps 1, 2, 4, 5 and 6 can be identified within a GIS, on kinematic test and thickness above SLBL maps, and aerial photographs. For a specific area, the number of satisfied criteria leads to a rating of the potential for large rockfall instability. It is assumed that the criteria of steps 1 and 2 are required, the others being conditional with respect to the first two. This is not straightforward because the different criteria detected through the 6 steps do not necessarily overlay on one point even if they are linked to the same instability. As a consequence the simple intersection of criteria is not sufficient. The count of criteria at a specific location (a cell) must include a spatial range around that point in which criteria are counted. This has not yet been included in the present release of the method. Thus we have mainly tested the method on known cases. The present stage of development of the method verifies if known instabilities possess those features. Note that the rockfall activity or the pre-existing instability are signs of an active slope, which means that slow processes are made visible by fastest manifestation.

3 CASE STUDIES

Different case studies have been selected to check if the proposed method is effective. Most of the arguments are based on the Randa rockfall experience.

3.1 *Randa*

The Randa cliff is the frontal part of a spur inherited from glacial erosion, located above the village of Randa (10 km north of Zermatt, Switzerland). The lower part of the spur is made of competent orthogneiss of Permian age. The upper part is made of less competent paragneiss. On April 18, 1991, 22 million m^3 of rock fell from the slope. A second rock mass of 7 million m^3 fell down on May 9, 1991. The main characteristics of the Randa rockfall are summarized below and can be found in detail in Sartori et al. (2003).

The Randa rockslide was mainly controlled by a large discontinuity (J$_3$) lying at the bottom of the cliff and belonging to a regional fault system at the scale of the valley (Fig. 4). Four other discontinuity sets subdivide the unstable volume into large blocks, creating
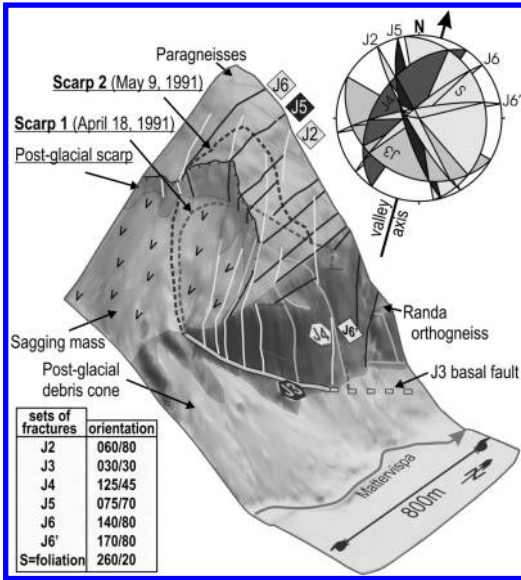
Figure 4. Main structural features of the pre Randa rock-fall topography (modified after Sartori et al. 2003).

a composite backward failure surface (Sartori et al. 2003). J_3 faults are also one of the main features forming the landscape of the area (Jaboyedoff et al. 2004b).

Twenty years before the rockslide event, the cliff of Randa had been affected by increasing rockfall activity. It is clear that a large sagging mass developed on the south side of the Randa spur during the last several hundred or thousand years (Sartori et al. 2003).

The Randa spur represents the largest and thickest potential erodible volume defined by the SLBL within a surrounding region of more than $400\,km^2$ (Jaboyedoff et al. 2004b, c). The fixed points used for the SLBL computation are the streams calculated from a $25 \times 25\,m$ DEM. Some artifacts of the stream generation routine have been removed by hand after computation (Fig. 5). The Randa spur appears as a large unique volume. A flat area situated on the top of the spur confirms the actual physical existence of the SLBL (Fig. 6). The simulations of Eberhardt et al. (2004) have also confirmed that the calculated SLBL is located along the most stressed zone (Fig. 1). Furthermore, a second planar surface delimits an imbricated second surface (SLBL' in Fig. 6).

3.2 *Arvel*

The rock face of Arvel is located 2 km eastward from the eastern part of the lake of Geneva (Switzerland) within Rhone valley. The rock is an alternation of limestone and marl of Lower Jurassic age (Fig. 7).
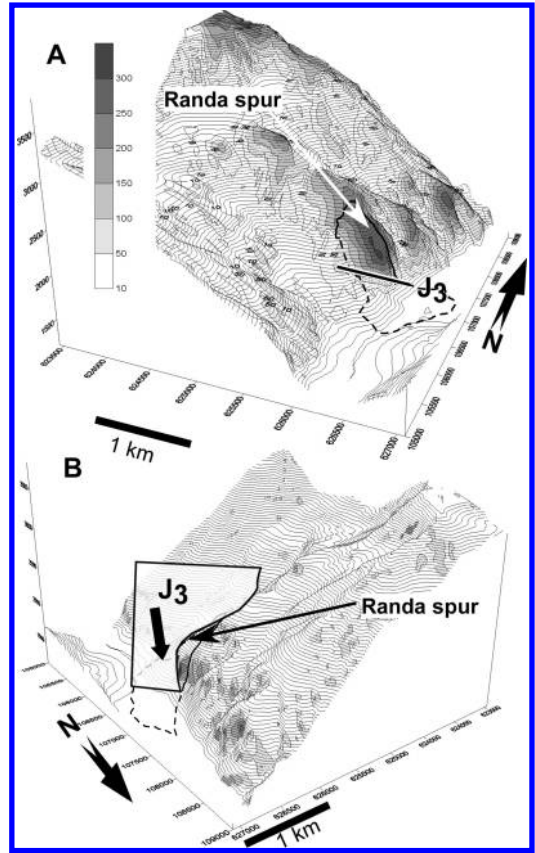
Figure 5. (A) Rock mass thickness above the SLBL in meters and location of the basal discontinuity J_3 on the pre-rockfall topography of Randa. Note the agreement between the locations of highest thickness values, J_3 and rockfall scars. (B) The grey scale represents the relative density of J_3 discontinuities where the kinematics condition of sliding is verified (DHM25© 2004 swisstopo (BA045928)).

At 4 PM, on 14th March, 1922, a $615,000\,m^3$ rock mass fell down on the alluvial plain of the Rhone valley (Choffat 1929, Jaboyedoff 2003). The main destabilizing factor was a quarry situated at the foot of the cliff. The workers were evacuated because of anomalous rock fall activity.

The slope is controlled by two main persistent discontinuity sets (J3 and faults system F2), forming a quite flat wedge with the movement direction parallel to the slope direction (Locat et al., in prep.). Both discontinuity sets crosscut the cliff. A third discontinuity set (J1) is steeper and acts as a lateral limit. The kinematic analysis for wedges indicates clearly that the area close to the rockslide is characterized by a relatively high fracture density (Fig. 8). From the cross-section after Choffat (1929), it is clear that the slope was in a

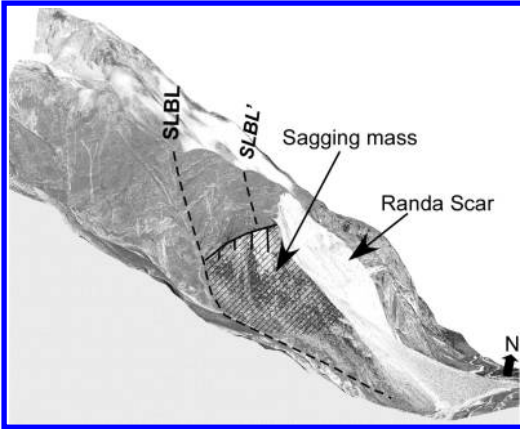Figure 6. 3-D representation of the main morphologic feature of the Randa rockfall area (DHM25© 2004 swisstopo (BA045928)).

Figure 7. Rock face after the rockfall of Arvel (form Choffat 1929, reproduced with the authorization of the Société vaudoise des Sciences naturelles). The rock face width measures approximately 250 m.

destabilizing phase. A scarp is clearly visible on the top of the fallen mass. The rockfall scar has clearly the highest available erodible volume above the SLBL within the entire slope (Fig. 8). Furthermore, a failure surface crosscuts the present outcrop and can be considered as a physical manifestation of the SLBL,
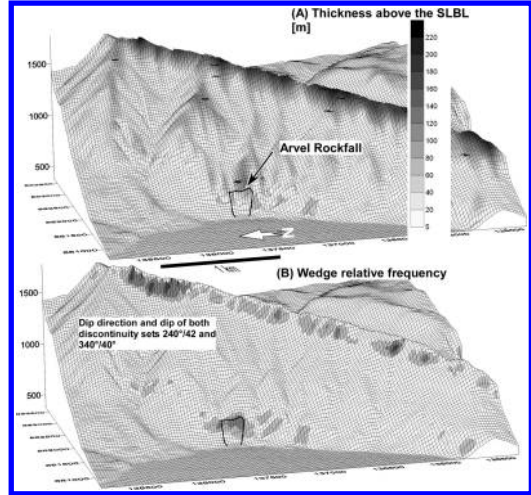

Figure 8. (A) Thickness above the SLBL. The crest presents high SLBL and can be considered as an artifact of the method; nevertheless it is an active zone of rockfall. (B) Wedge density showing the particular situation of the cliff of Arvel.

because it joins the small valley on both sides on the spur (Jaboyedoff et al. in prep.).

3.3 Frank slide

The eastern slope of Turtle Mountain fell down on April 29, 1903, in a 30 M m^3 rock avalanche killing 70 people of the mining town of Frank situated in the Canadian Rockies (southern Alberta). Turtle Mountain cuts an asymmetric anticline affecting a Paleozoic series thrusted over a Mesozoic series. Slope destabilization by coal mining is suspected, but is certainly not the main factor of causing slope destabilization (Cruden & Martin 2004).

The toe of the Frank slide is linked to either a sliding plane following bedding (Cruden & Krahn 1973) or other faults (Jones 1993). These major structures certainly weakened the slope. Several joint sets affect the slope (Cruden & Krahn 1973, Jaboyedoff et al. 2004d). A wedge with an axis direction parallel to the slope direction and dipping with an angle of about 30° has probably favored the toppling of the slope using the joints as shear surface. Furthermore, a subvertical fault system acts as a detachment surface for the wedges (Fig. 9).

Cruden & Martin (2004) suggested that the movement affecting Turtle Mountain began long before the rockslide. Pictures taken before the slide clearly indicate rockfall activity (McConnell & Brock 1904). On drawings from these pictures (Fig. 10a), the greyed area indicates the expected area of active rockfalls.

A DEM of the slope before the slide is not yet available; thus any considerations about the SLBL
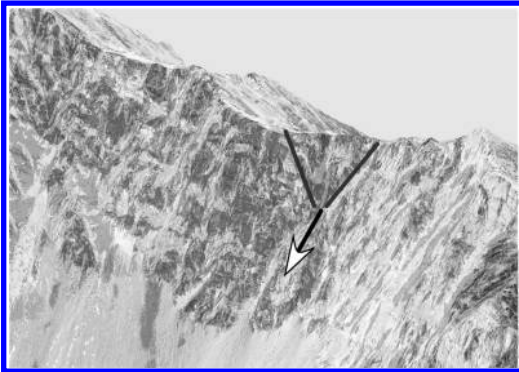
619

Figure 9. Wedge identified on the present scar of Frank slide (Source Geological Survey of Canada). [see Colour Plate XII]
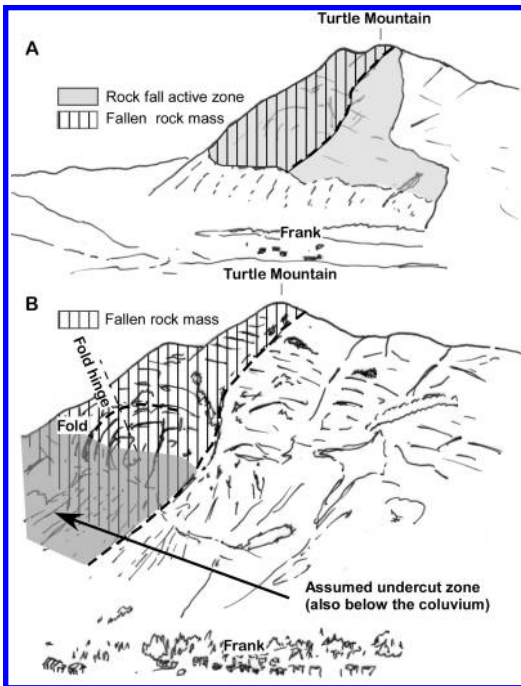

Figure 10. (A) Drawing after a picture from McConnell and Brock (1904) indicating active rockfall area before the rockslide. (B) Drawing after a postcard showing the future rockfall.

can only be very speculative Cruden & Martin (2004) state that Turtle Mountain was partly undercut by the river, which potentially generated a gravitational mass movement along the slope. Thus, as suggested by Figure 10, the SLBL computation on a pre-event topography would presumably indicate a large erodible volume at the location of Frank slide.

3.4 *Other examples for further assessments of the method*

On 28 July 1987, a rockslide occurred in northeastern Italy (Valtellina). Around 30 to 40 M m^3 fell down to the valley of Adda (Govi 1989). Regional discontinuities have clearly controlled the rockslide mechanism (Crosta, pers. comm.). Furthermore it is clear from pictures (Azzoni et al. 1992) that recent rockfall affected the slope and that pre-existing instabilities were present. The two streams along the instability indicate that the rock slope is incised. This suggests that the volume involved by the rockslide had certainly a high erodible volume above the SLBL.

The Ruinon slide, N-E Italy, is an active 30 M m^3 rockslide (Agliardi et al. 2001). This instability is part of a larger slope instability delimited by a basal sliding surface that can be identified as to a SLBL. Overlapping with regional faulting and discontinuity sets are also demonstrated. Recent rock falls are also reported.

4 DISCUSSION

From these examples, it is clear that the example instabilities can be part of larger unstable systems affecting in some cases entire slopes. Slope destabilization often initiated just after glacier retreat. But it seems also that some instabilities underlined by the SLBL, like in Randa, pre-date the last glaciation. The Randa rockfall area appears to be a large ancient instability that has been eroded and remodeled by the last glaciation.

The criteria proposed in the procedure are verified at all the study sites, at least qualitatively. Most of the unstable volumes are detected with the SLBL and are undercut. The link to preexisting structures is always made clear, by controlling either the geometry of the instability or the destabilization mechanism (wedge toppling, fragmentation). In any case, there are large structures with orientations that favor sliding. Preexisting instabilities are always present, underlining the slow slope evolution. But usually the catastrophic instability itself is the result of an acceleration of the slope movements. It happens at a particular location belonging to a larger destabilization system that evolves because of continuously changing conditions. Often the last stage (days to years) of destabilization leads to rock fall.

The rate at which the slope stability can change is controlled by other parameters than those presented here (e.g. water infiltration, which is function of the dismantling slope; water table level changes; weathering of the slope).

The idea is that where the structure is favorable, slope destabilization increases greatly if the volume

620

above the SLBL is large. This mass creates a zone of high stress near an unfavorable structure as demonstrated by Eberhardt et al. (2004). This is more or less a retrogressive failure process.

Combining the use of the SLBL with the kinematic analysis permits the analysis of large areas. Aerial photographs and detailed inspections can be used to find other indications (e.g. pre-existing instabilities, rock falls and large structures). At present, this procedure is not entirely automatic because all the parameters used are not necessarily located at the same points, but they can be distributed over the entire slope system. Moreover new technologies, such as *InSAR*, can provide the rate of slope movement as a new parameter.

It must also be underlined that some geological settings affect a slope in a similar way as undercutting or structures. For example packing down and/or dissolution can generate slope gravitational movement, as for example the La Clapière mass movement, where anhydrite dissolution is expected (Guglielmi et al. 2000).

5 CONCLUSIONS

As mentioned, the different criteria presented here can be implemented in a GIS. Nevertheless, some improvements are needed in order to reach an automatic procedure.

It is clear that a thick mass above the SLBL induces high stresses at the slope toe, which progressively leads to failure. The expression of such slope activity has been observed in large unstable systems. Then the detection of large potentially unstable volumes is important. The procedure successfully identifies rock masses that have failed and it can be considered promising.

ACKNOWLEDGMENTS

REFERENCES

Agliardi, F., Crosta, G. & Zanchi, A. 2001. Structural constraints on deep-seated slope deformation kinematics. *Engineering Geology* 59(1–2): 83–102.

Azzoni, A., Chiesa, S., Frassoni, A. & Govi, M. 1992. The Valpola landslide. *Engineering Geology* 33: 59–70.

Baillifard, F., Jaboyedoff, M., Rouiller, J.D., Couture, R., Locat, J., Locat, P., Hamel, G. & Robichaud, G. 2004. Towards a GIS-based rockfall hazard assessment along the Quebec City Promontory, Quebec, Canada.

In: Lacerda, W.A., Ehrlich, M., Fontoura, A.B. and Sayo, A. (eds): *Landslides Evaluation and stabilization*. 207–213. Balkema.

Burrough, P.A. & McDonnell, R.A. 1998, Principals of Geographical Information Systems: Oxford University Press.

Castelli, M. 2000. A simplified methodology for stability analysis of rock slopes with non-persistent discontinuity systems. In Yufin (ed.), *Geoecology and computers*: 185–190. Rotterdam: Balkema.

Chigira, M. & Kiho, K. 1994. Deep-seated rockslide-avalanches preceded by mass rock creep of sedimentary rocks in the Akaishi Mountains, central Japan. *Engineering Geology* 38: 221–230.

Choffat, Ph. 1929. L'écroulement d'Arvel (Villeneuve) de 1922. *Bull. Soc vaudoise Sci. Nat.* 57: 5–28.

Cruden, D.M. 1982. The Brazeau Lake slide, Jasper National Park, Alberta. *Canadian Geotechnical Journal* 19: 975–981.

Cruden, D.M. 1988. Thresholds for catastrophic instabilities in sedimentary rock slopes. *Zeitschrift fur Geomorphologie* 67: 67–76.

Cruden, D.M. & Martin, C.D. 2004. Before The Frank Slide: Preparatory & Triggering Causes from Maps and Photographs. *Proceedings 57th Canadian Geotechnical Conference, GeoQuébec 2004*.

Cruden, D.M. & Krahn, J. 1973. A re-examination of the geology of Frank slide. *Canadian Geotechnical Journal* 10: 581–591.

Eberhardt, E., Stead, D. & Coggan, J.S. 2004. Numerical analysis of initiation and progressive failure in natural rock slopes – the 1991 Randa rockslide. *International Journal of Rock Mechanics and Mining Sciences* 41(1): 69–87.

Gokceoglu, C., Sonmez, H. & Ercanoglu, M. 2000. Discontinuity controlled probabilistic slope failure risk maps of the Altindag (settlement) region in Turkey. *Eng. Geol.* 55: 277–296.

Govi, M. 1989. The 1987 Landslide on Mount Zandila in the Valtellina, Northern Italy. *Landslide News* 3: 1–3.

Guglielmi, Y., Bertrand, C., Compagnon, F., Follacci, J.P. & Mudry, J. 2000. Acquisition of water chemistry in a mobile fissured basement massif: its role in the hydrogeological knowledge of the La Clapière landslide (Mercantour massif, southern Alps, France. *J. Hydrology* 229: 138–148.

Günther, A. 2003. SLOPEMAP: programs for automated mapping of geometrical and kinematical properties of hard rock hill slopes. *Computers and Geosciences* 29(7): 865–875.

Hoek, E. & Bray, J. 1981. Rock slope engineering, revised third edition, *E & FN Spon*, London.

Jaboyedoff, M. 2003. The rockslide of Arvel caused by human activity (Villeneuve, Switzerland): Summary, partial reinterpretation and comments of the work of Choffat, Ph. (1929): L'écroulement d'Arvel (Villeneuve) de 1922. Bull. SVSN 57, 5–28. *Quanterra OPEN FILE REPORT – NH-03 (http://www.quanterra.org/erosion_hazard.htm)*.

Jaboyedoff, M., Baillifard, F., Philipossian, F. & Rouiller, J.-D. 2004a. Assessing fracture occurrence using "weighted fracturing density": a step towards estimating rock instability hazard. *Natural Hazards and Earth System Sciences* 4: 83–93.

Jaboyedoff, M., Baillifard, F., Couture, R., Locat, J. & Locat, P. 2004b. New insight of geomorphology and landslide prone area detection using DEM. In: Lacerda et al. (eds), *Landslides Evaluation and stabilization*: 199–205. Balkema.

Jaboyedoff, M., Baillifard, F., Couture, R., Locat, J. & Locat, P. 2004c. Toward preliminary hazard assessment using DEM topographic analysis and simple mechanic modeling. In Lacerda et al. (eds), *Landslides Evaluation and stabilization*: 191–197. Balkema.

Jaboyedoff, M., Couture, R. & Locat, P. 2004d. Structural Analysis of Turtle Mountain (Alberta) Using Digital Elevation Model (DEM). *Proceedings 57th Canadian Geotechnical Conference, GeoQuébec* 2004.

Jaboyedoff, M. et al. (in prep.). Evidence of the sloping local base level. *Natural Hazards and Earth System Sciences*.

Jones, P.B. 1993. Structural geology of the modern Frank Slide and ancient Bluff Mountain Slide, Crownest, Alberta. *Bulletin of Canadian Petroleum Geology* 41: 232–243.

Leroueil, S. 2001. Natural slopes and cuts: movement and failure mechanisms. *Geotechnique* 51: 197–243.

Locat, P, Couture, R., Locat, J., Leroueil, S. & Jaboyedoff, M. (in prep.). Fragmentation energy in rock avalanches. *Can. J. Geotech.*

Locat, J., Leroueil, S. & Picarelli, L. 2000. Some considerations on the role of geological history on slope stability and estimation of minimum apparent cohesion of a rock mass. In Bromhead et al. (eds), *Landslides in research, theory and practice,* 8th International Symposium on Landslides, Cardiff, 935–942.

Mazzoccola, D.F. & Hudson, J.A. 1996. A comprehensive method of rock mass characterization for indicating natural slope instability, *Quarterly Journal of Engineering Geology* 29: 37–56.

McConnell, R.G. & Brock, R.W. 1904. Report on the great landslide at Frank, Alberta, Department of the Interior, Annual Report for 1903, Ottawa, Part 8.

Meentemeyer, R.K. & Moody, A. 2000. Automated mapping of conformity between topographic and geological surfaces, *Computers & Geosciences* 26 (7): 815–829.

Miller, D.J. 1995. Coupling GIS with physical models to assess deep-seated landslide hazards. *Environmental & Engineering Geoscience* 1: 263–276.

Roering, J.J., Kirchner, J.W. & Dietrich, in press. Characterizing structural and lithologic controls on deep-seated landsliding: Implications for topographic relief and landscape evolution in the Oregon Coast Range, USA, *Geological Society of America Bulletin*.

Romana, M.R. 1993. A geomechanical classification for slopes: Slope mass rating. In: J.A. Hudson (Editor), *Rock testing and site characterization*: 575–600. Pergamon Press, Oxford, United Kingdom.

Rouiller, J.-D., Jaboyedoff, M., Marro, C., Philippossian, F. & Mamin, M. 1998. Pentes instables dans le Pennique valaisan. Matterock: une méthodologie d'auscultation des falaises et de détection des éboulements majeurs potentiels. Rapport final du PNR31. VDF, Zürich.

Sartori, M., Baillifard, F., Jaboyedoff, M. & Rouiller, J.-D. 2003. Kinematics of the 1991 Randa rockfall (Valais, Switzerland). *Natural Hazards and Earth System Sciences* 3(5): 423–433.

Schmidt, K.M. & Montgomery, D.R. 1995. Limits to relief. *Science* 270: 617–620.

Terzaghi, K. 1962. Stability of steep slopes in hard unweathered rock. *Géotechnique* 12: 251–270.

van Westen, C.J. 2004. Geo-information tools for landslide risk assessment : an overview of recent developments. In Lacerda et al. (eds), *Landslides Evaluation and Stabilization*: 39–56. Balkema.

Wagner, A., Leite, E. & Olivier, R. 1988. Rock and debris-slides risk mapping in Nepal – A user-friendly PC system for risk mapping, in: Landslides. In Bonnard, C. (Ed.) *Proceedings of the 5th International Symposium on Landslides, Lausanne, Switzerland, 10–15 July 1988*: 1251–1258. Balkema, Rotterdam.

Reliability analysis of iron mine slopes

J.A.C. Maia & A.P. Assis
University of Brasília, Brazil

ABSTRACT: This paper aims to analyse the reliability of typical slopes of the Timbopeba Iron Mine, which is one of the deepest open pits in Brazil, with a maximum depth of more than 500 meters. As usual in most open pits, the behavior of its slopes has been structurally controlled by discontinuities. Using data of typical slopes of the Timbopeba Mine, related to slope and discontinuity geometry, and others related to shear strength, reliability analyses were developed using both the First-Order Second-Moment (FOSM) and Point-Estimate (Rosenblueth) methods to evaluate the reliability of the slopes. The reliability and use of the probabilistic approach were assessed in comparison to the traditional deterministic one, pointing out that higher values of the factor of safety do not exclude higher risks of slope failures.

1 INTRODUCTION

The Timbopeba Iron Mine is one of the deepest open pits in Brazil, with a maximum depth over 500 meters. The pit is aligned approximately in the North-South trend (52°/030°) and a major geology feature, called West Fault, can be observed. The eastern section of the mine is generally composed of sound rock, where only some local fractures are noticed due to blast operations. On the other hand, the western section presents a more complex geology, ranging from sound rock to highly weathered rock.

The behavior of rock masses is structurally governed by its discontinuities, which may be characterized by several parameters, such as number of families, dip and dip direction, spacing, roughness, strength, presence of filling etc. Some of these parameters are related to the discontinuities themselves, mostly affecting their shear strength, stiffness and permeability properties.

This paper presents the statistical characterization of the geometric and strength parameters of the discontinuities existing in the South Slope of the Timbopeba Mine. These data were used in slope stability analyses, following the probabilistic approach, applying both the First-Order Second-Moment (FOSM) and Point-Estimate (Rosenblueth) methods, in order to evaluate the reliability, and consequently, failure risk of this slope.

2 SLOPE STABILITY ANALYSES

Slope stability analyses performed were limited to the southern and southeastern slopes. However, only the
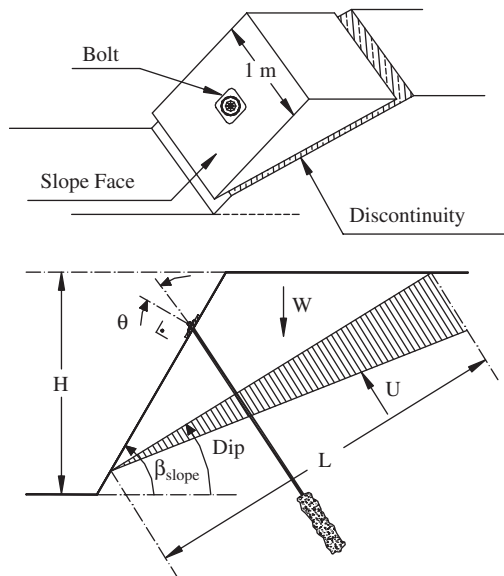

Figure 1. Southern slope geometry.

results related to the southern slope (52°/030°) are presented in this paper. Figure 1 shows the geometry of the southern slope. Other results can be found in Maia (2003).

As dip directions of the southern slope face and discontinuities are sub-parallel (within 20°), stability analyses were calculated by spreadsheet, based on the

623

single-block mechanism, as presented by Hoek & Bray (1981), given by the following equation:

$$FS = \frac{cL + \left[W\cos(Dip) - U + T\sin\theta \right]\tan\phi}{W\sin(Dip) - T\cos\theta} \quad (1)$$

where:
FS – Factor of safety;
c – Cohesion of the discontinuity;
L – Length of the discontinuity;
W – Weight of the sliding block;
Dip – Dip angle of the discontinuity;
U – Water force acting on the sliding surface;
T – Load of bolts;
θ – Installation angle of bolts;
φ – Friction angle of the discontinuity.

In order to calculate some of these parameters (L, W and U), it is also necessary the height (H), face angle (β_{slope}) and direction of the slope, and unit weights of the rock and water. Data presented in Table 1 are the summary of the statistical analyses carried out by Durand (1995), Cavalcante (1997) and Lauro (2001), reporting the average of values (means), standard deviation (σ) and the coefficient of variation (CV), which is the ratio between the standard deviation and the mean.

The adopted bolt for these studies presents a maximum load capacity of 200 kN, with an installation angle of 10 degrees, upwards to the perpendicular line to the sliding plane. Stability analyses treated the slope as being either dry or under saturated conditions.

Table 1. Summary of the statistical analyses of the slope geometry and discontinuity shear strength parameters (modified from Maia 2003).

	Mean	Standard deviation (σ)	CV (%)
c′ (MPa)	2.1	1.4	67
φ′ (degree)	38.2	13.3	35
H (m)	255.6	6.7	3
β_{slope} (degree)	45.4	6.1	13

Table 2. Conventional and vector analyses data of discontinuity family 1 (modified from Maia 2003).

Data type	Dip (degrees)		Dip direction (degrees)	
	mean	σ	mean	σ
Conventional	42.0	08.7	045.0	012.9
Vector	44.1	04.0	030.8	082.6

Regarding the discontinuities, the only family noticed in the southern slope is the one called F1, as presented in Table 2. As a discontinuity plane is defined by a vector (dip and dip direction), its data were treated by two different means, conventional and vector analyses in order to calculate the mean and standard deviation values. Conventional data were obtained by stereo nets, using the program Dips (Hoek & Diederichs 1991). Vector data analysis followed that proposed by Priest (1985).

3 RELIABILITY INDEX

The conformity of a Project is generally determined by evaluating the capacity of the system to deal with demands imposed upon the project, by users and the environmental. Acceptable levels of conformity, or of risk, are subject to judgments, taking into account social and economic aspects (Ang & Tang 1975). The evaluation of risk and safety in civil and environmental engineering projects is traditionally based on factors of safety (FS). Factors of safety values are established by designers and clients based on their experiences on similar projects (Kottegoda & Rosso 1997).

Another alternative for evaluating a project is the reliability index (β). In terms of factor of safety, when it is less than 1, projects are potentially subject to failure. The reliability index, given by the following equation, establishes the distance from the mean factor of safety (μ_s) to the critical one (FS = 1), in terms of standard deviations (σ_s):

$$\beta = \frac{\mu_s - 1}{\sigma_s} \quad (2)$$

where β is the reliability index; μ_s the mean of the FS distribution and σ_s the standard deviation of the FS distribution.

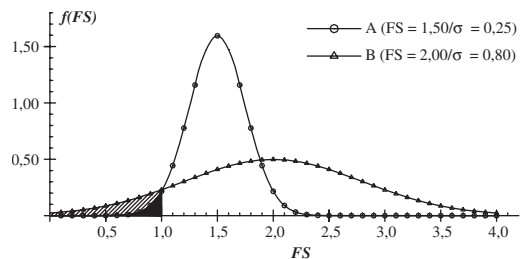Christian *et al*. (1994) define the probability failure (p_r) as been the area (integral) of the factor of

Figure 2. Two hypothetical projects with different FS and σ values (Christian *et al*. 1994).

624

safety distribution for FS values less than 1. The Figure 2 presents two hypothetical FS distribution curves (Project A and B). Project A, with lower FS value, but also lower standard deviation value, is safer than Project B, because it presents lower value of p_r.

4 ROSENBLUETH'S PROBABILISTIC METHOD

Initially the Rosenblueth's probabilistic method, also known as point estimate, was limited to analyses of three variables, but later was adapted for any number of statistical variables (Giani 1992). For Rosenblueth (1975) the distribution of one random variable X_i is concentrated in two specific points:

$$X_{i+} = \overline{X}_i + \sigma_i \qquad (3)$$

$$X_{i-} = \overline{X}_i - \sigma_i \qquad (4)$$

where $\overline{X}_i$ represent the value mean of the distribution of X_i and σ_i the standard deviation of the distribution of X_i.

The probabilities associated for these points are P_+ e P_-, which are function of no symmetry of distribution. In case of n variables, the Rosenblueth's probabilistic method need have 2^n estimated values for each combination of particular points X_{i+} e X_{i-} Figure 3. After realization of combination of particular points, start the probabilistic work through deterministic calculations, for this group of 2^n values. Therefore, for each new step of the probabilistic process, deterministic calculations are loaded for new values, i.e., new data are utilized in the next calculation.

Figure 3. Combination (2^n) of the particulars points X_{i+} and X_{i-} (Harr 1987).

5 PROBABILISTIC ANALYSES

For the probabilistic analyses, the Point-Estimate Method of Rosenblueth (1975) was adopted. Statistical variables are those listed in Table 1 and Table 2, related to the slope geometry (H and β_{slope}) and discontinuity family F1 ("Dip", c and ϕ). Besides these five statistical variables, it was also included the presence or not of bolts, and the presence or not of water pressure. The total number of runs would be 128 ($2^7 = 128$), as each variable has two point-estimates (mean plus standard deviation and mean minus standard deviation).

5.1 Parameter-relevance analyses

After considering all possible relevant parameter to this slope stability problem, the First-Order Second-Moment (FOSM) Method was used to verify the variables that may affect more the results (FS values). As described by Harr (1987), this method evaluates the variance of the FS distribution (V[FS]), as well as the contribution of each variable, as given by the following equation:

$$V[FS] = \left(\frac{\delta FS_{ii}}{\delta X_i}\right)^2 \times V[\delta X_i] \qquad (5)$$

where:
V[FS] – Variance of the FS distribution;
δFS_{ii} – Change in the FS value due to a small change of a certain statistical variable (δX_i);
δX_{ii} – Small change in certain statistical variable;
V[FS] – Variance in certain statistical variable (X_i).

To carry out a FOSM analysis, it is necessary $n + 1$ runs, where n is the number of statistical variables. The first run is done using the Equation. 1 and imputing all mean values of the statistical variables X_i (Table 3). Then, n runs are calculated evaluating the change in the FS value due to small changes in each statistical variable. The Table 3 presents the FOSM results for the southern slope and Figure 4 depicts the percentages of the influence of each statistical variable,

Table 3. FOSM results for the southern slope (Maia 2003).

X_i	δX_i	δFS_{ii}	$\dfrac{\delta FS_i}{\delta X_i}$	$V[X_i]$	Eqn 5
I Dip $= 42°$	$+4.2°$	0.192	0.046	$1.37°$	0.00287
c′ $= 2.1\,\mathrm{MPa}$	$+0.21$	0.011	0.054	1.92	0.00566
$\phi = 38.2°$	$+3.82°$	0.127	0.033	$2.91°$	0.00321
II Dip $= 45.4°$	$+4.54$	0.062	0.014	$0.64°$	0.00012
H $= 256\,\mathrm{m}$	$+25.6$	0.010	0.0004	44.7	0.00001

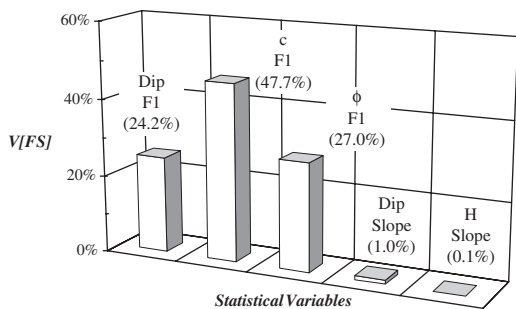I – Family 1 (F1); II – Slope. $V[FS]_{total} = 0.0119$

625

Figure 4. Influence of the statistical variables on the FS distribution variance.

Table 4. Summary of the FOSM analyses (Maia 2003).

	Data type	Without bolt	With bolt
V[FS]	Conventional	0.0119	0.0123
	Vector analysis	0.0423	0.0429
E[FS]	Conventional	0.989	0.993
	Vector analysis	1.105	1.115
σ[FS]	Conventional	0.10	0.11
	Vector analysis	0.17	0.18
β	Conventional	−0.10	−0.07
	Vector analysis	0.60	0.64

in relation to the total variance of the FS distribution variance is governed by the strength parameter (cohesion and friction angle) and dip of the discontinuity.

Table 4 presents a summary of results using conventional and vector analysis data of the statistical variables of southern slope, with and without bolts. These results are expressed in terms of variance of the FS distribution (V[FS]), mean of the FS distribution (E[FS]), standard deviation of the FS distribution (σ[FS]) and reliability index (β). Negative values of β were found, what means that the mean FS (E[FS]) is less than 1.

5.2 *Reliability analysis*

The probabilistic analyses were calculated by spreadsheet mentioned in Item 2. The data introduced from statistical variables, and its respective standard deviation was realized in a unique phase. However, for each new run four different slope situations were impost at a program, manually. The Table 5 shows those situations which represent the mobilized forces in the slope.

Table 6 shows input data utilized in the probabilistic analyses. In this table, it is possible to identify the constant and statistical data variables considered for this study.

After the calculate FS phase, its results were treated for knowledge the E[FS], σ[FS] and p_r which

Table 5. Summary of situations utilized in the probabilistic analyses.

Situation	Bolt	Water pressure
1	without	without
2	without	with
3	with	without
4	with	with

Table 6. Summary of input data utilized in the probabilistic analyses.

Data		Description
Constants		γ_{rock}
		γ_{water}
		Direction of the slope
		Load of bolt
		Installation angle of bolt
Statistical variables	Slope	Height – H (m)
		Face angle – β_{slope}
	Discontinuity	Dip – Dip (degrees)
		Cohesion – c (MPa)
		Friction angle – ϕ (degrees)

Table 7. Results from the probabilistic analyses.

Data	sup-port	Water pres-sure	Determ. E[FS]	Probabilistic E[FS]	σ[FS]	p_r (%)
Means	Without	I	0.99	1.20	0.61	2.42
		II	0	0.16	0.29	28.69
	With	I	0.99	1.21	0.61	2.43
		II	0	0.16	0.29	28.67
Vectors	Without	I	1.105	1.06	0.53	2.21
		II	0	0.01	0.02	32.07
	With	I	1.115	1.07	0.53	2.27
		II	0	0.01	0.02	31.99

I – Without; II – With.

behavior is descript by a log-normal distribution. The results are summarized in Table 7.

The results indicate a influence of the geometry of rock masses in the actuation of bolt, as well as the influence of water pressure in the FS, and consequently in the failure probability.

6 CONCLUSIONS

For mean and vector data, the slopes presented results within expected, then it indicates a good behavior of discontinuity. The lower standard deviation is responsible by that good behavior of discontinuity, which

626

can mean a small variation around its mean orientation. Then, the deterministic and probabilistic approach resulted in next values. Consequently, advantages have been observed of working with probabilistic tools for forecast and evaluation of events.

Other conclusion was that σ[FS] present values less than zero, in the great number. Thus, it reinforced the certain that studies, where variables present a higher variability, are perfectly predispose at use of probabilistic methods.

After to know the results of analysis, comparisons were realized between deterministic and probabilistic methods. It was observed satisfactory factor safety values from deterministic analyses. This is because a little variation of geometric discontinuity families data, as well as the strength data from own discontinuity.

7 FINAL COMMENTS

The applicability of the probabilistic methods is notorious when they are compared with the traditional deterministic methods, especially when the available data are well known and reliable, generating in this way little distortion of standard deviation in relation to the mean value of these data. Therefore, a highest number of data is necessary, which in certain times is impossible.

The great advantage of probabilistic methods is in its capacity in calculating the failure probability inherent at the engineering design. This capacity is contrary the idea that higher values of the factor of safety imply in projects more safe.

Finally, although have been observed higher values of the factor of safety do not exclude higher risks of slope failures. Because, higher natural variability of parameters presents in slope, as well as variability due local geology of at Timbopeba Mine.

REFERENCES

Ang, A.H.S. & Tang, W.H. 1975. Probability Concepts in Engineering Planning and Design: Basic Principles. John Wiley & Sons, New York, USA, vol. 1, 422 pp.

Cavalcante, R.F. 1997. Analysis of Pit Mine Slope Stability by Limit Equilibrium and Stress-Strain Methods (in Portuguese). M.Sc. Thesis, Publishing G.DM–046/97, Department of Civil and Environmental Engineering, University of Brasília, Brazil, 113 pp.

Christian, J.T., Ladd, C.C. & Baecher, G.B. 1994. Reliability Applied to Slope Stability Analysis. Journal of Geotechnical Engineering, ASCE 120(12): 2180–2207.

Durand, A.F. 1995. Slope Stability Study in Pit Mine Using Rock Mass Classification (in Portuguese). M.Sc. Thesis, Publishing G.DM–023/95, Department of Civil and Environmental Engineering, University of Brasília, Brazil, 192 pp.

Giani, G.P. 1992. Rock Slope Stability Analysis. Balkema, Rotterdam, Netherlands, 361 pp.

Harr, M.E. 1987. Reliability – Based Design in Civil Engineering. McGraw-Hill Publishing Company, New York, USA, 291 pp.

Hoek, E. & Bray, J.W. 1981. Rock Slope Engineering. Institution of Mining and Metallurgy, London, UK, 358 pp.

Hoek, E. & Diederichs, M. 1989. DIPS – Version 5.1. Rock Engineering Group Department of Civil Engineering, University of Toronto, Toronto, Ontario, Canada, 60 pp.

Kottegoda, N.T. & Rosso, R. 1997. Statistics Probability and Reliability for Civil and Environmental Engineers. McGraw-Hill Publishing Company, New York, USA, 735 pp.

Lauro, C.A. 2001. Probabilistic Model of 3D Distribution of Joints in the Mass Failure Rock (in Portuguese). D.Sc. Thesis, Publishing G.TD–008/01, Department of Civil and Environmental Engineering, University of Brasília, Brazil, 253 pp.

Maia, J.A.C. 2003. Probabilistic Methods Applied to Rock Slope and Underground Excavation Stability (in Portuguese). M.Sc. Thesis, Publishing G.DM–099/03, Department of Civil and Environmental Engineering, University of Brasília, Brazil, 192 pp.

Priest, S.D. 1985. Hemispherical Projection Methods in Rock Mechanics. George Allen & Unwin (Publishers) Ltd, London, UK, 124 pp.

Rosenblueth, E. 1975. Point Estimates for Probability Moments. Proceedings of the National Academy of Sciences of the United States of America 72(10): 3812–3814.

Evaluation of catastrophic landslide hazard on gentle slopes in liquefiable soils during earthquakes

A.C. Trandafir
Slope Conservation Section, Geohazards Division, Disaster Prevention Research Institute, Kyoto University, Japan

K. Sassa
Research Centre on Landslides, Disaster Prevention Research Institute, Kyoto University, Japan

ABSTRACT: This paper outlines a methodology for evaluating the likelihood of catastrophic landslide occurrence on gentle slopes in liquefiable soils during earthquake. The approach is based on a modified Newmark sliding block model of assessing the earthquake-induced undrained landslide displacements for conditions of no shear stress reversals on the sliding surface. By employing the shear resistance-displacement relationship from undrained monotonic ring shear tests, the simulation model incorporates the sensitivity of computed displacements to variations in yield acceleration. The proposed approach involves an examination of undrained seismic slope performance under various horizontal seismic waveforms scaled to different specific values of the peak earthquake acceleration. An example problem illustrates how the proposed methodology may be used to demarcate, based on the magnitude of permanent seismic displacement, the levels of low, moderate and high risk of catastrophic landslide on a gentle slope in a saturated cohesionless soil susceptible to liquefaction during earthquake.

1 INTRODUCTION

Catastrophic landslides occurred repeatedly on gentle slopes during past earthquakes in Japan causing significant damage to the local environment and posing serious threat to inhabitants' lives. The January 1995 Nikawa landslide (Hyogo Prefecture), January 1995 Takarazuka landslide (Hyogo Prefecture) or May 2003 Tsukidate landslide (Miyagi Prefecture) are representative examples of such seismically-induced catastrophic slope failures. Typically, the sliding surface of these landslides was comprised of saturated cohesionless materials, and the slope gradient was greater than 10° but not exceeding 20°.

Laboratory studies consisting of undrained ring shear tests on soil samples from Nikawa (Sassa 1996) and Tsukidate (Trandafir & Sassa 2004) landslides revealed a gradual loss in undrained shear resistance after failure with progress of shear displacement. This so-called "sliding surface liquefaction" phenomenon (Sassa 1996) culminated in undrained ultimate steady state strengths smaller than static (gravitational) driving shear stress on the sliding surface of the investigated landslides. Thus, the experimental results demonstrated the susceptibility of the sliding mass to an accelerated motion under static conditions (i.e., catastrophic

failure) if the shear strength loss due to some transient disturbance (e.g., earthquake) was large enough to bring definitively the shear resistance on the sliding surface below the gravitational driving shear stress.

The sensitivity of undrained yield resistance to progressive shear displacement noted in the case of previously mentioned landslides, suggests that a performance-based methodology is necessary to assess the slope vulnerability against an earthquake-induced catastrophic failure, rather than a pseudo-static traditional limit equilibrium approach based on the concept of safety factor. Accordingly, a modified formulation of the Newmark (1965) sliding block model was developed by Trandafir & Sassa (2004, 2005) to assess the earthquake-induced undrained displacements on shear surfaces in a saturated cohesionless soil for conditions of no shear stress reversals on the sliding surface.

Basically, under conditions of no shear stress reversals, a catastrophic failure will take place when the earthquake-induced shear displacement exceeds a critical level associated with a definitive drop of undrained shear strength to a value equal to the gravitational (static) driving shear stress, and smaller yield resistances characterize the undrained shear behavior of the soil beyond this stage of deformation (Trandafir & Sassa 2004, 2005). However, seismic stability analyses

carried out for various hypothetical infinite slopes by using the modified Newmark sliding block procedure (Trandafir & Sassa 2005) revealed that estimated permanent displacements smaller than the critical value should also be regarded as dangerous for the post-earthquake slope serviceability. In this framework, the present paper describes, via an example problem, a performance-based approach that could be used to evaluate for conditions of no shear stress reversals the earthquake-induced catastrophic landslide hazard on shear surfaces in liquefiable soils. The numerical study is conducted for the case of Tsukidate landslide triggered by the 26-May-2003 Sanriku-Minami earthquake in Tsukidate town, Miyagi Prefecture, Japan. This translational slide with a volume of about $10,000\,m^3$ is characterized by a horizontal traveling distance of about 180 m, and a maximum velocity of about 6–7 m/sec (Konagai et al. 2003). The landslide occurred on a gentle slope of about 14°, and according to the post-earthquake reconnaissance survey, failure took place along a shear surface located in fully saturated silty sand.

2 EXAMPLE PROBLEM

2.1 *Features of slide mass used in dynamic calculations*

The configuration of Tsukidate slide mass before failure is shown in Figure 1a. However, in order to be able

to study the seismic slope performance in undrained conditions, the geometry from Figure 1a is approximated by the equivalent infinite slope model depicted in Figure 1b. The main reason for this approximation is that the material on the sliding surface is a liquefiable soil showing a significant amount of generated excess pore pressure even at the incipient stages of deformation, and a gradual loss in undrained strength after failure (Fig. 1c) due to excess pore pressure built-up with progressive shear displacement (Trandafir & Sassa 2004). As noted later in the paper, for the infinite slope model shown in Figure 1b, the undrained yield resistance-displacement curve given in Figure 1c was employed to perform the undrained dynamic calculations. This relationship incorporates therefore the effects of excess pore pressure generation on the soil undrained shear strength. On the other hand, the influence of initial effective normal stress, σ'_0, and driving shear stress, τ_0, on the liquefaction resistance of saturated cohesionless soils attested by several researchers (e.g., Castro 1969, Kramer & Seed 1988, Vaid et al. 1995, Ishihara et al. 1999, Matsuo et al. 2002, Sivathayalan & Vaid 2002), is also representative for the material on the sliding surface of Tsukidate landslide (Trandafir & Sassa 2004). Obviously, for the real geometry of the investigated failure mass (Fig. 1a), the distribution of the initial (static) stresses (σ'_0, τ_0) generated by the gravitational forces is non-uniform along the actual sliding surface. Thus, after dividing the sliding mass in an appropriate number of
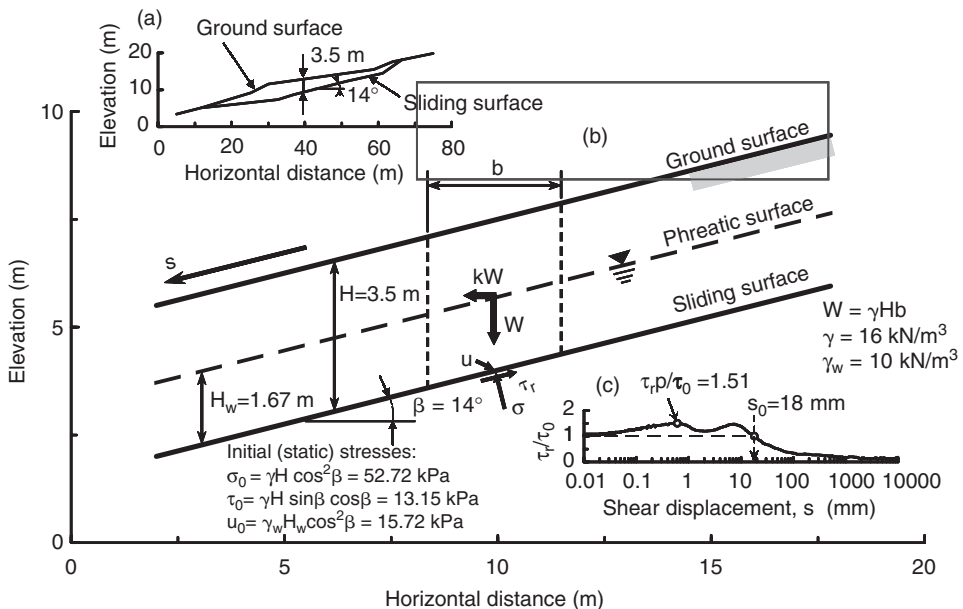

Figure 1.   Infinite slope characteristics (*b*) derived from the original configuration of the slide mass (*a*), and yield resistance-displacement curve (*c*) used in the seismic analysis.

630

slices and assuming, eventually, a uniform distribution of the initial stresses (σ'_0, τ_0) at the base of each slice, we would need to obtain the undrained yield resistance-displacement curves (such as the relationship in Fig. 1c) for every combination of initial stresses (σ'_0, τ_0) encountered at the base of the slices within the slide mass. These curves would enable us to estimate and update the undrained yield acceleration of the slide mass based on the undrained yield resistances mobilized at the base of the slices along the sliding surface at a specific shear displacement during earthquake. However, such an approach requires a generalized soil model that could reproduce the undrained shear behavior (and provide the undrained yield resistance-displacement relationship) for any combination of initial stresses (σ'_0, τ_0). The development of a soil model for the undrained monotonic shear behavior, especially in the ring shear apparatus, represents a quite difficult task, and at present, such model is not available. As an alternative, the equivalent infinite slope model (Fig. 1b) was considered for the seismic stability analysis carried out in undrained conditions. For the particular geometry of the investigated translational landslide (Fig. 1a), this simplification seems quite reasonable, and offers the advantage of a uniform distribution of stresses along the sliding surface under static conditions, which may be described by a single pair of values (σ'_0, τ_0), as seen in Figure 1b. Consequently, for a given location of the groundwater table, only one undrained monotonic ring shear test was necessary to obtain the undrained yield resistance-displacement relationship required for the seismic stability analysis. The groundwater level considered in Figure 1b is relatively close to the location of the phreatic surface found in the field at sites adjacent to Tsukidate landslide.

Figure 1c depicts the relationship between shear displacement, s, and yield resistance ratio, τ_r/τ_0, utilized in the subsequent numerical analysis. These data were obtained by Trandafir & Sassa (2004) from an undrained monotonic ring shear test conducted on the soil specimen sampled from the sliding surface of Tsukidate landslide. The test was carried out under initial stress conditions on the sliding surface associated with the infinite slope characteristics shown in Figure 1b, for a dry density after consolidation relatively close to the value estimated in the field (i.e., 1.1 g/cm^3). The experimental data (Fig. 1c) indicate a peak yield strength ratio, τ_r^p/τ_0, of 1.51, and a critical shear displacement (Trandafir & Sassa 2004, 2005), s_0, necessary to induce a catastrophic failure of about 18 mm. For earthquake-induced displacements greater than s_0, the slide mass is expected to develop an accelerated motion under static conditions due to the static driving shear stress (τ_0) exceeding the undrained yield resistance (τ_r) on the sliding surface (i.e., $\tau_r/\tau_0 < 1$ in Fig. 1c).

2.2 Equation of motion for undrained conditions on the shear surface

Assuming the slide mass in Figure 1b as a rigid body in translation driven downslope by a horizontal seismic force, the equation of motion may be written as (Trandafir & Sassa 2005):

$$\ddot{s} = (a - k_y\, g)\, \cos\beta \tag{1}$$

where $\ddot{s}$ represents the relative acceleration on the direction parallel to the sliding surface, β is the infinite slope angle, while a, g and k_y stand for the horizontal earthquake acceleration, gravitational acceleration and yield coefficient, respectively. The horizontal earthquake acceleration coefficient, k, rendering the inertia force, kW, in a soil column of width b and weight W (Fig. 1b), represents the ratio between the horizontal earthquake acceleration and gravitational acceleration (i.e., $k = a/g$). It is worth mentioning that parameters a and consequently, $\ddot{s}$ in Equation 1 are functions of time, t (i.e., $a = a(t)$, $\ddot{s} = \ddot{s}(t)$).

The horizontal yield coefficient for undrained conditions on the sliding surface is given by the following equation (Trandafir & Sassa 2005):

$$k_y = \left(\frac{\tau_r}{\tau_0} - 1\right)\tan\beta \tag{2}$$

Equation 2 makes use of the τ_r/τ_0-s relationship shown in Figure 1c in order to update the value of the undrained yield coefficient of the slide mass at a specific value of shear displacement during earthquake. The experimental outcomes of a laboratory study based on undrained monotonic and cyclic ring shear tests on soil specimens from Tsukidate landslide (Trandafir & Sassa 2004) demonstrated the accuracy of using (in dynamic calculations) the shear resistance-displacement relationship from undrained monotonic shearing (such as the one in Fig. 1c) as an estimate of the undrained yield resistance under seismic conditions for conditions of no shear stress reversals on the sliding surface. The step-by-step numerical integration procedure to calculate the dynamic displacements given the expression of relative acceleration, $\ddot{s}$, is explained in detail elsewhere (Trandafir & Sassa 2005).

Trandafir & Sassa (2004) investigated the influence of the vertical component of earthquake acceleration on the undrained seismic performance of the sample slope depicted in Figure 1b. According to the computational results, the accuracy of estimated undrained seismic displacements was not significantly affected by neglecting in dynamic calculations the vertical component of earthquake acceleration. In these circumstances, the simplification made in the present study by

631

considering only the horizontal component of earthquake acceleration seems reasonable.

2.3 *Seismic records used in the analysis*

The undrained seismic performance of the sliding mass shown in Figure 1*b* was investigated using ten input horizontal earthquake records depicted in Figure 2. Each seismic record was scaled to different specific values of the peak earthquake acceleration, $k_m g$, and the corresponding earthquake-induced undrained permanent displacements were estimated. As illustrated in Figure 2, the peak earthquake acceleration ($k_m g$) is defined in this study as the maximum value of earthquake acceleration on the positive side of an input accelerogram, irrespective of whether this value is smaller or greater than the maximum absolute value of earthquake acceleration on the negative side of the accelerogram. Positive values of the accelerograms shown in Figure 2 are associated in this analysis with horizontal inertia forces due to earthquake driving the sliding mass downslope; thus corresponding to the direction of kW shown in Figure 1*b*. For all of the numerical results presented herein, the condition of no shear stress reversals on the sliding surface (which is essential in the applicability of the previously introduced sliding block formulation) was satisfied during the calculated dynamic response.

3 OPERATION CHARTS

Figure 3 provides the relationship between the earthquake-induced undrained permanent displacement, s_p, (relative to the critical displacement, s_0, given in Fig. 1*c*) and the acceleration ratio, k_{yp}/k_m, for three input seismic records (i.e., Gilroy (337°), Gilroy (247°) and Sanriku-Minami (90°)). k_{yp} (constant = 0.127) stands for the peak yield coefficient in undrained conditions obtained by substituting in Equation 2 the corresponding values of τ_r^p/τ_0 and β given in Figure 1, whereas k_m represents the peak earthquake acceleration coefficient of the scaled input seismic record. Due to the non-linear nature of the diagrams depicted in Figure 3, this type of chart may be utilized to differentiate for a particular slope, the levels of risk associated with the onset of a catastrophic landslide during earthquake. Apparently, for permanent displacements in excess of $0.53s_0$ (i.e., zone III in Fig. 3), the relationships start to increase asymptotically towards the critical level s_0 with subsequent decrease in the acceleration ratio, indicating that from this stage of deformation, insignificantly larger peak accelerations (k_m) could trigger a catastrophic landslide. Therefore, estimated permanent displacements exceeding $0.53s_0$ should be regarded as unsafe, and associated with a high risk of catastrophic

failure. The slide mass could be considered safe against a catastrophic shear failure if the calculated earthquake-induced permanent displacement is smaller than $0.3s_0$ (i.e., zone I in Fig. 3), whereas estimated permanent displacements located within the transition interval ranging from $0.3s_0$ to $0.53s_0$ (i.e., zone II in Fig. 3) should represent a warning signal indicating the necessity for a careful evaluation of the dynamic stability of the analyzed slope.

We define the critical peak earthquake acceleration, $k_{mc} g$, as the peak earthquake acceleration required to induce an undrained permanent displacement equal to the critical displacement, i.e., $s_p = s_0$. Hence, $k_{mc} g$ stands for the minimum peak earthquake acceleration necessary to trigger a catastrophic failure. We also define the $k_{ms} g$ parameter as the value of the peak acceleration required to trigger a permanent displacement of $0.3s_0$ which represents the upper limit of zone I (i.e., safe zone) in Figure 3.

As the displacement curves from Figure 3, determined for different earthquake records, approach the s_0 and $0.3s_0$ levels at different acceleration ratios, it appears that, for the analyzed slope, k_{mc} and k_{ms} depend strongly on the characteristics of the input accelerogram. In the present investigation, the k_{mc} and k_{ms} parameters were estimated for all of the seismic records shown in Figure 2, considering both the positive and negative orientations of each accelerogram. For the considered earthquakes, these data were compiled in relation to the Arias intensity parameter, I_a, as seen in Figure 4. Arias intensity represents a commonly used energy-based measure of earthquake shaking severity, and offers the advantage of incorporating both the amplitude and duration elements of ground motion, as well as all frequencies of recorded motion. For a single component of motion in a given direction, Arias intensity (I_a) is defined as (Arias 1970)

$$I_a = \frac{\pi}{2g} \int_0^{t_s} a^2(t) \; dt \tag{3}$$

where t_s represents the duration of earthquake-shaking. The Arias intensity values used in the diagram given in Figure 4, were estimated by Equation 3 from the input accelerogram scaled to a peak acceleration ($k_m g$) of $0.5 g$. In this representation, the lower bounds of k_{mc} and k_{ms} values are used to separate the regions of peak earthquake accelerations that may cause a catastrophic failure, bring the slope near the brink of a catastrophic failure (i.e., zone II + III in Fig. 4) or on the contrary, showing no danger for the post-earthquake slope serviceability (i.e., zone I in Fig. 4). The diagram illustrated in Figure 4, offers the advantage of a quick assessment of the earthquake-induced catastrophic landslide hazard by knowing only the characteristics of the design earthquake (i.e., k_m and I_a).
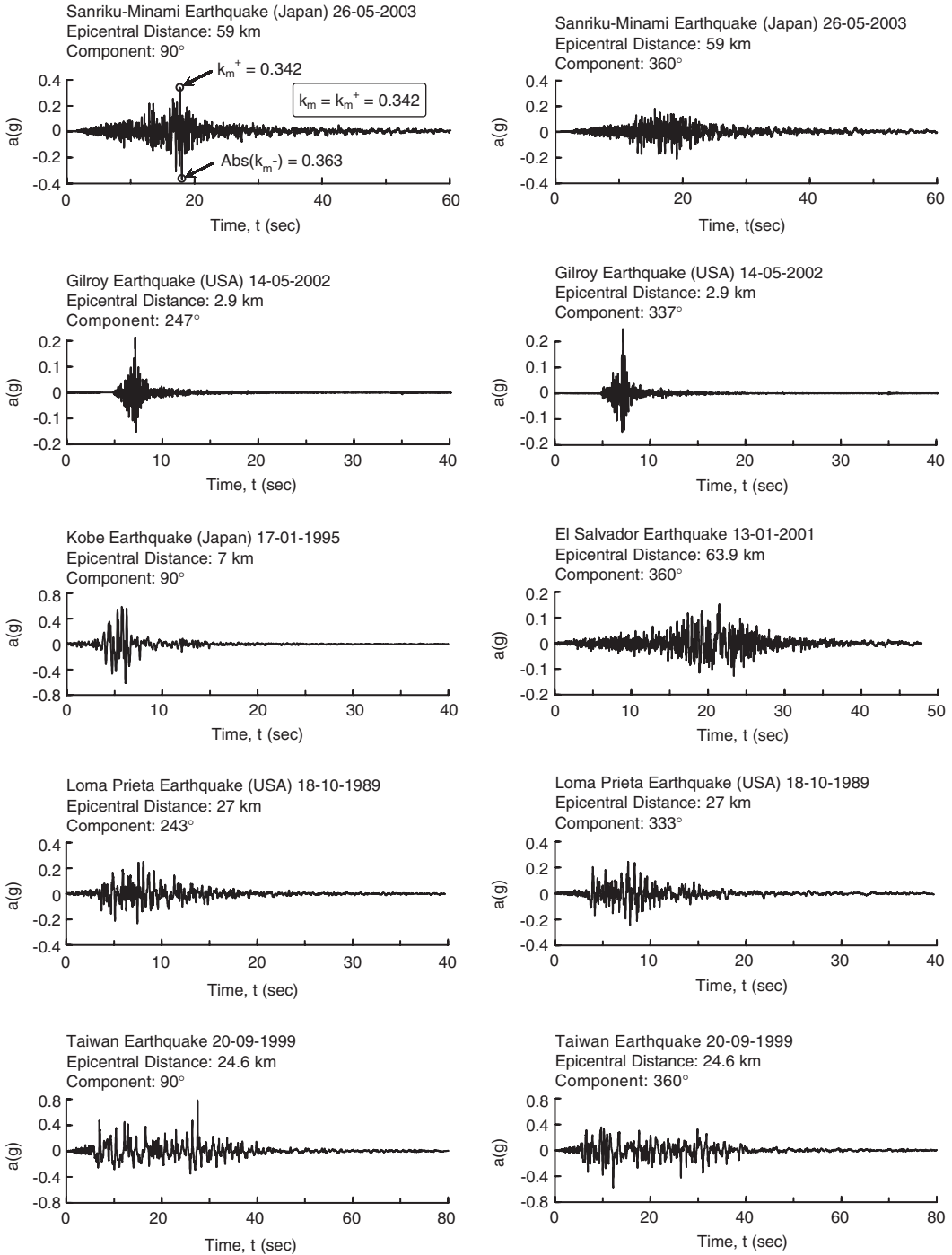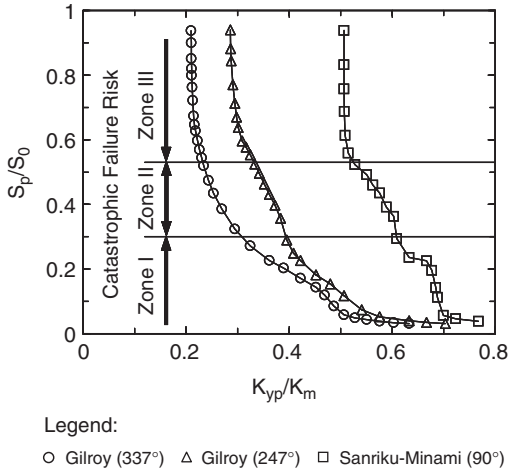
Figure 2. Input earthquake records.

Figure 3. Earthquake-induced permanent displacement, s_p, (relative to the critical displacement, s_0) versus acceleration ratio, k_{yp}/k_m.

4 CONCLUDING REMARKS

The performance-based approach described in this paper may be used to identify unacceptable permanent deformations, and estimate the minimum peak earthquake acceleration that could endanger the stability of gentle slopes in liquefiable soils susceptible to catastrophic failure under seismic conditions. By employing an easy-to-use sliding block model of evaluating the undrained seismic displacements, the proposed methodology represents for the practitioners a useful tool in performing quick and yet quantitative preliminary assessments of the earthquake-induced catastrophic landslide hazard. This information may be useful in deciding whether a more refined stability analysis based on comprehensive field and laboratory investigations, as well as numerical studies using more complex computational techniques (e.g., finite element method) should be undertaken in a subsequent stage to evaluate, in a more accurate manner, the slope vulnerability and eventually plan the mitigation measures against an earthquake-induced catastrophic failure.
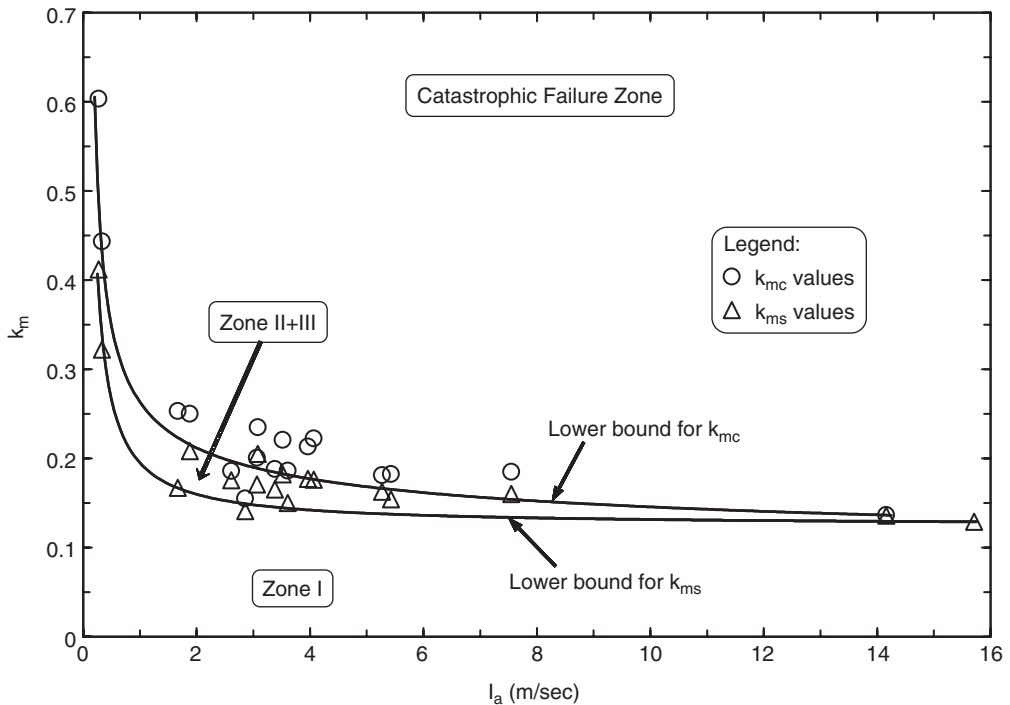

Figure 4. Coefficients of peak earthquake acceleration k_{mc} and k_{ms} (required to trigger levels of permanent displacement equal to s_0 and $0.3s_0$, respectively) in relation to Arias intensity, I_a, estimated for the corresponding seismic records scaled to $k_m g = 0.5\,g$.

634

REFERENCES

Arias, A. 1970. A measure of earthquake intensity. *R.J. Hansen, ed. Seismic design for nuclear power plants*. MIT Press, Cambridge, Mass.

Castro, G. 1969. Liquefaction of sands. *Ph.D. thesis*. Harvard University. Cambridge, Mass.

Ishihara, K., Tsukamoto, Y. & Nakayama, S. 1999. Flow-type failure of slopes based on behavior of anisotropically consolidated sand. *Proc. Int. Symp. Slope Stability Engng–IS-SHIKOKU'99, Matsuyama, Shikoku, Japan*, 1: 3–12.

Konagai, K., Ito, H. & Johansson, J. 2003. Features of Tsukidate landslide mass in the May 26, 2003, South-Sanriku earthquake. *Proc. 42nd Annual Conf. Japan Landslide Society, Toyama, Japan, 20–21 August*, 1: 233–236.

Kramer, S.L. & Seed, H.B. 1988. Initiation of soil liquefaction under static loading conditions. *Journal of Geotechnical Engineering, ASCE* 114(4): 412–430.

Matsuo, O., Saito, Y., Sasaki, T., Kondoh, K. & Sato, T. 2002. Earthquake-induced flow slides of fills and infinite slopes. *Soils and Foundations* 42(1): 89–104.

Newmark, N.M. 1965. Effects of earthquakes on dams and embankments. *Géotechnique* 15(2): 139–159.

Sassa, K. 1996. Prediction of earthquake induced landslides. *Proc. 7th Int. Symp. Landslides, Trondheim, Norway, 16–21 June*, 1: 115–132. Rotterdam: Balkema.

Sivathayalan, S. & Vaid, Y.P. 2002. Influence of generalized initial state and principal stress rotation on the undrained response of sands. *Canadian Geotechnical Journal*, 39(1): 63–76.

Trandafir, A.C. & Sassa, K. 2004. Newmark deformation analysis of earthquake-induced catastrophic landslides in liquefiable soils. *Proc. 9th Int. Symp. Landslides, Rio de Janeiro, June 28-July 2*, 1: 723–728. Rotterdam: Balkema.

Trandafir, A.C. & Sassa, K. 2005. Seismic triggering of catastrophic failures on shear surfaces in saturated cohesionless soils. *Canadian Geotechnical Journal* (*in press*).

Vaid, Y.P., Sivathayalan, S., Uthayakumar, M. & Eliadorani, A. 1995. Liquefaction potential of reconstituted Syncrude sand. *Proc. 48th Canadian Geotech. Conf., Vancouver, B.C.*, 1: 319–330.

Methodology: hazard characterization

Assessing landslide hazard on medium and large scales, using self-organizing maps

M.D. Ferentinou & M.G. Sakellariou
National Technical University of Athens, Athens, Greece

ABSTRACT: In recent years, experience has been accumulated in assessing and treating landslide hazard, though our knowledge still remains fragmentary. Consequently landslides and related instability phenomena in natural and manmade slopes remain an engineering geological problem. The study of basic landslide processes and mechanisms, as well as the rating of the critical parameters is crucial in order to carefully select the appropriate mitigation measures and finally predict future events. In the present paper, both quantitative and qualitative factors leading to landsliding were examined in terms of a holistic approach of instability phenomena. Causal factors such as geological formation, slope orientation, human intervention, number of soil raptures etc. were integrated in the model. Self Organizing Maps (SOM) training algorithms, which are unsupervised learning algorithms, were used in order to discover new knowledge offered through informative patterns. The research focused on the examination of the importance of the related factors, their dominance and interaction intensity. A landslide hazard assessment methodology is finally introduced, which couples both Geographical Information Systems (GIS) and Artificial Neural Networks (ANN). The study area is located in Evrytania district in Greece, an area that depicts high landslide frequency. The proposed methodology is valuable in the field of decision making and decision support studies for engineers, planners, developers, and other disciplines.

1 INTRODUCTION

Due to the population growth and the expansion of settlements and life-lines over hazardous areas the occurrence of landslides has increased. Landslide occurrence is a serious constraint on economic development both in the developed and developing world.

The assessment of landslide hazard and risk has become a topic of major interest for geoscientists and engineers as well as the local authorities. It is well known that landslide susceptibility mapping relies on a deep knowledge of slope movements and their causal factors.

In the current paper, both qualitative and quantitative factors involved in the abolition of equilibrium for natural or manmade slopes are implemented in a landslide hazard assessment model, in terms of a holistic approach of instability phenomena. Furthermore the dominance and interaction intensity of the factors is investigated through the use of computational tools called Artificial Neural networks (ANN). A ranking of the factors is calculated in an objective approach.

2 DETERMINATION OF THE PHYSICAL PROBLEM

Considering the various factors involved in slope instability, the practice of landslide hazard assessment requires in general:

– study of the instability processes
– analysis of the triggering factors
– representation of the spatial distribution of these factors

Landslide hazard zonation requires a detailed knowledge of the processes that are or have been active in a study area and the factors leading to the occurrence of a potentially damaging phenomenon. The objective is usually to assess the critical factors contributing to landsliding in order to both decide on the appropriate remedial measures and predict future events.

The factors leading to landsliding according to Varnes (1984) are the following:

– Geological conditions, lithological units and structures.

– Data describing the geometry of the slope and the morphometry of the entire study area.
– External factors (slope angle change, loading of slope, artificial vibration, rapid drawdown, weathering, etc.).

According to Working Party on World Landslide Inventory – WL/PLI (1990), landslide causal factors are the following:

– Geological causes (weak materials, jointed or fissured materials, contrast in permeability, contrast in stiffness, adversely oriented structural discontinuities).
– Morphological causal factors (tectonic uplift, fluvial or wave erosion of slope toe, deposition loading).
– Physical causal factors (intense rainfall, prolonged precipitation, earthquake loading and weathering).
– Human causes (excavation of slope toe, loading of slope or its crest, deforestation, etc.).

In order to execute the investigation on landslide processes we implemented in the analysis the factors leading to instability phenomena for which we had adequate data. The data come from Ziourkas (1989) and Ziourkas & Koukis (1989) and the main research focuses on the assignment of the weighting values of the various parameters, their dominance and interaction intensity.

3 INTRODUCED METHODOLOGY

The present work aims at contributing to advance our knowledge on the predominant factors weighting up, as objectively as possible, the influence of the various factors on landsliding in order to construct a realistic map of potential landslide hazard.

The introduced hazard assessment methodology could be characterized as a logical analytical model. In this kind of model landslide hazard is expressed by an equation in which the independent variables (causal factors) are tied together by various weights, depending upon the influence they exert on the independent value slope movement. This particular methodology is also categorized in quantitative methods because it uses computational neural networks in order to assign weigh values to the various factors contributing to landsliding.

The factors are selected cautiously in terms of a holistic approach in order to describe the phenomenon utterly. Subsequently the interaction intensity and the sequence the factors are determined using self organizing maps and generic matrix coding (Hudson 1992). Overlay and combination of the selected factors leads to the production of landslide hazard maps.

The introduced methodology comprises the following steps:

1. Determination of the list of causal factors that will be included in the analysis.
2. Determination of the thematic layers.
3. Assessment of reference system – data transformation.
4. Logical and physical database design, data input and verification and data manipulation.
5. Overlay of thematic layers.
6. Application of exploratory data analysis using self organizing maps algorithm.
7. Assignment of weighting values to the various causal factors.
8. Database output and presentation through landslide hazard maps and evaluation of the results taking into consideration the engineering geological regime of the study area.

3.1 Determination of the list of causal factors that will be included in the analysis

The study area is divided into terrain units, the size of which is related to the scale of the Digital Terrain Model and the scale of the geological mapping. Then, the causative factors considered are chosen after a careful bibliographical review. These factors for the current study are shown in Table 1.

3.2 Determination of the thematic layers

Maps deriving from topographical – geological maps are first digitized to obtain vectorical maps, which are then rasterized by dividing the area into cells of 40 m at the side. Each factor implemented in the analysis is stored in a different thematic layer and afterward is stored in the GIS. Construction of the steepness slope, aspect maps, altitude and relief maps, referring to morphometrical information, is practically automatic beginning from the Digital Elevation Model, (DEM), which in its turn was automatically constructed by

Table 1. Causal factors investigated.

Classification	Nr	Symbol	Causal factor
Geological conditions	1	LIT	Lithology
	2	GM	Layers orientation compared to slope
Geometrical conditions	3	SL	Slope steepness, slope angle
	4	ALT	Altitude
	5	REL	Relief
	6	RAI	Mean annual rainfall
	7	MANT	Weathering mantle thickness
External factors	8	AZI	Slope orientation
	9	ACT	Effect of human activity to vegetation
	10	DEN	Maximum seismic intensity

digitizing the contour lines with contour intervals of 40 m. These maps are obtained from a simple rasterizing of the digitized maps. In case of data coming from mean annual rainfall maps, seismic intension maps they are obtained in a similar method, first digitizing the original maps and then rasterizing them.

3.3 *Determination of scale and reference system*

Following the selection of the parameters, all the information is georeferenced in the geographic reference system Universal Transverse Mercator (UTM) since the topographical maps used were based on this Cartesian system. The overall of data layers which refer to the morphometric, geological characteristics and external factors information of the study area should follow the identical reference system. The scale required in order to construct the final landslide hazard map should be the same for all the thematic maps and is defined according to the scale of the geological and the accuracy of the DEM.

3.4 *Data base design and development*

Data base design follows the steps of the determination of the logical and physical design of a data base. Transformations are necessary to convert the variables from symbolic data to such a form that the modeling method can best utilize them. The proposed modeling tool can only utilize numerical information. Subsequently data referring to quantitative information must be coded into numerical data. Data must retain their scalability and physical meaning after the transformations.

3.5 *Overlay of thematic maps*

An overlay of the thematic maps is accomplished and a geographical database is constructed. Each terrain unit that is each record in the data base has information for the whole of the factors involved in the analysis that is for all the items of the data base.

3.6 *Application of exploratory data analysis using self organizing maps*

Data elements are exported from the GIS and are imported in a neural network system of unsupervised learning. We used Self Organizing Map (SOM) Toolbox. The self organizing map (Kohonen 1995a, b, Kohonen et al. 1999) is a special type of neural network that can learn from complex, multi-dimensional data and transform them into visually decipherable clusters. This specific algorithm has been used for a wide variety of applications, mostly for engineering problems but also for data analysis. It has been essentially applied in various engineering applications in system recognition, image analysis, process monitoring and fault diagnosis.

Basically, the SOM is a visualization, clustering and projection tool. The SOM has properties of both vector quantization and vector projection algorithms. It is found to be essentially suitable for data understanding and it has proven to be a valuable tool in data mining especially in high dimensional data. The self organizing maps illustrate structures in the data in a different manner than, for example, multidimensional scaling, a more traditional multivariate data analysis methodology. The SOM algorithm concentrates on preserving the neighborhood relations in the data instead of trying to preserve the distances between the data items. It illustrates structures, multivariate relations between data items, in high-dimensional data sets. Thus it is suitable for cluster analysis and it reveals non-linear relations between data.

Cluster analysis is a technique for grouping subjects into clusters of similar elements. In cluster analysis, we try to identify similar elements comparing their attributes. Groups or clusters are formed that are homogenous and different from other groups. SOM networks combine competitive learning with dimensionality reduction by smoothing the clusters with respect to an "a priori" grid and provide a powerful tool for data visualization.

Due to all above mentioned characteristics of this specific training algorithm we decided to apply it in the field of landslide hazard assessment in order to investigate the non-linear relations and tendency of cluster creation among the causative factors of instability phenomena. SOM toolbox offers efficient visualization techniques in a form that large amounts of detailed information are presented in an efficient and easy to understand approach.

There are a number of techniques for visualization offered from SOM. One of these is small multiples or scattered diagrams. In this kind of visualization objects in small multiples can be linked together using similar position or place. These scatter diagrams can be coded appropriately and become generic interaction matrices (Hudson 1992). Other kinds of visualizations offered from SOM and used in the current work are U-matrices and distance matrices. Analyzing and processing these diagrams produced from SOM the factors are evaluated objectively according to their interaction intensity and dominance in the system of landsliding.

3.7 *Assignment of weighting values to the various causal factors, synthesis based on an overlay combination of the thematic maps*

Subsequent to dominance and interaction intensity attributed to each parameter, the following operations should be carried out:

1. Subdivision of each parameter into a number of relevant classes.
2. Attribution of a weighted value to each class. In the present study the highest value is attributed towards

the direction of landslide manifestation. This coding is subjective and is taking into account the pre-existing knowledge about landslide frequency in each class and results from statistical analysis performed in a large data base of 802 events in the Greek territory (Koukis & Ziourkas 1989).

3. Overlay mapping of the weighted maps. In this case, the map classes occurring on each input map are assigned different scores.
4. Development of the final maps showing hazard classes.

The weighting values and the rating of the parameters combined with the rating of the class intervals of the parameters demonstrate the value of landside hazard for each map unit. The values of landslide hazard for each map unit are calculated as the product of parameter dominance multiplied by the score values which have come from the rating of the class intervals of the whole of the factors. According to the specific model the various thematic layers are overlaid in such a way that each map unit of the final map takes its value according to weighing value of each factor and the score of the class interval. For the final product (OUTPUT), for each map unit $n \in$ N it is:

$$output_1 = \frac{(w_1 item_1) + (w_2 item_2) + ... + (w_n item_n)}{n} \quad (1)$$

where w_1 to w_n are the weighting values according to exploratory data analysis and interaction matrix; $item_1$ to $item_n$ = the items of the data base for each parameter. The final map is constructed using the following classes of hazard: very high, high, medium, low and very low.

4 EVRYTANIA LANDSLIDE HAZARD ASSESSMENT

4.1 *Study area*

Evrytania district (Fig. 1) is one of the smaller in the Greek territory and depicts high landslide frequency. Almost every year landslides and reactivated landslides occur, responsible for the high landslide risk of the area. Often, villages had to be moved and relocated in most stable sites.

Flysch and chert formations prevail along with thin bedded folded limestones. They belong to Pindos zone. Flysh formations are usually covered with weathering mantle. The flysh structure, the intense morphology and the climate conditions (high and prolonged rainfalls) favor the intense weathering and the frequent manifestation of landslide phenomena. Landslides are mostly translational slides, earth flows, or rock slides and rock falls in a lesser extend. Particularly the flysch along the upthrusting fronts of Pindos isopic zone is highly fractured, demonstrating reduced mechanical features.
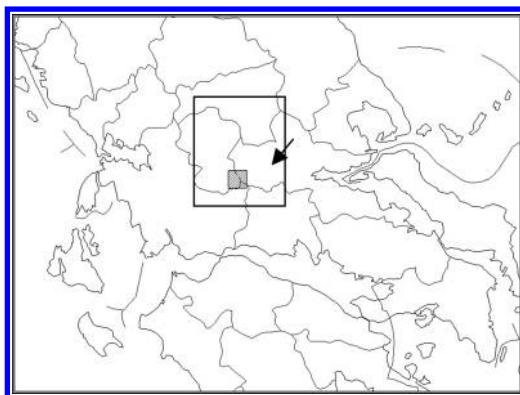

Figure 1.   Evrytania district – study area.

Table 2.   Classification of the morphometric factors.

ALT (m)	Score	SL (°)	Score	AZI (°)	Score
0–800	3	0–5	1	0–45	7
800–1200	2	5–15	2	45–90	8
<1200	1	15–40	4	90–135	4
		>40	3	135–180	3
				180–225	6
				225–270	2
				270–315	1
				315–360	5

Table 3.   Classification of relief type.

Type of relief	Score
Low	1
Medium	2
Intense	3

4.2 *Modeling and application*

In the case of Evrytania area landslide hazard mapping the model uses a maximum of ten (10) parameters involved. In Tables 2 to 7, the class intervals are established for each parameter and the score attributed to each class interval. The parameters altitude (ALT), slope (SL), slope orientation (AZI) were subdivided in a number of relevant classes (Table 2) and the appropriate maps were created. Each class was attributed a score. The highest value is attributed towards the direction of landslide manifestation.

Following the same procedure, relative relief (REL), mean annual rainfall (RAI), lithological units (LIT) and data related to weathering mantle thickness (MANT) and the effect of human activity on vegetation (ACT) are classified in Tables 3 to 6.

Considering slope orientation, combined with geological mapping data we evaluated the general dip

642

Table 4. Classification of mean annual rainfall.

Mean annual rainfall (mm)	Score
600–1300	8
1300–1400	7
1400–1500	6
1500–1600	5
1600–1700	4
1700–1800	3
1800–1900	2
>1900	1

Table 5. Classification of lithological units.

Main lithological units	Score
Thin bedded limestones	1
Sandstones and conglomerates	3
Clay marlstones	4
Scree material	2

Table 6. Classification of effect of human activity on vegetation, weathering mantle thickness.

Weathering mantle thickness (mm)	Score	Effect of human activity on vegetation	Score
<0.50	1	Low – medium	1
0.50–1.50	3	Intense – absence of vegetation	2
1.50–3.00	4	Cultivated areas, urban areas	3
>3.00	2	–	–

direction and strike of layers and subdivided the information into three classes in Table 7.

Seismic density DEN was assumed the same in the whole study area. Each of the parameters became a different thematic map.

The investigation of the interrelation of the above parameters combined with the absence or presence of landslides in the study area was another thematic layer. Ziourkas (1991) has constructed a landslide inventory map using aerial photos. We implemented this information in the GIS as an eleventh parameter, and overlaid with the 10 thematic maps together.

Data were imported in SOM Toolbox in order to perform cluster analysis and rate the 10 parameters according to their dominance to the system. Using the visualization tool SOM Toolbox offers one can easily investigate large multidimensional data sets and

Table 7. Classification of layers bedding, dip direction compared to slope orientation.

Orientation of bedding compared to slope	Score
Favourable	1
Horizontal or diagonal	2
Unfavourable	3

discover novelty. Matrix dimension is n × 10 και n × 11 where n is n = 34.406.

4.3 Data preparation

Data preparation in general is a diverse and difficult issue. It aims to:

– Select variables and data sets to be used for building the model.
– Filter erroneous or uninteresting data.
– Generate new features which capture interesting problem characteristics better than the raw data.
– Transform the data into a format which the modeling tool can best utilize.
– Define a prepared information environment.
– Normalize the values in order to accomplish a unique scale and avoid problems of parameter prevalence according to high values.

In the apparent data set a series of normalizations have been applied and it was found that the value of topographical error (t_e) and quantization errors (q_e) after the training varied according to the kind of normalization method that was applied. In the projection methods it is aimed to minimize the mean square error, that is the distance between a sample x and its map unit $m_c(x)$ in the self organizing map. These two values express the rate of convergence of the neural network. Table 8 shows the results of the methods of normalizations applied with the related topographical and quantization errors. Logistic normalization gives the best results. With this method all values need to be coded between zero and one [0,1].

4.4 Initializing and training

A SOM is formed of neurons located on a regular grid. The neurons are connected to adjacent neurons by a neighborhood relation dictating the structure of the map. Neighborhood function determines how strongly the neurons are connected to each other. Each neuron i of the SOM has an associated d dimensional prototype vector m_i, where d is equal to the dimension of the input space of the prototype vector and another in the output space, on the map grid. Each neuron has actually two

Table 8. Errors calculated for different normalization methods.

Normalization method	Quantization error (t_e)	Topographical error (q_e)
1 'var' variance	1.3	0.08
2 'log' logarithmic	0.27	0.09
3 'logistic' softmax normalization	0.20	0.07
4 'range'	0.22	0.11
5 'hisC' Continuous Histogram	0.23	0.07
6 'histD' Discrete histogram	0.23	0.12

Figure 2. Clustering visualizations using similarity coloring.

positions, one in the input space and another in the output space. Thus, SOM is a vector projection method from the input space to a lower dimension outer space.

In order carry out the following analysis using SOM Toolbox scripts were executed originally written by Vesanto (2000) in Matllab v.6.5 and altered in order to satisfy the needs of the specific data set by (Ferentinou 2004).

Training algorithm that was used was batch training algorithm. A grid with dimension 40×25 (1000 neurons) was created. The initialization of the initial weights was random. Training took place in two phases. The initial phase is a robust one and then a second one is fine-tuning with a smaller neighborhood radius and smaller (learning rate). Quantization error and topographic error were calculated $q_e = 0.2$ και $t_e = 0.07$. The neighborhood function that was used was Gauss. The whole methodology aims to:

– Cluster detection (projection in a lower dimension space).
– Discovery of non linear relations between data base items.

4.5 Presentation and evaluation of results: distance matrices – component layer – label map

In Figure 2, a map display is constructed using SOM algorithm. A multiple visualization is demonstrated which consists of 12 hexagonal grids. The first map on the upper left is a self organizing map, a U-matrix with values indicated using similarity coloring. This map is visualizing the results of training. From this map one can discover information about the general structure of data and clustering tendency. The last map on the right is called label map and defines two main clusters.

The best mapping unit is selected among the whole data set for each input vector. For the specific data set 9 units have been selected. These are (REL, MANT, SL, DEN, AZI, GM, LIT, ALT, RAIN).
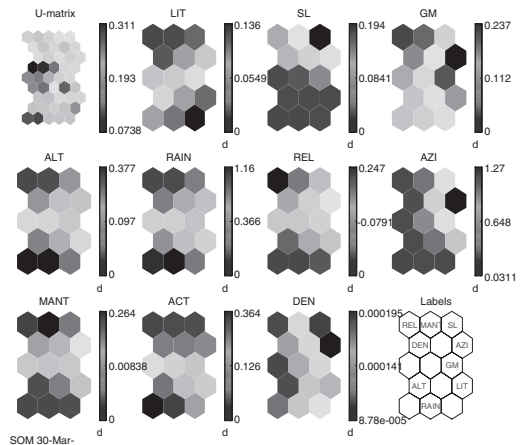
The multiple visualization is completed with the 10 maps which are called component planes. Each component plane refers to different factor. It these self organizing maps high values (hot colors), indicate the borders of the clusters though (low colors) characterize clusters themselves. In this multiple visualization one can reveal three clusters. According to the label map we refer to the following combinations of parameters. The first refers to the factors ALT-RAIN, and could be named as "climatic – morphological". The second refers to the factors REL-DEN-MANT – and could be named "morphological", and the third refers to the parameters AZI-GM-SL-LIT, and could be called "morphological – geological".

Using the method of exploratory data analysis there is revealed in an apparent method the tendency of the parameters to clustering, which clusters have a clear physical meaning. According to the results (Fig. 3) altitude ALT, mean annual rainfall RAIN, relative relief REL, orientation of layers compared to slope strata GM are the most important. This multiple visualization gives information about the intensity of each parameter. Reading the numbers in the hexagon on the left map on can discover which are the most predominant factors.

Koukis et al. (1996), have studied systematically landslide inventories covering the period 1953 to 1991. They statistically analysed them, and found that in Achaia County located in southwestern Greece, an area of high mean annual rainfall the dominant factor contributing to landsliding is precipitation and lithology. The same authors established that there is high correlation between landslide manifestation and rainfall events. This area is a typical sample of an area belonging to Pindos isopic zone.

Another very important visualization offered from SOM training algorithm is scatter diagrams and
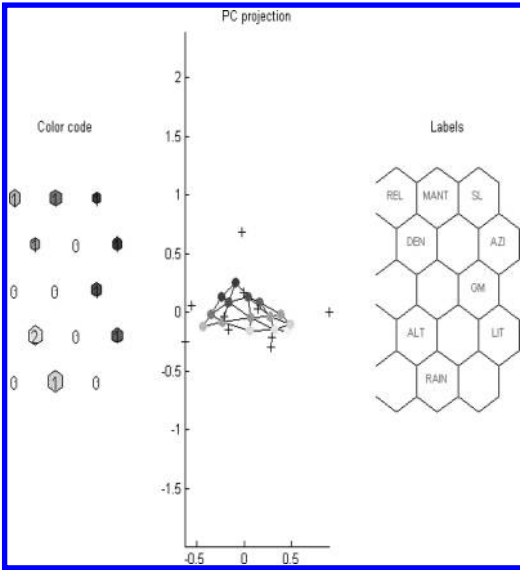
644

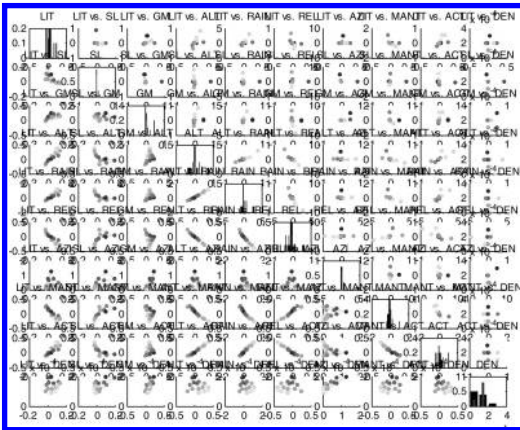Figure 3. Color coding, principal component projection, label map.

Figure 4. Scatter diagram 10 × 10.

histograms (Fig. 4) When studying them thoroughly one can detect novelties in data and information about the interrelations of the various parameters.

When investigating multidimensional data, it is necessary to visualize the parameters and their correlation. For the specific data set a matrix of 10 × 10 was created. The parameters are projected in the leading diagonal of the matrix and refer to the lines and columns of the matrix. In the leading diagonal the histograms of the variables are demonstrated. With red color are represented the vectors after training and with black

color are represented the data before training. The matrix is symmetric. In the upper triangle are visualized the data before training and in the lower triangle are visualized the data after training.

According to the diagram we arrive at the following conclusions for the correlations of the parameters:

– LIT-SL element (2,1).
– LIT-GM elements (3,1), (1,3).
– LIT-ALT elements (4,1), (1,4).
– LIT-RAIN elements (5,1), (1,5).
– LIT-REL elements (6,1), (1,6).
– LIT-MANT elements (8,1), (1,8).
– LIT-ACT elements (9,1), (1,9).
– SL-ALT elements (4,2).
– SL-RAIN element (5,2).
– SL-REL element (6,2).
– SL-MANT element (8,2).
– SL-ACT (9,2).
– GM-ALT element (4,3).
– GM-RAIN element (5,3).
– GM-REL element (6,3).
– GM-AZI elements (7,3), (3,7).
– GM-MANT elements (8,3), (3,8).
– GM-ACT elements (9,3), (3,9).
– ALT-RAIN elements (5,4), (4,5).
– ALT-REL elements (6,4), (4,6).
– ALT-MANT elements (8,4), (4,8).
– ALT-ACT elements (9,4), (4,9).
– RAIN-REL elements (6,5), (5,6).
– RAIN-MANT elements (8,5), (5,8).
– RAIN-ACT elements (9,5), (5,9).
– REL-MANT elements (8,6), (6,8).
– REL-ACT element (9,6).
– AZI-MANT element (8,7).
– AZI-ACT element (9,7).
– AZI-DEN elements (10,7).
– MANT-ACT element (9,8).

where:
LIT = lithology
SL = slope angle
GM = layer orientation compared to slope
ALT = altitude
RAIN = mean annual rainfall
REL = relative relief
AZI = slope orientation
MANT = weathering mantle thickness
ACT = effect of human activity on vegetation

4.6 *Parameter rating*

The scatter diagram in Figure 4 can be sophisticated coded and become an interaction matrix.

Hudson (1992), established an analytical method in order to consider problems of rock engineering or soil mechanics. This method is basically using matrices and

645

Table 9. Interaction matrix.

		P1	P2	P3	P4	P5	P6	P7	P8	P9	P10	Σj
Cause	1	LIT	0	0	1	1	1	0	1	1	0	5
	2	1	SL	0	0	0	0	0	0	0	0	1
	3	1	0	GM	0	0	0	1	1	1	1	5
	4	1	1	1	ALT	1	1	0	1	1	0	7
	5	1	1	1	1	RAI	1	0	1	1	0	7
	6	1	1	1	1	1	REL	0	0	1	0	6
	7	0	0	1	0	0	0	AZI	0	0	0	1
	8	1	1	0	1	1	1	1	MANT	1	0	7
	9	1	1	1	1	1	1	1	1	ACT	0	8
	10	0	0	0	0	0	0	1	0	0	DEN	1
Σi		7	5	5	5	5	5	4	5	6	1	

was named interaction matrix method. This type of visualization is an efficient and easy to understand way of ranking parameters involved in a system. In such matrices the elements of the leading diagonal are the main parameters which do not actually interact, but the rest of the elements reflect the parameters with high interaction. The method proposes an appropriate encoding of the matrix in order to define how important is the parameter to the system. This is defined by two characteristics, the interaction intensity and the dominance. Each system is characterized from parameters belonging to the space of cause effect. Effect is considered the impact of the parameter to the system, though effect is considered the impact of the system to the parameter 9element of the leading diagonal). The basic characteristics of the interaction matrices used in every geotechnical problem are symmetry and matrix dimensions. The projection of these characteristics is illustrated to a cause (C) – effect (E) plot.

A binary approach has been followed in order to code the scatter diagram of Figure 4. The 47 elements not belonging to the main diagonal have severe correlation and have been attributed a value of 1. The elements of the leading diagonal have been attributed the values of zero. Consequently the system is interactive as 47 out of 100 elements depict an open mechanism. In the following Table 9 are presented the interaction matrix after binary coding. Column Σj is the sum for each line and represents the cause value *C*. Line Σi is the sum for each column and represents the effect value *E*. Following this methodology a cause – effect diagram is produced (Cause–Effect C,E). The sum of the parameter values are presented as points coordinates at the diagram.

The cause effect plot refers to the influence of each parameter on the system and the effect refers to the influence of the system on the parameters. On Tables 9 and Table 10 the generation of the cause effect coordinates is presented. In Table 9 the main parameters are listed along the leading diagonal with parameter construction as the last box.

Table 10. Cause effect coordinates.

	C	E	C + E	C − E
LIT	5	7	12	−2
SL	1	5	6	−4
GM	5	5	10	0
ALT	7	5	12	2
RAI	7	5	12	2
REL	6	5	11	1
AZI	1	4	5	−3
MANT	7	5	12	2
ACT	8	6	14	2
DEN	1	1	2	0

One can reveal the meaning of the rows and the columns of the matrix by the row and the column through each parameter Pi. From the construction of the matrix it is clear that row passing through Pi represents the influence of Pi on all the other parameters in the system.

Conversely the column through Pi represents the influence of the other parameters on Pi. Once the matrix has been constructed, one can find the sum of each row and each column. The parameter interaction intensity and the parameter dominance are illustrated in the plot diagram of (Fig. 5).

Parameter interaction intensity increases from zero to the maximum parameter interaction. The associated maximum possible parameter dominance values rise from zero to a maximum of 50% parameter interaction intensity and then reduce back to zero at a maximum parameter intensity value.

The specific numerical values of the two characteristics are (C + E) and C − E. For the studied data base the maximum coordinate values are (20, 20). The most interactive parameters are projected along the leading diagonal C = E. According to the diagram the most dominant parameters are altitude (ALT), mean annual rainfall (RAI), weathering mantle thickness
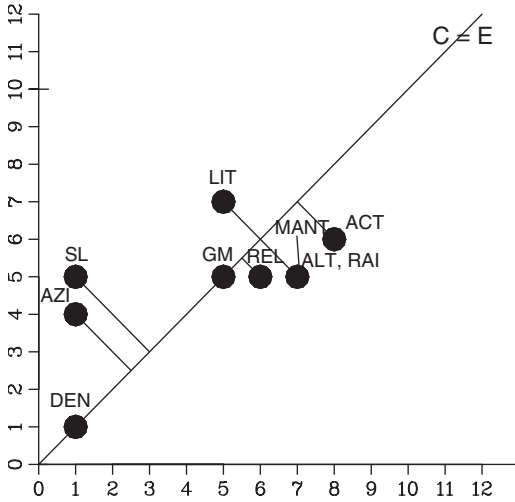
646

Figure 5. Cause effect plot.

(MANT), effect of human activity on vegetation (ACT) (highest value C − E = 2). The less dominant parameter is slope angle (SL) (value C − E = −4), and slope orientation (value C − E = −3). The dominant parameters follow the rule C > E, and are projected on the right of the line C = E. The most interactive parameters human interaction with vegetation, (ACT), (value C + E = 14), mean annual rainfall (RAI), altitude (ALT), and weathering mantle thickness, value C + E = 12). The least interactive parameters are seismic intensity (DEN), (value C + E = 2), slope orientation (AZI) (value C + E = 5).

4.7 Construction of landslide hazard maps

The dominance attributed to each parameter through the interaction matrix reflects the weighting value and the importance of the parameter in the manifestation of landslides. The weighting values combined with class scores, reflect the landslide hazard for each map unit. The final product (OUTPUT) follows equation (1) for each map unit (Fig. 6).

Figure 7 shows a histogram of the number of polygons classified according to landslide hazard class.

4.8 Verification and validation of the model

The resulting map was compared with the landslide inventory map constructed from Ziourkas (1989) in the study area. It was assumed that the majority of the map units in which landslides have been manifested belong to the category of low to high hazard.

The results of the comparison are presented in Table 11.

In this model only 10 parameters were examined, and we believe that we could achieve a more realistic
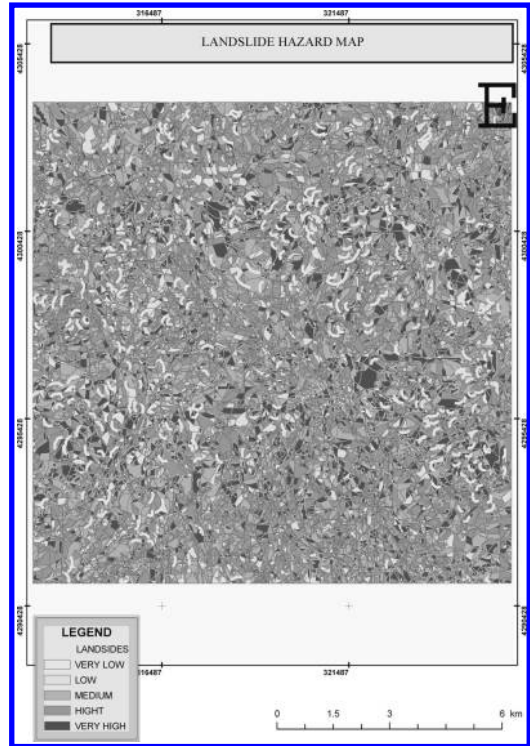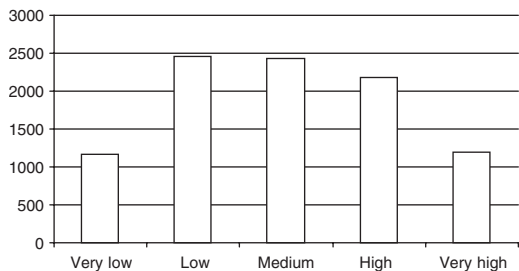

Figure 6. Landslide hazard map.

Figure 7. Number of polygons of the study area belonging to each hazard class interval.

Table 11. Comparison of landslide hazard and landslide inventory map.

Hazard class	Area (km^2)	Nr of polygons	Landslide density
Very low	31	140	4.52
Low	39	267	6.85
Medium	43	298	6.93
High	33	237	7.18
Very high	14	93	6.64

647

result when feeding the model with more data referring to more parameters.

One of the advantages of the applied methodology is the possibility of dynamically feedback the model and re-assess parameter weights whenever changes concerning their values take place.

5   CONCLUDING REMARKS

- Unsupervised artificial neural networks were developed which use knowledge discovery methods in order to detect the trend of the data to cluster according to the mechanism of failure and the status of stability.
- The importance and the interaction intensity of the factors contributing to landsliding procedures were investigated, in an objective and quantified approach using a coupled model of artificial neural networks and interaction matrix, the results were again reasonable.
- Self Organising Maps detect clusters in a data set in a different approach than multidimensional statistical analysis techniques. There is a tendency of the data to preserve their neighborhood distances than the distances between the items of the data base and create clusters around the most important factors, which portray a clear physical meaning.
- Geographical information systems offer the prospect of an integrated analysis and they are also the necessary tools in order to organize data coming from neural networks, in order to produce landslide hazard models.

REFERENCES

Ferentinou, M. 2004. Landslide hazard assessment using artificial neural networks in a geographical information system environment. PhD thesis, School of Rural and Surveying Engineering , National Technical University of Athens.

Hudson, J.A. 1992. Rock Engineering Systems: Theory and Practice, Horwood, Chisesteractice.

Ziourkas, K. 1989. Landslide phenomena in the Greek Territory, Ph.D. thesis, Dept. of Geology, University of Patras.

Kohonen, T. 1995a. Self-Organizing Map, 2nd ed., Springer-Verlag, Berlin, 113.

Kohonen, T. 1995b. Self – Organising Maps, Vol. 30 of Springer Series in Information Sciences.

Koukis, G., Rozos, D. & Hadzinakos, I. 1996. Rainfall induced Landslides in Achaia county, Greece. In: Proc. of the 7th Int. Symposium on Landslides, Trondheim, Norway. pp. 1929–1934. Rotterdam, Balkema.

Varnes, D.J. 1984. Landslide Hazard Zonation: a renew of principles and practice. Commission on Landslides of the IAEG, UNESCO, Natural Hazards No. 3.

Vesanto, J. 2000. http://www.cis.hut.fi/projects/somtoolbox.

WL/PLI 1990. A suggested method for reporting a landslide. *Bull. of the Int. Assos. Engineering Geology* 41: 5–12.

Assessment of slope failure susceptibility using Fuzzy Logic

F. Saboya Jr., W.D. Pinto & C.E.N. Gatts
State University of Norte Fluminense Darcy Ribeiro – UENF, Campos, Rio de Janeiro, Brazil

ABSTRACT: Generally, the occupation process of urban space involves unsuitable areas for construction, which are subject to landslides. Therefore, it is important to develop measures to evaluate the susceptibility of occurrence of landslides in large areas. For this, the model should be able to capture the known local factors affecting the slope stability and also the relationship amongst them. Therefore, the model based on Fuzzy Logic seems to be suitable to assess the susceptibility of landslides of large and spread areas, once the vagueness in information and the relationship among factors affecting slope stability can be easily be taken into account in the analysis. The possibility of capturing the judgment and the possibility of modeling linguistic variables are the main advantages of using Fuzzy Logic. This methodology has been used to identify the susceptibility of landslides in the urban area of Itaperuna City in northeastern of Rio de Janeiro, Brazil.

1 INTRODUCTION

Slope failures are responsible for thousands of deaths and vital infrastructure destruction each year throughout the world. This is particularly important in developing countries where the land occupation is generally chaotic. In crowded cities most of the suitable places for construction have already been occupied pushing new constructions to geologically unsuitable areas, where the population lives under constant disaster threats. Therefore, it becomes critical the development of a mapping of slope failure susceptibility in order to guide authorities in the establishment of an occupation plane of hillside areas. In Rio de Janeiro, Brazil, several studies have found a direct relationship amongst the number of failure occurrence and the density of hillside occupied areas (slums), where 60% of failures were due to cuts, embankments over steep slopes, lack of drainage systems, domestic waste disposal and deforesting.

In order to deal with this problem it is proposed herein the promotion of a smart model aiming to evaluate the susceptibility of landslides in large areas, based upon essentially qualitative and observational data. This methodology is based on susceptibility analysis, which has the Fuzzy Logic as the theoretical background.

In order to evaluate the sliding susceptibility, Fuzzy Logic was chosen due to its capability of transporting to the mathematical field, judgments that are essentials in such a comprehensive study. This is especially important and attractive in cases where data are imprecise and the available information is somewhat vague as, for instance, height of slope, steepness,

density of vegetation, rainfall etc. Fuzzy Logic also allows one to take into account the relationship among these factors, which is crucial in assessing the potentiality of failure.

This methodology is then applied to a hillside area in Itaperuna city in the State of Rio de Janeiro, Brazil, where several cases of sliding have been reported recently, with casualties.

2 FUZZY LOGIC

Fuzzy Logic is the only mathematical theory with capability of processing linguistic terms. Despite the fact that Fuzzy Logic was developed three decades ago (Zadeh 1975, Sundararajan 1998), its use in Geotechnical Engineering is still incipient.

Fuzzy Logic is a method based on fuzzy sets concept and fuzzy operations. The most notable aspect of this methodology is the possibility of capturing, in a mathematical field, intuitive concepts which are the base of consistent judgment.

Fuzzy Logic, first proposed by Zadeh (1965), has as the main characteristic, the possibility of modeling the vagueness in information. In the classical Boolean Logic a given element can either belong or not to a specific set, i.e., there is no possibility to modeling a degree of "belonging". On the other hand, Fuzzy Logic uses the membership function to ascertain the "belonging degree" of a element to a specific set, that can varies from 0 to 1, where the extreme values represent the Boolean Logic (Fig. 1). This methodology makes possible to capture in a mathematical model, intuitive
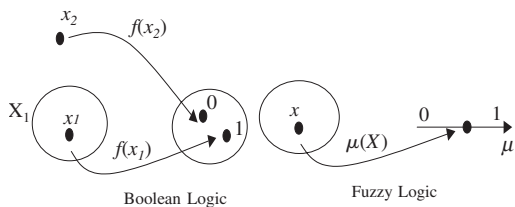
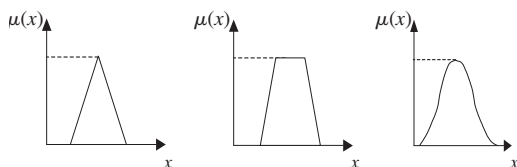Figure 1. Boolean and Fuzzy Logic representation (after Bueno et al. 2000).

Figure 2. Example of membership functions.

concepts as *old, hot, tall, etc.* which can constitute themselves in vague information with ill-defined domain or boundaries.

Despite not being popular in civil engineering, this methodology has a great field of development, as long as, most of time, the variables involved on certain problems are of uncertain definition with high degree of subjectivity.

In the case of soil slope stability the basic idea is to try to "model" those particular items that the experts take into account when inspecting the slope conditions in order to construct a comprehensive model.

2.1 *Membership functions and arithmetic operation*

Membership Functions define the value of membership for each element of a fuzzy set. They relate, by means of ordered pairs, the linguistic variable with ambiguity in information as shown in Eq. 1.

$$C = \sum_{i=1}^{n} \frac{\mu_A(x_i)}{x_i} \qquad (1)$$

where $\mu_A(x_i)$ is the membership function of the variable A whose value is x_i; and n is the number of linguistic variables of that particular membership function.

This function can assume any convex shape, however the most common are bell-shape, trapezoidal and triangular (Fig. 2).

The most common mathematical operations involving Fuzzy Logic are *intersection* and *union*.

The intersection corresponds to a *minimum* operator, as following:

(*a*) *Intersection*. If A and B are two fuzzy sets, the intersection *C* is also a fuzzy set. This operation

corresponds to a *minimum* operator, as following:

$$\mu_C(x) = \min[\mu_A(x), \mu_B(x)]$$

or $\qquad (2)$

$$\mu_C(x) = \mu_A(x) \wedge \mu_B(x)$$

(*b*) *Union*: If A and B are two fuzzy sets, the union *C* is also a fuzzy set. This operation corresponds to a *maximum* operator, as following:

$$\mu_C(x) = \max[\mu_A(x), \mu_B(x)]$$

or $\qquad (3)$

$$\mu_C(x) = \mu_A(x) \vee \mu_B(x)$$

According to Grima e Verhoef (1999), the three main stages must be followed in order to set up a Fuzzy Logic model:

- Selection of *input* and *output* variables:
- Establishing a relationship among input and output variables (*rule base*) represented generically by the algorithm given by Eq. 4:

$$\boxed{\begin{array}{l} \text{if } x_1 \text{ is } A_{i,1} \text{ and } x_2 \text{ is } A_{i,2} \text{ and},........, x_p \text{ is } A_{i,p} \\ \text{then y is } B_i, i = 1,......,k \end{array}} \qquad (4)$$

where $x_1, x_2,......, x_p$ are the input variables and y is the output variable for the desired inference. $A_{i,j}$ are the terms that linguistic variables can assume and i is the number of rules. B_i is the term assumed by the output linguistic variable.

This stage defines the dependency of the output variable to the relationship amongst input variables through organized *If- then* rules.

- Defuzzyfication: It is the step transforming output linguistic variables into *crisp* values. The most common defuzzyfication method is the *Centre of Gravity* method (Jager 1995, Babuska 1996) given by:

$$CoG(B') = \frac{\int_y \mu_{B'}(y) y \, dy}{\int_y \mu_{'B'}(y) \, dy} \qquad (5)$$

where:
B' = output fuzzy set
μ_B' = membership function

3 METHODOLOGY

Lee & Juang (1992) have developed a qualitative evaluation system in order to assess the slope failure potential of large areas in Honk Kong based on fuzzy sets. Selection of the factors contributing for the

650

Table 1. Antecedents and their linguistic terms.

Linguistic variables (factors)	Linguistic values (terms)
Angle of slope	Very low, low, average, high, very high, extremely high
Height	Small, average, high, very high
Type of vegetation	None, grass, shrub, tree
Density of vegetation	Very low, low, average, high, very high
Case history (failure nearby)	None, few, some, many
Permeability of top soil	Very low, low, average, high
Top soil thickness	None, very thin, thin, thick, very thick
Maximum daily precipitation	Low, average, high, very high
Frequency of movements	Low, average, high
Signs of movements	Weak, average, strong
Stabilization works	None, some, many
Drainage works	None, some, many
Contribution area	Small, average, big

Table 2. Linguistic values for failure potential index.

Linguistic variables (factor)	Linguistic values (terms)
Failure Potential Index (FPI)	Very low, low, medium, high, very high

instability and their corresponding influence on triggering failures are based on results obtained from a questionnaire filled by specialists (Juang et al. 1992).

Thus, the first step in establishing a fuzzy model for mapping landslide susceptibility is the definition of factors affecting the stability of slope inside the surveyed area. These factors are defined herein by means of both, case-history data and a questionnaire letter sent to several experienced specialists.

The modeling concept requires initially the definition of the factors influencing the stability of slope. However, the actual influence of these factors and the inter-relationship among them are not consensus amongst expert engineers. Therefore, the modelling of factors and their influence on stability will constitute the main challenge in applying Fuzzy Logic theory in this field of engineering.

To overcome this uncertainty in establishing the role of these factors, a data-base review was carried out in order to make possible to establish a list of factor to be presented to experts (Table 1).

All these antecedent terms are linked to a rule base, in order to form the consequent variables and their linguistic values. The consequent considered herein is the Failure Potential Index (FPI) and its linguistic values are presented in Table 2.
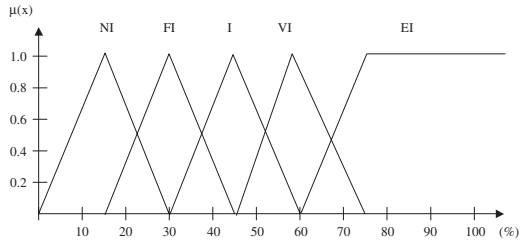

Figure 3. Fuzzy number for factors degree of importance.

The rule base that links "antecedents" to "consequents" is given by Eq. 5 and it has to be as most comprehensive as possible, in order to take into account the influence of all factors influencing the instability and the interaction among them, as well. The FPI, after defuzzyfication is directly associated to Linguistic Terms to describe the "Instability Level" (Very Unstable, Unstable, Fairly Unstable, Stable, Too Stable).

This "Instability Level" can certainly lead to misinterpretation regarding the words themselves, because the word "stable" can be understood as ultimate condition and therefore, "too stable" could have no meaning. However, a good reasoning sense allied to a proper criteria, would undoubtedly get rid of any uncertainty associated to this dichotomy.

The FPI is directly associated to the centre of the cell under consideration, allowing thus, the next step to be taken, which is the "Instability Chart" that represents the susceptibility of the analysed area.

The Linguistic Variables related to slope stability were defined by experts who were invited to give weight to the factors presented in Table 1.

Each Linguistic Term used to contemplate the relative importance of those factors shown in Table 1, as EI (Extremely Important), VI (Very Important), I (Important), FI (Fairly Important) and NI (Not Important) has to be converted into Fuzzy Numbers. These Standard Fuzzy Numbers, representing the terms were assumed to follow a triangular fuzzy distribution as shown in Figure 3.

The next step is to convert different opinions (different weight/terms) to a given factor in order to come up with a global opinion. This was done considering the simple mean of three points of fuzzy distribution: Minimum and maximum points A and C and vertex point B of triangle that defines fuzzy numbers. Using the similarity concept (Juang et al. 1996), the mean obtained was compared to standard fuzzy numbers presented in Figure 3 and the adopted weight will be that fuzzy number that shows the smallest distance (highest similarity) from the standard fuzzy number as shown in Figure 4.
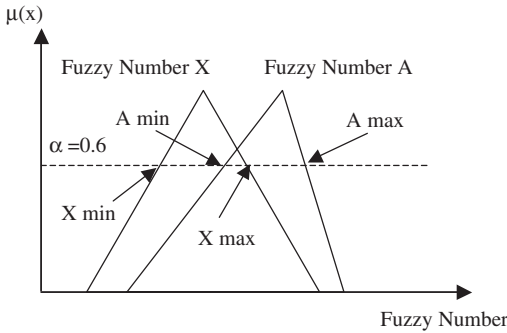
651

Figure 4. Similarity concept.

Table 3. Expert's opinion survey.

Linguistic variables (factors)	E1	E2	E3	E4	E5	E6
Angle of slope	I	EI	I	EI	FI	EI
Height	I	VI	FI	I	VI	FI
Type of vegetation	I	I	NI	VI	FI	MI
Density of vegetation	I	FI	VI	VI	FI	I
Case history (failure nearby)						
Permeability of top soil	VI	—	VI	I	VI	VI
Top soil thickness	VI	I	VI	FI	VI	VI
Maximum daily precipitation	FI	EI	VI	EI	EI	EI
Frequency of movements	VI	VI	EI	EI	FI	I
Signs of movements	EI	EI	EI	EI	NI	EI
Stabilization works						
Drainage works	VI	EI	VI	VI	VI	VI
Contribution area	I	FI	I	I	VI	FI
Shear strength						VI

The similarity for N levels of membership degree α is defined in (Fig. 4) and given by the following equation:

$$d_{x \to A} = \dfrac{\displaystyle\sum_{\alpha=0}^{1.0} \sqrt{\dfrac{\left(A_{min} - X_{min}\right)^2 + \left(A_{max} - X_{max}\right)^2}{2}}}{N}$$

(6)

Only one α level was considered because the triangles were regulars.

The questionnaire letter was sent to 16 experts, but it was answered by 6 of them. This was used as a source to infer the degree of importance of those factors listed in Table 1, and the expert's opinion can be seen in Table 3.

As long as the invited experts were free to include or exclude factors, Table 3 shows that none of them

Table 4. Opinions transformed into fuzzy numbers.

Linguistic Variables (factors)	Mean values of fuzzy numbers		
	A	B	C
Angle of slope	50	65	80
Height	35	50	65
Type of vegetation	31.7	46.7	61.7
Density of vegetation	35	50	65
Permeability of top soil	47	62	77
Top soil thickness	42.5	57.5	72.5
Maximum daily precipitation	58.3	73.3	88.3
Frequency of movements	49.2	64.2	79.2
Signs of movements	58.3	73.3	88.3
Stabilization works			
Drainage works	53.3	68.3	83.3
Contribution area	32.5	47.5	62.5
Shear strength	50	65	80

has considered the Case History and Stabilization Works. Moreover, one of the experts found worthy to include shear strength, despite the fact that this factor is a localized characteristic and most of the time cannot be interpolated for large areas where observational factors should be priority. However, the most noticeable characteristic of opinion poll was the high degree of unevenness in establishing weights for those factors listed in Table 3 where some of them varied from EI to FI.

The next step was the translation of those linguistic variables into fuzzy by using the similarity concept described in Eq. 6. As formerly stated, the mean fuzzy numbers can be calculated for each factor through the simple mean of maximum, minimum and vertex points of the linguistic values indicated by experts. Therefore, it can be said that the mean fuzzy number is a combined expert's opinions. The transformed fuzzy numbers are presented in Table 4.

With the numbers shown in Table 4, the fuzzy distance or similarity is calculated for each factor using membership degree for $\alpha = 0$ (Fig. 4). The weight that shows minor fuzzy distance is that weight chosen as the most representative of the influence of that specific factor. The calculated weights in according to fuzzy distance are presented in Table 5.

For "Top Soil Thickness" there was a tie and, thus, an untie criteria should be necessary. Therefore, it has been considered that the Linguistic Variable which was most cited for that factor would prevail giving, thus, the weight of VI.

Once the weights were qualitatively defined, it is now necessary to turn them back to numbers considering firstly that the sum of cited Linguistic Variables equals to 1 defining thus a relationship amongst them as follows:

$5(I)+8(VI)=1$ (7)

Table 5. Similarity degree for weights.

Linguistic variables (factors)	Fuzzy distance of each weight						
	NI	FI	I	VI	EI	Min diff.	
Angle of slope	50	30	15	0	20	0	VI
Height	35	15	0	15	35	0	I
Type of vegetation	31.7	11.7	3.3	18.3	38.3	3.3	I
Density of vegetation	35	15	0	15	35	0	I
Permeability of top soil	47	27	12	3	23	3	VI
Top soil thickness	42.5	22.5	7.5	7.5	27.5	7.5	VI
Maximum daily precipitation	58.3	38.3	23.3	8.3	11.7	8.3	VI
Frequency of movements	49.2	29.2	14.2	0.8	20.8	0.8	VI
Signs of movements	58.3	38.3	23.3	8.3	11.7	8.3	VI
Drainage works	53.3	33.3	18.3	3.3	16.7	3.3	VI
Contribution area	32.5	12.5	2.5	17.5	37.5	2.5	I
Shear strength	50	30	15	0	20	0	VI

Reasoning is used to define the others equations established amongst Linguistic Variables, taken the value of "Important" (I) as a basis, as follows:

$$NI = I/3 \quad (8)$$

$$FI = I/2 \quad (8a)$$

$$VI = 2I \quad (8b)$$

$$EI = 3I \quad (8c)$$

Thus, the weights of Linguistic Variables I and VI are 0.048 and 0.096 respectively. It is important to mention that these criteria are based on experience and intuition (engineering judgment) and can be modified at any time for better adjustment.

4 FAILURE POTENTIAL INDEX (FPI)

As stated before, the reaching of defuzzyfied value of FPI gives the cell (area) under consideration a classification ranking regarding its susceptibility of sliding. Now, one needs to obtain a numerical value that reflects this stability condition. For this, it is necessary to define fuzzy intervals of FPI, as presented in Figure 5.

The criteria used to define FPI is made up of weighing the membership values for all Linguistic Terms laying emphasis on those with higher susceptibility and under-weighing those which shows lower susceptibility using the following expression:

$$FR = 0.05 * p\_fail\_VL + 0.15 * p\_fail\_L + \\ + 0.20 * p\_fail\_me + 0.25 * p\_fail\_H + \\ + 0.35 * p\_fail\_VH \quad (9)$$

Figure 5. Panoramic view of Vinhosa Square.

and

$$FPI = FR * (FPI\_Max - FPI\_Min) + FPI\_Min \quad (10)$$

The pondered Eq. 9 reflects the idea of "susceptibility". Thus, the membership values of terms associated to the higher susceptibility classes are weighed by the coefficients p_fail_VL (failure potential Very Low), p_fail_L (failure potential Low) and so on … to give a weight ratio (FR) that will be the weighting factor of susceptibility class as shown in Eq. 10. If all terms are with maximum membership degree (1), the FPI value will corresponds to the maximum value of interval. On the other hand, if all membership degree is a minimum (~0) the value of FPI will correspond to the minimum value of interval.

In order to apply this methodology to actual cases, a computer program in Pascal was developed. This program allows user to define the membership functions, the rule base and calibrating the susceptibility classes according to user's experience.

5 STUDIED AREA

This methodology was applied in Itaperuna City, located in northeastern Rio de Janeiro, Brazil. The city of Itaperuna has a population of 120 000 inhabitants where predominates a tropical humid climate that combined to its geological features are responsible to many cases landslides resulting in loss of lives in the last 10 years. In 1997 and 2004, due to heavy rains, the city was severely hurt by several considerable slides in urban areas. This called for a comprehensive study in order to identify potentially dangerous areas. However, to cover great areas, this study should be essentially visual, i.e., identification of critical areas based only on visual inspection and, with rare exceptions, samples were taken.
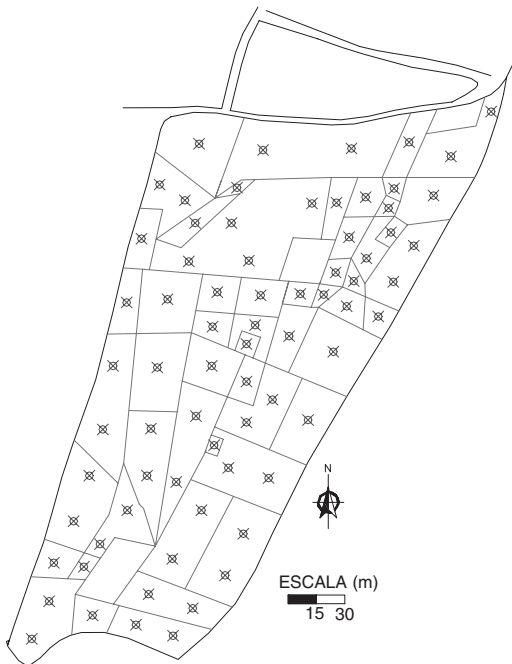
653

Figure 6.   Vinhosa Square mesh.

In order to illustrate the methodology, one unaffected colluvial area was chosen: Vinhosa Square. This area is chaotically occupied and the possibility of a sliding event could have catastrophic results with considerably loss of lives.

5.1   *Vinhosa square*

This area (Fig. 5) has approximately 51 thousand square meters and it is 150 m above downstream streets, where two minor occurrences of sliding were taken place. The Vinhosa area has a straight geometry and remaining scars have indicated a thin layer of top soil.

5.2   *Area mesh*

The criteria for defining the cell mesh was resulting from the terms presented in Table 1 along with declivity charts and refined during field inspections (Fig. 6). For each cell, only one value of FPI is assigned.

However, to facilitate interpolation, in some large cells more that one point was considered. It is important to mention that the criteria for establishing the number of points and cells was strongly based on judgment and personal field evaluation.

6   RESULTS

The results of the analysis generally have as a final product charts whose features are dependent, not only
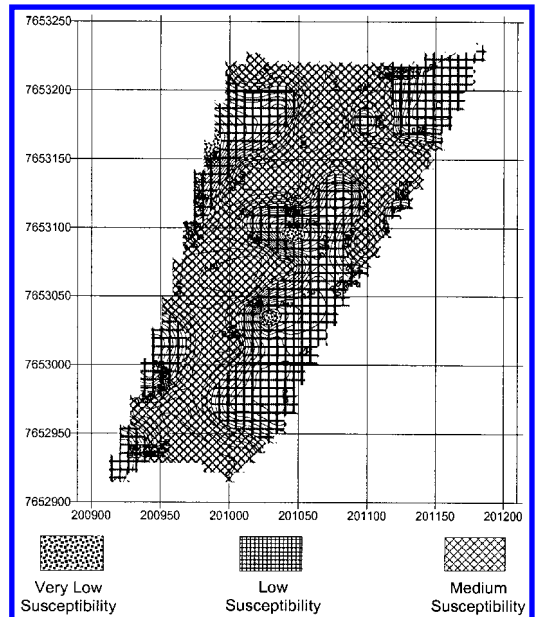

Figure 7.   Susceptibility map of Vinhosa Square.

to the model response, but also to the interpolation method and cell mesh. However these charts should be seen as a guide to indicate dangerous areas, where field investigation should be carried out to better calibrate the model.

For the Vinhosa Square (Fig. 7), it can be seen as controversy the fact by which there is no sector with high or very high susceptibility, once two slides had been reported in 1997 during heavy rains. However it is worthy to mention that these sliding were taken place during heavy rains and the model was applied to a normal daily precipitation of 10 years of recurrence period, around 126 mm/day. Therefore, for the recurrence period used herein, it seems coherent that zones pointed as of medium susceptibility might deserve special attention under exceptional precipitation.

It should be emphasized that sectors that presented medium susceptibility, can be dealt with worry and care by public defense department. On the other hand, sectors of high and/or very high susceptibility are closely associated to imminent sliding events and rains with lower recurrence time could easily trigger the rupture.

7   REMARKS

This paper intends to present a straight methodology based on fuzzy logic for the assessment of sliding susceptibility of natural slopes. With appropriate calibration and adjusts in the rule base it is possible to

654

apply this methodology for other types of sliding as mudflow, debris flow, avalanches, rockfalls, etc.

The model proposed herein has 13 factors in which the degree of importance of each one was inferred through a questionnaire survey filled by engineers (and geologists) experts in slope stability.

The results show that this methodology is particularly attractive when analyzing large areas where the study has to be essentially based on field inspection.

REFERENCES

Babuska, R. 1996. Fuzzy Modelling and Identification. Ph.D. Thesis. Delft University of Technology. Delft, the Netherlands.

Bueno, M.L., Stemmer, M.R. & Borges, P.S.S. 2000. Automatic visual inspection of ceramic pieces by means of "artificial intelligence". *Ceramica Industrial* 5: 29–37 (In Portuguese).

Grima, M.A. & Verhoef, P.N.W. 1999. Forecasting rock trencher performance using fuzzy logic. *International Journal of Rock Mechanics and Mining Sciences* 36: 413–432.

Jager, R. 1995. Fuzzy Logic in Control. Ph.D. Thesis. Delft University of Technology. Delft, the Netherlands.

Juang, C.H., Huang, X.H., Holtz, R.D. & Chen, J.W. 1996. Determining of relative density of sands from CPT using fuzzy sets. *J. Geotech. Eng.* 122(1): 1–16.

Lee, D.H. & Juang, C.H. 1992. Evaluation of failure potential in mudstone slopes using fuzzy sets. ASCE Geotechnical Special Publication 31, Stability and Performance of Slopes and Embankment-II, 2, 1137–1151.

Suarez, J.D. 1997. La Vegetación en la Estabilización de Deslizamientos. II Pan-American Simposium on Landslide, Rio de Janeiro, Vol. 2. 961–966.

Zadeh, L.A. 1965. Fuzzy sets. *Information and Control* 8: 338–353.

Landslide and debris flow characteristics and hazard mapping in mountain hill-slope terrain using GIS, central Nepal

T. Esaki, P.B. Thapa, Y. Mitani & H. Ikemi
Faculty of Engineering, Kyushu University, Japan

ABSTRACT: This paper presents an innovative approach of deriving landslide and debris flow characteristics and hazard mapping in mountain hill-slope terrain of the Himalayan region by using GIS. A comprehensive study of landslide and debris flow processes is carried out to identify and quantify the most influential geological and geomorphological variables and their relative contributions. GIS based spatial prediction model for landslide hazard assessment has been developed and the statistical probabilities of sampling units (e.g. grid, slope unit) are used to derive the predicted hazard of slope stability. Validity of prediction result is performed by overlaying hazard map to the map of spatial distribution of landslide episodes that have occurred in the past. The prediction model has demonstrated the capability of covering large areas, and has the objectivity and reproducibility of the results to improve the landslide hazard mapping.

1 INTRODUCTION

Hazards are inherent but dangerous and costly element of mountain environments. Landslides and debris flows in mountainous terrains often occur during or after heavy rainfall which results in the loss of life and damage to the natural and/or built environment. It has been estimated that nearly 600 people are killed every year worldwide as a consequence of slope failure (Varnes 1981).

Including landslides, a wide variety of slope movements exist such as soil slips, deep-seated slides, mudflows, debris flows, rockfalls, etc. (Varnes 1978, Hutchinson 1988, Cruden & Varnes 1996, Hungr et al. 2001). In last few decades, different methods and techniques for evaluating landslides occurrence have been developed and proposed worldwide (Hansen 1984, Varnes 1984, Hutchinson 1995). They can be grouped into the inventory, heuristic, statistical, and deterministic approaches (Soeters & Van Westen 1996, Van Westen et al. 1997, Atkinson & Massari 1998). Despite the methodological and technical differences, most proposed methods consider that geological and geomorphological conditions of future landslides should be similar to those conditions that led to past and present slope movements, together with the identification and mapping of the conditioning or preparatory factors of slope instability, and are the keys in predicting future landslides (Carrara et al. 1998).

Conventional maps of the mountain hazards provide useful inventories of hazardous sites but provide little insight into the operation of hazards. Furthermore, this approach tends to rely heavily on subjective interpretation of the landscape, which means that the results can not be replicated or transformed to other areas. Therefore, alternative approach employing the quantitative capabilities of Geographic Information Systems (GIS) is used to model and predict slope stability in the Agra Khola watershed of central Nepal. Since the middle of 1980s, GIS have become a very popular technology for analyzing natural hazards, including landslides (Coppock 1995). The GIS techniques are capable of facilitating various functions of geospatial data handling, analysis, and management and have been employed to model and predict landslide susceptibility or hazard. However, the reliability of the hazard analysis does not depend on which GIS software or platform is used but on what analysis method is employed (Carrara et al. 1999, Guzzetti et al. 2000).

Due to significant limitation of deterministic models, there is need for geo-material data (mechanical properties, water saturation, etc.) that are difficult to obtain over large areas (Terlien et al. 1995). The second general quantitative approach of statistical analysis is selected to develop a spatial prediction model for landslide and debris flow hazard. In the model, the relation between the potential for landsliding (dependent variable) and a set of intrinsic properties (independent variables) is constructed using statistical techniques and is then applied to map the regional landslide hazard (Hansen 1984, Wang & Unwin 1992).

2 DESCRIPTION OF THE STUDY AREA

The Agra Khola watershed lies in central Nepal and is bounded by the latitudes 27°45′ and 27°36′ N, and the longitudes 84°58′ and 85°7′ E (Fig. 1). The Agra Khola is the main draining river in the study area.

2.1 Geomorphological and geological setting

The study area is highly dissected and exhibits rugged topography in the south whereas it is smooth in the north. Hillslope comprises the residual soils and colluvium, including debris flow and other slope debris deposits. Surficial deposits which found in the area are mostly of thin residual soil and colluvium. The effects of weathering vary with rock types, being reflected in topographic relief.

The bedrock geology of the study area consists predominantly of low- to medium-grade metamorphic rocks. The rocks are meta-sandstone, slate, phyllite, marble, schist, quartzite, and their age ranging from Precambrian to Paleozoic (Stöcklin 1980). Intrusive rock granite is found southwestern part of the area whereas sedimentary strata comprising the limestone are outcropping in eastern region.
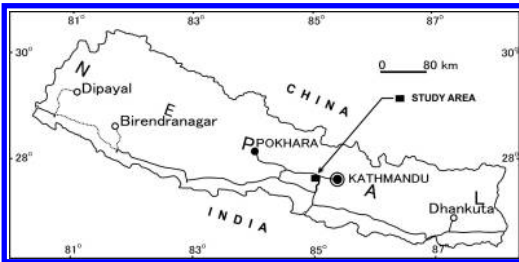

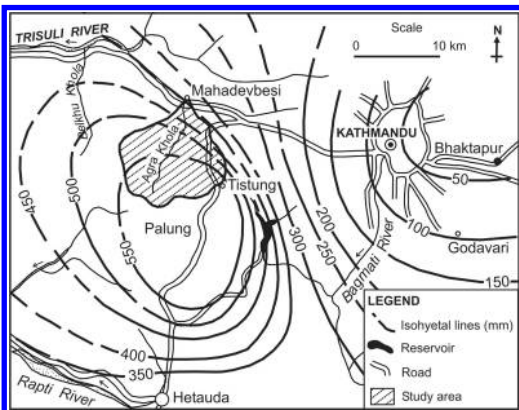Figure 1. Location map of the study area.

Figure 2. Isohyatal Map of Agra Khola area, central Nepal (DHM 1993).

2.2 Assessment of landslide and debris flow events of 19–21 July 1993

The high intensity rainfall due to cloudburst of 19–21 July 1993 triggered off numerous rock- and soil slides in the Agra Khola watershed. During 19–21 July 1993, the volume of maximum precipitation within 24 hours recorded in the nearest station Tistung is 540 mm. The entire catchment received intense rainfall of 300–500 mm between 19 and 21 July of 1993 with the major cloudburst near Tistung-Palung region of the central Nepal.

The Agra Khola catchment area especially the upper portion was severely damaged. The four span bridge located along the main highway connecting to Kathmandu was washed away early in the morning of July 20, 1993.

3 SPATIAL DATABASE AND CONSTRUCTION IN GIS

3.1 GIS data source and database creation

GIS data have been acquired from many sources: existing shapefiles and themes, interpretation aerial photographs and detailed field surveying. Thus, the data have been gathered and manipulated automatically or semi-automatically.

Database creation involves several stages: input of spatial data, attribute data, and linking spatial and attribute data. Spatial data is entered via digitization of field surveyed data or directly from existing digital sources. Once point, line, and polygon features are created, topology has built and other relevant attributes are keyed in or imported from other digital databases. Desired spatial extent of area under analysis is obtained with the use of geoprocesing wizard of ArcMap by clipping the shapefiles.

The basic data layers produced from GIS procedure include landslide inventory, factors responsible

Table 1. Basic data layers of the study area.

Classification	Coverage	Spatial	Attribute
		Data type	
Geological hazard	Landslide	Point, Polygon	Nominal
Damageable object	Road, building	Point, Polyline	Nominal
Basic map	Topographic map	Point, Polyline	Nominal Interval
	Geological map	Polygon	Nominal
	Engineering geol. map	Polygon	Nominal
	Landuse	Polygon	Nominal

for causing slope failures, and damageable objects (elements at risk) (Table 1).

3.1.1 Landslide database and attribute assignment

A total of 138 polygons and 61 points are generated by the process of vectorization. The point data represent those failures than can not be mapped as polygon feature at scale of 1:25,000. Each landslide is attributed with a unique ID and a link to the landslide database is established allowing the direct production of layers reflecting any variable from the database.

Assignment of the various kinds of attributes to individual landslides is a key to quantitatively analyze the relationship between landslides and their causative factors. In this study, the spatial overlay function of the GIS is adopted to carry out for such a task. For example, overlaying lithological shapefile with landslide shapefile (coverage) through the Union operator in Arcmap will tag each landslide with a rock type.

3.1.2 GIS digital thematic maps and spatial analysis

Landslide conditioning variable maps are obtained as derivative layers by spatial analysis or digitized layer of field surveyed maps with various attribute data.

3.1.2.1 Spatial derivative of terrain attributes

A Triangulated Irregular Network (TIN) model is created from digital terrain map (polylines of 20 m interval and elevation points) that is initially in digital vector format at 1:25,000 scale. TIN generation is done by overlaying the two themes of the line and point data in a single file using union function of ArcMap. The TIN model is used to construct a detailed Digital Elevation Model (DEM) at a resolution of 10 m ($100\,\mathrm{m}^2$) grid (pixel) size. DEM is utilized to produce very significant derivative layers, including slope angle and slope aspect, which are main predisposing factors for the landslide activity.

The slope angle layer is directly derived from the DEM. A sensitivity study of the grid size influence on calculated slope angle is carried out by using grid size of 2, 5, 10, 20 and 50 m. It is found that the slope angle distributions are not remarkably changed when grid size is less than 20 m.

The slope aspect layer is also based on the DEM. This variable represents the angle between the Geographic North and a horizontal plain for a certain point, classified in eight major orientations (N, NE, E, SE, S, SW, W, NW) with the addition of flat areas.

Drainage lines are automatically generated from DEM using ArcHydro Tool "ESRI". Strahler classification function is used to rank the stream orders.

3.1.2.2 Spatial properties of thematic layers

Physical variables, such as lithology, landuse, and engineering geological map are prepared. Lithology is obtained from the geological map of the region. Depending on the strength characteristics of rock, they are grouped in six different lithological domains.

Engineering geological map information is represented in a discrete way which consists of mapping unit conveying the spatial distribution of soils and rock types (Rengers et al. 1991). The engineering geological map units include alluvium, colluvium, thin residual soil, thick residual soil, low rock mass strength, medium rock mass strength, and high rock mass strength. An estimation of the deposit depth is made in the field and two different subclasses are considered: thickness of 1–3 m is thin soil and >3 m is thick soil. The thickness of soil less than 1 m is considered as rocky terrain.

The land use layer classifies the land use type in to five different categories of polygon shapefile which include forest, shrub land, grassland, cultivated land, debris, and water bodies along drainage network. The obtained data are the result of editing existing polygon coverage shapefile together with field verification data.

4 SPATIAL OCCURRENCE OF MASS MOVEMENTS

Occurrence of mass movements can be visualized in detailed digital landslide inventory map created in GIS. Spatially localized mass movements are seen in the upper and middle parts of the watershed (Fig. 3). The mass movements are varying in type and size, some of which are periodically reactivated that affect the areas of the Agra Khola watershed.

The dominant mode of failure is rotational slide, while the other modes of failure are debris or soil flow and shallow translational slide according to the
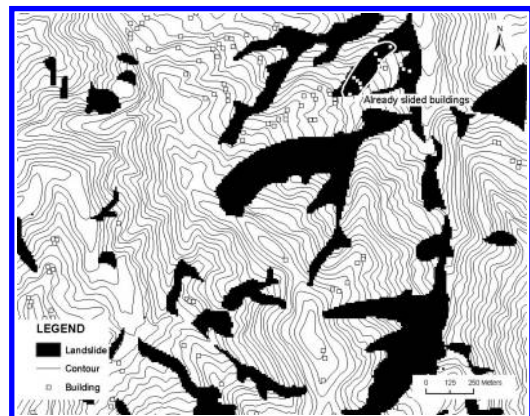

Figure 3. Densely distributed landslides and debris flows in the upper-middle reaches of the Agra Khola watershed.

659

Figure 4. Slope failure initiating as a plane translational movement.

Figure 5. Procedure of combining GIS map layers to derive landslide characteristics.

classification of Varnes (1978). Some common failures are initially failed along the rock discontinuity as planar failure and are gradually converting into debris flows downstream (Fig. 4). There were many tension cracks at the proximity of the crowns of the slides and the amount of debris deposited along the river course was so great that it formed about five meters high terraces in the Agra Khola.

5 LANDSLIDES AND DEBRIS FLOW CHARACTERISTICS DERIVATION

After preparing the landslide inventory and causative variable maps in digital format, a database representing the landslide characteristics is needed. To determine the landslide characteristics, landslide inventory and parameter data files are analyzed. If any grid is exposed to a landslide, each parameter feature at this grid is stored in the landslide database.

A pixel size of 10 m (100 m^2) is adopted to the DEM layer as well as the other themes and analytical spatial integration of data is demonstrated by an example application in order to allow the concise procedure to develop the approach (Fig. 5). Analysis data include the vector data as well as raster data which are integrated by the definition of hybrid data model.

5.1 *GIS data analysis procedures*

The information stored in digital maps consists of vector coverages as represented by point, line, and polygon features. GIS data analysis procedures include rasterization and attribute discretization.

5.1.1 *Rasterization of variable maps*
All the thematic vector layers are imported to Arc GIS 9.0 and rasterized for analytical purposes. A vector-to-raster conversion is undertaken to provide a raster data of landslide areas with 10×10 m pixels. This
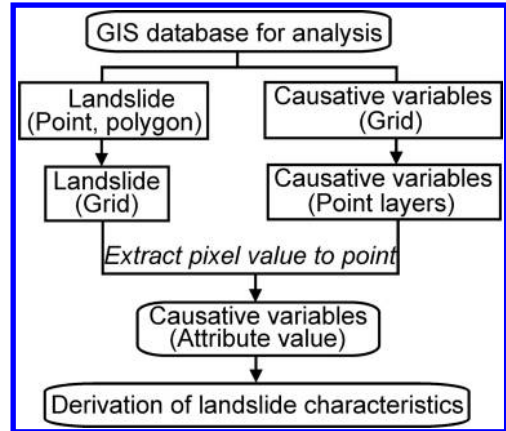
resolution allows to fully exploiting the detailed morphological information, as topographic variables like slope are known to play a very important role in landslides and debris flows triggering. The grid format is considered optimum for this kind of process, as the sizes of the landslides and debris flows are similar to the grid cells. Rasterization of linear element is done by creating arbitrary buffer around the linear features.

5.1.2 *Attribute discretisation (Re-classification)*
Continuous attributes such as altitude and slope are significant variables to slope failure. For such cases, the spatial data is not only rasterized, but the attribute data is also mapped into discrete classes, that is, it is "discretized". Spatial Analysis Module is used for the transformation. In establishing reclassification criteria for continuous variables, a compromise has been made between the need to have a limited number of classes which sufficiently represent the wide range of original categories in each class. Natural slope angle is classified into <15°, 15°–25°, 25°–35°, 35°–45°, and >45°. Slope aspect is divided into nine categories.

5.2 *Spatial relationship between slope instability and causative variables*

To examine the physical variables contributing to the initiation of landslides, the landslides which occurred in the study area are correlated with those parameters considered to have influence on their occurrence. The univariate probability analysis is adopted to quantify the relationship between landslide frequency and the each variable class.

5.2.1 *Lithology*
The correlation of landslide frequency with lithology showed that relatively high landslide frequency found in quartzite and schist unit (Fig. 6). The occurrence of
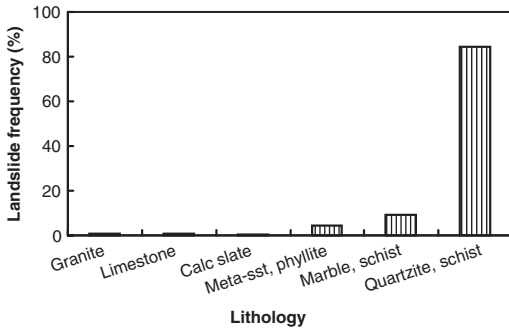
660

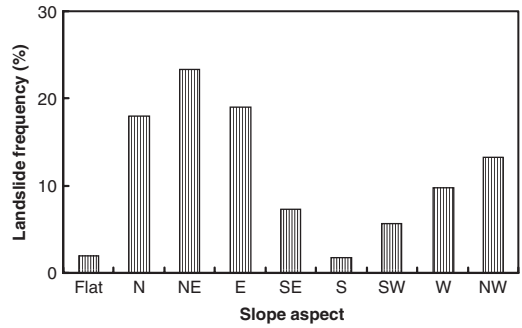Figure 6. Landslide distribution in lithological units.

Figure 7. Landslide occurrence in various slope angles.
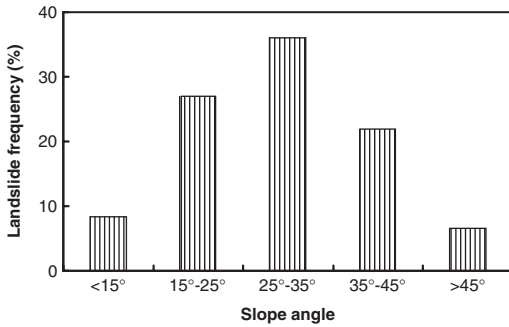

Figure 8. Landslides occurrence with respect to slope aspects.

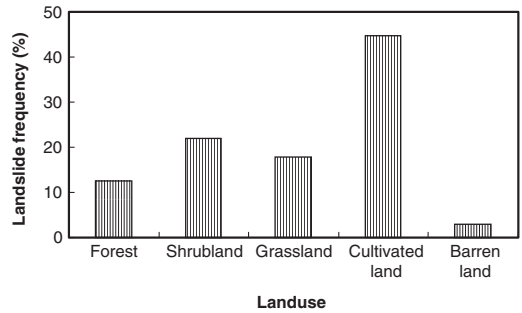Figure 9. Landslide frequency according to landuse.

Figure 10. Effect of stream order on landslide frequency (within 20 m buffer).

large number of slope failures in the quartzite and schist is due to steep hill-slope and favorable orientation of foliation in the direction of slope face.

5.2.2 *Slope angle*
Slope gradient has a great influence on the susceptibility of a slope to landslide phenomena. Examination of landslide frequency with the corresponding slope angles categories shows that maximum frequency is reached into the slope angles of 25°–35° and 35°–45° (Fig. 7).

5.2.3 *Slope aspect*
Moisture retention and vegetation is reflected by slope aspect, which in turn may affect soil strength and susceptibility to landslides. From the distribution of aspect among the mapped landslides, it is found that northward facing slope faces have predominant slope failures compared to southward facing slopes (Fig. 8).

5.2.4 *Landuse*
Many investigations have shown that landuse cover or vegetation cover, especially of a woody type with strong and large root systems, helps to improve stability of slopes (Greenway 1987). The correlation between landuse type and landslide frequency is given in Figure 9.
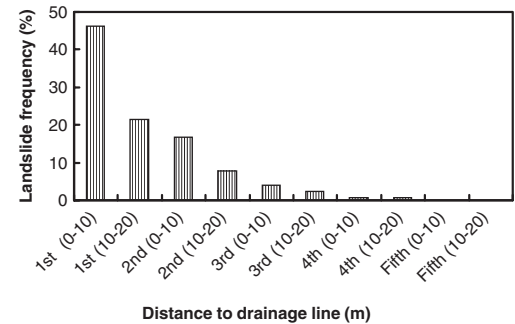
5.2.5 *Proximity to drainage line*
An analysis has been carried out to assess the influence of drainage lines on landslide occurrence. For this purpose, proximity to drainage line is identified with 20 m buffer from the central drainage line and the results are divided into ten categories. The analysis showed that first order drainage has caused the more triggering mechanism of landslides than the successive streams of higher orders (Fig. 10).

661

6 MOUNTAIN HILL-SLOPE ANALYSIS FOR DEBRIS FLOWS

Debris flow characteristics and its hazard consequences in mountainous hill-slope have been illustrated by using GIS. The analysis of debris flows in the natural hill-slope terrain based on post-event field measurements of deposited and eroded debris materials. General analytical approach of GIS procedure is applied to evaluate the debris flows in mountain hill-slope but not like the dynamic flow model "DAN" developed by Hungr (1995).

Present study mainly focuses on an innovative method to estimate debris flow that integrates easily obtained input data which incorporates theoretical concepts with empirical analysis. Debris flow characteristics and associated hazard is estimated from the several slope profiles along the section of spatial occurrence of past debris.

6.1 Source recognition and spatial mode of flow occurrence

The triggering area of the debris flows are in the upper catchment of the basin. A DEM of the terrain and the potential debris flow sources are used in GIS to provide the required terrain and source data. On the basis of DEM and field survey, potential source zones are identified in the watershed.

Various modes of failures and occurrence of debris along the drainage, slope, and hill-slope are described. Two main forms of landslides are distinguished. Hillslope debris flows, for example in the middle and lower reaches of the area form a single track on a steeper open slope and debouch onto the plain below or onto a fan slope. Channeled debris flows are found in the uppermost catchment which flow through a preexisting channel or gully.

Identifying the flow path is fundamental to understanding the areas affected by debris flow. The characteristics of the downhill path traversed by the debris can affect the mode of debris travel. The DEM is used to analyze the debris flow paths. The direction of flow is determined by finding the steepest descent, or maximum drop from each cell. Two different flow paths are seen: an ordinary path following the stream channel and an anomalous path spilling over obstacles or embankments along the hill-slope.

6.2 Drainage profile analysis in natural hill-slope

It would be appear that drainage class has a significant influence on the slope angle at which movement initiates. Basically, the analysis required two different input data sets. The topographic surface strongly influences which area affected and can be described by
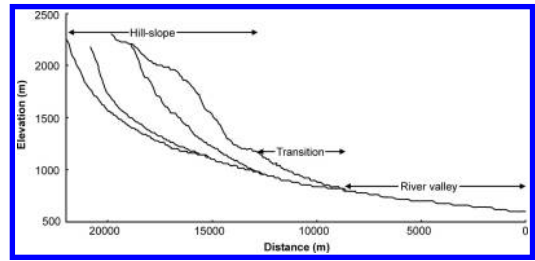

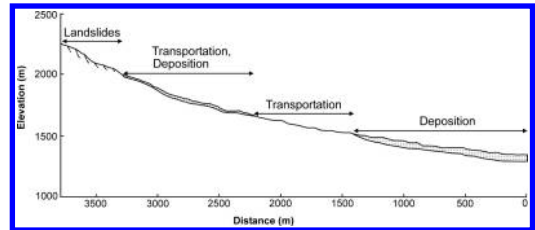Figure 11. Major river profiles derived from DEM

Figure 12. Typical cross profile illustrating erosion, transportation, and deposition.

DEM. As source of the debris, the locations of streams as well as the location of settlement areas which might be in particular affected by debris are taken in to consideration. Data of the factors that are considered critical to debris flow initiation are processed using the spatial analysis features of GIS. The procedure involves several steps. The first is to choose the variables that are critical to the occurrence of debris flows. The second step is to obtain data for each attribute by GIS data derived from field survey. The third step is to define a quantitative measure of debris flow characteristics and hazardous events. It can be argued that just the landslide failure area or the landslide volume would be preferable, but these quantities are often difficult to determine.

Major river profiles are extracted from DEM to visualize relationship of drainage with natural slope (Fig. 11) and the characteristics of the events relating to initiation, transportation, and deposition are examined along the various stream profiles in the hill-slope (Fig. 12). The morphology of area is largely controlled by lithology, which in turn influences the transportation and deposition mechanism of the debris in the mountainous terrain (Fig. 13).

Interpretation of the results of this analysis also considers erosion, transportation, and deposition of debris. Events in the study area exhibit several characteristics of deposition. Generally, the gradient of a depositional area on an open slope is greater than that of the fan at the exit of a gully. The average gradient of depositional area of debris in the area as channel bed predominantly up to 20° and minor variation exists in
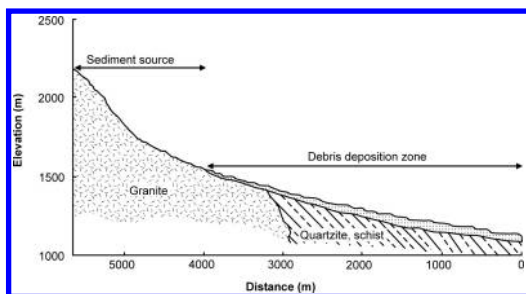
662

Figure 13. Geological section profile demonstrating the lithological influence on transportation and deposition.
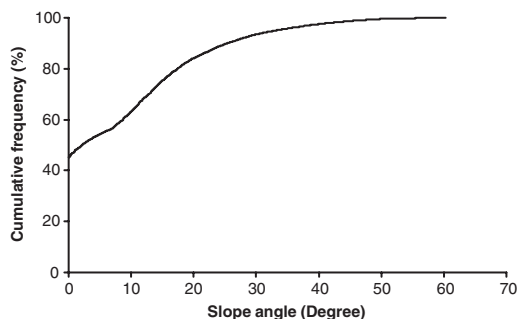

Figure 14. Spatial relationship of debris deposition and natural slope angles along the drainage network channels.

lower and upper slope angles (Fig. 14). The variation of debris deposited areas at lower and steeper slope gradients clarified the evidence that stream channel is not the only factor controlling the onset of deposition, and confinement of channel may influence deposition with similar gradient.

6.3 *Evaluation of landslide and debris flow characteristics*

Natural slope angle of 25°–35° degrees and quartzite and schist zone with dip-slope regions are the most susceptible to failure. Most of the landslides are seen in cultivated land according to landuse type.

Examination of hill-slope profiles indicates that natural slope and lithology has significant contribution for erosion, transportation, and deposition of debris along the hill-slope. The 45 per cent of debris is deposited on the flat areas and other debris deposit occurred with average gradient of up to 20° slope angle (Fig. 14). Quatzitic and granitic regions forming the steep slope are more favorable to slope failure and producing the sediment debris. But in the case of granite and quartzite-schist area, granitic hill is delivering the debris sediment to the quartzite-schist zone of low topographic relief (Fig. 13).

7 SPATIAL PREDICTION MODELLING OF LANDSLIDE HAZARD

Spatial prediction modeling is evaluated by several spatial data layers (i.e., variables). Aiming at a higher degree of objectivity and better reproducibility of the hazard prediction, quantitative technique of statistical prediction models have been developed for assessment of landslide hazard.

7.1 *Analysis variables and their acquisition*

The analysis variables comprises the terrain, geo-material and other useful variables that have been linked to slope failure. The variables entered in the model come from very different sources. In the model, two categories of variables are defined:

– Derived from DEM (elevation, slope angle, slope aspect, illumination)
– Not derived from DEM (lithology, engineering geology, landuse)

All locations of the landslides studied are used to extract from the existing data layers of the physical parameters that characterize landslide locations.

7.2 *Spatial design in prediction model*

Automated cartography and GIS-based spatial operations have demonstrated their usefulness in partitioning a territory into mapping units. Grids are acquired through rasterization and slope units are automatically identified in the watershed from the DEM using GIS-based hydrologic tools: "Arc Hydro Tool" ESRI and "Slope Unit Tool" (Esaki et al. 2004).

7.3 *Quantitative prediction model*

Several quantitative spatial prediction models for identifying hazardous areas to be affected by future landslides have been developed (Carrara et al. 1991, Montgomery & Dietrich 1994, Mark & Ellen 1995). In these quantitative models, the hazard levels of the prediction results were expressed in terms of mathematical functions such as probability functions. The probability function is used to express future landslides as the quantitative measures of the hazard.

The geological and geomorphological variables considered relevant to the occurrence of landslides have been extracted for all landslides of the event. The result from the overlays is then transferred to a matrix of causative variables. The main steps in the procedure are shown in Figure 15 which discusses the flow chart for hazard prediction.
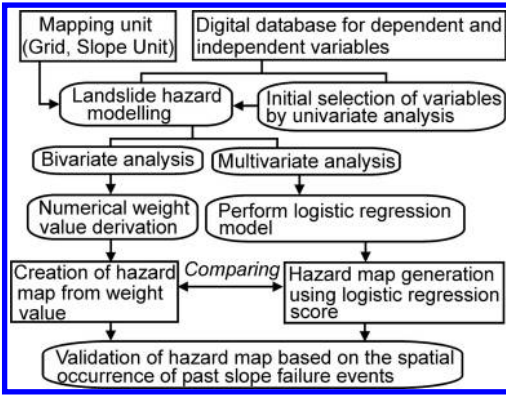
663

Figure 15. GIS procedure for predicting landslide hazard adopted in this study.

Figure 16. An illustrative example of matrix conversion from integer variable to dummy variable coding.

7.3.1 *Bivariate analysis and hazard map creation*

Bivariate statistical analysis is carried out to generate statistically derived numerical weights for all classes of the variable maps. The weights of the variables are calculated to compare the calculated density of variable class with the overall density in the parameter map of the whole catchment area (Van Westen 1993). Using these weight values, the most relevant variable maps are selected for combination into landslide susceptibility maps. Although weight calculation procedure is apparently complex, it can easily be coded and automatized by using the GIS functions, allowing a fast execution of the entire process.

7.3.2 *Multivariate analysis and hazard prediction*

All input variables are grouped into a few meaningful classes. For categorical data, such as geology, engineering geology, and landuse did not involve any subjective judgment. For continuous variables, such as slope angle or elevation, the selection of the number of classes and class limits requires a significant amount of guess work guided by previous knowledge of the causal relationships between slope failures and instability factors (Guzzetti et al. 1999).

Using the overlay capabilities of GIS, the attribute data are georeferenced to the slope units. The GIS regional database is then exported to a statistical software package for analysis, from which a regional landslide hazard model is developed. An important aspect is the conversion of various parameters from nominal to numeric, e.g., lithology, landuse. This can be done through the creation of dummy variable matrix automatically (Fig. 16).

Due to the binary character of the response and some predictor variables, and the dubious normality of some of the variables, a logistic regression procedure is selected. Logistic regression model is a multivariate technique which considers several physical parameters (variables) that may affect probability. It accepts both binary and scalar values as the independent variables, which allows for the use of variables that are not continuous or qualitatively derived.

The technique of logistic multiple regression yields coefficients for each variable based on data derived taken across a study area (SPSS 1997). These coefficients serve as weights in an algorithm which are used in the GIS database to produce a map depicting the probability of landslide occurrence. Quantitatively, the relationship between the occurrence and its dependency on several variables can be expressed as (Equation 1):

$$\mathrm{Pr(event)} = 1/(1+e^{-Z}) \qquad (1)$$

where Pr(event) is the probability of an event occurring. Z varies from $-\infty$ to $+\infty$ and the probability varies from 0 to 1 on an S-shaped curve. Z is the linear combination (Equation 2):

$$Z = B_0 + B_1 X_1 + B_2 X_2 + ... + B_n X_n \qquad (2)$$

Where B_i ($i = 0, 1, ..., n$) is the coefficient estimated from the sample data, n is the number of independent variables (i.e. landslide-related physical parameters), and X_i ($i = 1, 2, ..., n$) is the independent variable. The coefficients for the logistic regression model are shown in Table 2.

Finally, the calculated logistic regression scores of slope stability from SPSS are imported back into GIS for further analysis and a predicted hazard map is obtained.

7.4 *Visualization of hazard scenario*

Hazard maps that resulted from bivariate analysis are based on numerical weight values and multivariate analysis is based on logistic regression scores in probability value. The hazard map generated from the analysis is classified into different levels of hazard for the general use. Practically, there is no straightforward statistical rule to categorize continuous data automatically and this is always unclear in landslides and debris flows hazard mapping. Most researchers use their

664

Table 2. Regression coefficients for the prediction model.

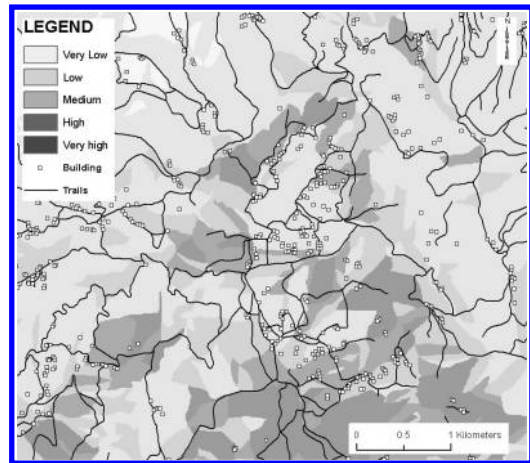| Variables	Coefficients
Geology	
Quartzite, schist (KF)	0.764
Marble, schist (MF)	−0.261
Meta-sandstone, phyllite (TF)	−0.708
Calc. shale, slate (SF)	−1.516
Limestone (CL)	−1.683
Granite (AG)	−1.600
Slope angle	
0°–15°	−0.284
15°–25°	−0.041
25°–35°	0.790
35°–45°	0.603
>45°	0.084
Slope aspect	
North (N)	0.087
Northeast (NE)	0.297
East (E)	0.400
Southeast (SE)	−0.228
South (S)	0.219
Southwest (SW)	−0.239
West (W)	−0.025
Northwest (NW)	0.320
Engineering geological unit	
Thin soil (TnSl)	0.013
Thick soil (TkSl)	0.238
Colluvium (Clv)	0.003
Alluvium (Alv)	0.252
High rock mass strength (HRMS)	−0.970
Medium rock mass strength (MRMS)	0.233
Low rock mass strength (LRMS)	1.642
Debris deposit (Dd)	0.853
Water bodies (Wb)	−0.663
Landuse	
Forest (Fo)	1.389
Shrubland (SrL)	−0.437
Grassland (GrL)	0.652
Cultivated land (CuL)	0.346
Barren land (BaL)	2.174
Debris (D)	0.671
Constant	−3.407

Figure 17. Visualization of hazard map that resulted from spatial prediction modeling (upper-middle part of the study area).

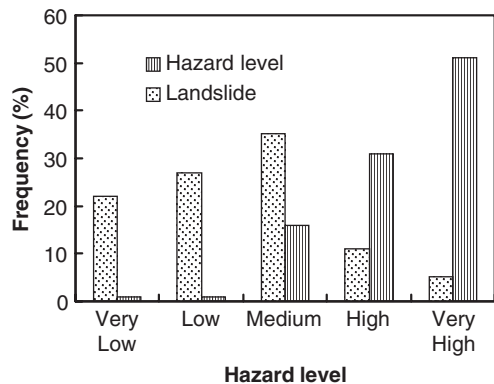Figure 18. Validation of hazard prediction by using spatial distribution of past slope failure events.

expert opinion basis along with available classification methods to develop class boundaries. The range of the susceptibility (hazard) to landslides is classified into five hazard levels based on the histogram of the estimated susceptibility. The hazard levels categorized are very low, low, medium, high, and very high hazard levels applying classification methods found in GIS and with overlaying of past landslide and debris flow map for the adjustment of boundaries (Fig. 17).

7.5 *Validation of the prediction model*

In prediction modelling, the most important and the absolutely essential component is to carry out a validation of the prediction results. Some works have addressed the issue of map validation (Carrara 1983, Brabb 1984, Yin & Yan 1988, Carrara et al. 1991, Van Westen 1993, Carrara *et al.* 1995, Chung et al. 1995, Luzi & Pergalani 1996, Chung & Fabbri 2003, Remondo et al. 2003).

We presented here rather simple and useful procedures for the validation, so that the prediction results can be interpreted meaningfully with respect to the future landslide hazard. Map crossing between predicted hazard map and slope failure of past events was carried out on raster maps. The calculated and classified hazard levels are found in good agreement with occurrence of preexisting landslides because the higher the hazard level, the greater the frequency of landslide occurrence found (Fig. 18). Figure 18.

Validation of hazard prediction by using spatial distribution of past slope failure events.

8 DISCUSSION AND CONCLUSIONS

Analysis of landslide hazard requires evaluation of the relationships between various terrain conditions and landslide occurrences. An experienced earth scientist has the capability to assess the overall slope conditions and to extract the critical parameters. However, an objective procedure is often desired to quantitatively support the slope instability assessment. For this purpose, A GIS technique is adopted and has proved the capability of improving the hazard models by evaluating their results and adjusting the input variables in interactive manner.

Concerning methodological approaches, a quantitative statistical approach is used which showed the successful modelling of landslide and debris flow hazard in the area by spatial integration of easily accessible data and sets of data that linked to actual behavior of slope movements. The analysis indicated that the use of geomorphological and geological variables in the statistical analysis improved the overall accuracy of the final hazard map considerably. Also, the comparison of hazard modelling result demonstrated that statistical modeling minimizes the effect of error in selecting input variables.

Therefore, the spatial prediction model result in this study is applicable to decisions makers dealing with multipurpose use of space for human activity in the mountainous terrains of the Himalayan region. The advantage of the model is that it allows rapid assessment of spatial correlation of the geomorphological and geological attributes over large areas.

The modelling results shows that very high hazardous are mainly confined to upper and middle reaches of the study area. Also the spatially localized scattered distribution of very high hazardous zones are found to be embedded in the medium to high hazardous zones over the rest of the area.

ACKNOWLEDGEMENTS

REFERENCES

Atkinson, P.M. & Massari, R. 1998. Generalized linear modeling of susceptibility to landsliding in the central Apennines, Italy. *Computers and Geosciences* 24(4): 373–385.

Brabb, E.E. 1984. Innovative approaches to landslide hazard and risk mapping. In *Proc. 4th Int. Symp. on Landslides*, 1: 307–324, Toronto.

Carrara, A. 1983. A multivariate model for landslide hazard evaluation, *Mathematical Geology* 15: 403–426.

Carrara, A., Cardinali, M., Detti, R., Guzetti, F., Pasqui, V. & Reichenbach, P. 1991. GIS techniques and statistical models in evaluating landslide hazard. *Earth Surface Processes and Landforms* 16: 427–445.

Carrara, A., Cardinali, M., Guzzetti, F. & Reichenbach, P. 1995. GIS-based techniques for mapping landslide hazard. In A. Carrara & F. Guzzetti (eds), *GIS in Assessing Natural Hazards*: 135–176, Kluwer Publications, Dordrecht.

Carrara, A., Guzzetti, F., Cardinali, M. & Reichenbach, P. 1998. Current limitations in modeling landslide hazard. In A. Buccianti et al. (eds), *Proc. of IAMG'98*: 195–203.

Carrara, A., Guzzetti, F., Cardinali, M. & Reichenbach, P. 1999. Use of GIS Technology in the Prediction and Monitoring of Landslide Hazard. *Natural Hazards* 20: 117–135.

Chung, C.F., Fabbri, A.G. & VanWesten C.J. 1995. Multivariate regression analysis for landslide hazard zonation. In A. Carrara & F. Guzzetti (eds), *GIS in Assessing Natural Hazards*: 107–133, Kluwer, Dordrecht.

Chung, C.F. & Fabbri, A.G. 2003. Validation of Spatial Prediction Models for Landslide Hazard Mapping. *Natural Hazards* 30: 451–472.

Coppock, J.T. 1995. GIS and natural hazards: An overview from a GIS perspective. In A. Carrara & F. Guzzetti (eds), *GIS in Assessing Natural Hazards*: 21–34, Kluwer Academic Publishers, Dordrecht.

Cruden, D.M. & Varnes, D.J. 1996. Landslide types and processes. In Schuster, R.L. & Turner, A.K. (eds), *Landslides, investigation and mitigation*, TRB Special Report 247: 36–75, National Academy Press, Washington, DC.

D.H.M. 1993. *Climatological Records of Nepal, 1963–1993*. Department of Hydrology and Meteorology, Ministry of Water Resources, Kathmandu, Nepal.

Esaki, T., Xie, M., Mitani, Y. & Zhou, G. 2004, Development of GIS-based spatial three-dimensional slope stability analysis system: 3DSlopeGIS. *J. of Appl. Computing in Civil Engineering* 13: 21–32.

Greenway, D.R. 1987. Vegetation and slope stability. In M.G. Anderwon & K.S. Richards (eds), *Slope Stability*: 187–230, Wiley, New York.

Guzzetti, F., Carrarra, A., Cardinali, M. & Reichenbach, P. 1999. Landslide hazard evaluation: A review of current techniques and their application in a multi-scale study, central Italy, *Geomorphology* 31: 181–216.

Guzzetti, F., Cardinali, M., Reichenbach, P. & Carrara, A. 2000. Comparing landslide maps: A case study in the Upper Tiber River Basin, Central Italy. *Environmental Management* 25(3): 247–263.

Hansen, A. 1984. Landslide Hazard Analysis. In D. Brunsden & D.B. Prior (eds), *Slope Instability*: 523–602, Wiley & Sons, New York.

Hungr, O. 1995. A model for the runout analysis of rapid flow slides, debris flows and avalanches. *Can. Geotech. J.* 32(4): 610–623.

Hungr, O., Evans, S.G., Bovis, M. & Hutchinson, J.N. 2001. Review of the classification of landslides of the flow

type. *Environmental and Engineering Geoscience*, VII: 221–238.

Hutchinson, J.N. 1988. General report: morphological and geotechnical parameters of landslides in relation to geology and hydrology. *Proc. 5th Int. Symp. on Landslides*, Lausanne, 1: 3–35.

Hutchinson, J.N. 1995. Keynote paper: Landslide hazard assessment, In *Proc. 6th Int. Symp. on Landslides*, 3: 1805–1841, Christchurch, 1992, Balkema, Rotterdam.

Luzi, L. & Pergalani, F. 1996. A methodology for slope instability zonation using a probabilistic method. *Actas VI Congreso Nacional y Conferencia Internacional de Geología Ambiental y Ordenación del Territorio*, 1: 537–556.

Mark, R.K. & Ellen, S.D. 1995. Statistical and simulation models for mapping debris-flows hazard. In A. Carrara & F. Guzzetti (eds), *GIS in Assessing Natural Hazards*: 93–106, Kluwer Academic Publisher, Dordrecht.

Montgomery, D.R. & Dietrich, W.E. 1994. A physically based model for the topographic control of shallow landsliding. *Water Resources Research* 30(4): 1153–1171.

Remondo, J., González, A., DeTerán, J.R.D., Cendrero, A., Fabbri, A. & Chung, C.F. 2003. Validation of landslide susceptibility maps: Examples and applications from a case study in Northern Spain. *Natural Hazards* 30: 437–449.

Rengers, N., Soeters, R., Van Riet P.A.L.M., & Vlasblom, E. 1991. Large scale engineering geological mapping in the central Spanish Pyrenees. *ITC Journal,* 1991–4: 262–268.

Soeters, R. & Van Westen, C.J. 1996. Slope Instability Recognition, Analysis and Zonation. In A.K. Turner & R.L. Schuster (eds), *Landslides, investigation and mitigation*, TRB Special Report 247: 129–177, National Academy Press, Washington, D.C.

SPSS 1997. *SPSS advanced statistics 7.5*. SPSS, Chicago.

Stöcklin, J. 1980. Geology of Nepal and its Regional Frame, *J. Geol. Soc., London* 137: 1–34.

Terlien, M.T.J., Van Westen, C.J. & van Asch, T.W.J. 1995. Deterministic modeling in GIS based landslide hazard assessment. In A. Carrara & F. Guzzetti (eds), *GIS in Assessing Natural Hazards*: 57–78, Kluwer Academic Publishers, Dordrecht.

Van Westen, C.J. 1993. *GISSIZ: Training package for geographic information systems in slope instability zonation. Volume 1 – Theory*, International Institute for Aerospace Survey and Earth Sciences (ITC), 15: 245.

Van Westen, C.J., Rengers, N., Terlien, M.T.J. & Soeters, R. 1997. Prediction of the occurrence of slope instability phenomena through GIS-based hazard zonation. *Geologische Rundschau*, 86: 404–414.

Varnes, D.J. 1978. Slope movements, type and processes. In R.L. Schuster & R.J. Krizek (eds), *Landslide Analysis and Control*, TRB Special Report 176: 11–13, National Academy Press, Washington, DC.

Varnes, D.J. 1981. Slope stability problems of the circum Pacific region as related to mineral and energy resource. In M.T. Halbouty (ed.), *Energy Resources of the Pacific Region*, AAPG Studies in Geology 12: 489–505.

Varnes, D.J. 1984. *Landslide Hazard Zonation: A Review of Principles and Practice*, UNESCO Press, Paris.

Wang, S.Q. & Unwin, D.J. 1992. Modelling landslide distribution on loess soils in China: an investigation. *Int. J. of Geographical Information Systems*, 6: 391–405.

Yin, K.L. & Yan, T.Z. 1988. Statistical prediction models for slope instability of metamorphosed rocks. In *Proc. 5th Int. Symp. on Landslides, Lausanne*, 2: 1269–1272, Rotterdam: Balkema.

Hazard assessment of landslides triggered by heavy rainfall using Artificial Neural Networks and GIS

H.B. Wang, K. Sassa, H. Fukuoka & G.H. Wang

Research Centre on Landslides, Disaster Prevention Research Institute, Kyoto University, Japan

ABSTRACT: This paper proposes Back Propagation Neural Networks (BPNN) to predict the probability of landslide occurrence in scenario of rainfall in Minamata area, the southern Kyushu Island of Japan. In this study, datasets of the geospatial database were chosen for the input variables of the presented model, including lithology, topography, soil, land use and rainfall parameters such as cumulative precipitation and maximum daily precipitation in heavy rainfall events of six or seven days. The training sample consists of 602 cells with landslide occurrence and 1600 cells in the stable areas. Using the trained BPNN with 49 input nodes, three hidden layers and one output node, all the 239,589 cells obtained by overlaying were processed to produce a map of landslide probability for a maximum daily precipitation of 329 mm and a maximum cumulative precipitation of 581 mm, in a heavy rainfall event in the future. The resultant hazard map was classified into four hazard levels: high, moderate, low and very low.

1 INTRODUCTION

1.1 *The study area*

Minamata city, as the study area, is located on the coast of the southern island of Kyushu (Fig. 1). The site lies between the latitudes 32°6′30″N and 32°14′10″N, and longitudes 130°21′40″E and 130°36′E, and covers an area of 162.6 km². The bedrocks of the study area crop out mainly andesite from the Pliocene to the Early Pleistocene, such as lava, tuff breccia, etc. The topography of this area is characterized by mountainous areas with few hilly lands in northwest Minamata. With an average annual temperature of 16.8 Celsius and an average precipitation of 1,711 millimeters, it is characterized by a temperate oceanic climate with abundant rainfall.

1.2 *Geospatial database*

In the area studied, the dominant landslides have been shallow with debris flows that occurred during days of high intensity rainfall or shortly thereafter. Aerial

Figure 1. Location of the study area.

photographs taken in Feb. of both 1999 and 2002 at a scale of 1:30,000 were adopted for the interpretation of landslides, which occurred in 1998 and 2001. Landslides were identified at Hougawachi and Fukugawa areas using aerial photographs taken after disaster of July 2003. A total of 65 landslides were distinguished in three periods, 11 of which were extracted from aerial photographs taken in 1998 and 39 landslides in 2001.

A regularly spaced DEM was created from 1:25,000-scale digitized topographical maps at a spatial resolution of 25 m. Two thematic maps of slope and aspect were classified from raster of the DEM data. The geological setting of the study area is relatively uncomplicated, and the bedrock outcrops are mainly andesite, most of which is extremely weathered and susceptible to landsliding. The 1:50,000-scale map of geology was downloaded from an official website of Land and Water Bureau, Ministry of Land, Infrastructure and Transport (MLIT), Japan, and then used to construct the lithology database. For ease of analysis, rock types were categorized into 9 classes. A soil distribution map was also downloaded from the same website and digitized at a scale of 1:50,000. Land use/cover was extracted from the ortho-images dated February 29, 1999 and February 25, 2002, to update a land use map of the study area generated before 1984.

1.3 *Rainfall conditions*

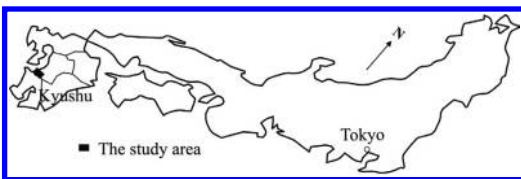In Minamata area, rainfall data from two gauges near the areas most affected by the landsliding were available,

669

the Minamata gauge of the Japan Meteorological Agency and the Fukugawa gauge owned by the Kumamoto prefecture. All the rainfall data in other 26 gauges extracted to construct the rainfall database were downloaded from the Internet library of the Japan Meteorological Agency, including intensity, duration of rainfall from 1979 to 2004, and some statistical results about climatic conditions.

1.3.1 *The July 20, 2003 event*

The Minamata area experienced heavy rainfall with cumulative totals over 397 mm within 24 hours recorded at the Fukugawa gauge on July 19 to 21, 2003 (Fig. 2). The spatial distribution of cumulative rainfall within 48 hours elucidated that the area of study was a centre of intensive rainfall up to 430 mm. During the July 20 event, rainfall was concentrated during the first six hours early morning, in which the hourly precipitation exceeded 72 mm at 2 am and the cumulative rainfall at 7 am reached up to 224 mm measured at the Minamata gauge. Due to the high intensity of rainfall, debris flows occurred at Hougawachi and Fukugawa at 4:20 am, resulting in 19 persons dead, 7 injured persons and 15 damaged houses.

1.3.2 *Historical rainfall events*

Precipitation observations of the Japan Meteorological Agency were made from 1979 until now. As aforementioned, the Minamata area was characterized as a temperate oceanic climate with abundant rainfall. Analysis of the historical daily-rainfall records reveals that high-intensity rainfall was very common, especially during the months of June and July in the Kyushu Island, and many landslides triggered by rainfall were reported causing deaths and property damage. On the basis of detailed analysis of rainfall data from 1979 to 2003, it can be assumed that landslides which occurred in 1998 and 2001 were due to intensive rainfall from 18 to 24 June, 1998 and 18 to 23 June, 2001 respectively. At Minamata gauge, for 25 years for which the
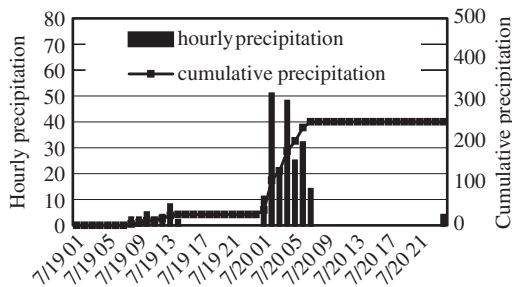
information is available, the maximum daily rainfall exceeded 329 mm, which triggered debris flows causing 21 deaths in Izumi of Kagoshima prefecture in July of 1997, whilst maximum hourly rainfall reached up to 91 mm recorded at Fukugawa gauge, which caused the disaster of July 20, 2003. Comprehensive analyses of the data recorded over 25 years can reveal, moreover, that average daily precipitation varied from a low of 6.17 mm in 1981 to a high of 96.83 mm in 1979, and the maximum of cumulative rainfall exceeded 581 mm measured at Minamata gauge during the six-day heavy rainfall events. It is also clarified that monthly precipitation was mainly concentrated from June to August, the maximum of which was 962 mm in August 1993. Maximum daily precipitations reached 81 mm in June 1998 and 125 mm in June whilst maximum hourly precipitations exceeded 25 mm on 21 June 1998 and 53 mm on 23 June 2001 (Fig. 3). All the isohyets were made by interpolating data on daily rainfall measurements available for the surrounding areas of Minamata city. In the study area, the maximum daily precipitation reached 79 mm and 125 mm, while the cumulative precipitation was 273 mm and 329 mm in heavy rainy days of June in 1998 and 2001 (Fig. 4).
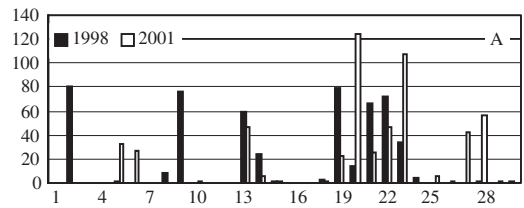

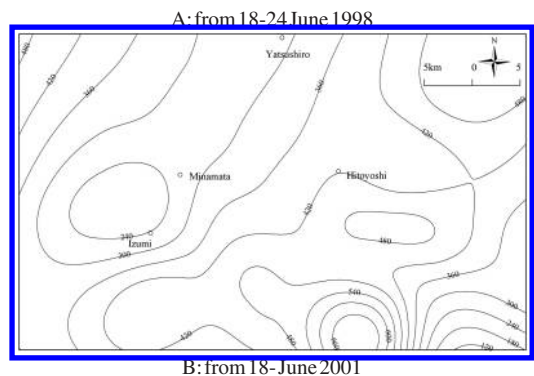Figure 3. Daily precipitation of June 18998 and 2001 (mm).

Figure 2. Average daily precipitations in heavy rainfall events of June between 1979 and 2003 (mm).

Figure 4. Cumulative precipitation in intensive rainfall events.

670

2 METHODS

2.1 *Back propagation Neural Networks*

Artificial Neural Networks (ANN) are a powerful tool for the prediction of nonlinearities. They can learn some target values (desired output) from a set of chosen input data that have been introduced to a network under both supervised and self-adjusted or unsupervised learning algorithms. There are many kinds of ANN models, among which Back Propagation Neural Networks (BPNN) are the most widely applied. In a feed-forward network, the layers are completely connected to one another. The most common configuration of the BPNN is composed of three layers, and this method can be expended to multi-layer models. The model adjusts the connection weights between the nodes by learning to memorize every one of the network learning and training patterns, each of which is composed of an input-output pair.

In the BPNN model, highly non-linear correspondence relations of input and output can be generated by self-adaptive learning of a large number of training patterns. The results of the first layer are passed to the next layer. This process is repeated for each layer until an output is generated. The difference between the generated output and a training set output is calculated. This difference is fed back to the network where it is used for connection weight readjustment by iteratively attempting to minimize the difference to within a predefined tolerance. The fundamental back-propagation algorithm of BPNN can be found in the literature (Rumelhart et al. 1986).

2.2 *BPNN application*

Input variables in a BPNN model are the factors influencing an evaluation target. However, main causes of slope stability or landslide occurrence depend on different regions and different types of slopes. For instance, important considerations for the rain-induced slope are density, strength and annual, monthly volume of rain as the external causes, and friction coefficients and cohesions as mainly internal causes. There are also different factors between soil slopes and rocky slopes contributing to a failure of a slope. In this study, data sets of the geospatial database were chosen for the input variables as listed in Table 1, including

Table 1. The factors selected to BPNN from the geospatial database.

Attribute	Description	Code	Attribute	Description	Code
Lithology	Reclaimed land	1	Slope	0–10	1
	Gravel sand, and mud (lowland sediments)	2		10–15	2
	Alternating beds of sandstone & mudstone, sandstone and mudstone	3		15–20	3
	Sandstone and conglomerate	4		20–30	4
	Mainly sandstone with subordinate slump deposit	5		30–40	5
	Mainly slump deposits	6		40–50	6
	Limestone	7		50–60	7
	Pyroclastics	8		≥60	8
	Andesitic rock (lava, tuff breccia)	9			
Land use	Irrigated field	1	Elevation	0–100	1
	Non-irrigated farmland	2		100–200	2
	Garden	3		200–300	3
	Forested land	4		300–400	4
	Grassed land/barren land	5		400–500	5
	Residential area	6		500–600	6
	Water	7		≥600	7
Soil	Lithosol	1	Aspect	Flat	1
	Ando soil	2		N	2
	Dry brown forested soil	3		NE	3
	Brown forested soil	4		E	4
	Red soil	5		SE	5
	Yellow soil	6		S	6
	Dark red soil	7		SW	7
	Gray lowland soil	8		W	8
	Other soil	9		NW	9
Rainfall	Maximum daily precipitation				
	Average daily precipitation				

lithology, slope, aspect, elevation, soil and land use, as well as rainfall conditions such as cumulative precipitation and maximum daily precipitation in heavy rainfall events of six or seven days.

In this BPNN modelling, input variables of all the training samples were described with qualitative and quantitative indices such as categorical and continuous. The presence or absence of landslide occurrence can be represented by 1 or 0 indicating the probability of landsliding, whilst the presence of the attributes as binary in a cell within the geospatial database is 1 and the absence is 0. To predict the probability of landslide occurrence, the number of input variables in the training data sets was 49 apart from the maximum daily precipitation and the cumulative precipitation. The quantitative indices can be processed with different normalization methods to analyze data, for example, the rainfall parameters as continuous can be normalized by dividing each observation x_i by the maximum.

The maps of factors which influence the landslide occurrence are overlaid to obtain a combined map with intra-unit homogeneity. The study area contains 239×589 cells, each with a variable indicating the presence or absence of a landslide. Thus, the training sample size consisted of all 602 cells with landslide occurrence, in which 219 indicated the slope failure in 1998, 283 in 2001 and 100 in 2003, and 1600 cells in the stable areas, of which each 600 represented the areas without landslide in 1998 and 2001 respectively. As the training data described the probability of landslide occurrence as binary, which should be continuous in natural slope failure, many cells with landslide occurrence were assigned values of 0.75 to 1 ranking as high probability, some cells in the stable areas with 0 to 0.5 as low probability.

Rainfall parameters were obtained from the database of precipitation, and then 273 mm, 329 mm and 288 mm were determined for the cumulative precipitations in rainfall events of 1998, 2001 and 2003; 79 mm, 125 mm and 228 mm of maximum daily rainfall in 1998, 2001 and 2003. The data sets of 2202 cells were then input to the BPNN program for iteration to converge.

A five-layer BPNN with 49 input nodes and one output node was then constructed. Hidden nodes and the number of hidden layers were decided to obtain reasonable errors from repeated trainings. Consequently, hidden nodes were 36, 10 and 16 in 3 hidden layers respectively. Repeated trainings were completed and convergences were obtained until ε was considered to be a reasonable error. In the training model, the learning ratio was 0.9, the learning step was 0.7, the individual error was 0.01 and the collective error was 0.0001. Learning results correlated with the expected after 16,490 iterations and a trained BPNN model was generated.

3 RESULTS AND DISCUSSIONS

Using this model, when trained, all 239,589 cells were calculated to produce a map of landslide probability by applying it to all cell locations across the entire map in the case of 329 mm for the maximum daily precipitation and 581 mm, the maximum cumulative precipitation in an heavy rainfall event of the future. This involved reformatting the raster map images into a single input file which was fed through the trained network. The output was then converted into a digital image in the Arc/GIS and the resultant hazard map was classified into four probability levels, namely very low ($<$0.25), low (0.25–0.5), moderate (0.5–0.75), and high ($>$0.75), as shown in Fig. 5.

Throughout this study, the BPNN was applicable to predict the probability of landslide occurrence on the assumption of the rainfall as one trigger on June 1998 and 2001. Compared with statistical analysis commonly used, the BPNN is more suitable to produce the map of landslide hazard. Since the BPNN is independent of statistical distributions of data, there is no need for a specific statistical variable, and it can improve the accuracy of prediction and classification of landslides after learning like a human being. Owing to a large amount of data to be trained, however, the training of the BPNN needs considerable execution time and computer capacity.

In the BPNN model adopted to predict the landslide probability, some cells with landslide occurrence were randomly assigned with values of 0.75 to 1 ranking high probability of landsliding and some cells in the stable areas with 0 to 0.5 as low probability. In a strict sense, this model can not predict the probability of landslide occurrence, and the result can be better explained as landslide susceptibility. It can be seen that 81% of the total area were classified as very low susceptibility to landsliding and the high susceptibility zones were predicted nearly 18%.

These results can be interpreted so that the maximum of rainfall parameters, which were used in the predictive model, together with steep valley-side slopes make great contribution to high susceptibility of landslide occurrence. Another explanation of this result map is that the number of sampling cells with landslide absence is much more than that of cells with the presence of landsliding so that this data distribution pattern could account for the concentration of stable areas, or high densities of landslide occurrence, despite of the independence of BPNN on the statistical distribution of data. However, the high landslide susceptibility classes cover all the landslides present in this area, and it thus can be noted that the model is a success in assessing landslide susceptibility.

Nevertheless, there are some inevitable errors because of difficulties with prediction of the spatial and temporary distribution of landslides. Firstly, the
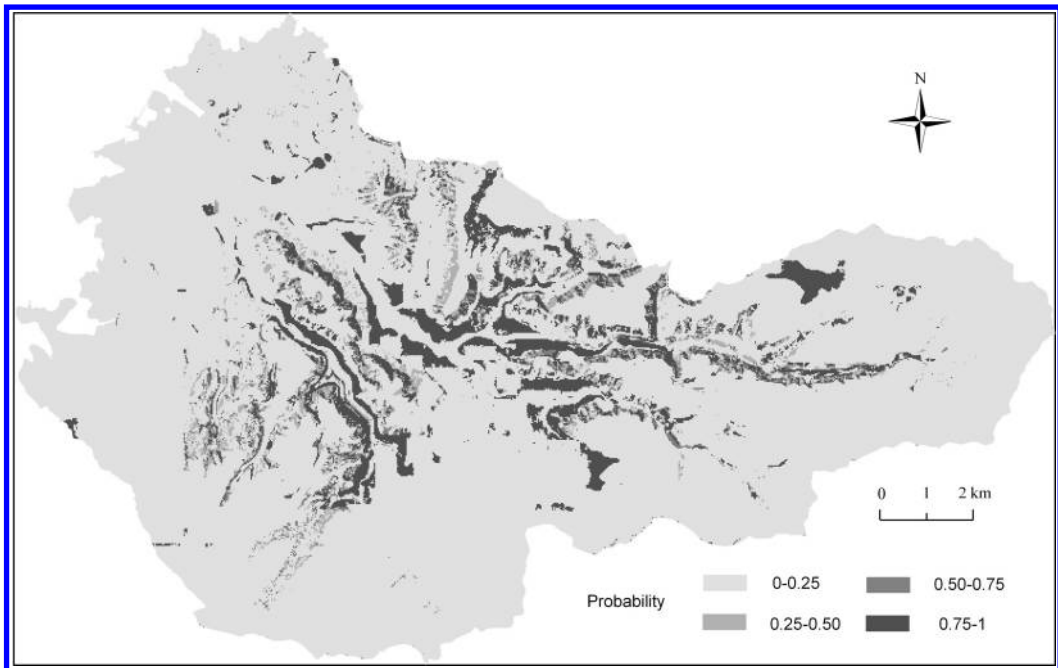
672

Figure 5.   The resultant map of rainfall-induced landslide assessment.

particular problem with uncertainty is that the 1: 25,000-scale topographic map used to generate a DEM of 25 m resolution cannot fully reflect micro-topographic conditions prerequisite for the occurrence of landslides, because landslide occurrence in the study area is to some extent characterized by small failure volumes. It should be also kept in mind that the reliability and accuracy of data during collection and storage is crucial to assess landslide probability correctly, for example, some landslides interpreted from aerial photographs were probably not triggered by the rainfall events of 1998 and 2001. In the case of rainfall triggered landslides, the intensity, duration and frequencies, as well as antecedent rainfall, may have some influence on the slope failures, but this effect is not completely taken into account by the predictive model as described above. If the relationship between rainfall and landslide occurrence in this area can be improved much more in further research, the ANNs may provide a robust evaluation of landslide hazard.

However, the probability of landslide occurrence should be evaluated on a site-specific scale in this area, and accurate information on geological details, geotechnical parameters and pore water pressures should be obtained because it is of paramount importance for detailed studies concerning individual sites. This suggests that further research should focus on the soil-hydrology, hydraulic conductivity, geotechnical features of materials, rainfall characteristics and

failure patterns, etc., and reasonable models should be utilized to predict the probability or evaluate the Factor of Safety using the GIS in a small area.

4   CONCLUDING REMARKS

This paper proposed a BPNN model to predict the probability of landslide occurrence triggered by rainfall after the interpretation of landslide locations from aerial photographs. Using the trained neural networks, all 239,589 cells were converted to landslide probabilities in the case of 329 mm for the maximum daily precipitation and 581 mm, the max of the cumulative precipitation in a six-day intensive rainfall event of the future. The resultant hazard map was generated showing the four probability levels of landslide occurrence. The study indicates the convenience of using GIS and the BPNN to delineate the areas prone to landsliding from complex phenomena, and expands the models used for landslide hazard/susceptibility assessment. If necessary, the model as presented can also combine different parameters of rainfall with different characteristics to predict the probability of landslides. The information on the hazard map can assist land use planners in making planning decisions for community development of the study area, in which areas believed with high susceptibility to rainfall-triggered landslide activity should be studied

673

carefully on a site-specific scale before planning any development.

REFERENCES

Cruden, D.M. & Varnes, D.J. 1996. Landslide Types and Processes. In Turner, A.K., Schuster, R.L. (eds.), *Landslides Investigation and Mitigation*. Transportation Research Board Special Report 247, National Research Council, Washington, D.C., National Academy Press.

Guzzetti, F., Carrarra, A., Cardinali, M. & Reichenbach, P. 1999. Landslide hazard evaluation: a review of current techniques and their application in a multi-scale study, Central Italy. *Geomorphology* 3: 181–216.

IDNHR, Advisory Committee. 1987. *Confronting Natural Disasters*. National Academy Press, WA.

Lee, S., Ryu, J.H., Min, K. & Won, J.S. 2003. Landslide susceptibility analysis using GIS and artificial neural network. *Earth Surface Processes and Landforms* 28(12): 1361–1376.

Rumelhart, D.E., Hinton, G.E. & Williams, R.J. 1986. Learning representations by back-propagating errors. *Nature* 323: 533–536.

Ushiyama, M. 2004. Characteristics of heavy rainfall disaster in the Kyushu district from July 19 to 21 2003. *Journal of Natural Disaster Science* 22(4): 376–385.

Varnes, D.J., IAEG Commission on landslides and other Mass-Movements. 1984. *Landslide hazard zonation: A review of principles and practices*. UNESCO Press, Paris.

A general landslide distribution: further examination

D.L. Turcotte
Department of Geology, University of California, Davis, CA, USA

B.D. Malamud
Environmental Monitoring and Modeling Research Group, Department of Geography, King's College London, Strand, London, UK

F. Guzzetti & P. Reichenbach
CNR–IRPI Perugia, Perugia, Italy

ABSTRACT: Large numbers of landslides can be associated with a trigger, i.e. an earthquake or a large storm. We have hypothesized (Malamud *et al.* 2004a) that the frequency-area statistics of landslides triggered in an event are well approximated by a three-parameter inverse-gamma distribution, irrespective of the trigger type. The use of this general distribution was established using three substantially complete and well-documented landslide event inventories: 11,000 landslides triggered by the Northridge California Earthquake, 4,000 landslides triggered by a snowmelt event in the Umbria region of Italy, and 9,000 landslides triggered by heavy rainfall associated with Hurricane Mitch in Guatemala. In this paper, we examine further this general landslide distribution by using an inventory of 165 landslides triggered by a rainfall event in the region of Todi, Central Italy. Our previous studies have shown the applicability of our general landslide distribution to events with 4,000–11,000 landslides. This smaller inventory provides a critical step in examining the applicability of the general landslide distribution. We find very good agreement of the Todi event with our general distribution. This also provides support for our further hypothesis that the mean area of landslides triggered by an event is approximately independent of the event size.

1 INTRODUCTION

Landslides are complex phenomena influenced by many factors, including soil and rock types, bedding planes, topography, and moisture content. Landslide events are single to many thousands of landslides, generally associated with a trigger such as an earthquake, a large storm, a rapid snowmelt, or a volcanic eruption. A landslide event may be quantified by the frequency-area distribution of the triggered landslides. We have recently shown (Malamud *et al.* 2004a) that the frequency-area statistics of three substantially complete landslide inventories are well approximated by the same probability density function, a three-parameter inverse-gamma distribution. We also introduced a landslide-event magnitude scale $m_L = \log(N_{LT})$, with N_{LT} the total number of landslides associated with the landslide event, in analogy to the Richter earthquake magnitude scale. We argue that the statistics of triggered-landslide events under a wide variety of conditions follow a general statistical behaviour to a good approximation. Such a 'general' statistical behaviour

is widely accepted for the frequency-magnitude statistics of earthquakes, which are also complex, but generally follow a power-law relationship between the number of earthquakes and the earthquake rupture area, the Gutenberg-Richter relation.

In this paper, we will first discuss our 'general' probability distribution of landslide areas for triggered landslide events, and then several implications of having a 'general' distribution, including (i) a magnitude scale for landslide events, (ii) the same theoretical average area of landslides associated with any given landslide event, and (iii) the ability to extrapolate for incomplete landslide events or historical inventories. We will also present a fourth, much smaller, landslide inventory from Todi, central Italy.

2 FREQUENCY-AREA DISTRIBUTIONS

In order to give the statistical distribution of landslide areas, a probability density function $p(A_L)$ is defined

675

according to

$$p(A_L) = \frac{1}{N_{LT}} \frac{\delta N_L}{\delta A_L} \qquad (1)$$

with the normalization condition

$$\int_0^\infty p(A_L) dA_L = 1 \qquad (2)$$

where A_L is landslide area, N_{LT} is the total number of landslides in the inventory, and δN_L is the number of landslides with areas between A_L and $A_L + \delta A_L$.

In Figure 1 we present the probability densities $p(A_L)$ for three substantially complete landslide inventories, from the USA, Italy and Guatemala. A detailed discussion of each inventory is found in Malamud *et al.* (2004a).

The three sets of probability densities given in Figure 1 exhibit a characteristic shape (Guzzetti *et al.* 2002, Malamud *et al.* 2004a), with densities increasing to a maximum value (most abundant landslide size) and then decreasing with a power-law tail. The inventories were estimated to be nearly complete (Harp & Jibson 1995, 1996, Cardinali *et al.* 2000, Bucknam *et al.* 2001, Guzzetti *et al.* 2002) for landslides with length scales greater than 5–15 m ($A_L \approx 25$–$225\,\mathrm{m}^2$), therefore the 'rollover' in Figure 1 is regarded as real. Based on the good agreement between these three sets of probability densities, we proposed (Malamud *et al.* 2004a) a general probability distribution for landslides, a three-parameter inverse-gamma distribution, given by (Johnson & Kotz 1970, Evans *et al.* 2000)

$$p(A_L; \rho, a, s) = \frac{1}{a\Gamma(\rho)} \left[\frac{a}{A_L - s} \right]^{\rho+1} \exp\left[-\frac{a}{A_L - s} \right] \qquad (3)$$

where $\Gamma(\rho)$ is the gamma function of ρ. The inverse-gamma distribution has a power-law decay with exponent $-(\rho + 1)$ for medium and large areas and an exponential rollover for small areas. The maximum likelihood fit of Equation 3 to the three data sets in Figure 1 yields $\rho = 1.40$, $a = 1.28 \times 10^{-3}\,\mathrm{km}^2$, and $s = 1.32 \times 10^{-4}\,\mathrm{km}^2$, with coefficient of determination $r^2 = 0.965$; the power-law tail has exponent $\rho + 1 = 2.40$. Many authors (see Malamud *et al.* 2004a for a review) have also noted that the frequency-area distribution of large landslides correlate with a power-law tail. This common behaviour is observed despite large differences in landslide types, topography, soil types, and triggering mechanisms.

On the basis of the good agreement between the three landslide inventories and the inverse-gamma distribution illustrated in Figure 1, Malamud *et al.* (2004a) hypothesized that the distribution given in
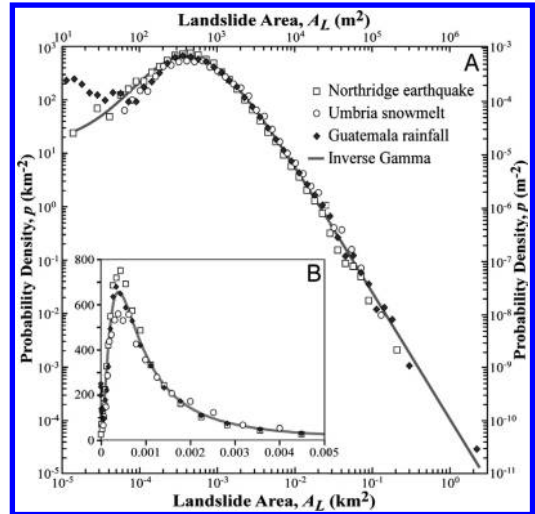

Figure 1. Dependence of landslide probability densities p on landslide area A_L, for three landslide inventories (figure after Malamud *et al.* 2004a): (i) 11,111 landslides triggered by the 17 January 1994 Northridge earthquake in California (Harp & Jibson 1995, 1996); (ii) 4,233 landslides triggered by rapid snowmelt in the Umbria region of Italy in January 1997 (Cardinali *et al.* 2000, Guzzetti *et al.* 2002); (iii) 9,594 landslides triggered by heavy rainfall from Hurricane Mitch in Guatemala in late October and early November 1998 (Bucknam *et al.* 2001). Probability densities are given on logarithmic axes in **A** and linear axes in **B**. Also included is our proposed general landslide probability distribution. This is the best-fit to the three landslide inventories of the three-parameter inverse-gamma distribution (Eq. 3), with $\rho = 1.40$, $a = 1.28 \times 10^{-3}\,\mathrm{km}^2$, and $s = 1.32 \times 10^{-4}\,\mathrm{km}^2$ (coefficient of determination $r^2 = 0.965$).

Equation 3 is general for landslide events. It is not expected that all landslide-event inventories will be in as good agreement as the three considered, but we do argue that the quantification, if only approximate, is valuable in assessing the landslide hazard.

In this paper we present the probability densities $p(A_L)$ for a fourth landslide inventory consisting of $N_{LT} = 165$ rainfall-triggered landslides in the vicinity of Todi, central Italy, with landslides occurring in the period March to May 2004. The inventory was complied through reconnaissance field surveys, and is reasonably complete. Probability densities for these landslides are given in Figure 2, along with the inverse-gamma distribution from Equation 3 with $\rho = 1.40$, $a = 1.28 \times 10^{-3}\,\mathrm{km}^2$, and $s = 1.32 \times 10^{-4}\,\mathrm{km}^2$, the best-fit to the three inventories in Figure 1.

A reasonable agreement is obtained between this fourth set of data (Fig. 2) from Todi, Italy, and the inverse-gamma distribution. It should be emphasized that the total number of landslides in the Todi event, $N_{LT} = 165$, is a factor of thirty to eighty less than the
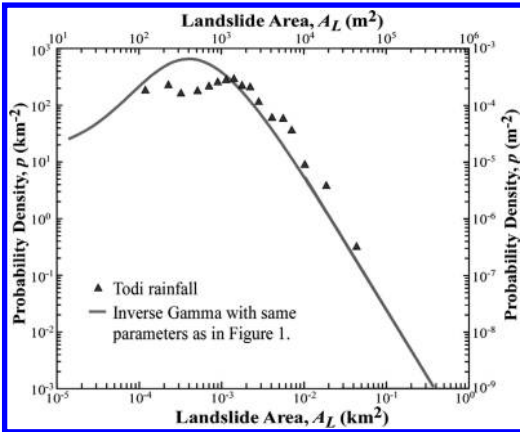
Figure 2. Dependence of landslide probability densities p on landslide area A_L, for 165 rainfall-triggered landslides in the vicinity of Todi, central Italy, occurring March to May 2004. Probability densities are given on logarithmic axes. Also included is the three-parameter inverse-gamma distribution (Eq. 3) with $\rho = 1.40$, $a = 1.28 \times 10^{-3} \text{km}^2$, and $s = 1.32 \times 10^{-4} \text{km}^2$, the best-fit to the three inventories in Figure 1.

number of landslides in the three substantially complete inventories given in Figure 1.

Before discussing implications of a 'general' landslide distribution we briefly discuss rockfall inventories. It has been shown (Dussauge *et al.* 2003, Malamud *et al.* 2004a) that the frequency-size statistics of rockfalls are very different than the statistics for other types of landslides as discussed above. Malamud *et al.* (2004a) examined three rockfall inventories, and found that the noncumulative frequency-volume relationship is best described by a power-law with exponent -1.93, with no 'rollover' for smaller rockfall volumes; the equivalent tail for the medium and large landslides in our 'general' distribution (Eq. 3, with $\rho = 1.40$), with areas converted to volumes, would be a power-law exponent of -1.07. There is a significant difference in slope for the medium and large landslides, compared to rockfalls, and the rockfalls have no 'rollover' for the smaller landslides. This difference has been attributed to different applicable physics, with rockfalls controlled by processes of fragmentation, compared to landslides that are primarily controlled by process of slope stability. We now discuss the implication of our general landslide distribution for the 'average' landslide area in the landslide event.

3 AVERAGE LANDSLIDE AREA

Assuming the validity of Equation 3 for the probability distribution of landslide areas in individual triggered

landslide events, Malamud *et al.* (2004a) used the distribution to derive a theoretical mean landslide area $\overline{A}_L$. This is the mean of all landslide areas that occur during a landslide event. The theoretical mean area is obtained by taking the first moment of the probability distribution function, giving

$$\overline{A}_L = \int_0^\infty A_L p(A_L) dA_L \tag{4}$$

Substitution of the three-parameter inverse-gamma distribution from Equation 3 into Equation 4 and integrating gives

$$\overline{A}_L = \frac{a}{\rho - 1} + s \tag{5}$$

For the landslide probability distribution given in Figure 1 we have $\rho = 1.40$, $a = 1.28 \times 10^{-3} \text{km}^2$, and $s = 1.32 \times 10^{-4} \text{km}^2$, so that $\overline{A}_L = 3.07 \times 10^{-3} \text{km}^2$. One implication of our landslide distribution is that since the probability distribution always has the same mean, all landslide events should have the same mean landslide area $\overline{A}_L = 3.07 \times 10^{-3} \text{km}^2 = 3{,}070 \text{m}^2$. This follows directly from the applicability of our proposed landslide distribution, and is independent of the number of landslides associated with a landslide event. Malamud *et al.* (2004a) found that the measured mean landslide areas $\overline{A}_L$ for the three event inventories, Northridge, Umbria, and Guatemala are $\overline{A}_L = 3.01 \times 10^{-3} \text{km}^2$, $2.14 \times 10^{-3} \text{km}^2$, and $3.07 \times 10^{-3} \text{km}^2$, in good agreement with the value predicted by our general landslide distribution. The mean landslide area for the fourth inventory from Todi, Italy, given in Figure 2, is $\overline{A}_L = 4.05 \times 10^{-3} \text{km}^2$. This is also in reasonably good agreement with the theoretical $\overline{A}_L = 3.07 \times 10^{-3} \text{km}^2$, particular for a triggered landslide event with so few landslides, and is potential further confirmation of our general landslide distribution.

4 LANDSLIDE MAGNITUDE SCALE

A second implication of having a 'general' landslide probability distribution, is the ability to create a landslide event magnitude scale. Measures of event sizes are useful for natural hazards. For example, the Richter magnitude scale for earthquakes is universally used and the general public has some understanding of the implications of an $M = 7.0$ earthquake. Over a dozen magnitude scales are available for other natural hazards, including the Saffir–Simpson scale (hurricanes), the Fujita scale (tornadoes), and the Volcanic Explosivity Index. Malamud *et al.* (2004a) proposed a magnitude scale m_L for a landslide event based on the logarithm to the base 10 of the total

677

number of landslides associated with the landslide event:

$$m_L = \log N_{LT} \tag{6}$$

Keefer (1984) and later Rodríguez *et al.* (1999) used a similar scale to quantify the number of landslides in earthquake-triggered landslide events: 100–1,000 landslides were classified as a two, 1,000–10,000 landslides a three, etc. The landslide event magnitudes for the three event inventories considered by Malamud *et al.* (2004a) are (i) Northridge earthquake triggered event, $m_L = 4.05$; (ii) Umbria snow-melt triggered event, $m_L = 3.63$; (iii) Guatemala rainfall triggered event, $m_L = 3.98$. These are in the range of $m_L = 3.6$–4.0.

While observed earthquakes span a wide range on the Richter scale, available landslide-event inventories are often restricted to a relatively narrow magnitude range. There are several reasons for this. Accurate inventories are restricted to populated areas and have been carried out only during the last ten years or so. Thus, very few large landslide events with $m_L > 4.0$ have occurred in regions where studies have been carried out. In addition, there has been little incentive to carry out studies of small magnitude landslide events, $m_L < 3.6$. A limited range was also the case for earthquakes in the 1940s when instrumental limitations limited studies to large earthquakes and the time span for studies was short so few large earthquakes had occurred. Therefore, one of the purpose of this paper was to introduce a fourth 'substantially' complete landslide inventory, but with a low magnitude. The Todi rainfall triggered event has $m_L = 2.22$.

Given several hundred landslide events and their magnitudes in a given region and time period, we hypothesize that there will be many more 'smaller' magnitude events compared to the larger ones. In analogy to earthquakes, we further hypothesize that these will follow a relationship such that $\log N_C = -bm_L + a$, where N_C is the number of landslide events with magnitudes greater than or equal to m_L, and b and a are constants. To partially confirm (or disprove) this hypothesize, we will need to assign landslide event magnitudes using substantially complete inventories, or making extrapolations based on 'incomplete' inventories, which we now discuss.

5 HISTORICAL AND INCOMPLETE INVENTORIES

A historical landslide inventory include the sum of many landslide events that have occurred over time. Assuming that our landslide probability distribution is applicable to all landslide events, the sum of events over time (the historical inventory) will also satisfy this

distribution (Malamud *et al.* 2004a). However, in historical inventories, the evidence for the existence of many smaller and medium landslides will have been lost due to wasting processes over time. Therefore, for the historical inventories, we attribute the deviation from our general landslide distribution to the incompleteness of the inventories. Using the general landslide distribution (Eq. 3) we can extrapolate an inventory, which contains just the largest landslides to give the total number and total volume of all landslides in the region.

Malamud *et al.* (2004b) used this extrapolation by considering two examples. Frequency densities were used since the inventories are incomplete and the normalization given in Equation 2 no longer holds. From Equation 1, the frequency density $f(A_L)$ is

$$f(A_L) = \frac{\delta N_L}{\delta A_L} = N_{LT}\, p(A_L) \tag{7}$$

Theoretical curves of $f(A_L)$ for various landslide-event magnitudes m_L are obtained by multiplying the probability distribution $p(A_L)$ given in Equation 3 by the total number of landslides in the event N_{LT}. Curves are given in Figure 3 for $m_L = 1$ ($N_{LT} = 10$) to $m_L = 8$ ($N_{LT} = 10^8$).
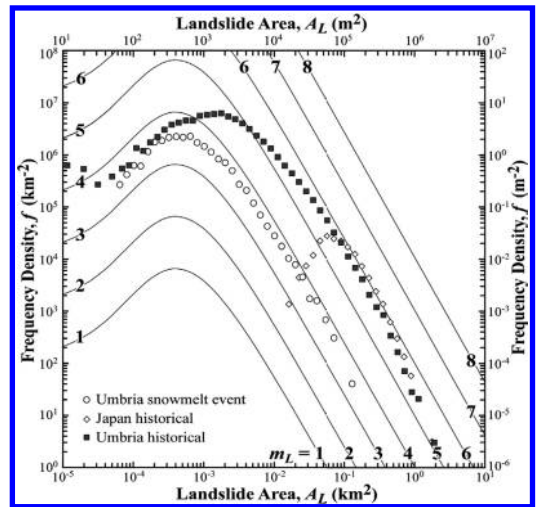

Figure 3. Dependence of the landslide frequency density f on landslide area A_L, both on logarithmic axes (figure after Malamud *et al.* 2004a). Landslide frequency distributions corresponding to our proposed landslide probability distribution (Eqs. 3 and 18) are given for landslide magnitudes $m_L = 1, 2, \ldots, 8$ ($N_{LT} = 10, 10^2, \ldots, 10^8$). Also included are the frequency densities for three landslide inventories: (i) Umbria snowmelt-triggered landslides as in Figure 1; (ii) 3,424 historical landslides in the Akaishi Ranges of central Japan (Ohmori & Sugai 1995) estimated to have occurred in the last 10 ky; (iii) 44,724 historical landslides in the Umbria region of Italy (Guzzetti *et al.* 2003) estimated to have occurred in the last 5–10 ky.

The same method can be used for a single incomplete landslide event inventory where only the largest landslides have been measured (e.g. those largest landslides that comprise just 1–2% of the total inventory) and the medium and smaller landslide sizes are not known. Using the general landslide distribution (Eq. 3) we can extrapolate the frequency densities of the largest landslides to give the total number of all landslides in the event, and estimate of the equivalent landslide event magnitude.

Figure 3 includes frequency densities for two historical landslide inventories, from Italy and Japan. Also included, for reference, are frequency densities for the snowmelt-triggered Umbria landslide event (Fig. 1). The first historical inventory includes 44,724 landslides in Umbria, Italy (Guzzetti *et al.* 2003) estimated to have occurred in the last 5–10 ky (thousand years). The power-law tail of the frequency densities is in good agreement with the landslide-event probability distribution (Eq. 3). With a landslide magnitude $m_L = 5.8 \pm 0.1$, we estimate that over the last 5–10 ky the total number of landslides that have occurred is $N_{LT} = 650{,}000 \pm 150{,}000$. The second historical inventory in Figure 3 includes 3,424 landslides in the Akaishi Ranges of central Japan (Ohmori & Sugai 1995) estimated to have occurred in the last 10 ky. The power-law tail of the frequency densities gives $m_L = 6.0 \pm 0.2$, corresponding to $N_{LT} = 1{,}100{,}000 \pm 500{,}000$.

Malamud *et al.* (2004b) related the landslide-event magnitude for individual events to the total area and volume of associated landslides, as well as the area and volume of the maximum landslides. They then used the historical landslide inventories just discussed (Fig. 3) from Italy and Japan, and made estimates of total area and volumes of landslides involved over time for each of the regions, and from these a lower bound estimate on regional erosion rates due to landslides. They inferred long-term erosion rates due to landslides in these two regions of Italy and Japan, as 0.4 and 2.2 mm yr^{-1}, respectively.

6 CONCLUSIONS

Landslide events display large variations in landslide types, sizes, distributions, patterns and triggering mechanisms. Many would question whether such complex phenomena can be quantified. Malamud *et al.* (2004a) showed that three well-documented and substantially complete landslide-event inventories from different parts of the world, each with different triggering mechanisms, have frequency-area statistics that are well approximated by a three-parameter inverse-gamma distribution (Eq. 3). In this paper, we have shown that a forth, much smaller landslide inventory, is also well-approximated by our proposed

'general' landslide inventory. It is clearly desirable to test this distribution using other substantially complete landslides inventories.

There are several important implications of the applicability of a general landslide distribution. It provides the basis for defining a landslide-event magnitude scale $m_L = \log(N_{LT})$, with N_{LT} the total number of landslides in the landslide event. The direct determination of the landslide-event magnitude requires that the landslide inventory be substantially complete. However, the general landslide distribution can be used to determine a landslide-event magnitude from a partial inventory, where the inventory is complete only for landslide areas greater than a specified value. It can also be used for historical inventories, which include the sum of landslide events over time. Using the general landslide distribution, the total area and volume of associated landslides in the event or sum of events over time, as well as the area and volume of the maximum landslides, can be directly related to the landslide-event magnitude m_L. These can then be used to estimate regional erosion due to landslides.

REFERENCES

Bucknam, R. C., Coe, J. A., Chavarría, M. M., Godt, J. W., Tarr, A. C., Bradley, L.-A., Rafferty, S., Hancock, D., Dart, R. L. & Johnson, M. L. 2001. *Landslides triggered by Hurricane Mitch in Guatemala – inventory and discussion*, U.S. Geological Survey Open File Report 01–443, 38 p.

Cardinali, M., Ardizzone, F., Galli, M., Guzzetti, F. & Reichenbach, P. 2000. Landslides triggered by rapid snow melting: The December 1996–January 1997 event in Central Italy. In Claps, P. P. & Siccardi, F. (eds) *Proceedings 1st Plinius Conference on Mediterranean Storms*, Maratea, Italy, 14–16 October 1999, Consenza: Editorial BIOS, 439–448.

Dussauge, C., Grasso, J.-R. & Helmstetter, A. 2003. Statistical analysis of rockfall volume distributions: Implications for rockfall dynamics. *Journal of Geophysical Research* 108(B6): 2286, doi.:10.1029/2001JB000650.

Evans, M., Hastings, N. & Peacock, J.B. 2000. *Statistical Distributions*, 3rd ed., New York: John Wiley, 248 pp.

Guzzetti, F., Malamud, B. D., Turcotte, D. L. & Reichenbach, P. 2002. Power-law correlations of landslide areas in central Italy. *Earth and Planetary Science Letters* 195: 169–183.

Guzzetti, F., Reichenbach, P., Cardinali, M., Ardizzone, F. & Galli, M. 2003 Impact of landslides in the Umbria Region, Central Italy, *Natural Hazards and Earth System Sciences* 3: 469–486.

Harp, E. L. & Jibson, R. L. 1995. *Inventory of landslides triggered by the 1994 Northridge, California earthquake*, U.S. Geological Survey Open File Report 95–213, electronic database.

Harp, E. L. & Jibson, R. L. 1996. Landslides triggered by the 1994 Northridge, California earthquake, *Seismological Society of America Bulletin* 86: S319–S332.

Johnson, N. L. & Kotz, S. 1970. *Continuous Univariate Distribution*, John Wiley, New York, 300 pp.

Keefer, D. K. 1984. Landslides caused by earthquakes, *Geological Society of America Bulletin* 95: 406–421.

Malamud, B. D., Turcotte, D. L., Guzzetti, F. & Reichenbach, P. 2004a. Landslide inventories and their statistical properties. *Earth Surface Processes and Landforms* 29: 687–711, doi 10.1002/esp.1064.

Malamud, B. D., Turcotte, D. L., Guzzetti, F. & Reichenbach, P. 2004b. Landslides, earthquakes, and erosion. *Earth and Planetary Science Letters* 229: 45–59.

Ohmori, H. & Sugai, T. 1995 Toward geomorphometric models for estimating landslide dynamics and forecasting landslide occurrence in Japanese mountains, *Zeiscrift fur Geomorphology (Suppl. Bd.)* 101: 149–164.

Rodríguez, C. E., Bommer, J. J. & Chandler, R. J. 1999. Earthquake-induced landslides: 1980–1997, *Soil Dynamics and Earthquake Engineering* 18: 325–346.

Developing and using landslide size frequency models

A.T. Moon & R.A. Wilson
Coffey Geosciences Pty Ltd, Australia

P.N. Flentje
University of Wollongong, Australia

ABSTRACT: Predicting the size and frequency of landslides is essential in landslide risk assessment. Records of past landslides are invariably incomplete and often provide little guidance on infrequent events. Presenting size frequency models graphically has the advantage of showing how observations, interpretations and judgements are interrelated, allows patterns to be recognized and understood, and models for different situations to be easily compared. Slope retreat rates were used to calibrate landslide size frequency models for individual slope units on an oversteepened escarpment above a road threatened by landslides in Australia. Evidence based models should be developed early and should be based on how slopes form and fail over a range of time scales. The size of deposits, historical records and measured movements can be used to help assess landslide process rates. Regional models can help in the judgment of how a particular slope may behave.

1 INTRODUCTION

1.1 *Limitations of the historical record*

Predicting the size and frequency of landslides is essential in landslide risk assessment. Records of past landslides can provide some information on what has happened, but are invariably incomplete and often provide little or no guidance on less frequent events that may occur. In landslide risk assessment, one of the most important questions to ask is what might happen in the future and often judgements have to be made about the likelihood of infrequent events with serious consequences with little, or no help from historical records.

1.2 *Using slope models*

Slope models can be used to support judgements about what might happen which go beyond the limitations of the historical record. Lee & Jones (2004) and Baynes & Lee (1998) discuss and give examples of the essential role of slope models in assessing the probability of landslides. Although slope models provide simplified views of reality, they enable prediction and they can be tested and updated with local and regional knowledge and relevant knowledge from elsewhere.

The slope models need to answer questions like:

– How did the slope form?
– How fast is it eroding?
– What proportion of the erosion is by landslides?

– What is the size frequency distribution of the landslides?

1.3 *Scope of this paper*

We have found landslide size frequency models useful in practice. This paper shows how models can be presented graphically, gives an example of their recent application and discusses the knowledge and evidence on which models are based.

2 PRESENTING JUDGEMENTS ABOUT THE SIZE AND FREQUENCY OF LANDSLIDES

Observations and judgements about the size and frequency of landslides can be presented in words, tables or diagrams. Presenting size frequency models graphically has the advantage of showing how observations, interpretations and judgements are interrelated, allows patterns to be recognized and understood, and models for different situations to be easily compared. Figure 1 is an example of the graphical presentation of a landslide size frequency model.

2.1 *Explanation of figure 1*

2.1.1 *Log-log histogram*

The underlying structure of Figure 1 is a histogram on a log-log scale. Showing the underlying log-log structure

Volume is product of annual frequency and average volume on log scale (e.g. 20 x 0.3 = 6 m³)

Volume to be consistent with overall landslide process rate

Average landslides per year

Totals

| Volume (m³) | - | 4.5 | 6 | 6 | 3 | 0.3 | - | 19.8 m³ |
| Number | - | 150 | 20 | 2 | 0.1 | 0.001 | - | 172 landslides |

Often good evidence of small frequent events (on project time scale)

Maximum credible volume and Shape of curve depend on slope geometry, geology and failure mechanisms

Landslide frequency - average number of landslides in each volume category per year (on log scale)

Shown as curve, but actually a histogram

Area of histogram (or area under curve) is average annual volume which is the landslide process rate

Often good knowledge / evidence of large events - easier to see, evidence lasts longer and people remember them

Often critical size below which landslides are unlikely to be a problem

Landslide volume categories (on log scale)

May include different mechanisms

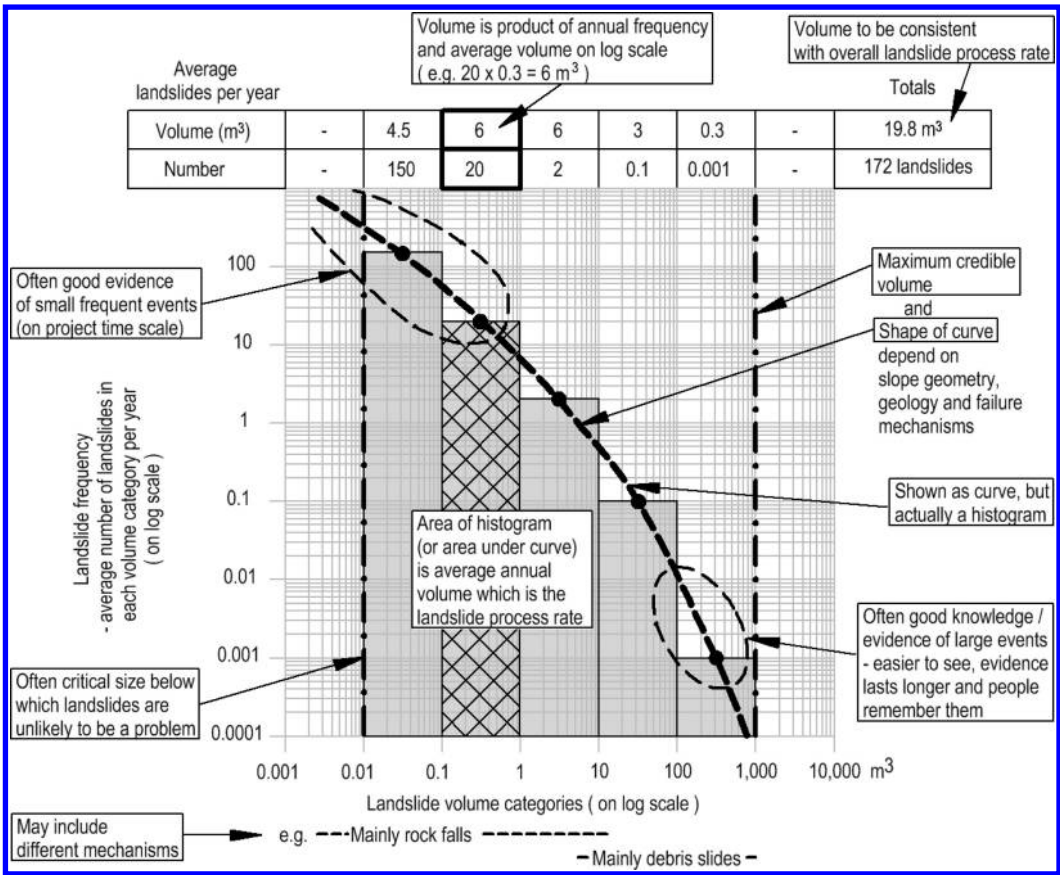e.g. ---·Mainly rock falls ----------

−Mainly debris slides −

Figure 1.   Explanation of the graphical presentation of a landslide size frequency model.

is useful when developing the graph but does not need to be shown on the final drawing.

The *x* axis shows landslide volume in order of magnitude categories, although smaller divisions (such as half order of magnitude) can be used if more useful for particular projects.

The *y* axis shows the landslide frequency which is the average number of landslides per year in each of the landslide volume categories. For example, the highlighted column on Figure 1 indicates that, on average there are judged to be 20 landslides per year with volumes in the range 0.1 m³ to 1 m³ (which usually means that there will be less than 20 landslides in most years). Different periods (such as design life) can be used on the *y* axis if required.

When developing a model it is often useful to show the average annual number of landslides in each volume category above the graph. The average annual volume of landslides in each volume category can be calculated by multiplying the number of landslides by the average volume on a log scale (e.g. the log average

of the 0.1 m³ to 1 m³ category is 0.3 m³). As shown on Figure 1, the average annual total number and volume of landslides (the area of the histogram) can also be calculated.

Although Figure 1 is a histogram with discrete volume categories, we have also shown the model as a curve (points separated by a dashed line so the actual judged numbers of landslides in each volume category can be clearly seen). Showing the model as a curve rather than columns allows several models to be presented and compared on the same graph. The average volume of landslides per year (or landslide process rate) can then be thought of as the area under the curve (calculated from the histogram as described above).

2.1.2   Critical project element and critical landslide size

Before developing a size frequency model for use in risk assessment it is important to understand the potential consequences of landslides and consider what are the critical project elements or locations at risk. The model

682

can then be developed to focus on the likelihood of landslides of different sizes reaching or affecting critical elements. Critical elements for particular projects may include roads, railways, buildings, footpaths, fences, reservoirs etc.

Defining the critical element or elements for a particular project helps define the critical landslide size (below which landslides are unlikely to be a problem). The potential speed of a landslide may also influence the judgment of critical size. For example, if the critical project element is a road, a large but very slow landslide may present little risk (if minor damage can be periodically repaired) compared to a fast very small landslide (e.g. boulder falling vertically on to traffic).

2.1.3 *Defining and calibrating the size frequency model*

Other notes on Figure 1 point out that:

– For any particular slope the maximum credible volume and the shape of the landslide size frequency curve depends on the slope geometry (e.g. height and orientation), slope geology and failure mechanisms.
– Landslide size frequency models may include several failure mechanisms.
– When developing size frequency models there is often good evidence of small frequent events (sometimes on a project timescale) which is helpful in developing and calibrating the model.
– There is also sometimes good knowledge or evidence of some of the larger landslide events which affect the slope of concern (or similar slopes in the area). Depending on the time scale, this is because people remember the larger events and the evidence of larger events is easier to see and lasts longer.
– The average annual volume (or area under the size frequency curve) needs to be consistent with the overall landslide process rate (which can vary with time) as represented by slope retreat rate models or other slope evolution models.

The above aspects of landslide size frequency models are illustrated by the examples given or referred to in the remainder of the paper.

2.2 *An example of size frequency models*

Figure 2 is an example of landslide size frequency models for toppling failures from rock slopes (Moon et al. 1996). In this project, rock falls from a 48 year old, very steep, 30 m high railway cutting in granite at Bethungra in New South Wales, Australia had damaged trains and caused at least one derailment. Most falls resulted from toppling of individual blocks or columns defined by persistent near vertical joints. As part of the design of slope stabilization works, landslide size frequency models were developed based on a
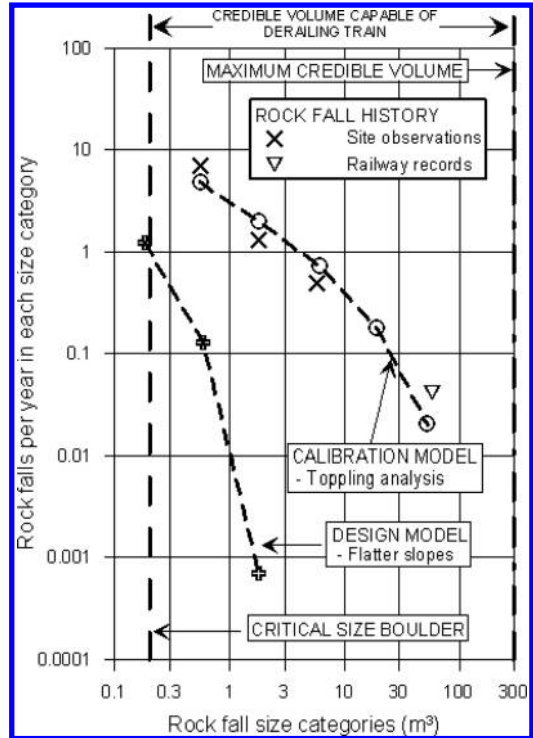

Figure 2. Rock fall size frequency relationship at Bethungra (adapted from Moon et al. 1996).

probabilistic toppling failure model calibrated against the history of rock falls.

For this project:

– Half order of magnitude landslide volume categories were used.
– The critical project element was the railway track.
– The critical size landslide was judged to be 0.2 m^3 (anything smaller on the track was unlikely to derail a train traveling at the low speed limit in place at the site).
– The maximum credible landslide volume was judged to be 300 m^3 (based on slope height, potential column widths and stability analysis).
– There was a good record of rock falls (of up to 10 m^3) for the previous two years and knowledge of two past failures in the 30 m^3 to 100 m^3 range.
– Long term railway inspectors were able to confirm that there had been no decrease in rock falls with time.
– It was possible to assess the average annual landslide volume (landslide process rate) with knowledge of how many wagon loads of rocks had been removed.

The probabilistic toppling failure model, using information on the orientation, continuity and spacing of

683

joints and calibrated against the rock fall history was used to assess the size and frequency of landslides for redesigned slopes with varying amounts of overbreak.

2.3 *Other ways of presenting size frequency observations and judgements*

Hungr et al. (1999) point out that magnitude cumulative frequency relationships are used widely in natural hazard assessments (e.g Gunther-Richter relationship for earthquakes) and present magnitude cumulative frequency relationships on a log-log scale for rock falls and slides along road and rail corridors in British Columbia. Dussauge-Peisser et al. (2002) use a similar approach for rock falls at sites in France and the USA.

We have found the size frequency histogram approach useful because:

– The log-log histogram directly shows the actual number of landslides (point on graph and, if useful, number at the top of the graph) in each size category. This makes the model completely transparent and easier to develop and manipulate in workshops (particularly with non specialists).
– When developing a model, and/or trying to elicit information from non-specialists who have seen landslides, judging whether a landslide is in a particular size category is easier than trying to estimate its actual size.
– Landslides of different sizes usually have different consequences and need to be treated differently. Keeping the size categories separate helps to better understand (and show graphically) the relationship between size of landslide and risk and remediation options (e.g. Wilson et al., in prep.).

The method of presenting observations or models depends partly on what best suits a particular application. For example, Whitehouse & Griffith (1983) present rock avalanche deposit volume against return period (on log-Gumbel paper), Morgan et al. (1992) graphically present a variety of size frequency relationships for debris flows and Baynes (1997) presents a recurrence interval curve for kinetic energies of landslides at critical locations. Graphical presentation of observations and models is invariably useful and some of the aspects of presentation discussed for log-log histograms also apply to other methods of presentation.

3 LANDSLIDE SIZE FREQUENCY MODELS AT THE LAWRENCE HARGRAVE DRIVE PROJECT

A 1.3 km section of Lawrence Hargrave Drive (LHD) south of Sydney, Australia is at the base of an oversteepened coastal escarpment (Figs. 3–4). Following a long history of landslides the road has been temporarily closed while bridges are built to avoid the higher risk areas and slope stabilization measures are being carried out elsewhere. The hazard and quantitative risk assessments for the project are described by Hendrickx et al. (in prep.) and Wilson et al. (in prep.) respectively.

3.1 *Geological and geomorphological history*

The 320 m high coastal escarpment in the project area is made up of a sequence of near horizontal interlayered sandstone and claystone units of Permian and Triassic age. The stronger sandstone units form prominent near vertical cliffs and the intervening claystones and some of the weaker sandstones, overlain by colluvium, form the intervening slopes (Figs. 3–4).

The most prominent regional geomorphological feature is the escarpment at the edge of the 300 m to 500 m high plateau. In the project area the escarpment has been oversteepened by marine erosion. To the south the escarpment is further inland, the Bulgo Sandstone does not form cliffs and there are flatter lower slopes with a well developed coastal plain (Fig. 3).

Much of the marine erosion that has oversteepened the escarpment in the project area probably occurred during sea level highs during the many interglacial periods in the last 2 million years. During the colder glacial periods colluvium is likely to have repeatedly buried some of the cliffs.

3.2 *Escarpment retreat rates in the region and landslides in the project area*

The University of Wollongong has a database of landslides in the region (Flentje 1998) and have been monitoring some of the larger debris slides with inclinometers. Slope retreat rate estimates have been made on the basis of knowledge of rock falls from the Hawkesbury Sandstone, debris flows from steeper slopes and monitored debris slides (Hendrickx et al., in prep.). The estimates (which range from about 0.2 m to 2 m per 1000 years) confirm that regional slope retreat rates are higher where the escarpment is closer to the sea and the regional estimates are consistent with the slope retreat rate estimates for the project area.

Hendrickx et al. (in prep.) discuss landslide mechanisms and the landslide record in the project area.

3.3 *Slope retreat rate*

Knowledge and interpretation of evidence on the geological and geomorphological history of the region and project area (including escarpment retreat rates and the landslide record) were used to develop a slope retreat rate model for the LHD Project. Figure 4 shows average slope retreat rates (in m/1000 years) for the different slope units (labeled 1 to 7) above the road. Figure 4 also shows the total volume of material

684

Figure 3. 1967 aerial photograph looking south at Lawrence Hargrave Drive (near the base of the escarpment). The geological units which make up the escarpment are shown on Figure 4. The Bulgo sandstone (centre right of photo) only forms cliffs in the project area (foreground) where the escarpment has been oversteepened by coastal erosion. In the distance there is a mature escarpment with a coastal plain. Other features described by Hendricks et al. (in prep.). Photo courtesy of RTA photo archive.
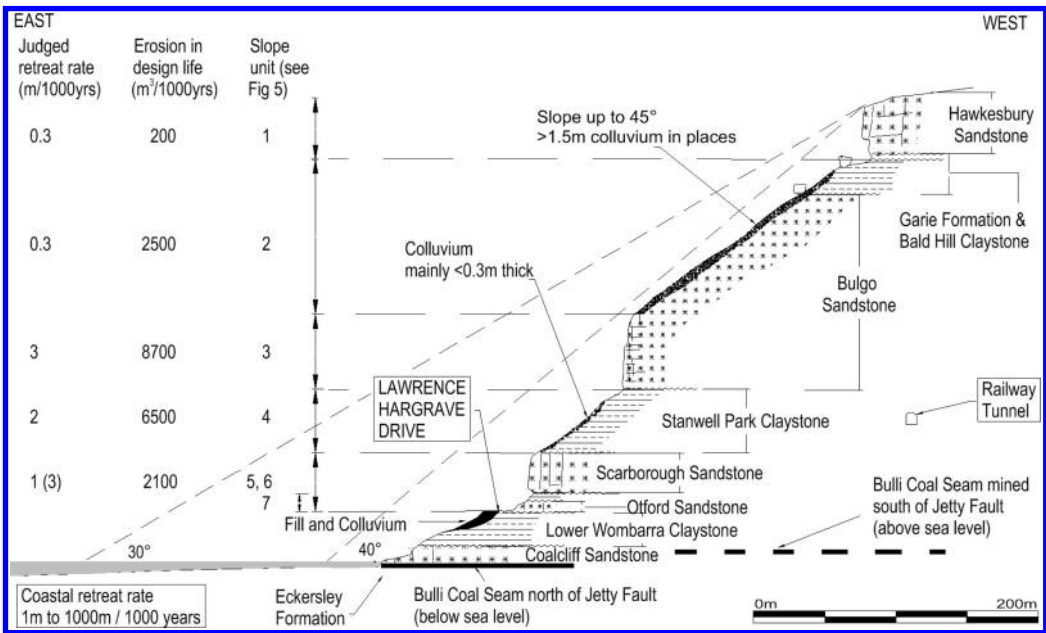

Figure 4. Cross section of coastal escarpment at Lawrence Hargrave Drive showing slope units and slope retreat rates. The section is through the highest Bulgo Sandstone cliff (second bay from foreground in Fig. 3).
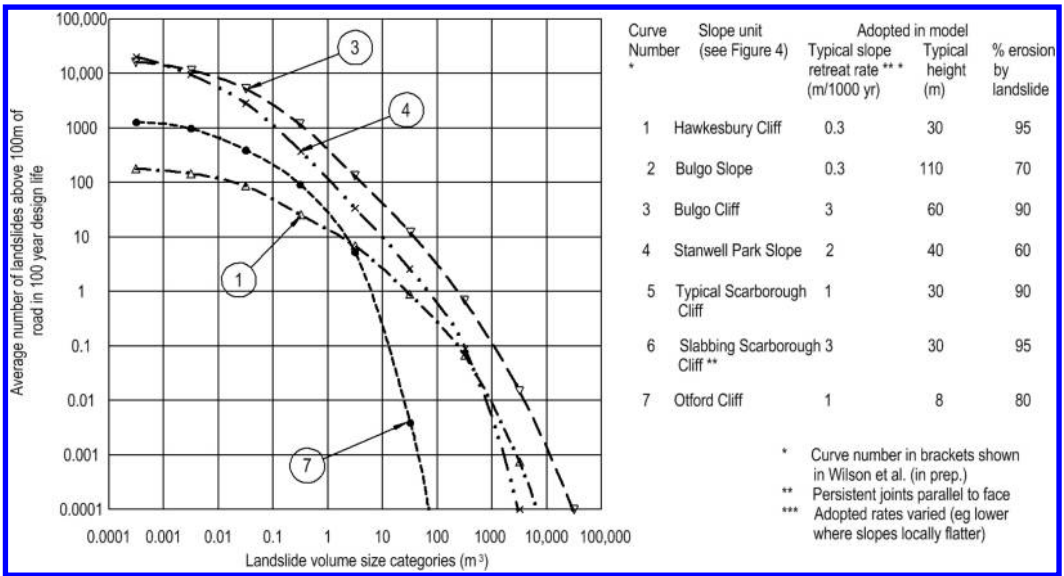
685

Curve Number [*]	Slope unit (see Figure 4)	Adopted in model		% erosion by landslide
		Typical slope retreat rate [** *] (m/1000 yr)	Typical height (m)	
1	Hawkesbury Cliff	0.3	30	95
2	Bulgo Slope	0.3	110	70
3	Bulgo Cliff	3	60	90
4	Stanwell Park Slope	2	40	60
5	Typical Scarborough Cliff	1	30	90
6	Slabbing Scarborough Cliff [**]	3	30	95
7	Otford Cliff	1	8	80

[*]   Curve number in brackets shown in Wilson et al. (in prep.)
[**] Persistent joints parallel to face
[***] Adopted rates varied (eg lower where slopes locally flatter)

Figure 5.   Selected size frequency judgements at Lawrence Hargrave Drive.

derived from each slope unit which would be removed from the slopes during the 100 year project life (calculated by multiplying the slope retreat rate by the length and average vertical height of slope unit in the project area). The model implies that there would be about $20,000\,m^3$ of erosion. Most of the erosion would be by landslides which would cross the road if no preventive measures were in place. Additional material would be lost from below the road.

The initial slope retreat model (and size frequency models for each slope unit) was developed early in the project. During the design period, the knowledge gained from new landslides and new historical information enabled the models to be reviewed and improved.

3.4 Size frequency models and risk analysis

The size frequency judgements for some of the different slope units are shown as curves on Figure 5.

The curves have been normalized to show the size and frequency of landslide debris passing 100 m of road in the design life (100 years). The landslide process rate or yield (area under the curves) is the product of the slope retreat rate, the typical height, the length (100 m) and the judged proportion of erosion that is by landslides (some of the erosion is by other processes such as slope wash following rain and wind action).

In the risk analysis described by Wilson et al. (in prep.) the size frequency distributions shown were adjusted for the actual length, height and rate applicable to the location and slope unit being considered.

The process rate model describes the amount of material removed from the escarpment by landslides but does not imply that all debris from every landslide crosses the road. Some debris is transported by series of landslides and often material will locally accumulate on flatter slopes. In the risk analysis (Wilson et al., in prep.), this process was modeled by making judgements about the number and proportion of each landslide reaching the road.

3.5 Shape of size frequency curves

The location and shape of the size frequency curves on Figure 5 are related to the landslide process rate, the slope geometry, the geology and failure mechanisms involved. For example:

– Curve 1 is the flattest curve because joints and other defects are widely spaced in the Hawkesbury Cliff and there are relatively few small failures.
– Curve 7 is the steepest curve because the Otford Cliff is not very high and large failures will not occur. It is also the tightest curve because joints are generally widely spaced and so there will also be relatively few small failures.
– Curve 3 yields potentially larger failures because the Bulgo Cliff is the highest cliff. It also has the highest overall yield and a relatively large proportion of smaller landslide because it is relatively closely jointed and includes beds of low strength material.
– Curve 4 is a relatively steep curve with a high proportion of smaller landslides because the Stanwell

686

Park Slope generates many small debris slides and debris flows particularly near the top of the Scarborough Cliff.

The orientation of a slope can also have a big effect on the size frequency curve. Wilson et al. (in prep) show the size frequency curves for the typical and slabbing (where there are persistent joints parallel to the face) Scarborough Cliffs. While the overall landslide process rate is higher for the slabbing cliff, the increase in frequency of landslides is much more pronounced for the larger failures (collapse of slabs larger than $1000\,m^3$ judged to be 15 times more likely than for the typical cliff).

4 DEVELOPING AND USING LANDSLIDE SIZE FREQUENCY MODELS

4.1 Slope evolution models

4.1.1 Understand the processes

The key to developing slope models is to understand how slopes are formed. Selby (1993) describes the materials and processes that form slopes, models of slope evolution and provides quantitative information on slope retreat and general erosion rates in a variety of environments. Lee & Jones (2004) describe slope hazard models (including simulation models for cliff recession) and landslide triggers and Hutchinson (2001) also gives examples of quantified slope development models. Dahlhaus & Miner (2000) describe how judgements about cliff retreat rates were used to help assess the frequency of rock falls.

4.1.2 Models must be evidence based

Slope models must be based on evidence from the slope or slopes in question and similar slopes in similar environments elsewhere. Moon & Wilson (2004) point out that the evidence has to be assembled, understood and interpreted. They describe the range of skills and knowledge bases required to develop a sound knowledge of how slopes are formed, how they have behaved in the past and how they might behave in the future. Geological and geomorphological skills and knowledge of failure mechanisms are essential and the quality of the model often depends more on the expertise and experience of those preparing the model than the quantity of the evidence available.

4.1.3 Develop early

Whatever the scale of the project there is always knowledge available on the regional geological and geomorphological history which can form the starting point for a landslide process rate model. It is best to develop an initial model early and use as many different approaches for development and calibration as possible. The advantage of an early model is that it demonstrates where the uncertainty lies and enables subsequent effort to be concentrated on collecting and interpreting evidence that improves and calibrates the model.

4.1.4 Time scales involved

The importance of understanding how slopes are formed applies to both natural and man made slopes. Slope forming and slope failure processes occur over timescales ranging from seconds to many millions of years. A new slope (e.g. a cliff formed by a river in flood or a temporary excavation on a construction site) may fail instantly while other slopes change very little over very long periods. Twidale (1998) points out erosion rates can be very slow and that some slopes in Africa, Australia and elsewhere are many hundreds of millions of years old. Knowledge of the age of the landscape or slope, whether natural or man made, is essential to the calibration of judgements about overall landslide process rates.

4.2 Landslide process rates

For the LHD Project, landslide process rates were derived from slope retreat rate models calibrated with a lot of evidence. Other examples and approaches to assessing or calibrating overall landslide process rates and the need to understand how they can change with time are discussed below.

4.2.1 Size of deposits

Colluvial fans may represent deposits that have formed by a variety of processes in a variety of environments over a long period. If the origin and age of particular components of the fans (e.g. Holocene debris flow deposits) can be identified, they can be used to help calibrate landslide process rates in the catchment.

Whitehouse & Griffith (1983) used knowledge of the size of Holocene debris deposits (dated by various methods) to help develop a size return period relationship for rock avalanches in the Central Southern Alps of New Zealand.

Volumes of material accumulating over a known period at the base of a cliff or cut slope can also help calibrate landslide process rates. At Bethungra, the size frequency model was derived initially from the events shown on Figure 2. Reliable information on the smaller events was only available for two years but the overall process rate (area under the curve) was also found to be consistent with the number of wagon loads of rocks removed from the cutting over a much longer period. This knowledge helped confirm the long term railway inspector's observations that the overall process rate had not changed significantly over the life of the cutting. Hungr et al. (1999) used deposit volumes to help develop size frequency relationships for landslides in British Columbia.

687

In other projects, accumulations of debris against fences or walls of known age has helped calibrate landslide process rates.

4.2.2 *Historical information*

On the LHD Project (see Section 3 and Hendrickx et al. in prep.), newspaper reports, old photographs and other old records helped calibrate the landslide process rate. In another project in Australia rock falls from a natural cliff threatened an historic railway bridge. The cliff was in the background of a 19th century photograph of a train. Comparison with the present day cliff revealed the size, number and location of rock falls in the previous 100 years. Old maps in Britain have been used to help assess slope retreat rates (Holmes 1972, Brunsden & Jones 1975) and Lee & Jones (2004) give other examples of the value of historical records.

4.2.3 *Measured movements*

Measured slope movements can be used to help calibrate landslide process rates. At Roxburgh Gorge in New Zealand many large pre-existing landslides were partially flooded by the reservoir formed behind Roxburgh dam which was completed in 1956. Movement monitoring by survey and air photo interpretation helped establish an overall landslide process rate and calibrate a landslide size frequency model. The model was used to help assess the likelihood of a rapid landslide and landslide dam (Moon 1997).

Inclinometer monitoring of debris slides by the University of Wollongong helped establish slope retreat rates for the LHD Project (Section 3.2). Real time monitoring of inclinometers is now in place (Flentje et al., in prep.).

4.2.4 *Demonstrating slow process rates*

Developing landslide process rate models is easier when landslides are frequent and there are plenty of observations and evidence available. Where slope processes are slow, slope models based on a thorough understanding of slope processes, slope evolution and regional knowledge are even more important. In some cases, demonstrating lack of evidence can help put an upper limit on the overall landslide process rate and point to low likelihood of particular events.

At Montrose in Victoria, Australia, historical records of a large landslide prompted concerns about debris flow risk in the area (Moon et al., 1991). Mapping of one colluvial fan in the area led to recognition of a surface debris flow deposit which could be traced back to the precursor landslide. Elsewhere on that fan and on other colluvial fans an older well developed soil profile (dated to be of Pleistocene age) occurred at the surface. The lack of debris flow deposits overlying the old soil profile elsewhere in the region helped demonstrate that large debris flows are an unusual event in the area (i.e. the debris flow process rate is slow).

In another project in a mountainous area, the likelihood of debris flows from slopes above a small town needed to be assessed. A review showed that similar slopes (similar geology, vegetation, climate, aspect, similar or steeper slope) are widespread in the region and a review of 13 sets of aerial photographs covering a period of 50 years revealed no evidence of past debris flows in the region. The area reviewed was about 50 times the area of the slopes of concern. The evidence from the aerial photographs and other evidence (old valley, little colluvium, well developed soil profile and historical information) helped to demonstrate that the debris flow process rate in the region, and above the town, is slow.

4.2.5 *Process rates change with time*

Baynes & Lee (1998) discuss geomorphological principles in landslide risk analysis and point out that the controls on landslide activity are not constant in time and space. Landslide process rate and size frequency models are predictions for defined periods (usually the design life). Process rates change with time and rate changes in the design life must be anticipated and understood.

Cruden (1997) describes a cutting where there was a reduction in the annual average volume of rock falls over time partly because of the effects of remedial measures. Cruden points out that there was insufficient evidence to assess whether rock falls would have reduced anyway as available loose rock failed. Hungr et al. (1999) also report a reduction in rock fall frequency in transportation corridors following remedial measures. At Bethungra (Sections 2.2 & 4.2.1), the average annual volume of rock falls did not decrease over time. This was probably because time dependent processes such as stress relief, root jacking, and other forms of mechanical weathering caused joints to open.

The LHD Project provides an example where landslide process rates may increase in time (beyond the project design life). The Bulgo Sandstone is a weak rock mass which only forms cliffs because of local over-steepening in the project area caused by marine erosion (Figs. 3–4). In time, as the Bulgo Sandstone cliff fails and begins to flatten, slope retreat rates (and landslide processes) in the higher slope units will increase as the escarpment tends towards the profile in the background of Figure 3 (i.e. no Bulgo cliff). The slope retreat rate of the upper units is likely to increase even if further marine erosion is prevented (e.g. by engineering works). This increase in process rate was not an issue for the project because of the long time scale involved (many hundreds of years) and the risk will be largely avoided below the highest Bulgo Sandstone cliffs with a bridge.

4.3 *Regional and site specific studies*

Landslide process rate models are particularly applicable to route or regional studies but can also be useful in

site specific studies by ensuring that regional evidence/knowledge is brought together and incorporated into the judgements of how a particular slope might behave.

The LHD Project shows how regional knowledge helped develop and calibrate models for particular slopes. While the overall slope rates were identified, it was possible to develop size frequency models for whatever individual part of the escarpment was required.

Tse et al. (1999) also suggest using evidence from areas of similar geological setting when trying to assess the likelihood of infrequent events at particular locations.

While knowledge of the regional performance history is essential, the particular characteristics of the specific slope in question need to be understood. The variety of models shown in Figure 5 for some of the different components of the escarpment at LHD shows how misleading too much mixing of models and observations from different sites could be.

4.4 *Interpretation and quality issues*

4.4.1 *Incomplete observations*
Hungr et al. (1999) discuss why data on the size and frequency of landslides is usually incomplete and how such data can be interpreted to reduce errors and Brunsden et al. (1995) discuss how "rules of interpretation" can help in the evaluation of old records. The interpretation of incomplete data depends on the individual circumstances of the project but it is usually possible to work out what the deficiencies are and take them into account when calibrating size frequency models.

4.4.2 *Size observations and judgements*
In order to develop size frequency models it is necessary to make judgements about the volume of landslides. When only the plan area is known (or anticipated), the landslide depth can be judged by assessing typical length/depth and width/depth ratios for the geology and geometry and failure mechanism involved and where appropriate using the relationship given by Cruden & Varnes (1996) to calculate volume.

Where a volume has to be estimated from a past event observed by a non-specialist, providing typical dimensions, order of magnitude size categories or comparisons (e.g. the size of a small car) can help assess the size category.

In risk assessment for rock falls it may be the volume of individual blocks at impact which are most relevant. If a jointed rock mass has failed the individual block volume will be smaller than the volume of the intact mass prior to failure and the final mass of debris after bulking. If rocks break on impact and the debris is observed later, the number of rock falls may be overestimated and the largest individual block size at impact may be underestimated. Dents in the road and other evidence can help assess what actually happened (Bunce et al., 1995).

To help understand the risk at the LHD Project, size frequency models were developed for in situ, impact and debris volumes (based on failure mechanisms, defect spacing, fall trajectories and rock strength calibrated against observations). Judgements of individual boulder size at impact helped develop kinetic energy return period relationships for parts of the project where rock shelters and rock fall fences were being considered.

4.4.3 *Recognizing patterns and building models*
The overall pattern of the inverse relationship between the size and frequency of landslides has been established by many studies (e.g. Dussauge-Peisser et al., 2002, Hungr et al., 1999, Whitehouse & Griffiths 1983). The pattern has also been demonstrated at Bethungra (Moon et al., 1996 and Fig. 2) by probabilistic toppling failure stability analysis based on measured defect characteristics (including orientation, spacing, length). Yokoi et al. (1995) describe how the relative dimensions of landslides are repeated on different scales (self-similar geometry) and establish a similar inverse relationship pattern (for numbers of landslides and lengths and widths) from both observations and fractal models. The well calibrated models developed for the LHD Project (Fig. 5) demonstrate how the size frequency distribution is related to the geometry, geology and failure mechanisms involved.

The body of knowledge developed (including the patterns established graphically) can provide guidance when models have to be developed for new projects where records and observations are limited.

5 CONCLUSIONS

Knowledge of geology, geomorphology and landslide processes can be used to develop landslide process rate and landslide size frequency models. Such models can be developed for both natural and man-made slopes and calibrated against observations. Graphical presentation can be used to show how observations, interpretations and judgements are interrelated and allows different models to be compared.

If the models are based on sound knowledge of slope evolution, slope materials and slope processes they can be used to help make defensible, evidence based judgements of landslide likelihood which go beyond the limitations of the historic record. The approach has worked for a wide range of time scales, landslide sizes and processes.

REFERENCES

Baynes, F.J. 1997. Problems associated with geological characterisation for quantitative landslide risk assessment. In D.M. Cruden & R. Fell (eds), *Landslide Risk Assessment*: 153–163. Rotterdam: Balkema.

Baynes, F.J. & Lee, M. 1998. Geomorphology in landslide risk analysis, an interim report. In Moore & Hungr (eds) *Proc. of the Eighth Congress of the Int. Assoc. of Engineering Geologists*. 1129–1136. Rotterdam: Balkema.

Brunsden, D., Ibsen, M-L., Lee, E.M. & Moore, R. 1995. The validity of temporal archive records for geomorphological purposes. *Quaestiones Geographicae Special Issue* 4: 79–92.

Brunsden, D & Jones, D.K.C. 1976. The evolution of landslide slopes in Dorset. *Phil. Trans. Roy. Soc.* A283: 605–631.

Bunce, C.M., Cruden, D.M. & Morgenstern, N.R. 1997. Assessment of the hazard from rock fall on a highway. *Canadian Geotechnical Journal* 34: 344–356.

Cruden, D.M. 1997. Estimating the risks from landslides using historical data. In D.M. Cruden & R. Fell (eds), *Landslide Risk Assessment*: 177–184. Rotterdam: Balkema.

Cruden, D.M. & Varnes, D.J. 1976. Landslide types and processes. In A.K. Turner & R.L. Schuster (eds), *Landslides; investigation and mitigation*: Special Report 247, Transportation Research Board, National Research Council (US).

Dahlhaus, P.G & Miner, A.S. 2000 Estimating the occurrence of rockfalls in columnar basalt. *Proc. Int. Conf. On Geotechnical Engineering (GeoEng 2000)*.

Dussauge-Peisser, C., Helmstetter, A., Grasso, J-R., Hantz, D., Desvarreaux, P., Jeannin, M. & Giraud, A. 2002. Probabilistic approach to rock fall hazard assessment: potential of historical data analysis. *Natural Hazards and Earth System Sciences* 2: 15–26.

Flentje, P. 1998. *Computer based landslide hazard and risk assessment.* PhD Thesis, Faculty of Engineering, University of Wollongong, Australia.

Flentje, P., Chowdhury, R.N., Tobin, P. & Brizga, V. in prep. Towards real-time landslide risk management in an urban area.

Hendrickx, M., Wilson, R., Moon, A., Stewart I. & Flentje, P. In prep. Slope hazard assessment on a coast road in New South Wales, Australia.

Holmes, S.C.A. 1972. Geological application of early large scale cartography. *Proc Geol. Assn.* 83: 121–138.

Hungr, O., Evans, S.G. & Hazzard, J. 1999. Magnitude and frequency of rock falls and rock slides along the main transportation corridors of southwestern British Columbia. *Canadian Geotechnical Journal* 36: 224–238.

Hutchinson, J.N. 2001. Reading the ground: Morphology and geology in site appraisal. *Quarterly Journal of Engineering Geology and Hydrogeology* 34: 7–50.

Lee, E.M. & Jones, D.K.C. 2004. *Landslide risk assessment.* London: Thomas Telford.

Moon, A.T. 1997. Predicting low probability rapid landslides at Roxburgh Gorge, New Zealand. In D.M. Cruden & R. Fell (eds) *Landslide Risk Assessment*: 277–284. Rotterdam: Balkema.

Moon, A.T., Olds, R.J., Wilson, R.A. & Burman, B.C. 1991. Debris flow risk zoning at Montrose, Victoria. In D.H. Bell (ed) *Landslides*: Vol. 2, 1015–1022. Rotterdam: Balkema.

Moon, A.T., Robertson, M.D. & Davies, W.N. 1996. Quantifying rockfall risk using a probabilistic toppling failure model. In K. Senneset (ed) *Landslides*: Vol 2, 1311–1316. Rotterdam: Balkema.

Moon, A.T. & Wilson, R.A. 2004. Will it happen? – Quantitative judgements of landslide likelihood. *Proc. Australia New Zealand Conf. On Geomechanics. Univ. of Auckland*: (2): 754–760.

Morgan, G.C., Rawlings, G.E. & Sobkowicz, J.C. 1992. Evaluating total risk to communities from large debris flows. In *Geotechnique and natural hazards*: Canadian Geotechnical Society: 225–236. Bitech Publishers.

Selby, M.J. 1993. *Hillslope materials and processes.* Oxford University Press.

Tse, C.M., Chu, T., Lee, K., Wu, R., Hungr, O. & Li, F.H. 1999. A risk-based approach to landslide hazard mitigation measure design. In *Proc. Hong Kong Institution of Engineers Geotech. Division annual seminar on geotech. risk management*: 32–42. Hong Kong Inst. of Engineers.

Twidale, C.R. 1998. Antiquity of landforms – an extremely unlikely concept vindicated. *Australian Journal of Earth Sciences* 45(5): 657–668.

Whitehouse, I.E. & Griffiths, G.A. 1983. Frequency and hazard of large rock avalanches in the central Southern Alps, New Zealand. *Geology* 11: 331–334.

Wilson, R., Moon, A., Hendrickx, M. & Stewart, I. In prep. Application of quantitative risk assessment to the Lawrence Hargrave Drive Project, New South Wales, Australia.

Yokoi, Y., Carr, J.R. & Watters, R.J. 1995. Fractal character of landslides. *Environmental & Engineering Geoscience* 1(1): 75–81.

The morphology and sedimentology of valley confined rock-avalanche deposits and their effect on potential dam hazard

S.A. Dunning, D.N. Petley & N.J. Rosser
International Landslide Centre, Department of Geography, University of Durham, Durham, UK

A.L. Strom
Institute of Geospheres Dynamics, Moscow, Russia

ABSTRACT: Rock avalanches are high magnitude, low frequency mass movements involving the failure of over $1 \times 10^6 \, m^3$ of bedrock and weathered mountainside. They present an ever-present, unpredictable hazard within high mountains areas. Although rock avalanches commonly show long travel distances, the morphology and sedimentology of the landslide deposits are dependent upon local morphological constraints, with three key assemblages commonly being observed: primary spread, secondary two-phase, and stalled. The potential to create a landslide dam, which can pose a significant hazard to life and property if rupture occurs, is vastly different between the three assemblages. Results of a sedimentological study using direct measurement and predictive plots have provided a facies-based approach that is applicable to these three deposit morphologies. The distribution and relative properties of the facies prove critical to the safety of rock-avalanche dams against failure. The result of the combination of a morphological classification and their varied sedimentological properties is a pro-forma approach that allows rapid quantification of the hazard posed by the three morphological variations. The approach allows an estimate of the material properties of the facies contained within the three morphologies of rock-avalanche dam that can be used as direct input into computer modelling of the dam's reaction to rapidly increasing lake levels and its long-term safety.

1 INTRODUCTION

1.1 *Rock avalanches*

A rock avalanche is a catastrophic, high magnitude, low frequency, long-runout form of landslide that involves a commonly-agreed minimum volume of $1 \times 10^6 \, m^3$ of bedrock and associated cover (Dunning, unpubl.). Rock avalanches can be triggered by seismic shaking, intense and/or prolonged rainfall, human activity or accelerating creep. However, the trigger mechanism appears to have no discernable effect on the resulting mass movement or final deposit. Rock avalanches are often considered anomalous due to travel distances well in excess of what is expected from the normal laws of friction (Melosh 1987). It is debatable if excess travel distance is a true distinctive feature of rock avalanches though. Rock avalanches can be shown to occur within a continuous spectrum of mass movement transport processes, and not as an anomalously mobile event requiring exotic modification of the laws of friction (Corominas 1996). Whether a rock avalanche shows 'excessive' travel distance or not, the precise

mechanisms acting during motion and emplacement are poorly understood.

The initial phase of motion has been termed collapse (Eisbacher 1979, McSaveney & Davies 2002), where the trigger releases a volume of bedrock that dilates along preexisting discontinuity surfaces such as jointing or foliation during the initial fall and/or slide to the valley floor. It is the mechanism of motion acting as the rock avalanche travels along, across, or even up-valley at high speed that remains controversial. Current theories range from the entrainment and subsequent alteration of the rheology of the moving mass (Hungr & Evans 2004) to dynamic fragmentation and spreading under a non-exotic frictional regime (Davies et al. 1999, Davies & McSaveney 2004).

1.2 *Rock-avalanche dams*

Rock avalanches commonly interact with rivers. If a sufficiently large volume of material is emplaced quickly, with the correct distribution of mass, a valley-blocking deposit can be formed. This process is as

much dependent upon the river characteristics and valley morphology as it is upon the landslide properties. In this paper we briefly review the classification of rock-avalanche dam morphology, before presenting a simple classification that accounts for sedimentology as well as morphology. The novel combination of these two factors is intended to provide a rapid tool for dam stability assessment as the distribution of facies in rock-avalanche dams is critical to failure prediction.

2 ROCK-AVALANCHE DEPOSITS

2.1 *Sedimentology*

The deposit resulting from a rock avalanche is sedimentologically distinctive and can thus form an important basis for classification. Generally, they are inversely graded (Cruden & Hungr 1986), preserve source stratigraphy in the final deposit (Strom 1999), and contain highly fragmented but relatively undisaggregated clasts (Davies et al. 1999). More detailed discussion of the sedimentology of rock-avalanche deposits can be found in Dunning & Armitage (in press).

2.2 *Rock-avalanche deposit morphology*

The morphology of valley-confined rock-avalanche deposits has been a key research topic and numerous classification systems are in use. The simplest use just three morphological types (Strom 1999) based upon cross-sectional profile and the distribution of mass. Nicoletti & Sorriso-Valvo (1991) noted that rock-avalanche deposits conform to the local valley morphology, and presented a three-fold classification based primarily on geomorphic control and interpreted energy dissipation. However, the classification most commonly used (Ermini & Casagli 2003) is that of Costa & Schuster (1988), in which six morphologies of possible valley blocking land-slides are described, of which four are commonly formed by rock avalanches. The Costa & Schuster (1988) classification has recently been modified by Hermanns et al. (2004) with the addition of four more morphological types. However, the classes added in reality are not new morphological forms of rock-avalanche deposit, but instead represent varied river response to the Type II blockages of Costa & Schuster (1988). Both the Costa & Schuster (1988) and the Hermanns et al. (2004) classifications consider entry of a rock avalanche at near right angles into the main river drainage, and its subsequent effect on that major drainage. Recent examples have shown that single rock-avalanche deposits can interact and dam several tributaries (Dunning et al. in review), or alternatively, the rock avalanche can be channelised along a drainage line instead of the simple representation of lateral spreading upon entering the main

drainage as shown in Type III of Costa & Schuster (1988). This may, in reality reflect the fact that this sort of channelised flow does not sufficiently frequently result in a river damming deposit to be considered.

2.3 *Geomorphological considerations*

In addition to the classification systems outlined above, a number of indexes and statistical relationships based upon geomorphological parameters are available. However, care is needed as measurement errors are inherent within geomorphic parameters as they are often interrelated. Korup (2004) noted that numerous correlations, for instance, between landslide dam volume, landslide height, landslide length and landslide width can be interpreted to actually represent statistical replication of the original data collation technique. Many morphometric parameters are originally inter-calculated; for example landslide volume is usually calculated from plan morphology using an estimate of average unit depths. This does not restrict the use of measured geometric parameters so long as erroneous relationships are identified, as in Korup (2004), rather than all statistically valid results being treated as true physical relationships between parameters.

The aims of such statistical and graphical treatments of geomorphic parameters are to provide information on the geomorphic configurations that create an 'unstable' or 'stable' landslide dam, and delimit some of the controlling and independent geomorphic variables. The final outputs are often graphical domains of dam properties, usually in terms of being stable and unstable, based on either the measured properties or a mathematical relationship of several variables (Casagli & Ermini 1999, Ermini & Casagli 2003, Korup 2004).

The classification of unstable and unstable is of primary importance because the evacuation of vulnerable populations is often the only possible defense against a large outburst flood. The problem is that in much of the work under discussion, a state of being unstable is only a notion. The unstable field represents past dam events that have failed, for example in the case of Korup (2004) those deposits that no longer retain a lake, whilst stable dams are those that still retained a lake when the dataset was compiled. This cannot account for those dams that have failed, often multiple times, and so must be unstable, yet still retain sizeable lakes (Dunning et al. in review) Such an empirical approach provides no indication of the possible future evolution of 'stable' dams into the 'unstable' field. Instead, they are a measure of simply of whether the dam is stable or unstable at the time of measurement. The work of Casagli & Ermini (1999), Ermini & Casagli (2003) and Korup (2004) all rely upon the well established fact that the failure of most landslide dams, is a rapid process, with 50% failing within 10 days and 85% within 1 year (Costa & Schuster 1988).

In process terms, the geomorphic approach outlined above is essentially a black-box. Once all data have been plotted, an envelope is created. This envelope can be represented by an associated equation, resulting in an absolute value of a defined index or indices above/below which landslide dams are considered to be stable/unstable Points plotted close to the envelope might be considered to be inconclusive; a necessary precaution for risk assessment (Korup, 2004). The position of these envelopes, and so the critical index values, vary from region to region. Thus, different envelopes have been defined for Italy (Casagli & Ermini 1999, Ermini & Casagli 2003) and New Zealand (Korup 2004), and a further envelope would be required for Canada.

The above brief review is not intended to unduly criticize the approach. Korup (2004) fully acknowledged the limitations of the approach, noting that it is often limited by incomplete case study examples from the literature. The approach is, however, deemed useful (Korup 2004) for the first approximation of the stability of landslide dams and as a comparison of the conditions necessary for the formation of stable dams between regions with varied geomorphic and bounding conditions.

3 ROCK-AVALANCHE DAM FAILURE

If a dam is considered to be unstable then regression equations, computer-based models and physical models calibrated on past events can be used to evaluate the potential outburst flood (Manville 2001). Interestingly, the form of failure often does not affect the peak discharge, Qmax, of the outburst flood at the dam site (Davies, pers. comm.). The most commonly reported mechanism of dam failure is overtopping (Costa & Schuster 1988) (Fig. 1). Failure due to seepage and

internal erosion (piping) or downstream slope failure is considered to be rare but has been noted to be responsible for several rock-avalanche dam failures (Glazyrin & Reyzvikh 1968, Costa & Schuster 1988, Dunning et al., in review), (Fig. 2 for example).

With the sedimentology of rock-avalanche dam deposits becoming ever better constrained (Dunning, unpubl., Dunning & Armitage, in press) the failure style of landslide dams can be modeled more satisfactorily. Sedimentologically-correct finite-element seepage and method of slices limit-equilibrium slope stability models of rock-avalanche dams can be simulated under lake filling conditions based on case study examples (Dunning & Armitage, in press). The preliminary results show the critical importance of the dam geometry and the dam sedimentology, factors previously noted to be key factors in the stability of such dams (Costa & Schuster 1988, Casagli et al. 2003).
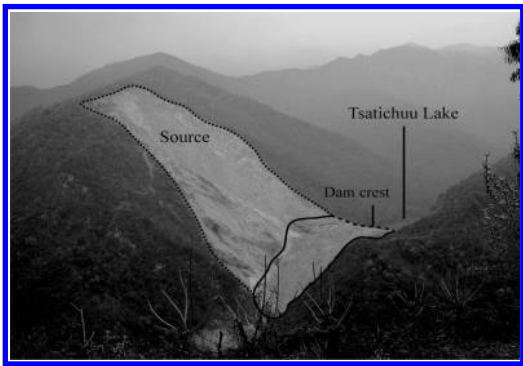

Figure 2. The Stalled Tsatichuu rock-avalanche dam, Bhutan, the downstream face failed 2 months after this picture was taken releasing most of the $15 \times 10^6 \text{m}^3$ impounded reservoir as a catastrophic flood with Qmax estimated at $\sim 5900 \text{m}^3\text{sec}^{-1}$ 35 km from the dam site (photo C. Massey).
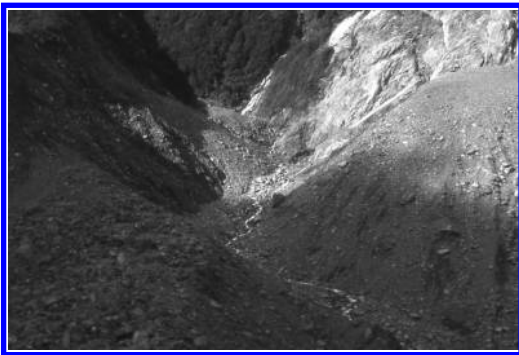

Figure 1. Breach channel (20 m deep) cut after overtopping failure through schistose, Stalled Poerua deposit, New Zealand, exposing the *Body facies* (described in Section 5.2).

Figure 3. Downstream face of the Tsatichuu deposit with seep point. The face failed catastrophically after seep progression in combination with heavy rainfall (photo C. Massey).

693

Alteration of the sedimentology of a dam geometry based on the 1999 Poerua (Fig. 1), Westland, New Zealand, rock-avalanche dam (Hancox et al. 1999), from a homogenous mass, as used within most forms of modeling, to the *Carapace* and *Body facies* of Dunning (unpubl.) yields interesting results. As the reservoir fills, 'phreatic tonguing' occurs as the lake reaches the highly permeable *Carapace facies*. The downstream dam face, deposited below the angle of repose of the gravel grade material beneath, drops below a Factor of Safety (FoS) of 1 in respect to a slope failure in just 48 hours. In contrast, a homogenous mass remains stable to this style of failure for 18 days (Dunning & Armitage, in press). The extended time is sufficient for such a dam to fail via overtopping, as the reservoir fills above the dam crest under the lake inflow and dam seepage conditions specified. It would appear that the thickness of the *Carapace* facies, the reservoir filling rate and valley morphology are key variables for failure timing and style.

A recently described rock-avalanche dam in the Bhutan Himalaya (Dunning et al. in review) showed similar dam geometry to Poerua. Notable differences were the lower river input and considerable seepage discharge, which broadly balanced, other than during several brief periods of overflow, each of which was insufficient to initiate a catastrophic breach channel. However, the seepage progressed up the downstream dam face gradually (Fig. 10), partially in response to increased monsoonal inputs and led ultimately to catastrophic dam failure via multiple slope failures after 10 months (Dunning et al. in review).

4   RESEARCH AIMS

At present there are numerous morphological classification systems based on the landslide footprint, and there are empirical relationships and associated equations for stability analysis. As illustrated above, case study examples can also be modeled using the present understanding of the sedimentology and relative geotechnical properties and specific site variables such as lake input. The key is linkage; the modeling of a dam's precise sedimentology, geometry and system inputs/outputs is the best form of specific hazard assessment. However, case study by case study hazard and risk assessment is not the answer to understanding why landslide dams remain stable or fail. The approach has to be scaled up to the level of empirical studies and indices proposed by research such as Korup (2004). This would require the collection of a detailed data set at each rock-avalanche deposit, be it damming or not, as it is just as important to study those deposits that cannot form a lake-impounding blockage. With the information gained from sedimentological

investigation, geomorphic data, and case study computer modeling, distinct categories of dam geometry, sedimentology and associated failure styles and timing can be identified.

The aim of this research is to outline the morphological and sedimentological assemblages of valley confined rock-avalanche deposits and to describe the damming potential associated with them. This will then form the basis of future proforma data collection for assessment of the key controls on the stability of such deposits.

5   VALLEY-CONFINED ASSEMBLAGES

5.1   *Morphological classification scheme*

It is entirely possible to over-classify a phenomena – the danger is in creating a system too specialized to extract the higher order relationships. The morphology of valley-confined rock-avalanche deposits is a continuous spectrum. It is far more useful to identify a small number of near end-member morphologies with minor overlap between them than tens of morphological types with the overlap between each being as large as the category itself.

For the purposes of this research a classification scheme of three morphological types has been proposed, adapting and furthering the work of Strom (1999) and Strom & Pernik (2004). Each has its own sedimentological assemblage and dam forming potential. The three morphological types are termed Primary Stalled, Secondary Two-Phase, and Spread, with subtypes divided by the mass distribution of the final deposit, which is important for the positioning and timing of failure and the impoundment potential, here defined as the volume of the lake at first possible overtopping level (Fig. 5).

5.2   *Sedimentological classification scheme*

The detailed sedimentology of rock-avalanche deposits has been outlined in Dunning & Armitage (in press). The key point of interest is the development of a three facies approach, the *Carapace*, *Body*, and *Basal facies*; the more detailed sub-facies are not of importance here. The *Carapace facies* (Fig. 4) is the surface and near-surface material. These facies can account for as much as 30% of a deposit by thickness, but for considerably less by mass due to the large void spaces present. The carapace is an assemblage of large, angular interlocking blocks created during the collapse of the bedrock slope and transported along the near surface of the rock avalanche. The sizing of the carapace blocks is a function of the original rock properties such as strength and discontinuities, and the time in

motion – a proxy for distance traveled, and so related to the morphology in the scheme outlined. The carapace is characterized by high hydraulic conductivities, in the region of $0.1\,\mathrm{m\,s^{-1}}$ for a relatively fine carapace of argillite (Falling Mountain, New Zealand). The *Carapace facies* is sharply bounded below by the *Body facies*. This is in direct contrast to previous reports of the interior of rock avalanche deposits being crudely inversely graded (Cruden & Hungr 1986). It is this abruptness of the boundary that becomes critical to dam stability in particular morphological situations.

The *Body facies*, beneath the carapace (Figs. 4, 6), forms the bulk of most rock avalanche deposits. The material is angular, poorly sorted, and highly fragmented but in places relatively undisaggregated – giving rise to the description of jigsaw texture (Hewitt 1999, 2001). The *Body facies* retains the original source stratigraphy (Fig. 6) in the final deposit, often as a series of sub-horizontal bands stretched during motion regardless of the original source rock orientations (Dunning, unpubl., Hodgson et al. 1998). This preservation of stratigraphy affects the grain-size distribution and material properties of each band above

Figure 4. Well developed *Carapace facies* (people for scale) above the finer *Body facies*, Karakujdor rock-avalanche deposit, Kyrgyzstan.
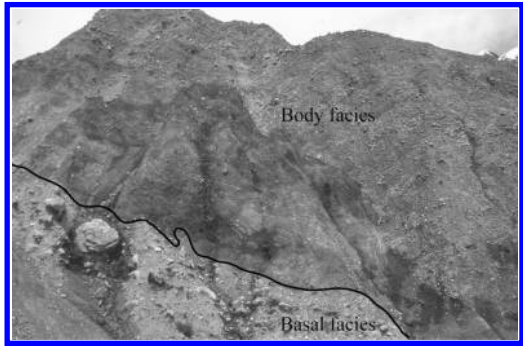
Figure 6. Complete ~35 m surface to basal exposure at the Secondary Two-phase Falling Mountain rock-avalanche deposit, New Zealand showing sub-horizontal preserved stratigraphy and entrained material in the *Basal facies*.
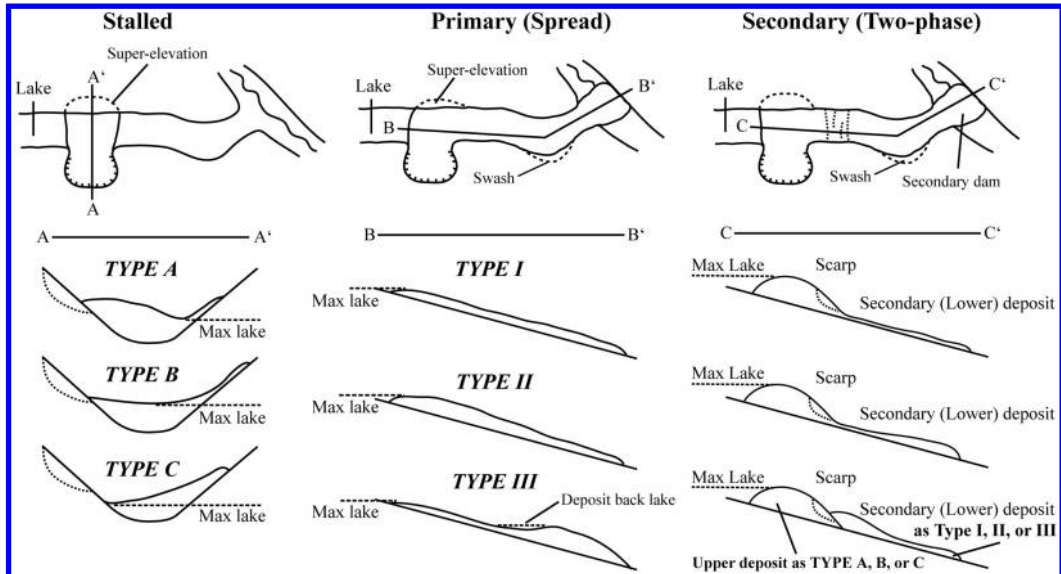
Figure 5. The three principle morphological types identified, sub-types based on mass distribution. Super-elevation is common but not compulsory in Type A–C.

all other variables (Dunning, unpubl.). For the purposes of simple dam-break modelling these variations due to lithology are not considered as important as the contrast between the *Carapace* and *Body facies*. Hydraulic conductivities for the interior vary based upon the lithology present and the time in motion, both controls on final grain-size distribution. Two predictive plots applicable to all lithologies based on a measure of weight percent gravel can be used to provide estimates of the median grain size, sorting, fractal dimension and hydraulic conductivity of rock-avalanche deposits (Dunning, unpubl., Dunning & Armitage, in press). For the purposes of comparison, an argillite sample in the interior of the Falling Mountain rock-avalanche deposit yielded hydraulic conductivity values of around $3 \times 10^{-3} \mathrm{ms}^{-1}$ and porosity of around 20% . It is sufficient to say that the hydraulic conductivity increases at coarser grain size assemblages, all of which are fractal in nature rather than following other forms of distribution such as the Weibull as previously considered (Strom & Pernick 2004).

5.3 *Stalled morphology*

The Stalled morphology (Fig. 5) of a valley confined rock-avalanche deposit involves the smallest geometric footprint for a given volume of debris. It is an end member morphology showing the shortest possible run-out for a rock avalanche. Consequently, if the width and length of deposit are relatively low, the dam height must be high to accommodate the end member morphology showing the shortest mass. As such, the configuration creates a narrow, high blockage (Figs. 2–3) in a confined valley setting. The mass can be distributed as an evenly crested deposit or biased toward opposing slopes or the source region. Such details should always be recorded as any low point in the crest affects both impoundment potential and failure timing. Frontal portions of the mass can super-elevate to vast heights above the former valley floor on the opposing valley slopes to the source. A notable Canadian example of such super-elevation is the 640 m run-up at the Avalanche Lake rock-avalanche dam deposit (Evans 1989). A controlling limit on the footprint of the deposit is the angle of repose of the debris. Observations suggest that rock avalanches usually deposit with dam face angles below the angle of repose (Costa & Schuster 1988), therefore stable to slope failure unless forced by pore pressure.

The interpreted process by which a Stalled morphology deposit is created is the direct impact of the moving mass on opposing slopes. This impact serves to stall the mass due to the high energy dissipation, as noted by Nicoletti & Sorriso-Valvo (1991) in similar situations. The active mechanism of motion is reduced to a level where spreading along valley is restricted, resulting in the morphology described.

The pre-failure valley morphology is critical to formation of a Stalled morphology, as is the angle of incidence of the failing mass into the valley. Near right angle impacts have been observed to produce the most spectacular examples of restricted spreading and super-elevation. It is interesting to note that this sort of impact usually results in super-elevated debris falling directly back onto the surface of the landslide, partially obscuring the true surface texture with finer material, as for example at Val Pola (Crosta et al. 2004).

The detailed surface morphology varies with bedrock properties and failure style. Progressive phases of failure result in a series of lobate features, with the long axis orientated toward the source. The length to width ratio of such lobes tends towards values of 2. Surface lobes can have relative relief of meters to tens of meters and can significantly affect the pathways available for overtopping water before discharges are reached whereby carapace blocks cannot resist erosion.

5.3.1 *Stalled sedimentology*

The sedimentology of a Stalled rock avalanche deposit consists of a thick *Carapace facies*, up to 30% by depth. The carapace is usually, lithology allowing, the coarsest observed due to the time in motion restricting time for large blocks to disintegrate along pre-existing discontinuities or develop new ones. The body facies is the typical highly fragmented gravel, sand, and finer material, even during such relatively restricted run-outs (Fig. 5). Decrease in grain size during motion is statistically valid for rock-avalanche deposits (Dunning, 2004) but it starts from a point of highly fragmented material proximal to the source; presumably formed during any period of free-fall and/or the active flow mechanism as the mass travels to the valley floor from the failure scar. This results in a large contrast in sedimentological and geotechnical properties between the two facies, critical for stability analyses.

5.4 *Primary spread morphology*

The Spread form of rock-avalanche deposit morphology (Fig. 5) is the opposite end-member to the Stalled type. It is this form of rock-avalanche deposit that can be interpreted to show the excessive run-out often noted as characteristic. For a particular volume of failed mass, it is the Spread morphology that creates the largest geometric footprint, with run-outs usually in the order of kilometers. As a result, the lowest deposit thickness of all of the morphologies is observed. The long cross-sectional form can be varied, with a distribution of mass biased toward the proximal or terminal regions (Fig. 7) of runout. This distribution of mass should be noted as it affects the damming potential. The morphological type can be applied to non-valley confined rock-avalanches; in this case the resulting deposit is
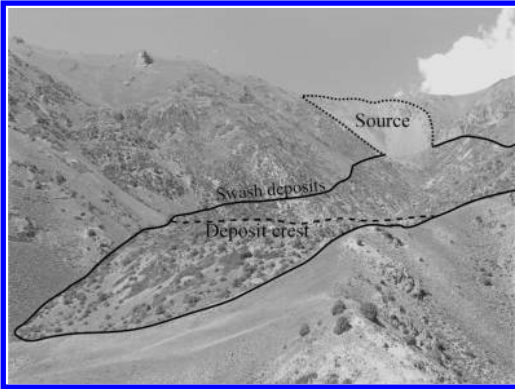
696

Figure 7. The Primary Spread Seit rock-avalanche deposit, Kyrgyzstan. In this case the bulk of the mass deposited terminally and would be capable of forming a minor dam and deposit back lake.
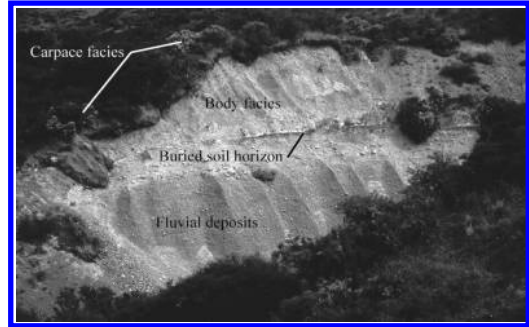

Figure 8. Internal section through the Primary Spread Acheron rock-avalanche deposit, New Zealand overlying fluvial deposits. The deposit is only ~8 m thick with a thin *Carapace facies* and was only capable of forming a low dam across several tributary valleys.

lobate in plan form due to unrestricted spreading in all directions. In the case of valley confinement, the mass spreads and thins in the available accommodation space, usually down gradient.

During runout, Spread morphologies deposit numerous morphological features. The most prominent are swash deposits (Fig. 7), here termed as debris retained on the valley side after a portion of super-elevating material has passed. Swash deposits are distinct from the super-elevation of material on slopes directly opposite to the source region, often shown at all forms of deposit. Swash deposits are found on the outside of valley bends and represent the rock avalanche motion around those bends via adjustment of the flow direction; super-elevation deposits represent a frontal wedge of material climbing directly up-slope and ceasing in motion or falling back onto the surface below. Super-elevation deposits at Spread deposits are controlled by valley morphology and angle of incidence of failure. Failures entering the valley at sufficient angles may exhibit no super-elevation, only swash. Lateral levees, a product of dilation of the mass during motion and not of flow direction adjustment are common. They occur both along straight portions of the valley plan geometry and on the inside of valley bends. The levees deposit on the valley sides as motion ceases, remaining several meters or more above the main deposit mass in the valley floor that settles from the higher dilation levels achieved during motion.

The detailed surface morphology of Spread deposits is similar to that of Stalled deposits. Lobe-like features are common, though often more elongate than those discussed above. The surface morphology can be complicated by a relatively thin deposit. Previous valley features are mantled by the depositing rock avalanche, although many features will have lower relief due to

the base of the rock avalanche interacting with the substrate. The *Basal facies* where this interaction takes place shows mixed features of both the *Body facies* and substrate material and is highly dependent upon substrate material, in particular whether or not it can be entrained.

5.4.1 *Primary spread sedimentology*

Spread deposits have *Carapace facies* that may be in the same ratio of thickness as Stalled deposits, but as the actual deposit depth is the minimum for a given volume the carapace thickness may only be in the order of the block size (Fig. 8). The block size is again dictated by lithology and discontinuity spacing. The time in motion also allows for a greater degree of carapace disintegration along discontinuity surfaces. This can result in an inversely graded Carapace with the action of kinematic sieving (Bianchi-Fascini, unpubl.). This grading does not extend below the *Carapace facies*, the sedimentological character beneath the sharply bounded carapace is the distinctive highly fragmented but relatively disaggregated texture of the *Body facies* (Fig. 8). However, it is possible that observation of an inversely graded carapace lying above finely fragmented debris that leads to the erroneous interpretation that rock-avalanche deposits are inversely graded.

5.5 *Secondary two-phase morphology*

The Two-phase morphological type (Fig. 5) appears as an intermediate between the two forms presented so far. In plan form it appears as the Spread class, with a lower runout for a specified setting. A number of important features distinguish the two morphologies. The level of super-elevation (Fig. 9) on the slopes opposite the source region is considered greater than for Spread deposits and less than for Stalled deposits for a given
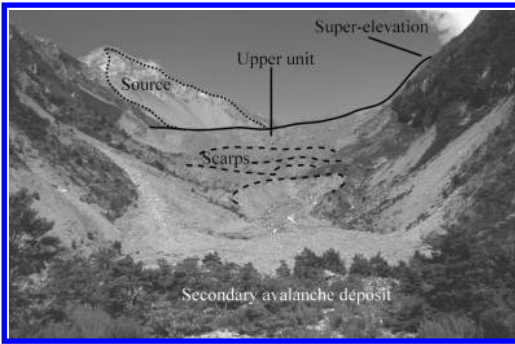
697

Figure 9. Secondary Two-phase Falling Mountain deposit looking up-flow toward the source from the finer grained, Secondary avalanche. Both Super-elevation and swash are apparent (marked) and the Secondary avalanche source clear.

Figure 10. The upper unit of the Secondary Two-phase Falling Mountain deposit showing the debris that stalled on impact with the valley side (flow is from right to left). Width of view is approximately 1 km. The surface is formed of coarser *Carapace facies* material than the Secondary deposit in Figure 9.

failure volume and valley geometry. Along with this high super-elevation, a significant portion of the mass stalls on impact against the valley floor and opposite side (Figs. 9–10). The result is an upper deposit similar in character to a Stalled morphology deposit.

What sets the Two-phase deposit apart is a portion of material not stalled by the impact on opposing slopes. This portion or portions of the mass retain sufficient energy to continue spreading and thinning run-out along the valley (Fig. 9). Observations suggest that this can occur on one or both sides of the stalled mass. The most spectacular have involved volumes of debris with enough energy retained to travel for several kilometers. This more mobile mass is termed the Lower deposit or Secondary avalanche deposit (Strom 1999, Strom & Pernik 2004) and shows all of the morphological features of a Spread deposit including swash deposits, lateral levees, and

an abrupt terminal margin. It is debatable whether the mobile lower deposit is a syn-depositional or post-depositional slope instability feature of the deposit. The boundary between upper and lower units is often characterized by a number steep rotational scar features. We favor a syn-depositional failure of a portion of the mass unstable under the depositional regime of the Upper deposit that stalled.

The presence of a number of scars suggests successive pulses of failure evacuating completely or flank settling of the upper unit along the valley gradient. It is often the down valley side of the upper unit that is noted to continue run-out.

The surface morphology of a Two-phase deposit reflects its two origins. The upper unit shows the lobate features of Stalled deposits, again orientated toward the source and reflecting failure style. The Secondary deposit mantles the valley floor and sides, lobes are present, reflecting the multiple failure scars and their interaction, though relief is orders of magnitude lower than the upper unit.

5.5.1 *Secondary two-phase sedimentology*

As the morphology of a Two-phase deposit is intermediate between the two end members presented, so is the sedimentology. The Upper unit shows a coarse carapace overlying a highly fragmented interior (Fig. 6), with the grain-size distribution and geotechnical properties being lithologically dependent. The Secondary deposit is characterized by the finer carapace of a Spread morphology and decreasing internal grain size, again at a rate too low to gain importance over the contrast between the *Carapace* and *Body facies*. The boundary between the Upper and Lower unit is more complex. The presence of distinct evacuation scars affects both the surface and interior sedimentology and individual site evaluations are usually required.

If the runout it sufficient, spreading and thinning increases the importance of the *Basal facies* leading to a deposit that may have equal depths of all three facies identified, a situation more common at Spread deposits. The *Basal facies* shows mixed sedimentological and geotechnical character of both the rock avalanche and substrate material. Dependent upon the substrate this can include smears of alluvial mud, rip-up alluvial boulders and gravel, and valley side screes and landslide deposits. Granular material entrained is subject to the same transport processes, including fragmentation of clasts incorporated (Dunning, unpubl.).

6 DAM FAILURE HAZARD

6.1 *Introduction*

Each of the three morphologies and their associated sedimentologies outlined are capable of impounding

698

lakes. Significant differences can be interpreted for each in terms of the hazard posed – affected by the impoundment potential, the failure style, and the time to that failure, ranging from hours to thousands of years.

This section is intended to outline the uses that study of the morphology and sedimentology can have for the assessment of the stability of rock-avalanche dams. At present there is a dearth of case studies with the relevant morphological and sedimentological details to statistically test the interpretations below. Collection of such a dataset is ongoing.

6.2 *Hazard related to classification*

Common sense dictates that the greatest secondary hazard are posed by Stalled and Two-phase morphologies, for a given volume and suitable valley geometry they form the highest possible dams (Figs 2, 9). The higher a dam crest above the former valley floor, the greater the possible lake impoundment volume, and so the greater the maximum possible outburst flood, again dependent upon the valley gradient and valley side morphology upstream of the dam site, and of course dam stability. Conversely, the dam created by a valley blocking Spread morphology will be extremely low for the same volume, and so too will be the impoundment potential. The primary hazard (due to run-out) will be high, the secondary (due to an outburst flood) low. The rate of emplacement of all is high enough to reduce any possible river sluicing of debris upon entering the drainage; in essence the dam is formed near instantaneously. A Two-phase morphology is capable of forming a high crested dam in the Upper unit backed by the Lower unit of material as toe weight (Figs. 9–10).

The maximum hazard is therefore created by both Stalled and Two-phase morphologies. The only possible configuration to increase the secondary hazard present at a Spread deposit is an extremely low valley gradient increasing the possible lake volume. Spread deposits are more likely to produce numerous minor dams against tributary valleys due to the runout rather than a hazardous single blockage.

6.3 *Failure style*

Dam height and valley geometry determine the maximum lake size possible at lake full level, but it is the inflow/outflow that determine the actual rate of filling and failure style. If the river inflow sufficiently exceeds seepage outflow the lake can fill to crest level, resulting in overtopping breach formation and dam failure. However, this is not always the case, case studies show examples stable to limited overflow conditions, with the flow confined to the *Carapace facies* and not eroding to failure (Dunning et al., in review, Hancox

et al. 1999). This overflow can continue and increase to create a failing breach, or stabilize to below crest level, as observed in a Stalled landslide dam in the Bhutanese Himalaya (Dunning et al., in review). In such cases the role of seepage becomes critical to dam stability, and so too does the role of morphology and sedimentology.

Preliminary investigation has focused upon Stalled morphology case studies due to the hazard posed, with the collection of the relevant morphological and sedimentological data complete (Dunning, unpubl., Dunning et al., in review). As discussed, the main aim of modelling was to confirm the effect of the correct sedimentology on the time to failure of rock-avalanche dam deposits. The failure style was defined as downstream face slope failure (Fig. 3) based on case study observation (Dunning & Armitage, in press). This is true for those deposits that do not over-top due to the equilibrium of input and outputs, or those that are deemed stable to low overflow conditions. Under these conditions the role of sedimentology is crucial, it is the contrast in properties of the *Carapace* and *Body facies* that allows for the rapid destabilization of the downstream face.

7 CONCLUSIONS AND FURTHER WORK

The morphological classification scheme of Strom (1999) and Strom & Pernik (2004) has been modified with the inclusion of sedimentology. The hazard posed by a rock avalanche itself is low when compared to that of a potential outburst flood when a lake is impounded behind a deposit. Preliminary investigation suggests that of the three assemblages identified the Stalled and Two-phase create the greatest hazard, both in terms of the reservoir potential and instability to both overtopping and slope failure.

The numerical modelling technique applied to the Stalled morphology and sedimentology is to be applied to the Two-phase and Spread classes. It is anticipated that the mode of failure and relative time to failure will be significantly different. In particular, Spread deposits are interpreted to be stable against slope failure due to their geometry, but to be susceptible to breach via enlarging channel formation. Evaluation of the sensitivity of failure style to reservoir filling rate is underway, high rates are deemed to favor fast overtopping breach channel failure and head-cutting, low rates favor slope failure for a specified setting.

Both the Poerua (Fig. 1) and Bhutan Himalaya rock-avalanche dams (Figs. 2–3) were of similar geometry, lithology and sedimentology, and can be classified as Stalled deposits. Poerua failed in days via lake overtopping (Hancox et al. 1999), but physical modelling (Davies, pers. comm.) and computer based modelling (Dunning & Armitage, in press) suggest that a breach

via slope failure was a possibility. The Bhutan Himalaya dam failed after 10 months through large scale slope failure of the downstream face (Fig. 3) (Dunning et al. in review). The critical variables between the two appear to be reservoir filling and seepage rates.

Key to the evaluation of the hazard posed by the three classes identified is a dataset of past and present rock-avalanche dams. Such a dataset will allow empirical relationships against which model outputs can be tested. For this purpose a proforma has been created to collect all necessary morphological and sedimentological data utilizing predictive plots for the often unobtainable interior sedimentology (Dunning & Armitage, in press). Physical modelling is to be undertaken using the three morphologies and associated sedimentological characteristics in collaboration with Canterbury University, New Zealand. The physical modelling will also allow greater insight into the correlation of failure styles and timing with varied reservoir filling conditions. Previous models have yielded varied failure styles under identical conditions (Davies, pers. comm.) with little effect on Qmax, suggesting that failure style cannot be identified based upon discharge downstream of dam failures. To be borne in mind is that failure style is difficult to interpret from post-failure site evaluation, much of the evidence is destroyed during the failure sequence.

REFERENCES

Bianchi-Fasani, G. unpublished. *Security of Natural and Artificial Rockslide Dams*, NATO Advanced Research Workshop, Bishkek, Kyrgyzstan, June 8–13, 2004, oral presentation.

Casagli, N. & Ermini, L. 1999. Geomorphic analysis of landslide dams in the northern Apennine. *Transactions of the Japanese Geomorphological Journal* 2: 219–249.

Casagli, N., Ermini, L. & Rosati, G. 2003. Determining grain size distribution of the material composing landslide dams in the Northern Apennines: sampling and processing methods. *Engineering Geology* 69(1–2): 83–97.

Corominas, J. 1996. The angle of reach as a mobility index for small and large landslides. *Canadian Geotechnical Journal* 33: 260–271.

Costa, J.E. & Schuster, R.L. 1988. The formation and failure of natural dams. *Geological Society of America Bulletin* 100: 1054–1068.

Crosta, G.B., Chen, H. & Lee, C.F. 2004. Replay of the 1987 Val Pola landslide, Italian Alps. *Geomorphology* 60: 127–146.

Cruden, D.M. & Hungr, O. 1986. The debris of the Frank Slide and theories of rockslide-avalanche mobility. *Canadian Journal of Earth Sciences* 23(3): 425–432.

Davies, T.R., McSaveney, M.J. & Hodgson, K.A. 1999. A fragmentation-spreading model for long-runout rock avalanches. *Canadian Geotechnical Journal* 36: 1096–1110.

Davies, T.R. & McSaveney, M.J. 2004, in press. Rock-avalanche size and runout- implications for landslide dams. In Evans, S.G., Hermanns, R, Scarascia Mugnozza, G. & Strom, A.L. (eds) *Security of Natural and Artificial Rockslide Dams*; *NATO Science Series: IV Earth and Environmental Sciences*. Dordrecht: Kluwer Academic Publishers.

Dunning, S.A. 2004, unpublished. Rock Avalanches in High Mountains. PhD Thesis, University of Luton, United Kingdom.

Dunning, S.A. & Armitage, P.J. 2004, in press. The grain-size distribution of rock-avalanche dams. In Evans, S.G., Hermanns, R, Scarascia Mugnozza, G. & Strom, A.L. (eds) *Security of Natural and Artificial Rockslide Dams*; NATO Science Series: IV Earth and Environmental Sciences. Dordrecht: Kluwer Academic Publishers.

Dunning, S.A., Rosser, N.J., Petley, D.N. & Massey, C.J. 2005, in review. The formation and failure of the Tsatichhu rock-avalanche dam, Bhutan.

Eisbacher, G.H. 1979. Cliff collapse and rock avalanches (sturzstroms) in the Mackenzie Mountains, north-western Canada. *Canadian Geotechnical Journal* 16: 309–334.

Ermini, L. & Casagli, N. 2003. Prediction of the behaviour of landslide dams using a geomorphological dimensionless index. *Earth Surface Processes and Landforms* 28: 31–47.

Evans, S.G. 1989. Rock avalanche run-up record. *Nature* 340: 271.

Glazyrin, G. & Reyzvikh, V.N. 1968. Computation of the flow hydrograph from the breach of landslide lakes. *Soviet Hydrology* 5: 592–596.

Hancox, G.T., McSaveney, M.J., Davies, T.R. & Hodgson, K. 1999. Mt Adams rock avalanche of 6 October 1999 and subsequent formation and breaching of a large landslide dam in Poerua River, Westland, New Zealand. Institute of Geological and Nuclear Sciences Science Report 99/19, 22 pp.

Hermanns, R.L., Niedermann, S., Gonzalez Diaz, F.E., Faque, L., Folguera, A., Ivy-Ochs, S. & Kubik, P. 2004, in press. Landslide dams in the Argentine Andes. In Evans, S.G., Hermanns, R, Scarascia Mugnozza, G. & Strom, A.L. (eds) *Security of Natural and Artificial Rockslide Dams*; *NATO Science Series: IV Earth and Environmental Sciences*. Dordrecht: Kluwer Academic Publishers.

Hewitt, K. 1999. Quaternary moraines vs catastrophic rock avalanches in the Karakoram Himalaya, Northern Pakistan, *Quaternary Research* 51: 230–237.

Hewitt, K. 2001. Catastrophic rockslides and the geomorphology of the Hunza & Gilgit River Valleys, Karakoram Himalaya, *Erdkunde*, Band 55.

Hodgson, K.A., Davies, T.R. & McSaveney, M.J. 1998. Experimental granular flows and their relationship to large rock avalanches. GSNZ, In: *New Zealand Geophysical Society 1998 Joint Annual Conference, 30 Nov. – 3 Dec.. programme and abstracts*, 260 pp.

Hungr, O. & Evans, S.G. 2004. Entrainment of debris in rock avalanches; an analysis of a long run-out mechanism. Geological Society of America Bulletin 9/10: 1240–1252.

Korup, O. 2004. Geomorphic characteristics of New Zealand landslide dams. *Engineering Geology* 73: 13–35.

Manville, V. 2001. Techniques for evaluating the size of potential dam-break floods from natural dams. Institute of Geological and Nuclear Sciences Science Report 2001/28, 72 pp.

McSaveney, M.J. & Davies, T.R. 2002. Dynamic simulation of the motion of fragmenting rock avalanches. *Canadian Geotechnical Journal* 39(4): 789–798.

Melosh, 1987. The mechanics of large rock avalanches. *Geological Society of America Reviews in Engineering Geology*, VII: 41–49.

Nicoletti, P.G. & Sorriso-Valvo, M. 1991. Geomorphic controls of the shape and mobility of rock avalanches. *Geological Society of America Bulletin* 103: 1365–1373.

Strom, A.L. 1999. The morphology and internal structure of large rockslides as indicators of their formational mechanisms. *Dolkady Earth Sciences* 369(8): 1079–1081.

Strom, A.L. & Pernik, L.M. 2004. Utilization of the data on rockslide dams formation and structure for blast-fill dams design. In Abdrakhmatov, K., Evans, S.G., Hermanns, R., Scarascia Mugnozza, G. & Strom, A.L. (eds) *Security of Natural and Artificial Rockslide Dams, extended abstracts volume, NATO Advanced Research Workshop, Bishkek, Kyrgyzstan, June 8–13, 2004*, 177–182.

Remedial works and early warning systems

Development and implementation of a warning system for the South Peak of Turtle Mountain

C.R. Froese, C. Murray, D.S. Cavers, W.S. Anderson & A.K. Bidwell
AMEC Earth & Environmental, Edmonton/Burnaby, Canada

R.S. Read
RS Read Consulting Inc., Okotoks, Alberta, Canada

D.M. Cruden
University of Alberta, Edmonton, Alberta, Canada

W. Langenberg
Alberta Geological Survey, Edmonton, Alberta, Canada

ABSTRACT: Since the original catastrophic slide at Turtle Mountain in 1903 that buried the Town of Frank, killing 70 people, government and public attention has shifted to the potential for a second large failure originating from the South Peak. In 2003, on the centennial of the initial slide, the design, installation and commissioning of a real time monitoring system for the South Peak was launched by the Alberta Provincial Government to provide first and foremost the framework for a real time monitoring system to warn of the development of a second large failure. In addition, the monitoring system will also be an educational tool for the public. This paper outlines the review of recently obtained data from a series of tiltmeters, surface extensometers, prisms and differential GPS, as well as surface and subsurface microseismic instrumentation installed in 2003/2004, coupled with a review of historic monitoring data obtained from the early 1900's to present. Synthetic Aperture Radar Interferometery (InSAR) has also been utilized to map deformations over a six-month period in 2004. Included as part of this assessment is an update of the structural geology of the South Peak obtained from a combination of detailed mapping, ground penetrating radar surveys and borehole televiewer data. All this information, coupled with the recent and historical movement data, was utilized to develop preliminary alarm threshold values and alarm and notification protocols to be incorporated into the Emergency Response Planning for the Municipality of Crowsnest Pass.

1 INTRODUCTION

After the catastrophic 1903 rock slide at Turtle Mountain that buried parts of the town of Frank and killed 70 people (Fig. 1), studies of the remaining portions of the mountain highlighted a series of large cracks around the South Peak (Fig. 2). Studies by Allan (1933) estimated that a failure of the mass at South Peak could potentially have a volume up to 5 million cubic meters of material and impact on municipal development and infrastructure below.

Although numerous studies have been undertaken since the early 1900's, there was not conclusive evidence of the overall movements of the peak and no way to provide a predictive warning should an acceleration of movements occur. In 2003, during a ceremony marking the centennial of the Frank Slide, the

government of Alberta committed $1.1 million (CDN) to develop and deploy a real time monitoring system and develop a warning and response plan for the Municipality of Crowsnest Pass.

This paper provides an overview of the system design and installation, a review of the historical and current data trends and discusses the basis on which the monitoring, warning and response plan is being developed.

2 BACKGROUND

In 1998, AGRA Earth & Environmental (1998) was retained by Alberta Environmental Protection to assess the hazards related to the Frank Slide and Turtle Mountain. Following a review of the historical
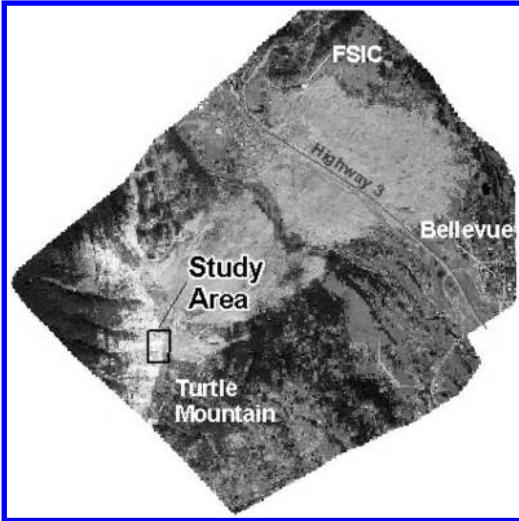
705

Figure 1. The location of the South Peak study area, in relation to the 1903 Frank Slide.
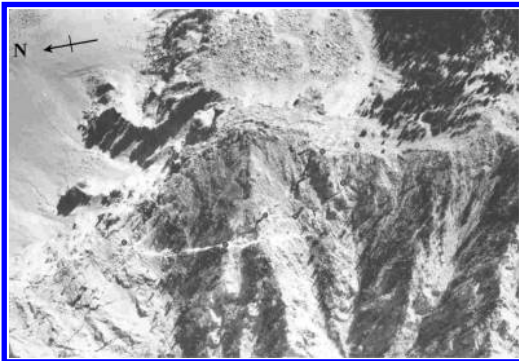

Figure 2. Photo of cracks around South Peak red dots indicate fissures that are greater than 30 metres in depth.

Figure 3. Predicted range of danger zones for runout from South Peak (BGC 2000).

instrumentation installed on Turtle Mountain, the findings indicated that only near surface, localized features were being monitored for displacement, and the near surface instrumentation was strongly influenced by fluctuations in the weather. Since displacements were occurring on Turtle Mountain, it was recommended that more sophisticated instrumentation be installed with an increased monitoring frequency to provide warning of slope failure. It was considered unlikely that even sophisticated instrumentation would provide a tool to forecast time to failure.

Monitoring systems considered appropriate to monitor movement at Turtle Mountain included a remotely monitored Differential Global Positioning System (DGPS) to monitor surface movements. In addition, borehole extensometers and In-Place inclinometers,

which could also be set up for remote reading, were considered feasible to monitor displacements at depth.

Following the 1998 study, a geotechnical hazard assessment of the south flank of Frank Slide was undertaken by BGC Engineering (2000). The assessment included a site reconnaissance partly to confirm the geological structure and fissure patterns in the South Peak and to assess the state of the existing instrumentation on Turtle Mountain. Six of Allan's original 18 gauging stations were identified and aperture measurements taken. No significant displacements were interpreted from these measurements. It was observed that the TM-71 Moiré crack gauges had been completely destroyed through vandalism.

In addition, in order to refine the empirically based rock slide runout danger zones provided by Allen (1933), BGC (2000) undertook dry avalanche computer simulations and an updated zonation was provided (Fig. 3).

As a continuation of the earlier studies RSRCI (Read 2003) addressed the development of a framework for future monitoring of Turtle Mountain, particularly South Peak.

Conceptual monitoring system options were proposed for three systems. An educational system including seismic stations and a weather station, would provide broad seismic coverage of Turtle Mountain but not attempt to measure surface or subsurface deformations. An investigative system including an EDM total station and prisms and crack monitors, would correlate seismic and surface deformation data, but not provide information on subsurface deformations or pore pressure. A predictive system including boreholes containing microseismic monitors, extensometers and inclinometers has been proposed in conjunction with the educational and investigative systems to provide a predictive monitoring system that would measure seismicity, surface and subsurface

706

deformations, pore pressure, temperature, climate data and surface water flow data.

It was proposed that these instrumentation devices be set up with a data acquisition system whereby raw data would be received at the Frank Slide Interpretive Centre (FSIC), which would act as a control centre, where long term data monitoring and assessment would be undertaken for long term monitoring. This conceptual framework was the basis for the system discussed in this paper.

3 UPDATED GEOLOGICAL MAPPING

During the system design refinement in winter 2004, the existing information on the structural geology of the South Peak and postulated mechanisms and contributing factors for the 1903 Frank Slide were re-examined. Previous work by Norris (1955), Allan (1933) and Cruden & Krahn (1973) had highlighted that the mountain consisted of an anticlinal fold and that the east limb of this fold had failed during the 1903 slide. Figure 4 shows the hinge of the anticline exposed in the scarp of the 1903 slide below South Peak.

More recently, studies of the structural geology of South Peak by Fossey (1988) and as part of Turtle Mountain Monitoring Project (TMMP) by the Alberta Geological Survey and University of Calgary have been undertaken. Detailed mapping of the structure and fracture patterns of the peak have confirmed the structural framework. In addition, downhole optical techniques and surface geophysics have been utilized to gather information on subsurface structure within the peak.

Theune et al. (2005) completed a series of surface ground penetrating radar (GPR) surveys of South Peak during the summer of 2004. These surveys were able to map rock structure to depths of 40 metres and observe bedding and fracture orientations and frequency.

In addition, during drilling of test holes on South Peak during the summer of 2004 an optical televiewer was utilized to photograph the test hole wall (Bidwell et al., in press). A hole 62 metres deep was drilled using a helicopter portable air rotary drilling rig and a Mount Sopris optical televiewer was utilized to obtain a complete photo record of the downhole conditions and to map geologic structure. Significant zones of highly fractured rock and cavities were encountered within the peak. Figure 5 shows one of the televiewer images illustrating the nature of the bedrock within South Peak.

The recent detailed information has confirmed the highly fractured nature of the bedrock on the surface and within South Peak but has not changed the overall view of the range of postulated mechanisms for potential large movements of South Peak.
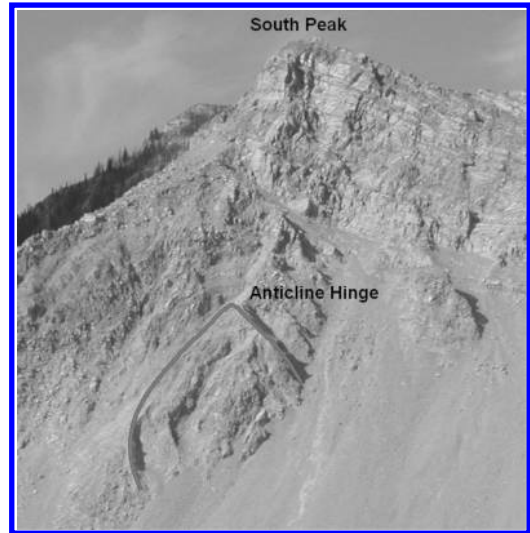

Figure 4. View across 1903 slide scarp toward South Peak showing exposed hinge of anticline.
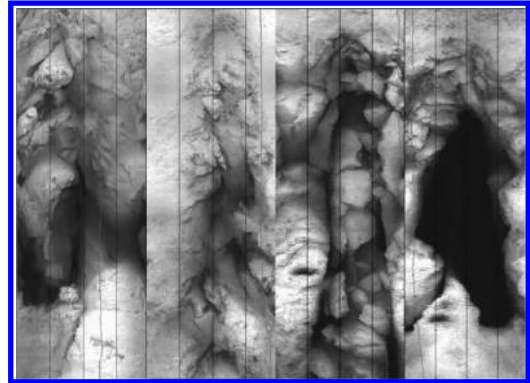

Figure 5. Optical televiewer logs from a borehole drilled on South Peak in summer 2004 showing highly fractured bedrock containing large cavities. The photos show 4 logs side by side of different portions of the 100 mm diameter hole unwrapped to a flat surface.

4 SYSTEM DESIGN AND INSTALLATION

Based on this understanding of the geology and rock structure, the following are the main postulated movement mechanisms that may exist at South Peak:

1 Rotation and Toppling
2 Progressive development of a displacement plane
3 A combination of the above mechanisms

In reviewing the existing information followed by a detailed reconnaissance of South Peak, the overall mechanism and style of movement could not be

707

Table 1. Sensors installed on South Peak in 2004.

Ten uniaxial tiltmeters

Four surface wire extensometers

Five differential GPS hubs

A series of prisms with a theodolite set up at the Frank Slide Interpretive Centre (FSIC)

Twenty-two crack gauges

Five surface microseismic sensors

Two downhole microseismic sensors

One borehole thermistor string and vibrating wire piezometer

A meteorological station providing information on temperature, wind speed and direction, barometric pressure, precipitation and rock temperature
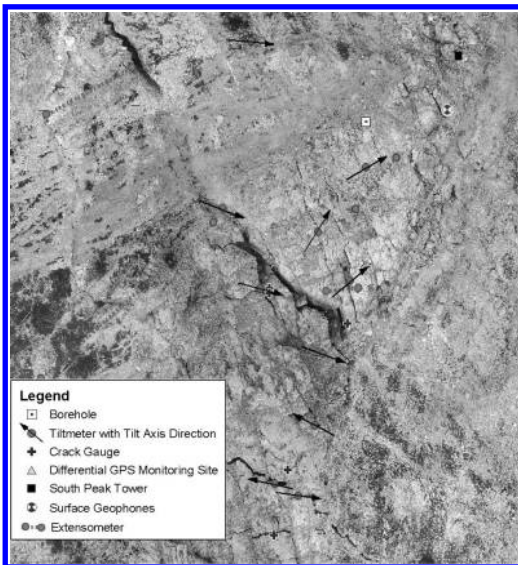
Figure 6. Plan layout of newly installed instrumentation on South Peak.

conclusively determined and therefore the design of a system that maximized the spatial deformation information on South Peak within the specified project budget was recommended. The array of sensors was chosen to provide the most complete information possible as to the kinematics of movement. The overall system was comprised of the sensors shown in Table 1. The layout of the instruments is provided on Figure 6.

As can be seen on Figure 6, a certain amount of redundancy was built into the system as a check on sensors. The concept was that if one sensor shows deformation then another type of sensor should also reflect the deformation if it is real and not an erroneous reading caused by instrument malfunction, atmospheric effects or vandalism. Data from each of the sensors are collected by automatic data loggers on the mountain and transmitted via telemetry to the FSIC (in some cases via Blairmore due to sight lines) where the data are received on a server that can be accessed remotely for data review.

5   DATA REVIEW

While the monitoring system provides an educational system for the public at the FSIC, the main purpose was to provide a real time monitoring system to better understand the deformations at South Peak and to provide warning for the Municipality of Crowsnest Pass in the event of an apparently significant increase in movement rates.

In order to develop threshold alarm levels for the various instruments installed on South Peak a review of previously installed instruments was undertaken in conjunction with the more recently installed sensors. The following provides a summary of the data review.

5.1   *Historical data*

As part of a Master of Engineering project at the University of Alberta, Murray (2005) completed a detailed review of the literature and available instrumentation readings between 1911 and 1996. The following constitutes the main findings of this study.

Following the devastation resulting from the Frank Slide at Turtle Mountain in 1903 within the Crowsnest Pass region of Alberta, many observations and investigations have been undertaken throughout various time frames over the past 100 years to understand the geological setting and delineate whether subsequent slope movements would be detected to establish an understanding of the stability of the mountain.

From these investigations and visual observations, the general conclusion has been that on-going small surface displacements are occurring. New cracking has been observed at the surface since soon after the slide, however, consistent monitoring has not been maintained over a sufficient period of time to allow for a more complete assessment.

Many attempts were made to monitor surface displacements with inconclusive results. Surface monitoring stations including reference mounds, reference points, Allan crack width stations, survey benchmarks and trilateral signs have been implemented, each affected by system accuracy issues. Since displacement measurements in the order of millimetres were detected, rather than centimetres, much of the data showed significant scatter due to climactic cycles and measurements issues, which made the information difficult to assess.

708

Crack gauges were installed as a trial in 1980 where slope movements were again detected in the millimetre scale, indicating horizontal shear and crack closure, however the data were also affected by annual climactic cycles. The rates of movements detected were not considered to be alarming.

5.2 *New instruments*

As many of the instruments were only installed in the summer/fall of 2004, there is not a large baseline of data to establish trends and the seasonal effects of climatic fluctuations on the instruments. To this point it is clear that climatic effects have a significant impact on the instruments. The following provides a brief summary of observations from the sensors to this time.

Temperature fluctuations have been observed to directly impact on deformations on both the tiltmeters and crack gauges. As can be seen on the plot in Figure 7, increases in air and rock temperature after periods of cold weather have apparently resulted in the opening of cracks.

Snow and frost also have impacts on the instruments. Recently it has been determined that some of the crack gauges are no longer operational as snow loading within the cracks had loaded the crack gauge rods and extended the gauges beyond their allowable movement limits, rendering them temporarily inoperable. Although protective housings have been built over each set of crack gauge triplets, the high winds on the west side of the peak have blown snow in and around the gauges. This has been confirmed with field assessments during the winter months. With respect to frost, field assessments have also encountered significant build up of hoar frost on the faces of the prisms mounted on the peak, likely indicating that readings may not be possible from these instruments in the winter months.

The impacts of lightning also required significant attention during planning of installations. In July 2004, a total of seven crack gauges were destroyed by a lightening strike. After this, all crack gauges and tiltmeters were fitted with surge arrestors to minimize the potential for a future strike to incapacitate the sensors. However, adequate grounding of the surge arrestors remains a significant problem.

The information regarding the seasonal effects also has a bearing on the weighting of the reliance on each of the sensors if deformations are observed in different seasons. Overall to this point the extensometers, tiltmeters and the majority of the crack gauges have provided continuous reliable data flow since installation. Notably, the extensometers, primarily constructed of aircraft cable with a very low thermal expansion coefficient enclosed in an armored conduit, have not yielded any variations due to climatic effects.
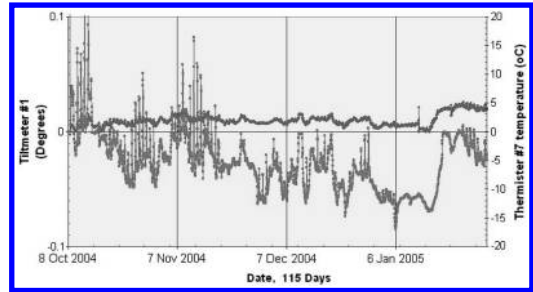

Figure 7. Data plot showing tiltmeter plotted versus surface air temperature showing correlation between changes in air temperature and observed deformations.

As seen in the above discussion, the primary focus for the development of the warning system is the performance of the instruments that provide measurable deformations and are considered primary sensors. Other sensors installed as part of the project, including the meteorological station, thermistors, geophones and an outflow weir at the mine opening near the slope toe, are complimentary systems that are utilized to better understand the nature of the deformations observed on the primary sensors but not specifically relied upon for warnings.

5.3 *InSAR*

Another technology utilized for the assessment of deformations on Turtle Mountain was Synthetic Aperture Radar Interferometry (InSAR). InSAR is a technique that utilizes repeat pass radar satellites to map subcentimetre level deformations between successive satellite passes. A more detailed description of the application of this technology to slope movements is provided by Froese et al. (2004).

For the InSAR assessment, a technique called Coherent Target Monitoring (CTM) was utilized. This technique uses a large number of satellite scenes and identifies permanently coherent (points that maintain radar coherency) points that can be referenced on these scenes. By collecting a large number of readings of these points over time, trends can be identified and data noise statistically filtered in order to obtain millimeter level deformation data. Figure 8 shows the number of points utilized for the CTM assessment on Turtle Mountain.

At the time of the preparation of this paper, 21 scenes had been specifically tasked for RADARSAT-1 between spring and fall 2004 and nine scenes were utilized for the assessment. Over this time period there were not yet sufficient data to identify trends and filter out noise in the data and therefore conclusive deformation data were not yet available. As this portion of the project is being primarily funded by the
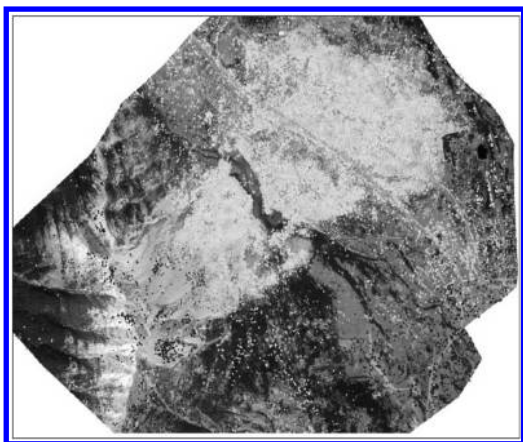
709

Figure 8. Data points utilized for the CTM assessment overlain on the DEM.

Canadian Space Agency, with support from the Alberta Geological Survey, ongoing data collection and review is planned to develop a better understanding of spatial deformations on Turtle Mountain.

The goal of the InSAR assessment is to provide a better understanding of the spatial deformations of the mountain and provide another level of redundancy for the deformation sensors on the mountain.

6 MONITORING AND RESPONSE PLAN DEVELOPMENT

Based on the nature of failures in rock slopes the most effective method of managing the risks associated with a rock slope movement is the development of an effective warning system. As indicated by Crosta & Agliardi (2003) "remedial countermeasures are not often useful when coping with a large rockslide because of the extremely high kinetic energy potentially involved in the phenomena. In these conditions, suitable emergency planning is the only effective tool to reduce the vulnerability of the potentially involved areas by means of evacuation or road closure." Therefore the challenge is to develop a systematic approach to monitoring and system refinement, along with the development of realistic monitoring thresholds that are not too conservative resulting in excessive false alarms, but provides adequate warning should an event occur.

The overall approach to the monitoring and response program for the South Peak of Turtle Mountain is comprised of four overall components:

1 *Monitoring procedure*: This is the structure under which regular data review and acknowledgement is undertaken. This specifies who undertakes the

monitoring at what frequency and under what circumstances these frequencies are altered in response to ongoing data trends or anomalies. For the TMMP, the ongoing management of the data is to be undertaken by personnel from the Government of Alberta (GOA) with specialist input to review data trends, refine instrumentation thresholds and to determine when various alert levels are to be triggered. An essential component of this system will be the specialist review, especially within the first few years of system operation in order to utilize experience and judgment with similar systems to identify data trends and realistically refine instrument specific thresholds.

2 *Threshold development/evolution*: This component includes the establishment of thresholds against which the results obtained from the sensors are evaluated. Both absolute exceedence values and velocity-based values will be used. Guidance is also provided for the continued revision of these thresholds over time as more data are obtained and data trends are better understood. As the instrumentation has only been recently installed and there is only minimal baseline information (in some cases the sensors are still not operational), the challenge is to develop initial trigger alarm levels that are neither too conservative, leading to numerous false alarms, nor fail to catch real events and provide adequate warning. Based on the initial sensor data, specific absolute and velocity-based triggers were developed. In the initial stages, these levels have been based largely on two standard deviations above the background sensor noise with velocity thresholds that are set at a low enough level that at least one of each type of sensor could trigger annually during the system training stage. At this time no attempt has been made to undertake analysis to determine velocity thresholds due to the complex nature of the rock mass and the influence of seasonal fluctuations on the readings. As outlined by Crosta & Agliardi (2003) during the development of alert velocity thresholds for the Ruinon rock slide, the development of a model to predict failure breaks down when external conditions that are not time invariant and deviations induced by seasonal variations and temperature and rainfall regime take place. Further, Crosta & Agliardi (2003) indicate that the prediction provided by threshold values should be supported by expert judgment able to take into account factors such as the reliability of the monitoring network, the complexity of the displacement patterns, and the short-time evolution of meteorological and loading conditions.

3 *Alert levels and notification protocols*: These provide standardized terminology and appropriate responses to trends in the data deemed by a specialist

Table 2. Alert level framework for South Peak.

Condition	Activity level	Instrumentation behaviour	response
Green – No Immediate Risk	Background noise or seasonal fluctuations	No change in monitoring data from background levels, no concern	Normal operation plus information calls to GOA and local authorities for weak through strong unrest as appropriate
	Ongoing trends independent of seasonal effects	No significant change noted in data trends, no immediate concern	Continue monitoring
	Alarm Triggers on one sensor	Change noted in data, no immediate need for concern.	Continue monitoring/field check instrument. Further evaluate as to whether a Yellow condition is appropriate.
Yellow – Watch	Multiple sensors develop movements that are non seasonal but low level compared to threshold levels.	Some movement potential, some potential concern	Increase frequency of data review and/or data acquisition. Heads up notification to GOA and municipal officials
Orange – Warning	Multiple sensors exhibit acceleration of data trends exceeding threshold values (non-seasonal)	Accelerated movements, elevated concern	Increase data review frequency, site visit to check conditions, communicate findings with key decision makers
Red – Event in Progress	High or catastrophic acceleration on several. Initiation of full scale movement	Acceleration of movements and visual observations of movement	Evaluate. Trigger Emergency Response Plan, including evacuations and mobilization of emergency services

as constituting a raised level of alert with respect to a potential rock slope movement. For South Peak, the alert framework provided in Table 2 has been proposed in order to couple the instrumentation readings on the displacement based sensors and threshold exceedence with appropriate levels of action.

4 *Emergency response*: This task is to provide guidance and suggested alterations to the existing Emergency Response Plan based on the latest data. For the TMMP, the existing Emergency Response Plan for the Municipality of Crowsnest Pass was reviewed and recommendations for revisions that incorporate the warning framework developed were provided. This refinement was developed in conjunction with Emergency Management Alberta and the municipality. Covered under this portion of the study was the development of call-out lists and procedures including the use of email and telephone for various levels of alerts.

7 CONCLUSIONS

The Turtle Mountain Monitoring Project (TMMP) was undertaken over a period of twenty months

between summer 2003 and winter 2005. The purpose of the TMMP was to establish a series of sensors on the South Peak of Turtle Mountain in order to provide an enhanced understanding of the kinematics of a movement of South Peak and to provide a system to provide warning of the development of a catastrophic failure. The sensor layout was designed such that there was adequate surface coverage of the peak and sufficient redundancy of the layout in order to provide a higher level of confidence in interpreting the kinematics of movement and the impending failure of the peak than would be available from single sensor readings. For the sensors, specific absolute and velocity based triggers were set with the intention of continuously refining these triggers based on ongoing data review.

(Andrew Bidwell, Joyce Chen), Danaus Corporation (Dan Kenway, Douglas Bingham), Gennix Corporation (Henry Bland, Rob Stewart), Monica Field, David McIntyre, Greg Carter, Dave Redman, Weir Jones Engineering (Iain Weir-Jones, Joe Seraphim), Advanced Geotechnology (Pat McLellan, Ulrich Zimmer), University of Calgary (Deb Spratt, Malcolm Lamb), Alberta Geological Survey (Dinu Panu), University of Alberta (Derek Martin, Emily Herd).

REFERENCES

Allan, J.A. 1933. Third Report on the Stability of Turtle Mountain for Department of Public Works, Government of Alberta, Edmonton, Alberta. Department of Geology, University of Alberta. 28 pp.

AMEC Earth & Environmental 1998. Assessment of hazards and land-use related to the Frank Slide and Turtle Mountain. Report to Alberta Environmental Protection, Agreement Number 98-0317.

AMEC Earth & Environmental 2005a. Turtle Mountain Monitoring Project, Summary Report – WP11.03 and 12.03, Subsurface Geotechnical and Microseismic Monitoring System. Report to Alberta Municipal Affairs, February 2005.

AMEC Earth & Environmental 2005b. Turtle Mountain Monitoring Project, Summary Report – WP 7b/7c, Data Presentation Summary Report, South Peak, Turtle Mountain. Report for Alberta Municipal Affairs.

Atlantis Scientific Inc (ASI) 2005. Frank Slide, Alberta InSAR Monitoring: Set-up and Demonstration for 2004. Report for AMEC Earth & Environmental, February 11, 2005.

BGC Engineering Inc. 2000. Geotechnical hazard assessment of the south flank of Frank Slide, Hillcrest, Alberta. Report to Alberta Environment, No. 00–0153.

Bidwell, A.K., Froese, C.R., Anderson, W.S. & Cavers, D.S. 2005. Geotechnical drilling at the South Peak of Turtle Mountain. Proceedings of the 58th Canadian Geotechnical Conference. Saskatoon, Saskatchewan. (in press).

Crosta, G.C. & Agliardi, F. 2003. Failure forecast for large rock slides by surface displacement measurements. *Canadian Geotechnical Journal* 40:176–191.

Cruden, D.M. & J. Krahn. 1973. A re-examination of the geology of the Frank Slide. *Canadian Geotechnical Journal* 10:581–91.

Fossey, K.W. 1986. Structural geology and slope stability of the southeast slopes of Turtle Mountain. Master of Science Thesis, Department of Geology, University of Alberta.

Froese, C.R., Kosar, K. & van der Kooij, M. 2004. Advances in the Application of InSAR to Complex, Slowly Moving Landslides in Dry and Vegetated Terrain. Invited Lecture. Proceedings of the 9th International Symposium on Landslides. Rio de Janeiro, Brasil: 1255–1264. Rotterdam: Balkema.

Murray, C. 2005. Historical Summary: Crack Monitoring Data for Turtle Mountain, Crowsnest Pass, Alberta. Master of Engineering Report. Department of Civil Engineering. University of Alberta.

Norris, D.K. 1955. Blairmore, Alberta. Geological Survey of Canada, Paper 55–18.

Read, R.S. 2003. A framework for monitoring the South Peak of Turtle Mountain – the aftermath of the Frank Slide. Proceedings, 3rd Canadian Conference on Geotechnique and Natural Hazards, pp. 261–268.

Theune, U., deGroot, M., Rokosh, C.D., Sacchi, M.D., Schmitt, D.R., Welz, M. & Holzhauer 2005. Looking inside Turtle Mountain: Mapping fractures with GPR. University of Alberta, Department of Physics.

Frank Slide a century later: the Turtle Mountain monitoring project

R.S. Read
RSRead Consulting Inc, Okotoks, Alberta, Canada

W. Langenberg
Alberta Geological Survey, Edmonton, Alberta, Canada

D.M. Cruden
Dept. of Civil & Environmental Engineering, University of Alberta, Edmonton, Alberta, Canada

M. Field, R. Stewart, H. Bland, Z. Chen, C.R. Froese, D.S. Cavers, A.K. Bidwell, C. Murray,
W.S. Anderson, A. Jones, J. Chen, D. McIntyre, D. Kenway, D.K. Bingham, I. Weir-Jones,
J. Seraphim, J. Freeman, D. Spratt, M. Lamb, E. Herd, D. Martin, P. McLellan & D. Pana
Turtle Mountain Monitoring Project Participants, Edmonton/Calgary/Burnaby/Crowsnest Pass, Canada

ABSTRACT: Turtle Mountain in southwest Alberta, Canada – the site of the 1903 Frank Slide – has been the focus of many studies over the past century. Geotechnical investigations have concluded that there is potential for a subsequent rock avalanche from the South Peak of Turtle Mountain. To reduce the risk associated with a second rock avalanche, the Government of Alberta initiated a two-year multi-disciplinary monitoring project in 2003. The Turtle Mountain Monitoring Project involves implementation of a predictive monitoring system comprising a variety of geotechnical, geophysical, hydrological and other instruments operating in near real-time. The system incorporates an integrated data management strategy linked to emergency response protocol. Site-specific alarm and warning criteria being developed on the basis of monitoring data from Turtle Mountain are the subject of a companion paper. The project represents a state-of-the-art application of geotechnical monitoring technology in an area of significant historical interest from a landslide perspective. Long-term monitoring is planned following completion of the current project.

1 INTRODUCTION

1.1 *Background*

The Frank Slide occurred at 4:10 AM on April 29, 1903 in what is now southwest Alberta. The slide lasted 90 seconds, and involved some 30 million cubic metres of limestone from the east face of Turtle Mountain. It covered an area of 3 km^2 with an average depth of 14 m of rock debris, burying the south end of the town of Frank, the main road, and the CPR mainline, and damming the Crowsnest River (Stewart 1903). The slide killed about 70 people.

The 1903 Slide left two prominent peaks on Turtle Mountain (Fig. 1). South Peak comprises Paleozoic limestone, and rises about 1000 m above the valley floor to an elevation of 2200 m. Studies of South Peak conducted since the 1903 Slide have identified a rock volume of about 5 million cubic metres that could be the source of a future rock avalanche from Turtle Mountain.

The area of attendant risk (Fig. 2) is bounded by the 1903 Slide runout area, Bellevue to the east, and the Hillcrest cemetery to the south. This area currently contains residences, transportation corridors, recreational facilities, commercial buildings, historic sites, agricultural activities, and utilities. There are currently no land use restrictions outside the 1903 Slide runout area to prevent further development in this area (BGC 2000).

To reduce the risk associated with a second rock avalanche, a two-year multi-disciplinary monitoring project was announced by the Government of Alberta on April 29, 2003 – the 100th anniversary of the Frank Slide. The Turtle Mountain Monitoring Project involves implementation of a predictive monitoring system comprising microseismic, displacement, pore pressure, temperature, and other monitoring instruments operating in near real-time. The system incorporates an integrated data management strategy, including operational
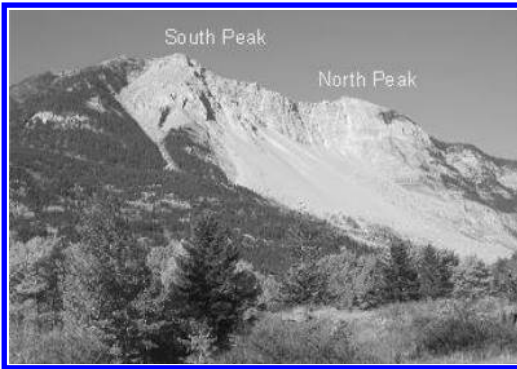
Figure 1. East face of Turtle Mountain showing the 1903 Frank Slide and the prominent North and South Peaks.
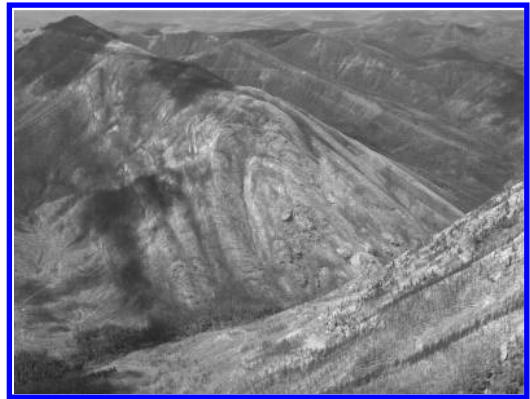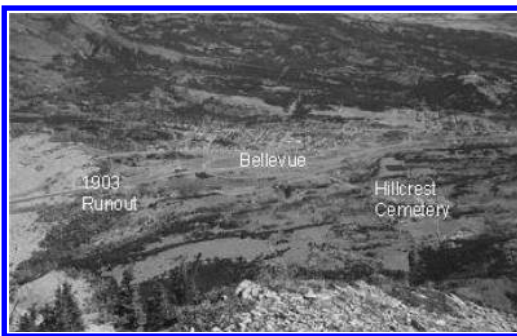

Figure 2. View looking east from South Peak of the potential runout area associated with a rock avalanche from South Peak.

procedures and planning guidelines linked to emergency response protocol. Site-specific alarm and warning criteria are being developed on the basis of background and baseline monitoring data from Turtle Mountain, and are the subject of a companion paper (Froese et al. 2005). The project represents a state-of-the-art application of geotechnical monitoring technology in an area of significant historical interest from a landslide perspective.

This paper presents an overview of the Turtle Mountain Monitoring Project in the context of prior monitoring efforts, geotechnical investigations, and recent field studies. Instrumentation installed for the project, and plans for ongoing operation of the monitoring system, are also described.

2 GEOTECHNICAL CONSIDERATIONS

2.1 Factors contributing to the Frank Slide

The factors contributing to the 1903 Frank Slide have been identified as the geological structure of Turtle

Figure 3. Turtle Mountain anticline exposed in Hillcrest Mountain looking south across Drum Creek.

Mountain, deformation due to coal mining at the toe of the mountain, above-average precipitation in the months prior to the slide, water and ice accumulation in cracks at the top of the mountain, remote natural and blast-induced seismicity, thermal variations and freeze-thaw cycles, and karst development.

The geological structure of the mountain, dominated by the Turtle Mountain anticline (Fig. 3) and several thrust faults, is considered the prime contributing factor (Cruden & Krahn 1973). However, mining-related deformation at the toe of the slide, in combination with water and ice accumulation in cracks, is considered a key trigger of the 1903 Slide. The relative importance of these contributing factors continues to be a source of debate amongst experts, and is one of the aspects being studied as part of the Turtle Mountain Monitoring Project.

2.2 Geotechnical studies of South Peak

The 1903 Slide created a network of deep subvertical tension cracks (fissures) at the crest of Turtle Mountain around South Peak (Fig. 4), extending to within a few metres of North Peak. Monitoring of these fissures commenced shortly after the 1903 Slide as a means of identifying the onset of a subsequent rock avalanche.

Between 1931 and 1933, three investigations of the stability of South Peak were conducted, including detailed mapping of the fissure network at the top of Turtle Mountain (Allan 1931, 1932, and 1933). Allan (1931) defined a large and a small "danger zone" associated with runout of a rock avalanche of 5 million cubic metres from South Peak. Based on these studies, the Provincial Government issued a Notice of Danger in February 1933 to residents in the small "danger zone" advising them of the potential risk associated with South Peak. Relocation of residents to neighbouring communities started in 1934.
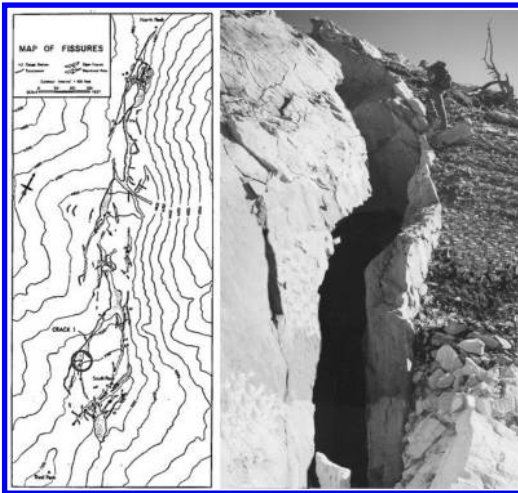
714

Figure 4. Junction of crack 1 and a major splay on the west side of South Peak (right), and its approximate location shown by the circle on a reduced copy of Allan's fissure map (left).
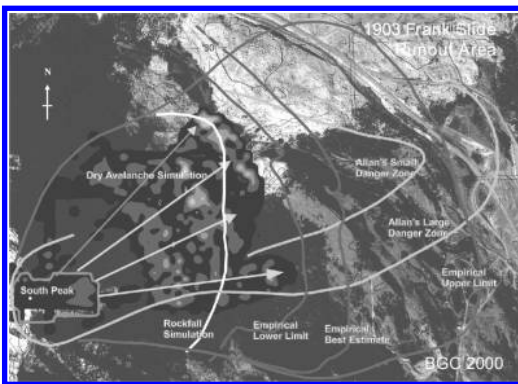

Figure 5. Summary of results from rockfall and rock avalanche analyses performed by BGC Engineering (2000) and earlier estimates by Allan (1931). The empirical upper limit represents the probable maximum hazard zone. [see Colour Plate XV]

Subsequent studies of the geotechnical hazard posed by South Peak were conducted by Agra Earth and Environmental (1998) and BGC Engineering (2000). The annual probability of occurrence of a rock avalanche from Turtle Mountain was estimated to be between 10^{-2} and 10^{-4} depending on the assumed contribution of coal-mining to the 1903 Frank Slide. With a population base between 1 and 100 people in the possible runout area, reduction of risk associated with a second rock avalanche from Turtle Mountain was considered warranted.

The 2000 study produced an updated estimate of the potential runout area associated with a rock avalanche from South Peak, and possible means of reducing the attendant risk. As shown in Figure 5, Allan's estimates of "danger zones" are generally consistent in distal extent with these recent estimates, but not in shape or lateral extent (Read et al. 2000).

Options identified to reduce risk within the probable maximum hazard zone associated with a rock avalanche from South Peak include consultation with those potentially affected by the hazard, restrictions on land use and development within the hazard zone, and installation of a predictive monitoring system. Mitigative measures such as engineered barriers, controlled blasting, or rock mass stabilization were not considered feasible given the large volume of the potential sliding mass (BGC 2000).

3 MONITORING

3.1 *Framework for monitoring*

Based on the recommendations of the geotechnical hazard assessment of South Peak (BGC 2000, Read et al. 2000), RSRead Consulting Inc. (RSRCI) was retained by Alberta Municipal Affairs in 2002 to develop a framework for monitoring the South Peak of Turtle Mountain. This planning framework was intended to provide a blueprint for possible future actions aimed at reducing the risk associated with a rock avalanche from South Peak.

The 2002 study included a review of options for landslide monitoring, a summary of historical monitoring of South Peak, a proposed predictive monitoring system for Turtle Mountain, and an overview of the associated operational logistics, implementation strategy, schedule, and costs. Read (2003) provides an overview of the monitoring framework report.

3.2 *Historical monitoring of South Peak*

Intermittent monitoring of Turtle Mountain has been conducted since 1903. Shortly after the Frank Slide occurred, reference mounds were installed to monitor changes in aperture of the major fissures at the top of the mountain (Dowlen 1903). Daly et al. (1912) recommended that monuments be established for future monitoring of fissures.

As part of Allan's studies, 18 manual gauging stations were established across major fissures in 1933. By 1994, eight of these stations had been destroyed by local rockfalls (Cruden 1986). Readings taken at six of these gauging stations in 1999 showed a maximum of 4 cm change from Allan's original measurements. The nature of movement associated with this aperture change (episodic versus gradual) is unknown.

Starting in 1980, several monitoring systems were deployed on Turtle Mountain. Two TM 71 crack motion

715

detection (Moiré) gauges were installed in the major fissure (Crack 1) between South and Third Peaks (Kostak & Cruden 1990). Between 1980 and 1988, total movement of about 3 mm was detected by these instruments. Tape extensometer measurements across Crack 1 were also taken at nine different locations (Cruden 1986).

In 1981, Alberta Environment installed a seismic monitoring array on the east flank of Turtle Mountain. The array comprised six seismometers in two linked triangular sub-arrays (Bingham 1996). The system used low power radio telemetry to transmit data to an acquisition system at the Frank Slide Interpretive Centre (FSIC).

The seismic monitoring system recorded nearly 350 local events between 1983 and 1992 from different sources including local earth tremor events, rockfall events, blast events, teleseisms, sonic events, noise, and other unidentified sources. Source locations of these events were typically uncertain. It was concluded that induced seismicity is ongoing in Turtle Mountain, pri-

marily west of the abandoned Frank Mine up to 1 km below surface (Bingham 1996). This seismicity is believed to be related primarily to deformation and stress relief within Turtle Mountain, and to ongoing collapse of the mine workings at the base of the mountain.

Recent work by Chen et al. (2005) reinterpreted these results, and shows correlation between event location swarms and some geological structures within Turtle Mountain (Fig. 6).

Subsequent monitoring of Turtle Mountain included displacement measurements using high-precision photogrammetry (Fraser & Gruendig 1985, Chapman 1986), electronic distance measurement (EDM) surveys (Anderson & Stoliker 1983), and strain gauges (Peterson & Cruden 1986). Meteorological observations were also recorded at a solar-powered weather station on the mountain. Regular monitoring of Turtle Mountain was discontinued by the early to mid-1990's. Historical instruments and monitoring stations were located and inspected in 1999 as part of a field investigation (BGC 2000). It was found that many of the instruments had been vandalized or destroyed (Fig. 7).

In addition to quantitative measurements, observations, and anecdotal evidence (Allan 1933, Kerr 1990, Cruden 1986, Bingham 1996) indicate that rockfalls have been ongoing from the steep scarp left by the 1903 Slide, and from the northeast side of South Peak. Of those rockfalls observed, debris has in some cases reached, but not crossed, the Crowsnest River at the foot of the mountain (consistent with predictions from geomechanical analyses). A rockfall of about 15,000 tonnes from the vicinity of North Peak occurred on June 3, 2001. Active collapse of mine workings at the base of the mountain was also observed in 2001 (M. Field, Alberta Community Development, pers. com.).

These observations and measurements confirm that ongoing deformation and microseismic activity
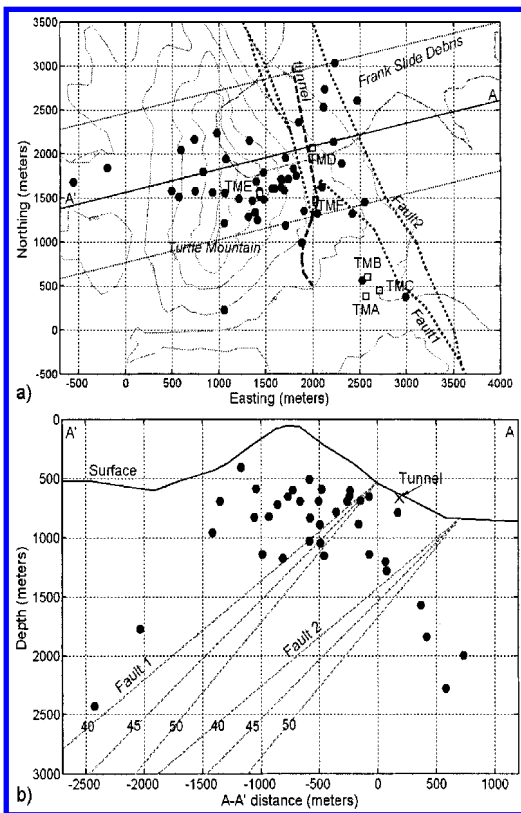

Figure 6. Microseismic results in (a) plan and (b) cross section through Turtle Mountain showing hypocentres of well-resolved events (Chen et al. 2005).

Figure 7. Defaced photogrammetry target (left) and vandalized Moiré crack gauges (right) observed in 1999.

716

are occurring at various locations on and within Turtle Mountain.

3.3 *Predictive monitoring of South Peak*

Past monitoring of Turtle Mountain has been sporadic and relatively short-lived, generally involving manual readings and intermittent analysis. There has been limited coordination of past research projects, and no commitment to ongoing funding for long-term monitoring. The result has been inconclusive information on the background levels of deformation and microseismic activity expected as a result of normal climatic variation versus significant changes associated with the geological and man-made structures (i.e., mine openings) within Turtle Mountain.

The implementation of a predictive monitoring system followed by committed long-term monitoring is expected to provide the data required to identify trends in deformation and microseismic activity associated with degrading stability conditions on Turtle Mountain.

The four objectives of a predictive monitoring system on Turtle Mountain are to advance or improve public safety, public education, scientific research, and tourism/economy in the Crowsnest Pass. Such a system is envisioned as an integrated collection of different types of instruments communicating in near real-time to a data acquisition/processing control centre at FSIC, and other designated sites. Public safety is the primary concern; educational, research, and tourism/economic aspects are lower in order of priority.

3.4 *Critical monitoring parameters*

In developing a predictive monitoring system for Turtle Mountain, monitoring systems and approaches used by BC Hydro at hydroelectric sites in British Columbia (Moore et al. 1991), experimental monitoring systems used to monitor brittle rock failure in Switzerland (Willenberg et al. 2002), and other types of systems were reviewed. Based on this review and observations from the 1903 Frank Slide, the critical monitoring parameters associated with Turtle Mountain were identified as:

- Shear deformation along joints and flexural slip surfaces,
- Extensional deformation across subvertical tension cracks and joints near South Peak,
- Deformation and induced seismicity due to mine collapse at the toe of the potential sliding mass,
- Seismicity induced by progressive development of a basal sliding surface,
- Natural seismicity that might act as a triggering mechanism for a rock avalanche,
- Pore pressure at the basal sliding surface and at various depths in the rock mass,

- Temperature at various depths in the rock mass,
- Precipitation at the top of Turtle Mountain,
- Surface temperature and other climatic data; and
- Outflow at springs connected to the fracture network on South Peak.

As in the case of the Wahleach power tunnel (Baker 1991), it is entirely possible that a continuous basal sliding plane does not currently exist beneath South Peak, but may develop progressively with time. As such, microseismic monitoring in combination with deformation monitoring is considered an important diagnostic component of the monitoring system. Additional system components to measure climatic data and outflow are also needed to help diagnose causative mechanisms associated with observed data trends (e.g., freeze-thaw effects, pore pressure increase due to ice-damming of fissures, and temperature variations).

4 THE TURTLE MOUNTAIN MONITORING PROJECT

4.1 *Project synopsis*

On April 29, 2003, during the ceremony commemorating the 100th anniversary of the Frank Slide, the Government of Alberta announced that it would commit $1.1 million to implement a state-of-the-art monitoring system on Turtle Mountain. The Turtle Mountain Monitoring Project was established as a collaborative effort between the Government of Alberta, contractors, Universities, stakeholders and interested third parties. Ongoing communication with stakeholders and the public was considered an integral part of the project.

Three Alberta government departments were involved in the project. Emergency Management Alberta, through Alberta Municipal Affairs, was responsible for initiating and administering the project. Alberta Geological Survey, through the Alberta Energy and Utilities Board and in conjunction with selected contractors, was tasked with providing necessary technical expertise to implement the monitoring system. Alberta Community Development agreed to house part of the system at FSIC.

The monitoring framework developed for Turtle Mountain (Read 2002) was used as the basic blueprint for the project. The project timeline was compressed from the proposed 3 years to about 20 months as a result of necessary project start-up activities and a major forest fire in Crowsnest Pass in summer 2003.

Development of the monitoring system was originally planned around the idea of three consecutive implementation phases, using information from earlier phases to help refine plans for the later phases. The first phase involved replacing the existing seismic stations and weather station on Turtle Mountain,

717

and establishing a control centre at FSIC. The second phase involved deploying electronic or laser-based distance measurement systems, differential GPS-based instruments, and a series of crack gauge monitors to assess surficial deformation and aperture changes in the major fissures around South Peak. The third phase involved deploying borehole-based instruments to measure displacement, pore pressure, temperature, and microseismicity. Outflow monitoring at springs near the toe of the mountain was also planned as part of the third phase.

Several supporting investigative studies and repeated surveys were planned to provide new site-specific characterization data, compile historical monitoring data and information on mining development, assess the influence of mine collapse on the stability of South Peak, and assess gross deformation patterns using radar-based satellite imagery.

The three implementation phases were scheduled for completion between April 1, 2003 and March 31, 2005. The compressed timeline associated with the project required reorganization of field activities and overlap of the three implementation phases. Eighteen distinct work packages involving eleven contractor/subcontractor companies, two Universities, and several Government agencies, were defined to complete the project over the approved time frame.

The Turtle Mountain Monitoring Project is expected to be followed by ongoing long-term monitoring in order to define baseline deformation and microseismic characteristics of the site, and developing trends that might indicate degrading stability conditions.

4.2 *Microseismic monitoring systems*

Two complementary microseismic systems were installed as part of the Turtle Mountain Monitoring Project: a surface-based system and a borehole-based system. These systems both communicate with the control centre at FSIC via two-way radio telemetry operating at 2.4 GHz.

The surface microseismic system was designed and deployed by Gennix Technology Corp. of Calgary, Alberta between October 2003 and March 2004. Six motion sensing stations (Fig. 8) were installed at various locations on Turtle Mountain. Three 28 Hz triaxial geophones connected in series were cemented into outcrops at each of the stations. Station locations were selected on the basis of array design analysis and consideration of sunlight available to provide solar power.

There are a number of components associated with each surface seismic station, including a microprocessor, power control unit, A/D converters, a GPS antenna and receiver, a radio transceiver and a telemetry antenna. Each station is powered by four 12 V deep-cycle batteries, charged by a 100 W solar panel. One station near the old Frank Mine entrance (River

Figure 8. Typical surface seismic station installed on South Peak of Turtle Mountain.

Station) is also powered by a wind turbine as this location is the most shaded of all of the stations.

In addition to the three channels of input from the geophone, the microprocessor receives timing and positional data from a GPS receiver whose antenna is mounted on the solar-panel mast. Seismic and GPS data are wirelessly transmitted to the control centre at FSIC.

The FSIC control centre has four separate installations: 1) the roof-mounted antenna assembly to receive digital data from the mountain stations, 2) an administration and analysis workstation, 3) an equipment rack housing the central network switch, and three computers (one for data acquisition, one for web serving, and one for SQL and file storage), and 4) a computer-based display centre on the FSIC exhibition floor.

The data received at FSIC are transferred via cable to the equipment rack network hub. Data from all sensors are processed in near-real-time on the acquisition computer and then inserted into an SQL database on a database server system.

In addition to the surface seismic system, two 28 Hz triaxial geophones supplied by Weir Jones Engineering Corp. of Vancouver, BC were installed by AMEC Earth and Environmental in an air rotary drillhole completed to a depth of 62.5 m on South Peak. The borehole was drilled using a helicopter portable drill rig (Fig. 9) operated by Bertram Drilling Limited of Carbon, Alberta.

The subsurface geophones were positioned at 23.9 and 38.2 m depth. The lower geophone was grouted in place by first setting an inflatable borehole packer to isolate the upper portion of the borehole from large cavities visible by televiewer. Geophone signal cables were routed through watertight conduit to data

Figure 9. Air rotary drill used on South Peak during installation of subsurface geophones.

acquisition equipment in an instrument enclosure near the South Peak borehole.

The acquisition board and GPS module for the subsurface seismic system digitize seismic sensor and GPS data, and send data via ethernet cable to a network hub at the South Peak surface seismic station. Data are merged with the surface seismic data and sent to FSIC using the existing telemetry equipment at South Peak.

At the FSIC control centre, the data acquisition computer receives via wireless ethernet the telemetered data transmitted from the South Peak acquisition system, merges the data from the surface and subsurface seismic systems, and runs event detection, source location and visualization software to analyze seismic events. These data are stored as event files, and interpreted data associated with each event are stored in the SQL database.

4.3 *Deformation monitoring systems*

Several deformation monitoring systems were designed and deployed as part of the Turtle Mountain Monitoring Project to provide redundant measurements of rock mass movement.

A series of 20 vibrating wire crackmeters (Fig. 10) were installed by Danaus Corp. of Edmonton, Alberta between October 2003 and November 2004. These instruments were located in eight clusters across major fissures on the west side of Turtle Mountain downslope of South Peak. Five of these clusters had crackmeters installed in triplets to determine a true movement vector.

Of the installed crackmeters, five were donated to the project by Dr. Neal Iverson of Iowa State University following completion of a precursor research project. A lightning strike in July 2004 destroyed six of the installed instruments, necessitating replacement of these crackmeters and installation of lightning protection. Data from all crackmeters are captured by a Campbell Scientific CR-10X datalogger installed on South Peak, and transmitted via 900 kHz radio telemetry

Figure 10. Vibrating wire crackmeters installed across a major fissure. The metal snow roof is to protect the instruments.

to the Provincial Building in Blairmore, then relayed via a 5 GHz radio link to FSIC for storage in the SQL database.

Although protective metal snow roofs were installed at each crackmeter cluster to shed snow, several instruments were affected by drifting snow and ice build-up in late 2004. Further protective measures are planned next field season.

To supplement the information from crackmeters, a robotic optical survey system was deployed by Danaus Corp. in 2004. A computer-automated Trimble theodolite was mounted in a protected area at FSIC, and ten prisms (Fig. 11) were mounted at strategic points on South Peak and Third Peak. Readings of the position of each prism are taken hourly, and relative changes in position between each prism on South Peak and that on Third Peak (considered a stable benchmark) are calculated. These data are stored in the SQL database

In addition to these prism installations, six GPS stations were erected by Danaus Corp. in the vicinity of South Peak in summer 2004. Each station comprises a reinforced concrete pillar mounted with a dual metal plate assembly and a fixed GPS antenna (Fig. 11).

The GPS antenna receives satellite-based time and positional data, which is stored and transmitted via telemetry to FSIC or, for those stations on the west side of Turtle Mountain, via a 900 kHz radio link to the Provincial Building in Blairmore, then via a 5 GHz radio link to FSIC. Data are stored in the SQL database, and compared to measurements taken at a fixed FSIC base station to calculate movement.

As part of one of the major work packages for the Turtle Mountain Monitoring Project, AMEC Earth

719

Figure 11. Combination theodolite prism and GPS antenna mounted on a concrete pillar near South Peak.

and Environmental (in cooperation with Durham Geo Slope Indicator) installed 10 surface-mounted tiltmeters in the vicinity of South Peak in October 2004 to detect angular deformations.

Each tiltmeter is designed to measure tilt in a vertical plane, therefore the installation surfaces were selected to be as close to vertical as possible, striking in the same direction as the possible tilt direction. The signal cable for each tiltmeter was conveyed via protective conduit to a Campbell Scientific CR-10X data logger in an instrument enclosure near the borehole collar. Data were transmitted via telemetry to the Provincial Building in Blairmore, and then relayed to FSIC. Measurements of angular deformation are stored in the SQL database at the FSIC control centre.

AMEC Earth and Environmental was also responsible for the installation of four surface-mounted extensometers in October 2004. The cable associated with these instruments (Fig. 12) is anchored to bedrock at one end, then pinned to the ground surface. A suspended weight at the fixed up-slope end of the assembly provides a constant load to the metal cable, which is housed inside a protective plastic sheath. Rock mass deformation results in a change in position of the suspended weight, which is recorded as movement. These instruments are expected to be sensitive down to 1 or 2 mm.

Extensometer locations were selected such that the head assembly (upslope end) and anchor (downslope end) were installed in exposed bedrock, with the extensometer cable roughly parallel to the possible direction of movement. The signal cable from the head assembly of each extensometer was run through protective conduit to the Campbell Scientific CR-10X data logger at the enclosure near the South Peak borehole. Displacement data from these instruments is transmitted to the control centre at FSIC via the Provincial Building in Blairmore.

To complement these other deformation systems, a TDR cable installation was originally planned for the South Peak borehole to determine the depth of a

Figure 12. Typical surface extensometer head assembly with housing removed to show suspended weight.

possible basal sliding plane. The hole did not reach its target depth of 120 m due to fractured rock conditions, so the TDR cable installation was aborted.

4.4 Climatic monitoring systems

The original weather station installed on South Peak in the 1980s was refurbished by Danaus Corp. in December 2003. The weather station (Fig. 13) monitors barometric pressure, air temperature, relative humidity, wind speed, wind direction, solar radiation, precipitation, and rock temperature near the station. Additional temperature data are measured by each of the vibrating wire crackmeters. These data are collected on a Campbell Scientific CR-10X data logger near the weather station and transmitted to the FSIC control centre by radio telemetry via Blairmore.

To complement the weather station data with subsurface information, a 14.3 m long thermistor string with seven temperature measurement points was installed in the borehole drilled on South Peak. These instruments are expected to provide information on the depth of influence of freeze-thaw cycles, and correlations between melting and rock mass movement.

4.5 Hydrological monitoring system

Hydrological monitoring for the Turtle Mountain Monitoring Project is focused on pore pressures at depth in the rock mass, and outflow from a spring at the entrance to the old Frank Mine.

A single vibrating wire piezometer was installed at 21.1 m depth in the South Peak borehole by AMEC

720

Figure 13. Refurbished weather station on the west side of South Peak.

Figure 14. Outflow weir installed at the Frank Mine entrance.

Earth and Environmental. Two other piezometers of this type were deployed in one of the major fissures as part of the precursor Iowa State University research project. These three instruments provide pore pressure data that are collected by Campbell Scientific data loggers on South Peak, and transmitted to FSIC by radio telemetry via Blairmore.

The entrance to the old Frank Mine was identified as the location of a spring. As the mine workings are connected to the fracture network on Turtle Mountain, monitoring of outflow from this spring provides insight on the connection between precipitation events on the mountain and outflow. Variations in outflow response times during the year may indicate changes in the fracture network, possibly associated with freezing and ice-damming of cracks.

Matrix Solutions of Calgary, Alberta fabricated and installed a metal weir across the outflow path from the mine entrance (Fig. 14). A Keller pressure transducer installed inside a piece of screened PVC pipe bored into the streambed provides a continuous measure of water level. Data from the outflow monitoring system are collected on a Campbell Scientific CR510-55 datalogger connected to the telemetry system at the nearby surface seismic station (River Station). Data are transferred by radio telemetry to FSIC and stored in the SQL database.

4.6 *Other monitoring systems and related studies*

In addition to these continuous monitoring methods, satellite radar interferometry (InSAR) is being investigated by Atlantis Scientific as a complementary tool to identify deformation over the area encompassed by the new digital elevation model of Turtle Mountain. Repeated photogrammetric surveys of existing repainted targets were deferred due to budget limitations. However, this technique could be used to provide additional periodic assessments of surface deformation in the study area.

Supporting studies conducted under the Turtle Mountain Monitoring Project include surface and subsurface characterization of structural geology and fracture patterns on Turtle Mountain from surface mapping and televiewer logging of the South Peak borehole (Alberta Geological Survey and University of Calgary), compilation of mine opening information into a GIS-based system for visualization and analysis of the effects of mine opening collapse on stability of South Peak (University of Alberta), compilation of historical monitoring data (University of Alberta), and evaluation of ground-penetrating radar as a means of characterizing subsurface fractures on Turtle Mountain (University of Alberta).

5 OPERATIONAL LOGISTICS

5.1 *Data management*

A well-defined data management strategy is critical to ensure long-term data integrity. The database is accessible through a three-tier web-based interface designed for expert users, technical users, and the general public. The database can only be changed using the expert access protocol. Visualization of recent data can be accomplished using the other two access

721

protocols. Ongoing regular review of the data by qualified individuals is required to identify developing trends and anomalous data. Alarm and warning conditions require immediate review of data and subsequent action defined by emergency response protocol.

5.2 *Quality assurance*

During the initial commissioning of the monitoring system, standard operating procedures will be in place and followed for future component installation, wiring, calibration, diagnostic checks, and maintenance. Quality assurance procedures for regularly checking the overall functionality of the system, including sensor operation and alarms, are also necessary. These procedures include both automatic system diagnostic checks of each station, and regular manual inspection to check for damage.

5.3 *Alarm and warning criteria*

Predictive monitoring systems require data analysis and logic that determine when a warning should be given. According to Bell (2001), emergency warning should never be based on the results of only one sensor reading. Typically, warning logic is based on majority vote, and allows for sensor and transmitter failures in alarm determination. Alarm thresholds can be programmed to consider absolute readings, relative changes in readings, or rate of change in readings. Several alarm thresholds for each sensor can be defined.

Alarm thresholds require site-specific baseline data. A combination of criteria based on total displacement, velocity, and acceleration is possible for the displacement sensors. Likewise, alarm criteria based on pore pressure, precipitation, or other measurements can be established. Alarm thresholds for seismic data can be developed on the basis of event magnitude, event frequency, localization (clustering) of events, or some combination of these parameters. The initial alarm and warning for the Turtle Mountain Project will be based primarily on displacement measurements. Froese et al. (2005) describe the development of alarm thresholds for Turtle Mountain.

5.4 *Emergency response protocol*

Emergency response protocol is a vital link between long-term monitoring of Turtle Mountain and response to a warning of a rock avalanche from South Peak. The relevant legislation related to Emergency preparedness for this project includes the Federal Emergency Preparedness Act (1985), the Alberta Disaster Services Act (1995), and supporting regulations. The Municipality of Crowsnest Pass Peacetime Emergency Operations Plan provides procedures for prompt and coordinated response to peacetime emergencies affecting the municipality. Development of specific emergency plans and planning guidelines based on the monitoring system is part of the project being undertaken by AMEC Earth and Environmental.

6 LONG-TERM MONITORING

Long-term monitoring of Turtle Mountain will require ongoing funding to maintain the monitoring system, to upgrade or replace components, and to conduct ongoing analysis and reporting of the recorded data. The long-term monitoring plan involves regular site visits to manually inspect instruments and stations, and to visually check geotechnical conditions on Turtle Mountain.

Readings from all sensors are to be checked daily to identify possible system malfunctions or sensors operating out of range. Any observed anomalies are to be reported immediately to qualified personnel to initiate diagnosis and repair of the system. Data are to be analyzed weekly, or more frequently during critical periods, to identify trends that might indicate decreasing stability of South Peak. Data are to be summarized monthly in a short data summary report. An annual report will summarize the key observations and data trends to establish if conditions on Turtle Mountain are deteriorating from year to year.

7 CONCLUSIONS

Recent studies of the South Peak of Turtle Mountain have identified the potential for a large rock avalanche. Based on previous monitoring and recent observations, deformation and induced seismicity are ongoing on and within Turtle Mountain. Past monitoring of the mountain has been sporadic and short-lived. The Turtle Mountain Monitoring Project has implemented a combination of deformation, microseismic, hydrological and climatic monitoring systems suitable for planned long-term monitoring. This project represents an integrated state-of-the-art application of geotechnical monitoring technology in an area of significant historical interest. The multi-disciplinary focus of the project addresses issues of public safety, scientific research, public education, and local tourism/economy.

REFERENCES

Agra Earth & Environmental 1998. Assessment of hazards and land-use related to the Frank Slide and Turtle Mountain. Report to Alberta Environmental Protection, No. 98-0317.

Allan, J.A. 1931. Report on stability of Turtle Mountain, Crowsnest District, Alberta. Dept. of Public Works, Edmonton, Alberta. Alberta Provincial Archives.

Allan, J.A. 1932. Second report on stability of Turtle Mountain, Crowsnest District, Alberta. Dept. of Public Works, Edmonton, Alberta. Alberta Provincial Archives.

Allan, J.A. 1933. Report on stability of Turtle Mountain, Alberta and survey of fissures between North Peak and South Peak. Dept. of Public Works, Edmonton, Alberta. Alberta Provincial Archives.

Anderson, E.G. & Stoliker, P.C. 1983. Remote EDM monitoring of fractures on Turtle Mountain, Phase 1. Research Management Division, Alberta Environment, 24 p.

Baker, D.G. 1991. Wahleach power tunnel monitoring. In Field Measurements in Geotechnics, Balkema: Rotterdam, pp. 467–479.

Bell, W. 2001. Design of a warning and monitoring system. Proceedings of the Annual CDA Conference, Fredericton.

BGC Engineering Inc. 2000. Geotechnical hazard assessment of the south flank of Frank Slide, Hillcrest, Alberta. Report to Alberta Environment, No. 00-0153.

Bingham, D.K. 1996. Seismic monitoring of Turtle Mountain. Unpublished report, Hydrogeology Branch, Alberta Environmental Protection.

Chapman, M.A. 1986. Deformation monitoring of Turtle Mountain by high-precision photogrammetry, epoch 4. Research Management Division, Alberta Environment, 37 p.

Chen, Z., Stewart, R., Bland, H. & Thurston, J. 2005. Microseismic activity and location at Turtle Mountain, Alberta. In Proc. CSEG National Convention, Calgary, Canada.

Cruden, D.M. & Krahn, J. 1973. A re-examination of the geology of the Frank Slide. *Can. Geotech. J.* 10: 581–591.

Cruden, D.M. 1986. Monitoring the South Peak of Turtle Mountain, 1980 to 1985. Research Management Division and Earth Sciences Division, RMD Report 86/37. 70 pp.

Daly, R.A., Miller, W.G. & Rice, G.S. 1912. Report of the commission appointed to investigate Turtle Mountain, Frank, Alberta. Can. Geol. Surv. Mem. 27, 34 pp.

Dowlen, W.E. 1903. The Turtle Mountain rock slide. *Engineering and Mining Journal* 77: 10–12.

Fraser, C.S. & Gruendig, L. 1985. The analysis of photogrammetric deformation measurements on Turtle Mountain. *Photogrammetric Eng. & Remote Sensing* 51(2): 207–216.

Froese, C.R., Murray, C.M., Cavers, D.S., Anderson, W.S., Bidwell, A.K., Read, R.S., Cruden, D.M. & Langenberg, W. 2005. The development of a warning system for the South Peak of Turtle Mountain. Proceedings of the International Conference on Landslide Risk Management, Vancouver, B.C. Canada. Balkema Publishers, Netherlands.

Kerr, J.W. 1990. Frank Slide. Barker Publishing, Calgary.

Kostak, B. & Cruden, D.M. 1990. The Moiré crack gauges on the crown of the Frank Slide. *Can. Geotech. J.* 27: 835–840.

Moore, D.P., Imrie, A.S. & Baker, D.G. 1991. Rockslide risk reduction using monitoring. In Proc., Canadian Dam Safety Conf., Whistler B.C., Canadian Dam Safety Association.

Peterson, A.E. & Cruden, D.M. 1986. Review of strain gauge and other records. Research Management Division, Alberta Environment.

Read, R.S., Savigny, K.W., Oboni, F., Cruden, D.M. & Langenberg, W. 2000. Geotechnical hazard assessment of the south flank of Frank Slide. In Proc. Geo Canada 2000, Calgary, AB.

Read, R.S. 2003. A framework for monitoring the South Peak of Turtle Mountain – the aftermath of the Frank Slide. In Proc. 3rd Canadian Conference on Geotechnique and Natural Hazards, Edmonton, Canada, pp. 261–268.

Stewart, D.A. 1903. A disaster in the Rockies. *The Canadian Magazine* 4: 227–233.

Willenberg, H., Spillmann, T., Eberhardt, E., Evans, K., Loew, S. & Maurer, H.R. 2002. Multi-disciplinary monitoring of progressive failure processes in brittle rock slopes – concepts and system design. In Proc. 1st European Conference on Landslides, Prague, Czech Republic, pp. 477–483.

The significance of climate on deformation in a rock-slope failure – the Åkerneset case study from Norway

G. Grøneng & B. Nilsen
Norwegian University of Science and Technology (NTNU), Dept. of Geology and Mineral Resources Engineering/International Centre for Geohazards (ICG), Trondheim, Norway

L.H. Blikra
Geological Survey of Norway (NGU)/International Centre for Geohazards (ICG), Trondheim, Norway

A. Braathen
University of Bergen (UiB) Centre for Integrated Petroleum Research/International Centre for Geohazards (ICG), Bergen, Norway

ABSTRACT: The significance of climate on the long-term deformation (creep) of large rock-slope failures is widely discussed in the literature. A possible relationship between the data from climate and patterns of deformation has been studied for the Åkernes landslide area. This site is located in the fjord region of western Norway, (Møre and Romsdal County). Estimated area and volume of the landslide is $780\,000\,\text{m}^2$ and 30–45 million m^3, respectively. Should a rockslide of this size occur, it is expected to cause a tsunami that would cause great damage to the small communities along the fjord. This has made it essential to monitor and study the locality. The upper boundary of the unstable area is determined by a distinct, more or less continuous tension fracture that is about 500 m long. This fracture is seen as a back scarp, which has been monitored since 1986. These data show an annual downhill creep in the order of approximately 3–4 cm per year. A continuous surveillance program was started in 1993 with three extensometers. The datasets from the extensometers have been correlated with climate data from a weather station, aiming on the relationship between the pattern of deformation in the moving rock mass and precipitation or periods of extensive snow melting. Preliminary results are discussed and plans for future, more comprehensive investigations and measurements are presented.

1 INTRODUCTION

The importance of climate on stability is illustrated by the fact that most rock falls and slides take place during heavy rainfall, and particularly when repeated freezing-thawing is much in effect. The most catastrophic rock slides in Norway, Loen and Tafjord, have all taken place during such conditions (Bjerrum & Jørstad 1968). For very large rock slides like these it is also a general experience that the failure does not occur without warning – it is preceded by a period of increased rockfall activity. Thus, creep effects and time dependent behaviour are key issues in stability assessment.

There are many examples that climate and water have been decisive factors for long-term deformation and slope stability. One of the best known cases is Vajont, where a catastrophic rock slide of 250 million m^3, killing over 2 000 people due to a huge wave caused by the slide overtopping the dam of the Vajont reservoir, took place in 1963 (Goodman 1993). Stability problems were monitored in the reservoir slope as early as 1960, and a system for surveillance was established prior to the main slide. An example of the surveillance recordings, convincingly illustrating the relationship between rainfall and deformation, is shown in Figure 1. The figure also shows that not only the precipitation, but also the elevation of the reservoir, influenced the slide movement.

Failures of large slopes are normally not sudden events, but more a successive process where creep and time dependant deformation play important roles. In Norway there are numerous locations where considerable creep has taken place or is still in effect in rock slopes (Braathen et al. 2004). One of them is the Åkerneset site, which will be discussed in this paper. The effect of climate on creep and long-term deformation will particularly be emphasized.
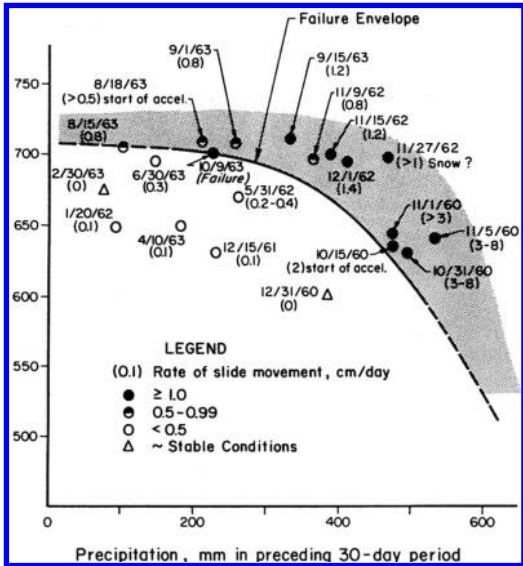
725

Figure 1. Stability of the vajont slide for combinations of reservoir elevation and precipitation (Hendron & Patton 1985).

2 EFFECTS OF CLIMATE

Water may destabilize large rock slopes in many different ways. The most obvious is that water pressure in joints and fractures will reduce stability by directly representing a driving force, and also by reducing normal force and thus the frictional resistance on potential sliding planes (see Nilsen 2005 for more details on this).

For gouge materials in a potential sliding plane, water may considerably reduce the internal friction, and thus the stability. In cases with rock to rock contact along a potential sliding plane, water will reduce stability by reducing the strength of irregularities.

When water freezes, it expands by approximately 10%, causing considerable displacement and forces that may greatly reduce slope stability. Freezing may also cause blockage of drainage ways for water in joints and fractures, and thus reduce stability.

In the Norwegian climate, characterized by great annual variations in precipitation and temperature, the effects caused by water and freezing may accumulate. A common stability problem in this country is deep fractures parallel to the valley, playing an important role for stability, and for this situation Bjerrum & Jørstad (1968) argue that due to the variations in rainfall, and variation in possibility for drainage due to freezing, the water pressure will fluctuate considerably during a year. Such fluctuation may cause fatigue fracturing and thus fracturing of intact rock, and the effect is likely to be enhanced by pieces of unstable rock falling down and blocking for relaxation when water pressure is being reduced.

For other types of stability problems, for instance typical sliding, the process of accumulated deformation will be slightly different from that discussed earlier. The basic principle, with "jacking" due to fluctuating water pressure and freezing-thawing, is believed however to be much the same as described above.

Although it is not a main topic of this paper, it should be emphasized here that in addition to climate, the long term effects of high rock stresses are believed to be very important for creep and long term deformation.

3 DESCRIPTION OF THE ÅKERNESET SLIDE

Currently large attention is being drawn to the Åkernes sliding area. The area (Fig. 2) is located in the Møre and Romsdal County in the West of Norway, in a fjord system where some 30 rockslides with a volume exceeding 1 million m^3 have occurred since the last ice age (c. 10 000 years BP) (Blikra et al. in press). In this particular landslide area, there have been at least three smaller rockslides, the latest in 1960.

The sliding area at Åkerneset was first visited and described by the Norwegian Geotechnical Institute (NGI 1987, 1989). The upper boundary of the unstable area is determined by a distinct, more or less continuous tension fracture of about 500 m in length (Fig. 3). Furthermore, it is now believed that the unstable area is divided into at least two separate blocks, moving in different directions. Several weak layers containing clay and brecciated material are documented, and are believed to be of importance for the overall stability of the slope.

The downhill creep probably started in the 1960's, and downhill creep rates in the order of 3–4 cm/year have been monitored at the back scarp since 1986 (Sandersen et al. 1996, Larsen 2002). By the end of 2004 the following investigations have been carried out in addition to the recordings described in Chapter 4:

– Detailed mapping of the topography by the use of laser scan from helicopter.
– Geological field studies including geomorphic mapping and collection of structural data as well as studies of potential sliding planes and fractures at the surface.
– Geophysical measurements (2D resistivity, refraction and reflection seismics and penetrating radar) in order to map the thickness of the unstable slope.
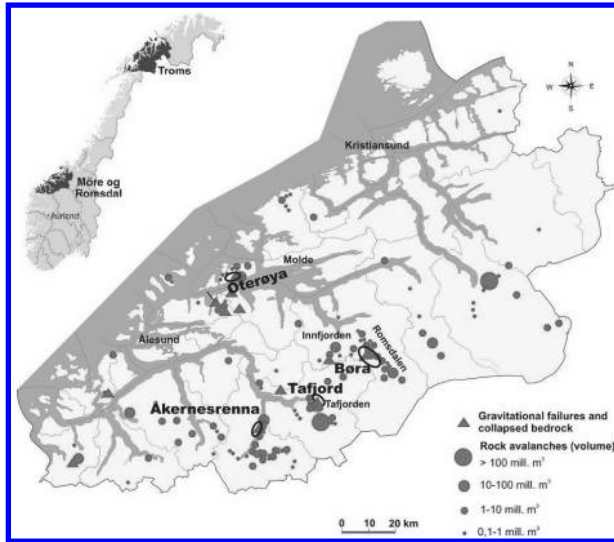
726

Figure 2.   Historical events in Møre and Romsdal County (revised after Blikra et al., in press).
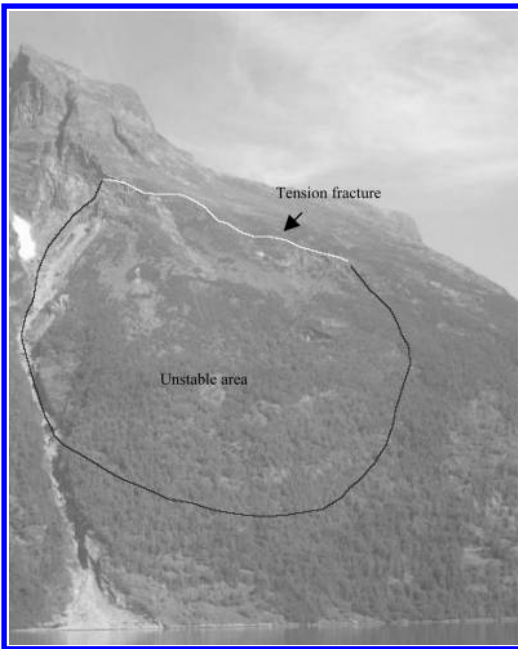

Figure 3.   The Åkerneset locality shown with the tension fracture seen as a back scarp and the unstable area indicated.

Figure 4.   Location of the 5 extensometers on the back scarp.

4   PREVIOUS RECORDINGS OF DISPLACEMENT FOR ÅKERNESET

For monitoring of movement in the creeping rock mass, 4 bolts for manual reading were installed on the back scarp in 1986 and 1989. A continuous surveillance program was started in 1993 with three extensometers (ext. 1, 2 & 3). Two additional extensometers (ext. 4 & 5) were installed recently (summer 2004). The locations of the extensometers in the back scarp are shown in Figure 4.

The extensometers are placed in telescopic steel pipes and fixed to solid rock on each side of the rupture. The data is sampled once daily and stored locally in a datalogger.

Measurement data for the period 1993–1995 have been analysed and show movement every year. There is no evident relation between precipitation and displacement in this period, but there are indications of increased movement during the snow melt season. This
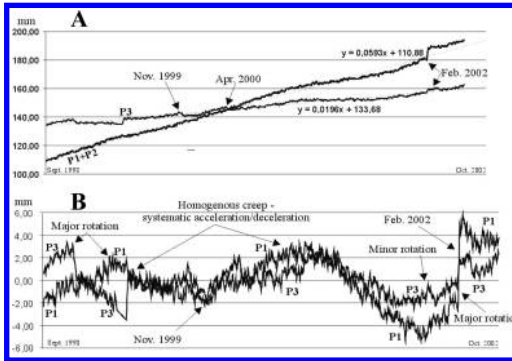
727

Figure 5. A) Plot that shows cumulative displacement (mm) for three sites (ext. 1,2 & 3) between September 1998 and October 2002 (data from the municipality of stranda). Noise is reduced by a running average of 5 neighbouring recordings. The approximate linear trends for the dataset is indicated. B) plot of variations in cumulative displacement for ext. 1 & 3, seen as variations around the linear trend line (0-line in the plot), as established above (Braathen et al. 2004).

Figure 6. Recordings from the daily surveillance program, Aug. 1993–Jun. 1996, Oct. 1998–Aug. 2003.

suggests that water pressure does not play any important role during increased precipitation in the autumn, but may be of importance during springtime (Sandersen 1996, Larsen 2002).

Deformation data at the three extensometers for 1998–2002 have been studied by Braathen et al. (2004) and confirm a continuous creep of the block studied, with slightly greater movements at two of the extensometers (ext. 1 & 2). In general, the rate of movement has been more or less steady for 1998–2002, with linear movement patterns, although local events appear in the dataset (Fig. 5).

One major local event was recorded during a 6 day period in February 2002. This event showed fast acceleration followed by equal deceleration of ext. 1 and 2, whereas a minor change was recorded at extensometer 3. This is consistent with internal block deformation, as well as rotation of the entire block around a fixed point at its sole (Braathen et al. 2004).

When the entire dataset is evaluated with respect to variations from the observed linear movement trend, two patterns emerge: 1) For a long period the entire block seems to have moved homogeneously (c. 750 days), 2) In two shorter periods, changes in movement have been faster and more complex, which is consistent with periods of either major or minor block rotation. The overall, detailed movement pattern suggests that friction along the sole structure varies both through time and in space, and that the block in periods rotates around sticky spots/areas on the basal shear surface.

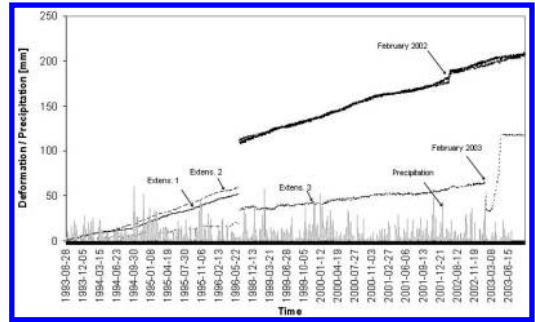Deformation data from the daily surveillance period from August 1993 to August 2003 are shown

in Figure 6. The recordings are available for two periods, from August 1993 to June 1996 and from October 1998 to August 2003. The recordings show that the fast acceleration followed by equal deceleration of ext. 1 and 2 in February 2002 described by Braathen et al. 2004 is followed by an equal pattern of acceleration and deceleration of ext. 3. The deformation has however a time-lag in the order of 1 year and is not visible until the beginning of February 2003.

The precipitation data presented in the same figure is from a weather station located at the fjord level, 6 km northwest of the Åkerneset locality. As mentioned earlier, the precipitation does not seem to play an important role due to deformation in the sliding area.

5 FUTURE RECORDINGS OF DEFORMATION

There is a great demand for more detailed investigations and installations of new monitoring systems due to the complexity of the Åkernes area and the large consequences of a potential slide. The plans for the coming 2–5 years concerning investigations and monitoring include primarily:

– Further studies of aerial photos of different ages, including new aerial photographs, in order to detect movements in larger areas.
– Extensive mapping of fractures, sliding planes and physical features of importance for stability evaluations.
– Additional geophysical profiles in order to verify geometry of the slide area (resistivity, seismics and georadar).
– Drilling through the base of the unstable rock mass at two localities, geophysical logging of the 2 drill holes.
– Mapping of groundwater pattern and velocity.

In order to obtain a more complete understanding of the deformation patterns in the area a network of GPS points and reflectors (a total of 22 points) were

728

established during the summer of 2004 throughout the area. Information on the patterns of movement will be available in the summer of 2005. Instrumentation of drill holes in order to map and monitor movements has been suggested. Such instrumentation with a series of inclinometers and piezometers may make it possible to identify weak layers, measure movement in different areas and measure pore pressure. A climate station recording data on precipitation, temperature and wind speed was established in the summer of 2004. This will make it possible to further verify possible relationships between precipitation/snow melting and slide movements.

6 CONCLUDING REMARKS

Recordings of creep movement related to meteorological factors may give valuable information on climatic influence on rock stability. An attempt to study this relationship has previously been made for the Åkerneset locality. These studies, carried out by Sandersen et al. (1996) and Larsen (2002), conclude that there is no evident relationship between precipitation and displacement in the period 1993–1995, but increased movement has been observed due to snow melting in the spring time. The displacement patterns in the period 1995–2002 show similar tendencies, with a stable rate of creep in the order of 3–4 cm per year.

One explanation for this somewhat surprising, weak influence of climate may be the fact that increased precipitation during autumn does not play an important role for the water pressure in the area, and thereby not for the movement. The movements are more related to ice activity and freezing/thawing. The basis for this theory is however not very solid. The two additional extensometers that were installed in the summer of 2004 in addition to new monitoring systems that will be installed in 2005, as well as the climate station that has been established at the locality will make it possible to study this relationship in greater detail. The network of GPS points and reflector points will also provide additional deformation data which can be correlated with the climate data. A comprehensive study, based on all these data will be done in the near future, and hopefully will make it possible to draw a more accurate conclusion of the relationship or lack of relationship between the meteorological factors such as precipitation and snow melting and deformation of the unstable rock-slope at Åkerneset.

REFERENCES

Bjerrum, L. & Jørstad, F. 1968. Stability of rock slopes in Norway. Norwegian Geotechnical Institute Publication 79, pp. 1–11.

Blikra, L. H., Longva, O., Braathen, A., Anda, E., Dehls, J. & Stalsberg, K. in press. Rock slope failures in Norwegian fjord areas: Examples, spatial distribution and temporal pattern. In Evans et al. (Eds.): *Massive rock slope failures*. NATO Advanced Research Workshop. Kluwer.

Braathen, A., Blikra, L.H., Berg, S.S. & Karlsen, F. 2004. Rock-slope failures in Norway; type, geometry and hazard. Norwegian Journal of Geology 84: 67–88.

Goodman, R. E. 1993. *Engineering geology: Rock in engineering construction*. John Wiley & Sons Inc, pp. 170–172.

Hendron, A. J. Jr. & Patton, F. D. 1985. The Vajont Slide, a geotechnical analysis based on new geological observations of the failure surface, U.S. Army, Corps of Engineers, Waterways Experiment Station, Geotechnical Laboratory Report GL-85-5.

Larsen, J. O. 2002. Some aspects of physical weather related slope processes. Dr. Ing. – thesis, Norwegian University of Science and Technology, Department of Geotechnical Engineering Mining, pp. 31–37.

Nilsen, B. 2005. The significance of groundwater pressure estimation in rock slope stability analysis. Paper published: 2005 International Conference on Landslide Risk Management, Vancouver. In press (this volume).

Sandersen, F., Bakkehøi, S., Hestnes, E. & Lied, K. 1996. The influence of meteorological factors on the initiation of debris flows, rockslides and rockmass stability. In Senneset (ed) Proceedings in Landslides. Seventh International Symposium on Landslides, Trondheim, Norway, pp. 97–114.

Tveten, E., Lutro, O. & Thorsnes, T. 1998. Bedrock map Ålesund, M 1:250 000. Geological Survey of Norway.

Early warning of landslides for rail traffic between Seattle and Everett, Washington, USA

R.L. Baum, J.W. Godt, E.L. Harp & J.P. McKenna
U.S. Geological Survey, Denver, CO, USA

S.R. McMullen
Shannon & Wilson, Inc. Seattle, WA, USA

ABSTRACT: Landslides on coastal bluffs between Seattle and Everett Washington, USA, have repeatedly interrupted rail traffic and at times have posed a serious threat to the safety of railway operations. Historical records of landslides in the Seattle area indicate that a background rate of landslide activity exists due to various causes, such as erosion, ground-water fluctuation, and grading, but widespread activity results from periods of intense rainfall on already damp soil. Results of three years of monitoring precipitation, near-surface soil wetness (water content) and pore pressure on the coastal bluffs between Edmonds and Everett, Washington, combined with results of other ongoing research have identified conditions upon which to base an early warning system for widespread precipitation-induced landslide activity. Monitoring data show that the soil wetness is generally less than about 20% by volume at the end of the dry season in October and increases to 25–30% with the beginning of the winter rainy season in November or December. Subsequent winter precipitation maintains this level of soil wetness until March or April. Prolonged or intense rainfall tends to further elevate soil wetness 2–3% above the winter background level. Wet soil conditions (about 60–80% saturated) that occur at times of frequent or prolonged rainfall during the winter rainy season appear to be a necessary prerequisite for widespread landslide activity. When the soil is wet, periods of intense rainfall that exceed a threshold defined by $I \geqslant 82.73D - 1.13$, in which I is mean intensity in mm and D is duration in hours, can cause multiple landslides. Continuous monitoring of precipitation, soil water content and pore pressure, combined with this empirical rainfall threshold can form the basis for a landslide early warning system that could enable the railway to identify times of high landslide probability and adjust its operations accordingly.

1   INTRODUCTION

Landslides on coastal bluffs between Seattle and Everett, Washington have posed a major hazard to transportation since the 1800s (Fig. 1). Recently, more than 100 landslides resulted in damage to property and temporary disruption of railroad service in 1996 and 1997 (Baum et al. 2000). The majority were shallow landslides that resulted from a rain-on-snow event about January 1, 1997. The January 15, 1997, Woodway landslide, which was one of the largest recent slides on the coastal bluffs, derailed several cars of a freight train (Fig. 2, W.A. Hultman & D.N. McCulloch, Shannon & Wilson, Inc. written comm. 1997, Baum et al. 1998). Additional landslides resulted from heavy rainfall on March 18–19, 1997. Rainstorms also triggered significant numbers of landslides from mid November 2001 through January 2002 (Chleborad 2003, Baum et al. 2005) and at least one of them covered the railway and temporarily interrupted rail traffic near Edmonds on November 29, 2001 (Seattle Times 2001).

Passenger and freight rail traffic in the Seattle-to-Everett corridor has steadily increased as population of the Puget Sound region has grown. On December 21, 2003, commuter rail service began between Seattle and Everett. Long-range plans for transportation in the region call for increased rail traffic in the corridor and Sound Transit is already investing heavily in improvements to support commuter rail (Puget Sound Regional Council 2004).

In 2001, a cooperative monitoring effort between the U.S. Geological Survey (USGS), the Burlington Northern Santa Fe Railway (BNSF), BNSF's geotechnical consultant, Shannon & Wilson, Inc. and the Washington Department of Transportation was begun to determine whether near real-time monitoring of rainfall and shallow subsurface hydrologic conditions
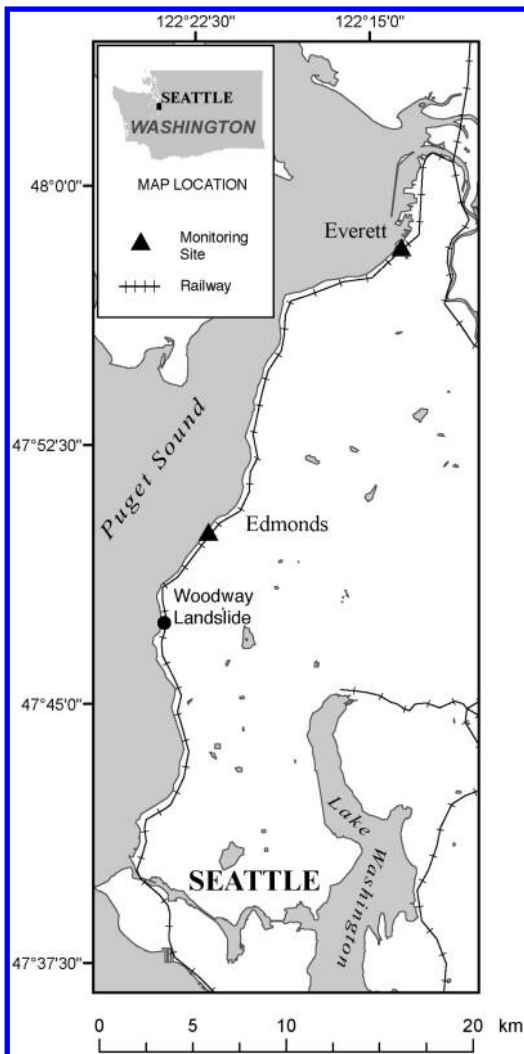
Figure 1. Map showing location of the rail corridor from Seattle to Everett and coastal bluff monitoring sites, landslides have occurred along most of the corridor.
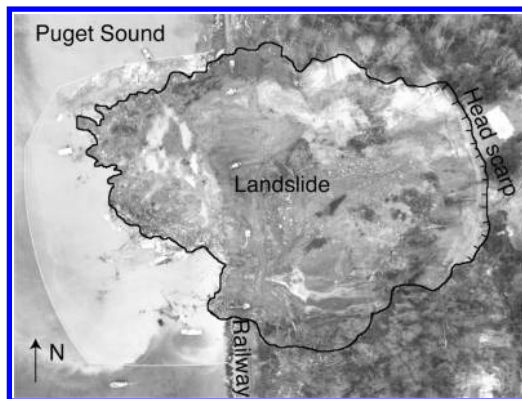

Figure 2. Aerial photograph of the January 15, 1997, Woodway landslide that covered the railway and derailed several cars of a passing freight train near Edmonds, Washington, white polygons in water next to landslide are shipping containers from the derailed train, hachures on headscarp (Washington Department of Transportation photograph, January 16, 1997). The landslide was about 150 m wide and 210 m long.

could be used to anticipate landslide activity on the bluffs. Monitoring currently occurs at two sites, one near Edmonds and the other near Everett, Washington (Fig. 1). Data and experience gained during three seasons of monitoring (2001–2004) show the relationships between precipitation, soil wetness, and landslide activity, and identify characteristics of field monitoring stations needed to support a landslide early warning system (Baum et al. 2005). This report summarizes results from our monitoring, describes an empirical rainfall threshold developed for anticipating landslide activity in Seattle, and outlines development of an

operational system for monitoring, forecasting, and early warning of impending landslide activity.

1.1 *Rainfall intensity-duration thresholds*

Rainfall conditions that lead to shallow slope failure have been investigated for regions where rainfall is generally of much higher intensity than in the Seattle area and where orographic enhancement can be a significant effect. For example, landslide-triggering rainfall thresholds have been reported for Puerto Rico (Larsen & Simon 1993), Hong Kong (Au 1993, Finlay et al. 1997) central and southern California (Campbell 1975, Cannon & Ellen 1985, Wieczorek 1987, Cannon 1988, Wilson & Wieczorek 1995), the Blue Ridge in Virginia (Wieczorek et al. 2000), New Zealand (Crozier 1986, 1999, Glade et al. 2000), and the Piedmont Region in Italy (Aleotti 2004). These empirical relations between rainfall intensity and rainstorm duration are region specific and often take the form of a power-law function. Caine (1980) analyzed precipitation data associated with 73 failures of natural hillslopes from several mountainous regions throughout the world and developed one of the earliest examples of such a threshold above which shallow landslides may be expected that is described by

$$I = 14.82 D^{-0.39} \tag{1}$$

where I is the rainfall intensity (mm/hr) and D is the duration of precipitation in hours. The threshold is defined for rainstorm durations of more than

732

10 minutes and less than 10 day; however, few data were available for durations greater than about 24 hours.

1.2 *Operational landslide warning systems*

Intensity-duration thresholds, in combination with rainfall forecasts and real-time rainfall measurements, have been the basis for operational landslide warning systems in several areas. These systems are typically operated over broad regions where people and infrastructure are at risk from shallow landslides. The Hong Kong Geotechnical Engineering Office established a warning system in 1977 (Chan et al. 2003); continuous data collection and periodic review has resulted in significant improvement of the criteria for issuing and canceling warnings of impending landslides. The USGS, in cooperation with the National Weather Service, operated a debris-flow warning system in the San Francisco Bay region during the later 1980s until the early 1990s (Keefer et al. 1987, Wilson 1997). In Rio de Janeiro, the Alerta Rio System consists of a network of 30 telemetered rain gauges and weather radar and has been used by operational forecasters to issue 42 warnings between 1998 and 2003 for landslides and/or flash flooding to government agencies and the public during severe rainstorms (d'Orsi et al. 2004). The State of Oregon operates a landslide warning system in western Oregon (Mills 2002). At a local scale, data from an extensive instrumental network to detect movement in a large landslide complex at Lyme Regis, UK are combined with rainfall information to warn residents of periods when landslide activity can be expected (Cole & Davis 2002).

2 GEOLOGIC SETTING

The coastal bluffs between Seattle and Everett are underlain by subhorizontally bedded glacial and interglacial sediments, which include glacial advance outwash sand overlying glaciolacustrine silt deposits (Minard 1983, 1985). Shallow landslides commonly occur in weathered glacial and interglacial deposits and slope deposits (colluvium) on the bluffs after periods of relatively heavy rainfall or snowmelt (Baum et al. 2000). Lack of significant runoff from natural (unpaved) slopes during rainfall indicates that water enters the slopes by infiltration. Within the bluffs, water also flows laterally through sandy layers that rest on less permeable layers of silt or clay, as indicated by the presence of seeps and springs (Baum et al. 2005). Shallow landslides commonly have depths less than 3 m, with a majority having depths less than 2 m. Seeps in landslide scars indicate that the bluffs are dominantly unsaturated, with localized saturated zones (Baum et al. 2005).

3 HYDOLOGIC MONITORING AND LANDSLIDE ACTIVITY

Historical records show that most landslides in the Seattle area occur during the rainy season, which lasts from November through April, and most are strongly correlated with rainfall events (Chleborad 2000, 2003, Godt 2004). In the fall of 2001, we began monitoring rainfall and hydrologic conditions in the shallow subsurface of coastal bluff sites near Edmonds and Everett to better define the relationship between precipitation, soil wetness and landslide activity (Baum et al. 2005). The near-real-time field data collection system at each site consists of commercially available geotechnical and environmental sensors connected to a field datalogger that is equipped with a radio for data transmission. The dataloggers normally record hourly, but they have been programmed to record precipitation and other data on 15-minute intervals during times of high precipitation (>2.54 mm/hour). Regardless of the time interval, recording data triggers radio transmission of the most recent data. The data are relayed over a commercial line-of-site radio network based in Kent, Washington, where the network operator places the raw data on an Internet server. USGS computers in Golden, Colorado, retrieve the data by hourly File Transfer Protocol (FTP) download, reduce and graph the data and copy the graphs to a web server, which provides access to graphs of the most recent data in near real time.

We have experimented with various kinds of sensors at the two sites in an effort to find a combination that provide monitoring data of sufficient quality, reliability, and relevance to be suitable for anticipating landslide activity (Baum et al. 2005). At the time of this writing, each site is equipped with two tipping bucket rain gauges. The site near Everett, which operates on solar power, uses three water content reflectometers. The reflectometers use time-domain reflectometry to measure the soil bulk dielectric constant, which varies with volumetric water content. The site near Edmonds, which operates on AC power, has two water content profilers equipped with eight sensors each at depths ranging from 20 cm to 200 cm, and two nests of six tensiometers to measure soil suction, ranging in depth from 20 cm to 150 cm (Baum et al. 2005). The water content profilers measure soil capacitance, which varies with soil water content. A similar configuration would be used at Everett, if AC power were available.

Our monitoring has shown that soil wetness, as measured by volumetric water content, and pore pressure are strongly related to rainfall (Baum et al. 2005). At each, soil wetness at some depths is higher throughout the year than at others. These long-term differences in absolute value of the soil wetness at different depths are indicative of spatial variations in

733

porosity and other properties of the soil as well as differences between individual sensors, which were not individually calibrated for soil at the sites. Consequently, our description and analysis of soil wetness data in succeeding paragraphs focus primarily on the changes through time, rather than absolute value of the soil wetness, in order to identify flow directions and characterize subsurface water movement in response to rainfall.

Figure 3 shows precipitation and water content at Everett from June 1, 2002 through October 15, 2003. Precipitation was markedly seasonal, with most falling from November through April, and the soil was significantly wetter during the rainy season (Fig. 3). Soil wetness increased episodically over several weeks at the beginning of the rainy season and remained elevated 4–10% above the dry-season water content for the remainder of the rainy season. During the rainy season, soil wetness increased rapidly by an additional 1–4% following rainfall that exceeded about 12 mm in 24 hours. During the dry season, the same amount of rainfall produced smaller increases in soil wetness (Baum et al. 2005).

Changes in soil wetness and pore pressure depended on depth and initial conditions as shown by monitoring at the Edmonds site where sensors extend to greater depths than at Everett (McKenna et al. 2004, Baum et al. 2005). We installed the water-content profilers and tensiometers on September 25, 2003, and began receiving data on October 17, 2003. Installation caused minimal disturbance of the relatively permeable soils, so we estimate that soil water equilibrated around the water content profilers in a matter of hours and that pore pressure at the tensiometers equilibrated within a few days. During October 2003, the soil was dry at depths greater than 0.5 m (e.g. 11–19% water at

various depths and suction of 0.8–1.0 m water at 80–120 cm depth, Fig. 4, 5) (Baum et al. 2005) and wetting fronts moved slowly downward in response to rainfall as indicated by the increasing time lag between precipitation and peak soil wetness at increasing depth (Fig. 4). In mid-October, record 24-hr rainfall (127.5 mm at Seattle-Tacoma airport) produced a few shallow landslides and debris flows. This storm produced 74.4 mm of rain in 32 hr at Edmonds and the soil wetness peaked within hours at 0.5 and 0.8 m depths, but after four days at 1.2 m depth and after 8 days at 2 m depth (Fig. 4). However, pore pressure at 1.2 m depth peaked after only 22 hours. The storm triggered a few landslides that were probably related to the elevated pore pressures that occurred despite initial dryness of the soil.

As soil wetness increased throughout the winter season, pore pressure and soil wetness at depth responded more rapidly to heavy rainfall (Fig. 4-5). In mid-November 90.9 mm of rain fell in 29 hr resulting in a 2–4% increase in soil wetness at 2 m depth in only one day (Fig. 4). The rounded peaks at depths of 120 and 200 cm for the mid October storm compared with

Figure 4. Soil water content recorded by water content profilers and rainfall at the Edmonds site October 17, 2003 to December 31, 2003. Instruments were installed on September 25, 2003, and data collection began on October 17, 2003.
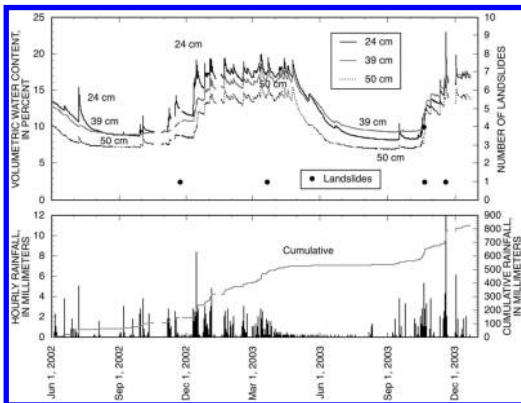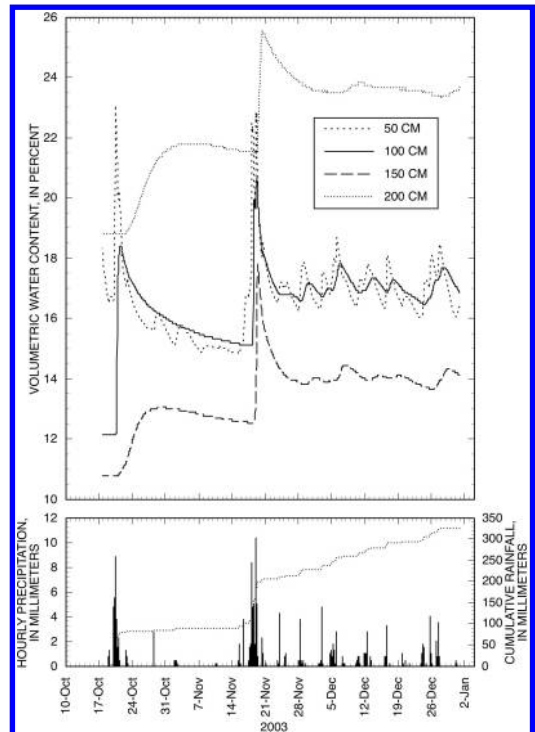
Figure 3. Soil water content recorded by water content reflectometers and rainfall at the Everett site compared to the number of landslides in Seattle from June 1, 2002 to December 31, 2003. Gaps indicate periods of no data.

734

sharp peaks at the same depths for the mid November storm clearly depict this difference in response between dry conditions at the beginning of monitoring and wet conditions from November 2003 onward (Fig. 4). Pore pressure at all depths down to 120 cm peaked within a few hours of the peak rainfall intensity, which occurred between midnight and 2:00 a.m. on November 19, 2003. The pore pressure response during this and subsequent rain storms was more rapid than during the mid October rainfall (Fig. 5). Soil wetness at 1–2 m depth differs by 4–5% from before the mid October storm to the end of December.

Most landslide activity between autumn 2001 and summer 2004 occurred during the 2001–2002 rainy season (Fig. 6), and relatively few landslides occurred during the 2002–2003 and 2003–2004 seasons (Baum et al. 2005). Most landslides during 2001 occurred when antecedent soil wetness was at or above the winter background level. Although problems with instrumentation during the 2001–2002 rainy season resulted in significant data loss (a poor connection resulted in no data from the water content reflectometer at 46 cm before Nov 29, 2001, Fig. 6); all landslides recorded that season occurred after several days of rainfall in late October caused soil at the Everett site at 74 cm depth to become significantly wetter than it had been previously. The sandy clay soil at the site was previously dry enough that the sensor did not respond to moderate precipitation during early and mid October 2001. Most historical landslides have occurred during the November-April rainy season (Chleborad 2003). Measurements of soil wetness appear to be a useful indicator of when hillside materials have absorbed enough rainfall to become susceptible to rainfall-induced landslides. Soil wetness at a given depth might be best characterized relative to soil wetness near the end of the dry season (August and September), because absolute values of soil wetness indicated by our measurements are so variable. Antecedent soil wetness during the 2001–2002 season when most landslides occurred was several percent higher than the dry season wetness at the same depth (Baum et al. 2005). Except for a few early season landslides that resulted from very intense rainfall, similar patterns were observed during 2002–2003 and 2003–2004 (Baum et al. 2005). The rainfall that triggered clusters of three or more landslides raised soil wetness an additional 2–4% within several hours (Fig. 6). These observed increases in soil wetness correspond to two- to three-fold greater increases in the degree of saturation of the soil because the wetness, Θ, is the volume of water, V_w, divided by the bulk volume of the soil, V_B, but the degree of saturation, S, is V_w divided by the volume of the pore space, V_v, and the porosity of uniform sand like that found at the
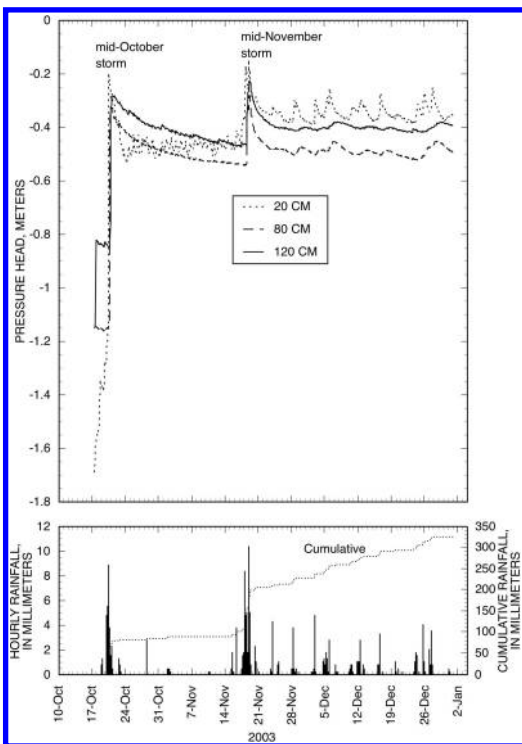

Figure 5. Pressure head recorded by tensiometers and rainfall at the Edmonds site from October 17, 2003 to December 31, 2003. Instruments were installed on September 25, 2003, and data collection began on October 17, 2003. Large diurnal fluctuations recorded after mid February 2004 resulted from tensiometers beginning to dry out.
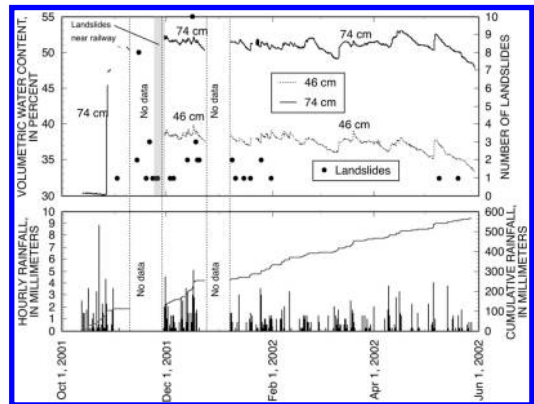

Figure 6. Soil water content and rainfall at the Everett site compared to the number of landslides in Seattle from October 2001 through May 2002 (after Baum et al. 2005). Water content here is not directly comparable to that shown in Figure 3 because instruments were moved a short distance to soil that contained fewer fines on May 28, 2002.

735

monitoring sites is generally between 30–50% of the bulk volume (Lambe & Whitman 1969). Thus, at 40% porosity, $V_v = 0.4V_B$ and $S/\Theta = 1/0.4$, or 2.5. Comparison of field and experimental data (Godt 2004) indicates that the degree of soil saturation at times of landslide activity is at least 80%.

4 INTENSITY-DURATION THRESHOLD FOR THE SEATTLE AREA

We have developed a rainfall intensity-duration threshold for anticipating widespread landslide activity. The dates and locations of shallow landslide occurrence since hourly rainfall records became available in Seattle (1978) were determined from a landslide database compiled from the records of the Seattle Engineering Department, the Seattle Department of Planning and Development, and Shannon & Wilson Inc. (Laprade et al. 2000) and from reports by Chleborad (2000, 2003). The database also contains information describing the geologic setting, dimensions, style of failure, and the apparent influence of drainage modification or slope engineering for most of the entries. Landslides reported in the database are primarily those that caused damage to private property or infrastructure, and in general the accuracy and completeness of the record increases with time (Coe et al. 2004). The dates of landslides that occurred during the years of 1978 to 1997 were selected for use in developing the threshold if: (1) at least two landslides were recorded on the same date in different geographic areas of the city; (2) available information indicated the landslides were not deep seated; and (3) the landslides were not directly caused by excavation or other construction activities. Accurate information on the timing of shallow landslides is generally only available from first-hand accounts, and for the purposes of this study, we assume that the shallow landslides were a direct result of the recorded rainfall.

Mean rainfall intensity, I, and duration, D, were compiled from data collected by the City of Seattle rain-gauge network (Fig. 7) for the six rainstorms that meet the three selection criteria outlined in the previous paragraph. Rainstorms were bounded by periods of no rainfall at least 3 hours in duration. Mean intensities were calculated by dividing the total rainfall by the rainstorm duration. The rain-gauge network consists of 17 tipping-bucket rain gauges maintained by the Seattle Public Utilities and provides dense coverage (2–5 km between-gauge distance) of the city. The mean-annual precipitation recorded by this network is about 850 mm. The maximum between-gauge difference of the mean-annual precipitation is about 20% with no trend related to gauge elevation. The gauges do not directly measure snowfall and are not equipped with windscreens.
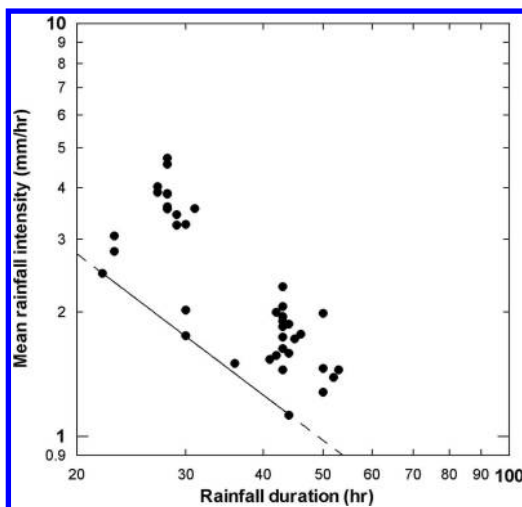

Figure 7. Mean rainfall intensity, I, versus duration, D, near the locations of landslides caused by the six storms that produced two or more shallow landslides in different geographic locations in Seattle during the period from 1978 to 1997. The threshold fit through the three points closest to the origin is described by I = 82.73D − 1.13.

Two rainstorms (1/18/1986 and 3/19/1997) produced widespread shallow landslides in the Seattle area. A third event over the New Year holiday of 1996–1997 also produced widespread shallow landslides, but resulted from rainfall in combination with melting snow (Gerstel et al. 1997). The approach we outline here does not account for melting snow, and this event is ignored in the determination of the threshold. This is a shortcoming of this approach as the New Years 1996–1997 event caused significant damage, however, the presence of a 600–900 mm deep snowpack in the Seattle area is quite rare and the Seattle rain-gauge network does not collect snow-depth information.

Figure 7 shows the mean rainfall intensity and duration determined at the rain gauges nearest each landslide triggered by the six rainstorms. A line defining the intensity-duration threshold was fit through the three points closest to the origin of the graph and can be represented by

$$I = 82.73D^{-1.13} \qquad (2)$$

where the intensity is measured in mm/hr and the storm duration is in hours.

Rain gauge number one is the most northerly gauge in the Seattle network. The intensity-duration threshold (I-D) was exceeded at gauge one 0.11% of the time for an average of 0.84 exceedances per year for the period 1978 to 2003. Other gauges in the

736

Table 1. Probability of landslide occurrence in Seattle relative to the intensity-duration threshold, I-D, and antecedent water index (AWI) of Godt (2004) based on number of days conditions exceeded from 1978–2003.

Landslides per day N	Probability, P, of N or more landslides on a day when conditions satisfied					
	I-D exceeded		I-D and AWI exceeded		I-D not exceeded	
	P (%)	Days	P (%)	Days	P (%)	Days
2	46.0	12	63.9	12	0.4	38
3	30.7	8	42.6	8	0.1	13
5	23.0	6	32.0	6	0.02	3
50	7.7	2	10.7	2	0.01	1

Seattle network had similar levels of exceedance. Using a database compiled by Chleborad (2003, written comm. 2004) we estimated the probability of landslides occurring when the I-D has been exceeded alone and when combined with an empirical antecedent water index (AWI) defined by Godt (2004) (Table 1). The AWI is computed from hourly rainfall and was modeled to mimic variations in soil wetness as observed by our instrumentation; we use it here as a substitute for instrumentally observed high soil wetness, which is available only for the Edmonds and Everett sites, but not for Seattle. We estimated the probability of N or more landslides on a given day when the I-D and AWI have been exceeded by dividing the total number of days when N or more landslides had occurred in Seattle while the thresholds were exceeded by the average number of continuous periods (typically less than 24 hours, but may overlap two contiguous dates) when the I-D or combined I-D and AWI were exceeded at all the gauges in the Seattle network. We also estimated the probability of landslides on any given day when the I-D has not been exceeded (Table 1) by dividing the number of days on which N or more landslides occurred while the thresholds were not exceeded by the average number of days on which the thresholds had not been exceeded. Though small, the probability of landslides occurring without conditions exceeding the I-D is significant (as indicated by the number of days, Table 1) and increases as the number of landslides decreases. Widespread events with 50 or more landslides exceeded the I-D and AWI at all gauges in the network. Events with fewer landslides typically exceeded the thresholds only at gauges near the landslides; sometimes rainfall at only one gauge exceeded the threshold. Thus, having gauges located near areas of frequent landslide activity is critical to anticipating smaller events.

5 LANDSLIDE EARLY WARNING SYSTEM

Our research indicates that several components are needed to reliably forecast landslide activity in the Seattle area. These components include (1) field monitoring of precipitation and subsurface water conditions, (2) analyzing quantitative precipitation forecasts in the context of empirical rainfall thresholds (Chleborad 2000, 2003, Godt 2004) or a coupled transient rainfall infiltration and slope stability model (Savage et al. 2003, 2004), and (3) comparing current and recent precipitation with empirical rainfall thresholds. (4) Criteria for issuing warnings. Such a system could be adapted to other transportation routes and residential developments in landslide-prone areas of Puget Sound communities as well as other geographic locations that have seasonal rainfall and frequent precipitation-induced landslides.

Installation, operation, and maintenance of an early warning system for landslides would be done most effectively by some combination of the rail operators and appropriate state and local agencies, aided by geotechnical specialists. Analysis to determine the point at which rail traffic in this corridor will have sufficient exposure to landslides that such a system becomes a cost-effective means of reducing landslide risk is beyond the scope of this paper.

5.1 *In situ monitoring systems*

Based on analysis of monitoring data and instrument performance, an ideal monitoring system for early warning of shallow landslide activity on coastal bluffs of Puget Sound would consist of stations for continuously monitoring precipitation and soil wetness between the ground surface and 2-m depth (Baum et al. 2005). Water content profilers appear to be the most reliable way of monitoring when the soil is wet enough to be susceptible to shallow landslides. Site-specific calibration of these instruments is needed to measure absolute values of soil wetness accurately. Tensiometers would provide a valuable addition at sites that can be accessed easily for maintenance, because tensiometers show actual changes in pore pressure, which typically happen more rapidly than changes in soil wetness. Furthermore, pore pressure is more directly related to slope instability than water content alone. However, piezometers do not appear to be useful on Puget Sound coastal bluffs, unless a perennial saturated zone is present at a particular site because piezometers provide little useful data in the unsaturated zone. Permanent AC power sources, direct-burial cable or wireless communications between the datalogger and hillside sensors, and redundant sensors and dataloggers, would be needed to develop existing monitoring systems into permanent, reliable installations for long-term use in early warning of landslide activity.

Table 2. Warning criteria.

Warning level	Lead time	Tools
"Advisory"	Days	Field monitoring
"Watch"	3–72 hours	QPF and Intensity-Duration Threshold (I-D) or TRIGRS
"Warning"	Near real time	Intensity-Duration Threshold

A regular maintenance program for the field sites would help ensure reliable operations. Analysis of hourly precipitation and landslide activity from Seattle indicates that uncertainty increases with distance between rain gauges and historical landslides. Ideal spacing for monitoring stations in areas of historical landslide activity is 2–3 km (Chleborad 2000, 2003, Godt 2004). Based on the distribution of historical landslides (Baum et al. 2000), about ten stations would adequately cover the Seattle-Everett rail corridor.

5.2 *Warning criteria*

Based on our field observations and analysis of rainfall thresholds, it is possible to specify three levels of warning, with successively shorter lead times, for use in a landslide early warning system between Seattle and Everett (Table 2). Field observation of a high degree of soil saturation ($>$60–80%), which indicates that the hillside materials are wet enough to be susceptible to landslide activity, leads to the lowest level of warning, "Advisory." In the event of prolonged, intense rainfall, shallow landslides are likely during this lowest level of warning. An "Advisory" combined with a forecast of rainfall that is sufficient to exceed the empirical intensity-duration threshold leads to the intermediate level of warning, "Watch." Reliable quantitative precipitation forecasts (QPF) for use in determining the intermediate warning level are available from the University of Washington Department of Atmospheric Sciences (http://www.atmos.washington.edu/mm5rt/) or the National Weather Service. The TRIGRS model (Savage et al. 2003, 2004) could be used as an alternative to the rainfall threshold for estimating landslide potential from the quantitative precipitation forecast (Godt 2004). If near real-time field data indicate that actual rainfall conditions are approaching the threshold and that soil wetness and pressure head are high, so that landslides are likely at any time, then the level of warning is elevated to the highest level, "Warning."

6 DISCUSSION

Our field observations have important implications for modeling infiltration, subsurface water flow, and slope instability of the bluffs for the purpose of forecasting landslide activity. Instrumental observations indicate that the upper two meters of soil rarely becomes saturated and that the flow of soil water there has a strong downward component during and directly after storms. Rainfall-induced pore-pressure changes propagate more rapidly than wetting fronts and both move more rapidly in initially damp soils than in initially dry ones. Consequently, time-dependent, vertical infiltration models for unsaturated soils should be able to explain most of the features of our soil-wetness and pore-pressure data (Srivastava & Yeh 1991, Simunek et al. 1998), but entrapped air may play a role in driving pore-pressure response ahead of wetness. Unsaturated soil mechanics principles and data may be required to understand occurrence of shallow landslides on the bluffs. Visual observations indicate that saturated zones and lateral flow of ground water do exist locally in the bluffs (Baum et al. 2005); consequently, two-or three-dimensional models probably would be needed to represent conditions at sites larger than the vertical profiles represented by our field measurements.

Increasing reliance on rail transportation between Seattle and Everett for local commuters, long-distance travelers, and freight will increase exposure of rail traffic to potentially hazardous landslides associated with heavy rainfall. Our observations indicate that field measurement of precipitation, soil wetness, and pore pressure (soil suction) is useful in identifying conditions under which landslides are likely to occur. These measurements combined with rainfall forecasts and an intensity-duration threshold for anticipating landslide activity provide the tools needed to operate a landslide early warning system that could be used to reduce landslide risk for rail traffic or other activities. The probability of landslide occurrence when the I-D and AWI are exceeded is sufficient to make early warnings based on them useful for planning and emergency preparedness, and the highest level of warning might be used to make short-term decisions about rail operations. Continued observations and analysis will likely result in improvements (increased level of certainty) to the warning criteria. Additional work is needed to determine how the antecedent precipitation threshold of Chleborad (2000, 2003) might improve the ability to anticipate low-level landslide activity. However, landslides having immediate causes other than intense rainfall, such as snow melt, long-term low-intensity rainfall, earthquakes, and man-made disturbances, may still occur without warning. A landslide early warning system like that proposed here would be supplemental to the trip-wire system (slide fences) already in use by BNSF to detect landslides when they approach the railway between Seattle and Everett. A landslide early warning system based on components we have described could be adapted readily to other areas or applications.

738

REFERENCES

Aleotti, P. 2004. A warning system for rainfall-induced shallow failures. *Engineering Geology* 73: 247–265.

Au, S.W.C. 1993. Rainfall and slope failure in Hong Kong. *Engineering Geology* 36: 141–147.

Baum, R.L. Chleborad, A.F. & Schuster, R.L. 1998. Landslides triggered by the December 1996 and January 1997 storms in the Puget Sound area, Washington. *U.S. Geological Survey Open-File Report* 98–239.

Baum, R.L. Harp, E.L. & Hultman, W.A. 2000. Map showing recent and historic landslide activity on coastal bluffs of Puget Sound between Shilshole Bay and Everett, Washington. *U.S. Geological Survey Miscellaneous Field Studies Map* MF 2346.

Baum, R.L. McKenna, J.W. Godt, J.P. Harp, E.L. & McMullen, S.R. 2005. Hydrologic monitoring of landslide-prone coastal bluffs near Edmonds and Everett, Washington, 2001–2004. *U.S. Geological Survey Open-File Report* 2005–1063.

Caine, N. 1980. The rainfall intensity-duration control of shallow landslides and debris flows. *Geografiska Annaler* 62A: 23–27.

Campbell, R.H. 1975. Soil slips, debris flows and rainstorms in the Santa Monica Mountains and vicinity, southern California. *U.S. Geological Survey Professional Paper* 851.

Cannon, S.H. 1988. Regional rainfall-threshold conditions for abundant debris-flow activity. In Ellen, S.D. & Wieczorek, G.F. (eds.) Landslides, Floods, and Marine Effects of the Storm of January 3–5, 1982. In the San Francisco Bay Region, California. *U.S. Geological Survey Professional Paper* 1434.

Cannon, S.H. & Ellen, S.D. 1985. Rainfall conditions for abundant debris avalanches, San Francisco Bay region, California. *California Geology* 38(12): 267–272.

Chan, R.K.S. Pang, P.L.R. & Pun, W.K. 2003. Recent developments in the Landslip Warning system in Hong Kong. In *Proceedings of the 14th Southeast Asian Geotechnical Conference*. Lisse: Balkema.

Chleborad, A.F. 2000. A method for anticipating the occurrence of precipitation-induced landslides in Seattle, Washington. *U.S. Geological Survey Open-File Report* 00–469.

Chleborad, A.F. 2003. Preliminary evaluation of a precipitation threshold for anticipating the occurrence of landslides in the Seattle, Washington, area. *U.S. Geological Survey Open-File Report* 03–463.

Coe, J.A. Michael, J.A. Crovelli, R.A. Savage, W.Z. Laprade, W.T. & Nashem, W.D. 2004. Probabilistic assessment of precipitation-triggered landslides using historical records of landslide occurrence, Seattle, Washington. *Environmental and Engineering Geoscience* 10(2): 103–122.

Cole, K. & Davis, G.M. 2002. Landslide warning and emergency planning systems in West Dorset, England. In McInnes, R.G. & Jakeways, J. (eds.) *Instability: Planning and Management*. London: Thomas Telford.

Crozier, M.J. 1986. *Landslides: causes, consequences and environment*. London: Routledge.

Crozier, M.J. 1999. Prediction of rainfall-triggered landslides: A test of the antecedent water status model. *Earth Surface Processes and Landforms* 24: 825–833.

d'Orsi, R.N. Feijo, R.L. & Paes, N.M. 2004. 2,500 operational days of Alerta Rio System: history and technical improvements of Rio de Janeiro Warning System for severe weather. In Lacerda, W.A. Ehrlich, M. Fontana, G.D. & Sayao, A.S.F. (eds.) *Landslides: Evaluation and Stabilization*. London: Taylor & Francis Group.

Finlay, P.J. Fell, R. & Maguire, P.K. 1997. The relationship between the probability of landslide occurrence and rainfall. *Canadian Geotechnical Journal* 34: 811–824.

Gerstel, W.J. Brunengo, M.J. Lingley, W.S. Logan, R.L. Shipman, H. & Walsh, T.J. 1997. Puget Sound bluffs: The where, why, and when of landslides following the holiday 1996/97 storms. *Washington Geology* 25: 17–31.

Glade, T. Crozier, M. & Smith, P. 2000. Applying probability determination to refine landslide- triggering rainfall thresholds using an empirical "Antecedent Daily Rainfall Model". *Pure and Applied Geophysics* 157(6–8): 1059–1079.

Godt, J.W. 2004. *Observed and modeled conditions for shallow landsliding in the Seattle, Washington, area (Ph.D. dissertation)*. Boulder: University of Colorado.

Keefer, D.K. Wilson, R.C. Mark, R.K. Brabb, E.E. III, W.M.B. Ellen, S.D. Harp, E.L. Wieczorek, G.F. Alger, C.S. & Zatkin, R.S. 1987. Real-time landslide warning during heavy rainfall. *Science* 238(13): 921–925.

Lambe, T.W. & Whitman, R.V. 1969. *Soil Mechanics*. New York: Wiley.

Laprade, W.T. Kirkland, T.E. Nashem, W.D. & Robertson, C.A. 2000. *Seattle landslide study (Internal Report W-7992-01)*. Seattle: Shannon & Wilson, Inc.

Larsen, M.C. & Simon, A. 1993. A rainfall intensity-duration threshold for landslides in a humid-tropical environment, Puerto Rico. *Geografiska Annaler* 75A (1–2): 13–23.

McKenna, J.P. Godt, J.W. & Baum, R. L. 2004. Instrumental observations of unsaturated zone hydrology and slope stability – Puget Sound coastal bluffs. *Geological Society of America Abstracts with Programs* 36(4): 15.

Mills, K.A. 2002. Oregon's debris flow warning system. *Geological Society of America Abstracts with Programs* 34(5): 25.

Minard, James P. 1983. Geologic Map of the Edmonds East and part of the Edmonds West Quadrangles, Washington. *U.S. Geological Survey Miscellaneous Field Studies Map* MF-1541.

Minard, James P. 1985. Geologic Map of the Everett 7.5-Minute Quadrangle, Snohomish County, Washington. *U.S. Geological Survey Miscellaneous Field Studies Map* MF-1748.

Puget Sound Regional Council, 2004. *Destination 2030–2004 review and progress report (to the Federal Highway Administration and the Federal Transit Administration)*. Seattle: Puget Sound Regional Council.

Savage, W.Z. Godt, J.W. & Baum, R.L. 2003. A model for spatially and temporally distributed shallow landslide initiation by rainfall infiltration. In Rickenmann, D. & Chen, C. (eds.) *Debris-Flow Hazards Mitigation – Mechanics, Prediction, and Assessment; Proceedings of the 3rd International conference on Debris Flow Hazards, Davos, Switzerland, September 10–13, 2003*. Rotterdam: Millpress.

Savage, W.Z. Godt, J.W. & Baum, R.L. 2004. Modeling time-dependent aerial slope stability. In Lacerda, W.A.

Erlich, M. Fontoura, S.A.B. & Sayao, A.S.F. (eds.) *Landslides – evaluation and stabilization; Proceedings of the 9th International Symposium on Landslides.* London: A.A. Balkema Publishers.

Seattle Times, 2001. *Transportation windfall for state*, November 30. Seattle: Seattle Times.

Simunek, J. Huang, K. & van Genuchten, M.Th. 1998. The HYDRUS code for simulating 1-dimensional movement of water, heat and multiple solutes in variably saturated media, version 6.0. *Research Report* 144. Riverside: U.S. Salinity Laboratory.

Srivastava, R. & Yeh, T.-C. J. 1991. Analytical solutions for one-dimensional, transient infiltration toward the water table in homogeneous and layered soils. *Water Resources Research* 27: 753–762.

Wieczorek, G.F. 1987. Effect of rainfall intensity and duration on debris flows in central Santa Cruz Mountains, California. In Costa, J.E. & Wieczorek, G.F. (eds.) *Debris Flows/Avalanches: Process, Recognition, and Mitigation. Reviews in Engineering Geolog*y. Boulder: Geological Society of America.

Wieczorek, G.F. Morgan, B.A. & Campbell, R.H. 2000. Debris-flow hazards in the Blue Ridge of Central Virginia. *Environmental and Engineering Geosciences* 6: 3–23.

Wilson, R.C. 1997. Operation of a landslide warning system during the California storm sequence of January and February 1993. In Larson, R.A. & Slosson, J.E. (eds.) *Reviews in Engineering Geology*. Boulder, CO: Geological Society of America.

Wilson, R.C. & Wieczorek, G.F. 1995. Rainfall thresholds for the initiation of debris flows at La Honda, California. *Environmental and Engineering Geoscience* 1(1): 11–27.

Towards real-time landslide risk management in an urban area

P.N. Flentje & R.N. Chowdhury
Faculty of Engineering, University of Wollongong, Wollongong, NSW, Australia

P. Tobin
Wollongong City Council, Wollongong, NSW, Australia

V. Brizga
Roads and Traffic Authority of New South Wales, Wollongong, NSW, Australia

ABSTRACT: With an average annual rainfall in the range 1200 mm–1800 mm, landslides in Wollongong are triggered by periods of prolonged heavy rainfall. During such events, real-time pore water pressure, slope movement and rainfall data can be extremely useful for risk assessment and emergency management. A network of continuously monitored real-time landslide field stations has been established in Wollongong. This network will facilitate risk management operations, enhance our understanding of landslide triggering mechanisms and improve quantitative assessment of landslide hazard. Four stations have been established and additional stations are proposed. Data collection and management is fully automated yet manually accessible as required. The major benefit of this system is the accessibility and availability of fully automated graphical output via the web immediately as the data is received from the field stations. The widespread accessibility of this information in near real-time has clear benefits for risk management and emergency response decisions.

1 INTRODUCTION

This paper is primarily concerned with the management of landslide hazard and risk with the aid of a network of real-time continuously monitored web-enabled landslide field stations. The importance of an observational approach is implicit in this strategy. Four such stations are currently operating in Wollongong, in the state of New South Wales, Australia. A wider network of field stations is proposed for the study area and extending to other landslide sites outside of the study area. The key features of these field stations are outlined here and some data from three of the stations are presented and discussed. Utilising the data from such stations requires the development of multi-agent strategies to facilitate the efficient dissemination of information and response. These implementations of the observational approach are one component of a comprehensive strategy for the management of landslide hazard and risk employed within the Wollongong area.

1.1 *The Wollongong area*

The city of Wollongong is nestled on a narrow coastal plain approximately 70 km south of Sydney in the state of New South Wales (NSW), Australia as shown in Figure 1. Over the last 150 years of settlement the population of the Wollongong area has increased to about 200,000 people. The coastal plain is triangular in shape with a coastal length of 45 km. The coastal plain is up to 17 km wide in the south and narrows sharply towards the north, disappearing north of Thirroul. The coastal plain is bounded to the north, west and south by an erosional escarpment ranging in height from 300 m up to 500 m

The escarpment consists of slopes with moderate to steep inclinations with several intermediate benches and cliff lines. Spectacular cliffs of Hawkesbury Sandstone (of Middle Triassic age) cap the escarpment and there is dense vegetation over most of the escarpment below these cliffs.

The main road link to Sydney is the F6 Freeway that traverses the escarpment via Mount Ousley Road. There are several other road links from the coastal plain to the top of the escarpment such as at Bulli Pass (refer Fig. 1). Lawrence Hargrave Drive links the northern suburbs to the F6 freeway via the spectacular near vertical 200 m high cliffs near Clifton, although one section of this road is currently closed due to landsliding (Hendrickx, et al. 2005, in prep).
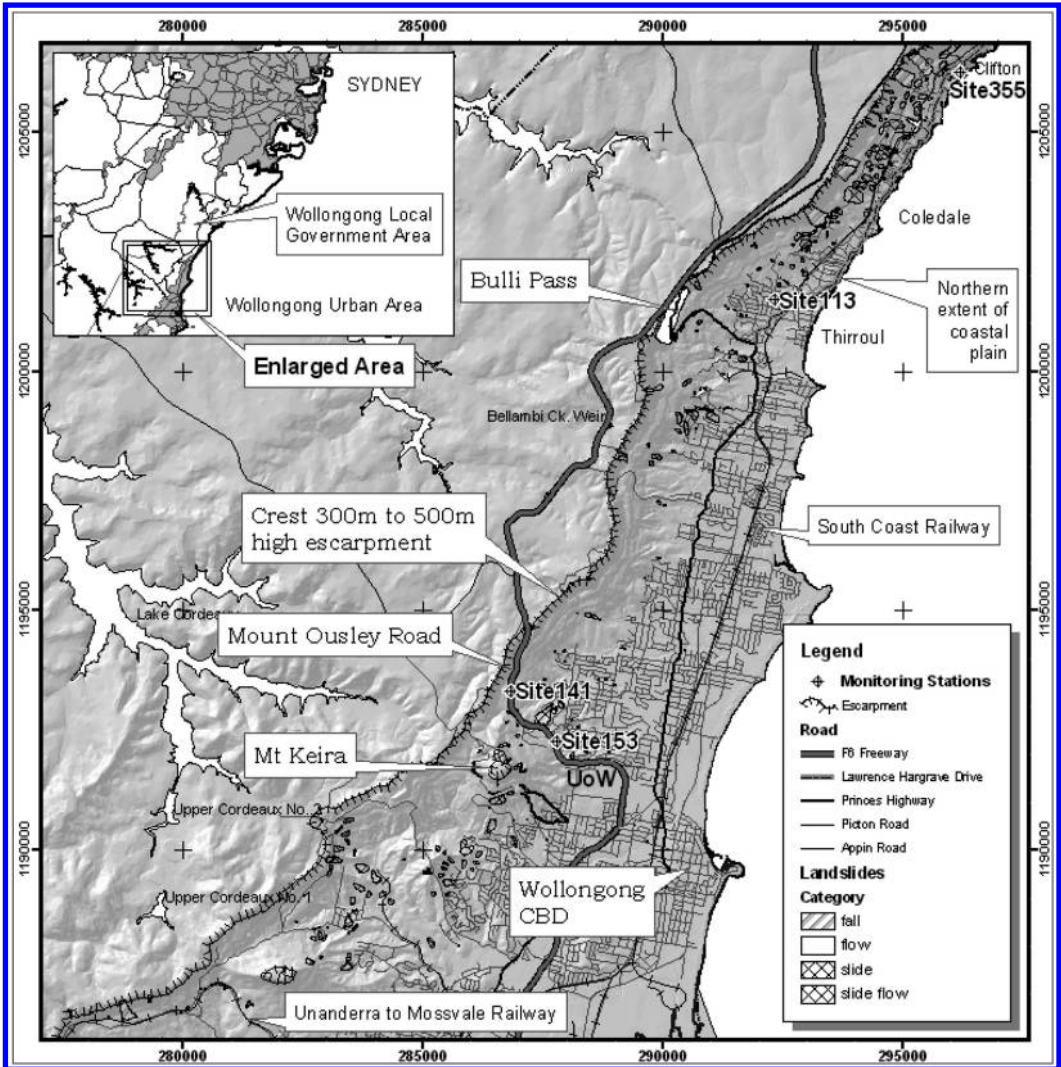
Figure 1.   Location plan for the city of Wollongong showing the four field stations discussed in this paper.

The South Coast and the Unanderra to Mossvale railway lines also traverse the escarpment slopes and coastal plain and both provide important freight and passenger services between Sydney, Wollongong and the surrounding areas.

Processes and mechanisms of slope failure are controlled in Wollongong by factors such as stratigraphy and geotechnical strength parameters, hydrogeology, geomorphology, slope inclination and pore water pressure. Prolonged and/or intense rainfall is typically the trigger for significant landsliding. The average annual rainfall for Wollongong varies from 1200 mm on the coastal plain near the city centre up to 1800 m along the top of the escarpment.

1.2 Background

The landslide research team at the University of Wollongong (UoW) has carried out systematic research over the last twelve years with funding from the Australian Research Council (ARC) as well as significant support from several external industry

742

partners. These include the Wollongong City Council (WCC), the Rail Corporation (RC), Geoscience Australia (GA) and, more recently, the Roads and Traffic Authority (RTA). During this research a number of aspects have been covered including the following:

1 The development of a comprehensive GIS-based datasets including boreholes and structural geology
2 The development of a comprehensive landslide inventory containing 570 landslide sites (Flentje 1998, Chowdhury & Flentje 2002)
3 The development of comprehensive GIS-based maps of geology and landslides
4 Geological and geotechnical modelling, deterministic and probabilistic studies
5 GIS-based and numerical modelling of the spatial variability and recurrence of rainfall
6 Development of a strategic framework for assessment of landslide hazard and risk including qualitative and quantitative methods and including scope for both site-specific and area-specific studies (Ko Ko 2001, Ko Ko et al. 2004)
7 Knowledge-based modelling, using 'data mining' techniques, facilitating the preparation of GIS-based susceptibility maps for specific landslide types for a whole region (Chowdhury et al. 2002).

2 ESTABLISHING A REAL-TIME MONITORING STATION

Equipment used to monitor a landslide in real-time currently starts at approximately $18,000 AUS in 2004 and this does not include installation costs. This is clearly an inexpensive means of monitoring any landslide which poses a significant or moderate risk to infrastructure and especially if there is a moderate or even low risk to human safety. At present, four remotely accessible continuous monitoring stations have been built in Wollongong and selected data obtained from three of these stations are discussed in this paper.

The instruments used in the Wollongong applications include In-Place-Inclinometers (IPI's) and vibrating wire piezometers (vwp) installed at depth in boreholes. Rainfall Pluviometers have been installed at all the field stations to record rainfall as it occurs (0.2 mm or 0.5 mm bucket tips).

The stations are all powered by small solar panels which charge 12 Volt 7.0 Ah sealed lead-acid batteries housed in Campbell Scientific PS/12 Power Supply/regulator units. Tele-communications are performed by Wavecom WMOD2 digital cellular mobile phones. Datalogging and on-site data management is carried out with Campbell Scientific CR10X data loggers. Slope Indicator has bundled these systems together and supplied them to the University of Wollongong together with the programming for the CR10X data loggers. Slope Indicator staff have completed the CR10X programming incorporating our research-based landslide triggering rainfall thresholds and other troubleshooting as required.

A discussion concerning the installation of inclinometer casing and vibrating wire piezometers is beyond the scope of this paper. However, it is worth noting that the IPI instrument itself is approximately 44 cm from wheel to wheel centre and approximately 38.2 mm in diameter. These dimensions highlight two important points. Firstly, the length can be extended by the addition of stainless steel tubing to whatever gauge length movement is to be monitored over. In one instance during local trials a 3 m-gauge length was used, as the precise depth interval of shearing was not known. As landslide shearing progressed over a 1 m depth interval within this 3 m interval, inaccurate A axis values were recorded as the stainless steel gauge tubing flexed within what has turned out to be a poorly backfilled inclinometer casing which also flexed in undesirable (upslope) orientations, as discussed below. Clearly, as the depth and style of shearing is confirmed, the inclinometer gauge length should be reduced to an appropriate minimum length. Secondly, the 38.2 mm diameter occupies more than half of the typical 70 mm OD casing (approximately 58.5 mm ID) restricting the amount of displacement that can occur with the instruments remaining accessible and serviceable from the ground surface. Wider diameter 85 mm OD casing (73 mm ID) inclinometer casing allows greater movement before serviceability issues will be encountered.

2.1 Real-time data acquisition and data management

Data management in real-time is an integral aspect of this monitoring and the key component of the University of Wollongong system. The LoggerNet and MultiMon software from Campbell Scientific and Slope Indicator respectively enable remote access to the field stations from an office based PC with a modem and a telephone connection.

The programmable CR10X data logger is the intelligent component of each field station. The data loggers are setup to record data hourly and in low rainfall/dry times download data to the office weekly. When rainfall intensity increases the frequency of data download is increased to daily and even up to 4 hourly (at which time the datalogger also starts recording data at 5 minute intervals). The rainfall intensity thresholds to trigger the varied data logger responses are coded in the software over antecedent intervals spanning 6 hours up to 120 days.

The office based PC can contact the field stations at any time and download data. Alarm conditions can be set on the office PC software whereby colour coded
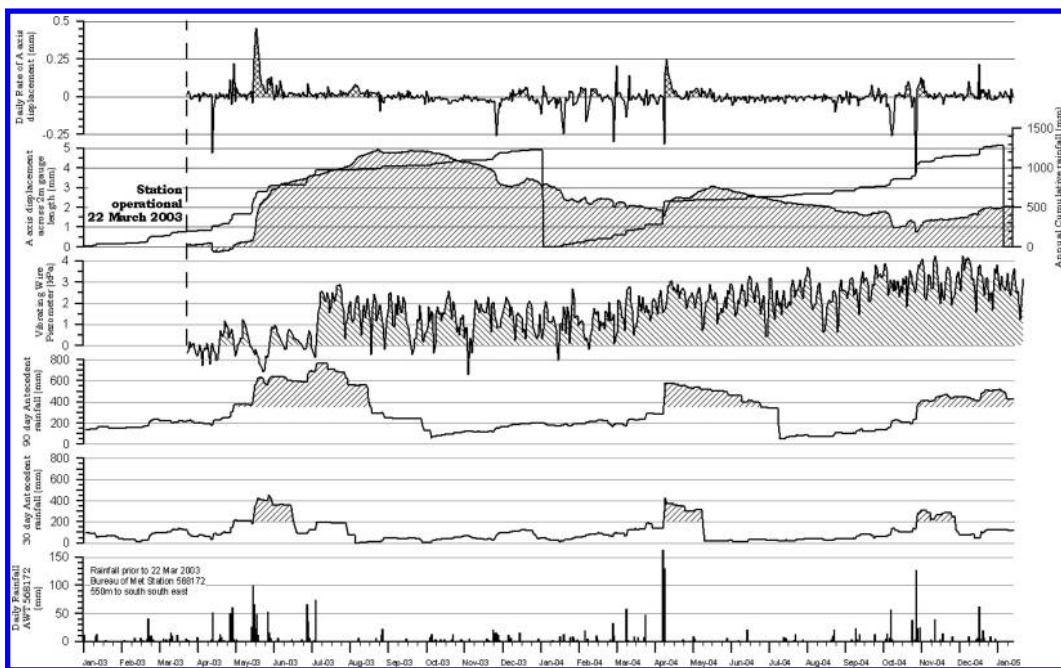
743

Figure 2. Continuous monitoring history, landslide Site 113, 22nd March 2003 to 7 Jan 2005. Rainfall, pore water pressure, landslide cumulative displacement and rate of shear.

data boxes on the graphical displays change colour as thresholds are reached and or exceeded.

The real challenge is then to disseminate this data to geotechnical colleagues and other managers in a timely fashion. This innovative aspect of the strategy adopted by the landslide research team is discussed in Section 7 below.

3 DATA FROM REAL-TIME MONITORING STATION INSTALLED AT SITE 113

Site 113 is a 3 m deep slide category landslide having a volume of approximately 25,000 m³ that was selected as the first trial research site for several reasons as summarised below:

1 It is an active shallow slide category landslide that has destroyed 5 houses and 1 school building during the last 50 years
2 It has been reactivated 14 times over a period of 50 years (highest known frequency of 570 landslides in study area) and was therefore likely to produce useful data in a short time frame
3 It exposes a school yard to landslide risk
4 A geotechnical investigation is currently ongoing at this site

5 There is existing inclinometer casing at this site and the depth of sliding is relatively well known.

The instrumentation (one IPI, one vwp and one pluviometer) was installed during February 2003 and the station was fully commissioned on 22nd March 2003.

The continuous monitoring record shown in Figure 2 highlights a number of important features. The rainfall over the 2-year period is close to average and this is supported by the approx 1200 mm annual cumulative totals for both years. Still the period has produced three relatively minor rainfall events during May 2003, April and October 2004, which triggered some landslide movement at this site. The May 2003 event is discussed below. The pore water pressure curve also displays two important points. The vibrating wire piezometer was installed on the 3rd February 2003 and did not indicate 'reasonable' pore water pressure until late June 2003, a period of 4 months after installation. However, since that time the pore water pressure data has shown considerable daily variation and superimposed on this variation a slow and steady rise in pressure. As this piezometer is installed at 3.9 m depth the variability displayed is considered to be partly related to atmospheric pressure variation.

The hourly continuous monitoring record for May 2003 is shown in Figure 3 and this clearly shows that the landslide accelerated during the afternoon of the
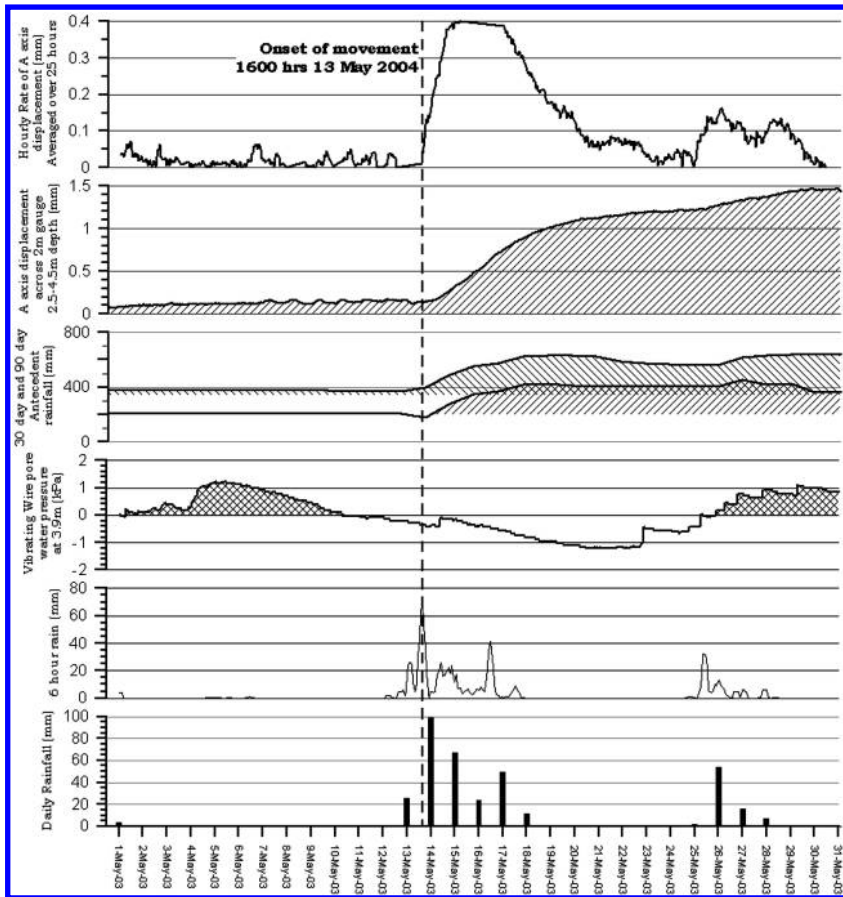
744

Figure 3.　Continuous monitoring record Site 113 for the May to August period 2003.

13th May, reached a peak velocity of 0.4 mm/25 hours on the 15th May and slowed to 0.022 mm/day by the 25th May 2003.

The landslide then briefly accelerated again up to 0.15 mm/25 hours in response to 53.4 mm of rain on the 26th May and slowed essentially to zero on the 30th May. However, as shown in Figure 2, the slide did continue moving episodically at extremely slow rates until late August 2003.

4　DATA FROM REAL-TIME MONITORING STATION INSTALLED AT SITE 355

Site 355 is a deep-seated slow moving 'slide' category landslide with a volume of approximately 35,000 m³. A comprehensive geotechnical investigation of this landslide, carried out by the University of Wollongong, has shown that this landslide presents a high risk of loss of life for adjacent residential dwellings, the

proximity of which are clearly visible in Figure 4. This assessment was an important factor that resulted in the construction of this continuous monitoring station. Three IPI's, two vibrating wire piezometers and one rainfall pluviometer were installed at the site.

The continuous monitoring record of Site 355 is shown as Figure 5. Manual inclinometer profiles recorded from borehole GUOWsc02, as shown in Figures 4 and 6, have recently confirmed that the depth of sliding in borehole 2 is between 4 and 5 m depth.

Up until 2nd November 2004, the upper IPI 11567 at this site spanned the interval 4 m to 7 m that encompassed the base of the fill material and upper colluvium whilst the two deeper IPI's spanned the base of the colluvium and colluvium-bedrock interface.

The manual profiles also display two prominent upslope deflections in the casing over the 5 to 6 m and 9 to 13 m depths. The inclinometer was installed following difficult drilling operations and partially grouted and
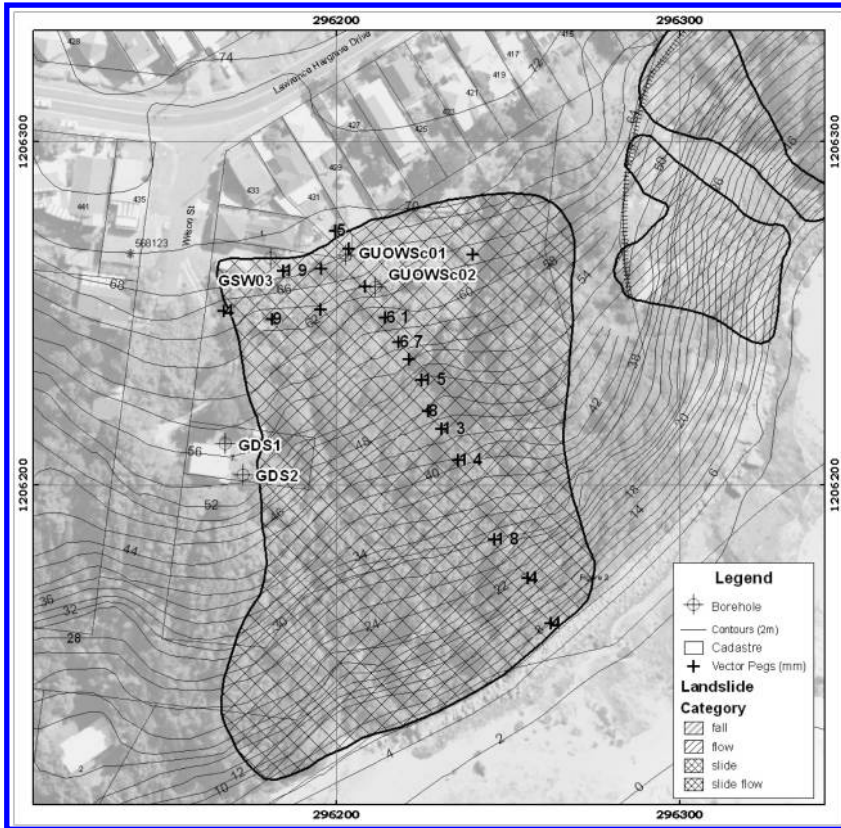
745

Figure 4. Site 355 landslide. Continuously recording field station is located at site of borehole GUOWSc02. Crosses indicate the array of vector pegs.

then backfilled with sand. Hence the upslope deflections are considered to be the result of poor annulus support. Hence any deflections indicated by IPI's 11568 and 11569 have been ignored.

This continuous dataset has highlighted several important issues. Firstly, the IPI's provide data regarding the relative displacement of two locations (per IPI instrument) in a borehole, as opposed to the full borehole profile obtained from running a manual inclinometer. Hence, the style (or profile) of landslide shear displacement experienced in a borehole should be known before an IPI can be strategically placed.

Secondly, apparent negative displacement of IPI 11567 as shown in Figure 5, was a concern. However, a review of the manual profiles displayed in Figure 6 highlights the cause of the problem. IPI 11567 includes the IPI instrument itself, as mentioned above, a 0.45 m long instrument with the bottom wheels at the base of the 4 m to 7 m monitoring interval with a stainless steel tube 2.55 m long above that at the top of which is affixed the top wheels of the monitored depth at 4 m. Figure 6 clearly shows that IPI 11567 was indeed being

rotated uphill (indicated negative displacement) approximately 18 mm whilst the soft stainless steel tubing was flexing in the inclinometer casing and actually masking the real landslide shear displacement. This situation has been rectified after the latest manual profile was recorded by removing all three IPI's and simply reinstalling one IPI (IPI 11568 was arbitrarily selected) at the 4 m to 5 m depth interval. Preliminary data from this revised installation has already exhibited 2 mm downslope displacement. Interestingly, the Inclinometer casing has now exhibited a total displacement of approximately 90 mm over this 4 m to 5 m interval and the IPI was difficult to reinstall. Consequently we have already commissioned the installation of a new borehole in which we will tremmie grout in place the larger diameter 85 mm inclinometer casing. A new vibrating wire piezometer will also be installed to monitor pore water pressure at this shallow depth.

Notwithstanding these problems, the IPI's have provided excellent data. The IPI 11567 rate of shear displacement curve in Figure 3 clearly displays two
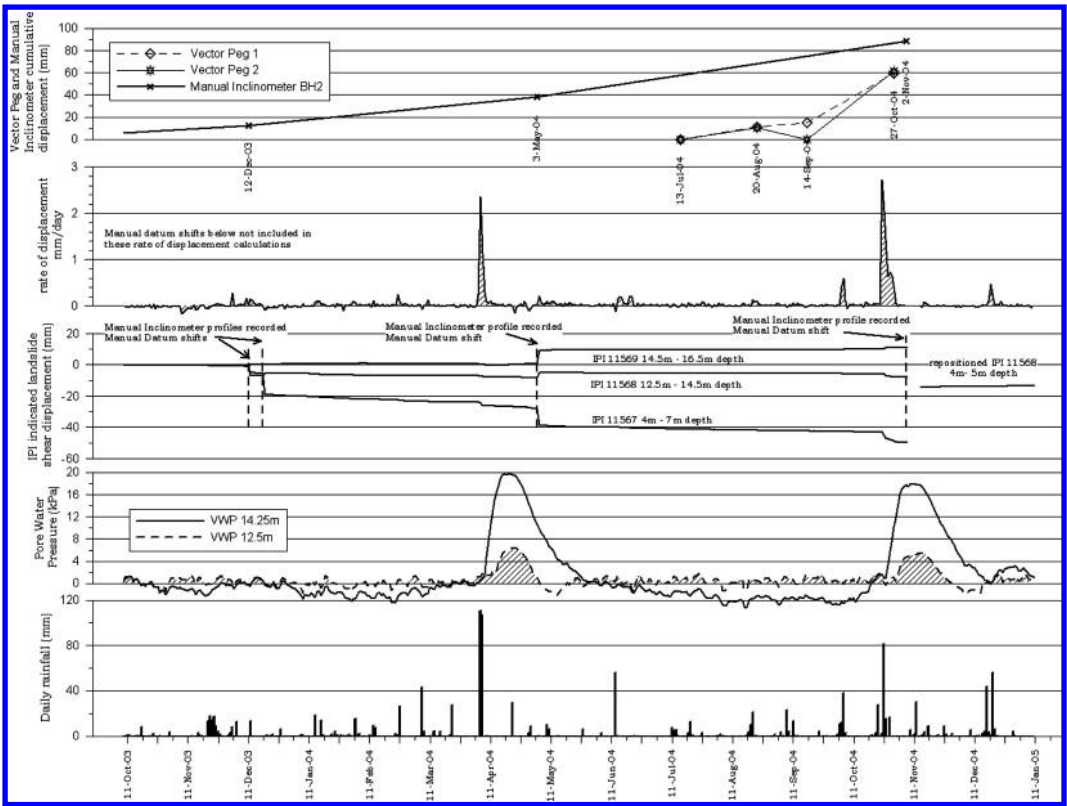
746

Figure 5. Continuous monitoring history, landslide Site 355, 11th October 2003 to 2 Dec 2004. Rainfall, pore water pressure, landslide cumulative displacement, rate of shear, vector Peg displacement and manual inclinometer displacement at 4 m depth.
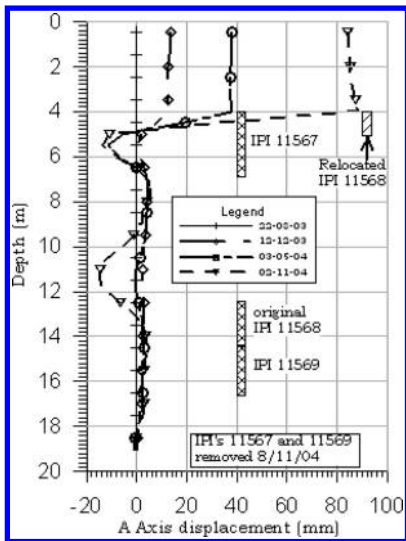

Figure 6. Manual inclinometer profiles, borehole GUOWSc02, Site 355.

prominent spikes of accelerated displacement commencing on the 4th April and the 21st October 2004. The movement event, which commenced on The 4th April, continued for 5 days and peaked at 2.4 mm per day. This was triggered by rainfall of 110 mm and 106 mm on consecutive days.

The movement event, which commenced on the 21st October 2004, lasted for 7 days and peaked at 2.7 mm per day (although this may have actually been almost 4 times higher at around 10 mm per day because of the problems discussed above) on the second day. A maximum daily rainfall of 81.5 mm and several other days of 15 mm to 30 mm triggered this short duration of movement.

The vibrating wire piezometers (vwp) have both shown quite strong responses to the rainfall. However, it is important to note that these two instruments were installed immediately above and below the bedrock colluvium interface, 7 m and 9 m below the current slide plane. As noted previously a new vwp will be installed at the depth of the slip surface in the near future.
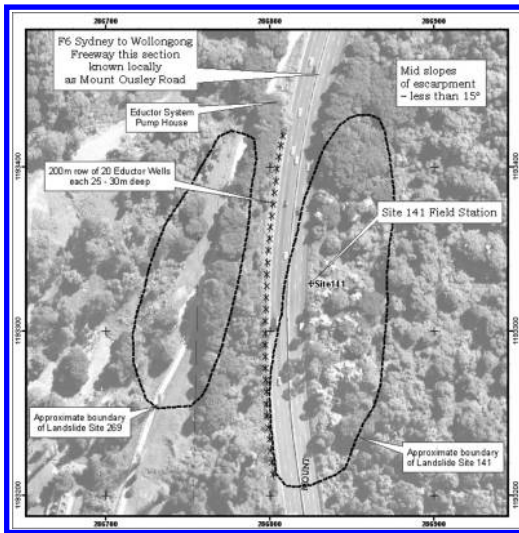
747

Figure 7. Site 141 on Mount Ousley Road (see Fig. 1).

5 SITE 141 – INTRODUCTION

Site 141 has been installed on a landslide that has previously disrupted three lanes of the six lane dual carriageway of the F6 Sydney to Wollongong Freeway (Fig. 7). This field station is one of two that has been installed on this road in collaboration with the Southern Region of the Roads and Traffic Authority (RTA) of New South Wales during 2004. The second station is Site 153, 1.5 km south of Site 141 and as no movement has occurred at this since the installation date, data from Site 153 is not being discussed in this paper.

The Site 141 landslide is approximately 200 m wide, 60 m long downslope and up to 22 m of colluvium has been encountered in boreholes drilled on the site. These dimensions indicate an approximate volume of 150,000 m^3.

During 1988 a series of twenty 100 mm diameter vertical eductor wells were installed at this landslide site on the uphill side of the carriageway as shown in Figure 7 in an attempt to "de-water" and therefore, stabilize the landslide area. Each borehole was drilled to a depth of 25–30 m and at 10 m centers spanned a 200 m length of the road. Electrical pumps have been installed in each eductor well and the outlet of each is interconnected so that the daily volume of pumped water is logged.

Existing inclinometer records from this site spanning 15 years since the installation of the eductor wells however, show an average annual displacement at this site of approximately 10 mm, with more movement in wet years and less in drier years.

The RTA is collaborating with the University and has funded the stations as part of a strategy to; (a) gain a better understanding of how both sites are performing, (b) examine means of reducing maintenance costs and (c) improve methods of managing risk to infrastructure and life.

5.1 *Data from real-time monitoring station installed at Site 141*

The two field stations on Mount Ousley Road were fully commissioned at 10:00am on Friday 30th July 2004 and since that time negligible movement has been detected as shown in Figure 8. However, two rainfall events, 76.2 mm and 164.8 mm on the 2nd and 22nd October 2004 respectively have resulted in significant rises in pore water pressure at Site 141. Two vibrating wire piezometers have been installed at this site in the same borehole, one at 17.9 m depth within the colluvium material, and the second at 22.5 m depth within the bedrock material with existing manual inclinometer profiles showing shear displacement is occurring between these two depths.

The rise in pore water pressure on the 2nd October and the subsequent 3 days was striking and some cause for concern. However, the rapid drop in pore pressure on the 5th October was even more surprising. This process was repeated following the heavy rainfall of the 22nd October although this time it was accompanied by curious pore water pressure fluctuations.

The field station does not log the eductor well flow rate at present (may in the future), rather this data is acquired at 6 monthly intervals via data exchange with another organisation. It is only upon viewing this data together with the pore water and rainfall data that a better understanding of the inter-relationships develops. On the 12th July 2004, prior to the field station being commissioned, the eductor wells pumping flow rate had dropped below the pre-set threshold of 90 Kilolitres per day whereby the pumps were turned off, being re-activated again on the 4th October, following the rainfall on the 2nd October.

At this early stage it is clear that pumping from the eductor wells inhibits the rise in pore water pressure at both vibrating wire instrument levels (i.e., both above and below the slide plane) and that the pore water pressure rises that do occur are dissipated rapidly. This of course has the positive effect of at least mitigating landslide movement at this site.

6 DISCUSSION – PROPOSED ARRAY OF STATIONS DISTRIBUTED THROUGHOUT THE STUDY AREA

There are four field stations operating in Wollongong at the present time and these represent the early stages
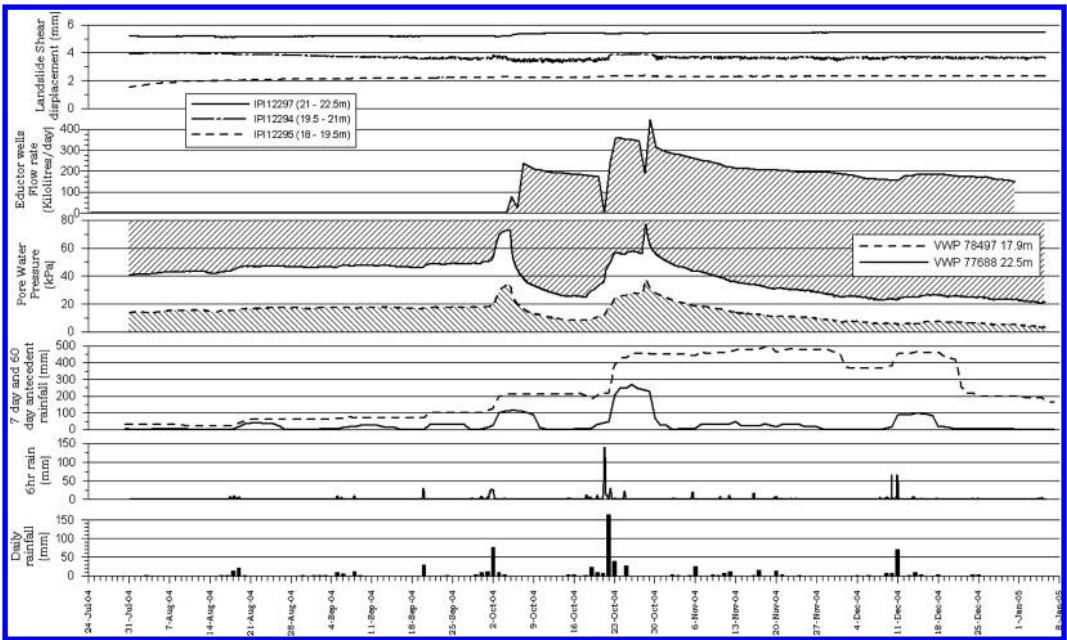
Figure 8. Continuous monitoring history, landslide Site 141 30th July to 7th Jan 2005. Daily and 6 hourly rainfall, pore water pressure, eductor wells daily volumetric output, landslide cumulative displacement and rate of shear.

of the University of Wollongong proposed network of real-time continuous monitoring stations. We propose to install up to 15 additional stations at some of the nearly 600 landslides documented within the area that pose a risk to residential areas or certain infrastructure components.

The need for such an array of stations has been well demonstrated during the August 1998 Wollongong rainfall event. During this event the city experienced 750 mm of rainfall during 5 days and the city was isolated from adjacent urban centres including Sydney for 24 hours. A total of 142 landslides were activated during and in the weeks following this event. However, during the emergency response phase, accurate information regarding rainfall was limited and information regarding landslide movement was not available, other than incoming reports of damage.

The proposed network of stations will facilitate the availability of accurate information in real-time especially during emergency management situations and thereby enhance the rational allocation of limited resources during these peak demand situations.

The stations provide real-time information regarding the onset of landslide movement that is particularly important because of the episodic 'slip and stick' nature of many of the Wollongong landslides. This is well demonstrated by the performance of Site 355 during the recent late October 2004 rainfall event as discussed above. The landslide accelerated on the

21st of October and the writers were aware at 9.00am on the morning of the 21st that this was occurring. Local government authorities were informed immediately and inspections were carried out that morning. Over the next 7 days the event was monitored continuously and updated information was provided several times a day.

7 WEB BASED MANAGEMENT OF CONTINUOUS REAL-TIME DATA

Having fully automated the data collection process at the landslide sites and the transfer of that data to the office, the World Wide Web was considered to be the most appropriate way of managing the inbound data and its dissemination. This is especially important given the desired audience for the data being geotechnical colleagues, managers of essential infrastructure, managers of emergency services, police and their technical advisers and in some cases, other stakeholders.

Using the web to manage the data has important benefits. Firstly managing the data from the field stations has proven to take considerable time in the office using the commercial software described previously. Secondly, using the commercial software in the office does not in itself get the essential data out to the required audience.

749

Using the ASP.NET framework with a database created in MS Access, the landslide research team in collaboration with the University of Wollongong Centre for Educational Development and Interactive Resources (CEDIR) has developed web-based software to provide real-time graphical updates of the incoming data as it arrives from the field stations. The web-based facility is available via the University of Wollongong web portal *http://landres.uow.edu.au/* which opens as shown in Figure 9. At present four sites are available and these can be selected from the menu on the left by clicking on the site locations on the index map.

The site specific pages open as shown in the upper part of Figure 10, in this case Site 355 has been selected. The most recent 2 weeks of data is always available at a glance by selecting the 2 week overview

Figure 9. University of Wollongong continuous real-time landslide monitoring web page.
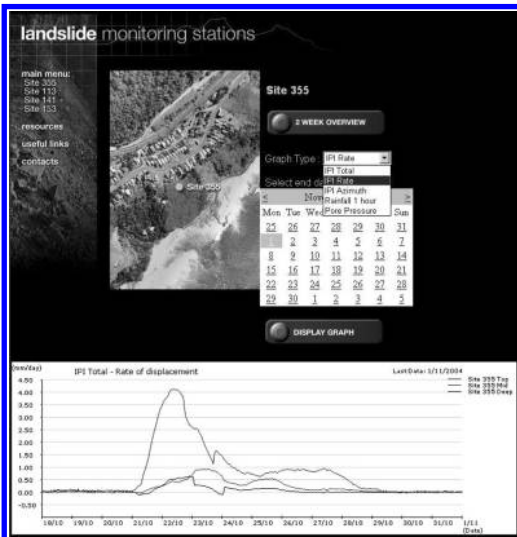

Figure 10. Site 355 continuous real-time monitoring web page with IPI rate of displacement graph for the 2 weeks up to 12:00 am hours on the 1st November 2004.

button. Furthermore, the database of existing landslide performance data is also available for review by selecting from a range of graphical outputs. The web-based hourly continuous monitoring record of In Place Inclinometers displacement at Site 355 for the 14 days up to 1st November 2004 12.00am is also shown in Figure 10. This 2 week period includes the 21st–23rd October movement event at this site. Graphs of hourly data displaying IPI Total displacement, IPI rate, IPI azimuth, hourly rainfall and pore water pressure for any 14 day period can be simply generated. The 5 graph types are soon to be extended to 18 graph types and the display period is being extended up to 180 days with a fully interactive graphical user interface.

8 FUTURE DEVELOPMENTS

The web-based real-time facility is to be upgraded on several fronts during 2005. Firstly, due to the sensitive nature of the material presented the access will be password protected. At present the data supply from the field is based on a pre-programmed regional rainfall intensity. As experience with the landslide sites and instrumentation performance develops, the reporting of data could also be activated on the basis of specified magnitudes of (a) landslide displacement, or (b) rates of displacement, or (c) pore water pressure, or (d) refined site-specific rainfall thresholds.

The web-based software will, with the appropriate experience, also be configured to provide alerts based on rainfall, pore water pressure and or displacement thresholds. These alerts will be sent automatically to designated staff via a range of media including email and telephone (voice and text). Tabulated downloads of data will also be enabled.

The network of field monitoring stations is also proposed to be extended beyond Wollongong to other landslide areas within the state NSW and even interstate.

On a more general note the html address will also be expanded to access other areas of our landslide research at the Faculty of Engineering at the University of Wollongong.

9 CONCLUSIONS

Continuous real-time monitoring is an important component of quantitative landslide risk management especially during high magnitude (longer return period) rainfall events and emergency management operations. However, it is also important for risk assessment work in helping to quantitatively assess landslide frequency and hazard. In addition the data provides an important research component as the landslide performance data together with pore water

pressure and rainfall contributes greatly to the understanding of landslide processes and triggering mechanisms. Such data recorded at 5 minute and 1 hour intervals is providing an unparalleled database of information.

Whilst Pedrozzi (2004) has recently suggested that the regional prediction of triggering of landslides is not possible using rainfall intensity/frequency methods in an area such as Canton Ticino in Switzerland, the writers strongly believe that a regional landslide triggering rainfall threshold (intensity/frequency) curve is relevant for the Illawarra area of New South Wales in Australia. In fact a preliminary threshold has already been proposed for this area (Flentje 1998, Flentje & Chowdhury 2001). It is understood that rainfall threshold curves for specific landslide sites will differ from a regional curve.

The continuous real-time monitoring discussed in this paper will lead to a refinement of the existing regional landslide triggering rainfall threshold (intensity/frequency) curve and the refinement and or development of specific threshold curves for the four sites. These are important developments as they will enhance our ability to provide early warning of landslide activity.

Coupled with these developments is the improved quantitative assessment of landslide frequency and hazard that this data will provide. With experience as the data record builds the rates of landslide displacement and frequency of events will be reviewed in comparison with structural damage and vulnerability tables.

REFERENCES

Chowdhury, R., Flentje, P., Hayne, M. & Gordon, D. 2002. Strategies for Quantitative Landslide Hazard Assessment. Proceedings of the International Conference on Instability – Planning and Management. McInnes & Jakeways (eds.), Isle of Wight, UK, Thomas Telford, London, pp 219–228.

Chowdhury, R. & Flentje, P. 2002b. Keynote Address - Modern Approaches for Assessment and Management of Urban Landslides. Proceedings of the 3rd International Conference on Landslides, Slope Stability and the Safety of Infrastructures. July 11–12, Singapore. CI-Premier Conference Organisation, pp 23 – 36.

Flentje, P. 1998. Computer Based Landslide Hazard and Risk Assessment. PhD Thesis, University of Wollongong, Australia.

Flentje, P. & Chowdhury, R.N. 2001. Aspects of Risk Management for Rainfall – Triggered Landsliding. Proceedings of the Engineering and Development in Hazardous Terrain Symposium, New Zealand Geotechnical Society Inc. University of Canterbury, Christchurch, New Zealand. The Institution of Professional Engineers New Zealand. August 24–25, pp 143–150.

Hendrickx, M., Wilson, R., Moon, A., Stewart I. & Flentje, P. in prep. Slope hazard assessment on a coast road in New South Wales, Australia.

Ko Ko, C. 2001. Landslide Hazard and Risk Assessment Along a Railway Line, Ph.D. thesis, University of Wollongong, New South Wales, Australia

Ko Ko, C., Flentje, P. & Chowdhury, R. 2004. Interpretation of Probability of landsliding triggered by rainfall. Landslides 1(4): 263 – 275.

Pedrozzi, G. 2004. Triggering of landslides in canton Ticino (Switzerland) and prediction by the rainfall intensity and duration method. Bulletin of Engineering Geology and the Environment 63(4): 281 – 291.